

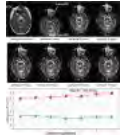
The VIP Cancer MR Session

Exhibition Hall

Monday, May 9, 2016: 10:45 - 11:45

2635

Computer #1



Longitudinal Diffusion MRI for Treatment Response Assessment: Preliminary Experience using an MRI-Guided tri-Cobalt 60 Radiotherapy System

Yingli Yang¹, Minsong Cao¹, Ke Sheng¹, Yu Gao², Allen M Chen¹, Mitchell Kamrava¹, Percy Lee¹, Nzhde Agazaryan¹, James Lamb¹, David H Thomas¹, Daniel A Low¹, and Peng Hu²

¹Radiation Oncology, University of California, Los Angeles, Los Angeles, CA, United States, ²Radiological Sciences, University of California, Los Angeles, Los Angeles, CA, United States

Diffusion weighted MRI is promising for early prediction of response to radiotherapy 1, 2, and for adaptive radiotherapy, wherein the treatment plan is adapted during treatment based on patients' response assessed by imaging. Currently DWI-based adaptive radiotherapy is not widely adopted because of scientific and practical challenges. Most importantly, the timing for DWI imaging is not well studied without longitudinal diffusion MRI data at a finer time interval (every 2-5 days) throughout the course of treatment. A recently commercialized MRI-guided radiotherapy system (ViewRay) may eliminate the current challenges and bring diffusion MRI-guided adaptive radiation therapy closer to clinical utility.

2636

Computer #2



MR T1p imaging study on normal-appearing brain in patients with nasopharyngeal carcinoma after radiotherapy

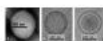
Xiang Xiao¹, Yikai Xu¹, Yuankui Wu¹, Yingjie Mei², and Queenie Chan³

¹Department of Medical Imaging Center, Nanfang Hospital, Southern Medical University, Guangzhou, China, People's Republic of, ²Philips Healthcare, Guangzhou, China, People's Republic of, ³Philips Healthcare, HongKong, China, People's Republic of

Radiation induced encephalopathy is one of the most serious complications of radiotherapy (RT) for treatment of nasopharyngeal carcinoma (NPC). In order to detect early radiation-induced changes in gray matter (GM) and white matter (WM) of NPC patients after RT, we recruited NPC patients before RT and after RT with normal-appearing brain for MR T1p examination. We found abnormal microstructure changes of WM had already happened in NPC patients after RT even when routine MRI findings are negative. MR T1p imaging can be used to detect early radiation-induced changes of WM following RT for NPC patients.

2637

Computer #3



Targeted MRI contrast guided drug delivery: Magnevist and doxorubicin encapsulated into liposomes for detection and treatment of glioma

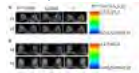
Xiaoli Liu¹, A. B. Madhankumar², Patti A. Miller¹, Becky Webb², James R. Connor², and Qing X. Yang¹

¹Radiology, College of Medicine Penn State University, Hershey, PA, United States, ²Neurosurgery, College of Medicine Penn State University, Hershey, PA, United States

Glioma in its early stage is hard to detect and treat because MRI contrast agent and chemotoxin are not able to cross the blood brain barrier (BBB). The conventional MRI contrast agent such as Magnevist (GD-DTPA) is limited to the cases where the BBB is significantly compromised by the tumor. Present study reports the development of a novel theranostic tool, interleukin-13-liposomes-Magnevist-doxorubicine (IL-13-lip-magnevist-dox) for detection and treatment of glioma. Our results demonstrated that IL-13-lip-magnevist-dox own the potential to specifically target, concomitantly detect and treat glioma in its early stage when BBB is still intact.

2638

Computer #4



Early Prediction and Evaluation of Breast Cancer Response to Neoadjuvant Chemotherapy Using Quantitative DCE-MRI

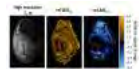
Alina Tudorica¹, Karen Y Oh¹, Stephen Y-C Chui¹, Nicole Roy¹, Megan L Troxell¹, Arpana Naik¹, Kathleen Kemmer¹, Yiyi Chen¹, Megan L Holtorf¹, Aneela Afzal¹, Charles S Springer, Jr¹, Xin Li¹, and Wei Huang¹

¹Oregon Health & Science University, Portland, OR, United States

DCE-MRI was performed in 28 breast cancer patients (29 tumors) before, during, and after neoadjuvant chemotherapy (NACT). Several DCE-MRI pharmacokinetic (PK) parameters were found to be good early predictors of pathologic complete response (pCR) vs. non-pCR after only one NACT cycle. In addition, several PK parameters and tumor size were significantly correlated with pathologically measured residual cancer burden (RCB).

2639

Computer #5



The USPIO GEH121333 as a dual R1 and R2 Contrast Agent for Imaging Response to Anti-angiogenic Therapy

Jana Cebulla¹, Eugene Kim¹, Dan E Meyer², Karina Langseth³, Tone F Bathen¹, Siver A Moestue¹, and Else Marie Huuse^{1,4}

¹Department of Circulation and Medical Imaging, Norwegian University of Science and Technology, Trondheim, Norway, ²Diagnostics, Imaging and Biomedical Technologies, Niskayuna, NY, United States, ³GE Healthcare AS, Oslo, Norway, ⁴Department of Medical Imaging, St. Olavs University Hospital, Trondheim, Norway

Preclinical-phase iron oxide particles (GEH121333), with a high r_1/r_2 ratio compared to other iron oxide nanoparticles, were used for monitoring vascular response to bevacizumab treatment in ovarian cancer xenografts. Susceptibility contrast MRI using T_2 and T_2^* mapping revealed a treatment induced decrease in blood volume and vessel density, but not in vessel size. Additionally, DCE-MRI using gadodiamide detected a decrease in perfusion and/or permeability. In combination, these two methods provide a comprehensive assessment of anti-angiogenic treatment effects.

Lastly, GEH121333 particles induced a strong signal increase in T_1w images, which shows promise for its use also as a positive contrast agent.

2640

Computer #6



Assessment of anti-angiogenic efficacy of targeted ECO/siHIF-1 α nanoparticles with DCE-MRI and a biodegradable macromolecular contrast agent

Anthony Malamas¹ and Zheng-Rong Lu¹

¹Biomedical Engineering, Case Western Reserve University, Cleveland, OH, United States

To apply DCE-MRI with a biodegradable macromolecular contrast agent in assessment of the efficacy of targeted ECO/siRNA nanoparticles for silencing HIF-1 α expression for cancer therapy in a mouse colon cancer model. DCE-MRI non-invasively revealed that the treatment resulted in over 70% reduction in average tumor blood flow (Fp), permeability-surface area product (PS), and plasma volume fraction (Vp) in the treatment group as compared to the saline control group ($p < 0.05$). The treatment was effective to inhibit tumor angiogenesis and proliferation.

2641

Computer #7



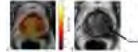
Inhibiting 2-hydroxyglutarate production reverses some, but not all, of the MRS-detectable metabolic markers of mutant IDH1 in glioma Pavithra Viswanath¹, Russell Pieper², and Sabrina M Ronen¹

¹Radiology, University of California San Francisco, San Francisco, CA, United States, ²Neurological Surgery, University of California San Francisco, San Francisco, CA, United States

Mutations in IDH1 are predominant in low-grade gliomas, and inhibitors of the mutant IDH1 enzyme are under investigation as therapeutic agents. Beyond 2-HG production, the IDH1 mutation also induces a broader pattern of ¹H-MRS-detectable metabolic alterations. In this study, we investigated whether inhibiting mutant IDH1 using AGI-5198 reverses the metabolic reprogramming observed in IDH1 mutant glioma cells. Our results indicate that AGI-5198 treatment, while completely inhibiting 2-HG production, nevertheless only partially reverses other metabolic alterations and results in a moderate effect on clonogenicity of IDH1 mutant cells.

2642

Computer #8



Assessment of R1 Relaxation Rate Error in DCE-MRI Using Bookend Measurements

Michael Josef Dubec¹ and Lucy Elizabeth Kershaw^{1,2}

¹CMPE, The Christie NHS Foundation Trust, Manchester, United Kingdom, ²Institute of Cancer Sciences, University Of Manchester, Manchester, United Kingdom

Dynamic contrast enhanced MRI (DCE-MRI) allows quantitative assessment of tumour status. The addition of a relaxation rate (R_1) measurement following the dynamic acquisition in DCE-MRI studies allows the uncertainty in the conversion from signal intensity (S) to R_1 to be assessed. In this work the effect of errors in flip angle and pre-contrast signal estimation on the S(t) to $R_1(t)$ conversion were evaluated. Results indicated that uncertainty in the measurement of S_{pre} had greater effect than realistic flip angle variations on the S(t) to $R_1(t)$ conversion, and that the error was tissue dependent.

2643

Computer #9



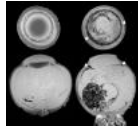
Spatial Overlapping between the Subvolumes with Elevated CBV and with Hypercellularity in Glioblastoma Hemant Parmar¹, Daniel Wahl², Priyanka Pramanik², Michelle Kim², Theodore S Lawrence², and Yue Cao^{1,2}

¹Radiology, University of Michigan, Ann Arbor, MI, United States, ²Radiation Oncology, University of Michigan, Ann Arbor, MI, United States

Standard imaging for glioblastoma relies on post-contrast T1 and T2 FLAIR MRI sequences, which do not accurately reflect tumor biology. Advanced MRI techniques can define biologically relevant and prognostic features of glioblastoma including perfusion-based volumes with high cerebral blood volume (V_{hCBV}) and high b-value diffusion-based hypercellular subvolume (HCV). We defined V_{hCBV} and HCV in 24 patients with glioblastoma prior to undergoing chemoradiation. Surprisingly, there was little overlap between V_{hCBV} and HCV within individual patients, which suggests that these volumes represent distinct aspects of tumor biology and may be independently prognostic. Analysis of failure patterns and prognostic relevance is ongoing.

2644

Computer #10



Ultrahigh-field (9.4T and 17.6T) magnetic resonance imaging of retinoblastoma: ex vivo evaluation of microstructural anatomy and disease extent

Marcus Christiaan de Jong¹, Pim de Graaf¹, Petra Pouwels¹, Jan-Willem Beenakker², Jeroen Geurts¹, Annette C. Moll¹, Jonas A. Castelijns¹, Paul van der Valk¹, and Louise van der Weerd²

¹VU University Medical Center, Amsterdam, Netherlands, ²Leiden University Medical Center, Leiden, Netherlands

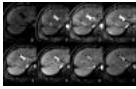
Staging of retinoblastoma – the most common pediatric eye cancer – is currently performed in vivo at 1.5 or 3.0 T and allows for images with voxel sizes $< 0.5 \times 0.5 \times 2 \text{ mm}^3$. We performed ex vivo ultrahigh-resolution MRI at 9.4 and 17.6 T of enucleated retinoblastoma eyes. This method allowed us to generate high-resolution images (voxel size: $59 \times 59 \times 59$ to $100 \times 100 \times 100 \mu\text{m}^3$) of different aspects of retinoblastoma showing the potential of ultrahigh-resolution MRI for staging retinoblastoma and gaining insight in anatomical details.

2645

Computer #11

Improved Detection of Recurrent Hepatocellular Carcinomas in Arterial Phase with Multiple Arterial-Phase Volume-Interpolated Breath-Hold Examination

Jinrong Qu¹, Hui Liu², Zhaoqi Wang³, Ihab R Kamel⁴, Kiefer Berthold⁵, Nickel Marcel Dominik⁵, and Hailiang Li¹



¹Radiology, Henan Cancer Hospital, Zhengzhou, China, People's Republic of, ²MR Collaboration, Siemens Healthcare, Shanghai, China, People's Republic of, ³Radiology, the affiliated Cancer Hospital of Zhengzhou University, Zhengzhou, China, People's Republic of, ⁴Radiology, Johns Hopkins University School of Medicine, Baltimore, MD, United States, ⁵MR Pre-development, Siemens Healthcare, Erlangen, Germany

Overall, 6 arterial sub-phases TWIST-VIBE showed higher detection of recurrent HCCs compared with the equivalent-to-conventional single arterial phase exams by providing an optimized wide observation window for tumor vascularity evaluation. This is especially valuable in improving the detection of hypervascular recurrent HCCs with diameters of less than 2cm.

2646

Computer #12



Multi-parametric MRI at 3.0 Tesla for the Prediction of Treatment Response in Rectal Cancer

Trang Pham^{1,2,3}, Michael Barton^{1,2,3}, Dale Roach⁴, Karen Wong^{1,2,3}, Daniel Moses^{2,5}, Christopher Henderson^{2,6,7}, Mark Lee¹, Robba Rai¹, Benjamin Schmitt⁸, and Gary Liney^{1,3,9,10}

¹Radiation Oncology, Liverpool Hospital, Sydney, Australia, ²Faculty of Medicine, University of New South Wales, Sydney, Australia, ³Ingham Institute for Applied Medical Research, Sydney, Australia, ⁴Faculty of Physics, University of Sydney, Sydney, Australia, ⁵Radiology, Prince of Wales Hospital, Sydney, Australia, ⁶Anatomical Pathology, Liverpool Hospital, Sydney, Australia, ⁷Faculty of Medicine, Western Sydney University, Sydney, Australia, ⁸Siemens Healthcare Pty Ltd, Sydney, Australia, ⁹Faculty of Radiation and Medical Physics, University of Wollongong, Wollongong, Australia, ¹⁰University of New South Wales, Sydney, Australia

A complete protocol using quantitative diffusion weighted imaging (DWI) and dynamic contrast enhanced (DCE) imaging in combination, and a voxel-by-voxel histogram analysis strategy was successfully developed for multi-parametric MRI prediction of treatment response in rectal cancer. In good responders, the week 3 histograms showed a combined shift in distribution of ADC of voxels to higher values and K^{trans} of voxels to lower values compared to the pre-CRT. Multi-parametric histogram analysis of ADC and K^{trans} appears to be a promising and feasible method of assessing tumour heterogeneity and its changes in response to CRT in rectal cancer.

2647

Computer #13 Chang-Zheng Shi¹, Dong Zhang², Liang-Ping LUO³, and Yong Zhang⁴



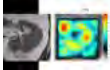
The study of vascular disrupting agent A64 combined with bevacizumab in the treatment of NSCLC using Multiple b-value DWI

¹Jinan University, Guangzhou, China, People's Republic of, ²Guangzhou, China, People's Republic of, ³Guangzhou, China, People's Republic of, ⁴GE Healthcare MR People's Republic of

Studies showed that vascular disrupting agents and angiogenesis inhibitors had a synergistic effect for the treatment of cancer. Few previous reports on angiogenesis drugs in non-small cell lung cancer (NSCLC). MR multi-b value diffusion-weighted imaging can be used to monitor the treatment of tumor angiogenesis drugs. In our study, the nude mice xenograft model was used to evaluate the role of vascular disrupting agents combining angiogenesis inhibition value diffusion weighted imaging (DWI).

2648

Computer #14



Characterization of Renal Tumors: Initial Experience Integrating Biomechanical and Morphological Assessment Using 3 Tesla Magnetic Resonance Imaging and Elastography (MRE)

Davide Prezzi¹, Radhouene Neji², James Stirling¹, Sami Jeljeli¹, Hema Verma³, Tim O'Brien⁴, Ben Challacombe⁴, Ashish Chandra⁵, Vicky Goh¹, and Ralph Sinkus¹

¹Division of Imaging Sciences and Biomedical Engineering, King's College London, London, United Kingdom, ²MR Research Collaborations, Siemens Healthcare, Frimley, United Kingdom, ³Department of Radiology, Guy's and St Thomas' NHS Foundation Trust, London, United Kingdom, ⁴Urology Centre, Guy's and St Thomas' NHS Foundation Trust, London, United Kingdom, ⁵Department of Histopathology, Guy's and St Thomas' NHS Foundation Trust, London, United Kingdom

Incidentally detected renal tumors are overtreated surgically, as up to 15% of them are benign, most frequently oncocytomas. We hypothesize that integrating biomechanical with morphological MRI assessment can improve lesion characterization, precluding unnecessary surgery. Initial experience and pathological correlation in four resected renal oncocytomas and renal cell carcinomas (RCC) demonstrate that 30Hz MRE with shear modulus elastography parametric mapping is feasible, correlating spatially with gross pathology, with lower viscosity/elasticity (γ) ratios [mean = 0.22] in malignant RCCs compared to oncocytomas [mean = 0.46], showing promise for clinical application.

2649

Computer #15



Integrating dynamic contrast-enhanced magnetic resonance imaging and diffusion kurtosis imaging for neoadjuvant chemotherapy assessment in nasopharyngeal carcinoma

Dechun Zheng¹, Yunbin Chen¹, Meng Liu¹, Qiuyuan Yue¹, Xiaoxiao Zhang¹, Hao Lin¹, Xiangyi Liu¹, Wang Ren¹, Weibo Chen², and Queenie Chan³

¹Radiology, Fujian Provincial Cancer Hospital, Fuzhou, China, People's Republic of, ²Philips Healthcare, Shanghai, China, People's Republic of, ³Philips Healthcare, Hong Kong, Hong Kong

DKI is an emerging technique and shows advantage than traditional DWI. Prior DCE-MRI studies suggested it had utility in early monitoring radiotherapy and chemotherapy sensitivity in anti-tumor treatment. However, there are a few studies investigated whether a combination of multi-modalities functional MRI techniques could improve diagnostic efficacy for prediction of anti-tumor outcome. This study enrolled 53 patients who received both DCE-MRI and DKI exams during NAC courses and suggested there were collaboration between DCE-MRI and DKI to early monitor NAC treatments in NPC. In addition, two NAC cycles is a better time point to non-invasive assess NAC response using fMRI.

2650

Computer #16



Apparent Diffusion Coefficient Features Predict Response to Chemoradiation Treatment of Locally Advanced Cervical Cancer
Daisy Q Huang¹, Daniel Margolis¹, Daniel Grossi Marconi², José Humberto Tavares Guerreiro Fregnani², Ana Karina Borges², FR Lucchesi², Rodrigo Rossini², Pechin Lo³, Bharath Ramakrishna³, Grace Lee³, and Mitchell Kamrava⁴

¹Radiology, Ronald Reagon UCLA Medical Center, Los Angeles, CA, United States, ²Radiation Oncology, Barretos Cancer Hospital, Barretos, Brazil, ³Radiological Sciences, Ronald Reagon UCLA Medical Center, Los Angeles, CA, United States, ⁴Radiation Oncology, Ronald Reagon UCLA Medical Center, Los Angeles, CA, United States

FDG-PET is optimal for evaluating and predicting treatment response in cervical cancer; however, developing countries where cervical cancer remains prevalent are more likely to have access to MR than radiotracer. Our prospective study explores the utility of MR for predicting treatment response. Patients with locally advanced cervical cancer underwent MR at baseline, midway through chemoradiation and after chemoradiation. Patients demonstrated robust tumor volume reduction (>93%) and increase in ADC values after treatment. The discriminatory value of the standard deviation of ADC at baseline suggests that tumor heterogeneity may be predictive of response, supporting MR's role in identifying more aggressive tumors.

2651

Computer #17



Evaluation of the tCho and β -catenin concentration with different molecular biomarkers in breast cancer patients
Khushbu Agarwal¹, Gururao Hariprasad², Komal Rani², Uma Sharma¹, Sandeep Mathur³, Vurthaluru Seenu⁴, Rajinder Parshad⁴, and Naranamangalam R Jagannathan¹

¹Department of NMR and MRI Facility, All India Institute of Medical Sciences, Delhi, India, ²Department of Biophysics, All India Institute of Medical Sciences, New Delhi, India, ³Department of Pathology, All India Institute of Medical Sciences, Delhi, India, ⁴Department of Surgical Disciplines, All India Institute of Medical Sciences, Delhi, India

We evaluated the correlation of tCho and β -catenin concentrations were correlated with molecular biomarkers (ER, PR and Her2neu) in breast cancer patients. The nuclear β -catenin expression was significantly higher compared to cytosolic expression. A positive correlation between tCho and β -catenin (cytosolic and nuclear fractions) concentrations was seen. The PR- tumors had significantly higher cytosolic β -catenin compared to PR+ tumors. This may be because progesterone acts as an inhibitor of Wnt pathway and thus its absence may lead to increased cytosolic β -catenin in PR- tumors. Results demonstrated role of tCho, β -catenin and progesterone in breast cancer progression.

2652

Computer #18



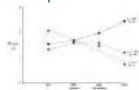
MRI/MRS-based assessment of lipid metabolism: a new tool for better detection and characterization of breast tumors?
Ileana Hancu¹, Elizabeth Morris², Christopher Sevinsky¹, Fiona Ginty¹, and Sunitha Thakur²

¹GE Global Research Center, Niskayuna, NY, United States, ²Memorial Sloan Kettering Cancer Center, New York City, NY, United States

Differential expression of lipid metabolism genes was recently reported in breast cancer patients. In this pilot study, single voxel MRS data was used to assess the spatial and spectral lipid profile of normal volunteers and subjects undergoing neo-adjuvant chemotherapy. Statistically significant differences in lipid profiles from different voxels in single volunteers and between volunteers were found. Moreover, some lipid peak ratios provided good tumor/normal tissue separation. MRI/MRS-based profiling of lipid metabolism may provide a unique tool for better breast cancer tumor detection and characterization.

2653

Computer #19



Metabolic Imaging Biomarker k_{10} Discriminates Breast Tumor Therapy Time-Courses

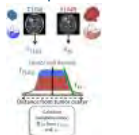
Wei Huang^{1,2}, Alina Tudorica³, Karen Y. Oh³, Stephen Y-C. Chui^{2,4}, Nicole Roy³, Megan L. Troxell^{2,5}, Arpana Naik^{2,6}, Kathleen A. Kemmer⁴, Yiyi Chen^{2,7}, Megan L. Holtorf², Aneela Afzal¹, Xin Li¹, and Charles S. Springer, Jr.¹

¹Advanced Imaging Research Center, Oregon Health & Science University, Portland, OR, United States, ²Knight Cancer Institute, Oregon Health & Science University, Portland, OR, United States, ³Diagnostic Radiology, Oregon Health & Science University, Portland, OR, United States, ⁴Medical Oncology, Oregon Health & Science University, Portland, OR, United States, ⁵Pathology, Oregon Health & Science University, Portland, OR, United States, ⁶Surgical Oncology, Oregon Health & Science University, Portland, OR, United States, ⁷Public Health and Preventive Medicine, Oregon Health & Science University, Portland, OR, United States

The new DCE-MRI biomarker k_{10} measures on-going vital metabolic activity. For subjects with biopsy-proven breast IDC, it monitors the course of neoadjuvant therapy. While k_{10} decreases for most tumors, for a sub-set it increases during therapy.

2654

Computer #20



Glioblastoma growth and invasion kinetics correlate with MRI ADC metrics

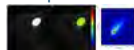
Pamela R Jackson¹, Andrea Hawkins-Daarud¹, Joshua Jacobs², Timothy Ung³, Hani Malone³, Joo Kim⁴, Olya Stringfield⁵, Lauren DeGirolamo¹, Emilio Benbassat⁶, Anthony Rosenberg⁶, Joseph Crisman⁶, Robert Gatenby⁴, Savannah Partridge⁷, Peter Canoll³, and Kristin Swanson¹

¹Neurological Surgery, Mayo Clinic, Scottsdale, AZ, United States, ²Mayo Clinic, Rochester, MN, United States, ³Pathology, Columbia University, New York City, NY, United States, ⁴Diagnostic Imaging and Interventional Radiology, H. Lee Moffitt Cancer Center, Tampa, FL, United States, ⁵Cancer Imaging and Metabolism, H. Lee Moffitt Cancer Center, Tampa, FL, United States, ⁶Chicago, IL, United States, ⁷Radiology, Seattle Cancer Care Alliance, Seattle, WA, United States

We hypothesize that tumors with different invasiveness indices (D/p), as predicted by the Proliferation-Invasion (PI) mathematical model, will exhibit differences in ADC. Segmented tumor volumes were determined on T1Gd and FLAIR MRIs for six GBM patients. The ROIs were used to mask registered ADC maps and parameterize the PI model for calculating D/p . Lower quartile ADC values within the FLAIR and FLAIR penumbra ROIs were positively correlated with D/p ($p=0.041$ and $p=0.026$, respectively). ADC skewness within the T1Gd ROI negatively correlated with D/p ($p=0.021$). Understanding the relationship between D/p and ADC could be important for targeting brain

2655

Computer #21



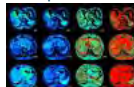
Characterization of Myxoid Soft Tissue Tumors as Benign or Malignant Using Texture Analysis of the Apparent Diffusion Coefficient
Hyun Su Kim¹, Jae-Hun Kim¹, and Young Cheol Yoon¹

¹Radiology, Samsung medical center, Seoul, Korea, Republic of

Myxoid soft tissue tumors (STTs) are histologically unique group of tumors that have been proven to have significantly higher ADC values than nonmyxoid counterparts. In addition, no significant difference of mean ADC value exists between benign and malignant myxoid STTs. We propose texture of ADC value as a new parameter for differentiating benign and malignant myxoid STTs. The global (mean, standard deviation, skewness and kurtosis), regional (intensity variability and size-zone variability), and local features (energy, entropy, correlation, contrast, homogeneity, variance and maximum probability) were extracted from ADC values of each tumor group for texture analysis and statistical comparisons were performed.

2656

Computer #22



Intravoxel incoherent motion (IVIM) imaging for differential diagnosing hepatocellular carcinoma (HCC), hepatic hemangioma and hepatic metastasis.

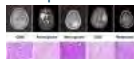
Ye Ju¹, Ai-lian Liu¹, Qing-wei Song¹, Mei-yu Sun¹, Jing-hong LIU¹, Li-hua Chen¹, Zheng Han¹, Yi-min WANG¹, and Li-zhi Xie²

¹The First Affiliated Hospital of Dalian Medical University, Dalian, China, People's Republic of, ²GE Healthcare, MR Research China, Beijing, Beijing, China, People's Republic of

The diffusion property of tumor tissues largely depends on cell density, which may also be predictive features of malignancy in some types of tumors. Intravoxel incoherent motion (IVIM) imaging is an extension of diffusion weighted imaging (DWI) that can be used to investigate both diffusion and perfusion changes in tissues. Comparing the IVIM parameters between carcinoma (HCC), hepatic hemangioma and hepatic metastasis, we found that IVIM can facilitates understanding of tumor tissue characteristics of perfusion and diffusion, and it may provide more useful information to distinguish hemangiomas from other two malignant tumors.

2657

Computer #23



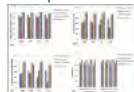
Pairwise metabolite-metabolite correlation analysis (MMCA) of HR-MAS 1H NMR spectra from 407 human brain tumours
Basetti Madhu¹, Sean McGuire¹, Alexandra Jauhiainen², and John R Griffiths¹

¹Molecular Imaging (MRI & MRS), Cancer Research UK Cambridge Institute, Cambridge, United Kingdom, ²Early Clinical Biometrics, AstraZeneca AB R&D, Molndal, Sweden

Human brain tumour tissues from glioblastoma multiforme, astrocytoma, meningioma, oligodendroglioma and metastatic tumours were analyzed by metabolite-metabolite correlation analysis of HRMAS 1H NMR spectra from the eTumour database. The following metabolites were quantified using a modified LC-Model basis set: alanine (Ala), choline (Cho), creatine (Cr), lactate (Lac), glutamine (Gln), glutamate (Glu), glycine (Gly), N-acetylaspartate (NAA), phosphocholine (PCh), phosphocreatine (PCr), taurine (tau), myo-inositol (Ino) and various lipids/macromolecules. The estimated metabolite concentrations from LCModel fittings were used in the investigation of pairwise metabolite-metabolite correlations. Pairwise metabolite-metabolite correlations can serve as an overview of metabolism and can be helpful in understanding the cellular metabolism.

2658

Computer #24



Imbalanced learning techniques for improved classification of paediatric brain tumours from magnetic resonance spectroscopy
Niloufar Zarinabad^{1,2}, Christopher Bennett^{1,2}, Simrandip Gill^{1,2}, Martin P Wilson¹, Nigel P Davies^{1,2,3}, and Andrew Peet^{1,2}

¹Institute of Cancer and Geonomic Sciences, University of Birmingham, Birmingham, United Kingdom, ²Birmingham Children's Hospital NHS foundation trust, Birmingham, United Kingdom, ³Department of Medical Physics, University Hospitals Birmingham NHS Foundation Trust, Birmingham, United Kingdom

Classification of paediatric brain tumours from Magnetic-Resonance-Spectroscopy has many desirable characteristics. However the imbalanced nature of the data introduces difficulties in uncovering regularities within the small rare tumour type group and attempts to train learning algorithms without correcting the skewed distribution may be premature. By fusing oversampling and classification techniques together, an improved classification performance across different classes with a good discrimination for minority class can be achieved. The choice of learning algorithm, use of oversampling-technique and classifier input (complete spectra versus metabolite-concentration) depends on the data distribution, required accuracy in discriminating specific groups and degree of post-processing complexity.

Electronic Poster

Educational E-Poster

Exhibition Hall

Monday, May 9, 2016: 10:45 - 11:45

2659

Computer #25



In vitro Imaging of Alanine: Application of CEST MRI

Puneet Bagga¹, Srisha Bolledula¹, Harsith Reddy¹, Rishika Reddy¹, Apoorva Sudini¹, Hari Hariharan¹, and Ravinder Reddy¹

¹Department of Radiology, University of Pennsylvania, Philadelphia, PA, United States

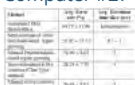
Alanine is a highly abundant non-essential amino acid which provides an alternate source of TCA cycle intermediates for energy and cell survival. It has been shown that myc-driven tumors utilize alanine as an energy source over lactate. Currently, alanine can be detected *in vivo* only by ^{13}C NMR spectroscopy. Chemical Exchange Saturation Transfer (CEST) MRI is an imaging technique which exploits the properties of exchangeable protons on the molecule for imaging. In the present study, we have shown the *in vitro* CEST effect of solution containing alanine.

2660 Computer #26 UTILITY OF PET-MRI IN INITIAL STAGING, TREATMENT PLANNING AND FOLLOW UP OF GYNECOLOGIC CANCERS
RAJ MOHAN PASPULATI¹, KARIN HERMAN¹, and AMIT GUPTA¹

¹RADIOLOGY, UNIVERSITY HOSPITALS, CASE WESTERN RESERVE UNIVERSITY, CLEVELAND, OH, United States

In this exhibit we share our 3 year experience of sequential design PET-MR (Phillips Ingenuity TF PET/MR) application in staging and follow up of gynecologic cancers. Hybrid PET-MR imaging is a new evolving technique and has a useful role in staging, treatment planning and follow up of gynecologic cancers. Standardization of the imaging protocol and understanding its limitations and pit falls is essential before considering regular clinical application.

2661 Computer #27 Automated Segmentation of Ewing's Sarcoma using Diffusion Weighted Imaging
Amit Mehndiratta^{1,2}, Abhimanyu Sahai¹, Esha Baidya Kayal¹, Jayendra Tiru Alampally³, Sameer Bakhshi⁴, Devasenathipathy K³, and Raju Sharma³



¹Center for Biomedical Engineering, Indian Institute of Technology Delhi, New Delhi, India, ²Department of Biomedical Engineering, All India Institute of Medical Sciences, New Delhi, India, ³Department of Radiology, All India Institute of Medical Sciences, New Delhi, India, ⁴BRA IRCH, All India Institute of Medical Sciences, New Delhi, India

Accurate demarcation of tumors on DWI MRimages could play a crucial role in diagnosis and prognosis when using quantitative image analysis like ADC or IVIM. Manual demarcation of tumour on each slice of a 3D stack is usually not feasible. Automated or semi-automated methods of segmentation are thus desirable specifically for DWimages that can be used to identify the tumor region, optimizing on both speed and accuracy. Our results reveals that semi-automated algorithms based on both Otsu-threshold or Active-Contours based region growing perform tumour segmentation with acceptable level of accuracy in diffusion MRimages and reduce time and manual effort required.

2662 Computer #28 How to make a diagnosis and differential diagnoses for superficial soft-tissue solid masses by magnetic resonance imaging: our experiences and initial results
Jingfeng Zhang¹, lingxiang Ruan², Qidong Wang², and Bingying Lin²



¹Dept. of Radiology, 1st Affiliated Hospital, School of Medicine, Zhejiang University, Hangzhou, China, People's Republic of, ²Hangzhou, China, People's Republic of

Superficial soft-tissue masses are common in clinical practice, and most of them are solid. The radiological imaging is available to provide more detailed information, which is more helpful to make a diagnosis and differential diagnosis. Additionally, analysis of imaging features is useful in distinguishing between benign and malignant lesions, which can help make a strategy for therapy, such as preoperative planning of the extent of surgery and whether adjuvant chemotherapy/radiotherapy. Lesions that are assigned benign can be followed expectantly, whereas indeterminate or malignant lesions can be subjected to histological evaluation. The location of a solid mass within the superficial tissue is best described as cutaneous (epidermis and dermis); subcutaneous (adipose tissue, nerve tissue, fibrous tissue and vascular tissue etc.); or fascial (overlying the muscle). Cutaneous lesions may arise in association with the epidermis or dermis, and subcutaneous lesions may arise in the adipose tissue, or the fascia overlying the muscle. However, some lesions can invade the cutaneous and subcutaneous tissue simultaneously. For purposes of comprehensive understanding and analysis, it is most useful to categorize superficial soft-tissue solid masses by histology as skin appendage tumors, mesenchymal tumors and metastatic tumors.

2663 Computer #29 Physics in Motion: Diffusion Weighted Imaging - An Illustrated Review
Yi Xiong Ong¹, Fang Yang Sim¹, and Le Roy Chong¹

¹Changi General Hospital, Singapore, Singapore

An educational video which uses simple animations to describe the random thermal molecular motion that is diffusion, and how the diffusion process can be demonstrated with the magnetic resonance signal.

Electronic Poster

Atherosclerosis Imaging

Exhibition Hall

Monday, May 9, 2016: 10:45 - 11:45

2664 The Ability to Detect Intracranial Arterial Calcifications: Evaluation of 3D TOF MRA and SNAP

Computer #31 Mahmud Mossa-Basha¹, Haining Liu¹, Dan S. Hippe¹, Niranjan Balu¹, Jie Sun¹, Dean Shibata¹, and Chun Yuan¹

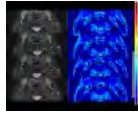


¹Radiology, University of Washington Medical Center, Seattle, WA, United States

Intracranial arterial calcification evaluation has shown increasing importance in the literature based on associations with current and future stroke events, dementia and cognitive decline. We hypothesize that the proton-density image, SNAP Ref, that is generated with Simultaneous Non-contrast Angiography and intraPlaque hemorrhage (SNAP) can more adequately assess calcifications compared to 3D TOF MRA relative to the reference standard, thin slice CTA.

2665

Computer #32



Simultaneous multi-slice carotid vessel wall MRI with DIR-FSE

Sagar Mandava¹, Mahesh Bharath Keerthivasan¹, Kevin Johnson², Diego R. Martin³, Ali Bilgin^{1,3,4}, and Maria I. Altbach³

¹Electrical and Computer Engineering, University of Arizona, Tucson, AZ, United States, ²Siemens Healthcare, Tucson, AZ, United States, ³Medical Imaging, University of Arizona, Tucson, AZ, United States, ⁴Biomedical Engineering, University of Arizona, Tucson, AZ, United States

The DIR-FSE sequence is popularly used to assess plaque build up but is known to be a single slice technique due to a non-selective inversion pulse used in the DIR module. In this work we present a technique to improve the SNR efficiency of DIR-FSE sequences by multi-band excitation. The proposed technique can generate multiple slices at the exact null point of blood and the acquired data can be used to create upto 16 TE images and T2 maps for all the acquired slices.

2666

Computer #33



Post-Contrast T1w Black Blood Images of Atherosclerotic Plaque using 3D DANTE prepared Stack of Stars (3D DANTE-SOS) Sequence and ciné Reconstruction Method using Retrospective Ordering and Compressed Sensing (ciné-ROCS)

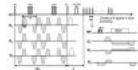
Seong-Eun Kim¹, John A Roberts¹, J Scott McNally¹, Bradley D Bolster, Jr.², Gerald S Treimam^{3,4}, and Dennis L Parker¹

¹Department of Radiology, UCAIR, University of Utah, Salt Lake City, UT, United States, ²Siemens Healthcare, Salt Lake City, UT, United States, ³Department of Surgery, University of Utah, Salt Lake City, UT, United States, ⁴Department of Veterans Affairs, VASLCHCS, Salt Lake City, UT, United States

Contrast enhanced T1 imaging has been used to aid in the detection of the fibrous cap overlying the necrotic core. We have implemented 3D SOS with retrospective cardiac cycle gated compressed sensing reconstruction to minimize, characterize artifacts in post-contrast imaging. Radial based k-space trajectory may offer reduced motion sensitivity and more robust ciné-ROCS reconstructions due to its inherent oversampling of central k-space. Ciné-ROCS reconstruction from 3D SOS acquisition demonstrates improved demonstration of fine plaque structures and vessel wall movement due to cardiac motion to the regular reconstruction and may help provide information on symptomatic plaque development and response to treatment.

2667

Computer #34



Motion insensitive high resolution in vivo DWI of Carotid Artery Wall Imaging using 3D Diffusion Weighted Driven Equilibrium Stack of Stars (3D DW-DE SOS) sequence

Seong-Eun Kim¹, J Scott McNally¹, Bradley D Bolster, Jr.², Gerald S Treimam^{3,4}, and Dennis L Parker¹

¹Department of Radiology, UCAIR, University of Utah, Salt Lake City, UT, United States, ²Siemens Healthcare, Salt Lake City, UT, United States, ³Department of Surgery, University of Utah, Salt Lake City, UT, United States, ⁴Department of Veterans Affairs, VASLCHCS, Salt Lake City, UT, United States

DWI might provide a tool for discriminating intraplaque hemorrhage and lipid core from other components. Motion insensitive 3D DW-DE SOS has been developed to acquire high resolution DWI to improve the accuracy of ADC measurements. This technique was able to yield high resolution ADC that could provide clear ROI selection for important plaque components. Increased spatial resolution in motion insensitive 3D DW-DE SOS can improve the sensitivity of ADC maps in plaque component identification. The results obtained indicate that an ADC map may be of substantial value in identifying lipid and hemorrhage within overall plaque burden.

2668

Computer #35



Motion Insensitive 3D technique for simultaneous measurement of in-vivo ADC and T2* in Atherosclerotic plaque using a 3D Multiple Echo Diffusion Weighted Driven Equilibrium Stack of Stars (3D ME-DW-DE SOS) Sequence.

Seong-Eun Kim¹, J Scott McNally¹, Bradley D Bolster, Jr.², Gerald S Treimam^{3,4}, and Dennis L Parker¹

¹Department of Radiology, UCAIR, University of Utah, Salt Lake City, UT, United States, ²Siemens Healthcare, Salt Lake City, UT, United States, ³Department of Surgery, University of Utah, Salt Lake City, UT, United States, ⁴Department of Veterans Affairs, VASLCHCS, Salt Lake City, UT, United States

DWI has the potential to provide complementary information that will allow better discrimination of plaque components such as lipid core. Iron has consistently been found in higher concentrations in atherosclerotic plaque compared to vessel tissue. In previous studies, intraplaque T2* distinguished symptomatic from asymptomatic plaques in patients with carotid atherosclerosis. In this work we introduce simultaneous measurement of ADC and T2* using a motion insensitive high resolution 3D multiple echo diffusion weighted driven equilibrium Stack of Stars sequence. This technique can provide high resolution T2* and ADC values simultaneously, which may provide important clinical information to detect plaque progression.

2669

Computer #36

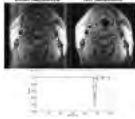
Characterization of carotid plaque using sampling perfection with application-optimized contrast using different flip angle evolution (SPACE) sequence

Yoshimitsu Ohgiya¹, Nobuyuki Ohike², Naomi Yagi¹, Hiroto Sasamori¹, Jiro Munechika¹, Masanori Hirose¹, and Takehiko Gokan¹

The purpose of this study was to investigate whether 3D turbo spin-echo (TSE) SPACE sequence can evaluate plaque characteristics of the carotid artery. Mann-Whitney test was used to examine differences in the contrast ratio (CR) between soft plaques and fibrous plaques on T1- and T2-weighted images. The mean CR of the soft plaques (1.54 ± 0.25) was significantly higher than that of the fibrous plaques (1.17 ± 0.13) ($p < 0.001$) on T1-weighted images. In conclusion, T1-weighted TSE SPACE sequence can evaluate main components of plaques in the carotid artery with high sensitivity and specificity.

2670

Computer #37



Selective reacquisition for motion artifact reduction in quantitative T2 mapping of carotid artery vessel wall
Robert Frost¹, Aaron T. Hess², Linqing Li³, Matthew D. Robson², Luca Biasioli², and Peter Jezzard¹

¹FMRIB Centre, Nuffield Department of Clinical Neurosciences, University of Oxford, Oxford, United Kingdom, ²Oxford Centre for Clinical Magnetic Resonance Research, Division of Cardiovascular Medicine, University of Oxford, Oxford, United Kingdom, ³Section on Magnetic Resonance Spectroscopy, National Institute of Mental Health, Bethesda, MD, United States

Ghosting and blurring artifacts caused by swallowing or coughing can be a significant problem in quantitative T2 mapping of atherosclerotic plaque in the carotid artery. The method is based on a multi-slice multiple spin-echo sequence which acquires k-space lines sequentially with a 2 s gap between lines. A navigator echo was added at the end of the echo-train to identify and reacquire data corrupted by motion. The selective reacquisition reduced ghosting and blurring artifacts in healthy volunteer scans with intentional swallowing motion.

2671

Computer #38



Feasibility of Vessel Wall Imaging of the Superficial Palmar Arch using 7T and 3T MRI

Alison N. Pruzan^{1,2}, Audrey Kaufman^{1,2}, Claudia Calcagno^{1,2}, Yu Zhou^{1,2}, Zahi A. Fayad^{1,2}, and Venkatesh Mani^{1,2}

¹Department of Radiology, Icahn School of Medicine at Mount Sinai, New York, NY, United States, ²Translational and Molecular Imaging Institute, Icahn School of Medicine at Mount Sinai, New York, NY, United States

Evaluation of atherosclerosis in smaller arteries in the hand may be clinically useful in certain disease conditions such as Diabetes. We sought to demonstrate feasibility of vessel wall imaging of the superficial palmar arch using 7T and 3T MRI in comparison with very high frequency micro ultrasound. Results indicated that 7T imaging of the palmar arch was feasible and subjective image quality analysis was better than 3T and ultrasound.

Electronic Poster

MRA

Exhibition Hall

Monday, May 9, 2016: 10:45 - 11:45

2672



Computer #49



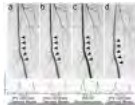
Four-Dimensional, Multiphase, Steady-State Imaging with Contrast Enhancement (MUSIC) with Improved Functional Assessment
Ziwu Zhou¹, Fei Han¹, Takegawa Yoshida¹, Kim-Lien Nguyen¹, Paul Finn¹, and Peng Hu¹

¹Radiological Sciences, University of California, Los Angeles, Los Angeles, CA, United States

A recent proposed technique called four dimensional, multiphase, steady-state imaging with contrast enhancement (MUSIC) enables detailed anatomical assessment of cardiovascular system. However, limited available cardiac phase prevents accurate functional assessment of the heart. In this study, we compared original MUSIC with an improved MUSIC technique that generates double cardiac phases. Initial results suggest a more accurate left ventricular volume measurement and better appreciation of cardiac wall motion can be achieved with more cardiac phases.

2673

Computer #50



Effect of Gadolinium-Induced Susceptibility on First-Pass Single-echo Dixon CE-MRA and Methods for Correction
Eric G. Stinson¹, Joshua D. Trzasko¹, and Stephen J. Riederer¹

¹Radiology, Mayo Clinic, Rochester, MN, United States

Single-echo Dixon imaging for contrast-enhanced MR angiography (CE-MRA) can provide the advantages of multi-echo Dixon without the tradeoff of longer acquisitions and reduced temporal resolution. Single-echo Dixon imaging assumes that both the water and fat signals are real and have known initial phase and phase due to field inhomogeneities. However, when a paramagnetic Gadolinium-based contrast agent is injected for CE-MRA, the field may be perturbed and render the a priori phase estimates invalid. The purpose of this study is to demonstrate the effect of Gd-induced field perturbations on first-pass single-echo Dixon CE-MRA and describe strategies to avoid or correct artifacts.

2674

Computer #51



Preliminary evaluation of Respiratory Self Navigated Whole-Heart Angiography in Combination with Ultra-small Super-paramagnetic Iron Oxide Particles

Davide Piccini^{1,2}, Peter J. Weale³, Saeed Mirsadraee⁴, Rachel O. Forsythe⁵, Annette S. Cooper⁶, and Scott Semple^{5,6}

¹Advanced Clinical Imaging Technology, Siemens Healthcare, Lausanne, Switzerland, ²Department of Radiology, University Hospital (CHUV) and University of Lausanne (UNIL), Lausanne, Switzerland, ³Siemens Healthcare Ltd, Camberley, United Kingdom, ⁴NHS Lothian & Clinical Research

Respiratory self-navigated 3D-radial MRA is an efficient and robust method for the depiction of coronary luminal anatomy at 1.5T. Higher magnetic fields are more challenging, due to off-resonance artifacts. Contrast-enhanced imaging is usually beneficial. However, variable contrast during prolonged scans can deteriorate the self-navigation signal. Here we investigate the use of an ultra-small super-paramagnetic iron oxide particles (USPIO) contrast agent with longer half-life in combination with self-navigation at 3T. Systolic and diastolic datasets from 10 volunteers were acquired and analyzed. We show that USPIO contrast-enhanced self-navigated coronary MRA is feasible at 3T with good image quality and reliable motion correction.

2675

Computer #52



Feasibility of Subtractionless Three-Station First-Pass Peripheral MRA at 3 T

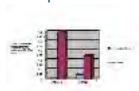
Holger Eggers¹, Bernhard Schnackenburg², Marc Kouwenhoven³, Alan Huang³, Tim Leiner⁴, Rolf Gebker⁵, and Sebastian Kelle⁵

¹Philips Research, Hamburg, Germany, ²Philips Healthcare, Hamburg, Germany, ³Philips Healthcare, Best, Netherlands, ⁴Department of Radiology, University Medical Center Utrecht, Utrecht, Netherlands, ⁵German Heart Institute Berlin, Berlin, Germany

Chemical shift encoding-based water-fat imaging, or Dixon imaging, has recently been demonstrated to permit first-pass peripheral MRA without subtraction. While previous work focused on an evaluation at 1.5 T, this work explores the feasibility of this subtractionless method at 3 T. Results on the first six patients are presented and are compared with the established subtraction method. Substantial improvements in image quality are seen, and the use of three stations is, despite particular challenges at 3 T, preliminarily found to be practicable.

2676

Computer #53



International, Multicenter Phase 3 Blinded Study of the Structural Visualization, Diagnostic Efficacy and Safety of Gadobutrol (Gadavist) Enhanced MRA of the Renal Arteries compared to Time-of-Flight MRA using CTA as the standard of reference (SoR)

Jacob Agris¹, Neda Rastegar², Kelly Fabrega-Foster², Sheela Agarwal^{1,3}, Daniel Haverstock⁴, and Ihab Kamel²

¹Radiology, Bayer, Whippany, NJ, United States, ²Radiology, Johns Hopkins, Baltimore, MD, United States, ³Radiology, Massachusetts General Hospital, Boston, MA, United States, ⁴Statistics, Bayer, Whippany, NJ, United States

International, multicenter phase 3 blinded study comparing the performance of CE-MRA with Gadobutrol, a high relaxivity and highly stable macrocyclic contrast agent, to 2D Time-of-flight MRA (ToF) using CTA as the standard of reference (SoR). 317 patients suspected of renal artery disease were enrolled. There was almost no error in the Gadobutrol MRA vessel measurements (0.0mm Gadobutrol vs 0.5mm ToF for stenosis measurements) and superior assessability as well as superior specificity was demonstrated reducing the need for additional imaging studies by 50%. Gadobutrol enhanced MRA of the renal arteries has superior visualization, more accurate measurements and is a valuable alternative to CTA without any ionizing radiation.

2677

Computer #54



Lung Perfusion: MRI vs SPECT for screening in suspected Chronic Thromboembolic Pulmonary Hypertension

Christopher S Johns¹, Smitha Rajaram², David Capener¹, David G Kiely³, Andrew J Swift^{1,4}, and Jim M Wild¹

¹Academic Unit of Radiology, University of Sheffield, Sheffield, United Kingdom, ²Radiology Department, Sheffield Teaching Hospitals, Sheffield, United Kingdom, ³Sheffield Pulmonary Vascular Clinic, Sheffield Teaching Hospitals, Sheffield, United Kingdom, ⁴Institute of In Silico Medicine, The University of Sheffield, Sheffield, United Kingdom

A comparison of perfusion SPECT and MRI in screening for chronic thromboembolic disease. To assess the role of MRI perfusion in the clinical imaging pathway in this patient group.

2678

Computer #55



Estimation of Error in Volume Measurement for 100 Intracranial Aneurysms Imaged Serially with CE-MRA at 1.5T and 3T

Farshid Faraji¹, Alastair Martin¹, and David Saloner¹

¹Department of Radiology, UCSF, San Francisco, CA, United States

Intracranial aneurysms are localized dilations in blood vessels occurring in 1-6% of the population which can have devastating consequences in the event of rupture. Many aneurysms are asymptomatic, found incidentally, and fall below the surgical size threshold. For this reason, physicians choose to follow aneurysms with imaging rather than opting for surgical or endo-vascular intervention. Here we further our analysis of a previously presented image processing technique using contrast-enhanced MRA to follow intracranial aneurysms longitudinally. We investigate the measurement error of this post-processing technique in 100 intracranial aneurysms, and evaluate the differential effects of imaging at 1.5T and 3T.

2679

Computer #56



Intra-individual quantitative and qualitative comparison of 4D-MRA- and dynamic CTA-bolus-time-curves of gadopentetate dimeglumine and gadobutrol in minipigs

Dariusch Reza Hadizadeh¹, Vera Catharina Keil¹, Gregor Jost², Hubertus Pietsch², Martin Weibrecht³, Bishr Agha¹, Christian Marx¹, Michael Perkuhn³, Hans Heinz Schild¹, and Winfried Albert Willinek⁴

¹Radiology, University of Bonn, Bonn, Germany, ²MR and CT Contrast Media Research, Bayer Healthcare, Berlin, Germany, ³Innovative Technologies, Research Laboratories, Philips Technologie GmbH, Aachen, Germany, ⁴Department of Radiology, Neuroradiology, Sonography and Nuclear Medicine, Brüderkrankenhaus Trier, Trier, Germany

In an animal model bolus kinetics and image quality after injection of 1M gadobutrol (standard and half-dose) and 0.5M gadopentetate

dimeglumine (standard-dose) had been investigated in 4D-MRA at 3T and dynamic CTA. The first pass arterial peak Gd-concentrations (quantified by CTA) were higher for standard-dose compared to half-dose gadobutrol. In 4D-MRA the first pass arterial peak enhancement was comparable for both gadobutrol doses and gadopentetate dimeglumine due to peak cut-off effects at high vascular Gd concentrations. Markedly higher venous bolus peaks were found for standard-dose gadobutrol. Image quality of 4D-MRA was rated significantly higher for both doses of gadobutrol.

2680

Computer #57



Evaluate Relative Helicity of Aortic Flow for Marfan Syndrome by 4D Flow Phase Contrast MRI

Pin-Chen Chen¹, Hsin-Hui Chiu², Wen-Yih Isaac Tseng³, and Hsu-Hsia Peng⁴

¹Institute of Systems Neuroscience, Hsinchu, Taiwan, ²Department of Pediatrics, Taipei, Taiwan, ³Center for Optoelectronic Biomedicine, Taipei, Taiwan, ⁴Department of Biomedical Engineering and Environmental Sciences, Hsinchu, Taiwan

We aim to evaluate relative helicity of aortic flow for patients with Marfan syndrome (MFS) by 4D flow phase-contrast MRI. An individual helicity_{AED} mapping was composed to provide the information of the spatiotemporal distribution of relative helicity. The E sign represents the relative helicity cores shown in the early diastole whereas D sign represents the relative helicity core shown time-delayed and downstream. The A sign represents an additional relative helicity core other than D, E, or the normal single cores. MFS patients showed abnormal relative helicity core in helicity_{AED} mapping, which provided promising approaches for patient managements in the future.

2681



Computer #58



Evaluation of Dual Agent Relaxation Contrast MR Lymphangiography (DARC-MRL) for Pre-surgical Identification of Lymphatic Channels

Beth Ripley¹, Gregory J Wilson¹, and Jeffrey H Maki¹

¹Department of Radiology, University of Washington Medical Center, Seattle, WA, United States

A new method of lymphatic channel mapping was evaluated in a retrospective review of pre-surgical lymphedema MR exams. Dual Agent Relaxation Contrast MR Lymphangiography (DARC-MRL) uses intracutaneous injection of a Gd contrast agent for enhancement of lymphatic channels and concomitant intravenous injection of USPIO (ferumoxytol) for suppression of (otherwise lymphatic-obscuring) veins. 43 MR exams using DARC-MRL were compared to 43 matched exams using conventional (no USPIO) MR lymphangiography. Exams were graded for degree of venous contamination, and DARC-MRL exams exhibited dramatically less obscuring venous contamination than the conventional method.

2682

Computer #59



Cardiac and Respiratory Motion-Resolved Free-Running Whole-Heart Coronary MRA of Patients Using 5D XD-GRASP Reconstruction.

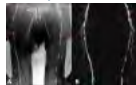
Giulia Ginami¹, Simone Coppo¹, Li Feng², Davide Piccini^{1,3}, Tobias Rutz⁴, Ricardo Otazo², Daniel Sodickson², Matthias Stuber^{1,5}, and Jerome Yerly^{1,5}

¹University Hospital (CHUV) and University of Lausanne (UNIL), Lausanne, Switzerland, ²Center for Advanced Imaging Innovation and Research (CAI2R), Department of Radiology, New York University School of Medicine, New York, NY, United States, ³Advanced Clinical Imaging Technology, Siemens Healthcare, Lausanne, Switzerland, ⁴Division of Cardiology and Cardiac MR Center, University Hospital of Lausanne (CHUV), Lausanne, Switzerland, ⁵Center for Biomedical Imaging (CIBM), Lausanne, Switzerland

Free-running self-navigated techniques have been introduced in order to allow for time resolved three-dimensional whole-heart MR acquisitions. A more recently proposed free-running 5D (x-y-z-cardiac-respiration) XD-GRASP (eXtra-Dimensional Golden-angle RAdial Sparse Parallel MRI) approach enables acquisition and reconstruction of cardiac- and respiratory-motion resolved 3D volumes. In this study, we investigated the potential of 5D XD-GRASP in a clinical setting.

2683

Computer #60



MRI of peripheral vascular calcifications using stack-of-stars 3D FLASH

Marcos Paulo Botelho¹, Shivraman Giri², Ioannis Koktzoglou^{1,3}, Alto Stemmer⁴, and Robert R. Edelman^{1,5}

¹Radiology, NorthShore University HealthSystem, Evanston, IL, United States, ²Siemens Healthcare, Chicago, IL, United States, ³Radiology, University of Chicago Pritzker School of Medicine, Chicago, IL, United States, ⁴Siemens Healthcare GmbH, Erlangen, Germany, ⁵Radiology, Feinberg School of Medicine, Northwestern University, Chicago, IL, United States

We evaluated a novel approach for visualizing and quantifying peripheral arterial calcifications using a stack-of-stars 3D FLASH pulse sequence. The technique permitted isotropic 1mm³ spatial resolution and displayed dark calcifications against a relatively uniform bright background. Banding artifacts relating to chemical shift were minimized by the use of radial in-plane spatial encoding and an in-phase echo time, while vascular signal was enhanced by the use of a low flip angle near the Ernst angle of blood. In patients with peripheral arterial disease, there was excellent correlation using CT angiography as the standard of reference.

2684

Computer #61



Non-Contrast Gate-Free Aortic MR Angiography with Robust Fat Suppression

Nobuyuki Toyonari¹, Masami Yoneyama², Seiichiro Noda¹, Yukari Horino¹, and Kazuhiro Katahira¹

¹Kumamoto Chuo Hospital, Kumamoto, Japan, ²Philips Electronics Japan, Tokyo, Japan

Non-contrast MR angiography (MRA) is a promising method to diagnose and follow-up of vascular diseases such as dissecting aortic aneurysm. Conventionally, 3D gated balanced steady-state free precession (bSSFP) is used for the aorta, but it has several limitations. To overcome bSSFP's limitations, we propose a new technique based on gradient echo DIXON sequence with flow-independent relaxation-enhanced non-contrast MRA technique (Relaxation-Enhanced Angiography without Contrast and Triggering: REACT). We showed that REACT could provide more robust and stable MRA without any artifacts and failed fat suppression compared with conventional bSSFP.

2685

Computer #62

Parameter	Value	Unit
Scanning pattern	axial	axial
FOV (mm)	400	mm
Time (min)	5:00	min
Time (min)	5:00	min
Time (min)	5:00	min
Time (min)	5:00	min
Time (min)	5:00	min
Time (min)	5:00	min
Time (min)	5:00	min
Time (min)	5:00	min
Time (min)	5:00	min

Time-of-flight unlimited: Novel self-gated unenhanced peripheral MR angiography with continuous table movement in less than 7 minutes

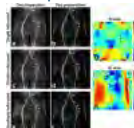
Michael O. Zenge¹, Justin Ream², Ankur Doshi², Mary Bruno², Christopher Stroehlein³, Peter Speier³, Hersh Chandarana², and Harald H. Quick^{4,5}

¹Siemens Healthcare, Malvern, PA, United States, ²Radiology, NYU Langone Medical Center, New York, NY, United States, ³Siemens Healthcare, Erlangen, Germany, ⁴Erwin L. Hahn Institute for MR Imaging, University Duisburg-Essen, Essen, Germany, ⁵High Field and Hybrid MR Imaging, University Hospital Essen, Essen, Germany

Although unenhanced MR angiography eliminates the need for contrast injection, it would use ECG triggering which adds extra time and complexity to patient preparation. In the current work, time-of-flight (TOF) unlimited introduces self-gated rapid, radial MR imaging with continuous table movement for seamless coverage of the peripheral vasculature. In-vivo experiments in five healthy volunteers and two patients were performed. Initial results are more than promising and TOF unlimited demonstrates similar image quality compared to conventional ECG triggered TOF despite sevenfold accelerated data acquisition. Thus, novel TOF unlimited may be a time efficient screening tool for peripheral arterial disease.

2686

Computer #63



Reduction of image artifacts in non-contrast-enhanced velocity-selective peripheral MRA at 3T

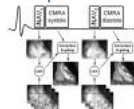
Taehoon Shin¹, Qin Qin², Jang-Yeon Park^{3,4}, Robert S. Crawford⁵, and Sanjay Rajagopalan⁶

¹Diagnostic radiology and nuclear medicine, University of Maryland, Baltimore, MD, United States, ²Radiology, Johns Hopkins University, Baltimore, MD, United States, ³Biomedical Engineering, Sungkyunkwan University, Suwon, Korea, Republic of, ⁴Center for neuroscience imaging research, Insititute for Basic Science, Suwon, Korea, Republic of, ⁵Vascular and endovascular surgery, University of Maryland, Baltimore, MD, United States, ⁶Cardiovascular Medicine, University of Maryland, Baltimore, MD, United States

Velocity-selective (VS) magnetization-prepared non-contrast-enhanced MR angiography has advantages of large 3D FOV, arbitrary 3D spatial resolution and need for single acquisition only. Peripheral VS-MRA has shown great potential at 1.5T but might be challenging at 3T due to large B₀ and B₁ inhomogeneity in the pelvis and legs. In this study, we show that the effects of B₀ and B₁ offsets are manifested as arterial signal loss, stripe artifact and background signal variation. We develop multiple-refocused VS excitation pulses and propose successive applications of two VS preparation pulses with shifted excitation profiles to suppress these artifacts.

2687

Computer #64



Dual-phase coronary MR angiography using image based respiratory navigation

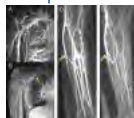
Markus Henningsson¹ and Rene Botnar¹

¹Imaging Sciences and Biomedical Engineering, King's College London, London, United Kingdom

Image-based navigation (iNAV) is a promising respiratory motion correction approach for coronary MR angiography (CMRA). However, for dual-phase CMRA the technique may fail due to the different cardiac motion states of the systolic and diastolic acquisition. Here we propose the use of separate independent systolic and diastolic iNAV acquisitions to address this issue. We compared iNAV to the conventional diaphragmatic one-dimensional navigator (1D NAV) in 8 healthy subjects. The proposed technique achieves similar or improved coronary vessel sharpness compared to 1D NAV while reducing dual-phase CMRA acquisition time.

2688

Computer #65



FSE-based Non-Contrast-enhanced Magnetic Resonance Venography for evaluation of the upper extremity veins compared with Contrast-enhanced MRV and Ultrasound

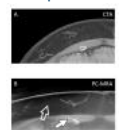
Ruth P Lim^{1,2,3}, Emma Hornsey¹, Dinesh Ranatunga^{1,2}, Huming Hao⁴, Lucy McKenna¹, Julie Smith¹, Tim Spelman⁵, Jason Chuen^{3,4}, and Mark Goodwin^{1,2}

¹Radiology, Austin Health, Melbourne, Australia, ²Radiology, The University of Melbourne, Melbourne, Australia, ³Surgery, The University of Melbourne, Melbourne, Australia, ⁴Surgery, Austin Health, Melbourne, Australia, ⁵Centre for Population Health, Burnet Institute, Melbourne, Australia

Venous mapping is important in end stage renal disease patients requiring vascular access for hemodialysis. We compare image quality (IQ) and measured vessel caliber of FSE based non-contrast MRV (NC-MRV) to contrast-enhanced MRV (CE-MRV) and US in available segments in 10 healthy volunteers. Central and arm vein IQ was diagnostic, but forearm vein IQ was suboptimal, inferior to CE-MRV. No difference in vessel caliber between sequences was demonstrated for most segments between NC-MRV and CE-MRV, but both MRV techniques yielded significantly larger caliber measurements than US, raising concern regarding application of MRV-derived measurements to clinical practice.

2689

Computer #66



Imaging Deep Inferior Epigastric Perforators with Phase Contrast Magnetic Resonance Angiography: A Feasibility Demonstration

Xiangyu Yang¹, Michael Miller², and Michael V Knopp¹

¹Radiology, The Ohio State University, Columbus, OH, United States, ²Plastic Surgery, The Ohio State University, Columbus, OH, United States

Currently, MRA is not considered the optimal technique for preoperative imaging of perforators before flap reconstructive plastic surgeries. In this prospective study, we demonstrate that the quality of perforator MRA can be greatly enhanced by using the phase contrast technique. Perforator imaging with PC-MRA not only generates images with better quality and contrast than X-ray and iodinated contrast based CTA, the current clinical gold-standard, but

also offers unique features, such as the capability to visualize venous flow and differentiate perforator arteries and veins, that are highly relevant to the design, planning, and execution of DIEP flap reconstructive surgery.

2690

Computer #67



Vessel-selective time-resolved cerebral angiograms in less than one minute

Eleanor S K Berry¹, Peter Jezzard¹, and Thomas W Okell¹

¹*FMRI Centre, Nuffield Department of Clinical Neurosciences, University of Oxford, Oxford, United Kingdom*

Vessel-encoded pseudo-continuous arterial spin labeling (VEPCASL) can be used to obtain vessel-selective time-resolved angiograms. Here we compare accelerated Cartesian and radial readouts to demonstrate the feasibility of speeding up their acquisition, enabling better prospects for use of the method in a clinical setting. It was possible to acquire 2D vessel-selective angiograms in less than one minute. Accelerated (undersampled) radial acquisition consistently led to angiograms with higher signal-to-noise ratio and better quality peripheral artery imaging versus accelerated Cartesian imaging.

2691

Computer #68



Clinically-Acceptable Non-Contrast Thoracic MRA using 3D Radial k-space Sampling and Compressed Sensing

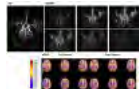
Marc D Lindley^{1,2}, Daniel Kim², Kristi Carlston², Leif Jensen², Daniel Sommers², Ganesh Adluru², Edward VR DiBella², Christopher J Hanrahan², and Vivian S Lee²

¹*Physics, University of Utah, Salt Lake City, UT, United States*, ²*Radiology, UCAIR, University of Utah, Salt Lake City, UT, United States*

As an alternative to contrast-enhanced (CE) MRA, we developed an accelerated non-contrast MRA of thoracic aorta using a combination of T2-prepared and fat saturation preparations, b-SSFP readout, 3D radial stack of stars sampling with tiny golden angles, and compressed sensing. This NC-MRA was compared with standard ECG-gated CE-MRA in 8 patients. Normalized signal difference and aortic diameters were not significantly different between CE- and NC-MRA methods.

2692

Computer #69



Non-Contrast MR Angiography with Arterial Spin Labeling: Initial Experience in Pediatric Patients With a 3D Spiral pCASL and CINEMA Protocol

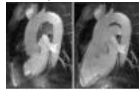
Amber Pokorney¹, Niccolo Stefani², Zhiqiang Li³, Jonathan M. Chia², John Condie⁴, Houchun Harry Hu¹, and Jeffrey H. Miller¹

¹*Radiology, Phoenix Children's Hospital, Phoenix, AZ, United States*, ²*Phillips, North America, Cleveland, OH, United States*, ³*Barrow Neurological Institute, Phoenix, AZ, United States*, ⁴*Neurology, Phoenix Children's Hospital, Phoenix, AZ, United States*

This pilot clinical study evaluates the diagnostic utility of a 3D spiral pCASL approach and a 3D dynamic PASL pulse sequence (i.e., CINEMA) in evaluating the neurovasculature in pediatric patients. With increasing recent concerns over the possible deposition of Gadolinium in the brain, a viable clinical protocol that can supplant traditional contrast-enhanced MR angiography is particularly relevant to the pediatric population. Our clinical results in patients ranging from 1 year of age to adolescents demonstrate that both 3D spiral pCASL and dynamic PASL are robust approaches and yield diagnostically useful information that supports clinical findings from conventional TOF angiography.

2693

Computer #70



Pseudocontinuous spin-labeled quiescent-interval slice-selective (QISS) magnetic resonance angiography

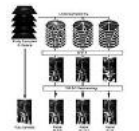
Ioannis Koktzoglou^{1,2}, Marcos P Botelho^{1,3}, Shivraman Giri⁴, Amit Pursnani⁵, and Robert R Edelman^{1,3}

¹*Radiology, NorthShore University HealthSystem, Evanston, IL, United States*, ²*University of Chicago Pritzker School of Medicine, Chicago, IL, United States*, ³*Northwestern University Feinberg School of Medicine, Chicago, IL, United States*, ⁴*Siemens Healthcare, Chicago, IL, United States*, ⁵*Medicine, NorthShore University HealthSystem, Evanston, IL, United States*

To describe a pseudocontinuous arterial spin-labeled quiescent-interval slice-selective (pCASL QISS) pulse sequence for vessel-selective nonenhanced MR angiography.

2694

Computer #71



Clinically-Feasible Non-Contrast Abdominopelvic MRA using 3D Radial Stack-of-Stars k-space Sampling and Compressed Sensing

Marc D Lindley^{1,2}, Daniel Kim², Kristi Carlston², Leif Jensen², Daniel Sommers², Ganesh Adluru², Edward VR DiBella², Christopher J Hanrahan², and Vivian S Lee²

¹*Physics, University of Utah, Salt Lake City, UT, United States*, ²*Radiology, UCAIR, University of Utah, Salt Lake City, UT, United States*

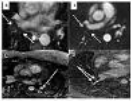
Quadruple inversion-recovery (QIR), non-contrast (NC) MRA was developed as an alternative to contrast-enhanced MRA, and its performance was evaluated in patients with peripheral arterial disease. The scan time for QIR with respiratory gating, however, is on the order of 10-15 minutes. We sought to accelerate QIR using a combination of 3D radial stack-of-stars sampling with tiny golden angles and compressed sensing (CS). This study shows that 5.3-fold accelerated QIR with radial k-space sampling and CS produces images that are comparable to those produced by original QIR (e.g., 2.7-fold acceleration using GRAPPA). In 10 human subjects, normalized signal difference and vessel dimensions were not significantly different between original QIR and 5.3-fold accelerated QIR with radial k-space sampling and CS.

2695

Computer #72

Pulmonary Magnetic Resonance Angiography: The direct and indirect findings of pulmonary embolism and their mimics

John Bisges¹, Scott K. Nagle¹, Christopher J. François¹, Peter Bannas², Michael D. Hope³, J. Paul Finn⁴, Karl Vigen¹, Thomas M. Grist¹, Scott



B. Reeder¹, and Mark L. Schiebler¹

¹Radiology, UW-Madison, Madison, WI, United States, ²Radiology, University of Hamburg-Eppendorf, Hamburg, Germany, ³Radiology, University of California at San Francisco, San Francisco, CA, United States, ⁴Radiology, University of California at Los Angeles, Los Angeles, CA, United States

The use of pulmonary magnetic resonance angiography (MRA) is playing an increasingly important role for the primary diagnosis of pulmonary embolism (PE) and other causes of acute chest pain. We will define appropriate imaging scenarios for the clinical use of this test. Then, using a pictorial essay approach, we will demonstrate the various imaging features that: (A) directly indicates the presence of PE; (2) indirectly suggests the presence of PE; (3) findings that directly show right heart strain; (4) indirect findings suggesting elevated central venous pressure and most importantly; (5) those findings that can mimic PE. After review of these teaching cases, imaging physicians will be able to confidently make the diagnosis of PE on pulmonary MRA examinations.

Electronic Poster

Velocity & Flow Quantification

Exhibition Hall

Monday, May 9, 2016: 10:45 - 11:45

2696

Computer #73



Performance of Self-Calibrated Phase Contrast Correction in Pediatric and Congenital Cardiovascular MRI

Ana Beatriz Solana¹, Erin A. Paul², Ek Tsoon Tan³, Ameer M. Shah², Wyman W. Lai², Christopher J. Hardy³, and Anjali Chelliah²

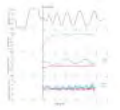
¹GE Global Research, Garching bei Muenchen, Germany, ²Dept of Pediatrics, New York-Presbyterian Morgan Stanley Children's Hospital of New York, New York, NY, United States, ³GE Global Research, Niskayuna, NY, United States

Phase contrast (PC) MR flow measurements are affected by multiple sources of error, including background phase offsets. The gold-standard approach to correct these offsets involves repeating PC measurements on a static phantom, prolonging each CMR study and impeding exam workflow. Here, we compared the performance of a self-calibrated correction to static-phantom corrected PC data obtained from a pediatric and congenital heart disease population. Self-calibrated correction results showed strong agreement with phantom-corrected data for all vessel types and differed from static-phantom correction by a mean difference in Qp/Qs values of only 0.069.

2697



Computer #74



Analysis and correction of eddy current induced artifacts in spiral phase contrast MRI using Point RESolved Spectroscopy

Rene Bastkowski¹, Kilian Weiss^{1,2}, David Maintz¹, and Daniel Giese¹

¹Department of Radiology, University Hospital of Cologne, Cologne, Germany, ²Philips Healthcare, Hamburg, Germany

A novel method based on single-voxel-spectroscopy (PRESS) for the analysis and correction of eddy-current induced artefacts in spiral phase-contrast MRI is presented. It is demonstrated, that 0th and 1st order corrections result in residual background offsets of less than 0.5cm/s, inherently correcting for geometrical misalignments between flow acquisitions as well as 2nd order spatial phase offsets. The method does not require special hardware and can be applied as a pre-scan.

2698



Computer #75



ktv-ARC reconstruction for 4D flow MRI using correlations between velocity encodings

Fatih Suleyman Hafalir^{1,2}, Ana Beatriz Solana², Peng Lai³, Malek Makki⁴, Anja C.S. Brau⁵, Axel Haase¹, and Martin A. Janich²

¹Technischen Universität München, Munich, Germany, ²GE Global Research, Munich, Germany, ³GE Healthcare, Menlo Park, CA, United States, ⁴MRI Research Center, University Children Hospital, Zurich, Switzerland, ⁵GE Healthcare, Munich, Germany

4D flow MRI is a powerful tool for visualization and quantification of blood flow. Repeated acquisition of 4 echoes with different velocity encoding is needed to measure flow in 3D. In this study, we propose a new ktv-ARC reconstruction by incorporating correlations between velocity encoded echoes (v) to the spatiotemporal correlations (kt). The error behavior of the method was analyzed on retrospectively undersampled in vivo cardiac data and resulted in more accurate velocity images with ktv-ARC compared to kt-ARC.

2699

Computer #76



Accuracy of relative pressure measurements from 3D PC-MR data using realistic aortic coarctation phantoms

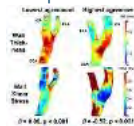
Jesús Urbina^{1,2}, Julio Sotelo^{1,3}, Cristian Montalba¹, Felipe Valenzuela^{1,3}, Cristián Tejos^{1,3}, Pablo Irrarrazaval^{1,3}, Marcelo Andia^{1,4}, Israel Valverde^{5,6}, and Sergio Uribe^{1,4}

¹Biomedical Imaging Center, Pontificia Universidad Católica de Chile, Santiago, Chile, ²School of Medicine, Pontificia Universidad Católica de Chile, Santiago, Chile, ³Electrical Engineering Department, Pontificia Universidad Católica de Chile, Santiago, Chile, ⁴Radiology Department, Pontificia Universidad Católica de Chile, Santiago, Chile, ⁵Pediatric Cardiology Unit, Hospital Virgen del Rocío, Seville, Spain, ⁶Institute of Biomedicine of Seville, Universidad de Sevilla, Seville, Spain

The aim of this work was to evaluate the accuracy of relative pressures obtained from 3D PC-MRI in a realistic aortic phantom with different grades of aortic coarctations at rest and stress conditions. We also evaluated the accuracy of the relative pressures when subjected to different aortic segmentation and spatial resolutions. The accuracy of the 3D PC-MRI is excellent compared with catheterization values with mild to moderate AoCo at rest and stress conditions. Also, relative pressures were in excellent accuracy with catheterization values when the aortic segmentation only included laminar flow and with higher spatial resolution at rest and stress conditions. However, its accuracy decreases for severe AoCo cases.

2700

Computer #77



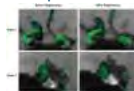
4D flow MRI-derived Wall Shear Stress Correlates with Vessel Wall Thickness: Atlases of the Carotid Bifurcation

Pim van Ooij¹, Merih Cibis², Wouter V. Potters¹, Oscar H Franco³, Meike Vernooij⁴, Aad van der Lugt⁴, Frank J Gijsen², Jolanda J Wentzel², and Aart J Nederveen¹¹Radiology, Academic Medical Center, Amsterdam, Netherlands, ²Biomedical Engineering, Erasmus MC, Rotterdam, Netherlands, ³Epidemiology, Erasmus MC, Rotterdam, Netherlands, ⁴Radiology, Erasmus MC, Rotterdam, Netherlands

The purpose of this study is to investigate if, already in early disease, a correlation exists between wall thickness (WT) and wall shear stress (WSS) in the carotid bifurcation. Eleven subjects with plaques in the left carotid arteries underwent 3D-flow-MRI and proton-density-weighted-EPI for WSS and WT quantification, respectively. Relationships between WT and WSS were investigated on an individual basis and using cohort-averaged maps (atlases). Spearman's ρ averaged over all subjects was -0.28, which was significantly different from 0 ($p < 0.001$). For the atlases, ρ was -0.66 ($p < 0.001$). The atlas approach facilitates more statistical power to show that wall thickening occurs in low WSS regions.

2701

Computer #78



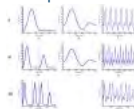
Flow and Structure with Simultaneous Visualization of Registered 4D Flow and Black Blood MRI

Dahan Kim^{1,2}, Carson Hoffman¹, Oliver Wieben^{1,3}, and Kevin M. Johnson¹¹Department of Medical Physics, University of Wisconsin, Madison, WI, United States, ²Department of Physics, University of Wisconsin, Madison, WI, United States, ³Department of Radiology, University of Wisconsin, Madison, WI, United States

In this work, we examined the feasibility of registering 4D-flow MRI scans with different scan sequences, and demonstrate how the incorporation of complementary, registered data can enhance characterization of hemodynamic information. Black blood (BB) and 4D-flow magnitude images demonstrated excellent registration between the pre- and post-rotation data sets, with high values of correlation and good overlap of the vessels between head rotation. Joint visualization of aneurysm 4D flow and BB shows accurate lesion depiction only after registration and is a promising technique for the comprehensive evaluation of vascular pathology.

2702

Computer #79



A Validation Study of Real-time Phase Contrast MRI with Low-Rank Modeling

Aiqi Sun¹, Bo Zhao², Yunduo Li¹, Qiong He¹, Zechen Zhou¹, Shuo Chen¹, Rui Li¹, and Chun Yuan^{1,3}¹Center for Biomedical Imaging Research, Department of Biomedical Engineering, School of Medicine, Tsinghua University, Beijing, China, People's Republic of, ²Martinos Center for Biomedical Imaging, Harvard Medical School, Chalestown, MA, United States, ³Department of Radiology, University of Washington, Seattle, WA, United States

Conventional phase-contrast (PC) MRI method relies on ECG-synchronized cine acquisition to acquire data over multiple cardiac cycles. The underlying spatiotemporal averaging limits this method to studying pathological irregularities. Real-time PC-MRI is a promising approach to overcome these limitations. Although several techniques have been developed to real-time PC-MRI, few have been fully validated due to the difficulty of acquiring a reference data set as gold standard. This study aims at validating the accuracy of a novel real-time PC-MRI technique through both flow phantom experiments and in vivo experiments.

2703

Computer #80



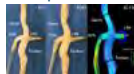
Validation of compressed sensing accelerated 2D flow MRI in the common carotid arteries

Eva S. Peper¹, Wouter V. Potters¹, Bram F. Coolen¹, Henk A. Marquering¹, Gustav J. Strijkers¹, Pim van Ooij¹, and Aart J. Nederveen¹¹Radiology, Academic Medical Center (AMC), Amsterdam, Netherlands

Flow MRI of the carotid arteries has emerged as an important imaging field during the last decade and has been shown valuable for the assessment of hemodynamics in the context of atherosclerosis. In this study a 2D flow acquisition was accelerated using random undersampling and compressed sensing reconstruction. For validation of the reconstructed flow a phantom experiment was performed at different acceleration factors followed by an in vivo scan of the carotid arteries.

2704

Computer #81



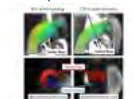
Effects of 3D-printing technology on flow measurements in patient-specific models of total cavo-pulmonary connection

Christopher J Francois¹, Zachary Borden¹, Sylvana Garcia-Rodriguez¹, Jon Wrobel¹, and Alejandro Roldan-Alzate¹¹Radiology, University of Wisconsin - Madison, Madison, WI, United States

This study investigated the effects of 3D printing technology on flow rates in patient-specific total cavo-pulmonary connection models. 4D flow MRI was used to quantify flow through the Fontan, Glenn, left pulmonary artery and right pulmonary artery in three models at four different flow rates. No statistically significant differences in flow in any of the regions of interest were observed.

2705

Computer #82



4D flow MR imaging for differentiation of pulmonary arterial hemodynamics in pre-capillary pulmonary hypertension

Hideki Ota¹, Koichiro Sugimura², Haruka Sato², Yuta Urushibata³, Yoshiaki Komori³, Hiroaki Shimokawa², and Kei Takase¹¹Diagnostic Radiology, Tohoku University Hospital, Sendai, Japan, ²Cardiovascular Medicine, Tohoku University Hospital, Sendai, Japan, ³Research&Collaborations, Siemens Japan KK, Tokyo, Japan

Etiologies of pre-capillary pulmonary hypertension may be associated with pulmonary arterial hemodynamics. This study included 64 patients (pulmonary arterial hypertension [PAH], 25, chronic thromboembolic pulmonary hypertension [CTEPH], 39) who underwent 4D flow and cardiac MR imaging. Backward flow ratio and forward flow eccentricity in the pulmonary trunk as assessed by 4D flow MR and

several cardiac MR parameters were different between two diseases. After controlling for age and mean pulmonary arterial pressure, backward flow ratio was the strongest differentiator of PAH from CTEPH. 4D flow has a potential to visualize different pulmonary arterial hemodynamics according to etiologies in pulmonary hypertension.

2706

Computer #83



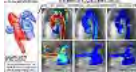
4D flow MRI Improves Computational Fluid Dynamics Analysis of Aortic Dissection
Sylvana García-Rodríguez¹, Jon Wrobel¹, Alejandro Roldán-Alzate^{1,2}, and Christopher J. François¹

¹Radiology, University of Wisconsin-Madison, Madison, WI, United States, ²Mechanical Engineering, University of Wisconsin-Madison, Madison, WI, United States

The effects of MRI-derived three-directional velocity profiles implemented at the inlet of aortic dissection (AD) computational fluid dynamics (CFD) simulations were investigated. Two AD models were generated from in vivo MRA data using 3D printing. In vitro 4D Flow MRI was performed on the AD phantoms at two flow rates. Normal and multidirectional blood flow vectors at the AD inlet was measured from 4D Flow MRI data and used in CFD simulations. Significant differences were found in pressure distribution in response to inlet boundary condition definitions. Peak velocity and wall shear stress were also affected by inlet condition definition.

2707

Computer #84



4D flow MRI derived energetic biomarkers are abnormal in repaired tetralogy of Fallot patients and may predict deteriorating hemodynamics

Joshua Daniel Robinson^{1,2}, Cynthia K Rigsby^{3,4}, Michael Rose³, Susanne Schnell⁴, Alex J Barker⁴, and Michael Markl^{4,5}

¹Pediatric Cardiology, Ann & Robert H Lurie Children's Hospital, Chicago, IL, United States, ²Pediatrics, Northwestern University Feinberg School of Medicine, Chicago, IL, United States, ³Medical Imaging, Ann & Robert H Lurie Children's Hospital, Chicago, IL, United States, ⁴Radiology, Northwestern University Feinberg School of Medicine, Chicago, IL, United States, ⁵McCormick School of Engineering, Northwestern University, Evanston, IL, United States

Tetralogy of Fallot (TOF) is the most common form of cyanotic heart disease. As life expectancy continues to increase, MRI plays a central role in evaluation for post-operative complications and reintervention. Current assessment is based on simplified parameters that measure late expression of underlying physiologic changes, with poor outcome prediction. In this study, we explore quantitative 4D flow metrics which may be important measures of hemodynamic efficiency. We found that energetic metrics are abnormal in TOF compared to healthy controls. While these metrics correlated only modestly with routine measurements of ventricular efficiency, they may represent earlier biomarkers of disease progression.

2708

Computer #85



Highly Accelerated 4D Flow MRI with CIRCular Cartesian UnderSampling (CIRCUS) in Patients with Intracranial Aneurysms
Jing Liu¹, Yan Wang¹, Farshid Faraji¹, Sarah Kefayati¹, Henrik Haraldsson¹, and David Saloner^{1,2}

¹University of California San Francisco, San Francisco, CA, United States, ²VA Medical Center, San Francisco, CA, United States

A highly accelerated 4D flow MRI method with a high spatiotemporal resolution has been validated in healthy volunteers by comparing to the conventional method. The proposed method been demonstrated to be very promising for imaging the patients with intracranial aneurysms, by achieving an isotropic resolution of 1.3mm and a temporal resolution of 26ms within a 5-minute scan time (R=12).

2709

Computer #86



Non-Contrast Cardiac 4D Flow with Bright Blood and Improved Robustness Using Multiple Thin Slab Acquisition and Variable Density Radial Sampling

Peng Lai¹, Ann Shimakawa¹, Joseph Yitan Cheng², Marcus T Alley², Shreyas S Vasanawala², and Anja C.S Brau³

¹Global MR Applications and Workflow, GE Healthcare, Menlo Park, CA, United States, ²Radiology, Stanford University, Stanford, CA, United States, ³Global MR Applications and Workflow, GE Healthcare, Munich, Germany

Cardiac 4D Flow suffers from blood signal saturation due to whole-volume imaging and limited accuracy if acquired without contrast agents. This work developed and investigated a new multiple thin slab scheme for non-contrast whole-chest 4D Flow. With in-flow enhancement and bright blood, the new sequence provides higher SNR and motion robustness than conventional 4D Flow. The proposed radial golden angle view order ensures smooth slab merging that is insensitive to cardiac and respiratory variations during the scan.

2710

Computer #87



Using MRI to Observe Increased Venous Flow Collateralization in Subjects with Anomalous Jugular Veins

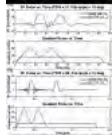
SEAN KUMAR SETHI¹, Giacomo Gadda², Ana M. Daugherty³, David T. Utriainen¹, Jing Jiang¹, Naftali Raz³, and Ewart Mark Haacke⁴

¹The MRI Institute of Biomedical Research, Detroit, MI, United States, ²Physics, University of Ferrara, Ferrara, Italy, ³Department of Gerontology, Wayne State University, Detroit, MI, United States, ⁴Biomedical Engineering, Wayne State University, Detroit, MI, United States

We have established in previous works that a subset of multiple sclerosis (MS) patients show abnormal structure and flow in the internal jugular veins (IJV) when measured with MRI. In this retrospective analysis, we classified and compared extracranial venous collateral flow in MS and normal control samples using MR venography and Phase-contrast flow quantification with a large, standardized dataset. Over 50% of the MS cohort shows a jugular anomaly. The stenotic-MS group shows reduced Type I venous flow compared to healthy controls and non-stenotic MS, while having elevated Type II and Type III flows.

2711

Computer #88



Design and Validation of a Minimum Time Verse Pulse for 4D Flow MRI

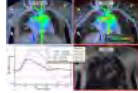
Patrick Magrath^{1,2}, Eric Aliotta^{1,3}, Shams Rashid¹, Yutaka Natsuaki⁴, Xiaoming Bi⁴, Zhe Wang^{1,2}, Kyung Sung^{1,2,3}, Peng Hu^{1,2,3}, Holden Wu^{1,2,3}, and Daniel B Ennis^{1,2,3}

¹Department of Radiological Sciences, University of California, Los Angeles, CA, United States, ²Department of Bioengineering, University of California, Los Angeles, CA, United States, ³Physics and Biology in Medicine IDP, University of California, Los Angeles, CA, United States, ⁴Siemens Healthcare, Los Angeles, CA, United States

4D-flow MRI is used to quantify blood flow in a variety of neurovascular pathologies including intracranial aneurysms [1], but is limited by long scan times as well as moderate spatial and temporal resolution. Conventional RF pulses have poor slab profiles that contribute to low sequence efficiency by increasing the field-of-view needed to avoid aliasing in the slab direction. Our objectives were to design a minimum time, high Time Bandwidth Product (TBW) VERSE pulse for 4D flow and to validate the improvement in sequence efficiency, confirm flow accuracy, and evaluate total SAR deposition for VERSE+4D-flow compared to our clinical 4D flow imaging protocol.

2712

Computer #89



Contrast-Enhanced 4D Flow Imaging with Reduced Fat Signal

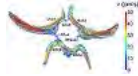
Joseph Y. Cheng¹, Tao Zhang¹, Adam B. Kerr², Michael Lustig³, John M. Pauly², and Shreyas S. Vasanawala¹

¹Radiology, Stanford University, Stanford, CA, United States, ²Electrical Engineering, Stanford University, Stanford, CA, United States, ³Electrical Engineering & Computer Sciences, University of California, Berkeley, CA, United States

Volumetric time-resolved velocity imaging (4D flow) can be used as a single comprehensive sequence to quantify blood flow, evaluate cardiac function, and assess anatomy. However, fat signal can reduce tissue contrast, introduce high-signal-intensity artifacts from motion, and cause errors in velocity quantification. Two approaches are presented for reducing fat signal in contrast-enhanced 4D flow imaging with minimal time penalty. The first approach is a short spectral-spatial RF pulse that reduces fat signal below the level of contrast-enhanced blood pool. The second approach is the introduction of one additional echo with a different TE to separate fat/water for all flow encoding echoes. The performance of these approaches are evaluated in a static phantom study and in patient volunteer studies.

2713

Computer #90



The Communicating Arteries Redistribute Blood Flow in the Circle of Willis with Hypoplastic Segments: Intracranial 4D flow MRI at 7 Tesla

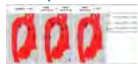
Pim van Ooij¹, Matthan Caan¹, Bart M. W. Cornelissen², Henk A Marquering², Pieter Buur³, Gustav J Strijkers², Jeroen Hendrikse⁴, and Aart J Nederveen¹

¹Radiology, Academic Medical Center, Amsterdam, Netherlands, ²Biomedical Engineering & Physics, Academic Medical Center, Amsterdam, Netherlands, ³Spinoza Center for Neuroimaging, Amsterdam, Netherlands, ⁴Radiology, University Medical Center Utrecht, Utrecht, Netherlands

In this study it was investigated if the communicating arteries redistribute blood flow in the circle of Willis (coW) with hypoplastic arteries. For this purpose, 4D flow MRI at 7 Tesla was used in ten healthy volunteers. 50% of the participants had a full coW, whereas 50% had hypoplastic or missing segments. Significant correlations were found for time-averaged blood flow (mL/s) between the left /right posterior communicating artery and the left/right posterior cerebral artery and between the anterior communicating artery and the right anterior cerebral artery. This finding illustrates that flow is redistributed through the communicating arteries in the coW.

2714

Computer #91



Aortic hemodynamics in pediatric Marfan patients compared to healthy pediatric subjects: heterogeneity in the Marfan population

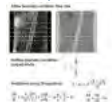
Roel LF van der Palen^{1,2}, Alex J Barker², Emilie Bollache², Michael J Rose³, Pim van Ooij⁴, Julio Garcia², Luciana Young⁵, Arno AW Roest¹, Michael Mark^{2,6}, Cynthia K Rigsby³, and Joshua D Robinson^{5,7}

¹Department of Pediatric Cardiology, Willem-Alexander Children and Youth Center, Leiden University Medical Center, Leiden, Netherlands, ²Department of Radiology, Feinberg School of Medicine, Northwestern University, Chicago, IL, United States, ³Department of Medical Imaging, Ann & Robert Lurie Children's Hospital of Chicago, Chicago, IL, United States, ⁴Department of Radiology, Academic Medical Center, Amsterdam, Netherlands, ⁵Division of Pediatric Cardiology, Ann & Robert Lurie Children's Hospital of Chicago, Chicago, IL, United States, ⁶Department of Biomedical Engineering, McCormick School of Engineering, Northwestern University, Chicago, IL, United States, ⁷Department of Pediatrics, Ann & Robert Lurie Children's Hospital of Chicago, Chicago, IL, United States

Marfan syndrome (MFS) is a connective tissue disease with high risk of aortic dissection/rupture. Two-thirds of dissections occur in the ascending aorta, one-third in the descending aorta. Diameter plays an important role in risk stratification. However, recent literature has shown diameter only accounts for 50% of the dissections in the descending aortic region. It is not well known how aortic hemodynamics interact with the altered vascular structure of these aortas and how it may impact dilatation. A cohort of MFS children and an age appropriate control group were evaluated with 4D flow MRI: already distinct abnormalities are present in childhood.

2715

Computer #92



Model-based estimation of arterial pulse wave velocity from MRI velocity data

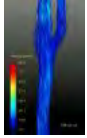
Prem Venugopal¹, Ek Tsoun Tan¹, Peter Lamb¹, Christopher J Hardy¹, and Thomas K Foo¹

¹GE Global Research, Niskayuna, NY, United States

Pulse wave velocity (PWV) is a commonly used surrogate for arterial stiffness. This abstract describes a new method to estimate arterial PWV by using MRI phase-contrast data to tune a 1D blood flow model describing the hemodynamics and propagation of the arterial pulse wave. Results obtained in a single volunteer indicate that the proposed approach could be used with low time resolution methods such as 4D Flow MRI to obtain PWV in the aorta with much lower variability than the foot-to-foot method.

2716

Computer #93



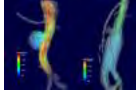
10 fold accelerated 4D flow in the carotid arteries at high spatiotemporal resolution in 7 minutes using a novel 15 channel coil
Eva S. Peper¹, Qinwei Zhang¹, Bram F. Coolen², Wouter V. Potters¹, Pim van Ooij¹, Dennis W.J. Klomp³, and Aart J. Nederveen¹

¹Radiology, AMC, Amsterdam, Netherlands, ²Biomedical Engineering and Physics, AMC, Amsterdam, Netherlands, ³Radiology, UMCU, Utrecht, Netherlands

Using a novel 15 channel coil for carotid artery imaging we could prove that the g-factor loss at higher acceleration factors is limited. This permits the use of higher parallel imaging factors than commonly exploited in carotid MRI. A 4D flow scan at high spatiotemporal resolution was accelerated 10 fold (SENSE 4 x 2.5), resulting in high quality images and consistent flow values acquired in a scantime as short as 7 min.

2717

Computer #94



Lower Wall Shear Stress and Abnormal Hemodynamics within the Saccular Aneurysm in Contrast to Fusiform Aneurysm in the Abdominal Aorta.

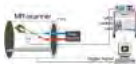
Masataka Sugiyama¹, Yasuo Takehara², Hatsuko Nasu¹, Shuhei Yamashita¹, Mika Kamiya¹, Nobuko Yoshizawa¹, Yuki Hirai¹, Takasuke Ushio¹, Naoko Hyodo¹, Yohei Ito¹, Naoki Oishi², Marcus Alley³, Tetsuya Wakayama⁴, and Harumi Sakahara¹

¹Radiology, Hamamatsu University School of Medicine, Hamamatsu, Japan, ²Radiology, Hamamatsu University Hospital, Hamamatsu, Japan, ³Department of Radiology, Stanford University School of Medicine, Stanford, CA, United States, ⁴Applied Science Laboratory Asia Pacific, GE Healthcare Japan, Hino, Japan

3D cine PC MRI (4D-flow) study of abdominal aorta was conducted to measure wall shear stress (WSS) and to characterize aortic blood flow dynamics within saccular and fusiform abdominal aortic aneurysm and non-dilated aorta. Peak systolic WSS was significantly lower within saccular aneurysm, and stream line analysis depicted separated vortex flow within the saccular aneurysm. The abnormal vortex flow and consequent low WSS of saccular aneurysmal wall may be reflecting the continuing risk of atherogenic changes of the saccular aneurysm in contrast to fusiform aneurysm.

2718

Computer #95



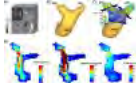
3D Printed Patient-Specific Model for In Vitro Hemodynamic Studies and Comparison with In Vivo Findings Using 4D Flow MRI
Rouzbeh R Ahmadian¹, Austin P Boyd², Jeremy D Collins¹, James C Carr¹, Alex J Barker¹, and Michael Markl³

¹Radiology, Northwestern University, Chicago, IL, United States, ²Northwestern University, Chicago, IL, United States, ³Radiology & Biomedical Engineering, Northwestern University, Chicago, IL, United States

The advent of 3D printing has opened exciting possibilities for biomedical applications. One of the most intriguing of these possibilities is the ability to use images obtained from radiology scanners (CT or MR) to create 3D models of patient anatomy followed by 3D printing. These models will have all the same geometries of patient anatomy to very high detail. In order to have practical applications, however, these 3D models need to behave similarly to human tissue under standard conditions. Our research utilizes patient-specific 3D printed models in an in vitro fluid dynamic circuit to compare 4D Flow MRI data to that of the patient (in vivo). This direct comparison will allow for validation of the 3D printed model for further biomedical application.

2719

Computer #96



Volumetric assessment of kinetic energy and vorticity in the pulmonary artery: alteration of flow hemodynamics in patients with repaired tetralogy of Fallot using 4D flow MRI

Julio Garcia¹, Silvia Hidalgo Tobon^{2,3}, Guadalupe Sagaon Rojas⁴, Benito de Celis Alonso⁵, Manuel Obregon², Porfirio Ibanez², Julio Erdmenger⁶, and Pilar Dies-Suarez²

¹Radiology, Northwestern University, Chicago, IL, United States, ²Investigacion en Imagen y Resonancia Magnetica Nuclear, Hospital Infantil de Mexico Federico Gomez, Mexico City, Mexico, ³Physics, Universidad Autonoma Metropolitana, Mexico, Mexico, ⁴Physics, Universidad Autonoma Metropolitana, Mexico City, Mexico, ⁵Faculty of Physics and Mathematics, Benemérita Universidad Autónoma de Puebla, Puebla, Mexico, ⁶Pediatric Cardiology, Hospital Infantil de Mexico Federico Gomez, Mexico City, Mexico

Flow alterations in the pulmonary artery (PA) of patients with repaired tetralogy of Fallot (rTOF) may be link with elevated kinetic energy (KE). 4D flow MRI allows for the non-invasive volumetric assessment of flow hemodynamics, vorticity, and KE in patients with rTOF in the pulmonary (PA). Thus, the aim was to investigate the impact of flow alterations in the PA and its association with KE and vorticity.

Electronic Poster

Breast Cancer

Exhibition Hall

Monday, May 9, 2016: 11:45 - 12:45

2720

Computer #1



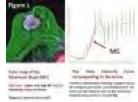
Fat suppression using water excitation for improved spatial resolution compared with 2-point Dixon at 3.0 T for DCE breast MRI
Courtney K Morrison¹, Leah C Henze Bancroft¹, Kang Wang², James H Holmes², Frank R Korosec^{1,3}, and Roberta M Strigel^{1,3}

¹Medical Physics, University of Wisconsin-Madison, Madison, WI, United States, ²Global MR Applications and Workflow, GE Healthcare, Madison, WI, United States, ³Radiology, University of Wisconsin-Madison, Madison, WI, United States

Fat suppression can be achieved in a variety of ways, including using water-only excitation or using a Dixon method. Each of these methods exhibits strengths and limitations. In this work, we evaluated the characteristics of water excitation compared to a 2-point Dixon fat suppression method used in high spatiotemporal resolution DCE breast MRI.

2721

Computer #2



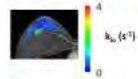
Diagnostic Performance of Maximum Slope as a Novel Kinetic Parameters in High Resolution Ultrafast Dynamic Contrast Enhanced Breast MRI using KWIC
Akane Ohashi¹, Masako Kataoka¹, Syotaro Kanao¹, Mami Iima¹, Onishi Natsuko¹, Makiko Kawai¹, Masakazu Toi², Elizabeth Weiland³, and Kaori Togashi¹

¹Department of Diagnostic Imaging and Nuclear Medicine, Kyoto University Graduate School of Medicine, Kyoto, Japan, ²Breast Surgery, Kyoto University, Kyoto, Japan, ³Siemens Healthcare GmbH, Erlangen, Germany

Maximum slope (MS) is a kinetic parameter obtained from the very early phase of ultrafast DCE MRI. Diagnostic performance of MS in breast lesions were compared to washout index (WI), a conventional semi-quantitative kinetic parameters obtained from standard DCE MRI. Ultrafast DCE MRI was obtained using KWIC and analyzed by TWIST Breast Viewer. MS demonstrated significantly higher AUC (0.91) than WI (0.80, $p=0.03$) with fewer false positive cases of fibrocystic changes than WI. MS is a promising kinetic parameters that provides information complimentary to WI in diagnosing breast lesions.

2722

Computer #3



Breast Tumor Metabolic Imaging Biomarker k_{10} Correlates with Histopathology Residual Cancer Measures
Charles S. Springer, Jr.^{1,2}, Xin Li¹, Alina Tudorica³, Karen Y. Oh³, Stephen Y-C. Chui^{2,4}, Nicole Roy³, Megan L. Troxell^{2,5}, Arpana Naik^{2,6}, Kathleen A. Kemmer⁴, Yiyi Chen^{2,7}, Megan L. Holtorf², Aneela Afzal¹, and Wei Huang^{1,2}

¹Advanced Imaging Research Center, Oregon Health & Science University, Portland, OR, United States, ²Knight Cancer Institute, Oregon Health & Science University, Portland, OR, United States, ³Diagnostic Radiology, Oregon Health & Science University, Portland, OR, United States, ⁴Medical Oncology, Oregon Health & Science University, Portland, OR, United States, ⁵Pathology, Oregon Health & Science University, Portland, OR, United States, ⁶Surgical Oncology, Oregon Health & Science University, Portland, OR, United States, ⁷Public Health and Preventive Medicine, Oregon Health & Science University, Portland, OR, United States

The new DCE-MRI biomarker k_{10} measures on-going vital metabolic activity. Whole breast tumor k_{10} correlates well with pathology determinations of residual cancer burden and tumor invasive cell volume fraction from surgical specimens obtained just a few days later.

2723

Computer #4



Pre-treatment DCE-MRI based tumour heterogeneity is associated with traditional prognostic parameters and provides an insight into early recurrence following neoadjuvant chemotherapy in locally advanced breast cancer
Martin D Pickles¹, Martin Lowry¹, and Peter Gibbs¹

¹Centre for Magnetic Resonance Investigations, Hull York Medical School at University of Hull, Hull, United Kingdom

Tumours can have high levels of heterogeneity. Lesions demonstrating high levels of heterogeneity have an 'aggressive' phenotype. Assessing heterogeneity might provide superior insights into treatment response than traditional mean/median values. The aims of this study were to determine if histogram analysis of pre-treatment DCE-MRI parameters are associated with traditional prognostic indicators and early breast cancer recurrence.

Breast dynamic datasets from 208 individuals underwent histogram analysis. U-tests and survival analysis indicated that DCE-MRI histogram parameters are associated with traditional prognostic indicators, have superior prognostic information than mean/median values and provide independent prognostic information regarding breast cancer recurrence prior to therapy initiation.

2724

Computer #5



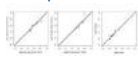
Amide proton transfer (APT) imaging of breast cancer at 3T MRI: a pilot study
Natsuko Onishi¹, Masako Kataoka¹, Shotaro Kanao¹, Mami Iima¹, Makiko Kawai¹, Akane Ohashi¹, Katsutoshi Murata², Benjamin Schmitt³, and Kaori Togashi¹

¹Dept of Diagnostic Imaging and Nuclear Medicine, Kyoto University Graduate School of Medicine, Kyoto, Japan, ²Research & Collaboration Dpt., Siemens Japan K.K., Tokyo, Japan, ³Healthcare Sector, Siemens Ltd, Melbourne, Australia

Amide proton transfer (APT) imaging is the representative endogenous chemical exchange saturation transfer (CEST) imaging that has been applied to some clinical cancer studies. However, little is known about the clinical usefulness of APT imaging in breast cancer. In this study, 3T MRI studies including APT imaging were performed for 24 breast cancer lesions, and the possible utility of APT imaging in evaluating biochemical information induced by breast cancer was demonstrated. APT CEST imaging is a potentially useful MRI technique for breast cancer.

2725

Computer #6



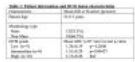
Repeatability of Diffusion MRI Measurements
Ella F Jones¹, Lisa J Wilmes¹, Wen Li¹, Jessica Gibbs¹, David C Newitt¹, John Kornak², Evelyn Proctor¹, Bonnie N Joe¹, and Nola M Hylton¹

¹Radiology and Biomedical Imaging, UCSF, San Francisco, CA, United States, ²Epidemiology and Biostatistics, UCSF, San Francisco, CA, United States

The purpose of this study was to assess breast tissue measurements using diffusion MRI techniques in repeated studies to evaluate the variability of ADC and FA measurements within- and between-subjects.

2726

Distinguishing pure ductal carcinoma in situ grade using quantitative DWI biomarkers at 3 Tesla

Computer #7

Jing Yuan¹, Gladys Lo², Oilei Wong¹, Helen H.L. Chan², Ting Ting Wong³, and Polly S.Y. Cheung³

¹Medical Physics and Research Department, Hong Kong Sanatorium&Hospital, Hong Kong, Hong Kong, ²Department of Diagnostic & Interventional Radiology, Hong Kong Sanatorium&Hospital, Hong Kong, Hong Kong, ³Breast Care Center, Hong Kong Sanatorium&Hospital, Hong Kong, Hong Kong

This study aims to explore the use of quantitative breast DWI at 3T to distinguish DCIS pathological grades. In a cohort of 30 pathology confirmed pure DCIS, the mean ADC was 1.26 ± 0.19 , 1.51 ± 0.29 and $1.13 \pm 0.26 \times 10^{-3} \text{ mm}^2/\text{s}$ for low (n=5), intermediate (n=9) and high-grade (n=16) DCIS respectively. The high-grade DCIS could be distinguished by the significantly lower mean ADC from non-high grade DCIS (low and intermediate grades, $1.42 \pm 0.28 \times 10^{-3} \text{ mm}^2/\text{s}$, $p=0.0057$). Quantitative DWI has potentials to aid DCIS risk stratification and management.

2727

Computer #8

MRI Biomarkers of breast cancer complete pathologic response to neoadjuvant chemotherapy

Elizabeth Jane Sutton¹, Duc A. Fehr², Brittany Z. Dashevsky^{1,3}, Sunitha B Thakur², Joseph O. Deasy², Elizabeth A Morris¹, and Harini Veeraraghavan²

¹Radiology, Memorial Sloan Kettering Cancer Center, New York, NY, United States, ²Medical Physics, Memorial Sloan Kettering Cancer Center, New York, NY, United States, ³Radiology, University of Chicago, Chicago, IL, United States

Neoadjuvant chemotherapy (NAC) is used in breast cancer and pathologic complete response (pCR) is associated with improved survival. Computer extracted MRI features generate quantitative metrics of treatment response. We used an interactive Grow-Cut method to volumetrically segment breast cancers on multiparametric breast MRI pre and post NAC and then computed Haralick features for each sequence. We found a difference in the MRI tumor texture features pre and post NAC. We also found this difference to be statistically significant between tumors with pCR and no-pCR. These metrics demonstrate changes in tumor microenvironment post NAC and are biomarkers for pCR.

2728

Computer #9

Multi-parametric MRI for predicting disease recurrence or death in breast cancer patients following neo-adjuvant chemotherapy.

Elizabeth Anne Maxine O'Flynn¹, Maria A Schmidt¹, David Collins¹, James D'arcy¹, and Nandita M deSouza¹

¹Cancer Research UK Cancer Imaging Centre, Institute of Cancer Research and Royal Marsden Hospital, Sutton, United Kingdom

The aim of this pilot study was to explore whether functional MRI metrics from a multi-parametric acquisition can predict for disease recurrence or death in breast cancer following neo-adjuvant chemotherapy. 60 months after commencement of the study, a lower R2* value was found at baseline in the women who are alive and disease free, suggesting that these tumours were less hypoxic and better oxygenated than those who developed metastatic disease or died in the interim

2729

Computer #10

Triexponential Diffusion Analysis in Breast Cancer

Masako Ohno¹, Tosiaki Miyati², Naoki Ohno², Hiroko Kawashima², Kazuto Kozaka¹, Yukihiko Matsuura¹, and Toshifumi Gabata¹

¹Kanazawa University Hospital, Kanazawa, Japan, ²Kanazawa University, Kanazawa, Japan

To acquire more detailed information on perfusion and diffusion in breast cancer, we analyzed three diffusion components using triexponential function. Perfusion-related diffusion (D_p), fast free diffusion (D_f), and slow restricted diffusion coefficients (D_s) were calculated from triexponential function. We compared these parameters between invasive ductal carcinoma (IDC) and ductal carcinoma in situ (DCIS) groups. D_s was significantly lower in the IDC group than those in the DCIS group because of difference in the cellularity. Triexponential analysis makes it possible to noninvasively obtain more detailed information on perfusion and diffusion in breast cancer, thereby assisting in the diagnosis.

2730

Computer #11

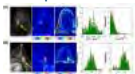
Analyzing the Texture of Suspicious Lesions in the Female Breast with ADC-mapping in DWIBS and DWI

Jana Tesdorff¹, Frederik Laun², Stefan Delorme¹, Wolfgang Lederer³, Heidi Daniel⁴, Heinz-Peter Schlemmer¹, and Sebastian Bickelhaupt¹

¹Radiology, German Cancer Research Center, Heidelberg, Germany, ²Medical Physics, German Cancer Research Center, Heidelberg, Germany, ³Heidelberg, Germany, ⁴Mannheim, Germany

Diffusion-weighted imaging (DWI) can be helpful to differentiate benign and malignant lesions in the female breast. We compared the diagnostic performance of conventional DWI and DWIBS (DWI with background suppression) derived ADC maps with different definitions of the region of interest used to measure the ADC value (1.5T Philips). Texture analysis of suspicious breast lesions was performed utilizing ADC mapping in 59 lesions. Statistical analysis revealed the highest accuracy for lesion differentiation if using the mean ADC-value calculated of three small regions-of interest in the DWIBS derived ADC.

2731

Computer #12

Histogram-metrical DCE-MRI based Quantitative Discrimination of Breast Masses

Chao Jin¹, Ting Liang¹, Hongwen Du¹, Gang Niu¹, Zihua Su¹, Peng Cao¹, Yonghao Du¹, Chenxia Li¹, Yitong Bian¹, and Jian Yang¹

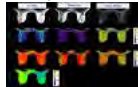
¹Department of Radiology, the First Affiliated Hospital of Xi'an Jiaotong University, Xi'an, China, People's Republic of

To clarify the diagnostic efficiency of histogram and mean in tumor detection, this study aims to compare the efficiency of mean and histogram metrics (i.e. skewness, kurtosis, median, variance, entropy and energy) of K^{trans} and k_{ep} at transverse slice with tumor biggest diameter in discriminating benign lesion, grade II- and III-invasive ductal carcinomas (IDC). The results indicate that in breast DCE-MRI,

both mean and histogram-metrics provide roughly comparable values in identifying malignancy from benignancy. However, histogram-metrics are considerably more informative and enable to discriminate pathological grade of IDCs. k_{ep} presented better diagnostic efficiency than K^{trans} .

2732

Computer #13



Dixon fat-water imaging based variable flip-angle T1 mapping quantification for breast cancer

Dattesh D Shanbhag¹, Parita Sanghani¹, Reem Bedair², Venkata Veerendranadh Chebrolu¹, Uday Patil¹, Sandeep N Gupta³, Scott Reid⁴, Fiona Gilbert², Andrew Patterson², Rakesh Mullick¹, and Martin Graves²

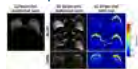
¹GE Global Research, Bangalore, India, ²University of Cambridge, Cambridge, United Kingdom, ³GE Global Research, Niskayuna, NY, United States, ⁴GE Healthcare, Leeds, United Kingdom

In DCE-MRI, T₁ map is necessary for signal to concentration conversion. In highly fat-water mixed tissue such as breast, contrast uptake primarily changes T₁ values of water protons. Therefore, DCE quantification in breast cancer must reliably measure water T₁. We evaluated T₁ maps obtained using Dixon based fat-water separated VFA method and compared values in fat, fibro-glandular tissue and tumors. We observed that T₁ mapping with Dixon based VFA method and non-linear fitting recovers T₁ values for tissue in breast by reducing partial volume. We conclude that water only T1 mapping will improve accuracy of PK modeling in breast cancer.

2733



Computer #14



Removing Silicone Artifacts in Diffusion-Weighted Breast MRI by Means of Shift-Resolved Spatiotemporally Encoding

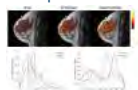
Eddy Solomon¹, Noam Nissan², Rita Schmidt¹, Edna Furman-Haran³, Uriel Ben-Aharon⁴, and Lucio Frydman¹

¹Chemical Physics Department, Weizmann Institute of Science, Rehovot, Israel, ²Biological Regulation Department, Weizmann Institute of Science, Rehovot, Israel, ³Unit of Biological Services, Weizmann Institute of Science, Rehovot, Israel, ⁴Breast Surgery Unit, Meuhedet Clinic, Ashdod, Israel

A new ADC-mapping methodology based on SPatio-temporal ENcoding (SPEN) was applied to augmented breasts, organs possessing multiple spectral components. SPEN provides a robust single-shot alternative to echo-planar-imaging (EPI) in terms of overcoming B0-inhomogeneities, while being able to resolve—and thereby suppress—the contributions of different chemical sites. Diffusion SPEN measurements were carried out at 3T on healthy volunteers with silicone-implant augmentation and compared against SE-EPI counterparts, confirming SPEN's ability to yield more reliable ADC maps, free from the dominant silicone signal contributions, in a single shot. This opens new screening possibilities for cancer detection in breast augmented patients.

2734

Computer #15



Detecting BOLD vasomotor contrast in healthy breast parenchyma and breast carcinoma

Tess E. Wallace¹, Andrew J. Patterson², Oshaani Abeyakoon¹, Reem Bedair¹, Roie Manavaki¹, Mary A. McLean³, James P. B. O'Connor⁴, Martin J. Graves², and Fiona J. Gilbert¹

¹Department of Radiology, University of Cambridge, Cambridge, United Kingdom, ²Cambridge University Hospitals NHS Foundation Trust, Cambridge, United Kingdom, ³Cancer Research UK Cambridge Institute, Cambridge, United Kingdom, ⁴Institute of Cancer Sciences, University of Manchester, Manchester, United Kingdom

Blood oxygenation level-dependent (BOLD) MRI with hyperoxic/hypercapnic gas stimuli has potential to non-invasively probe vascular function, which could help characterize tumors, predict treatment susceptibility and monitor response. This work evaluates BOLD contrast changes in healthy breast parenchyma in response to air and oxygen interleaved with 2% and 5% carbogen gas mixtures, relative to an all-air control. We found that oxygen vs. 5% carbogen was the most robust stimulus for inducing BOLD contrast in the breast. Measurements may be confounded by physiological fluctuations and menstrual cycle changes. Response in breast carcinoma was variable and may indicate underlying differences in vascular function.

2735

Computer #16



Comparisons of pre- and post-treatment intravoxel incoherent motion (IVIM) biomarkers to clinical response in breast cancer patients undergoing neoadjuvant treatment

Gene Young Cho^{1,2,3}, Lucas Gennaro², Elizabeth J Sutton², Emily C Zabor², Zhigang Zhang², Linda Moy¹, Daniel K Sodickson¹, Elizabeth A Morris², Eric E Sigmund¹, and Sunitha B Thakur²

¹Department of Radiology, Center for Advanced Imaging Innovation and Research (CAI2R) and Bernard and Irene Schwartz Center for Biomedical Imaging, New York University School of Medicine, New York, NY, United States, ²Memorial Sloan Kettering Cancer Center, New York, NY, United States, ³The Sackler Institute of Graduate Biomedical Sciences, New York University School of Medicine, New York, NY, United States

Using the intravoxel incoherent motion (IVIM) effect, one can characterize the tumor microenvironment in terms of vascularity and cellularity. Combined with histogram analysis of these IVIM biomarkers, these metrics are compared to clinical responders and nonresponders of neoadjuvant treatment (NAT) in breast cancer patients. We examine the prognostic capabilities of these IVIM metrics and find that (1) certain IVIM parameters significantly differentiate between responders and nonresponders to NAT and (2) IVIM parameters change between pre- and post-treatment MRI scans. This data shows IVIM MRI to be a potentially powerful prognostic tool in breast cancer.

2736

Computer #17

Quantitative magnetic resonance imaging of lymphatic function before and after manual lymphatic drainage in patients with breast cancer treatment-related lymphedema

Paula M.C. Donahue¹, Allison O. Scott², Rachele Crescenzi², Aditi Desai², Vaughn Braxton², and Manus J. Donahue²

¹Physical Medicine and Rehabilitation, Vanderbilt University Medical Center, Nashville, TN, United States, ²Radiology, Vanderbilt University Medical Center, Nashville, TN, United States

The overall goal of this work is to develop quantitative biomarkers of lymphatic system structure and function using noninvasive 3T MRI. Here, we focus on breast cancer treatment-related lymphedema (BCRL) where we hypothesize quantitative T2 is elevated in patients relative to controls resulting from greater fluid content in the region of interests, and which reduces following manual lymphatic drainage (a commonly performed therapy intervention). Findings suggest abilities to detect changes consistent with intervention-elicited lymphatic dynamics by using internal measures of tissue composition from MRI otherwise not detected using more common limb volume, bioimpedance spectroscopy and tissue dielectric constant measures.

2737

Computer #18



High Resolution DWI with Readout-segmented EPI and computed DWI as a potential alternative of High Resolution Dynamic Contrast Enhanced MRI in evaluating Breast Cancer

MASAKO Y KATAOKA¹, Shotaro Kanao¹, Mami Iima¹, Natsuko Onishi¹, Makiko Kawai¹, Akane Ohashi¹, Rena Sakaguchi¹, Masakazu Toi², and Kaori Togashi¹

¹Diagnostic Imaging and Nuclear Medicine, Kyoto University Graduate School of Medicine, Kyoto, Japan, ²Breast Surgery, Kyoto University, Kyoto, Japan

Eighteen breast lesions underwent high resolution (HR) diffusion-weighted MRI (DWI) with a resolution of 1.1 x 1.1 x 1.4 mm and b value of 0 and 850 sec/mm² using readout-segmented echo-planar imaging (rs-EPI). Computed (c) DWI with b value of 1200 sec/mm² were calculated. Lesion conspicuity and maximum size on these images were compared to those on HR DCE MRI. Masses showed relatively good lesion conspicuity on rs-EPI, slightly deteriorated on cDWI. Size was similar between rs-EPI and HR-DCE, while slightly smaller for cDWI. In contrast, NME is often poorly visualized on rs-EPI and cDWI, resulting in underestimation of NME.

2738

Computer #19



Breast MRI for early prediction of residual disease following neoadjuvant chemotherapy: optimization of response cut-point by tumor subtype

Wen Li¹, Vignesh Arasu¹, Ella F Jones¹, David C Newitt¹, Lisa J Wilmes¹, John Kornak², Laura Esserman³, and Nola M Hylton¹

¹Radiology & Biomedical Imaging, University of California San Francisco, San Francisco, CA, United States, ²Epidemiology and Biostatistics, University of California San Francisco, San Francisco, CA, United States, ³Surgery, University of California San Francisco, San Francisco, CA, United States

This study demonstrated the effect of changing the cut-point of the functional tumor volume measured in breast MRI on the prediction of pathologic complete response (pCR) for breast cancer patients undergoing neoadjuvant chemotherapy. The study was performed using the retrospective data of a multi-center clinical trial as a full cohort and in subsets defined by clinically-relevant breast cancer subtypes. Optimal cut-point was selected by minimizing a penalty equation that considered different relative consequences of false negative and false positive predictions. Results showed that the optimal cut-point chosen in subtype had superior negative predictive value than using the one chosen from the full cohort.

2739

Computer #20



Breast imaging changes of invasive cancers on dynamic contrast-enhanced and diffusion-weighted MR Imaging: correlation with molecular subtypes

Lina Zhang¹, Qingwei Song¹, Lizhi Xie², Ailian Liu¹, Yanwei Miao¹, Weisheng Zhang¹, Zhijin Lang¹, Jianyun Kang¹, Qiang Wei¹, and Bin Xu¹

¹The 1st affiliated hospital of Dalian Medical University, Da Lian, China, People's Republic of, ²GE Healthcare, MR Research China, Beijing, Beijing, China, People's Republic of

This work has evaluated the breast characteristics of invasive cancers on DCE-MRI and DWI assessed as parameters in comparison with different molecular subtypes, and found that they all could provide novel quantitative information reflecting invasive cancers microenvironment changes, with a potential role in the differentiation of molecular subtypes and to facilitate lesion-specific targeted therapies.

2740

Computer #21



Using MRI to assess changes in distribution and leakage of contrast media in murine mammary ducts after intra-ductal injection: intact ducts vs. ducts with in situ cancer

Erica Markiewicz¹, Xiaobing Fan¹, Devkumar Mustafi¹, Marta Zamora¹, Suzanne D. Conzen², and Gregory S Karczmar¹

¹Radiology, University of Chicago, Chicago, IL, United States, ²Medicine, Hematology/Oncology, University of Chicago, Chicago, IL, United States

Contrast media injected directly into mammary ducts clearly shows mammary gland structure with 3D-MRI. Development of in situ cancer causes changes in the leakage rates and contrast agent distribution in ductal lumens and surrounding tissue. Differences we describe here between FVB/N mice and the SV40Tag mammary cancer mouse model, indicate that in situ cancer significantly changes the permeability of the ductal epithelium. Information gained from imaging these glands following intra-ductal injection can be used to develop new MRI-detectable biomarkers for early detection of in situ cancer, improve understanding of mammary cancer biology, and guide the design of new therapy.

2741

Computer #22



Restriction Spectrum Imaging in Breast Cancer

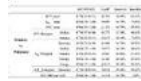
Rebecca Rakow-Penner¹, Nathan White¹, Boya Abudu¹, Joshua Kuperman¹, Hauke Bartsch¹, Natalie Schenker-Ahmed¹, David Karow¹, Haydee Ojeda-Fournier¹, and Anders Dale¹

¹Radiology, UCSD, San Diego, CA, United States

Restriction Spectrum Imaging (RSI) is an advanced diffusion imaging technique that has potential to correct for B0 distortions and non-invasively predict tumor grade. This abstract is an initial evaluation of RSI in breast imaging. We evaluated RSI on 11 patients with biopsy proven cancer. Our results indicate that RSI significantly increases conspicuity of cancer relative to the standard ADC.

2742

Computer #23



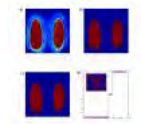
Combined strategy of histogram-metrical DCE-MRI and DWI in diagnosis of breast masses
Ting Liang^{1,2}, Chao Jin¹, Hongwen Du¹, Gang Niu¹, Peng Cao¹, Chenxia Li¹, Miaomiao Wang¹, and Jian Yang¹

¹Department of Radiology, the First Affiliated Hospital of Xi'an Jiaotong University, Xi'an, China, People's Republic of, ²School of Life Science and Technology, Xi'an Jiaotong University, Department of Biomedical Engineering, China, People's Republic of

The combined strategy of DCE-MRI and DWI shows promising diagnosis efficiency in breast cancer. This paper is to explore the diagnostic value of combined DCE-MRI and DWI based on histogram-metrical in discriminating breast masses. The results indicate that combined DWI and DCE-MRI based on histogram-metrical analysis have superior efficacy than either DCE-MRI or DWI alone in discriminating breast masses; moreover, the parameters based on histogram-metrical can offer additional features of tumor heterogeneity.

2743

Computer #24



Automated Breast MRI Segmentation Method for Background Parenchymal Enhancement
Vignesh A Arasu¹, Roy Harnish¹, Cody McHargue¹, Wen Li¹, Lisa J Wilmes¹, David Newitt¹, Ella Jones¹, Laura J Esserman², Bonnie N Joe¹, and Nola M Hylton¹

¹Radiology and Biomedical Imaging, University of California, San Francisco, San Francisco, CA, United States, ²Surgery, University of California, San Francisco, San Francisco, CA, United States

Automated measurements of whole breast segmentation are becoming an essential process to the development of quantitative and reproducible imaging biomarkers. We have developed a method for automated whole breast tissue segmentation and assess its performance using a test dataset, and found approximately 75% of cases had satisfactory segmentation requiring none to minimal manual modification. The current method can likely provide accurate assessment of mean background parenchymal enhancement, but further refinement of breast-chest wall boundary identification is required for other measurements (e.g. breast density).

Electronic Poster

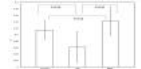
Prostate Cancer

Exhibition Hall

Monday, May 9, 2016: 11:45 - 12:45

2744

Computer #25



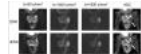
Diffusion and Perfusion Coefficients of Prostate Cancer: Using Intravoxel Incoherent Motion Bi-exponential model
Yu Guo¹, Penghui Wang¹, Xiaodong Ji¹, Chao Chai¹, Yu Zhang², and Wen Shen¹

¹Department of Radiology, Tianjin first center hospital, Tianjin, China, People's Republic of, ²Phillips Healthcare, Beijing, China, People's Republic of

The purpose of the study was to investigate the diffusion and perfusion coefficients among prostate cancer (PCa), normal peripheral zone (PZ) and benign prostatic hyperplasia (BPH) using the IVIM technique. The IVIM was performed at 11 b values of 0, 10, 20, 30, 50, 75, 100, 250, 500, 750 and 1000s/mm². The perfusion fractions in prostate cancer were significantly higher than those found in the PZ and lower than BPH, which different with some studies. But our results are more consistent with some DCE-MRI studies in tumors. Future work will recruit more volunteers and subjects and combined with DCE-MRI for further validation.

2745

Computer #26



Prostate DWI: comparison of a shorter diagonal acquisition to standard 3-scan-trace acquisition
Stefanie Hectors¹, Idoia Corcuera-Solano², Mathilde Wagner¹, Sara Lewis², Nicholas Titelbaum³, Ashutosh Tewari⁴, Ardeshir Rastinehad⁴, and Bachir Taouli^{1,2}

¹Translational and Molecular Imaging Institute, Icahn School of Medicine at Mount Sinai, New York, NY, United States, ²Department of Radiology, Icahn School of Medicine at Mount Sinai, New York, NY, United States, ³Department of Medicine, Icahn School of Medicine at Mount Sinai, New York, NY, United States, ⁴Department of Urology, Icahn School of Medicine at Mount Sinai, New York, NY, United States

Diagonal single shot EPI (SS-EPI) diffusion-weighted imaging (DWI) potentially allows for reduced acquisition time with preserved image quality. In this study, diagonal DWI was compared to standard SS EPI 3-scan-trace DWI of the prostate in terms of image quality and quantitative ADC. ADC values were similar between the 2 sequences (coefficient of variation <4%). Significant fewer artifacts were observed in the diagonal acquisition. These results show that diagonal DWI can provide substantial reduction in acquisition time (40%) while maintaining adequate image quality.

2746

Computer #27



Feasibility Study of 3-T diffusion tensor imaging of the prostate transition zone: fractional anisotropy Versus apparent diffusion coefficient
Zan Ke¹ and Liang Wang¹

¹Radiology, Tongji Hospital of Tongji Medical College, Huazhong University of Science and Technology, Wuhan, China, China, People's Republic of

This study is to investigate the diagnostic utility of fractional anisotropy(FA) and apparent diffusion coefficient(ADC) values of diffusion tensor imaging(DTI) to differentiate and classify abnormal signal nodules in prostate transition zone. Eighty-four patients were included in our study and divided into 5 groups: BPH,Gleason score(GS) ≤ 6 ,GS=7,GS=8,GS ≥ 9 ,measured FA and ADC of the region of interest, using one-way ANOVA to compare the difference among groups. There was significant statistical difference between the groups of FA and ADC values($F=20.986,P=0.000$; $F=26.560,P=0.000$).Comparison among five groups: just BPH had significant statistical difference($P=0.000$) with other four groups. The FA and ADC values of DTI had higher value for distinguishing benign and malignant nodules, but no obvious advantages in the further classification.

2747

Computer #28



Comparison of performance of quantitative ADC versus PI-RADS v2 assessment for differentiating high-grade from low-grade prostate cancer

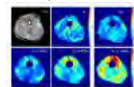
Elmira Hassanzadeh¹, Olutayo I Olubiyi¹, Andriy Fedorov¹, Daniel I Glazer¹, Clare M Tempany¹, and Fiona M Fennessy^{1,2}

¹Brigham and Women's Hospital, Boston, MA, United States, ²Dana-Farber Cancer Institute, Boston, MA, United States

One of the challenges in prostate cancer (PCa) management is the ability to differentiate aggressive tumors that require prompt treatment from indolent tumors that can safely undergo active surveillance. To promote global standardization and diminish variation in the acquisition, interpretation, and reporting of prostate multi-parametric MRI (mpMRI) examinations, Prostate Imaging Reporting and Data System (PI-RADS) has been introduced. The second version of PI-RADS (PI-RADS v2) was released early in 2015, but requires clinical validation. Here, we present the results of a study investigating the performance of PI-RADS v2 compared to quantitative ADC (qADC) values in discriminate high-grade from low-grade PCa.

2748

Computer #29



Prostate tissue microstructure: Complementary assessment using multifrequency MR elastography and diffusion tensor imaging in ex vivo human prostate tissue.

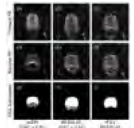
Lynne E. Bilston^{1,2}, Lauriane Jugé^{1,3}, and Roger Bourne⁴

¹Neuroscience Research Australia, Randwick, NSW, Australia, ²Prince of Wales Clinical School, University of New South Wales, Kensington, NSW, Australia, ³School of Medical Sciences, University of New South Wales, Kensington, NSW, Australia, ⁴Discipline of Medical Radiation Sciences, Faculty of Health Sciences, University of Sydney, Lidcombe, NSW, Australia

MR elastography (MRE) and diffusion weighted imaging (DWI) techniques are sensitive to microstructural changes, as reflected in the tissue stiffness and water diffusion properties respectively. These results showed that mechanical and diffusion properties varied between fresh and fixed prostate tissue, but were not highly correlated with each other, suggesting that multifrequency MRE and DWI have the potential to be complementary imaging tools for tracking the alterations in soft tissue microstructure, such as those that occur in cancer and other diseases.

2749

Computer #30



Time-Efficient Reduced-Distortion Prostate Diffusion MRI Using Reduced Field-of-View Readout-Segmented EPI

Novena Rangwala¹, Kyunghyun Sung¹, and Holden Wu¹

¹Department of Radiological Sciences, David Geffen School of Medicine, University of California Los Angeles, Los Angeles, CA, United States

The purpose of this study was to minimize echo planar imaging (EPI)-related distortion artifacts while maintaining the time-efficiency for prostate diffusion-weighted MRI (DWI) using a reduced field of view (rFOV) readout-segmented EPI (RESOLVE) technique. Image distortions in clinical standard DW single-shot (ss) EPI (5:52min) were compared with a matched RESOLVE protocol (seven segments, 7:03min) and rFOV RESOLVE (five segments, 4:59min) using the Dice similarity coefficient (DSC) on forward and reverse phase-encoded images. DSC was significantly higher (0.91 ± 0.05) in rFOV RESOLVE compared with the other protocols, indicating that rFOV RESOLVE can improve DWI quality and visualization in the prostate compared with ss-EPI, with higher time efficiency than regular RESOLVE.

2750

Computer #31



Multimodality multiparametric 18F-Fluciclovine PET/MRI for computer-assisted detection of primary prostate cancer: is there a role for SUV?

Mattijs Elscho¹, Elise Sandsmark¹, Kirsten Margrete Selnæs^{1,2}, Jose Teruel¹, Brage Krüger-Stokke^{1,3}, Øystein Størkersen⁴, Helena Bertilsson^{5,6}, May-Britt Tessem¹, Siver Andreas Moestue^{1,2}, and Tone Frost Bathen^{1,2}

¹Department of Circulation and Medical Imaging, Norwegian University of Science and Technology, Trondheim, Norway, ²St Olavs Hospital, Trondheim, Norway, ³Department of Radiology, St Olavs Hospital, Trondheim, Norway, ⁴Department of Pathology, St Olavs Hospital, Trondheim, Norway, ⁵Department of Urology, St Olavs Hospital, Trondheim, Norway, ⁶Department of Cancer Research and Molecular Medicine, Norwegian University of Science and Technology, Trondheim, Norway

Computer-assisted algorithms have been proposed to support radiological reading of multiparametric MRI (mpMRI) images for detection of localized primary prostate cancer. In this work, we investigated if standardized uptake values (SUV) from combined ¹⁸F-Fluciclovine PET/mpMRI can improve automated classification of tumor and non-tumor voxels. We found that a PET/mpMRI model (features: T2W, ADC, K_{trans} , V_e and SUV) did not significantly improve the area under the receiver operating curve in comparison with an mpMRI-only model (features: T2W, ADC, K_{trans} , V_e), suggesting limited additional value of SUV in voxel classification for computer-assisted detection of primary prostate cancer.

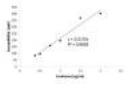
2751

Computer #32

Quantitative susceptibility mapping of prostate cancer xenografts

Kofi Deh¹, Marjan Zaman¹, Padraic O'Malley¹, Richard Lee¹, Pascal Spincemaille¹, and Yi Wang¹

¹Weill Cornell Medicine, New York, NY, United States



Quantitative susceptibility mapping (QSM) is a recently developed technique for quantifying magnetic susceptibility and it may be useful in quantifying super-paramagnetic iron oxide (SPIO) nanoparticles for prostate cancer therapy. Previously, researchers have been hampered in extending the use of this technique to cancers outside the brain because of problems such as chemical shift and a large dynamic susceptibility range. Recently developed algorithms, however, allow us to overcome these problems and we demonstrate their use for quantifying SPIO in a prostate cancer xenograft model for magnetic hyperthermia.

2752

Computer #33



Logistic Regression Models May Predict Gleason Grade of Prostate Cancer in the Peripheral Zone but Not the Transition Zone
Edward William Johnston¹, Kenneth Cheung¹, Nikolas Dikaios¹, Harbir Singh Sidhu¹, Mrishta Brizmohun Appayya¹, Lucy Simmons², Alex Freeman³, Hashim Ahmed², David Atkinson¹, and Shonit Punwani¹

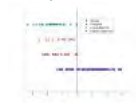
¹UCL Centre for Medical Imaging, London, United Kingdom, ²Department of Urology, University College Hospital, London, United Kingdom, ³Cellular Pathology, University College Hospital, London, United Kingdom

Quantitative imaging metrics forming multiparametric prostate MRI have been shown to correlate with Gleason grade. We therefore aimed to develop logistic regression models which predict aggressive prostate cancer in focal lesions using quantitative MRI parameters. Models were constructed separately for the transition and peripheral zones, using data from 176 examinations.

In the peripheral zone, a combination of 3 simple parameters were found to predict a Gleason 4/5 component with a similar sensitivity and specificity to experienced radiologists. However, performance was relatively poor in the transition zone. Logistic regression models may therefore prove useful when training radiologists to characterise prostate cancer.

2753

Computer #34



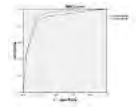
Principal Component Analysis Applied to Magnetic Resonance Fingerprinting Data in Prostate
Debra F. McGivney¹, Alice Yu², Chaitra Badve³, Mark A. Griswold^{1,4}, and Vikas Gulani^{1,3}

¹Radiology, Case Western Reserve University, Cleveland, OH, United States, ²School of Medicine, Case Western Reserve University, Cleveland, OH, United States, ³Radiology, University Hospitals, Cleveland, OH, United States, ⁴Biomedical Engineering, Case Western Reserve University, Cleveland, OH, United States

MR fingerprinting provides a way to generate quantitative information on tissue parameters, giving a set of multidimensional data at each pixel. Having a method to interpret this multidimensional data will aid in an objective and efficient means for differentiating between normal and healthy tissues, or variations between disease states. We apply principal component analysis (PCA) to MRF data along with the apparent diffusion coefficient (ADC) to differentiate between normal and diseased (prostate cancer, prostatitis) tissue within the prostate.

2754

Computer #35



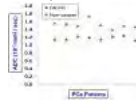
The efficiency of multiparametric MRI using PI-RADS version 2 in the diagnosis of clinically significant prostate cancer
chenglin zhao¹, ge gao¹, dong fang¹, he wang¹, xuedong yang¹, feiyu li¹, and xiaoying wang¹

¹Peking University First Hospital, Beijing, China, People's Republic of

Multiparametric MRI (mpMRI) has been well used for detecting prostate cancer and provides helpful information before biopsy. Prostate Imaging Reporting and Data System (PI-RADS version 2), which is a standard protocol for it, need to be evaluated. In this study, we aim to investigate the efficiency and accuracy of mpMRI using PI-RADS version 2 in the diagnosis of clinically significant prostate cancer. Finally, the diagnostic efficiency for clinically significant cancer of mpMRI using PI-RADS version 2 shows good accuracy using PI-RADS. However the consistency of interobserver should be improved in the future.

2755

Computer #36



Prostate Cancer Detection Using Accelerated 5D EPJRESI - sLASER Combined With DWI
Rajakumar Nagarajan¹, Zohaib Iqbal¹, Neil Wilson¹, Daniel J Margolis¹, Steven S Raman¹, Robert E Reiter², and M.Albert Thomas¹

¹Radiological Sciences, University of California Los Angeles, Los Angeles, CA, United States, ²Urology, University of California Los Angeles, Los Angeles, CA, United States

Prostate cancer (PCa) is the second leading cause of cancer related death in Western countries. Conventional 3D MRSI in PCa using weighted encoding and long echo time. One dimensional MRSI suffers from overlapping of metabolites. In this study, a non-uniformly undersampled (NUS) five dimensional (5D) echo planar J-Resolved spectroscopic imaging (EP-JRESI) sequence using semi LASER radio-frequency pulses for optimal refocusing was used to record 2D J-resolved spectra from multiple prostate locations and to quantify changes in prostate metabolites, Cit, Cr, Ch and ml after compressed sensing reconstruction of the NUS 5D EP-JRESI data by minimizing total variation method. Also, we found the prostate metabolites ratios (Ch+Cr/Cit and Ch+Cr/ml) were inversely correlated with ADC values.

2756

Computer #37



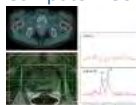
Prostate tumor growth in patients on active surveillance: is a change in the apparent diffusion coefficient an indicator of an accelerated growth rate?
Veronica A Morgan^{1,2}, Chris Parker³, and Nandita M deSouza^{1,2}

¹MRI, Royal Marsden Hospital, Sutton, United Kingdom, ²Clinical Magnetic Resonance Unit, Institute of Cancer Research, London, United Kingdom, ³Urology, Royal Marsden Hospital, Sutton, United Kingdom

We evaluated relationship between tumor doubling time and ADC in prostate cancer patients managed by active surveillance. Tumor (defined as a low signal-intensity T2-W region showing restricted diffusion and a Type3 contrast-enhanced curve within a biopsy positive octant) volume was calculated at 3 time-points ~12-24mths apart in 22 patients by drawing regions-of-interest on the T2-W images. Mean tumor ADC was estimated centrally through the tumor. Five of 22 tumors (22.7%) showed growth acceleration after the second time-point. A 10% decrease in ADC identified 3 of 4 tumors and missed 1 of 22 cases with a doubling time of <12 months.

2757

Computer #38



Choline metabolism in prostate cancer: relationship between 1H-MRS measured concentrations and uptake of 18F-Choline on PET-CT in the dominant tumor nodule

Mihaela Rata¹, Monica Celli², Veronica Morgan¹, Geoffrey Payne¹, Jonathan Gear², Emma Alexander¹, Sue Chua², David Dearnaley¹, and Nandita deSouza¹

¹Radiotherapy and Imaging, CR-UK and EPSRC Cancer Imaging Centre, The Institute of Cancer Research and Royal Marsden Hospital, London, United Kingdom, ²Department of Nuclear Medicine and PET/CT, Royal Marsden Hospital, Sutton, United Kingdom

Intracellular choline, a putative marker of prostate cancer, may be measured using ¹H-MRS, while uptake of extrinsic radiolabelled choline derivatives (¹¹C-choline and ¹⁸F-choline) on PET is used to identify prostate cancer. We compared the steady-state concentrations of total choline (¹H-MRS) with the uptake of ¹⁸F-Choline on PET in a cohort of 11 prostate cancer patients. The measured choline/water ratio in tumor was $0.09 \pm 0.02 \times 10^{-3}$ units; the normalized ¹⁸F-Choline uptake was 2.69 ± 1 . There was a weak negative correlation between measured MRS and early PET uptake (-0.61 , $p=0.04$) suggesting an increased avidity of prostate tumors for choline when internal concentrations are low.

2758

Computer #39



Consistent T1 Quantification in a Multiscanner Setting using Reference Region Variable Flip Angle B1+ Mapping

Novena Rangwala¹, Isabel Dregely¹, Holden Wu¹, and Kyunghyun Sung¹

¹Department of Radiological Sciences, David Geffen School of Medicine, University of California Los Angeles, Los Angeles, CA, United States

The purpose of this study was to demonstrate improved T_1 estimation in the prostate using the Reference Region Variable Flip Angle (RR-VFA) B_1+ mapping and correction across multiple MRI scanners with different RF transmission modes. Prostate T_1 measurements were compared in four volunteers on three MRI scanners before and after B_1+ correction. The results showed that, for each volunteer, T_1 variations across scanners decreased by 62% after RR-VFA correction, to an average of 10% among scanners, highlighting the need for B_1+ correction and the ability to effectively yield precise T_1 estimations in a multi-scanner setting using RR-VFA.

2759

Computer #40



Metabolic dynamics of hyperpolarized [1-13C] pyruvate in human prostate cancer

Kristin L Granlund^{1,2}, Hebert A Vargas¹, Serge K Lyashchenko³, Phillip J DeNoble³, Vincent A Laudone⁴, James Eastham⁴, Ramon A Sosa¹, Matthew A Kennedy¹, Duane Nicholson¹, YanWei W Guo¹, Albert P Chen⁵, James Tropp⁶, Hedvig Hricak^{1,2}, and Kayvan R Keshari^{1,2}

¹Radiology, Memorial Sloan Kettering Cancer Center, New York, NY, United States, ²Molecular Pharmacology, Memorial Sloan Kettering Cancer Center, New York, NY, United States, ³Radiochemistry & Imaging Probes (RMIP) Core, Memorial Sloan Kettering Cancer Center, New York, NY, United States, ⁴Surgery, Memorial Sloan Kettering Cancer Center, New York, NY, United States, ⁵GE Healthcare, Toronto, ON, Canada, ⁶GE Healthcare, Fremont, CA, United States

Hyperpolarized (HP) pyruvate has the potential to improve tumor grading and evaluate response to treatment by probing the metabolism of lesions. Three patients with biopsy-proven prostate cancers have been scanned with a 2D dynamic hyperpolarized pyruvate protocol. Repeatability has been evaluated in 2 patients to date. The data from these first 5 injections confirm that HP prostate imaging is feasible and reproducible, and the 2D dynamics will inform 3D static acquisition timing.

2760

Computer #41



Proposal of a novel co-registration and 3D visualization method for comparing prostate tumors on pre-treatment MRI and ablation cavities on post-treatment DCE as a measure of treatment efficacy

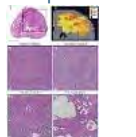
Nicole Wake¹, Samir S Taneja², Daniel K Sodickson¹, and Andrew B Rosenkrantz¹

¹Bernard and Irene Schwartz Center for Biomedical Imaging, Center for Advanced Imaging Innovation and Research, Department of Radiology, New York University School of Medicine, New York, NY, United States, ²Department of Urology, New York University School of Medicine, New York, NY, United States

Strategies for the follow-up of focal ablation of prostate cancer combine serial post-procedural PSA, multiparametric MRI examinations, and biopsy, although the optimal follow-up regimen remains controversial. In this study, we propose a co-registration and 3D visualization method for comparing prostate tumors on pre-treatment T2W-MRI and ablation cavities on post-treatment DCE-MRI as a measure of proper treatment coverage. Our preliminary findings suggest that this co-registration method may be used to help assess treatment efficacy.

2761

Computer #42



Voxel level radiologic-pathologic validation of Restriction Spectrum Imaging cellularity index with Gleason grade in Prostate Cancer

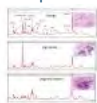
Natalie M Schenker-Ahmed¹, Ghiam Yamin¹, Ahmed Shabaik¹, Dennis Adams¹, Hauke Bartsch¹, Joshua Kuperman¹, Nathan S White¹, Rebecca A Rakow-Penner¹, Kevin McCammack¹, J Kellogg Parsons¹, Christopher Kane¹, Anders Dale¹, and David Karow¹

¹UC-San Diego, La Jolla, CA, United States

Current multiparametric magnetic resonance imaging techniques for detecting prostate cancer are limited with respect to tumor

conspicuity assessment, in vivo characterization and localization. We demonstrate that a novel diffusion-based MRI technique, restriction spectrum imaging (RSI-MRI), differentiates among benign, low-grade and high-grade PCa at voxel-level resolution. Using an RSI-MRI index to differentiate between low- and high-grade categories of tumor PCa aggressiveness may help improve and refine diagnosis and staging of PCa. Additionally, because it can detect intratumor variation, RSI-MRI may have particular relevance for planning targeted therapies such as radiation seed therapy placement, MR-guided focused ultrasound surgery, and MR-guided targeted biopsy.

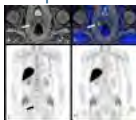
2762 **Computer #43** Response of degarelix treatment in human prostate cancer monitored by HR-MAS 1H NMR spectroscopy
Basetti Madhu¹, Greg Shaw¹, David Neal¹, and John R Griffiths¹



¹Molecular Imaging (MRI & MRS), Cancer Research UK Cambridge Institute, Cambridge, United Kingdom

Absolute concentrations of metabolites were measured in samples of Benign Prostate Hypertrophy (BPH) and high grade prostate cancer tissues from intact and castrate patients (Degarelix treated). Lactate, alanine, choline compounds concentrations were significantly elevated in high-grade prostate cancer biopsies when compared to BPH samples. Castration resulted in the significant decrease of lactate and t-choline concentrations in high grade prostate cancer biopsies. The reduced metabolite concentrations of lactate and t-choline observed in this study due to Degarelix shows that there is a potential application of *in vivo* ¹H MRS to monitor non-invasively the effects of castration in prostate cancer .

2763 **Computer #44** Early detection of recurrent prostate cancer with 18F-Fluciclovine PET/MRI
Kirsten Margrete Selnaes^{1,2}, Mattijs Elschot¹, Brage Krüger-Stokke^{1,3}, Håkon Johansen⁴, May-Britt Tessem¹, Siver Andreas Moestue^{1,2}, Arne Solberg⁵, Helena Bertilsson^{6,7}, and Tone Frost Bathen^{1,2}



¹Department of Circulation and Medical Imaging, Norwegian University of Science and Technology, Trondheim, Norway, ²St. Olavs Hospital, Trondheim University Hospital, Trondheim, Norway, ³Department of Radiology, St. Olavs Hospital, Trondheim University Hospital, Trondheim, Norway, ⁴Department of Nuclear Medicine, St. Olavs Hospital, Trondheim University Hospital, Trondheim, Norway, ⁵Clinic of Oncology, St. Olavs Hospital, Trondheim University Hospital, Trondheim, Norway, ⁶Department of Urology, St. Olavs Hospital, Trondheim University Hospital, Trondheim, Norway, ⁷Department of Cancer Research and Molecular Medicine, Norwegian University of Science and Technology, Trondheim, Norway

Prostate cancer patients with biochemical relapse (rising PSA) after initial treatment are a diagnostic challenge. Simultaneous PET/MRI combines the excellent soft-tissue contrast of MRI with the high molecular sensitivity of PET in a single imaging session. The aim of this exploratory study is to evaluate detection rate of simultaneous 18F-Fluciclovine PET/MRI for recurrent prostate cancer. The overall detection rate in an initial cohort of 16 patients was 43.8% for combined 18F-Fluciclovine PET/MR. Combined 18F-Fluciclovine PET/MR can detect areas suspicious for prostate cancer recurrence even in patients with very low PSA levels.

2764 **Computer #45** MRI-guided prostate biopsies at 3 T – clinical experience with a navigation option
Harald Busse¹, Josephin Otto¹, Alexander Schaudinn¹, Nicolas Linder¹, Simone Mucha¹, Nikita Garnov¹, Minh Do², Roman Ganzer², Jens-Uwe Stolzenburg², Lars-Christian Horn³, Thomas Kahn¹, and Michael Moche¹



¹Diagnostic and Interventional Radiology Department, Leipzig University Hospital, Leipzig, Germany, ²Urology Department, Leipzig University Hospital, Leipzig, Germany, ³Institute of Pathology, University of Leipzig, Leipzig, Germany

Multiparametric MRI has been shown to improve the detection and localization of prostate cancer and is therefore ideally suited for targeting as well. While biopsy guidance in an MRI system typically requires more efforts and time (30-120 min) than under ultrasound imaging, MRI provides unparalleled contrast of the prostate substructures. Diagnostic detection rates show large variability between patient groups and sites (about 10-60%). With a custom-made navigation option for a commercial device, any intraprocedural MRI data can be used for stereotactic real-time biopsy targeting. This work presents navigation features, indications and clinical biopsy results for a total of 75 patients.

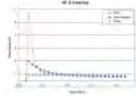
2765 **Computer #46** MRI-guided and Tumor-Targeted Biopsy to Inform Focal Therapy in Prostate Cancer
Andrew McPartlin¹, Peter Chung¹, Anna Simeonov¹, Theodor van der Kwast¹, Sangeet Ghai¹, Charles Catton¹, Robert Bristow¹, Andrew Bayley¹, Padraig Warde¹, Mary Gospodarowicz¹, and Cynthia Menard^{1,2}



¹Princess Margaret Cancer Centre, Toronto, ON, Canada, ²CHUM, Montreal, QC, Canada

We performed MRI-guided biopsy in patients with known localized prostate cancer to confirm MRI findings and guide focal therapy. We found that MRI-guided biopsy had limited impact on the treatment planning process for dose-painted radiotherapy with dose-escalation to tumor-bearing regions.

2766 **Computer #47** Comparison of different population-averaged arterial-input-functions in dynamic contrast-enhanced MRI of the prostate: effects on pharmacokinetic parameters and their diagnostic performance
Ahmed Othman¹, Florian Falkner¹, Petros Martirosian¹, Jakob Weiss¹, Stephan Kruck², Robert Grimm³, Konstantin Nikolaou¹, and Mike Notohamiprodo¹

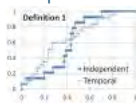


¹Department of Diagnostic and Interventional Radiology, University Hospital Tübingen, Tübingen, Germany, ²Department of Urology, University Hospital Tübingen, Tübingen, Germany, ³Siemens Healthcare, Siemens Healthcare, Erlangen, Germany

The Choice of arterial input function (AIF) is a potential source of variability in DCE-MRI studies. In clinical practice, it's not always possible to estimate individual AIFs due to artifacts or difficulties in vessel detection, particularly in transversal slices, which are typically acquired for prostate MRI. Therefore, population averaged AIFs (pAIFs) are often used. In the present study we assessed the effect of different pAIFs on parameter estimates in DCE-MRI of the prostate. We found that choosing various pAIF types causes high variability in pharmacokinetic parameter estimates. Therefore, it is important to keep AIF type selection constant in DCE-MRI studies.

2767

Computer #48



Validation of a diagnostic transition zone prostate cancer model trained in a 1.5T MRI scanner on an independent cohort of patients scanned on a 3T MRI scanner.

Nikolaos Dikaaios¹, Ed William Johnston¹, Hashim Ahmed², Lucy, Simmons³, Alex Freeman⁴, Clare Allen⁵, David Atkinson¹, and Shonit Punwani¹

¹Centre of Medical Imaging, UCL, London, United Kingdom, ²Department: Research Department of Urology, UCL, London, United Kingdom, ³Div of Surgery & Interventional Sci, UCL, London, United Kingdom, ⁴Histopathology, UCL, London, United Kingdom, ⁵Radiology, UCL, London, United Kingdom

Diagnostic models for classifying prostate cancer within the transition zone based on multi-parametric magnetic resonance imaging (mp-MRI) have been proposed to improve radiologist's performance. Such diagnostic models are trained on mp-MRI data acquired at 1.5T or 3T MRI scanners, but to the best of our knowledge no-one has yet examined whether these magnet specific models are interchangeable. This work applied a previously published diagnostic model trained on mp-MRI data acquired at a 1.5T scanner, on an independent cohort of patients with mp-MRI data acquired at a 3T and found that the performance of the model doesn't drop significantly.

Electronic Poster

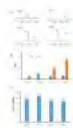
Novel MR Applications in Cancer

Exhibition Hall

Monday, May 9, 2016: 11:45 - 12:45

2768

Computer #49



Ethanolamine Kinase-1 as a Potential Therapeutic Biomarker in Pancreatic Cancer

Tariq Shah¹, Balaji Krishnamachary¹, Flonne Wildes¹, Jannie Wijnen², Kristine Glunde¹, and Zaver M Bhujwalla¹

¹Radiology, Johns Hopkins University, Baltimore, MD, United States, ²Utrecht, Netherlands

In understanding the aberrant choline metabolism of cancer, significant effort has been focused on phosphocholine (PC) but the role of phosphoethanolamine (PE) is relatively underexplored, even though tumors show increased PE as consistently as increased PC. Our previous findings in breast cancer cells have led us to expand our study to understand the role of ethanolamine kinase-1 (EtnK-1) and PE in pancreatic cell lines. We have demonstrated that EtnK-1 is the major contributor to PE levels in these cells and may be a potential therapeutic target.

2769

Computer #50



Pancreatic cancer stromal characterization using diffusion tensor imaging and collagen 1 fibers in xenograft model

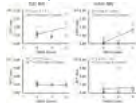
Samata Kakkad¹, Desmond Jacob¹, Marie-France Penet^{1,2}, Jiangyang Zhang¹, Kristine Glunde^{1,2}, and Zaver M. Bhujwalla^{1,2}

¹JHU ICMIC program, Division of Cancer Imaging Research, The Russell H. Morgan Department of Radiology and Radiological Science, The Johns Hopkins University School of Medicine, Baltimore, MD, United States, ²Sidney Kimmel Comprehensive Cancer Center, The Johns Hopkins University School of Medicine, Baltimore, MD, United States

The dense desmoplastic stroma present in pancreatic ductal adenocarcinoma (PDAC) limits the delivery of diagnostic imaging probes and therapeutic agents leading to poor prognosis of PDAC from a combination of late-stage diagnosis and limited response to chemotherapy. Collagen 1 (Col1) fibers form a major component of this desmoplastic stroma. By combining noninvasive diffusion MRI with optical imaging we characterized the relationship between Col1 fibers and diffusion MRI in PDAC. A good correlation was observed between Col1 fibers and diffusion MRI parameters providing a rationale for detecting PDAC with diffusion MRI, and characterizing the relationship between Col1 fibers and diffusion MRI.

2770

Computer #51



Measurement of Arteriolar Blood Volume in Brain Tumors Using MRI without Exogenous Contrast Agent Administration at 7T

Yuankui Wu^{1,2,3}, Shruti Agarwal⁴, Craig K Jones^{2,3}, Andrew G Webb⁵, Peter C.M. van Zijl^{2,3}, Jun Hua^{2,3}, and Jay J Pillai⁴

¹Department of Medical Imaging, Nanfang Hospital, Southern Medical University, Guangzhou, China, People's Republic of, ²Neurosection, Div. of MRI Research, Dept. of Radiology, Johns Hopkins University School of Medicine, Baltimore, MD, United States, ³F.M. Kirby Research Center for Functional Brain Imaging, Kennedy Krieger Institute, Baltimore, MD, United States, ⁴Division of Neuroradiology, Russell H. Morgan Department of Radiology and Radiological Science, Johns Hopkins University School of Medicine, Baltimore, MD, United States, ⁵Department of Radiology, C.J.Gorter Center for High Field MRI, University Medical Center, Leiden, Netherlands

The purpose of this study is to evaluate the potential diagnostic value of inflow-based vascular-space-occupancy (iVASO) MRI in brain tumor patients by comparing it with the widely used dynamic-susceptibility-contrast (DSC) MRI. The iVASO approach can measure arteriolar cerebral blood volume (CBVa) without using an exogenous contrast agent. The measured CBVa by iVASO showed a stronger association with tumor grade than DSC CBV. As the total scan times for iVASO and DSC are comparable, iVASO MRI may be a useful alternative for the assessment of tumor perfusion, especially when exogenous contrast agent administration is difficult or contraindicated in certain patient populations.

2771

Computer #52



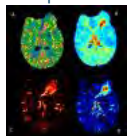
An Extended Linear Reference Region Model that accounts for plasma volume in Dynamic Contrast Enhanced MRI

Zaki Ahmed¹ and Ives Levesque^{1,2}¹Medical Physics Unit, McGill University, Montreal, QC, Canada, ²Research Institute of the McGill University Health Centre, Montreal, QC, Canada

The reference region model allows quantification of tumour perfusion through DCE-MRI without needing an arterial input function. One limitation is that the model does not account for plasma volume which could be non-negligible in highly vascularized tissues such as tumours. This study introduces a reference region model that accounts for the plasma volume. The performance of this model is evaluated in simulation and in vivo data.

2772

Computer #53



Test-retest stability of MTT insensitive CBV leakage correction in DSC-MRI

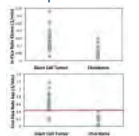
Atle Bjørnerud^{1,2}, Magne Mørk Kleppestø¹, Tracy T Batchelor^{3,4}, Patrick Y Wen⁵, Gregory Sorensen⁶, and Kyrre Eeg Emblem^{1,7}

¹The Intervention Centre, Oslo University Hospital, Oslo, Norway, ²Dept. of Physics, University of Oslo, Oslo, Norway, ³Department of Neurology, Massachusetts General Hospital and Harvard Medical School, Boston, MA, United States, ⁴Department of Radiology, Massachusetts General Hospital and Harvard Medical School, Boston, MA, United States, ⁵Center for Neuro-Oncology, Dana-Farber Cancer Institute and Harvard Medical School, Boston, MA, United States, ⁶Siemens Healthcare Health Services, Malvern, MA, United States, ⁷MGH-HST A.A. Martinos Center for Biomedical Imaging, Massachusetts General Hospital and Harvard Medical School, Boston, MA, United States

Contrast agent extravasation is known to be a serious confounder in estimations of cerebral blood volume (CBV) analysis of primary brain tumors using DSC-MRI. We here propose a modified MTT-insensitive method for correction of contrast agent extravasation based on parametric analysis of the tissue impulse response function from a two-compartment kinetic model combined with automated global arterial input function (AIF) approximation. Using DSC-MRI data from 28 patients with recurrent glioblastoma which were scanned twice prior to treatment initiation, we show that the proposed method yields test-retest stability similar to the current reference method, but with the added advantage of reduced MTT sensitivity.

2773

Computer #54



Differential Diagnosis of Giant Cell Tumor and Chordoma in the Spine by Using Morphological Features and Pharmacokinetic Parameters Analyzed from DCE-MRI

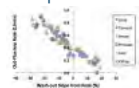
Ning Lang¹, Hon J. Yu², Huishu Yuan¹, and Min-Ying Su²

¹Department of Radiology, Peking University Third Hospital, Beijing, China, People's Republic of, ²Center for Functional Onco-Imaging, Department of Radiological Sciences, University of California, Irvine, CA, United States

26 patients with giant cell tumor in the spine and 12 patients with chordoma received DCE-MRI were analyzed. The morphological features (lesion location, vertebral compression, paraspinal soft tissue mass, bone expansion change, fiber separation, and MR signal on T1W1 and T2W1) and DCE pharmacokinetic parameters were compared. Several typical morphological features could be used for differential diagnosis, but there was a substantial overlap. DCE-MRI may provide very helpful information. Giant cell tumor had a significantly higher K_{trans} and k_{ep} compared to chordoma, and by using a cut-off value of $k_{ep}=0.43/\text{min}$, it could achieve a very high accuracy of 95%.

2774

Computer #55



Characterization of Metastatic Cancer in the Spine by DCE-MRI: Comparison of Heuristic and Pharmacokinetic Parameters Analyzed from DCE Kinetics

Ning Lang¹, Hon J. Yu², Huishu Yuan¹, and Min-Ying Su²

¹Department of Radiology, Peking University Third Hospital, Beijing, China, People's Republic of, ²Center for Functional Onco-Imaging, Department of Radiological Sciences, University of California, Irvine, CA, United States

A retrospective DCE-MRI of 76 patients with different metastatic cancers in the spine (35 lung, 11 thyroid, 12 breast, 7 prostate, 7 liver and 4 kidney) were studied. Three heuristic parameters: the maximum and steepest wash-in signal enhancement ratio and the wash-out slope were measured. Two-compartmental pharmacokinetic analysis was performed to obtain K_{trans} and k_{ep} . The maximum and wash-in SE ratio were highly correlated with K_{trans} ; and the wash-out slope was highly correlated with k_{ep} . The lung cancer had the widest variation, the breast cancer had the highest wash-in SE ratio, and the thyroid cancer had the greatest wash-out slope.

2775

Computer #56



DCE-MRI Evidence of Biological Changes in Irradiated Healthy Muscle Following Chemoradiotherapy Treatment of Head and Neck Cancer

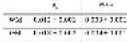
Kimberly Li^{1,2}, Abdallah S.R. Mohamed³, Yao Ding⁴, Musaddiq J Awan⁵, Steven J Frank³, Jihong Wang⁶, John D Hazle⁴, Kate Hutcheson⁷, Stephan Y Lai⁷, Jayashree Kalpathy-Cramer⁸, Xin Li², Clifton D Fuller³, and Wei Huang²

¹International School of Beaverton, Beaverton, OR, United States, ²Advanced Imaging Research Center, Oregon Health & Science University, Portland, OR, United States, ³Department of Radiation Oncology, U.T. MD Anderson Cancer Center, Houston, TX, United States, ⁴Department of Imaging Physics, U.T. MD Anderson Cancer Center, Houston, TX, United States, ⁵Department of Radiation Oncology, Case Western Reserve University, Cleveland, OH, United States, ⁶Department of Radiation Physics, U.T. MD Anderson Cancer Center, Houston, TX, United States, ⁷Department of Head and Neck Surgery, U.T. MD Anderson Cancer Center, Houston, TX, United States, ⁸Harvard Medical School, Boston, MA, United States

Head and neck cancer patients are commonly treated with chemoradiotherapy as standard of care. Although the conventional wisdom is that radiation does not cause long-term adverse effects in healthy, well-perfused tissues such as muscle, few studies have evaluated potential biological changes in irradiated muscle tissues longitudinally during the course of treatment. Here, we report preliminary findings of such changes as measured by Dynamic Contrast Enhanced Magnetic Resonance Imaging (DCE-MRI) before, during, and after chemoradiotherapy treatment of a subset of human papilloma positive (HPV+) oropharyngeal cancer (OPC).

2776

Computer #57



Reliability of DCE pharmacokinetic parameter values for quantitative longitudinal assessment of brain tumors

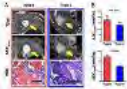
Moran Artzi¹, Gilad Liberman^{2,3}, Deborah Blumenthal⁴, Orna Aizenstein¹, and Dafna Ben Bashat^{1,5}

¹Functional Brain Center, Tel Aviv Sourasky Medical Center, Tel-Aviv, Israel, ²Functional Brain Centerasky Medical Cente, Tel Aviv Sourasky Medical Center, Tel-Aviv, Israel, ³Department of Chemical Physics, Weizmann Institute, Rehovot, Israel, ⁴Neuro-Oncology Service, Tel Aviv Sourasky Medical Center, Tel-Aviv, Israel, ⁵Sackler Faculty of Medicine and Sagol School of Neuroscience, Tel Aviv University, Tel-Aviv, Israel

DCE-MRI parameters have been shown to be useful for therapy response assessment in patient with glioblastoma, yet the estimated parameters may show high variation in their values. This study investigated the reliability of DCE parameters for quantitative longitudinal assessment of brain tumors. 14% standard-deviation in the WM and 12% in the GM, were detected for v_p in healthy subjects(n=27). Results from six patients showed mean differences of 3.2%/9.7% in v_p for WM/GM in the hemisphere contralateral to the lesion, comparing two longitudinal scans. Parametric-response-maps calculated within lesion areas based on the threshold values from the healthy controls supported radiological assessment.

2777

Computer #58



DWI and DCE-MRI for imaging diagnosis on vasculogenic mimicry and predicting responses to vascular-disrupting therapy on primary liver cancers in rats

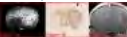
Yewei Liu^{1,2}, Ting Yin¹, Yuanbo Feng¹, Jie Yu¹, Gang Huang², Jianjun Liu², Shaoli Song², Johannes V Swinnen³, Guy Bormans⁴, Uwe Himmelreich⁵, Raymond Oyen⁶, and Yicheng Ni¹

¹Theragnostic Laboratory, MoSAIC, Department of Imaging and Pathology, Faculty of Medicine, KU Leuven, Leuven, Belgium, ²Renji Hospital, Shanghai Jiao Tong University, School of Medicine, Department of Nuclear Medicine, Shanghai, China, People's Republic of, ³Laboratory of Lipid Metabolism and Cancer, Department of Oncology, Faculty of Medicine, KU Leuven, Leuven, Belgium, ⁴Radiopharmacy, Department of Pharmaceutical and Pharmacological Sciences, Faculty of Medicine, KU Leuven, Leuven, Belgium, ⁵Biomedical MRI, MoSAIC, Department of Imaging and Pathology, Faculty of Medicine, KU Leuven, Leuven, Belgium, ⁶Radiology, Department of Imaging and Pathology, Faculty of Medicine, KU Leuven, Leuven, Belgium

Vasculogenic mimicry (VM) refers to tumor cells mimicking endothelial cells and directly participating in blood vessel formation, which appears in 2 distinctive forms, namely, the tubular type and the patterned matrix type. In liver cancer, VM is associated with tumor aggressiveness and poor clinical outcome. DENA-induced primary liver cancer model in rat appears an optimal VM model with both the 2 VM types. DWI and DCE-MRI were used to characterize and distinguish different VM types, and sensitively predicting diverse therapeutic responses to a vascular-disrupting agent CA4P.

2778

Computer #59



MR prediction of Tumor Burden in Patient-Derived Mouse Xenografts Model of Glioblastoma using an Adaptive Model

Hassan Bagher-Ebadian^{1,2}, Ana deCarvalho¹, Tavarékere Nagaraja¹, Azimeh NV Dehkordi³, Susan Irtenkauf¹, Swayamparva Panda¹, Robert Knight¹, and James R Ewing^{1,2}

¹Henry Ford Hospital, Detroit, MI, United States, ²Oakland University, Rochester, MI, United States, ³Shahid Beheshti University, Tehran, Iran

In human glioblastoma multiforme (GBM), infiltrating cells are found in remote locations, even in the hemisphere contralateral to the primary lesion. Although MRI allows approximation of the extent of tumor cell infiltration, the actual extent of infiltration may be greater or less than the edema, and there is no standard MRI practice that can be used to assess the infiltrating tumor burden. This pilot study investigates the feasibility of using a set of MR modalities for the development of an MRI estimate of infiltrating tumor burden in Patient-Derived Mouse Xenografts model of GBM using an adaptive model.

2779

Computer #60



Automatic Segmentation and Classification of Glioblastoma using DCE-MRI

Moran Artzi¹, Gilad Liberman^{2,3}, Deborah Blumenthal⁴, Felix Bokstein⁴, Orna Aizenstein¹, and Dafna Ben Bashat^{1,5}

¹Functional Brain Center, Tel Aviv Sourasky Medical Center, Tel-Aviv, Israel, ²Functional Brain Centerasky Medical Cente, Tel Aviv Sourasky Medical Center, Tel-Aviv, Israel, ³Department of Chemical Physics, Weizmann Institute, Rehovot, Israel, ⁴Neuro-Oncology Service, Tel Aviv Sourasky Medical Center, Tel-Aviv, Israel, ⁵Sackler Faculty of Medicine and Sagol School of Neuroscience, Tel Aviv University, Tel-Aviv, Israel

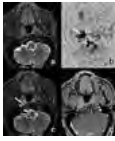
Segmentation of lesion area in patients with glioblastoma (GB) into active tumor, tissue necrosis, vasogenic edema and infiltrative disease, is highly important for patient monitoring, yet is challenging using standard radiological assessment. The aim of this study was to segment the lesion area into these four tissue types in GB patients. Voxel-wise classification was performed using support-vector-machine based on anatomical and DCE-MRI parameters. Significant differences were detected between the tissue types for FLAIR, v_p , and k^{trans} . Sensitivity and specificity of the training-set were measured based on 2-fold-cross-validation analysis, showing high sensitivities and specificities of 94-100% for the different tissue types.

2780

Computer #61

Can FS-T2/ASL fusion image be an alternative to T1 enhanced imaging in Nasopharyngeal carcinoma?

Meng Lin¹, Xiaoduo Yu¹, Han Ouyang¹, Dehong Luo¹, Chunwu Zhou¹, and Bing Wu²



¹Cancer Hospital, Chinese Academy of Medical Sciences, Beijing, China, People's Republic of, ²GE Healthcare MR research China, Beijing, Beijing, China, People's Republic of

Tumor extent assessment of NPC is critical for delineating the radio-therapeutic target region. We aimed to investigate the use of the fusion images of fat suppressed (FS)-T2 with arterial spin labeling (ASL) in measuring the volume of NPC. Two observers measured the volume of 21 untreated NPC using FS-T2, FS-T2/ASL (with PLD=1.0, 1.5 and 2.0s) fusion images and enhanced-T1WI separately. Compared to those obtained using FS-T2 alone, measurements made using FS-T2/ASL were more consistent with those made using enhanced-T1WI. The FS-T2/ASL fusion image has the potential to be an alternative to enhanced-T1WI, when contrast administration can not be performed.

2781

Computer #62



Comparison of DCE-MRI using Gd-EOB-DTPA and Gd-DTPA for tumor vascularity evaluation for hepatoma: preclinical study using rat orthotopic hepatoma model.

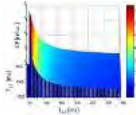
Jimi Huh¹, Kyung Won Kim¹, Chang Kyung Lee¹, Jisuk Park¹, In Seong Kim², Su Jung Ham¹, and Bumwoo park¹

¹radiology, Asan medical center, Seoul, Korea, Republic of, ²Siemens Healthcare, Seoul, Korea, Republic of

For evaluation of tumor vascularity of hepatoma, we aim to compare the DCE-MRI using Gd-EOB-DTPA and Gd-DTPA. When we perform DCE-MRI twice with 24-hours interval: first scan using Gd-DTPA and second scan using Gd-EOB-DTPA, the time-intensity curve patterns were quite different between the two scans. These findings imply that Gd-DTPA distributes between blood vessels and EES, working as an extracellular contrast agent, whereas Gd-EOB-DTPA distribute blood vessels, EES, and intracellular space in the hepatoma, working as a hepatobiliary contrast agent. Therefore, the conventional two-compartment model does not fit DCE-MRI using Gd-EOB-DTPA in subjects with hepatoma which may express OATP receptors.

2782

Computer #63



Similarity of *In Vivo* Lactate T₁ and T₂ Relaxation Times in Different Preclinical Cancer Models Facilitates Absolute Quantification of Lactate

Ellen Ackerstaff¹, Nirilanto Ramamonjisoa¹, H. Carl LeKaye¹, Kristen L. Zakian¹, Ekaterina Moroz¹, Inna S. Serganova¹, Ronald G. Blasberg¹, and Jason A. Koutcher¹

¹Memorial Sloan Kettering Cancer Center, New York, NY, United States

Aggressive, treatment-resistant tumors have been associated with high tumor lactate. For the absolute quantification of *in vivo* tumor lactate by the substitution method, it is essential to correct for differences between reference phantom and *in vivo* lactate T₁ and T₂ relaxation times (LacT₁/T₂). The LacT₁/T₂ acquisition requires specialized MR sequences and is hampered *in vivo* by long acquisition times and low lactate SNR. Here, we measure LacT₁/T₂ for various orthotopic breast and subcutaneous prostate cancer models in immune-competent and immune-compromised hosts. Our results indicate that using an average LacT₁/T₂ correction factor introduces less than 20% error in the lactate quantification.

2783

Computer #64

Parameter	Value
Field Strength	3T
Sequence	3D T1-weighted
Resolution	1.0mm x 1.0mm x 1.0mm
TR	1000ms
TE	150ms
Flip Angle	9 degrees
Matrix	256 x 256 x 128
FOV	256 x 256 mm
Bandwidth	12.5kHz
Phase Encoding	128
Parallel Imaging	2x
Contrast	Non-contrast
Reference	Phantom
Subject	Transgenic mouse
Region	Brain
ROI	Lesion
Measurement	T1, T2, ADC

Multiparametric MRI of a transgenic mouse model of neuroblastoma using an asymmetric high resolution 3-channel/3-animal RF coil on a clinical 3T platform

Gilberto S Almeida¹, Rafal Panek^{1,2}, Albert Hallsworth³, Hannah Webber³, Efthymia Papaevangelou¹, Jessica KR Boulton¹, Yann Jamin¹, Louis Chesler³, and Simon P Robinson¹

¹Radiotherapy and Imaging, The Institute of Cancer Research, London, United Kingdom, ²The Institute of Cancer Research/ Royal Marsden NHS Foundation Trust, London, United Kingdom, ³Cancer Therapeutics and Clinical Studies, The Institute of Cancer Research, London, United Kingdom

The use of clinical MRI scanners to conduct preclinical research facilitates a more direct or matched comparison with clinical studies. The increased use of orthotopic and transgenic mouse tumour models in cancer research demands non-invasive methods to accurately assess their progression and treatment response *in vivo*. The purpose of this study was to evaluate the utility and sensitivity of anatomical and functional MRI data/biomarkers acquired from transgenic mouse models of neuroblastoma using a non-bespoke asymmetric high resolution RF coil on a clinical 3T scanner.

2784

Computer #65

Parameter	Value
Field Strength	3T
Sequence	3D T1-weighted
Resolution	1.0mm x 1.0mm x 1.0mm
TR	1000ms
TE	150ms
Flip Angle	9 degrees
Matrix	256 x 256 x 128
FOV	256 x 256 mm
Bandwidth	12.5kHz
Phase Encoding	128
Parallel Imaging	2x
Contrast	Non-contrast
Reference	Phantom
Subject	Animal
Region	Brain
ROI	Lesion
Measurement	T1, T2, ADC

Early MRI findings after Near Infrared Photoimmunotherapy in an animal model

Yuko Nakamura¹, Marcelino Bernardo¹, Tadanobu Nagaya¹, Kazuhide Sato¹, Toshiko Harada¹, Peter L. Choyke¹, and Hisataka Kobayashi¹

¹Molecular Imaging Program, Center for Cancer Research, National Cancer Institute, Bethesda, MD, United States

Near infrared photoimmunotherapy (NIR-PIT) is a new cancer treatment that combines the specificity of antibodies for targeting tumors with the toxicity induced by photon absorbers after irradiation with NIR light. The purpose of this study was to determine if MR imaging can detect changes in the MR properties of tumor within several hours of NIR-PIT in an animal model. Prolongation of T₂, reductions in apparent diffusion coefficient (ADC) and increased enhancement using gadofosveset are seen within 2 hours of NIR-PIT treatment of tumors. Thus, MRI can be a useful imaging biomarker for detecting early therapeutic changes after NIR-PIT.

2785

Computer #66

Imaging of Nuclear Overhauser Enhancement in Human Brain Tumor at 3 Tesla

Yuanyu Shen¹, Gang Xiao², Zhiwei Shen¹, Xiaolei Zhang¹, Wei Hu¹, Xiangyong Tang¹, Zhiyan Zhang¹, Jitian Guan¹, and Renhua Wu¹

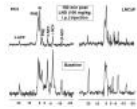


¹2nd Affiliated Hospital, Shantou University Medical College, Shantou, China, People's Republic of, ²Hanshan Normal University, Chaozhou, China, People's Republic of

Our aim was to demonstrate the feasibility of nuclear Overhauser enhancement (NOE) imaging to detect the characteristic of patients with brain tumors. Six healthy volunteers and eleven patients with brain tumors were recruited for undergoing MRI scan at 3T. As a result, we found NOE value was greater in white matter compared to gray matter. However, in human brain tumors, NOE value was slightly hypointense in glioma and little difference in meningioma. NOE imaging may help to distinguish the heterogeneity of benign or malignant tumors, and it is important in diagnosis and treatment planning for patients with brain tumors.

2786

Computer #67



31P and 1H MRS of Androgen-Independent and Androgen-Dependent Prostate Cancer Xenografts: Lonidamine Selectively Decreases Tumor Intracellular pH, Bioenergetics and Increases Lactate

Kavindra Nath¹, David Nelson¹, Dennis Leeper², and Jerry Glickson¹

¹University of Pennsylvania, Philadelphia, PA, United States, ²Thomas Jefferson University, Philadelphia, PA, United States

Lonidamine (LND) effects were measured *in vivo* by ³¹P and ¹H MRS in androgen-independent (PC3) and androgen-dependent (LNCaP) prostate cancer xenografts indicating a sustained and tumor-selective decrease in intracellular pH (pHi) and extracellular pH (pHe), and decrease in tumor bioenergetics (β NTP/Pi) by 75.0 % and 79.0 % in PC3 and LNCaP, respectively, relative to the baseline levels. Steady-state levels of tumor lactate were significantly increased ~ 2 fold at 60 min. post-LND. The decline of pHi, pHe, bioenergetics and increase in lactate produced increased therapeutic efficacy when LND was combined with other therapeutic interventions (chemotherapy, radiation, and hyperthermia).

2787

Computer #68



Assessment of radiation damaged mouse lungs using perfluorohexane liquid MRI.

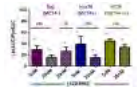
Alexandre A Khrapitchev¹, James R Larkin¹, Stavros Melemenidis¹, Peter E Thelwall², and Nicola R Sibson¹

¹Department of Oncology, University of Oxford, Oxford, United Kingdom, ²Newcastle Magnetic Resonance Centre, Newcastle University, Newcastle upon Tyne, United Kingdom

The imaging of lungs with MRI is difficult owing to low proton density. Imaging with hyperpolarized noble gases has overcome some of these limitations but at great expense and effort. We have investigated damage caused by radiation of mouse lungs using ¹⁹F MRI of perfluorohexane – a cheap biocompatible liquid at room temperature. Using lungs filled with perfluorohexane, we were able to obtain high resolution scans with comparable SNRs to hyperpolarized xenon imaging and high resolution. These bright and stable lung images provide a very sensitive tool to monitor the lung damage development.

2788

Computer #69



Monocarboxylate transporter 1 (MCT1) inhibition with AZD3965 leads to MRS-detectable MCT4-dependent blockade of lactate efflux and pyruvate-lactate exchange in human cancer cells providing potential for non-invasive imaging

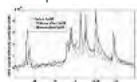
Mounia Belouèche-Babari¹, Slawomir Wantuch¹, Harold G Parkes¹, Markella Koniordou¹, Vaitha Arunan¹, Thomas R Eykyn¹, Paul D Smith², and Martin O Leach¹

¹CRUK Cancer Imaging Centre, The Institute of Cancer Research & Royal Marsden NHS Foundation Trust, London, United Kingdom, ²AstraZeneca, Cambridge, United Kingdom

The monocarboxylate transporter 1 (MCT1), which mediates the bidirectional movement of molecules such as lactate and pyruvate, is upregulated in cancer and constitutes a promising drug target. Using MRS we investigate the impact of the MCT1 inhibitor AZD3965, currently in phase-I clinical trials, on human cancer cell metabolism to assess potential for pharmacodynamic biomarker discovery. We show that AZD3965 inhibits lactate efflux and blocks hyperpolarised ¹³C-pyruvate-lactate exchange in human cancer cells in an MCT4-dependent manner. Thus, intracellular lactate and hyperpolarised ¹³C-pyruvate-lactate exchange are promising metabolic imaging biomarkers for monitoring the action of AZD3965 and potentially other MCT1 inhibitors.

2789

Computer #70



Measuring the effect of CA-IX inhibition on tumor pH in patient-derived xenografts (PDX) of breast cancer.

William Dominguez-Viqueira¹, Pedro Miguel Enriquez Navas¹, Gary Martinez¹, Epifanio Ruiz¹, David Morse¹, Robert Gillies¹, and Susan Frost²

¹Department of Cancer Imaging and Metabolism, Moffitt Cancer Center, Tampa, FL, United States, ²Biochemistry and Molecular Biology, University of Florida, Gainesville, FL, United States

Membrane-bound carbonic anhydrase (CA-IX) plays an important role in maintaining an acidic extracellular pH (pHe) in tumors. We investigate the effect of inhibiting CA-IX on the pHe of patient derived xenografts (PDX) from a triple negative breast cancer using ³¹P MRS of 3-aminopropylphosphonate (3-APP) as a pH biomarker. Mice were imaged before the injection of the ureido-sulfonamide CA-IX inhibitor (cpd25) and again at 2.5 and 24 hours after injection. There was an increase in pH in 5/6 animals in the first 24 hours. This is first *in vivo* evidence that CA-IX inhibition disrupts pH *in vivo*.

2790

Computer #71



Investigation of the mouse colon wall using endoscopic MRI and confocal endomicroscopy

Hugo Dorez¹, Raphaël Sablong¹, Laurence Canaple², Sophie Gaillard¹, Hervé Saint-Jalmes^{3,4}, Driffa Moussata⁵, and Olivier Beuf¹

¹CREATIS, Université de Lyon ; CNRS UMR5220 ; Inserm U1044 ; INSA-Lyon ; Université Claude Bernard Lyon 1, Villeurbanne, France, ²IGFL, ENS Lyon, Lyon, France, ³LTSI - Inserm U642, Rennes, France, ⁴CRLCC, Rennes, France, ⁵Hôpital Régional Universitaire de Tours, Tours, France

The purpose of this project is to provide new tools and protocols to evaluate digestive pathologies. To this end, endoscopic MRI, using endoluminal coils, was combined with confocal endomicroscopy (CEM). Both modalities provide complementary information. CEM is well suited to investigate the surface of the colon wall whereas endoscopic MRI can assess deeper structures. It allows characterizing and staging the first steps of cancer development. The study was performed on a mouse model of colitis following 24 animals. This opens perspectives to better understand digestive pathologies such as colorectal cancer and inflammatory bowel disease.

2791

Computer #72



Tissue positional repeatability in head and neck revealed by a dedicated MR simulator: Is positioning verification using bony landmarks adequate in radiotherapy treatment?

Abby Y. Ding¹, Oi Lei Wong¹, Jing Yuan¹, Max W.K. Law¹, K.F. Cheng², K. T. Chan², Gladys G. Lo³, K.Y. Cheung¹, and Siu Ki Yu¹

¹Medical Physics & Research Department, Hong Kong Sanatorium & Hospital, Hong Kong, China, People's Republic of, ²Department of Radiotherapy, Hong Kong Sanatorium & Hospital, Hong Kong, China, People's Republic of, ³Department of Diagnostic & Interventional Radiology, Hong Kong Sanatorium & Hospital, Hong Kong, China, People's Republic of

Current positioning verification in radiotherapy mainly relies on bony structures using X-ray based imaging techniques, where visualization of tumor and soft organ-at-risk is relatively poor. This study aimed to assess the positional repeatability of soft and bony structures, and investigate the correlation between the positional deviations of various head and neck (H&N) tissues. Our results suggested that the current positioning verification practice for radiotherapy relying mainly on bony structure may be inadequate and inefficient in H&N. MR-simulator may play a potential role in improving H&N radiotherapy by enabling positional verification directly on target tissues rather than simply on bony structure.

Electronic Poster

Tumour Response to Therapy

Exhibition Hall

Monday, May 9, 2016: 11:45 - 12:45

2792

Computer #73



Effects of Temporal Resolution on Quantitative DCE-MRI Prediction of Breast Cancer Therapy Response

Wei Huang¹, Aneela Afzal¹, Alina Tudorica¹, Yiyi Chen¹, Stephen Y-C Chui¹, Arpana Naik¹, Megan Troxell¹, Kathleen Kemmer¹, Karen Y Oh¹, Nicole Roy¹, Megan L Holtorf¹, and Xin Li¹

¹Oregon Health & Science University, Portland, OR, United States

15 breast cancer patients undergoing neoadjuvant chemotherapy (NACT) consented to two DCE-MRI studies at the same time points before, during, and after NACT: one with high temporal resolution (tRes) and the other with low tRes. There were systematic errors in estimated pharmacokinetic (PK) parameters from the low tRes data compared to the high tRes data. However, the abilities of PK parameters for early prediction of pathologic response to NACT were not affected by poorer tRes.

2793

Computer #74

Effect of Neoadjuvant Chemotherapy on in-vivo MRS determined tCho and Membranous and Cytoplasmic b-catenin Expression in Breast Cancer Patients

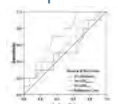
Naranamangalam R Jagannathan¹, Khushbu Agarwal¹, Uma Sharma¹, Sandeep Mathur², Vurthalaru Seenu³, and Rajinder Parshad³

¹Department of NMR and MRI Facility, All India Institute of Medical Sciences, New Delhi, India, ²Department of Pathology, All India Institute of Medical Sciences, New Delhi, India, ³Department of Surgical Disciplines, All India Institute of Medical Sciences, New Delhi, India

We evaluated the changes in tCho levels and β -catenin expression (membrane and cytoplasm) after III neoadjuvant chemotherapy in breast cancer patients. Significant reduction in β -catenin expression (membranous and cytoplasmic) was observed after therapy. Post-therapy, tCho reduced significantly in tumors with Grades 1 and 2 membranous β -catenin expression and also in tumors with IRS 0 and Grade 1 cytoplasmic β -catenin. Prior to therapy, tCho was positively associated with cytoplasmic β -catenin while negatively with membranous protein. However post-therapy tCho was negatively associated with both cytoplasmic and membranous β -catenin. This signifies antiproliferative and apoptosis induction effects of chemotherapy drugs on breast cancer patients.

2794

Computer #75



Correlation of diffusion weighted MR imaging with the prognosis of locally advanced gastric carcinoma to neoadjuvant chemotherapy

Lei Tang¹, Ying-Shi Sun¹, Zi-Yu Li², Xiao-Ting Li¹, Fei Shan², Zi-Ran Li², and Jia-Fu Ji²

¹Radiology, Peking University Cancer Hospital & Institute, Beijing, China, People's Republic of, ²GI surgery, Peking University Cancer Hospital & Institute, Beijing, China, People's Republic of

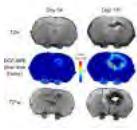
The percentage changes of ADC after neoadjuvant chemotherapy of gastric carcinoma have correlation with long-term prognosis. The significantly increased ADC after chemotherapy is more prone to signify long-term survival, and has potential to be a surrogate imaging biomarker for the prediction of the prognosis. ADCentire for the whole lesion is better than ADCmin for high signal area in the prognosis prediction.

2795

Computer #76

T2*-weighted imaging and DCE-MRI as complementary tools to characterize the continuous process of radionecrosis and neovascularization

J r mie P. Fouquet¹, Julie Constanzo¹, Laurence Masson-C t ^{1,2}, Luc Tremblay¹, Philippe Sarret³, Sameh Geha⁴, Kevin Whittingstall⁵, Benoit Paquette¹, and Martin Lepage¹

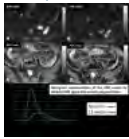


¹Department of Nuclear Medicine and Radiobiology, Université de Sherbrooke, Sherbrooke, QC, Canada, ²Service of Radiation Oncology, Centre Hospitalier Universitaire de Sherbrooke, Sherbrooke, QC, Canada, ³Department of Pharmacology-Physiology, Université de Sherbrooke, Sherbrooke, QC, Canada, ⁴Department of Pathology, Université de Sherbrooke, Sherbrooke, QC, Canada, ⁵Department of Diagnostic Radiology, Université de Sherbrooke, Sherbrooke, QC, Canada

Radiation dose delivered to healthy tissues during brain tumors radiosurgery can cause important side effects. We imaged an animal model of brain irradiation with DCE-MRI and T2*-weighted imaging at different time points after treatment. DCE-MRI allowed the discrimination of areas with high vessel permeability and necrotic regions. T2*-weighted imaging enabled the visualization of a necrotic core and micro-lesions at its periphery. Micro-lesions were initially co-localized with permeable vessels and later evolved into necrosis. Together, DCE-MRI and T2*-weighted images provided a coherent picture on the phenomena involved in radionecrosis progression, which could help in the management of associated problems.

2796

Computer #77



DIFFUSION-WEIGHTED IMAGING (DWI) AS A TREATMENT RESPONSE BIOMARKER IN PROSTATE CANCER BONE METASTASES

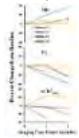
Raquel Perez-Lopez^{1,2}, Matthew D. Blackledge^{1,2}, Joaquin Mateo^{1,2}, David J. Collins^{1,2}, Veronica A. Morgan^{1,2}, Alison MacDonald^{1,2}, Diletta Bianchini^{1,2}, Zafeiris Zafeiriou^{1,2}, Pasquale Rescigno^{1,2}, Michael Kolinsky^{1,2}, Daniel Nava Rodrigues^{1,2}, Helen Mossop¹, Nuria Porta¹, Emma Hall¹, Martin O. Leach^{1,2}, Johann S. de Bono^{1,2}, Dow-Mu Koh^{1,2}, and Nina Tunariu^{1,2}

¹The Institute of Cancer Research, Sutton, United Kingdom, ²The Royal Marsden NHS Foundation Trust, Sutton, United Kingdom

We hypothesized that changes in the median apparent diffusion coefficient (mADC) and volume of bone metastases (BM), quantified by whole body (WB) diffusion-weighted imaging (DWI), are response biomarkers in metastatic castration-resistant prostate cancer (mCRPC). 21 patients completed WB-DWI at baseline and after 12 weeks of treatment in a sub-study within a clinical trial of olaparib in mCRPC, performed on a 1.5-T Siemens Avanto scanner. Four different segmentation techniques were explored including axial skeleton analyses and simpler methods including 5 target lesions. Changes in mADC and volume of BM associated with response to therapy. The simplified approach also showed promising results, warranting further evaluation.

2797

Computer #78



Response Assessment to Tumor Treating Fields in Patients with Glioblastoma using Physiologic and Metabolic MR Imaging

Sanjeev Chawla¹, Sumei Wang¹, Gaurav Verma¹, Aaron Skolnik¹, Sulaiman Sheriff², Katelyn M Reilly¹, Lisa Desiderio¹, Andrew Maudsley², Steven Brem³, Katherine Peters⁴, Harish Poptani⁵, and Suyash Mohan¹

¹Radiology, Perelman School of Medicine at the University of Pennsylvania, Philadelphia, PA, United States, ²Radiology, University of Miami, Miami, FL, United States, ³Neurosurgery, Perelman School of Medicine at the University of Pennsylvania, Philadelphia, PA, United States, ⁴Neurology, Duke University Medical Center, Durham, NC, United States, ⁵Department of Cellular and Molecular Physiology, University of Liverpool, Liverpool, United Kingdom

Tumor treating fields (TTFields) are a novel antimitotic treatment modality for treatment of patients with glioblastoma (GBM). To assess response to TTFields, 4 GBM patients underwent diffusion, perfusion and 3D-echo-planar spectroscopic imaging prior to initiation of TTFields and at one and two month follow-up periods. A trend towards increased MD and a decrease in FA and rCBV_{max} was noted in most patients at 2-month relative to baseline indicating inhibited tumor growth and vascularity. Cho/Cr values did not exhibit any trend probably due to heterogeneity in response. These preliminary data indicate the potential of advanced MR imaging in assessing response to TTFields.

2798

Computer #79

The value of functional MRI on predicting therapeutic outcome of TACE on hepatocellular carcinoma

Ma Xiaohong¹, Zhao Xinming¹, Ouyang Han¹, and Zhou Chunwu¹

¹Diagnostic Radiology, Cancer Hospital, Chinese Academy of Medical Sciences, Peking Union Medical College, Beijing, China, People's Republic of

The purpose of this study was to explore the efficacy of functional MRI (diffusion-weighted imaging (DWI), IntraVoxel incoherent motion (IVIM) and perfusion-weighted imaging (PWI)) quantitative analysis in predicting therapeutic outcome of TACE on HCC. The D_{fast} , K^{trans} , ΔD_{fast} and ΔK^{trans} of HCC acquired before and after TACE obviously correlated with PFS and was valuable in the prediction of the clinical outcome of HCC treated with TACE.

2799

Computer #80



Early Assessment of Antiangiogenic Effects of Sorafenib using IVIM in Mouse Model with Hepatocellular Carcinoma

Yong Zhang¹, Bing Wu¹, Xin Chen², and Zaiyi Liu²

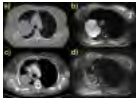
¹GE Healthcare MR Research China, Beijing, China, People's Republic of, ²Radiology, Guangdong General Hospital, Guangzhou, China, People's Republic of

Antiangiogenic therapy is efficient to treat hypervascular tumor such as hepatocellular carcinoma (HCC). Unlike chemotherapy and radiation therapy, tumor dimension doesn't change in its early phase. Hence traditional response criteria based on morphological change fails to early assess the therapeutic response of antiangiogenic treatment. This study used intravoxel incoherent motion (IVIM) theory to separate perfusion and diffusion characteristics in HCC over several time points after antiangiogenic Sorafenib administration. It was found that IVIM-derived pure diffusivity and pseudo-diffusivity were able to detect the microvascular collapse and cellular edema in HCC at early phase of antiangiogenic medication.

2800

Computer #81

Lung tumour radiotherapy treatment response assessment using Active Breathing Coordinated (ABC) Diffusion-Weighted Magnetic Resonance Imaging



Evangelia Kaza¹, Matthew Blackledge¹, David John Collins¹, Erica Scurr², Helen McNair³, Richard Symonds-Taylor¹, Fiona McDonald², Martin Osmund Leach¹, and Dow-Mu Koh²

¹The Institute of Cancer Research and Royal Marsden Hospital, London, United Kingdom, ²The Royal Marsden NHS Foundation Trust, London, United Kingdom, ³Department of Radiotherapy, Royal Marsden NHS Foundation Trust and Institute of Cancer Research, London, United Kingdom

Imaging with an Active Breathing Coordinator (ABC) modified for MR use was performed on lung cancer patients to acquire spatially matching diffusion-weighted images (DWI) before, during and after Radiotherapy. DWI spatially matched the CT and depicted mediastinal nodal involvement as well as internal tumour heterogeneity. ADC maps provided information about changes in solid and fluid components throughout therapy. Treatment response was evaluated by applying multi-parametric tumour heterogeneity characterisation using Gaussian Mixture Modelling. Differences in ADC and volume behavior of separate cancerous tissue components at various treatment time points may indicate tumour sub-volumes and provide detailed cancer characterisation.

2801

Computer #82



Defining the baseline functional imaging characteristics of retroperitoneal sarcomas

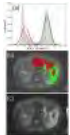
Jessica M Winfield^{1,2}, Aisha Miah³, Dirk Strauss⁴, Khin Thway⁵, Andrew Hayes⁴, Daniel Henderson³, David J Collins^{1,2}, Nandita M deSouza^{1,2}, Martin O Leach^{1,2}, Sharon L Giles^{1,2}, Veronica A Morgan^{1,2}, and Christina Messiou^{1,2}

¹MRI, Royal Marsden Hospital, Sutton, United Kingdom, ²Division of Radiotherapy and Imaging, Cancer Research UK Cancer Imaging Centre, Institute of Cancer Research, London, United Kingdom, ³Department of Radiotherapy, Royal Marsden Hospital, London, United Kingdom, ⁴Department of Surgery, Royal Marsden Hospital, London, United Kingdom, ⁵Department of Histopathology, Royal Marsden Hospital, London, United Kingdom

Soft tissue sarcomas are often highly heterogeneous tumours and post-treatment changes cannot be described by standard size criteria. Functional imaging may provide a non-invasive method of assessing response to treatment. Knowledge of baseline functional imaging characteristics and the repeatability of estimated parameters is essential in development of future studies. In this study, 22 patients with retroperitoneal sarcoma were imaged before treatment. Whole-tumour assessments of apparent diffusion coefficient (ADC), parameters of the intra-voxel incoherent motion model (IVIM: diffusion coefficient D , fraction f , fast exponential component D^*), transverse relaxation rate (R_2^*), fat fraction and enhancing fraction (EF) showed large ranges of median estimates, indicating wide inter-tumour heterogeneity. The large standard deviation of parameters within tumours reflects the intra-tumour heterogeneity. In 21 patients, a second examination was carried out to assess repeatability of ADC, D , f , D^* and R_2^* . Excellent repeatability of fitted parameters, particularly ADC, indicates high sensitivity to treatment-induced changes.

2802

Computer #83



Gaussian mixture modelling of combined functional imaging parameters provides new insight into tumour heterogeneity

Jessica M Winfield^{1,2}, Matthew D Blackledge², Aisha Miah³, Dirk Strauss⁴, Khin Thway⁵, David J Collins^{1,2}, Martin O Leach^{1,2}, Sharon L Giles^{1,2}, Daniel Henderson³, and Christina Messiou^{1,2}

¹MRI, Royal Marsden Hospital, Sutton, United Kingdom, ²Division of Radiotherapy and Imaging, Cancer Research UK Cancer Imaging Centre, Institute of Cancer Research, London, United Kingdom, ³Department of Radiotherapy, Royal Marsden Hospital, London, United Kingdom, ⁴Department of Surgery, Royal Marsden Hospital, London, United Kingdom, ⁵Department of Histopathology, Royal Marsden Hospital, London, United Kingdom

Multi-parametric functional imaging may enable non-invasive assessment of response to treatment in soft tissue sarcomas. Image analysis is complicated, however, by the highly heterogeneous nature of these tumours, which can include regions of cellular tumour, fat, necrosis and cystic change that may respond differently to treatment. In this study, patients with retroperitoneal sarcoma were imaged before and after radiotherapy using DW-MRI, Dixon and pre-/post-contrast T_1 -w imaging for evaluation of enhancing fraction (EF). Gaussian mixture modelling was applied to classify pixels in the tumour volume according to their functional imaging behaviour, combining ADC, fat fraction and EF to characterise tumour components. This method enabled segmentation of highly heterogeneous tumours and estimation of mean ADC and volume of each tumour component. Heterogeneous changes post-radiotherapy were summarised in tissue classification maps, which combine multiple functional imaging parameters. Combined analysis of functional imaging parameters may provide greater insight into tumour behaviour, for example identification of viable tumour.

2803

Computer #84



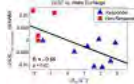
Threshold functional imaging maps depict intra-tumour heterogeneity of response to radiotherapy in retroperitoneal sarcomas

Jessica M Winfield^{1,2}, Aisha Miah³, Dirk Strauss⁴, Khin Thway⁵, David J Collins^{1,2}, Martin O Leach^{1,2}, Sharon L Giles^{1,2}, Daniel Henderson³, Shane Zaidi⁶, and Christina Messiou^{1,2}

¹MRI, Royal Marsden Hospital, Sutton, United Kingdom, ²Division of Radiotherapy and Imaging, Cancer Research UK Cancer Imaging Centre, Institute of Cancer Research, London, United Kingdom, ³Department of Radiotherapy, Royal Marsden Hospital, London, United Kingdom, ⁴Department of Surgery, Royal Marsden Hospital, London, United Kingdom, ⁵Department of Histopathology, Royal Marsden Hospital, London, United Kingdom, ⁶Department of Clinical Oncology, Royal Marsden Hospital, London, United Kingdom

Functional imaging provides scope for non-invasive assessment of response to radiotherapy and/or systemic agents in retroperitoneal sarcomas and investigation of heterogeneity of response in this highly heterogeneous tumour type. In this study 9 patients with retroperitoneal sarcoma were imaged before treatment and 2-4 weeks after radiotherapy. Whilst some tumours exhibited large increases in median ADC and enhancing fraction after radiotherapy, the overall changes for the cohort were not significant and there were no clear changes in fat fraction. Thresholded ADC maps and enhancement maps, however, reveal localised post-radiotherapy changes in ADC and enhancement that are not fully characterised by whole-tumour metrics.

Computer #85



Chemical exchange saturation transfer (CEST) and relaxometry as biomarkers for assessing response of brain metastases to stereotactic radiosurgery

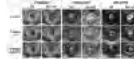
Hatef Mehrabian^{1,2}, Kimberly L Desmond³, Anne L Martel^{1,2}, Arjun Sahgal^{1,4}, Hany Soliman^{1,4}, and Greg J Stanisz^{1,2}

¹Physical Sciences, Sunnybrook Research Institute, Toronto, ON, Canada, ²Medical Biophysics, University of Toronto, Toronto, ON, Canada, ³Medical Physics and Applied Radiation Sciences, McMaster University, Hamilton, ON, Canada, ⁴Radiation Oncology, Odette Cancer Centre, Toronto, ON, Canada

Quantitative MRI techniques that probe the metabolic and micro-structural changes in the tumor have the potential to assess response of brain metastases to stereotactic radiosurgery early after treatment. Two techniques were investigated here: **a)** Chemical Exchange Saturation Transfer (CEST), **b)** Relaxometry.

Among all model parameters, early changes in the intracellular-extracellular water exchange rate in relaxometry, and peak amplitude of nuclear overhauser effect at the ipsilateral normal appearing white matter in CEST provided the strongest correlation with tumor volume change one-month post-treatment. We also demonstrated that these two parameters were highly correlated suggesting they could provide complementary information about treatment effects.

Computer #86



MRI in Assessing Response to Neoadjuvant Chemo-radiation in Locally Advanced Rectal Cancer Using DCE-MR and DWI Data Sets: Before, During and After the Treatment

Ke Nie¹, Liming Shi², Ning Yue¹, Jabbour Salma¹, Xi Hu², Liwen Qian², Tingyu Mao², Qin Chen², Xiaonan Sun², and Tianye Niu^{2,3,4}

¹Radiation Oncology, Rutgers-Cancer Institute of New Jersey, Rutgers-Robert Wood Johnson Medical School, New Brunswick, NJ, United States, ²Radiation Oncology, Sir Run Run Shaw Hospital, Zhejiang University of Medicine, Hangzhou, China, People's Republic of, ³Institute of Translational Medicine, Hangzhou, China, People's Republic of, ⁴Radiology, Sir Run Run Shaw Hospital, Zhejiang University of Medicine, Hangzhou, China, People's Republic of

We are one of the first to investigate the predictive value of combined anatomical, DCE-MRI and DWI for good pathological response at different time points during the pre-operative chemo-radiation treatment (CRT) in patients with locally advanced rectal cancer (LARC). The pre-treatment ADC and internal heterogeneity enhancement measured by texture features from DCE-MRI and the relative change of the ADC values during the treatment showed good prognostic value with pathological response. Overall, this study provides new information of the optimal use of MRI in predicting response to the pre-operative CRT, which may further help tailor the treatment into the era of personalized medicine.

Computer #87



Altered lipid metabolism on 1H NMR as response biomarkers in prostate cancer cells and tumors following radiotherapy

Gigin Lin¹, Yu-Chun Lin¹, Hsi-Mu Chen¹, and Chiun-Chieh Wang²

¹Medical Imaging and Intervention, Chang Gung Memorial Hospital, Taoyuan, Taiwan, ²Radiation Oncology, Chang Gung Memorial Hospital, Taoyuan, Taiwan

The intracellular storage and utilization of lipids are critical for cancer cells to maintain energy homeostasis. In this study, we investigated the changes of lipid metabolites in murine TRAMP-C prostate cancer cells and tumors following radiotherapy. The lipid profile following radiotherapy demonstrated increased levels of fatty acids and triacylglycerols, before the change of tumor size. The increase of lipids signals can potentially serve as early response biomarkers in clinical setting for prostate cancer patients following radiotherapy.

Computer #88



Impact of T1 and B1 correction on quantitative DCE-MRI for assessing longitudinal therapy response in breast cancer

Dattesh D Shanbhag¹, Parita Sanghani¹, Reem Bedair², Venkata Veerendranadh Chebrolu¹, Sandeep N Gupta³, Scott Reid⁴, Fiona Gilbert², Andrew Patterson², Rakesh Mullick¹, and Martin Graves²

¹GE Global Research, Bangalore, India, ²University of Cambridge, Cambridge, United Kingdom, ³GE Global Research, Niskayuna, NY, United States, ⁴GE Healthcare, Leeds, United Kingdom

In this work, we investigated the impact of incorporating T₁ and/or B₁ maps on PK parameters in breast cancer patients and impact of these PK maps on assessing therapy response in longitudinal data. DCE-MRI PK parameters in six breast cancer patients was investigated with four different processing schemes comprising combinations of T₁ and B₁ map with DCE and its trend assessed in longitudinal data. We demonstrate that in breast tumor imaging, a DCE protocol incorporating T₁ and B₁ mapping can be more reliable in reflecting tumor heterogeneity and predicting therapy response longitudinally.

Computer #89



Monitoring Breast Cancer Response to Neoadjuvant Chemotherapy by Diffusion Tensor Imaging

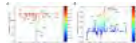
Edna Furman-Haran¹, Noam Nissan², Hadassa Degani², and Julia Camps Herrero³

¹Department of Biological Services, The Weizmann Institute of Science, Rehovot, Israel, ²Department of Biological Regulation, The Weizmann Institute of Science, Rehovot, Israel, ³Radiology, Hospital de la Ribera, Alzira, Spain

We have evaluated the ability of diffusion tensor imaging (DTI) to assess breast cancer response to neoadjuvant chemotherapy. Changes in lesion size and diffusion parameters in response to therapy were determined. Diameter and volume measurement derived from DTI were compared to those derived from dynamic contrast enhanced (DCE) MRI and to post surgery pathological reports. A high congruence was found between DTI and DCE-MRI for tumor size and response evaluation, with both methods showing a good agreement with pathology results.

2809

Computer #90



Evaluation of neoadjuvant chemotherapy combined with bevacizumab in breast cancer using MR metabolomics

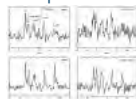
Leslie R. Euceda¹, Tonje H. Haukaas^{1,2}, Guro F. Giskeødegård¹, Riyas Vettukattil¹, Geert Postma³, Laxmi Silwal-Pandit^{2,4}, Jasper Engel⁵, Lutgarde M.C. Buydens³, Anne-Lise Børresen-Dale^{2,4}, Olav Engebraaten⁶, and Tone F. Bathen^{1,2}

¹Department of Circulation and Medical Imaging, The Norwegian University of Science and Technology, Trondheim, Norway, ²K.G. Jebsen Center for Breast Cancer Research, Institute of Clinical Medicine, University of Oslo, Oslo, Norway, ³Institute for Molecules and Materials, Radboud University Nijmegen, Nijmegen, Netherlands, ⁴Department of Genetics, Institute for Cancer Research, Oslo University Hospital, The Norwegian Radium Hospital, Oslo, Norway, ⁵NERC Biomolecular Analysis Facility Metabolomics Node (NBAF-B), School of Biosciences, University of Birmingham, Birmingham, United Kingdom, ⁶Department of Oncology, Department of Tumor Biology, Oslo University Hospital, Oslo, Norway

This study used HR MAS magnetic resonance based metabolic profiles from breast tumor tissue to explore the metabolic changes occurring as an effect of overall neoadjuvant therapy, discriminate therapy responders from nonresponders, and determine metabolic differences between patients receiving or not receiving the antiangiogenic drug bevacizumab. Changes as an effect of chemotherapy were detected and responders were successfully discriminated from nonresponders after treatment, showing potential for assessment of patient benefit to treatment and the understanding of underlying mechanisms affecting response. Although metabolic differences based on bevacizumab administration were not prominent, glutathione was identified to be possibly affected by the drug.

2810

Computer #91



Early detection of changes in phospholipid metabolism during neoadjuvant chemotherapy using phosphorus magnetic resonance spectroscopy at 7 tesla

Erwin Krikken¹, Wybe J.M. van der Kemp¹, Hanneke W.M. van Laarhoven², Dennis W.J. Klomp¹, and Jannie P. Wijnen¹

¹Radiology, University Medical Center Utrecht, Utrecht, Netherlands, ²Medical Oncology, Academic Medical Center Amsterdam, Amsterdam, Netherlands

Neoadjuvant chemotherapy plays an important role in the treatment of breast cancer patients. During chemotherapy, the phospholipid metabolism changes which can be measured by ³¹P-MRS at 7 tesla. Eight patients were examined, using the AMESING sequence to receive metabolic signals in the tumor. The ³¹P-MRS data were analyzed on group level, which enables the detection of changes the levels of phospholipid metabolites in an early stage of the treatment, directly after the first cycle of chemotherapy.

2811

Computer #92



The Role of Heterogeneity Analysis for Differential Diagnosis in Diffusion-Weighted Images of Meningioma Brain Tumors

Mojtaba Safari¹, Anahita Fathi Kazerooni^{1,2}, Maryam Babaie³, Mahnaz Nabil⁴, Mahsa Rostamie¹, Parvin Ghavami¹, Morteza Saneie Taheri³, and Hamidreza Saligheh Rad^{1,2}

¹Quantitative MR Imaging and Spectroscopy Group (QMISG), Research Center for Molecular and Cellular Imaging (RCMCI), Tehran University of Medical Sciences, Tehran, Iran, ²Department of Medical Physics and Biomedical Engineering, School of Medicine, Tehran University of Medical Sciences, Tehran, Iran, ³Radiology Department, School of Medicine, Shahid Beheshti University of Medical Sciences, Tehran, Iran, ⁴Department of Mathematics, Islamic Azad University, Qazvin Branch, Qazvin, Iran

Meningioma brain tumors constitute the majority of adult primary brain tumors, in which the role of apparent diffusion coefficient (ADC) is controversial. We hypothesize that analysis of the heterogeneity within a tumorous ecological region can reveal biological tissue properties, which could further assist decision making about the optimum patient-specific treatment strategy. In the present work, we propose an automated computer-aided diagnosis method for phenotyping meningioma brain tumors, based on features representing spatial heterogeneity in ADC-maps, with classification accuracy of 85.1%. In conclusion, it is demonstrated that heterogeneity of meningioma brain tumors can be a potential discriminating biomarker of tumor malignancy.

2812

Computer #93



Microvascular Heterogeneity Assessed Using DCE-MRI Predicts Disease-Free Survival in Cancers of the Cervix, Bladder, and Head and Neck

Ben R Dickie^{1,2}, Lucy E Kershaw^{1,2}, Bernadette M Carrington³, Suzanne Bonington³, Susan E Davidson³, Catharine ML West¹, and Chris J Rose⁴

¹Institute of Cancer Sciences, The University of Manchester, Manchester, United Kingdom, ²Christie Medical Physics and Engineering, Christie NHS Foundation Trust, Manchester, United Kingdom, ³Diagnostic Radiology, Christie NHS Foundation Trust, Manchester, United Kingdom, ⁴Centre for Imaging Sciences, The University of Manchester, Manchester, United Kingdom

There is a clinical need for non-invasive imaging biomarkers capable of accurately predicting outcomes in locally advanced cancers. Microvascular heterogeneity measurements obtained from dynamic contrast enhanced-MRI have shown prognostic utility however no attempt has been made to compare the prognostic value of the available methods across disease and identify which type of heterogeneity (statistical or spatial) is important for survival. In this study we identify heterogeneity biomarkers that are universally prognostic across cancers of the cervix, bladder, and head and neck and compare their prognostic value to standard clinicopathologic factors such as disease stage.

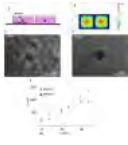
2813

Computer #94

Oscillatory shear strain impacts metastatic cancer cell spread

Marlies Christina Hoelzl¹, Marco Fiorito², Ondrej Holub³, Gilbert Fruhwirth⁴, and Ralph Sinkus¹

¹Biomedical Engineering, King's College London, London, United Kingdom, ²Imaging Chemistry and Biology, King's College London, London, United Kingdom, ³London, United Kingdom, ⁴Imaging Chemistry and Biology, King's College London, London, United Kingdom



Major reasons of cancer related deaths are repercussion of the dissemination of cancer cells from the primary tumour site and an outgrowth at the secondary metastatic site. The microenvironment where the cancer cells reside with various signals, are central factors to provide cancer cell spread throughout the body; signals can be (bio)chemical or mechanical nature. Translation of mechanical forces, displacements and deformations into biochemical signals (i.e. mechanotransduction) affects their adhesion, spread and survival. We show here, that focussed shear waves operating at specific frequency and amplitude affects the metastatic behaviour of cancer cells by reducing the invasive behaviour and growth.

2814

Computer #95



Can Diffusion Weighted MRI Assess Early Response of Lymphadenopathy to Induction Chemotherapy in Nasopharyngeal Cancer: A Heterogeneity Analysis Approach

Manijeh Beigi¹, Anahita Fathi Kazerooni¹, Mojtaba Safari², Marzieh Alamolhoda³, Ahmad Ameri⁴, Shiva Moghadam⁵, Mohsen Shojaaee Moghadam⁶, and Hamidreza SalighehRad²

¹ Tehran University of Medical Sciences, Quantitative MR Imaging and Spectroscopy Group, Research Center for Cellular and Molecular Imaging, Institute for Advanced Medical Imaging, Tehran, Iran, ²Tehran University of Medical Sciences, Quantitative MR Imaging and Spectroscopy Group, Research Center for Cellular and Molecular Imaging, Institute for Advanced Medical Imaging, Tehran, Iran, ³Statistics, Shiraz University of Medical Science, Shiraz, Iran, ⁴Jorjani Radiotherapy Center, Shahid Beheshti of Medical Science, Tehran, Iran, ⁵Shahid Beheshti University of Medical Science, Tehran, Iran, ⁶Payambaran MRI center, Tehran, Iran

Induction chemotherapy is an effective way to control subclinical metastasis in locally-advanced nasopharyngeal cancer patients. Diffusion-weighted MRI is a noninvasive imaging technique allowing some degree of tissue characterization by showing and quantifying molecular diffusion. Histogram analysis on ADC map could be carried out to reveal physiological alterations early after IC. For this purpose, several quantitative metrics from ADC-map were explored to obtain the most accurate feature(s) as potential predictive biomarker for early response of the lymphnode to IC. If the outcome can be predicted at an early stage of the treatment, the patient could be spared from unnecessary treatment toxicity.

2815

Computer #96



Monitoring Changes of the Tumor Microenvironment Following Administration of a Novel Vascular Disrupting Agent OXi6197 Using Multi-parametric MRI

Heling Zhou¹, James Campbell¹, Zhang Zhang², Debabrata Saha², Rebecca Denney¹, Mary Lynn Trawick³, Kevin G Pinney³, and Ralph P Mason¹

¹Radiology, UT Southwestern Medical Center, Dallas, TX, United States, ²Radiation Oncology, UT Southwestern Medical Center, Dallas, TX, United States, ³Chemistry and Biochemistry, Baylor University, Waco, TX, United States

Vascular disrupting agents (VDAs), selectively damage the endothelial cells of tumor blood vessels, inducing ischemia and consequent hypoxia and cell death. We investigated the impact of a novel indole-based VDA (OXi6197) to tumor perfusion and oxygenation using multi-parametric MRI on a lung tumor animal model. DCE MRI showed decreased blood flow after administration of VDA. Oxygen sensitive MRI, BOLD and TOLD, showed progression of hypoxia at 24 hours. Multimodality imaging provides useful information to evaluate the efficacy of VDA. The findings in this study will be important for dose optimization and potential combination therapy in the future.

Electronic Poster

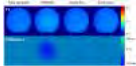
Relaxation Applications

Exhibition Hall

Monday, May 9, 2016: 14:15 - 15:15

2816

Computer #1



trueFLASH: Model-Based Iterative T1 Mapping using Variable-Flip-Angle Fast Low-Angle Shot

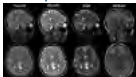
Tom Hilbert^{1,2,3}, Damien Nguyen^{4,5}, Jean-Philippe Thiran^{2,3}, Gunnar Krueger^{2,3,6}, Tobias Kober^{1,2,3}, and Oliver Bieri^{4,5}

¹Advanced Clinical Imaging Technology (HC CMEA SUI DI BM PI), Siemens Healthcare AG, Lausanne, Switzerland, ²Department of Radiology, University Hospital (CHUV), Lausanne, Switzerland, ³LTSS, École Polytechnique Fédérale de Lausanne, Lausanne, Switzerland, ⁴Radiological Physics, Department of Radiology, University of Basel Hospital, Basel, Switzerland, ⁵Department of Biomedical Engineering, University of Basel, Basel, Switzerland, ⁶Siemens Medical Solutions USA, Inc., Boston, MA, United States

Various methods have been published to quantify the longitudinal relaxation T1; amongst others, a variable-flip-angle fast low-angle shot acquisition can be used. Here, we suggest applying an 8-fold undersampling to such an acquisition, subsequently using a model-based iterative optimization to estimate T1 maps. This approach allows the acquisition of whole-brain 1.3mm isotropic T1 maps within 3:20min using 16 different flip angles. Aliasing artifacts due to the undersampling were successfully removed by the iterative reconstruction. However, the T1 maps show a slight overestimation of T1 values and require a B1-field correction as it is typical for variable-flip-angle approaches.

2817

Computer #2



Fast 3D Acquisition for Quantitative Mapping and Synthetic Contrasts Using MIRACLE and trueCISS

Tom Hilbert^{1,2,3}, Damien Nguyen^{4,5}, Jean-Philippe Thiran^{2,3}, Gunnar Krueger^{2,3,6}, Oliver Bieri^{4,5}, and Tobias Kober^{1,2,3}

¹Advanced Clinical Imaging Technology (HC CMEA SUI DI BM PI), Siemens Healthcare AG, Lausanne, Switzerland, ²Department of Radiology, University Hospital (CHUV), Lausanne, Switzerland, ³LTSS, École Polytechnique Fédérale de Lausanne, Lausanne, Switzerland, ⁴Radiological Physics, Department of Radiology, University of Basel Hospital, Basel, Switzerland, ⁵Department of Biomedical Engineering, University of Basel, Basel, Switzerland, ⁶Siemens Medical Solutions USA, Inc., Boston, MA, United States

Quantitative imaging promises to be a good biomarker of disease but requires long acquisition times, especially when 3D acquisition techniques are used. Here we propose to use a highly undersampled 3D phase-cycled balanced steady-state free-precession sequence in combination with the reconstruction methods MIRACLE and trueCISS, providing quantitative maps (T2,T1,M0). Additionally, synthetic contrasts can be generated using the previously calculated quantitative maps and signal models, exemplarily shown for bSSFP, T2- and T1-weighted contrast. In summary, the proposed method provides a set of quantitative maps and various conventional contrasts using a single 3:31min acquisition.

2818

Computer #3



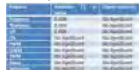
Rapid Multislice T1 Mapping of Contrast-Enhanced Mouse Tumor Using Saturation Recovery Look-Locker Method with Spiral Readout
Yuchi Liu¹, Zheng Han¹, Kai Jiang², Yun Jiang¹, Yajuan Li¹, Zheng-Rong Lu¹, and Xin Yu^{1,3,4,5}

¹Biomedical Engineering, Case Western Reserve University, Cleveland, OH, United States, ²Division of Nephrology and Hypertension, Mayo Clinic, Rochester, MN, United States, ³Radiology, Case Western Reserve University, Cleveland, OH, United States, ⁴Physiology and Biophysics, Case Western Reserve University, Cleveland, OH, United States, ⁵Case Center for Imaging Research, Case Western Reserve University, Cleveland, OH, United States

In this study, a rapid multislice saturation-recovery Look-Locker (MSRLL) T₁ mapping method with spiral readout was developed for the application on tissues with long T₁ value, such as tumor. This method was validated in vitro and evaluated in a dynamic contrast-enhanced MRI (DCE-MRI) study on mouse tumor. The spiral MSRLL method showed a strong agreement with Cartesian method, and achieved temporal resolution of 2 min 40s with a voxel size of 0.23×0.23×1 mm³ in vivo.

2819

Computer #4



Comparison of Signal intensity measures with absolute T1 value quantification in patients undergoing serial follow up imaging in patients with neurocysticercosis

Pradeep Kumar Gupta¹, Prativa Sahoo², Alok Kumar Singh³, Ravindra Kumar Garg³, Rupsa Bhattacharjee⁴, and Rakesh Kumar Gupta¹

¹Radiology and Imaging, Fortis Memorial Research Institute, Gurgaon, India, ²Healthcare, Philips India Ltd, Bangalore, India, ³Department of Neurology, KG Medical University, Lucknow, India, ⁴Healthcare, Philips India Ltd, Gurgaon, India

Gadolinium based contrast agents are necessary for MRI for disease detection and therapy. Studies reported gadolinium remains in brain for long time after injecting contrast particularly in follow up patients undergoing serial contrast applications. T1 signal intensity increases slowly due to contrast accumulation in brain. Our study quantifies T1 relaxation time as a measure for follow up contrast patients. Results show absolute T1 significantly decreases in Gray Matter regions, putamen, thalamus and globus pallidus. We conclude that absolute T1 quantification can efficiently pick up deposition of gadolinium much earlier than T1 signal intensity changes as observed in Gray matter regions.

2820

Computer #5



NOVIFAST: A fast non-linear least squares method for accurate and precise estimation of T1 from SPGR signals

Gabriel Ramos-Llordén¹, Arnold J. den Dekker^{1,2}, Marcus Björk³, Marleen Verhoye¹, and Jan Sijbers¹

¹University of Antwerp, Antwerp, Belgium, ²Delft University of Technology, Delft, Netherlands, ³Uppsala University, Uppsala, Sweden

The longitudinal relaxation time T1 can be estimated from a set of spoiled gradient recalled echo (SPGR) magnetic resonance images acquired over a range of flip angles with constant repetition time (TR). While linear estimators are widely used because of their low computation time, they are less accurate than their slower nonlinear counterpart¹. In this work, we introduce a novel NON-linear Variable Flip Angle data baSed T1 (NOVIFAST) estimator that combines the best of both worlds: high accuracy and precision in a low computation time.

2821

Computer #6



The effect of through-plane gradients on 2D gradient-echo acquisitions: are sinc-term corrections appropriate for R2* mapping?

Mukund Balasubramanian^{1,2} and Robert V. Mulkern^{1,2}

¹Department of Radiology, Boston Children's Hospital, Boston, MA, United States, ²Harvard Medical School, Boston, MA, United States

We made slice profile measurements and acquired 2D multi-gradient-echo data on a phantom in the presence of various through-plane gradients. The sinc-term correction for R₂* mapping that is commonly used to compensate for the dephasing effects of these gradients was substantially outperformed by a correction based on the measured slice profiles. Our results highlight the importance of incorporating realistic slice profiles into the estimation of "intrinsic" R₂* values, which may contain information about tissue structure at microscopic-to-mesoscopic spatial scales.

2822

Computer #7



Molecular Mechanism of Transverse Relaxation in Whole Blood with Plasma Contrast Reagent: Simulations of Bulk Magnetic Susceptibility and Water Exchange

Gregory J Wilson¹, Charles S Springer², Sarah Bastawrous^{1,3}, and Jeffrey H Maki¹

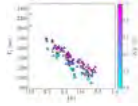
¹University of Washington, Seattle, WA, United States, ²Oregon Health and Science University, Portland, OR, United States, ³Puget Sound VA HCS, Seattle, WA, United States

Previously reported T₂* values in oxygenated whole blood with gadolinium based contrast reagents are very small. This has important implications for optimization of contrast-enhanced MR angiography and quantification of arterial input functions. To investigate the molecular mechanism of these short T₂* values, we have performed Monte Carlo simulations of signal dephasing that predict the reported values remarkably well. Intracellular water signal experiences a frequency shift that is dependent on the orientation of the RBC

in the magnetic field. The resulting frequency distribution in combination with trans-membrane water exchange results in rapid dephasing of water signal.

2823

Computer #8



Relaxation Properties of Human Umbilical Cord Blood at 1.5 Tesla

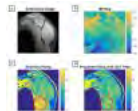
Sharon Portnoy¹, Mark Osmond², Meng Yuan Zhu³, Mike Seed⁴, John G. Sled^{1,2,5}, and Christopher K. Macgowan^{1,4}

¹Department of Medical Biophysics, University of Toronto, Toronto, ON, Canada, ²Department of Obstetrics and Gynaecology, University of Toronto, Toronto, ON, Canada, ³Institute of Medical Science, University of Toronto, Toronto, ON, Canada, ⁴Diagnostic Imaging, The Hospital for Sick Children, Toronto, ON, Canada, ⁵Mouse Imaging Centre, The Hospital for Sick Children, Toronto, ON, Canada

Relaxometry measurements were performed on umbilical cord blood samples ($N=88$) spanning a broad range of hematocrits ($0.19 < \text{Hct} < 0.76$) and oxygen saturations ($4\% < s\text{O}_2 < 100\%$). Simple biophysical models were used to describe variations in T_1 and T_2 as a function of these blood properties. The data and fitted model parameters presented here can be used for calibration of future MRI investigations of fetal and neonatal blood physiology.

2824

Computer #9



Quantitative T2 mapping using a modified BIR-4 T2 preparation in the presence of large B0 offsets

Dominik Weidlich¹, Hendrik Kooijman², Peter Börner³, Jan S. Kirschke⁴, Ernst J. Rummeny¹, Axel Haase⁵, and Dimitrios C. Karampinos¹

¹Department of Diagnostic and Interventional Radiology, Technische Universität München, Munich, Germany, ²Philips Healthcare, Hamburg, Germany, ³Philips Research Laboratory, Hamburg, Germany, ⁴Section of Neuroradiology, Technische Universität München, Munich, Germany, ⁵Zentralinstitut für Medizintechnik, Technische Universität München, Garching, Germany

T2 mapping has been emerging as a tool to quantitatively assess tissue edema and inflammation. Sequences employing T2 preparation have been suggested for accurate and precise T2 quantification. The use of the modified BIR-4 pulse has been proposed to minimize the sensitivity of T2 mapping to B1 inhomogeneities. However, in the presence of large B0 offsets, part of the magnetization can experience both T1 and T2 relaxation during the BIR-4 pulse leading to T2 quantification errors. The present work proposes a novel methodology to make T2 quantification based on the modified BIR-4 robust to the presence of large B0 offsets.

2825

Computer #10



Contrast optimization using Fast Field Cycling techniques and fast low angle sequences

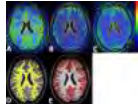
Nicolas Chanut¹ and Ludovic De Rochefort¹

¹IR4M (Imagerie par Résonance Magnétique Médicale et Multi-modalités), Univ. Paris-Sud, CNRS, UMR8081, Université Paris-Saclay, Orsay, France

Fast Field Cycling MRI offers the possibility to explore new contrasts generated from NMR dispersion (NMRD) profiles of tissue or contrast agents. Here, it is shown that dreMR contrast can be generated and optimized in fast low flip angle sequences extending the range of sequences that can be used with this new degree of freedom. The expression of a generalized Ernst angle maximizing signal with dreMR pulses is derived as well as the angle maximizing the dispersive contrast.

2826

Computer #11



Whole brain adiabatic T1rho and Relaxation Along a Fictitious Field imaging in healthy volunteers: feasibility and initial findings

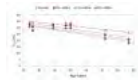
Aida Kiviniemi¹, Harri Merisaari¹, Marko Pesola¹, Timo Liimatainen², Hannu Juhani Aronen¹, and Ivan Jambor¹

¹University of Turku, Turku, Finland, ²A.I. Virtanen Institute for Molecular Sciences, Kuopio, Finland

The adiabatic $T_{1\rho}$ and RAFF measurements, RAFF2 and RAFF4, were performed in 28 healthy volunteers (24-69 years) and four of them had repeated MR scan within 4 weeks to evaluate short term repeatability. The relative differences on the voxel level were below 5% in gray and white matter for all of the relaxation parameters except of T_{RAFF4} in gray matter which was 7.3%. No statistically significant age related changes in white and gray matter were present as evaluated by adiabatic $T_{1\rho}$, RAFF2 and RAFF4 imaging.

2827

Computer #12



T1rho dispersion in human calf muscle

Ping Wang^{1,2}, Henry Zhu^{1,2}, Hakmook Kang³, Jake Block², and John C. Gore^{1,2}

¹Institute of Imaging Science, Vanderbilt University Medical Center, Nashville, TN, United States, ²Department of Radiology and Radiological Sciences, Vanderbilt University Medical Center, Nashville, TN, United States, ³Department of Biostatistics, Vanderbilt University Medical Center, Nashville, TN, United States

$T_{1\rho}$ imaging is sensitive to slow macromolecular interactions which may be generally characterized by a correlation time (τ_c) but also varies with the strength of the locking field used (ω_1). At higher fields (3T and beyond) $T_{1\rho}$ is also strongly influenced by chemical exchange processes and the dispersion of the relaxation rate $R_{1\rho} (=1/T_{1\rho})$ with locking field may be used to quantify exchange processes. We imaged normal muscles from individuals of different ages and found that $R_{1\rho}$ value is negatively correlated with age in normal muscle, and there is a small dispersion of $R_{1\rho}$ that appears to increase with age.

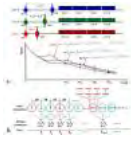
2828

Computer #13

Evaluation of Renal Oxygenation using a Simultaneous Dynamic R2, R2' and R2* Quantification Approach - Under the Influence of Hyperoxic Challenge

CY Wang¹, R Zhang², L Jiang³, R Wang⁴, XD Zhang⁴, H Wang³, K Zhao⁴, LX Jin³, J Zhang^{1,2}, XY Wang^{1,4}, and J Fang^{1,2}

¹Academy for Advanced Interdisciplinary Studies, Peking University, Beijing, China, People's Republic of, ²College of Engineering, Peking University, Beijing, China, People's Republic of, ³Philips Healthcare, Suzhou, China, People's Republic of, ⁴Department of Radiology, Peking University, Beijing, China, People's Republic of

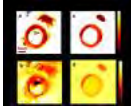


University First Hospital, Beijing, China, People's Republic of

This study demonstrates the feasibility of dynamic renal R_2 , R_2' and R_2^* measurement with the proposed psMASE-ME method. High temporal resolution was achieved by combining psMASE sequence and moving estimation strategy. The superiorities of this method could potentially be used in the renal oxygenation evaluation.

2829

Computer #14



Highly Accelerated, Intravascular T_1 , T_2 , and Proton Density Mapping with Linear Algebraic Modeling and Sensitivity Profile Correction at 3T

Guan Wang^{1,2}, Yi Zhang², Shashank Sathyanarayana Hegde^{2,3}, and Paul A. Bottomley²

¹Dept. of Electrical & Computer Engineering, Johns Hopkins University, Baltimore, MD, United States, ²Russell H. Morgan Dept. of Radiology & Radiological Sciences, Johns Hopkins University, Baltimore, MD, United States, ³(currently) Philips Innovation Campus, Bangalore, India

Vessel wall MRI with intravascular (IV) detectors can produce superior local signal-to-noise ratios (SNR) and generate high-resolution T_1 , T_2 , and proton density (PD) maps that could be used to automatically classify atherosclerotic lesion stage. However, long acquisition times potentially limit multi-parametric mapping. Here, for the first time, spectroscopy with linear algebraic modeling (SLAM) is applied to yield accurate compartment-average T_1 , T_2 and PD measures at least 10 times faster compared to a standard full k-space reconstructed MIX-TSE sequence at 3T. Simple phase and magnitude sensitivity corrections are incorporated into the SLAM reconstruction to compensate for IV detector non-uniformity.

2830

Computer #15



A Pulse Sequence for $T_1\rho$ Imaging of Liver in Human Subjects

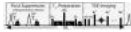
Weitian Chen¹, Queenie Chan², Min Deng¹, and Yixiang Wang¹

¹Imaging and Interventional Radiology, the Chinese University of Hong Kong, New Territory, Hong Kong, ²Philips Healthcare, New Territory, Hong Kong

$T_1\rho$ is a potential biomarker for evaluation of liver fibrosis. However, the application of $T_1\rho$ imaging for liver disease in human subjects remains challenging. We propose a pulse sequence based on single shot Turbo (Fast) Spin Echo (SSTSE or SSFSE) acquisitions to address the problems.

2831

Computer #16



Fast Fluid Suppressed $T_{1\rho}$ Imaging of the Human Brain

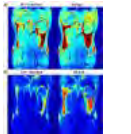
Eberhard Daniel Pracht¹ and Tony Stöcker^{1,2}

¹German Center for Neurodegenerative Diseases (DZNE), Bonn, Germany, ²University of Bonn, Department of Physics and Astronomy, Bonn, Germany

The longitudinal relaxation time in the rotating frame ($T_{1\rho}$) is a non-invasive biomarker, which is sensitive to slow macromolecular interactions. It might potentially be useful to detect pathological changes in neurodegenerative diseases such as Alzheimer's Disease. However, long scan times and high SAR limit the application of this technique in a routine setting. Furthermore, high CSF signal modulates the image intensity at CSF/tissue boundaries leading to an overestimation of $T_{1\rho}$ in these regions. To overcome these issues we developed a fast and robust approach to assess $T_{1\rho}$ in the human brain at high image resolution.

2832

Computer #17



Colloidal Nanoparticles for MRI Contrast Agents

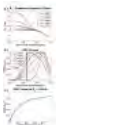
Akbar Alipour^{1,2,3}, Vijay Kumar Shamra^{3,4}, Zeliha Soran Erdem³, Zaliha Gamze Aykut⁵, and Hilmi Volkan Demir^{2,3,4}

¹UMRAM-National Magnetic Resonance Research Center, Bilkent University, Ankara, Turkey, ²Department of Electrical and Electronics Engineering, Bilkent University, Ankara, Turkey, ³UNAM - Institute of Materials Science and Nanotechnology, Bilkent University, Ankara, Turkey, ⁴School of Mathematical and Physical Sciences, Nanyang Technological University, Singapore, Singapore, ⁵Department of Molecular Biology and Genetics, Bilkent University, Ankara, Turkey

Magnetic resonance imaging (MRI) contrast agents, employed as image contrast enhancement mechanism, are able to change either negative or positive signal intensity. T_2 contrast normally offers magnetic susceptibility artifacts and decreases the resolution. On the other hand, T_1 contrast provides high spatial resolution, but it suffers from the deficiency of high contrast-to-noise ratio, which limits their clinical applications. To overcome the aforementioned limitations, we offer cubic shape super-paramagnetic iron oxide nanoparticles (SPIONs) as dual-mode colloidal MRI contrast agents. The in vitro and in vivo T_1 and T_2 MR images promise the great potential clinical application of SPIO nanocubes as dual-mode MR contrast agent.

2833

Computer #18



Quantifying Chemical Exchange Contributions in Mixtures Using Spin-Lock MRI

John Thomas Spear^{1,2} and John Gore^{1,2,3,4}

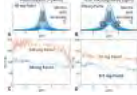
¹Physics and Astronomy, Vanderbilt University, Nashville, TN, United States, ²Institute of Imaging Science, Vanderbilt University, Nashville, TN, United States, ³Radiology, Vanderbilt University, Nashville, TN, United States, ⁴Biomedical Engineering, Vanderbilt University, Nashville, TN, United States

$R_{1\rho}$ dispersion provides insight into the rates of molecular processes that give rise to relaxation, and a technique called Exchange Rate Contrast (ERC) can differentiate proton pools based on chemical exchange rates. Double dispersion phenomena may occur when three exchanging proton pools are present, and parametric images may be calculated in which the image intensity scales with the concentration of the exchanging pools. A theoretical equation was derived for this contrast and shown to align well with Bloch-

McConnell simulations. Various applications with exogenous contrast agents present a great deal of potential for utilizing this technique in practice.

2834

Computer #19



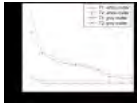
Paradoxical Narrowing of the Spectroscopy Water Peak in the Presence of Iron Overload
Diego Hernando¹, Samir D Sharma¹, Debra E Horng², and Scott B Reeder^{1,2,3,4,5}

¹Radiology, University of Wisconsin-Madison, Madison, WI, United States, ²Medical Physics, University of Wisconsin-Madison, Madison, WI, United States, ³Biomedical Engineering, University of Wisconsin-Madison, Madison, WI, United States, ⁴Medicine, University of Wisconsin-Madison, Madison, WI, United States, ⁵Emergency Medicine, University of Wisconsin-Madison, Madison, WI, United States

In phantoms with large iron particles, as well as in patients with liver iron overload, a paradoxical relationship was observed where the linewidth measured from MRS was smaller than the linewidth obtained from multi-echo spoiled gradient echo MRI. Assuming a model of “apparent” R2 decay in the presence of iron where single-echo acquisitions are essentially diffusion-weighted by the iron-induced B0 heterogeneities, we speculate that different isochromats within the observed spectra undergo different diffusion weighting related to their location relative to nearby large iron particles. These observations may have implications for the characterization of iron deposition in tissue.

2835

Computer #20



Towards Optimized Experiment Design for Magnetic Resonance Fingerprinting
Bo Zhao¹, Justin P. Haldar², Kawin Setsompop¹, and Lawrence L. Wald¹

¹Martinos Center for Biomedical Imaging, Cholestown, MA, United States, ²Signal and Image Processing Institute, University of Southern California, Los Angeles, CA, United States

A principled framework is proposed to optimize the experiment design for magnetic resonance fingerprinting (MRF) based on the Cramer-Rao bound. Within this framework, we optimize the acquisition parameters (flip angle, TR, etc.) to maximize the SNR efficiency of quantitative parameter estimation. Preliminary results indicate that the optimized experiments allow for substantially reducing the length of an MRF acquisition and substantially improving estimation performance for the T2 map, while maintaining similar accuracy level for the T1 map. The proposed framework should prove useful for fast quantitative MR imaging with MRF.

2836

Computer #21



Myelin Water Imaging using 3D Radial multi-echo GRE acquisition

Hongpyo Lee¹, Yoonho Nam², Min-Oh Kim¹, Dongyeob Han¹, Sung-Min Gho¹, and Dong-Hyun Kim¹

¹School of Electrical and Electronic Engineering, Yonsei University, Seoul, Korea, Republic of, ²Department of Radiology, Seoul St. Mary Hospital, College of Medicine, The Catholic University of Korea, Seoul, Korea, Republic of

Recently, myelin water fraction was investigated using multi-echo GRE data. In case of complex model fitting for MWF, only a small fraction of the total signal is used, small artifacts caused by physiological motion can induce severe noise in MWF. To overcome this problem, radial trajectory which is known to have robustness against object motion can be used. Also, this trajectory has the additional advantage of acquiring the more center of k-space than Cartesian trajectory which is helpful for detecting accurate T2* decay curve, and it may provide higher SNR and improved quantification. In this abstract, we demonstrated that the radial acquisition can reduce artifacts and improve image quality in MWF.

2837

Computer #22



Myelin Water Imaging in Multiple Sclerosis Post-Mortem Spinal Cord

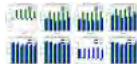
Amy McDowell¹, Natalia Petrova¹, Irene Vavasour², David Thomas³, Daniele Carassiti¹, Marc Miquel⁴, Shannon Kolind², and Klaus Schmierer^{1,5}

¹Neuroscience and Trauma, Queen Mary University of London, London, United Kingdom, ²University of British Columbia, Division of Neurology, Department of Medicine, Vancouver, BC, Canada, ³Neuroimaging Analysis Centre, Department of Brain Repair and Rehabilitation, London, United Kingdom, ⁴Clinical Physics, Barts Health Trust, London, United Kingdom, ⁵Department of Neurology, Barts Health Trust, London, United Kingdom

Evidence obtained from *post mortem* multiple sclerosis (MS) brain suggest that ‘myelin water fraction’ (MWF) acquired using the CPMG sequence is strongly associated with myelin. However, relaxation times differ significantly between brain and spinal cord (SC), a key area of the clinical manifestations of MS. We investigated the histological correlates of MWF in *post mortem* MSSC. Good separation of the short T₂ components, and correlation between MWF and myelin content detected using immunohistochemistry were observed.

2838

Computer #23



Linear models for estimating myelin and iron content in the brain

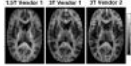
Riccardo Metere¹ and Harald E. Möller¹

¹Max Planck Institute for Human Cognitive and Brain Sciences, Leipzig, Germany

Quantitative MRI maps are believed to strongly correlate with myelin and ferritin content. Recently, a model combining prior information from non-MRI quantitative techniques was proposed for the quantification of myelin and ferritin based on relaxometry information $R_{1\rho}$ and R_2^* in post mortem human brain samples. Here, we propose four different simple linear models for tentatively obtaining semi-quantitative information using simultaneous quantitative acquisitions under in vivo conditions. Three of the four model are relatively consistent, but do not agree with previously published measurements. A fourth model, although not validated, is compatible with previous works.

2839

Computer #24



Inter-scanner reproducibility of 4 minute whole brain myelin mapping using FAST-T2

Thanh D. Nguyen¹, Kofi Deh¹, Sneha Pandya¹, Yi Wang¹, and Susan A. Gauthier¹

¹Weill Cornell Medical College, New York, NY, United States

The purpose of this study was to measure the inter-scanner reproducibility of fast myelin water fraction (MWF) mapping using a 4 min FAST-T2 sequence on three scanners from two vendors at 1.5T and 3T. Regional MWF measurements obtained in 7 healthy volunteers were highly reproducible with excellent inter-scanner correlation ($R > 0.95$) and small MWF bias of less than 1%.

Electronic Poster

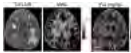
Magnetic Susceptibility

Exhibition Hall

Monday, May 9, 2016: 14:15 - 15:15

2840

Computer #25



Absolute quantification of white matter lesion iron and myelin using QSM and FAST-T2 at 3 Tesla

Thanh D. Nguyen¹, Pascal Spincemaille¹, Sneha Pandya¹, Susan A. Gauthier¹, and Yi Wang¹

¹Weill Cornell Medical College, New York, NY, United States

The purpose of this study was to develop a clinically feasible method for quantifying myelin and iron distribution in white matter lesions by integrating absolute myelin water mapping using Fast Acquisition using Spiral Trajectory and T2prep (FAST-T2) sequence with Quantitative Susceptibility Mapping (QSM). Preliminary results from 8 healthy volunteers and 3 MS patients demonstrated the feasibility of the developed method.

2841

Computer #26



Susceptibility Changes in Dentate Nucleus on Quantitative Susceptibility Mapping due to serial GBCAs administration.

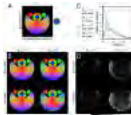
Takuya Hinoda¹, Yasutaka Fushimi¹, Tomohisa Okada^{1,2}, Tsutomu Okada¹, Akira Yamamoto¹, and Togashi Kaori¹

¹Radiology, Graduate school of Medicine, Kyoto University, Kyoto, Japan, ²Human Brain Research Center, Graduate school of Medicine, Kyoto University, Kyoto, Japan

Gadolinium-based contrast agents (GBCAs) have been widely used for contrast material-enhanced magnetic resonance (MR) imaging. However, gadolinium accumulation in the dentate nucleus (DN) has gained attention due to recent studies. In this study, we retrospectively evaluated the susceptibility values of DN, using quantitative susceptibility mapping. The susceptibility values of the patients with GBCA administration were significantly higher than those of normal controls.

2842

Computer #27



The Absence of Phase Information in the Signal-Deprived Image Background is an Important Source of Error in Susceptibility Mapping

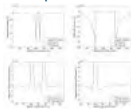
Russell Dobb^{1,2} and Chunlei Liu^{3,4}

¹Center for In Vivo Microscopy, Duke University, Durham, NC, United States, ²Biomedical Engineering, Duke University, Durham, NC, United States, ³Brain Imaging & Analysis Center, Duke University, Durham, NC, United States, ⁴Radiology, Duke University, Durham, NC, United States

Susceptibility mapping is limited in part due to reconstruction artifacts spawning from errors in tissue frequency data. Through simulations of susceptibility tensor imaging (STI) data, we show that a lack of phase information in the image background (where there is typically no signal) engenders artifacts in reconstructed susceptibility property maps. These errors are most egregious in the boundary regions of the object and affect mean susceptibility, susceptibility anisotropy, and tissue structure orientation measurements. Greater understanding of susceptibility mapping artifacts will aid in developing the tools necessary for accurate and reliable susceptibility imaging techniques.

2843

Computer #28



Improved magnetic dipole kernel for reconstruction methods in quantitative susceptibility mapping

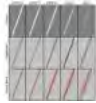
Carlos Milovic^{1,2}, Jose Miguel Pinto^{1,2}, Julio Acosta-Cabronero³, Petr Dusek^{4,5}, Vince Istvan Madai⁶, Till Huelnhagen⁷, Thoralf Niendorf⁷, Jens Wuerfel⁸, and Cristian Tejos^{1,2}

¹Department of Electrical Engineering, Pontificia Universidad Catolica de Chile, Santiago, Chile, ²Biomedical Imaging Center, Pontificia Universidad Catolica de Chile, Santiago, Chile, ³German Center for Neurodegenerative Diseases (DZNE), Magdeburg, Germany, ⁴Institute of Neuroradiology, University Medicine Goettingen, Goettingen, Germany, ⁵Department of Neurology and Center of Clinical Neuroscience, Charles University in Prague, 1st Faculty of Medicine and General University Hospital in Prague, Praha, Czech Republic, ⁶Department of Neurology and Center for Stroke Research Berlin (CSB), Charité-Universitaetsmedizin, Berlin, Germany, ⁷Berlin Ultrahigh Field Facility (B.U.F.F.), Max-Delbrueck Center for Molecular Medicine, Berlin, Germany, ⁸Medical Image Analysis Center, Basel, Switzerland

We propose a new magnetic dipole kernel for QSM reconstructions based on the discrete cosine transform and discrete derivative operators. The method minimises aliasing artefacts, reduces noise and improves detection of small objects and tissue interfaces. This is demonstrated numerically with a synthetic phantom and qualitatively with an ultra-high resolution QSM of post-mortem brain tissue.

2844

Computer #29



Simultaneous Quantification of Blood Vessel Caliber and Oxygenation via Multi-Voxel Joint Utilization of Magnitude and Phase (MV-JUMP)

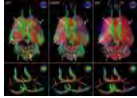
Patrick McDaniel¹, Berkin Bilgic², Audrey Fan³, Jeffrey Stout⁴, and Elfar Adalsteinsson^{1,4}

¹Electrical Engineering and Computer Science, MIT, Cambridge, MA, United States, ²Athinoula A Martinos Center for Biomedical Imaging, Massachusetts General Hospital, Charlestown, MA, United States, ³Richard M Lucas Service Center for Imaging, Stanford University, Stanford, CA, United States, ⁴Health Sciences and Technology, Harvard/MIT, Cambridge, MA, United States

Accurate, quantitative determination of blood vessel oxygenation and caliber from GRE data would be useful for assessing local perfusion and oxygen consumption. However, partial-volume effects confound both measurements. Vessel edges are blurred and discretized, hampering assessment of vessel size. Oxygenation can be measured from GRE phase, but partial-volume effects with other tissues often contaminate these measurements. In this work, we present a novel approach that simultaneously obtains accurate measurements of vessel caliber and oxygenation state for vessels nearly parallel to B_0 . This approach is demonstrated in numerical and in vivo experiments.

2845

Computer #30



Estimating Shared Relaxation and Susceptibility Tensor Eigenvectors Enhances STI Tractography in the Heart, Kidney, and Brain

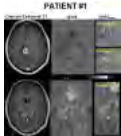
Russell Dobb^{1,2}, Luke Xie^{1,3}, and Chunlei Liu^{4,5}

¹Center for In Vivo Microscopy, Duke University, Durham, NC, United States, ²Biomedical Engineering, Duke University, Durham, NC, United States, ³Utah Center for Advanced Imaging Research, University of Utah, Salt Lake City, UT, United States, ⁴Brain Imaging & Analysis Center, Duke University, Durham, NC, United States, ⁵Radiology, Duke University, Durham, NC, United States

Conjoint relaxation and susceptibility tensor imaging (CRSTI) uses both magnitude- and phase-derived tensor data to compute susceptibility-based tractography in magnetically anisotropic tissues. CRSTI reduces image artifacts that appear in traditional susceptibility tensor imaging by taking advantage of mutual eigenvector data in relaxation and susceptibility tensors. We present an efficient conjoint tensor estimation algorithm and demonstrate improved susceptibility-based tractography in myofibers, renal tubules, and axon fiber bundles. As susceptibility imaging is sensitive to both microstructure and cellular content, CRSTI is a potential tool for studying disease in tissues throughout the body.

2846

Computer #31



Assessing Response to Hyperoxic Respiratory Challenges with Quantitative Susceptibility Mapping in Primary Malignant Brain Tumors

Pinar Senay Özbay^{1,2}, Cristina Rossi¹, Sonja Stieb³, Oliver Riesterer³, Andreas Boss¹, Klaas Paul Pruessmann², and Daniel Nanz¹

¹Department of Radiology, University Hospital Zurich, Zurich, Switzerland, ²Institute of Biomedical Engineering, ETH Zurich, Zurich, Switzerland, ³Department of Radio-Oncology, University Hospital Zürich, Zurich, Switzerland

Glioblastoma multiforme and anaplastic astrocytoma are aggressive brain tumors which can form large heterogeneous lesions, parts of which respond with varying sensitivity to radiotherapy. The long-term goal of the current study is to characterize the oxygenation state of tumors or parts of heterogeneous large tumors by quantitative-susceptibility-mapping, under hyperoxic respiratory challenge, and yield valuable information, e.g., for an improved dose shaping, which may lead to an improved therapy outcome. The preliminary results suggest that QSM may indeed be capable of differentiating the response of well vascularized tumor-tissue volumes to respiratory-induced hypoxia from the response of likely necrotic and edematous volumes.

2847

Computer #32



High-Resolution Quantitative Susceptibility Mapping of Free-Breathing Human Lung

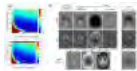
Hongjiang Wei¹, Luke Xie², Yuyao Zhang¹, and Chunlei Liu^{1,3}

¹Brain Imaging and Analysis Center, Duke University, Durham, NC, United States, ²Utah Center for Advanced Imaging Research, Department of Radiology, University of Utah, Salt Lake City, UT, United States, ³Department of Radiology, School of Medicine, Duke University, Durham, NC, United States

In the pulmonary tissue, strong-susceptibility-induced field perturbation is mostly a source of artifact resulting in severe distortion. Breathing artifacts pose further challenges, especially in pediatric populations. These artifacts coupled with the intrinsic low proton SNR make it extremely difficult to perform quantitative susceptibility mapping in the lung. State-of-the-art STAR-QSM method combined with the recently developed locally low rank parallel imaging method could further reduce motion artifacts and allow free-breathing high resolution QSM of the lung.

2848

Computer #33



How to compare SHARP parameters? New definitions in physical rather than numerical space

Pinar Senay Özbay^{1,2}, Andreas Deistung³, Xiang Feng^{3,4}, Daniel Nanz², Jürgen Reichenbach^{3,5}, and Ferdinand Schweser^{4,6}

¹Institute of Biomedical Engineering, ETH Zurich, Zurich, Switzerland, ²Department of Radiology, University Hospital Zurich, Zurich, Switzerland, ³Medical Physics Group, Institute of Diagnostic and Interventional Radiology, Jena University Hospital - Friedrich Schiller University Jena, Jena, Germany, ⁴Buffalo Neuroimaging Analysis Center, Department of Neurology, Jacobs School of Medicine and Biomedical Sciences, The State University of New York at Buffalo, Buffalo, NY, United States, ⁵Friedrich Schiller University Jena, Michael Stifel Center for Data-driven and Simulation Science Jena, Jena, Germany, ⁶MRI Clinical and Translational Research Center, Jacobs School of Medicine and Biomedical Sciences, The State University of New York at Buffalo, Buffalo, NY, United States

Sophisticated Harmonic Artifact Reduction for Phase data (SHARP) is a method widely used for removal of background fields, which is one of the steps of Quantitative susceptibility mapping (QSM). In this work we analyzed SHARP using different radii between 1 and 15mm, with varying regularization parameters in mm^{-1} , determined optimum values and showed two cases that can arise due to wrong interpretation of the original parameters. A direct conversion of the old-parameters-scheme to the new one is presented. Best and

extreme cases for parameters are demonstrated for simulated models and an in-vivo case, and the effects on images are discussed.

2849

Computer #34



Automated tissue phase and QSM estimation from multichannel data
Berkin Bilgic¹, Jonathan R Polimeni¹, Lawrence L Wald¹, and Kawin Setsompop¹

¹Martinos Center for Biomedical Imaging, Charlestown, MA, United States

An automated method for tissue phase and susceptibility estimation from multichannel data is proposed. Using ESPIRiT with virtual body coil calibration on multichannel data, phase-sensitive coil combination is achieved without an additional reference acquisition. This is shown to perform similarly to SNR-optimal Roemer combination that requires additional reference body and head coil acquisitions. Estimation of the tissue phase from the combined data is posed as a regularized inverse problem using the spherical mean value property. The extension of the technique to single-step Quantitative Susceptibility Mapping is also demonstrated on 2D, 3D and Simultaneous MultiSlice data.

2850

Computer #35



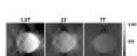
Susceptibility-driven oscillations in Multi-Gradient-Echo MRI reflect axonal microstructures
Daniel Nunes¹, Tomás Cruz¹, Sune Nørhøj Jespersen², and Noam Shemesh¹

¹Champalimaud Neuroscience Program, Champalimaud Center for the Unknown, Lisbon, Portugal, ²CFIN/MindLab, Aarhus Universitet, Århus C, Denmark

Characterizing white matter (WM) microstructure in terms of axon size and volume fraction remains elusive and typically requires extremely strong gradients to resolve water diffusion in micron-sized axons. Here, we develop and apply a new approach for quantifying WM microstructure using a simple multi-gradient-echo (MGE) sequence. We use rat spinal cord as our experimental system, and show that, at long echo times, oscillations in the signal decay emerge, which can be used to robustly quantify the WM microstructure. The ensuing parametric maps segment the SC into its underlying microstructures. The simplicity of the approach bodes well for many future applications.

2851

Computer #36



Magnetic Saturation and Field Dependency on Magnetic Susceptibility of Ferumoxytol
Jean-Christophe Brisset¹, Pippa Storey¹, Saifeng Liu², E. Mark Haacke³, and Yulin Ge¹

¹Radiology, New York University School of Medicine, New York, NY, United States, ²The MRI Institute for Biomedical Research, Waterloo, ON, Canada, ³Radiology, Wayne State University, Detroit, MI, United States

The magnetization of diamagnetic and paramagnetic materials is proportional to the strength of the applied magnetic field, with a constant of proportionality (χ) known as the magnetic susceptibility. While the magnetization of ferromagnetic and superparamagnetic materials is much higher than that of diamagnetic and paramagnetic materials, it becomes saturated in strong magnetic fields. We show that the magnetization of USPIO agents such as Ferumoxytol saturates at around 1.5T. This introduces a perceived inverse correlation between apparent susceptibility and field strength. By contrast, the magnetization of GdDTPA is proportional to field strength up to 7T, as expected for a paramagnetic material.

2852

Computer #37



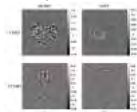
Evaluation of an Iterative Phase Replacement Method for Susceptibility Mapping in Regions with no MRI Signal
Emma Dixon¹, Anna Barnes², and Karin Shmueli¹

¹Department of Medical Physics and Biomedical Engineering, University College London, London, United Kingdom, ²Institute of Nuclear Medicine, UCLH-NHS Foundation Trust, London, United Kingdom

Magnetic susceptibility mapping has the potential to facilitate segmentation of air and teeth in the head due to their different magnetic susceptibilities, though there is no phase signal in these regions. An iterative phase replacement method to improve the calculation of susceptibility distributions in regions with no phase signal is validated using a numerical phantom consisting of three classes: air, teeth and tissue with the phase image set to zero in the air and teeth to simulate the real case. Calculated susceptibility distributions in regions with no phase signal were not accurate and standard deviations were seen to increase in some regions, though the iterative technique improved a simple segmentation.

2853

Computer #38



Quantitative susceptibility mapping with discrete wavelet transform at 7T & 3T MRI
Young Joong Yang^{1,2}, Jong-Hyun Yoon¹, Jinho Park¹, Hyeon-Man Baek², and Chang-Beom Ahn¹

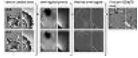
¹Kwangwoon University, Seoul, Korea, Republic of, ²Korea Basic Science Institute, Ochang, Korea, Republic of

A tissue characterization with susceptibility e.g., susceptibility weighted imaging (SWI), quantitative susceptibility mapping (QSM), susceptibility tensor imaging (STI), gets more attention in high field MRI. Using a numerical phantom, various processing elements for QSM are analyzed. We propose a method to remove background phase using a discrete wavelet transform (DWT). The proposed DWT method shows superb performances over exiting techniques including SHARP in the QSM experiments with volunteer subjects at 7.0T and 3.0T MRI, without distortions at the susceptibility maps.

2854

Computer #39

Preserving vessel conspicuity and contrast in local frequency maps by processing channel phase images prior to combination
Zahra Hosseini¹, Junmin Liu², and Maria Drangova³



¹Biomedical Engineering Graduate Program, Western University, London, ON, Canada, ²Imaging Research Laboratories, Robarts Research Institute, London, ON, Canada, ³Department of Medical Biophysics, Western University, London, ON, Canada

Local frequency shift (LFS) mapping from multi-channel acquisition is traditionally performed with channel-combined data set prior to background field removal. In this work we utilize inter-echo variance channel combination to evaluate the effect of pre-channel combination (pre-CC) phase image processing on the quality of LFS maps. We compare our results with post-channel combination (post-CC) LFS maps. The results illustrate superior performance in the contrast of LFS maps resulting from pre-CC processing compared to the post-CC LFS maps. Several examples where vessel conspicuity is lost through post-CC processing but preserved through pre-CC processing are presented.

2855

Computer #40



WHOLE-BODY QUANTITATIVE SUSCEPTIBILITY MAPPING IN HEALTHY SUBJECTS AND IN PATIENTS WITH IRON OVERLOAD

Samir D. Sharma¹, Jens-Peter Kühn², Marie-Luise Kromrey², Scott B. Reeder^{1,3}, and Diego Hernando¹

¹Radiology, University of Wisconsin - Madison, Madison, WI, United States, ²Experimental Radiology, Greifswald University, Greifswald, Germany, ³Medical Physics, University of Wisconsin-Madison, Madison, WI, United States

Magnetic susceptibility is a fundamental property of all tissues. The presence of biomaterials (e.g. iron, gadolinium) changes the susceptibility of the tissue in a direct and well-understood manner, allowing quantification of biomaterial concentration. Quantitative susceptibility mapping (QSM) techniques have been developed, largely to investigate iron and calcium deposits in the brain. The development and application of whole-body QSM may enable improved characterization and quantification of tissue pathophysiology based on a fundamental property of tissue. Thus, the purpose of this work was to develop and demonstrate the feasibility of whole-body QSM in healthy subjects and in patients with suspected iron overload.

2856

Computer #41



Gauging the stability of susceptibility and R2* mapping across ten sites

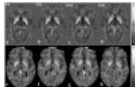
Bing Wu¹, Dandan Zheng¹, and Zhenyu Zhou¹

¹GE healthcare MR Research China, Beijing, China, People's Republic of

In this work, the stability of simultaneously obtained R2* and susceptibility are investigated and compared across 10 sites with identical experiment setup and post-processing hardware, as may be the case for a multi-center study.

2857

Computer #42



Investigation of intrascanner reproducibility of quantitative susceptibility mapping (QSM) and R2* at 3T

Xiang Feng¹, Andreas Deistung¹, Marianne Cleve¹, Ferdinand Schweser^{2,3}, and Juergen Reichenbach¹

¹Medical Physics Group, Institute of Diagnostic and Interventional Radiology, Jena University Hospital - Friedrich Schiller University Jena, Jena, Germany, ²Buffalo Neuroimaging Analysis Center, Department of Neurology, Jacobs School of Medicine and Biomedical Sciences, The State University of New York at Buffalo, Buffalo, NY, United States, ³MRI Molecular and Translational Research Center, Jacobs School of Medicine and Biomedical Sciences, The State University of New York at Buffalo, Buffalo, NY, United States

In the present work, we quantitatively assessed the reproducibility of Quantitative susceptibility mapping (QSM) and effective transverse relaxation rate (R2*) in healthy volunteers at 3T scanner during multiple scanning sessions. We also investigated the QSM normalization based on 2 reference structures, Cerebrospinal fluid (CSF) and frontal White Matter (fWM). Our results indicated that QSM using CSF as reference region reveals increased scan-rescan reliability than referencing with fWM.

2858

Computer #43



Optimising SWI in neonates

Rui Pedro A. G. Teixeira^{1,2}, Christopher Kelly¹, Tomoki Arichi¹, Shaihan J. Malik², Serena Counsell¹, and Joseph V. Hajnal^{1,2}

¹Perinatal Imaging and Health, King's College London, London, United Kingdom, ²Imaging Sciences and Biomedical Engineering, King's College London, London, United Kingdom

Susceptibility-weighted imaging (SWI) is sensitive to susceptibility changes associated with blood and shows excellent performance in detecting hemorrhage. Infants born preterm and those with congenital heart disease are at risk of parenchymal, cerebellar or intraventricular/germinal layer haemorrhage. As such, there is a clinical need for rapid, high resolution SWI to assess brain injury in these infants. In this work a dedicated neonatal SWI protocol is proposed that aims to maximize the obtainable signal while minimizing the expected WM/GM contrast to improve sensitivity to local field variations.

2859

Computer #44



Quantification of Liver Iron Concentration using the Apparent Susceptibility of Vessels

Saifeng Liu¹, Chaoyue Wang², Xiaoqi Zhang³, Hongyan Ni³, Panli Zuo⁴, Jiani Hu⁵, and E. Mark Haacke^{1,2,5}

¹The MRI Institute for Biomedical Research, Waterloo, ON, Canada, ²School of Biomedical Engineering, McMaster University, Hamilton, ON, Canada, ³Tianjin First Central Hospital, Tianjin, China, People's Republic of, ⁴Siemens Healthcare, MR Collaborations NE Asia, Beijing, China, People's Republic of, ⁵Department of radiology, Wayne State University, Detroit, MI, United States

Quantification of liver iron concentration (LIC) is critical for the diagnosis of patients with liver iron overload. LIC is conventionally

measured using R_2/R_2^* mapping methods which have limited accuracy and precision, partly due to the non-linear relation between relaxation rate and iron concentration. Quantitative susceptibility mapping (QSM) has been shown to be effective in quantifying cerebral iron deposition. For LIC quantification using QSM, the challenges include dealing with air-tissue interface in the abdomen in background field removal and solving the ill-posed inverse problem. Here we show a method which uses the apparent susceptibility of liver vessels for LIC quantification.

2860

Computer #45



Investigating the magnetic susceptibility of skeletal muscle at 7 T

Benjamin Tandler¹ and Richard Bowtell¹

¹Sir Peter Mansfield Imaging Centre, University of Nottingham, Nottingham, United Kingdom

There has been longstanding interest in the anisotropic magnetic properties of muscle tissue, but to date there has been little examination of these properties using MRI. Here we describe an initial examination of muscle via field mapping measurements carried out at 7T on phantoms containing small pieces of muscle embedded in agar. The results indicate that the susceptibility of this muscle is diamagnetic (~ -100 ppb) with respect to agar and only weakly anisotropic (<5 ppb). There was a significant uniform and orientation-independent positive frequency offset inside the muscle of 30 ppb most likely due to chemical exchange effects.

2861

Computer #46



Quantitative susceptibility mapping including a white matter Lorentzian correction

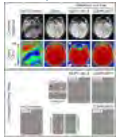
Diana Khabipova^{1,2}, Rita Gil², Marcel Zwiers², and José Pedro Marques²

¹CIBM-AIT, EPFL, Lausanne, Switzerland, ²Centre for Cognitive Neuroimaging, Donders Institute, Nijmegen, Netherlands

Quantitative susceptibility mapping (QSM) has been shown to provide quantitative measures of iron concentration in deep gray matter structures. In white matter, QSM is affected not only by local susceptibility but also by the local organized microstructure of axons and its myelin coating where reduced water signal exists. Recently, the anisotropic effect of myelin susceptibility was shown to be minor compared to the effect of its compartmentalization. In this work, the Lorentzian correction was, for the first time, implemented in a COSMOS like QSM reconstruction. The correction does not affect deep gray matter structure values, but creates QSM maps of isotropic susceptibility and maps of the susceptibility of cylindrically organized inclusion spaces.

2862

Computer #47



Combining phase information from multi-channel coils using a short TE reference scan (COMPOSER): evaluation with a range of coils and comparison with other approaches at 7T

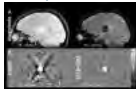
Simon Daniel Robinson^{1,2}, Barbara Dymerska^{1,2}, Wolfgang Bogner^{1,2}, Markus Barth³, Zoric Olgica^{1,2}, Sigrun Goluch^{1,4,5}, Günther Grabner^{1,2}, Xeni Deligianni^{6,7}, Oliver Bierl^{6,7}, and Siegfried Trattnig^{1,2}

¹High Field Magnetic Resonance Centre, Medical University of Vienna, Vienna, Austria, ²Department of Biomedical Imaging and Image-guided Therapy, Medical University of Vienna, Vienna, Austria, ³Centre for Advanced Imaging, The University of Queensland, Brisbane, Australia, ⁴Center for Medical Physics and Biomedical Engineering, Medical University of Vienna, Vienna, Austria, ⁵Division of Endocrinology and Metabolism, Department of Internal Medicine III, Medical University of Vienna, Vienna, Austria, ⁶Department of Radiology, Division of Radiological Physics, University of Basel Hospital, Basel, Switzerland, ⁷Department of Biomedical Engineering, University of Basel, Basel, Switzerland

A new method for combining phase images from multi-channel radio-frequency coils in the absence of a volume reference coil is presented and tested with calf, breast and head coils at 7 Tesla. This approach, called COMbining Phased array data using Offsets from a Short Echo-time Reference, or COMPOSER, is shown to yield phase matching between channels which is better than a rival, widely adopted reference-free method (MCPC-3D) and comparable with the reference-based Roemer method. COMPOSER can be used with all coil arrays, including the next generation of PTx coils where the transmit array may not be engineered to receive signal.

2863

Computer #48



Quantitative susceptibility mapping (QSM) as a means to monitor cerebral hematoma treatment

Hongjiang Wei¹, Yuyao Zhang¹, Yan Zhou², Yawen Sun², Jianrong Xu², Nian Wang¹, and Chunlei Liu^{1,3}

¹Brain Imaging and Analysis Center, Duke University, Durham, NC, United States, ²Department of Radiology, Ren Ji Hospital, Shanghai Jiaotong University, Shanghai, China, People's Republic of, ³Department of Radiology, School of Medicine, Duke University, Durham, NC, United States

Quantitative susceptibility mapping (QSM) based on GRE phase data can provide an accurate measurement of the hemorrhage volumes by removing blooming artifacts inherent in traditional T2* weighted imaging. It is shown here that new developed STAR-QSM can effectively remove the streaking artifact and provide more reliable measure for hematoma volume and susceptibility quantification, e.g., for evaluating the patients per- and post-treatment. By taking the advantage of high quality susceptibility maps, susceptibility information can help to provide further classification of the hemorrhage stage.

Electronic Poster

Perfusion & Permeability

Exhibition Hall

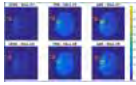
Monday, May 9, 2016: 14:15 - 15:15

2864

Computer #49

Magnetic Resonance Perfusion Quantification using QR-based Deconvolution

Phaneendra Kumar Yalavarthy¹, Kasireddy Viswanatha Reddy¹, and Junki Lee²



¹Samsung R & D Institute, Bangalore, India, ²Medical System Lab, Samsung Electronics, Suwon, Korea, Republic of

The standard approaches for performing the deconvolution in post-processing of DSC-MRI data is singular value decomposition (SVD) and Frequency-Domain Deconvolution (FDD), which are known to be relatively less accurate and requires a careful choice of threshold to obtain physiologically meaningful results. In this work, a method that utilizes QR decomposition to perform the deconvolution is proposed. The QR method is a well-known dimensionality reduction technique for solving ill-conditioned linear system of equations and known to have better numerical properties in obtaining a regularized solution. It is shown that the proposed method provides superior results compared to the standard deconvolution methods.

2865

Computer #50



Assessment of an automated method for AIF voxel selection for renal filtration rate estimation from DCE-MRI data.

Anita Banerji¹, Derek Magee², Constantina Chrysochou³, Philip Kalra³, David Buckley¹, and Steven Sourbron¹

¹Department of Biomedical Imaging, The University of Leeds, Leeds, United Kingdom, ²School of Computing, The University of Leeds, Leeds, United Kingdom, ³Department of Renal Medicine, Salford Royal hospital NHS foundation trust, Salford, United Kingdom

In this work we present an automated arterial input function voxel selection method for estimation of glomerular filtration rate (GFR) from renal DCE-MRI data. We assessed the agreement of GFR values estimated using the automated method with values estimated using semi-automatic expert selection and nuclear medicine techniques using 16 acquired data sets. The automated method successfully selected voxels within the aorta in all cases. The agreement between the expert and automated method was in some cases poor. However, the agreement of the automated method with the nuclear medicine results was similar to that of the expert method.

2866

Computer #51



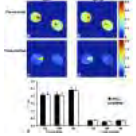
The quantitative research of the vertebral microvascular permeability and fat fraction in alloxan-induced diabetic rabbits lei hu¹, fei yun zha¹, dong xing¹, wei gong¹, jiao wang¹, yuan lin¹, hui lin², and xiao xu²

¹Renmin Hospital of Wuhan University, wuhan, China, People's Republic of, ²GE healthcare, wuhan, China, People's Republic of

To estimate the effect of diabetes on vertebral bone marrow, twelve young New Zealand White rabbits including alloxan-induced diabetic rabbits (n=6) and the controls (n=6) underwent sagittal magnetic resonance imaging (IDEAL-IQ, DCE-MRI) of lumbar at each time point. At the week of 16, all rabbits were killed. L7 sampling, HE staining and immunoperoxidase CD31 labeling were performed. According to statistical analysis, there were statistically significant differences of the vertebral DCE-MRI parameters and fat fraction (FF) between the diabetic groups and controls at each time point. The variety of vertebral microvascular permeability was strongly associated with the increasing vertebral fat deposition.

2867

Computer #52



Saturation Recovery Fast Spin Echo Method for Rapid T1 Mapping of Mouse Kidney

Kai Jiang¹, Hui Tang¹, Prassana K. Mishra², Slobodan I. Macura², and Lilach O. Lerman¹

¹Division of Nephrology and Hypertension, Mayo Clinic, Rochester, MN, United States, ²Department of Biochemistry and Molecular Biology, Mayo Clinic, Rochester, MN, United States

In this study, a saturation recovery fast spin echo method was developed for fast T₁ mapping of mouse kidney at a temporal resolution of ~3 min. The validity of this method was first demonstrated *in vitro* on a phantom with different concentrations of MnCl₂ by comparing to the conventional spin echo T₁ mapping method and a previously validated saturation recovery Look-Locker (SRLL) method and then *in vivo* on mouse kidneys at both pre- and post-MnCl₂ infusion by comparing to SRLL.

2868

Computer #53



SPIO-enhanced MRI as a nondestructive *in vivo* Method to assess Vascularization of a 3D Matricel Collagen Scaffold planted on the Chorioallantoic Membrane of the Chick Embryo *in ovo*

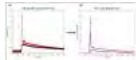
Conny F. Waschkies^{1,2}, Fatma Kivrak Pfiffner³, Yinghua Tian¹, Maurizio Calcagni³, Pietro Giovanoli³, Markus Rudin², and Johanna Buschmann³

¹Division of Visceral and Transplantation Surgery, University Hospital Zurich, Zurich, Switzerland, ²Institute for Biomedical Engineering, ETH and University Zurich, Zurich, Switzerland, ³Plastic Surgery and Hand Surgery, University Hospital Zurich, Zurich, Switzerland

MRI has been presented as a nondestructive *in vivo* readout to report perfusion capacity in biomaterials planted on the CAM in the living chick embryo *in ovo*. Perfusion capacity was assessed through changes in T₁ relaxation pre and post injection of a paramagnetic contrast agent, Gd-DOTA (Dotarem®, Guerbet S.A.). Hence local contrast agent concentration was dependent on perfusion, vascular permeability and extravascular compartment size. In the present study we explore intravascular SPIO particles of 30-40 nm size (FeraSpin series M, Viscover™, Miltenyi Biotec, Germany) that stay in the vasculature to deliver a more direct measure of vascularization.

2869

Computer #54



Influence of Linear and Non-linear Conversions of T1-weighted Signal Intensity to Gadolinium Concentration on Contrast Kinetic Model Parameters: A Simulation Study

Nicole Wake¹, Hersh Chandarana¹, Koji Fujimoto¹, Daniel K Sodickson¹, and Sungheon Gene Kim¹

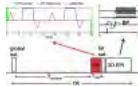
¹Bernard and Irene Schwartz Center for Biomedical Imaging, Center for Advanced Imaging Innovation and Research, Department of Radiology, New York University School of Medicine, New York, NY, United States

The purpose of this study was to assess the effect of linear and non-linear signal-to-concentration conversion methods on the estimation of contrast kinetic parameters in T₁-weighted dynamic contrast-enhanced MRI. A simulation study was conducted, using the

Generalized Kinetic Model with a population-based arterial input function, to compare the two conversion methods in terms of the uncertainty in contrast kinetic parameter estimation, influence by the error in the pre-contrast T1 value, and the effect of flip angle, one of the important scan parameters. The results provide useful information on how to interpret the results with the linear conversion method.

2870

Computer #55



Measurement of Absolute Cerebral Blood Volume using Velocity-Selective Pulse Trains
Feng Xu^{1,2} and Qin Qin^{1,2}

¹Radiology, Johns Hopkins University, Baltimore, MD, United States, ²F.M. Kirby Research Center for Functional Brain Imaging, Kennedy Krieger Institute, Baltimore, MD, United States

Current MRI techniques for quantification of absolute cerebral blood volume (CBV) are all contrast-based. To reduce associated risks and cost, we proposed a non-contrast-enhanced (NCE) MRI method using a velocity-selective (VS) spin labeling approach for CBV measurement at 3T. Gray matter CBV values across 5 subjects are 2.4 ± 0.2 mL/100g for blood flowing between the encoded cutoff velocities of 0.5cm/s and 3.1cm/s, with a GM/WM ratio of 1.9 ± 0.3 .

2871



Computer #56



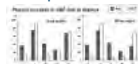
Pulmonary Perfusion using pseudo-Continuous Arterial Spin Labeling
Joshua S. Greer^{1,2}, Xinzeng Wang², Ivan Pedrosa^{2,3}, and Ananth J. Madhuranthakam^{2,3}

¹Bioengineering, University of Texas at Dallas, Richardson, TX, United States, ²Radiology, UT Southwestern Medical Center, Dallas, TX, United States, ³Advanced Imaging Research Center, UT Southwestern Medical Center, Dallas, TX, United States

Cardiac triggering is regularly used in arterial spin labeled (ASL) pulmonary perfusion imaging to minimize pulsatile flow effects. A cardiac-triggered pseudo-continuous ASL (pCASL) sequence was previously implemented to improve the SNR of lung perfusion, but was found to be sensitive to variations in heart rate due to the prolonged TR, causing the data acquisition to occasionally occur during systole. The purpose of this study was to investigate methods to reduce this cardiac cycle sensitivity in pulmonary perfusion images using pCASL, including cardiac triggering the acquisition and alternative readouts such as a projection acquisition.

2872

Computer #57



Comparison of pseudo-continuous arterial spin labeling with [15O]-water PET at baseline and after Diamox: a simultaneous PET-MRI study

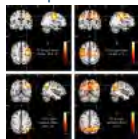
Audrey Fan¹, Praveen Gulaka¹, Mohammad Mehdi Khalighi², Bin Shen¹, Aileen Hoehne¹, Prachi Singh¹, Jun H Park¹, Dawn Holley¹, Frederick T Chin¹, and Greg Zaharchuk¹

¹Radiology, Stanford University, Stanford, CA, United States, ²Applied Science Lab, GE Healthcare, Menlo Park, CA, United States

The ability to noninvasively image cerebral blood flow (CBF) would help with assessment of many cerebrovascular disorders including stroke. We compared simultaneous PET-MRI measurements of CBF by arterial spin labeling MRI and the [15O]-water PET reference standard in healthy volunteers. ASL and PET revealed similar spatial distributions of perfusion in the brain and reliably detected CBF augmentation due to Diamox administration. ASL MRI also demonstrated lower scan-rescan coefficient of variation across the gray matter relative to PET. Going forward, we will perform kinetic modeling of absolute CBF from [15O]-water PET and consider potentially different radiotracer arterial input functions (derived from the PET-MRI images themselves) that occur in different brain perfusion states.

2873

Computer #58



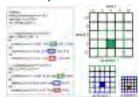
Improving ASL Perfusion MRI-based Functional Connectivity Analysis with Robust Principal Component Analysis
Ze Wang¹

¹Hangzhou Normal University, Hangzhou, China, People's Republic of

ASL perfusion fMRI has much less neurovascular effects than BOLD fMRI, but its application in time-series analysis is still depreciated due to the low signal-to-noise-ratio (SNR). Robust principal component analysis (RPCA) decomposing the original data into a smoothly varying low-rank component and a residual component with sparse signal. In this study, we used RPCA to denoise ASL MRI. Our results showed that RPCA can markedly increase the sensitivity of ASL MRI-based functional connectivity analysis.

2874

Computer #59



Reduction of motion artefacts in multi-shot 3D GRASE Arterial Spin Labelling using Autofocus

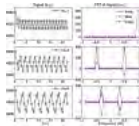
David L Thomas^{1,2}, Fabio Nery³, Isky Gordon³, Chris A Clark³, Sebastien Ourselin², Xavier Golay¹, David Atkinson⁴, and Enrico De Vita^{1,5}

¹Department of Brain Repair and Rehabilitation, UCL Institute of Neurology, London, United Kingdom, ²Translational Imaging Group, UCL, London, United Kingdom, ³Developmental Imaging and Biophysics Section, UCL Institute of Child Health, London, United Kingdom, ⁴Centre for Medical Imaging, UCL, London, United Kingdom, ⁵Lysholm Department of Neuroradiology, National Hospital for Neurology and Neurosurgery, London, United Kingdom

Multi-shot 3D acquisition schemes offer an efficient method to obtain ASL data with good SNR and spatial resolution. However, multi-shot techniques are susceptible to motion-induced artefacts that can severely degrade image quality. In this work, we investigate the use of the autofocus algorithm to correct k-space phase inconsistencies caused by inter-shot motion, and demonstrate its effectiveness at improving image sharpness and removing artefacts in motion-corrupted 3-shot 3D GRASE data. As such, autofocus offers a retrospective approach to improve the quality of multi-shot ASL data, with the associated improvements in CBF quantification accuracy and reproducibility.

2875

Computer #60



The potential of arterial spin labeling with full labeling duty cycle (FDC-ASL) to measure blood flow and transit delay simultaneously with substantially improved sensitivity and efficiency

Jia Guo¹, Richard B. Buxton¹, and Eric C. Wong^{1,2}

¹Radiology, UC San Diego, La Jolla, CA, United States, ²Psychiatry, UC San Diego, La Jolla, CA, United States

Pulsed arterial spin labeling (PASL) has the potential to achieve full labeling duty cycle with almost instant labeling. We explore here a new PASL-based fast labeling and imaging method for measuring blood flow (BF) and transit delay (TD) simultaneously, through a series of simulations. The results show that the BF and the TD can be accurately estimated. This new approach shows promise for substantially improved sensitivity and efficiency compared with conventional methods using PASL or pseudo-continuous ASL.

2876

Computer #61



CBF correction in vessel selective ASL perfusion using vessel selective MRA as a calibration

Bing Wu¹, Jianxun Qu¹, Ziyang Meng², and Zhenyu Zhou¹

¹GE healthcare MR Research China, Beijing, China, People's Republic of, ²Department of Precision Instrument, Tsinghua University, Beijing, China, People's Republic of

CBF quantification in territorial arterial spin labeling (tASL) is difficult in practice due to unknown labeling efficiency as compared to non-selective ASL perfusion. It is also difficult to derive this labeling efficiency based on perfusion map due to the irregular cerebral region and potential multi-vessel supply. In this work, tASL MRA is used as a reference scan to derive the needed labeling efficiency for correct derivation of the CBF quantification.

2877

Computer #62



ASL in the MriCloud: a platform-independent, installation-free tool for arterial-spin-labeling analysis

Peiyang Liu¹, Yue Li², Angelica Herrera³, Andreia Vasconcelos Faria¹, Can Ceritoglu⁴, Michael Miller⁴, Susumu Mori⁵, and Hanzhang Lu¹

¹Department of Radiology, Johns Hopkins University School of Medicine, Baltimore, MD, United States, ²AnatomyWorks, LLC, Baltimore, MD, United States, ³Department of Biomedical Engineering, Johns Hopkins University, Baltimore, MD, United States, ⁴Center for Imaging Science, Johns Hopkins University, Baltimore, MD, United States, ⁵Radiology, Johns Hopkins University School of Medicine, Baltimore, MD, United States

There has been a surging interest in using arterial spin labeling (ASL) MRI to measure cerebral perfusion. Current downloadable ASL analysis toolboxes are still primitive compared those for fMRI and DTI, and involves issues of software compatibility and computational burden. Here we describe a cloud-computing-based tool for comprehensive analysis of ASL-MRI. With this tool, the user can obtain CBF maps and ROI-averaged CBF values without having to install any software on the local computer. The maintenance of software upgrades will be performed by the developer. This tool may prove valuable and timely in accommodating the recent surging interest in ASL-MRI.

2878

Computer #63



Partial Volume Effects Correction for QUASAR ASL: A Spatially Regularised Approach

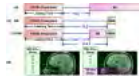
Moss Y Zhao¹, Egill Rostrup^{2,3}, Otto Mølby Henriksen³, and Michael A Chappell¹

¹Institute of Biomedical Engineering, University of Oxford, Oxford, United Kingdom, ²Functional Imaging Unit, Department of Clinical Physiology, Nuclear Medicine and PET, Copenhagen University Hospital Rigshospitalet Glostrup, Glostrup, Denmark, ³Department of Clinical Physiology, Nuclear Medicine and PET, Copenhagen University Hospital Rigshospitalet Blegdamsvej, Copenhagen, Denmark

The precise quantification of cerebral blood flow (CBF) using ASL MRI is affected by signal contaminations and partial volume (PV) effects. Among the numerous ASL techniques, QUASAR ASL exhibits unique characteristics of separating tissue and arterial blood components, allowing the bias from the arterial blood component being controlled. However, PV effects remain a critical issue that has not been fully addressed for QUASAR ASL. Here, we investigate a spatially regularised method to correct PV effects in QUASAR ASL using a three-component model. The results indicate that the proposed method preserves more spatial variations than the linear regression method.

2879

Computer #64



Time Efficient ASL Imaging with Segmented Multiband-acquisition (TEAISM)

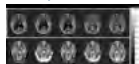
Xiufeng Li¹, Dingxin Wang^{1,2}, Edward J. Auerbach¹, Steen Moeller¹, Gregory J. Metzger¹, and Kamil Ugurbil¹

¹Center for Magnetic Resonance Research, University of Minnesota, Minneapolis, MN, United States, ²Siemens Medical Solutions USA Inc., Minneapolis, MN, United States

Recent studies have demonstrated the benefits of multi-band (MB) EPI for high-resolution whole brain PCASL imaging. However, the intrinsic nature of spatially interleaved simultaneous slice acquisition of MB-EPI requires a post-labeling delay larger than the longest arterial transit time in the brain, resulting in SNR efficiencies in the inferior or middle-inferior slices only comparable to or lower than those in SB-EPI PCASL imaging. To overcome the limitations of traditional MB-EPI and further improve SNR efficiencies of whole-brain high-resolution PCASL imaging, an alternative imaging acquisition strategy has been proposed and demonstrated: Time Efficient ASL Imaging with Segmented Multiband-acquisition (TEAISM).

2880

Computer #65



SCRUB: A Structural Correlation and Empirical Robust Bayesian Method for ASL Data

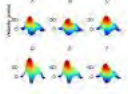
Sudipto Dolui^{1,2}, David A. Wolk², and John A. Detre^{1,2}

¹Department of Radiology, University of Pennsylvania, Philadelphia, PA, United States, ²Department of Neurology, University of Pennsylvania,

Philadelphia, PA, United States

We propose SCRUB, a data cleaning technique to improve cerebral blood flow (CBF) estimation based on arterial spin labeling (ASL) data. The method consists of (i) an outlier detection and removal stage and (ii) a subsequent voxel-wise empirical robust Bayesian estimation step. Compared to alternative options, SCRUB provided (i) better retest agreement between CBF values obtained from ASL scans of elderly Controls in ADNI database acquired 3 months apart, and (ii) better discrimination between Controls and patients with Alzheimer's disease (AD) based on CBF values in several regions of interest which are sensitive to AD related changes.

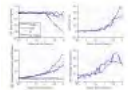
2881 Computer #66 Time Varying Velocity Labeling Efficiency Correction in Arterial Spin Labeling
Adam Bush¹, Yaqing Chia², Julie Coloigner², Thomas Coates³, Natasha Lepore⁴, and John Wood¹



¹Biomedical Engineering/ Cardiology, University of Southern California/ Children's Hospital Los Angeles, Los Angeles, CA, United States, ²Cardiology, Children's Hospital Los Angeles, Los Angeles, CA, United States, ³Hematology, Children's Hospital Los Angeles, Los Angeles, CA, United States, ⁴Children's Hospital Los Angeles, Los Angeles, CA, United States

In this study we propose a time varying correction technique for pseudo continuous arterial spin labeling efficiency. We compare this correction method to other correction methods and phase contrast MRI.

2882 Computer #67 A Theoretical Comparison of Multi-Delay Arterial Spin Labeling Methods
Joseph G Woods¹, Michael A Chappell², and Thomas W Okell¹



¹FMRI Centre, NDCN, University of Oxford, Oxford, United Kingdom, ²Institute of Biomedical Engineering, University of Oxford, Oxford, United Kingdom

This study aims to investigate the ideal labeling and delay parameters for single-delay, multi-delay and time-encoded pCASL and compare their theoretical performance in cerebral blood flow (CBF) and bolus arrival time (BAT) estimation under realistic noise levels over two BAT ranges: healthy (500ms-1500ms) and disease (500ms-3000ms).

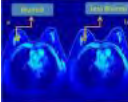
2883 Computer #68 Effect of labeling position on MT effects and Bolus Arrival Time
Marta Vidorreta^{1,2}, Yulin V Chang², and John A Detre^{1,2}



¹Neurology, University of Pennsylvania, Philadelphia, PA, United States, ²Radiology, University of Pennsylvania, Philadelphia, PA, United States

The effects of labeling location were assessed in pseudo-continuous ASL by performing kinetic modeling of data acquired at multiple post-labeling delays and by assessing the ratio of mean ASL intensity to M0. Labeling location differences resulted in significant MT effects on raw ASL data, and produced nonlinear effects on bolus arrival time across vascular distributions.

2884 Computer #69 Pharmacokinetic modeling driven Rapid Adaptive Spatio-Temporal Resolution for Accelerated (RASTRA) DCE-MRI
Rashmi Reddy¹, Imam Shaik¹, Nithin N Vajuvalli¹, Dharmendra Kumar K C¹, and Sairam Geethanath¹



¹Dayananda Sagar Institutions, Bangalore, India

The proposed method combines Compressed Sensing (CS) framework with view sharing to accelerate Dynamic Contrast Enhanced Magnetic Resonance Imaging (DCEMRI). A novel method to combine k-spaces of different regions (Temporal Region (TR) and Spatial Region (SR)) is carried out in this work. View sharing is adapted to combine the kspace, by mapping samples from SR region frames onto corresponding frames in TR region to improve the edge information, achieving better reconstruction with higher acceleration. It is shown that the proposed method provides better Pharmacokinetic(PK) maps at higher acceleration rates than existing methods with minimum error, as qualified by NRMSE values.

2885 Computer #70 A simple and low cost Dynamic contrast enhancement MRI perfusion phantom
Nithin N Vajuvalli¹, Amaresh Konar¹, Shivaprasad Ashok Chikop¹, Darshan S Keelara¹, Ashwini Kumnoor¹, and Sairam Geethanath¹



¹Medical Imaging Research Centre, Dayananda Sagar Institutions, Bangalore, India

DCE MRI technique is widely used in tissue characterization and tissue perfusion. Current work focuses on the design and development of a low cost in vivo DCE phantom for providing a reference standard for quantitative validation and the ability to generate Signal Intensity curves similar to arterial input functions. Poly vinyl Alcohol material was used in the phantom to mimic tissue perfusion characteristics and obtain signal intensity curves for different flow rates. We obtained similar curves compared to Arterial Input Function and were able to control flow rates through different tube and pore sizes.

2886 Computer #71 A Correlation Study between DCE-MRI Quantitative Parameters and Immunohistochemical Labeling Indices in Nasopharyngeal Carcinoma



Yunbin Chen¹, Meng Liu², Dechun Zheng¹, Qiuyuan Yue¹, Xiaoxiao Zhang¹, Hao Lin¹, Weibo Chen³, Queenie Chan⁴, Wang Ren¹, and Xiangyi Liu¹

¹Fujian Provincial Cancer hospital, Fuzhou, China, People's Republic of, ²Fujian Provincial Cancer Hospital, Fuzhou, China, People's Republic of, ³Philips Healthcare, Shanghai, China, People's Republic of, ⁴Philips Healthcare, Hong Kong, China, People's Republic of

We assessed correlations between DCE-MRI quantitative parameters with immunohistochemical labeling indices which reflect tumor hypoxia (HIF-1 α), tumor angiogenesis (VEGF, MVD) and tumor proliferation (Ki67) in nasopharyngeal carcinoma(NPC). We found that HIF-1 α positive group was significantly correlated with VEGF positive expression and MVD count respectively. K^{trans} and K_{ep} was positively associated with HIF-1 α positive expression, VEGF positive expression and MVD respectively. There were significantly positive correlations between vp and the VEGF expression, MVD count respectively. However, there were no significant relationship between the Ki67 expression and any DCE-MRI quantitative parameters in our study.

2887

Computer #72



The effect of blood brain barrier disruption on the cerebral blood flow measurement with dynamic susceptibility contrast MRI: Comparison study between SPION and Gd-DOTA
SEOKHAJIN¹ and HyungJoon Cho²

¹UNIST, Ulsan, Korea, Republic of, ²Ulsan, Korea, Republic of

Dynamic susceptibility contrast MRI (DSC MRI) is widely used for cerebral blood flow (CBF) measurement for diseases, such as stroke and cancer.¹⁻² Fundamental assumption of DSC-MRI based CBF measurement is that contrast agent is non-leaking with intact blood brain barrier (BBB).³ Here, we investigate the effect of BBB disruption on the CBF measurement, especially for stroke model utilizing serial dual acquisitions using DOTAREM and SPION. As SPION remains as intravascular agent, while DOTAREM becomes extravasating agent with BBB disruption, dual CBF acquisitions with both agents provide quantitative way to characterize the effect of BBB disruption on CBF measurements with DSC-MRI.

Electronic Poster

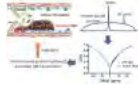
CEST & MT

Exhibition Hall

Monday, May 9, 2016: 14:15 - 15:15

2888

Computer #73



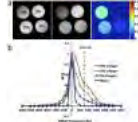
Staging deep vein thrombosis using quantitative Magnetization Transfer
Huanling Liu^{1,2}, Wenbo Li^{1,3}, Yuguo Li^{1,3}, Dexiang Liu^{1,2}, Hanwei Chen^{2,3}, Peter C.M Van Zijl^{1,3}, and Guanshu Liu^{1,3}

¹F.M. Kirby Research Center for Functional Brain Imaging, Kennedy Krieger Institute, Baltimore, MD, United States, ²Department of Radiology, Guangzhou Panyu Central Hospital, Guangzhou, China, People's Republic of, ³The Russell H. Morgan Department of Radiology and Radiological Science, Division of MR Research, Johns Hopkins University School of Medicine, Baltimore, MD, United States

There is an urgent need for a quantitative imaging technique that can stage deep vein thrombosis (DVT) and guide thrombolysis treatment. In the present study, we explored the ability of quantitative Magnetization transfer (qMT) technique as a non-invasive means to stage thrombi based on their macromolecular content. Thrombi in the inferior vena cava were formed using a Mouse Complete Stasis Model. A two-pool MT mathematical model was adapted to fit high-resolution MT data of excised thrombi samples. The results clearly showed that bound proton fraction (BPF) is a useful parameter for distinguishing aged blood clots from freshly formed ones.

2889

Computer #74



Noninvasive Assessment of Renal Fibrosis Using Magnetization Transfer MRI in Murine Renal Artery Stenosis
Kai Jiang¹, Christopher M. Ferguson¹, Behzad Ebrahimi¹, Hui Tang¹, Timothy L. Kline², Prassana K. Mishra³, Joseph P. Grande⁴, Slobodan I. Macura³, and Lilach O. Lerman¹

¹Division of Nephrology and Hypertension, Mayo Clinic, Rochester, MN, United States, ²Department of Radiology, Mayo Clinic, Rochester, MN, United States, ³Department of Biochemistry and Molecular Biology, Mayo Clinic, Rochester, MN, United States, ⁴Department of Laboratory Medicine and Pathology, Mayo Clinic, Rochester, MN, United States

In this study, magnetization transfer was used to measure renal fibrosis in a murine model of renal artery stenosis. A collagen phantom study was performed to optimize the irradiation-offset frequency of MT pulses. Renal fibrosis by *in vivo* MT and *ex vivo* histology or hydroxyproline assay showed a good correlation, suggesting that MT could be used to assess renal fibrosis. In addition, MT successfully captured the physiological changes at different stages of renal fibrosis, indicating that MT was capable of monitoring the longitudinal development of functionally significant renal fibrosis.

2890

Computer #75



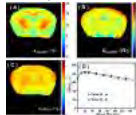
Increasing the inhomogeneous magnetization transfer (ihMT) signal in vivo with high amplitude, low duty cycle irradiation
Gopal Varma¹, Olivier M Girard², Valentin H Prevost², Guillaume Duhamel², and David C Alsop¹

¹Radiology, Division of MR Research, Beth Israel Deaconess Medical Center, Harvard Medical School, Boston, MA, United States, ²CRMBM-CEMEREM UMR 7339, CNRS-AMU, Aix Marseille Université, Marseille, France

High power, off-resonance irradiation as utilized in ihMT/MT can saturate pools of bound magnetization before they exchange in tissues. Observation of such saturation phenomena is limited by power constraints in-vivo and by attenuation of the free pool magnetization. A technique for studying and enhancing saturation effects using relatively short bursts of higher power irradiation is evaluated. The results provided 2-5 fold increases in ihMTR (depending on average power and offset frequency). Such short duration, high power pulses offer a new window to probe exchange kinetics and dipolar order effects, as well as enhancing the quality and feasibility of ihMT imaging.

2891

Computer #76



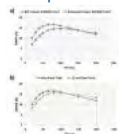
On-resonance Variable Delay Multi Pulse Scheme for Imaging of Fast-exchanging Protons and semi-solid Macromolecules
Jiadi Xu^{1,2}, kannie W. Y. Chan^{1,2}, Xiang Xu², Nibhay Yadav^{1,2}, Guanshu Liu^{1,2}, and Peter C. M. van Zijl^{1,2}

¹F. M. Kirby Center, Kennedy Krieger Institute, Baltimore, MD, United States, ²Russell H. Morgan Department of Radiology and Radiological Science, Johns Hopkins University School of Medicine, Baltimore, MD, United States

An on-resonance variable delay multi-pulse (onVDMP) scheme was developed for separation and quantification of magnetization transfer contrast (MTC) and total fast-exchanging protons (TFP) contributions. Phantom studies of glucose, bovine serum albumin (BSA) and hair conditioner show the capability of onVDMP to separate out exchangeable protons with different exchange rates by their unique signal buildup curves. Quantitative MTC and TFP maps acquired on healthy mouse brains showed strong gray/white matter contrast for the slowly transferring MTC protons while the TFP map was more uniform across the brain.

2892

Computer #77



Theoretical and Experimental Optimization of a 3D Steady-State Inhomogeneous Magnetization Transfer (ihMT) Gradient Echo Sequence: Boosting the ihMT Sensitivity with Sparse Energy Deposition

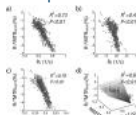
Olivier M. Girard^{1,2}, Gopal Varma³, Samira Mchinda^{1,2}, Valentin Prevost^{1,2}, Arnaud Le Troter^{1,2}, Stanislas Rapacchi^{1,2}, Maxime Guye^{1,2}, Jean-Philippe Ranjeva^{1,2}, David C. Alsop³, and Guillaume Duhamel^{1,2}

¹CRMBM, UMR 7339 CNRS, Aix-Marseille University, Marseille, France, ²Pôle d'Imagerie Médicale, CEMEREM, APHM, Marseille, France, ³Radiology, Division of MR Research, Beth Israel Deaconess Medical Center, Harvard Medical School, Boston, MA, United States

Inhomogeneous Magnetization Transfer (ihMT) has shown improved specificity for myelinated tissue as compared to conventional MT. Recently, fundamental developments have led to theoretical modeling of the ihMT effect. In this study forward modeling of a steady-state ihMT gradient echo (GRE) sequence is used to guide experimental optimization for various TRs, power levels and ihMT pulse-train duration. An efficient RF-energy deposition scheme is demonstrated for relatively long TRs, leading to ihMTRs as high as 15-17% and 10-12% in WM at 1.5T and 3T, respectively. This opens new perspectives for patient studies at clinical field strength and ihMT implementation at higher field strength.

2893

Computer #78



Stratification of graded acute stroke metabolic injury with magnetization transfer and relaxation-normalized amide proton transfer (MRAPT) pH-weighted MRI

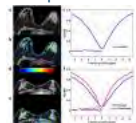
Phillip Zhe Sun¹, Yingkun Guo^{1,2}, Iris Yuwen Zhou¹, Suk-Tak Chan¹, Yu Wang³, Emiri Mandeville⁴, Eng H Lo⁴, and Xunming Ji³

¹Athinoula A. Martinos Center for Biomedical Imaging, Department of Radiology, Massachusetts General Hospital and Harvard Medical School, Charlestown, MA, United States, ²Department of Radiology, Key Laboratory of Obstetric & Gynecologic and Pediatric Diseases and Birth Defects of Ministry of Education, West China Second University Hospital, Sichuan University, Chengdu, China, People's Republic of, ³Cerebrovascular Diseases Research Institute, Xuanwu Hospital of Capital Medical University, Beijing, China, People's Republic of, ⁴Neuroprotection Research Laboratory, Department of Radiology and Neurology, Massachusetts General Hospital and Harvard Medical School, Charlestown, MA, United States

Amide proton transfer (APT) MRI probes amide protons from endogenous proteins/peptides, which has shown promising results in defining tissue acidosis. pH MRI complements perfusion and diffusion MRI for enhanced stratification of heterogeneous ischemic tissue injury. However, the endogenous APT effect depends not only on pH but also on tissue water content, MRI relaxation rates, and experimental conditions. There are also concomitant RF irradiation effects including direct RF saturation, magnetization transfer and nuclear overhauser effects (NOE). Our study evaluated magnetization transfer and relaxation-normalized APT (MRAPT) MRI in an animal model of acute ischemic stroke that enabled semiautomatic segmentation of graded ischemic tissue injury.

2894

Computer #79



CEST-mDixon for Breast Lesion Characterization at 3T

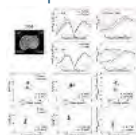
Shu Zhang¹, Stephen Seiler¹, Ananth Madhuranthakam^{1,2}, Jochen Keupp³, Ivan E Dimitrov^{2,4}, Robert E Lenkinski^{1,2}, and Elena Vinogradov^{1,2}

¹Radiology, UT Southwestern Medical Center, Dallas, TX, United States, ²Advanced Imaging Research Center, UT Southwestern Medical Center, Dallas, TX, United States, ³Philips Research, Hamburg, Germany, ⁴Philips Medical Systems, Cleveland, OH, United States

In this work, the feasibility of mDixon-based CEST-MRI for breast lesions characterization at 3T was explored. The mDixon technique was used to acquire pure water CEST images without fat contamination. The B_0 maps derived from mDixon technique were used for field inhomogeneity correction. Human studies demonstrated marked differences in MTR_{asym} between malignant and healthy tissue in hydroxyl range (0.8-1.8 ppm) and amide range (3.1-4.1 ppm). In addition, the width of the Z-spectrum was reduced in malignant vs healthy breast tissue. The results suggest that the CEST-mDixon has the potential as a robust detection and characterization tool of breast malignancy.

2895

Computer #80



Identification of the Origin for Amide Proton Transfer (APT) Imaging Signals in Multiple Pathologies

Dong-Hoon Lee¹, Hye-Young Heo¹, Yi Zhang¹, Shanshan Jiang¹, and Jinyuan Zhou¹

¹Department of Radiology, Johns Hopkins University School of Medicine, Baltimore, MD, United States

APT imaging can provide endogenous contrast related to the mobile amide proton concentration, amide proton exchange rate (depending on tissue pH), and other tissue and experimental parameters. Here, based on the correlations between quantified APT signals and combined parameter of water proton concentration and water T_1 (T_{1w} [water proton]), we attempted to reveal the origin for APT imaging signals in multiple disease models. The results showed no significant correlations between APT signals and the T_{1w} [water proton]. Our findings clearly indicated that the APT signals is primarily related to the mobile amide proton concentration and amide

2896

Computer #81



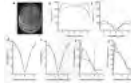
B0-calibrated and motion-registered dynamic CEST MRI of muscles undergoing exercise

Alessandro M Scotti^{1,2,3}, Rong-Wen Tain^{1,3}, Xiaohong Joe Zhou^{1,2,3}, and Kejia Cai^{1,3}¹Radiology, University of Illinois, Chicago, IL, United States, ²Bioengineering, University of Illinois, Chicago, IL, United States, ³Center for MR Research, University of Illinois, Chicago, IL, United States

Artifacts arising from tissue motion and static field inhomogeneities can heavily impact the measurement of metabolites concentration in CEST-MRI experiments in vivo. We present a correction strategy applied to CEST-MRI of creatine concentration during muscle exercise. Corrections consisted in image registration by means of a demons algorithm and signal calibration over static field offsets map at baseline, without the need of additional scanning. After correction, results are in accord with conventionally corrected data and published results. This method is shown to be effective in dynamic studies, where a high temporal resolution and coverage is required.

2897

Computer #82



Localized, gradient-reversed ultrafast z-spectroscopy in vivo at 7T

Neil Wilson¹, Kevin D'Aquila¹, Catherine Debrosse¹, Hari Hariharan¹, and Ravinder Reddy¹¹Department of Radiology, Center for Magnetic Resonance and Optical Imaging (CMROI), University of Pennsylvania, Philadelphia, PA, United States

Ultrafast z-spectroscopy can be collected by saturating the nuclear spins with an RF pulse in the presence of a gradient, effectively encoding the offset frequency spatially across a voxel and allowing full z-spectra to be collected in a single shot. When asymmetry analysis is applied, frequencies on one physical side of the voxel are compared with those on the other physical side. This can be a problem if there is inhomogeneity or partial voluming. By acquiring an additional z-spectrum with the gradient polarity reversed, mixed z-spectra can be created in which the positive and negative offset frequencies come from the same side of the voxel. This method is more robust to inhomogeneity and partial voluming typically found in vivo as demonstrated here with studies on 7T in human brain.

2898

Computer #83



Can CEST be used as biomarker in Huntington's disease?

Marilena Rega^{1,2}, James Fairney¹, Francisco Torrealdea^{1,3}, Blair Leavitt⁴, Rachel Schahill¹, Raymund Roos⁵, Bernhard Landwehrmeyer⁶, Beth Borowsky⁷, Sarah Tabrizi¹, and Xavier Golay¹¹Institute of Neurology, University College London, London, United Kingdom, ²Medical Physics, University College London Hospital, London, United Kingdom, ³Center of Medical Imaging, University College London, London, United Kingdom, ⁴Department of Medical Genetics, University of British Columbia, Vancouver, BC, Canada, ⁵Department of Neurology, University Medical Center, Leiden, United Kingdom, ⁶Department of Neurology, Ulm University, Ulm, Germany, ⁷HighQ foundation, CHDI, New York, NY, United States

Huntington's is a hereditary disease caused by the HTT gene, resulting in the aggregation of mutant huntingtin in the cytoplasm. CEST, known to be affected by protein concentration and structure, was considered a potential biomarker for a clinical trial and comparison with MT, T1 and T2 relaxometry. Data were acquired in n=54 HD patients and n=46 healthy individuals. Comparison of CEST revealed significant differences (p<0.05) in the putamen and globus pallidus regions which did not correlate with any changes in relaxometry or MT, suggesting that CEST might be able to provide additional contrast to the already existing methods.

2899

Computer #84



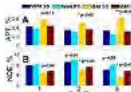
Imaging the pH by means of CEST-responsive iopamidol: normal and AKI model studies

Wei Hu¹, Zhuozhi Dai¹, Zhiwei Shen¹, Yuanyu Shen¹, Xiangyong Tang¹, Zhiyan Zhang¹, Gang Xiao², Phillip Zhe Sun³, and Renhua Wu¹¹2nd Affiliated Hospital, Shantou University Medical College, Shantou, China, People's Republic of, ²Hanshan Normal University, Chaozhou, China, People's Republic of, ³Massachusetts General Hospital and Harvard Medical School, Charlestown, MA, United States

The promising imaging technique of chemical exchange saturation transfer (CEST) MRI, which is sensitive to microenvironment properties including pH, metabolites, temperature, metal ions, and enzymatic activities, has been increasingly applied in vivo such as acute ischemia, infection and cancer. The aim of this work was to observe the differentiation between normal and acute kidney injury (AKI) using echo-planar imaging sequence (EPI) as well as the sensitive ratiometric methods under 7T magnetic field.

2900

Computer #85



Comparison of 3D CEST acquisition schemes: steady state versus pseudo-steady state

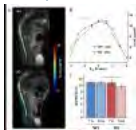
Vitaliy Khlebnikov¹, Nicolas Geades², Dennis WJ Klomp¹, Hans Hoogduin¹, Penny Gowland², and Olivier Mougin²¹Radiology, University Medical Center Utrecht, Utrecht, Netherlands, ²Sir Peter Mansfield Imaging Centre, University of Nottingham, Nottingham, Nottinghamshire, United Kingdom, Nottingham, United Kingdom

Chemical Exchange Saturation Transfer (CEST) has gained much popularity due to its unmatched sensitivity to dilute labile protons when compared to other MRI techniques. Of particular interest are two CEST effects: Amide Proton Transfer (APT, CEST of amides) and Nuclear Overhauser Enhancement (NOE). Fast-paced developments for CEST resulted in the design of multiple CEST imaging sequences. This raises the obvious question as to which sequence to use and in what particular applications. Two pulsed volumetric CEST acquisition schemes are currently available in the literature. The first is based on the standard Magnetization Transfer imaging technique: a steady-state (SS) acquisition with alternating brief saturation and image acquisition. The second is based on the preparation of the magnetization before a long readout, where the prolonged saturation reaches a pseudo-steady state (PS) before the image acquisition. In this report, these two CEST acquisition schemes, optimized for maximum sensitivity to APT and NOE effects

through Bloch-McConnell simulations, were systematically compared for the same spatial resolution, brain coverage and scan time.

2901

Computer #86



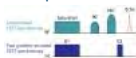
GluCEST imaging of spinal cord in a mouse model of Friedreich ataxia
Jérémy Pépin^{1,2}, Françoise Piguet^{3,4,5,6}, Hélène Puccio^{3,4,5,6}, and Julien Flament^{1,7}

¹CEA/DSV/I2BM/MIRcen, Fontenay-aux-Roses, France, ²CNRS Université Paris-Saclay UMR 9199, Fontenay-aux-Roses, France, ³Department of Translational Medicine and Neurogenetics, Institut de Génétique et de Biologie Moléculaire et Cellulaire, Illkirch, France, ⁴INSERM U596, Illkirch, France, ⁵CNRS UMR7104, Illkirch, France, ⁶Université de Strasbourg, Strasbourg, France, ⁷INSERM UMS 27, Fontenay-aux-Roses, France

Friedreich Ataxia (FA) is the most common form of recessive inherited ataxia which induces severe neurological disabilities and reduced life expectancy. As glutamate has been shown to be a potential biomarker of neurodegenerative diseases, we used Chemical Exchange Saturation Transfer imaging of glutamate (gluCEST) in order to characterize our mouse model of FA and to monitor glutamate alterations in the spinal cord. GluCEST images revealed decrease of glutamate level in FA mouse model compared to control littermates, especially in the lumbar part. These results demonstrate the potential of gluCEST in providing innovative and relevant biomarkers of FA.

2902

Computer #87



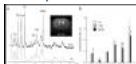
Tissue Characterization with Fast High Resolution Magic Angle Spinning (HRMAS) CEST Spectroscopy
Iris Yuwen Zhou¹, Taylor Fuss^{1,2}, Gang Xiao³, Takahiro Igarashi¹, Lin Li¹, Leo L. Cheng^{1,2}, and Phillip Zhe Sun¹

¹Athinoula A. Martinos Center for Biomedical Imaging, Department of Radiology, Massachusetts General Hospital and Harvard Medical School, Charlestown, MA, United States, ²Department of Pathology, Massachusetts General Hospital and Harvard Medical School, Boston, MA, United States, ³Department of Mathematics and Statistics, Hanshan Normal University, Chaozhou, China, People's Republic of

Z-spectrum is conventionally acquired through multiple experiments with selective saturation at different frequency offsets of interest, leading to extreme long acquisition time. Here, we employ gradient-encoding to substantially accelerate the acquisition of Z-spectrum. This speedup in combination with higher spectral resolution provided by high resolution magic angle spinning (HRMAS) allows rapid quantification of chemical exchange rates of CEST agents, monitoring dynamic processes and fast tissue characterization. The approach was validated in phantom and used for characterization of brain tissues after ischemic stroke.

2903

Computer #88



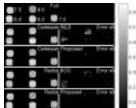
GluCEST imaging: a relevant biomarker of Huntington's disease.
Jérémy Pépin^{1,2}, Laetitia Francelle^{1,2}, Maria-Angeles Carillo-de Sauvage^{1,2}, Huu Phuc Nguyen^{3,4}, Nicole El Massioui^{5,6}, Valérie Doyère^{5,6}, Emmanuel Brouillet^{1,2}, and Julien Flament^{1,7}

¹CEA/DSV/I2BM/MIRcen, Fontenay-aux-Roses, France, ²CNRS Université Paris-Saclay UMR 9199, Fontenay-aux-Roses, France, ³Institute of Medical Genetics and Applied Genomics, University of Tuebingen, Tuebingen, Germany, ⁴Centre for Rare Diseases, University of Tuebingen, Tuebingen, Germany, ⁵Paris-Saclay Institute of Neuroscience, Université Paris-Sud, UMR 9197, Orsay, France, ⁶Centre National de la Recherche Scientifique, Orsay, France, ⁷INSERM UMS 27, Fontenay-aux-Roses, France

Huntington's disease (HD) is an inherited neurodegenerative disease characterized by motor, cognitive and psychiatric symptoms. As glutamate has been shown to be a potential biomarker of neurodegenerative diseases, we used Chemical Exchange Saturation Transfer imaging of glutamate (gluCEST) to map cerebral glutamate distribution in mouse and rat models of HD. A decrease of [Glu] was measured in the striatum by MRS and gluCEST. In addition, good spatial resolution of gluCEST over MRS allowed identification of other afflicted brain regions such as corpus callosum. These results demonstrate the potential of gluCEST in providing relevant biomarkers of HD in the whole brain.

2904

Computer #89



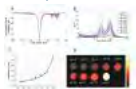
Accelerating CEST Imaging with Spatial-Temporal Sparse Dictionary Learning
Huajun She¹, Bian Li¹, Robert Lenkinski¹, and Elena Vinogradov¹

¹Radiology, Advanced Imaging Research Center, UT Southwestern Medical Center, Dallas, TX, United States

This work investigates accelerating CEST imaging. The original blind compressive sensing method assumes that a few functions are enough to represent the dynamic behavior, and the coefficient matrix should be sparse. In CEST imaging, z-spectrum shows group sparsity in the same compartment. So not only the coefficients matrix is sparse but also the transformation of the coefficients matrix is sparse, such as total variation and wavelets. The proposed method addresses this prior information and further improves the original BCS method, demonstrating a better estimation of the CEST effect at high reduction factors for both Cartesian and radial sampling patterns.

2905

Computer #90



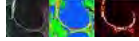
Use of Yb-HPDO3A probe for CEST-MRI pH mapping in glioblastoma mouse models
Giuseppe Ferrauto¹, Michel Sarraf², Enza Di Gregorio¹, Vincent Aboiroux³, Ulysse Gimenez², François Berger², Silvio Aime¹, and Hana Lahrech²

¹Dept of Molecular Biotechnologies & Health Sciences, University of TORINO (IT), Torino, Italy, ²CLINATEC-CEA-INSERM UA01 - CHU -UJF Grenoble (FR), Grenoble, France, ³CLINATEC-CEA Grenoble (FR), Grenoble, France

MRI maps of extracellular/extravascular pH distribution in glioblastoma mouse model (U87 cells) have been obtained by administrating YbHPDO3A CEST probe. This molecule has potential in a clinical setting as it displays analogue properties (stability and in vivo pharmacokinetic) of its analogue clinically approved Gd-HPDO3A (ProHance). Furthermore, glioblastoma pH maps have been correlated with histology (H/E, Hif-1a and Ki-67 staining). The assessment of glioblastoma pH could be used to monitor tumor development and to target acidic tumor regions using innovative responsive pH therapies.

2906

Computer #91



Comparison of gagCEST and sodium MRI in evaluating knee cartilage in vivo at 7 Tesla

Vladimir Mlynarik^{1,2}, Stefan Zbyn¹, Markus Schreiner³, Vladimir Juras¹, Pavol Szomolanyi¹, Didier Laurent⁴, and Siegfried Trattnig^{1,2}

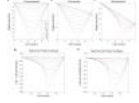
¹Department of Biomedical Imaging and Image-Guided Therapy, High Field MR Center, Medical University of Vienna, Vienna, Austria, ²CD Laboratory for Clinical Molecular MR Imaging, Vienna, Austria, ³Department of Orthopedic Surgery, Medical University of Vienna, Vienna, Austria, ⁴Novartis Institutes for Biomedical Research, Basel, Switzerland

There are several methodological and data processing issues in gagCEST, which complicate the translation of this method into clinical practice. For assessing performance of the gagCEST protocol optimized in our laboratory, corrected signal intensities from sodium images were used as a reference. The results demonstrate a good correlation between both methods, although the small magnitude of the gagCEST effect and the low resolution in sodium images require carefully optimized methodology and long measurement times. It can be concluded that the gagCEST method can be useful in evaluating early degeneration of articular cartilage at 7 Tesla.

2907



Computer #92



Chemical shift artifact of the third kind: Implications for gradient-echo based contrast enhanced imaging

Jamal J. Derakhshan¹, Elizabeth S. McDonald², Evan S. Siegelman³, Mitchell D. Schnall³, and Felix W. Wehrli⁴

¹Radiology, Hospital of the University of Pennsylvania, Philadelphia, PA, United States, ²Radiology, Breast Imaging Division, Hospital of the University of Pennsylvania, Philadelphia, PA, United States, ³Radiology, Abdominal Imaging Division, Hospital of the University of Pennsylvania, Philadelphia, PA, United States, ⁴Radiology, University of Pennsylvania, Philadelphia, PA, United States

A common subtraction band artifact in breast MRI was not understood, causing reduced confidence in clinical interpretation. The source of the artifact is shown to be a subtle chemical shift effect between fat and water in the presence of contrast enhancement. The phenomenon is now generalized and characterized at all off-resonance angles. Strong echo-time and fat signal dependence may lead to enhancement errors as a function of scanner hardware, field strength and fat suppression limitations. A time and SNR-equivalent in-phase VIBE sequence eliminates the artifact; gradient-echo based contrast enhanced imaging can be performed to eliminate these important potential pitfalls.

2908

Computer #93



Fixed Angle Single Rotation CEST (FASR-CEST) sequence for reducing saturation time

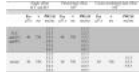
Yi Wang¹, Yang Fan², Bing Wu², and Jia-Hong Gao¹

¹School of Physics, Peking University, Beijing, China, People's Republic of, ²MR Research Group, GE Healthcare China, Beijing, China, People's Republic of

In CEST imaging, when saturation time is not sufficient long (empirically smaller than 0.8s), rotation effect would appear and contaminate with saturation effect, making the signal unavailable for further analysis. Considering the inhomogeneity of B_0 and B_1 in reality, we propose a novel Fixed Angle Single Rotation CEST (FASR-CEST) sequence to overcome the restriction, successfully reducing the saturation time to about 0.5s while keeping identical effect as CEST sequence with long saturation time, with the help of analytical calibration method in another abstract. Effect of the sequence is verified with *in vitro* and *in vivo* data.

2909

Computer #94



T1D-w ihMT: Dipolar Relaxation time weighted imaging using inhomogeneous Magnetization Transfer

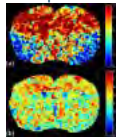
Guillaume Duhamel¹, Valentin H Prevost¹, Gopal Varma², David C Alsop², and Olivier M Girard¹

¹CRMBM / CNRS 7339, Aix Marseille University, Marseille, France, ²Radiology, Division of MR Research, Beth Israel Deaconess Medical Center, Harvard Medical School, Boston, MA, United States

The inclusion of a dipolar reservoir in the existing two pool model for MT allowed interpreting the inhomogeneous MT (ihMT) signal as a dipolar order effect -characterized by a relaxation time T_{1D} - within motion restricted molecules. In this study, we demonstrate that an ihMT signal can actually be evidenced in any component with non-trivial T_{1D} value. Adjustment of the dual frequency irradiation efficiency by increase of Δt , the repetition rate of consecutive saturation pulses, filters the signal of shorter T_{1D} components. This provides a means to realize T_{1D} -weighted imaging, a new source of MR contrast between tissues.

2910

Computer #95



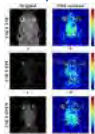
Improvement of in vivo glucoCEST imaging in rat brain using inverse z-spectrum analytical scheme at 7.0 T

Ping-Huei Tsai^{1,2,3}, Hua-Shan Liu^{4,5}, Fei-Ting Hsu⁶, Yu-Chieh Kao³, Chia-Feng Lu³, Li-Chun Hsieh², Pen-Yuan Liao², Hsiao-Wen Chung⁷, and Cheng-Yu Chen^{1,2,3}

¹Department of Radiology, School of Medicine, College of Medicine, Taipei Medical University, Taipei, Taiwan, ²Department of Medical Imaging, Taipei Medical University Hospital, Taipei Medical University, Taipei, Taiwan, ³Translational Imaging Research Center, Taipei Medical University, Taipei, Taiwan, ⁴Graduate Institute of Clinical Medicine, Taipei Medical University, Taipei, Taiwan, ⁵Department of Medical Imaging, Taipei Medical University Hospital, Taipei, Taiwan, ⁶Taipei Medical University Hospital, Taipei Medical University, Taipei, Taiwan, ⁷Graduate Institute of Biomedical Electronics and Bioinformatics, National Taiwan University, Taipei, Taiwan

GlucoCEST have been proposed to assess the discrepant concentrations of glucose *in vitro*. However, it is still a challenge to obtain accurate signals from glucose *in vivo*. Our preliminary finding demonstrated that the proposed analytical scheme provides an alternative to extract glucose profile and could be more robust to the field inhomogeneity, which may be helpful in further implementation in disease models.

2911 Computer #96 A fast chemical exchange saturation transfer imaging scheme based on spatiotemporal encoding
Jianpan Huang¹, Miao Zhang¹, Shuhui Cai¹, Congbo Cai², Lin Chen¹, and Ting Zhang¹



¹Department of Electronic Science, Xiamen University, Xiamen, China, People's Republic of, ²Department of Communication Engineering, Xiamen University, Xiamen, China, People's Republic of

Chemical exchange saturation transfer (CEST) is widely exploited in magnetic resonance imaging (MRI) because of its special quantitative contrast mechanisms. To overcome the long acquisition time required by fast spin-echo multi-slice imaging and alleviate the sensitivity to field inhomogeneity and chemical shift effects appeared in echo planar imaging, we proposed a CEST imaging scheme based on spatiotemporally encoded magnetic resonance imaging (SPEN MRI). Experimental results validated the feasibility and capability of the new scheme.

Electronic Poster

Pulmonary, Mediastinum & Hyperpolarized Gas MRI

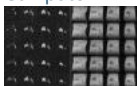
Exhibition Hall

Monday, May 9, 2016: 15:15 - 16:15

2912



Computer #1



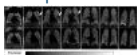
Ventilation imaging with sulfur hexafluoride in free-breathing mice: initial experience
Marta Tibiletti¹, Martin Tschecne¹, Andrea Bianchi², Detlef Stiller², and Volker Rasche^{1,3}

¹Core Facility Small Animal MRI, Ulm University, Ulm, Germany, ²Target Discovery Research, In-vivo imaging laboratory, Boehringer Ingelheim Pharma GmbH & Co. KG, Biberach an der Riss, Germany, ³Department of Internal Medicine II, Ulm University, Ulm, Germany

Functional information of the lung is of great importance for staging and monitoring lung disease. Imaging of lung ventilation has been addressed by inhalation of polarized gases like Helium or Xenon. Major limitation of this technique rises from the high costs of equipment and gases. As an efficient alternative to polarized gases, the use of fluorinated gases has been proposed. In pre-clinical application these have always been used in combination with intubation, which does not realistically reflect the ventilation during free breathing. In this contribution the imaging of ventilation in mice with fluorinated gases during free-breathing is addressed.

2913

Computer #2



3D Lung Ventilation 1H Imaging Using a Respiratory Self-Navigated Stack-of-Stars Sequence in Comparison to 2D Fourier Decomposition
Andreas Voskrebenez^{1,2}, Marcel Gutberlet^{1,2}, Frank Wacker^{1,2}, and Jens Vogel-Clausen^{1,2}

¹Institute of Diagnostic and Interventional Radiology, Hanover, Germany, ²German Centre for Lung Research, Hanover, Germany

Fourier Decomposition (FD) is a lung function imaging technique with a high clinical potential. Nevertheless the 2D acquisition leads to long acquisition times for complete lung scans and the 3D breathing motion might lead to errors in the ventilation measurements. Self-navigated sequences offer the possibility to reconstruct images in different respiratory states. Using a stack-of-stars sequence, a method for 3D fractional ventilation (FV) imaging is demonstrated for six healthy volunteers and compared with FV calculated by 2D FD. The two methods show a good agreement. Additionally, 3D FV depicts 3D lung motion, which is not adequately detected with 2D FD.

2914

Computer #3



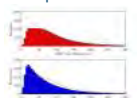
PETRA Lung MRI: Towards Robust Lung Imaging with Patient Comfort and with Improved Contrast
Yutaka Natsuaki¹, Xiaoming Bi¹, Gerhard Laub¹, and David Grodzki²

¹Siemens Healthcare, Los Angeles, CA, United States, ²Siemens Healthcare, Erlangen, Germany

With recent developments in ultra-short TE (UTE) MRI sequences such as PETRA with the respiratory triggering and the segmented acquisition, MRI has shown a potential of being a viable radiation-free alternative to the incumbent gold standard CT lung imaging. Within a volunteer validation study (n=14), the current work demonstrates a recent progress in the PETRA lung MRI towards its robustness and its applicability to all patient populations. The proposed solution improves patient comfort and image contrast by suppressing the unintended high intensity signals from surrounding tissues.

2915

Computer #4



Histogram based Analysis of Lung Perfusion of Children after Congenital Diaphragmatic Hernia Repair
Nora Kassner¹, Meike Weis², Katrin Zahn³, Thomas Schaible⁴, Stefan O Schoenberg², Lothar R Schad¹, K Wolfgang Neff², and Frank G Zöllner¹

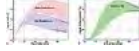
¹Computer Assisted Clinical Medicine, Medical Faculty Mannheim, Heidelberg University, Mannheim, Germany, ²Institute of Clinical Radiology and Nuclear Medicine, University Medical Center Mannheim, Heidelberg University, Mannheim, Germany, ³Department of Pediatric Surgery, University Medical Center Mannheim, Heidelberg University, Mannheim, Germany, ⁴Department of Neonatology, University Medical Center Mannheim, Heidelberg University, Mannheim, Germany

Reported measured lung perfusion data of 2-year old children after congenital diaphragmatic hernia repair was evaluated by regions of interest (ROI) within the acquired 3D volume. In this work a histogram based approach is used to characterize the distribution of perfusion in the whole left and right lung, and suitable quantities to characterize the distribution are extracted.

2916



Computer #5



Balanced SSFP pulmonary signal enhancement after contrast agent injection
Orso Pusterla^{1,2}, Grzegorz Bauman^{1,2}, and Oliver Bieri^{1,2}

¹Radiological Physics, Dep. of Radiology, University of Basel Hospital, Basel, Switzerland, ²Department of Biomedical Engineering, University of Basel, Basel, Switzerland

In contrast to the common view that Gd-based contrast agents have only marginal/limited effect on balanced steady state free precession (bSSFP) from its T_2/T_1 signal properties, we will demonstrate that especially for lung imaging single-dose contrast agent administration increases the parenchymal signal nearly up two fold.

2917



Computer #6



Fast 3D quantitative ¹H ventilation imaging of the human lung at 1.5T with SSFP

Orso Pusterla^{1,2}, Grzegorz Bauman^{1,2}, Mark Wielpütz^{3,4}, Claus Heussel^{3,4}, and Oliver Bieri^{1,2}

¹Radiological Physics, Dep. of Radiology, University of Basel Hospital, Basel, Switzerland, ²Department of Biomedical Engineering, University of Basel, Basel, Switzerland, ³Department of Diagnostic and Interventional Radiology with Nuclear Medicine, Thoraxklinik at University Hospital Heidelberg, Heidelberg, Germany, ⁴Department of Diagnostic and Interventional Radiology, University Hospital of Heidelberg, Heidelberg, Germany

Monitoring lung ventilation is of great interest to assess pulmonary function and disease progression. Here, a novel, fast, and simple three-dimensional (3D) quantitative in vivo ¹H imaging method is introduced, reflecting regional ventilation information. To this end, typically five ultra-fast balanced steady state free precession (ufSSFP) scans are repetitively performed in breath-hold from which a respiratory index map, γ , is derived. The new measure γ shows high reproducibility in healthy volunteers and high sensitivity to respiratory defects, such as in patients with COPD.

2918



Computer #7



Four-Dimensional Respiratory Motion-Resolved Sparse Lung MRI

Li Feng¹, Jean Delacoste², Hersh Chandarana¹, Davide Piccini^{2,3}, Francis Girvin¹, Matthias Stuber^{2,4}, Daniel K Sodickson¹, and Ricardo Otazo¹

¹Center for Advanced Imaging Innovation and Research (CAI2R), New York University School of Medicine, New York, NY, United States, ²University Hospital (CHUV) and University of Lausanne (UNIL), Lausanne, Switzerland, ³Advanced Clinical Imaging Technology, Siemens Healthcare, Lausanne, Switzerland, ⁴Center for Biomedical Imaging (CIBM), Lausanne, Switzerland

A four-dimensional (4D) respiratory motion-resolved UTE MRI method is presented for free-breathing lung MRI with isotropic spatial resolution. Center-out radial half-projection k-space data are continuously acquired using a 3D golden-angle UTE sequence. The radial k-space data are retrospectively sorted into distinct respiratory states, resulting in an undersampled 4D dataset ($k_x k_y k_z$ -respiration) using a respiratory motion signal extracted from the acquired data. The undersampled 4D data are reconstructed by exploiting sparsity along the new respiratory dimension. The proposed approach enables free-breathing lung MRI with 100% scan efficiency, allowing for assessment of lung tissue in arbitrary orientations at different respiratory states.

2919

Computer #8



Fourier Decomposition MRI using the SENCEFUL Approach for Non-Contrast-Enhanced Ventilation Imaging in Cystic Fibrosis Patients

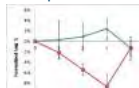
Simon Veldhoen¹, Andreas Max Weng¹, Clemens Wirth¹, Andreas Steven Kunz¹, Janine Nicole Knapp¹, Daniel Stäb^{1,2}, Florian Segerer³, Helge Uwe Hebestreit³, Thorsten Alexander Bley¹, and Herbert Köstler¹

¹Department of Diagnostic and Interventional Radiology, University Hospital Würzburg, Würzburg, Germany, ²The Centre for Advanced Imaging, The University of Queensland, Brisbane, Australia, ³Department of Pediatrics, University Hospital Würzburg, Würzburg, Germany

Fourier Decomposition MRI using the SENCEFUL approach is a recent development in functional lung MRI allowing for site-resolved assessment of lung function. The purpose of the present study is to evaluate its feasibility for ventilation imaging in patients with cystic fibrosis. Seven cystic fibrosis patients and 7 healthy volunteers were examined, lung ventilation maps were reconstructed and quantitative ventilation measurements were performed in tidal and deep breathing. Mean quantitative ventilation was significantly lower for patients with cystic fibrosis when compared to the healthy controls. The ventilation maps indicated increased ventilation inhomogeneity in cystic fibrosis patients.

2920

Computer #9



Tobacco smoke shortens T1 in a mouse model of COPD

Daniel Alamidi¹, Amir Smailagic², Abdel Bidar², Nicole Parker², Marita Olsson², Sonya Jacksson², Linda Swedin², Paul Hockings^{3,4}, Kerstin Lagerstrand¹, and Lars E Olsson⁵

¹Department of Radiation Physics, Institute of Clinical Sciences, Sahlgrenska Academy, University of Gothenburg, Gothenburg, Sweden, ²AstraZeneca R&D, Mölndal, Sweden, ³Medtech West, Chalmers University of Technology, Gothenburg, Sweden, ⁴Antaros Medical, BioVenture Hub, Mölndal, Sweden, ⁵Department of Medical Physics, Lund University, Translational Sciences, Malmö, Sweden

Tobacco smoking is the main cause of COPD. MRI may improve the characterization of COPD where lung T1 mapping has been used to study lung disease. We investigated whether tobacco smoke exposure affects lung T1 in a mouse model with repeated T1 readouts and biological measurements. Free breathing 3D-UTE T1 maps of the lungs were weekly performed over one month in mice exposed to air or tobacco smoke. The lung T1 was shortened in the tobacco smoke exposed mice, most likely due to early signs of smoking-induced lung pathology. Consequently, T1 is a potential biomarker of lung disease.

2921



Computer #10



Respiratory self-gating in 3D UTE lung acquisition in small animal imaging

Marta Tibiletti¹, Andrea Bianchi², Åsmund Kjørstad³, Detlef Stiller², and Volker Rasche^{1,4}

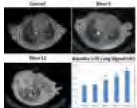
¹Core Facility Small Animal MRI, Ulm University, Ulm, Germany, ²Target Discovery Research, In-vivo imaging laboratory, Boehringer Ingelheim Pharma GmbH & Co. KG, Biberach an der Riss, Germany, ³Department of Neuroradiology, University Hospital Hamburg-Eppendorf, Hamburg, Germany, ⁴Department of Internal Medicine II, Ulm University, Ulm, Germany

1D (k-space center) and 3D (sliding window 3D reconstruction) have been evaluated for respiratory retrospective self-gating for Quasi Random UTE-3D lung acquisition in freely breathing rats. Low-resolution 3D GRASP reconstruction allowed the extraction of an effective gating signal from changes in lung-liver interface position. The 1D center-of-k-space method did not yield sufficient gating signal fidelity, most likely caused by the only limited changes of the anatomy in the investigated volume, and to a lesser extent intensity modulations introduced by residual eddy-currents.

2922



Computer #11



Longitudinal Assessment of Pulmonary Permeability in a Mouse Model of Lung Fibrosis

Iliyana P Atanasova¹, Pauline Desogere¹, Clemens K Probst², Nicholas Rotile¹, Andrew M Tager², and Peter Caravan¹

¹A. A. Martinos Center for Biomedical Imaging, Massachusetts General Hospital, Charlestown, MA, United States, ²Center for Immunology and Inflammatory Diseases, Massachusetts General Hospital, Boston, MA, United States

Idiopathic pulmonary fibrosis is a fatal condition without effective treatment. Given evidence that vascular leak promotes fibrosis, we assessed whether pulmonary leak could be quantified using dynamic MRI and an intravascular tracer. In a mouse model we observed that permeability to albumin rose sharply on day 3 after insult, returned to baseline by day 5 and increased moderately between days 5-13. To our knowledge this is the first report of the time course of vascular leak in pulmonary fibrosis. The proposed method could be useful for studying the role of lung permeability in fibrosis and for monitoring of treatment response.

2923

Computer #12



Imaging of Lung Conductivity Using Ultrashort Echo-Time Imaging

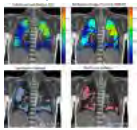
Ulrich Katscher¹ and Peter Börnert¹

¹Philips Research Europe, Hamburg, Germany

Reliable MR imaging of lung tissue could be an important element of diagnosing lung-related diseases. The very short T2 components of lung tissue, one of the main problems of lung imaging, can be visualized using ultrashort echo times (UTE). Furthermore, UTE sequences allow the determination of conductivity of the imaged tissue. This study shows the principle feasibility of UTE to image lung conductivity, examining healthy volunteers. Obtained conductivity was lower for inspiration breath hold than expiration breath hold, which is the expected behaviour due to corresponding fraction of air (with nearly zero conductivity) inside lungs during inspiration and expiration.

2924

Computer #13



Pulmonary Fourier decomposition MRI compared to multiple breath washout and spirometry: A preliminary study in Primary Ciliary Dyskinesia

Grzegorz Bauman^{1,2}, Sylvia Nyilas^{2,3,4}, Orso Pusterla^{1,2}, Christoph M Heyer⁵, Cordula Koerner-Rettberg⁶, Philipp Latzin^{3,4}, and Oliver Bieri^{1,2}

¹Division of Radiological Physics, Department of Radiology, University Hospital of Basel, Basel, Switzerland, ²Department of Biomedical Engineering, University of Basel, Basel, Switzerland, ³Department of Pediatric Pneumology, University Children's Hospital Basel (UKBB), Basel, Switzerland, ⁴Division of Respiratory Medicine, Department of Pediatrics, University Children's Hospital of Bern, Bern, Switzerland, ⁵Institute of Diagnostic Radiology, Interventional Radiology and Nuclear Medicine, Ruhr-University of Bochum, Bochum, Germany, ⁶Department of Pediatric Pneumology, University Children's Hospital of Ruhr University Bochum at St Josef-Hospital, Bochum, Germany

In this work, the feasibility of contrast-media-free pulmonary Fourier decomposition (FD) MRI is assessed in patients with primary ciliary dyskinesia (PCD). An automatic evaluation of regional functional defects on fractional ventilation and perfusion FD maps has been developed. Furthermore, the lung function evaluated using FD MRI is compared to the parameters obtained using multiple breath washout technique and spirometry. Statistical analysis was used to find significant correlations between FD MRI and lung function techniques.

2925

Computer #14

Whole Lung Morphometry with Hyperpolarised ³He Gas Diffusion MRI - 3D Multiple b-value Acquisition and Compressed SensingHo-Fung Chan¹, Neil J. Stewart¹, Juan Parra-Robles¹, Guilhem J. Collier¹, and Jim M. Wild¹

¹Academic Unit of Radiology, University of Sheffield, Sheffield, United Kingdom

Compressed sensing (CS) was implemented to reduce scan time and facilitate acquisition of 3D multiple b-value ³He diffusion-weighted (DW) MRI data for whole lung morphometry. A fully-sampled 3D DW-MRI dataset was retrospectively undersampled using CS simulations to determine optimal k-space undersampling patterns. Whole lung morphometry measurements derived from prospective 3-fold undersampled 3D multiple b-value DW-MRI were compared to 3D and 2D fully-sampled equivalents. Good agreement was obtained between lung morphometry measurements indicating 3D multiple b-value ³He DW-MRI with CS can provide reliable measurements of whole lung morphometry within a single breath-hold.

2926

Single breath washout imaging – regional phase III slope mapping with rapid hyperpolarized gas MRI

Computer #15 Felix C Horn¹ and Jim M Wild¹



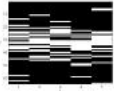
¹University of Sheffield, Sheffield, United Kingdom

Single breath washout (SBW) is a whole lung pulmonary function test that has been shown to be sensitive to early changes in lung disease. Of particular clinical interest has been the Phase III slope (S_{III}) as the concentration decay between 25-75% of the exhaled volume.

In this work rapid lung imaging of exhaled hyperpolarized gas is used to acquire 2D images of SBW of subjects expiring to residual lung volume. The ability to calculate regional S_{III} from those time resolved images is demonstrated in healthy volunteers.

2927

Computer #16



Incorporation of prior knowledge of the signal behavior into the compressed sensing framework for accelerated acquisition in hyperpolarized gas diffusion MRI

Juan FPJ Abascal^{1,2}, Manuel Desco^{1,2,3}, and Juan Parra-Robles^{1,2}

¹Department of Bioengineering and Aerospace Engineering, Universidad Carlos III de Madrid, Madrid, Spain, ²Instituto de Investigación Sanitaria Gregorio Marañón, Madrid, Spain, ³Centro de Investigación en Red de Salud Mental (CIBERSAM), Madrid, Spain

Diffusion MRI measurements using hyperpolarized gases are generally acquired during patient breath hold, which yields a compromise between achievable image resolution, lung coverage and number of b-values. In this work, we propose a novel method that incorporates the knowledge of the signal decay into the reconstruction (SIDER) to accelerate the acquisition of MR diffusion data by undersampling in both spatial and b-value dimensions. SIDER is assessed by retrospectively undersampling diffusion datasets of normal volunteers and COPD patients. Results suggest that accelerations of at least x7 are achievable with negligible effect in the estimates of diffusion parameters.

2928

Computer #17



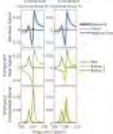
3D Multi-Parametric Acquisition of ³He Lung Ventilation Images, Lung Diffusion Morphometry and T₂* Maps with Compressed Sensing Ho-Fung Chan¹, Neil J. Stewart¹, Guilhem J. Collier¹, and Jim M. Wild¹

¹Academic Unit of Radiology, University of Sheffield, Sheffield, United Kingdom

Whole-lung coverage ³He ventilation images, maps of ADC, alveolar dimension (Lm_D), and T₂* were acquired in a single breath-hold using a multiple-interleaved 3D sequence with compressed sensing (CS). A fully-sampled three-interleaved ADC and T₂* dataset was acquired for CS simulations, to determine the optimal k-space undersampling patterns. A prospective, 3-fold undersampled 3D five-interleaved dataset was acquired with CS and parametric maps were compared to those calculated from fully-sampled datasets. CS-derived ADC and Lm_D values showed good agreement with fully-sampled equivalents. CS-derived T₂* values were lower than fully-sampled ones due to the smoothing process of the CS reconstruction.

2929

Computer #18



Improved fitting of ¹²⁹Xe spectroscopy identifies three dissolved-phase resonances in the human lung

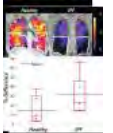
Scott H. Robertson^{1,2}, Elianna A. Bier^{1,2}, Rohan S. Virgincar^{1,3}, and Bastiaan Driehuys^{1,2,3,4}

¹Center for In Vivo Microscopy, Duke University Medical Center, Durham, NC, United States, ²Medical Physics Graduate Program, Duke University, Durham, NC, United States, ³Department of Biomedical Engineering, Duke University, Durham, NC, United States, ⁴Department of Radiology, Duke University Medical Center, Durham, NC, United States

Hyperpolarized ¹²⁹Xe experiences chemical shifts between the lung airspaces, interstitium, and capillary beds, enabling functional information to be directly probed. However, in order to realize the potential of these chemical shifts, the spectrum must be carefully decomposed. Previous methods have assumed only two dissolved-phase resonances exist in the human lung and have used inconsistent 0 ppm reference frequencies. Here we present novel non-linear fitting of complex exponentially decaying FIDs and demonstrate that the dissolved phase signal can be robustly decomposed into three dissolved-phase resonances. We present updated frequencies and widths using and appropriately adjusted 0 ppm reference value.

2930

Computer #19



Improving quantitative Hyperpolarized ¹²⁹Xe gas exchange MRI in idiopathic pulmonary fibrosis

Scott H. Robertson^{1,2}, Jennifer Wang¹, Geoffrey Schrank¹, Holman P. McAdams³, and Bastiaan Driehuys^{1,2,4,5}

¹Center for In Vivo Microscopy, Duke University Medical Center, Durham, NC, United States, ²Medical Physics Graduate Program, Duke University, Durham, NC, United States, ³Department of Radiology, Duke University Medical Center, Durham, NC, United Kingdom, ⁴Department of Biomedical Engineering, Duke University, Durham, NC, United States, ⁵Department of Radiology, Duke University Medical Center, Durham, NC, United States

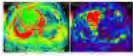
While gas-exchange imaging with ¹²⁹Xe holds great potential for enhancing both the diagnosis and followup of IPF, the quantitative ability of these techniques is currently limited by the SNR and spatial resolution afforded by the limited dissolved-phase signal and highly undersampled acquisition. Here we tune our reconstruction for these challenging conditions, and demonstrate improvements in image quality. We then quantify the loss of gas exchange in the apex and base of the lung and show that there is significantly reduced gas exchange in the basal regions of subjects with IPF relative to healthy controls.

2931

Computer #22

Magnetic Resonance Elastography of the Anterior Mediastinal Mass at 3T: a Preliminary Study

Wei Tang¹, Yao Huang¹, Ning Wu¹, Wenwen Lu¹, Linlin Qi¹, and Bing Wu²

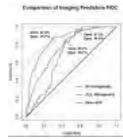


¹Diagnostic Radiology, Cancer Hospital, Chinese Academy of Medical Sciences, Peking Union Medical College, Beijing, China, People's Republic of, ²GE healthcare MR research China, Beijing, China, People's Republic of

Magnetic resonance (MR) elastography depicts the elastic properties of tissues of interest has been primarily applied in the work-up of diagnosis for hepatic fibrosis. Theoretically, interference fringes could be visualized on the elastogram due to the miscalculation of the interaction between the attenuated propagations of shear wave and the tissue overlying or surrounding to the investigated subject, which might be one of the main concern that limited the clinical potentials of MRE. We propose an investigation on the feasibility of MR elastography in characterizing the mechanical properties of anterior mediastinal masses with the consideration of the relatively superficial location of these entities, therefore few interactions between the shear wave and subject unexpected were produced during the process of elasticity mapping. It was demonstrated in our study that anterior mediastinal mass in various etiology of thymic carcinoma, thymoma, and lymphoma has distinct elastic properties. MR elastography was helpful in distinguishing the thymic carcinoma from lymphoma.

2932

Computer #20



Prediction of Longitudinal FEV1 Decline in Smokers with Hybrid Hyperpolarized 3He MRI

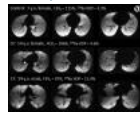
Hooman Hamedani^{1,2}, Yi Xin¹, Stephen J Kadlecck¹, Heather Gatens¹, Maurizio Cereda³, Sarmad M Siddiqui^{1,2}, Mehرداد Pourfathi^{1,4}, Joseph Naji¹, Masaru Ishii⁵, and Rahim R Rizi¹

¹Radiology, University of Pennsylvania, Philadelphia, PA, United States, ²Bioengineering, University of Pennsylvania, Philadelphia, PA, United States, ³Anesthesiology and Critical Care, University of Pennsylvania, Philadelphia, PA, United States, ⁴Electrical and Systems Engineering, University of Pennsylvania, Philadelphia, PA, United States, ⁵Johns Hopkins University, Baltimore, MD, United States

Aside from the superior diagnostic power that HP gas MRI provides through imaging unique aspects of lung function, it is evident that the underlying mechanisms that lead to subsequently evident global changes in the lung function in future are detectable through regional and functional imaging using HP gas MRI.

2933

Computer #21



Hyperpolarized 129Xe MRI ventilation in pediatric cystic fibrosis lung disease: safety and sensitivity

Laura L Walkup¹, Robert P Thomen^{1,2}, Teckla Akinyi^{1,3}, Wolfgang Loew⁴, Kai Ruppert¹, John P Clancy⁵, Zackary I Cleveland¹, and Jason C Woods¹

¹Center for Pulmonary Imaging Research, Division of Pulmonary Medicine and Department of Radiology, Cincinnati Children's Hospital Medical Center, Cincinnati, OH, United States, ²Department of Physics, Washington University in St. Louis, St. Louis, MO, United States, ³Department of Biomedical Engineering, University of Cincinnati, Cincinnati, OH, United States, ⁴Imaging Research Center, Department of Radiology, Cincinnati Children's Hospital Medical Center, Cincinnati, OH, United States, ⁵Division of Pulmonary Medicine, Cincinnati Children's Hospital Medical Center, Cincinnati, OH, United States

We demonstrate hyperpolarized ¹²⁹Xe MRI in healthy pediatric control subjects and cystic fibrosis patients as young as age 7, for the first time. Subjects experienced a transient nadir in SpO₂ that quickly returns to baseline with normal breathing. Despite having similarly high lung function (i.e., normal FEV₁), CF patients had nearly 4-fold increase in ¹²⁹Xe ventilation defect volume compared to their healthy peers, with statistical significance. Importantly, ventilation defects were present even in CF patients with FEV₁ near or exceeding 100% predicted, suggesting that ¹²⁹Xe MRI is more sensitive to early CF lung disease than traditional clinical spirometry.

2934

Computer #23



Assessment of Pleural Effusion in Dengue Fever

Therese Sjöholm¹, Benjamin A Thomas¹, Yin Mo², Louisa Sun², Ashley St. John³, Paul Anantharajah Tambyah², and John J Totman¹

¹A*STAR-NUS Clinical Imaging Research Centre, Singapore, Singapore, ²Department of Medicine, National University Hospital Singapore, Singapore, Singapore, ³Duke-NUS Graduate Medical School, Singapore, Singapore

In this study we assess the feasibility of using MRI for measurement of pleural effusion in Dengue Fever. 30 subjects with confirmed Dengue infection were scanned using T2-weighted HASTE MRI and chest x-rays (CXRs) at baseline and 4-8 days follow-up. Fluid accumulation in the pleural cavity was assessed for both modalities. For MRI, significantly different fluid accumulations were measured between baseline and follow-up (p=0.002). The fluid accumulations were all below the detectability limit of CXR. As such, MRI provides a sensitive measurement of pleural effusion in dengue fever and can be used to track fluid accumulation over time.

Electronic Poster

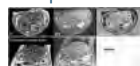
Hepatobiliary 2

Exhibition Hall

Monday, May 9, 2016: 15:15 - 16:15

2935

Computer #25



Quantitative assessment and follow-up of hepatocellular carcinoma in rat livers using clinical 3T MRI.

Lorenzo A Orci¹, Graziano Oldani¹, Stephanie Lacotte¹, Florence Slits¹, Iris Friedli², Wolfgang Wirth³, Jean-Paul Vallée², Christian Toso¹, and Lindsey Alexandra Crowe²

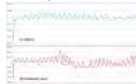
¹Division of Abdominal and Transplantation Surgery, Hepato-pancreato-biliary Centre, Department of Surgery, Geneva University Hospital and Faculty of Medicine, Geneva, Switzerland, ²Division of Radiology, Geneva University Hospital and Faculty of Medicine, Geneva, Switzerland, ³Institute of Anatomy, Paracelsus Medical University, Salzburg, Austria

In vivo liver cancer research commonly uses rodent models of liver tumor growth. One of the limitations of such models is the lack of

accurate and reproducible endpoints for dynamic assessment tumor nodules. We used 3T clinical MRI to quantify tumor volume over time and correlate to gold standard histological volumes and blood levels of α -fetoprotein in two rat orthotopic models of hepatocellular carcinoma (HCC). Combination of 3D isotropic gradient echo for accurate volume and T2 for contrast provided appealing correlation. We have developed a 3D volume quantification method that enables follow-up and analysis of complex tumor morphology.

2936

Computer #26



Clinical feasibility of free-breathing gadoxetic acid-enhanced liver MRI using incoherent undersampling in patients with transient dyspnea

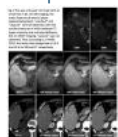
Jeong Hee Yoon¹, Jeong Min Lee¹, Robert Grimm², Son Yohan³, Kiefer Berthold², Tobias Kai Block⁴, Hersh Chandarana⁴, and Joon Koo Han¹

¹Radiology, Seoul National University Hospital, Seoul, Korea, Republic of, ²Siemens Healthcare, Erlangen, Germany, ³Siemens Healthcare Korea, Seoul, Korea, Republic of, ⁴Radiology, NYU School of medicine, New York, NY, United States

Acquisition of optimal late arterial phase is essential for focal liver lesion diagnosis and detection at gadoxetic acid-enhanced liver magnetic resonance imaging (MRI). However, it is often challenging to obtain late arterial phase due to short arterial window and frequent involuntary motion during arterial phase. We attempted to characterize the frequency, onset, and duration of the involuntary motion after gadoxetic acid injection and whether acceptable quality of late arterial phase can be obtained using incoherent undersampling technique.

2937

Computer #27



A Retrospective, Multicenter, Intra-individual Study Based on LI-RADS 2014: Unenhanced combined contrast-enhanced MRI Elevates the HCC probability Category Compared with Multiphasic CT in Patients with Cirrhosis Induced by HBV Infection

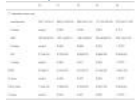
Ke Wang¹ and Xiaoying Wang²

¹Radiology, Peking University First Hospital, Beijing, China, People's Republic of, ²Beijing, China, People's Republic of

This study was to compare the category of unenhanced combined contrast enhanced MR imaging (MR) and Multiphasic CT (CT) in the diagnosis of HCC based on LI-RADS 2014 in patients with cirrhosis induced by HBV infection. We retrospectively collected patients who had both undergone CT and MR imaging within 30 days and had pathologically proved HCC. A radiologist using LI-RADS 2014 recored the imaging features and the category of all the lesions. The result showed that MR showed higher LI-RADS category compared with CT, and had better ability for the showing of some imaging features. Thus, we concluded that MRI can elevate the LI-RADS category and is recommended in the initial evaluation of suspected HCC priority to CT.

2938

Computer #28



Assessing Liver Fibrosis in Patients with Chronic Hepatitis B: Comparison of T1 Mapping with Gd-EOB-DTPA-enhanced 1.5T MRI, Aspartate Aminotransferase-to-Platelet Ratio Index and Fibrosis-4

Li Yang¹, Ying Ding², Mengsu Zeng³, Shengxiang Rao³, and Ruofan Sheng³

¹Shanghai Institute of Medical Imaging, Zhongshan Hospital of Fudan University, Shanghai, China, People's Republic of, ²Zhongshan Hospital of Fudan University, Shanghai Institute of Medical Imaging, Shanghai, China, People's Republic of, ³Zhongshan Hospital of Fudan University, Shanghai, China, People's Republic of

Hepatobiliary-phase gadoxetic acid-enhanced MR imaging may reflect liver function and was reported to be able to predict liver fibrosis stage with higher reliability. Aspartate aminotransferase-to-platelet ratio index (APRI) and fibrosis-4 (FIB-4) are widely used non-invasive tests that estimate liver fibrosis. We compared the diagnostic performance of T1 mapping on Gd-EOB-DTPA-enhanced 1.5T magnetic resonance imaging (MRI), APRI and FIB-4 for evaluating the severity of liver fibrosis in 118 patients with chronic viral hepatitis B, and the results showed The HBP T1 relaxation time measurement on gadoxetic acid-enhanced appears superior to unenhanced, D% (the reduction rate) of T1 relaxation times, the APRI and FIB-4 index in differentiating advanced liver fibrosis.

2939

Computer #29



Multiparametric functional MR imaging for evaluation of hepatic warm ischemia-reperfusion injury in rabbit models

Qian Ji¹, Zhi-Qiang Chu², Tao Ren¹, Pan-Li Zuo³, Thorsten Feiweier⁴, Andre de Oliveira⁴, and Wen Shen¹

¹Radiology, Tianjin First Central Hospital, Tianjin, China, People's Republic of, ²Transplantation, Tianjin First Central Hospital, Tianjin, China, People's Republic of, ³MR Collaborations NE Asia, Siemens Healthcare, Beijing, China, People's Republic of, ⁴Siemens Healthcare GmbH, Erlangen, Germany

Hepatic warm ischemia-reperfusion injury (WIRI) is clinically relevant in liver transplantation. We undertook this study to determine the feasibility of using IVIM, DTI, and BOLD MR imaging for the characterization of hepatic WIRI. 20 hepatic WIRI models and control rabbits were examined using a 3T clinical MR scanner, which followed by biochemical and histopathological analysis. There were significant differences of Dfast, Dslow, PF, ADC, and R2* values between the two groups. There were significant correlations between MR parameters and biochemical parameters. This indicated that multiparametric functional MR imaging are noninvasive and valuable techniques for assessing the pathophysiologic changes of hepatic WIRI.

2940

Computer #30



Apparent Relaxivity of Gd-BOPTA in A Mixture of Water, Gd-BOPTA and Fat

Yuan Le¹

¹Radiology and Imaging Science, Indiana University School of Medicine, Indianapolis, IN, United States

This paper is to discuss the impact of fat on the Gd-based contrast behavior in a mixture of water based Gd-BOPTA solution and fat. A set of vials, contains such mixtures with various fat fraction and Gd-BOPTA concentration, was constructed and scanned using both

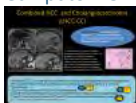
Turbo Spin Echo (TSE) with 3 point Dixon, and VIBE-Dixon. With VIBE-Dixon, the slopes of the regression (relaxivity) of R1 vs. [Gd] in water were very close among groups with various fat fraction; while with TSE image, the slopes of R1 vs. [Gd] in whole mixture were close among vial groups.

- 2941
Computer #31
Usefulness of Short Breath Hold High Resolution Technique (CAIPIRINHA) in Gadoteric acid-enhanced Liver MRI: To Overcome Degraded Arterial Phase
Chang-Hee Lee¹ and Cheol Min Park²

¹Radiology, Korea University Guro Hospital, Seoul, Korea, Republic of, ²Korea University Guro Hospital, Seoul, Korea, Republic of

The short breath-hold high-resolution MR technique shows better HAP image quality with less degraded HAP and lower incidences of breath-hold difficulty and gadoteric acid related dyspnea than the conventional long breath-hold MR technique.

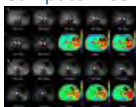
- 2942
Computer #32
MRI Characteristics of Primary Liver Malignancies: Common and Uncommon Mimics with Histopathological Correlation - A Practical Approach
Nikhil Kinger¹, Sadhna Nandwana¹, Courtney Moreno¹, Kelly Cox¹, and Pardeep Mittal¹



¹Radiology and Imaging Sciences, Emory University School of Medicine, Atlanta, GA, United States

The liver is an important oncologic organ. Primary liver tumors can arise from a variety of different liver components such as hepatocytes, bile duct epithelium, neuroendocrine cells, and mesenchymal cells. We will discuss imaging and histopathological features of primary liver tumors and their common and uncommon mimics.

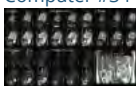
- 2943
Computer #33
The potentiality of MR T1rho as a biomarker for liver fibrosis evaluation
shuangshuang xie¹, qing li¹, yu zhang², wenjing hou¹, yue cheng¹, and wen shen¹



¹Radiology, Tianjin First Center Hospital, Tianjin, China, People's Republic of, ²Philips healthcare, Beijing, China, People's Republic of

This study evaluated the potential of T1rho for liver fibrosis evaluation and to explore the best TSL points with good B0 and B1 inhomogeneity. Thirteen healthy control subjects and eight patients with clinically diagnosed liver fibrosis were scanned 3D b-TEF sequence. T1rho map were constructed by using 7-TSLs, 6-TSLs or 3-TSLs and compared between groups. Our results showed both 7-TSLs and 6-TSLs had moderate diagnostic efficacy, and AUC of 7-TSLs was slightly higher than 6-TSLs. We conclude 7-TSLs and 6-TSLs are recommended for the diagnosis of liver fibrosis, and 7-TSLs has slightly higher diagnostic performance.

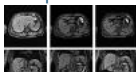
- 2944
Computer #34
Measurement of Liver Perfusion using Pseudo-Continuous Arterial Spin Labeling with Background Suppression: Approaches to Separate Portal-Venous and Arterial Perfusion
Petros Martirosian¹, Rolf Pohmann², Christina Schraml³, Holger Schmidt³, Nina F Schwenzer³, Martin Schwartz¹, Klaus Scheffler², Konstantin Nikolaou³, and Fritz Schick¹



¹Section on Experimental Radiology, University of Tübingen, Tübingen, Germany, ²Max Planck Institute for Biological Cybernetics, Tübingen, Germany, ³Department of Diagnostic and Interventional Radiology, University Hospital of Tübingen, Tübingen, Germany

The separation of portal-venous and hepatic arterial blood supply is important for the evaluation of chronic liver diseases and the characterization of liver lesions. The aim of this study was to investigate the capability of a pseudo-continuous arterial spin labeling sequence, to separate arterial and portal venous perfusion of the liver using a background suppression technique and different tagging plane orientations. It was demonstrated that the presented method provides high quality perfusion images of the liver without application of intravenous contrast agent and offers promising approaches for the separation of arterial and portal-venous perfusion fractions.

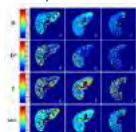
- 2945
Computer #35
A 3D non-rigid registration method for liver in DCE MR images
Yang Feng¹, He Wang¹, and Junbo Li¹



¹Philips Healthcare, Shanghai, China, People's Republic of

The shape and position of liver is varied through respiratory movement in DCE MR liver images. A robust 3D deformable registration was employed to define the distortion between them and compensate it. As a result, the liver and vessels will be located at the exact position with the exact shape (include vessels) of the reference image after registration.

- 2946
Computer #36
MRI-based Estimation of Liver Function by Intravoxel Incoherent Motion Diffusion-weighted Imaging
Jing Zhang¹, Yikai Xu¹, Yihao Guo², Yanqiu Feng², Queenie Chen³, Yingjie Mei^{2,4}, Xiangliang Tan¹, Jiajun Zhang¹, Xixi Zhao¹, Zeyu Zheng¹, and Chunhong Wang¹



¹Department of Medical Imaging Center, Nanfang Hospital, Southern Medical University, Guangzhou, China, People's Republic of, ²School of Biomedical Engineering and Guangdong Provincial Key Laboratory of Medical Image Processing, Southern Medical University, Guangzhou, China, People's Republic of, ³Philips Healthcare, Hong Kong, China, People's Republic of, ⁴Philips Healthcare, Guangzhou, China, People's Republic of

The quantitative evaluation of hepatic function is important for monitoring patients and preoperative assessment of the hepatic reserve. This work aims to assess the sensitivity of IVIM in evaluating liver function in patients with chronic liver disease. The results demonstrate that perfusion-related parameters (D^* and f) are useful for indicating the severity of liver disease, and may have the potential to become a promising non-invasive tool for monitoring liver function.

2947

Computer #37



Liver IVIM MR imaging: improved reproducibility of pseudo-diffusion coefficient D^* via proper signal modeling

Shih-Han Hung¹, Meng-Chieh Liao¹, Cheng-Ping Chien¹, Wen-Chau Wu², and Hsiao-Wen Chung³

¹Graduate Institute of Biomedical Electronics and Bioinformatics, National Taiwan University, Taipei, Taiwan, ²Graduate Institute of Oncology, National Taiwan University, Taipei, Taiwan, ³Electrical Engineering, National Taiwan University, Taipei, Taiwan

A new scheme was proposed to analyze intravoxel incoherent motion MR imaging data of the liver. The method integrated the combined use of single- and bi-exponential signal decaying models to deal with regions with absence of prominent vasculature, and the removal of data obtained at b-values less than 15s/mm^2 to avoid contamination from large vessels. Results from ten healthy subjects scanned twice at 3T showed substantially improved reproducibility in the pseudo-diffusion coefficient D^* , while those of the true diffusion coefficient and the perfusion fraction were unaltered. Using our scheme the estimated D^* mostly fall within 38 to $85 \times 10^{-3} \text{mm}^2/\text{s}$.

2948

Computer #38



Value of Whole-Liver Apparent Diffusion Coefficient Histogram Analysis for Quantification of Liver Fibrosis Stages

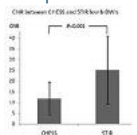
Zhaoxia Yang¹, Xinxing Hu¹, Heyue Liang¹, Robert Grimm², Caixia Fu³, Xu Yan⁴, Hui Liu⁴, Mengsu Zeng¹, and Shengxiang Rao¹

¹Department of Radiology, Zhongshan Hospital, Fudan University, Shanghai, China, People's Republic of, ²MR Application Predevelopment, Siemens Healthcare, Erlangen, Germany, ³Application department, Siemens Shenzhen Magnetic Resonance Ltd., Shenzhen, China, People's Republic of, ⁴MR Collaboration NE Asia, Siemens Healthcare, Shanghai, China, People's Republic of

Histogram analysis of whole-liver ADC maps was applied for patients with liver fibrosis to assess its diagnostic value and correlation with fibrosis stages achieved from liver biopsy. Our study shows that the mean and the 75th percentile ADC were significantly lower with the increasing grade of liver fibrosis. The median, standard deviation (SD), 5th, 10th, 25th, 90th and 95th percentiles also showed statistical differences among pathological fibrosis grades. In conclusion, histogram analysis of whole-liver ADC maps has a potential value for quantifying liver fibrosis grades.

2949

Computer #39



Conspicuity of malignant liver tumors on STIR low b diffusion-weighted imaging with gadolinium ethoxybenzyl dethylenetriaminepentaacetic acid

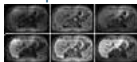
Takashi Iwanaga¹, Yoshihiko Fukukura², Tomonori Saito¹, Masashi Sasaki¹, Yuichi Kumagae², Koji Takumi², Takuro Fujisaki¹, and Takashi Yoshiura²

¹Department of Radiological Technology, Kagoshima University Hospital, Kagoshima, Japan, ²Department of Radiology, Kagoshima University Graduate School of Medical and Dental Sciences, Kagoshima, Japan

When liver MRI is performed using Gd-EOB-DTPA, DWI is often obtained after Gd-EOB-DTPA injection to shorten examination time in the busy clinical practice. We compared malignant tumor conspicuity on low b-value DWI after contrast between chemical shift selective (CHES) and short inversion time inversion recovery (STIR) sequences. Malignant liver tumors were more conspicuous with STIR than with CHES. DWI with STIR is useful for visualizing malignant liver tumors after Gd-EOB-DTPA injection, thus decreasing overall scan time.

2950

Computer #40



Non-uniformity correction of Gd-EOB-DTPA-enhanced magnetic resonance imaging of the liver at 3T

Yusuke Inoue¹, Gou Ogasawara¹, Keiji Matsunaga¹, Kaoru Fujii¹, Hirofumi Hata², and Yuki Takato²

¹Kitasato University School of Medicine, Sagami-hara, Japan, ²Kitasato University Hospital, Sagami-hara, Japan

We evaluated two commercially available methods for non-uniformity correction, an image-based method (SCIC) and a calibration-based method (PURE), in Gd-EOB-DTPA-enhanced MR imaging using a 3T scanner. SCIC improved uniformity for the precontrast images; however, artificial hyperintensity in the liver surface was evident especially in the hepatobiliary-phase images. Quantitative evaluation of contrast effects were severely distorted by SCIC. PURE improved uniformity in the precontrast and hepatobiliary-phase images, and appeared to aid quantitative evaluation of the signal intensity after contrast administration. PURE is indicated to be a useful non-uniformity correction method in Gd-EOB-DTPA-enhanced MR imaging using a 3T scanner.

2951

Computer #41



Noninvasive MR diffusion and perfusion analysis of liver fibrosis using comprehensive parameters

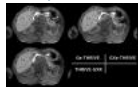
qing li¹, shuangshuang xie¹, yu zhang², wenjing hou¹, yue cheng¹, and wen shen¹

¹Radiology, Tianjin First Center Hospital, Tianjin, China, People's Republic of, ²Philips healthcare, Beijing, China, People's Republic of

This study investigated the value of multi-parametric analysis using MR IVIM, BOLD MRI and DKI for the diagnosis of liver fibrosis. Eight patients with clinically diagnosed liver fibrosis and thirteen healthy control subjects were scanned with DKI, IVIM, BOLD. IVIM derived D^* , D , f , DKI derived MD, K value and BOLD derived $R2^*$ were compared between the two groups. Our results showed D^* , D , f , MD decreased, $R2^*$ and K value increased in patients with liver fibrosis, but only D^* and D demonstrated significant difference ($P < 0.05$). We therefore conclude D^* and D could be useful in the diagnosis of liver fibrosis.

2952

Computer #42



Robust free-breathing hepatic MRI using respiratory-gated 3D stack-of-stars sequence

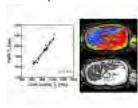
Takashige Yoshida^{1,2}, Yuki Furukawa¹, Hiroaki Tsuchiya¹, Kohei Yuda¹, Masami Yoneyama³, Nobuo Kawauchi¹, and Haruo Saito⁴

¹Radiology, Tokyo metropolitan police hospital, Tokyo, Japan, ²Graduate school of Medicine, Tohoku university, Miyagi, Japan, ³Marketing, Philips Electronics Japan, Tokyo, Japan, ⁴Division of Diagnostic Image Analysis, Graduate school of Medicine, Tohoku University, Miyagi, Japan

An extension of slice direction and high resolution imaging cannot help to increase scan time in hepatic MRI. The hepatic MRI is necessary to hold their breath, and breath holding influenced on image quality. Hence improved image quality on hepatic MRI is a required free breath sequence. Our study using 3D stack-of-stars trajectory with respiratory navigator is objective that perfectly eliminates respiratory motion effect. A sequence combined motion averaging by stack-of-stars and correction by navigator is possible to eliminate respiratory motion.

2953

Computer #43



Liver MR imaging using 3D phase-sensitive inversion recovery (PSIR) sequence

Yasuhiro Fujiwara¹, Hirotooshi Maruyama², Nobuyuki Kosaka³, Yoshiyuki Ishimori⁴, and Noriyuki Furukawa²

¹Department of Medical Imaging, Faculty of Life Sciences, Kumamoto University, Kumamoto, Japan, ²Radiological Center, National Hospital Organization Kumamoto Medical Center, Kumamoto, Japan, ³Department of Radiology, University of Fukui, Fukui, Japan, ⁴Department of Radiological Sciences, Ibaraki Prefectural University of Health Sciences, Ibaraki, Japan

We applied 3D phase-sensitive inversion recovery (PSIR) sequence to liver MR imaging. Experiments with phantom and healthy subjects revealed that this sequence improved contrast enhancements of Gd-based agents and liver-to-spleen or muscle contrasts while simultaneously providing an accurate T1 map of the liver. Better Gd contrast enhancements and liver contrasts may improve tumor-to-liver contrasts in the hepato-biliary phase with Gd-based hepatocyte-specific contrast agents, and the accurate T1 map may be useful for liver-function assessments. Although a clinical study is required to evaluate its utility, this sequence may have potential to improve liver MR imaging.

2954

Computer #44



Reducing bias due to B0 inhomogeneity in abdominal T2* mapping

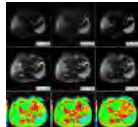
Pippa Storey¹ and Dmitry S. Novikov¹

¹Radiology Department, New York University School of Medicine, New York, NY, United States

T2* measurements in the abdomen are often corrupted by macroscopic magnetic susceptibility effects from air in the lung and bowel. We show that sensitivity to linear B0 variations can be eliminated by tailoring the 2D slice profile appropriately and truncating the echo train where the phase difference between adjacent voxels within or across slices exceeds $\pi/2$. This improves T2* accuracy without the need for post hoc corrections. When compared with a conventional approach, the proposed technique demonstrates reduced sensitivity to B0 inhomogeneity in the liver caused by magnetic susceptibility differences in the lung.

2955

Computer #45



Comparison of Three Different DiffusionWeighted Imaging Acquisitions for Focal Liver Lesions

Zhuo Shi¹, Xinming Zhao¹, Ouyang Han¹, and Lizhi Xie²

¹Department Of Imaging Diagnosis, Cancer Hospital, Chinese Academy of Medical Sciences & Peking Union Medical College, Beijing China, Beijing, China, People's Republic of, ²GE Healthcare, MR Research China, Beijing, Beijing, China, People's Republic of

By comparing the breath-hold, respiratory-triggered, and free-breathing techniques in diffusion-weighted magnetic resonance imaging (MRI) for the evaluation of focal liver lesions on a 3.0T system, we found that: The free-breathing DWI is better than others for the patients who want to do the whole liver examination; but for the patients with focal liver lesions who need to do the DWI scan to evaluate the local lesions, the breath-hold DWI was optimal. Generally speaking, the respiratory-triggered DWI of the 3T MRI system had higher SNR and CNR in any case, and it was the best DWI acquisition technique.

2956

Computer #46

Effects of ancillary features of gadoxetic acid-enhanced MRI on the categorization of hepatocellular carcinoma: validation of the Liver Imaging Reporting And Data System v2014

Ijin Joo¹, Jeong Min Lee¹, Dong Ho Lee¹, Su Joa Ahn¹, Eun Sun Lee², and Joon Koo Han¹

¹Radiology, Seoul National University Hospital, Seoul, Korea, Republic of, ²Radiology, Chung-Ang University Hospital, Seoul, Korea, Republic of

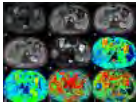
The latest Liver Imaging Reporting And Data System (LI-RADS v2014) incorporates gadoxetic acid-enhanced MRI into the diagnostic algorithm of hepatocellular carcinoma (HCC). In this study, we investigated the effects of ancillary features of gadoxetic acid-enhanced MRI in the determination of LI-RADS categories of HCCs. On gadoxetic acid-enhanced MRI, LI-RADS showed sensitivities of 69.0% and 67.8% in the diagnosis of HCCs (LR-5/5v) in two reviewers, respectively. Ancillary features of HCCs on gadoxetic acid-enhanced MRI including hepatobiliary imaging features frequently resulted in upgrade LR-3 to LR-4.

2957

Computer #47

Use of Intravoxel Incoherent Motion (IVIM) in Evaluation of Histological Differentiation of Hepatocellular Carcinoma (HCC) in Patients with Hepatitis B Virus Infection

Qungang Shan¹, Tianhui Zhang¹, Yong Zhang², Yunhong Shu³, Zhuang Kang¹, Bingjun He¹, Jingbiao Chen¹, Zhenyu Zhou², and Jin Wang¹



¹Department of Radiology, The Third Affiliated Hospital of Sun Yat-Sen University, Guangzhou, China, People's Republic of, ²GE Healthcare China, Beijing, China, People's Republic of, ³Mayo Clinic, Rochester, MN, United States

Among the various causes of hepatocellular carcinoma (HCC), hepatitis B virus (HBV) infection is the most common one in Asian countries including China. We assessed the correlation of ADC and IVIM parameters with the histological differentiation of HBV-related HCCs. Our results showed that ADC, D and f coefficients are significantly correlated with histological differentiation of HBV-related HCC. According to ROC analysis, ADC, D and f were useful parameters for the evaluation of histological differentiation of HCCs. ADC showed better diagnostic performance compared with D and f IVIM is a promising tool for predicting histological differentiation of HBV-related HCC.

2958

Computer #48



Short-Term Reproducibility of Intravoxel Incoherent Motion Parameters and Apparent Diffusion Coefficient of Large Hepatocellular Carcinoma
Lifang Wu¹

¹Fudan University, Shanghai, China, People's Republic of

More and more studies have been attributed to the evaluation of IVIM analysis for disease characterization or response assessment, but its measurement reproducibility when applied in clinical practice and research still be in controversial. There is only few prior research on repeatability of IVIM-derived parameters of hepatocellular carcinoma (HCC) as well as the choice of free-breathing (FB). In this study we used our own data to explore the reproducibility of IVIM-derived parameters, $ADC_{(0,500)}$ and ADC_{total} of HCC.

Electronic Poster

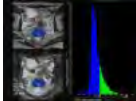
Gastrointestinal

Exhibition Hall

Monday, May 9, 2016: 15:15 - 16:15

2959

Computer #49



Correlation of Pre -Treatment Volumetric Apparent Diffusion Coefficient Histogram Analysis of Diffusion Weighted MRI in Rectal Cancer with Post ChemoRadiation Treatment Response and Clinical Outcomes.

Kartik Jhaveri¹, Vijay Chidambaram², James Brierley¹, Bernard Cummings^{1,3}, Rajesh Bhayana¹, Ravi Menezes¹, Erin Kennedy⁴, and Richard Kirsch⁴

¹UHN, university of Toronto, Toronto, ON, Canada, ²Royal Liverpool Hospital, Liverpool, United Kingdom, ³Toronto, Canada, ⁴Mt.Sinai Hospital, University of Toronto, Toronto, Canada

Rectal cancer patients treated with preoperative chemoradiation therapy with complete treatment response can be considered for individualised therapies such as 'wait and watch' avoiding surgery. However this currently can only be definitely identified by postoperative histopathology. Diffusion weighted-MRI has been well correlated to tumor biology and treatment response. Volumetric ADC histogram analysis eliminates errors resulting from tumor heterogeneity and variable diffusivities by including the tumor volume and could provide promise for prediction of treatment response and clinical outcomes, thereby providing means for individualised therapy.

2960

Computer #50



Correlation between apparent diffusion coefficients and HER2 status in gastric cancers: pilot study
Zhengyang Zhou¹, Jian He¹, Song Liu¹, and Weibo Chen²

¹Department of Radiology, Drum Tower Hospital, School of Medicine, Nanjing University, Nanjing, China, People's Republic of, ²Philips Healthcare Greater China, Shanghai, China, People's Republic of

Forty-five patients with gastric cancer underwent DWI prior to surgery to evaluate whether ADC value correlates with the HER2 status. HER2 status was compared among tumors with various histopathological features. Meanwhile, the ADC values of gastric cancers with positive and negative HER2 were compared. The mean ADC value of HER2-positive gastric cancers was significantly higher than those of HER2-negative tumors. The minimal ADC value of HER2-positive gastric cancers was significantly higher than those of HER2-negative tumors. The ADC values of gastric cancer correlate with the HER2 status. DWI can predict HER2 status and help in tailoring therapy for gastric cancer.

2961

Computer #51



Spatial registration improves parametric mapping of abdominal MRI and may allow assessment of extent of fibrosis in intestinal lesions of patients with Crohn's Disease

Elizabeth Li¹, Tim Lu¹, Alexandre Coimbra¹, and Alex de Crespigny¹

¹Genentech Inc., South San Francisco, CA, United States

Parametric mapping may provide estimates of extent of fibrosis in Crohn's Disease (CD) patients but are subject to respiratory and peristaltic motion. Various image registration strategies and their impact on quality and robustness of parametric maps of gain of enhancement (GE) and magnetization transfer ratio (MTR) were compared. Healthy test-retest and CD image datasets were evaluated. Spatial registration improved quality and test-retest reliability of GE and MTR maps. In a limited cohort, extent of fibrosis estimated with GE and MTR maps were correlated. Cross validation of MR enterography-based fibrosis estimates with histological data will be conducted as data becomes available.

2962

Computer #52



Prospective Comparison of a Contrast-Enhanced MRI Protocol with Contrast-Enhanced CT for the Primary Diagnosis of Acute Appendicitis

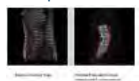
Michael Dean Replinger¹, Perry J Pickhardt², Jessica B Robbins², Tim J Ziemlewicz², Doug R Kitchin², John Brian Harringa¹, Scott Hetzel³, and Scott Brian Reeder²

¹Emergency Medicine, University of Wisconsin - Madison, Madison, WI, United States, ²Radiology, University of Wisconsin - Madison, Madison, WI, United States, ³Biostatistics and Medical Informatics, University of Wisconsin - Madison, Madison, WI, United States

The aim of our study was to determine the test characteristics of an MRI protocol consisting of unenhanced, contrast-enhanced, and DWI to diagnose appendicitis. This was a prospective study including patients ≥ 12 years old being evaluated for appendicitis. We enrolled 226 patients; all images were interpreted by three fellowship-trained abdominal radiologists. Sensitivity and specificity (95% CI) were 95.2% (86.5-99%) and 89.4% (83.2-94%) for unenhanced MRI with DWI, 96.8% (89-99.6%) and 89.9% (83.7-94.4%) for CE-MRI, and 98.4% (91.6-100%) and 93.7% (88.3-97.1%) for CE-CT. We conclude that this MRI protocol is as accurate as CE-CT to diagnose appendicitis.

2963

Computer #53



Assessment of flow in the human colon in health and constipation using an MR tagging technique

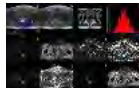
Susan Pritchard¹, Joe Paul¹, Giles Major^{2,3}, Luca Marciani^{2,3}, Penny Gowland¹, Robin Spiller^{2,3}, and Caroline Hoad^{1,2}

¹Sir Peter Mansfield Imaging Centre, University of Nottingham, Nottingham, United Kingdom, ²Nottingham Digestive Diseases Centre, University of Nottingham, Nottingham, United Kingdom, ³Nottingham Digestive Diseases Biomedical Research Unit, University of Nottingham, Nottingham, United Kingdom

Assessment of colonic motility may be extremely useful in understanding the symptoms of constipation. Current techniques (manometry, cine-MRI) can only detect wall movements and not the effect this motion may have on mixing of colonic contents. We report the use of an MR tagging technique to assess flow and mixing in the human colon following ingestion of a 500ml macrogol preparation. This technique successfully identified differences in intracolonic mixing between 11 healthy and 11 constipated subjects and shows potential to generate novel insights into the physiology and mechanisms of disease and the environmental pressures on, and effects of, gut microbiota.

2964

Computer #54



Perfusion and Diffusion Weighted Magnetic Resonance Imaging in Rectal cancer: How is the Correlation between Multiple Methods?

Xiaojuan Xiao¹, Baolan Lu¹, Xinyue Yang¹, Shenping Yu¹, Yanhong Yang¹, and Xu Yan²

¹Department of Radiology, The First Affiliated Hospital, Sun Yat-sen University, Guangzhou, China, People's Republic of, ²MR Collaboration NE Asia, Siemens Healthcare, Shanghai, China, People's Republic of

DCE-MRI, IVIM and DKI are emerging as promising tools for tumor diagnostic or therapy-predictive purposes. We performed these three methods in patients with rectal cancer simultaneously to find out their correlations. Our results showed significant correlation between perfusion sensitive parameters of IVIM and DCE-MRI. In addition, DKI parameters were calculated from data with a low (0-1000) and high (200-2000) b-value range, and the parameters from low b-value range showed significant correlation with IVIM parameters, but not for the high b-value range.

2965

Computer #55



Radiomic Features on Diagnostic Magnetic Resonance Enterography Appear to Predict Patient Outcome Following Treatment of Crohn's Disease: Preliminary Results

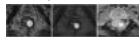
Cheng Lu¹, Maneesh Dave², H. Matthew Cohn², Prateek Prasanna¹, Jeffrey Katz², Rajmohan Paspulati³, Anant Madabhushi¹, and Satish Viswanath¹

¹Biomedical Engineering, Case Western Reserve University, Cleveland, OH, United States, ²Digestive Health Institute, University Hospital, Case Western Reserve University, Cleveland, OH, United States, ³Dept of Radiology, University Hospital, Case Western Reserve University, Cleveland, OH, United States

We present initial results of identifying radiomic features (computer-extracted image features from radiography) from baseline diagnostic Magnetic Resonance Enterography (MRE) scans to discriminate patients who will and will not respond to initial therapy for Crohn's Disease. Feature selection was employed to identify the most discriminatory features, followed by principal component analysis to identify an optimal combination of these features. In a cohort of 11 patients, the radiomic feature combination was able to successfully distinguish between responders and non-responders with only 1 misclassification. Multi-scale oriented gradient (Gabor) features appeared to best capture subtle inflammation-related imaging characteristics on MRE and hence most predictive of patient outcome.

2966

Computer #56



Application of Magnetic Resonance Fingerprinting (MRF) for assessment of rectal cancer: a feasibility study

Shivani Pahwa¹, Ziang Lu¹, Sara Dastmalchian¹, Yun Jiang², Mital Patel³, Neal Meropol³, Mark Griswold⁴, and Vikas Gulani⁵

¹Radiology, Case Western Reserve University, Cleveland, OH, United States, ²Biomedical Engineering, Case Western Reserve University, Cleveland, OH, United States, ³Hematology and Oncology, University Hospitals Case Medical Center, Cleveland, OH, United States, ⁴Radiology and Biomedical Engineering, Case Western Reserve University, Cleveland, OH, United States, ⁵Radiology, University Hospitals Case Medical Center, Cleveland, OH, United States

Accurate delineation of tumor extent and early assessment of response to treatment are open challenges in imaging evaluation of

colorectal tumors. Quantitative imaging methods as relaxometry have been explored to fulfill this unmet need, but not adopted in clinical practice due to long acquisition time. In this feasibility study, we examined the relaxation time of rectal tumors, mesorectum and rectal wall using magnetic resonance fingerprinting (MRF)

2967



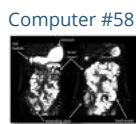
Volumetric dynamic MR-defecography

Valentin Ratz¹, Tobias Wech¹, Andreas Schindele², Alexander Sauer¹, Alexander Dierks¹, Joachim Reibetanz³, Alfio Borzi², Thorsten Bley¹, and Herbert Köstler¹

¹Institute of Diagnostic and Interventional Radiology, University Hospital Würzburg, Würzburg, Germany, ²Institute of Mathematics, University Würzburg, Würzburg, Germany, ³Department of General-, Visceral-, Vascular- and Pediatric Surgery, University Hospital Würzburg, Würzburg, Germany

Current 2D MR-defecography techniques lack information about lateral localized pathologies. The purpose of this project was to implement a dynamic 3D MR-defecography which covers a larger area and thereby gathers more detailed information on the anatomy during defecation. Therefore we implemented a radial 3D TrueFISP Stack of Stars sequence with density-weighting and view-sharing. The highly undersampled datasets, which we have acquired in 5 patients, were reconstructed using a modified FISTA compressed sensing algorithm. The proposed method allows for a dynamic 3D examination of the fast defecation process. Therefore the detection of lateral localized pathologies is possible as well.

2968



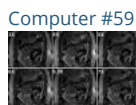
Use of magnetic resonance imaging to assess the effects of corticotrophin releasing factor on fructose malabsorption

Kathryn Murray¹, Ching Lam², Sumra Rehman³, Caroline Hoad¹, Luca Marciani², Carolyn Costigan¹, Melanie Lingaya², Rawinder Banwait², Stephen Bawden¹, Robin Spiller², and Penny Gowland¹

¹Sir Peter Mansfield Imaging Centre, School of Physics and Astronomy, University of Nottingham, Nottingham, United Kingdom, ²NIHR Nottingham Digestive Diseases Biomedical Research Unit, University of Nottingham, Nottingham, United Kingdom, ³University of Nottingham, Nottingham, United Kingdom

A link between FODMAP malabsorption and stress has been suggested. Here, the effects of corticotrophin releasing factor (CRF) on fructose malabsorption are investigated in this randomised, placebo-controlled, crossover study in healthy volunteers.

2969



Compressed Sensing and Parallel Imaging (CS-PI) Reconstruction of Prospectively Undersampled Dynamic MRI for Faster Imaging of Bowel Motility

Abdallah G. Motaal¹, Catharina S. de Jonge¹, Wouter V. Potters¹, Bram F. Coolen¹, Aart J. Nederveen¹, and Jaap Stoker¹

¹Radiology Department, 3T Lab, Academic Medical Center, Amsterdam, Netherlands

Motility assessment of the small bowel using dynamic MRI can only be acquired with either a limited coverage of the intestines or relatively low temporal resolution, which obscures details of motion during contraction and relaxation. Compressed sensing and parallel imaging (CS-PI) techniques allow higher temporal resolution imaging by acquiring and reconstructing undersampled acquisitions. In this abstract we show that by using CS-PI, accelerations up to 7X could be achieved, which outperforms conventional approaches based on parallel imaging only. As a consequence, CS-PI provides a valuable tool for improved assessment of small bowel motility.

2970



R2* estimation with CSI: A Pilot and Feasibility Study

Eamon K Doyle, MS¹, Jonathan M Chia, MS², Krishna S Nayak, PhD^{3,4}, and John C Wood, MD, PhD^{4,5}

¹Biomedical Engineering, University of Southern California, Sierra Madre, CA, United States, ²Philips Healthcare, Cleveland, OH, United States, ³Electrical Engineering, University of Southern California, Los Angeles, CA, United States, ⁴Biomedical Engineering, University of Southern California, Los Angeles, CA, United States, ⁵Cardiology, Children's Hospital of Los Angeles, Los Angeles, CA, United States

R2 (1/T2) and R2* (1/T2*) are useful metrics related to tissue iron loads. Clinical iron estimation at 3T is limited by the achievable echo times in Cartesian spin echo and gradient echo imaging. We present a modified CSI spectroscopy sequence robust to motion for high SNR liver R2* estimation with the potential for simultaneous R2 estimation.

2971



Correlation between intravoxel incoherent motion (IVIM) and dynamic contrast-enhanced magnetic resonance imaging (DCE-MRI) parameters in rectal cancer

Yanyan Xu¹, Hongliang Sun¹, Kaining Shi², and Wu Wang¹

¹Radiology, China-Japan Friendship hospital, Beijing, China, People's Republic of, ²Philips Healthcare China, Beijing, China, People's Republic of

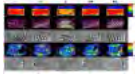
Dynamic contrast-enhanced magnetic resonance imaging (DCE-MRI) has been applied in rectal cancer for the purpose of characterizing tumor perfusion[1]. However, DCE-MRI should use intravenous contrast media based gadolinium, which will increase the risk of kidney systemic fibrosis[2]. The bi-exponential analysis in intravoxel incoherent motion (IVIM) model can separate microscopic circulation perfusion with pure water diffusion[3-4]. Correlation has been derived between the IVIM perfusion parameters f and D* and the classical perfusion parameters[5-6]. However, its relationship with DCE-MRI parameters in rectal cancer has not been clarified.

2972



Simple improvement method of uniformity of MR elastography on liver

Yuki Kanazawa¹, Yuki Matsumoto², Hiroaki Hayashi¹, Tsuyoshi Matsuda³, Mungunbagana Ganbold⁴, and Masafumi Harada⁴



¹Tokushima University, Tokushima, Japan, ²School of Health Sciences, Tokushima University, Tokushima, Japan, ³MR Applications and Workflow, Asia Pacific GE Healthcare Japan Corporation, Hino, Japan, ⁴Department of Radiology and Radiation Oncology, Tokushima University, Tokushima, Japan

The purpose of this study was to development and evaluate a dual passive driver system to improve non-uniformity of liver MRE. This study was performed using a phantom and a volunteer. The standard deviation on unwrapped phase image (S.D._{unwrap}) for the dual driver system has shown higher values than that of a single system. Moreover, the shear stiffness value of a system having a high S.D._{unwrap} showed the highest correlation with actual measurement values ($P < .05$). In conclusion, MRE with a dual driver system may render it possible to obtain more detailed information for the evaluation of liver conditions.

2973

Computer #63



Contrast-Enhanced Perianal Fistula Imaging with Dixon-Based Fat Suppression

Eric G. Stinson¹, Joshua D. Trzasko¹, Eric A. Borisch¹, Phillip M. Young¹, Joel G. Fletcher¹, and Stephen J. Riederer¹

¹Radiology, Mayo Clinic, Rochester, MN, United States

Perianal fistula images with high spatial resolution, high SNR, and excellent fat suppression were achieved with a multi-TE interleaved acquisition and a constrained-phase graph cuts-based Dixon fat/water separation.

2974

Computer #64



FDG-PET-MR acquisition in systemic sclerosis for the assessment of gastrointestinal involvement: a pilot study

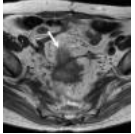
Stephanie Marchesseau¹, Sue-Ann P.L Ng², Andrea H.L. Low^{2,3}, YT Wang⁴, Jamie X.M Ho¹, Josh D. Schaefferkoetter¹, and John J. Totman¹

¹Clinical Imaging Research Centre, NUS, Singapore, Singapore, ²Departement of Rheumatology and Immunology, SGH, Singapore, Singapore, ³Duke-National University, Singapore, Singapore, ⁴Department of Gastroenterology and Hepatology, SGH, Singapore, Singapore

Systemic sclerosis (SSc) is a multi-system disease characterized by immune dysregulation, fibrosis and vascular damage that affects the gastrointestinal tract in most patients. In this study, we investigate simultaneous FDG-PET/MR imaging for the diagnosis of SSc GIT involvement. Our preliminary results show that FDG-PET can detect inflammation in the bowels while T1 MOLLI mapping could be able to distinguish healthy from fibrotic GIT tissue.

2975

Computer #65



Rectal Cancer: Apparent Diffusion Coefficient Value and Clinical-Pathologic Factors Associated with Local Recurrence or Distant Metastases

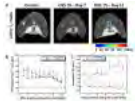
Yoshifumi Noda¹, Satoshi Goshima¹, Hideto Tomimatsu¹, Haruo Watanabe¹, Hiroshi Kawada¹, Nobuyuki Kawai¹, Hiromi Ono¹, Masayuki Matsuo¹, and Kyongtae T Bae²

¹Radiology, Gifu University Hospital, Gifu, Japan, ²Radiology, University of Pittsburgh Medical Center, Pittsburgh, PA, United States

To determine the ADC value and clinical-pathologic risk factors associated with postoperative local recurrence or distant metastases in patients with rectal cancer. The plasmatic CA19-9 level ($P = 0.0027$), pathological N stage ($P = 0.0018$), lymphatic invasion ($P < 0.0001$), and ADC value ($P = 0.0076$) were independently associated with postoperative local recurrence or distant metastases in the patients with rectal cancer. Among the several indicators, the tumor ADC values and plasmatic CA19-9 level can be useful for the preoperative prediction of high risk cases for postoperative local recurrence or distant metastases in patients with rectal cancer.

2976

Computer #66



Assessing mucosal inflammation in a DSS-induced colitis mouse model by MR Colonography

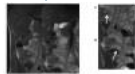
Inbal E Biton¹, Noa Stettner¹, Ayelet Erez², Alon Harmelin¹, and Joel R Garbow³

¹Department of Veterinary Resources, Weizmann Institute of Science, Rehovot, Israel, ²Department of Biological Regulation, Weizmann Institute of Science, Rehovot, Israel, ³Biomedical Magnetic Resonance Laboratory, Mallinckrodt Institute of Radiology, Washington University, St. Louis, MO, United States

Inflammatory bowel disease (IBD) is characterized by uncontrolled inflammation of the gastrointestinal tract [1]. Determining the inflammatory state of the colon is critical for defining the disease activity. Endoscopy in human IBD allows visualization of mucosal inflammation [2]. However, the technique is based on grading of the entire colon, which is operator dependent. The mucosa is very fragile, therefore endoscopic evolution is problematic. Therefore, the development of an improved, noninvasive, objective MRI technique may provide a non-invasive assessment tool to depict pathologies in the small intestinal mucosa and, more specifically, along the colon, and to assess the bowel wall and surrounding structures. In this study, dextran sodium sulphate (DSS) polymer treatment was used to induce acute colitis in mice that was subsequently characterized by multi-slice MR colonography.

2977

Computer #67



Application of variable refocusing flip angle SSFSE T2 for improved MR Enterography in Pediatric Patients

Yi Li¹, Daniel Litwiller², Pauline Worters³, Ersin Bayram⁴, John MacKenzie¹, and Jesse Courtier¹

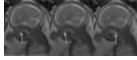
¹Department of Radiology, University of California San Francisco, San Francisco, CA, United States, ²Global MR Applications and Workflow, GE Healthcare, Rochester, MN, United States, ³Global MR Applications and Workflow, GE Healthcare, Menlo Park, CA, United States, ⁴Global MR Applications and Workflow, GE Healthcare, Houston, TX, United States

MR enterography is the modality of choice for the imaging of inflammatory bowel disease, but presents unique challenges in the pediatric population, particularly with respect to motion degradation. Variable refocusing flip angle single shot fast spin echo (vrfSSFSE), an improvement upon the traditional single shot fast spin echo (SSFSE) sequence, allows for shortened acquisition times and improved

contrast and spatial resolution. Clinical use of vrfSSFP in pediatric MR enterography has led to subjective improvements in image quality and has allowed for improved identification of many imaging findings related to inflammatory bowel disease.

2978

Computer #68



Evaluation of bSSFP for the visualisation of Human fetal esophageal and tracheal obstruction and swallowing
Andrew Fry¹, Elspeth Whitby², and Peter Wright¹

¹Medical Physics, Sheffield Teaching Hospitals NHS Foundation Trust, Sheffield, United Kingdom, ²Academic Unit of reproductive and developmental medicine, University of Sheffield, Sheffield, United Kingdom

A balanced steady-state free precession (bSSFP) sequence gives excellent fluid/tissue contrast and allows rapid repeat acquisition of a single slice, resulting in a cine image dataset. We evaluate the bSSFP sequence to image fetal swallowing action and passage of fluid in the esophagus and airway in 7 human fetuses. Regurgitation of amniotic fluid is observed where major or total obstruction is present. Optimised bSSFP sequences are demonstrated at 1.5T and 3.0T and can be used in assessment of obstruction and swallowing in a wide variety of cases including esophageal atresia, neck masses, CHAOS and cleft palate.

2979

Computer #69



Correcting for the Effect of Motion using Simultaneous Image Registration and Model Estimation (SIR-ME) in Abdominal DW-MRI
Sila Kurugol¹, Moti Freiman¹, Onur Afacan¹, Liran Domachevski², Jeanette M. Perez-Rossello¹, Michael J. Callahan¹, and Simon K. Warfield¹

¹Radiology, Boston Children's Hospital and Harvard Medical School, Boston, MA, United States, ²Nuclear Medicine, Rabin Medical Center, Petah-Tikva, Israel

Quantitative diffusion-weighted MRI (DW-MRI) has been increasingly used for the detection and characterization of abdominal abnormalities. However, respiratory, cardiac and peristalsis motion deteriorates robustness and reproducibility of parameter estimation in DW-MRI. Current solutions do not entirely correct for motion and have disadvantages such as increased scan time. In this work, we introduce a simultaneous image registration and model estimation (SIR-ME) framework for motion-compensated parameter estimation. The proposed method improved the goodness-of-fit by more than 50% and estimated model parameters more precisely, resulting in better discrimination between normal and diseased bowel loops, which will potentially impact clinical utilization.

2980

Computer #70



DWIBS Improves the Detection of Extra-Hepatic Colorectal Cancer Metastases. A Prospective Study.

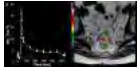
Kim Sivesgaard¹, Maria Louise Jöhnk², Lars Peter Skovgaard Larsen¹, Michael Sørensen³, Stine Kramer³, Flemming Hansen², and Erik Morre Pedersen¹

¹Department of Radiology, Aarhus University Hospital, Aarhus, Denmark, ²Department of Oncology, Aarhus University Hospital, Aarhus, Denmark, ³PET-centre, Aarhus University Hospital, Aarhus, Denmark

A whole body (WB) MRI protocol added to a dedicated liver MRI in one scan session, could alleviate the need for a PET/CT for staging patients prior to local treatment of colorectal liver metastases. With the aim of developing a disease optimised WB protocol, 30 patients with extra-hepatic metastases from colorectal cancer were prospectively recruited and scanned on a 1.5 T scanner and using a PET/CT scan within an average of 1.33 days as reference. Preliminary results show that combining a traditional whole body MRI protocol with DWIBS produces superior results compared to the traditional protocol alone.

2981

Computer #71



Dynamic multi-echo MRI of rectal cancer: Quantitative tumor R_2^* analysis predicts lymph node status

Endre Grøvik^{1,2}, Kathrine Røe Redalen³, Sebastian Meltzer^{3,4}, Anne Negård⁵, Stein Harald Holmedal⁵, Anne Hansen Ree^{3,4}, Tryggve Holck Storås¹, Atle Bjørnerud^{1,2}, and Kjell-Inge Gjesdal⁶

¹The Intervention Centre, Oslo University Hospital, Oslo, Norway, ²Department of Physics, University of Oslo, Oslo, Norway, ³Department of Oncology, Akershus University Hospital, Lørenskog, Norway, ⁴Faculty of Medicine, University of Oslo, Oslo, Norway, ⁵Department of Radiology, Akershus University Hospital, Lørenskog, Norway, ⁶Sunnmøre MR klinikk AS, Ålesund, Norway

The purpose was to evaluate the association between the dynamic change in R_2^* , obtained from a multi-echo dynamic contrast-based acquisition, and clinicopathologic data in patients with rectal cancer. Twenty patients were examined using a high temporal resolution multi-echo EPI sequence. Dynamic R_2^* images were calculated by assuming a mono-exponential dependence of signal change on echo-time, and parametric images representing the maximum peak change in R_2^* , ΔR_2^* -peak, were generated. Tumor ΔR_2^* -peak significantly differentiate between rectal cancer patients with and without nodal metastases ($P=0.01$), with an area under the ROC curve of 0.94.

Electronic Poster

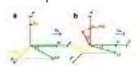
Contrast Mechanisms: Electromagnetic Based & Others

Exhibition Hall

Monday, May 9, 2016: 15:15 - 16:15

2982

Computer #73



Spectral analysis enhances the detectability of rotary saturation contrast

Jingwei Sheng¹, Yuhui Chai¹, Bing Wu², Yang Fan², and Jia-Hong Gao¹

¹Center for MRI Research, Peking University, Beijing, China, People's Republic of, ²GE Healthcare MR Research China, Beijing, China, People's Republic of

Traditional rotary saturation based methods requires triggered phases to create a robust signal change, which may not be satisfied in practical application. In this work, based on the analysis of magnetization in the double rotating frame, we proposed detecting the signal fluctuations of proposed SLOE method by manipulating TRs, which needs no triggering. Further, a spectral statistical test in the frequency domain was proposed and verified, which featured an enhanced detection sensitivity than that of deviation test.

2983

Computer #74



QUANTITATIVE SUSCEPTIBILITY MAPPING OF THE LIVER AND SPLEEN IN SUBJECTS WITH FERUMOXYTOL INJECTION

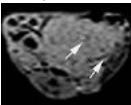
Samir D. Sharma¹, Timothy J. Colgan¹, Camilo A. Campo¹, Tilman Schubert¹, Utaroh Motosugi², Diego Hernando¹, and Scott B. Reeder^{1,3}

¹Radiology, University of Wisconsin - Madison, Madison, WI, United States, ²Radiology, University of Yamanashi, Yamanashi, Japan, ³Medical Physics, University of Wisconsin-Madison, Madison, WI, United States

Ferumoxytol is an ultrasmall superparamagnetic iron oxide (USPIO) agent that is taken up by the reticuloendothelial system where it accumulates in organs such as the liver, spleen, and bone marrow. Given the superparamagnetic properties of ferumoxytol, it may be possible for quantitative susceptibility mapping (QSM) techniques to detect and quantify the concentration of ferumoxytol in these organs. Recent technical developments have demonstrated the feasibility of a QSM technique for magnetic susceptibility mapping of the abdomen. Thus, the purpose of this work was to test the feasibility of QSM to assess the longitudinal changes of ferumoxytol in the liver and spleen.

2984

Computer #75



Contrast-Enhanced Susceptibility Weighted Imaging with Ultrasmall Superparamagnetic Iron Oxide Improves the Detection of Tumour Vasculature in A HCC-LM3 Nude Mouse Model

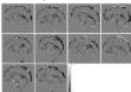
Shuohui Yang¹, Jiang Lin¹, Fang Lu², Yuanyuan Dai¹, Zhihong Han³, and Caixia Fu⁴

¹Radiology, Zhongshan Hospital, Shanghai Medical College, Fudan University, Shanghai, China, People's Republic of, ²Radiology, Shuguang Hospital, Shanghai University of Traditional Chinese Medicine, Shanghai, China, People's Republic of, ³Pathology, Shuguang Hospital, Shanghai University of Traditional Chinese Medicine, Shanghai, China, People's Republic of, ⁴Siemens Shenzhen Magnetic Resonance Ltd., Shenzhen, China, People's Republic of

Hepatocellular carcinoma (HCC) is a hyper-vascular tumor and knowledge of the intratumoral vasculature is essential. Susceptibility weighted imaging (SWI) uses magnitude and filtered-phase information to provide high sensitivity to susceptibility changes caused by hemorrhage, calcium, iron, and small veins. It has been used to visualize normal or pathologic vascular structures that are not visible on conventional MRI. Ultrasmall superparamagnetic iron oxide (USPIO) is an intravascular blood pool contrast medium. After intravenous administration, it can cause a greater effect on local magnetic field inhomogeneities and results in higher susceptibility differences between all intratumoral vessels and the tumor on SWI. This study showed that USPIO-enhanced SWI could further enhance the demonstration of tumor vasculature inside HCC when compared to unenhanced SWI in an orthotopic xenograft nude mice HCC model.

2985

Computer #76



Using frequency difference mapping to assess white matter microstructure in the human corpus callosum

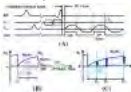
Benjamin Tandler¹ and Richard Bowtell¹

¹Sir Peter Mansfield Imaging Centre, University of Nottingham, Nottingham, United Kingdom

Frequency difference mapping (FDM) is a recently developed phase-based technique that takes advantage of the non-linear temporal evolution of the phase in GE sequences to produce images that are sensitive to white matter microstructure. Images can be produced simply from raw phase data, with minimal post-processing. In this study 10 subjects underwent six repeats of a single-slice, sagittal multi-echo GE scan on the mid-line. Frequency difference maps reproducibly depicted white matter tracts oriented perpendicular to the applied field. Fitting the FD and magnitude data to a three-pool model provided insight into the variation of microstructure along the corpus callosum.

2986

Computer #77



Can myelin protons be directly imaged with the adiabatic inversion recovery prepared ultrashort echo time (IR-UTE) sequence - a validation study based on D2O exchange in sheep brain specimens

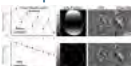
Hongda Shao¹, Soorena Azam ZAnganeh¹, Rong Luo¹, Jun Chen¹, Graeme Bydder¹, and Jiang Du¹

¹Radiology, University of California, San Diego, San Diego, CA, United States

Directly assessing the integrity of myelin in white matter is important for diagnosis and assessment of prognosis in multiple sclerosis (MS). However, the protons in myelin have extremely short T₂s and cannot be directly imaged with conventional clinical MRI sequences. Adiabatic inversion recovery prepared ultrashort echo time (IR-UTE) sequences can detect signal from myelin protons and efficiently suppress the signal from water. In this study we aimed to further validate the IR-UTE technique in sheep brain using a D₂O exchange model.

2987

Computer #78



Phase Correction of a Bipolar Gradient-Echo Acquisition for Quantitative Susceptibility Mapping

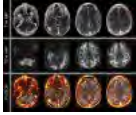
Hongfu Sun¹, M. Ethan MacDonald¹, and G. Bruce Pike¹

¹University of Calgary, Calgary, AB, Canada

A method to remove phase offsets in bipolar gradient-echo readouts is proposed. Their effects on Quantitative Susceptibility Mapping (QSM) reconstruction are demonstrated by comparing QSM before and after phase offsets removal.

2988

Computer #79



High Resolution Blood Vessel Imaging with USPIOs in the Human Brain: T1 vs T2* contrast.

Thomas Christen¹, Samantha Holdsworth¹, Samuel Cheshier², Michael Moseley¹, Greg Zaharchuk¹, and Kristen Yeom¹¹Radiology, Stanford University, Palo Alto, CA, United States, ²Neurosurgery, Stanford University, Stanford, CA, United States

In this study, we probed the potential of ultrasmall superparamagnetic iron oxide particles (USPIOs) to provide high-resolution angiographic images of the human brain using T2* and T1 contrasts. 10 paediatric patients suspected of arteriovenous malformations (AVM) were scanned pre and post intravenous USPIOs injection as part of their clinical exam. To test the influence of USPIOs concentration on both T2* and T1 images, a healthy volunteer was scanned before and after injections of 7 incremental doses of the contrast agent. The results suggest that both approaches can provide exquisite details of the neurovascular anatomy while offering complementary information.

2989

Computer #80

Artifacts Affecting Derivative of σ maps for EPT ReconstructionsStefano Mandija¹, Alessandro Sbrizzi¹, Astrid L.H.M.W. van Lier¹, Peter R. Luijten¹, and Cornelis A.T. van den Berg¹¹Center For Image Sciences, UMC Utrecht, Utrecht, Netherlands

EPT conductivity reconstruction is affected by difficulties to reliably calculate spatial derivatives on voxelized MRI data. Here, we explore the impact of several numerical approximations. In particular: the different size of finite-difference kernels and the k-space truncation (always present in MR images). We also explore a Fourier-domain alternative, which does not require finite-difference approximation kernels.

2990

Computer #81



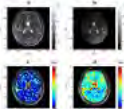
Comparison of Multi-transmit Microstrips and Loops for Electrical Properties Tomography (EPT) in the Breast at 3T

Yicun Wang¹, Gregor Adriany², Jiaen Liu¹, Xiaotong Zhang¹, Pierre-Francois Van de Moortele², and Bin He^{1,3}¹Department of Biomedical Engineering, University of Minnesota, Minneapolis, MN, United States, ²Center for Magnetic Resonance Research, University of Minnesota, Minneapolis, MN, United States, ³Institute for Engineering in Medicine, University of Minnesota, Minneapolis, MN, United States

Electrical Properties Tomography (EPT) is a promising technique to provide high specificity in breast cancer diagnosis. Previous studies have demonstrated that multi-transmit coils array enables reconstruction of the electrical properties free of transmit phase and local homogeneity assumptions. In this study, the strengths and drawbacks of a microstrip array and a loop array for EPT reconstruction in the breast at 3T were investigated based on numerical simulations. It has been discovered that with the same driving power, a loop array provides higher signal to noise ratio on the reconstructed image while a microstrip array performs better at delineating tissue boundaries.

2991

Computer #82



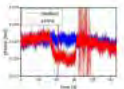
Generalized Phase based Electrical Conductivity Imaging

Necip Gurler¹ and Yusuf Ziya Ider¹¹Electrical and Electronics Engineering, Bilkent University, Ankara, Turkey

In this study, a new formulation for phase based electrical properties tomography (EPT) has been proposed to eliminate the boundary artifact issue and to provide robustness against noise. The feasibility of the proposed method, which is called "generalized phase based EPT", has been demonstrated using simulation, experimental phantom, and in vivo experiments.

2992

Computer #83



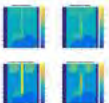
Applying „Electric Properties Tomography“ to Low Frequency Conductivity Using Magnetic Particle Imaging

Ulrich Katscher¹, Jürgen Rahmer¹, Christian Stehning¹, Peter Vernickel¹, and Bernhard Gleich¹¹Philips Research Europe, Hamburg, Germany

MRI-based "Electric Properties Tomography" (MRI-EPT) determines electric conductivity measuring and post-processing the spatial distribution of the TX RF field. Obtained conductivity corresponds to Larmor frequency, reflecting biochemical content of tissue, but not its specific cellular structure. Cellular tissue structure is reflected by conductivity at low frequency (LF, 100-500 kHz), as used for "Magnetic Particle Imaging" (MPI). Similar to MRI, MPI is able to determine the spatial distribution of applied LF field, and thus, a reconstruction of LF conductivity should be possible ("MPI-EPT") in analogy to MRI-EPT. This study investigated the principle feasibility of MPI-EPT and compared results with MRI-EPT.

2993

Computer #84



Global Maxwell Tomography: a novel technique for electrical properties mapping without symmetry assumptions or edge artifacts

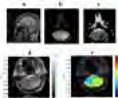
Jose E.C. Serralles¹, Athanasios Polimeridis², Manushka V. Vaidya^{3,4}, Gillian Haemer^{3,4}, Jacob K. White¹, Daniel K. Sodickson^{3,4}, Luca Daniel¹, and Riccardo Lattanzi^{3,4}¹Research Laboratory of Electronics, Massachusetts Institute of Technology, Cambridge, MA, United States, ²Center for Computational and Data-Intensive Science and Engineering, Skolkovo Institute of Science and Technology, Moscow, Russian Federation, ³Center for Advanced Imaging Innovation and Research (CAI2R) and Center for Biomedical Imaging, Department of Radiology, New York University School of Medicine, New York, NY, United States, ⁴The Sackler Institute of Graduate Biomedical Science, New York University School of Medicine, New York, NY, United States

We introduce Global Maxwell Tomography (GMT), a novel volume integral equation-based technique for the extraction of electric

properties from MR data. GMT is framed as an unconstrained optimization problem in which the error between measured and simulated B1+ magnitude maps is minimized. Due to its global nature, GMT is not subjected to edge artifacts. By using exclusively B1+ magnitude, GMT does not rely on symmetry assumptions to estimate B1+ phase. In one numerical example, three tumors were inserted into a head model, and starting from a tumorless initial guess, GMT accurately inferred the electrical properties and locations of these tumors.

2994

Computer #85



Application of Generalized Phase based Electrical Conductivity Imaging in the Subacute Stage of Hemorrhagic and Ischemic Strokes
Necip Gurler¹, Omer Faruk Oran¹, Hava Donmez Keklikoglu², and Yusuf Ziya Ider¹

¹Electrical and Electronics Engineering, Bilkent University, Ankara, Turkey, ²Department of Neurology, Yıldırım Beyazıt University Atatürk Education and Research Hospital, Ankara, Turkey

In this study, clinical applicability of the recently proposed generalized phase based EPT method has been investigated for two patients with neurovascular diseases in the subacute phase, i.e. hemorrhagic and ischemic stroke. In the case of ischemia, conductivity was found to be increased in the lesion area. In the case of hematoma, although the conductivity of the surrounding edema region was found to be increased, the conductivity in the hematoma region itself was found to be similar to that of brain tissue.

2995

Computer #86



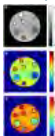
Investigation and Reduction of the Effects of Gibbs Ringing in SSFP Phase Based MR-EPT
Gokhan Ariturk¹, Necip Gurler¹, and Yusuf Ziya Ider¹

¹Electrical and Electronics Engineering, Bilkent University, Ankara, Turkey

Phase based MR-EPT methods mainly make use of the balanced SSFP since it is a fast MRI sequence. As SSFP sequence yields high magnitude contrast variations, Gibbs artifacts occur at tissue boundaries. This artifact manifests itself as phase spikes and oscillations at and near tissue boundaries respectively. The commonly used image enhancement methods, for reducing the ringing artifact, mainly focus on the magnitude images, leaving out the phase images. Throughout simulation and phantom experiment results, we investigate and propose a method for the reduction of the effect of ringing artifact on phase based MR-EPT studies.

2996

Computer #87



Validation study of water-content-assisted electrical properties tomography (wEPT) with an electrolyte protein phantom and B1 inhomogeneity consideration
Eric Michel¹ and Soo Yeol Lee¹

¹Kyung Hee University, Suwon, Korea, Republic of

New MRI-based tissue electrical properties (EPs) mapping techniques had achieved higher accuracy and resolution increasing its chances to be used in several clinical applications. In this work, we describe a validation study for a technique called water-content-assisted electrical properties tomography (wEPT) based on in situ measurements of a brain-tissue-like phantom created by electrolytic protein solutions. The influence of inhomogeneous radiofrequency field distributions and its impact in wEPT reconstructions is also analyzed. Significant consistency between in vivo brain tissue estimations and phantom measurements was found, supporting the formalism and validity of wEPT for EPT studies.

2997

Computer #88



Peripheral Nerve Imaging using 2-point Dixon 3D Fast Spine Echo (CUBE-FLEX) with Flow-Saturation Preparation (FSP): Initial Feasibility Study
Darryl Sneag¹, Mitsuharu Miyoshi², Maggie Fung³, Daniel Litwiller³, and Hollis Potter¹

¹Hospital for Special Surgery, New York, NY, United States, ²GE Healthcare, Hino, Japan, ³GE Healthcare, New York, NY, United States

High-resolution MRI currently plays an important role in diagnostic management of peripheral nerve pathology. Peripheral nerves, however, pose particular imaging challenges that conventional sequences frequently cannot address. Their small size and oblique course between muscles and alongside vessels may inhibit reliable identification. We propose a 2-point Dixon fat/water separation 3D fast spin echo technique to achieve uniform fat suppression, combined with a flow-saturation prep pulse to suppress moving vascular spins to improve nerve visualization. The objective of this study was to assess the technique's feasibility and potential diagnostic utility in evaluating peripheral nerves throughout the body.

2998

Computer #89



Enforcing a Physical Tissue Model for Partial Volume MR Fingerprinting
Anagha Deshmane¹, Debra F. McGivney², Yun Jiang¹, Dan Ma², and Mark A. Griswold²

¹Biomedical Engineering, Case Western Reserve University, Cleveland, OH, United States, ²Radiology, Case Western Reserve University, Cleveland, OH, United States

We present a method to compute fraction maps of tissue types using a subset of three dictionary entries chosen specifically for each individual, enforcing consistency with a physical tissue model. This approach removes erroneous partial volumes in the fraction maps, and reduces noise and distortions in T1, T2, and M0 maps.

2999

Computer #90

Continuously Adjustable Fat Suppression Image Contrast with one MRI Acquisition
Kecheng Liu¹, Xiaodong Zhong¹, Dan Ma², Brian Dale¹, and Mark Griswold²



¹Siemens Healthcare USA Inc., Malvern, PA, United States, ²Case Western Reserve University, Cleveland, OH, United States

Fat suppression or saturation (FatSat) is widely used in MRI applications, which reduces the fat signal and preserves water signal for clinical diagnosis, enhancing potential pathological changes. Different degree of FatSat yields different image contrast. However, when radiologists read FatSat images, they have different contrast preferences. To provide such variable preferences is not trivial because it typically costs more imaging time to re-acquire another contrast of FatSat image by adjusting imaging parameters. This work presents an alternative approach to provide continuously adjustable image contrast of FatSat images with only one acquisition.

3000

Computer #91



Spin Echo Dynamics as Codes for Quantitative Imaging
Gigi Galiana¹

¹Diagnostic Radiology, Yale University, New Haven, CT, United States

Recent work has highlighted the complicated and distinctive dynamics that shape the signal observed during an irregularly-spaced train of spin echoes. Here, we use those signals as codes that allows us to identify mixtures of molecules that are too similar to distinguish by standard spectroscopy. Extensions to water based systems, where relaxation mechanisms are the primary driver of signal dynamics, will also be presented.

3001

Computer #92



Dual-pathway sequences for MR thermometry: When and where to use them

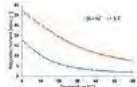
Pelin Aksit Ciris¹, Cheng-Chieh Cheng², Chang-Sheng Mei³, Lawrence P. Panych², and Bruno Madore²

¹Department of Biomedical Engineering, Akdeniz University, Antalya, Turkey, ²Department of Radiology, Brigham and Women's Hospital, Harvard Medical School, Boston, MA, United States, ³Department of Physics, Soochow University, Taipei, Taiwan

Dual-pathway sequences have been proposed to improve the temperature-to-noise-ratio (TNR) in MR thermometry. The present work establishes how much improvement these sequences may bring for various tissue types. Simulation results were validated against analytical equations, phantom and in vivo human results. PSIF-FISP thermometry allowed TNR improvements for kidney, pelvis, spleen or gray matter, and up to 2-3 fold reductions in TR with 20% TNR gains were achievable. Further TNR benefits are expected for heated tissues, due to heating-related changes in relaxation rates. In other tissue types such as liver, muscle or pancreas improvements were observed only for short TR settings.

3002

Computer #93



T2* Based MRI Temperature Contrast

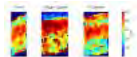
Janusz Henryk Hankiewicz¹, Jason Nobles¹, Zbigniew Celinski¹, Karl Stupic², and Robert Camley¹

¹UCCS Center for Biofrontiers Institute, University Colorado Colorado Springs, Colorado Springs, CO, United States, ²National Institute of Standards and Technology, Boulder, CO, United States

The aim of this study was to develop a novel temperature-sensitive MRI contrast agent based on temperature changes of the magnetic moment of magnetic particles. Gadolinium was used to test the hypothesis that magnetic particles will create a temperature-dependent local dipole magnetic field. This effect was locally visible as a temperature dependent darkening on gradient-echo MRI images. Shades of gray within the images can then be calibrated to map the local temperatures in specific areas of tissue during medical procedures. The estimated accuracy of temperature determination deep in the phantom using MR image intensity is $\pm 1.8^\circ\text{C}$, at 37°C .

3003

Computer #94



Correlation time mapping of degenerated human and bovine articular cartilage reveals tissue structure and degenerative changes

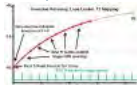
Hassaan Elsayed^{1,2,3,4}, Matti Hanni^{2,3,4}, Jari Rautiainen^{2,3,5}, Mikko Johannes Nissi^{5,6}, and Miika Nieminen^{2,3,4}

¹Computer Science and Engineering, University of Oulu, Oulu, Finland, ²Research Unit of Medical Imaging, Physics and Technology, University of Oulu, Oulu, Finland, ³Medical Research Center, University of Oulu and Oulu University Hospital, Oulu, Finland, ⁴Department of Diagnostic Radiology, Oulu University Hospital, Oulu, Finland, ⁵Department of Applied Physics, University of Eastern Finland, Kuopio, Finland, ⁶Diagnostic Imaging Center, Kuopio University Hospital, Kuopio, Finland

Correlation time (τ_c) maps were obtained by fitting τ_c from T_2^* dispersion measurements of human articular cartilage specimens and enzymatically digested bovine samples to develop a new MRI contrast which characterizes tissue properties at molecular level. τ_c revealed the laminar appearance in control and PG depleted bovine specimens, which was not observable in the collagen-digested specimens. The laminar appearance was also visible in the early OA human specimens, in contrast to the advanced OA group. The results demonstrated that τ_c mapping is a potential method for providing information about the articular cartilage structure and associated changes with degeneration.

3004

Computer #95



Cardiac in vivo T1-Mapping with Novel Reactive Oxygen Species Sensing Agent Specifically Detects Cardiac Oxidative Stress in Doxorubicin-treated Rats

Ronald J Beyers¹, Meng Yu², Dean Schwartz³, Nouha Salibi^{1,4}, Christian Goldsmith⁵, and Thomas Denney¹

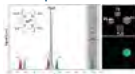
¹MRI Research Center, Auburn University, Auburn University, AL, United States, ²Chemistry & Biochemistry, Auburn University, Auburn University, AL, United States, ³Anatomy, Physiology and Pharmacology, Auburn University, Auburn University, AL, United States, ⁴MR R&D, Siemens Healthcare, Malvern, PA, United States, ⁵Chemistry and Biochemistry, Auburn University, Auburn University, AL, United States

Pathological cardiac oxidative stress causes cardiac dysfunction and possible cardiac failure. We developed a novel reactive oxygen

species sensing T1 agent (H4qpt2) and applied it with *in vivo* cardiac T1 mapping MRI at 7T in a doxorubicin-treated (Dox) rat model. Cardiac T1 mapping with H4qpt2 specifically detected significantly shortened myocardial T1 in Dox rats while no change in T1 occurred in skeletal muscle or control rats with H4qpt2. This new H4qpt2 agent combined with cardiac or non-cardiac T1 mapping may advance the early detection of oxidative stress in multiple pathologies and promote their early treatment.

3005 Heteronuclear Proton MRI - SNR, temperature effects and frequency separation of UTE versus CSI readout
Tim Klasen¹, Carsten Hölte¹, and Cornelius Faber¹

Computer #96



¹Department of Clinical Radiology, University of Münster, Münster, Germany

Heteronuclear proton MRI is a recent method for MRI cell tracking and opens up the possibility for Multicolor MRI when using different Ln-DOTMA complexes. Here, we compare UTE and CSI as readout with regard to SNR efficiency, sensitivity towards temperature changes and performance in separating resonance lines from different Ln-DOTMA complexes at 9.4 T. UTE readout provides faster image acquisition and higher SNR efficiency than CSI. CSI on the other hand is insensitive to temperature changes. Multicolor MRI was possible with both readout schemes. Further studies will use these methods for *in vivo* cell tracking experiments.

Electronic Poster

Diffusion: Acquisition

Exhibition Hall

Monday, May 9, 2016: 16:30 - 17:30

3006 Imaging Restrictive Pore Geometry with Asymmetrical Chirped Pulses

Computer #1



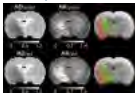
Qutaibeh Katatbeh¹, Alexey Tonyshkin², and Andrew Kiruluta³

¹Jordan University of Science and Technology, Irbid, Jordan, ²MGH, Boston, MA, United States, ³Harvard, Cambridge, MA, United States

Presents a practical way of recovering the phase of diffusing spins to recover the underlying restrictive geometry through a Fourier transform

3007 Enhanced efficiency and sensitivity in detection of acute ischemic brain injury using fast diffusion kurtosis imaging

Computer #2



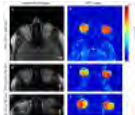
Yin Wu^{1,2}, Jinsuh Kim³, Suk-Tak Chan¹, Iris Yuwen Zhou¹, Yingkun Guo¹, Takahiro Igarashi¹, Hairong Zheng², Gang Guo⁴, and Phillip Zhe Sun¹

¹Athinoula A. Martinos Center for Biomedical Imaging, Department of Radiology, Massachusetts General Hospital and Harvard Medical School, Charlestown, MA, United States, ²Paul C. Lauterbur Research Centre for Biomedical Imaging, Shenzhen Key Laboratory for MRI, Shenzhen Institutes of Advanced Technology, Chinese Academy of Sciences, Shenzhen, China, People's Republic of, ³Department of Radiology, University of Illinois at Chicago, Chicago, IL, United States, ⁴Department of Radiology, Xiamen 2nd Hospital, Xiamen, China, People's Republic of

We systematically compare the diagnostic value of conventional tensor-based DKI and recently proposed fast DKI protocols using an acute stroke rodent model. The measures and volumes of diffusion and kurtosis lesions were in good agreement between the two DKI methods. Importantly, contrast-to-noise ratio (CNR) of mean kurtosis using the fast DKI protocol was significantly higher than that of the routine method with its CNR efficiency approximately doubles. Therefore, our results demonstrated excellent performance of the fast DKI protocol in characterizing acute ischemic tissue injury, which may facilitate translation of the fast DKI approach in the acute stroke setting.

3008 Towards Fast Diffusion-Sensitized MR Imaging of the Eye and Orbit with High Anatomic Fidelity: Combining a Segmented RARE variant with Inner Volume Imaging

Computer #3



Katharina Paul¹, Till Huelnhagen¹, Oliver Stachs², and Thoralf Niendorf^{1,3}

¹Berlin Ultrahigh Field Facility (B.U.F.F), Max Delbrück Center for Molecular Medicine in the Helmholtz Association (MDC), Berlin, Germany, ²Department of Ophthalmology, University Medicine Rostock, Rostock, Germany, ³Experimental and Clinical Research Center, a joint cooperation between the Charité Medical Faculty and the Max-Delbrueck-Center for Molecular Medicine in the Helmholtz Association, Berlin, Germany

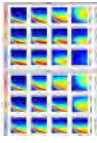
Diffusion-weighted imaging of the eye and orbit is an emerging MRI application to provide guidance during diagnostic assessment and treatment of ophthalmological diseases. It has been shown that RARE based diffusion-sensitized imaging (ms-RARE) provides images free of geometric distortions. Though, artifacts induced by involuntary eye motion remain a concern. Applying inner volume imaging (IVI) offers the possibility to shorten acquisition times by reducing the number of acquired phase encoding lines. This study examines the applicability of IVI in conjunction with ms-RARE with the goal to reduce the propensity to bulk eye motion in diffusion-sensitized ophthalmic imaging.

3009 Impact of sequence parameters on the sensitivity of DDE and DODE sequences to microscopic anisotropy

Computer #4

Andrada Ianuş¹, Ivana Drobnjak¹, Noam Shemesh², and Daniel C. Alexander¹

¹CMIC, University College London, London, United Kingdom, ²Champalimaud Neuroscience Programme, Champalimaud Centre for the Unknown, Lisbon, Portugal

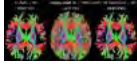


In the long mixing time regime, double-diffusion-encoding (DDE) sequences provide contrast capable of reflecting microscopic anisotropy, which may have added value for highly heterogeneous tissues such as the gray matter. Recently, double-oscillating-diffusion-encoding (DODE) sequences, which combine oscillating waveforms and varying gradient orientation, have been proposed to improve sensitivity to microscopic anisotropy. This work investigates the effect of varying different sequence parameters and shows that DODE sequences provide higher sensitivity to pore size for elongated pores, while DDE sequences are more sensitive to pore eccentricity.

3010



Computer #5



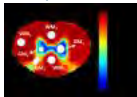
A novel iterative approach to reap the benefits of multi-tissue CSD from just single-shell ($+b=0$) diffusion MRI data
Thijs Dhollander¹ and Alan Connelly^{1,2}

¹The Florey Institute of Neuroscience and Mental Health, Melbourne, Australia, ²The Florey Department of Neuroscience, University of Melbourne, Melbourne, Australia

Constrained spherical deconvolution (CSD) is a robust approach to resolve the fibre orientation distribution (FOD) from diffusion MRI data. However, the FOD from CSD only aims to represent "pure" white matter (WM) and is inappropriate/distorted in regions of (partial voluming with) grey matter (GM) or cerebrospinal fluid (CSF). Multi-shell multi-tissue CSD was proposed to solve this issue by estimating WM/GM/CSF components, but requires multi-shell data to do so. In this work, we provide the *first* proof that similar results can also be obtained from *only* simple single-shell ($+b=0$) data, and propose a novel *specialised* optimiser that achieves this goal.

3011

Computer #6



Double-Pulsed-Field Gradient MRI in the Long Evans shaker rats' spinal cords
Debbie Anaby¹, Darya Morozov¹, Ian D. Duncan², and Yoram Cohen^{1,3}

¹School of Chemistry, The Raymond and Beverly Sackler Faculty of Exact Sciences, Tel Aviv University, Tel Aviv, Israel, ²Medical Sciences, The University of Wisconsin-Madison, Madison, WI, United States, ³Sagol School of Neurosciences, Tel Aviv University, Tel Aviv, Israel

Double pulsed-field gradient (d-PFG) MRI has recently been suggested as an additional methodology for studying microstructure in the CNS. The Long Evans shaker (*les*) rats' CNS has been previously studied by q-space diffusion (QSI) and more recently by angular d-PFG MRI. Here, we characterize the microstructure of the *les* spinal cords by fitting the angular d-PFG MRI data to the multiple correlation function (MCF) and extracting the unique parameter L/R ratio and its fractions. Clearly, the angular d-PFG methodology is capable of distinguishing between the *les* and their controls, in white matter and even in some gray matter ROIs.

3012

Computer #7



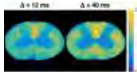
Effects of the Number of Diffusion Directions in Diffusion Kurtosis Imaging: a Structural Connectivity Study using in vivo data
Ricardo Loução¹, Karolina Elsner¹, Rita G. Nunes¹, Rafael Neto-Henriques², Marta Correia², André Ribeiro³, and Hugo Ferreira¹

¹Instituto de Biofísica e Engenharia Biomédica, Lisbon, Portugal, ²Cognition and Brain Science Unit, MRC, Cambridge, United Kingdom, ³Centre for Neuropsychopharmacology, London, United Kingdom

Diffusion Kurtosis Imaging Tractography Reconstructions (DKI-TR) are often performed using high quality data. In clinical practice, that is often not possible, as only a lower number of b-values and diffusion gradient directions can be acquired. This study assessed the performance of DKI-TR for the two algorithms currently proposed for DKI-TR using variable amounts of data, and looked at their respective structural connectivity metrics. A 64 gradient direction data set was acquired in six healthy subjects, and down-sampled to 21 and 32 directions. Differences were found between gradient sets and also between algorithms, regarding the reconstructions and the connectivity metrics.

3013

Computer #8



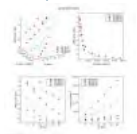
Assessment of Diffusion Time Dependence of Diffusion Kurtosis in Rat Spinal Cord
Nathaniel D Kelm^{1,2}, Kevin D Harkins², and Mark D Does^{1,2,3,4}

¹Biomedical Engineering, Vanderbilt University, Nashville, TN, United States, ²Vanderbilt University Institute of Imaging Science, Vanderbilt University, Nashville, TN, United States, ³Radiology and Radiological Sciences, Vanderbilt University School of Medicine, Nashville, TN, United States, ⁴Electrical Engineering, Vanderbilt University, Nashville, TN, United States

Diffusion kurtosis imaging (DKI) is an extension of DTI with the ability to provide additional information about tissue microstructure. To evaluate the diffusion time dependence of diffusion kurtosis, kurtosis is measured perpendicular to white matter tracts in rat spinal cord for diffusion times ranging from 12 to 100 ms. In this study, kurtosis increased as a function of diffusion time in white matter, yet decreased in gray matter. Assessing the change in diffusion kurtosis across diffusion time could potentially inform upon the underlying white matter microstructure.

3014

Computer #9



Time-dependent diffusion on in vivo human brain data from the Connectom scanner
Uran Ferizi¹, Claudia Wheeler-Kingshott², Daniel Alexander³, and Jose Raya¹

¹Department of Radiology, New York University School of Medicine, New York, NY, United States, ²Institute of Neurology, University College London, London, United Kingdom, ³Department of Computer Science, University College London, London, United Kingdom

Diffusion MRI models for brain microstructure do not currently incorporate time-dependent diffusivity. Previous studies with ex vivo tissue (muscle and brain) have observed such dependency. The advent of high diffusion gradient scanners have enabled us to probe the tissue to unprecedented. Here we examine and observe the time dependency of the measured diffusion using data from the live human brain.

3015

Computer #10



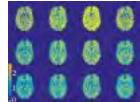
Between-Session Variability of Diffusion Kurtosis Metrics in in vivo Brains
Nino Kobalia¹, Farida Grinberg^{1,2}, Ezequiel Farrher¹, Xiang Gao¹, and N. Jon Shah^{1,2}

¹Institute of Neuroscience and Medicine - 4, Forschungszentrum Jülich GmbH, Jülich, Germany, ²Department of Neurology, Faculty of Medicine, JARA, RWTH Aachen University, Aachen, Germany

The knowledge of intra- and inter-subject variability of diffusion kurtosis imaging metrics plays an important role in the interpretation of the results in clinical trials. However, it has not been sufficiently studied thus far. The purpose of this work is to investigate between-session variability of a single subject with N-repeated measurements with an identical experimental protocol, and thus to provide the baseline for comparison with phantom measurements and inter-subject in vivo variability. We quantified variability in terms of the coefficient of variation and studied how its value varies between various diffusion tensor and kurtosis metrics estimated in twenty anatomical regions.

3016

Computer #11



The importance of b-values selection and the precision of diffusion kurtosis estimation by the conventional schemes
Andrey Chuhutin¹, Noam Shemesh², Brian Hansen¹, and Sune Nørhøj Jespersen^{1,3}

¹CFIN, Aarhus University, Aarhus, Denmark, ²Champalimaud Neuroscience Programme, Champalimaud Centre for the Unknown, Lisbon, Portugal, ³Department of Physics and Astronomy, Aarhus University, Aarhus, Denmark

In DKI imaging studies, a wide range of different gradient strengths is used, which is known to affect the estimated kurtosis. Being driven by a need to assess the validity of the DKI expression and the accuracy of the estimated parameters as a function of b-value we both evaluated the variability of the kurtosis parameter for the in vivo and ex vivo data for different fitting techniques and studied the error in a mean kurtosis parameter with respect to the ground truth. The results and conclusions suggest circumspection while preferring a specific technique.

3017

Computer #12



Diffusion Kurtosis Breast Imaging model – Which should be the highest b-value?

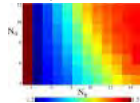
Filipa Borlinhas¹, Luísa Nogueira², Sofia Brandão³, Rita G. Nunes¹, Raquel Conceição^{1,4}, Joana Loureiro³, Isabel Ramos³, and Hugo A. Ferreira¹

¹Instituto de Biofísica e Engenharia Biomédica, Faculdade de Ciências da Universidade de Lisboa, Lisboa, Portugal, ²Escola Superior de Tecnologia da Saúde do Porto, ESTSP/IPP, Porto, Portugal, ³Hospital de São João, Porto, Portugal, ⁴Institute of Biomedical Engineering, University of Oxford, United Kingdom, Oxford, United Kingdom

For the application of the Diffusion Kurtosis Imaging (DKI) model, the use of higher b values is advised. Here, the diagnostic performance of the DKI model in the differentiation of benign and malignant breast tumors was studied for the first time regarding the most suitable higher b-value (2000, and 3000 s/mm²). In this study were included 36 benign and 75 malignant lesions, assessed using combinations of b-values 50 to 2000, and to 3000s/mm². The b-value range 50 to 3000 s/mm² showed the best results regarding diagnostic performance and so this range is suggested for use in future DKI breast cancer studies.

3018

Computer #13



A new framework for the optimisation of multi-shell diffusion weighting MRI settings using a parameterised Cramér-Rao lower-bound
Ezequiel Farrher¹, Ivan I. Maximov², Vincent Gras¹, Farida Grinberg^{1,3}, Rüdiger Stirnberg^{1,4}, and N. Jon Shah^{1,3}

¹INM 4 - Medical Imaging Physics, Forschungszentrum Jülich, Jülich, Germany, ²Experimental Physics III, TU Dortmund University, Dortmund, Germany, ³Department of Neurology, Faculty of Medicine, RWTH Aachen University, Aachen, Germany, ⁴German Center for Neurodegenerative Diseases (DZNE), Bonn, Germany

We propose a parameterisation for multi-shell diffusion gradient settings which is sufficiently flexible to cover a broad range of experimental configurations, on the one hand, but uses only 6 degrees of freedom, on the other. Thus, such parameterisation enables a robust optimisation of the diffusion weighting settings by minimising the Cramér-Rao lower bound of the parameters of interest. Finally, we demonstrate its performance in the context of the biexponential diffusion tensor analysis.

3019



Computer #14



A Robust Reconstruction Method for High Resolution Multishot DWI: SPIRiT-based SYMPHONY
Zijing Dong¹, Fuyixue Wang¹, Xiaodong Ma¹, Erpeng Dai¹, Zhe Zhang¹, and Hua Guo¹

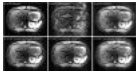
¹Center for Biomedical Imaging Research, Department of Biomedical Engineering, School of Medicine, Tsinghua University, Beijing, China, People's Republic of

SYnergistic iMAGE reconstruction using PHase variatiOns and seNsitivity (SYMPHONY) is a reconstruction method for multi-shot DWI which can provide high resolution diffusion weighted images. In this study, we proposed a SPIRiT-based SYMPHONY method in which a self-consistency constraint is applied instead of the conventional GRAPPA kernel to further improve the robustness of SYMPHONY. Simulation and in-vivo experiment validated the benefits of the proposed method which can improve the accuracy of reconstruction with less navigator data.

3020

Self-calibrated K-space Phase Correction Method for Multi-shot Diffusion Imaging

Computer #15 Zhe Zhang¹, Xiaodong Ma¹, Erpeng Dai¹, Hui Zhang¹, and Hua Guo¹



¹Center for Biomedical Imaging Research, Department of Biomedical Engineering, School of Medicine, Tsinghua University, Beijing, China, People's Republic of

Multi-shot EPI can achieve high resolution diffusion imaging, but the ghost artifacts caused by shot-to-shot phase variations must be corrected. In recent works, k-space phase correction methods have been proposed, which require navigator acquisitions for each excitation for calibrating the k-space interpolation parameters. In this work, a self-calibrated method for multi-shot DWI correction in k-space is proposed, which does not require navigator acquisitions for efficient scanning and does not suffer from the potential mismatch between image and navigator echoes. Experiments on liver DWI demonstrate that the proposed method can correct the motion induced artifacts in diffusion imaging.

3021

Computer #16



Diffusion Weighted 3D UTE Imaging Using Stimulated Echoes: Technical Considerations

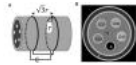
Michael Carl¹, Yajun Ma², Graeme M Bydder², and Jiang Du²

¹Global MR Applications & Workflow, General Electric, San Diego, CA, United States, ²University of California San Diego, San Diego, CA, United States

Due to the fast decay rate of the transverse magnetization, diffusion weighting is challenging in short T2 tissues; only very limited b-values can be achieved before the signal decays to zero. In this work, we used stimulated echoes to allow spin diffusion while the magnetization is stored along the longitudinal axis, therefore achieving useful b-values and allowing examination of short T2 tissues. Several technical challenges have to be addressed however, such as minimizing the oscillatory signal banding due to the low diffusion gradient area and reducing T1 contamination in multi-spoke UTE acquisition. This initial proof-of-principle study shows good quantitative agreement with clinical EPI diffusion sequences.

3022

Computer #17



EPI-based diffusion-weighted MR imaging of the neck at 3 Tesla: Comparison of sequence technologies for the reduction of susceptibility-related artifacts.

Sergios Gatidis¹, Mike Notohamiprodjo¹, Alto Stemmer², Konstantin Nikolaou¹, and Petros Martirosian¹

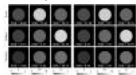
¹University of Tuebingen, Tuebingen, Germany, ²Siemens Healthcare AG, Erlangen, Germany

The aim of this study was to compare different EPI-based MR sequence techniques (conventional EPI, zoomed EPI, readout-segmented EPI and integrated 2D shim EPI (iShim)) for diffusion weighted imaging of the neck at 3 Tesla. To this end, MR measurements of a dedicated phantom and in-vivo measurements in volunteers were performed.

Our results suggest that iShim is the best option for DWI of the neck at 3 Tesla yielding good image quality and efficiently reducing spatial distortions and off-resonance artifacts.

3023

Computer #18



Optimization of b-value sampling using error propagation methods for intravoxel incoherent motion imaging for various organs

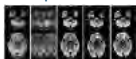
Suguru Yokosawa¹, Hisaaki Ochi¹, and Yoshitaka Bito²

¹Research & Development Group, Hitachi, Ltd., Tokyo, Japan, ²Healthcare Company, Hitachi, Ltd., Chiba, Japan

In this study, we proposed a method for optimizing b-value sampling using error propagation methods for IVIM imaging. We investigated the difference in an optimal set of b-values depending on the organ and the effect of b-value sampling on the precision of IVIM parameters. The results show that the optimal b-values were divided into four b-values and the combination of b-values varied with the organ. The SNR increased 1.2–1.6 times by optimization. We concluded that the optimization of b-value sampling corresponding to an organ can improve the fitting precision of IVIM parameters.

3024

Computer #19



Multi-shot Cartesian TSE DWI with Inherent 2D Phase Correction

Zhe Zhang¹, Xiaodong Ma¹, Bing Zhang², Ming Li², Chun Yuan^{1,3}, and Hua Guo¹

¹Center for Biomedical Imaging Research, Department of Biomedical Engineering, School of Medicine, Tsinghua University, Beijing, China, People's Republic of, ²Department of Radiology, The Affiliated Drum Tower Hospital of Nanjing University Medical School, Nanjing, China, People's Republic of, ³Vascular Imaging Laboratory, Department of Radiology, University of Washington, Seattle, WA, United States

Single-shot EPI DWI suffers from geometric distortion which can mask the pathology. Single-shot TSE DWI can help settle the distortion problems, but the spatial resolution is limited. In this work, a multi-shot Cartesian TSE DWI method with improved in-plane resolution is proposed. The ghost artifacts from shot-to-shot phase variations are corrected using an image domain correction method. The results show that the proposed method provides diffusion images with improved resolution and insensitivity to susceptibility induced distortion artifacts.

3025

Computer #20



3D Ultrashort Echo Time Cones Sequence with Diffusion Weighted Imaging (3D UTE-Cones-DWI): Evaluation of the Angular Dependence of Diffusion in the Achilles Tendon

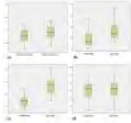
Yajun Ma¹, Michael Carl², Graeme Bydder¹, and Jiang Du¹

¹Department of Radiology, UCSD, San Diego, CA, United States, ²Global MR Application & Workflow, General Electric, San Diego, CA, United States

Diffusion weighted imaging (DWI) has been widely used to evaluate the rate of water diffusion in long T_2 tissues such as the white matter of the brain. Tissues such as cortical bone, tendons, ligaments and menisci have short T_2 and have little or no signal with conventional clinical MR sequences. Water diffusion in these tissues is inaccessible. Ultrashort echo time (UTE) sequences with TEs down to 8 μ s have been employed to image the short T_2 tissues. The combination of UTE and stimulated echo diffusion preparation (UTE-DWI) allows water diffusion to be evaluated in short T_2 tissues. In this study we report the use of a novel stimulated echo (STE) diffusion prepared 3D UTE Cones sequence (3D UTE-Cones-DWI) for assessment of water diffusion in the Achilles tendon using a clinical 3T scanner. The magic angle dependence of apparent diffusion coefficients (ADC) determined through this sequence was also investigated.

3026

Computer #21



Quantitative evaluation of Apparent Diffusion Coefficient (ADC) from two DWI sequences – echo planar spin echo (EPSE) and read-out segmented echo planar (RESOLVE) imaging

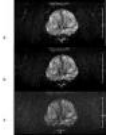
Yo-jin Hwang¹, Hyun-Seok Choi¹, Yoon-Ho Nam¹, and Joon-Yong Jung¹

¹Department of Radiology, St.Mary Hospital, Seoul, Korea, Republic of

The purpose of this study was to quantitatively evaluate ADCs from two different DWI sequences – echo planar spin echo (EPSE) and read-out segmented echo planar (RESOLVE) imaging. The mean ADCs of the whole brain, GM, WM and CSF were compared based on masking templates generated from T2-weighted images. Our results demonstrated that although difference between the two ADCs was statistically significant over the whole brain regions, ADCs from msDWI and ssDWI were highly correlated ($R^2 = 0.989$). The relationship between the two ADCs should be considered to utilize it as an effective quantitative metric.

3027

Computer #22



The Optimization of Zoomed Field of View DWI (iZOOM) with Echo Planar Imaging (EPI) Sequence Excited by a Two Dimensional Radiofrequency Pulse (2D RF) on Prostate at 3.0 T

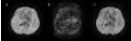
Kangjie Xu¹, Xiaodong Zhang¹, Chengyan Wang², Hongxia Sun¹, Yu Zhang³, Zhigang Wu⁴, and Xiaoying Wang¹

¹The Department of Radiology, Peking University First Hospital, Beijing, China, People's Republic of, ²Academy for Advanced Interdisciplinary Studies, Peking University, Beijing, China, People's Republic of, ³Philips Healthcare, Beijing, China, People's Republic of, ⁴Philips Healthcare (Suzhou) Co., Ltd, Suzhou, China, People's Republic of

This study aims to demonstrate the feasibility of iZOOM using a 2D RF pulse EPI sequence in the application of prostate DWI and the optimization of iZOOM at 3.0 T MRI. 58 patients took prostate MRI examination with 3 iZOOM sequences (1. b=1000, resolution: 1.4x1.4mm; 2. b=1000, resolution: 1.0x1.0mm; 3. b=2000, resolution: 1.4x1.4mm). Images were evaluated with the basic image quality, the display of lesions and overall image quality. The result shows iZOOM is feasible on prostate DWI. High b value and high resolution iZOOM are both favored by radiologists.

3028

Computer #23



Efficient Macroscopic Motion Correction for Multi-shot DTI

zhongbiao xu¹, Yanqiu Feng¹, Wufan Chen¹, Zhigang Wu², Ha-kyu Jeong³, Wenxing Fang², Yingjie Mei^{1,4}, Li Guo¹, and Feng Huang²

¹School of Biomedical Engineering and Guangdong Provincial Key Laboratory of Medical Image Processing, Southern Medical University, Guangzhou, China, People's Republic of, ²Philips Healthcare (Suzhou), Suzhou, China, People's Republic of, ³Philips Korea, Seoul, Korea, Republic of, ⁴Philips Healthcare, Guangzhou, China, People's Republic of

Though cMUSE proposed by our group tackles the pixels mismatch of macroscopic motion in multi-shot EPI by clustering and registration, it neglects altered gradient directions. In this work, we treat motion induced variations in gradient direction as additional diffusion direction(s). The proposed method simply and effectively solves the gradient direction alternation due to macroscopic motion in multi-shot DTI.

3029

Computer #24



Acceleration motion compensation DWI for measuring intraventricular temperature

Shuhei Shibukawa^{1,2}, Toshiaki Miyati², Naoki Ohno², Tetsuo Niwa³, Yutaka Imai³, Tetsuo Ogino⁴, and Isao Muro¹

¹Department of Radiology, Tokai university hospital, Isehara, Japan, ²Division of Health Sciences, Graduate School of Medical Sciences, Kanazawa University, Ishikawa, Japan, ³Department of Radiology, Tokai University School of Medicine, Isehara, Japan, ⁴Healthcare, Philips Electronics Japan Ltd., Tokyo, Japan

Although it has been reported a method for monitoring the intraventricular cerebrospinal fluid (CSF) temperature calculated from the DWI, this method was affected by the CSF pulsation. We proposed the acceleration-motion compensation DWI (aMC-DWI) to the determination of the intraventricular temperature to improve that accuracy and precision. Compared with conventional DWI, measurement of intraventricular temperature using aMC-DWI was accuracy even in ventricles with high flow, e.g., third ventricle, fourth ventricle. These results suggested that aMC-DWI is a suitable method for analyzing the intraventricular temperature.

Electronic Poster

Diffusion: Analysis

Exhibition Hall

Monday, May 9, 2016: 16:30 - 17:30

3030

Graph theoretical analysis of abnormal structural networks in obese patients using DTI tractography

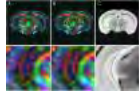


¹Department of Medical Imaging and Radiological Sciences, Chung Shan Medical University, Taichung, Taiwan, ²Department of Psychiatry, Chang Gung Memorial Hospital, Chiayi, Taiwan, ³Taiwan Center for Metabolic and Bariatric Surgery, Jen-Ai Hospital, Taichung, Taiwan, ⁴Department of Psychology, Chung Shan Medical University, Taichung, Taiwan, ⁵Department of Medical Imaging, Chung Shan Medical University Hospital, Taichung, Taiwan

Obesity is one of the most serious public health concerns among adults and children in the 21st century, which increases risk of many other diseases, including cardiovascular risks, hypertension, dyslipidemia, endothelial dysfunction, etc., and it is commonly measured with body mass index (BMI). Previously studies about obesity mainly used diffusion tensor imaging (DTI) to examine the relationship between BMI and DTI parameters, and found that white matter integrity was reduced in obesity. However, the research about the particular structural brain network change of obese patients was tended to be less. Hence, our study aimed to map the structural connectomic changes over obese patients based on DTI tractography using graph theoretical and network-based statistic (NBS) analyses. In the result of graph theoretical analysis, poor ability of local segregation, global integration, and transitivity in the obese patients was found. In the result of NBS, decreased connections in structural connectivity network, and alterations in the corpus callosum region was observed.

3031

Computer #26



Automated rejection of motion-corrupted slices and optimised retrospective ghost correction for multi-shot DTI
Malte Hoffmann¹ and Stephen J Sawiak^{1,2}

¹Wolfson Brain Imaging Centre, University of Cambridge, Cambridge, United Kingdom, ²Behavioural and Clinical Neuroscience Institute, University of Cambridge, Cambridge, United Kingdom

DTI sequences based on EPI allow rapid acquisitions of image slices by traversing k-space lines in opposite directions following a single RF excitation. During long acquisition trains, phase errors caused by field inhomogeneity can lead to distortion. Acquiring slices in multiple shots can mitigate this effect. Motion between shots, however, results in ghosting that cannot be corrected. We show that slice-wise phase correction by entropy minimisation reduces ghosting compared to the manufacturer software (ParaVision 4.0, Bruker). Second, we propose an algorithm to automatically detect and reject slices with residual motion-induced ghosting, and validate it in a large cohort of mice.

3032

Computer #27



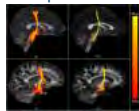
Using A Hyperspherical Harmonic Basis for Sparse Multi-Voxel Modeling of Diffusion MRI
Evan Schwab^{1,2}, Hasan Ertan Cetingul², Rene Vidal³, and Mariappan Nadar²

¹Electrical and Computer Engineering, Johns Hopkins University, Baltimore, MD, United States, ²Medical Imaging Technologies, Siemens Healthcare, Princeton, NJ, United States, ³Biomedical Engineering, Johns Hopkins University, Baltimore, MD, United States

For diffusion magnetic resonance imaging (dMRI), 3D signals are acquired at each voxel to estimate neuronal fiber orientation in the brain. Traditionally, dMRI signals are reconstructed using the same basis for each voxel with added spatial regularization and sparsity constraints. By repeating the same basis for each voxel, there exist millions of redundant parameters to represent an entire brain volume. In this work, we reconstruct dMRI signals jointly across multiple voxels to reduce the number of parameters needed to represent a brain volume by 65%. Sparse dMRI representation is important for storage, information extraction, and reduction of clinical scan times.

3033

Computer #28



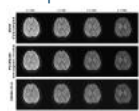
Caveats of probabilistic tractography for assessing fiber connectivity strength
Hamed Y. Mesri¹, Anneriet M. Heemskerk¹, Max A. Viergever¹, and Alexander Leemans¹

¹Image Sciences Institute, University Medical Center Utrecht, Utrecht, Netherlands

Despite previous reviews on the limitations of using probabilistic fiber tractography techniques for assessing the “strength” of brain connectivity, these tractography techniques are still being used for this purpose. The objective of this work is to characterize the reliability of probabilistic tractography for investigating connectivity “strength”. To this end, we demonstrate that the sensitivity of reconstructing fiber tracts with respect to the noise level and/or the choice of number of gradient directions is high, suggesting that the interpretation of such results for assessing the “strength” of connectivity should be used with extreme caution.

3034

Computer #29



Joint reconstruction of high-SNR multiple b-values diffusion-weighted images using projection onto convex sets based multiplexed sensitivity-encoding (POCSMUSE)
Hing-Chiu Chang^{1,2}, Mei-Lan Chu², and Nan-Kuei Chen²

¹Department of Diagnostic Radiology, The University of Hong Kong, Hong Kong, Hong Kong, ²Brain Imaging and Analysis Center, Duke University Medical Center, Durham, NC, United States

Intra-voxel incoherent motion (IVIM) MRI utilizes diffusion-weighted echo-planar imaging (DW-EPI) technique to acquire a set of image data with multiple b-values. The major limitation of IVIM is due to long acquisition time for multiple b-values that can lower the feasibility of clinical use, especially it requires multiple averaging of high-b value to compensate SNR loss. In this study, we propose a joint reconstruction framework of POCSMUSE algorithm, to simultaneously reconstruct under-sampled multi-b interleaved DW-EPI data with reduced noise amplification.

3035

Sparse re-parametrization of continuous Fibre Orientation Distributions using spherical harmonic delta functions

Computer #30 Robert Elton Smith¹ and Alan Connelly^{1,2}



¹The Florey Institute of Neuroscience and Mental Health, Melbourne, Australia, ²The University of Melbourne, Melbourne, Australia

Constrained Spherical Deconvolution (CSD) estimates the Fibre Orientation Distribution (FOD) in each voxel in the Spherical Harmonic (SH) basis. Although features of the underlying fibre configuration are captured within the FOD, the SH basis is not wholly appropriate for their analysis. We propose a re-parametrization of the FOD, fitting a sparse set of SH delta functions to each FOD, that additionally captures the anisotropic dispersion of each discrete fibre bundle.

3036

Computer #31



Reliable estimation of Diffusional kurtosis in the skeletal muscle needs perfusion correction.

Alberto De Luca^{1,2,3}, Alessandra Bertoldo¹, and Martijn Froeling³

¹Department of Information Engineering, University of Padova, Padova, Italy, ²Neuroimaging Lab, Scientific Institute IRCCS Eugenio Medea, Bosisio Parini (LC), Italy, ³Department of Radiology, University Medical Center, Utrecht, Netherlands

Perfusion is known to affect the estimation of Diffusion Tensor Imaging (DTI) measures on the skeletal muscle. However, no previous works evaluated its effects on kurtosis estimation. Therefore, in this study we investigated the influence of perfusion on kurtosis. Synthetic signals for different perfusion levels with and without isotropic kurtosis were generated and then fitted with and without taking IVIM into consideration. Results showed that IVIM correction was essential to estimate non-biased values of kurtosis in case of increased perfusion. Real data showed that the simultaneous estimation of kurtosis and IVIM is robust and feasible.

3037

Computer #32



High field DTI and NODDI imaging to assess the effects of systemic inflammation on the pup rat brain.

Yohan van de Looij^{1,2}, Justin M Dean³, Alistair J Gunn³, Petra S Hüppi¹, and Stéphane V Sizonenko¹

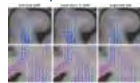
¹Division of Child Growth & Development, Department of Pediatrics, University of Geneva, Geneva, Switzerland, ²Laboratory for Functional and Metabolic Imaging, Ecole Polytechnique Fédérale de Lausanne, Lausanne, Switzerland, ³Department of Physiology, University of Auckland, Auckland, New Zealand

Infection-induced inflammation is a major cause of injury to the white matter and grey matter structures of the brain in the early preterm infant. In the present study, we assessed the long-term effects of early-life inflammation on white and grey matter microstructure using diffusion tensor imaging (DTI) and neurite orientation dispersion and density imaging (NODDI) at 9.4T. In this study, we characterized the microstructural consequences of LPS exposure in newborn pup rats recovered to P21. Mild changes in white matter and cortical development were observed without ventriculomegaly. DTI and NODDI can be used to assess subtle changes following LPS exposure.

3038



Computer #33



Unsupervised multi-tissue decomposition of single-shell diffusion-weighted imaging by generalization to multi-modal data

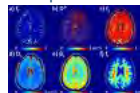
Daan Christiaens^{1,2}, Frederik Maes^{1,2}, Stefan Sunaert^{2,3}, and Paul Suetens^{1,2,4}

¹ESAT/PSI, Department of Electrical Engineering, KU Leuven, Leuven, Belgium, ²Medical Imaging Research Center, UZ Leuven, Leuven, Belgium, ³Translational MRI, Department of Imaging & Pathology, KU Leuven, Leuven, Belgium, ⁴Medical IT Department, iMinds, Leuven, Belgium

Recent method developments have improved the reconstruction of fibre orientation distributions in white matter by incorporating partial voluming with isotropic grey matter and CSF. Yet, their use is limited to multi-shell data. Here, we present a generalization of convexity-constrained non-negative spherical factorization to multi-modal data, and illustrate its use for decomposing single-shell diffusion-weighted data and T1 anatomical data in three tissue components. Results show that we can effectively reconstruct fibre orientation distributions and separate isotropic volume fractions of grey matter and CSF in single-shell data, even at low b-values.

3039

Computer #34



A Trimodal non-Gaussian Diffusion Model for the Full Spectrum of Multi-b Diffusion MRI in Brain Tissue

Nicholas W. Damen^{1,2}, Kejia Cai^{2,3,4}, Yi Sui^{2,4}, Muge Karaman², and Frederick C. Damen^{2,3}

¹Illinois Math and Science Academy, Aurora, IL, United States, ²Center for Magnetic Resonance Research, University of Illinois at Chicago, Chicago, IL, United States, ³Radiology, University of Illinois Medical Center, Chicago, IL, United States, ⁴Bioengineering, University of Illinois at Chicago, Chicago, IL, United States

When examining brain diffusion weighted MRI (DW-MRI) images acquired at multiple diffusion weightings, i.e., b-values, it has become apparent that the DW-MRI measurements may not be completely explained with a Gaussian mono-exponential model. A trimodal model is proposed to fit the full spectrum of multi-b DW-MRI (from 0 to 5000 s/mm²) by incorporating a perfusion component, a stretch exponential component, and a 3rd distinct diffusion component. The trimodal model reduced the χ^2 fitting residuals, provided an additional 3rd diffusion component with good white matter contrast without sacrificing contrast in the perfusion and stretch exponential components.

3040

Computer #35



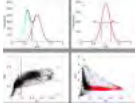
Voxel Level Comparison of Two Anomalous Diffusion Models: Continuous-Time Random-Walk Model versus Fractional Motion Model

Muge Karaman¹, Ying Xiong^{1,2}, Kejia Cai^{1,3}, and X. Joe Zhou^{1,4}

¹Center for MR Research, University of Illinois at Chicago, Chicago, IL, United States, ²Department of Radiology, Tongji Hospital, Tongji Medical College, Huazhong University of Science and Technology, Wuhan, China, People's Republic of, ³Department of Radiology, University of Illinois at

Over the past decades, several non-Gaussian diffusion models have been developed to reveal the underlying structures of the complex and heterogeneous tissue by measuring the anomalous diffusion behavior. Within these, continuous-time random-walk (CTRW) and fractional motion (FM) models have actively been studied by several groups to compare them at *cellular* or *molecular* level. In this study, we provide a comparison between the CTRW and FM models on human brain *in vivo* at the voxel level using high *b*-value diffusion MRI. It was observed that all CTRW and FM parameters exhibit characteristic contrasts, reflecting different aspects of the complex diffusion process.

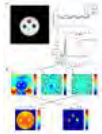
3041 Computer #36 Novel Diffusion-Kurtosis-Informed Template to Reduce Partial Volume Effects in the Atlas-Based Analysis
Farida Grinberg^{1,2}, Xiang Gao¹, Ezequiel Farrher¹, and N. Jon Shah^{1,2}



¹Institute of Neuroscience and Medicine - 4, Forschungszentrum Juelich GmbH, Juelich, Germany, ²Department of Neurology, Faculty of Medicine, RWTH Aachen University, Aachen, Germany

Between-group comparisons of diffusion tensor and diffusion kurtosis imaging metrics are important for elucidation of differences between pathology and healthy state. However, thus far, the methodology of such comparisons has not been well established. Frequently used methods, such as region-of-interest analysis or atlas-based analysis are subject to errors due to partial volume effects, whereas the track-based spatial statistics reduces consideration to a small amount of voxels along the skeleton, thus diminishing useful information. In this work we represent a simple, robust diffusion-kurtosis-informed template effectively reducing partial volume effects in the atlas-based analysis using less restrictive approach.

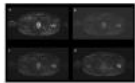
3042 Computer #37 Differentiating Contributions To Diffusional Kurtosis with Symmetrized Double-PFG MRI
Jeffrey Louis Paulsen¹, Iris Yuwen Zhou², Yi-Qiao Song¹, and Phillip Zhe Sun²



¹Schlummerger-Doll Research, Boston, MA, United States, ²Department of Radiology, Athinoula A. Martinos Center for Biomedical Imaging, Charlestown, MA, United States

Kurtosis imaging enables valuable diagnostics of stroke and other tissue pathologies. It can arise both directly from restricted diffusion, and indirectly from averaging multiple microscopic environments. We develop an EPI imaging sequence utilizing double diffusion contrast that isolates the direct contribution. We demonstrate consistency with traditional kurtosis imaging in phantoms yet unique contrast in-vivo in a live rat brain.

3043 Computer #38 Whole-body diffusion weighted imaging in multiple myeloma: Temporal changes of Gaussian and non-Gaussian diffusion parameters following treatment. Initial experience at 3.0T

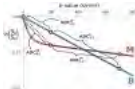


Arash Latifoltojar¹, Margaret Hall-Craggs², Nikolaos Dikaios¹, Kwee Yong¹, Neil Rabin², Alan Bainbridge², Magdalena Sokolska², and Shonit Punwani¹

¹University College London, London, United Kingdom, ²University College London Hospital, London, United Kingdom

Diffusion weighted imaging's apparent diffusion coefficient (ADC) has been shown to be a potential imaging biomarker for monitoring treatment response in multiple myeloma. However, in most instances, a mono-exponential fitting model is used to assess temporal changes. In this work, we investigated the Gaussian and non-Gaussian fitting algorithms and their respective quantitative biomarkers for assessing response in multiple myeloma using whole body diffusion weighted imaging.

3044 Computer #39 Relative enhanced diffusivity in terms of intravoxel incoherent motion
Peter T. While¹, Jose R. Teruel^{2,3}, Igor Vidić⁴, Tone F. Bathen², and Pål E. Goa⁴



¹Department of Radiology and Nuclear Medicine, St. Olav's University Hospital, Trondheim, Norway, ²Department of Circulation and Medical Imaging, Norwegian University of Science and Technology (NTNU), Trondheim, Norway, ³St. Olav's University Hospital, Trondheim, Norway, ⁴Department of Physics, Norwegian University of Science and Technology (NTNU), Trondheim, Norway

Relative enhanced diffusivity (RED) is a recently proposed parameter for DWI that is strongly weighted by pseudo-diffusion and provides good tissue discrimination using only three *b*-values. In this work we perform a theoretical study on the link between the RED parameter and the intravoxel incoherent motion (IVIM) model, and we derive a simple approximate expression for describing this relationship.

3045 Computer #40 Angular Complexity and Fractional Displacement Probability: New metrics for diffusion propagator imaging
Luis Miguel Lacerda¹, Gareth Barker¹, and Flavio Dell'Acqua¹

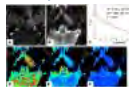


¹Department of Neuroimaging, The Institute of Psychiatry, Psychology & Neuroscience, King's College London, London, United Kingdom

Several methods have been used to represent the diffusion signal, and recently novel multi-shell approaches like SHORE, have allowed analytical and continuous reconstruction of the diffusion propagator. In this study, we propose two new metrics to better characterize the propagator at different displacement radii, the Angular Complexity Index (ACI), as a measure of propagator anisotropy, and the Fractional Displacement Probability (FDP), as index of relative mean displacement probability within fixed displacement bands. Furthermore, we display preliminary results that suggest sensitivity to microstructural organisation at different displacement scales, as opposed to traditional propagator metrics that reduce it to single scalar maps.

3046

Computer #41



Emerging applications of intravoxel incoherent motion MRI in primary nasopharyngeal carcinoma
Shuixing Zhang¹, Long Liang¹, Bin Zhang¹, Barbara Dong¹, Kannie W.Y. Chan², Guanshu Liu², and Changhong Liang¹

¹Department of Radiology, Guangdong Academy of Medical Sciences/Guangdong General Hospital, Guangzhou, Guangdong Province, China, Guangzhou, China, People's Republic of, ²Russell H. Morgan Department of Radiology and Radiological Sciences, Division of MR Research, The Johns Hopkins University School of Medicine, Baltimore 21287, USA, Baltimore, AL, United States

Worldwide, nasopharyngeal carcinoma (NPC) is a rare malignancy, but it shows marked geographic and racial variation in incidence and is particularly endemic in southern China. The aim of our study is to compare pure molecular diffusion (D), perfusion-related diffusion (D*), perfusion fraction (f) and apparent diffusion coefficient (ADC) based on intravoxel incoherent motion (IVIM) theory in patients with NPC. Our results revealed that IVIM DWI is a feasible technique for investigating primary NPC. D was significantly decreased in primary NPC, and increased D* reflected increased blood vessel generation and parenchymal perfusion in primary NPC.

3047

Computer #42



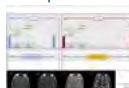
Computed FLAIR-DWI Technique combined with DWI, PDW, T2W and T1W Imagings
Yuki Takai¹ and Tokunori Kimura²

¹MRI development department, Toshiba Medical Systems, Otawara, Japan, ²Clinical Application Research and Development Dept., Toshiba Medical Systems, Otawara, Japan

We proposed a new computed DWI technique allowing to provide quantitative maps of ADC, T2, T1 and DWI images with arbitrary contrast of PDW, T2W, and T1W. We clarified that our techniques enabled to provide FLAIR-DWI images with higher SNR than actually measured FLAIR-DWI, and furthermore enhanced by using SE-based ADC map and SE- or IR-based T1 map with optimal T1 for brain tissue. Although further optimization is required, it is expected to be especially useful for clinical brain diagnosis.

3048

Computer #43



Correlation Time Diffusion Brain Mapping at 1.5T vs. 3.0T
Hernan Jara¹, Arnaud Guidon², Lloyd Estkowski³, Jorge A Soto¹, and Osamu Sakai¹

¹Radiology, Boston University, Boston, MA, United States, ²Global MR Applications and Workflow, GE Healthcare, Boston, MA, United States, ³Global MR Applications and Workflow, GE Healthcare, Menlo Park, CA, United States

Purpose: To test the hypothesis that correlation time diffusion coefficient (DCT) MRI is not be dependent of the main magnetic field strength B₀. Methods: A healthy volunteer was scanned (head) at 1.5T and 3.0T with the same diffusion mapping capable scans: quadrature FSE for DCT mapping and DW-SE-sshEPI for DPGF mapping. Results: Despite the B₀ dependent shifts of the relaxation time (T₁, T₂) histograms, the DCT, DPGF, and PD histograms do not exhibited significant B₀ shifts. Conclusion: The correlation time diffusion coefficient is theoretically and experimentally a genuine physical property inherent to biological tissue and independent of experimental variables including B₀.

3049

Computer #44



Non-invasive characterization of BI-RADS 4/5 X-ray mammography findings using unenhanced breast MRI with fusion of diffusion weighted and morphological T2-weighted images

Sebastian Bickelhaupt¹, Jana Tesdorff¹, Frederik Bernd Laun², Wolfgang Lederer³, Heidi Daniel⁴, Tristan Amseln Kuder², Susanne Teiner³, Stefan Delorme², and Heinz-Peter Schlemmer²

¹Department of Radiology, German Cancer Research Center, Heidelberg, Germany, ²Department of Medical Physics in Radiology, German Cancer Research Center, Heidelberg, Germany, ³Radiological Practice at the ATOS Clinic Heidelberg, Heidelberg, Germany, ⁴Radiology Center Mannheim (RZM), Mannheim, Germany

Additive unenhanced breast MRI prior to biopsy might reduce false positive x-ray mammograms. Therefore we evaluated the adjunctive diagnostic value of unenhanced breast MRI with image fusion of DWI and T2-weighted images and compared it to a side-by-side analysis of the sequences. 30 patients were included undergoing a 1.5 T breast MRI examination prior biopsy. We found that reading DWI/T2w-fused images alone decreased the accuracy (81.6% ± 2.8%) compared to the side-by-side analysis (91.6% ± 2.3%) and significantly reduced the reader confidence significantly (p < 0.001). Therefore fused image series should currently be considered always in addition to morphologic images since they could miss important morphologic information.

3050

Computer #45

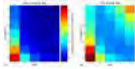


Inherent correction of both geometric distortion and motion-induced aliasing artifacts in multi-shot diffusion-weighted EPI
Mei-Lan Chu¹, Arnaud Guidon², Hing-Chiu Chang³, and Nan-kuei Chen¹

¹Brain Imaging and Analysis Center, Duke University, Durham, NC, United States, ²Global MR Applications and Workflow, GE Healthcare, Boston, MA, United States, ³Department of Diagnostic Radiology, The University of Hong Kong, Hong Kong, Hong Kong

A new reconstruction framework is developed to simultaneously correct geometric distortion and motion-induced aliasing artifacts in multi-shot DW-EPI data without relying on additional calibration scan or field mapping. Through reversing the polarity of phase-encoding gradient between interleaves in multi-shot EPI, the field inhomogeneities and segment-specific phase information can be inherently estimated from DW-EPI data. High-quality DWI images free from distortions and aliasing artifacts can then be reconstructed with our new POCSMUSE method that uses coil sensitivity profiles, shot-to-shot phase variations, and field inhomogeneities as the input.

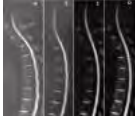
3051 Computer #46 The effect of subject motion on fractional anisotropy estimates: A simulation study of angular bias Szabolcs David¹, Anneriet Heemskerk¹, Max Viergever¹, and Alexander Leemans¹



¹Image Sciences Institute, UMC Utrecht, Utrecht, Netherlands

Subject motion during diffusion weighted MRI acquisition is a well-known confounding factor which can affect diffusion tensor metrics. In this simulation study, we investigated whether this confound is related to the change in distribution of diffusion gradient orientations due to the required "B-matrix rotation" during subject motion. According to our findings, subject motion can indeed generate a significant angular bias in addition to the noise bias, suggesting that subject motion itself may cause group differences in diffusion metrics.

3052 Computer #47 High-Resolution DWI using reduced FOV multi-shot EPI with IRIS reconstruction Wenxing Fang¹, Zhigang Wu¹, Feng Huang¹, and Jeong Ha-Kyu²



¹Philips Healthcare (Suzhou), Suzhou, China, Suzhou, China, People's Republic of, ²Philips Healthcare Korea, Seoul, Republic of Korea, Seoul, Korea, Republic of

Multi-shot EPI using IRIS technique works fantastically in reduced FOV, which can enhance high resolution diffusion images. It can be a potential application for the research and clinical diagnosis in diffusion imaging.

3053 Computer #48 Highly accelerated graph theory implementations show benefits of finer cortical parcellations for group connectomic analyses Greg D Parker¹, Mark Drakesmith^{1,2}, and Derek K Jones^{1,2}



¹CUBRIC, School of Psychology, Cardiff University, Cardiff, United Kingdom, ²Neuroscience and Mental Health Research Institute (NMHRI), School of Medicine, Cardiff University, Cardiff, United Kingdom

Graph theoretical connectome analysis¹ is an increasingly important research area. There is, however, high computational overhead required to: (a) produce whole or partial brain tractographies; (b) convert tractographies into binary or weighted graphs; and (c) analyse those graphs according to multiple, often complex graph metrics. We have developed GP-GPU accelerated implementations of each step. Exploiting the resultant increase in computational power, we examined the effects of increasing streamline sampling densities and number of cortical parcellations on separability of connectomes between first episode psychosis patients and controls. We show finer cortical parcellation increases separability (while increasing streamline density reduces it).

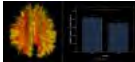
Electronic Poster

Diffusion: Analysis & Tractography

Exhibition Hall

Monday, May 9, 2016: 16:30 - 17:30

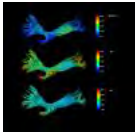
3054 Computer #49 Novel diffusion markers for tract-based spatial statistics and bundle-specific analysis – feasibility study in patients with schizophrenia Stefan Sommer¹, Matthias Kirschner², Oliver Hager^{2,3}, Stefan Kaiser², Sebastian Kozerke¹, Erich Seifritz², and Philipp Stämpfli²



¹Institute for Biomedical Engineering, ETH and University of Zurich, Zurich, Switzerland, ²Department of Psychiatry, Psychotherapy and Psychosomatics Psychiatric Hospital, University of Zurich, Zurich, Switzerland, ³Laboratory for Social and Neural Systems Research, Department of Economics, University of Zurich, Zurich, Switzerland

In the last few years, tract base spatial statistics (TBSS) become prominent tools for analyzing diffusion data in group studies. In this study, we introduce optimized high-resolution tract density (optTD) images based on tractograms. In order to avoid tractography bias, the tractograms are optimized using the convex-optimization modeling for microstructure informed tractography (COMMIT). The optTD were analyzed in a group of patients with schizophrenia and healthy controls using TBSS. Additionally, we have shown significant group differences comparing fiber weights derived from the COMMIT optimization. The introduced measures provide promising tools for investigating white-matter abnormalities in mental disorders.

3055 Computer #50 Mapping fibre dispersion and tract specific metrics in multiple fibre orientation using multi Bingham distributions Rafael Neto Henriques¹, Marta Morgado Correia¹, and Flavio Dell'Acqua²

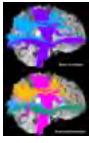


¹Cognition and Brain Sciences Unit, MRC, Cambridge, United Kingdom, ²Netbrainlab, Centre for Neuroimaging Sciences, Institute of Psychiatry, Psychology & Neuroscience, King's College London, London, United Kingdom

In this study, a new approach to obtain improved fiber dispersion estimates by simultaneously fitting multi-Bingham distributions to the FODF is presented.

3056 Computer #51 Color this! An automatic algorithm to assign visually distinct colors to white matter bundles Jean-Christophe Houde¹ and Maxime Descoteaux¹

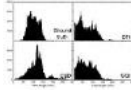
¹Sherbrooke Connectivity Imaging Lab (SCIL), Université de Sherbrooke, Sherbrooke, QC, Canada



We propose a new technique to automatically assign visually distinct colors to streamlines bundles. Our technique takes into account spatial positioning of bundles to avoid assigning similar colors to neighboring bundles. This will help researchers visually disambiguate close bundles. We show that basic techniques simply trying to spread the colors through the available spectrum often fail to take neighbors into consideration, and assign visually indistinguishable colors to close bundles. Our technique is fully automatic and stable, giving the same color assignments for any subject with the same bundles and similar structure.

3057

Computer #52



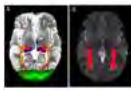
Evaluation of tractography using Fiberfox for whole brain connectome analysis
Hu Cheng¹, Ahmad Abdulrahman M Alhulail², and Sharlene Newman¹

¹Department of Psychological and Brain Sciences, Indiana University, Bloomington, IN, United States, ²Department of Physics, Indiana University, Bloomington, IN, United States

Due to the complexity of brain microstructure and organization, the validation of tractography results remains a challenging problem. In this work, effect of SNR and b value of diffusion imaging on the variability and errors of tractography was evaluated through a software phantom developed by Tractometer. Three fiber tracking algorithms based on DTI, CSD, and Q-sampling were tested. Large false positive and false negative rate was seen for all methods, regardless of SNR or b value. A moderate thresholding can reduce false positive rate and total error rate.

3058

Computer #53



Comparison of Automated and Hand-Drawn Tractography of the Optic Radiations in Children with NF1-Associated Optic Pathway Gliomas

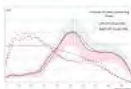
Peter de Blank^{1,2}, Greg Russell³, Michael J Fisher⁴, and Jeffrey I Berman⁵

¹Pediatrics, University Hospitals, Cleveland, OH, United States, ²Case Western Reserve University, Cleveland, OH, United States, ³Boston, MA, United States, ⁴Pediatrics, Children's Hospital of Philadelphia, Philadelphia, PA, United States, ⁵Radiology, Children's Hospital of Philadelphia, Philadelphia, PA, United States

Previous studies demonstrate that hand-drawn tractography of the optic radiations correlates with visual acuity in children with optic pathway glioma (OPG). However, automated tractography using a structural atlas would require less time and user expertise. We evaluated 50 children with OPG using both tractography methods. Both methods demonstrate significant differences in MD and RD between children with and without visual acuity loss. On multivariable analysis, both methods demonstrate a similar association between DTI measures and visual acuity. Automated tractography is a valid method to assess the optic radiations in children with OPG that requires less time and expertise.

3059

Computer #54



Improvement of probabilistic tractography of the corticospinal tract in human brain

David Neil Manners¹, Claudia Testa¹, Stefania Evangelisti¹, Stefano Zanigni¹, Mariagrazia Popeo^{2,3}, Caterina Tonon¹, and Raffaele Lodi¹

¹Department of Biomedical and Neuromotor Sciences, University of Bologna, Bologna, Italy, ²Istituto Italiano di Tecnologia, Rovereto, Italy, ³Center for Neurosciences and Cognitive Systems, University of Trento, Rovereto, Italy

We performed an along tract analysis of the cortico-spinal tract in a group of healthy subjects using a probabilistic tractography algorithm. We were able to evaluate CST reconstruction along the tract using appropriate performance metrics, based on the congruence of fibre paths in the subject population, and the presence or absence of fibre tracks identified as originating from the precentral gyrus. The method was compatible with clinical protocols given spatial definition and tract localization obtained.

3060

Computer #55



Diffusion Tensor Imaging (DTI) of the myopathic and dystrophic skeletal muscle

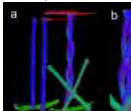
Sarah Keller¹, Jerry Zhiyue Wang², Amir Golsari³, Adam Gerhard¹, Hendrick Kooijman⁴, Mathias Gelderblom³, and Jin Yamamura¹

¹Diagnostic and Interventional Radiology, University Medical Center Hamburg Eppendorf (UKE), Hamburg, Germany, ²Radiology, University of Texas Southwestern Medical Center, Dallas, TX, United States, ³Neurology, University Medical Center Hamburg Eppendorf (UKE), Hamburg, Germany, ⁴MRI, Philips GmbH, Hamburg, Germany

MRI-Diffusion tensor imaging (DTI) based fiber tracking is an emerging tool for the evaluation of alterations in the skeletal muscle architecture caused by trauma and various inflammatory or hereditary diseases. It remains still a matter of debate, whether dystrophic conditions of the skeletal muscle, which are frequently associated with fatty infiltration, can be reliably assessed by DTI, as previous studies showed the potential biasing effect of the fat fraction (%FF) and the concomitant decrease of the signal to noise ratio (SNR) [1, 2]. The goal of this study was to analyze the DTI based apparent diffusion coefficient (ADC), fractional anisotropy (FA) and tractography data in various conditions of muscular disease, either with or without increase of the FF in comparison to healthy controls on a 3T system.

3061

Computer #56



A novel diffusion tensor imaging phantom that simulates complex neuro-architecture for potential validation of DTI Processing
Greg Whitton¹, Timotheus Gmeiner¹, Chad Tyler Harris¹, and Fergal Kerins¹

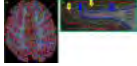
¹Synaptive Medical, Toronto, ON, Canada

In this work a DTI phantom containing complex geometries and anisotropic microstructure to mimic fiber bundles is presented. The phantom consists of ten individual fiber bundles distributed in different orientations to best test and confirm proper DTI processing. Each fiber bundle contains 4.4 million fibers within a flexible casing. The phantom was imaged using a 2D EPI DTI sequence, and

tractography was generated using BrightMatter™ Plan. Agreement was found between fiber location and tractography: FA values averaging 0.51, were within +/- 10% of the overall FA average within the fibers demonstrating consistent diffusion throughout the fiber bundles.

3062

Computer #57



Uncover of fiber reorientation in the medial human cortex *in vivo*
Oleg Posnansky¹, Myung-Ho In¹, and Oliver Speck¹

¹*Department of Biomedical Magnetic Resonance, Institute of Experimental Physics, Magdeburg, Germany*

Higher spatial resolution at ultra-high field ($\geq 7T$) magnetic resonance imaging (UHF MRI), with consequent reduction of partial volume effects, enables diffusion tensor imaging (DTI) to visualize sharp turns of the white matter (WM) fibers into grey matter cortex (CTX), which are challenging to see in the lower main magnetic field data. More, UHF DTI data also recover rather high fractional anisotropy (FA) in several CTX regions, which may help to minimize the strong gyral bias in tractography that are found even in the relatively high resolution 3T DTI. In this work we analyse statistical properties of DTI major eigenvectors at UHF as in WM-CTX interface as in medial CTX to understand fiber orientation characteristics in the *whole* human brain *in vivo* and allow connectivity analysis from white matter into the cortex.

3063

Computer #58



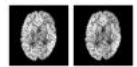
Construction of a diffusion MRI brain template using Human Connectome Project database
Yung-Chin Hsu¹ and Wen-Yih Isaac Tseng¹

¹*Institute of Medical Device and Imaging, National Taiwan University College of Medicine, Taipei, Taiwan*

The present study uses the diffusion data of the human connectome project (HCP) as well as a state-of-the-art registration strategy to develop a diffusion template in the ICBM-152 space. A total of 489 diffusion datasets were included in the template construction. The HCP diffusion template matches to the ICBM-152 space well, in both the deep and superficial white matter regions. In addition, this template is capable of revealing detailed diffusion-dependent structures, such as the cortical-depth dependence of general fractional anisotropy (GFA). The HCP diffusion template is potentially useful in segmenting fine fiber tracts and parceling thalamic nuclei or hippocampal subfields.

3064

Computer #59



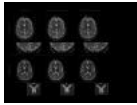
Examining Global White Matter Development via the Sparse Coding Properties of Diffusion-Weighted MRI
Vishal Patel¹, Mariko Fitzgibbons¹, Paul M Thompson², Arthur W Toga², and Noriko Salamon¹

¹*University of California, Los Angeles, Los Angeles, CA, United States*, ²*University of Southern California, Los Angeles, CA, United States*

To avoid the assumptions inherent in diffusion modeling and tractography, we develop a new approach for studying global white matter development that operates on diffusion-weighted MR images directly. We apply a sparse coding method, K-SVD, to decompose a diffusion-weighted series. We quantify the efficiency of the resulting encoding by computing the Gini coefficient. We then show that this measure increases in a predictable manner throughout normal pediatric development. Our results support the hypotheses that more organized white matter can be more sparsely encoded and that the sparsity of the encoding may thus be used to infer the state of development.

3065

Computer #60



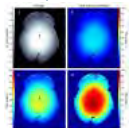
DTI with embedded PLACE: geometric distortion correction with no extra scan time and reduced motion sensitivity
Jordan Chad¹, Andrew Curtis¹, Qing-San Xiang^{2,3}, and Sofia Chavez^{1,4}

¹*Centre for Addiction and Mental Health, Toronto, ON, Canada*, ²*Department of Radiology, University of British Columbia, Vancouver, BC, Canada*, ³*Department of Physics and Astronomy, University of British Columbia, Vancouver, BC, Canada*, ⁴*Department of Psychiatry, University of Toronto, Toronto, ON, Canada*

A phase-based method, PLACE, is embedded into a stock DTI sequence to enable geometric distortion correction without the need for extra scans. We show that geometric distortion correction via this embedded PLACE DTI sequence performs like the more traditional B0-map based correction schemes when there is no motion between scans. Furthermore, when motion occurs, embedded PLACE yields superior results. This embedded PLACE DTI is thus more efficient and less sensitive to motion than traditional B0 mapping methods.

3066

Computer #61



A comparison of multiple acquisition strategies to overcome B1 inhomogeneities in diffusion imaging of post-mortem human brain at 7T
Sean Foxley¹, Saad Jbabdi¹, Moises Hernandez Fernandez¹, Connor Scott², Olaf Ansorge², and Karla Miller¹

¹*FMRIB Centre, University of Oxford, Oxford, United Kingdom*, ²*Nuffield Department of Clinical Neurosciences, University of Oxford, Oxford, United Kingdom*

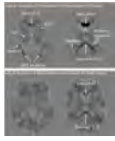
In this work we compare a single flip angle and dual flip angle approach to overcome B1 inhomogeneities in DW-SSFP data of post mortem human brain at 7T. Both approaches were designed and optimized to achieve optimal CNR with whole brain coverage. The single flip angle approach displayed slight improvements in orientation estimates; however, the dual flip angle approach is being further investigated as a potential source of microstructural estimates with little to no cost in orientation.

3067

Computer #62

Deformation Based Morphometry using Diffusion Tensor MRI (DTI) Data

Neda Sadeghi¹, Cibu P. Thomas^{1,2,3}, M. Okan Irfanoglu^{1,3}, Amritha Nayaka^{1,3}, Maria Grazia D'Angelo⁴, Filippo Arrigoni⁵, and Carlo Pierpaoli¹

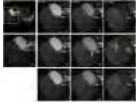


¹Section on Quantitative Imaging and Tissue Sciences, National Institute of Child Health and Human Development, National Institutes of Health, Bethesda, MD, United States, ²Center for Neuroscience and Regenerative Medicine, Uniformed Services University of the Health Sciences, Bethesda, MD, United States, ³Henry Jackson Foundation, Bethesda, MD, United States, ⁴Functional Rehabilitation Unit - Neuromuscular Disorders, IRCCS E.Medea Institute, Bosisio Parini, Italy, ⁵Neuroimaging Lab, IRCCS E.Medea Institute, Bosisio Parini, Italy

Tensor based morphometry (TBM) is a class of deformation based morphometry (DBM) methods that is traditionally performed on T1-weighted images (T1W). Here, we investigate the sensitivity of TBM, based on T1W and diffusion tensor imaging (DTI) data in patients diagnosed with SPG11, a neurological condition with a known genetic basis. TBM based on T1W and diffusion data captured the volumetric changes along the corpus callosum, which is a known characteristic of SPG11 patients, but does not fully explain the disorder. In contrast, only DTI-TBM identified volumetric changes in several association and projection pathways suggesting greater sensitivity of DTI-TBM.

3068

Computer #63



Motion correction for abdominal diffusion weighted images by using fitting accuracy guided free-form deformation.

Yihao Guo¹, Zhentai Lu¹, Yingjie Mei², Jing Zhang³, and Yanqiu Feng^{1,4,5}

¹School of Biomedical Engineering and Guangdong Provincial Key Laboratory of Medical Image Processing, Southern Medical University, GuangZhou, China, People's Republic of, ²Philips Healthcare, GuangZhou, China, People's Republic of, ³Department of Medical Imaging Center, Nanfang Hospital, Southern Medical University, GuangZhou, China, People's Republic of, ⁴Laboratory of Biomedical Imaging and Signal Processing, The University of Hong Kong, Hong Kong SAR, China, People's Republic of, ⁵Department of Electrical and Electronic Engineering, The University of Hong Kong, Hong Kong SAR, China, People's Republic of

Free-form deformation registration has been widely used but would lead to unwanted bias in the registration of different b-value images to b0 image, especially high-b-value images, due to signal attenuation dependent on b values. We use fitting accuracy to guide free-form deformation registration. The results of our proposed method can well realign the different b-value images in liver edges and improve the fitting accuracy.

3069

Computer #64



A New Method to Construct and Validate an Optic Radiation Template using Probabilistic Tractography

Chenyu Wang^{1,2}, Alexander Klistorner^{1,3,4}, Linda Ly^{1,2}, Ruth A Oliver^{1,2}, and Michael H Barnett^{1,2}

¹Sydney Neuroimaging Analysis Centre, Camperdown, Sydney, Australia, ²Brain and Mind Centre, University of Sydney, Camperdown, Sydney, Australia, ³Ophthalmology, Save Sight Institute, University of Sydney, Sydney, Australia, ⁴Australian School of Advanced Medicine, Macquarie University, Sydney, Australia

In-vivo delineation the white matter (WM) fibre bundles with diffusion-weighted imaging (DWI) and tractography facilitates the study of tract-specific damage due to neurological disease. However, this approach is limited by suboptimal or absent DWI datasets. Accurate atlas based white matter segmentation may provide an alternative method that can be broadly applied to existing neuroimaging datasets. Using the optic radiation as an example, we propose a new framework for the mapping and validation of white matter tracts in healthy subjects using probabilistic tractography.

3070

Computer #65



Recovery of Lost Connectivities in the Human Brain Connectome as Enabled by Ultra High Spatial Resolution Diffusion MRI

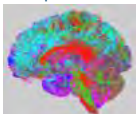
Iain P Bruce¹, Christopher Petty¹, Nan-Kuei Chen¹, and Allen W Song¹

¹Brain Imaging and Analysis Center, Duke University Medical Center, Durham, NC, United States

Typical diffusion tensor imaging datasets are acquired at relatively low spatial resolutions (~2 mm) because of limitations in commonly used single-shot echo-planar imaging (EPI) protocols. However, within a relatively coarse voxel, it is often difficult for fiber tracking algorithms to accurately resolve short association fibers (e.g. cortical u-fibers) with very high curvature. As these fibers play an important role in linking adjacent gyri and constructing the human connectome, this report aims to quantify the recovery of lost connections and the improved accuracy of mutual connectivities between ROIs through high spatial resolution (enabled by multi-shot EPI based on multiplexed sensitivity encoding).

3071

Computer #66



Assessment of Rotationally-Invariant Clustering Using Streamlet Tractography

Matthew George Liptrot^{1,2} and Francois Lauze¹

¹Department of Computer Science, University of Copenhagen, Copenhagen, Denmark, ²DTU Compute, Technical University of Denmark, Lyngby, Denmark

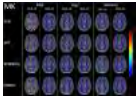
We present a novel visualisation-based strategy for the assessment of a recently proposed clustering technique for raw DWI volumes which derives rotationally-invariant metrics to classify voxels. The validity of the division of all brain tissue voxels into such classes was assessed using the recently developed streamlets visualisation technique, which aims to represent brain fibres by collections of many short streamlines. Under the assumption that streamlines seeded in a cluster should stay within it, we were able to assess how well perceptual tracing could occur across the boundaries of the clusters.

3072

Computer #67

Comparing the performances of three diffusion kurtosis tensor estimation algorithms via a ground truth diffusion template derived from HCP data

Daniel V. Olson¹, Volkan Arpinar², and L. Tugan Muftuler²

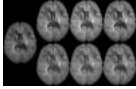


¹*Biophysics, Medical College of Wisconsin, Milwaukee, WI, United States,* ²*Neurosurgery, Medical College of Wisconsin, Milwaukee, WI, United States*

A diffusion weighted imaging template is proposed, which is derived from the in vivo data from the HCP database. Diffusion weighted signals are generated from this template using the DKI tensor model, and diffusion tensor and kurtosis tensor metric maps are produced. These maps established the ground truth, against which the outputs of different DKI tensor estimation algorithms were compared. Rician noise is added to simulate typical diffusion MRI acquisitions with different SNR levels. The performances of the algorithms are then compared via voxel-wise Mean Square Error and bias-plus-variance decomposition to determine the optimal algorithm for the desired application.

3073

Computer #68



Automatic DWI denoising using TGV with local dependent noise estimate

Gernot Reishofer¹, Kristian Bredies², Karl Koschutnig³, Christian Langkammer⁴, Margit Jehna¹, and Hannes Deutschmann¹

¹*Neuroradiology, Medical University of Graz, Graz, Austria,* ²*Mathematics and Scientific Computing, University of Graz, Graz, Austria,* ³*Psychology, University of Graz, Graz, Austria,* ⁴*Neurology, Medical University of Graz, Graz, Austria*

High-resolution diffusion weighted imaging (DWI) with reduced susceptibility artifacts can be acquired using readout-segmented echo planar imaging (rs-EPI). The poor SNR that limits the applicability of this technique increases the need for denoising strategies. We introduce a novel user independent algorithm for denoising DWI data utilizing total generalized variation (TGV) regularization under consideration of the spatial dependent noise distribution. The feasibility of the proposed method was tested on synthetic DWI data at different noise levels and compared with non-local-means (NLM) filtering.

3074

Computer #69



Cortico-Subcortical motor network integrity relates to functional recovery after stroke

Silvia Obertino¹, Lorenza Brusini¹, Ilaria Boscolo Galazzo^{2,3}, Mauro Zucchelli¹, Alessandro Daducci⁴, Gloria Menegaz¹, and Cristina Granziera^{5,6}

¹*Computer Science, University of Verona, Verona, Italy,* ²*Institute of Nuclear Medicine, UCL, United Kingdom,* ³*Neuroradiology, University Hospital Verona, Italy,* ⁴*École polytechnique fédérale de Lausanne, Switzerland,* ⁵*Martinos Center for Biomedical Imaging, Massachusetts General Hospital and Harvard Medical School, Chalestown, MA, United States,* ⁶*Advanced Clinical Imaging Technology (HC CMEA SUI DI BM PI), Siemens Healthcare AG, Lausanne, Switzerland*

In this work, we investigated whether the structural properties of cortico-subcortical (CS) motor circuits are related to motor outcome after stroke. To do this, we acquired Diffusion Spectrum Imaging data in 10 stroke patients at 3 time points after stroke. We then performed tractographic reconstruction and estimated a number of microstructural indices, derived from the 3D Simple Harmonic Oscillator based REconstruction and Estimation (SHORE) model, in the cortico-subcortical motor fiber tracts. Linear regression analysis showed that that SHORE metrics of thalamo-cortical and intrastriatal connections in the first week after stroke are strongly related to stroke recovery at 6 months follow-up.

3075

Computer #70



Comparisons of cortical depth dependence of diffusion properties over the whole human brain in-vivo

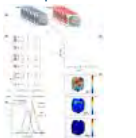
Oleg Posnansky¹, Myung-Ho In¹, and Oliver Speck¹

¹*Department of Biomedical Magnetic Resonance, Institute of Experimental Physics, Magdeburg, Germany*

Ultra-high field (≥ 7 T) magnetic resonance imaging possesses substantial sensitivity to depict patterns of tissue cytoarchitecture. Recent studies have shown a cortex depth dependence of diffusion tensor invariants such as fractional anisotropy and mean diffusivity. In this study we further probe the potential of diffusion tensor imaging for the *whole* human brain *in vivo* by mapping it on the segments of Desikan-Killiany atlas. Such analysis complied via very precise distortion correction procedure and building a series of lamellae, allows one to understand a spatial specificity of marginal distribution of diffusion tensor invariants and reveal unusual effects in fiber topology.

3076

Computer #71



Asymmetrical cerebral response to appetite in mice

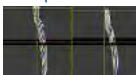
Ania Benítez^{1,2}, Blanca Lizarbe³, Pilar López-Larrubia¹, Luis Lago-Fernández², Manuel Sánchez-Montañés², and Sebastián Cerdán¹

¹*Instituto de Investigaciones Biomédicas "Alberto Sols", Madrid, Spain,* ²*Universidad Autónoma de Madrid, Madrid, Spain,* ³*École Polytechnique Fédérale de Lausanne EPFL, Lausanne, Switzerland*

We investigate the global cerebral response to appetite in mice by functional Diffusion Weighted Imaging, implementing two independent, but complementary, methods of data analysis; a) Model-free classification algorithm and b) Biexponential diffusion parameter fittings. The model-free approach allowed the pixel by pixel calculation of appetite index maps, used to classify the brain between fed and fasted conditions. Biexponential model fittings allowed the calculation of diffusion parameter maps, revealing significant increases in diffusion parameters through the whole fasted brain. Both methods detected an asymmetric cerebral response to appetite with the right cerebral hemisphere becoming more responsive.

3077

Computer #72



3D Curvature of Medial Gastrocnemius (MG) Muscle Fibers Tracked from Diffusion Tensor Images (DTI): Age Related Differences in 3D fiber curvature.

Yanjie Xue¹, Usha Sinha¹, Vadim Malis², Robert Csapo³, and Shantanu Sinha³

¹*Physics, San Diego State University, San Diego, CA, United States,* ²*Physics, University of California at San Diego, San Diego, CA, United States,* ³*Radiology, University of California at San Diego, San Diego, CA, United States*

Muscle fiber curvature influences muscle function but 3D curvature of the MG remains unexplored. This study determines 3D fiber curvature from young and old cohorts from MG fibers tracked using DTI data. The fiber coordinates are fit to a 2nd or 3rd order polynomial before extracting curvature using the Frenet-Serret relationship. The order of the polynomial affects curvature values and the choice may depend on muscle fiber shape. Regional curvature changes were significant between distal and central in the deep, middle and superficial compartments. No significant changes were seen in the curvature between young and old subjects

Electronic Poster

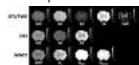
Diffusion: Microstructure

Exhibition Hall

Monday, May 9, 2016: 16:30 - 17:30

3078

Computer #73



Longitudinal Comparison of Diffusion Imaging Modeling in Rat Spinal Cord Injury

Nathan P Skinner^{1,2,3}, Sean D McGarry⁴, Shekar N Kurpad^{3,5}, Brian D Schmit⁶, and Matthew D Budde^{3,5}

¹*Biophysics Graduate Program, Medical College of Wisconsin, Milwaukee, WI, United States*, ²*Medical Scientist Training Program, Medical College of Wisconsin, Milwaukee, WI, United States*, ³*Department of Neurosurgery, Medical College of Wisconsin, Milwaukee, WI, United States*, ⁴*Neuroscience Doctoral Program, Medical College of Wisconsin, Milwaukee, WI, United States*, ⁵*Clement J. Zablocki Veteran's Affairs Medical Center, Milwaukee, WI, United States*, ⁶*Department of Biomedical Engineering, Marquette University, Milwaukee, WI, United States*

A rat model of graded spinal cord injury was used to evaluate several diffusion models for the ability to detect injury at acute and chronic time points. Parameters from diffusion tensor imaging, free water estimation, diffusion kurtosis imaging, and white matter tract integrity models demonstrated that higher order modeling showed better separation of injury severity, especially in the chronic time point. Furthermore, parameters sensitive to volume changes associated with edema and inflammation demonstrated the greatest separation of these injury groups, indicating the importance of these processes in altering diffusion characteristics in spinal cord injury.

3079

Computer #74



Intracellular metabolites exhibit non-Gaussian diffusion in the healthy human brain using magnetic resonance spectroscopy at 7 Tesla

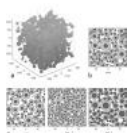
Carson Ingo¹, Wyger M. Brink¹, Ece Ercan¹, Andrew G. Webb¹, and Itamar Ronen¹

¹*C.J. Gorter Center for High Field MRI, Department of Radiology, Leiden University Medical Center, Leiden, Netherlands*

Since choline mostly resides in astrocytes, N-acetyl-aspartate mostly resides in axons, and creatine is distributed between both neural cell types, these intracellular metabolites can provide more specific microstructural compartment information compared to water. In this study, we apply diffusion-weighted spectroscopy to analyze axonal and glial structures by identifying non-Gaussian movement of intracellular metabolites in both white and gray matter of the healthy human brain at b-values up to ~17,000 s/mm². We establish that all measured metabolites exhibited non-Gaussian subdiffusion in both tissue types with the gray matter intracellular space appearing more heterogeneous than white matter, opposite to water diffusion dynamics.

3080

Computer #75



Relations between the stretched exponential DWI model and tumor malignancy related microstructural changes

Chu-Yu Lee¹, Kevin M Bennett², Josef P Debbins³, In-Young Choi^{1,4,5}, and Phil Lee^{1,5}

¹*Hoglund Brain Imaging Center, University of Kansas Medical Center, Kansas city, KS, United States*, ²*Department of Biology, University of Hawaii, Manoa, HI, United States*, ³*Neuroimaging research, Barrow Neurological Institute, Phoenix, AZ, United States*, ⁴*Department of Neurology, University of Kansas Medical Center, Kansas City, KS, United States*, ⁵*Department of Molecular & Integrative Physiology, University of Kansas Medical Center, Kansas City, KS, United States*

Diffusion weighting imaging (DWI) has been shown to be useful in differentiating low- and high-grade tumors in the brain. The decreased apparent diffusion coefficient (ADC) has been associated with increased tumor cellularity. However, tumor malignancy involves multiple microstructural changes that may also affect changes in the ADC. The alternative way to assess water diffusion in the complex microstructure is through the diffusion heterogeneity measured by the stretched exponential model (α -DWI). Recent studies using the α -DWI model have shown the increased diffusion heterogeneity in high-grade tumors. However, it remains unclear about the microstructural information provided by the α . The purpose of this study was to investigate how the α -DWI model responds to tumor malignancy related microstructural changes. We simulated a 3-D microenvironment in tumors and a DWI experiment. We studied how ADC and the fitted parameters of the α -DWI model responded to microstructural changes related to tumor malignancy.

3081

Computer #76



Validation and comparison of diffusion MR methods measuring transcytolemmal water exchange rate

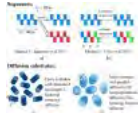
Xin Tian^{1,2}, Hua Li¹, Xiaoyu Jiang¹, Jingping Xie¹, John C Gore¹, and Junzhong Xu¹

¹*Radiology and Radiological Sciences, Vanderbilt University, Nashville, TN, United States*, ²*Radiology, The Second Hospital of Hebei Medical University, Shijiazhuang, China, People's Republic of*

Two diffusion-based method, the CG (constant gradient) and FEXI (filtered exchange imaging) methods, have been developed to provide a flexible and safer means to measure transcytolemmal water exchange rate k_{tr} non-invasively in vivo. However, neither methods have been fully validated up to date. In the present work, computer simulations and in vitro experiments with well-controlled cultured cells with different sizes and permeabilities were performed to evaluate the accuracy of the CG and FEXI methods. The results suggest that k_{tr} can be accurately estimated when $k_{tr} < 10$ Hz. Although the FEXI method provides less accurate results, the linear dependence of AXR on k_{tr} suggesting it is still a reliable method.

3082

Computer #77



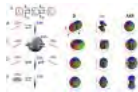
Metrics of microscopic anisotropy: a comparison study

Andrada Ianus¹, Noam Shemesh², Daniel C. Alexander¹, and Ivana Drobnjak¹¹CMIC, University College London, London, United Kingdom, ²Champalimaud Neuroscience Programme, Champalimaud Centre for the Unknown, Lisbon, Portugal

Microscopic anisotropy disentangles the effects of pore shape from orientation distribution, and thus can serve as a valuable metric for underlying microstructural configurations. Recent developments in diffusion MRI proposed different approaches to acquire and analyse data for extracting information regarding microscopic anisotropy. This work compares in simulation two recently introduced metrics of microscopic anisotropy: fractional eccentricity (FE), derived from double-diffusion-encoding (DDE) sequences and microscopic fractional anisotropy (μ FA), derived from a combination of sequences with isotropic and directional diffusion weighting. We find that DDE-derived metrics are more reliable for quantifying underlying microstructures if diffusion is restricted, while μ FA is closer to the ground truth values when individual micro-domains feature Gaussian diffusion.

3083

Computer #78



Apparent Exchange Rate in Multi-compartment Anisotropic Tissue

Samo Lasič¹, Sune N. Jespersen^{2,3}, Henrik Lundell⁴, Markus Nilsson⁵, Tim B. Dyrby⁴, and Daniel Topgaard⁶¹CR Development, AB, Lund, Sweden, ²CFIN/MINDLab, Department of Clinical Medicine, Aarhus University, Aarhus, Denmark, ³Department of Physics and Astronomy, Aarhus University, Aarhus, Denmark, ⁴Danish Research Centre for Magnetic Resonance, Copenhagen University Hospital, Hvidovre, Copenhagen, Denmark, ⁵Lund University Biomaging Center, Lund University, Lund, Sweden, ⁶Physical Chemistry, Lund University, Lund, Sweden

Filter exchange imaging (FEXI) is a noninvasive method to probe Apparent Exchange Rate (AXR). Understanding how diffusion anisotropy affects AXR is fundamental in experimental design and interpretation of results. In case of only two compartments, AXR is isotropic regardless of diffusion anisotropy. The key finding of this work is that AXR is anisotropic even in systems with a single exchange rate if there are more than two orientationally dispersed compartments. These findings may guide identification of different fiber populations and their directions and could be useful for analysis of fiber-specific characteristics.

3084

Computer #79



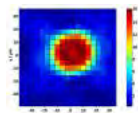
Simulating axon packing for investigating white matter tissue characteristics with diffusion MRI

Hamed Y. Mesri¹, Dmitry S. Novikov², Max A. Viergever¹, and Alexander Leemans¹¹Image Sciences Institute, University Medical Center Utrecht, Utrecht, Netherlands, ²Bernard and Irene Schwartz Center for Biomedical Imaging, Department of Radiology, New York University School of Medicine, New York, NY, United States

A novel algorithm for simulating axon packing in nerve bundles is proposed. Statistical analysis of the results demonstrates that, in contrast to conventional methods, the proposed method eliminates the bias in the estimated distribution and achieves higher packing densities, while preserving the random nature of the axon packing structure. The resultant tissue models can be used subsequently to study the Brownian motion of water molecules within nerve bundles. With our novel axon packing simulation framework, the effect of axon properties on the derived diffusion-weighted MR signal can be investigated more reliably now.

3085

Computer #80



Magnetic Resonance Diffusion Pore Imaging on Preclinical 9.4T-Animal-Scanner

Marco Bertleff¹, Sebastian Domsch¹, Frederik Laun², Tristan Kuder², and Lothar Schad¹¹Computer Assisted Clinical Medicine, Heidelberg University, Medical Faculty Mannheim, Mannheim, Germany, ²Department of Medical Physics in Radiology, German Cancer Research Center (DKFZ), Heidelberg, Germany

The study of porous microstructures is of high interest in medical imaging. Diffusion pore imaging (DPI) has recently been proposed as a means to acquire images of the average cell shape in a voxel or region of interest. In this work, we present the feasibility of DPI phantom measurements on a preclinical 9.4T animal scanner for the first time and preliminarily compare two different sequence implementations. The shown feasibility on a preclinical system opens the possibility of a potential in-vivo measurement realization.

3086

Computer #81



Diffusion microstructure in the population: variability and effect size of biophysical compartment model parameters over 100 subjects

Robbert Harms¹, Rainer Goebel¹, and Alard Roebroeck¹¹Maastricht University, Maastricht, Netherlands

Statistical power in neuroscience studies is often limited, leading to, among others, low reproducibility of results[1]. Robust effect size estimates over a large subject group are crucial for power assessments. Here, we computed these estimates for microstructural differences in splenium, body and genu of the Corpus Callosum (CC) using diffusion MRI microstructure modeling over 100 subjects. We fitted Tensor, Ball&Stick, NODDI and CHARMED using GPU-accelerated software (MDT) and extracted subject specific parameters for the CC for each model. We observe medium to large effect sizes (Cohen's $d=1-3$) for dMRI microstructure measures, promising for power and reproducibility of dMRI microstructure studies.

3087

Computer #82

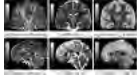
Obtaining geometrical information from the time-dependent apparent diffusion coefficient

Simona Schiavi¹, Housseem Haddar¹, and Jing-Rebecca Li¹

Diffusion MRI (dMRI) has been established as a useful tool to obtain voxel-level information on the tissue micro-structure. An important quantity measured in dMRI is the apparent diffusion coefficient (ADC), and it has been well established by in-vivo brain imaging experiments that the ADC depends significantly on the diffusion time. We derive an explicit formula for the time-dependent ADC, and, using the ADCs at multiple diffusion times and gradient directions, we estimate the surface to volume ratio, the eigenvalues and the first moment of the dominant eigen-functions associated to the geometry of the biological cells.

3088

Computer #83



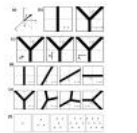
Precise Inference of Cellular and Axonal Structural Organization (PICASO) using diffusion MRI
Lipeng Ning^{1,2}, Carl-Fredrik Westin^{1,2}, and Yogesh Rathi^{1,2}

¹Brigham and Women's Hospital, Boston, MA, United States, ²Harvard Medical School, Boston, MA, United States

We propose a novel model termed PICASO for investigating the microstructural layout of brain tissue using in vivo diffusion MRI (dMRI) measurements. Our method provides a direct connection between the structural organization of biological tissue and a function representing the disorder in the evolution of magnetization density. This is achieved by extending the Bloch-Torrey equation to include variability in diffusivity due to restrictions and hindrances. Using in vivo data from the Human Connectome Project (HCP), we show that the PICASO model can provide novel information about the microstructural layout of the axonal packing in human brain. Thus, our method can be applied in clinical settings to investigate brain abnormalities.

3089

Computer #84



Simulation study investigating the effect of diffusion, susceptibility, and vessel topology in characterizing normal and tumorous vasculature using R2*

Mohammed Salman Shazeeb^{1,2}, Jayashree Kalpathy-Cramer¹, and Bashir Issa²

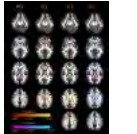
¹Athinoula A. Martinos Center for Biomedical Imaging, Massachusetts General Hospital and Harvard Medical School, Boston, MA, United States,

²Department of Physics, UAE University, Al-Ain, Abu Dhabi, United Arab Emirates

Brain vasculature is conventionally represented as straight cylinders when simulating BOLD contrast effects in fMRI. In reality, the vasculature is more complicated with branching and coiling especially in tumors. We applied a cylinder fork model to reflect the bifurcation, tortuosity, and size of vessels and performed simulations to study the effect of the rotation angle (ϕ) on R2* at different bifurcation angles (β), vessel diameters, diffusion constants, and susceptibility values. This model clearly showed an R2* dependence on ϕ , which could potentially be used as a tool to differentiate between normal and tumor vessels.

3090

Computer #85



Anomalous diffusion parameters are sensible to microstructural variations in brain due to aging

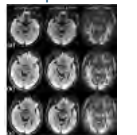
Michele Guerrerri^{1,2}, Alessandra Caporale^{1,2}, Marco Palombo^{1,3}, Ivan De Berardinis¹, Emiliano Macaluso⁴, Marco Bozzali⁴, and Silvia Capuani¹

¹Department of physics, CNR ISC UOS Roma Sapienza, Rome, Italy, ²Department of anatomical, histological, forensic and of the locomotor system science, Morphogenesis & Tissue Homeostasis, Sapienza University, Rome, Italy, ³MIRcen, CEA/DSV/I2BM, Fontenay-Aux Roses, France, ⁴Neuroimaging Laboratory, Santa Lucia Foundation, Rome, Italy

We investigated the anomalous diffusion (AD) stretched exponential γ -imaging model to overcome the sensitivity limitations of conventional DTI approach based on the assumption of the Gaussian model with regard to displacements of water molecules in tissues. The benefits of this approach are illustrated with an in-vivo diffusion study of the human brain performed on 18 healthy volunteers in the age range (23-70 years). Mean γ (M_γ) and anisotropic γ (A_γ) maps are obtained and compared with DTI maps. The current study suggests that M_γ and A_γ are more sensitive to micro-structural changes caused by normal aging, compared to DTI metrics.

3091

Computer #86



Diffusion Microstructure Imaging With High-Performance Head-Only Gradient: Preliminary Results

Ek T Tan¹, Jonathan I Sperl², Miguel Molina Romero^{2,3}, Seung-Kyun Lee¹, Matt A Bernstein⁴, and Thomas KF Foo¹

¹GE Global Research, Niskayuna, NY, United States, ²GE Global Research, Munich, Germany, ³Technical University of Munich, Munich, Germany, ⁴Mayo Clinic, Rochester, MN, United States

A high-performance head-only gradient coil ($G_{\max}=80$ mT/m, SR=700 T/m/s) allows diffusion imaging at substantially shorter echo-time and echo-spacing than conventional whole-body gradient coil systems. This greatly benefits microstructure imaging with diffusion EPI, providing reduced echo spacing by up-to two-fold and shorter TE by up-to 30%. Imaging results demonstrate reduced distortion and improved white matter SNR. Preliminary results on axonal radius mapping with high b-value imaging (up-to $b=12,000$ s/mm²) demonstrate the feasibility of 2 mm-isotropic imaging with the head-gradient.

3092

Computer #87

Quantifying White Matter Microstructure with a Unified Spatio-Temporal Diffusion Weighted MRI Continuous Representation

Demian Wassermann¹, Alexandra Petiet², Rutger Fick¹, Mathieu Santin², Anne-Charlotte Philippe², Stephane Lehericy², and Rachid Deriche¹

¹Athena, Inria, Sophia-Antipolis, France, ²CENIR, Brain and Spine Institute, Paris, France

A current problem Diffusion MRI (dMRI) based microscopy faces under the narrow pulse approximation is how to best exploit the 4D (q-space + diffusion time) nature of the signal. Assaf et al. showed that exploring the dMRI attenuation at different diffusion times provides information on the apparent distribution of axonal diameters within a voxel in their seminal work: AxCaliber¹. However, AxCaliber

requires knowing beforehand the predominant orientation of the axons within the analyzed volume to adjust the q-space sampling accordingly. In this work, we show that our novel sparse representation of the 3D+t dMRI signal² enables the recovery of axonal diameter distribution parameters with two main advantages. First, it doesn't require knowledge of the predominant axonal direction at acquisition time. Second, using the hypothesised dMRI signal symmetry, it allows computing the average attenuation on the plane perpendicular to the predominant axonal direction analytically. Hence, it takes advantage of the full 3D+t signal information to fit the AxCaliber model.

3093



Computer #88



Cytoarchitectonic abnormalities along white matter pathways in temporal lobe epilepsy: Combining diffusional kurtosis imaging and automated fiber quantification

Russell Glenn¹, Jens H Jensen¹, Simon S Keller², Joseph A Helpert¹, and Leonardo Bonilha³

¹Medical University of South Carolina, Charleston, SC, United States, ²University of Liverpool, Liverpool, United Kingdom, ³Charleston, SC, United States

Temporal lobe epilepsy (TLE) is the most common form of medically refractory epilepsy and is associated with focal brain abnormalities causing recurrent, unprovoked seizures originating from the temporal lobe. However, cytoarchitectonic changes can be detected outside of the temporal lobe and may be associated with the clinical course of the disease. We implement a novel neuroimaging approach which combines the strengths of diffusional kurtosis imaging and automated fiber quantification for the non-invasive characterization of white matter pathways and demonstrate its sensitivity to detect pathological alterations associated with TLE. The proposed technique may provide further insights into the clinicopathology of TLE.

3094

Computer #89



Short-term mindfulness-based stress reduction training increases tract integrity in right auditory radiation and anterior and posterior commissures

Chang-Le Chen¹, Yao-Chia Shih², Tzung-Kuen Wen³, Shih-Chin Fang⁴, Da-Lun Tang⁵, Si-Chen Lee⁶, and Wen-Yih Isaac Tseng^{1,7,8}

¹Graduate Institute of Brain and Mind Sciences, National Taiwan University College of Medicine, Taipei, Taiwan, ²Institute of Biomedical Engineering, National Taiwan University, Taipei, Taiwan, ³Department of Buddhist Studies, Dharma Drum Institute of Liberal Arts, New Taipei City, Taiwan, ⁴Department of Neurology, Cardinal Tien Hospital Yonghe Branch, New Taipei City, Taiwan, ⁵Department of Mass Communication, Tamkang University, Taipei, Taiwan, ⁶Department of Electrical Engineering, National Taiwan University, Taipei, Taiwan, ⁷Institute of Medical Device and Image, National Taiwan University College of Medicine, Taipei, Taiwan, ⁸Molecular Imaging Center, National Taiwan University, Taipei, Taiwan

Mindfulness-based stress reduction (MBSR) is an 8-week mindfulness meditation training which exerts beneficial effects on physical and mental health. Many researches showed that the changes in brain structure were related to mindfulness meditation. However, few studies have investigated the relationships between short-term mindfulness meditation and altered white matter tracts. Therefore, a longitudinal study was designed in this study to identify the effects of 8-week MBSR program on white matter tract integrity. We found that there was significant difference in three white matter tracts, right auditory radiation, anterior commissure and posterior commissure, in the novice practitioners.

3095

Computer #90



A physically-constrained model for diffusion kurtosis imaging

Darryl McClymont¹, Irvin Teh¹, Hannah Whittington¹, Vicente Grau², and Jurgen Schneider¹

¹Division of Cardiovascular Medicine, University of Oxford, Oxford, United Kingdom, ²Department of Engineering Science, University of Oxford, Oxford, United Kingdom

Diffusion kurtosis imaging provides higher-order information about diffusion. However, the quadratic term in the diffusion kurtosis model produces undesirable behaviour at high b-values as a result of the negative tails of the diffusivity distribution. A truncated normal distribution has been proposed to address this in one dimension. This work extends this concept to a multivariate truncated normal distribution, and extends the range of b-values over which kurtosis can be estimated. The proposed model is fit to diffusion data from rat hearts, and yields kurtosis values that are consistent with the DKI model.

3096

Computer #91



Intravoxel Incoherent Motion in Normal Pituitary Gland: Initial Study with Turbo Spin-echo Diffusion-weighted Imaging

Kiyohisa Kamimura¹, Masanori Nakajo¹, Yoshihiko Fukukura¹, Takashi Iwanaga², Tomonori Saito², Masashi Sasaki², Takuro Fujisaki², Atsushi Takemura³, Tomoyuki Okuaki³, and Takashi Yoshiura¹

¹Radiology, Kagoshima University Medical and Dental Hospital, Kagoshima, Japan, ²Clinical Engineering Department Radiation Section, Kagoshima University Hospital, Kagoshima, Japan, ³Philips Electronics Japan, Tokyo, Japan

Our purpose was to evaluate the feasibility of intravoxel incoherent motion (IVIM) assessment based on turbo spin-echo diffusion-weighted imaging (TSE-DWI) in the normal pituitary gland. In a validation study using normal brain white matter (WM), Bland-Altman analyses revealed fair to good agreement with conventional echo-planar-based DWI (EP-DWI) in the true diffusion coefficient (D) and perfusion fraction (f). In 7 volunteers, both D and f in the anterior pituitary lobe were significantly higher than those in WM, being consistent with high microvascular density in the pituitary gland. Results demonstrated that IVIM assessment based on TSE-DWI in the pituitary gland is feasible.

3097

Computer #92

White Matter Asymmetry During Development Using Diffusion Kurtosis Imaging

Xiang Gao¹, Farida Grinberg^{1,2}, Ezequiel Farrher¹, Fei Li¹, Eileen Oberwelland^{3,4}, Irene Neuner^{1,5,6}, Kerstin Konrad^{4,6,7}, and N.Jon. Shah^{1,2,6}

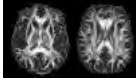


¹Institute of Neuroscience and Medicine - 4, Forschungszentrum Juelich GmbH, Juelich, Germany, ²Department of Neurology, Faculty of Medicine, RWTH Aachen University, Aachen, Germany, ³Translational Brain Research in Psychiatry and Neurology, Department of Child and Adolescent Psychiatry, Psychosomatics and Psychotherapy, RWTH Aachen University, Aachen, Germany, ⁴Institute of Neuroscience and Medicine - 3, Forschungszentrum Juelich GmbH, Juelich, Germany, ⁵Department of Psychiatry, Psychotherapy and Psychosomatics, RWTH Aachen University, Aachen, Germany, ⁶JARA - BRAIN, Translational Medicine, Juelich, Germany, ⁷Child Neuropsychology Section, Department of Child and Adolescent Psychiatry, Psychosomatics and Psychotherapy, RWTH Aachen University, Aachen, Germany

We compare changes in the white matter asymmetry index in conventional fractional anisotropy (FA) and other diffusion kurtosis imaging (DKI) metrics in adults and children. For some fibres, such as cingulate gyrus, hippocampus and superior longitudinal fasciculus, other DKI parameters show significant asymmetry where FA fails. When compared to adults, children showed more laterality in cingulate gyrus, superior longitudinal fasciculus and superior longitudinal fasciculus in temporal parts, which indicate that the degree of asymmetry in these fibres is higher during childhood.

3098

Computer #93



Anisotropy measure from High angular resolution diffusion imaging Data Using Higher Order Diffusion Tensor model
Getaneh Bayu Tefera¹ and Ponnada A. Narayana¹

¹Diagnostic & Interventional Imaging, University of Texas at Houston, Houston, TX, United States

Different anisotropy indices such as generalized anisotropy (GA) and generalized fractional anisotropy (GFA) for HARDI data have been reported, but they have their own limitations. Here we propose a new anisotropy measure (HFA) for the HARDI data that is rotationally invariant. The new proposed measure is compared with GA and GFA using the contrast-to-noise ratio and coefficient of variation as the metrics for three white matter regions. HFA and GFA have shown better CNR than FA and GA in two and three crossing regions. The results described above were very similar across all the five subjects.

3099

Computer #94



Tract Orientation and Angular Dispersion Deviation Indicator (TOADDI): A framework for single-subject analysis in diffusion tensor imaging

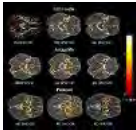
Cheng G. Koay^{1,2}, Ping-Hong Yeh^{2,3}, John M. Ollinger², M. Okan İrfanoğlu^{1,3}, Carlo Pierpaoli¹, Peter J. Basser¹, Terrence R. Oakes², and Gerard Riedy²

¹Eunice Kennedy Shriver National Institute of Child Health and Human Development, National Institutes of Health, Bethesda, MD, United States, ²National Intrepid Center of Excellence, Walter Reed National Military Medical Center, Bethesda, MD, United States, ³The Henry M. Jackson Foundation for the Advancement of Military Medicine, Bethesda, MD, United States

The purpose of the proposed framework is to carry out single-subject analysis of diffusion tensor imaging (DTI) data. This framework is termed **T**ract **O**rientation and **A**ngular **D**ispersion **D**eviation **I**ndicator (TOADDI). It is capable of testing whether an individual tract as represented by the major eigenvector of the diffusion tensor and its corresponding angular dispersion are significantly different from a group of tracts on a voxel-by-voxel basis. This work develops two complementary statistical tests (orientation and shape tests) based on the elliptical cone of uncertainty, which is a model of uncertainty or dispersion of the major eigenvector of the diffusion tensor.

3100

Computer #95



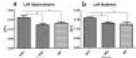
Assessment of brain structural abnormalities and the correlation with inhibitory control in betel nut chewers with DTI
Te-Wei Kao¹, Ming-Chou Ho², and Jun-Cheng Weng^{1,3}

¹Department of Medical Imaging and Radiological Sciences, Chung Shan Medical University, Taichung, Taiwan, ²Department of Psychology, Chung Shan Medical University, Taichung, Taiwan, ³Department of Medical Imaging, Chung Shan Medical University Hospital, Taichung, Taiwan

Betel nut is one of the common addictive substances in many countries. The brain influence of cocaine, alcohol, and tobacco cigarette have been studied by several studies. However, only few studies focused on the brain influence of betel nut, and most of them used fMRI or PET. Thus, our study aim was to use diffusion tensor imaging (DTI) to evaluate the impact of neurological structure of white matter caused by betel nut. The brain structural differences between the betel nut chewers and healthy controls and the correlation with inhibitory control were also discussed. Our results pointed out the significant neurological structural differences in the insula, amygdala and putamen of DTI indices between the betel nut chewers and healthy controls.

3101

Computer #96



Assessment of pharmacotherapy effects on APP/PS1 mice brain by Diffusion Spectrum Imaging
Chih-Hsien Tseng^{1,2}, Yu-Jen Chen¹, and Wen-Yih Isaac Tseng^{1,2,3,4}

¹Institute of Medical Device and Imaging, National Taiwan University College of Medicine, Taipei, Taiwan, ²Institute of Biomedical Engineering, National Taiwan University College of Medicine, Taipei, Taiwan, ³Graduate Institute of Brain and Mind Sciences, National Taiwan University College of Medicine, Taipei, Taiwan, ⁴Molecular Imaging Center, National Taiwan University, Taipei, Taiwan

To determine the effects of a novel neuroprotective drug on white matter integrity in Alzheimer's disease (AD), generalized fractional anisotropy (GFA) was assessed in mice brains using diffusion spectrum imaging (DSI). The mice included 5 AD mice without medication, 4 AD mice with medication, and 5 control mice. Comparing with the control mice, the AD mice without medication showed significantly increased GFA in the hippocampus and thalamus, whereas the AD mice with medication showed no significant difference. Our findings imply that DSI can be used to monitor the drug effects in AD mice.

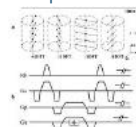
Novel Cardiovascular Techniques

Exhibition Hall

Monday, May 9, 2016: 17:30 - 18:30

3102

Computer #1



Accelerated 3D self-gated cardiac cine imaging at 3T using a tiny golden angle and compressed sensing

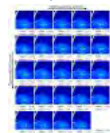
Xiaoyong Zhang^{1,2}, Guoxi Xie², Yanchun Zhu², Zijun Wei², Caiyun Shi², Shi Su², Fei Yan², Hairong Zheng², Bensheng Qiu¹, Xin Liu², and Zhaoyang Fan³

¹University of Science and Technology of China, Hefei, China, People's Republic of, ²Shenzhen Institutes of Advanced Technology, Shenzhen, China, People's Republic of, ³Cedars-Sinai Medical Center, Los Angeles, CA, United States

An accelerated self-gating (SG) technique, SparseSG, was developed to realize whole-heart coverage of 3D cardiac cine imaging at 3T without ECG and breath-holding. Preliminary in vivo study demonstrated that a whole heart coverage of 3D cine imaging can be achieved within 1 min and the technique had excellent performance compared to the standard ECG-triggering and conventional SG methods.

3103

Computer #2



Two-Dimensional Respiratory-Motion Characterization for Continuous MR Measurements Using Pilot Tone Navigation

Lea Schroeder¹, Jens Wetzl^{1,2}, Andreas Maier^{1,2}, Robert Rehner³, Matthias Fenchel⁴, and Peter Speier⁴

¹Pattern Recognition Lab, Department of Computer Science, Friedrich-Alexander-Universität Erlangen-Nürnberg, Erlangen, Germany, ²Erlangen Graduate School in Advanced Optical Technologies, Friedrich-Alexander-Universität Erlangen-Nürnberg, Erlangen, Germany, ³Magnetic Resonance, Research and Development, Hardware, Siemens Healthcare GmbH, Erlangen, Germany, ⁴Magnetic Resonance, Product Definition and Innovation, Siemens Healthcare GmbH, Erlangen, Germany

Pilot Tone signals, generated by a commercial signal generator and received with standard MR local coils, were analyzed for multidimensional respiratory information. The ground truth for respiratory motion in two orthogonal directions ($\boldsymbol{g}_{\text{SI}}$ and $\boldsymbol{g}_{\text{AP}}$), generated by sagittal image streams of the right liver dome using standard fluoroscopic sequences, showed excellent correlation with the PT signal derived from a separate measurement (for $\boldsymbol{g}_{\text{SI}}$: 0.90 \pm 0.13; for $\boldsymbol{g}_{\text{AP}}$: 0.82 \pm 0.21). Our results demonstrate that PT navigation can provide two-dimensional characterization of regular and irregular respiratory motion without interfering with the MR measurement.

3104

Computer #3



Fetal Cardiac MRI with self-gated iGRASP

Kostas Haris^{1,2}, Erik Hedstrom^{2,3}, Sebastian Bidhult², Frederik Testud⁴, George Kantasis^{1,2}, Henrik Engblom², Marcus Carlsson², Nicos Maglaveras¹, Einar Heiberg², Stefan R Hansson⁵, Hakan Arheden², and Anthony H Aletras^{1,2}

¹Laboratory of Medical Informatics, Department of Medicine, Aristotle University of Thessaloniki, Thessaloniki, Greece, ²Lund Cardiac MR Group, Department of Clinical Physiology and Nuclear Medicine, Skåne University Hospital, Lund University, Lund, Sweden, ³Department of Diagnostic Radiology, Skåne University Hospital, Lund University, Lund, Sweden, ⁴Siemens Healthcare AB, Malmö, Sweden, ⁵Department of Obstetrics and Gynecology, Skåne University Hospital, Lund University, Lund, Sweden

The aim of this study was to demonstrate the feasibility of CINE fetal MRI within a breath-hold with self-gated retrospective binning applied with continuous golden angle radial sampling and iGRASP acceleration. A bSSFP radial acquisition scheme was applied with 0.7x0.7mm² in-plane resolution and a small golden angle of 23.1°. A total of 3800 radial spokes were acquired within a breath hold of 15s. Cardiac triggering was obtained from the centers of the readouts via Principal Component Analysis. The final images were obtained by using iGRASP. Good quality CINE images from the fetus in the third trimester were acquired.

3105

Computer #4



Cardiac Phase-Resolved B1 Mapping at 3T

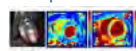
Sebastian Weingartner^{1,2,3}, Greg Metzger², Pierre-Francois Van de Moortele², and Mehmet Akcakaya^{1,2}

¹Electrical and Computer Engineering, University of Minnesota, Minneapolis, MN, United States, ²Center for Magnetic Resonance Research, University of Minnesota, Minneapolis, MN, United States, ³Computer Assisted Clinical Medicine, University Medical Center Mannheim, Heidelberg University, Mannheim, Germany

For various cardiac MRI applications, having B1 maps that are cardiac phase-resolved may be beneficial at high fields. In this work, we develop a retrospectively ECG-gated sequence based on the actual flip angle imaging technique for 2D cardiac phase-resolved B1 mapping at 3T.

3106

Computer #5



CMR Assessment of an Isoproterenol Infusion Mouse Model of Myocardial Hypertrophy and Fibrosis

Haiying Tang¹, Matthew Fronheiser¹, Harold Malone¹, Paul Slep², Adrienne Pena¹, Thomas Petrone¹, Thomas Bradstreet¹, Patrick Chow¹, Lei Zhao², David Gordon², Feng Luo³, and Wendy Hayes¹

¹Bristol Myers Squibb, Princeton, NJ, United States, ²Bristol Myers Squibb, Hopewell, NJ, United States, ³Bristol Myers Squibb, Wallingford, CT, United States

Recent advances in cardiovascular MRI (CMR) technologies such as T1-mapping or extracellular volume (ECV) fraction (derived from T1-mapping) offer robust techniques to assess diffuse fibrosis in patients with myocardial infarction and heart failure. In the present study, CMR assessment of myocardial fibrosis and hypertrophy was evaluated in an isoproterenol infusion model in Balb/c mice. The CMR techniques including T1-mapping and the ECV quantification provide a translational non-invasive imaging marker to assess diffuse

3107

Computer #6



Gamma Knife Radiosurgery Treatment of in Vivo Rabbit Model Aneurysms

Mark David Meadowcroft^{1,2}, Timothy Cooper³, Michele Ferenci², Elizabeth B Neely¹, Ephraim Church¹, Thaddeus Wright¹, Sebastian Rupprecht², Weimin kang¹, Jenelle Tretter³, Qing X Yang², Robert E Harbaugh¹, James R Connor¹, and James Mcinerney¹

¹Neurosurgery, The Pennsylvania State University - College of Medicine, Hershey, PA, United States, ²Radiology, The Pennsylvania State University - College of Medicine, Hershey, PA, United States, ³Comparative Medicine, The Pennsylvania State University - College of Medicine, Hershey, PA, United States

Current treatment options for un-ruptured intracranial aneurysms typically include open clipping, endovascular embolization, or observation. We undertook this study to examine the effects of GKRS on an in vivo rabbit aneurysm model. Involution of aneurysms after GKRS could provide a safer and more cost-effective treatment alternative for patients harboring un-ruptured intracranial aneurysms. The results of the study reveal a 40 percent reduction in aneurysm total volume, internal volume, and surface area over the 24-month period. Targeted GKRS is successful in promoting histological and hemodynamic changes to the rabbit carotid aneurysm, linearly reducing size over time.

3108

Computer #7



Assessment of longitudinal reproducibility of mice LV functional parameters @11.7T derived from self-gated CINE MRI

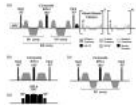
Zhi Zuo^{1,2,3}, Anne Subgang^{2,3}, Alireza Abaei³, Gen-shan Ma¹, and Volker Rasche^{2,3}

¹Department of Cardiology, Zhongda Hospital, Medical School of Southeast University, Nanjing, China, People's Republic of, ²Department of Internal Medicine II, University Hospital Ulm, Ulm, Germany, ³Core Facility Small Animal MRI, Medical Faculty, Ulm University, Ulm, Germany

Cardiovascular magnetic resonance (CMR) has emerged as the most accurate imaging modality for noninvasive assessments of left ventricular (LV) structure and function in mice. However, data on the longitudinal variability of LV systolic function assessment in mice is still limited. In this contribution, a one year follow-up of the longitudinal reproducibility of the LV function and mass has been performed at 11.7T with self-gated CINE MRI. The investigated protocol was proven reliable for the evaluation of EF, EDV, ESV, SV and LVM data.

3109

Computer #8



In Vivo Cardiac DTI on a 3T Clinical Scanner: An Optimized M2 Approach

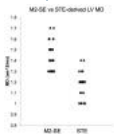
Christopher Nguyen¹, Zhaoyang Fan¹, Yibin Xie¹, Jianing Pang¹, Xiaoming Bi², Peter Speier³, Jon Kobashigawa⁴, and Debiao Li^{1,5}

¹Biomedical Imaging Research Institute, Cedars-Sinai Medical Center, Los Angeles, CA, United States, ²MR R&D, Siemens Healthcare, Los Angeles, CA, United States, ³Siemens Healthcare GmbH, Erlangen, Germany, ⁴Heart Institute, Cedars-Sinai Medical Center, Los Angeles, CA, United States, ⁵Bioengineering, University of California Los Angeles, Los Angeles, CA, United States

Optimized second order motion compensated (M2) diffusion tensor prepared cardiac magnetic resonance (DT-CMR) was applied in healthy volunteers and heart failure patients at 3T. The pulse sequence design focused on B1 robustness at high main field. In healthy volunteers, the proposed M2 DT-CMR was compared to zero order (M0) and first order (M1) motion compensations. In addition, heart rate dependency of the proposed M2 DT-CMR was explored with contextual comparison to M0 and M1. M2 DT-CMR was the only technique capable of application in heart failure patients without bulk motion artifacts.

3110

Computer #9



Comparison Between Spin Echo and Stimulated Echo Diffusion Encoding for Diffusion-Weighted Cardiac Magnetic Resonance (DW-CMR) at 3T

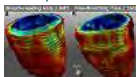
Christopher Nguyen¹, Peter Speier², Xiaoming Bi³, and Debiao Li^{1,4}

¹Biomedical Imaging Research Institute, Cedars-Sinai Medical Center, Los Angeles, CA, United States, ²Siemens Healthcare GmbH, Erlangen, Germany, ³Siemens Healthcare, Los Angeles, CA, United States, ⁴Bioengineering, University of California Los Angeles, Los Angeles, CA, United States

Clinical application of diffusion-weighted cardiac magnetic resonance (DW-CMR) has demonstrated promise in detecting and characterizing the tissue microphysiology and/or microstructure. The aim of this study is to compare a recently developed SE diffusion-prepared approach with a conventional STE DW-CMR technique in normal volunteers on a 3T system. M2-SE derived MD values were significantly higher than STE derived values despite the same prescribed b-value and the difference is not dependent on heart rate. Both DW-CMR techniques were reproducible and motion corruption was seen to be overall less in M2-SE.

3111

Computer #10

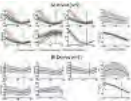


Diffusion Tractography of the Entire Heart using Free-Breathing Accelerated Simultaneous Multislice Imaging

Choukri Mekkaoui¹, Timothy G Reese¹, Marcel P Jackowski², Stephen F Cauley¹, Kawin Setsompop¹, William J Kostis³, Himanshu Bhat⁴, and David E Sosnovik¹


¹Harvard Medical School - Massachusetts General Hospital, Boston, MA, United States, ²University of São Paulo, São Paulo, Brazil, ³Rutgers Robert Wood Johnson Medical School, New Brunswick, NJ, United States, ⁴Siemens Healthcare, Boston, MA, United States

We introduce an approach to perform free-breathing DTI and tractography of the whole heart based on simultaneous multislice excitation, sequential reordering of the diffusion-encoding gradients, combined with a retrospective entropy-based image alignment and selection method. The approach was tested in 7 healthy volunteers, in whom breath-hold and free-breathing scans were performed. Coherent tracts of the entire heart could be derived in all cases, and no significant differences were seen in mean diffusivity, fractional anisotropy, or myofiber helix angle. Accelerated free-breathing DTI of the entire heart could be performed in less than 15 minutes without significant loss of image quality.

- 3112 **Computer #11** Transmural heterogeneity of in-vivo whole heart diffusion parameters: architecture, physiology or artifact?
Martijn Froeling¹, Tim Leiner¹, Laura W M Vergoossen², Eibert A ten Hove², Aart J Nederveen³, Gustav J Strijkers⁴, and Peter R Luijten¹
- 

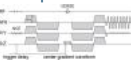
¹Radiology, UMC Utrecht, Utrecht, Netherlands, ²Biomedical Engineering, Eindhoven University of Technology, Eindhoven, Netherlands, ³Radiology, AMC Amsterdam, Amsterdam, Netherlands, ⁴Biomedical Engineering & Physics, AMC Amsterdam, Amsterdam, Netherlands

A recent study by McGill et al. showed in-vivo spatial and transmural heterogeneity of cardiac diffusion parameters. The aim of this study was to investigate the origin of DWI-parameter heterogeneity using whole heart in- and ex-vivo SE-DWI. Based on our results, transmural heterogeneity is partially explained by variations in transmural and spatial perfusion signal fraction and, partially seems to have its origin in cardiac architecture during systole.

- 3113 **Computer #12** Comprehensive comparison of in- and ex-vivo whole heart fiber architecture: similar yet different
Martijn Froeling¹, Gustav J Strijkers², Laura W M Vergoossen³, Eibert A ten Hove³, Aart J Nederveen⁴, Tim Leiner¹, and Peter R Luijten¹
- 


¹Radiology, UMC Utrecht, Utrecht, Netherlands, ²Biomedical Engineering & Physics, AMC Amsterdam, Amsterdam, Netherlands, ³Biomedical Engineering, Eindhoven University of Technology, Eindhoven, Netherlands, ⁴Radiology, AMC Amsterdam, Amsterdam, Netherlands

The aim of this study was to provide a comprehensive description of whole heart in-vivo myocardial fiber architecture using the fiber architecture matrix, and to validate results using ex-vivo and simulated data. We showed that whole heart fiber architecture described by the FAM can be obtained from in-vivo DWI. However, compared to ex-vivo data the direction of ϵ_2 and ϵ_3 are exchanged.

- 3114 **Computer #13** Second-order motion-compensated spin echo diffusion tensor imaging of the in vivo human heart – considerations on gradient performance requirements
Christian T Stoeck^{1,2}, Constantin von Deuster^{1,2}, and Sebastian Kozerke^{1,2}
- 

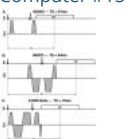
¹King's College London, London, United Kingdom, ²University and ETH Zurich, Zurich, Switzerland

In vivo cardiac DTI using spin-echoes has been demonstrated on MR systems equipped with powerful gradients. In this study we investigate the dependency of helix and transverse angle error on maximum gradient amplitude for second order motion compensated diffusion encoding of the in-vivo heart. Root-mean-square errors for helix and transverse angles were $15.0 \pm 3.7^\circ$, $11.0 \pm 1.8^\circ$, $10.3 \pm 2.4^\circ$, and $11.7 \pm 3.8^\circ$, $9.0 \pm 2.0^\circ$, $8.1 \pm 2.2^\circ$ for gradient strengths of 30mT/m, 40mT/m and 60mT/m when compared to data obtained at 74.5 mT/m gradient strength. From the data it is concluded that second order motion compensated diffusion encoding allows for in vivo cardiac DTI even on MR systems with standard gradient amplitudes of 40 mT/m.

- 3115 **Computer #14** A comparison of M012 compensated spin-echo and STEAM cardiac DTI at multiple cardiac phases
Andrew David Scott^{1,2}, Sonia Nielles-Vallespin^{1,3}, Pedro Ferreira^{1,2}, Peter Gatehouse^{1,2}, Zohya Khaliq¹, Philip Kilner^{1,2}, Dudley Pennell^{1,2}, and David Firmin^{1,2}
- 


¹Cardiovascular Biomedical Research Unit, Royal Brompton and Harefield Foundation NHS Trust, London, United Kingdom, ²National Heart and Lung Institute, Imperial College London, London, United Kingdom, ³National Heart Lung and Blood Institute, National Institutes of Health, Bethesda, MD, United States

In-vivo cardiac diffusion tensor imaging (cDTI) performed with a stimulated echo (STEAM) sequence is considered strain sensitive and low SNR. Alternatively, motion compensated spin-echo (M012-SE) sequences are thought to be strain insensitive and high SNR, but suffer from long echo times and short mixing times. In this work we compare the reliability of and the cDTI parameters derived from STEAM and M012-SE data in 20 volunteers at multiple points in the cardiac cycle on a standard clinical scanner. We show systematic differences between the sequences and show that there are few correlations between these differences and strain and/or T1/T2.

- 3116 **Computer #15** Convex Optimized Diffusion Encoding (CODE) Gradient Waveforms for Bulk Motion Compensated Cardiac Diffusion Weighted MRI
Eric Aliotta^{1,2}, Holden H Wu^{1,2}, and Daniel B Ennis^{1,2}
- 

¹Radiological Sciences, UCLA, Los Angeles, CA, United States, ²Biomedical Physics IDP, UCLA, Los Angeles, CA, United States

Bulk motion compensated diffusion encoding is critical for accurately measuring diffusion in the heart. However, the diffusion encoding gradient waveforms required to suppress bulk motion artifacts can extend TE and limit SNR. We have developed a Convex Optimized Diffusion Encoding (CODE) framework to design time-optimal, motion compensated diffusion encoding gradients that remove sequence dead times and minimize TE. CODE gradients were designed and implemented for cardiac DWI on a 3.0T clinical scanner in healthy volunteers and patients. CODE reduced bulk motion artifacts compared with conventional monopolar encoding.

- 3117 **Computer #16** Right Ventricular Myofiber Architecture
Benoit Scherrer¹, Amara Majeed², Onur Afacan¹, Jolene M. Singh¹, Simon K. Warfield¹, and Stephen P. Sanders²
- 

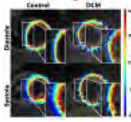
¹Department of Radiology, Boston Children's Hospital, Harvard Medical School, Boston, MA, United States, ²Departments of Cardiology and Pathology, Boston Children's Hospital, Harvard Medical School, Boston, MA, United States

While the left ventricle (LV) myofiber architecture has been studied extensively, there have been fewer studies of right ventricle (RV)

myofiber architecture, and there is no established convention for reporting RV myofiber anatomy. Establishing the normal RV myofiber architecture is critical to facilitate our understanding of the impact of congenital microstructural defects in diseased hearts. In this work, we fixed a juvenile swine heart and imaged it with magnetic resonance diffusion compartment imaging (MR-DCI). We describe the detailed myofiber pattern of the RV with both MR-DCI and stained histological microscopy, and propose a standardized convention for describing the myofiber anatomy.

3118

Computer #17



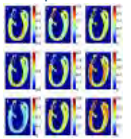
Mapping Dynamic Myocardial Fibre Reorientation in Dilated Cardiomyopathy using Dual-Phase In-Vivo Cardiac Diffusion Tensor Imaging
Constantin von Deuster^{1,2}, Eva Sammut¹, Christian T. Stoeck^{1,2}, Reza Razavi¹, and Sebastian Kozerke^{1,2}

¹Division of Imaging Sciences and Biomedical Engineering, King's College London, London, United Kingdom, ²Institute for Biomedical Engineering, University and ETH Zurich, Zurich, Switzerland

In vivo cardiac diffusion tensor imaging (DTI) was employed to study dynamic alterations of myocardial microstructure in patients with dilated cardiomyopathy (DCM) relative to healthy controls using dual-phase cardiac DTI. A reduction in dynamic change of fiber orientation between diastole and systole compared to the controls was observed. Steeper diastolic helix angles in DCM patients relative to controls were associated with a larger pre-stretch of the left ventricle. It is speculated that this larger pre-stretch alongside with reduced myocyte shortening compromises the ability to dynamically reorient fiber aggregates during systolic contraction.

3119

Computer #18



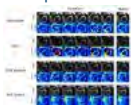
Assessing non-Gaussian diffusion in cardiac tissue
Darryl McClymont¹, Irvin Teh¹, Hannah Whittington¹, Vicente Grau², and Jurgen Schneider¹

¹Division of Cardiovascular Medicine, University of Oxford, Oxford, United Kingdom, ²Department of Engineering Science, University of Oxford, Oxford, United Kingdom

Non-Gaussian diffusion MRI allows the quantification of diffusion signals that deviate from mono-exponential decay. In cardiac MRI, very little has been reported on non-Gaussian models. In this work, the diffusion tensor, stretched exponential, bi-exponential, and diffusion kurtosis models were fit to data from fixed rat hearts. Performance was measured using the Akaike Information Criterion (AIC). All models demonstrated the presence of non-Gaussian diffusion, particularly in the right ventricle. The bi-exponential model fit the data best and had the lowest AIC. Non-Gaussian diffusion was greater perpendicular, rather than parallel, to cardiac fibers, corresponding to greater restrictions to diffusion.

3120

Computer #19



Quantification of residual motion in diffusion-weighted cardiac MR (DW-CMR): objective quality metrics and validation using 3 diffusion encoding schemes under free breathing conditions.

Kévin Moulin^{1,2}, Alban Chazot³, Pierre Croisille^{1,3}, and Magalie Viallon^{1,3}

¹CREATIS, Université de Lyon ; CNRS UMR5220 ; Inserm U1044 ; INSA-Lyon ; Université Claude Bernard Lyon 1, Lyon, France, ²Siemens Healthcare France, Paris, France, ³Department of Radiology, Centre Hospitalier Universitaire de Saint-Etienne, Université Jean-Monnet, Saint-Etienne, France

DW-CMR remains challenging due to respiratory and heart motion. Recent developments in cardiac diffusion imaging proposed Acceleration Motion Compensation (AMC) spin echoes encoding scheme to tackle cardiac motion. In addition, free breathing acquisition with prospective motion correction like slice following technique has been shown to reduce efficiently and significantly the scan time. Here, we proposed a method to quantify the remaining cardiac or breathing motion corruption in DW-CMR measurement and we evaluated it using 3 diffusion encoding scheme: AMC, Stjegal-Tanner and Twice Refocused Spin Echo. Error maps were also compared to physiological motion indicators: cardiac motion using strain measurement and breathing phase using navigator information.

3121

Computer #20

Physiological Parameters Measurements of Normal and Infarcted Myocardium with Ultrasound and MR imaging
Tamer Mohamed¹, Yu Huang¹, Maythem Saeed², Deepark Srivastava¹, and Sergey Magnitsky³

¹Gladstone Institute, San Francisco, CA, United States, ²UCSF, San Francisco, CA, United States, ³Radiology, UCSF, San Francisco, CA, United States

In this study we compared two in vivo imaging techniques to obtain anatomical and physiological parameters of mice heart. Our results suggest that measurements of ejection fraction and mass of left ventricle were easier and cheaper with ultrasound echocardiography however evaluation of a scar tissue and re-muscularization of infarcted myocardium are only possible with MRI method

3122

Computer #21



Applying Origami Coil Design for Deployable Intra-cardiac MRI Catheter
Austin James Taylor¹, Zion Tse¹, Ehud Schmidt², Matthew Miller¹, Mable Fok¹, and Kent Nilsson³

¹Engineering, The University of Georgia, Athens, GA, United States, ²Department of Radiology, Brigham and Women's Hospital, Boston, MA, United States, ³Medicine, The University of Georgia, Athens, GA, United States

Catheter ablation is a common electrophysiological (EP) procedure to treat irregular heart rhythm conditions, such as atrial fibrillation. Catheter ablation can be assisted through the use of imaging coils under magnetic resonance imaging (MRI) which provides a roadmap for preoperative preparation and intraoperative catheter navigation. Intra-cardiac imaging coils allow for ablated lesions to be observed in real time with excellent soft tissue contrast, providing electrophysiologists better control over the result of the procedure. We present a novel catheter design which integrates a unique origami deployable mechanism for enabling parallel MR imaging in MRI guided EP procedures.

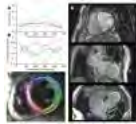
Myocardial Perfusion & Function

Exhibition Hall

Monday, May 9, 2016: 17:30 - 18:30

3123

Computer #25



Short-breath hold cine DENSE

Andrew David Scott^{1,2}, Upasana Taya^{1,2}, Sonia Nelles-Vallespin^{1,3}, Pedro Ferreira^{1,2}, Xiaodong Zhong⁴, Frederick Epstein⁵, Sanjay Prasad^{1,2}, and David Firmin^{1,2}

¹NIHR funded Cardiovascular Biomedical Research Unit, Royal Brompton Hospital, London, United Kingdom, ²National Heart and Lung Institute, Imperial College London, London, United Kingdom, ³National Heart Lung and Blood Institute, National Institutes of Health, Bethesda, MD, United States, ⁴MR R&D Collaborations, Siemens Healthcare, Atlanta, GA, United States, ⁵University of Virginia, Department of Biomedical Engineering, Charlottesville, VA, United States

Displacement encoding with stimulated echoes (DENSE) can provide valuable strain information, but acquisitions are typically too long for patient cohorts who have difficulty breath holding. In this work we accelerate 2D cine spiral DENSE acquisitions by selectively exciting a small field of view around the heart. We compare strain data derived from DENSE acquired with unaccelerated and up to 2.5x acceleration in a cohort of healthy subjects and show minimal differences when the acquisition is accelerated. We also show an example from a patient with a myocardial infarction where the accelerated DENSE data shows abnormal strain in the infarcted regions.

3124

Computer #26



Biventricular Cardiac Mechanics in Healthy Subjects using 3D Spiral Cine DENSE and Mesh-Free Strain Analysis

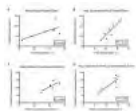
Jonathan D Suever^{1,2}, Gregory J Wehner³, Christopher M Haggerty^{1,2}, Linyuan Jing^{1,2}, David K Powell³, Sean M Hamlet⁴, Jonathan D Grabau², Dimitri Mojsenjenko², and Brandon K Fornwalt^{1,2,3}

¹Institute for Advanced Application, Geisinger Health System, Danville, PA, United States, ²Pediatrics, University of Kentucky, Lexington, KY, United States, ³Biomedical Engineering, University of Kentucky, Lexington, KY, United States, ⁴Electrical Engineering, University of Kentucky, Lexington, KY, United States

Cardiac mechanics have been extensively characterized in the left ventricle (LV). However, the right ventricle (RV) is rarely studied due to both acquisition and post-processing challenges. In this study, we combined 3D displacement-encoded (DENSE) imaging with custom post-processing that utilizes a local coordinate system to extract advanced measures of cardiac mechanics in an effort to characterize healthy biventricular function. We found that torsion as well as circumferential and longitudinal strain vary throughout the RV, but globally were comparable to their LV counterparts. This data can be used to better understand how biventricular function is disrupted by disease.

3125

Computer #27



Myocardial Strain Analysis With CMR in Breast Cancer Patients with Iatrogenic Cardiotoxicity Using Heart Deformation Analysis: Comparison to DENSE

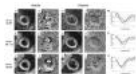
Abraham Bogachkov¹, Kai Lin², Ahmadreza Ghasemiesfe², Amir Ali Rahsepar³, Bruce Spottiswoode³, Ben Freed⁴, Michael Mark², James Carr², and Jeremy Collins²

¹Northwestern University Feinberg School of Medicine, Chicago, IL, United States, ²Radiology, Northwestern University, Chicago, IL, United States, ³Cardiovascular MR R&D, Siemens Healthcare, Chicago, IL, United States, ⁴Cardiology, Northwestern University, Chicago, IL, United States

Strain imaging at cardiac MR has been shown to be a powerful tool in the pre-clinical detection of early cardiac dysfunction in the heart failure population, but has been only minimally studied in cardiotoxicity patients. This study evaluated a semi-automatic heart deformation analysis (HDA) tool in the assessment of left ventricular myocardial strain in patients with known cardiotoxicity, and found very good to excellent agreement with global strain values calculated using displacement encoding with stimulated echoes (DENSE). HDA analysis of conventional cine sequences has the potential to play a significant role in the evaluation of patients at risk for cardiotoxicity.

3126

Computer #28



Free-breathing 2D cine DENSE MRI using localized signal generation, image-based navigators, motion compensation and compressed sensing

Xiaoying Cai¹, Xiao Chen², Yang Yang¹, Michael Salerno³, Daniel S. Weller⁴, Craig H. Meyer¹, and Frederick H. Epstein¹

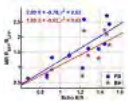
¹Biomedical Engineering, University of Virginia, Charlottesville, VA, United States, ²Medical Imaging Technologies, Siemens Healthcare, Princeton, NJ, United States, ³University of Virginia, Charlottesville, VA, United States, ⁴Electrical and Computer Engineering, University of Virginia, Charlottesville, VA, United States

Current cine DENSE protocols require breath-holding, which limits the use of this technique to patients with good breath-holding capabilities and excludes many pediatric and heart failure patients. To accomplish free-breathing scans with high efficiency and quality, we developed a 2D cine DENSE acquisition and reconstruction framework that utilizes localized signal generation, image-based self-navigated motion estimation, k-space motion correction and compressed sensing. Reconstructions and Bland-Altman analysis from 5 volunteers demonstrated that the proposed method recovered high-quality images and strain data from free-breathing data, showing better agreement than conventional reconstructions of the same data with breath-holding scans.

3127

Computer #29

Effect of Respiratory Suspension on the Computation of Left Ventricular (LV) Volume and Rate of Volume Change (dV/dt)-based Diastolic Indices with Echocardiography as a Reference



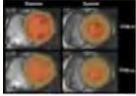
Amol Pednekar¹, Jiming Zhang², Debra Dees³, Benjamin Y Cheong³, and Raja Muthupillai³

¹Phillips Healthcare, Cleveland, OH, United States, ²Diagnostic and interventional Radiology, CHI St Luke's Health, Houston, TX, United States, ³Diagnostic and Interventional Radiology, CHI St Luke's Health, Houston, TX, United States

Diastolic functional indices based on trans-mitral blood flow velocities are pre-load dependent and early diastolic filling can be diminished by activities such as inspiration or Valsalva maneuver. Cardiac cine MR images are typically acquired during suspended respiration and thus could induce systemic bias. In this study, we evaluate the impact of respiratory suspension on the computation of volume-based diastolic indices using peak velocity-based Doppler echo measurements as the reference. The volume based diastolic indices derived from high temporal resolution cine MR correlated well with velocity based E/A ratio from echo while indicating the direct impact of respiratory suspension.

3128

Computer #30



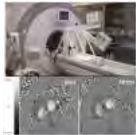
Peak Filling Rates assessed by Cardiac Magnetic Resonance Imaging indicate Diastolic Dysfunction from Myocardial Iron Toxicity
Jin Yamamura¹, Sarah Keller¹, Roland Fischer^{2,3}, Regine Grosse⁴, Gregory Kurio³, Gunnar Lund¹, Joachim Graessner⁵, Gerhard Adam¹, and Bjoern Schoennagel¹

¹Diagnostic and Interventional Radiology, University Medical Center Hamburg-Eppendorf, Hamburg, Germany, ²Biochemistry, University Medical Center Hamburg-Eppendorf, Hamburg, Germany, ³Department of Radiology, UCSF Benioff Children's Hospital Oakland, Oakland, CA, United States, ⁴Department of Pediatric Hematology/Oncology, University Medical Center Hamburg-Eppendorf, Hamburg, Germany, ⁵Siemens Healthcare, Hamburg, Germany

The diastolic peak filling rate ratio (PFRR) is a sensitive marker to indicate diastolic dysfunction from myocardial iron toxicity in patients with systemic iron overload disease. Precise assessment of the PFRR by CMR requires a volumetric approach with exclusion of trabeculae and papillary muscles from the LV cavity. The PFRR assessed by CMR may be a valuable parameter for the screening and monitoring of myocardial iron toxicity due to iron deposition in patients with preserved systolic function.

3129

Computer #31



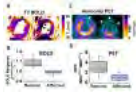
Exercise stress cardiac MR assessment of diastolic function in healthy volunteers and pulmonary hypertension
Thomas Kennedy¹, Omid Forouzan², Oliver Wieben^{1,3}, Naomi C Chesler², Jacob Macdonald³, and Christopher J Francois¹

¹Radiology, University of Wisconsin- Madison, Madison, WI, United States, ²Biomedical Engineering, University of Wisconsin- Madison, Madison, WI, United States, ³Medical Physics, University of Wisconsin- Madison, Madison, WI, United States

Dyspnea on exertion is a common manifestation of systolic and diastolic heart failure. Using an MRI-compatible exercise device allowing subjects to exercise while in the bore of the scanner, we assessed exercise-induced changes in diastolic transmitral flow in younger and older healthy volunteers and subjects with pulmonary hypertension. The measurements we obtained demonstrated decreased E/A ratios for older healthy volunteers and PH subjects when compared to younger healthy volunteers, however these differences were not statistically significant.

3130

Computer #32



Quantitative, Time-efficient, Heart-Rate Independent Myocardial BOLD MRI with Whole-heart Coverage at 3T in a Canine Model of Coronary Stenosis with Simultaneous ¹³N-Ammonia PET Validation

Hsin-Jung Yang¹, Damini Dey¹, Jane Sykes², John Butler², Xiaoming Bi³, Behzad Sharif¹, Sotirios Tsaftaris⁴, Debiao Li¹, Piotr Slomka¹, Frank Prato², and Rohan Dharmakumar¹

¹Cedars Sinai Medical Center, Los Angeles, CA, United States, ²Lawson Health Research Institute, London, ON, Canada, ³Siemens Healthcare, Los Angeles, CA, United States, ⁴IMT Institute for Advanced Studies Lucca, Lucca, Italy

Current myocardial BOLD MR methods are limited by: (a) poor spatial coverage and imaging speed; (b) imaging confounders; and (c) imaging artifacts, particularly at 3T. To address these limitations, we developed a heart-rate independent, free-breathing 3D T2 mapping technique at 3T that utilizes near 100% imaging efficiency, which can be completed in 3 minutes with full LV coverage. We tested our method in a canine model of coronary stenosis and validated our findings with simultaneously acquired ¹³N-ammonia PET perfusion data in a whole-body PET/MR system.

3131

Computer #33



Spiral SPIRIT Tissue Phase Mapping enables the acquisition of myocardial motion with high temporal and spatial resolution during breath-hold

Marius Menza¹, Daniela Föll², Jürgen Hennig¹, and Bernd Jung³

¹University Medical Center Freiburg, Dept. of Radiology - Medical Physics, Freiburg, Germany, ²University-Heart Center Freiburg, Cardiology and Angiology I, Freiburg, Germany, ³University Hospital Bern, Institute of Diagnostic, Interventional and Pediatric Radiology, Bern, Switzerland

MR Tissue Phase Mapping (TPM) is a powerful approach to assess left ventricular (LV) function. Conventional Cartesian acquisition-strategies with k-t-based parallel imaging acceleration allow the acquisition of a single slice within a breath-hold, but suffer from low spatial resolution. In this work a comparison with undersampled high-resolution spiral SPIRIT TPM for different trajectory designs within one breath-hold and free breathing Cartesian k-t-accelerated PEAK TPM is presented. High image quality, comparable peak velocity values and time to peaks of spiral SPIRIT TPM for high resolution within a breath-hold might enhance myocardial functional analysis.

3132

Computer #34

Comparison Between Radial and Cartesian Sampling Patterns in Accelerated Real-Time Cardiac Cine MRI

Elwin Bassett¹, Ganesh Adluru², Brent D. Wilson³, Cory Nitzel³, Tobias Block⁴, Hassan Haji-Valizadeh⁵, Edward VR DiBella², and Daniel



Kim²

¹Physics, University of Utah, Salt Lake City, UT, United States, ²Radiology, UCAIR, University of Utah, Salt Lake City, UT, United States, ³Internal Medicine, Division of Cardiology, University of Utah, Salt Lake City, UT, United States, ⁴School of Medicine, Radiology, New York University, New York, NY, United States, ⁵Bioengineering, University of Utah, Salt Lake City, UT, United States

To date, no study has compared 12-fold accelerated real-time cine MRI with compressed sensing (CS) between Cartesian and radial k-space sampling schemes. We sought to compare their performance in patients and volunteers. We compared point spread functions (PSF) to determine which sampling pattern generates more incoherent aliasing artifacts. We also compared their performance in a group of 15 patients and one volunteer, where 3-fold accelerated product real-time MRI was used as reference. Two cardiologists independently graded images from each subject.

PSF analysis showed that radial produces more incoherent aliasing artifacts. Image quality was better for radial than Cartesian sampling schemes.

3133

Computer #35



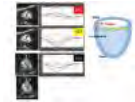
Wideband Cardiac MR Perfusion Pulse Sequence for Imaging Patients with implantable cardioverter defibrillator
KyungPyo Hong^{1,2} and Daniel Kim¹

¹Radiology, UCAIR, University of Utah, Salt Lake City, UT, United States, ²Bioengineering, University of Utah, Salt Lake City, UT, United States

Patients with end-stage heart failure (HF) often require advanced therapeutics, but current clinical profiles and biomarkers are not adequate for predicting outcomes. Myocardial perfusion reserve may be an important predictor, but it is technically challenging to perform perfusion MRI in patients with end-stage HF because they often have implantable cardioverter defibrillator (ICD), which generates significant image artifacts. We developed a novel cardiac perfusion pulse sequence using a wideband saturation pulse. Compared with standard perfusion MRI, wideband perfusion MRI suppresses image artifacts induced by ICD.

3134

Computer #36



Feature tracking imaging (FTI) for right ventricular strain assessment in patients with chronic thromboembolic pulmonary hypertension (CTEPH)

Yoshiaki Morita¹, Naoaki Yamada¹, Makoto Amaki², Emi Tateishi², Asuka Yamamoto², Masahiro Higashi¹, and Hiroaki Naito¹

¹Department of Radiology, National Cerebral and Cardiovascular Center, Suita, Osaka, Japan, ²Division of Cardiology, National Cerebral and Cardiovascular Center, Suita, Osaka, Japan

Right ventricular (RV) function has a significant impact on the prognosis of chronic thromboembolic pulmonary hypertension (CTEPH), as it does with other forms of pulmonary arterial hypertension (PH). In this study, we demonstrated that feature tracking imaging (FTI) is fast, simple, and has potential for clinical use for assessing RV strain in CTEPH. The global longitudinal strain (GLS) showed better correlation with the RV ejection fraction (RVEF) and mean pulmonary artery pressure (mPAP). FTI-derived strain measurement might offer a modality for good detection of RV dysfunction and repeatable monitoring after therapeutic intervention.

3135

Computer #37



Cardiac MR Assessment of Diastolic Function

Thomas Kennedy¹, Niti Aggarwal², Christopher Francois¹, Mark Schiebler¹, and Jeremy Collins³

¹Radiology, University of Wisconsin- Madison, Madison, WI, United States, ²Cardiology, University of Wisconsin-Madison, Madison, WI, United States, ³Radiology, Northwestern University, Chicago, IL, United States

Diastolic dysfunction is the primary cause of CHF in 40-60% of patients with heart failure in the United States and has been shown to lead to poor outcomes. Early diagnosis and treatment of the causes of diastolic dysfunction is effective in relieving symptoms and reducing mortality. The non-invasive methods which can be used to assess diastolic function include cardiac magnetic resonance (CMR) imaging. The purpose of this educational poster is to describe the CMR techniques which can be used to evaluate diastolic function and review the CMR findings of this disorder.

3136

Computer #38



Finite Element Digital Image Correlation for Cardiac Strain Analysis from 3D Whole-Heart Tagging

Martin Genet^{1,2}, Christian T Stoeck^{3,4}, Constantin von Deuster^{3,4}, Lik Chuan Lee⁵, Julius M Guccione⁶, and Sebastian Kozerke^{3,4}

¹École Polytechnique, Palaiseau, France, ²Institute for Biomedical Engineering, ETHZ, Zurich, Switzerland, ³KCL, London, United Kingdom, ⁴ETHZ, Zurich, Switzerland, ⁵MSU, East Lansing, MI, United States, ⁶UCSF, San Francisco, CA, United States

The objective of the present work was to develop, validate and analyze a finite element digital image correlation approach of extracting ventricular strain data from MR images, which can be applied to both 3D CSPAMM images and conventional multi-slice cine images. Cine and 3D CSPAMM data was acquired on a normal human volunteer, and analyzed. The proposed method provided similar circumferential strain data compared to already validated SinMod method. In contrast to strain mapping from cine images, strain mapping from 3D CSPAMM images captures ventricular twist and torsion in agreement with physiological values, and is less sensitive to image misregistration.

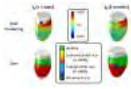
3137

Computer #39

A data analysis framework to study remodeling after myocardial infarction

Freddy Odille^{1,2,3}, Lin Zhang^{1,2}, Bailiang Chen^{1,2,3}, Jacques Felblinger^{1,2,3,4,5}, Damien Mandry^{1,2,4}, and Marine Beaumont^{3,5}

¹U947, Inserm, Nancy, France, ²IADI, Université de Lorraine, Nancy, France, ³CIC-IT 1433, Inserm, Nancy, France, ⁴Pôle imagerie, CHRU de Nancy,

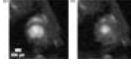


Nancy, France, ⁵Pôle S2R, CHRU de Nancy, Nancy, France

A data analysis framework is proposed to study the relation between scar severity and regional myocardial function during the process of remodeling after acute myocardial infarction (MI). The framework includes registration steps to correct for slice-to-slice inconsistencies, to align cine with late gadolinium enhancement (LGE) data and to align data from follow-up scans. The framework was evaluated in 114 patients with CMR scans within 3 days after MI and at 6 months. Registration accuracy was below 3 mm. Results show that function at 6 months was inversely associated with scar transmuralty at both 3 days and 6 months.

3138

Computer #40



High-resolution MR Imaging of Left-ventricular Function in Newborn Mice

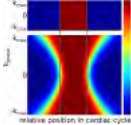
Mahon L Maguire¹, Mala Rohling², Megan Masters², Debra McAndrew¹, Paul Riley², and Jurgen E Schneider¹

¹Radcliffe Department of Medicine, University of Oxford, Oxford, United Kingdom, ²Department of Physiology, Anatomy, and Genetics, University of Oxford, Oxford, United Kingdom

The neonatal mouse heart has been reported to regenerate following myocardial injury during the first days of life. Research into this regenerative capability is being actively pursued for translation into the clinic. This study presents cardiac cine imaging of one-day old mice using retrospectively gated, accelerated MR imaging with recovery. Images were acquired with 78x78x500 μm resolution. Left ventricular functional parameters were derived from the images and are presented. This proof of concept study demonstrates that cardiac functional MR imaging with recovery in newborn mice is practical. It also allows the investigation of myocardial regeneration during the first days of life.

3139

Computer #41



Fast myocardial perfusion mapping in mice using heart cycle dependent data weighting

Fabian Tobias Gutjahr¹, Thomas Kampf¹, Stephan Michael Guenster¹, Volker Herold¹, Patrick Winter¹, Xavier Helluy², Wolfgang Bauer³, and Peter Jakob¹

¹Experimental Physics V, University of Wuerzburg, Wuerzburg, Germany, ²NeuroImaging Centre, Ruhr University, Bochum, Germany, ³Department of Internal Medicine 1, Universitaetsklinikum Würzburg, Wuerzburg, Germany

A fast method for the measurement of myocardial perfusion in mice is presented. Using an efficient retrospective data selection and weighting process in combination with a model based reconstruction perfusion maps can be acquired within 3.5min.

3140

Computer #42



A preliminary study of Intravoxel Incoherent Motion MR for quantitative evaluation of myocardial perfusion in diabetes and/or hypertension

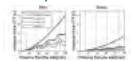
Anna Mou¹, Zhiyong Li¹, Mengying Li², Qingwei Song², Chen Zhang², and Ailian Liu²

¹Radiology, The First Affiliated Hospital of Dalian Medical University, Dalian, China, People's Republic of, ²Dalian, China, People's Republic of

Myocardial microcirculation perfusion dysfunction plays an important role in assessment cardiac disease especially diabetes and hypertension because of their high incidence in the world. We preliminarily investigated the difference of myocardial micro-vascular perfusion between patients with diabetes/hypertension and normal volunteers with IVIM (0, 20, 50, 80, 120, 150, 200, 300, 500 s/mm²) diffusion weighted imaging. We found that Fast ADC values in patients were significant lower than in healthy volunteers. We concluded that IVIM CMR could quantitatively and noninvasively evaluate perfusion status in patients with diabetes and/or hypertension.

3141

Computer #43



A Computational Fluid Dynamics Simulation Study on the Influence of the Tortuosity of the Coronary Arteries on Contrast Agent Bolus Dispersion in Contrast-Enhanced Myocardial Perfusion MRI

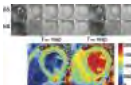
Regine Schmidt¹, Hanns-Christian Breit¹, and Laura Maria Schreiber^{1,2}

¹Section of Medical Physics, Department of Radiology, Johannes Gutenberg University Medical Center, Mainz, Germany, ²Department of Cellular and Molecular Imaging, Comprehensive Heart Failure Center (CHFC), Wuerzburg, Germany

The dispersion of the contrast agent bolus at T1-weighted contrast-enhanced first-pass myocardial perfusion MRI was examined by means of computational fluid dynamics simulations. In this study simulations in idealized coronary artery geometries with different extent of vessel tortuosity and in a straight reference vessel geometry have been performed for the condition of rest and stress. The contrast agent bolus dispersion was larger at rest compared to stress. Furthermore, a negative correlation between the extent of tortuosity and the contrast agent bolus dispersion was found.

3142

Computer #44



Myocardial ASL Perfusion Imaging using MOLLI

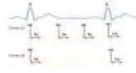
Hung Phi Do¹ and Krishna S Nayak²

¹Department of Physics and Astronomy, University of Southern California, Los Angeles, CA, United States, ²Ming Hsieh Department of Electrical Engineering, University of Southern California, Los Angeles, CA, United States

Modified Look-Locker Inversion Recovery (MOLLI) provides the highest precision and reproducibility for myocardial T₁ mapping, and extracellular volume (ECV) mapping. In this work, we determine its effectiveness for measuring myocardial blood flow (MBF), based on apparent-T₁ mapping under two conditions, slice-selective inversion and non-selective inversion. We demonstrate that MOLLI provides measured MBF comparable to the reference FAIR-SSFP ASL method.

3143

Computer #45



High-resolution myocardial perfusion imaging with radial simultaneous multi-slice imaging and constrained reconstruction
Ganesh Adluru¹, Chris Welsh¹, John Roberts¹, and Edward DiBella¹

¹Radiology, University of Utah, Salt Lake City, UT, United States

High-resolution myocardial perfusion imaging offers improved delineation of subendocardial ischemic regions and can lead to improved diagnosis. Here we use undersampled radial simultaneous multi-slice (SMS) acquisitions in conjunction with constrained reconstruction with temporal total variation and spatial block-matching 3D (BM3D) constraints to obtain high in-plane spatial resolution perfusion imaging. Promising results are shown with two types of myocardial perfusion acquisitions (i) a set of 3 simultaneous slices after a saturation pulse, repeated several times per beat at different cardiac phases, and (ii) a 'hybrid' perfusion acquisition with one saturation pulse per beat and the reconstructed cardiac phase of the 3 slices chosen retrospectively.

3144

Computer #46



3D first-pass myocardial perfusion stack-of-stars imaging using balanced steady state free precession

Merlin J Fair^{1,2}, Peter D Gatehouse^{1,2}, Liyong Chen^{3,4}, Ricardo Wage², Edward VR DiBella⁵, and David N Firmin^{1,2}

¹NHLI, Imperial College London, London, United Kingdom, ²NIHR Cardiovascular BRU, Royal Brompton Hospital, London, United Kingdom, ³UC Berkeley, Berkeley, CA, United States, ⁴Advanced MRI Technologies, Sebastopol, CA, United States, ⁵UCAIR, University of Utah, Salt Lake City, UT, United States

A method for enabling a balanced steady-state free precession 3D stack-of-stars approach to whole-heart first-pass myocardial perfusion imaging is investigated. Consideration is made of the impact of potential off-resonance effects at 3T and sequence-based modifications to rectify this are examined. Demonstration of the feasibility of this approach is then performed in-vivo.

3145

Computer #47



Double-gated Myocardial ASL Perfusion Imaging provides Insensitivity to Heart Rate Variation

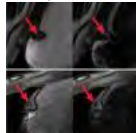
Hung Phi Do¹, Andrew J Yoon², Michael W Fong², Farhood Saremi³, Mark L Barr⁴, and Krishna S Nayak⁵

¹Department of Physics and Astronomy, University of Southern California, Los Angeles, CA, United States, ²Department of Medicine, Division of Cardiology, Keck School of Medicine of USC, University of Southern California, Los Angeles, CA, United States, ³Department of Radiology, Keck School of Medicine of USC, University of Southern California, Los Angeles, CA, United States, ⁴Department of Cardiothoracic Surgery, Keck School of Medicine of USC, University of Southern California, Los Angeles, CA, United States, ⁵Ming Hsieh Department of Electrical Engineering, University of Southern California, Los Angeles, CA, United States

Double-gating in myocardial ASL allows for variations in the post-labeling delay in order to ensure that both labeling and imaging occur in the same cardiac phase. Originally proposed by Poncelet et al. in 1999, this was believed to provide insensitivity to heart rate variation. Despite this, most groups have utilized single-gating with a fixed post-labeling delay for pairs of control and tagged images, since this allows for simpler quantification of myocardial blood flow. In this study, we demonstrate that the double-gating is indeed more robust to heart rate variation compared to single-gating for myocardial ASL, based on experiments in healthy volunteers and heart transplant recipients.

3146

Computer #48



Demonstration of Velocity Selective Myocardial Arterial Spin Labeling

Terrence Jao¹ and Krishna Nayak²

¹Biomedical Engineering, University of Southern California, Los Angeles, CA, United States, ²Electrical Engineering, University of Southern California, Los Angeles, CA, United States

Arterial spin labeled CMR is a non-contrast myocardial perfusion imaging technique capable of assessing coronary artery disease. A limitation of current methods is potential underestimation of blood flow to myocardial segments that have coronary arterial transit time longer than 1 R-R, which are found in regions with significant collateral development from chronic myocardial ischemia. In this work, we demonstrate the feasibility of a velocity selective labeling scheme for ASL-CMR that is insensitive to arterial transit time.

Electronic Poster

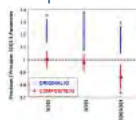
Myocardial Tissue Characterisation

Exhibition Hall

Monday, May 9, 2016: 17:30 - 18:30

3147

Computer #49



Modified Look-Locker Inversion Recovery (MOLLI) \$\$\$T_1\$\$\$ Mapping with High Precision Composite Inversion Group (IG) Fitting

Marshall Stephen Sussman^{1,2} and Bernd Juergen Wintersperger^{1,2}

¹Medical Imaging, University Health Network, Toronto, ON, Canada, ²Medical Imaging, University of Toronto, Toronto, ON, Canada

The MOLLI \$\$\$T_1\$\$\$ mapping technique has been used to characterize a variety of cardiac pathologies. However, a significant limitation of this technique is the requirement for rest periods between inversion groups. This increases scan time, and limits the choice of possible inversion groups. A new technique, inversion group (IG) MOLLI fitting, has been recently shown to eliminate the requirement for rest periods, and permits complete flexibility of inversion group selection. However, a significant limitation of this technique is that the resulting \$\$\$T_1\$\$\$ maps have low precision. In this study, a method is presented for high precision IG fitting.

3148

Computer #50



Systolic Myocardial T1- and ECV-Mapping using Saturation-Recovery at 3 Tesla

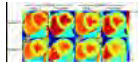
Nadja M Meßner^{1,2}, Sebastian Weingärtner^{1,3,4}, Johannes Budjan⁵, Dirk Loßnitzer⁶, Theano Papavassiliu^{2,6}, Lothar R Schad¹, and Frank G Zöllner¹

¹Computer Assisted Clinical Medicine, Medical Faculty Mannheim, Heidelberg University, Mannheim, Germany, ²DZHK (German Centre for Cardiovascular Research) partner site Mannheim, Mannheim, Germany, ³Department of Electrical and Computer Engineering, University of Minnesota, Minneapolis, MN, United States, ⁴Center for Magnetic Resonance Research, University of Minnesota, Minneapolis, MN, United States, ⁵Institute of Clinical Radiology and Nuclear Medicine, Medical Faculty Mannheim, Heidelberg University, Mannheim, Germany, ⁶1st Department of Medicine Cardiology, Medical Faculty Mannheim, Heidelberg University, Mannheim, Germany

Partial volume artifacts in myocardial T₁-mapping are a major source of quantification inaccuracy. In this study, saturation-recovery T₁-mapping at 3T was adapted to allow for systolic imaging in order to take advantage of the increased myocardial wall thickness. Estimated T₁- and ECV- values for SR T₁-mapping during systole were 1554±3ms/0.29±0.03 compared to 1581±35ms/0.31±0.04 at diastole. In conclusion, our results show that SR T₁-mapping in systole might be an alternative to derive T₁- and ECV-values with reduced effects of partial volume.

3149

Computer #51



Ungated, Free-breathing Native T1 Mapping in Multiple Cardiac Phases in Under One Minute: A Proof of Concept

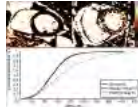
Jaime L. Shaw^{1,2}, Anthony G. Christodoulou^{1,3}, Behzad Sharif¹, and Debiao Li^{1,2}

¹Biomedical Imaging Research Institute, Cedars-Sinai Medical Center, Los Angeles, CA, United States, ²Department of Bioengineering, University of California, Los Angeles, Los Angeles, CA, United States, ³Heart Institute, Cedars-Sinai Medical Center, Los Angeles, CA, United States

Current cardiac T1 mapping techniques are generally limited to single-shot 2D images acquired in a breath hold with ECG gating. Heart rate variability or poor ECG triggering are sources of error and reduced reproducibility in the widely used MOLLI T1 mapping technique. To mitigate the dependence of T1 mapping on heart rate and breath-holds, we propose an ungated, free-breathing, continuous IR approach using low-rank tensors modeling the image as partially separable in space, cardiac phase, respiratory phase, and inversion time. We show the feasibility of the ungated, free-breathing approach in producing T1 maps in multiple cardiac phases in under 1 minute.

3150

Computer #52



Cardiac Tissue Characterization in End Stage Renal Disease Patients with Non-Contrast MRI and Myocardial Mechanics

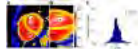
Tori A Stromp^{1,2}, Joshua C Kaine^{2,3}, Tyler J Spear², Kristin N Andres^{2,3}, Brandon K Fornwalt⁴, Vincent L Sorrell⁵, Steve W Leung⁵, and Moriel H Vandsburger^{1,2,6}

¹Department of Physiology, University of Kentucky, Lexington, KY, United States, ²Saha Cardiovascular Research Center, University of Kentucky, Lexington, KY, United States, ³College of Medicine, University of Kentucky, Lexington, KY, United States, ⁴Institute for Advanced Application, Geisinger Health System, Danville, PA, United States, ⁵Gill Heart Institute, University of Kentucky, Lexington, KY, United States, ⁶Biomedical Engineering, University of Kentucky, Lexington, KY, United States

Patients with end stage renal disease (ESRD) suffer from high rates of sudden cardiac death, often attributed to development of reactive fibrosis. This study aims to integrate cardiac tissue characterization via non-contrast 2-pt bSSFP with myocardial mechanical analysis. ESRD patients demonstrate elevated myocardial signal with magnetization transfer-weighted 2-pt bSSFP, indicating increased fibrosis. This elevated signal correlates with delayed time to peak contraction and septo-lateral dyssynchrony, which are both elevated in ESRD patients. Combining non-contrast 2-pt bSSFP for tissue characterization with analysis of regional contractile function offers a promising approach to identify potential MRI biomarkers of cardiac risk in ESRD.

3151

Computer #53



3D Free Breathing Whole Heart T1 mapping at 3 T

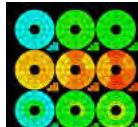
Rui Guo¹, Zhensen Chen¹, Jianwen Luo¹, and Haiyan Ding¹

¹Center for Biomedical Imaging Research, Department of Biomedical Engineering, School of Medicine, Tsinghua University, Beijing, China, People's Republic of

In this study, we developed a free-breathing, three-dimensional (3D) T1 mapping method at 3T based on the saturation-prepared, inversion-prepared radiofrequency-spoiled gradient echo (SPGR) sequence, which achieved 3D T1 maps with whole heart coverage. Excellent correlation for the T1 values typically observed in myocardium pre and post contrast was obtained with little residual ($R^2 = 0.99$) and a regression slope 0.93. Homogeneous T1 maps were obtained from in-vivo study. Whole left ventricle T1 mapping was finished in around ~10 minutes with about 40% navigator efficiency without using any parallel imaging. Measured normal myocardium T1 values were comparable to those previously published.

3152

Computer #54



Myocardial T1- and ECV- Mapping at 3 Tesla using the Saturation-Recovery Techniques SASHA and SAPPHERE

Nadja M Meßner^{1,2}, Sebastian Weingärtner^{1,3,4}, Johannes Budjan⁵, Dirk Loßnitzer⁶, Uwe Mattler⁵, Theano Papavassiliu^{2,6}, Lothar R Schad¹, and Frank G Zöllner¹

¹Computer Assisted Clinical Medicine, Medical Faculty Mannheim, Heidelberg University, Mannheim, Germany, ²DZHK (German Centre for Cardiovascular Research), partner site Heidelberg/Mannheim, Germany, ³Department of Electrical and Computer Engineering, University of Minnesota, Minneapolis, MN, United States, ⁴Center for Magnetic Resonance Research, University of Minnesota, Minneapolis, MN, United States, ⁵Institute of Clinical Radiology and Nuclear Medicine, Medical Faculty Mannheim, Heidelberg University, Mannheim, Germany, ⁶1st Department of Medicine Cardiology, Medical Faculty Mannheim, Heidelberg University, Mannheim, Germany

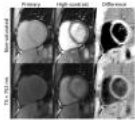
Myocardial T₁- and ECV-mapping for the detection of fibrosis is commonly performed at 1.5T with inversion-recovery (IR) techniques such as MOLLI.

As an alternative, we studied the robustness and precision of the saturation-recovery (SR) T₁-mapping techniques SAPHIRE and SASHA at 3T in 20 healthy volunteers. The resulting T₁- and ECV- reference values for SR T₁-mapping were 1578±42ms/0.30±0.03 (SAPHIRE) and 1523±46ms/0.31±0.03 (SASHA), revealing the underestimation of T₁-times by MOLLI to be approximately 20-29%.

Therefore, we suggest SR T₁-mapping with its high accuracy, low precision-loss, and good inter-subject variability as a valuable alternative to IR T₁-mapping at 3T.

3153

Computer #55



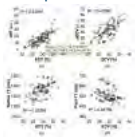
Free-breathing SASHA T₁ mapping using high-contrast image registration has greater precision than MOLLI T₁ mapping
Kelvin Chow¹, Yang Yang², and Michael Salerno^{1,2}

¹Medicine, Division of Cardiology, University of Virginia, Charlottesville, VA, United States, ²Biomedical Engineering, University of Virginia, Charlottesville, VA, United States

The robustness of SASHA T₁ mapping to systematic errors provides more accurate T₁ measurements, but SASHA is less precise than the more commonly used MOLLI sequence. Free-breathing SASHA acquisitions can increase precision in T₁ maps, but motion correction of SASHA images is challenging due to poor blood-tissue contrast. We present a novel approach for robust image registration by acquiring additional high-contrast data in a keyhole fashion without affecting T₁ accuracy. In 10 healthy subjects, a SASHA T₁ maps acquired in <90 seconds of free-breathing had a lower myocardial T₁ standard deviation than MOLLI (46.1±3.8 ms vs. 55.3±7.7 ms, p<0.05).

3154

Computer #56



Sensitive Non-contrast CMR Index for Quantifying Myocardial Fibrosis

Jiayu Sun¹, Simeng Wang¹, Robert O'Connor², David Muccigrosso³, Yucheng Chen⁴, Wei Cheng¹, Charles Hildebolt³, Fabao Gao¹, and Jie Zheng³

¹Radiology, West Hospital, Chengdu, China, People's Republic of, ²NIH, Bethesda, MD, United States, ³Radiology, Washington University in St. Louis, St. Louis, MO, United States, ⁴Cardiology, West Hospital, Chengdu, China, People's Republic of

The purpose is to develop and evaluate a non-contrast CMR approach for sensitive and quantitative assessment of myocardial fibrosis. Ten patients with cardiomyopathy were scanned with and without contrast injection. A quantitative fibrosis index derived from native T₁p dispersion contrast was obtained and compared with extracellular volume calculated by T₁ mapping. A strong correlation was shown between two indexes and superior sensitivity was observed for fibrosis index to detect myocardial diffuse fibrosis.

3155

Computer #57



Fat Signal Removal in LGE using Phase-Sensitive Chemical Selection (PiSCES)

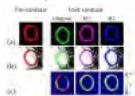
Martin A Janich¹, Steven D Wolff², Oleg Shubayev², and Anja CS Brau³

¹GE Global Research, Munich, Germany, ²Advanced Cardiovascular Imaging, New York, NY, United States, ³GE Healthcare, Munich, Germany

Late Gadolinium Enhancement (LGE) with fat suppression typically leaves traces of fat signal in the image. The goal of the present work is to completely remove fat signal from the LGE image and to visualize fat separately. The PiSCES method applies phase sensitive image reconstruction and customized timing of fat-selective RF pulses. In 19 out of 22 patient examinations PiSCES better removed fat compared to conventional magnitude fat-suppressed LGE.

3156

Computer #58



Automatic extracellular volume fraction mapping in the myocardium: multiple initial T₁ values and deformable image registration combined with LV segmentation

Chiao-Ning Chen¹, Hsiao-Hui Huang¹, Ming-Ting Wu², and Teng-Yi Huang¹

¹Electrical Engineering, National Taiwan University of Science and Technology, Taipei, Taiwan, ²Radiology, Kao-Hsiung Veterans General Hospital, Kao-Hsiung, Taiwan

This study attempted to improve the accuracy of T₁ fitting and image registration for automatic extracellular volume fraction mapping. We proposed to use multiple initial values in the T₁ fitting procedure and the results prominently exhibited less errors. For the image registration, we first performed the automatic segmentation of left-ventricle (LV) walls based on an image synthesis approach and then used the obtained LV masks for the deformable image registration. The results supported that the method significantly improved the overlap rate between the pre- and postcontrast images as well as the accuracies of the obtained ECV maps.

3157

Computer #59

Native myocardial T₁ correlates with right ventricular mass and invasive catheter measurement in patients with Pulmonary Hypertension

Laura Claire Saunders¹, Neil J Stewart¹, Charlotte Hammerton¹, David Capener¹, Valentina O Puntmann², David G Kiely³, Martin J Graves⁴, Andy Swift¹, Jim M Wild¹, and Laura Claire Saunders¹

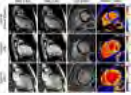
¹Academic Unit of Radiology, The University of Sheffield, Sheffield, United Kingdom, ²Department of Cardiovascular Imaging, Kings College London, London, United Kingdom, ³The University of Sheffield, Sheffield, United Kingdom, ⁴University of Cambridge School of Clinical Medicine, University of Cambridge, Cambridge, United Kingdom

Patients with pulmonary hypertension (n=102, 58±16 years, 56% female) and age and sex matched volunteers (n=34, 51±14 years, 58% female) underwent functional cardiac MR and MOLLI T₁ mapping at 1.5T. MOLLI images were registered to correct for respiratory

motion. Patients had elevated myocardial T1 at the right ventricular (RV) insertion point ($p < 0.001$) and left ventricular free wall when compared to healthy volunteers ($p = 0.013$). RV insertion point T1 and pulmonary artery pressure correlated significantly ($r = 0.406$, $p = 0.016$). Correlations were found between RV free wall and septal T1 and diastolic mass index (corrected for age and sex) ($r = 0.305$, $p = 0.003$ and $r = 0.281$, $p = 0.006$ respectively). Patients with pulmonary hypertension ($n = 102$, 58 ± 16 years, 56% female) and age and sex matched volunteers ($n = 34$, 51 ± 14 years, 58% female) underwent functional cardiac MR and MOLLI T1 mapping at 1.5T. MOLLI images were registered to correct for respiratory motion. Patients had elevated myocardial T1 at the right ventricular (RV) insertion point ($p < 0.001$) and left ventricular free wall when compared to healthy volunteers ($p = 0.013$). RV insertion point T1 and pulmonary artery pressure correlated significantly ($r = 0.406$, $p = 0.016$). Correlations were found between RV free wall and septal T1 and RV mass index (corrected for age and sex) ($r = 0.305$, $p = 0.003$ and $r = 0.281$, $p = 0.006$ respectively).

3158

Computer #60



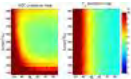
Characterization of Compacted Myocardial Abnormalities by Cardiac Magnetic Resonance with Native T1 Mapping in Left Ventricular Non-compaction Patients: A Comparison with Late Gadolinium Enhancement
Hongmei Zhou¹, Xue Lin¹, Haiyan Ding², and Quan Fang¹

¹Cardiology, Peking Union Medical College, Beijing, China, People's Republic of, ²Center for Biomedical Imaging Research, Department of Biomedical Engineering, School of Medicine, Tsinghua University, Beijing, China, People's Republic of

Left Ventricular Non-compaction (LVNC) manifesting with myocardial fibrosis can cause cardiac dysfunction, arrhythmia, and sudden death. Native T1 mapping is an emerging CMR technique in quantitative evaluation of myocardial fibrosis. This study aims to investigate the usefulness of native T1 mapping in characterization of myocardial abnormalities in LVNC patients by comparing with late gadolinium enhancement. It may suggest that native T1 mapping may provide information for early detection of fibrosis in compacted myocardium and stratification of severity in Left Ventricular Non-compaction.

3159

Computer #61



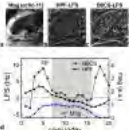
Optimized Acquisition for Joint T2 and ADC mapping in the Heart
Zhaohuan Zhang^{1,2}, Eric Aliotta^{2,3}, and Daniel B Ennis^{2,3}

¹Department of Physics and Astronomy, Shanghai Jiao Tong University, Shanghai, China, People's Republic of, ²Department of Radiological Sciences, University of California, Los Angeles, CA, United States, ³Physics & Biology in Medicine Graduate Program, University of California, Los Angeles, CA, United States

Myocardial T₂ and Apparent Diffusion Coefficient (ADC) can be used to evaluate the presence of edema and myocardial infarction^{1,2}. We recently developed a technique for joint acquisition and reconstruction of T₂ and ADC maps using a spin-echo EPI diffusion weighted sequence (SE-EPI DWI) with a total acquisition time short enough to accommodate measurement in a single breath-hold. The objective of this study was to optimize the joint T₂/ADC acquisition to enhance sensitivity to myocardial infarction and to evaluate performance in simulations and phantom experiments.

3160

Computer #62



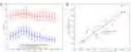
Myocardial Local Frequency Shift Mapping
Junmin Liu¹, James W Goldfarb², and Maria Drangova^{1,3}

¹Imaging Research Laboratories, Robarts Research Institute, Schulich School of Medicine & Dentistry, University of Western Ontario, London, ON, Canada, ²Department of Research and Education, Saint Francis Hospital, Roslyn, NY, United States, ³Medical Biophysics, Schulich School of Medicine & Dentistry, University of Western Ontario, London, ON, Canada

Local Frequency Shift (LFS) mapping of the myocardium may provide information about the integrity and organization of myofibers, which contribute anisotropic magnetic susceptibility. We present a myocardial LFS mapping method by explicitly removing the unwanted phase terms caused by B₀ inhomogeneity and chemical-shift (CS) between fat and water. The proposed method was tested with human data and compared with the established high-pass filtering technique. The results demonstrate a gradient across the myocardial wall suggesting that LFS maps of the myocardium may enable visualization of myofiber orientation.

3161

Computer #63



Myocardial Effective Transverse Relaxation Time at 7.0 T Correlates with Left Ventricular Wall Thickness
Till Huelnhagen¹, Teresa Serradas Duarte¹, Fabian Hezel¹, Erdmann Seeliger², Bert Flemming², Marcel Prothmann³, Jeanette Schulz-Menger³, and Thoralf Niendorf^{1,4}

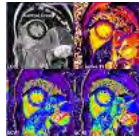
¹Berlin Ultrahigh Field Facility (B.U.F.F), Max Delbrück Center for Molecular Medicine in the Helmholtz Association (MDC), Berlin, Germany, ²Institute for Physiology, Charité University Medicine, Berlin, Germany, ³Working Group on Cardiovascular Magnetic Resonance, Experimental and Clinical Research Center, a joint cooperation between the Charité Medical Faculty and the Max Delbrück Center for Molecular Medicine in the Helmholtz Association, Berlin, Germany, ⁴Experimental and Clinical Research Center, a joint cooperation between the Charité Medical Faculty and the Max Delbrück Center for Molecular Medicine in the Helmholtz Association, Berlin, Germany

This work examines the relationship of ventricular septal wall thickness and T₂* at 7.0T in healthy volunteers. Results show, that T₂* changes periodically over the cardiac cycle, increasing in systole and decreasing in diastole. A strong correlation between mean septal T₂* and wall thickness was found. Temporally resolved field mapping showed that macroscopic magnetic field fluctuations can be excluded as source of the observed changes. While T₂* is often regarded as surrogate for tissue oxygenation, the found systolic increase of T₂* cannot be explained by increased oxygenation. Instead changes in blood volume fraction are assumed to be responsible for the observed T₂* fluctuations.

3162

Myocardial Extracellular Volume Measurements using a shorter post-contrast T1 mapping delay time for Diagnosis of Cardiac

Computer #64 Amyloidosis in 3.0T Cardiac Magnetic Resonance



Yan Yi¹, Lu Lin¹, Yining Wang¹, Jian Cao¹, Lingyan Kong¹, Jing An², Tianjing Zhang², and Bruce Spottiswoode³

¹Peking Union Medical College Hospital, Beijing, China, People's Republic of, ²Siemens Shenzhen Magnetic Resonance Ltd., Beijing, China, Beijing, China, People's Republic of, ³MR Research and Development, Siemens Healthcare, Chigago, IL, United States

The study aim was to explore the diagnostic value of ECV for cardiac amyloidosis calculated by 5 min post-contrast T1-mapping compared with conventional 15-20 min post-contrast T1 mapping. The results showed ECV calculated by 5min post-contrast T1 mapping had similarly promising diagnosis value for cardiac amyloidosis compared with 15-20 min post-contrast T1 mapping.

3163

Computer #65



Free-breathing 3D myocardial T2 mapping using image-based respiratory motion correction

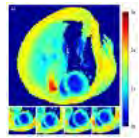
Joao Luis Tourais¹, Markus Henningsson¹, and Rene Botnar¹

¹King's College London, London, United Kingdom

Image navigator based free-breathing whole heart 3D T2prep-based T2 mapping achieved similar accuracy to a conventional 2D-BH T2prep-based mapping approach, and can be performed within less than 5 minutes. With this approach the limitations of conventional 2D T2 mapping (low resolution, mis-registration and diaphragmatic motion between BH) as well as 3D T2 mapping (unpredictable scan time because of navigator gating) have been overcome. These promising results warrant further investigation in patients with myocardial pathologies.

3164

Computer #66



Rapid T1-Mapping of Mouse Hearts using Real-Time MRI

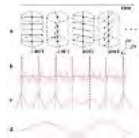
Tobias Wech¹, Nicole Seiberlich², Andreas Schindele³, Alfio Borzi³, Herbert Köstler¹, and Jürgen E. Schneider⁴

¹Department of Diagnostical and Interventional Radiology, University of Würzburg, Würzburg, Germany, ²Department of Biomedical Engineering, Case Western Reserve University, Cleveland, OH, United States, ³Institute of Mathematics, University of Würzburg, Würzburg, Germany, ⁴Radcliffe Department of Medicine, University of Oxford, Oxford, United Kingdom

The feasibility of using real-time MRI to determine T_1 relaxation times in mouse hearts was explored. An inversion recovery prepared and highly undersampled radial acquisition was applied and data were reconstructed using a combination of through-time radial GRAPPA and compressed sensing. The ECG in combination with the DC-signal recorded for each projection was used to eliminate cardiac and respiratory motion, which allowed for fitting T_1 -values in every voxel. The method was applied to five mice in vivo and the measured T_1 -values found for myocardial tissue agreed well with literature. Our work indicates that it is possible to accurately measure T_1 in mice using real-time MRI.

3165

Computer #67



3D T1-weighted self-gated cardiac MRI for assessing myocardial infarction in mouse models

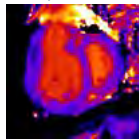
Xiaoyong Zhang^{1,2}, Guoxi Xie², Zijun Wei², Yanchun Zhu², Shi Su², Caiyun Shi², Fei Yan², Bensheng Qiu¹, Xin Liu², Hairong Zheng², and Zhaoyang Fan³

¹University of Science and Technology of China, Hefei, China, People's Republic of, ²Shenzhen Institutes of Advanced Technology, Shenzhen, China, People's Republic of, ³Cedars-Sinai Medical Center, Los Angeles, CA, United States

A 3D self-gating technique was developed for assessing myocardial infarction (MI) in mouse model. The preliminary in vivo study has demonstrated that the technique can correctly detect the MI, which may outperform the conventional MR techniques with ECG-triggering and respiratory gating.

3166

Computer #68



Cardiac Magnetic Resonance T1 mapping in pulmonary hypertension. Is Native T1 mapping an alternative to Late Gadolinium Enhancement?

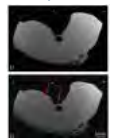
Geesath Jayasekera¹, Colin Church¹, Martin Johnson¹, Andrew Peacock¹, and Aleksandra Radjenovic²

¹Scottish Pulmonary Vascular Unit, Golden Jubilee National Hospital, Glasgow, United Kingdom, ²Institute of Cardiovascular and Medical Sciences, University of Glasgow, Glasgow, United Kingdom

Pulmonary hypertension is a rare progressive disorder characterised by elevated pulmonary artery pressure leading to right ventricular failure and death. Native T1 mapping is a CMR technique for myocardial tissue characterisation that does not require MRI contrast administration. We investigated whether native T1 values relate to invasive pressure measurements and markers of RV dysfunction in patients with pulmonary hypertension.

3167

Computer #69



High resolution Magnetic Resonance Imaging (MRI) combined with Magnetization Transfer (MT) for the visualization of the cardiac structure: an ex vivo proof of concept

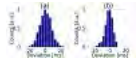
Julie Magat¹, Arnaud Fouillet¹, Jérôme Naulin¹, David Benoist¹, Yunbo Guo¹, Olivier Bernus¹, Bruno Stuyvers¹, and Bruno Quesson¹

¹IHU LIRYC, Université de Bordeaux, Pessac, France

The motivation of this study was to investigate Magnetization Transfer MRI as a technique of contrast for visualization of the Purkinje Fiber (PF) network in ex vivo cardiac sample of a large animal. We first optimized MT parameters to obtain the best contrast: offset frequency, duration of the module and radiofrequency field. We performed 2D and 3D acquisition on pig ex vivo heart. We were able to enhance contrast between PF network and muscle and visualize insert points inside the myocardium in 3D.

3168

Computer #70



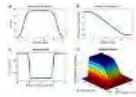
Self-navigated cardiac T₁ mapping using an ultra short echo time (UTE) inversion recovery acquisition
Patrick Winter¹, Thomas Kampf¹, Fabian Tobias Gutjahr¹, Cord Bastian Meyer¹, Volker Herold¹, Wolfgang Rudolf Bauer², and Peter Michael Jakob¹

¹Experimental Physics 5, University of Wuerzburg, Wuerzburg, Germany, ²Medizinische Klinik und Poliklinik I des Universitaetsklinikums Wuerzburg, Wuerzburg, Germany

Radial trajectories enable self-navigated cardiac T₁ measurements without the necessity of external ECG signals. However, the extracted cardiac synchronization signals and the reconstructed images can be susceptible to B₀ inhomogeneities and flow. In order to improve the robustness of the self-navigated method a 2D - UTE inversion recovery sequence is introduced that minimizes the echo time to 0.57 ms and reduces the susceptibility to B₀ inhomogeneities. Steady state cines and a T₁ map were derived from the UTE measurement. Comparisons with a self-navigated gradient echo measurement indicate more reliable self-navigation signals and better image quality when using shorter echo times.

3169

Computer #71



Wideband Adiabatic Inversion with a Hyperbolic Secant 4 (HS4) Pulse for Late Gadolinium Enhancement MRI of Patients with Implanted Cardiac Devices

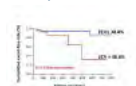
Shams Rashid¹, Jiaxin Shao¹, and Peng Hu^{1,2}

¹Radiological Sciences, University of California, Los Angeles, Los Angeles, CA, United States, ²Biomedical Physics Inter-Departmental Graduate Program, University of California, Los Angeles, Los Angeles, CA, United States

We present a wideband inversion pulse of 8kHz bandwidth designed with a hyperbolic secant 4 (HS4) adiabatic inversion pulse, for use in wideband late gadolinium enhancement (LGE) MRI in patients with implantable cardioverter-defibrillators (ICDs). This HS4 wideband pulse has more than twice the bandwidth of the previously reported wideband hyperbolic secant (HS) adiabatic inversion pulse for wideband LGE. We demonstrate that the wideband HS4 pulse is superior to the wideband HS pulse in eliminating hyperintensity artifacts resulting from off-resonance induced by an ICD in the myocardium.

3170

Computer #72



Myocardial T₁-map-derived extracellular volume fraction (ECV) measurement can represent the disease severity and prognostic information in patients with dilated cardiomyopathy (DCM)

Yoshiaki Morita¹, Naoaki Yamada¹, Emi Tateishi², Teruo Noguchi², Masahiro Higashi¹, and Hiroaki Naito¹

¹Department of Radiology, National Cerebral and Cardiovascular Center, Suita, Osaka, Japan, ²Division of Cardiology, National Cerebral and Cardiovascular Center, Suita, Osaka, Japan

Myocardial fibrosis is closely related to clinically evident cardiac dysfunction and worse outcomes, such as heart failure and arrhythmia. Therefore, non-invasive methods, which can reliably quantify fibrosis, would be preferable. In this study, we demonstrated that T₁-map-derived ECV measurement is a significant independent predictor of major adverse cardiovascular events (MACEs) when compared with the presence of LGE and other risk factors. ECV may thus represent a novel prognostic indicator in patients with DCM.

Electronic Poster

Pulse Sequences

Exhibition Hall

Tuesday, May 10, 2016: 10:00 - 11:00

3171

Computer #1



Accelerated Multi Echo based Correlated spectroscopic imaging of calf muscle in three spatial dimensions

Manoj Kumar Sarma¹, Zohaib Iqbal¹, Rajakumar Nagarajan¹, and M. Albert Thomas¹

¹Radiological Sciences, UCLA School of Medicine, Los angeles, Los Angeles, CA, United States

Multi-echo based echo-planar correlated spectroscopic imaging (ME-EP-COSI) has been an innovative method to study muscle lipid content in T2D and a variety of other metabolic conditions. In this study we implemented accelerated ME-EP-COSI and validated in a corn oil phantom and in healthy human calf muscle. Both phantom and human calf muscle results show that 5D ME-EP-COSI has the potential to be a powerful tool for human calf muscle examination. Further studies will investigate various pathologies, including obesity and type 2 diabetes, using the 5D ME-EP-COSI method.

3172

Computer #2



Frequency Shift Imaging (FSI) for characterization of cells labeled with superparamagnetic iron-oxide nanoparticles

Judy Alper^{1,2}, Priti Balchandani¹, Francois Fay¹, and Hadrien Dyvorne¹

¹Translational and Molecular Imaging Institute, Icahn School of Medicine at Mount Sinai, New York, NY, United States, ²Department of Biomedical Engineering, City College of New York, New York, NY, United States

MRI has long been used as a detection tool for cells labeled with superparamagnetic iron-oxide nanoparticles (SPIOs). Positive contrast

imaging of off-resonance SPIO signal provides benefits over negative contrast methods and imaging the SPIOs at 7 Tesla (7T) allows for leveraging greater off-resonance sensitivity for quantitative imaging of smaller cell populations. In this study, we imaged a cell phantom containing SPIO labeled macrophages at 7T. We demonstrated the performance of frequency shift imaging (FSI), a new acquisition technique, for characterizing the magnetic signature of SPIOs, as compared to negative contrast methods.

3173

Computer #3



Trajectory design of optimized repeating linear and nonlinear gradient encoding using a k-space point spread function metric
Nadine Luedicke Dispenza¹, Hemant Tagare^{1,2}, Gigi Galiana², and Robert Todd Constable¹

¹Biomedical Engineering, Yale University, New Haven, CT, United States, ²Radiology and Biomedical Imaging, Yale University, New Haven, CT, United States

Accelerated imaging with nonlinear gradients can result in undersampling artifacts. A computationally efficient k-space point spread function metric that reflects the qualitative features of interest in the object is used to design a repeating nonlinear gradient trajectory that can be added to the linear trajectory. The nonlinear gradient solution is found through optimization of the metric calculated for only a few time points in the linear trajectory over a subregion of k-space containing the linear encoding. Images reconstructed from data simulated with the optimized nonlinear trajectories result in less undersampling artifacts compared to linear trajectories.

3174

Computer #4



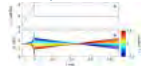
COBRA - Continuously Ordered B0 Readout Acquisition
Martyn Paley¹, Steven Reynolds¹, Sarah Calvert², and Allan Pacey²

¹Immunity, Infection and Cardiovascular Disease, University of Sheffield, Sheffield, United Kingdom, ²Oncology and Metabolism, University of Sheffield, Sheffield, United Kingdom

A novel encoding method known as Continuously Ordered B0 Readout acquisition or COBRA is described. The method uses an additional B0 coil with a unique field at every point in space to perform Volume Frequency Encoding. The field increases as a monotonic function within the coil and can be sorted to the appropriate 3D location for reconstruction. 3D data sets have been acquired and reconstructed at 9.4T.

3175

Computer #5



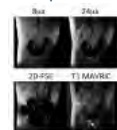
Application of Spin Echoes in the Regime of Weak Dephasing to Oxygen Enhanced T1-Quantification in the Lung
Jakob Assländer¹, Steffen Glaser², and Jürgen Hennig¹

¹Dept. of Radiology - Medical Physics, University Medical Center Freiburg, Freiburg, Germany, ²Dept. of Chemistry, Technische Universität München, Munich, Germany

This paper proposes an inversion-recovery spin-echo SNAPSHOT-FLASH sequence for quantifying proton-density and T_1 of the lung. It is shown that T_1 is reduced compared to the standard gradient-echo sequence. Similar results have been previously reported for UTE sequences. In combination with an iterative algorithm that is similar to MR-fingerprinting reconstructions, the feasibility of acquiring quantitative maps of the entire lung with a resolution of 5 mm x 5 mm x 10 mm within 5.5 s is demonstrated.

3176

Computer #6



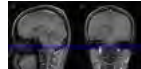
Single Point Imaging with Broadband Excitations and Ultra-Short Echo Times for Imaging near Metallic Implants
Curtis Wiens¹, Nathan S. Artz^{1,2}, Hyungseok Jang¹, Alan McMillan¹, Kevin Koch³, and Scott B. Reeder^{1,4,5,6,7}

¹Radiology, University of Wisconsin, Madison, WI, United States, ²Diagnostic Imaging, St. Jude Children's Research Hospital, Memphis, TN, United States, ³Biophysics and Radiology, Medical College of Wisconsin, Milwaukee, WI, United States, ⁴Medical Physics, University of Wisconsin, Madison, WI, United States, ⁵Biomedical Engineering, University of Wisconsin, Madison, WI, United States, ⁶Medicine, University of Wisconsin, Madison, WI, United States, ⁷Emergency Medicine, University of Wisconsin, Madison, WI, United States

Large magnetic susceptibility differences between metallic implants and tissue generate severe B_0 inhomogeneities that present several challenges for MR: excitation of the entire off-resonance spectrum, distortion in the frequency encoding direction, and severe intra-voxel dephasing. In this work we propose an ultra-short echo time acquisition with broadband excitation. Single point encoding was used to avoid in-plane distortions while 3D undersampling facilitated clinically feasible acquisition times. The effects of RF pulse duration on signal loss near the implant and T_1 weighting were evaluated in a total hip replacement phantom and a volunteer with a total knee replacement.

3177

Computer #7



Artery selective 3D TOF by Using Asymmetrically RF-shimmed Pre-saturation pulse with 4-channel RF Transmit at 3T
Kosuke Ito¹, Atsushi Kuratani¹, Yukio Kaneko², and Masahiro Takizawa¹

¹Healthcare Company, Hitachi Ltd., Chiba, Japan, ²Research and Development Group, Hitachi Ltd., Tokyo, Japan

A technique of ICA-selective 3D TOF imaging using asymmetrically RF-shimmed Pre-saturation pulse is presented. By using 4-channel RF transmit coil, spatially asymmetric RF transmission is achieved. Then apply RF shimming parameter to Pre-saturation pulse, the saturation effect becomes spatially asymmetric, and achieved selectively visualize blood flow from each ICA. This technique provides high contrast between blood and brain parenchyma because it does not make TR longer.

3178

Computer #8

Spectrally selective 3D dynamic bSSFP for hyperpolarized C-13 metabolic imaging at 14.1T

Hong Shang^{1,2}, Subramaniam Sukumar¹, Robert A. Bok¹, Irene Marco-Rius¹, Cornelius von Morze¹, Adam B. Kerr³, Galen Reed⁴, Michael Ohliger¹, John Kurhanewicz¹, Peder E. Z. Larson¹, John M. Pauly³, and Daniel B. Vigneron¹

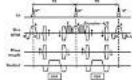


¹Radiology and Biomedical Imaging, UCSF, San Francisco, CA, United States, ²Bioengineering, UC Berkeley - UCSF, San Francisco / Berkeley, CA, United States, ³Electrical Engineering, Stanford University, Stanford, CA, United States, ⁴HeartVista, Menlo Park, CA, United States

Balanced SSFP sequences can provide superior SNR efficiency for hyperpolarized ¹³C imaging, by efficiently utilizing the non-recoverable magnetization. A spectrally selective bSSFP sequence was developed to enable fast mapping of hyperpolarized metabolites. A novel approach for bSSFP spectral selectivity was developed utilizing a combination of optimized multiband RF pulses and a bSSFP pulse train with a carefully chosen TR to avoid banding artifact. The sequence enabled 3D dynamic imaging of HP resonances generated in studies with co-polarized pyruvate and urea (with ~1% selectivity), attaining 2mm isotropic resolution and <1s temporal resolution.

3179

Computer #9



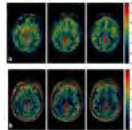
Interleaving SSFP Signal Acquisition
Ke Jiang¹, Wen Song¹, Chao Zou¹, and Yiu Cho Chung¹

¹Paul C. Lauterbur Research laboratory for Biomedical imaging, Shenzhen Institutes of Advanced Technology, Shenzhen, China, People's Republic of

We propose to acquire the different components in the steady state signal by interleaving. Using DESS as an example, we show that through appropriate gradient design, the two major components (S+ and S-) in the SSFP signal can be separately acquired in alternate TR and form images similar to those conventionally acquired by DESS. The new technique shortens TR and reduces motion and diffusion sensitivity.

3180

Computer #10



Fast 3D Magnetic Resonance Fingerprinting (MRF) For Whole Brain Coverage in Less Than 3 Minutes

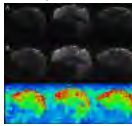
Dan Ma¹, Jesse Hamilton², Yun Jiang², Nicole Seiberlich², and Mark Griswold¹

¹Radiology, Case Western Reserve University, Cleveland, OH, United States, ²Biomedical Engineering, Case Western Reserve University, Cleveland, OH, United States

The purpose of this study is to accelerate the acquisition time of 3D MRF scans. A simple acquisition scheme was applied to allow a total factor of 144 acceleration as compared to the Nyquist rate, such that 3D T1, T2 and proton density maps can be acquired from a whole brain scan at clinical resolution in 2.6 minutes.

3181

Computer #11



A Multishot, Hadamard-Encoded Autocalibration Scan for Multiband EPI at 7T

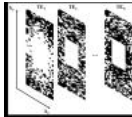
Alexander D. Cohen¹, Andrew S. Nencka^{1,2}, and Yang Wang^{1,2}

¹Radiology, Medical College of Wisconsin, Milwaukee, WI, United States, ²Biophysics, Medical College of Wisconsin, Milwaukee, WI, United States

A multiband (MB) echo planar imaging (EPI) sequence with multishot autocalibration was developed and implemented at 7T. Slices were unaliased using the principles of Hadamard encoding, resulting in a fully-sampled calibration scan reconstructed without parallel imaging techniques. A Hadamard unaliasing procedure was demonstrated with an acceleration factor of lower rank than the Hadamard encoding matrix. Using this sequence, a functional MRI protocol at 7T was introduced to obtain a sufficient calibration volume, that was then utilized to unalias the remaining repetitions using a slice-GRAPPA technique. Preliminary resting state data acquired using this protocol has generated reliable connectivity networks.

3182

Computer #12



3D Metabolite and Neurotransmitter Mapping Using Multiple-TE Encoding with Sparse Sampling

Fan Lam¹, Qiang Ning^{1,2}, Chao Ma¹, Bryan Clifford^{1,2}, and Zhi-Pei Liang^{1,2}

¹Beckman Institute, University of Illinois at Urbana-Champaign, Urbana, IL, United States, ²Department of Electrical and Computer Engineering, University of Illinois at Urbana-Champaign, Urbana, IL, United States

We present an integrative subspace-based sampling and reconstruction method for 3D high-resolution mapping of brain metabolites and neurotransmitters using MRSI. An echo-planar spectroscopic imaging sequence with J-resolved encoding capability has been developed to implement the proposed sparse sampling strategy for fast spatio-spectral encoding. An explicit subspace model-based reconstruction scheme that incorporates J-resolved spectral prior to enable joint reconstruction of the metabolite and neurotransmitter signal components from the sparse data is described. Results from experimental data are used to demonstrate the capability of the proposed method in producing high-resolution and high-SNR spatio-spectral distributions of both metabolites and neurotransmitters.

3183

Computer #13



Three Minute Whole-heart Magnetic Resonance Angiography with Prospective Heart Tracking and Compressed Sensing Parallel Image Reconstruction

Mehdi Hedjazi Moghari^{1,2}, Martin Uecker^{3,4}, Sébastien Roujol⁵, Tal Geva^{1,2}, and Andrew J Powell^{1,2}

¹Pediatrics, Harvard Medical School, Boston, MA, United States, ²Cardiology, Boston Children's Hospital, Boston, MA, United States, ³German Center for Cardiovascular Research (DZHK), Goettingen, Germany, ⁴Department of Diagnostic and Interventional Radiology, University Medical Center, Goettingen, Germany, ⁵Division of Imaging Sciences and Biomedical Engineering, King's Health Partners, St. Thomas' Hospital, King's College London, London, United Kingdom

To accelerate whole-heart magnetic resonance angiography, we implemented a variable density Poisson disc undersampling pattern and compressed sensing parallel image reconstruction, and compared it to a standard parallel image (SENSE) acquisition in 15 patients.

The compressed sensing technique was faster (mean 3.4 ± 1.0 minutes vs 7.6 ± 1.7 minutes) and had similar objectively measured sharpness in 4 designated regions (all $p > 0.05$) but a lower subjective image quality scores (all $p \leq 0.05$).

3184

Computer #14



MR relaxometry with an interleaved SSFP sequence

Chao Zou¹, Wensha Guo¹, Xin Liu¹, Hairong Zheng¹, and Yiu-Cho Chung¹

¹Paul C. Lauterbur Research Center for Biomedical Imaging, Shenzhen Institutes of Advanced Technology, CAS, Shenzhen, China, People's Republic of

A novel SSFP sequence with interleaved acquisition for F0, F- and F+ was proposed and applied to T1/T2 relaxometry. The good agreement with analytical solution of SSFP implies that steady state is maintained at different TR. Compared to TESS, TEs of the three echoes can be identical to eliminate T2* effect. The reduced TR decreases susceptibility induced signal void and motion sensitivity. The crusher in slice select direction avoids the unwanted diffusion effect for high resolution imaging. The phantom study shows that the T1/T2 relaxometry results are consistent with the traditional IR-TSE and SE results.

3185

Computer #15



Feasibility of Abdominal k-t GRAPPA Accelerated Dual-Venc 4D flow MRI in the Setting of Portal Hypertension

Eric James Keller¹, Susanne Schnell¹, James C Carr¹, Michael Markl^{1,2}, and Jeremy Douglas Collins¹

¹Radiology, Northwestern University, Chicago, IL, United States, ²Biomedical Engineering, Northwestern University, Evanston, IL, United States

Abdominal 4D flow MRI is currently limited by long acquisition times required to capture the wide range of velocities and flows present in the abdomen with separate low and high velocity encoding gradient (venc) acquisitions. By instead using a single 4D flow sequence with two different velocity encodings (dual-venc), we were able to quantify abdominal hemodynamics with similar accuracy in a total of 21% less time. Overall, this is encouraging as it directly addresses scan time, a major limitation of 4D flow MRI, increasing its clinical utility.

3186

Computer #16



Gradient Optimization for arbitrary k-space trajectories using Active Contour (GO-Active)

Pavan Poojar¹, Bikkemane Jayadev Nutandev², Ramesh Venkatesan³, and Sairam Geethanath¹

¹Medical Imaging Research Centre, Dayananda Sagar College of Engineering, Bangalore, India, ²Bangalore, India, ³Wipro-GE Healthcare, Bangalore, India

K-space trajectories such as cartesian, radial, spiral are not optimal for traversing arbitrary k-space shapes. GO-Active is a novel acquisition technique which is a combination of active contour and convex optimization where active contour was used to obtain arbitrary k-space trajectory and convex optimization was employed to optimize the gradients based on hardware constraints. Reconstruction was performed using Non Uniform Fast Fourier Transform and compressed sensing. Retrospective study was performed on six brain datasets and phantom, where as prospective study was carried out on the phantom respectively. Current and Future work involves application of GO-Active on in vivo data prospectively.

3187

Computer #17



Beachball: A fast and efficient 3D k-space trajectory with time optimal gradients

Pavan Poojar¹ and Sairam Geethanath¹

¹Medical Imaging Research Centre, Dayananda Sagar College of Engineering, Bangalore, India

3D Variable density spiral (VDS)-"beachball" was designed and generated to cover 3D k-space efficiently. Beachball is obtained by rotating along one axis of a 2D VDS for various number of shots. Beachball was demonstrated in-silico by analyzing point spread function and retrospective analysis of a in-vitro water phantom. Reconstruction was done using NUFFT. Optimal gradient waveforms were generated for beachball by using convex optimization formulations based on the constraints of maximum gradient amplitude and slew rate. This trajectory provides for smoother coverage and densely sampled at the centre of k-space and allows implementation of silent MR.

3188

Computer #18



Design of a k-space trajectory allowing the reconstruction of both standard and accelerated data in fat-suppressed DCE-MRI of breast

Julie POUJOL^{1,2}, Pierre-André VUISSOZ^{1,2}, Jacques FELBLINGER^{1,2,3}, and Freddy ODILLE^{1,2,3}

¹Imagerie Adaptative Diagnostique et Interventionnelle, Université de Lorraine, Nancy, France, ²U947, INSERM, Nancy, France, ³CIC-IT 1433, INSERM, Nancy, France

DCE-MRI protocol is the reference technique to detect and characterize breast lesions. Due to the high spatial resolution needed to detect small lesions, the temporal resolution of the DCE-MRI protocol is limited to 90 seconds. A good fat suppression is also needed and a spectral inversion preparation is commonly used for it. To provide more information about lesion vascularization, temporal resolution need to be increased. We have developed a method to implement a smart k-space trajectory allowing both standard DCE-MRI protocol reconstruction and accelerated DCE-MRI protocol via Compressed-Sensing reconstruction compatible with fat suppression.

3189

Computer #19

Dual Echo Trajectory for Novel Fast Acquisition

Jeehun Kim¹ and Jongho Lee¹

¹Laboratory for Imaging Science and Technology, Department of Electrical and Computer Engineering, Seoul national university, Seoul, Korea,

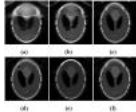


Republic of

In this study, we propose a new fast acquisition trajectory, Dual Echo Trajectory (DuET), to accelerate spin echo imaging. The proposed method allowed a 2-fold increase in acquisition speed with minimum image artifacts.

3190

Computer #20



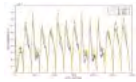
Composite pulses for RF phase encoded MRI
Somaie Salajeghe¹, Paul Babyn², and Gordon E. Sarty¹

¹Biomedical Engineering, University of Saskatchewan, Saskatoon, SK, Canada, ²Medical Imaging, University of Saskatchewan, Saskatoon, SK, Canada

RF phase encoded MRI uses spatial RF phase gradients in place of B_0 gradients coils to encode information. Using a nonlinear RF phase gradient coil instead of linear one leads to a larger field of view. However, this coil will generate an in-homogeneous B_1 field which result in pulse imperfection. To minimize the effect of pulse imperfection, the application of composite pulses is required. Current composite pulses were designed to use in current MRIs (having gradient coils and uniform RF coil), so the feasibility of working composite pulses with an RF encoded coil needs to be checked.

3191

Computer #21



B1-sensitive Encoding for Magnetic Resonance Fingerprinting
Gregor Körzdörfer¹, Thorsten Feiweier¹, Yun Jiang², and Mathias Nittka¹

¹Siemens Healthcare GmbH, Erlangen, Germany, ²Department of Biomedical Engineering, Case Western Reserve University, Cleveland, OH, United States

Quantitative parameter maps obtained from Magnetic Resonance Fingerprinting (MRF) are sensitive to B_1+ inhomogeneities. In principle, one could reduce this dependency by using a dictionary with an additional B_1+ dimension. However, if the dictionary entries are not well distinguishable, the simultaneous pattern matching of three parameters (T_1 , T_2 , B_1+) will not work reliably. In order to improve the separation of data in the B_1+ dimension, we implemented a novel B_1+ sensitive encoding. This approach employs a dedicated composite RF excitation pulse which directly encodes B_1+ magnitude information into the phase of the acquired signal. Here we present an experimental proof of principle using a 1D projection MRF sequence.

3192

Computer #22



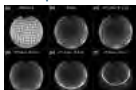
Selective Hepatic Artery Imaging Using Beam IR pulse
Takashi Nishihara¹, Kuniaki Harada¹, Noriko Itabashi¹, Kuniharu Oka¹, and Hiroyuki Itagaki¹

¹Healthcare Company, Hitachi, Ltd., Chiba, Japan

We confirmed that 2D beam excitation presaturation-pulse (hereafter Beam Sat pulse) can saturate the vessels selectively and visualized hemodynamics in brain and liver. Although Beam Sat can visualize portal vein and hepatic artery, right hepatic artery (RHA) cannot visualize clearly because T_1 relaxation of saturated blood magnetizations is short. In this study, 2D excitation pulse was used as IR pulse (hereafter Beam IR pulse), and we showed that the Beam IR pulse can clearly visualize a flow phantom and RHA of healthy volunteers.

3193

Computer #23



Accelerated imaging of sub-volumes using region-of-interest focused O-Space: Experimental verification of rOi-Space
Emre Kopanoglu¹, Haifeng Wang¹, Gigi Galiana¹, Dana C. Peters¹, and Robert Todd Constable^{1,2}

¹Diagnostic Radiology and Biomedical Imaging, Yale University, New Haven, CT, United States, ²Neurosurgery, Yale University, New Haven, CT, United States

rOi-Space is a region-of-interest imaging technique. The method uses a nonlinear gradient field for improved accelerated imaging similar to O-Space but focuses the encoding effort to the region-of-interest rather than imaging the whole field-of-view. Simulations showed improved reconstruction compared to radial acquisitions for acceleration factors between 2.2 and 14.2 and up to 70% reduction in reconstruction error, for acceleration factors of around 4. Noise performance comparisons demonstrate some degraded SNR performance due to intra-voxel dephasing. Experiments showed improved resolution inside the ROI at the expense of SNR performance. Hence, the method can be used for resolution enhancement in applications with adequate SNR.

Electronic Poster

A Mixed Bag: Sequence Simulations & Analyses / Dynamic Imaging

Exhibition Hall

Tuesday, May 10, 2016: 10:00 - 11:00

3194

Computer #25

Teaching MRI using Tuning Forks and Speakers
Sophie Shermer^{1,2} and Aled Issac¹

¹College of Science (Physics), Swansea University, Swansea, United Kingdom, ²Medical Imaging, Swansea University, Swansea, United Kingdom

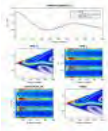
We illustrate some key basic concepts in MRI such as resonance, frequency-based slice selection and readout, as well as relaxation using tuning forks and sound waves.

3195 Computer #26 EPGspace: A Flexible Framework for Extended Phase Graphs of Periodic and Non-Periodic MRI Sequences
Matthias Weigel¹

¹Dept. of Radiology, Radiological Physics, University of Basel Hospital, Basel, Switzerland

The Extended Phase Graph (EPG) calculus can be understood as a solution of the Bloch equation using its k-space representation. The ability to represent magnetization in phase state configurations frequently enables an intuitive and pictorial understanding of echo formation and assignment. A class of functions that allows for the easy calculation and simulation of EPGs for arbitrary MR sequences was developed (EPGspace) and its key points are presented. The *EPGspace* source code is made publically available for download in the internet.

3196 Computer #27 Equivalence of EPG and Isochromat-based simulation of MR signals
Shaihan J Malik¹, Alessandro Sbrizzi², Hans Hoogduin², and Joseph V Hajnal¹



¹Imaging Sciences & Biomedical Engineering, King's College London, London, United Kingdom, ²Imaging Division, University Medical Centre, Utrecht, Utrecht, Netherlands

Extended Phase Graphs and Isochromat-summation are two leading methods for simulating MR signals. The latter method is more intuitive, but choice of the number and distribution of isochromats significantly affects results. It is well known that the two methods are related by Fourier Transform, but precise equivalence is not widely understood. We demonstrate conditions under which they are exactly equivalent and related by DFT. Choice of isochromats is shown to be a sampling problem and conditions for accurate isochromat-based simulations are given. Matlab code is provided as a direct illustration.

3197 Computer #28 PolyFT: a Freely-Available Optimized MATLAB Implementation of the Polyhedral Fourier Transform for Analytical Simulations in MRI
Shuo Han¹ and Daniel A. Herzka¹



¹Department of Biomedical Engineering, Johns Hopkins University School of Medicine, Baltimore, MD, United States

Analytical Fourier transforms (FT), such as FT of 2D and 3D Shepp-Logan phantoms, enable accurate arbitrary k-space sampling of digital phantoms. Here, we present and demonstrate a computationally efficient MATLAB implementation of the analytical FT of polyhedral phantoms with uniform intensity or non-uniform intensities. The computation time of the implementation is presented, as well as demonstrations showing its feasibility of simulating physiologically relevant phantoms and evaluating non-Cartesian sampling trajectories and parallel imaging algorithms. The implementation is now available through the Mathworks user community and GitHub.

3198 Computer #29 Parameter Dependency in Modular MR Sequences using Directed Graphs
Cristoffer Cordes¹, Thorsten Honroth¹, Daniel Hoinkiss¹, Saulius Archipovas¹, David Porter¹, and Matthias Günther^{1,2}



¹Fraunhofer MEVIS, Bremen, Germany, ²University of Bremen, Bremen, Germany

The interactions of MRI sequence components within complex techniques are hard to explain, grasp and extend using common modularity approaches. This results in poor developability and calculation efficiency. The proposed algorithm yields a new sequence description approach that resolves the component parameter dependencies and enables the calculation of arbitrary module parameters using the least amount of calculation steps. The algorithm has been used on a twice-refocused, spin-echo diffusion MRI sequence to simplify its description and boost the calculation of critical parameters during sequence preparation calculation.

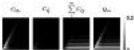
3199 Computer #30 Fast Realistic MRI Simulations Based on Generalized Exchange Spin Model
Fang Liu¹, Richard Kijowski¹, Wally Block², and Alexey Samsonov¹



¹Department of Radiology, University of Wisconsin-Madison, Madison, WI, United States, ²Department of Medical Physics, University of Wisconsin-Madison, Madison, WI, United States

Numerical simulation dramatically improves the understanding and development of new MR imaging methods. We proposed an improved version of MR simulation package named as MRiLab with the feature of incorporating a generalized exchange tissue model to facilitate flexible and realistic MR signal simulation for complex tissue structures.

3200 Computer #31 Using Cellular Automata to Represent MRI Signal Progression
Nicholas Dwork¹, Brian A. Hargreaves², and John M. Pauly¹



¹Electrical Engineering, Stanford University, Stanford, CA, United States, ²Radiology, Stanford University, Stanford, CA, United States

In this document we show that we can represent MRI signal progression as a sum of Cellular Automata processes.

3201 Computer #32 Convolutional Forward Modeling for Actual Slice Profile Estimation
Xiaoguang Lu¹, Peter Speier², and Ti-chiun Chang³

¹Medical Imaging Technologies, Siemens Healthcare, Princeton, NJ, United States, ²Siemens Healthcare, Erlangen, Germany, ³Siemens Corporate



Technology, Princeton, NJ, United States

Resolving slice thickness for better MR reconstruction is desirable, where actual slice profile plays a crucial role. Conventional blind deconvolution formulation includes both original signals and slice profile as unknowns, which is an ill-posed problem with high complexity. We propose a convolutional forward model (CFM), leveraging additional orthogonal stack(s) with an added convolution process in the formulation to fit actual forward imaging process accurately, resulting in a significantly simplified slice profile estimation problem. The actual slice profile is calculated through a data-driven approach. Experimental results demonstrate that the proposed method is robust to handle various challenges.

3202

Computer #33



GPU optimized fast 3D MRI simulator

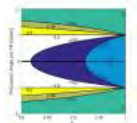
Ryoichi Kose¹ and Katsumi Kose²

¹MRTechnology Inc., Tsukuba, Japan, ²University of Tsukuba, Tsukuba, Japan

We have developed a GPU optimized fast 3D MRI simulator for pulse sequence developments. We compared simulation and experimental results for gradient echo images of water phantoms that contains an air-filled cylinder and air-filled sphere. The agreements between simulation and experiments were good if the calculation matrix was more than two times that of original images. Because the processing speed of our simulator varied from 2.2 to 3.1 TFLOPS, we concluded that our simulator is useful for development of MRI pulse sequences.

3203

Computer #34



Geometric solution to the fully balanced SSFP signals

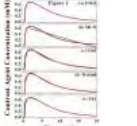
Hao Song¹, John Hazle¹, and Jingfei Ma¹

¹Imaging Physics, The University of Texas MD Anderson Cancer Center, Houston, TX, United States

Fully-balanced steady-state free precession (bSSFP) is clinically useful because of its high SNR efficiency, imaging speed and unique T_2/T_1 contrast. A geometric solution to bSSFP has been derived and provides a simple and intuitive understanding of how the complex steady-state signals are formed. However, T_1 and T_2 relaxation has generally been ignored. In this work, we present an exact geometric solution to the bSSFP signals by including the T_1 and T_2 relaxation effects. The results are consistent with those based on matrix calculations, and are useful in understanding different aspects of bSSFP signal behavior.

3204

Computer #35



Using numerical simulations to compare and evaluate different mathematical models for analyzing dynamic contrast enhanced MRI data

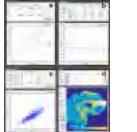
Dianning He^{1,2}, Wei Qian^{1,3}, Lisheng Xu^{1,4}, and Xiaobing Fan²

¹Sino-Dutch Biomedical and Information Engineering School, Northeastern University, Shenyang, China, People's Republic of, ²Radiology, University of Chicago, Chicago, IL, United States, ³Electrical and Computer Engineering, University of Texas at El Paso, El Paso, TX, United States, ⁴Key Laboratory of Medical Image Computing, Ministry of Education, Shenyang, China, People's Republic of

Numerical simulations were performed to study analytical mathematical models for fitting tissue contrast agent concentration curves obtained from DCE-MRI. Randomly generated K^{trans} and v_e were used to calculate the curves using the Tofts model. A total of five analytical mathematical models, empirical mathematical model, modified logistic model, modified sigmoidal function, Weibull model, and extended phenomenological universalities were compared and evaluated in terms of how well they fitted to 100 curves. Statistical analysis showed that the empirical mathematical model provided the best fit out of those models. The analytical mathematical models were different despite having the same number of parameters.

3205

Computer #36



Quantitative Magnetization Transfer Imaging Made Easy with qMTLab: Software for Data Simulation, Analysis and Visualisation

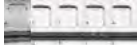
Jean-François Cabana¹, Ye Gu², Mathieu Boudreau³, Yves R. Levesque³, Yaaseen Atchia⁴, John G. Sled⁴, Sridar Narayanan³, Douglas L. Arnold³, Bruce G. Pike⁵, Julien Cohen-Adad⁶, Tanguy Duval⁶, Manh-Tung Vuong⁶, and Nikola Stikov⁶

¹Medical Physics, University of Montreal, Montreal, QC, Canada, ²NeuroRX, Montreal, QC, Canada, ³McGill University, Montreal, QC, Canada, ⁴University of Toronto, Toronto, ON, Canada, ⁵University of Calgary, Calgary, AB, Canada, ⁶Ecole Polytechnique, Montreal, QC, Canada

We have developed a free, open source software (*qMTLab*) that unifies the most widely used quantitative magnetization transfer imaging (qMTI) methods in a simple and easy to use graphical interface. *qMTLab* allows to easily simulate qMTI data, compare the performance of the methods under various experimental conditions, define new acquisition protocols, fit acquired data, and visualize the fitted parameter maps. In this presentation, we will offer a brief introduction on the theory behind qMTI, present the current acquisition and analytical methods, and present the functionality of the qMTLab software and its utility in basic and clinical research.

3206

Computer #37



Modelling intra-voxel dephasing in MR simulations

Stefan Kroboth¹, Katharina E. Schleicher¹, Kelvin J. Layton¹, Axel J. Krafft^{1,2,3}, Klaus Düring⁴, Feng Jia¹, Sebastian Littin¹, Huijun Yu¹, Jürgen Hennig¹, Michael Bock¹, and Maxim Zaitsev¹

¹Medical Physics, University Medical Center Freiburg, Freiburg, Germany, ²German Cancer Consortium (DKTK), Heidelberg, Germany, ³German Cancer Research Center (DKFZ), Heidelberg, Germany, ⁴MaVis Medical GmbH, Hannover, Germany

In order to capture intra-voxel dephasing in simulations, the object has to be modeled with a very large number of spins per voxel. We present a method to improve and speed up simulations by explicitly modelling intra-voxel dephasing. The method is evaluated by

simulating an MR-safe guidewire. The iron particles in the wire create dipole fields, which lead to dephasing in the proximity of the wire. We show that a substantial reduction of the required number of spins by a factor of ~5.4 is possible, without sacrificing image quality. This reduces the memory requirements and speeds up simulations.

3207

Computer #38



Platform-independent, rapid prototyping of MR sequences without code compilation

Thorsten Honroth¹, Cristoffer Cordes^{1,2}, Saulius Archipovas¹, Daniel Christopher Hoinkiss¹, Matthias Günther^{1,2,3}, and David Porter¹

¹Fraunhofer MEVIS, Bremen, Germany, ²University of Bremen, Bremen, Germany, ³mediri GmbH, Heidelberg, Germany

A platform-independent rapid clinical prototyping environment for MR sequences is demonstrated. Fully interactive product-like sequences can be defined without coding or compiling software. They are saved as plain text files and run by a generic pre-installed software module at the scanner that never needs modifications by a user. Sub-groups of sequence elements can be exported as *macros* and reused in other sequences.

3208

Computer #39



Real-time speech MRI: what is the optimal temporal resolution for clinical velopharyngeal closure assessment?

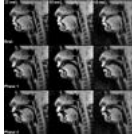
Matthieu Ruthven^{1,2}, Andrea C. Freitas³, Stephen F. Keevil^{2,4}, and Marc E. Miquel¹

¹Clinical Physics Department, Barts Health NHS Trust, London, United Kingdom, ²Imaging Sciences & Biomedical Engineering Research Division, King's College London, London, United Kingdom, ³William Harvey Research Institute, Queen Mary University of London, London, United Kingdom, ⁴Medical Physics Department, Guy's and St Thomas' NHS Foundation Trust, London, United Kingdom

Clinical velopharyngeal closure assessment involves imaging patients while they perform standard speech tasks. Real-time MRI could offer an alternative to the imaging techniques used at present, however, there is currently no consensus on the optimal temporal resolution. The purpose of this study is to determine an optimal temporal resolution by comparing the numbers of velopharyngeal closures in high temporal resolution and simulated lower temporal resolution datasets of healthy adult volunteers. The results of this study suggest that the optimal temporal resolution is between 7.5 and 10 frames per second. Future work will aim to pinpoint and validate this resolution.

3209

Computer #40



Real-time MRI of Speech at Very High Temporal Resolution

Arun Antony Joseph^{1,2}, Dirk Voit¹, Klaus-Dietmar Merboldt¹, and Jens Frahm^{1,2}

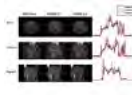
¹Biomedizinische NMR Forschungs GmbH, Max-Planck-Institute for Biophysical Chemistry, Goettingen, Germany, ²DZHK, German Center for Cardiovascular Research, Goettingen, Germany

MRI has become the preferred technique to study the dynamics of tongue and vocal tract during speech, singing or instrument playing. Recent advances provide access to qualitative information of fast tongue movements at very high temporal resolution. In this study, real-time MRI using highly undersampled radial FLASH with regularized nonlinear inverse reconstruction was used to monitor the dynamics of the tongue at 10 ms, 18 ms and 33 ms resolution. The effect of different temporal resolutions on the tongue and oral cavity during speech will be compared and analyzed.

3210



Computer #41



Ultrafast volumetric cine MRI (VC-MRI) for real-time 3D target localization in radiation therapy

Wendy Harris^{1,2}, Fang-Fang Yin^{1,2}, Chunhao Wang^{1,2}, Zheng Chang^{1,2}, Jing Cai^{1,2}, You Zhang^{1,2}, and Lei Ren^{1,2}

¹Department of Radiation Oncology, Duke University, Durham, NC, United States, ²Medical Physics Graduate Program, Duke University, Durham, NC, United States

A novel technique has been developed to generate ultra-fast high-quality volumetric cine MRI (VC-MRI) using patient prior information. The VC-MRI was generated by deforming the prior volumetric MRI images based on ultra-fast on-board 2D-cine MRI and patient PCA-based respiratory breathing model. The ultra-fast 2D-cine images were acquired by sampling about 10% of k-space. The undersampled cine images were reconstructed using an iterative MR reconstruction algorithm with a total generalized variation penalty. The technique was evaluated using both anthropomorphic digital phantom and patient data. Results demonstrated the feasibility of generating ultrafast-VC-MRI for both inter- and intra-fraction verification of moving targets in radiotherapy.

3211

Computer #42



Intracranial Dual-Venc 4D flow MRI at 7T: Effect of low versus high spatial resolution in combination with k-t GRAPPA acceleration

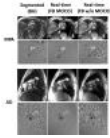
Susanne Schnell¹, Can Wu¹, Pierre-Francois Van de Moortele², Bharathidasan Jagadeesan³, Kâmil Uğurbil², Michael Markl¹, and Sebastian Schmitter²

¹Radiology, Northwestern University, Chicago, IL, United States, ²Center for Magnetic Resonance in Research, University of Minnesota, Minneapolis, MN, United States, ³Neurosurgery Department, University of Minnesota, Minneapolis, MN, United States

Dual-*venc* 4D flow MRI was applied in 6 healthy volunteers at a 7T MRI scanner at two different approximately isotropic spatial image resolutions, low resolution with (1.1mm)³ and high resolution with (0.8mm)³ voxel volumes. The aim of this study was to systematically investigate the potential of high-resolution k-t GRAPPA accelerated dual-*venc* 4D flow MRI compared to the low-resolution scan with standard GRAPPA with respect to improved image quality (vessel sharpness and depiction of small intracranial vessels) and quantification of intracranial flow parameters (net flow, peak velocity).

3212

Computer #43



Unsupervised motion correction for real-time free-breathing flow acquisitions: high SNR, single heart-beat, pseudo-breathheld flow images easy to quantify

Haris Saybasili¹ and Ning Jin²

¹MR R&D, Siemens Healthcare USA, Inc., Chicago, IL, United States, ²MR R&D, Siemens Healthcare USA, Inc., Columbus, OH, United States

Flow quantification on uncooperative patients that cannot hold their breath may be performed by real-time free-breathing flow acquisitions that generally cover multiple heart-beats. However, heart-rate fluctuations, low SNR, and respiratory motion associated with such acquisitions may impede flow quantification process. In this study, we are extending our unsupervised motion correction method for real-time free-breathing cine imaging to flow imaging, and comparing the results with gold standard ECG gated, breath-held, segmented flow acquisition. Preliminary results indicate net forward volumes in agreement with the reference, with comparable image quality.

3213

Computer #44



Improved Assessment of Left Ventricular Diastolic Function using High-Temporal Cine-CMR

Keigo Kawaji¹, Mita B. Patel¹, Marco Marino¹, Roberto M. Lang^{1,2}, Hui Wang³, Yi Wang⁴, and Amit R. Patel^{1,2}

¹Medicine, The University of Chicago, Chicago, IL, United States, ²Radiology, The University of Chicago, Chicago, IL, United States, ³Philips Healthcare, Cleveland, OH, United States, ⁴Biomedical Engineering and Radiology, Cornell University, New York, NY, United States

Assessment of diastolic function using cine-CMR is limited by its temporal resolution. A high-temporal cine-CMR approach that yields comparable temporal resolution to echocardiography was recently developed using radial trajectories with a custom spoke ordering that exploits the property of prime numbers (Modulo-Prime Spokes, or MoPS), as well as a radial UNFOLD-type streaking artifact removal step. In this study, we validate the functional cine-assessment parameters associated with systolic and diastolic performance of the left ventricle (LV) by comparing the measurements derived from time-volume curves between the proposed radial MoPS-Cine and the clinically employed Cartesian Cine reference.

3214

Computer #45



Breath-Held Phase-Cycled Cardiac Cine MRI using Slow Frequency Modulation

Anjali Datta¹, Corey A Baron¹, R Reeve Ingle², Joseph Y Cheng¹, and Dwight G Nishimura¹

¹Electrical Engineering, Stanford University, Stanford, CA, United States, ²HeartVista, Inc., Menlo Park, CA, United States

bSSFP is commonly used for cardiac cine imaging due to its high myocardium-blood contrast but suffers from signal nulls due to off-resonance. By modifying the slow frequency modulation scheme for use in the heart, we acquire interleaved phase-cycles within a breath-hold for banding artifact reduction. Because a constant heart rate cannot be assumed, the phase increment increases slowly for a time equal to the shortest expected RR interval and then remains constant until the next trigger. In vivo results indicate that the proposed method is comparable to standard phase-cycling but with shorter scan time and interleaved phase-cycle acquisition.

Electronic Poster

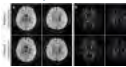
Parallel Imaging

Exhibition Hall

Tuesday, May 10, 2016: 10:00 - 11:00

3215

Computer #49



Shot-Coil Compression for Accelerated K-Space Reconstruction in Interleaved EPI DWI

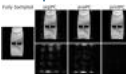
Zijing Dong¹, Fuyixue Wang¹, Xiaodong Ma¹, Erpeng Dai¹, Zhe Zhang¹, and Hua Guo¹

¹Center for Biomedical Imaging Research, Department of Biomedical Engineering, School of Medicine, Tsinghua University, Beijing, China, People's Republic of

A novel compression method, shot-coil compression, is developed and implemented to a k-space reconstruction method SYMPHONY for computation acceleration. By this technique, high resolution multishot diffusion images can be reconstructed with much less reconstruction time. The basic idea of the proposed method is to remove the redundant multi-coil and multi-shot data while reserving most useful information. Simulation and in-vivo experiment were designed and the results validated the effectiveness of the shot-coil compression method.

3216

Computer #50



Robust GRAPPA Calibration in Phase Cycled bSSFP

Corey Allan Baron¹, Tiffany Jou¹, Anjali Datta¹, John M Pauly¹, and Dwight G. Nishimura¹

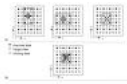
¹Electrical Engineering, Stanford University, Stanford, CA, United States

In phase cycled bSSFP, there is considerable motivation to use undersampling to mitigate long scan times. Direct application of a GRAPPA or SPIRiT reconstruction involves performing calibration separately for each phase cycled image. However, the receiver sensitivities are equivalent for all phase cycles, and this redundancy should be accounted for to improve calibration quality. Here, we describe a method for calculation of a single GRAPPA kernel over all phase cycles simultaneously, which is shown to improve calibration quality.

3217

Effects of ACS line geometry in volumetric GRAPPA: A Comparative Study

Computer #51 JungHyun Song¹, Seon Young Shin¹, Yeji Han¹, and Jun-Young Chung¹



¹Gachon Advanced Institute for Health Science and Technology, Gachon University, Incheon, Korea, Republic of

In this study, the effects of the aspect ratio of ACS lines with respect to the phase-encoding and partition-encoding steps are investigated for 3D GRAPPA reconstruction algorithms such as EX-3D-GRAPPA and SK-3D-GRAPPA. When the ACS lines are acquired by carefully considering the dimensions of the image matrices, the quality of the reconstructed images can be improved.

3218

Computer #52 Steen Moeller¹, Sudhir ramanna¹, Kamil ugurbil¹, and Essa Yacoub¹

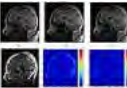


¹Center for Magnetic Resonance Research, University of Minnesota, Minneapolis, MN, United States

Investigation on the effect of reference or calibration scans needed to reconstruct undersampled MRI data. The study covers 3 different acceleration factors, and 6 different reference acquisitions. It is found that scan to scan variability for common acceleration factors is larger than any difference in tSNR between FLASH and FLEET, and that segmented EPI and single-shot are inferior to FLASH and FLEET acquisitions.

3219

Computer #53 Parallel Imaging Reconstruction from Undersampled K-space Data via Iterative Feature Refinement
Jing Cheng¹, Leslie Ying², Shanshan Wang¹, Xi Peng¹, Yuanyuan Liu¹, Jing Yuan³, and Dong Liang¹



¹Paul C. Lauterbur Research Center for Biomedical Imaging, Shenzhen Institutes of Advanced Technology, Chinese Academy of Sciences, shenzhen, China, People's Republic of, ²University at Buffalo, The State University of New York, New York, NY, United States, ³Medical Physics and Research Department, Hong Kong Sanatorium & Hospital, Hong Kong, Hong Kong

Compressed sensing based parallel imaging is an essential technique for accelerating MRI scan. However, most existing methods are still suffering from fine structure loss. This paper proposes an iterative feature refinement scheme for improving the reconstruction accuracy. We have incorporated the feature descriptor into the self-feeding sparse SENSE (SFSS) framework. Results on in-vivo MR dataset have shown that the descriptor is capable of capturing image structures and details that are discarded by SFSS and thus presents great potential for more effective parallel imaging.

3220

Computer #54 The influence of sampling density and randomness in Variable Density Poisson Disk undersampling on Parallel Imaging Compressed Sensing
Frank Zijlstra¹ and Peter R Seevinck¹



¹Image Sciences Institute, UMC Utrecht, Utrecht, Netherlands

We studied the effect of sampling density and randomness in Variable Density Poisson Disk (VDPD) undersampling patterns on Parallel Imaging Compressed Sensing (PICS) reconstruction errors. PICS reconstructions were performed on 3 datasets (knee, prostate, and brain) which were retrospectively undersampled with 110 VDPD undersampling patterns each. We found major differences in Normalized Root Mean Squared Errors when using different sampling densities, while the influence of randomness in patterns of the same sampling density was minor. Furthermore, the optimal sampling density varied per dataset. This shows that ad hoc choices of VDPD sampling density can result in significantly worse PICS reconstructions.

3221

Computer #55 Improved aliasing suppression in steady-state, parallel imaging using inner volume excitation Introduction
Tianrui Luo¹, Jon-Fredrik Nielsen¹, and Douglas C. Noll¹

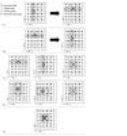


¹University of Michigan, Ann Arbor, MI, United States

A method of suppressing incomplete aliasing artifacts in accelerated MRI by combining inner-volume steady-state imaging with parallel imaging (GRAPPA) is proposed. Its effectiveness is evaluated across different net acceleration factors ($R=1.75-3.64$). The normalized root mean squared error inside the region of interest is generally suppressed by approximately a factor of 2 when inner volume excitation is adopted.

3222

Computer #56 A comparison of volumetric GRAPPA algorithms for in-vivo MRI
Seon Young Shin¹, JungHyun Song¹, Yeji Han¹, and Jun-Young Chung¹

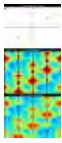


¹Gachon Advanced Institute of Health Sciences and Technology, Gachon University, Incheon, Korea, Republic of

To compare the volumetric GRAPPA algorithms in the presence of physiological artifacts, five different algorithms were used, i.e., 2D-GRAPPA-OP, 3D-GRAPPA, EX-3D-GRAPPA and SK-3D-GRAPPA. The performance of algorithms were compared using the root mean squared error (RMSE) of the image reconstructed from fully acquired 3D in-vivo k-space data and the image reconstructed using different reconstruction algorithms from undersampled dataset.

3223

Computer #57 Revisiting adaptive regularization for self-calibrated, dynamic parallel imaging reconstruction
Mark Chiew¹ and Karla L Miller¹



¹FMRIB, University of Oxford, Oxford, United Kingdom

In this work we demonstrate a simple method for reducing error in k-t under-sampled parallel imaging by subtracting a dynamic, low-rank time-series estimate prior to un-aliasing reconstruction. This estimate is generated directly from the under-sampled data by selecting the first r components of a singular value decomposition after sliding-window reconstruction, and removes signal variance that might otherwise contribute to residual aliasing. This method is motivated by the observation that the highest variance components in time-series data are typically low-frequency, and well characterised by a sliding window filter.

3224

Computer #58



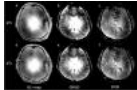
Improved robustness of parallel imaging in 3D multi-slab diffusion imaging using an adapted FLEET approach
Wenchuan Wu¹, Karla L Miller¹, Benedikt A Poser², and Peter J Koopmans¹

¹FMRIB, Nuffield Department of Clinical Neurosciences, University of Oxford, Oxford, United Kingdom, ²Maastricht Brain Imaging Center, Department of Cognitive Neuroscience, Maastricht University, Maastricht, Netherlands

In this work, we developed and evaluated a method for reducing motion sensitivity of auto-calibration data for parallel imaging in 3D MRI, with application to high-resolution diffusion imaging at ultra-high field. With the proposed Slice-FLEET method, we successfully achieve high resolution (1mm isotropic) diffusion MRI with high SNR and high b values.

3225

Computer #59



Improved Homogeneity of B1+ and Signal Intensity at 7T Using a Parallel Transmission on Human Volunteers

Taisuke Harada^{1,2}, Kohsuke Kudo¹, Ikuko Uwano³, Fumio Yamashita³, Hiroyuki Kameda^{1,3}, Tsuyoshi Matuda⁴, Makoto Sasaki³, and Hiroki Shirato²

¹Department of Diagnostic and Interventional Radiology, Hokkaido University Hospital, Sapporo, Japan, ²Department of Radiation Medicine, Hokkaido University Graduate School of Medicine, Sapporo, Japan, ³Division of Ultrahigh Field MRI, Institute for Biomedical Sciences, Iwate Medical University, Yahaba, Japan, ⁴MR Applications and Workflow, GE Healthcare, Tokyo, Japan

The aim of our study was to compare the homogeneity of B1+ map and clinical gradient-echo images at 7T between two-channel pTx and qTx. MRS phantom with a water pack and six volunteers were scanned by 7T MRI, and the homogeneity was evaluated by coefficient of variation of region-of-interest analysis. The signal homogeneities of B1+ map and GRASS image were better in pTx than in qTx, however the homogeneity of SPGR images had no difference between pTx and qTx, in both phantom and volunteer studies. These results might facilitate the development of pTx.

3226

Computer #60

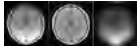


Image Intensity Corrections in ESPIRiT from Eigenvalue Based Spatially Variant Sensitivity Map Rescaling Modifications
Wang Bin¹, Zhu Gaojie¹, Luo Hai¹, Zhou Xiang¹, and Zha Leping^{1,2}

¹Alltech Medical Systems, Chengdu, China, People's Republic of, ²Alltech Medical Systems America, Cleveland, OH, United States

Images from accelerated acquisition and ESPIRiT reconstruction show inhomogeneous intensity from the original array coil sensitivity distributions, because of the arbitrarily scaled sensitivity (eigenvector) maps. We propose to use the corresponding eigenvalues to restore the proper relative sensitivity scaling in the maps as a method of intensity bias correction, to help better visualization of the anatomies.

3227

Computer #61



Fast dynamic imaging using multi-shell sampling for variable k-space density k-t acquisitions
Kilian Weiss^{1,2}, David Maintz², and Daniel Giese²

¹Philips Healthcare, Hamburg, Germany, ²Department of Radiology, University Hospital of Cologne, Cologne, Germany

In this work a new multi shell variable density k-t space sampling scheme for highly accelerated acquisitions with sheared grid k-t space sampling and an adapted reconstruction framework based on a linear reconstruction is proposed. The proposed method is evaluated on numerical phantom data and compared to a conventional k-t PCA acceleration. The proposed method is shown to be comparable to conventional k-t PCA for moderate acceleration factors while outperforming conventional k-t PCA for high accelerations factors allowing for ultra-fast dynamic MRI.

3228

Computer #62



Accelerating Real-time MRI of speech using spiral through-time GRAPPA

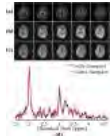
Sajan Goud Lingala¹, Yinghua Zhu¹, Yunhua Ji², Asterios Toutios¹, Wei-Ching Lo³, Nicole Seiberlich³, Shrikant Narayanan¹, and Krishna Nayak¹

¹Electrical Engineering, University of Southern California, Los Angeles, CA, United States, ²Biomedical Engineering, University of Southern California, Los Angeles, CA, United States, ³Biomedical Engineering, Case Western Reserve University, Cleveland, OH, United States

Real-time MRI (RT-MRI) is a powerful tool to safely assess and quantify the vocal tract dynamics during speech production. In this work, we evaluate the potential of a fast linear reconstruction method through-time GRAPPA (TT-GRAPPA) to efficiently exploit the acceleration capabilities offered by a custom 8-channel upper-airway coil and spiral trajectories and utilize it to improve RT-MRI of speech in visualizing rapid articulatory dynamics. We report feasibilities of 3 to 4 fold acceleration, and demonstrate up to 52 frames per second (18ms/frame) in single slice (2.4 mm²), and three-slice (4.5mm²) imaging.

3229

Computer #63



SENSE-SPICE: Integrating Parallel Imaging with Subspace-Based 3D 1H-MRSI

Bryan Clifford¹, Fan Lam², Qiegen Liu², Chao Ma², and Zhi-Pei Liang¹

¹Electrical and Computer Engineering, University of Illinois at Urbana-Champaign, Urbana, IL, United States, ²Beckman Institute, University of Illinois at Urbana-Champaign, Urbana, IL, United States

We present a method which reduces the acquisition time of 3D 1H-MRSI through the integration of parallel imaging and subspace-based imaging. The proposed method enables a better combination of speed, resolution, and SNR than can be provided by parallel imaging or subspace-based imaging alone; however, the removal of nuisance signals from under-sampled MRSI data requires significantly higher reconstruction accuracy than in conventional parallel imaging applications. We solve this problem by incorporating spatial and spectral constraints as well as sensitivity encoding into a recently proposed Union-of-Subspace model. We demonstrate the effectiveness of our method using in vivo data of the brain.

3230

Computer #64



Improved In-plane SENSE PROPELLER with Multi-Step Joint-Blade Reconstruction

Mengye Lyu^{1,2}, Yilong Liu^{1,2}, Victor B. Xie^{1,2}, Yanqiu Feng^{1,2}, Zhe Zhang³, Hua Guo³, and Ed X. Wu¹

¹Laboratory of Biomedical Imaging and Signal Processing, The University of Hong Kong, Hong Kong SAR, China, People's Republic of, ²Department of Electrical and Electronic Engineering, The University of Hong Kong, Hong Kong SAR, China, People's Republic of, ³Department of Biomedical Engineering, Tsinghua University, Beijing, China, People's Republic of

This work addresses three problems for in-plane SENSE-accelerated PROPELLER: generally amplified noise, increased artifact with narrow blades, and degraded motion correction with wide blades. We show that a novel reconstruction method - multi-step joint-blade (MJB) SENSE can lead to higher SNR and less narrow-blade artifact than conventional SENSE reconstruction. In addition, k-space truncation is used to improve the motion correction robustness. We also show that additional iterations can enhance MJB SENSE. This new method can greatly benefit future SENSE PROPELLER studies with improved image quality.

3231

Computer #65



Super Slice Interpolation (SSI) from Parallel MRI Data

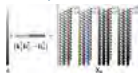
Yanqiu Feng^{1,2,3}, Mengye Lyu^{1,2}, Yilong Liu^{1,2}, Victor X Bin^{1,2}, and Ed X Wu^{1,2}

¹Laboratory of Biomedical Imaging and Signal Processing, The University of Hong Kong, Hong Kong SAR, China, People's Republic of, ²Department of Electrical and Electronic Engineering, The University of Hong Kong, Hong Kong SAR, China, People's Republic of, ³School of Biomedical Engineering and Guangdong Provincial Key Laboratory of Medical Image Processing, Southern Medical University, Guangzhou, China, People's Republic of

This work develops a novel super slice interpolation (SSI) method that exploits sensitivity variation along the slice direction to decrease slice thickness in multi-slice MRI. The phantom and in vivo head imaging results demonstrate that SSI successfully generates thinner slice images from a set of thick images acquired with multiple receiver coils, without the need of modifying pulse sequences. The proposed SSI method has potential to obtain more slices with decreased thickness in scenarios where acquisition window or specific absorption rate limits the available number of slices.

3232

Computer #66



Calibration-free Parallel Imaging Using Randomly Undersampled Multichannel Blind Deconvolution (MALBEC)

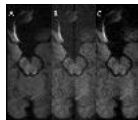
Jingyuan Lyu¹, Ukash Nakarmi¹, Yihang Zhou¹, Chaoyi Zhang¹, and Leslie Ying^{1,2}

¹Electrical Engineering, The State University of New York at Buffalo, Buffalo, NY, United States, ²Biomedical Engineering, The State University of New York at Buffalo, Buffalo, NY, United States

This abstract presents a novel reconstruction method for parallel imaging that does not require auto-calibration data. The method formulates the image reconstruction problem as a multichannel blind deconvolution problem in k-space where the data are randomly undersampled in all channels. Under this formulation, the k-spaces of the desired image and coil sensitivities are jointly recovered by finding a rank-1 matrix subject to the data consistent constraint. Experimental results demonstrate that the proposed method is able to achieve better reconstruction results than the state-of-the-art calibration-less parallel imaging methods.

3233

Computer #67



A novel reconstruction method for high-resolution DWI in zoomed FOV imaging with parallel acquisitions at 1.5T

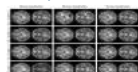
Jisu Hu^{1,2}, Zhigang Wu³, Wenxing Fang³, Ming Li⁴, Bing Zhang⁴, and Feng Huang³

¹Suzhou Institute of Biomedical Engineering and Technology, Chinese Academy of Sciences, Suzhou, China, People's Republic of, ²The Laboratory for Medical Electronics, School of Biological Sciences and Medical Engineering, Southeast University, Nanjing, China, People's Republic of, ³Philips Healthcare, Suzhou, China, People's Republic of, ⁴Department of Radiology, the Affiliated Drum Tower Hospital of Nanjing University Medical School, Nanjing, China, People's Republic of

A new reconstruction method is presented for high-resolution DWI in zoomed FOV imaging with parallel acquisitions. this method can reduce noise and artifact in the reconstructed images compared to conventional SENSE magnitude average.

3234

Computer #68



Can multi-slice information improve the conditioning of in-plane acceleration?

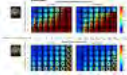
José P. Marques¹ and David G. Norris¹

¹Donders Centre for Cognitive Neuroimaging, Radboud University, Nijmegen, Netherlands

To improve the conditioning of GRAPPA enabled in-plane acceleration by using phase encoding shifts of spatially neighbouring slices. Parallel imaging offers the possibility to reduce acquisition time or echo train lengths needed to fully encode a given object. New k-space trajectories and reconstruction techniques offer the possibility of large acceleration factors in the slice direction (in the case of SMS) or in either of the two phase encoding directions in volumetric imaging. While 2D and 3D reconstructions can be seen on a common framework, it is not straightforward to, in conventional multi-slice imaging, have more than 3-4 fold inplane acceleration.

3235

Computer #69



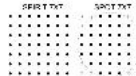
The potential of 256 channel high density receive arrays in combination with 2DCAIPIRINHA at 7T
Arjan D. Hendriks¹, Cezar B.S. Alborahal², Michel G.M. Italiaander², Dennis W.J. Klomp^{1,2}, and Natalia Petridou¹

¹Department of Radiology, University Medical Center Utrecht, Utrecht, Netherlands, ²MR Coils B.V., Drunen, Netherlands

There is an overall drive to high speed, high resolution brain MRI. High density receive arrays have proven to be a very valuable tool in this process. However, alternative acquisition strategies like 2DCAIPIRINHA have shown to be highly effective in acceleration. We investigated whether a 256ch high density receive array with or without 2DCAIPIRINHA can still outperform a 32ch array with 2DCAIPIRINHA.

3236

Computer #70



SPOT: SPIRiT Image Reconstruction with Custom Kernel Geometry

Yulin V Chang¹, Marta Vidorreta², Ze Wang³, and John A Detre²

¹Radiology, University of Pennsylvania, Philadelphia, PA, United States, ²Neurology, University of Pennsylvania, Philadelphia, PA, United States, ³Hangzhou Normal University, Hangzhou, Zhejiang, China, People's Republic of

In SPIRiT image reconstruction the kernel usually consists of all elements within a square. The number of elements in such a kernel increases rapidly as the kernel size increases, especially for 3D reconstructions. Thus, a large kernel requires a sizable calibration region in k-space and demands significant time for calibration. In this work we proposed and validated a new image reconstruction approach that uses a custom SPIRiT kernel geometry, which we call SPOT. We show that a SPOT kernel is much faster to compute and results in no loss of image quality compared to the traditional SPIRiT kernel.

3237

Computer #71



Increasing Temporal Resolution of DSC-perfusion MRI using 3D Distributed Spirals and Through-Time GRAPPA

Dallas C Turley¹ and James G Pipe¹

¹Neuroimaging Research, Barrow Neurological Institute, Phoenix, AZ, United States

DSC-MRI requires high temporal resolution to accurately measure perfusion parameters in vivo. Using GRAPPA parallel imaging, it is possible to achieve whole-brain coverage while maintaining high temporal sampling. The proposed method combines a 3D dual echo spiral sequence with through-time GRAPPA for whole-brain coverage with < 1 second temporal resolution.

Electronic Poster

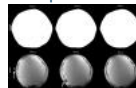
Simultaneous Multi-Slice

Exhibition Hall

Tuesday, May 10, 2016: 11:00 - 12:00

3238

Computer #1



Simultaneous Multi-Slice Imaging with ESPIRiT

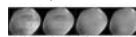
Gaojie Zhu¹, Hai Luo¹, Bin Wang¹, Xiang Zhou¹, and Leping Zha^{1,2}

¹Advanced Application, Alltech Medical Systems, Chengdu, China, People's Republic of, ²Advanced application, Alltech Medical Systems America, Cleveland, OH, United States

Simultaneous multi-slice (SMS) acquisitions with SENSE reconstruction rely greatly on the fidelity of coil sensitivity maps. Due to the difficulty on choosing polynomial orders, traditional polynomial fitting method often results in residual spatial oscillations or influence from imaging content, which compromise the reconstruction quality. ESPIRiT (An Eigenvalue approach to auto-calibrating parallel MRI) is a new technique to estimate sensitivity map from auto-calibration signal. It is a sub-space based method that is highly robust to many types of errors because the estimated subspace automatically adapts to inconsistencies in the data. We propose to extend the simultaneous multi-slice imaging with ESPIRiT for higher-fidelity sensitivity distribution estimation and highly robust reconstruction.

3239

Computer #2



Comprehensive CG-SENSE reconstruction of SMS-EPI

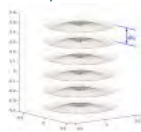
Lucilio Cordero-Grande¹, Anthony Price¹, Jana Hutter¹, Emer Hughes¹, and Joseph V. Hajnal¹

¹Center for the Developing Brain, King's College London, London, United Kingdom

A 2D CG-SENSE framework is proposed aiming at an integrated treatment of the main error sources in SMS-EPI reconstruction. Our pipeline jointly estimates the sensitivity profiles, Nyquist ghosting parameters, and image to be unfolded. In addition, an artifact-SNR tradeoff is established at a pixel level. Assessment by a phantom experiment has shown that all the main functionalities of the method do help diminish reconstruction artifacts. Stable results have been obtained when applying the framework in a large cohort of motion corrupted fMRI and DWI neonatal studies.

3240

Computer #3



Improved Radial Sampling using Wave-CAIPI
Weiran Deng¹, Michael Herbst¹, and V Andrew Stenger¹

¹University of Hawaii JABSOM, Honolulu, HI, United States

This abstract presents a method that applies sine waveforms to the imaging gradients in radial sampling. This concept is similar controlled aliasing in Parallel Imaging (CAIPI). It enhances the encoding power of coil sensitivities by introducing spatially varying convolution. Improvement in image quality are observed in images reconstructed from undersampled (R=8) wave-radial data compared to images from undersampled (R=8) radial data acquired at 3T.

3241

Computer #4

Multi-Step Joint-Blade SENSE Reconstruction for Simultaneous Multislice PROPELLER
Mengye Lyu^{1,2}, Yilong Liu^{1,2}, Victor B. Xie^{1,2}, Yanqiu Feng^{1,2}, Zhe Zhang³, Hua Guo³, and Ed X. Wu¹

¹Laboratory of Biomedical Imaging and Signal Processing, The University of Hong Kong, Hong Kong SAR, China, People's Republic of, ²Department of Electrical and Electronic Engineering, The University of Hong Kong, Hong Kong SAR, China, People's Republic of, ³Department of Biomedical Engineering, Tsinghua University, Beijing, China, People's Republic of

For simultaneous multislice (SMS) PROPELLER, we propose multi-step joint-blade (MJB) SENSE reconstruction. In MJB SENSE, all blades are jointly reconstructed in three steps without relying on iterations. Compared to separately reconstructing individual blades, MJB SENSE substantially reduces noise amplification and narrow-blade artifact. MJB SENSE is also compatible with motion correction. With these advantages, MJB SENSE can be used to achieve very high MB factors in SMS PROPELLER.

3242

Computer #5

An iterative reconstruction method for dual-band EPI in small-animal studies
Hiroshi Toyoda¹, Naoya Yuzuriha², Sosuke Yoshinaga², and Hiroaki Terasawa²

¹CINet, National Institute of Information and Communications Technology, Suita, Japan, ²Department of Structural Bioluminescence Imaging, Kumamoto University, Kumamoto, Japan

We proposed an iterative reconstruction method which was effective and valid in reducing artifacts in dual-band EPI in animal scanners. This iterative reconstruction method could accurately separate collapsed k-space data acquired simultaneously from multiple slice locations. Our findings give rise to a more efficient multi-band EPI technique that can be used even with a scanner system equipped with relatively few receiver coil elements.

3243

Computer #6



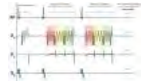
Simultaneously Multi-Slice (SMS) Accelerated Interleaved EPI DWI using 3D K-space Reconstruction
Erpeng Dai¹, Xiaodong Ma¹, Zhe Zhang¹, Chun Yuan^{1,2}, and Hua Guo¹

¹Center for Biomedical Imaging Research, Department of Biomedical Engineering, School of Medicine, Tsinghua University, Beijing, China, People's Republic of, ²Vascular Imaging Laboratory, Department of Radiology, University of Washington, Seattle, WA, United States

Simultaneously multi-slice (SMS) has been a powerful tool for single-shot EPI DWI acceleration, but still not well established for interleaved EPI (iEPI) DWI acceleration. The main challenge is how to effectively combine slice un-folding and inter-shot phase correction. In this study, a 3D k-space reconstruction method for navigated SMS accelerated iEPI DWI has been proposed. An optimized acquisition for navigator is designed. Then slice un-folding and inter-shot phase correction are performed in a SMS 3D k-space. The performance is compared with ssEPI and un-accelerated iEPI DWI, and has been shown to be applicable for both 4-sh and 8-sh iEPI DWI.

3244

Computer #7



Simultaneous Multi-Slice Acquisition with Multi-Contrast Segmented EPI for Dynamic Contrast-Enhanced Imaging
Klaus Eickel^{1,2,3}, Lutz Lüdemann³, David Porter¹, and Matthias Günther^{1,2}

¹Fraunhofer MEVIS, Bremen, Germany, ²mediri GmbH, Heidelberg, Germany, ³University Hospital Essen, Essen, Germany

The application of simultaneous multi-slice imaging to a segmented EPI allows the acquisition of multiple contrasts while retaining sufficient temporal resolution and spatial coverage. Contrast-enhanced perfusion measurements were performed on a pig's hip/leg resulting in mainly muscle-perfusion images with separated S_0 and T_2^* maps. The separation of the different signal contributions potentially allows for a quantitative analysis in contrast-enhanced dynamic imaging.

3245

Computer #8

Reconstruction of Simultaneous Multi-Slice EPI data using Dual-Polarity GRAPPA Kernels.
W. Scott Hoge¹, Kavin Setsompop², and Jonathan R. Polimeni²

¹Radiology, Brigham and Women's Hospital, Boston, MA, United States, ²Athinoula A. Martinos Center for Biomedical Imaging, Massachusetts General Hospital, Charlestown, MA, United States

This work presents a new approach to reconstruct SMS-EPI data that employs Dual-Polarity GRAPPA (DPG). DPG accurately models non-linear EPI phase errors between data sampled on positive versus negative readout gradients. When applied to SMS-EPI data, DPG can simultaneously and robustly perform slice separation, recovery of missing data from in-plane acceleration, and slice-specific ghost correction. Phantom and *in vivo* results are compared to a conventional SMS reconstruction, and demonstrate that DPG reduces residual ghosts and ghosting-related phase interference artifacts.

-
- 3246
Computer #9 Echo-Shift wave-CAIPI with Simultaneous MultiSlice imaging for rapid susceptibility weighted FLASH
Huihui Ye^{1,2}, Berkin Bilgic¹, Stephen Cauley¹, Borjan Gagoski³, Jianghui Zhong², Yiping Du², Lawrence L. Wald¹, and Kawin Setsompop¹
- ¹MGH/A.A. Martinos Center for Biomedical Imaging, Charlestown, MA, United States, ²Zhejiang University, Hangzhou, China, People's Republic of, ³Boston Children's Hospital, Charlestown, MA, United States
- Susceptibility weighted FLASH imaging provides exquisite soft tissue contrast at high spatial resolution and low distortion, but at a cost of lengthy acquisition time. In this work, we developed a highly efficient Echo-Shift wave-CAIPI technique and demonstrated its ability to provide 18-fold acceleration for FLASH acquisitions with minimal noise and artifact penalties. Instead of conventional single slice or slab echo-shift, we propose an echo-shift Simultaneous MultiSlice method to enable improved controlled aliasing and desirable volumetric noise averaging while avoiding slab edge artifacts. With this technique, we demonstrated high-quality 1.5 mm isotropic whole-brain susceptibility weighted FLASH at 3T and 7T in 36s.
-
- 3247
Computer #10 A Circular Echo Planar Sequence for Simultaneous Multi-Slice Imaging
V. Andrew Stenger¹, Weiran Deng¹, Michael Herbst¹, and Andrii Petrov¹
- ¹John A Burns School of Medicine, University of Hawaii, Honolulu, HI, United States
- This abstract presents a circular echo planar imaging sequence for simultaneous multi-slice imaging. A generalized SENSE reconstruction framework with ghost correction was utilized. Different sampling strategies including wave modulation, blipped-CAIPI, and hexagonal were examined. Phantom as well as human fMRI scanning at 3T are shown.
-
- 3248
Computer #11 Evaluating The Performance of Four Reconstruction Algorithms for Simultaneous Multi-Slice Imaging
Kangrong Zhu¹, Hua Wu², Robert F. Dougherty², Matthew J. Middione³, John M. Pauly¹, and Adam B. Kerr¹
- ¹Electrical Engineering, Stanford University, Stanford, CA, United States, ²Center for Cognitive and Neurobiological Imaging, Stanford University, Stanford, CA, United States, ³Applied Sciences Laboratory West, GE Healthcare, Menlo Park, CA, United States
- Several parallel imaging reconstruction algorithms have been proposed for simultaneous multi-slice (SMS) imaging, yet a thorough comparison of the algorithms still awaits investigation. In this study, the performance of four reconstruction algorithms are compared. Relative root-mean-squared error, g-factor, signal leakage, and reconstruction time are used as metrics for evaluating the performance. This work may provide a reference for the SMS community to choose from different reconstruction algorithms.
-
- 3249
Computer #12 Multiband TSE Imaging of the Fetal Brain at 3T
Anthony N Price^{1,2}, Shaihan J Malik², Jana Hutter², Martin B  hrer³, Lucilio Cordero-Grande², Rui Teixeira², Emer J Hughes¹, Mary A Rutherford¹, and Joseph V Hajnal^{1,2}
- ¹Centre for the Developing Brain, King's College London, London, United Kingdom, ²Biomedical Engineering, King's College London, London, United Kingdom, ³GyroTools, Zurich, Switzerland
- Single-shot Turbo Spin-Echo (ss-TSE) sequences can provide excellent anatomical images of the fetal brain. However, due to the surrounding maternal tissue, full field of view encoding leads to long echo train lengths, impacting efficiency, causing high SAR and increased risk of motion artefact. In this abstract we present the implementation of multiband accelerated ss-TSE of the fetal brain, with a zoom variant that reduces both overall scan time and the need to encode a large FOV. In addition simultaneous sampling multiple slice locations should benefit the image registration step in subsequent 3D slice-to-volume reconstructions.
-
- 3250
Computer #13 Multiplexed multiband EPI for increased efficiency in fetal fMRI and dMRI
Anthony N Price¹, Jana Maria Hutter¹, Lucilio Cordero Grande¹, Emer Judith Hughes¹, Kelly Pegoretti¹, Andreia Oliveira Gaspar¹, Laura McCabe¹, Mary Rutherford¹, and Joseph V Hajnal¹
- ¹Centre for the developing brain, King's College London, London, United Kingdom
- This abstract demonstrates combined multiband and multiplex imaging for fetal EPI based sequences such as used in diffusion and functional MRI. This application lends itself naturally to multiplex imaging, due to PNS and noise restrictions, EPI readout speeds are inherently limited so offsets the inevitable TE penalty from multiplex imaging.
-
- 3251
Computer #14 Ultrafast multi-slice MRI with segmented spatiotemporal encoding
Ting Zhang¹, Congbo Cai², Lin Chen¹, Jianpan Huang¹, and Shuhui Cai¹
- ¹Department of Electronic Science, Xiamen University, Xiamen, China, People's Republic of, ²Department of Communication Engineering, Xiamen University, Xiamen, China, People's Republic of
- As a recently launched method, spatiotemporally encoded (SPEN) magnetic resonance imaging (MRI) has been broadened from single-slice scan to multi-slice scan. A new single-shot multi-slice full-refocusing SPEN MRI sequence was proposed. By utilizing a segment-selective pulse and a 180° chirp pulse and sequentially acquiring the signals of every slice among the encoded segment, the new method can lower the specific absorption rate (SAR) and improve the image quality compared to the existing one. Experimental results

of phantom and in vivo rat brain verified the above conclusion.

-
- 3252
Computer #15 Half Fourier Acquisition Single Shot Turbo Spin Echo (HASTE) imaging using multiband (MB) excitation and Power Independent of Number of Slices (PINS) refocusing pulses at 3 Tesla
Jenni Schulz¹, Lauren J Bains¹, José P Marques¹, and David G Norris¹
- ¹*Donders Institute for Cognitive Neuroimaging, Radboud University Nijmegen, Nijmegen, Netherlands*
- HASTE sequences have high RF power deposition which particularly limits their use at high resolutions and high field strengths. In this work, TRAPS and fixed SAR Power Independent of Number of Slices (PINS)-refocusing pulses were used to reduce the power deposition. Multiband excitation pulses were added to enable arbitrary user-defined slice orientations, with the added benefit of accelerating the acquisition due to the simultaneous excitation of multiple slices. Good image quality was obtained for a MB4-HASTE protocols with 3.1 and 1.1 mm resolution, and a whole-brain MB6-HASTE protocol with 1.1 mm resolution.
-
- 3253
Computer #16 Shortening nonlinear phase multiband refocusing pulses with VERSE
Naoharu Kobayashi¹, Kamil Ugurbil¹, and Xiaoping Wu¹
- ¹*CMRR, Radiology, University of Minnesota, Minneapolis, MN, United States*
- Current high resolution, whole brain diffusion MRI protocol at 7T for the Human Connectome Project uses linear phase multiband (MB) refocusing pulses that have duration longer than 10 ms. Recent studies show that shorter duration can be obtained by designing nonlinear phase MB refocusing pulses. In this study, we designed root-flipped MB and hyperbolic secant (HS1) based MB refocusing pulses and investigated how the variable rate selective excitation (VERSE) principle can be used to further reduce the pulse duration. Our results suggest that both root-flipped and HS1 based MB refocusing pulses can be shortened by VERSE.
-
- 3254
Computer #17 Effects of Multiband Acceleration on High Angular Resolution Diffusion Imaging data collection, processing, and analysis.
Adam Scott Bernstein¹, Derek PISner², Aleksandra Klimova², Lavanya Umaphathy³, Loi Do¹, Scott Squire⁴, Scott Killgore², and Theodore Trouard¹
- ¹*Biomedical Engineering, University of Arizona, Tucson, AZ, United States*, ²*Psychiatry, University of Arizona, Tucson, AZ, United States*, ³*Electrical and Computer Engineering, University of Arizona, Tucson, AZ, United States*, ⁴*Radiology, University of Arizona, Tucson, AZ, United States*
- Multiband imaging allows for greater imaging speeds when collecting diffusion weighted MR images. As shown in this work, this saving in time results in small changes in several stages of diffusion image processing including tensor fitting and the associated calculation of scalar values such as FA, fiber orientation distribution calculation as in constrained spherical deconvolution, and tractography.
-
- 3255
Computer #18 Multiband Echo-Shifted EPI (MESH) fMRI
Rasim Boyacioglu^{1,2}, Jenni Schulz¹, and David G. Norris^{1,3}
- ¹*Radboud University, Donders Institute for Brain, Cognition and Behaviour, Nijmegen, Netherlands*, ²*Radiology, Case Western Reserve University, Cleveland, OH, United States*, ³*Erwin L. Hahn Institute, University Duisberg-Essen, Essen, Germany*
- Multiband Echo-Shifted EPI (MESH) is a combination of echo shifted 2D multi-slice EPI, in-plane and multiband acceleration. An additional EPI readout is inserted in the dead-time between slice selection and the multiband EPI readout. It is useful especially for low static magnetic field strengths (long optimal TE) and lower spatial resolutions (short EPI readout). It is shown that echo shifting gradients do not affect tSNR. Compared to standard and multiband EPI similar RS fMRI results are obtained at the group and individual subject level. MESH offers a further acceleration in image acquisition for fMRI at no loss in sensitivity.
-
- 3256
Computer #19 Revisited Multislice Distributed Inversion Recovery towards an Efficient Neonatal MR Examination.
Giulio Ferrazzi¹, Rui Pedro A. G. Teixeira¹, Jana M. Hutter¹, Lucilio Cordero-Grande¹, Emer Hughes¹, Anthony N. Price¹, and Joseph V. Hajnal¹
- ¹*Centre for the Developing Brain, Department of Perinatal Imaging and Health, King's College London, London, United Kingdom*
- Multislice multishot Inversion Recovery sequences as implemented in standard systems are often not optimized for efficiency. This becomes a critical factor when imaging neonates, where T1 is longer and the Inversion Time needs to increase to maintain the desired contrast. In this study, we have optimized a standard Inversion Recovery sequence and used it for an optimised neonatal protocol. The proposed sequence provides a total scan time reduction of 44% with identical imaged contrast and resolution.
-
- 3257
Computer #20 RF-Encoding for Simultaneous Multi Slab Imaging
Benjamin Zahneisen¹, Murat Aksoy¹, Julian Maclaren¹, Christian Wuerslin¹, and Roland Bammer¹
- ¹*Stanford University, Stanford, CA, United States*
- Simultaneous-Multi-Slab-Imaging is a promising approach for high resolution DW-EPI (<1mm) where the slice profile of a typical multi-band RF-pulse limits the spatial resolution for single-shot DW-EPI. Like every multi-band technique, slab separation during a parallel

imaging reconstruction requires a combination of coil sensitivity variation and k-space encoding. The most prominent way is blipped-CAIPIRINHA where k-space encoding along the slice direction is achieved by adding small gradient blips in z-direction to the EPI readout. Here we demonstrate how multi-band RF phase modulation can be used as an alternative way to encode along the slab dimension without affecting intra-slab phase encoding. The use of phase modulated RF-pulses decouples encoding between the logical intra- and inter-slab directions that are otherwise linked because there is only one physical z-gradient axis.

3258 Computer #21 Accelerated Simultaneous Multi-Slice (SMS) fMRI using spiral acquisition and low rank plus sparse (L+S) image reconstruction
Andrii Y Petrov¹, Michael Herbst^{1,2}, and V Andrew Stenger¹

¹Department of Medicine, University of Hawaii, Honolulu, HI, United States, ²Department of Radiology and Medical Physics, University Medical Center Freiburg, Freiburg, Germany

Sub-second whole brain imaging using Simultaneous Multi-Slice (SMS) imaging is of particular interest in Blood Oxygen Level Dependent (BOLD) functional Magnetic Resonance Imaging (fMRI). Faster acquisitions with higher temporal sampling of the BOLD time course provides several advantages including increased sensitivity in detecting functional activation, the possibility of filtering out physiological noise for improving temporal SNR, and freezing out head motion. The most commonly used strategy to accelerate image acquisition time using SMS involves using parallel imaging methods. We propose to accelerate SMS imaging by under sampling the number of excited slices in the k_z -t domain and L+S matrix decomposition method for reconstruction of slice aliased functional images. We present human fMRI results at 3T using 3D spiral sampling with SMS excitation and L+S reconstruction of the aliased slice data.

3259 Computer #22 Reconstruction of multiband MRI data using Regularized Nonlinear Inversion
Sebastian Rosenzweig¹ and Martin Uecker^{1,2}

¹Department of Diagnostic and Interventional Radiology, University Medical Center Göttingen, Göttingen, Germany, ²German Centre for Cardiovascular Research (DZHK), University Medical Center Göttingen, Göttingen, Göttingen, Germany

Multiband MRI can be used to acquire several slices at the same time. Here, we propose a new method of multiband MRI based on Regularized Nonlinear Inversion (NLINV). This method does not require a priori knowledge about the coil sensitivities. Simultaneous estimation of images and coil sensitivities of two slices is demonstrated from six-fold undersampled data for a simulated multi-band acquisition.

3260 Computer #23 Optimization of High-Resolution Slice-Accelerated Inversion Recovery T1 Mapping at 7T
John Grinstead¹, Valerie Anderson², Manoj Sammi², and William Rooney²

¹Siemens Healthcare, Portland, OR, United States, ²Oregon Health & Science University, Portland, OR, United States

Parametric T₁ mapping using inversion recovery has competing requirements for speed, SNR, spatial resolution, anatomical coverage, and adequate sampling of the longitudinal magnetization recovery. Potential sources of slice-to-slice variability in quantitative T₁ maps are investigated, including slice cross talk due to imperfect slice profiles, and the range of TIs used to fit each slice. It is demonstrated that T₁ relaxometry benefits significantly from slice acceleration techniques in not only scan time & slice coverage, but in its ability to reduce quantitative errors by allowing the same TI sampling across all slices.

3261 Computer #24 Noise amplification vs. resolution tradeoff in the SLIDER technique
Steen Moeller¹, Sebastian Schmitter¹, and Mehmet Akcakaya^{1,2}

¹Center for Magnetic Resonance Research, University of Minnesota, Minneapolis, MN, United States, ²Department of Electrical and Computer Engineering, University of Minnesota, Minneapolis, MN, United States

An investigation into the noise and resolution performance of SLIDER using a series of shifted low-resolution images to obtain a single high-resolution. The evaluation is performed both theoretical and experimentally using a FLASH acquisition, to remove experimental limitations from understanding the merits of the technique.

Electronic Poster

Fat/Water Imaging

Exhibition Hall

Tuesday, May 10, 2016: 11:00 - 12:00

3262 Computer #25 Improving Time Efficiency for T2-weighted Fat-Water Imaging by Using Multiband Simultaneous Multi-Slice Accelerated TSE Dixon
Dingxin Wang^{1,2}, Xiufeng Li², Xiaoping Wu², and Kamil Ugurbil²

¹Siemens Healthcare, Minneapolis, MN, United States, ²Center for Magnetic Resonance Research, University of Minnesota, Minneapolis, MN, United States

Dixon technique requires at least two images with different echo times, which increases TSE echo spacing and TR, and therefore prolongs total acquisition time. Slice acceleration may help improve imaging efficiency of TSE fat-water Dixon imaging. In this study, we develop a multiband slice accelerated TSE Dixon sequence and demonstrate the feasibility of SMS TSE Dixon acquisition for efficient T2-

-
- 3263
Computer #26 High Performance Volumetric 3T Breast Acquisition: A Foundation for Multi-Parametric Imaging
Jorge E Jimenez¹, Kevin M Johnson¹, Leah C Henze Bancroft¹, Diego Hernando², Roberta M Strigel^{1,2}, Scott B Reeder^{2,3}, and Walter F Block^{1,2,3}
- ¹Department of Medical Physics, University of Wisconsin-Madison, Madison, WI, United States, ²Department of Radiology, University of Wisconsin School of Medicine and Public Health, Madison, WI, United States, ³Department of Biomedical Engineering, University of Wisconsin-Madison, Madison, WI, United States*
- We present a 3D T1-Weighted radial trajectory suited to work with IDEAL fat/water separation. Some relevant characteristics are: rapid acquisition, reliable fat suppression, and high resolution despite significant data undersampling. The method is demonstrated in 3T bilateral breast MR imaging where isotropic resolution of 0.8 mm is achieved. In addition, we show the value of high count channel array for breast imaging.
-
- 3264
Computer #27 Bipolar time-interleaved multi-echo gradient echo imaging for high-resolution water-fat imaging
Stefan Ruschke¹, Holger Eggers², Hendrik Kooijman³, Houchun H. Hu⁴, Ernst J. Rummeny¹, Axel Haase⁵, Thomas Baum¹, and Dimitrios C. Karampinos¹
- ¹Department of Diagnostic and Interventional Radiology, Technische Universität München, Munich, Germany, ²Philips Research, Hamburg, Germany, ³Philips Healthcare, Hamburg, Germany, ⁴Radiology, Phoenix Children's Hospital, Phoenix, AZ, United States, ⁵Zentralinstitut für Medizintechnik, Technische Universität München, Garching, Germany*
- As the spatial resolution of a multi-echo gradient-echo imaging sequence increases, the echo time step increases resulting in an increased echo time step and an echo time selection that degrades the noise performance of water-fat separation. Time-interleaved gradient echo imaging combined with bipolar (flyback) gradients can achieve reasonable echo time steps at high resolution without dramatically increasing scan time. However, bipolar gradients are associated with known phase errors problems, which can lead to fat quantification errors. The present work develops a methodology for acquiring bipolar time interleaved multi-echo gradient echo data and for correcting the relevant phase errors.
-
- 3265
Computer #28 Silicone, fat, and water separation using a single-pass 3D Dixon acquisition
Ken-Pin Hwang¹, Jingfei Ma¹, Lloyd Estkowski², Ann Shimakawa², Kang Wang², Daniel Litwiller², Zachary Slavens², Ersin Bayram², and Bruce Daniel³
- ¹Department of Imaging Physics, The University of Texas M.D. Anderson Cancer Center, Houston, TX, United States, ²MR Applications and Workflow, GE Healthcare, Waukesha, WI, United States, ³Department of Radiology, Stanford University, Stanford, CA, United States*
- Separation of silicone, fat, and water is performed by using a two-step Dixon processing algorithm and a bipolar triple-echo readout in a 3D FSE sequence. The echoes are spaced for conventional water-fat separation, but the first and last echoes are also used to generate a phase map with double the phase evolution for resolving fat from silicone, which are relatively close in terms of chemical shift. Individual images of each of the three species are reconstructed in phantom and human data. The proposed method demonstrates improved SNR efficiency and robustness to field inhomogeneity compared to conventional saturation and inversion recovery techniques.
-
- 3266
Computer #29 Incorporation of Prior Knowledge of Main Field Inhomogeneity in Dixon Methods
Holger Eggers¹, Liesbeth Geerts-Ossevoort², Gert Mulder², and Clemens Bos³
- ¹Philips Research, Hamburg, Germany, ²Philips Healthcare, Best, Netherlands, ³Imaging Division, University Medical Center Utrecht, Utrecht, Netherlands*
- The robustness of Dixon methods often deteriorates close to large main field inhomogeneity. To resolve this problem, the exploitation of prior knowledge of magnet imperfections is considered in this work. Magnet-induced main field inhomogeneity is modeled to predict and correct spatial variations of the phase in single-echo images before the separation of water and fat signal. Improved fat suppression is demonstrated with this approach in first-pass peripheral angiography, in particular in the corners of the large FOVs.
-
- 3267
Computer #30 Comparison of Gradient Echo MRI Water-Fat separation and single voxel 1H MRS for liver fat fraction measurements in a dietary intervention study at 3T
Stephen Bawden^{1,2}, Carolyn Chee³, Caroline Hoad¹, Guruprasad Aithal², Ian Macdonald³, Richard Bowtell¹, and Penny Gowland¹
- ¹Sir Peter Mansfield Imaging Centre, University of Nottingham, Nottingham, United Kingdom, ²NIHR Nottingham Digestive Diseases Research Unit, University of Nottingham, Nottingham, United Kingdom, ³School of Life Sciences, University of Nottingham, Nottingham, United Kingdom*
- This study compared hepatic fat fraction measured using MRS and gradient echo MRI at 3T. Fitting algorithms using a single fat peak and multiple fat peaks were compared with MRS data at TE=20ms and also T2-corrected MRS. Individual differences between T2 values of water and fat calculated from MRS were also used to estimate the difference between R2*-water and R2*-fat and included in the multi peak fitting per subject. The results showed a good correlation between multi-peak and MRS data ($R^2 = 0.9$), but applying T2-

correction to MRS increased the scatter ($R^2 = 0.67$) and systematic error (gradient = 1.34). Using the new R2* corrected fitting algorithm resulted in similar scatter ($R^2 = 0.66$) but improved systematic error (gradient = 1.09). The results from this study indicate the dual-R2* fitting is important at 3T and further developments should be made to optimize these methods.

3268

Computer #31 Path based phase estimation for fat suppression near metal implants
Laura Jane King¹, Rick Millane¹, Hans Weber², Brian Hargreaves², and Phil Bones¹

¹Electrical and Computer Engineering, University of Canterbury, Christchurch, New Zealand, ²Radiology, Stanford University, Stanford, CA, United States

Being able to perform robust Dixon imaging near metal implants would allow for improved contrast-enhanced fat suppression. This requires accurate calculation of the phase shift due to the B0 field variation. We present a new technique where the phase is first estimated at the outer edges of the image. The method works inwards along a set of adjacent paths, finishing at the boundary of the implant. The described method is used to successfully separate fat and water in the vicinity of a titanium hip replacement, with phantom results shown.

3269

Computer #32 Improving Parameter Mapping in MRI Relaxometry and Multi-Echo Dixon using an Automated Spectral Denoising
Felix Lugauer^{1,2}, Dominik Nickel³, Stephan A. R. Kannengiesser³, Samuel Barnes⁴, Barbara Holshouser⁴, Jens Wetzl¹, Joachim Hornegger¹, and Andreas Maier^{1,2}

¹Pattern Recognition Lab, Department of Computer Science, Friedrich-Alexander Universität Erlangen-Nürnberg, Erlangen, Germany, ²Research Training Group 1773 "Heterogeneous Image Systems", Erlangen, Germany, ³MR Applications Predevelopment, Siemens Healthcare GmbH, Erlangen, Germany, ⁴Department of Radiology, Loma Linda University Medical Center, Loma Linda, CA, United States

Magnitude-based parameter fitting is commonly used for relaxometry and multi-echo Dixon but introduces a bias for relaxation and fat fraction estimates, particularly for a low signal-to-noise ratio and high relaxation. The application of an automated, patchwise denoising to the multi-echo image series prior to parameter fitting, considerably increased the SNR; thus, reducing the bias and standard deviation in the estimates of the fit. Our findings were validated on both numerical and in-vivo experiments.

3270

Computer #33 Two-point fat water separation using safest path region growing with self-feeding phasor estimation algorithm
Chuanli Cheng^{1,2}, Chao Zou¹, Hairong Zheng¹, and Xin Liu¹

¹Shenzhen Institutes of Advanced Technology, Chinese Academy of Sciences, Shenzhen, China, People's Republic of, ²University of Chinese Academy of Sciences, Beijing, China, People's Republic of

A novel two-point fat water separation method using safest path region growing with self-feeding phasor estimation algorithm is proposed. The phasor map is estimated by multiresolution region growing scheme where the seed pixels identification and region growing scheme is performed independently between coarser resolutions, avoiding the erroneous propagation between resolutions. The "self-feeding" mechanism when merging the phasor maps ensures the reliability of seed pixels selection at the finest resolution. The algorithm was tested on c-spine and abdomen data and shown to be robust in fast varying field and disjoint areas.

3271

Computer #34 Increased measurement precision for fatty acid composition mapping by parameter reduction
Johan Berglund¹, Henric Rydén¹, and Mikael Skorpil¹

¹Karolinska University Hospital, Stockholm, Sweden

An imaging method for mapping Fatty Acid Composition using three triglyceride spectrum model parameters (FAC3) was modified into mapping Fatty Acid Composition with only one spectrum model parameter (FAC1), namely the average number of double bonds per triglyceride (*ndb*). Images of a patient with a lipoma were reconstructed using both methods. The FAC3 *ndb* map showed large-scale variation from left to right, giving significant variation between subcutaneous adipose tissue locations. Measurements from the FAC1 *ndb* map were consistent within the adipose tissue, offering a higher level of confidence and more precise measurements.

3272

Computer #35 A Fast and Globally Optimal 3-D Graph Search Algorithm for Phase Unwrapping in MRI with Applications in Quantitative Susceptibility Mapping (QSM)
Chen Cui¹, Abhay Shah¹, Cameron M. Cushing², Vince Magnotta³, Xiaodong Wu^{1,2}, and Mathews Jacob¹

¹Electrical and Computer Engineering, University of Iowa, Iowa City, IA, United States, ²Radiology Oncology, University of Iowa Hospitals and Clinics, Iowa City, IA, United States, ³Radiology, University of Iowa Hospitals and Clinics, Iowa City, IA, United States

Phase wrapping is a classic problem in many fields of study. In MRI, Unwrapping the phase in the estimation of B0 field inhomogeneity maps is challenging commonly due to the presence of a large field inhomogeneity, anatomical discontinuities or low SNR in certain regions of the map (e.g. boundaries). We propose a general phase unwrapping method that exploits the smoothness of the field map in three spatial dimensions. The method is solved using a linear-convex constrained graph search algorithm that provides the globally guaranteed optimal solution without over-smoothing effect. The proposed scheme aims to produce a robust solution for field map estimation that will further improve the quality of quantitative susceptibility mapping (QSM).

- 3273
Computer #36 Analysis of Bias with SNR in Multi-echo Chemical Shift Encoded Fat Quantification
James H Holmes¹, Diego Hernando², Kang Wang¹, Ann Shimakawa³, Nate Roberts², and Scott B Reeder^{2,4,5,6}
- ¹MR Applications and Workflow, GE Healthcare, Madison, WI, United States, ²Radiology, University of Wisconsin-Madison, Madison, WI, United States, ³MR Applications and Workflow, GE Healthcare, Menlo Park, CA, United States, ⁴Medical Physics, University of Wisconsin-Madison, Madison, WI, United States, ⁵Biomedical Engineering, University of Wisconsin-Madison, Madison, WI, United States, ⁶Emergency Medicine, University of Wisconsin-Madison, Madison, WI, United States
- Multi-echo chemical shift encoded techniques provide accurate fat quantification over a broad range of fat-fractions and acquisition parameters. In order to be accurate, these techniques must correct for all relevant confounding factors. Emerging applications (eg: fat quantification with high spatial resolution or in iron overloaded tissues) can result in data with significantly lower signal-to-noise ratio (SNR) compared to previously established applications. In this work, we characterize the accuracy of current noise bias correction techniques for fat quantification in the low SNR regime and show simple modifications may enable accurate fat quantification for a wider range of SNR.
-
- 3274
Computer #37 DEVELOPMENT AND MULTI-CENTER VALIDATION OF A NOVEL WATER-FAT-IRON PHANTOM FOR JOINT FAT AND IRON QUANTIFICATION
Samir D. Sharma¹, Diego Hernando¹, Takeshi Yokoo², Mustafa R. Bashir^{3,4}, Jean Shaffer^{3,4}, Qing Yuan², Stefan Ruschke⁵, Dimitrios C. Karampinos⁵, Jean H. Brittain¹, and Scott B. Reeder^{1,6}
- ¹Radiology, University of Wisconsin - Madison, Madison, WI, United States, ²Radiology, UT Southwestern Medical Center, Dallas, TX, United States, ³Radiology, Duke University, Durham, NC, United States, ⁴Center for Advanced Magnetic Resonance Development, Duke University, Durham, NC, United States, ⁵Diagnostic and Interventional Radiology, Technische Universität München, Munich, Germany, ⁶Medical Physics, University of Wisconsin-Madison, Madison, WI, United States
- The need for rapid and non-invasive assessment of fat and iron deposition has become increasingly important given the high prevalence of obesity and obesity-related comorbidities as well as the need for monitoring chelation treatment in patients with iron overload. Recent advances in gradient-echo imaging have enabled the simultaneous quantification of fat and iron concentrations throughout the body. To ensure fidelity of these quantitative techniques, validation studies must be performed, ideally with initial testing in phantoms. In this work, we report on the development of a water-fat-iron MRI phantom that exhibits single-R2* decay, with controllable proton-density fat fraction (PDFF) and iron concentration. The purpose of this work is: 1) to describe the development of the water-fat-iron phantom, and 2) to assess the multi-center, multi-vendor reproducibility of joint fat and iron quantification using this phantom.
-
- 3275
Computer #38 A Novel Phase Unwrapping Method Based on Pixel Clustering and Local Surface Fitting with Application to Water-Fat Separation
Junying Cheng^{1,2}, Yingjie Mei^{2,3}, Biaoshui Liu², Xiaoyun Liu¹, Ed. X. Wu^{4,5}, Wufan Chen^{1,2}, and Yanqiu Feng^{2,4,5}
- ¹School of Automation Engineering, University of Electronic Science and Technology of China, Chengdu, China, People's Republic of, ²School of Biomedical Engineering and Guangdong Provincial Key Laboratory of Medical Image Processing, Southern Medical University, Guangzhou, China, People's Republic of, ³Philips Healthcare, Guangzhou, China, People's Republic of, ⁴Laboratory of Biomedical Imaging and Signal Processing, The University of Hong Kong, Hong Kong SAR, China, People's Republic of, ⁵Department of Electrical and Electronic Engineering, The University of Hong Kong, Hong Kong SAR, China, People's Republic of
- Current phase-unwrapping algorithms are challenged by rapid phase variations, noise and disconnected regions. We propose a novel phase-unwrapping method based on the observation the phase local difference (pLD) and complex local difference (cLD) maps. The proposed algorithm first clusters pixels into disconnected regions by thresholding the cLD map and then performs local polynomial surface fitting (LPSF) to unwrap phase with the knowledge of wrapping locations identified by thresholding the pLD map. Both simulation and in vivo results demonstrate that the proposed method can correctly unwrapped phase even in the presence of rapid phase variation, low SNR, and disconnected regions, and has great potential application to phase-related MRI in practice.
-
- 3276
Computer #39 Modified Single-Echo Dixon Imaging for Improved SNR and CNR in Contrast-Enhanced MRA
Holger Eggers¹
- ¹Philips Research, Hamburg, Germany
- Chemical shift encoding-based water-fat imaging, or Dixon imaging, is of recent interest in MRA. Single-echo Dixon methods are particularly appealing for this application because of their potential for decreasing scan times. This work suggests modifications to existing single-echo Dixon methods and demonstrates their benefits, primarily improvements in SNR and CNR, in contrast-enhanced peripheral MRA.
-
- 3277
Computer #40 Separation of Abdominal Subcutaneous Adipose Tissue (SAT) and Visceral Adipose Tissue (VAT) based on Wheel-Template in MRI
Steve Cheuk Ngai Hui¹, Teng Zhang¹, Defeng Wang¹, and Winnie Chiu Wing Chu¹
- ¹Dept. of Imaging and Interventional Radiology, The Chinese University of Hong Kong, Hong Kong, Hong Kong
- This abstract introduces the use of wheel-template to perform segmentation on subcutaneous adipose tissue (SAT) and visceral adipose tissue (VAT) at the abdominal region. The proposed method detects narrow regions between SAT and VAT, and uses line cut to separate two types of tissues based on MRI data. It performs well on obese individuals and the obtained results are correlated to those obtained from a semi-automatic method. A quantitative measurement of SAT and VAT is important as they are developed from different pathways and suggested to be related to different chronic diseases.

-
- 3278
Computer #41 Analytical Three-Point Dixon Method Using a Global Graph Cut
Jonathan Andersson¹, Filip Malmberg¹, Håkan Ahlström¹, and Joel Kullberg¹
¹Radiology, Uppsala University, Uppsala, Sweden
- When reconstructing chemical shift encoded water-fat images so called water-fat swaps due to incorrect phase maps can be a significant problem, limiting clinical assessment and quantitative measurements. A method is presented for solving the problem in the case of 3 echoes, assuming only a fix intra-echo spacing. Two possible solutions are analytically calculated for each voxel. The correct global solution is then found using a graph-cut method. The method succeeds where a region-growing reference method fails at low SNR. The presented method runs quickly and uses only one parameter that can be set automatically, which should allow for online implementation.
-
- 3279
Computer #42 Fat Residue Removal by SENSE in EPI and DW-EPI
Victor B. Xie^{1,2}, Mengye Lyu^{1,2}, Yilong Liu^{1,2}, Yangqiu Feng^{1,2}, Hua Guo³, and Ed X. Wu^{1,2}
¹Laboratory of Biomedical Imaging and Signal Processing, The University of Hong Kong, Hong Kong SAR, China, People's Republic of, ²Department of Electrical and Electronic Engineering, The University of Hong Kong, Hong Kong SAR, China, People's Republic of, ³Center for Biomedical Imaging Research, Department of Biomedical Engineering, School of Medicine, Tsinghua University, Beijing, China, People's Republic of
- In this abstract, we proposed to use parallel imaging method to remove the fat residue in EPI applications. In EPI, fat is shifted along the phase encoding direction and can be treated as another simultaneously excited slice with controlled aliasing together with the water image. By applying SENSE, water and fat residue can be effectively separated. We have presented this simple method to separate water and fat in EPI images and successfully applied it to remove fat residue in the brain and abdomen fat-suppressed EPI and DW-EPI images.
-
- 3280
Computer #43 Characterization of Brown Adipose Tissue using Multi-Varying-Peak MR Spectroscopy (MVP-MRS)
Gregory Simchick¹, Jinjian Wu², Guangming Shi², Hang Yin³, and Qun Zhao¹
¹Bioimaging Research Center, University of Georgia, Athens, GA, United States, ²Xidian University, Xian, China, People's Republic of, ³Department of Biochemistry and Molecular Biology, University of Georgia, Athens, GA, United States
- Differentiation of brown adipose tissue (BAT) from white adipose tissue (WAT) using magnetic resonance imaging (MRI) is clinically important to treat obesity, diabetes and heart disease. In contrast to the traditional Dixon model of single fat- and water-peak or fixed multi-fat-peak models, we propose a Multi-Varying-Peaks MR Spectroscopic (MVP-MRS) model, based on MR imaging data acquired with multiple echoes, to better characterize chemical structures of the fatty acid (saturated vs. unsaturated). Compared with traditional classification of BAT and WAT using fat fraction or proton relaxation time, the proposed MVP-MRS model can achieve a correct classification rate of 95% between BAT and WAT for in vivo mouse data implying great potentials in future longitudinal imaging of BAT and WAT.
-
- 3281
Computer #44 High-resolution imaging of muscular fat fraction - comparison of chemical shift-encoded imaging and T2-based imaging
Lena Trinh¹, Emelie Lind¹, Pernilla Peterson¹, and Sven Månsson¹
¹Dept. of Translational Medicine, Medical Radiation Physics, Skåne University Hospital, Lund University, Malmö, Sweden
- Chemical shift-encoded imaging is a quantitative method commonly used to estimate fat fraction (FF) in various body parts. However, for a reliable assessment, this technique requires short inter echo spacing which can be challenging if high spatial resolution is desirable. An alternative quantitative method, based on the difference in T2-relaxation time between fat and water, was examined and compared to the chemical shift-encoded imaging method. This T2-based technique successfully estimated FF in phantoms at high resolution and large matrix size, when the chemical shift-encoded method failed.
-
- 3282
Computer #45 Resolving Phase Ambiguity in Two-point Dixon Imaging Using a Projected Power Method
Tao Zhang^{1,2}, Yuxin Chen³, Marcus Alley¹, Brian Hargreaves^{1,2}, John Pauly², and Shreyas Vasanawala¹
¹Radiology, Stanford University, Stanford, CA, United States, ²Electrical Engineering, Stanford University, Stanford, CA, United States, ³Statistics, Stanford University, Stanford, CA, United States
- Dixon techniques offer robust water/fat separation in the presence of static field inhomogeneity. Two-point Dixon imaging with flexible echo times is desirable because of its high scan efficiency and flexibility. A major challenge in two-point Dixon imaging is how to estimate the phase error resulting from field inhomogeneity. In this work, we formulate a binary quadratic optimization and propose a fast projected power method to resolve the phase ambiguity in two-point Dixon imaging.
-
- 3283
Computer #46 A comprehensive approach for effective motion artifact reduction in Dixon
Gabriele Beck¹, Alan Huang¹, Adri Duijndam¹, and Lars van Loon¹
¹Philips Healthcare, Best, Netherlands

While Dixon provides superb fat suppression over large imaging volumes, motion can be a challenge in specific anatomies. This work evaluates a comprehensive approach to reduce motion artifacts in Dixon TSE and FFE sequences, combining a novel Dixon decorrelation approach, partial averaging, modulus in-phase (IP) – out-phase (OP) combinations and saturation of the physiological motion artifact sources by the means of saturation pulses and variable refocusing flip angle sweeps. We are able to show that this approach allows us to effectively remove motion artifacts improving the diagnostic quality of Dixon scans.

Electronic Poster

New Techniques: Evaluations & Applications

Exhibition Hall

Tuesday, May 10, 2016: 11:00 - 12:00

3284 Developing a free-breathing dynamic contrast enhanced scan for Lung Cancer using radial 'stack-of-stars' technique
Computer #49 Shivani Kumar^{1,2,3}, Robba Rai², Daniel Moses^{1,4}, Armia George^{2,3}, Lois Holloway^{1,2,3,5,6}, Shalini Vinod^{1,2}, and Gary Liney^{1,2,3,7}

¹The University of New South Wales, Sydney, Australia, ²Liverpool Cancer Therapy Centre, Liverpool, Australia, ³Ingham Institute of Applied Medical Research, Liverpool, Australia, ⁴Prince of Wales Hospital, Randwick, Australia, ⁵Institute of Medical Physics, University of Sydney, Sydney, Australia, ⁶Centre for Medical Radiation Physics, University of Wollongong, Wollongong, Australia, ⁷University of Wollongong, Wollongong, Australia

Dynamic contrast enhanced (DCE) MRI is becoming an increasingly important tool for assessing tumour response, however it's application in lung is limited by respiratory motion. We propose the use of radial acquisition technique to minimise motion by oversampling the centre of k-space albeit with reduced temporal resolution. The initial results show that the radial k-space trajectory is a suitable method for motion compensation which provided a DCE scan of sufficient image quality and temporal resolution which can be used as part of a complete free breathing lung MRI protocol.

3285 Robust in vivo DTI by Spatiotemporal Encoding
Computer #50 Eddy Solomon¹, Gilad Liberman¹, Noam Nissan², and Lucio Frydman¹

¹Chemical Physics Department, Weizmann Institute of Science, Rehovot, Israel, ²Biological Regulation Department, Weizmann Institute of Science, Rehovot, Israel

A recently proposed single-shot MRI methodology, SPatio-temporal ENcoding (SPEN), was evaluated for its usefulness in DTI experiments. SPEN's direct image acquisition is not bound by k-space sampling criteria, thereby enabling the use of stronger gradients during its monitoring of the low-bandwidth dimension. This helps it to overcome image distortions arising from field inhomogeneities, eddy currents and heterogeneous chemical environments. Single-shot and interleaved DTI SPEN measurements were tested under various pre-clinical and clinical settings, and the formalism needed to extract reliable DTI maps from SPEN data was derived. Substantial advantages in terms of overcoming EPI distortions were observed.

3286 Precision and Accuracy of Multi-Echo Based T_2 mapping: Fitted vs Measured B_1
Computer #51 Christopher L Lankford¹ and Mark D Does^{1,2}

¹Biomedical Engineering, Vanderbilt University, Nashville, TN, United States, ²Electrical Engineering, Vanderbilt University, Nashville, TN, United States

This abstract provides a simple criterion by which to determine whether refocusing pulse flip angle should be fitted or constrained to a measured B_1^+ map in multiple spin echo (MSE) based T_2 mapping protocols. Using propagation of error theory including the Cramér-Rao lower bound, it was discovered that T_2 estimate precision is improved through constraint when the signal-to-noise ratio (SNR) of the B_1^+ map is at least one-half the SNR of the MSE measurement. The accuracy cost of constraint is also evaluated and presented.

3287 3D Magnetic resonance fingerprinting microscopy using a vertical wide bore superconducting magnet
Computer #52 Yasuhiko Terada¹

¹Institute of Applied Physics, University of Tsukuba, Tsukuba, Japan

NMR microscopy provides a variety of image contrast with a high spatial resolution. However, 3D NMR multi-parameter mapping with large matrix sizes is time consuming and practically difficult to apply to living samples. Here we introduced magnetic resonance fingerprinting (MRF) technique to 3D NMR multi-parameter microscopy, which could reduce the scan time largely. We verified the feasibility of the relaxation and proton density mapping using a vertical wide bore superconducting magnet. The 3D MRF for a grape berry provided the T_1 , T_2 , and proton density maps in the short measurement time that can be used to extract important structural information.

3288 Feasibility of 4D MRI for Assessment of Regional Hepatic Blood Flow
Computer #53 Eric James Keller¹, Laura Kulik², James C. Carr¹, Michael Markl^{1,3}, and Jeremy Douglas Collins¹

¹Radiology, Northwestern University, Chicago, IL, United States, ²Gastroenterology and Hepatology, Northwestern University, Chicago, IL, United States, ³Biomedical Engineering, Northwestern University, Chicago, IL, United States

The success of surgical and transarterial therapies for hepatocellular carcinoma relies on hepatic hemodynamics. Non-contrast 4D flow MRI can quantify hepatic blood flow at the lobar arterial and portal vein levels with a low relative error and clearly evaluate portosystemic shunts; however, segmental flow quantification remains limited. By pairing 4D flow MRI with HCC surveillance MR imaging, lobar flow per volume can also be assessed, providing valuable information for surgical planning.

3289 How to minimize motion-induced phase and magnitude modulation in diffusion-prepared sequences?

Computer #54 Anh Tu Van¹, Barbara Cervantes², Ernst J Rummeny², Axel Haase¹, and Dimitrios Karampinos²

¹Zentralinstitut für Medizintechnik, Technische Universität München, Garching, Germany, ²Diagnostic and Interventional Radiology, Technische Universität München, Munich, Germany

Diffusion-preparation is regaining popularity recently thanks to its compatibility with any type of readout scheme. Using Bloch simulations, the current work provides understanding of the motion-induced magnitude and phase modulation of the signal obtained with diffusion-prepared sequences. When motion induces a constant phase across the voxel, dephasing signal before tipping up and rephasing it before readout should be used to remove motion-induced magnitude modulation. When the induced phase is not constant, smaller voxel sizes assist towards stabilizing both magnitude and phase of the signal. In vivo data using diffusion-prepared 3D TSE are shown supporting the observations of the Bloch simulations.

3290 Multi-site, multi-vendor comparison of T1 measurement using ISMRM/NIST system phantom

Computer #55 Kathryn E Keenan¹, Karl F Stupic¹, Michael A Boss¹, Stephen E Russek¹, Tom L Chenevert², Pottumarthi V Prasad³, Wilburn E Reddick⁴, Kim M Cecil⁵, Jie Zheng⁶, Peng Hu⁷, Edward F Jackson⁸, and Ad Hoc Committee for Standards in Quantitative MR⁹

¹Physical Measurement Laboratory, National Institute of Standards and Technology, Boulder, CO, United States, ²University of Michigan, Ann Arbor, MI, United States, ³NorthShore University Health System, Evanston, IL, United States, ⁴St. Jude Children's Research Hospital, Memphis, TN, United States, ⁵Cincinnati Children's Hospital Medical Center, Cincinnati, OH, United States, ⁶Washington University in St. Louis, St. Louis, MO, United States, ⁷University of California Los Angeles, Los Angeles, CA, United States, ⁸University of Wisconsin, Madison, WI, United States, ⁹ISMRM, Berkeley, CA, United States

We used the ISMRM/NIST system phantom to assess variations of T1 measurements across MRI systems at 1.5 T and 3 T, to determine the repeatability and reproducibility of the T1 measurements. This study demonstrates that T1 variations from NMR-measured value are correlated site-to-site within a vendor and by position within the head coil. The deviation from the NMR-measured values is greater at 3 T than at 1.5 T. The VFA data has a larger variation than IR; B1 inhomogeneity could contribute to the larger systematic error in VFA measurements. The ISMRM/NIST system phantom is an excellent tool for evaluating multi-site MRI acquisition protocols.

3291 Detection of Metabolic Brain Activation with High Spatiotemporal Resolution T1 ρ -Weighted MRI without Statistical Parametrization and without Exogenous Tracer Administration

Computer #56 Dharmesh Tailor, MSE, MD, PhD¹

¹Radiology Specialists of Florida, Florida Hospital, Adventist Health System, Orlando, FL, United States

Accurate and precise mapping of metabolically active eloquent foci in the brain, differentiating recurrent neoplasm from pseudo-progression, differentiating tumefactive demyelination from neoplasm, delineating the actual stroke penumbra, and early detection of neurodegenerative disease, all require high-resolution imaging of underlying relative brain oxygen metabolism. At the present time, however, there is no robust technique that can map brain metabolism at a high spatiotemporal resolution. This work derives and demonstrates a model for imaging of relative CMRO₂ with T₁ ρ -weighted MRI which can be readily performed on any clinical MRI scanner with a simple pulse sequence and without the need for hardware modification. This novel approach is optimized to yield a spatial resolution of 0.2 mm³ and temporal resolution of 3.2 sec, and developed to work without exogenous tracer or contrast agent administration, blood sampling, or statistical parametrization of the image data.

3292 Repeatability of Magnetic Resonance Fingerprinting on T1 and T2 quantification with the NIST/ISMRM standardized relaxation phantom

Computer #57 Yun Jiang¹, Dan Ma², Kathryn E. Keenan³, Karl Stupic³, Vikas Gulani^{1,2}, and Mark A. Griswold^{1,2}

¹Department of Biomedical Engineering, Case Western Reserve University, Cleveland, OH, United States, ²Department of Radiology, Case Western Reserve University, Cleveland, OH, United States, ³Physical Measurement Laboratory, National Institute of Standards and Technology, Boulder, CO, United States

In order to promote the clinical acceptance of quantitative relaxometry techniques as a valid biomarker, a fast quantitative method that can measure the relaxation parameters with high repeatability is needed. This study evaluates the repeatability of MRF with the standardized relaxometry phantom developed through collaboration between the ISMRM Ad Hoc Committee on Standards for Quantitative MR and the National Institute of Standards and Technology (NIST) over 35 consecutive days. A less than 5% variation on T₁ and T₂ estimations of MRF was observed in NIST standardized phantoms with a wide range of T1 and T2 values.

- 3293
Computer #58 Bloch-Siebert B1-mapping Improves Accuracy and Precision of T1 Measurements in the Breast at 3T
Jennifer G Whisenant¹, Richard D Dortch¹, Lori A Arlinghaus¹, William A Grissom¹, Hakmook Kang¹, and Thomas E Yankeelov¹
¹Vanderbilt, Nashville, TN, United States
- This study evaluated the ability of Bloch-Siebert B1 mapping to improve the accuracy and precision of variable flip angle (VFA)-derived T1 measurements of the breast at 3.0 T. Accuracy was evaluated by comparing VFA T1 values to inversion recovery measurements in a cohort of 16 healthy women. A reproducibility analysis from test-retest sessions within the same cohort was used to evaluate precision. After Bloch-Siebert B1 correction, accuracy of T1 measurements in the fat and fibroglandular tissue improved and measurement variability decreased. Thus, these results suggest that Bloch-Siebert B1 mapping is an attractive correction method for quickly obtaining accurate and precise measurements of T1 values of the breast at 3.0 T.
-
- 3294
Computer #59 Influence of multi-compartment effects on T2 mapping using multiecho steady state imaging
Dian Liu¹, Andreas Steingoetter^{1,2}, Jelena Curcic^{1,2}, and Sebastian Kozerke¹
¹Institute for Biomedical Engineering, University and ETH Zurich, Zurich, Switzerland, ²Division of Gastroenterology and Hepatology, University Hospital Zurich, Zurich, Switzerland
- Dual and triple echo steady state (DESS and TESS) schemes have enabled rapid measurements of transverse relaxation times (T₂). However, it has been shown that TESS may result in erroneous T₂ values when applied to articular cartilage. Since cartilage is a multi-compartment tissue, chemical shift-related signal fluctuations in the TESS echo modes need to be considered. The purpose of this work was to investigate the accuracy of T₂ quantification of multi-compartmental tissue using DESS and TESS based on computer simulations, *in vitro* and *in vivo* measurements. Results show that multi-compartment effects can significantly limit the accuracy of T₂ quantification and hence require careful attention.
-
- 3295
Computer #60 Accelerated 3D Acquisition for Susceptibility Weighted Imaging Using Spread Spectrum Encoding and Compressive Sensing
Sulaiman A Al Hasani¹, Zhaolin Chen², Gary F Egan², and Jingxin Zhang³
¹Department of ECSE, Monash University, Melbourne, Australia, ²Monash Biomedical Imaging, Melbourne, Australia, ³Swinburne University of Technology/School of Software and Electrical Engineering, Melbourne, Australia
- Spread spectrum based encoding methods have recently been investigated to spread the energy of MR signal in k-space and hence allowing for optimal incoherent sampling and hence higher performance of CS reconstruction. In this work, we extend the use of spread spectrum based encoding to 3D GRE sequence. The proposed encoding scheme can enhance the performance of multi-receive CS reconstruction at high acceleration factors and preserve resolution of small anatomical structures and preserve susceptibility contrast for Susceptibility-weighted imaging (SWI).
-
- 3296
Computer #61 Comparison of a novel, motion-robust MPRAGE imaging sequence with conventional MPRAGE imaging
Manojkumar Saranathan¹, Puneet Sharma¹, Unni Udayasankar¹, and Rihan Khan¹
¹Dept. of Medical Imaging, University of Arizona, Tucson, AZ, United States
- Conventional MPRAGE imaging is an integral part of most neuroimaging protocols. We investigated a new radial fan beam ordered MPRAGE sequence for its motion robustness and compared it to conventional MPRAGE imaging on 29 patients. The radial fan beam ordering had significantly better image quality than conventional centric ordered MPRAGE when rated for motion artifacts and overall diagnostic quality by 2 trained neuroradiologists.
-
- 3297
Computer #62 Brain tissue pulsatility measured at 7T with high resolution and whole brain coverage
Ayodeji L. Adams¹, Peter R. Luijten¹, and Jaco J.M. Zwanenburg¹
¹Radiology, University Medical Center Utrecht, Utrecht, Netherlands
- Pulsatile brain tissue motion, driven by the cardiac cycle, is important for maintaining homeostatic processes in the brain, and increased pulsatility is linked to diseases such as dementia. In this study, we demonstrate the feasibility of measuring whole brain volumetric strain with 2 mm isotropic resolution at 7T MRI in 8 healthy volunteers. Maximum volumetric strain was $(2.3 \pm 1.5) \times 10^{-3}$, and showed considerable inter-subject and inter-slice variability that was much larger than could be explained from intrinsic measurement errors as assessed from a gel phantom. This method has potential for studying the brain pulsatility in disease.
-
- 3298
Computer #63 Filling the deadtime gap in zero echo time MRI: principles compared
Romain Nicolas Froidevaux¹, Markus Weiger¹, David Otto Brunner¹, Bertram Jakob Wilm¹, Benjamin Emanuel Dietrich¹, and Klaas Paul Pruessmann¹
¹Institute for Biomedical Engineering, University and ETH Zurich, Zürich, Switzerland
- Often used for the imaging of compounds with short relaxation times, 3D center-out sequences performing broadband excitation on a ramped-up strong gradient provide very short acquisition delays and high bandwidth. In turn, data located around the k-space center is missed and needs to be recovered. Different approaches, like algebraic ZTE, WASPI or PETRA are used today. An important but still open question is how the relation of the deadtime and the T₂s involved affect image quality. We show that critical situations occur for

similar values of deadtime and T2, frequently encountered when imaging ultra-short-T2s in solid tissues or hardware parts.

-
- 3299
Computer #64
- Method to Simultaneously Calibrate Flip Angles and Measure T1 of Hyperpolarized Gas during a Single Breath-hold
Jianping Zhong^{1,2}, Weiwei Ruan¹, Xianping Sun¹, Chaohui Ye^{1,2}, and Xin Zhou¹
- ¹State Key Lab Magnet Resonance & Atom & Mol Phys, Wuhan Inst Phys & Math, Chinese Acad Sci, Wuhan, China, People's Republic of, ²School of Physics, Huazhong University of Science and Technology, Wuhan, China, People's Republic of
- In hyperpolarized gas MRI, the accurate flip angle calibration and T₁ measurements are important. Traditional flip angle calibration methods are time-consuming and suffer from polarization losses during T₁ relaxation. In this study, we propose a method to simultaneously calibrate flip angles and measure T₁ *in vivo* during a breath-hold time of less than 4 seconds. The so-called single-breath method is magnitude based and simple to use. We demonstrate the accuracy of this method and contrast it with traditional methods. The results of the calibration verified that it is robust and repeatable.
-
- 3300
Computer #65
- 2D Constrained Point-Spread-Function in Magnetic Resonance Spectroscopic Imaging of Prostate
Shelley HuaLei Zhang¹, Jr-Yuan George Chiou¹, Robert Vincent Mulkern¹, Pelin Aksit Ciris², Stephan Maier¹, and Lawrence Panych¹
- ¹Radiology, Brigham and Women's Hospital, Boston, MA, United States, ²Department of Biomedical Engineering, Akdeniz University, Antalya, Turkey
- Magnetic resonance spectroscopic imaging (MRSI) technique is often plagued by signal contamination (e.g. from fat) from outside the tissue of interest, particularly near organ boundaries. The goal is to demonstrate and validate in phantoms and healthy volunteers a spatial localization technique that features localized signal excitation and therefore eliminates the need for post-processing filtering. Here we demonstrated superior PSFs at prostate-relevant metabolic peaks for a 2D Gaussian-based PSF-Choice encoding scheme. The reduction of contamination from signals in surrounding tissue was further demonstrated in an in-vitro phantom. The feasibility of the method was demonstrated in a small group of prostate MRSI studies with normal volunteers.
-
- 3301
Computer #66
- Performance of spin-echo MRE sequences in patients with signal-related failure of standard GRE MRE
Bogdan Dzyubak¹, Yogesh K. Mariappan², Kevin J. Glaser¹, Sudhakar K. Venkatesh¹, and Richard L. Ehman¹
- ¹Radiology, Mayo Clinic, Rochester, MN, United States, ²Royal Philips, Bangalore, India
- Specialized spin-echo-based sequences have been developed to perform MRE in patients with short T2* where traditional MRE fails. This work demonstrates that these sequences are able to salvage such exams by improving SNR and MRE inversion confidence to the levels of successful GRE MRE exams. Additionally, the stiffnesses calculated by spin-echo and spin-echo-echo-planar acquisitions are equivalent to each other.
-
- 3302
Computer #67
- Slice Profile Correction in 2D Magnetic Resonance Fingerprinting (MRF)
Dan Ma¹, Shivani Pahwa¹, Vikas Gulani¹, and Mark Griswold¹
- ¹Radiology, Case Western Reserve University, Cleveland, OH, United States
- The goal of this study is to characterize and improve the accuracy and repeatability of 2D MRF scans in the presence of slice profile imperfections. Slice profile imperfection causes deviation between the actual flip angles and nominal flip angles, which affects the accuracy of measured T1 and T2 values. This error can be corrected by simulating the RF excitation pulse in the dictionary. No extra scan time or post-processing time is needed once the new dictionary is simulated. The accuracy of both T1 and T2 is improved after slice profile correction. MRF also demonstrates good repeatability, with the coefficient of variance (CV) of 1.17% for T1 and 3.08% for T2.
-
- 3303
Computer #68
- Local peripheral lung tissue microstructure quantification through CPMG relaxation rate dispersion
Felix T Kurz^{1,2}, Thomas Kampf³, Lukas R Buschle², Sabine Heiland¹, and Christian H Ziener^{1,2}
- ¹Heidelberg University Hospital, Heidelberg, Germany, ²E010 Radiology, German Cancer Research Center, Heidelberg, Germany, ³Wuerzburg University, Wuerzburg, Germany
- Microscopically small early stage lung pathologies like emphysematous alterations of local lung tissue are usually not detectable on clinical MR images. The presented model connects defining tissue parameters for an MR imaging voxel, i.e. local alveolar radius and air-tissue ratio as well as diffusion coefficient and air-tissue susceptibility gradient, to CPMG relaxation rate dispersion over a range of inter-echo times. The model shows an excellent agreement with data from ageing hydrogel foam that mimics lung tissue.
-
- 3304
Computer #69
- Similarity based fusion of multiple Regions of Interests for MR sequence evaluation
Michael Goetz¹, Christian Weber¹, and Klaus H. Maier-Hein¹
- ¹Medical Image Computing, German Cancer Research Center (DKFZ) Heidelberg, Heidelberg, Germany
- To compare the information content of different MR sequences often regions of interests (ROI) are used. A way to avoid observer-dependencies is to use ROIs from different observer, but this leads to the question how to fuse them. We propose a new method to combine the information obtained by multiple ROIs depending on their similarity, making our method less sensitive to outlier. We

evaluate our method by comparing the results obtained from the traditional merging method with the proposed algorithm. The results indicate that our method can be a valuable extension to ROI-based, multi-observer studies.

- 3305
Computer #70 A standardised clinical multicentric whole brain T2* mapping protocol at 3T
David Gay¹, Marie Chupin^{1,2}, Jean-François Mangin^{1,3}, Cyril Poupon^{1,4}, Hugo Dary¹, Takoua Kaaouana², Paulo Loureiro de Sousa⁵, Christine Delmaire⁶, Ludovic De Rochefort⁷, Jean-Marie Bonny⁸, and Alexandre Vignaud⁴

¹CATI Multicenter Neuroimaging Platform, *cati-neuroimaging.com*, Paris, France, ²ICM - Institut du Cerveau et de la Moelle Epinière, Paris, France, ³CEA, DSV, I2BM, NeuroSpin, UNATI, Gif-sur-Yvette, France, ⁴CEA, DSV, I2BM, NeuroSpin, UNIRS, Gif-sur-Yvette, France, ⁵Université de Strasbourg, CNRS, ICube, FTMS, Strasbourg, France, ⁶Neuroradiology, CHRU Roger Salengro, Lille, France, ⁷Université Paris-Sud, CNRS, IR4M UMR8081, Université Paris-Saclay, Orsay, France, ⁸INRA, UR370 QuaPA, Saint-Genès Champanelle, France

The purpose of this work is to report the implementation of a T2* map in multicenter neuroimaging studies. We focus on T2* because it is an endogenous biomarker for paramagnetic products like iron or melanin, which is very interesting to assess, among other diseases, Parkinson's disease. We developed a MR sequence which meets several specific requirements. This sequence is accessible on 3 major manufacturer 3T MRI scanners and ensures good measurement accuracy at a standard millimeter isotropic resolution. This "universal" sequence allows to acquire, in a reliable and repeatable way, T2* maps of the whole brain.

- 3306
Computer #71 B0 shimming with constraints for DWI with a reduced FOV
Denis Kokorin¹, Jürgen Hennig¹, and Maxim Zaitsev¹

¹Medical Physics, University Medical Center Freiburg, Freiburg, Germany

In this work, we investigated the application of B₀ shimming with constraints, in order to accomplish an intrinsic fat suppression during 2D EPI-based pulses. For this purpose, we simulated shimming in an ROI confined to part of the abdomen. Our initial results along with the experimental tests demonstrate the possibility for such a fat suppression method. However, the residual inhomogeneity in the main excitation ROI might become very substantial, if the restriction area for fat frequencies is too narrow.

- 3307
Computer #72 SNR Optimization in ZTE Imaging
Dong Kyu Kim¹ and Mark D Does^{1,2,3}

¹Department of Biomedical Engineering, Vanderbilt University, Nashville, TN, United States, ²Vanderbilt University Institute of Imaging Sciences, Vanderbilt University, Nashville, TN, United States, ³Department of Electrical Engineering, Vanderbilt University, Nashville, TN, United States

Zero Echo Time (ZTE) imaging is a technique with clinical potential for imaging tissues with very short T2 relaxation times. Due to the presence of a gradient during RF excitation, there is a slice profile effect that creates artifacts in the reconstructed image. This can be corrected prior to image reconstruction, at the cost of image SNR. Increasing pulse duration increases the signal acquired while reducing it lessens this profile effect. Hence, there exists an optimal pulse duration that balances these sources of signal loss. Herein, we present an optimized approach to maximizing SNR in ZTE imaging.

Electronic Poster

Normal Brain: Methods 1

Exhibition Hall

Tuesday, May 10, 2016: 13:30 - 14:30

- 3308
Computer #25 3D arterial spin labeling imaging with DANTE preparation pulse
Tsuyoshi Matsuda¹, Hirohiko Kimura², Masayuki Kanamoto³, and Hiroyuki Kabasawa¹

¹MR Applications and Workflow, GE Healthcare Japan Corporation, Tokyo, Japan, ²Department of Radiology, University of Fukui, Fukui, Japan, ³Radiological Center, University of Fukui Hospital, Fukui, Japan

DANTE preparation pulse for the arterial spin-labeling (ASL) sequence was developed to reduce the intravascular signal based on the hypothesis that DANTE could enable sufficient vascular signal suppression without any technical drawback. Phantom and human volunteer experiments were performed to evaluate the proposed method. A similar level of vascular suppression effect was observed with both MSDE and DANTE-prepared ASL sequence from phantom experiment. A signal intensity uniformity of vascular suppressed perfusion weighted images was superior with DANTE compared to MSDE. These results indicated that DANTE-preparation could be used as a vessel signal suppression method for ASL.

- 3309
Computer #26 A DOUBLE ACQUISITION FOUR-CONTRAST IMAGING APPROACH TO DELINEATE HUMAN BRAINSTEM ANATOMY IN-VIVO AT 7 TESLA
Michael Wyss¹, Laetitia Vionnet¹, Mike Bruegger^{1,2}, Bernd Daeubler³, Lars Kasper^{1,4}, Daniel Nanz⁵, Marco Piccirelli³, David O. Brunner¹, and Klaas P. Pruessmann¹

¹Institute for Biomedical Engineering, University of Zurich and ETH Zurich, Zurich, Switzerland, ²Center of Dental Medicine, University of Zurich, Zurich, Switzerland, ³Department of Neuroradiology, University Hospital Zurich, Zurich, Switzerland, ⁴Translational Neuromodeling Unit, Institute for Biomedical Engineering, University of Zurich and ETH Zurich, Zurich, Switzerland, ⁵Institute of Diagnostic and Interventional Radiology, University Hospital Zurich and University of Zurich, Zurich, Switzerland

The human brainstem anatomy is challenging to image in vivo on a single subject basis. The densely-packed interspersed of nuclei and white matter tracts cannot typically be imaged with an image contrast strong enough for differentiation of relevant substructures. We present an MR imaging approach at 7 Tesla that requires two high resolution MR acquisitions. From the two data sets, four image series with varying contrast weightings can be derived and used to delineate brainstem anatomy. The proposed strategy resulted in exceptionally high image quality enabling differentiation of several brainstem substructures that are hardly discernible in commonly acquired MR images.

3310 Computer #27 A Novel Diffusion Tensor Imaging Strategy for Delineating the Neuroanatomical Boundaries of the Amygdala
Andre Obenaus^{1,2}, Eli Kinney-Lang^{1,3}, Duke Shereen⁴, Ana Solodkin^{3,4}, and Tallie Z Baram^{2,3}

¹Pediatrics, Loma Linda University, Loma Linda, CA, United States, ²Pediatrics, University of California, Irvine, Irvine, CA, United States, ³Anatomy/Neurobiology, University of California, Irvine, Irvine, CA, United States, ⁴Neurology, University of California, Irvine, Irvine, CA, United States

The amygdaloid complex, including the basolateral nucleus (BLA) are critically important in mediating emotional and adaptive responses to stress. However, lack of contrast between the BLA and the surrounding gray matter (GM) has hampered routine imaging. We report a novel DTI paradigm to identify the BLA in the rodent brain. We derived BLA volumes and confirmed these with histological measures. Our approach can be used to study the morphological and functional consequences of emerging neuropsychiatric diseases, both in experimental and clinical studies.

3311 Computer #28 Measurement of bolus arrival time and velocity in Circle of Willis using dynamic MR angiography

Isaac Huen¹, Joanne Beckmann¹, Yuriko Suzuki², Maria A Zuluaga³, Andrew Melbourne³, Matthias JP van Osch⁴, David Atkinson⁵, Sebastien Ourselin³, Neil Marlow¹, and Xavier Golay¹

¹Institute of Neurology, University College London, London, United Kingdom, ²Philips Medical Systems, Philips, Tokyo, Japan, ³Centre for Medical Image Computing, University College London, London, United Kingdom, ⁴C.J. Gorter Center for High Field MRI, Leiden University Medical Center, Leiden, Netherlands, ⁵Centre for Medical Imaging, University College London, London, United Kingdom

The properties of the cerebral vasculature are of clinical relevance and thus of interest for investigation. Here an ASL-based 3D angiographic technique (CINEMA-STAR) is used to measure blood arrival times and blood velocities of a bolus labeled in the neck. Results are shown to be in broad agreement with existing methods.

3312 Computer #29 Quantitative MRI explorations of the hyaluronan-based extracellular matrix in brain tissues
Riccardo Metere¹, Markus Morawski², Carsten Jäger², and Harald E. Möller¹

¹Max Planck Institute for Human Cognitive and Brain Sciences, Leipzig, Germany, ²Paul Flechsig Institute for Brain Research, University of Leipzig, Leipzig, Germany

The tissue composition of the brain can be related to different contrast sources in quantitative MRI. Particularly, myelin and iron are considered to be major sources of MRI contrast, with strong correlation to T_1 and T_2^* , respectively. However, other components, may also play a role in contrast generation. In this work, we present experiments in post-mortem human brain specimens to disentangle the potential contribution of the hyaluronan-based extracellular matrix from other contrast sources in quantitative relaxation maps. This was achieved by comparing images of digested and undigested samples that were otherwise subject to the same environmental conditions.

3313 Computer #30 Automatic assessment of corpus callosum malformation from structural MRI images to improve diagnosis reproducibility.
Denis Peruzzo¹, Umberto Castellani², Fabio Triulzi^{1,3}, Andrea Righini⁴, Cecilia Parazzini⁴, and Filippo Arrigoni¹

¹Neuroimaging Unit, Scientific Institute IRCCS "Eugenio Medea", Bosisio Parini, Italy, ²Department of Computer Science, University of Verona, Verona, Italy, ³Department of Neuroradiology, Fondazione IRCCS "Ca' Granda" Ospedale Maggiore Policlinico, Milano, Italy, ⁴Department of Pediatric Radiology and Neuroradiology, Children Hospital "Vittorio Buzzi", Milano, Italy

The diagnosis of brain malformations is usually based on the visual inspection of MRI images by trained neuroradiologists. The resulting procedure is therefore subjective and mainly provides a qualitative description of the detected malformations. In this study, we propose an assisted diagnosis tool (ADT) for the analysis of the corpus callosum from structural T1-weighted images. The method detects and characterizes different kind of malformations (local/diffuse, homogeneous/heterogeneous). Inter-subject reproducibility experiments showed that the agreement rate significantly improved from 67.5% to 79.3% using the proposed method.

3314 Computer #31 T2 mapping of ventricular cerebrospinal fluid (CSF) at 7 Tesla with comparison to 3T
Jolanda M Spijkerman¹, Esben T Petersen², Peter R Luijten¹, Jeroen Hendrikse¹, and Jaco J M Zwanenburg¹

¹Radiology, University Medical Center Utrecht, Utrecht, Netherlands, ²Centre for Functional and Diagnostic Imaging and Research, Danish Research Centre for Magnetic Resonance, Copenhagen University Hospital, Hvidovre, Denmark

The relaxation parameters of CSF may have potential as imaging markers in several diseases. In this work T₂ mapping of CSF in the lateral ventricles and in the fourth ventricle was performed in six volunteers at 7T, with comparison to 3T. The sensitivity for B₁ was assessed by comparing the T₂s in both regions, with equal B₁ at 3T and different B₁ at 7T. T₂ values were significantly lower at 7T



compared to 3T. No significant difference was found between the lateral and the fourth ventricular T₂s at 7T (and 3T), indicating negligible B₁-sensitivity for the used T₂-mapping sequences.

-
- 3315
Computer #32 A Generic Supervised Learning Framework for Fast Brain Extraction
Yuan Liu^{1,2}, Benjamin Odry², Hasan Ertan Cetingul², and Mariappan Nadar²
- ¹Vanderbilt Institute in Surgery and Engineering, Vanderbilt University, Nashville, TN, United States, ²Medical Imaging Technologies, Siemens Healthcare, Princeton, NJ, United States*
- Automatic brain extraction, as a standard pre-processing step, typically suffers from a long runtime and inaccuracies caused by brain variations and limited qualities of MR images. We propose a generic supervised learning framework that builds binary classifiers to identify brain and non-brain tissues at different resolution levels, hierarchically performs voxel-wise classifications for a test subject, and refines the brain boundary using narrow-band level set technique on the classification map. The proposed method is evaluated on multiple datasets with different acquisition sequences and scanner types using uni- or multi-contrast images and shown to be fast, accurate, and robust.
-
- 3316
Computer #33 Reduced Distortion Artifact Whole Brain CBF Mapping using Blip-Reversed Non-Segmented 3D Echo Planar Imaging
Neville D Gai¹, Yi Yu Chou^{1,2}, Dzung Pham^{1,2}, and John A Butman¹
- ¹Radiology & Imaging Sciences, NIH, Bethesda, MD, United States, ²Center for Neuroscience and Regenerative Medicine, Henry Jackson Foundation, Bethesda, MD, United States*
- Arterial spin labeling is typically performed with segmented k-space acquisition schemes to reduce B₀ inhomogeneity related distortion. Non-segmented techniques offer the advantage of higher SNR/time allowing greater brain coverage in shorter scan times. Here we use a modified 3D EPI acquisition scheme along with pseudo-continuous arterial spin labeling to correct for B₀ inhomogeneity related distortion. By employing phase encoding along opposite directions in alternating control-label pairs and with subsequent post-processing, we correct for the distortion. CBF images were compared with GM masks obtained from relatively distortion free MPRAGE images to show improved localization of the CBF maps.
-
- 3317
Computer #34 Imaging of thalamic substructures: T1 based approach using IR-EPI sequence at 7T
Se-Hong Oh¹, Ken Sakaie¹, Stephen E. Jones¹, and Mark J. Lowe¹
- ¹Imaging Institute, Cleveland Clinic Foundation, Cleveland, OH, United States*
- Accurate identification of the thalamus sub-structures is therefore important for localization of specific nuclei and for the understanding of brain function. However, sub-structures of the thalamus are so small and have intermediate signal characteristics between grey/white matter it has been difficult to identify them with conventional MR imaging technique. In this work, in-vivo T₁ value at 7T are measured using fast T₁ mapping technique in less than 2 min and optimized inversion time to generate optimal contrast from the thalamus. The optimized results reveal markedly improved anatomical detail of the sub-structures of the thalamus, including their detailed locations.
-
- 3318
Computer #35 Motion Range Grouping of Brain Regions Based on Displacement Measured with Displacement Encoding with Stimulated Echoes (DENSE)
Xiaodong Zhong¹, Tucker Lancaster², Zihan Ye³, Deqiang Qiu², Brian M. Dale⁴, John N. Oshinski^{2,3}, and Amit Saindane²
- ¹MR R&D Collaborations, Siemens Healthcare, Atlanta, GA, United States, ²Department of Radiology and Imaging Sciences, Emory University, Atlanta, GA, United States, ³Biomedical Engineering, Georgia Institute of Technology, Atlanta, GA, United States, ⁴MR R&D Collaborations, Siemens Healthcare, Cary, NC, United States*
- In this work, we demonstrated that the DENSE technique can be used to measure and group motion of different brain regions. Preliminary results in 9 volunteers showed that the brain regions near the CSF (midbrain, pons, medulla and optic chiasm) had larger motion magnitude than regions far away (frontal lobe, occipital lobe, parietal lobe and cerebellum). DENSE enables us to investigate brain motion to a level of detail that has not been previously possible. The findings in this study may bring new insight into brain motion and provide useful information to improve potential imaging and therapy techniques.
-
- 3319
Computer #36 Motor Learning Induced Neuroplasticity, Revealed By fMRI-Guided Diffusion Imaging
Lee Bremner Reid¹, Martin V Sale², Ross Cunningham^{2,3}, and Stephen E Rose¹
- ¹e-Health Research Centre, CSIRO Health and Biosecurity, Brisbane, Australia, ²Queensland Brain Institute, The University of Queensland, Brisbane, Australia, ³School of Psychology, The University of Queensland, Brisbane, Australia*
- Detecting neuroplasticity requires highly sensitive measurements that may be outside the bounds of standard parcellation-seeded tractography. Earlier attempts to measure neuroplasticity induced by motor learning have utilised voxelwise analyses. Such analyses are reliant on precise registration, can have low statistical power, and provide little certainty as to the functional relevance of areas of detected change. We have measured motor-learning-induced neuroplasticity along corticomotor and thalamocortical tracts using fMRI-seeded diffusion-MRI, finding that changes uniquely occur in the corticomotor tract. Unlike previous analyses, we reveal that these changes occur throughout the corticomotor tract, not just near the grey-/white-matter interface.
-



- 3320
Computer #37 Cerebral Tissue Characterization by Magnetic Resonance Elastography and Arterial Spin Labeling
Patric Birr¹, Andreas Fehlner², Sebastian Hirsch², Florian Dittmann², Jing Guo², Jürgen Braun², Ingolf Sack², and Stefan Hetzer³
¹Physics, Humboldt University Berlin, Berlin, Germany, ²Radiology, Charité - University Medicine Berlin, Berlin, Germany, ³Berlin Center for Advanced Neuroimaging, Berlin, Germany
- Two imaging modalities, magnetic resonance elastography (MRE) and arterial spin labeling (ASL), were used to compare mechanical properties of brain tissue with regional perfusion across subcortical brain regions. An inverse correlation of stiffness ($|G^*|$) and average perfusion (CBF) was observed in deep gray matter when accounting for structurally and functionally distinct areas. In the $|G^*|$ -CBF space, globus pallidus, hippocampus, thalamus and amygdala clearly clustered from putamen and nucleus accumbens highlighting their anatomical differences in network density and vasculature. Differences in the microstructure between the striatum and other analyzed regions are not apparent by MRE or ASL alone.
-
- 3321
Computer #38 A New High-Resolution Perfusion-Weighted Imaging Technique without exogenous tracer and Its Quantitative Model
Hyunseok Seo¹, Dongchan Kim¹, Jaejin Cho¹, Kinam kwon¹, Byungjai Kim¹, and HyunWook Park¹
¹Electrical Engineering, KAIST, Daejeon, Korea, Republic of
- The proposed method is based on the perfusion model of intravoxel incoherent motion (IVIM), which assumes that perfusion is a microcirculation of blood in the capillary network. The method introduces two-types of bi-polar gradients in a radial spin-echo sequence, a new ordering of bi-polar gradients for isotropic perfusion weighting, and signal models for quantitative analysis of perfusion. To verify the proposed method, *in-vivo* imaging in 3 T MRI was performed, and the proposed method offers the high-resolution quantitative perfusion map.
-
- 3322
Computer #39 Insula Cortex Parcellation with Q-ball Residual Bootstrap Tractography Algorithm
Maria Luisa Mandelli¹, Matteo Paoletti², Nico Papinutto³, Bagrat Amirbekian^{3,4}, Roland G Henry^{3,4,5}, Eduardo Caverzasi^{3,6}, and Maria Luisa Gorno-Tempini¹
¹Neurology, Memory Aging Center, UCSF, San Francisco, CA, United States, ²Radiology, Fondazione IRCCS Policlinico San Matteo, Pavia, Italy, ³Neurology, UCSF, San Francisco, CA, United States, ⁴Bioengineering Graduate Group, Berkeley, CA, United States, ⁵Radiology and Biomedical Imaging, San Francisco, CA, United States, ⁶Brain and Behavioral Sciences, Pavia, Italy
- The insula cortex is involved in different functions, however its cortical connections have not yet been extensively explored. Whole brain tractography with Q-ball residual bootstrap algorithm was performed in 17 controls. Insula and the cortex regions were used as ending-ROIs. We found structural connections between the insula and 22 cortical regions for each hemisphere. After registered the images to the MNI space, the parcellation of the insula was obtained based on the ending-tract connected with each of the cortex region. Availability of a template atlas of insular structural connectivity would contribute to a better understanding of its multiple functions.
-
- 3323
Computer #40 An Atlas Pre-selection Method for Multi-atlas Based Brain Segmentation
Hengtong Li¹, Heather T Ma¹, Jingbo Ma¹, Chenfei Ye¹, and Shuai Mao¹
¹Department of Electronic and Information Engineering, Harbin Institute of Technology Shenzhen Graduate School, Shenzhen, China, People's Republic of
- This study proposed 4L and LV-based methods to improve the brain segmentation accuracy and eddiciency of multi-atlas brain segmentation. The atlas database contains T1 images of brain from 77 subjects. These two methods were adopted to calculate the Dice between the target image and each atlas. We compared the proposed methods with MI-based method and randomly selected method for geriatric, adult and pediatric populations. The segmentation accuracy was evaluated by Dice and the results show that the accuracy of 4L and LV-based methods has great improvement. In addition, the proposed pre-selection is more efficient.
-
- 3324
Computer #41 Characterizing Cerebral Arterial Pulsatility and Flow Waveforms from the Proximal Internal Carotid Artery to Distal Middle Cerebral Artery in Adult Volunteers Using 4D Flow MRI
Liliana E. Ma¹, Can Wu^{1,2}, Susanne Schnell¹, Christophe Chnafa³, David Steinman³, and Michael Markl^{1,2}
¹Department of Radiology, Northwestern University, Chicago, IL, United States, ²Department of Biomedical Engineering, Northwestern University, Evanston, IL, United States, ³Department of Mechanical Engineering, University of Toronto, Toronto, ON, Canada
- Characterization of cerebral arterial flow waveforms in healthy subjects can help establish a comparison baseline in studies of cerebrovascular disease and provide key inputs for computational fluid dynamic studies. The purpose of this study was to quantitatively characterize cerebral arterial waveforms in healthy adult subjects by extracting arterial pulsatility and flow waveforms along the ICA and MCA using 4D flow MRI. Our findings demonstrated no significant changes in arterial pulsatility from proximal ICA to distal MCA, although a decreasing trend was observed from the proximal to distal carotid siphon in young adults.
-
- 3325
Computer #42 Effect of window length on quasi-periodic pattern template correlation with fMRI data
Anzar Abbas¹, Waqas Majeed², Garth Thompson³, and Shella Keilholz⁴
¹Neuroscience Program, Emory University, Atlanta, GA, United States, ²School of Science and Engineering, Lahore University of Management Sciences, Lahore, Pakistan, ³Radiology and Biomedical Imaging, Yale University, New Haven, CT, United States, ⁴Biomedical Engineering, Emory

Quasi-periodic patterns that include alternation between the default mode and task positive networks are known to occur in humans and their templates can be acquired using a previously developed QPP-finding algorithm. The algorithm, however, relies on a user-specified window length for the QPP, the optimal size of which is not known. We apply the QPP algorithm on rsfMRI scans using varying window lengths and compare properties of observed QPP templates. Our results indicate an optimal window length adequately depicting QPP occurrences in human functional data. This will allow us to accurately characterize QPPs and study how they may be affecting functional connectivity measurements and brain function.

3326

Computer #43

Coupled fitting of T2 relaxometry and multi-shell diffusion weighted image data
Andrew Melbourne¹, Enrico De Vita^{2,3}, John Thornton^{2,3}, and Sebastien Ourselin¹

¹Medical Physics and Biomedical Engineering, University College London, London, United Kingdom, ²Lysholm Department of Neuroradiology, National Hospital for Neurology and Neurosurgery, London, United Kingdom, ³UCL Institute of Neurology, University College London, London, United Kingdom

This work combines information from acquisitions of diffusion-weighted and T2 relaxometry data to allow improvements in separating out multiple compartments. This is particularly useful when fitting a multi-compartment diffusion model or a multi-component T2 relaxometry model. Work of this type might allow improved fitting of multi-modal derived parameters such as the g-ratio.

3327

Computer #44

Regional variation of total sodium concentration in the healthy human brain
Ferran Prados^{1,2}, Bhavana S Solanky², Patricia Alves Da Mota², Manuel Jorge Cardoso¹, Wallace J Brownlee², Frank Riemer³, David H Miller², Xavier Golay⁴, Sebastien Ourselin¹, and Claudia Angela Michela Gandini Wheeler-Kingshott^{2,5}

¹Translational Imaging Group, Medical Physics and Biomedical Engineering, University College London, London, United Kingdom, ²NMR Research Unit, Queen Square MS Centre, Department of Neuroinflammation, UCL Institute of Neurology, University College London, London, United Kingdom, ³Department of Radiology, University of Cambridge, Cambridge, United Kingdom, ⁴Brain Repair & Rehabilitation, UCL Institute of Neurology, University College London, London, United Kingdom, ⁵Brain Connectivity Center, C. Mondino National Neurological Institute, Pavia, Italy

Non-invasive measurement of in vivo total sodium concentration (TSC) has been possible due to advances in sodium MRI at clinical field strengths. Changes in white and grey matter concentrations have been reported in a number of different diseases like Multiple Sclerosis. However, the presence of regional differences in normal healthy brain TSC has not been yet investigated. Here we use Geodesic Information Flow technique for computing per subject brain parcellations to allow differentiation of these areas and subsequently characterization of regional TSC in healthy controls.

3328

Computer #45

Effect of Gabapentin Administration on GABA and BOLD Signal in Visual Cortex of Healthy Men and Women
Ravi Prakash Reddy Nanga^{1,2}, Kosha Ruparel², Dina Appleby², Mark Elliott¹, Hari Hariharan¹, Ravinder Reddy¹, and Neill C Epperson^{2,3,4,5}

¹Radiology, University of Pennsylvania, Philadelphia, PA, United States, ²Psychiatry, Perelman School of Medicine at the University of Pennsylvania, Philadelphia, PA, United States, ³Obstetrics and Gynecology, Perelman School of Medicine at the University of Pennsylvania, Philadelphia, PA, United States, ⁴Penn Center for the Study of Sex and Gender in Health, Perelman School of Medicine at the University of Pennsylvania, Philadelphia, PA, United States, ⁵Penn Center for Women's Behavioral Wellness, Psychiatry, Perelman School of Medicine at the University of Pennsylvania, Philadelphia, PA, United States

We explored the potential for sex differences in brain Gamma-aminobutyric acid (GABA), glutamate (Glut) and neural response to an acute dose of gabapentin by using proton magnetic resonance spectroscopy (¹H-MRS) followed by functional magnetic resonance imaging (fMRI) at 7T.

3329



Computer #46

Brain volume changes during hypercapnia: Volume Reactivity
Jeroen C.W. Siero¹, Jeroen H.J. de Bresser¹, Lisa van der Kleij¹, Jill B. de Vis¹, and Jeroen Hendrikse¹

¹Radiology, University Medical Center Utrecht, Utrecht, Netherlands

Here we investigate brain volume changes upon a vasodilatory hypercapnic stimulus as a potential alternative to obtain cerebral tissue reactivity information. Using relatively standard 3D T1-weighted scans (MP-RAGE) and segmentation software we show significant volume changes (in all subjects) in subcortical deep gray matter areas which were paralleled by decreases in ventricular volume. This approach (volume reactivity) could yield novel insights on cerebral tissue reactivity in healthy and disease and be a potential alternative in cases where BOLD or ASL CVR interpretation can be ambiguous.

3330

Computer #47

The IVIM signal: a combination of two vascular pools
Gabrielle Fournet^{1,2}, Luisa Ciobanu¹, Jing Rebecca Li², Alex Cerjanic³, Brad Sutton³, and Denis Le Bihan¹

¹CEA Saclay/Neurospin, Gif-sur-Yvette, France, ²INRIA Saclay, Palaiseau, France, ³Beckman Institute of Advanced Science and Technology, Urbana, IL, United States

IntraVoxel Incoherent Motion (IVIM) imaging allows to extract perfusion parameters from a series of diffusion weighted images. We show that the standard mono-exponential model used to describe the IVIM signal can be improved by switching to a bi-exponential

model. Multiple diffusion time rat brain images were acquired at 7T and compared to numerical simulations of blood flow through the microvascular network. Our results demonstrate that the bi-exponential model better describes the data especially at short diffusion times and suggest that the IVIM signal comprises the contributions from two different vascular pools: small vessels (capillaries) and medium sized-vessels.

3331

Computer #48 REPLICABILITY OF CEREBRAL PERFUSION WITH DIFFERENT ARTERIAL SPIN LABELLING METHODS
ZHE HAN TOH¹, WENG HANG WONG¹, QING LONG GU¹, KAI-HSIANG CHUANG², KUAN-JIN LEE², JULIAN GAN³, and PHUA HWEE TANG¹

¹Department of Diagnostic and Interventional Imaging, KK WOMEN'S AND CHILDREN'S HOSPITAL, SINGAPORE, Singapore, ²Singapore Bio-Imaging Consortium, A*STAR, SINGAPORE, Singapore, ³Siemens Healthcare, Regional Headquarter, SINGAPORE, Singapore

We compared 3 versions of Arterial Spin Labelling (ASL) available (single-TI 3D-PASL, multi-TI 3D-PASL and 2D-pCASL) on 3T Siemens MRI scanner Skyra in 10 normal healthy adults with normal body mass index (BMI) at 3 different time points (baseline, 1 week later, 2 to 3 month later). There was good replicability of all 3 ASL techniques (correlation coefficients range from 0.55 to 0.77). Values acquired with these ASL techniques agree with the published normal range of cerebral blood flow values in adults. There is no significant difference in the CBF obtained with single-TI 3D-PASL, multi-TI 3D-PASL and 2D-pCASL.

Electronic Poster

Normal Brain Methods 2

Exhibition Hall

Tuesday, May 10, 2016: 13:30 - 14:30

3332

Computer #1 In-vivo Simultaneous Brain 18F FDG PET Imaging and 13C MR Spectroscopy: Initial Experience
Colm McGinnity¹, Radhouene Neji², Jane MacKewn¹, James Stirling¹, Sami Jeljeli¹, Titus Lanz³, Christian Geppert⁴, Mark Oehmigen⁵, Harald Quick⁵, Gary Cook¹, and Alexander Hammers¹

¹King's College London, London, United Kingdom, ²Siemens Healthcare, Frimley, United Kingdom, ³Rapid Biomedical, Wuerzburg, Germany, ⁴Siemens Healthcare, Erlangen, Germany, ⁵University Duisburg-Essen, Essen, Germany

We investigate the feasibility of in-vivo simultaneous brain 18F FDG PET imaging and 13C MR spectroscopy using a dedicated dual-tuned 1H-13C coil with low PET attenuation. Simultaneous in-vivo 18F FDG PET imaging and 13C unlocalized natural abundance MR spectroscopy were performed on three patients. Initial results show the technical feasibility of the simultaneous in-vivo measurement with good spectral and PET image quality.

3333

Computer #2 Optimizing dynamic MRI of the orbit during eye movement for clinical use: patient aptitude considerations.
Marco Piccirelli¹, Christopher Bockisch², Marc Bovet³, and Roger Luechinger⁴

¹Department of Neuroradiology, University Hospital Zurich, Zurich, Switzerland, ²Department of Ophthalmology, University Hospital Zurich, Zurich, Switzerland, ³ICT, University Hospital Zurich, Zurich, Switzerland, ⁴Institute for Biomedical Engineering, University and ETH Zurich, Zurich, Switzerland

To improve neuro-ophthalmologic surgery, biomechanical inside about the pathophysiological dynamic of eye movements is needed. High spatiotemporal resolution dynamic MR imaging of the orbit during eye movement shall provide such information. To enable clinical use, the acquisition design needs to accommodate limited patient capabilities to perform repetitive eye movement accurately.

3334

Computer #3 Highly-Accelerated, Self-Calibrated Stack-of-Spirals Arterial Spin Labeling Using 3D SPIRiT Reconstruction
Yulin V Chang¹, Marta Vidorreta², Ze Wang³, and John A Detre²

¹Radiology, University of Pennsylvania, Philadelphia, PA, United States, ²Neurology, University of Pennsylvania, Philadelphia, PA, United States, ³Hangzhou Normal University, Hangzhou, Zhejiang, China, People's Republic of

3D coverage of the whole brain by using RARE-refocused stack-of-2D-spirals often suffers from low temporal/spatial resolution due to the long spiral readout or long echo train. In this work we present a method that allows whole-brain coverage at 3 mm isotropic spatial resolution with one- or two-segment, accelerated acquisitions in both partition and spiral directions. The technique was applied in conjunction with background-suppressed pCASL, resulting in improved temporal/spatial resolution for quantification of cerebral blood flow.

3335

Computer #4 Quantifying cerebral blood flow with distortion-corrected pseudo-continuous arterial spin labeling
Michael N Hoff¹, Swati R Levendovszky¹, and Jalal B Andre¹

¹Radiology, University of Washington, Seattle, WA, United States

Cerebral blood flow (CBF) may be quantified using pseudo-continuous arterial spin labeling (pCASL), but pCASL suffers from image distortion due to its long echo planar imaging (EPI) readout. Phase labeling for additional coordinate encoding (PLACE) is employed here to remove distortion. EPI images and pCASL subtraction images show improved spatial accuracy when compared to a T1-weighted, anatomical reference image. This results in improved accuracy in CBF quantification, which could potentially improve the assessment of disease-specific patterns indicated by regional CBF abnormalities.

-
- 3336
Computer #5
Conductivity Determination of Deep Gray Matter Nuclei Utilizing Susceptibility-Based Delineation
Ulrich Katscher¹, Mussa Gagiyev¹, and Jakob Meineke¹

¹Philips Research Europe, Hamburg, Germany
- Deep gray matter nuclei (DGMN) in the human brain play an important role for numerous diseases like Alzheimer's disease. Thus, the characterization of DGMN in the framework of multiple MR-based physiologic parameters (like magnetic susceptibility or electric conductivity) is expected to be helpful for understanding these diseases. This study investigates - to the best of our knowledge, for the first time - the electric conductivity of DGMN in healthy volunteers, reflecting the electrolyte content of these nuclei. Conductivity determination is boosted by utilizing geometry information obtained from susceptibility maps during conductivity reconstruction.
-
- 3337
Computer #6
Optimization of the tagging region profile in super selective arterial spin labeling
Jianxun Qu¹, Bing Wu¹, and Zhenyu Zhou¹

¹MR Research China, GE Healthcare, Beijing, China, People's Republic of
- This work investigates the gradient design scheme in ssASL labeling train to improve the labeling profile. Both numerical approach and MR studies were performed. Refocused labeling and unrefocused control could generate flatter labeling region compared to currently adopted method. This was verified in in-vivo MR study.
-
- 3338
Computer #7
Acute effects of caffeine on grey matter haemodynamics
Alberto Merola¹, Esther AH Warnert¹, Michael A Germuska¹, Sharmila Khot^{1,2}, Daniel Helme², Lewys Richmond², Kevin Murphy¹, and Richard G Wise¹

¹CUBRIC, Cardiff University, Cardiff, United Kingdom, ²Department of Anesthesia and Intensive Care Medicine, Cardiff University, Cardiff, United Kingdom
- The acute effects of caffeine on haemodynamics are not well characterized across the brain with MRI. We aim at measuring these in a double-blind, crossover, placebo-controlled study on sixteen healthy, moderate caffeine consumers using mTI PASL acquisitions and a two-compartment ASL model. Results show spatial variations in the CBF and TAT response across grey matter at different levels of resolution (grey matter, ROI and voxel), with the latter presenting mixed directions. Moreover we demonstrate that great attention must be paid to physiological assumptions when modelling ASL data to estimate CBF in studies on drugs that affect brain haemodynamics.
-
- 3339
Computer #8
Blood flow velocity and pulsatility in perforating arteries of cerebral white matter during hypercapnia
Lennart Geurts¹, Alex Bhogal¹, Jeroen C.W. Siero¹, Peter R. Luijten¹, and Jaco J.M. Zwanenburg¹

¹Radiology, UMCU, Utrecht, Netherlands
- An increased blood flow pulsatility index in large cerebral arteries is a prognostic factor in stroke and has been linked to small vessel disease. Along with increased pulsatility, these patients show decreased hypercapnia induced cerebrovascular reactivity. We hypothesize that dilated vessels lose their ability to stretch and passively dampen the pulse pressure wave. The aim of this study was to shed light on how autoregulation influences the damping of the pulse pressure wave in small vessels. Our approach was to measure blood flow velocity and pulsatility changes in the perforating arteries of the white matter, during a hypercapnic breathing challenge.
-
- 3340
Computer #9
Pushing the limits of speed and accuracy for 7T GABA MR spectroscopy to reveal GABA level fluctuations in resting brain
Arjan D. Hendriks¹, Natalia Petridou¹, Catalina S. Arteaga de Castro¹, Mark W.J.M. Gosselink¹, Alessio Fracasso¹, and Dennis W.J. Klomp¹

¹Department of Radiology, University Medical Center Utrecht, Utrecht, Netherlands
- By maximizing acquisition volume, using efficient semi LASER detection with editing and macro molecular nulling, GABA can be detected at high SNR within 3 minutes. GABA concentrations were measured in the visual cortex and in a phantom containing a known concentration of GABA. A bootstrapping method was used to determine the accuracy. The results indicate that the stability and fitting accuracy of the method is sufficient to detect concentration changes of GABA higher than 3% within a short scan time of less than 3 minutes. In resting state, GABA fluctuations up to 30% are found in in-vivo brain measurements.
-
- 3341
Computer #10
Metabolic changes in the activated human visual cortex during mild hypoxia
Felipe Barreto^{1,2}, Nicholas Evanoff³, Donald Dengel³, Petr Bednarik^{1,4,5}, Ivan Tkac¹, Lynn Eberly⁶, Carlos Salmon², and Silvia Mangia¹

¹CMRR, Department of Radiology, University of Minnesota, Minneapolis, MN, United States, ²Department of Physics, University of Sao Paulo, Ribeirao Preto, Brazil, ³School of Kinesiology, University of Minnesota, Minneapolis, MN, United States, ⁴Central European Institute of Technology, Masaryk University, Brno, Czech Republic, ⁵Department of Medicine, University of Minnesota, Minneapolis, MN, United States, ⁶Division of Biostatistics, University of Minnesota, Minneapolis, MN, United States
- Previous fMRI studies have demonstrated reduced evoked vascular responses during mild hypoxia, which might indicate smaller neuronal recruitment during activation. Here we used fMRS at 7T to quantify the effects of mild hypoxia on stimulus-induced metabolic changes during visual stimulation. Our preliminary findings obtained on 6 healthy volunteers show that mild hypoxia does not result in

detectable differences of functional metabolic changes as compared to normoxia, consistent with similar functional energy demands in both conditions. Together with previous fMRI findings, our results suggest that mild hypoxia alters the neurovascular coupling, but does not result in smaller neuronal recruitment during activation.

-
- 3342
Computer #11
Quantification and normalization of Cerebral Blood Flow in rat brain using Pseudo-continuous Arterial Spin Labeling with phase-contrast-based flow measurement at 7 Tesla.
Sankar Seramani¹, Xuan Vinh To¹, Saktivel Sekar¹, Boominathan Ramasamy¹, Kishore Bhakoo¹, and Kuan Jin Lee¹
¹Singapore Bioimaging Consortium, Singapore, Singapore
- pCASL is a modified form of CASL where a short train of RF pulses reproduces CASL. pCASL sequence uses flow driven adiabatic pulses to invert the spin. The labeling efficiency of the pCASL sequence has a dependency on the velocity of the blood at the labeling. Phase contrast MRI (PCMRI) was used to measure the velocity of the blood at the labeling plane and to normalize the CBF value. In this study, we tested pCASL and PCMRI acquisition on a cohort of control rats vs. hyperglycemic rats and documented effect of varied labeling efficiency.
-
- 3343
Computer #12
High field imaging of large-scale neurotransmitter networks: concepts, graph theoretical metrics, and preliminary results
Tamar M van Veenendaal^{1,2}, Desmond HY Tse^{1,3}, Tom WJ Scheenen⁴, Dennis W Klomp⁵, Dominique M Ijff^{2,6}, Paul AM Hofman^{1,2,6}, Rob PW Rouhl^{2,6,7}, Marielle CG Vlooswijk^{2,6,7}, Albert P Aldenkamp^{2,6,7}, Walter H Backes^{1,2}, and Jacobus FA Jansen^{1,2}
¹Departments of Radiology and Nuclear Medicine, Maastricht University Medical Center, Maastricht, Netherlands, ²School for Mental Health and Neuroscience, Maastricht University, Maastricht, Netherlands, ³Department of Neuropsychology and Psychopharmacology, Maastricht University, Maastricht, Netherlands, ⁴Department of Radiology and Nuclear Medicine, Radboud University Medical Center, Nijmegen, Netherlands, ⁵Department of Radiology, University Medical Center Utrecht, Utrecht, Netherlands, ⁶Epilepsy Center Kempenhaeghe, Heeze, Netherlands, ⁷Department of Neurology, Maastricht University Medical Center, Maastricht, Netherlands
- Many studies are performed to assess structural or functional brain connectivity. However, these studies do not provide direct information on neurochemical imbalances, which underlie abnormal neuronal functioning. In this study, the concept of 'large-scale neurotransmitter networks' is proposed. The spatial neurotransmitter network was assessed in fifteen healthy participants who underwent 7T MR spectroscopic imaging. The average glutamate and GABA concentrations were computed in thirty brain regions, which were considered connected if the concentrations showed a significant correlation over all thirty participants. Both glutamate and GABA networks showed small-world characteristics, but further exploration of this concept is currently ongoing.
-
- 3344
Computer #13
Cerebral Arterial Inflow and Venous Outflow: Flow Discrepancy and Relation to Cardiac Outflow in Children and Adult Volunteers
Can Wu^{1,2}, Susanne Schnell², Ryan Kuhn³, Samantha E Schoeneman⁴, Amir R Honarmand², Michael Markl^{1,2}, and Ali Shaibani^{2,3}
¹Department of Biomedical Engineering, Northwestern University, Chicago, IL, United States, ²Department of Radiology, Northwestern University, Chicago, IL, United States, ³Department of Medical Imaging, Ann & Robert H. Lurie Children's Hospital of Chicago, Chicago, IL, United States, ⁴Rush Medical College, Chicago, IL, United States
- Abnormal cerebral venous outflow patterns may cause severe cerebrovascular disease. We aim to investigate the relationships between cerebral venous outflow and arterial inflow and between cerebral arterial inflow and cardiac outflow in adult and children volunteers using 4D flow and 2D phase-contrast MRI. The results demonstrate significant discrepancies between cerebral arterial inflow and venous outflow with larger discrepancies in children than adults. Additionally, we observed a significant association of cerebral and cardiac flow parameters with age.
-
- 3345
Computer #14
A Potential Global Brain Network Identified Using Resting State Arterial Spin Labeling
Weiyang Dai^{1,2}, Li Zhao¹, and David Alsop¹
¹Radiology, Beth Israel Deaconess Medical Center, Boston, MA, United States, ²Computer Science, State University of New York at Binghamton, Binghamton, NY, United States
- ASL global signal fluctuations, uniformly correlated across gray matter, may reflect globally correlated neural activity that would suggest a global resting network. However, physiological noise, such as cardiac and respiratory motion, could potentially contribute to the global signal fluctuations. Our results indicate that the systemic noise does not contribute to the ASL global signal fluctuation significantly. Global signal fluctuations are the dominant resting fluctuations of the ASL signal, suggesting a separate globally correlated resting state network in addition to those region-specific resting state networks.
-
- 3346
Computer #15
High Resolution quantitative T1 mapping under graded hyperoxia at 7T
Alex Bhogal¹, Jeroen C.W. Siero¹, Jaco Zwannenbergh¹, Marielle E.P. Philippens², Peter R. Luijten³, and Hans Hoogduin⁴
¹Radiology, UMC Utrecht, Utrecht, Netherlands, ²Radiotherapy, UMC Utrecht, Utrecht, Netherlands, ³UMC Utrecht, Utrecht, Netherlands, ⁴Utrecht, Netherlands
- We use native T1 (qT1) mapping to measure tissue T1 changes in response to precisely targeted, graded hyperoxic respiratory challenges at 7T.
-

- 3347
Computer #16 Quantification of the effect of head-down tilt posture on intracranial condition using MRI
Naoki Ohno¹, Tosiaki Miyati¹, Shinnosuke Hiratsuka², Shota Ishida³, Noam Alperin⁴, Satoshi Kobayashi¹, and Toshifumi Gabata⁵
- ¹Faculty of Health Sciences, Institute of Medical, Pharmaceutical and Health Sciences, Kanazawa University, Kanazawa, Japan, ²Department of Radiology, Shiga University of Medical Science Hospital, Otsu, Japan, ³Division of Health Sciences, Graduate School of Medical Science, Kanazawa University, Kanazawa, Japan, ⁴Department of Radiology, University of Miami, Miami, FL, United States, ⁵Department of Radiology, Kanazawa University, Kanazawa, Japan
- To quantify the effect of posture on intracranial condition, we assessed intracranial volume change ($\Delta ICVC$), pressure gradient (ΔPG), intracranial compliance index (ICC), and apparent diffusion coefficient (ADC) change of the brain during the cardiac cycle (ΔADC) in head-down tilt (HDT) and horizontal supine positions. ΔPG was significantly increased on HDT compared with that in the horizontal supine position because of the intracranial pressure compensatory mechanism. However, there were no significant differences in other parameters between postures. ΔPG analysis in the HDT and horizontal supine positions makes it possible to evaluate intracranial conditions concerning the intracranial pressure compensatory faculty.
-
- 3348
Computer #17 Dexamethasone Effects on Brain Function in Normal Healthy Subjects: a Magnetic Resonance Imaging Approach
Trina Kok¹, Bernice Oh², Fatima Nasrallah¹, Mary Stephenson¹, Chin-lan Tay Tony², Edwynn Kean-Hui Chiew², Johnson Fam², and Allen Eng-Juh Yeoh²
- ¹A*STAR-NUS Clinical Imaging Research Centre, Singapore, Singapore, ²National University Hospital, Singapore, Singapore
- Dexamethasone (DEX) is commonly used at varying dosages to treat a range of diseases such as altitude sickness and leukemia. Current reports of neuropsychiatric and cognitive effects after DEX administration lack determination of the pathophysiological mechanism of such effects. This work aims to investigate the neurotoxic effects of DEX in healthy subjects by collecting MR structural and 1H spectroscopy data. Analysis showed a significant reduction in brain volume structures and hippocampal GABA/water ($p < 0.02$) ratio from start to end of DEX administration, which is recovered after a washout period.
-
- 3349
Computer #18 High-Speed Whole-Brain Oximetry with a Golden-Angle Radial Imaging Sequence
Wen Cao¹, Yulin Chang¹, Suliman Barhoum¹, Zachary B Rodgers¹, Michael C Langham¹, Erin K Englund¹, and Felix W Wehrli¹
- ¹Department of Radiology, University of Pennsylvania, Philadelphia, PA, United States
- The OxFlow imaging approach allows simultaneous quantification of whole-brain venous oxygen saturation and total cerebral blood flow for the cerebral metabolic rate of oxygen. However, the current Cartesian rendition of the sequence is not ideal as the achievable temporal resolution is limited and needs to be chosen upfront. Here, we designed a golden-angle radial (GAR) encoding sequence that yields an effective temporal resolution of 1.29s and evaluated it in six subjects who underwent a paradigm of repeated breath-holds. Good agreement exists between the two methods but GAR provided superior SNR and better delineation of the temporal dynamics during the stimulus.
-
- 3350
Computer #19 Cerebrovascular reactivity measured with quantitative susceptibility mapping and TRUST MRI under hypercapnia
Jean-Christophe Brisset¹, Olga Marshall¹, Louise E Pape¹, Hanzhang Lu², and Yulin Ge¹
- ¹Radiology, New York University School of Medicine, New York, NY, United States, ²Radiology, Johns Hopkins University, Baltimore, MD, United States
- Cerebrovascular reactivity (CVR) measures the capacity of regulation of blood flow in response to vasoactive stimuli (e.g., CO₂) via changes in cerebral arterial resistance. CVR is responsible for maintaining optimal blood flow to meet the energy demand by neurovascular coupling during neuronal tasks. The defected CVR can cause transient states of inefficient blood delivery during neural activity leading to subsequent neurodysfunction and degeneration. CVR is commonly measured with mild hypercapnia (5%CO₂) ASL or BOLD MRI. The purpose of this study was to test the feasibility to measure CVR using hypercapnia MRI with quantitative susceptibility mapping (QSM) and T2-relaxation-under-spin-tagging (TRUST) techniques.
-
- 3351
Computer #20 Functional MRS at 7T and long TE
Petr Bednařik^{1,2,3}, Ivan Tkáč¹, Dinesh Deelchand¹, Felipe Barreto^{1,4}, Lynn E. Eberly⁵, Shalom Michaeli¹, and Silvia Mangia¹
- ¹CMRR, Department of Radiology, University of Minnesota, Minneapolis, MN, United States, ²Central European Institute of Technology, Masaryk University, Brno, Czech Republic, ³Department of Medicine, University of Minnesota, Minneapolis, MN, United States, ⁴Department of Physics, University of Sao Paulo, Ribeirao Preto, Brazil, ⁵Division of Biostatistics, University of Minnesota, Minneapolis, MN, United States
- With the goal of evaluating whether relaxation influences functional MRS (fMRS) results, we conducted fMRS experiments at 7T during visual stimulation using semi-LASER at 7T at long TE and short TR. The functional concentration changes of lactate (37%±6%) and glutamate (~5%±1%) observed here were consistent with previous results obtained at long TR and ultra-short TE. Small functional changes in signal intensity of NAA and Cr were also found, consistent with small changes in relaxations of those metabolites during visual stimulation.
-
- 3352
Computer #21 T2 measurements during hyperoxia in the lateral ventricles and peripheral CSF
Jolanda M Spijkerman¹, Jill B de Vis¹, Esben T Petersen², Jeroen Hendrikse¹, and Jaco J M Zwanenburg¹

¹Radiology, University Medical Center Utrecht, Utrecht, Netherlands, ²Centre for Functional and Diagnostic Imaging and Research, Danish Research Centre for Magnetic Resonance, Copenhagen University Hospital, Hvidovre, Denmark

The oxygen tension in CSF and tissue is coupled, but may be easier to measure in CSF. This work investigated the effect of O₂ administration on the T₂ of CSF. In five subjects, T₂s were mapped in the lateral ventricles and the peripheral CSF during administration of a hyperoxic gas mixture (end-tidal O₂ level: 500mmHg). In the lateral ventricles no T₂ change was observed, in the periphery a significant T₂ reduction was found under O₂ administration (T₂=1.54s) compared to baseline (T₂=1.61s), showing the feasibility to use CSF relaxation parameter mapping to detect oxygen tension changes.

3353
Computer #22 Placebo modulation of brain activity associated with orthodontic pain: a single-blind fMRI Study
Jing Jiang¹, Xin Yang², Wenli Lai², Qiyong Gong¹, and Kaiming Li¹

¹Department of Radiology, Huaxi MR Research Center, West China Hospital of Sichuan University, Chengdu, China, People's Republic of, ²West China Hospital of stomatology, Sichuan University, Chengdu, China, People's Republic of

To investigate the neural mechanism of placebo effects in orthodontic pain, we conducted a fMRI study where twenty-three volunteers, under orthodontic pain induced by separators, were scanned without placebos and followed by another scan with placebos a month later. During both scans, participants were instructed to perform a bite (with maximum strength)/no-bite block design fMRI task. Compared with the non-placebo condition, the participants with placebos demonstrated significant reduced brain activities in multiple regions, including precentral gyrus, superior frontal gyrus, superior parietal lobule and supramarginal gyrus. This study may provide new insights into the neural mechanism of analgesia by placebo.

3354
Computer #23 Spatially inhomogeneous CBV-CBF relationship across human visual cortex
Jie Huang¹

¹Department of Radiology, Michigan State University, East Lansing, MI, United States

Cerebral blood volume (CBV) is related with cerebral blood flow (CBF), and knowing this relationship may play an important role in quantitative BOLD-fMRI studies. A recent MRI study reports a varied CBV-CBF relationship both spatially and with sex. This study investigated the behaviors of CBV and CBF across the visual cortex at both rest and activation states, and the analysis showed a spatially inhomogeneous CBV-CBF relationship across the visual cortex.

3355
Computer #24 To Investigate the Regional Functional Connectivity of DMN Alterations in Hypercapnia
Hou-Ting Yang¹, Yi-Jui Liu¹, Tzu-Cheng Chao^{2,3}, Wen-Chau Chen⁴, Teng-Yi Huang⁵, You-Chia Cheng¹, Hsiao-Wen Chung⁶, Chao-Chun Lin⁷, Chia-Wei Lin⁷, and Wu-Chung Shen⁷

¹Department of Automatic Control Engineering, Feng Chia University, Taichung, Taiwan, ²Department of Computer Science and Information Engineering, National Cheng-Kung University, Tainan, Taiwan, ³Institute of Medical Informatics, National Cheng-Kung University, Tainan, Taiwan, ⁴Graduate Institute of Oncology, National Taiwan University, Taipei, Taiwan, ⁵Department of Electrical Engineering, National Taiwan University of Science and Technology, Taipei, Taiwan, ⁶Department of Electrical Engineering, National Taiwan University, Taipei, Taiwan, ⁷Department of Radiology, China Medical University Hospital, Taichung, Taiwan

To investigate the relationships among regional activity of DMN in different hypercapnia affect using resting-state functional magnetic resonance imaging (rs-fMRI). 10 healthy males were enrolled in this study. A high-resolution T1WI image and BOLD-EPI were performed by a 3 Tesla MR scanner. The CO₂ gas mixture (air, 3%, 5% and 7%) was given at the different hypercapnic for each experiment. Our results show that the functional connectivity of DMN is changed in hypercapnia. FC is slight change in 3% CO₂ fractions and gradual reduction as the CO₂ fraction increases.

Electronic Poster

Microstructure in Health & Disease

Exhibition Hall

Tuesday, May 10, 2016: 13:30 - 14:30

3356
Computer #49 Hybrid Diffusion Imaging to Detect Acute White Matter Injury after Mild TBI
Sourajit Mitra Mustafi¹, Chandana Kodiweera², Laura A. Flashman³, Thomas W. McAllister⁴, and Yu-Chien Wu¹


¹Department of Radiology and Imaging Sciences, Indiana University School of Medicine, Indianapolis, IN, United States, ²Department of Psychological and Brain Sciences, Dartmouth College, Dartmouth, NH, United States, ³Department of Psychiatry, Dartmouth Hitchcock Medical Center and New Hampshire Hospital, Lebanon, NH, United States, ⁴Department of Psychiatry, Indian University School of medicine, Indianapolis, IN, United States

In the present study we used multi-shell Hybrid Diffusion Imaging (HYDI) to study white matter changes in the acute stage of mild traumatic brain injury (mTBI). Nineteen mTBI patients and 23 trauma-controlled subjects were recruited and studied within 1 month of injury. Non-parametric diffusion analysis, q-space imaging as well as parametric analyses including conventional DTI and novel neurite orientation dispersion and density imaging (NODDI) were used to analyze the HYDI data. Only intra-axonal volume fraction of the NODDI model showed significant and diffuse decrease in white matter of the mTBI patients.

-
- 3357
Computer #50
Aberrant Structural and Functional Networks Associated with Comorbidity of Depression and Mild Traumatic Brain Injury
Ping-Hong Yeh^{1,2}, Cheng Guan Koay², John Graner², Jamie Harper², Elyssa B. Sham², Jeannine Mielke², Tara Staver², Wei Liu², John Ollinger², Terrence Oakes², and Gerard Riedy²
- ¹Henry M Jackson Foundation for the Advancement of Military Medicine, Bethesda, MD, United States, ²National Intrepid Center of Excellence, Bethesda, MD, United States*
- Comorbid depression and PTSD are common among military traumatic brain injury population. This study assess brain structural and functional networks affected in military service members diagnosed with mild TBI.
-
- 3358
Computer #51
Acute white matter changes within 24 hours and at 8 days following sport-related concussion: a diffusion tensor and diffusion kurtosis imaging study
Daniel V. Olson¹, Melissa A. Lancaster^{2,3}, Michael A. McCrea^{2,3}, and L. Tugan Muftuler²
- ¹Biophysics, Medical College of Wisconsin, Milwaukee, WI, United States, ²Neurosurgery, Medical College of Wisconsin, Milwaukee, WI, United States, ³Neurology, Medical College of Wisconsin, Milwaukee, WI, United States*
- The aim of this study was to characterize acute white matter changes within 24 hours and at 8 days following sport-related concussion in a group of young adult athletes. Both diffusion tensor and diffusion kurtosis tensor parameters were compared between concussed athletes and controls. The concussed group demonstrated widespread decrease in mean, axial, and radial diffusivity and increased axial kurtosis compared to the controls. Although diffusion effects became more extensive between the two time points, clinical measure differences between groups were nonsignificant at the 8-day follow-up. These findings may have significant implications for the clinical management of sport-related concussions.
-
- 3359
Computer #52
Finding biomarkers of cognitive decline in active professional fighters with multimodal MRI and exploring the longitudinal relationship of these biomarkers with cognitive decline
Virendra R Mishra¹, Xiaowei Zhuang¹, Karthik Sreenivasan¹, Zhengshi Yang¹, Sarah Banks¹, Charles Bernick¹, and Dietmar Cordes¹
- ¹Cleveland Clinic Lou Ruvo Center for Brain Health, Las Vegas, NV, United States*
- Several cross-sectional MRI studies have shown structural differences in professional fighters but there has been no results reported in longitudinal studies of such active fighters. The professional fighters brain health study (PFBHS) is a longitudinal study of active professional fighters with age-matched healthy controls using multimodal MRI methods. In this study, we show that the features/biomarkers predicting cognitive decline at baseline are sensitive and specific over time in our cohort of longitudinal active fighters. Our study opens a new window to predict and monitor cognitive decline in patients with traumatic brain injuries.
-
- 3360
Computer #53
Robust fiber crossing invariant analysis of white matter microstructure in acute mild traumatic brain injury
Mehrbod Mohammadian^{1,2}, Timo Roine³, Jussi Hirvonen^{2,4}, Timo Kurki², and Olli Tenovuo^{1,2}
- ¹Department of Rehabilitation and Brain Trauma, Turku University Hospital, Turku, Finland, ²Department of Clinical Medicine, University of Turku, Turku, Finland, ³Minds-Vision Lab, Department of Physics, University of Antwerp, Antwerp, Belgium, ⁴Department of Radiology, Turku University Hospital, Turku, Finland*
- We used a robust diffusion MRI approach to analyze global microstructural abnormalities in mild traumatic brain injury (mTBI) without confounding effects of complex fiber configurations. Microstructural properties of white matter skeleton were investigated, but only voxels with a single fiber orientation detected with constrained spherical deconvolution were included. In addition, whole-brain fiber tractograms were investigated. We studied 107 patients with mTBI and 28 age-matched control subjects. We found that fractional anisotropy was significantly decreased in mTBI, while mean diffusivity and radial diffusivity were increased. These differences were more significant when the analysis was restricted to single-fiber voxels.
-
- 3361
Computer #54
Gray Matter Alterations Using Voxel-Based Morphometry May Not Reflect Changes In Morphometry: A Study of Mild Traumatic Brain Injury
Sohae Chung^{1,2}, Yadi Li³, Jacqueline Smith^{1,2}, Steven R Flanagan⁴, and Yvonne W Lui^{1,2}
- ¹Center for Advanced Imaging Innovation and Research (CAI2R), Department of Radiology, New York University School of Medicine, New York, NY, United States, ²Bernard and Irene Schwartz Center for Biomedical Imaging, Department of Radiology, New York University School of Medicine, New York, NY, United States, ³Department of Radiology, The Affiliated Ningbo Medical Treatment Center Lihuli Hospital of Ningbo University, Zhejiang, China, People's Republic of, ⁴Department of Rehabilitation Medicine, New York University Langone Medical Center, New York, NY, United States*
- Voxel-based morphometry (VBM) analysis has been used to detect morphometric changes of the GM after mild traumatic brain injury (mTBI). Spatially normalized and modulated GM density from VBM analysis is typically interpreted as GM volume. VBM is, however, sensitive not only to changes in volume but to variations in T1 relaxation. In this study, we investigated alterations in GM density using simulated images and VBM followed by an in vivo study of cortical GM morphometry using GM density and cortical thickness in mTBI patients and matched controls.
-



- 3362
Computer #55 Bi-directional changes in fractional anisotropy are associated with altered fiber tracts after experimental TBI
Neil G Harris¹, Derek R Verley², Boris A Gutman³, and Richard L Sutton¹
- ¹Neurosurgery, UCLA, Los Angeles, CA, United States, ²Neurosurgery, University of California at Los Angeles, Los Angeles, CA, United States, ³Engineering, Radiology, & Ophthalmology, University of Southern California, Los Angeles, CA, United States
- Diffusion tensor imaging (DTI) is now widely used in both clinical and experimental research for studying pathology related to traumatic brain injury. However, studies report a wide range of DTI indices that are not easily ascribed to post-injury time-point, injury severity or developmental stage. In order to provide further information to help interpret these often complex changes we obtained DTI data before and after TBI using the well-known, clinically relevant rodent controlled cortical impact (CCI) model of TBI. In addition to the expected decreases in fractional anisotropy (FA) around the primary injury site which were associated with myelin breakdown and neurofilament loss, we found significant increases in FA within subcortical regions that were not associated with gliosis or fiber tract degeneration. Fiber tract density was decreased in regions of lowered FA but significantly increased only in subcortical regions associated with increased FA. High FA region seeded for tractography yielded significantly increased fiber length compared to pre-injury. These data provide additional insight into the interpretation of DTI indices following TBI.
-
- 3363
Computer #56 White Matter Integrity In Acute Mild Traumatic Brain Injury: A Diffusion Kurtosis MRI Study
Sohae Chung^{1,2}, Els Fieremans^{1,2}, Dmitry S Novikov^{1,2}, Jacqueline Smith^{1,2}, Steven R Flanagan³, and Yvonne W Lui^{1,2}
- ¹Center for Advanced Imaging Innovation and Research (CAI2R), Department of Radiology, New York University School of Medicine, New York, NY, United States, ²Bernard and Irene Schwartz Center for Biomedical Imaging, Department of Radiology, New York University School of Medicine, New York, NY, United States, ³Department of Rehabilitation Medicine, New York University Langone Medical Center, New York, NY, United States
- Mild traumatic brain injury (mTBI) is a growing public health problem. Most patients recover quickly, but some patients may suffer from serious symptoms. In this study, we investigated white matter (WM) changes in mTBI in terms of compartment specific WM tract integrity (WMTI) metrics derived from diffusion kurtosis imaging (DKI), such as intra-axonal diffusivity (D_{axon}), extra-axonal axial and radial diffusivities ($D_{e,a}$ and $D_{e,r}$), and axonal water fraction (AWF). The observed decreases in D_{axon} and $D_{e,a}$ suggest that increased restrictions along the axons, both inside and outside, such as possible axonal beading, could occur acutely after injury.
-
- 3364
Computer #57 Diffusion tensor imaging analysis to assess stem cell therapy efficacy in traumatic brain injury
Nastaren Abad^{1,2}, Abdol Aziz O. Ould Ismail^{1,2}, Ali Darkazali³, Jens T. Rosenberg¹, Cathy Levenson³, and Samuel Colles Grant^{1,2}
- ¹Center for Interdisciplinary MR, National High Magnetic Field Laboratory, Tallahassee, FL, United States, ²Chemical & Biomedical Engineering, Florida State University, Tallahassee, FL, United States, ³Biomedical Sciences and Program in Neuroscience, Florida State University, Tallahassee, FL, United States
- Traumatic Brain Injury (TBI) interferes with the functionality of the brain due to heterogeneous complications that continue after the initial trauma. As a result, stem cell therapy is viewed as a potential treatment approach that can be instituted during the chronic phase of TBI. This study employs Diffusion Tensor Imaging (DTI) to non-destructively probe the pathological impacts of endogenous Neural Progenitor Cells (NPC) and exogenous Mesenchymal Stem Cells (MSC) in a rodent model of TBI. This study represents the first investigation of the efficacy of MSC treatment in TBI and the potential synergistic effect of MSC and NPC.
-
- 3365
Computer #58 Tract-based longitudinal analysis of microstructural diffusion changes of mild traumatic brain injury in sports
Maged Goubran¹, Wei Bian¹, Brian Boldt¹, Mansi Parekh¹, David Douglas¹, Eugene Wilson¹, Lex Mitchell¹, Scott Anderson², Gerry Grant³, Huy Do¹, and Michael Zeineh¹
- ¹Department of Radiology, Stanford University, Stanford, CA, United States, ²Sports Medicine, Stanford University, Stanford, CA, United States, ³Department of Neurosurgery, Stanford University, Stanford, CA, United States
- While many cross sectional DTI studies have been performed for mild TBI in sports, very few longitudinal investigations have been performed. We present here a large longitudinal study assessing white matter integrity in high vs. low contact sports employing whole brain automated tractography and NODDI. We performed a tract-based analysis at baseline and longitudinally over 3 years, with both experiments localizing diffusion changes along the callosum forceps minor, left thalamic radiation and the superior longitudinal fasciculus. We have also shown that diffusion metrics correlate with cognition as assessed by the SCAT scores.
-
- 3366
Computer #59 Decrease in myelin water fraction of global white matter and white matter tracts in traumatic brain injury (TBI).
Bretta Russell-Schulz¹, Irene Vavasour², Jing Zhang², Alex MacKay^{1,3}, Shaun Porter⁴, Delrae Fawcett⁵, Ivan Torres⁵, William Panenka⁵, Lara Boyd⁶, and Naznin Virji-Babul⁴
- ¹UBC MRI Research Centre, Radiology, University of British Columbia, Vancouver, BC, Canada, ²Radiology, University of British Columbia, Vancouver, BC, Canada, ³Physics & Astronomy, University of British Columbia, Vancouver, BC, Canada, ⁴Physical Therapy, University of British Columbia, Vancouver, Canada, ⁵Psychiatry, University of British Columbia, Vancouver, Canada, ⁶Physical Therapy, University of British Columbia, Vancouver, BC, Canada
- Chronic traumatic brain injury (TBI) was examined using myelin water fraction (MWF) in global white matter and tracts for subjects undergoing intensive cognitive training (Arrowsmith Program) compared to age and gender matched controls. MWF was significantly lower in TBI subjects and correlations were found between MWF and cognitive scores of fluid and crystallized ability. However, after 3 months of cognitive training no significant differences were found in MWF in TBI subjects.

-
- 3367
Computer #60 Cerebellar surface mapping using T1 and T2* relaxometry at ultrahigh-field MRI: from macroscale to microscale?
Yohan Boilat¹, Pierre-Louis Bazin², Kieran O'Brien^{3,4}, Mário João Fartaria de Oliveira^{5,6}, Guillaume Bonnier^{1,6,7}, Gunnar Krueger^{6,8}, Wietske van der Zwaag^{1,9}, and Cristina Granziera^{1,6,7,10}
- ¹Ecole Polytechnique Fédérale de Lausanne, Lausanne, Switzerland, ²Max Planck Institute for Human Cognitive and Brain Sciences, Leipzig, Germany, ³Siemens Healthcare Pty Ltd., Brisbane, Australia, ⁴University of Queensland, St-Lucia, Australia, ⁵University of Lausanne, Lausanne, Switzerland, ⁶Advanced Clinical Imaging Technology Group, Siemens, Lausanne, Switzerland, ⁷Centre Hospitalier Universitaire Vaudois, Lausanne, Switzerland, ⁸Healthcare Sector IM&WS S, Siemens Schweiz AG, Lausanne, Switzerland, ⁹Spinoza Centre for Neuroimaging, Amsterdam, Switzerland, ¹⁰Massachusetts General Hospital and Harvard Medical School, Charlestown, MA, United States*
- The quantitative properties of the cerebellum were assessed by acquiring T₁ and T₂*-contrasts at 7T and mapping these onto the cerebellar cortex. T₁ maps showed medial-lateral alternating stripes of different intensities while T₂* values were homogeneously distributed across the lobes. This study showed the heterogeneity of the cerebellar cortex in terms of tissue content, which in part parallels a well-established gene expression pattern.
-
- 3368
Computer #61 Characterizing the cortical terminations of the arcuate fasciculus with diffusion microstructure
Kirsten Mary Lynch¹, Arthur Toga¹, and Kristi Clark¹
- ¹USC Mark and Mary Stevens Neuroimaging and Informatics Institute, University of Southern California, Los Angeles, CA, United States*
- The arcuate fasciculus (AF) is a group of association fibers consisting of 3 subcomponents that link perisylvian language centers in the frontal, temporal, and parietal lobes. The purpose of this study is to characterize the diffusion microstructural properties and functional outcomes of the cortical AF terminations in the right and left hemispheres. Multi-shell diffusion models were used to extract relative compartment densities, which were compared in cortical regions where AF fibers terminated. The results of this study show that perisylvian language centers exhibit differential cytoarchitecture that can be measured with *in vivo* MRI measures.
-
- 3369
Computer #62 A simple method to scale the macromolecular pool size ratio for computing the g-ratio in vivo
Mara Cercignani^{1,2}, Giovanni Giulietti², Nick Dowell¹, Barbara Spano², Neil Harrison¹, and Marco Bozzali²
- ¹Clinical Imaging Sciences Centre, Brighton and Sussex Medical School, Brighton, United Kingdom, ²Neuroimaging Laboratory, Santa Lucia Foundation, Rome, Italy*
- previous work suggested that the myelin volume fraction (MVF) is proportional to the macromolecular pool size ratio, F, derived from Magnetization Transfer (MT). However the proportionality constant seems to be dependent on the specific MT model, and requires histological validation. Here we propose a simple method based to derive such a constant.
-
- 3370
Computer #63 Axon Loss Detected by Diffusion Basis Spectrum Imaging (DBSI) in the Absence of Atrophy
Tsen-Hsuan Lin¹, Peng Sun¹, Yong Wang^{1,2,3,4}, and Sheng-Kwei Song^{1,3,4}
- ¹Radiology, Washington University School of Medicine, St. Louis, MO, United States, ²Obstetric and Gynecology, Washington University School of Medicine, St. Louis, MO, United States, ³The Hope Center for Neurological Disorders, Washington University School of Medicine, St. Louis, MO, United States, ⁴Biomedical Engineering, Washington University in St. Louis, St. Louis, MO, United States*
- The extent of axonal loss plays a significant role in irreversible neurological impairment in optic nerve crush (ONC). We detected significant 15% axonal loss in the absence of statistically significant atrophy using diffusion basis spectrum imaging (DBSI) 7 days after ONC in mice.
-
- 3371
Computer #64 Oral citicoline treatment improves visuomotor response and white matter integrity in the visual pathway after chronic intraocular pressure elevation
Yolandi van der Merwe^{1,2}, Xiaoling Yang^{1,3}, Leon C. Ho^{1,4}, Yu Yu⁵, Christopher K Leung^{6,7}, Ian P. Conner^{2,3}, Seong-Gi Kim^{1,8}, Gadi Wollstein³, Joel S Schuman^{2,3}, Michael B Stokete³, and Kevin C Chan^{1,3}
- ¹Neuroimaging Laboratory, University of Pittsburgh, Pittsburgh, PA, United States, ²Department of Bioengineering, University of Pittsburgh, Pittsburgh, PA, United States, ³Department of Ophthalmology, School of Medicine, University of Pittsburgh, Pittsburgh, PA, United States, ⁴Department of Electrical and Electronic Engineering, University of Hong Kong, Hong Kong, China, People's Republic of, ⁵Division of Biomedical Engineering, Hong Kong University of Science and Technology, Hong Kong, China, People's Republic of, ⁶University Eye Center, Hong Kong Eye Hospital, Hong Kong, China, People's Republic of, ⁷Department of Ophthalmology and Visual Sciences, Chinese University of Hong Kong, Hong Kong, China, People's Republic of, ⁸Center for Neuroscience Imaging Research, Institute for Basic Science, Sungkyunkwan University, Kuwon, Korea, Democratic People's Republic of*
- Glaucoma is a neurodegenerative disease that can cause irreversible blindness. Lowering intraocular pressure (IOP) is currently the only clinically approved treatment method for glaucoma, however the disease may still progress in some patients after lowering IOP. Citicoline has been suggested as a potential therapeutic for neurodegenerative diseases including glaucoma, but its neuroprotective effect remains incompletely understood. In this study, we determined the effects of oral citicoline treatment on visual function and white matter preservation in an experimental glaucoma model. The results show that citicoline treatment slowed the worsening of visual acuity and preserved white matter integrity along the visual pathway
-
- 

3372

Computer #65 G-ratio distribution within the healthy population: the effect of age and gender
Mara Cercignani^{1,2}, Giovanni Giulietti³, Nick Dowell⁴, Matthew Gabel⁴, Rebecca Broad⁴, P Nigel Leigh⁴, Neil Harrison⁴, and Marco Bozzali³

¹Clinical Imaging Sciences Centre, Brighton and Sussex Medical School, Brighton, United Kingdom, ²Neuroimaging Laboratory, Santa Lucia Foundation, Rome, Italy, ³Santa Lucia Foundation, Rome, Italy, ⁴Brighton and Sussex Medical School, Brighton, United Kingdom

This paper investigates the variability of the g-ratio (the ratio of the inner to the outer diameter of a myelinated axon) as a function of age and gender in the healthy population. By combining magnetization transfer and diffusion MRI, the mean g-ratio of 20 white matter tracts was estimated, revealing no gender differences, and a systematic increase with age. Right vs left hemisphere differences were also detected.

3373

Computer #66 Transient Changes in White Matter Microstructure during Anesthesia
Cheuk Ying Tang¹, Victoria X Wang², Johnny C Ng², Stacie Deiner³, Rafael O'Halloran², Patrick McCormick³, Prantik Kundu², Lazar Fleyshe², Angela Sanchez³, Kleopoulos Steven⁴, and Mark Baxter⁵

¹Radiology & Psychiatry, Icahn School of Medicine at Mount Sinai, New York, NY, United States, ²Radiology, Icahn School of Medicine at Mount Sinai, New York, NY, United States, ³Anesthesiology, Icahn School of Medicine at Mount Sinai, New York, NY, United States, ⁴Icahn School of Medicine at Mount Sinai, New York, NY, United States, ⁵Neuroscience, Icahn School of Medicine at Mount Sinai, New York, NY, United States

The effect of general anesthesia was studied in brain white matter of healthy control elderly subjects. DTI measures were compared between awake and general anesthesia conditions. We found significant transient decreases in Fractional Anisotropy and increases in Mean Diffusivities throughout the brain.

3374

Computer #67 Mouse Brain Microscopy with Loop Gap Resonator at 15T
Ouri Cohen^{1,2}, Frederick A. Schroeder^{1,2}, and Jerome L. Ackerman^{1,2}

¹Athinoula A. Martinos Center, Charlestown, MA, United States, ²Radiology, Massachusetts General Hospital, Boston, MA, United States

Construction of a loop-gap-resonator RF coil for MR microscopy of ex vivo mouse brains at 15T is described. The large signal obtained allowed acquisition of 20 μ m³ isotropic voxels, the highest resolution yet achieved in MR mouse brain imaging. Importantly, the high resolution allowed clear identification of multiple brain structures and will be of interest to researchers working with various mouse models.

3375

Computer #68 Super-Resolution MR imaging of ex-vivo eye-globe structures at 7T
Se-Hong Oh¹, Stephen E. Jones¹, Arun Singh², and Mark J. Lowe¹

¹Imaging Institute, Cleveland Clinic Foundation, Cleveland, OH, United States, ²Department of Ophthalmic Oncology, Cole Eye Institute, Cleveland Clinic Foundation, Cleveland, OH, United States

We demonstrate a high-resolution ex-vivo globe image using 7T. With voxel size of 250 μ m isotropic resolution, detailed structures of the globe were clearly identified. Our results show that the high-resolution MR imaging is particularly useful in helping to visualize inner structure of eye-globe. Moreover, it is successfully demonstrated the sensitivity to choroidal melanoma. In addition, we have performed MRI scans using human globe specimens to investigate the contribution of fixation to the evolution of T₂ over time and measured SNR changes as function of the number of excitations to gain some insight into the optimal average number.

3376

Computer #69 An automated pipeline for mouse brain morphometric MRI
Marco Pagani^{1,2}, Mario Damiano¹, Alberto Galbusera¹, Sotirios A Tsafaris^{3,4}, and Alessandro Gozzi¹

¹Istituto Italiano di Tecnologia, Rovereto, Italy, ²Center for Mind and Brain Sciences, Rovereto, Italy, ³IMT - Institute for Advanced Studies, Lucca, Italy, ⁴Institute of Digital Communications, School of Engineering, The University of Edinburgh, Edinburgh, United Kingdom

We provide a detailed description of registration-based procedures for voxel based morphometry, cortical thickness estimation and automated anatomical labelling of the mouse brain. To illustrate our procedures, we described their application to quantify morphological differences in two inbred mouse strains characterised by different social behaviour. We show that our approach can reliably detect both focal and large scale gray matter alterations using complementary readouts. The operational workflows described here are expected to help the implementation of rodent morphoanatomical methods by non-expert users, and promote the use of these tools across the preclinical neuroimaging community.

3377

Computer #70 Magnetic Resonance Myelin G-ratio mapping for the Brain and Cervical Spinal Cord: 10 Minutes Protocol for Clinical Application
Masaaki Hori^{1,2}, Nikola Stikov³, Ryuji Nojiri², Yasuaki Tsurushima², Katsutoshi Murata⁴, Keiichi Ishigame², Kouhei Kamiya⁵, Yuichi Suzuki⁵, Koji kamagata¹, and Shigeki Aoki¹

¹Radiology, Juntendo University School of Medicine, Tokyo, Japan, ²Tokyo Medical Clinic, Tokyo, Japan, ³Ecole Polytechnique, University of Montreal, Montreal, QC, Canada, ⁴Siemens Japan, Tokyo, Japan, ⁵Radiology, The University of Tokyo, Tokyo, Japan

The purpose of this exhibit is to present the feasibility of MR g-ratio mapping for whole brain and cervical spinal cord using a 10 minute protocol. This protocol is appropriate for clinical use and provides reasonable image quality for clinical diagnosis. In vivo MR g-ratio



mapping warrants daily clinical use as it has potential to provide additional information about WM microstructure and its changes in pathology.

3378
Computer #71 Macromolecular proton fraction as an ultimate source of brain tissue contrast in ultra-high magnetic fields
Anna V Naumova^{1,2}, Andrey E Akulov³, Alexandr V Romashchenko³, Oleg B Shevelev³, Marina Yu Khodanovich², and Vasily L Yarnykh^{1,2}

¹Radiology, University of Washington, Seattle, WA, United States, ²National Research Tomsk State University, Tomsk, Russian Federation, ³Institute of Cytology and Genetics, Novosibirsk, Russian Federation

This study provides methodological background for neuroimaging applications of fast 3D MPF mapping in ultra-high magnetic fields and demonstrates that MPF presents the most effective source of high-field brain tissue contrast. Unique contrast features, high spatial resolution, and the capability to provide quantitative information about myelination make MPF mapping an ultimate tool for small animal neuroimaging in high magnetic fields.

3379
Computer #72 Whole human brain diffusion MRI at 450µm post mortem with dwSSFP and a specialized 9.4T RF-coil
Francisco Lagos Fritz¹, Sean Foxley², Shubharthi Sengupta¹, Robbert Harms¹, Svenja Caspers³, Karl Zilles³, Desmond HY Tse¹, Benedikt Poser¹, Karla L Miller², and Alard Roebroek¹

¹Dept. of Cognitive Neuroscience, Faculty of Psychology & Neuroscience, Maastricht University, Maastricht, Netherlands, ²FMRIB Centre, University of Oxford, Oxford, United Kingdom, ³Institute of Neuroscience and Medicine (INM-1), Research Centre Jülich, Jülich, Germany

The investigation of whole human brains post mortem with large bore systems can achieve a resolution considerably superior to that achievable in-vivo. However, the achievable resolutions and contrast are limited, especially for diffusion MRI (dMRI), by gradient performance, non-optimized RF-coils, and RF-field inhomogeneity and decreasing T2 with increasing B0. Here we report on ultrahigh resolution (450µm) diffusion imaging of the whole human brain showing exquisite spatial definition. This is achieved using a specialized 9.4T 8Ch parallel transmit (pTx), 24Ch receive RF-coil and a diffusion weighted steady state free precession (dwSSFP) sequence extended with a kt-points excitation pulse for B1+ homogenization

Electronic Poster

Neurodegeneration

Exhibition Hall

Tuesday, May 10, 2016: 13:30 - 14:30

3380
Computer #73 Does tau pathology play a role in abnormal iron deposition in Alzheimer's Disease? A quantitative susceptibility mapping study in the rTg4510 mouse model of Tauopathy
James O'Callaghan¹, Holly Holmes¹, Nicholas Powell¹, Jack Wells¹, Ozama Ismail¹, Ian Harrison¹, Bernard Siow¹, Michael O'Neill², Emily Catherine Collins³, Karin Shmueli⁴, and Mark Lythgoe¹

¹Centre for Advanced Biomedical Imaging, University College London, London, United Kingdom, ²Eli Lilly & Co. Ltd, Surrey, United Kingdom, ³Eli Lilly and Company, Indianapolis, IN, United States, ⁴Department of Medical Physics and Biomedical Engineering, University College London, London, United Kingdom

In this work, quantitative susceptibility mapping (QSM) and T2* mapping were used to investigate iron accumulation both *in-vivo* and *ex-vivo* in a mouse model of Alzheimer's Disease exhibiting tau pathology for the first time. Magnetic susceptibility increases relative to controls were identified in grey matter and white matter brain regions and may indicate sensitivity to tissue iron content. QSM in this mouse model may therefore provide a non invasive method by which to dissect the relationship between iron and tau pathology in Alzheimer's Disease.

3381
Computer #74 T2-weighted imaging of substantia nigra pars compacta shows increased iron deposition in ventral lateral tier
Jason Langley¹, Jan Sedlacik², Daniel E Huddleston³, Xiaoping Hu¹, Jens Fiehler², and Kai Boelmans⁴

¹Department of Biomedical Engineering, Emory University & Georgia Tech, Atlanta, GA, United States, ²Department of Neuroradiology, University Medical Center Hamburg-Eppendorf (UKE), Hamburg, Germany, ³Department of Neurology, Emory University, Atlanta, GA, United States, ⁴Department of Neurology, University Medical Center Würzburg, Würzburg, Germany

Recent results found that the SN seen in neuromelanin sensitive MRI and iron sensitive T₂-weighted contrasts is located in disparate spatial positions in controls. Since iron is known to be deposited in the SN after onset of Parkinson's disease(PD), we re-examine iron sensitive measurements with respect to these new findings in this abstract. Specifically, we find that the SN seen in T₂-weighted contrasts is enlarged in inferiorly and medially when compared to controls. Most of this discrepancy happens in the NM SN and we found the overlap to be an incredibly sensitive marker for PD ($p < 10^{-15}$).

3382
Computer #75 Association of Brain Iron Deposition in Parkinson's Disease with Comorbidities of Visual Hallucinations: An ROI-based Quantitative Susceptibility Mapping Study
Darrell Ting Hung Li¹, Edward Sai Kam Hui¹, Queenie Chan², Nailin Yao³, Siew-eng Chua⁴, Grainne M. McAlonan^{4,5}, Shu Leong Ho⁶, and Henry Ka Fung Mak¹

¹Department of Diagnostic Radiology, The University of Hong Kong, Hong Kong, Hong Kong, ²Philips Healthcare, Hong Kong, Hong Kong, ³Department of Psychiatry, Yale University, New Haven, CT, United States, ⁴Department of Psychiatry, The University of Hong Kong, Hong Kong, Hong Kong, ⁵Department of Forensic and Neurodevelopmental Science, King's College London, London, United Kingdom, ⁶Department of Medicine, The University of Hong Kong, Hong Kong, Hong Kong

Abnormal iron accumulation in the brain may cause oxidative-stress-induced neurodegeneration, which is one of the hypothesis of nigral cell death in PD. It was also believed that non-motor symptoms of PD patients are associated with the increased of brain iron content. This study examined the iron concentration in several subcortical structures of PD patients with visual hallucinations by using the QSM technique. Higher magnetic susceptibility was observed in the hippocampus of this patient group. The result supported the hypothesis that hippocampal abnormality could induce visuospatial memory impairment which may be the cause of visual hallucination in PD patients.

-
- 3383
Computer #76
Evaluation of gray matter degeneration in Parkinson's disease by using neurite-orientation dispersion and density imaging: Analysis by gray matter-based spatial statistics
Koji Kamagata¹, Kouhei Tsuruta², Taku Hatano³, Keigo Shimoji⁴, Masaaki Hori¹, Ayami Okuzumi³, Misaaki Nakazawa², Syo Murata², Ryo Ueda², and Shigeki Aoki¹
- ¹Department of Radiology, Juntendo University, Tokyo, Japan, ²Department of Radiological Sciences, Tokyo Metropolitan University, Tokyo, Japan, ³Department of Neurology, Juntendo University, Tokyo, Japan, ⁴Department of Diagnostic Radiology, Tokyo Metropolitan Geriatric Hospital, Tokyo, Japan
- In this study, neurite-orientation dispersion and density imaging were used to estimate structural changes of neurites in the gray matter of the brain, which is the earliest pathological change in patients with PD. The results showed a significant decrease in the intracellular volume fraction in the right amygdala and right putamen in PD, suggesting a decrease in neurite density that may reflect actual pathological change. Given that NODDI could detect pathological changes at the earliest stages in PD, it may be useful for early diagnosis.

-
- 3384
Computer #77
Evaluation of different high-pass filter on the susceptibility in patients Parkinson's disease and controls
Gerd Melkus^{1,2}, Santanu Chakraborty^{1,2}, and Fahad A Essbaiheen^{1,2,3}
- ¹Medical Imaging, The Ottawa Hospital, Ottawa, ON, Canada, ²Radiology, University of Ottawa, Ottawa, ON, Canada, ³King Saud University, Riyadh, Saudi Arabia
- Quantitative susceptibility mapping (QSM) was found as a useful method to evaluate neurodegenerative diseases such as Parkinson's disease. For QSM reconstruction background field removed phase data is needed, but for retrospective studies only high-pass filtered data might be available. In this study we analyzed the influence of different high-pass filtered phase images on the susceptibility assessment for volunteers and Parkinson's disease patients and compared the results to QSM estimation using background field removed phase data. With increasing high-pass filter strength consistently lower susceptibility results, but up to a certain filter strength differences in susceptibility can still be distinguished.

-
- 3385
Computer #78
Imaging effects of memantine treatment in a mouse model of Huntington disease using evoked and resting-state fMRI
Wei-Tang Chang¹, Fiftarina Puspitasari¹, Ling-Yun Yeow¹, Hui-Chien Tay¹, Marta Garcia Miralles², Katrianne Bethia Koh², Liang-Juin Tan², Mahmoud POULADI^{2,3}, and Kai-Hsiang Chuang¹
- ¹SBIC, A*STAR, Singapore, Singapore, ²TLGM, A*STAR, Singapore, Singapore, ³Department of Medicine, National University of Singapore, Singapore, Singapore
- Huntington disease (HD) is an incurable neurodegenerative disease. Recently, memantine (MMT) was found to be effective delaying the progression of disease phenotypes in a mouse model of HD. Here we applied resting-state fMRI to evaluate functional connectivity in HD and the MMT treatment effect and its behavioral correlates. The results of forepaw stimulation reduced evoked responses though significance was hampered by large individual variation. Interestingly, functional connectivity outside of DMN, but not within DMN, was decreased by HD. With MMT treatment, the connectivity increased in general. The FC relevant to the behavioral test also showed behavioral correlates.

-
- 3386
Computer #79
Developmental White Matter Alterations in Monkey Brains with Huntington's Disease
Yuguang Meng¹, Anthony W.S. Chan^{2,3}, and Xiaodong Zhang^{1,3}
- ¹Yerkes Imaging Center, Yerkes National Primate Research Center, Emory University, Atlanta, GA, United States, ²Department of Human Genetics, School of Medicine, Emory University, Atlanta, GA, United States, ³Division of Neuropharmacology and Neurologic Diseases, Yerkes National Primate Research Center, Emory University, Atlanta, GA, United States
- This study examined the developmental changes of white matter integrity in rhesus monkey brains with the HD gene mutation using diffusion tensor imaging (DTI). Widespread developmental alterations are seen in striatum, and the frontal, motor, sensory and visual brain areas. The findings reveal the temporal-spatial evolution of abnormal white matter maturation during the development of the brain with the Huntington's Disease, and suggest altered neural substrates associated with motor and cognitive dysfunctions in HD patients.

-
- 3387
Diffusion tensor imaging of the substantia nigra in Parkinson's disease revisited

Computer #80 Jason Langley¹, Daniel E Huddleston², Michael Merritt¹, Xiangchuan Chen¹, Rebecca McMurray², Michael Silver², Stewart A Factor², and Xiaoping Hu¹

¹Department of Biomedical Engineering, Emory University & Georgia Tech, Atlanta, GA, United States, ²Department of Neurology, Emory University, Atlanta, GA, United States

Inconclusive results from prior diffusion tensor imaging-based studies can be attributed to variability in location of regions of interest used to define the substantia nigra and its subcomponents. We apply recent findings from neuromelanin sensitive MRI to standardize regions of interest for the substantia nigra. Differences in fractional anisotropy and mean diffusivity were found in the neuromelanin sensitive substantia nigra but not in the substantia nigra defined in the b0 image.

3388 Computer #81 Diagnosis of Parkinsonism Using Nigrosome 1 Imaging at 3T: Comparison of Interobserver Agreement between GRE Magnitude Images (MEDIC) and Susceptibility Map-weighted Images (SMWI)

Eung Yeop Kim¹, Yoon Ho Nam², Young Noh³, Young Hee Sung³, Byeong Ho Goh¹, Joon Hyung Ann¹, and Jongho Lee⁴

¹Radiology, Gachon University Gil Medical Center, Incheon, Korea, Republic of, ²Radiology, Seoul St. Mary Hospital, Seoul, Korea, Republic of, ³Neurology, Gachon University Gil Medical Center, Incheon, Korea, Republic of, ⁴Electrical and Computer Engineering, Seoul National University, Seoul, Korea, Republic of

Susceptibility map-weighted imaging (SMWI) improves both CNR and SNR in comparison with conventional SWI. In this work, we compared SMWI with MEDIC (a multi-echo GRE imaging that combines magnitude images via sum of squares) for nigrosome 1 imaging at 3T in terms of interobserver agreement and diagnostic performance in 74 subjects (44 with Parkinson's disease). Two experienced and two less-experienced reviewers visually assessed both imaging sets separately. Compared with MEDIC, SMWI showed higher kappa values and larger AUCs, regardless of level of experience. As a result, nigrosome 1 imaging using SMWI significantly improved diagnostic performance as well as interobserver agreement.

3389 Computer #82 Sensitivity of volumetric MRI and MRS to onset and progression of neurodegeneration
Dinesh K Deelchand¹, James M Joers¹, Adarsh Ravishankar², Tianmeng Lyu³, Uzay Emir^{1,4}, Diane Hutter¹, Christopher M Gomez⁵, Khalaf O Bushara⁶, Christophe Lenglet¹, Lynn E Eberly³, and Gulin Oz¹

¹Center for Magnetic Resonance Research, University of Minnesota, Minneapolis, MN, United States, ²School of Physics and Astronomy, University of Minnesota, Minneapolis, MN, United States, ³Division of Biostatistics, University of Minnesota, Minneapolis, MN, United States, ⁴University of Oxford, Oxford, United Kingdom, ⁵Department of Neurology, University of Chicago, Chicago, IL, United States, ⁶Department of Neurology, University of Minnesota, Minneapolis, MN, United States

The goal of this study was to combine MRS with volumetric MRI to determine the sensitivity of these two techniques to onset and progression of neurodegeneration in patients with early-moderate spinocerebellar ataxia type 1. Subjects were scanned at baseline and followed up at ~18 and ~36 months at 3T. Both MRI and MRS measures were found to be more sensitive to disease progression than standardized clinical scores. This study shows that volumetric MRI was most sensitive to disease progression while MRS might be more sensitive to detect the disease's early stage.

3390 Computer #83 QSM and T2* Mapping in a Six Month Placebo-Controlled Clinical Trial of the Iron Chelator Deferiprone in Parkinson's Disease
Rexford Newbould¹, Courtney Bishop¹, Antonio Martin-Bastida², and David Dexter²

¹Imanova Centre for Imaging Sciences, London, United Kingdom, ²Imperial College London, London, United Kingdom

A double-blind placebo-controlled clinical trial of an iron chelation therapy was performed in 25 subjects with Parkinson's disease (PD) and 12 healthy matched controls. Two MRI measures of brain iron at each of three visits at baseline, 3 months, and 6 months were derived from a high resolution 3D multiecho volume: T2* and QSM maps. T2* values significantly lengthened in six of nine pre-defined ROIs by the final visit in the highest dose group. QSM values, however, did not change with treatment. This differential trajectory between relaxation and susceptibility may result from ferritin's complex relaxation behavior.

3391 Computer #84 Characterizing neurodegeneration in progressive supranuclear palsy using VBM and SVM classification
Karsten Mueller¹, Robert Jech^{2,3}, Cecilia Bonnet^{2,3}, Jaroslav Tintěra⁴, Harald E Möller¹, Klaus Fassbender⁵, Jan Kassubek⁶, Markus Otto⁶, Evžen Růžička^{2,3}, and Matthias L Schroeter^{1,7}

¹Max Planck Institute for Human Cognitive and Brain Sciences, Leipzig, Germany, ²Department of Neurology and Center of Clinical Neuroscience, Charles University in Prague, Prague, Czech Republic, ³1st Faculty of Medicine and General University Hospital in Prague, Prague, Czech Republic, ⁴Institute for Clinical and Experimental Medicine, Prague, Czech Republic, ⁵Clinic and Polyclinic for Neurology, Saarland University Homburg, Homburg, Germany, ⁶Clinic and Polyclinic for Neurology, University of Ulm, Ulm, Germany, ⁷Clinic for Cognitive Neurology, University Hospital Leipzig, Leipzig, Germany

Structural brain differences were investigated between patients with progressive supranuclear palsy (PSP) and healthy controls with T1-weighted images (MP-RAGE) acquired at four centers with different 3T scanners (Siemens). Using voxel-based morphometry, we found a major decline in gray matter density in brainstem, insula, striatum, and frontomedian regions that is in line with the current literature. Support-vector-machine classification provided a high sensitivity of disease detection when using relevant brain regions in feature selection.

- 3392
Computer #85 Robust global and widespread local white matter abnormalities in a longitudinal study of juvenile neuronal ceroid lipofuscinosis (CLN3)
Ulrika Roine¹, Timo Roine^{2,3}, Antti Hakkarainen³, Anna Tokola³, Marja H. Balk³, Minna Mannerkoski⁴, Tuula Lönnqvist⁵, and Taina Autti³
- ¹Department of Neuroscience and Biomedical Engineering, Aalto University, Espoo, Finland, ²Minds-Vision Lab, Department of Physics, University of Antwerp, Wilrijk (Antwerp), Belgium, ³HUS Medical Imaging Center, Radiology, University of Helsinki and Helsinki University Hospital, Helsinki, Finland, ⁴Child Psychiatry, University of Helsinki and Helsinki University Hospital, Helsinki, Finland, ⁵Department of Child Neurology, Children's Hospital, University of Helsinki and Helsinki University Hospital, Helsinki, Finland
- Juvenile neuronal ceroid lipofuscinosis (CLN3), is a progressive neurodegenerative lysosomal storage disease of the childhood, which manifests with loss of vision, seizures and loss of cognitive and motor functions, and leads to premature death. We investigated global and local white matter microstructure with diffusion MRI in 14 children with CLN3 imaged at two time points. Robust global analysis was performed using whole-brain tractography and white matter tract skeleton. Local microstructural abnormalities were investigated using tract-based spatial statistics. Significantly decreased fractional anisotropy and increased diffusivity values were found in subjects with CLN3 both at the global and local scale.
-
- 3393
Computer #86 Structural brain connectome and cognitive impairment in Parkinson's disease
Sebastiano Galantucci¹, Federica Agosta¹, Elka Stefanova², Silvia Basaia¹, Martijn van den Heuvel³, Tanja Stojković², Elisa Canu¹, Iva Stanković², Vladana Spica², Vladimir S. Kostic², and Massimo Filippi^{1,4}
- ¹Neuroimaging Research Unit, San Raffaele Scientific Institute, Vita-Salute San Raffaele University, Milan, Italy, ²Clinic of Neurology, Faculty of Medicine, University of Belgrade, Belgrade, Yugoslavia, ³Department of Psychiatry, Rudolf Magnus Institute of Neuroscience, University Medical Center Utrecht, Utrecht, Netherlands, ⁴Department of Neurology, San Raffaele Scientific Institute, Vita-Salute San Raffaele University, Milan, Italy
- To date, MRI biomarkers have been demonstrated extremely useful for detecting and monitoring the neurodegenerative processes. However, brain network analysis seems the most powerful approach to quantitatively describe the topological organization of the brain connectome even at early stages of neurodegenerative diseases. This study provided promising biomarkers to detect features of neurodegeneration in PD-MCI, being able to distinguish it from PD without MCI. This study shows that the presence of subtle cognitive deficits not causing a dementia, produces a huge alteration of brain networks suggesting the importance of the study of connectomics in the investigation of neurodegenerative diseases.
-
- 3394
Computer #87 fMRI reveals plasticity compensating for early dopaminergic loss at corticostriatal synapse
Chiao-Chi Chen¹, Yi-Hua Hsu¹, Nai-Wei Yao¹, and Chen Chang¹
- ¹Institute of Biomedical Sciences, Academia Sinica, Taipei, Taiwan
- The dopaminergic system possesses striking plasticity compensating for motor aberrations from neuronal loss. Little is known regarding the compensation mechanism during dopaminergic loss, preventing the aberration from being arrested and treated early. Here we present in vivo imaging evidence from functional magnetic resonance imaging showing that, after dopaminergic depletion, the dorsolateral striatum (DOLS) exhibited an early and transient vasodilation cluster in response to specific forepaw stimulation. Activation of DOLS NMDA receptors causes this vasodilation, protects dopaminergic fibers from denervation, and counteracts motor deficits. The findings have clinical implications for early detection and intervention in brain disorders such as Parkinson's disease.
-
- 3395
Computer #88 Dopaminergic therapy modulates cortical perfusion in Parkinson's disease with and without dementia according to ASL perfusion MRI
Chien-Yuan Eddy Lin¹, Wei-Che Lin², Pei-Chin Chen², Yung-Cheng Huang³, Nai-Wen Tsai⁴, Hsiu-Ling Chen², Hung-Chen Wang⁵, Tsu-Kung Lin⁴, Kun-Hsien Chou⁶, Meng-Hsiang Chen², Yi-Wen Chen², and Cheng-Hsien Lu⁴
- ¹GE Healthcare, Taipei, Taiwan, ²Department of Diagnostic Radiology, Kaohsiung Chang Gung Memorial Hospital, Kaohsiung, Taiwan, ³Department of Nuclear Medicine, Kaohsiung Chang Gung Memorial Hospital, Kaohsiung, Taiwan, ⁴Department of Neurology, Kaohsiung Chang Gung Memorial Hospital, Kaohsiung, Taiwan, ⁵Department of Neurosurgery, Kaohsiung Chang Gung Memorial Hospital, Kaohsiung, Taiwan, ⁶Brain Research Center, National Yang-Ming University, Taipei, Taiwan
- We examined the cerebral perfusion differences among 17 Parkinson's disease (PD) patients, 17 PD with dementia (PDD) patients, and 17 healthy controls and used noncontrast arterial spin labelling MRI to assess the effects of dopaminergic therapies on perfusion in the patients. We demonstrated progressive widespread cortical hypoperfusion in PD and PDD and robust effects for the dopaminergic therapies. These patterns of hypoperfusion could be related to cognitive dysfunctions and disease severity. Furthermore, desensitization to dopaminergic therapies in terms of cortical perfusion was found as the disease progressed, supporting the concept that long-term therapies are associated with the therapeutic window narrowing.
-
- 3396
Computer #89 Aberrant interhemispheric structural and functional connectivity in amyotrophic lateral sclerosis: converging evidences from DTI and resting-state fMRI
Jiuquan Zhang^{1,2}, Bing Ji^{2,3}, Zhihao Li², Jun Hu⁴, Jian Wang¹, Mingze Xu⁵, and Xiaoping Hu²
- ¹Department of Radiology, Southwest Hospital, Chongqing, China, People's Republic of, ²Department of Biomedical Engineering, Emory University & Georgia Institute of Technology, Atlanta, GA, United States, ³University of Shanghai for Science & Technology, Shanghai, China, People's Republic of, ⁴Department of Neurology, Southwest Hospital, Chongqing, China, People's Republic of, ⁵Department of Biomedical Engineering, Perking University, Beijing, China, People's Republic of
- The corpus callosum (CC) involvement is a consistent feature of Amyotrophic lateral sclerosis (ALS), thus suggesting a pathophysiology of reduced interhemispheric neural connectivity. In the current study, we directly examined the interhemispheric functional and structural

connectivities in ALS. In terms of functional connectivity, extensive alterations in voxel mirrored homotopic connectivity were found in ALS. With structural connectivity, while there were widespread reductions in DTI metrics, only the fiber probability index through CC subregion III in the ALS patients was significantly decreased compared with the controls. These findings provide further evidence for structural and functional interhemispheric connectivity impairment in ALS.

3397 Computer #90 Investigation of inter-hemispheric functional connectivity in Parkinson's disease with asymmetric onset using Voxel-Mirrored Homotopic Connectivity
Yong Zhang¹, Naying He², Hua-Wei Lin², Ajit Shankaranarayanan³, Zhenyu Zhou¹, and Fu-Hua Yan²

¹MR Research China, GE Healthcare, Beijing, China, People's Republic of, ²Radiology, Ruijin Hospital, Shanghai Jiaotong University School of Medicine, Shanghai, China, People's Republic of, ³GE Healthcare, Menlo Park, CA, United States

This preliminary study used voxel-mirrored homotopic connectivity (VMHC), a novel resting-state fMRI parameter to investigate inter-hemispheric functional connectivity in Parkinson's Disease (PD) with asymmetric onset. Fifteen left side onset (LPD) patients, sixteen right side onset (RPD) patients and nineteen healthy controls were recruited for comparison. Both of LPD and RPD patients showed decreased VMHC in post-central gyrus responsible for motor functions. The decreased VMHC in the cuneus and middle occipital gyrus in LPD patients might affect visual processing function. For RPD patients, VMHC changes in the middle and superior frontal gyrus could be relevant to advanced cognitive impairment.

3398 Computer #91 Can longitudinal diffusion-weighted imaging of the basal ganglia be used as a surrogate marker in preclinical Huntington's disease?
Chris Patrick Pflanz¹, Marina Charquero-Ballester², Adnan Majid³, Anderson Winkler¹, Emmanuel Vallee¹, Mark Jenkinson¹, Adam Aron³, and Gwenaelle Douaud¹

¹FMRIB Centre, University of Oxford, Oxford, United Kingdom, ²Oxford, United Kingdom, ³San Diego, CA, United States

Huntington's disease is a monogenetic, neurodegenerative movement disorder that is amenable to predictive genetic testing. Here, we investigated whether longitudinal diffusion-weighted imaging of the basal ganglia could be used to detect early microstructural changes in participants with presymptomatic Huntington's disease (preHD). We found the first results showing significant longitudinal changes in the microstructure of the basal ganglia within a preclinical HD population. We further showed that, while FA and MD might be less sensitive to longitudinal changes than volumetric measures, they provide mechanistic insights into the underlying physiopathological process that are complementary to the monotonic, non-specific changes in the volume of the basal ganglia.

3399 Computer #92 Brain Iron Deficiency in Restless Legs Syndrome Measured by Quantitative Susceptibility and its Relation to Clinical Features
Xu Li^{1,2}, Hongjun Liu^{1,2}, Richard P Allen³, Christopher J Earley³, Richard A.E. Edden^{1,2}, Peter B Barker^{1,2}, Tiana Cruz³, and Peter C.M. van Zijl^{1,2}

¹F.M. Kirby Research Center for Functional Brain Imaging, Kennedy Krieger Institute, Baltimore, MD, United States, ²Radiology, Johns Hopkins University School of Medicine, Baltimore, MD, United States, ³Neurology, Johns Hopkins University School of Medicine, Baltimore, MD, United States

Possible brain iron deficiency was assessed using quantitative susceptibility mapping at 7T in restless legs syndrome (RLS) and analyzed with clinical measurements including IRLS severity score, serum iron, serum ferritin and periodic limb movement during sleep (PLMS). Using magnetic susceptibility as a brain iron index and compared to control group, significantly decreased iron was found in RLS patients in dentate nuclei and thalamus, and in substantia nigra in a subset of RLS patients with severe clinical symptoms with PLMS larger than 100 times per hour. Significant correlation between PLMS and brain iron was only found in substantia nigra in RLS.

3400 Computer #93 Quantitative Susceptibility Mapping of the "Swallow tail" in Parkinson disease
Santanu Chakraborty^{1,2}, Gerd Melkus^{1,2}, Fahad Essbaiheen^{1,2,3}, David A Grimes⁴, and Tiago Mestre⁴

¹Medical Imaging, The Ottawa Hospital, Ottawa, ON, Canada, ²Radiology, University of Ottawa, Ottawa, ON, Canada, ³King Saud University, Riyadh, Saudi Arabia, ⁴Neurology, The Ottawa Hospital, Ottawa, ON, Canada

Parkinson disease (PD) continues to be diagnosed based on clinical findings. Recently, in SWI images, the loss of 'swallow tail' appearance in dorsolateral substantia nigra in PD patients yielded high diagnostic accuracy. In our study we measured susceptibility values using QSM in the 'swallow tail' area in seven Parkinson's disease patients and compared to five control subjects. The susceptibility in the swallow tail area was higher in the PD group (0.072 vs. 0.058). This likely suggests increased iron deposition causing a masking effect that contributes along with dopaminergic neurons loss to the disappearance of the 'swallow tail' in PD patients.

3401 Computer #94 MRI signatures in the brain of patients with PD and iRBD
Silvia Mangia¹, Philip Burton¹, Alena Svatkova^{2,3}, Igor Nestrasil⁴, Alejandra Sierra Lopez⁵, Karin Shmueli⁶, Lynn Eberly⁷, Michael Howell⁴, Paul Tuite⁴, and Shalom Michaeli¹

¹CMRR, Department of Radiology, University of Minnesota, Minneapolis, MN, United States, ²Department of Pediatrics, University of Minnesota, Minneapolis, MN, United States, ³Central European Institute of Technology (CEITEC), Masaryk University, Brno, Czech Republic, ⁴Department of Neurology, University of Minnesota, Minneapolis, MN, United States, ⁵A.I.Virtanen Institute for Molecular Sciences, University of Eastern Finland, Kuopio, Finland, ⁶Department of Medical Physics and Biomedical Engineering, University College London, London, United Kingdom, ⁷Division of Biostatistics, University of Minnesota, Minneapolis, MN, United States

The idiopathic rapid eye movement sleep behavior disorder (iRBD) is a condition that often evolves into Parkinson's disease (PD), therefore by monitoring iRBD one can track the neurodegeneration of individuals that may progress to PD. Here we used a battery of MRI contrasts to characterize brain tissue properties such as microstructural integrity, iron loads, and functional connectivity in 10 iRBD, 10 PD and 10 age-matched healthy subjects. Rotating frame relaxation methods adiabatic $T_{1,2\rho}$ and RAFFn, along with DTI and rsfMRI detected heterogeneous abnormalities in several subcortical structures of PD and iRBD subjects.

3402 Computer #95 A High b-Value Diffusion Study of Brainstem Abnormality in Patients with Parkinson's Disease Using a CTRW Model
Zheng Zhong^{1,2}, Muge Karaman¹, Douglas Merkitich³, Jennifer Goldman³, and Xiaohong Joe Zhou^{1,4}

¹Center for MR Research, Chicago, IL, United States, ²Bioengineering, University of Illinois at Chicago, Chicago, IL, United States, ³Neurological Sciences, Rush University Medical Center, Chicago, IL, United States, ⁴Radiology, Neurosurgery and Bioengineering, University of Illinois Hospital & Health Sciences system, Chicago, IL, United States

It has been known that the substantia nigra of brain stem shows structural abnormalities with the progression of Parkinson's disease. While high b-value diffusion imaging has the potential to reveal such structural changes, single-shot EPI suffers from unwanted geometric distortion which may result in poor analysis of the diffusion data. In this study, we use a recently developed reduced field of view imaging technique and analyze the abnormalities occurring in the substantia nigra of the Parkinson's disease patients by using the continuous-time random-walk (CTRW) model.

3403 Computer #96 The Effect of Primidone on Gamma-Aminobutyric Acid Concentration in the Dentate Nucleus in Patients with Essential Tremor
Ulrike Dydak^{1,2}, Ruoyun Ma^{1,2}, Nora Hernandez³, Johnathan P Dyke⁴, and Elan Louis^{3,5,6}

¹School of Health Sciences, Purdue University, West Lafayette, IN, United States, ²Department of Radiology and Imaging Sciences, Indiana University School of Medicine, Indianapolis, IN, United States, ³Department of Neurology, Yale School of Medicine, New Haven, CT, United States, ⁴Department of Radiology, Weill Cornell Medical College, New York, NY, United States, ⁵Center for Neuroepidemiology and Clinical Neurological Research, Yale School of Medicine, New Haven, CT, United States, ⁶Department of Chronic Disease Epidemiology, Yale School of Public Health, New Haven, CT, United States

Whether current use of the medication primidone affects dentate γ -aminobutyric acid (GABA) concentrations is unknown. Yet, this may be an important confounder in studies of the pathophysiology of essential tremor (ET). Using the MEGA-PRESS J-editing sequence, we found no difference in dentate GABA levels between patients taking primidone and patients not taking primidone. Furthermore, there was no association between daily primidone dose and dentate GABA concentration. These data suggest that it is not necessary to exclude ET patients on primidone from MRS studies of dentate GABA concentration.

Electronic Poster

The Aging Brain

Exhibition Hall

Tuesday, May 10, 2016: 14:30 - 15:30

3404 Computer #1 Ex-Vivo Diffusion Anisotropy of Human Brain Hemispheres
Yingjuan Wu¹, Robert J. Dawe², Arnold Moya Evia², Julie A. Schneider³, David A. Bennett³, and Konstantinos Arfanakis²

¹Department of Biomedical Engineering, Illinois Institute of Technology, Chicago, IL, United States, ²Department of Biomedical Engineering, Illinois Institute of Technology, Chicago, IL, United States, ³Rush Alzheimer's Disease Center, Rush University Medical Center, Chicago, IL, United States

The aims of this work were to: 1) longitudinally assess the diffusion anisotropy of various white matter regions measured with ex-vivo MRI, and 2) investigate the relationship between FA values measured in-vivo and ex-vivo on the same subjects. This work demonstrated that brain white matter diffusion anisotropy measured ex-vivo decreases with time postmortem, and that diffusion anisotropy measured ex-vivo is linearly related to the diffusion anisotropy measured in-vivo on the same subjects. Combination of ex-vivo MR diffusion anisotropy and histopathology may become an effective tool for the assessment of the neuropathologic correlates of structural brain abnormalities observed in-vivo.

3405 Computer #2 Faster brain atrophy is associated with accelerated cognitive decline in healthy older adults: the Singapore Longitudinal Ageing Brain Study
June Chi-Yan Lo¹, Ruth Li-Fang Leong¹, Jesisca Tandi¹, and Michael Wei-Liang Chee¹

¹Center for Cognitive Neuroscience, Duke-NUS Graduate Medical School, Singapore, Singapore

Although East Asia harbors the largest number of aging adults in the world, there is limited data on longitudinal changes in brain structure and its relationship with domain-specific cognition. We tracked changes in brain volume and 5 cognitive functions over 8 years among healthy older adults in the Singapore-Longitudinal Ageing Brain Study. After adjusting for intracranial volume, demographic factors, and blood pressure, total cerebral atrophy was associated with faster decline in verbal memory. Hippocampal atrophy and ventricular expansion were associated with greater decline in verbal memory and executive functions. These findings clarify the relationships between age-trends in neurobiology and cognition.

- 3406
Computer #3 Age-related alterations in glutamatergic neurotransmission in the anterior and posterior cingulate cortices
Pui Wai Chiu¹, Edward S Hui¹, Queenie Chan², Raja Rizal Azman Raja Aman³, Raymond Chuen Chung Chang⁴, Raymond Chor Kiu Chan⁵, Leung Wing Chu⁶, and Henry Ka Fung Mak¹
- ¹Diagnostic Radiology, The University of Hong Kong, Hong Kong, Hong Kong, ²Philips Healthcare, Hong Kong, Hong Kong, Hong Kong, ³Biomedical Imaging, University of Malaya, Kuala Lumpur, Malaysia, ⁴School of Biomedical Sciences, The University of Hong Kong, Hong Kong, Hong Kong, ⁵Neuropsychology and Applied Cognitive Neuroscience Laboratory, Chinese Academy of Sciences, Beijing, China, People's Republic of, ⁶Medicine, Queen Mary Hospital, Hong Kong, Hong Kong
- Glutamatergic neurotransmission has an interesting role in aging. The anterior cingulate cortex(ACC) and posterior cingulate cortex(PCC) are focuses for aging research due to their implicated role in cognition. In this study, proton magnetic resonance spectroscopy was used to investigate the changes in glutamatergic neurotransmission during aging by measuring absolute Glx concentration([Glx]_{abs}) in ACC and PCC in a local Chinese cohort at 3.0T. Significant age-related increases of [Glx]_{abs} in ACC and PCC might indicate age-related alterations in glutamatergic neurotransmission. Significantly higher overall [Glx]_{abs} was found in ACC compared with PCC might be attributed to the abundant glutamatergic neurons in the forebrain.
-
- 3407
Computer #4 Cumulative Mid-Life Framingham Stroke Risk Profile Predicts Reduced Structural Brain Integrity in Old Age
Enikő Zsoldos¹, Nicola Filippini¹, Abda Mahmood¹, Archana Singh-Manoux², Mika Kivimäki², Clare Mackay¹, and Klaus P Ebmeier¹
- ¹Psychiatry, University of Oxford, Oxford, United Kingdom, ²Epidemiology and Public Health, University College London, London, United Kingdom
- Research presented discusses the cumulative effects of Framingham Stroke Risk profile in mid-life on structural brain integrity reduction in older life.
-
- 3408
Computer #5 Early aging effect on the function of human central olfactory system
Jianli Wang¹, Xiaoyu Sun¹, and Qing X Yang¹
- ¹Penn State College of Medicine, Hershey, PA, United States
- We report an olfactory fMRI study of the aging effect on the functions of central olfactory system during normal adulthood and early aging. The smell identification function declined with age. Accordingly, the BOLD signal responding to odor stimulations was significantly decreased with age in bilateral DLPFC, left orbitofrontal cortex, and left insula. However, there was no significant age correlation was detected with the BOLD signal in the primary olfactory cortex. These results suggest that age-related olfactory functional decline in human brain is more prominent in the secondary and higher order central olfactory structures than the POC in early aging process.
-
- 3409
Computer #6 Distribution of principal diffusion direction orientations: a novel method to characterize age-related changes in the brain.
Maria Eugenia Caligiuri¹, Aldo Quattrone^{1,2}, and Andrea Cherubini¹
- ¹Institute of Bioimaging and Molecular Physiology (IBFM), National Research Council, Catanzaro, Italy, ²Institute of Neurology, University Magna Graecia, Catanzaro, Italy
- Diffusion-weighted MRI of the brain allows the assessment of tissue integrity at the microscale. The most commonly used technique to analyze diffusion-weighted data is diffusion tensor imaging (DTI), which relies on the reconstruction of the diffusion tensor at each MRI voxel by calculating its eigenvalues and eigenvectors. These quantities allow the estimation of scalar DTI maps measuring mean diffusivity (MD) and fractional anisotropy (FA), which are considered markers of structural tissue integrity. To date, DTI has been extensively used in the field of neuroimaging to study brain microstructural integrity in healthy subjects and patients with several different neurological conditions. However, despite the three-dimensional nature of the tensor, existing studies have focused on changes in DTI-derived scalar indexes, such as MD and FA, not considering the orientation of the principal eigenvector of the tensor, which could provide invaluable insight on the nature of tissue changes, but is still only used for color-coding FA maps for qualitative, visual purposes.
-
- 3410
Computer #7 Intra Voxel Incoherent Motion (IVIM) in Brain Regions: a Repeatability and Aging Study
Eric T Peterson¹, Natalie M Zahr^{1,2}, Dongjin Kwon¹, Matthew Serventi¹, Cheshire Hardcastle¹, Edith V Sullivan², and Adolf Pfefferbaum¹
- ¹Biosciences, SRI International, Menlo Park, CA, United States, ²Psychiatry and Behavioral Sciences, Stanford University, Stanford, CA, United States
- This work investigates the inter- and intra-session repeatability and the effects of age on intra voxel incoherent motion (IVIM) parameters. Atlas registration allowed for parcellation-based region specific brain analysis. A new and robust fitting approach reliably identified the perfusion fraction, diffusion, and pseudo-perfusion parameters from 15 healthy normal volunteers. The results show that IVIM is repeatable and that the perfusion fraction, diffusion, and pseudo-perfusion parameters are significantly higher in older than younger adults in several brain regions, most likely from perivascular CSF infiltration. This work serves to highlight how age is an important factor to consider when using IVIM.
-
- 3411
Computer #8 Altered neurochemical profile in the healthy elderly measured via 7 T ¹H MRS
Malgorzata Marjanska¹, J. Riley McCarten², Laura Hemmy², Dinesh K Deelchand¹, and Melissa Terpstra¹

The goal of this work was to characterize differences in the concentrations of neurochemicals beyond tNAA, tCr, and tCho in the OCC and PCC regions of healthy young and elderly subjects. The key innovation was scanning at ultra-high field (7 T) at very short echo time. The observed differences are consistent with compromised neurons (NAA, NAAG, Glu and GABA), membrane turnover (PE and tCho), oxidative stress (lower GSH in the OCC), inflammation (mIns), altered energy metabolism (tCho and Glc), and changes in large molecules (Mac).

-
- 3412
Computer #9 Frontal GABA concentrations predict cognitive function beyond age-related decline.
Eric C. Porges¹, Adam J. Woods¹, Richard A.E. Edden^{2,3}, Nicolaas A.J. Puts^{2,3}, Ashley D. Harris^{4,5,6}, Amanda Garcia¹, Huaihou Chen^{1,7}, Damon G. Lamb^{1,8}, John B. Williamson^{1,8}, and Ronald A. Cohen¹
- ¹Aging and Geriatric Research, Institute on Aging, Center for Cognitive Aging and Memory, University of Florida, Gainesville, FL, United States, ²Russell H. Morgan Department of Radiology and Radiological Science, The Johns Hopkins University School of Medicine, Baltimore, MD, United States, ³Kennedy Krieger Institute, FM Kirby Center for Functional Brain Imaging, Baltimore, MD, United States, ⁴Department of Radiology, University of Calgary, Calgary, AB, Canada, ⁵CAIR Program, Alberta Children's Hospital Research Institute, University of Calgary, Calgary, AB, Canada, ⁶Hotchkiss Brain Institute, University of Calgary, Calgary, AB, Canada, ⁷Department of Biostatistics, University of Florida, Gainesville, FL, United States, ⁸Brain Rehabilitation and Research Center, Malcom Randall Veterans Affairs Medical Center, Gainesville, FL, United States
- GABA levels measured with MRS have been associated with performance in numerous sensory and attention domains. Here we demonstrate in a healthy aging cohort that frontal GABA levels are predictive of general cognitive function. Furthermore, the previously reported age-related decrease in GABA levels continues into advanced age.
-
- 3413
Computer #10 Reduced White Matter Integrity in Cognitively Normal HFE Mutation Carriers
Mark David Meadowcroft^{1,2}, Jian-Li Wang², Carson J Purnell¹, Paul J Eslinger³, Elizabeth B Neely¹, David J Gill³, Megha Vasavada², Qing X Yang², and James R Connor¹
- ¹Neurosurgery, The Pennsylvania State University - College of Medicine, Hershey, PA, United States, ²Radiology, The Pennsylvania State University - College of Medicine, Hershey, PA, United States, ³Neurology, The Pennsylvania State University - College of Medicine, Hershey, PA, United States
- Mutations associated with iron dysregulation in the brain include the H63D and C282Y HFE missense mutations and transferrin C2 mutation, all of which have been associated with development of neurodegenerative diseases. Diffusion tensor metrics were further utilized to investigate the relationship between HFE/transferrin mutations and myelin integrity more precisely. The MRI data presented here demonstrate that cognitively normal H63D/C282Y HFE and transferrin C2 carriers have diffusivity changes in white matter compared to wild-type subjects. The observation that these alterations are located in late-myelinating frontal areas is hypothesized to be related to increased susceptibility within this region of HFE/Tf mutation carriers.
-
- 3414
Computer #11 The Relationship between White Matter Structure and Clinical Behavior in Different APOE Genotypes: A Preliminary Study in Cognitively Intact Elderly.
Xiao Luo¹, Yefan Jiaerken¹, and MinMing Zhang¹
- ¹Radiology, Second Affiliated Hospital of Zhejiang University School of Medicine, Hangzhou, China, People's Republic of
- The purpose of this research was to study the relationship of white matter hyperintensities (WMH) with cognitive performance in healthy elderly with different APOE genotypes. In total, 158 subjects were separated into 3 groups ($\epsilon 2$ carriers, $\epsilon 4$ carriers and $\epsilon 3$ homozygotes). Group differences of regional WMH volume were calculated. Subsequent correlation analysis between regional WMH burden and behavior data was performed. Detrimental effect of APOE $\epsilon 4$ allele on white matter structure was found while no protective effect of APOE $\epsilon 2$ was observed; WMH volume was significantly correlated with processing speed and executive ability, especially in APOE $\epsilon 4$ carriers.
-
- 3415
Computer #12 Longitudinal relationship between cerebrovascular reactivity and processing speed in young and elderly individuals
Shin-Lei Peng^{1,2}, Xi Chen³, Yang Li¹, Karen Rodrigue³, Yamei Cheng⁴, Denise Park³, and Hanzhang Lu¹
- ¹Johns Hopkins University School of Medicine, Baltimore, MD, United States, ²China Medical University, Taichung, Taiwan, ³University of Texas at Dallas, Dallas, TX, United States, ⁴University of Texas Southwestern Medical Center, Dallas, TX, United States
- Processing speed is a fundamental building block of cognition that declines reliably with age. Therefore, the goals of this study were to examine whether changes in cerebrovascular reactivity (CVR) to CO₂ inhalation, a marker of cerebrovascular function, is associated with changes in processing speed. The results showed that, in elderly, but not young individuals, the rate of change in CVR over four years predicted decline in processing speed, indicating that declines in vascular brain health contribute to changes in the information processing speed in older but not young and middle-aged adults.
-
- 3416
Computer #13 Development and Aging of Superficial White Matter Myelin from Young Adulthood to Old Age: Mapping by Vertex-Based Surface Statistics (VBSS)
Minjie Wu¹, Anand Kumar¹, and Shaolin Yang^{1,2,3}
- ¹Department of Psychiatry, University of Illinois at Chicago, Chicago, IL, United States, ²Department of Radiology, University of Illinois at Chicago, Chicago, IL, United States, ³Department of Bioengineering, University of Illinois at Chicago, Chicago, IL, United States

Using Magnetization transfer imaging (MT) and innovative multimodal analysis approach, the current study vertexwise mapped age-related changes of superficial white matter (SWM) from young adulthood to old age (30-85 years, N = 66). Results demonstrated regionally selective and temporally heterochronologic changes of SWM MTR with age, suggesting that myelin change in SWM occurs at varied paces across the cortex. SWM MTR regions including the rostral middle frontal and parahippocampus followed inverted U-shaped trajectories, with protracted maturation till age 40-50 years and accelerating demyelination after age 60 years, while the primary motor, somatosensory and auditory SWM regions did not show age-related deterioration.

3417 Computer #14 The relationship between White Matter Hyperintensities volume and cognition in normal ageing women
Rowa Aljondi¹, Patricia Desmond^{1,2}, Chris Steward^{1,2}, and Cassandra Szoeké³

¹The University of Melbourne, Melbourne, Australia, ²Department of Radiology, Royal Melbourne Hospital, Melbourne, Australia, ³Department of Medicine, The University of Melbourne, Melbourne, Australia

White Matter Hyperintensities (WMH) lesions on brain magnetic resonance imaging (MRI) are common findings in elderly people and contribute to cognitive impairments. Here we examine volumetric MRI measures of WMH volume in relation to neuropsychological measures of episodic memory, executive function, semantic memory and visuospatial abilities in 116 elderly women, their mean age 69 years. Linear regression analysis showed that greater WMH volume was correlated with lower performance on tests involving measures of executive function and visuospatial abilities. These results help elucidate the pathological process leading to cognitive decline in ageing.

3418 Computer #15 Normal aging effect on commissure fibers assessed with template-based tractography
Pin-Yu Chen^{1,2}, Jeng-Min Chiou³, Ya-Fang Yang³, Yu-Ting Chen³, Yu-Ling Chang⁴, Yu-Chun Lo¹, Yu-Jen Chen¹, Yung-Chin Hsu¹, and Wen-Yih I. Tseng^{1,2,5}

¹Institute of Medical Device and Imaging, National Taiwan University College of Medicine, Taipei, Taiwan, ²Department of Life Science, National Taiwan University, Taipei, Taiwan, ³Institute of Statistical Sciences, Academia Sinica, Taipei, Taiwan, ⁴Department of Psychology, National Taiwan University, Taipei, Taiwan, ⁵Molecular Imaging Center, National Taiwan University, Taipei, Taiwan

This study used template-based diffusion spectrum imaging (DSI) tractography to analyze the microstructural integrity of commissure fiber tracts, and applied functional data statistics to analyze the age effect on the tract integrity. The anterior commissure fibers were highly sensitive to the aging effect across the lifespan. The posterior commissure fibers became sensitive to the aging effect after 60 years old. In contrast, the age effect of posterior commissure fibers appears to occur after age of 60 years old. In conclusion, our study provides evidences for specific degenerative patterns of the commissure fibers tracts in normal ageing which may serve as a useful reference for neurodegenerative diseases.

3419 Computer #16 Coupled changes in hippocampal integrity and cognitive ability in later life
Devasuda Anblagan^{1,2}, Maria C Valdés Hernández¹, Stuart J Ritchie^{2,3}, Benjamin S Aribisala^{1,2}, Natalie A Royle^{1,2}, Iona F Hamilton¹, David A Dickie¹, Susana Muñoz Maniega¹, Mark E Bastin^{1,2}, Ian J Deary^{2,3}, and Joanna M Wardlaw^{1,2}

¹Centre for Clinical Brain Sciences, University of Edinburgh, Edinburgh, United Kingdom, ²Centre for Cognitive Ageing and Cognitive Epidemiology, University of Edinburgh, Edinburgh, United Kingdom, ³Department of Psychology, University of Edinburgh, Edinburgh, United Kingdom

We tested whether there were coupled changes in hippocampal volume, T1, MTR, FA and MD and three broad cognitive domains (Verbal Memory, Working Memory, and Speed) in a large sample of community-dwelling non-demented adults at 73 and 76 years of age. Hippocampal volume, FA, MTR and T1 declined from age 73 to 76, while MD increased with age. Higher baseline MD was correlated with steeper cognitive decline in all three cognitive measures, but individuals with higher MD increases (i.e. more apparent deterioration in tissue integrity) also tended to show increases in Working Memory.

3420 Computer #17 White Matter Structural Integrity and Cerebral Arterial Pathology in Normal Aging
Roman Fleysheer¹, Michael L Lipton¹, Tatjana Rundek², Richard Lipton³, and Carol Derby⁴

¹Department of Radiology, Albert Einstein College of Medicine, Bronx, NY, United States, ²Departments of Neurology and Public Health Sciences, University of Miami Miller School of Medicine, Miami, FL, United States, ³Saul R Korey Department of Neurology, Albert Einstein College of Medicine, Bronx, NY, United States, ⁴Saul R Korey Department of Neurology and Department of Epidemiology and Population Health, Albert Einstein College of Medicine, Bronx, NY, United States

Normal aging is associated with changes both in micro-structure of white matter of the brain and in cerebral vasculature. We test the hypothesis that these processes are related by examining the association between fractional anisotropy (a diffusion tensor imaging measure of structural integrity) and pulsatility index (a transcranial Doppler ultrasound measure of abnormal arterial flow) in 70 years old and older adults free of stroke and dementia. We identified clusters of significant correlations between the measures, supporting this hypothesis.

3421 Computer #18 Metabolic changes upon supervised aerobic exercise in old adults monitored with 1H MRSI.
Ulrich Pilatus¹, Bianca Lienerth², Katharina Dietz³, Sina Schwarz⁴, Johannes Fleckenstein⁴, Silke Matura³, Tobias Engeroff⁴, Eszter Füzéki⁴, Valentina A. Tesky³, Elke Hattingen¹, Ralf Deichmann², Lutz Vogt⁴, Winfried Banzer⁴, and Johannes Pantel³

¹Neuroradiology, Goethe-Universität Frankfurt, Frankfurt, Germany, ²Brain Imaging Center, Goethe-Universität Frankfurt, Frankfurt, Germany, ³Institute of General Practice, Goethe-Universität Frankfurt, Frankfurt, Germany, ⁴Institute of Sport Sciences, Goethe-Universität Frankfurt, Frankfurt, Germany

In an interventional study changes in metabolic profiles (NAA/tCr, NAA/tCho) upon aerobic exercise were studied comparing two subgroups of volunteers who performed/not-performed supervised aerobic exercise. We observed a difference between both groups which can mainly be assigned to increased NAA/tCho in the group performing exercise.

-
- 3422
Computer #19
Age-related variability of functional connectivity in the basal ganglia in healthy elderly subjects and its implications for research in Parkinson's disease
Ludovica Griffanti¹, Philipp Stratmann^{2,3}, Michal Rolinski², Nicola Filippini^{1,2}, Enikő Zsoldos², Abda Mahmood², Mika Kivimäki⁴, Archana Singh-Manoux⁴, Klaus P. Ebmeier², and Clare E. Mackay²
- ¹FMRIB centre, University of Oxford, Oxford, United Kingdom, ²Department of Psychiatry, University of Oxford, Oxford, United Kingdom, ³Department of Informatics, Technische Universität München, München, Germany, ⁴Department of Epidemiology and Public Health, University College London, London, United Kingdom
- This exploratory study aims to identify factors that may account for variability in functional connectivity within the basal ganglia resting state network (BGN) in healthy subjects, to help the development of an imaging biomarker for Parkinson's disease. To this purpose we explored the relationship between functional connectivity measures derived from resting state fMRI and several demographic, behavioral and motor variables, in a large population-based sample of healthy elderly subjects, participating in the Whitehall II imaging sub-study.
-
- 3423
Computer #20
Aging Increases Markers of Inflammation and Alters Brain-Gut Interactions
Jared Hoffman¹, Vikas Bakshi², Ishita Parikh², Janet Guo³, Rachel Armstrong³, Steve Estes⁴, and Ai-Ling Lin¹
- ¹Pharmacology and Nutritional Sciences, University of Kentucky, Lexington, KY, United States, ²University of Kentucky, Lexington, KY, United States, ³Lexington, KY, United States, ⁴Physiology, University of Kentucky, Lexington, KY, United States
- Aging is the perhaps the greatest risk factor for the development of numerous health concerns, namely neurological diseases such as Alzheimer's Disease (AD). Recently, certain variations in the gut microbiota have been implicated in the development of neurological disease. We hypothesize that alterations of the gut microbiome from age may cause dysregulated brain-gut communication, promoting inflammation and ultimately, disease. Indeed, our preliminary data found old mice to have a distorted gut microbiota, decreased cerebral blood flow and cognitive deficits, and distinct levels of certain brain metabolites than the young mice.
-
- 3424
Computer #21
The impact of HPG-axis activation to the brain morphometry: a combined surface-based and voxel-based study
Di Yang¹, Yaxin Zhu¹, Wenjing Zhang², Su Lui², and Zhihan Yan¹
- ¹Department of Radiology, Second Affiliated Hospital, Wenzhou Medical University, Wenzhou, Zhejiang, China, People's Republic, Wenzhou, China, People's Republic of, ²Department of Radiology, Huaxi MR Research Center (HMRR), Department of Radiology, West China Hospital of Sichuan University, Chengdu, Sichuan, China, People's Republic of China, Chengdu, China, People's Republic of
- We investigated the impact of HPG-axis activity on brain morphometry. A total number of 52 subjects were recruited and scanned structural MRI. HPG-axis activated girls had less cortical thickness in the left inferiorparietal relative to comparison subjects. Meanwhile, gray matter volume was greater in the left precuneus in the focused group, relative to the control group. We found a positive correlation between circulating FSH and volume after excluded one outlier. This study demonstrates that there is some puberty-related maturation of the brain morphometry that is not confounded by age in the earlier stage of puberty.
-
- 3425
Computer #22
Visceral Adiposity, Inflammation and Cortical Thickness in Midlife
Sonya Kaur¹, Stephanie Oleson¹, Evan Pasha², Carolyn Cassill¹, Hirofumi Tanaka², and Andreana Haley¹
- ¹Psychology, University of Texas Austin, Austin, TX, United States, ²Kinesiology, University of Texas Austin, Austin, TX, United States
- The number of individuals classified as obese or overweight has doubled in the last two decades. In addition to documented effects of obesity on physical health, obesity is also associated with significantly deleterious effects on the brain, including increased risk for dementia. It has been hypothesized that the negative effects of obesity on central nervous system functioning are driven by visceral fat, which is metabolically active. However, the mechanisms behind this relationship are poorly understood. Here, we propose to directly test the role of systemic inflammation as a mediator of the relationship between visceral fat and brain structure in middle aged adults
-
- 3426
Computer #23
Distinguishing Between Different Aging-Related Cognitive Impairments Using GABA and Glx
Dandan Huang¹, Hongyan Ni², Dan Liu², and Tianyi Qian³
- ¹First Central Clinical College, Tianjin Medical University, Tianjin, China, People's Republic of, ²Tianjin, China, People's Republic of, ³Beijing, China, People's Republic of
- Several previous studies have tried to use MRS to investigate changes in brain function. In this study, we used a MEGA-PRESS sequence to measure the GABA and Glx concentration of normal controls, normal elderly controls, and patients with mild cognitive impairment and Alzheimer's disease. In ACC, the Glx showed significant differences between each groups, and the GABA showed significant aging

effects in normal subjects.

- 3427
Computer #24 Diabetes Mellitus Alters Brain Iron Metabolism in Cognitive Impaired Patients: Quantitative Susceptibility Mapping (QSM) Study
Won-Jin Moon¹, Yeon Sil Moon², Jin Woo Choi¹, Won Sung Yoon¹, Ju Yeon Park¹, and Seol-Heui Han²
- ¹Department of Radiology, Konkuk University School of Medicine, Seoul, Korea, Republic of, ²Department of Neurology, Konkuk University School of Medicine, Seoul, Korea, Republic of
- We found that the presence of DM is not associated with vascular risk factors on imaging and brain volumes, but associated with decreased susceptibility in left thalamus. Our results indicate that there may be a region-specific alteration of iron accumulation and iron metabolism in patients with both AD and DM.

Electronic Poster

Diffusion: Other

Exhibition Hall

Tuesday, May 10, 2016: 14:30 - 15:30

- 3428
Computer #25 Does reduced FOV Diffusion Weighted Imaging inherently yield lower ADC ?
Suchandrima Banerjee¹, David Aramburu-Nunez², Ramesh Paudyal², Thomas Chenevert³, Michael Boss⁴, and Amita Shukla-Dave^{2,5}
- ¹Global MR Applications & Workflow, GE Healthcare, Menlo Park, CA, United States, ²Department of Medical Physics, Memorial Sloan-Kettering Cancer Center, New York, NY, United States, ³Department of Radiology, University of Michigan Health System, Ann Arbor, MI, United States, ⁴Applied Physics Division, National Institute of Standards and Technology, Boulder, CO, United States, ⁵Department of Radiology, Memorial Sloan-Kettering Cancer Center, New York, NY, United States
- The benefits of reduced field-of-view (rFOV) imaging with the single-shot echoplanar diffusion sequence such as lower distortion and better discrimination of tumor from benign tissue have been demonstrated in several anatomies. In most of these published works, lower ADC was reported using rFOV compared to the standard full FOV (fFOV) method, irrespective of the technique by which rFOV was achieved. In this work we conducted controlled experiments in 3 phantoms to avoid some of the confounding factors present *in vivo* and investigated if there is a systemic underestimation of ADC in rFOV DWI compared to fFOV DWI.
- 3429
Computer #26 Diffusion Tensor Imaging of the Cervical and Thoracic Spinal Cord in Pediatric Subjects using an inner FOV 2D RF pulse sequence.
Sona Saksena¹, Devon M Middleton², Laura Krisa³, Pallav Shah², Scott H Faro², Rebecca Sinko³, John Gaughan⁴, Jürgen Finsterbusch⁵, M J Mulcahey³, and Feroze B Mohamed¹
- ¹Department of Radiology, Thomas Jefferson University, Philadelphia, PA, United States, ²Department of Radiology, Temple University, Philadelphia, PA, United States, ³Department of Occupational Therapy, Thomas Jefferson University, Philadelphia, PA, United States, ⁴BioStatistics Consulting Center, Temple University School of Medicine, Philadelphia, PA, United States, ⁵Department of Systems Neuroscience, University Medical Center Hamburg-Eppendorf, Hamburg, Germany
- This is the first study in pediatric subjects investigating the DTI values and its reproducibility along the entire cervical and thoracic spinal cord (SC). DTI data was acquired from 22 typically developing (TD) children and 15 patients with spinal cord injury (SCI) using an inner field-of-view DTI sequence. Regions of interest were manually drawn on whole cord at every axial slice along the cervical and thoracic SC. Fractional anisotropy and radial diffusivity values were significantly different between TD and SCI suggesting that these appear to be the most sensitive parameter in assessing the state of SC in chronic phase of SCI. This study demonstrates that DTI has a potential to be used as an imaging biomarker for evaluating the extent of injury, which may be useful to prognosticate as well as monitor patients with SCI
- 3430
Computer #27 Time-dependent diffusion for assessment of treatment response in GL261 murine glioma model
Olivier Reynaud¹, Jin Zhang¹, Kerryanne Veronica Winters¹, Dmitry Novikov¹, and Sungheon Gene Kim¹
- ¹Center for Biomedical Imaging, Department of Radiology, NYU School of Medicine, New York, NY, United States
- In this study, we investigate the feasibility of using the recently proposed diffusion MRI method, POMACE (Pulsed and Oscillating gradient MRI Assessment of Cell size and Extracellular space) for characterization of tissue changes induced by chemotherapy. Surface-to-volume ratio (S/V), cell size (R_{cell}) and extracellular space volume fraction (ECS) are estimated prior to and after 5FU and bevacizumab treatment in GL261 murine glioma model. Preliminary results indicate an early ECS decrease two days after 5FU/bevacizumab administration. By combining OGSE and PGSE, POMACE provides non-invasive and quantitative metrics regarding tumor microstructure that can be applied to evaluate treatment response.
- 3431
Computer #28 Diffusion Tensor Imaging and Neuropsychological Study: Pilot Findings in HIV Adults
Rajakumar Nagarajan¹, Manoj K Sarma¹, Edward Xu¹, Paul M Macey², Mario Guerrero³, Vanessa Correa³, Eric S Daar³, and M.Albert Thomas¹
- ¹Radiological Sciences, University of California Los Angeles, Los Angeles, CA, United States, ²UCLA School of Nursing, University of California at Los Angeles, Los Angeles, CA, United States, ³Department of Medicine, Harbor-UCLA Medical Center, Torrance, CA, United States

Our current study examined whether neuroimaging abnormalities in HIV infected adults are associated with neuropsychological changes as measured by diffusion tensor imaging (DTI) and HIV Dementia scale (HDS). Several brain regions demonstrated significantly decreased values of fractional anisotropy and mean diffusivity. Also there was a significant decline of HDS scores observed in the construction abilities of HIV infected adults compared to healthy controls. This study indicates that DTI is a sensitive tool for correlating neuroanatomic pathologic features with specific cognitive deficits in patients with HIV infection.

3432 Computer #29 Temporal evolution of diffusion indices in white matter and grey matter of macaque brains with ischemic stroke
Chun-Xia Li¹, Yumei Yan¹, Frank Tong², Doty Kempf¹, Stuart Zola^{1,3,4}, Leonard Howell^{1,3}, and Xiaodong Zhang¹

¹Yerkes National Primate Research Center, Emory University, Atlanta, GA, United States, ²Department of Radiology, School of Medicine, Emory University, Atlanta, GA, United States, ³Department of Psychiatry and Behavioral Sciences, School of Medicine, Emory University, Atlanta, GA, United States, ⁴Atlanta Veterans Affairs Medical Center, Decatur, GA, United States

In the present study, adult macaque monkeys were utilized to characterize the temporal changes of DTI-derived diffusion indices in grey matter (GM) and white matter (WM) after ischemic stroke. Our results showed that mean diffusivity (MD), radial diffusivity (RD) and axial Diffusivity (AD) decreased significantly in GM and WM immediately post stroke while fractional anisotropy (FA) remained unchanged until 48-hour post stroke. The results demonstrate the sensitivity and robustness of MD, AD and RD to access the ischemic injury of GM and WM during hyperacute stroke, and also reveal the temporal evolution of the WM and GM microstructure following stroke onset.

3433 Computer #30 Clinical Evaluation of Simultaneous Multi-Slice Diffusion-weighted Magnetic Resonance Imaging of the Prostate
Jakob Weiss¹, Jana Taron¹, Ahmed E. Othman¹, Petros Martirosian¹, Sascha Kaufmann¹, Ulrich Kramer¹, Konstantin Nikolaou¹, and Mike Notohamiprodjo¹

¹Diagnostic and Interventional Radiology, University of Tuebingen, Tuebingen, Germany

To evaluate the clinical performance of simultaneous multi-slice (sms) diffusion-weighted imaging (DWI) of the prostate. A prototype sms-DWI sequence was utilized and compared to conventional DWI sequences. Sms acquisition is based on the recently introduced principle of simultaneously exciting and acquiring multiple slices by a single radiofrequency (RF) pulse, thus accelerating image acquisition directly by the number of simultaneously excited slices (MB-factor). Image analyses revealed similar image quality and lesion detection as compared to conventional DWI sequences at a substantially decreased acquisition time. Sms-DWI seems a valuable alternative to conventional DWI sequences for prostate imaging.

3434 Computer #31 Comparison of six different diffusion weighted MRI models in pancreatic cancer patients
Oliver J. Gurney-Champion^{1,2}, Remy Klaassen³, Martijn Froeling^{1,4}, Jaap Stoker¹, Johanna W. Wilmink^{3,5}, Arjan Bel², Hanneke W.M. van Laarhoven³, and Aart J. Nederveen¹

¹Radiology, Academic Medical Center, Amsterdam, Netherlands, ²Radiation Oncology, Academic Medical Center, Amsterdam, Netherlands, ³Medical Oncology, Academic Medical Center, Amsterdam, Netherlands, ⁴Radiology, University Medical Center Utrecht, Utrecht, Netherlands, ⁵Internal Medicine, Academic Medical Center, Amsterdam, Netherlands

We compare the performance of six models for diffusion weighted MRI (DWI) data signal intensity as a function of b-values. We obtained three DWI-datasets spread over two sessions from 9 pancreatic cancer patients. To characterize the fit parameters' sensitivity to abnormalities, we compared the difference in fit parameter values between tumorous and healthy tissue. To characterize repeatability, we obtained the coefficient of variation. Every model had exactly one parameter that was significantly sensitive to tumorous tissue ($p < 0.05$). From these parameters, the most sensitive parameter was f_2 from the tri-exponential model, whereas the best repeatable measure was the ADC from the mono-exponential model.

3435 Computer #32 Intravoxel incoherent motion analysis of renal allograft diffusion with clinical and histopathological correlation in pediatric kidney transplant patients
Clare B Poynton¹, Marsha Lee², Yi Li¹, Zoltan Laszik³, John D Mackenzie¹, Pauline W Worters⁴, and Jesse Courtier¹

¹Department of Radiology and Biomedical Imaging, University of California, San Francisco, San Francisco, CA, United States, ²Department of Pediatrics, University of California, San Francisco, San Francisco, CA, United States, ³Department of Pathology, University of California, San Francisco, San Francisco, CA, United States, ⁴GE Healthcare, Menlo Park, CA, United States

This study investigated the use of intravoxel incoherent motion (IVIM) analysis for characterizing diffusion in renal allografts of pediatric transplant recipients. Patients were separated into two groups according to whether or not a renal allograft biopsy resulted in a change in clinical management. Patients requiring a change in management (i.e., increase in immunosuppression) showed statistically significant differences in tissue diffusivity in the region of the biopsy relative to those that did not require any change. These results suggest IVIM analysis may be a useful non-invasive tool for guiding clinical management of pediatric kidney transplant patients.

3436 Computer #33 Tract-profiling and bundle statistics: a test-retest validation study
Martin Cousineau¹, Eleftherios Garyfallidis¹, Marc-Alexandre Côté¹, Pierre-Marc Jodoin¹, and Maxime Descoteaux¹

¹Computer Science, Université de Sherbrooke, Sherbrooke, QC, Canada

Tractometry is a hot topic in population analysis that combines diffusion MRI metrics along white matter bundles. Using a dataset of 11

healthy subjects with 3 different acquisitions collected within the same week, and a state of the art processing pipeline that removes outliers and splits bundles in separate parts by computing their centroid, we perform a test-retest study which validates that tractometry results are reproducible in terms of shape, volume, average metric value, and tract profiles.

3437

Computer #34 Methodological considerations on graph theoretical analysis of structural brain networks
Timo Roine¹, Ben Jeurissen¹, Daniele Perrone², Jan Aelterman², Wilfried Philips², Jan Sijbers¹, and Alexander Leemans³

¹*iMinds-Vision Lab, Department of Physics, University of Antwerp, Wilrijk (Antwerp), Belgium*, ²*Ghent University-iMinds/Image Processing and Interpretation, Ghent, Belgium*, ³*Image Sciences Institute, University Medical Center Utrecht, Utrecht, Netherlands*

We studied the reproducibility of whole-brain structural brain connectivity networks reconstructed with constrained spherical deconvolution based probabilistic fiber tractography. Our main finding is that a low spherical harmonics order decreases the reproducibility of graph measures in connectomics. This is most likely caused by the wider peaks in the fiber orientation distributions, which increase the variation in orientations sampled by the tractography algorithm. Based on our observations, we recommend using spherical harmonics decomposition with an order of at least eight whenever the data allows so. In addition, threshold value was important for binary networks, and some network properties were highly intercorrelated.

3438

Computer #35 Diffusion-Weighted Hyperpolarized ¹³C-Urea in a Murine Model of Liver Fibrosis
Irene Marco-Rius¹, Jeremy A Gordon¹, Peder EZ Larson¹, Romelyn delos Santos¹, Robert A Bok¹, Aras Mattis^{2,3}, Jacquelyn Maher^{3,4}, Daniel B Vigneron^{1,3}, and Michael A Ohliger^{1,3}

¹*Department of Radiology and Biomedical Imaging, University of California San Francisco, San Francisco, CA, United States*, ²*Department of Pathology, University of California San Francisco, San Francisco, CA, United States*, ³*Liver Center, University of California, San Francisco, San Francisco, CA, United States*, ⁴*Department of Medicine, Division of Gastroenterology, University of California San Francisco, San Francisco, CA, United States*

Diffusion weighted MRI has been widely used to measure the movement of water molecules and study tissue microstructure in order to characterize both diffuse and focal liver disease. In liver fibrosis, for instance, increased collagen formation is associated with restricted diffusion of water. However, the majority of water within the liver is either in the vascular or intracellular space, making the diffusion of water a potentially poor marker for fibrosis, which is an extracellular process. Here, we investigated applying diffusion-weighted MRI with an exogenously injected extracellular agent, hyperpolarized ¹³C-urea, as a potentially more sensitive probe of the extracellular space in the liver in a mouse model of liver fibrosis induced with CCl₄.

3439

Computer #36 Diffusion parameters derived from multi b-value DWI-data as surrogate marker for kidney function
Oliver J. Gurney-Champion^{1,2}, René van der Bel³, Martijn Froeling^{1,4}, C.T. Paul Krediet³, and Aart J. Nederveen¹

¹*Radiology, Academic Medical Center, Amsterdam, Netherlands*, ²*Radiation Oncology, Academic Medical Center, Amsterdam, Netherlands*, ³*Internal Medicine, Academic Medical Center, Amsterdam, Netherlands*, ⁴*Radiology, University Medical Center Utrecht, Utrecht, Netherlands*

In this study, we show the potential of the tri-exponential intravoxel incoherent motion (IVIM) model parameters as surrogates for kidney function. We show (n=8) that f_1 , f_2 and D (fit parameters) changed as function of angiotensin-II dose (0, 0.3, 0.9 and 3 ng/kg/min). The changes in f_1 and f_2 correlated (correlation coefficient $r=0.42$ and -0.62 ; $p=0.01$ and $p<0.001$) to changes in effective renal plasma flow (ERPF) and glomerular filtration rate (GFR) deduced from a ¹²⁵I-thalamate and ¹³¹I-hippuran clearing test. Finally, we showed (n=6) high inter-session and intra-session repeatability with coefficients of variation below 15% for all fit parameters.

3440

Computer #37 Inter-modality correlation of prostatic microenvironmental tissue stiffness and water diffusivity using quantitative functional imaging techniques.
Hugh Harvey¹, Jeremie Fromageau², Veronica Morgan¹, Liz Bancroft³, Ros Eeles³, Jeff Bamber², and Nandita deSouza¹

¹*Radiotherapy & Imaging, The Institute of Cancer Research and Royal Marsden NHS Foundation Trust, London, United Kingdom*, ²*The Institute of Cancer Research, London, United Kingdom*, ³*Oncogenetics, The Institute of Cancer Research and Royal Marsden NHS Foundation Trust, London, United Kingdom*

Location-matched ROI analysis of tissue stiffness (SWE) and water diffusivity (ADC) in 9 normal prostates demonstrated that both techniques can adequately differentiate between peripheral and transitional zonal microenvironments, and that there is a weak negative correlation between tissue stiffness and water diffusivity in the peripheral zone. This suggests that factors such as microvasculature, cell size, extracellular matrix and macromolecules may have a differential effect on tissue stiffness and diffusivity. Transitional zone stiffness is too heterogeneous to demonstrate significant inter-modality correlation.

3441

Computer #38 Dependence of DTI Measures on SNR in a Multicenter Clinical Trial
Xiaopeng Zhou¹, Ken Sakaie¹, Josef Debbins², Robert Fox¹, and Mark Lowe¹

¹*Cleveland Clinic, Cleveland, OH, United States*, ²*Barrow Neurological Institute, Phoenix, AZ, United States*

The dependence of DTI metrics on SNR was investigated in a longitudinal multicenter clinical trial. We presented a combined simulation and experimental analysis of the effect of SNR on DTI measures using 27 scanners over 15 months. Although the dependence of DTI measures on SNR is different for each type of scanner, we demonstrate the inverse relation between mean diffusivity and SNR and FA decreasing slightly with SNR. A sufficient SNR is essential for a reliable estimation of DTI parameters generally and the dependence of

- 3442
Computer #39 The effect of brain microbleeds on the structural brain network after stroke
Xiaopei Xu¹, Henry KF Mak¹, Raja Rizal Azman², Kui-Kai Lau³, and Edward S Hui¹
- ¹Department of Diagnostic Radiology, The University of Hong Kong, Hong Kong, Hong Kong, ²Department of Bio-Medical Imaging, University of Malaya, Kuala, Malaysia, ³Department of Medicine, The University of Hong Kong, Hong Kong, Hong Kong*

To explore the influences of brain microbleeds (BMBs) on structural brain network in stroke patients, we used DTI-based tractography and brain network analysis to investigate the brain structural network configuration in stroke patients with and without BMBs. Our results demonstrated disrupted balance between integrated and segregated process in global network, and enhanced specialized functions in stroke patients with BMBs. These findings suggested that the presence of BMBs is related to a disturbed brain network organization with imbalanced integrated and segregated information process ability, and brain network analysis is a sensitive tool to assess the impaired cognition caused by cerebral small vessel disease.

- 3443
Computer #40 DTI Association with Working Memory and Speed in Cognitive Network Pathways
Junyu Guo¹, John O. Glass¹, JungWon Hyun¹, Yimei Li¹, Conklin Heather¹, Lisa Jacola¹, Ching-Hon Pui¹, Sima Jeha¹, and Wilbrun E. Reddick¹
- ¹St Jude Children's Research Hospital, Memphis, TN, United States*

We investigate the relationship of structural diffusion tensor imaging (DTI) metrics with working memory and decision speed performance in children treated for acute lymphoblastic leukemia (ALL). We built a core neurocognitive network including a central executive network, a salience network, and subcortical cortex based on previous fMRI findings. We generated structural connectivity pathways based on high-resolution DTI data from the human connectome project, and applied those in ALL patients to quantify DTI measures in each pathway. We found that DTI measures in most pathways were significantly associated with working memory and decision speed performance suggesting an essential structural neurocognitive network.

- 3444
Computer #41 Clinical Application of Simultaneous Multi-Slice DWI: A Multi-Body-Part Comparison with Standard EPI DWI
Man Sun¹, Hongyan Ni², Xu Yan³, and Tianyi Qian⁴
- ¹First Central Clinical College, Tianjin Medical University, Tianjin, China, People's Republic of, ²Tianjin First Central Hospital, Tianjin, China, People's Republic of, ³MR Collaborations NE Asia, Siemens Healthcare, Shanghai, China, People's Republic of, ⁴MR Collaborations NE Asia, Siemens Healthcare, Beijing, China, People's Republic of*

Applying simultaneous-multi-slice EPI (SMS EPI) sequences in diffusion-weighted imaging (DWI) can reduce scanning time greatly, but its clinical-routine image quality in different body parts has not been broadly tested. This study compared multi-site DWI images acquired with a prototype SMS EPI sequence with those acquired with a traditional EPI sequence, computed SNR and CNR and conducted paired t-test. The results show there are no significant differences of SNR and CNR between the two kinds of sequence ($p > 0.05$). When the SMS EPI sequence was applied to the clinical DWI examination, it not only reduced scanning time, but also kept the SNR, CNR in the same level as standard EPI. The SMS sequence was able to satisfy the requirements of clinical disease diagnosis.

- 3445
Computer #42 Altered social communication network in boys with autism spectrum disorder
Yu-Chun Lo¹, Yu-Jen Chen¹, Yung-Chin Hsu¹, Susan Shur-Fen Gau², and Wen-Yih Isaac Tseng¹
- ¹Institute of Medical Device and Imaging, National Taiwan University College of Medicine, Taipei, Taiwan, ²Department of Psychiatry, National Taiwan University College of Medicine, Taipei, Taiwan*

Impaired social communication skills have been consistently reported in autism spectrum disorder (ASD). We used diffusion spectrum imaging to measure white matter integrity of the social communication network, and investigated its relationships with social communication and social interaction in 62 ASD and 55 typically developing (TD) boys. ASD showed partially reduced white matter integrity of the social communication network as compared to TD. Positive correlations were found between white matter integrity and the social interaction in ASD. In conclusion, altered microstructural property of the social communication network might be a structural correlate of social communication deficits in ASD.

- 3446
Computer #43 The negative residuals of diffusion kurtosis model: a study on rat brain imaging
Wei-Cheng Lee¹, Sheng-Min Huang¹, Cheng-He Li¹, Kung-Chu Ho², and Fu-Nien Wang¹
- ¹Department of Biomedical Engineering and Environmental Sciences, National Tsing Hua University, Hsinchu, Taiwan, ²Nuclear Medicine, Chang Gung Memorial Hospital, Taoyuan, Taiwan*

The well-behaved residual of a successful fitting model should present as an independent random variable in its histogram, otherwise it will contain structure that is not accounted for in this model. In the study, we found that there are two groups of fitting residuals. And the spatial mapping of these smaller negative pixels reveals that the overestimation of kurtosis model is related to the contribution of vessel signal. Therefore, we proposed a semi-kurtosis model to calculate the restricted diffusion adequately and obtain correct DKI information in these regions with vascular interference.

- 3447
Computer #44 Spherical Deconvolution of High-Resolution 7T Whole-Head Diffusion Magnetic Resonance Images shows reduced radial anisotropic diffusion in human primary somatosensory cortex
Ralf Lützkendorf¹, Robin M. Heidemann², Thorsten Feiweier², Michael Luchtmann³, Sebastian Baecke¹, Joern Kaufmann⁴, Joerg Stadler⁵, Eike Budinger⁵, and Johannes Bernarding¹
- ¹Biometry and Medical Informatics, University of Magdeburg, Magdeburg, Germany, ²Siemens Healthcare GmbH, Erlangen, Germany, ³Department of Neurosurgery, University of Magdeburg, Magdeburg, Germany, ⁴Department of Neurology, University of Magdeburg, Magdeburg, Germany, ⁵Leibniz Institute for Neurobiology, Magdeburg, Germany
- Diffusion anisotropy in cortical gray matter (GM) and adjacent white matter (WM) provides microanatomic information about the course of the neuronal structures within GM and when connecting to other brain regions. However, interwoven neuronal fiber orientations and complex folded structures render the analysis difficult. Ultra-high-field diffusion MR imaging (dMRI) overcomes these limitations as the improved SNR allowed acquiring 1.4 mm isotropic voxel with increased diffusion-weighting. Applying constrained spherical deconvolution (1) enabled resolving radial and tangential anisotropic diffusion in cortical gray matter confirming recent reports of reduced radial anisotropy in primary somatosensory cortex as compared to other cortical areas (2).
-
- 3448
Computer #45 Investigation of diffusion signal behavior at different diffusion times in a human hepatocellular carcinoma xenograft model
Mami Iima^{1,2}, Tomomi Nobashi¹, Hirohiko Imai³, Sho Koyasu¹, Akira Yamamoto¹, Yuji Nakamoto¹, Masako Kataoka¹, Tetsuya Matsuda³, and Kaori Togashi¹
- ¹Department of Diagnostic Imaging and Nuclear Medicine, Graduate School of Medicine, Kyoto University, Kyoto, Japan, ²The Hakubi Center for Advanced Research, Kyoto University, Kyoto, Japan, ³Department of Systems Science, Graduate School of Informatics, Kyoto University, Kyoto, Japan
- The relationship between diffusion time and diffusion parameters in a human hepatocellular carcinoma xenograft mouse model was investigated at 7T. There was an increase in K values and decrease in ADCo values in 27.6ms compared to 9.6 ms. Accordingly a remarkable difference in a composite index (sADC) was also found. The investigation of the water diffusion behavior at different diffusion times may provide valuable information on the contribution of the different compartments or tissue components to the overall diffusion MRI.
-
- 3449
Computer #46 Altered microstructural integrity of the white matter tracts in strabismus: A systematic tract-specific analysis over the whole brain
Hsien-Te Su¹, Tzu-Hsun Tsai², Yao-Chia Shih³, Yu-Shiang Tzeng⁴, Chien-Chung Chen⁴, and Wen-Yih Isaac Tseng^{1,5}
- ¹Institute of Medical Device and Imaging, National Taiwan University College of Medicine, Taipei City, Taiwan, ²Department of ophthalmology, National Taiwan University Hospital, Taipei City, Taiwan, ³Institute of Biomedical Engineering, National Taiwan University, Taipei City, Taiwan, ⁴Department of Psychology, National Taiwan University College of Science, Taipei City, Taiwan, ⁵Molecular Imaging Center, National Taiwan University, Taipei City, Taiwan
- To investigate whether the white matter tracts are altered in patients with strabismus, we used diffusion spectrum imaging to measure microstructural property of 78 major white matter tracts, and compared the property between 12 patients with strabismus adults and 24 matched controls. As compared to the controls, patients showed differences with large effect sizes in the left vertical occipital fasciculus, callosal fibers to bilateral precuneus, callosal fibers to bilateral inferior parietal lobules, and the left superior longitudinal fasciculus I. The altered white matter tracts support the hypothesis of underlying microstructural changes of the visual pathways in strabismus.
-
- 3450
Computer #47 Flip Angle Optimization in Diffusion-Weighted Imaging using Simultaneous Multi-Slice Acceleration
Wei Liu¹ and Kun Zhou¹
- ¹Siemens Shenzhen Magnetic Resonance Ltd, Shenzhen, China, People's Republic of
- In this study, an automatic optimization scheme was proposed in diffusion-weighted imaging using simultaneous multi-slice (SMS) acceleration to determine an appropriate flip angle based on a short TR, which is capable to obtain similar contrast of a pair of tissue type compared to the one with long TR scan. With this optimization scheme, minimal TR in SMS case is practically achievable and there is no obvious contrast deviation between images from long TR (FA = 90°) and short TR (FA < 90°).
-
- 3451
Computer #48 Investigation of Intravoxel Fiber Configuration Complexity in the Human Heart
Changyu SUN¹, Lihui WANG², Feng YANG³, and Yuemin ZHU¹
- ¹CREATIS; CNRS UMR 5220; Inserm U 1044; INSA of Lyon; University of Lyon, Lyon, France, ²School of computer science and technology, Guizhou University, Guiyang, China, People's Republic of, ³School of Computer and Information Technology, Beijing JiaoTong University, Beijing, China, People's Republic of
- Fiber crossing in the myocardium of the heart is controversial despite some reports on the heart of animals. The purpose of this study is to investigate the fiber configuration complexity in a voxel, such as fiber crossing, in the human heart. We applied two different reconstruction techniques commonly used in high angular resolution diffusion imaging (HARDI) to conventional diffusion tensor imaging (DTI) data of the human heart acquired on clinical MRI system. The results consistently demonstrated that the human myocardium exhibits some complex fiber configurations such as fiber crossing in a voxel.

Diffusion: Body

Exhibition Hall

Tuesday, May 10, 2016: 14:30 - 15:30

3452



Computer #49

Prediction of the development of distant metastases from nasopharyngeal carcinoma using Diffusion-Weighted Imaging
 Qi Yong Ai¹, Ann D. King¹, Benjamin King Hong Law¹, Lok Yiu Sheila Wong¹, Kunwar S. Bhatia¹, David Ka Wai Yeung², and Brigette B.Y. Ma²

¹Department of Imaging and Interventional Radiology, The Chinese University of Hong Kong, Shatin, Hong Kong, ²Department of Clinical Oncology, The Chinese University of Hong Kong, Shatin, Hong Kong

This study evaluated pre-treatment diffusion weighted imaging of primary nasopharyngeal carcinoma for the prediction of patients at risk of distant metastases, based on long-term follow-up for at least 5 years. Analysis was performed of ADC parameters using histogram analysis (ADC_{mean}, ADC_{skewness} and ADC_{kurtosis}), together with stage and volume of the primary tumour and nodes. Multivariate analysis showed pre-treatment ADC_{skewness}, T stage and nodal volume were significant (p = 0.026, 0.022 and 0.005, respectively), distant metastases being more likely in patients with tumours with ADC values skewed toward the higher ADC range, and higher T stage and nodal volume.

3453

Computer #50

Differentiation of prostate cancer in central gland with Histogram analysis of apparent diffusion coefficient
 Xiaohang Liu¹, Liangping Zhou¹, Weijun Peng¹, and Yong Zhang²

¹Radiology, Fudan university shanghai cancer center, Shanghai, China, People's Republic of, ²MR Research China, GE healthcare, Beijing, China, People's Republic of

The diffusion weighted imaging (DWI) is commonly used in the diagnosis of Prostate cancer, but the cancer in Central gland (CG) is considered harder to detected on conventional DWI, but histogram analysis of apparent diffusion coefficient could potentially improve the differentiation of prostate cancer in CG.

3454

Computer #51

Statistical evaluation of bi-exponential IVIM effect in healthy human liver and its dependence on the cut-off b-value for segmented biexponential fit
 Oi Lei Wong¹, Jing Yuan¹, Gladys Goh Lo², Thomas W. T. Leung³, Wai Ki Chung², and Benny W. H. Ho²

¹Medical Physics and Research Department, Hong Kong Sanatorium & Hospital, Hong Kong, Hong Kong, ²Department of diagnostic & interventional radiology, Hong Kong Sanatorium & Hospital, Hong Kong, Hong Kong, ³Comprehensive Oncology Center, Hong Kong Sanatorium & Hospital, Hong Kong, Hong Kong

The use of IVIM in assessing the microcapillary perfusion and true diffusion has attracted elevating attention. The segmented bi-exponential fitting has been widely adopted to calculate IVIM metrics, in which a cut-off b-value is pre-defined for perfusion and diffusion region separation. This study calculated the corrected Akaike Information Criterion (AICc) for bi-exponential IVIM model in the healthy human liver with varying cut-off b-values and then compared to the AICc for the mono-exponential model. The statistical preference of the bi-exponential model to mono-exponential model was demonstrated based on the lowest AICc. This bi-exponential model preference was independent of the choice of cut-off b-value and ROI location.

3455

Computer #52

Histogram analysis of apparent diffusion coefficient in characterizing solid pancreatic masses
 Yoshihiko Fukukura¹, Toshikazu Shindo¹, Yuichi Kumagai¹, Koji Takumi¹, Hiroto Hakamada¹, Masanori Nakajo¹, and Takashi Yoshiura¹

¹Radiology, Kagoshima University Graduate School of Medical and Dental Sciences, Kagoshima, Japan

This study focused on the potential of ADC histogram analysis on DW imaging to characterize solid pancreatic masses. Among the ADC histogram parameters, the entropy of ADC with every b-value combination showed the highest area under the receiver operating characteristic curve for distinguishing neuroendocrine tumors from pancreatic adenocarcinomas and mass-forming autoimmune pancreatitis. The entropy of ADC might add helpful information in differentiating neuroendocrine tumors from pancreatic adenocarcinomas and mass-forming autoimmune pancreatitis, especially in patients with contraindication to contrast agents or with solid pancreatic masses showing atypical findings at dynamic CT or MRI.

3456

Computer #53

Histogram analysis of apparent diffusion coefficient for non-small cell lung cancer: correlation with pathological grade.
 Mariko Doai¹, Naoko Tsuchiya¹, Hisao Tonami¹, and Katsuo Usuda²

¹Radiology, Kanazawa Medical University, Kahoku, Japan, ²Thoracic surgery, Kanazawa Medical University, Kahoku, Japan

The purpose of this study is to investigate the application of histogram analysis of ADC in determining the pathological grade of non-small cell lung cancer (NSCLC). The study included 54 patients and the histogram parameters were correlated with pathological grades. For the parameters that were significantly different between high- and low-grade tumors, ROC curve analysis was performed. The 95th percentile of ADC was the most beneficial parameter for distinguishing high-from low-grade tumors. ADC histogram analysis on the basis of the entire tumor volume is useful for predicting the pathological grade of NSCLC.

- 3457
Computer #54 The superiority of high b value iZOOM with a Two Dimensional Radiofrequency Pulse (2D RF) Echo Planner Imaging (EPI) Sequence in Prostate Compared with regular ss-EPI DWI at 3.0 T
Kangjie Xu¹, Xiaodong Zhang¹, Chengyan Wang², Hongxia Sun¹, Yu Zhang³, Zhigang Wu⁴, Juan Wei⁵, and Xiaoying Wang¹
- ¹The Department of Radiology, Peking University First Hospital, Beijing, China, People's Republic of, ²Academy for Advanced Interdisciplinary Studies, Peking University, Beijing, China, People's Republic of, ³Philips Healthcare, Beijing, China, People's Republic of, ⁴Philips Healthcare (Suzhou) Co., Ltd (Suzhou), Suzhou, China, People's Republic of, ⁵Philips research China, Beijing, China, People's Republic of*
- This study aims to assess the clinical feasibility of high b value iZOOM on prostate and to validate whether it is superior to regular DWI at 3.0 T with 58 patients recruited in the study. The scan protocol included iZOOM and DWI with b value of 2000s/mm². Subjective and objective evaluation was carried out from three aspects: the basic image quality, the display of lesions, and the overall image quality. Our study found that with the same high b value, iZOOM had better comprehensive image quality, less artifact and distortion yet similar contrast compared with regular DWI.
-
- 3458
Computer #55 Feasibility of vertebral bone Diffusion Weighted MR Imaging (DWI) for early diagnosis of hepatic osteodystrophy in Primary Sclerosing Cholangitis
Sarah Keller¹, Fabian Kording¹, Hendrick Kooijman², Christoph Schramm³, Roland Fischer⁴, Adam Gerhard¹, Ansgar Lohse³, Harald Ittrich¹, and Jin Yamamura¹
- ¹Diagnostic and Interventional Radiology, University Medical Center Hamburg Eppendorf (UKE), Hamburg, Germany, ²MRI, Philips GmbH, Hamburg, Germany, ³Department of Internal Medicine, University Medical Center Hamburg Eppendorf (UKE), Hamburg, Germany, ⁴Biochemistry, University Medical Center Hamburg Eppendorf (UKE), Hamburg, Germany*
- Hepatic osteodystrophy is a frequent complication in patients with chronic cholestatic and non-cholestatic liver disease, affecting up to 20-30% of patients [1, 2]. Besides conventional dual x-ray absorptiometry (DXA) scans, diffusion-weighted MRI (DWI) has been performed for the evaluation of osteoporosis and osteopenia in risk patients. Follow up MRI examinations of PSC patients, to exclude malignancy and identify bile duct stenosis, are frequently performed in clinical routine. The aim of this study was to test the feasibility of add-on DWI sequences during routine examination for the detection of early changes of the bone marrow density (BMD) in comparison to DXA T-score values of the vertebral bone and healthy controls.
-
- 3459
Computer #56 Readout-Segmented Echo-Planar Imaging Improves the Image Quality of Diffusion-Weighted MR Imaging in Rectal Cancer
Chunchao Xia¹, Panli Zuo², David Porter³, Zhenlin Li⁴, and Bin Song⁴
- ¹West China Hospital, Chengdu, China, People's Republic of, ²Beijing, China, People's Republic of, ³Erlangen, Germany, ⁴Chengdu, China, People's Republic of*
- Readout-segment EPI (rs-EPI) is a new approach to reduce susceptibility artifacts and blurring in DWI. In this study, we qualitatively and quantitatively compare the images quality of ss-EPI and rs-EPI for rectal cancer DWI
-
- 3460
Computer #57 Clinical application of quantitative DWI in the pathological grading of lipid-containing small HCC
Weimin An¹, Jing Lei¹, Changchun Liu¹, and Jinghui Dong¹
- ¹302 military hospital of China, Bei Jing, China, People's Republic of*
- This study is designed to investigate whether ADC values of lipid-containing small HCC with different pathological grading are the same as well as the correlation of ADC values with the pathological differentiate degree was significant difference between low-grade group and moderate-grade group, as well as between low-grade group and high-grade group (P <0.05), or there was obviously significant difference between moderate-grade and high-grade group (p <0.05). Meanwhile, there was moderately positive correlation between ADC value and pathological grading of lipid-containing small HCC (P=0.002, r=0.419) and the coefficient of association was 0.95. This study demonstrated ADC value can distinguish different pathological grading of lipid-containing small HCC, and there is moderately positive correlation between them.
-
- 3461
Computer #58 Implementing a fast MR screening protocol for pancreas in patients with mutations of BRCA1 and BRCA2: preliminary data on Diffusion-Weighted Images.
Andrea Agostini¹, Mitchell Raeside¹, Richard Do¹, Amita Shukla-Dave², David Aramburu Nunez², Ramesh Paudyal², Olga Smelianskaia¹, Maggie Fung³, Monika Khan¹, David Kelsen⁴, Gabriella Carollo⁵, and Lorenzo Mannelli¹
- ¹Department of Radiology, Memorial Sloan-Kettering Cancer Center, New York, NY, United States, ²Department of Medical Physics, Memorial Sloan-Kettering Cancer Center, New York, NY, United States, ³Global MR Applications and Workflow, GE Healthcare, New York, NY, United States, ⁴Department of Medicine, Memorial Sloan-Kettering Cancer Center, New York, NY, United States, ⁵Saint Vincent Ferrer High School, New York, NY, United States*
- The aim of the study is the qualitative and quantitative evaluation of Diffusion-weighted images (DWI) with reduced field-of-view (rFOV), that are incorporated into a fast rapid MR pancreas screening protocol (MRpsp). We are developing a fast rapid MRpsp to be performed in carriers of BRCA mutations after a breast MRI, using the built-in body coil of a 3T magnet without repositioning a patient who is in the prone position. 15 patients were scanned. For b-values <100 s/mm², b=20 s/mm² DWI had the best contrast-to-noise and signal-to-noise ratios. Among b-values >100 s/mm², b=250 s/mm² DWI showed the highest diagnostic information.

- 3462
Computer #59 Optimization of Direct-coronal Diffusion-weighted Whole Body Imaging with Background Suppression (DWIBS) Using Single-shot Turbo Spin-echo (TSE) at 3T MRI.
Makoto Suzuki¹, Tatsuya Kuramoto¹, Yuki Hachiman¹, Yu Nishina², Satoru Morita², Kayoko Abe², and Masami Yoneyama³
¹Department of radiological servece, Tokyo Women's Medical University Hospital, Tokyo, Japan, ²Department of Diagnostic Imaging and Nuclear Medicine, Tokyo Women's Medical University Hospital, Tokyo, Japan, ³IS Business Group, Philips electronics japan, Tokyo, Japan
- Direct-coronal diffusion-weighted whole body imaging with background body signal suppression using single-shot turbo spin-echo (TSE-DWIBS) with b-values of 400, 600, 800, and 1000 mm²/s, and DWIBS using echo-planner imaging (EPI-DWIBS) with b-value of 1000mm²/s were obtained using 3T MR scanner in 5 healthy volunteers. We investigated optimal b-value of TSE-DWIBS and compared image distortions, contrast, signal-to-noise ratio (SNR), and artifacts between TSE-DWIBS and EPI-DWIBS. Image contrast and SNR of TSE-DWIBS with b-value of 800 mm²/s were equivalent to those of EPI-DWIBS with b-value of 1000 mm²/s. TSE-DWIBS had less image distortions and artifacts than EPI-DWIBS. Direct-coronal TSE-DWIBS using 3T MRI can be applied for clinical cases.
-
- 3463
Computer #60 Repeatability on diffusion MRI measurements on the different numbers of b values and excitations of the breast and its comparison with lactating breasts
Mami Iima^{1,2}, Masako Kataoka¹, Shotaro Kanao¹, Natsuko Onishi¹, Makiko Kawai¹, Akane Ohashi¹, Rena Sakaguchi¹, and Kaori Togashi¹
¹Department of Diagnostic Imaging and Nuclear Medicine, Graduate School of Medicine, Kyoto University, Kyoto, Japan, ²The Hakubi Center for Advancer Research, Kyoto University, Kyoto, Japan
- The effects of different numbers of b values and excitations on the non-Gaussian DWI parameter estimates in the breast of normal volunteers was assessed. A good agreement of Do, K and synthetic ADC₂₀₀₋₁₅₀₀ was observed among different number of b values as well as excitations. Lower Do and sADC₂₀₀₋₁₅₀₀ were found in women with lactation period. Higher K and fIVIM were observed in lactating volunteers with some overlap. A limited protocol using only 5 b values could be relevant in clinical setting, resulting in a remarkable reduction in acquisition time.
-
- 3464
Computer #61 Zoomed EPI-DWI of the Kidney Using Two-Dimensional Spatially-Selective Radiofrequency Excitation Pulses
Yong-Lan He¹, Philipp Riffel², Daniel Hausmann², Stefan Schönberg², and Ulrike Attenberger²
¹Radiology, Peking Union Medical College Hospital, Beijing, China, People's Republic of, ²Department of Clinical Radiology and Nuclear Medicine, University Medical Center Mannheim, Heidelberg University, Mannheim, Germany
- This is the first MR study to evaluate the use of zoomed EPI technology for diffusion-weighted imaging in the kidney. Zoomed diffusion-weighted EPI leads to substantial image quality improvements with reduction of susceptibility artifacts in renal DWI. The combination of the two sequences for renal imaging might be recommended: a c-EPI scan to cover and screen the whole upper abdomen and a z-EPI scan focused on the targeted anatomical structure and suspected lesions.
-
- 3465
Computer #62 Non-invasive quantification of prostate cancer using AMICO framework for VERDICT MRI
Elisenda Bonet-Carne¹, Alessandro Daducci^{2,3}, Eleftheria Panagiotaki¹, Edward Johnston⁴, Nicola Stevens⁴, David Atkinson⁴, Shonit Punwani⁴, and Daniel C Alexander¹
¹Centre for Medical Image Computing, University College London, London, United Kingdom, ²Signal Processing Lab (LTSS), École Polytechnique Fédérale de Lausanne, Lausanne, Switzerland, ³University Hospital Center (CHUV) and University of Lausanne (UNIL), Lausanne, Switzerland, ⁴Centre for Medical Imaging, University College London, London, United Kingdom
- The aim of this study is to extend the AMICO framework to the VERDICT model-based diffusion-weighted MRI (DW-MRI) technique and to evaluate its performance to prostate cancer imaging. DW-MRI was acquired for 4 subjects and the VERDICT model was fitted to the data using both fitting procedures. In both cases similar differences in parameter values between tumour and normal tissue were found. The AMICO formulation reduces the computation time for VERDICT and produces parameter maps that are more homogeneous than those obtained with the original fitting. The AMICO formulation reflects the microstructural differences in a clinically practical time.
-
- 3466
Computer #63 Assessing micro- and macro-circulation of graft kidneys by using IVIM-DWI and Non-contrast MRA
Yung-Chieh Chang¹, Mu-Ch Chung², Kuo-Hsiung Shu², Hao-Chung Ho³, Yen-Chieh Ouyang⁴, Jyh-Wen Chai¹, and Clayton-Chi-Chang Chen¹
¹Department of Radiology, Taichung Veterans General Hospital, Taiwan, Taiwan, ²Division of Nephrology, Taichung Veterans General Hospital, Taiwan, Taiwan, Taiwan, ³Division of Urolog, Taichung Veterans General Hospital, Taiwan, Taiwan, Taiwan, ⁴Department of Electrical Engineering, National Chung Hsing University, Taiwan, Taiwan
- The goal of the present study was to perform IVIM-DWI and non-contrast MRA of graft kidneys to evaluate the micro- and micro-structural status in 17 patients within 48 hours after transplantation. Five of them had a second scan in six months later. The experimental results suggested that D*, D and f values in IVIM-DWI might considerably be useful in early detection of functional change graft kidneys and non-contrast MRA and PC-MRI could effectively assess patency and flow rates of graft vessels. Combination of both IVIM-DWI and non-contrast MRA would be potentially promising in clinical application for monitoring graft kidneys.
-
- 3467
Computer #64 The repeatability of IVIM with fuzzy clustering algorithm in liver imaging
Kaining Shi¹, Ying Liu², Yu Shi², and Qiyong Guo²

¹Imaging Systems Clinical Science, Philips Healthcare, Beijing, China, People's Republic of, ²Radiology department, Shengjing Hospital of China Medical University, Shenyang, China, People's Republic of

Fussy clustering technique (FCM) has been combined with IVIM to increase the stability and reduce the post-processing time of the nonlinear curve fitting in IVIM. Another problem of the widely used bi-exponential IVIM model is its poor repeatability. This work is to assess the repeatability of IVIM with FCM between two scans in healthy liver by calculating the coefficient of variation and the 95% Bland-Altman limits of agreements. Results proved that FCM could improve the repeatability of IVIM, especially for the parameter D^* , which was the most unstable among total 3 parameters.

3468 Computer #65 Preliminary Investigation: Gaussian and Non-Gaussian Diffusion Method in Diagnostic Differentiation of Prostate Cancer from Prostatic Hyperplasia
Chen lihua¹, Liu ailian¹, Song qingwei¹, wang heqing¹, sun meiyu¹, Li ye¹, Chen ailian¹, and Zheng dandan²

¹The Affiliated Hospital of Dalian Medical University, Dalian, China, Dalian, China, People's Republic of, ²GE Healthcare, MR Research China, Beijing, Beijing, China, People's Republic of

Prostate cancer is the second most common cancer for men, and it has high leading cause of cancer death among men. In this study, DKI and DWI MR measurements were performed to investigate the correlation of the MK, Ka, Kr, MD, Da, Dr, FA and ADC values in ROIs of the prostate and benign prostatic hyperplasia. DKI working at present scanning hardware are capable to detect the pathophysiological changes unattainable to conventional MRI techniques.

3469 Computer #66 Diffusion weighted imaging of prostate cancer: mathematical modeling of signal obtained using low b values
Harri Merisaari¹, Parisa Movahedi¹, Ileana Montoya¹, Jussi Toivonen¹, Marko Pesola¹, Pekka Taimen², Peter Boström², Tapio Pahikkala¹, Hannu Juhani Aronen¹, and Ivan Jambor¹

¹University of Turku, Turku, Finland, ²Turku University Hospital, Turku, Finland

Eighty-one patients with historically confirmed PCa underwent two repeated 3T DWI examinations performed using 14 b-values in the range of 0-500 s/mm² and diffusion time of 19.004 ms. Various fitting methods for IVIM and mathematical models were evaluated in the terms of fitting quality (Akaike information criteria), repeatability, and Gleason score prediction. Monoexponential model demonstrated the highest repeatability and clinical values in the regions-of-interest based analysis of PCa DWI, b-values in the range of 0-500 s/mm².

3470 Computer #67 Characterizing breast lesions by Using Mono-exponential, Bi-exponential, and Stretched Exponential Diffusion-weighted MR Imaging and Diffusion Kurtosis MR Imaging
Kun Sun¹, Xu Yan², and Fuhua Yan¹

¹Department of Radiology, Ruijin Hospital, Shanghai Jiao Tong University School of Medicine, Shanghai, China, People's Republic of, ²Application Dept, Siemens Healthcare, Shanghai, China, People's Republic of

DKI model may provide additional information and improve the characterizing of breast lesions compared with conventional diffusion parameters. The kurtosis and water molecular diffusion heterogeneity index derived from DKI and stretched Exponential DWI may be helpful for the preoperative differentiation of proliferative activity of breast cancer.

3471 Computer #68 Comparative analysis of diffusion models for glioma malignancy grade differentiation
Ivan I. Maximov¹, Aram Tonoyan², Daniel Edelhoff¹, Igor Pronin², and Dieter Suter¹

¹TU Dortmund University, Dortmund, Germany, ²Burdenko Neurosurgery Institute, Moscow, Russian Federation

Diffusion weighted imaging is very powerful technique allows one to diagnose and differentiate glioma malignancy *in vivo*. Recently, the non-Gaussian diffusion models exhibited their efficacy in a detection of microstructure changes for low and high grade gliomas. In this study we perform a comparative analysis of four diffusion models (DTI, DKI, two- and three-compartment models) in ability to provide a quantitative measure of the gliomas malignancy *in vivo*.

3472 Computer #69 Optimization of Single-shot Turbo Spin-echo Diffusion-weighted Imaging with Parallel Imaging in Healthy Pancreas
Yu Nishina¹, Satoru Morita¹, Tatsuya Kuramoto², Makoto Suzuki², Hitoshi Tadenuma², Yasuhiro Goto², Masami Yoneyama³, and Shuji Sakai¹

¹Diagnostic Imaging and Nuclear Medicine, Tokyo Women's Medical University Hospital, Tokyo, Japan, ²Radiological Service, Tokyo Women's Medical University Hospital, Tokyo, Japan, ³Philips Electronics Japan, Tokyo, Japan

We compared the image quality of single-shot turbo spin-echo diffusion-weighted imaging (TSE-DWI) with parallel imaging and conventional echo planar DWI (EPI-DWI) in the pancreas of healthy volunteers. TSE-DWI with a sensitivity encoding factor (SF) of 2, 4, 6, and EPI-DWI with SF2 (b-values = 0, 500, 1000 s/mm²) were obtained using a 3T MRI scanner. Two radiologists evaluated overall image quality, susceptibility artifacts, and aliasing artifacts. TSE-DWI with moderate SF had better image quality than conventional EPI-DWI for a medium b-value because of less susceptibility artifacts.

- 3473
Computer #70 7T diffusion MRI of the forearm nerves
Wieke Haakma^{1,2,3}, Jeroen Hendrikse¹, Anneriet M. Heemsker⁴, Peter R. Luijten¹, Michael Pedersen³, Alexander Leemans⁴, and Martijn Froeling¹
- ¹Radiology, University Medical Center Utrecht, Utrecht, Netherlands, ²Forensic Medicine, Aarhus University, Aarhus, Denmark, ³Comparative Medicine Lab, Department of Clinical Medicine, Aarhus University, Aarhus, Denmark, ⁴Image Sciences Institute, University Medical Center Utrecht, Utrecht, Netherlands
- In this work we present our results obtained at the 7T MRI scanner investigating the nerves in the forearm. We tested two DTI protocols and were able to visualize the median, ulnar and radial nerves with fiber tractography with resolution up to 0.75×0.75×2.0 mm³. We have demonstrated the potential of 7T to identify these nerves and quantify their diffusion characteristics in a reliable way. We expect that the use of high resolution DTI can be beneficial in the investigation of peripheral nervous tissue in the forearm and might aid in identifying changes due to pathology.
-

- 3474
Computer #71 Comparison of TSE and EPI for renal DTI
Fabian Hilbert¹, Tobias Wech¹, Henning Neubauer¹, Simon Veldhoen¹, Thorsten Alexander Bley¹, and Herbert Köstler¹
- ¹Department of Diagnostic and Interventional Radiology, University of Würzburg, Würzburg, Germany
- Echo-planar imaging (EPI) is usually applied to acquire diffusion-weighted images. While EPI is fast in acquiring an entire image, it brings along distortion artifacts. Turbo spin echo (TSE) acquisitions require more time than EPI, but avoid distortions. Purpose of this study was to compare TSE and EPI for diffusion tensor imaging of the human kidney. We found similar mean diffusivity with EPI and TSE. Fractional anisotropy provides good corticomedullary contrast with both methods TSE and EPI. TSE is a practicable alternative to EPI for diffusion tensor imaging of the kidney.
-

- 3475
Computer #72 Imaging bio-markers of Intervertebral disc degeneration by T2 Relaxometry and DTI A prospective Study with Multi parametric Imaging correlation
rammohan sai venkata vadapalli¹, Raghav dutt sai venkata Mulukutla², and abhinav sriiram Vadapalli³
- ¹Imaging, Vijaya diagnostics and research, Hyderabad 500020, India, ²Orthopaedic and Spine surgery, Udai orthopaedic Institute, Hyderabad 500020, India, ³Imaging, GH, Hyderabad 500020, India
- Surgeons want to know Predictive disc health proximal to the level of fusion or intervention. Conventional MR imaging using T2 weighted Imaging is insensitive to early morphological changes with no predictive quantitative biomarker profile of early degeneration. The Thompson scale or the Pfirrmann scale are discontinuous scales fail to demonstrate the Degeneration or regeneration of disc Objectively. Multiparametric Imaging using T2 relaxometry maps,DTI indices namely FA and qualitative FA maps offer both quantitative and qualitative biomarkers for predictive disc health
-

Electronic Poster

Diffusion Applications

Exhibition Hall

Tuesday, May 10, 2016: 14:30 - 15:30

- 3476
Computer #73 Simple and robust cardiac diffusion weighted imaging using single-shot Turbo Spin-Echo with peripheral pulse gating
Yasuhiro Goto¹, Kenji Fukushima², Masami Yoneyama³, Atsushi Takemura³, Hitoshi Tadenuma¹, Mamoru Takeyama¹, and Shuji Sakai²
- ¹Department of Radiological Service, Tokyo Women's Medical University Hospital, TOKYO, Japan, ²Department of Diagnostic imaging & Nuclear Medicine, Tokyo Women`s Medical University Hospital, Tokyo, Japan, ³Philips Electronics Japan, Tokyo, Japan
- We evaluated the feasibility of optimal gating method and imaging parameters for Single-Shot Turbo Spin Echo (ssTSE) diffusion weighted image (DWI). As a result, The Peripheral pulse gating (PPG) synchronization method was significantly higher in visual scoring than that of the ECG synchronization method (p=0.02) and ssTSE-DWI using SENSE-factor 4.0 brought about the best image quality. Refocusing Flip Angle (RFA) tended to be higher in images with higher visual score. Visualizing cardiac DWI was feasible under above conditions. In conclusion, it is expected that ssTSE-DWI using PPG has a possibility to detect abnormal signal from myocardium by non-contrast MRI.
-
- 3477
Computer #74 The Study of Vertebral Marrow Microstructure in Healthy Young Adults with Intravoxel Incoherent Motion Diffusion-weighted Imaging
Jinliang Niu¹, Wenqi Wu¹, Tong Gong¹, Wenjin Li¹, Dandan Zheng², Zheng Zhong³, Hongwei Wang¹, and Xiaohong Joe Zhou³
- ¹The Second Hospital of Shanxi Medical University, Taiyuan, China, People's Republic of, ²GE Healthcare MR Research China, Beijing, China, People's Republic of, ³Center for Magnetic Resonance Research, University of Illinois Hospital &Health Sciences System, Chicago, IL, United States
- MRI has become preferred over other imaging modalities in evaluating marrow compositions. Although the routine MRI can evaluate the cellularity of marrow according to signal intensity, it's not quantitative analysis. IVIM provides both diffusion and perfusion quantification using a single imaging study at the same time, without intravenous contrast injection. IVIM has been applied in various diseases, but the application of IVIM in marrow composition is less. As the preliminary study, we will adopt the parameters of IVIM to assess the vertebral bone marrow microstructure, then to investigate gender-related cellular and capillary network of vertebral marrow

-
- 3478
Computer #75
Corticospinal Tract Distribution in Motor Cortices of Adult Macaque Brains Revealed by High Angular Resolution Diffusion Imaging Tractography
Yuguang Meng¹ and Xiaodong Zhang^{1,2}
- ¹Yerkes Imaging Center, Yerkes National Primate Research Center, Emory University, Atlanta, GA, United States, ²Division of Neuropharmacology and Neurologic Diseases, Yerkes National Primate Research Center, Emory University, Atlanta, GA, United States
- Non-human primates mimic most aspects of humans and are widely used in preclinical or medical studies. Understanding the structural connectivity in non-human primate brains can provide essential reference for translational research. The characterization of the corticospinal tracts plays a crucial role in motor function and has been well studied in human brain. However, it remains not fully understood in non-human primates. In this work, high angular resolution diffusion imaging (HARDI) tractography was utilized to evaluate the corticospinal tracts distribution in sub-regions of motor cortices of adult macaque monkeys, and high similarity to prior ex-vivo results was observed.
-
- 3479
Computer #76
White matter lesions highly influence group comparison of diffusion tensor imaging metrics
Daniel Svård^{1,2}, Markus Nilsson³, Björn Lampinen⁴, Jimmy Lätt², Pia Sundgren^{1,2}, Erik Stomrud⁵, Lennart Minthon⁵, Katarina Nägga⁵, Oskar Hansson^{5,6}, and Danielle van Westen^{1,2}
- ¹Diagnostic Radiology, Clinical Sciences, Lund University, Lund, Sweden, ²Center for Medical Imaging and Physiology, Skåne University Hospital, Lund, Sweden, ³Lund University Bioimaging Center, Lund University, Lund, Sweden, ⁴Department of Medical Radiation Physics, Lund University, Lund, Sweden, ⁵Clinical Memory Research Unit, Clinical Sciences, Lund University, Malmö, Sweden, ⁶Neurology, Clinical Sciences, Lund University, Lund, Sweden
- White matter lesions (WML) are common in cognitively healthy elderly and their presence in a brain region is associated with elevated mean diffusivity (MD) and reduced fractional anisotropy (FA). We compared patients with amnesic mild cognitive impairment (aMCI) to control groups with different prevalence of WML. Our results showed that including subjects with WML in the control group highly influence the outcome of statistical analysis of diffusion tensor imaging (DTI) metrics. We conclude that WML should be taken into consideration when designing and interpreting DTI studies.
-
- 3480
Computer #77
Quantitative Diffusion MRI of Hematopoietic Acute Radiation Syndrome using a Minipig Model
Frederick C. Damen^{1,2}, Matthew Lindeblad³, Kejia Cai^{2,4}, Michael Flannery², Yi Sui², Amelia M Bartholomew⁵, Aleksander V Lyubimov³, and Xiaohong Joe Zhou^{2,4,6,7}
- ¹Radiology, University of Illinois at Chicago, Chicago, IL, United States, ²Center for Magnetic Resonance Research, University of Illinois at Chicago, Chicago, IL, United States, ³Pharmacology, University of Illinois Medical Center, Chicago, IL, United States, ⁴Bioengineering, University of Illinois at Chicago, Chicago, IL, United States, ⁵Surgery, University of Illinois Medical Center, Chicago, IL, United States, ⁶Radiology, Chicago, IL, United States, ⁷Neurosurgery, University of Illinois at Chicago, Chicago, IL, United States
- The purpose of this study is to characterize Hematopoietic Acute Radiation Syndrome (hARS) and assess the effect of total body irradiation in a Göttingen minipig model using quantitative diffusion MRI. The minipigs were irradiated at a total dose of either 1.65 Gy (LD30/45 days) or 1.90 Gy (LD70/45 days). The animals underwent diffusion MRI scans prior to and again at 8, 15, or 22 days following irradiation. The consistent diffusion value prior to irradiation and the significant changes post-irradiation, both observed in this study, suggest that quantitative diffusion MR can be a viable marker for studying the effect of total body irradiation.
-
- 3481
Computer #78
White matter microstructure among perinatally HIV-infected youth: A diffusion tensor imaging study
Manoj Kumar Sarma¹, Margaret Keller², Rajakumar Nagarajan¹, David E Michalik³, Judy Hayes², Karin Nielsen-Saines⁴, Jaime Deville⁴, Joseph A Church⁵, Irwin Walot⁶, and M. Albert Thomas¹
- ¹Radiological Sciences, UCLA School of Medicine, Los Angeles, Los Angeles, CA, United States, ²Pediatrics, Harbor-UCLA Medical Center, Torrance, CA, United States, ³Infectious disease-Pediatrics, Miller's Children's Hospital of Long Beach, Long Beach, CA, United States, ⁴Pediatrics, UCLA School of Medicine, Los Angeles, Los Angeles, CA, United States, ⁵Pediatrics, Children's Hospital Los Angeles, Los Angeles, CA, United States, ⁶Radiology, Harbor-UCLA Medical Center, Torrance, CA, United States
- DTI was used to derive in vivo tissue status measurements of subcortical brain regions that are vulnerable to injury in perinatally HIV-infected youths. Quantitative measurements, including the mean diffusivity (MD), fractional anisotropy (FA), axial diffusivity (AD) and radial diffusivity (RD) were determined in of the whole brain in 12 well-characterized HIV youths and in 12 healthy control subjects. We observed widespread brain regions with increased AD values in perinatally HIV-infected youths compared to healthy controls, indicating axonal changes. We also observed increased FA, MD and RD. To confirm these findings a correlation study with neurodevelopment and neurocognitive changes as well as ART effect is needed. Understanding the impact of HIV disease severity on white matter integrity provides potentially useful clinical tools for evaluating ART efficacy during a dynamic period of brain development.
-
- 3482
Computer #79
Intravoxel incoherent motion diffusion weighted imaging in evaluating the radio-sensitivity of nasopharyngeal carcinoma xenografts
Youqing Xiao¹, Yunbin Chen¹, Jianji Pan², Dechun Zheng¹, Xiang Zheng¹, and Ying Chen¹
- ¹Radiology, Fujian Provincial Cancer Hospital, Fuzhou, China, People's Republic of, ²Radiation Oncology, Fujian Provincial Cancer Hospital, Fuzhou, China, People's Republic of

In this present study, by applying the special mouse coil(4 channel), IVIM-DWI with 14 b-factors(0~1000s/mm²) was successfully conducted on nude mice with different radio-sensitive NPC xenografts(CNE-1 and CNE-2) during the course of fractional radiations. The IVIM-DWI parameters of xenografts were found to change characteristically after fractional radiations and were significantly different between different radio-sensitive NPC xenografts, and their corresponding changes also behaved significant correlations with the pathological features of NPC xenografts. Thus, it is suggested IVIM-DWI parameters be valuable in evaluating the micro-structures and radio-sensitivity of NPC xenografts.

3483
Computer #80 Combining Intravoxel Incoherent Motion Model and Reduced FOV for Evaluation of Single Renal Diffusion and Perfusion
CY Wang¹, R Zhang², L Jiang³, R Wang⁴, XD Zhang⁴, H Wang³, K Zhao⁴, LX Jin³, J Zhang^{1,2}, XY Wang^{1,4}, and J Fang^{1,2}

¹Academy for Advanced Interdisciplinary Studies, Peking University, Beijing, China, People's Republic of, ²College of Engineering, Peking University, Beijing, China, People's Republic of, ³Philips Healthcare, Suzhou, China, People's Republic of, ⁴Department of Radiology, Peking University First Hospital, Beijing, China, People's Republic of

The sequence most commonly used in renal DWI is based on single-shot echo-planar imaging (SS-EPI), which is prone to artifacts and distortions related to susceptibility and eddy currents. Reducing these artifacts and distortions in SS-EPI generally requires a reduced field of view (rFOV) in the phase-encoding direction and/or reduced spatial resolution. To resolve these problems, a 2D rFOV-DWI sequence was introduced for imaging and further IVIM modeling. Compared with conventional full-FOV single-shot DWI techniques, rFOV-DWI methods generally produced images of superior quality. With the application of IVIM model, it is possible to evaluate single renal diffusion and perfusion simultaneously.

3484
Computer #81 Super-Resolution Track Density Imaging of 1.4 mm isotropic 7T Whole-Brain Diffusion Magnetic Resonance Images
Ralf Lützkendorf¹, Robin M. Heidemann², Thorsten Feiweier², Michael Luchtmann³, Sebastian Baecke¹, Joern Kaufmann⁴, Joerg Stadler⁵, Eike Budinger⁵, and Johannes Bernarding¹

¹Biometry and Medical Informatics, University of Magdeburg, Magdeburg, Germany, ²Siemens Healthcare GmbH, Erlangen, Germany, ³Department of Neurosurgery, University of Magdeburg, Magdeburg, Germany, ⁴Department of Neurology, University of Magdeburg, Magdeburg, Germany, ⁵Leibniz Institute for Neurobiology, Magdeburg, Germany

Track-density imaging (TDI) is a method to generate super-resolution images from fiber-tracking data (1). Here, we applied this technique to 1.4 mm isotropic 7T whole brain diffusion MR imaging data (dMRI). Besides the well-known large and medium-sized fiber tracts the high resolution of the data allowed visualizing the complex interwoven courses of fiber tracts in the cerebellar-pontine angle as well as showing parts of the trigeminus nerve. Combining TDI with high-resolved diffusion data has a great potential for analyzing the anatomy in vivo of brain structures across different scales as well as the neuronal connectome throughout the whole brain.

3485
Computer #82 Multi-Center Validation of an Acetone-D₂O Quantitative Diffusion Phantom
Xiaoke Wang¹, Samir D Sharma², Mustafa R Bashir³, Jean H Brittain², Jean Shaffer³, Takeshi Yokoo⁴, Qing Yuan⁴, Scott B Reeder^{1,2,5,6,7}, and Diego Hernando²

¹Biomedical Engineering, University of Wisconsin-Madison, Madison, WI, United States, ²Radiology, University of Wisconsin-Madison, Madison, WI, United States, ³Radiology, Duke University, Durham, NC, United States, ⁴Radiology, University of Texas Southwestern Medical Center, Dallas, TX, United States, ⁵Medical Physics, University of Wisconsin-Madison, Madison, WI, United States, ⁶Medicine, University of Wisconsin-Madison, Madison, WI, United States, ⁷Emergency Medicine, University of Wisconsin-Madison, Madison, WI, United States

A recently proposed acetone-D₂O phantom, which has ADC tunable over the entire physiological range, has shown promise for the development and quality assurance of quantitative diffusion MRI. In this study, this phantom was shipped between three sites with different MRI vendors to demonstrate consistent diffusion quantification across imaging protocols, platforms, and field strengths. The results demonstrated consistent ADC measurements across sites/vendors, field strength, choice of b-values, intra-exam and inter-exam repetition. In conclusion, the acetone-D₂O phantom is a promising tool for future multi-center validation and quality assurance of quantitative diffusion MRI techniques.

3486
Computer #83 Measuring diffusion time dependence of pseudo-diffusion using flow compensated pulsed and oscillating gradient sequences
Dan Wu¹ and Jiangyang Zhang^{1,2}

¹Radiology, Johns Hopkins University School of Medicine, BALTIMORE, MD, United States, ²Radiology, New York University School of Medicine, New York, NY, United States

Intravoxel incoherent motion (IVIM) in the capillaries reflects capillary geometry and flow velocity, which may be probed by diffusion MRI measured at varying diffusion times. In this study, we employed flow-compensated pulsed and oscillating gradient sequences to investigate the diffusion time dependence of pseudo-diffusion in the mouse brain with diffusion times ranging from 2.5 ms to 40 ms. We used a simplified IVIM model to characterize the pseudo-diffusion compartment and flow compartment based on the relation between capillary segments and diffusion time/distance. Our results clearly demonstrated diffusion time dependence and suggested that the pseudo-diffusion fraction increased with increasing diffusion time.

3487
Computer #84 Diffusion weighted imaging of prostate cancer xenografts: comparison of bayesian modeling and independent least squares fitting
Parisa Movahedi¹, Hanne Hakkarainen², Harri Merisaari¹, Heidi Liljenbäck¹, Helena Virtanen¹, Hannu Juhani Aronen¹, Heikki Minn¹, Matti

Tumor growth in mice preclinical prostate cancer model (human prostate cancer cells, PC-3) was followed for 4 weeks by weekly DWI in control group (n=10) and treatment group (n=9) receiving Docetaxel. DWI data sets were acquired using 15 b-values in the range of 0-500s/mm² and 12 b-values the range of 0-2000 s/mm². The DWI signal decays were fitted using monoexponential, biexponential, kurtosis and stretched exponential models/functions. Bayesian shrinkage prior method and independent least squares fitting have been applied and fitting quality evaluated by corrected Akaike Information Criteria. Bayesian modeling improved quality of DWI parametric maps derived using high b-value DWI data sets. Our result does not support the use of biexponential, kurtosis and stretched exponential models/functions for low b value DWI data sets of PC-3 mice preclinical prostate cancer model.

-
- 3488 Computer #85 Intravoxel Incoherent Motion Diffusion-weighted Magnetic Resonance Imaging for Monitoring the Early Response to ZD6474 from Nasopharyngeal Carcinoma in Nude Mouse
Yong Zhang¹ and Yanfen Cui²

¹GE Healthcare China, Shanghai, China, Shanghai, China, People's Republic of, ²Department of Radiology, Shanghai Jiao Tong University School of Medicine, Shanghai, China, People's Republic of

This study was to investigate the feasibility of IVIM DWI to evaluate the early therapeutic effects of ZD6474 upon human NPC xenografts in nude mouse. NPC mice underwent IVIM DWI at baseline and after 1, 3, and 7 days of treatment. In the treated group, the f and D* decreased significantly on day 1 while the ADC and D were significantly higher from day 3 compared with the control group, demonstrating that IVIM DWI is sensitive to detect the ZD6474-induced changes in human NPC nude mouse, and the D* and f parameters could predict early response to anti-angiogenic treatment.

-
- 3489 Computer #86 Comparison of IVIM and BOLD MR imaging in Functional Evaluation of Diabetic nephropathy
Lihua Chen¹, Tao Ren¹, Yu Zhang², Chenglong Wen¹, and Wen Shen¹

¹Tianjin First Center Hospital, Tianjin, China, People's Republic of, ²Philips healthcare, Beijing, China, People's Republic of

To detect the changes of kidney diseases, magnetic resonance imaging(MRI) as a noninvasive approach has been proved to be more suitable for detecting and monitoring diabetic nephropathy(DN). Intravoxel incoherent motion (IVIM) and blood oxygenation level dependent (BOLD) MR imaging have been confirmed their high potential in detecting changes of renal function in patients with chronic renal diseases and transplanted kidneys. We compared the parameters of IVIM and BOLD in patients with DN and healthy controls. The results demonstrated the capacity of IVIM and BOLD for reflecting renal perfusion, diffusion and oxygenation changes in patients with DN.

-
- 3490 Computer #87 Diffusion Kurtosis Metrics as Biomarker of Fibre Maturity
Grinberg Farida^{1,2}, Ivan I. Maximov^{1,3}, Ezequiel Farrher¹, Irene Neuner^{1,4,5}, Eileen Oberwelland^{6,7}, Kerstin Konrad^{5,6,8}, and N. Jon Shah^{1,2,5}

¹Institute of Neuroscience and Medicine - 4, Forschungszentrum Juelich GmbH, Juelich, Germany, ²Department of Neurology, Faculty of Medicine, RWTH Aachen University, Aachen, Germany, ³Experimental Physics III, TU Dortmund University, Dortmund, Germany, ⁴Department of Psychiatry, Psychotherapy and Psychosomatics, RWTH Aachen University, Aachen, Germany, ⁵JARA - BRAIN - Translational Medicine, Aachen, Germany, ⁶Institute of Neuroscience and Medicine - 3, Forschungszentrum Jülich GmbH, Juelich, Germany, ⁷Translational Brain Research in Psychiatry and Neurology, Department of Child and Adolescent Psychiatry, Psychosomatics and Psychotherapy, RWTH Aachen University, Aachen, Germany, ⁸Child Neuropsychology Section, Department of Child and Adolescent Psychiatry and Psychotherapy, RWTH Aachen University, Aachen, Germany

Diffusion tensor imaging has enabled the examination of white matter connectivity and microstructural changes across the lifespan. However, the detection of subtle microstructural changes during typical brain maturation still remains challenging. Recently, diffusion kurtosis imaging has attracted much attention as an efficient method for characterising non-Gaussian water diffusion in brain tissue. Here, we tested whether diffusion kurtosis imaging can extend our knowledge of changes in brain tissue microstructure related to normal brain development. We showed that diffusion kurtosis imaging provides useful biomarkers sensitive to the level of maturity in association, projection and commissural fibres.

-
- 3491 Computer #88 Using intravoxel incoherent motion MR imaging to measure renal diffusion and perfusion in contrast-induced acute kidney injury
Bin Zhang¹, Long Liang¹, Yuhao Dong¹, Kannie W.Y. Chan², Guanshu Liu², Changhong Liang¹, and Shuixing Zhang¹

¹Department of Radiology, Guangdong Academy of Medical Sciences/Guangdong General Hospital, Guangzhou, China, People's Republic of, ²Russell H. Morgan Department of Radiology and Radiological Sciences, Division of MR Research, The Johns Hopkins University School of Medicine, Baltimore 21287, USA, Baltimore, AL, United States

Contrast-induced acute kidney injury (CI-AKI) is a common iatrogenic event caused by the injection of iodinated contrast agent, and remains the third major source of in-hospital acquired acute renal failure. The objective of our study is to examine the feasibility of using Intravoxel Incoherent Motion (IVIM) MRI to simultaneously measure the pathological changes in kidney diffusion and perfusion in the course of CI-AKI. Our results showed that the kidney perfusion and diffusion as measured by IVIM are well-correlated with those measured using conventional methods, indicating IVIM MRI can be used as an effective tool for the diagnosis and staging of CI-AKI.

- 3492
Computer #89
Assessment of brain structural network alterations in major depressive disorder using generalized q-sampling imaging and connectome analysis
Chao-Yu Shen^{1,2,3}, Zhen-Hui Li¹, Vincent Chin-Hung Chen⁴, Ming-Chou Ho⁵, Yeu-Sheng Tyan^{1,2}, and Jun-Cheng Weng^{1,2}
- ¹Department of Medical Imaging and Radiological Sciences, Chung Shan Medical University, Taichung, Taiwan, ²Department of Medical Imaging, Chung Shan Medical University Hospital, Taichung, Taiwan, ³Institute of Medicine, Chung Shan Medical University, Taichung, Taiwan, ⁴Department of Psychiatry, Chang Gung Memorial Hospital, Chiayi, Taiwan, ⁵Department of Psychology, Chung Shan Medical University, Taichung, Taiwan
- Major depressive disorder (MDD) is the most common mood disorder in the world and the most important precursor of suicide. Despite decades of research, the pathophysiology of MDD remains not well understood. Recently, several MRI studies have focused on structural and functional connectivity evaluation and suggested that alterations of some specific regions of the brain, in both gray and white matter structures and some specific cortical-subcortical neuronal circuits, may play important roles of MDD. Generalized q-sampling imaging (GQI) is a more accurate and sophisticated diffusion MR approach compared to diffusion tensor imaging (DTI), which can extract additional information about the altered diffusion environments to resolve the complicated neural structure changes of neural disease. In this study, we used GQI and graph theoretical analysis to evaluate brain structure and connectivity change of MDD compared to healthy controls and correlation with symptom severity. Our results indicated GQI indices can help to detect structural and connective abnormalities of MDD patients and these alterations are correlated with depressive severity.
-
- 3493
Computer #90
Evaluation of Acute Cerebral Infarction Using a Fast Kurtosis Diffusion imaging Protocol
Chengxu Li¹, Tianyi Qian², Jinsuh Kim³, Philip Zhe Sun⁴, Jie Lu¹, and Kuncheng Li¹
- ¹Department of Radiology, Xuanwu Hospital, Capital Medical University, Beijing, China, People's Republic of, ²MR Collaborations NE Asia, Siemens Healthcare, Beijing, China, People's Republic of, ³Department of Radiology, University of Illinois at Chicago, Chicago, IL, United States, ⁴Martinos Center for Biomedical Imaging, Department of Radiology, Massachusetts General Hospital and Harvard Medical School, Boston, MA, United States
- Conventional DKI is limited in use for detecting acute stroke because of its relatively long scan time and current need of offline processing. Here we used a 13 directions protocol combined with simultaneous multi-slice technique with inline reconstruction to test the diffusion pattern at different time points. The results shows the lesion size observed within 24hr on MK matched with the lesion size on T2-FLAIR after one month, which was better than lesion size observed within 24hr on DWI. Early application of the fast DKI to detect the anomalous range of MK was beneficial to predict the range of the eventual infarction for clinical treatment.
-
- 3494
Computer #91
High resolution tract density tract-based spatial statistics and automating fiber-tract quantification analysis in patients suffering from major depressive disorder
Stefan Sommer^{1,2}, Nadja Doerig^{3,4}, Janis Brakowski², Martin grosse Holtforth⁵, Sebastian Kozerke¹, Erich Seifritz^{2,4}, Simona Spinelli^{2,4}, and Philipp Stämpfli²
- ¹Institute for Biomedical Engineering, ETH and University of Zurich, Zurich, Switzerland, ²Department of Psychiatry, Psychotherapy and Psychosomatics Psychiatric Hospital, University of Zurich, Zurich, Switzerland, ³Division Neuropsychology, Department of Psychology, University of Zurich, Zurich, Switzerland, ⁴Neuroscience Center, University and ETH Zurich, Zurich, Switzerland, ⁵Department of Psychology, University of Bern, Bern, Switzerland
- In the last few years, tract base spatial statistics (TBSS) and automating fiber-tract quantification (AFQ) have become prominent tools for analyzing diffusion data in group studies. In this study, we introduce optimized high-resolution tract density (optTD) images and analyze these maps using TBSS and AFQ in patients with major depressive disorders. We show a higher sensitivity in the newly introduced optTD compared to traditional FA analyses. Significant group differences were found using both methods indicating robust findings. High resolution optTD maps derived from optimized tractograms provide a promising tool for investigating white-matter abnormalities in mental disorders.
-
- 3495
Computer #92
Diffusional Kurtosis Imaging Study Of Parkinson Disease
Xilun Ma¹, Jitian Guan¹, Zhiyan Zhang¹, Miaomiao Chen¹, Yanzi Chen¹, Zhiwei Shen¹, and Renhua Wu¹
- ¹Department of Medical Imaging, the 2nd Affiliated Hospital, Medical College of Shantou University, Shantou 515041, China, Shantou, China, People's Republic of
- Eighteen Parkinson Disease's (PD) patients and four healthy controls(HC) underwent the diffusional kurtosis imaging (DKI) and then we tested the PD's patients with Hoehn-Yahr scale and Unified Parkinson Disease Rating Scale(UPDRS). As a result, we found a significant decrease of Mean kurtosis (MK) values in the left substantia nigra between PD's patients and healthy controls. Moreover, the kurtosis fractional anisotropy (KFA) values in right red nucleus of the PD's patients were positively associated with the UPDRS scores in our study.
-
- 3496
Computer #93
Characterization of Clear Cell Renal Cell Carcinoma with Diffusion Kurtosis Imaging: Correlation between Diffusion Kurtosis Parameters and Tumor Cell
Guangyu Wu¹ and Yongming Dai²
- ¹renji hospital, shanghai, China, People's Republic of, ²MR, Philips Healthcare, Shanghai, China, People's Republic of

A wide spectrum of the use of DKI to characterize non-Gaussian diffusion pattern in microstructural tumor tissue has been developed involving a variety of tumors. However, the feasibility of DKI in kidney has been assessed in healthy volunteers only. The study was assigned to assess the quantitative DKI in grading of clear cell renal carcinoma (ccRCC) and to compare the correlation between DKI parameters and tumor cellularity and found that DKI could not only quantitatively characterize ccRCC with different grades but also provide valuable information on the diffusion properties related to tumor microenvironment changes or tissue complexity in tumor.

3497 Computer #94 Diffusional kurtosis imaging study in idiopathic normal pressure hydrocephalus patients, before and after shunt placement surgery analysis

Chanon Ngamsombat¹, Zhe Zhang², Hua Gao², Theerapol Witthiwej³, Weerasak Muangpaisan⁴, Sith Sathornsumtee⁵, Suwit Charoensak⁶, Panida Charnchaowanish¹, and Orasa Chawalparit¹

¹Department of Radiology, Faculty of Medicine Siriraj Hospital, Mahidol University, Bangkok, Thailand, Bangkok, Thailand, ²Center for Biomedical Imaging Research, Department of Biomedical Engineering, School of Medicine, Tsinghua University, Beijing, China, Beijing, China, People's Republic of, ³Department of Surgery, Faculty of Medicine Siriraj Hospital, Mahidol University, Bangkok, Thailand, Bangkok, Thailand, ⁴Department of Preventive and Social Medicine, Faculty of Medicine Siriraj Hospital, Mahidol University, Bangkok, Thailand, Bangkok, Thailand, ⁵Departments of Medicine, Faculty of Medicine Siriraj Hospital, Mahidol University, Bangkok, Thailand, Bangkok, Thailand, ⁶Department of Psychiatry, Faculty of Medicine Siriraj Hospital, Mahidol University, Bangkok, Thailand, Bangkok, Thailand

Idiopathic normal pressure hydrocephalus (iNPH) is an important reversible cause of dementia and gait abnormality in elderly patients. Diffusional kurtosis imaging (DKI) moreover explains the complexity of white matter abnormality with inclusion of non-Gaussian effects. We aim to identify the difference in complexity of white matter alteration in iNPH patients before and after shunt placement surgery by using high resolution DKI. We report a significant increase in mean diffusional kurtosis (K_{mean}), mean diffusivity (MD) and decrease in radial diffusional kurtosis (K_{rad}), fractional anisotropy (FA) after shunt placement surgery. High resolution DKI can be used for monitoring and detecting the complexity of white matter alteration in iNPH patients.

3498 Computer #95 The Investigation of Cerebral Microstructure Changes of Pediatric Patients With Type I Gaucher Disease Using Diffusion Kurtosis Imaging

Huiying Kang¹, Ningning Zhang, Kaining Shi², Yanqiu Lv¹, Di Hu¹, and Yun Peng¹

¹Imaging center, Beijing Children's Hospital, Capital Medical University, Beijing, China, People's Republic of, ²Imaging Systems Clinical Science, Philips Healthcare, Beijing, China, People's Republic of

Increasing clinical studies suggested that there are some type I Gaucher disease (GDI) patients suffering from neurological symptoms, which was originally defined as non-neuropathological involvement. This study recruited 38 patients and 32 normal children to investigate morphological changes of the brain in GDI patients by using Diffusion Kurtosis Imaging. Our results showed a significant decrease in MD in the bilateral olfactory gyri, an increase in MD in the right calcarine and substantia nigra, and a significant increase in MK in the right olfactory gyrus. Our study suggests a necessity of adjusting the opinion regarding the CNS involvement of GDI, and DKI analysis is a potential imaging marker in clinical studies of GDI.

3499 Computer #96 Differentiating Minimal Fat Angiomyolipoma from clear cell Renal Cell Carcinoma: comparison of monoexponential, biexponential, and stretched exponential Diffusion-weighted imaging

Haojie Li¹, Lili Liang¹, Anqin Li¹, Qiong Li¹, Yao Hu¹, Hui Lin², Daoyu Hu¹, and Zhen Li¹

¹Departments of Radiology, Tongji Hospital, Tongji Medical College, WU HAN, China, People's Republic of, ²GE Healthcare, MR Research China, WU HAN, WU HAN, China, People's Republic of

Since DWI with different models may demonstrate different aspects of tissue properties, it should be valuable to compare and explore their roles in renal tumors. To our knowledge, however, no comparison of these different diffusion imaging approaches for the differential diagnosis in renal tumors has been investigated so far. The purpose of this study was to quantitatively compare and evaluate the potential clinical value of various diffusion parameters obtained from monoexponential, biexponential, and stretched exponential DWI models for the differentiation of MFAML from ccRCC.

Electronic Poster

RF Coils & Arrays

Exhibition Hall

Tuesday, May 10, 2016: 16:00 - 17:00

3500 Computer #1 7 Tesla dual element ³¹P TxRx/1H Rx endorectal coil combined with an 8-channel 1H-TxRx body coil
Mark J. van Uden¹, Bart Philips¹, Miriam Lagemaat¹, and T.W.J. Scheenen^{1,2}

¹Radiology and Nuclear Medicine, Radboud University Medical Center, Nijmegen, Netherlands, ²Erwin L. Hahn Institute for Magnetic Resonance Imaging, Essen, Germany

Multiparametric MRI (mpMRI) is a valuable tool to assess aggressiveness and stage of localized prostate cancer. When combined with metabolic information from ¹H and ³¹P spectra, valuable information on the metabolism of the disease can be derived. Here we demonstrate a dual element endorectal coil with ¹H Rx and ³¹P TxRx capabilities combined with an external 8-channel transmit-receive body array. One patient (Gleason score 4+4) was measured. High quality proton spectra show elevated total choline in tumor tissue,

which corresponded with increased glycerophosphocholine, glycerophosphoethanolamine and phosphocholine in the ^{31}P spectra of the tumor.

-
- 3501
Computer #2 Prostate MRI at 7.0 Tesla using an actively-tuned endorectal coil
M. Arcan Erturk¹ and Gregory J Metzger¹
¹Center for Magnetic Resonance Research, University of Minnesota, Minneapolis, MN, United States

Using endorectal coils (ERC) in combination with external surface arrays (ESA) can improve the SNR inside the prostate at 7.0T. When used in transmit, ERC can provide higher B1+ levels at the expense of field uniformity. Here, we develop a novel actively-tuned ERC that can be used both in “transmit” and “receive-only” modes utilizing the high B1+ of the ERC and field uniformity of the ESA inside the prostate. Transmit capabilities of this approach are investigated using simulations in a human model. Prostate MRI is acquired using the combined ESA+ERC approach to demonstrate the feasibility for translational studies at 7.0T.

-
- 3502
Computer #3 The Trellis Coil: A Morphing, Size Adaptable Array Coil
Graham Wiggins^{1,2} and August Frank³
¹The Center for Advanced Imaging Innovation and Research (CAI2R), Department of Radiology, New York University School of Medicine, New York, NY, United States, ²The Bernard and Irene Schwartz Center for Biomedical Imaging, Department of Radiology, New York University School of Medicine, New York, NY, United States, ³University of Pennsylvania, Philadelphia, PA, United States

The sensitivity of surface coil arrays can be maximized by conforming them closely to the human body, maximizing coil loading and minimizing the contribution of coil noise. There is, however, great diversity in body shape and size. Rigid coils must adopt a compromise, allowing for the largest cases while not giving up too much sensitivity when imaging smaller examples. Flexible arrays can be wrapped tightly around the body, but if the overall array dimensions are fixed there will always be gaps or undesired overlaps depending on body habitus. We present here a geometrical approach based on a trellis-like lattice of interlinked slats which allows a surface coil array to be re-shaped while maintaining coil tuning, coil loading and decoupling of neighboring coils.

-
- 3503
Computer #4 Liquid metal based deformable transmitter for MR imaging: A feasibility study
Qi Duan¹, Hai Lu^{2,3}, Chris Cooper⁴, Xiaopeng Zong³, Jeff H. Duyn¹, Michael D. Dickey⁴, and Shumin Wang^{2,3}
¹Laboratory of Functional and Molecular Imaging, National Institute of Neurological Disorders and Stroke, National Institutes of Health, Bethesda, MD, United States, ²UNC/NCSSU Joint Department of Biomedical Engineering, University of North Carolina of Chapel Hill, Chapel Hill, NC, United States, ³Biomedical Research Imaging Center, University of North Carolina of Chapel Hill, Chapel Hill, NC, United States, ⁴Department of Chemical & Biomolecular Engineering, NC State University, Raleigh, NC, United States

Recent advances of liquid metal technology have made it possible to build deformable RF transmitters. Such coils have many attractive features for MR, such as easy reconfiguration, flexibility, and self-healing capabilities. However, given that the conductivity of liquid metal is more than an order of magnitude lower than the copper, it is unclear whether it is suitable to be used as a RF transmitter in MR applications. In this work, such feasibility was demonstrated by comparing the performance of two electric dipole antennas with similar size, one made of liquid metal and the other one made of copper, on a 7T scanner.

-
- 3504
Computer #5 RF coil design for multi-nuclear lung MRI of ^{19}F fluorinated gases and ^1H using MEMS
Adam Maunder¹, Madhwesha Rao¹, Fraser Robb², and Jim Wild¹
¹Unit of Academic Radiology, University of Sheffield, Sheffield, United Kingdom, ²GE Healthcare, Aurora, OH, United States

Muti-nuclear lung MRI using inhaled inert fluorinated ^{19}F gas and ^1H provide complementary structural-functional information. The close MR resonance frequencies of the two nuclei preclude the use of dual-tuned coils using trap circuits. Thus, we introduce the use of Micro-electromechanical systems (MEMS) in a quadrature transmit-receive RF coil to switch between two resonance frequencies of ^{19}F and ^1H at 1.5T. Characterization of the additional loss and co-registered imaging of ^{19}F and ^1H with a custom-built body sized phantom is demonstrated.

-
- 3505
Computer #6 Performance of 7 Tesla Normal Metal and Superconducting Cryo-coils for MRI of Rat Brain
Jarek Wosik^{1,2}, Kurt Bockhorst³, Tan I-Chih⁴, Kuang Qin¹, Krzysztof Nesteruk⁵, and Ponnada A Narayana³
¹Electrical and Computer Engineering, University of Houston, Houston, TX, United States, ²Texas Center for Superconductivity, University of Houston, Houston, TX, United States, ³Radiology, The University of Texas Health Science Center, Houston, TX, United States, ⁴The Brown Foundation Institute of Molecular Medicine, The University of Texas Health Science Center, Houston, TX, United States, ⁵Institute of Physics of Polish Academy of Science, Warsaw, Poland

We report on the performance of receive only 300-MHz planar cryogenic (both copper and superconducting) coils for MRI of rat brain at 7 T. The double-sided coils were fabricated by patterning Cu and YBCO on laminate and 0.33 mm thick sapphire substrate, respectively. Practical limits of the performance of the cryocoils (20 mm Cu and 17 mm superconducting) were tested using 3D-RARE, 2D-RARE, and RGB-FA maps recorded with EPI_DTI protocols. Both in-vivo and ex-vivo images were acquired. Twofold SNR gain was achieved at 65K. Cryo-system stability tests with over 11 hours of DTI ex-vivo scanning are presented.

-
- 3506
Computer #7 8CH $^{19}\text{F}/^1\text{H}$ Transceiver Array for Lung Imaging at 7T (pTX)
Helmar Waiczies¹, Andre Kuehne¹, Armin M. Nagel^{2,3}, Dennis Schuchardt¹, Darius Lysiak¹, Jan Rieger¹, and Thoralf Niendorf^{1,4}
- ¹MRI.Tools GmbH, Berlin, Germany, ²Division of Medical Physics in Radiology, Cancer Research Center (DKFZ), Heidelberg, Germany, ³Diagnostic and Interventional Radiology, University Medical Center Ulm, Ulm, Germany, ⁴Berlin Ultrahigh Field Facility (B.U.F.F.), Max Delbrück Center for Molecular Medicine, Berlin, Germany
- Lung MR-Imaging is challenging due to low proton density in the lung. Ventilation can only be visualized directly using exogenous contrast agents such as hyperpolarized noble gases or ^{19}F -containing gases as a “contrast agents”. This work proposes a multi-channel transmit and receive (TX/RX) radiofrequency (RF) coil that supports eight TX/RX channels (4 loop- and 4 dipole-elements) for ^{19}F and ^1H lung imaging at 7.0T using a pTX-array.
-
- 3507
Computer #8 Comparison between commercial RF head coils and a new hybrid transmit-array coil based on 12 transmit elements and 22 receive elements for an 8-channel transmission system at 7 T
Alexis Amadon¹, Guillaume Ferrand², Elodie Georget¹, Eric Giacomini¹, Edouard Chazel¹, Marie-France Hang¹, Jeremy Bernard¹, Nicolas Boulant¹, Vincent Gras¹, Alexandre Vignaud¹, and Michel Luong²
- ¹CEA, DSV, I2BM, NeuroSpin, UNIRS, Gif-sur-Yvette, France, ²CEA, DSM, IRFU, SACM, LISAH, Gif-sur-Yvette, France
- This work compares the performance of two commercial RF coils with a new transmit-array hybrid coil developed at NeuroSpin for the human head at 7T. This z-segmented coil uses 11 transceiver dipoles connected to 7 power channels via an SVD-box, one transceiver patch to cover the top of the head, and 10 receive-only 3D loops in-between the dipoles. Its performance outbeats that of the commercial coils both in terms of signal-to-noise ratio and dynamic RF shimming efficiency.
-
- 3508
Computer #9 A size-adaptable electric dipole array for 7T body imaging
Bei Zhang¹, Martijn Cloos¹, Gang Chen¹, and Graham C. Wiggins¹
- ¹Department of Radiology, The Bernard and Irene Schwartz Center for Biomedical Imaging, New York, NY, United States
- A major challenge in 7T coil array design for body imaging is to achieve optimum distribution in different body sizes with only one coil array. In this work, we propose a flexible 8 channel dipole array with trellis-like substrate which can expand and contract to fit various body sizes and hold electric dipole antenna elements in the optimum distribution around the body for all subjects. The performance of the trellis array was compared with a flexible yet fixed-element-spaced folded dipole body array [1] in terms of flip angle maps and SNR on two different sizes of body phantoms. Both phantom and in vivo images show that the trellis array does not have common nulls between the circular polarized (CP) and gradient modes.
-
- 3509
Computer #10 ^{13}C MRS in human calf muscles at 7T using a double tuned 4 channel ^{13}C -4 channel ^1H transceiver phased array.
Guillaume Donati¹, Eulalia Serés Roig¹, and Rolf Gruetter^{1,2}
- ¹Laboratory of Functional and Metabolic Imaging, École Polytechnique Fédérale de Lausanne, Lausanne, Switzerland, ²Department of Radiology, Universities of Lausanne and Geneva, Lausanne, Geneva, Switzerland
- The inherent low sensitivity of ^{13}C MRS makes direct ^{13}C detection challenging. Moreover, the ^{13}C - ^1H heteronuclear J coupling requires double tuned ^{13}C - ^1H coils to perform proton decoupling during ^{13}C signal acquisition. High sensitivity can be achieved over a large field-of-view using array coils. We aimed to design and build a 4 channel ^{13}C -4 channel ^1H transceiver phased-array coil for ^{13}C -MRS studies in humans at ultra-high field. Electromagnetic performance of the coil was evaluated by FDTD simulations in calf muscles at both frequencies. Finally, ^1H -decoupled ^{13}C resonance of Glycogen C_1 was successfully detected in volunteer calf muscles at 7T.
-
- 3510
Computer #11 Use of the ultimate signal-to-noise ratio to assess the impact of coil coverage for brain imaging
Bastien Guerin¹, Jorge F. Villena², Athanasios G. Polimeridis³, Elfar Adalsteinsson^{4,5,6}, Luca Daniel⁴, Jacob K. White⁴, and Lawrence L. Wald^{1,5}
- ¹A. A. Martinos Center for Biomedical Imaging, Massachusetts General Hospital, Charlestown, MA, United States, ²Cadence Design Systems, Feldkirchen, Germany, ³Skolkovo Institute of Science and Technology, Moscow, Russian Federation, ⁴Department of Electrical Engineering and Computer Science, Massachusetts Institute of Technology, Cambridge, MA, United States, ⁵Harvard-MIT Division of Health Sciences Technology, Cambridge, MA, United States, ⁶Institute for Medical Engineering and Science, Massachusetts Institute of Technology, Cambridge, MA, United States
- We assess the impact of coil coverage for brain imaging at 3 T and 7 T using the ultimate SNR (uSNR). We simulate three coil configurations that cover (i) the whole head (ultimate), (ii) the whole head but the neck (realistic ultimate) and (iii) the head except the neck and face (helmet geometry). We compute the maximum SNR (unaccelerated and accelerated) achievable by any coils with these head coverage using random excitations of a dense dipole cloud placed around the head. Not covering the face (eye/nose/mouth) and neck has little impact on unaccelerated and accelerated SNR compared to the ultimate.
-

- 3511
Computer #12 A multisegment detunable HEM-mode dielectric resonator for increased patient comfort at 7 T
Rita Schmidt¹, Wouter M. Teeuwisse¹, and Andrew Webb¹
- ¹Radiology, Leiden University Medical Center, Leiden, Netherlands
- At ultrahigh field ($\geq 7T$) cavity- and waveguide-based RF coils become possible to construct, and have the advantage that simple designs can be used. One such design uses materials with a high dielectric constant. So far only completely circular structures have been produced; to improve the usability of such a dielectric resonator, it is important to be able to design a splittable and easily detunable resonator. In this work, we tested designs that allow splitting of the cylinder to sections, while maintaining the circularly polarized RF field. In-vivo measurements of the knee at 7 Tesla showed the feasibility of this approach.
-
- 3512
Computer #13 Segmented Dipole: A Remotely Reconfigurable Near-Field Dipole Antenna Transmitter for Optimized 7 T Spine Imaging
Qi Duan¹, Jeff H. Duyn¹, and Hellmut Merkle¹
- ¹Laboratory of Functional and Molecular Imaging, National Institute of Neurological Disorders and Stroke, National Institutes of Health, Bethesda, MD, United States
- 7T spine array based on electric dipole antenna starts to gain attention recently. Nevertheless, the transmit efficiency of the dipole has a natural decay from the feeding point, which does not necessarily corresponding to the target imaging area. In addition, a variety of patient size requires the dipole to be reconfigured for optimum performance. In this work, we propose a concept of "segmented dipole" that can be remotely reconfigured for transmit field-of-view shifting, tuning, and impedance matching characteristics without the need of a parallel-transmit system. A prototype transmitter was built and the reconfiguration capability was demonstrated at a 7T scanner.
-
- 3513
Computer #14 Dedicated surface coils for MR studies in the temporal and the frontal lobes of the human brain at 7T
J r mie Daniel Cl ment¹, Lijing Xin², Rolf Gruetter^{3,4,5}, and  zlem Ipek²
- ¹CIBM-LIFMET, Ecole Polytechnique F d rale de Lausanne, Lausanne, Switzerland, ²CIBM-AIT, Ecole Polytechnique F d rale de Lausanne, Lausanne, Switzerland, ³LIFMET, Ecole Polytechnique F d rale de Lausanne, Lausanne, Switzerland, ⁴Department of Radiology, University of Geneva, Geneva, Switzerland, ⁵Department of Radiology, University of Lausanne, Lausanne, Switzerland
- The purpose of the study was to build dedicated surface coils for the temporal and the frontal lobes of the human brain at 7T. Their transmit field efficiency and single-voxel spectroscopy performances were compared with a birdcage coil with a dielectric pad. An increased B_1^+ -field for the brain regions was measured with the surface coils compared to the birdcage with the pad, which allows single-voxel SPECIAL spectroscopy and anatomical image acquisitions in the peripheral temporal and frontal lobes.
-
- 3514
Computer #15 A combined microcoil and microdialysis approach to measure metabolic response in real-time.
Stefan Gl ggler¹, Silvia Rizzitelli², Noel Pinaud³, G rard Raffard², V ronique Bouchaud², St phane Sanchez², Alan Wong⁴, and Yannick Cr millieux²
- ¹University of Southampton, Southampton, United Kingdom, ²CRMSB, Universit  Bordeaux, Bordeaux, France, ³Universit  Bordeaux, Bordeaux, France, ⁴CEA Saclay, Gif-sur-Yvette, France
- We present two highly sensitive microcoil probes (1H and ^{13}C) that are connected to microdialysis probes inside a MRI scanner. Under continuous flow conditions the metabolic response can be monitored in real-time in vitro and in vivo.
-
- 3515
Computer #16 High Spatial Resolution Functional Imaging of Human Temporal Lobe Cortical Layers at 3T
Pu-Yeh Wu¹, Ying-Hua Chu¹, Shang-Yueh Tsai², Wen-Jui Kuo³, and Fa-Hsuan Lin¹
- ¹Institute of Biomedical Engineering, National Taiwan University, Taipei, Taiwan, ²Institute of Applied Physics, National Chengchi University, Taipei, Taiwan, ³Institute of Neuroscience, National Yang Ming University, Taipei, Taiwan
- By using a dedicated 24-channel coil array and tailored sequence, we achieved human temporal lobe functional imaging with 1.5 mm isotropic resolution. Our coil array had two-fold SNR and tSNR improvement in the temporal lobe compared to a 32-channel whole-head coil array. Functional MRI showed more robust BOLD signals elicited by music stimuli in the primary auditory cortex. Tonotopic mapping revealed the clearest frequency progressions in the middle layer of auditory cortex gray matter, which was consistent with the result acquired by electrophysiological recordings on rodents.
-
- 3516
Computer #17 A Slot Antenna Concept for High Fidelity Body Imaging at Ultra High Field
Leeor Alon^{1,2,3,4}, Cem M. Deniz^{1,2,3,4}, Ryan Brown^{1,2}, Daniel Sodickson^{1,2,3}, and Christopher M. Collins^{1,2,3}
- ¹Center for Advanced Imaging Innovation and Research (CAI2R), New York University School of Medicine, New York, NY, United States, ²Center for Biomedical Imaging, New York University School of Medicine, New York, NY, United States, ³NYU Wireless, NYU-Poly, New York, NY, United States, ⁴RF Test Labs, New York, NY, United States
- In recent years dipoles and other radiative antenna structures have become popular for ultra high field MR imaging. In this work, we introduce the radiative slot antenna, which generates a horizontally polarized E field showing promise as a simple coil structure for high fidelity axial imaging.

- 3517
Computer #18 A Novel 8-channel transceive open knee coil for dynamic musculoskeletal imaging at 7 Tesla
Bassem Henin¹, Ewald Weber¹, and Stuart Crozier¹
¹ITEE, The University of Queensland, Brisbane, Australia
- Magnetic resonance imaging (MRI) is a very important non-invasive modality for the diagnosis of knee anatomy and pathology. The use of 7 Tesla systems for knee imaging can provide higher signal-to-noise ratios (SNR) than lower field systems. In this work, a novel 8-channel transceive open knee coil for dynamic musculoskeletal (MSK) MR imaging of the knee is simulated and constructed. The open design concept will facilitate the diagnostic and functional assessment of knee injuries and pathology, and allow for imaging of a moving knee.
-
- 3518
Computer #19 A 4-element dual-tuned ¹H/³¹P coil array for MR imaging and spectroscopy of the human heart at 3 Tesla
Adrianus J. Bakermans¹, Bart-Jan van den Berg², Gustav J. Strijkers³, Maarten J. Versluis⁴, Dennis W.J. Klomp^{2,5}, Aart J. Nederveen¹, and Jeroen A.L. Jeneson^{1,6}
¹Department of Radiology, Academic Medical Center, Amsterdam, Netherlands, ²MR Coils B.V., Drunen, Netherlands, ³Department of Biomedical Engineering and Physics, Academic Medical Center, Amsterdam, Netherlands, ⁴Philips Healthcare Benelux, Eindhoven, Netherlands, ⁵Department of Radiology, University Medical Center Utrecht, Utrecht, Netherlands, ⁶Neuroimaging Center, University Medical Center Groningen, Groningen, Netherlands
- Maximizing the signal-to-noise ratio (SNR) in *in vivo* cardiac phosphorus-31 magnetic resonance spectroscopy (³¹P-MRS) remains a major challenge in investigations of human myocardial energy metabolism. Here, we demonstrate that with a dual-tuned ¹H/³¹P coil array with 4 elements, it is feasible to achieve a higher SNR and a more homogeneous receive sensitivity distribution over the region of interest for cardiac ³¹P-MRS at 3 Tesla than with a standard linear single-turn ³¹P surface coil. Furthermore, the 4 channels available for ¹H signal reception allow for cardiac cine ¹H-MRI with parallel imaging.
-
- 3519
Computer #20 Assessment of coil arrays with small loop diameter at 7T for micron-scale resolution fMRI of human neocortex.
Alexander Beckett¹, An T Vu^{1,2}, Boris Keil³, Kavin Setsompop³, Lawrence L Wald³, Scott Schillak⁴, and David A Feinberg^{1,2}
¹Helen Wills Neuroscience Institute, University of California, Berkeley, CA, United States, ²Advanced MRI Technologies, Sebastopol, CA, United States, ³Martinos Center for Biomedical Imaging, Charlestown, MA, United States, ⁴Virtumed, LLC, Minneapolis, MN, United States
- The use of array coils with smaller loop sizes allows increased signal to noise ratio close to the coils with decreased coverage of the brain. By focusing on cortical imaging (MR Corticography, MRCoG), this increased SNR can be leveraged to allow ultra-high resolution neuroimaging and fMRI. We assess array coils with varying loop sizes (50mm-20mm) in phantom and with 8-channel arrays (70mm, 40mm, 30mm) in brain at ultra-high resolution (≤ 500 micron isotropic voxels), and show increases in SNR and BOLD contrast in the human cortex as loop size decreases.
-
- 3520
Computer #21 A larger subject Field-of-View and denser coil arrays at UHF: What do we gain?
Shubharthi Sengupta¹, Gregor Adriany², Valentin G Kemper¹, Rainer Goebel¹, and Alard Roebroeck¹
¹Dept. of Cognitive Neuroscience, Faculty of Psychology and Neuroscience, Maastricht University, Maastricht, Netherlands, ²Dept. of Radiology, Center for Magnetic Resonance Research, University of Minnesota, Minneapolis, MN, United States
- Functional magnetic resonance imaging (fMRI) of the human brain has now become the preferred method for mapping functional pathways in the human visual cortex, among other brain regions. At ultra-high fields of 7 Tesla and above, the increased Contrast-to-Noise ratio for blood oxygenation level dependent (BOLD) techniques further facilitates this acquisition methodology. We designed and constructed a frontally open RF coil with a phased array transmit and a dense receiver array layout for human visual cortical imaging at 7 Tesla, specifically for visual fMRI experiments at sub-millimeter resolutions. We compared the coil's performance to that of a standard 32-channel whole-brain volume coil to inquire into its efficacy as a suitable substitute for the whole-brain coil for high resolution fMRI.
-
- 3521
Computer #22 An investigation of coupling and loading effects for adaptive coil design
Barbara Dornberger¹, Markus Vester¹, Robert Rehner¹, Michael Zenge², Riccardo Lattanzi³, and Graham Wiggins³
¹Siemens Healthcare GmbH, Erlangen, Germany, ²Siemens Medical Solutions USA, Inc., Malvern, PA, United States, ³Department of Radiology, New York University School of Medicine, Center for Advanced Imaging Innovation and Research (CAI2R) and Center for Biomedical Imaging, New York, NY, United States
- This abstract examines the feasibility of an adaptive coil design to overcome the disadvantage of poorly loaded and non-fitting local coils. The coil adjusts to the circumference of e.g. a knee by changing the overlap between coil elements. Through bench measurements and simulation we investigated the tradeoff between maintaining optimal coil loading and signal-to-noise ratio (SNR) losses due to coupling. Broadband matching was considered to reduce SNR degradation. Although results show that an adaptive coil can minimize coil losses, the non-ideal overlap of this design leads to a larger SNR degradation than the coil losses of a non-perfect fitting coil.
-
- 3522
Decoupling between coils in a flexible phased-array using stacked circumferential shielding

¹*Institute of Biomedical Engineering, National Taiwan University, Taipei, Taiwan*

We propose a flexible coil array design consisting of circumferential shielding stacked on circular coils to achieve robust decoupling between coil when the array is either bended or on a flat plane. Two types of circumferential shielding were tested through numerical simulation. The results demonstrated that both types can have good decoupling on a curved surface with $S_{21} < -17.1$ dB. The maximum $|B_1|$ for the array coil with Type-II (two-parallel-ring) shielding was 63% larger than that with Type-I (single-strip) shielding. Future work will empirically construct these coils to compensate simulation inaccuracies and validate their performance In Vivo.

3523

Computer #24 Sensitive detection of hemodynamic responses to TMS pulse at human sensorimotor cortex
Pu-Yeh Wu¹, Ying-Hua Chu¹, Aapo Nummenmaa², Thomas Witzel², Shang-Yueh Tsai³, Wen-Jui Kuo⁴, and Fa-Hsuan Lin¹

¹*Institute of Biomedical Engineering, National Taiwan University, Taipei, Taiwan*, ²*Athinoula A. Martinos Center for Biomedical Imaging, Massachusetts General Hospital, Charlestown, MA, United States*, ³*Institute of Applied Physics, National Chengchi University, Taipei, Taiwan*, ⁴*Institute of Neuroscience, National Yang Ming University, Taipei, Taiwan*

We tested how TMS pulses and the separation between TMS pulse and RF excitation affect MRI SNR and tSNR using our tailored 8-channel TMS-compatible MRI coil array. Result from an in vivo experiment using this integrated system to record the BOLD signal elicited by TMS pulses at human primary motor cortex is also reported.

Electronic Poster

UHF Applications & Modeling

Exhibition Hall

Tuesday, May 10, 2016: 16:00 - 17:00

3524

Computer #49 Dipole Array Design Considerations for Head MRI at 10.5T
Jinfeng Tian¹, Russell Lagore¹, Lance Delabarre¹, and J. Thomas Vaughan¹

¹*U. of Minnesota, Minneapolis, MN, United States*

An 8-channel dipole array is a promising structure for human head imaging at 10.5T. In order to optimize the structure for efficiency and homogeneity over the brain, many variations of the dipole were numerically simulated and compared. The variations include varying dipole lengths, warping the dipole, adding shielding, adding dielectric padding or dielectric mirrors and including decoupling capacitors. Compared to a design in use, numerical results predict the RF homogeneity can be greatly improved with a 210 mm dipole array while simultaneously lowering the peak local 1 gram and 10 gram SAR.

3525

Computer #50 Analytical Modeling of the Coupling within a Human Head Surface Loop Transmit Phased Array at Ultra-High Fields
Nikolai I Avdievich¹, Andreas Pfrommer¹, Ioannis Giapitzakis¹, and Anke Henning^{1,2}

¹*High-field Magnetic Resonance, Max Planck Institute for Biological Cybernetics, Tübingen, Germany*, ²*Institute for Biomedical Engineering, UZH and ETH Zurich, Zurich, Switzerland*

Decoupling of multi-channel ultra-high field ($\geq 7T$) transmit and transceiver arrays is a major issue. Analytical modeling of the coupling can facilitate the array optimization. We developed an analytical model describing the impedance matrix for two rectangular loops placed on a cylindrical surface and mimicking the human head array geometry. The developed model was comprehensively validated and allows for the optimization of the geometry and positioning of the loops. The latter enabled simultaneous cancellation of resistive and inductive coupling without additional decoupling circuits. The resulting overlapped array element arrangement improves both transmit and receive performance in comparison to conventional gapped arrays.

3526

Computer #51 Optimization of the antenna-subject spacing for transceive surface arrays of dipole antennas at 7T
A.A. Hurshkainen¹, I.J. Voogt², A.A. Haghnejad², D.W. Klomp², P.R. Luijten², I.V. Melchakova¹, S.B. Glybovski¹, C.A.T. van den Berg², and A.J.E. Raaijmakers²

¹*Department of Nanophotonics and Metamaterials, ITMO University, Saint-Petersburg, Russian Federation*, ²*Imaging Division, UMC Utrecht, Utrecht, Netherlands*

Dipole antennas are being used increasingly for body imaging at 7T. For dipole antennas, SAR levels can be reduced by increasing the antenna-subject spacing. However, this will increase inter-element coupling. In this study we investigate the relationship between antenna-subject spacing, inter-element coupling and maximum local SAR levels for fractionated dipole antennas. We demonstrate that the originally presented antenna-subject spacing (2 cm) can be increased without significant scattering losses. We have realized an 8-element array of fractionated dipole antennas with 4 cm antenna-subject spacing and demonstrate uncompromised imaging performance with 45% lower local SAR levels in comparison to the original design.

3527

Computer #52 Evaluation of through-time radial GRAPPA for real-time cardiac MR imaging at 7 Tesla
Sascha Brunheim^{1,2}, Sören Johst¹, Stefan Maderwald¹, Stefan Rietsch^{1,2}, Stephan Orzada¹, Marcel Gratz^{1,2}, Juliane Goebel³, Kai

Nassenstein³, Nicole Seiberlich⁴, and Harald H. Quick^{1,2}

¹Erwin L. Hahn Institute for Magnetic Resonance Imaging, University Duisburg-Essen, Essen, Germany, ²High Field and Hybrid MR Imaging, University Hospital Essen, Essen, Germany, ³Department of Diagnostic and Interventional Radiology and Neuroradiology, University Hospital Essen, Essen, Germany, ⁴Department of Biomedical Engineering, Case Western Reserve University, Cleveland, OH, United States

Accelerated radial data acquisition of the myocardium in combination with through-time radial GRAPPA offers the opportunity for real-time visualization of cardiac motility without the need for additional ECG or pulse wave synchronization. This is particularly useful in an ultrahigh-field MR environment where conventional gating methods in combination with cardiac dysrhythmia tend to fail. In this work, the performance of through-time radial GRAPPA against an established Cartesian k-space encoding protocol featuring pulse-triggered cine-FLASH has been evaluated and its role as an alternative for real-time cardiac 7-Tesla MR imaging is shown.

3528 Computer #53 Enabling axial diffusion tensor imaging of the human cervical spinal cord at 7T
Aurélien Massire^{1,2}, Pierre Besson^{1,2}, Maxime Guye^{1,2}, Jean-Philippe Ranjeva^{1,2}, and Virginie Callot^{1,2}

¹Centre de Résonance Magnétique Biologique et Médicale (CRMBM), UMR 7339, CNRS, Aix-Marseille Université, Marseille, France, ²Centre d'Exploration Métabolique par Résonance Magnétique (CEMEREM), Hôpital de la Timone, Pôle d'imagerie médicale, AP-HM, Marseille, France

MRI at 7T has recently demonstrated its ability to provide high-quality anatomical images of the spinal cord (SC), yet no diffusion tensor imaging (DTI) study was reported so far. Single-shot echo-planar imaging (ss-EPI) is the method of choice for DTI but the sequence is seriously limited by strong susceptibility artifacts. This work demonstrates that a thoughtful implementation of ss-EPI at 7T combined with distortion correction post-processing from two acquisitions with opposed phase-encoding directions can generate high-resolution axial DTI images of the cervical SC with added value compared to lower field standard protocols making SC DTI ready for UHF clinical investigations.

3529 Computer #54 The traveling heads: Qualitative and quantitative evaluation of multicenter brain imaging at 7 Tesla
Maximilian N. Voelker¹, Oliver Kraff², Daniel Brenner³, Astrid Wollrab⁴, Oliver Weinberger⁵, Moritz C. Berger⁶, Simon Robinson⁷, Wolfgang Bogner⁷, Christopher Wiggins⁸, Robert Trampel⁹, Tony Stöcker³, Thoralf Niendorf^{5,10}, Harald H. Quick^{2,11}, David G. Norris^{2,12}, Mark E. Ladd^{2,6}, and Oliver Speck^{4,13}

¹Erwin L. Hahn Institute for Magnetic Resonance Imaging, University Hospital Essen, University of Duisburg-Essen, Essen, Germany, ²Erwin L. Hahn Institute for Magnetic Resonance Imaging, University of Duisburg-Essen, Essen, Germany, ³German Center for Neurodegenerative Diseases (DZNE), Bonn, Germany, ⁴Otto-von-Guericke-University, Magdeburg, Germany, ⁵Berlin Ultrahigh Field Facility (B.U.F.F.), Max-Delbrueck-Center for Molecular Medicine, Berlin-Buch, Germany, ⁶Medical Physics in Radiology, German Cancer Research Center (dkfz), Heidelberg, Germany, ⁷High Field MR Center, Department of Biomedical Imaging and Image-guided Therapy, Medial University of Vienna, Vienna, Austria, ⁸ScanNexus, Maastricht, Netherlands, ⁹Max Planck Institute for Human Cognitive and Brain Sciences, Leipzig, Germany, ¹⁰Experimental and Clinical Research Center, a joint cooperation between the Charité Medical Faculty and the Max Delbrück Center for Molecular Medicine, Berlin, Germany, ¹¹High Field and Hybrid MR Imaging, University Hospital Essen, University Duisburg-Essen, Essen, Germany, ¹²Donders Centre for Cognitive Neuroimaging, Nijmegen, Netherlands, ¹³Leibniz Institute for Neurobiology, Magdeburg, Germany

The "traveling heads" is an experiment started in 2014 to assess the comparability and reproducibility of multicenter human brain imaging at 7T. This is of particular interest as 7T MRI is currently being discussed to become a clinical system in the very near future. The number of installations continues to increase, with currently approximately 60 research sites in operation worldwide. As an advantage, this new technology provides higher SNR, yet the artifact-to-noise ratio is also increased. This can influence the image quality severely and may be different at individual UHF sites, where system hardware differences could diminish reproducibility.

3530 Computer #55 Very high order B0 Shimming of the human brain at 9.4 T considering Real B0 Shim Fields
Paul Chang^{1,2}, Sahar Nassirpour^{1,2}, and Anke Henning^{1,3}

¹Max Planck Institute for Biological Cybernetics, Tuebingen, Germany, ²IMPRS for Cognitive and Systems Neuroscience, Eberhard Karls University of Tuebingen, Tuebingen, Germany, ³Institute for Biomedical Engineering, UZH and ETH Zurich, Zurich, Switzerland

A highly homogeneous B0 field is essential if we are to exploit the advantages of higher field strengths for MR applications. In this work, we model the real field of each shim channel of a 4th order shim system for a 9.4T MR system for *in vivo* B₀ shimming applications. Each shim channel is modelled at a range of frequencies to account for the possibility of amplitude nonlinearities.

By modelling the fields generated by each shim channel, we were able to achieve better shim qualities than if perfect fields were assumed.

3531 Computer #56 B1+ homogenization at 7T using an innovative meta-atom
Lisa Leroi¹, Alexandre Vignaud¹, Pierre Sabouroux², Elodie Georget¹, Benoit Larrat¹, Stefan Enoch², Gérard Tayeb², Nicolas Bonod², Alexis Amadon¹, Denis Le Bihan¹, and Redha Abdeddaim²

¹UNIRS, CEA Saclay - DSV - I2BM - Neurospin - UNIRS, Gif-sur-Yvette, France, ²CNRS, Aix-Marseille Université, Centrale Marseille, Institut Fresnel, UMR 7249, Marseille, France

B₁⁺ heterogeneity at ultra-high field (UHF) can be tackled performing "passive shimming" with High-Dielectric Constant (HDC) pads. Nevertheless, HDC pads have shown structural, manufacturing and composition constraints. Here, we substitute HDC padding with a new meta-atom (MA) structure with a high equivalent dielectric constant, leaving behind the identified limitations. In this work, we

compare this MA structure to a classic BaTiO₃ pad used in UHF clinical routine. Results demonstrate this solution to strongly impact local B₁⁺ distribution. Implementing multiple MA structures into the coil design might suggest a good potential for brain global B₁⁺ inhomogeneity mitigation.

3532
Computer #57 Improving travelling wave efficiency at 7 T using dielectric material placed "beyond" the region of interest
Rita Schmidt¹ and Andrew Webb¹

¹Radiology, Leiden University Medical Center, Leiden, Netherlands

The concept of traveling-wave MRI has been introduced for ultra-high fields, enabling large field-of-view excitation and physical separation between the antenna and the subject. Several studies have shown that introducing additional materials/structures into the magnet bore or surrounding the subject can improve the efficiency. In this work we explore the use of high permittivity material placed behind the region of interest and show that it can be beneficial for traveling wave efficiency. Separating the region of improved efficiency from that of the dielectric allow positioning of a receive array in the close proximity to the region of interest, physically separate from the dielectric material.

3533
Computer #58 Tuning Microstrip Coil Field Patterns Using Capacitor-Segmented Ground Planes
Xinqiang Yan^{1,2}, John C. Gore^{1,2,3}, and William A. Grissom^{1,2,3}

¹Institute of Imaging Science, Vanderbilt University, Nashville, TN, United States, ²Radiology, Vanderbilt University, Nashville, TN, United States, ³Biomedical Engineering, Vanderbilt University, Nashville, TN, United States

At 7T and higher, the B₁ fields of loop and microstrip coils become asymmetric. However, B₁ fields of dipole antennas are still symmetric. The different behaviors of dipole and microstrip coils may be explained by the fact that they have similar magnetic-field vectors but different Poynting vectors. We propose to manipulate the Poynting vector and thus the symmetry of the B₁ patterns of microstrip coils using capacitor-segmented ground (CSG) planes. This concept has been validated by numerical studies and practical MRI experiments. The CSG method provides additional flexibility for manipulating the shape of the B₁ field, which may be advantageous for RF shimming and parallel transmission.

3534
Computer #59 Control of Excited Modes in Ultra High Magnetic Field MRI with Electrically Hard Surfaces
Patrick Bluem¹, Andrew Kiruluta², Pierre-Francois Van de Moortele³, Gregor Adriany³, and Zoya Popovic¹

¹Department of Electrical, Computer, and Energy Engineering, University of Colorado at Boulder, Boulder, CO, United States, ²Massachusetts General Hospital, Harvard Medical School, Boston, MA, United States, ³University of Minnesota, Center for Magnetic Resonance Research, Minneapolis, MN, United States

Traditional MRI reactive near-field probe design for B₁ field uniformity assumes quasi-static fields. However, for B₀>4T, the quasi-static approximation is no longer valid since the wavelength is smaller than the FOV and field wave modes appear, affecting image quality. This work presents the use of a copper strip waveguide structure combined with a traveling wave excitation at 7T, 10.5T human wide-bore and 16.4T small animal scanners, while observing the effect on a cylindrical distilled water phantom. A simple flexible copper strip wearable wrap is shown to improve SNR and field distribution in UHF-MRI.

3535
Computer #60 Theoretical and simulation verification of SNR enhancement in traveling wave MRI using free local resonators
Xinqiang Yan^{1,2} and Xiaoliang Zhang³

¹Institute of Imaging Science, Vanderbilt University, Nashville, TN, United States, ²Radiology, Vanderbilt University, Nashville, TN, United States, ³Department of Radiology and Biomedical Imaging, University of California San Francisco, San Francisco, CA, United States

Traveling wave MR is a promising method for large field-of-view imaging at ultrahigh fields. However, a major issue currently faced in traveling wave MR is low transmit efficiency and limited SNR. It was found that the SNR in traveling wave MRI can be significantly improved by using a free local resonator. In this study, we validated this finding in simulation and extended the single loop to a multi-channel array. Based on the simulation results, the SNR on the phantom has a 16-fold gain (56.8 VS 3.6) at near area and 3-fold gain at far area (9.7 VS 3.5) with the help of the free loop. This improvement can be attributed to the secondary magnetic field caused by induced current of the free resonator.

3536
Computer #61 Zeroth-Order Resonator with Stepped Impedance for 7T Magnetic Resonance RF Coil
Vijayaraghavan Panda^{1,2}, Sung-Min Sohn^{1,2}, Thomas J Vaughan^{1,2}, and Anand Gopinath¹

¹Department of Electrical and Computer Engineering, University of Minnesota, Minneapolis, MN, United States, ²Department of Radiology, Center for Magnetic Resonance Research, Minneapolis, MN, United States

A planar structure based on a metamaterial transmission line Zeroth Order Resonance (ZOR) and Stepped Impedance Structure is designed as a MRI RF coil element. It generates high uniform magnetic field in the 7T Magnetic resonance imaging (MRI) system at 298 MHz, which improves the signal to noise ratio and the quality of the images. The full wave simulation and measurements show comparable results with the microstrip TEM RF coil element [1]. Additionally, it can generate uniform and high H-field intensity for any physical length of the coil as the resonance of the ZORs is independent of its length [2].

- 3537
Computer #62 9.4T Animal Scanner for Translation Research with Binary Compatibility to Human Scanner and Clinical UI
Jörg Felder¹, Chang-Hoon Choi¹, Stefan Schwan¹, A. Avdo Celik¹, Seong Dae Yun¹, Nuno Andre da Silva¹, Ana Maria Oros-Peusquens¹, and N. Jon Shah^{1,2}
- ¹*INM-4, Forschungszentrum Jülich, Jülich, Germany,* ²*Faculty of Medicine, Department of Neurology, JARA, RWTH Aachen University, Aachen, Germany*
- In translational research going from animal model to in vivo human it is often desirable to change as few experimental parameters as possible. For this purpose a unique 9.4 T animal scanner has been assembled consisting of a dedicated small bore magnet and being operated with clinical software. Here we demonstrate an initial performance analysis of the system as well as some more advanced image acquisitions.
-
- 3538
Computer #63 Revised Transmit/Receive Loop Coil for 7T Usage
Zhiyong Zhai¹ and Michael Morich¹
- ¹*Philips, Cleveland, OH, United States*
- At 7T, T/R loop coils have challenges in transmit B_1^+ -field efficiency and receive B_1^- -field sensitivity in a spatial context, due to the increased tissue dielectric/wavelength effect. Here we propose a revised T/R loop coil schema which improves the B_1^- -field non-uniformity at 7T. The proposed modification may make the T/R loop coil construct yet more useful at ultra-high fields.
-
- 3539
Computer #64 Feasibility of crossed-dipole antenna to excite a circularly-polarized field for human brain imaging at 7T, A design study
Özlem Ipek¹ and Rolf Gruetter^{2,3,4}
- ¹*CIBM-AIT, EPFL, Lausanne, Switzerland,* ²*LIFMET, EPFL, Lausanne, Switzerland,* ³*Department of Radiology, University of Lausanne, Lausanne, Switzerland,* ⁴*Department of Radiology, University of Geneva, Geneva, Switzerland*
- The aim of this study was to investigate the crossed-dipole antenna by means of electromagnetic simulations and compare it with the surface quadrature head loop and volume head coils in terms of B_1^+ efficiency for 7T human brain imaging. The crossed-dipole antenna consists of two dipoles placed in a crossed form mounted upon/in an one-side conductor shielded dielectric. This antenna excites the circularly-polarized field and enhances the transmit efficiency in the occipital lobe in a larger FOV compared to the conventional coils. The comparison of the simulated B_1^+ maps of the coils showed that it is feasible to build it.
-
- 3540
Computer #65 Traveling Wave MRI at 7T Using Dielectric Wave-Guide
Zhiyue J Wang^{1,2}, Alexander Ivanishev¹, Keith M Hulsey¹, Dah-Jyuu Wang³, and Robert E Lenkinski¹
- ¹*UT Southwestern Medical Center, Dallas, TX, United States,* ²*Children's Medical Center Dallas, Dallas, TX, United States,* ³*Children's Hospital of Philadelphia, Philadelphia, PA, United States*
- Traveling wave MRI uses a wave-guide for RF transmission. The metal bore of the scanner magnet serves as a wave-guide and extensions using conductor sheets may be added. Although dielectric materials are frequently introduced into the system, their intended function has been to modify the behavior of the wave-guide. In this work, we show that a dielectric material may be used as a wave-guide by itself, in a fashion similar to optic fibers guiding light transmission. We conducted MRI experiments at 7T using an insulator wave-guide constructed by filling a PVC tube with deionized water.
-
- 3541
Computer #66 Optimizing high permittivity materials for SAR minimization in transmit arrays: influence of the phase distribution of the excitation profile
Gillian G Haemer^{1,2,3}, Manushka V Vaidya^{1,2,3}, Daniel K Sodickson^{1,2,3}, Graham C Wiggins^{1,2}, and Riccardo Lattanzi^{1,2,3}
- ¹*The Center for Advanced Imaging Innovation and Research (CAI2R), Department of Radiology, New York University School of Medicine, New York, NY, United States,* ²*The Bernard and Irene Schwartz Center for Biomedical Imaging, Department of Radiology, New York University School of Medicine, New York, NY, United States,* ³*The Sackler Institute of Graduate Biomedical Sciences, New York University School of Medicine, New York, NY, United States*
- Appropriate high-permittivity, low-conductivity materials placed between the RF coil and the sample can provide performance improvement in both transmission and reception. We employed a simulation framework based on dyadic Green's functions for multi-layered spherical geometries to analyze how HPMs affect the tradeoff between excitation homogeneity and global Specific Absorption Rate (SAR) for RF shimming at 7T using an L-curves analysis. Three target excitation profiles were analyzed, with uniform amplitude and varied phase, to determine the influence that target phase distribution has on the optimal relative permittivity results.
-
- 3542
Computer #67 Evaluation of potential improvements from high permittivity pads for imaging upper extremities at 7 Tesla
Oliver Kraff¹, Andrea Lazik-Palm^{1,2}, Wyger M Brink³, Andreas K Bitz⁴, Mark E Ladd⁴, and Harald H Quick^{1,5}
- ¹*Erwin L. Hahn Institute for MRI, University Duisburg-Essen, Essen, Germany,* ²*Department of Diagnostic and Interventional Radiology and Neuroradiology, University Duisburg-Essen, University Hospital, Essen, Germany,* ³*Radiology, Leiden University Medical Center, Leiden, Netherlands,* ⁴*Medical Physics in Radiology, German Cancer Research Center (DKFZ), Heidelberg, Germany,* ⁵*High Field and Hybrid MR Imaging, University Duisburg-Essen, University Hospital, Essen, Germany*

Two sets of dielectric pads with high permittivity (CaTiO_3 : 110 and BaTiO_3 : 286) were evaluated for potential improvements in imaging the shoulder joint and upper arm in combination with an 8-channel transmit/receive shoulder coil at 7 Tesla. In vivo images with structural PD TSE and DREAM flip angle maps were obtained and compared to measurements without pads present. Both a fixed RF shim as well as individual RF shimming were applied. For the investigated configurations, no substantial improvements in imaging upper extremities at 7 Tesla were found when applying high permittivity dielectric pads.

-
- 3543
Computer #68
Characterization of a breast gradient insert coil at 7 tesla with field cameras
Tijl van der Velden¹, Quincy van Houtum¹, Mark W.J.M. Gosselink¹, Peter R Luijten¹, Vincent O Boer², and Dennis W.J. Klomp¹
¹Radiology, UMC Utrecht, Utrecht, Netherlands, ²Danish Research Centre for Magnetic Resonance, Copenhagen University Hospital Hvidovre, Hvidovre, Denmark
- In this work a gradient insert coil for breast MRI has been constructed. Its behaviour inside a 7T whole body MR system was characterized using magnetic field cameras. Furthermore, the possibility to correct eddy currents from the gradient insert coil using the built-in gradient set has been investigated.
-
- 3544
Computer #69
Extending the Sensitivity of a Head Coil toward Simultaneous Head and Neck Imaging Using High Permittivity Materials at 7 T
Manushka V. Vaidya^{1,2,3}, Gillian G. Haemer^{1,2,3}, Christopher M. Collins^{1,2,3}, Gang Chen^{1,2,3}, Giuseppe Carluccio^{1,2}, Mary Bruno^{1,2}, Graham C. Wiggins^{1,2}, Daniel K. Sodickson^{1,2,3}, and Riccardo Lattanzi^{1,2,3}
¹Center for Advanced Imaging Innovation and Research (CAI2R), Department of Radiology, New York University School of Medicine, New York, NY, United States, ²Bernard and Irene Schwartz Center for Biomedical Imaging, Department of Radiology, New York University School of Medicine, New York, NY, United States, ³Sackler Institute of Graduate Biomedical Sciences, New York University School of Medicine, New York, NY, United States
- A standard head-coil may not be sufficient to examine regions inferior to the base of the skull. Previous work demonstrates that the field-of-view of a surface coil can be extended using high permittivity materials (HPM). In this work, we use calcium titanate bags to extend the sensitivity of a commercial head-coil, and demonstrate an increase in the signal-to-noise ratio in the neck muscles, brainstem and superior regions of the spinal cord and cervical vertebrae. Our results indicate that extending the sensitivity of any commercial coil may be possible using appropriately positioned HPMS.
-
- 3545
Computer #70
7T 8-channel pTx head coil with high B1+ efficiency optimized for MRS
Frank Seifert¹, Harald Pfeiffer¹, Ralf Mekte¹, Patrick Waxmann¹, and Bernd Ittermann¹
¹Physikalisch-Technische Bundesanstalt (PTB), Braunschweig and Berlin, Germany
- A 7T 8-channel transmit/receive head volume coil is introduced which is capable to produce transmit fields in the human brain of more than 50 μT necessary for single voxel MRS with acceptable chemical shift artifacts. Key to this good transmit field efficiency was careful design and material selection but also the choice of relatively short coil elements. From the simulation based design process appropriate input power limits were concluded which allow safe operation of the coil in compliance with IEC 60601-2-33.
-
- 3546
Computer #71
On the robustness and reproducibility of spatially selective excitation using parallel transmission at 7T – a multicenter study
Maximilian N. Voelker¹, Daniel Brenner², Martina Flöser³, Marcel Gratz^{4,5}, Soeren Johst⁴, Stephan Orzada⁴, Tony Stöcker², Harald H. Quick^{4,6}, Mark E. Ladd^{3,4}, and Oliver Kraff⁴
¹University of Essen, Erwin L. Hahn Institute for Magnetic Resonance Imaging, Essen, Germany, ²German Center for Neurodegenerative Diseases (DZNE), Bonn, Germany, ³Medical Physics in Radiology, German Cancer Research Center (dkfz), Heidelberg, Germany, ⁴Erwin L. Hahn Institute for Magnetic Resonance Imaging, University of Duisburg-Essen, Essen, Germany, ⁵High Field and Hybrid MR Imaging, University Hospital Essen, University of Duisburg-Essen, Essen, Germany, ⁶High Field and Hybrid MR Imaging, University Hospital Essen, University Duisburg-Essen, Essen, Germany
- Parallel transmission (pTx) allows the excitation of arbitrarily shaped patterns or reduced field-of-view imaging and is of particular interest in ultra-high field MRI where it is used to diminish artifacts caused by B1 inhomogeneities. However, calculation of arbitrarily shaped pulses is not included in standard pTx system procedures, is time consuming, and can only be done with knowledge of additionally acquired transmit B1 fields. To optimize this workflow, it might be advantageous to share pre-calculated pulses between different systems and/or coils. Image patterns were generated and optimized to assess image quality and to evaluate reproducibility and robustness of shared pulses.
-
- 3547
Computer #72
Simulated phase of driving voltage for travelling wave MRI with a parallel-plate waveguide at 7 T
Fabian Vazquez¹, Sergio Solis¹, Rodrigo Martin¹, and Alfredo O Rodriguez²
¹Physics Department, Faculty of Sciences, UNAM, Mexico, DF, Mexico, ²Dep Electrical Engineering, UAM Iztapalapa, Mexico DF, Mexico
- Travelling wave magnetic resonance imaging (twMRI) offers to overcome the inhomogeneities due to the standing wave patterns, and the use of coil arrays with multiple coil elements. The excitation of the spins have been commonly done with RF surface coils, dipole and patch antennas, etc. The resonant device should be able to generate an adequate magnetic field to transmit the signal to a distant object using a waveguide. In this paper, we numerically simulated the magnetic field of the principal mode (TM_0) as a function of the

Gradients & Systems, MR Electronics, MR/PET

Exhibition Hall

Tuesday, May 10, 2016: 16:00 - 17:00

3548



Computer #25 A multi-channel gradient driver system for matrix gradient coils
Huijun Yu¹, Kelvin Jon Layton¹, Sebastian Littin¹, Stefan Kroboth¹, Feng Jia¹, and Maxim Zaitsev¹

¹Dept. of Radiology, Medical Physics, University Medical Center Freiburg, Freiburg, Germany

The matrix gradient coils are showing its potential in offering high flexibility in generating customized spatial magnetic fields. However, the high demands on the amplifiers might become unacceptable for conventional one-coil one-amplifier drive method. We developed a 12 channel gradient driver system integrated with multi-channel switches for matrix gradient coils to drive a higher number of coil elements. The system was tested successfully with a home-built matrix gradient coil with its channels grouped in 12 clusters.

3549

Computer #26 Variation in strain characteristics for multiscale multi-physics models of a 1.5T conduction cooled MRI system based on a 36 filament MgB₂ composite wire
Abdullah Al Amin¹, Tanvir Baig², Robert J. Deissler², David Doll³, Michael Tomsic³, Ozan Akkus¹, and Michael Martens²

¹Department of Mechanical Engineering, Case Western Reserve University, Cleveland, OH, United States, ²Department of Physics, Case Western Reserve University, Cleveland, OH, United States, ³Hyper Tech Research Inc., Columbus, OH, United States

A higher field (>1.5T) MRI magnet system is usually constructed with composite superconducting wire. Usually, modeling of the strain development of this magnet system requires approximation of the material property of composite Magnesium diboride wire using the simple rule of mixture (ROM). The Rule of Mixture (ROM) is a straight forward and simple technique but the underestimation of the strain development may affect the accuracy of the analysis. This study compares the variation in hoop strain development as three different numerical homogenization methods are employed to estimate the material property of the composite wire.

3550

Computer #27 Imaging with a high-channel matrix gradient coil
Kelvin Layton¹, Huijun Yu¹, Stefan Kroboth¹, Sebastian Littin¹, Feng Jia¹, and Maxim Zaitsev¹

¹Department of Radiology, Medical Physics, University Medical Center Freiburg, Freiburg, Germany

Matrix gradient coils consist of many elements that can be combined to produce a wide variety of magnetic fields for spatial encoding and shimming applications. In this work, first imaging results are presented using a newly constructed 84-channel actively shielded matrix gradient coil. The coil elements are combined in groups and driven by 12 additional gradient power amplifiers to produce approximately linear gradient fields. Images are of comparable quality to the standard clinical system with relatively little calibration of the matrix coil. The integrated system is extremely flexible and enables new research into novel encoding techniques.

3551

Computer #28 Analysis and Prediction of Gradient Response Functions under Thermal Load
Benjamin E. Dietrich¹, Jonas Reber¹, David O. Brunner¹, Bertram J. Wilm¹, and Klaas P. Pruessmann¹

¹Institute for Biomedical Engineering, University and ETH Zurich, Zurich, Switzerland

Temperature dependent changes of gradient impulse response functions are analyzed by measurements with a recently proposed continuous field camera and the resulting data is used in a locally linear model approach to predict impulse response functions based on temperature data.

3552

Computer #29 Peripheral Nerve Stimulation Thresholds of a High Performance Insertable Head Gradient Coil
Trevor P Wade^{1,2}, Andrew Alejski¹, Charles A McKenzie², and Brian K Rutt³

¹Robarts Research Institute, Western University, London, ON, Canada, ²Medical Biophysics, Western University, London, ON, Canada, ³Dept. of Radiology, Stanford University, Stanford, CA, United States

A high performance insertable head gradient was evaluated for peripheral nerve stimulation and found to have PNS thresholds several times higher than body gradients and equal to or exceeding existing head gradients. The most sensitive axis (Y) had a threshold of $\Delta G_{\min} = 108 \pm 4$ mT/m and $SR_{\min} = 156 \pm 9$ T/m/s. This rapidly insertable coil has the hardware capability to reach ΔG_{\max} of 120mT/m single axis and 400mT/m triple axis with presently available clinical gradient amplifiers, meaning extremely high hardware performance but also that PNS thresholds are reached on most axes.

3553

Computer #30 Gradient input optimization based on the measured system frequency response
Signe Johanna Vannesjo¹, Christian Vogt¹, Lars Kasper^{1,2}, Maximilian Haeberlin¹, and Klaas P Pruessmann¹

¹Institute for Biomedical Engineering, University of Zurich and ETH Zurich, Zurich, Switzerland, ²Translational Neuromodeling Unit, Institute for Biomedical Engineering, University of Zurich and ETH Zurich, Zurich, Switzerland

Accurate gradient time-courses are crucial for MRI, yet actual waveforms generally deviate from ideal. We here propose to treat the task of finding the ideal gradient input for a targeted output gradient waveform as a case-by-case optimization problem, based on an LTI model of the gradient system. The method is aimed to achieve optimal gradient waveform fidelity that a given gradient system is capable of producing, considering both bandwidth and amplitude/slew rate limitations. We perform the optimization for an EPI and a spiral sequence and compare the resulting output to using non-optimized input on measured k-space trajectories.

3554
Computer #31 Vibroacoustic Noise Reduction in High Performance Head Gradient Coils Using Ceramic Inserts
Simone Angela Winkler¹, Andrew Alejski², Trevor Wade², Charles McKenzie², and Brian K Rutt¹

¹Dept. of Radiology, Stanford University, Stanford, CA, United States, ²Robarts Research Institute, The University of Western Ontario, London, ON, Canada

We hypothesized that ceramic inserts will reduce sound pressure levels (SPLs) in high performance head gradient coils. We used realistic multi-physics modeling methods (previously validated by experiments) to investigate this hypothesis, and in particular to evaluate vibroacoustic reductions as a function of ceramic insert geometry and frequency of excitation. Averaged over the range 0-3000Hz, we demonstrate a maximum overall SPL reduction of 10.9dB, with a substantially higher reduction in the high frequency regime (2000-3000Hz) of 20.7dB. We show that a uniform 15mm thick cylindrical insert is a practical design that yields the majority of the acoustic reduction benefit.

3555
Computer #32 Continuous SWIFT on a whole-body 7T system: Initial phantom and in vivo images
Florian Maier¹, Manuela Rösler^{1,2}, Armin M. Nagel^{1,3}, and Reiner Umathum¹

¹German Cancer Research Center (DKFZ), Heidelberg, Germany, ²Institute for Biomedical Engineering, University of Zurich and ETH Zurich, Zurich, Switzerland, ³Diagnostic and Interventional Radiology, University Medical Center Ulm, Ulm, Germany

Simultaneous excitation and acquisition is a promising approach to acquire MR images using very low transmission power. This concept is also well-suited for imaging tissues and materials with ultrashort T2* relaxation times since no echo time exists. In this work, a cSWIFT hardware setup, pulse sequence, and reconstruction were designed for and implemented on a whole-body 7T system. Spectroscopy and imaging of phantoms and in vivo imaging of the human forearm were successfully performed. Feasibility of cSWIFT with the implemented setup was demonstrated.

3556
Computer #33 Portable Magnet Design Optimization for Brain Imaging without Gradient Coils
Clarissa Zimmerman Cooley¹, Melissa Haskell^{1,2}, Jason P Stockmann¹, Cristen Lapierre¹, Chenoa Schatzki-McClain¹, Charlotte Sappo¹, Stephen F Cauley^{1,3}, Bastien Guerin^{1,3}, Matthew S Rosen^{1,3,4}, and Lawrence L Wald^{1,3,5}

¹A. A. Martinos Center for Biomedical Imaging, Massachusetts General Hospital, Charlestown, MA, United States, ²Biophysics, Harvard University, Cambridge, MA, United States, ³Harvard Medical School, Boston, MA, United States, ⁴Department of Physics, Harvard University, Cambridge, MA, United States, ⁵Harvard-MIT Division of Health Sciences Technology, Cambridge, MA, United States

The development of a low-cost portable MRI scanner for brain imaging could address the need for imaging at unconventional sites. We previously presented an appropriate method for 3D imaging in a portable magnet without gradient coils. In-plane image encoding was demonstrated using the natural field variation of a rotating prototype magnet. However, the magnet diameter must be increased for human brain imaging and the built-in encoding field should be tailored to improve image resolution uniformity. We present a method for designing an optimized magnet for this application using the Genetic Algorithm, and evaluate a chosen design via image simulations.

3557
Computer #34 Very low field MRI setup for brain imaging
Reina AYDE¹ and Claude Fermon¹

¹SPEC, CEA, CNRS, Université Paris-Saclay, Gif-sur-Yvette, France

Mixed sensors are at present competitive with classical tuned coils for the detection of MRI signals on a very low field range. A very low field head MRI system is developed without pre-polarization technique nor magnetic shielding room. Homogeneity of the system and gradients were characterized. A homogeneity of 115 ppm was achieved in a quasi-open configuration. Linearity of the gradients was verified. The amplitude of each gradient was 100 times lower than at high field but sufficiently high to achieve a resolution of 2 mm x 2 mm x 2 mm.

3558
Computer #35 Wireless Powering Using MRI Pulse Sequences
Madhav Venkateswaran¹, Kevin Johnson², Daniel van der Weide¹, and Sean Fain²

¹Electrical Engineering, University of Wisconsin-Madison, Madison, WI, United States, ²Medical Physics, University of Wisconsin-Madison, Madison, WI, United States

We present models for wirelessly powering implants using the transmit RF excitation for MRI. Detailed models were developed for all hardware components of the transmit chain, including actual MRI sequences. Candidate pulse sequences were compared to predict

how wireless powering could operate synchronously with imaging. The methods are useful in designing and optimizing wireless powering inside the MRI scanner.

-
- 3559
Computer #36 ZT-AC: Zero TE based PET/MR attenuation correction
Florian Wiesinger¹, Sandeep Kaushik², Dattesh Shanbhag², Venkata Chebrolu², Vivek Vaidya², Sangtae Ahn³, Lishui Cheng³, Andrew Leynes⁴, Jaewon Yang⁴, Thomas Hope⁴, and Peder Larson⁴
- ¹GE Global Research, Munich, Germany, ²GE Global Research, Bangalore, India, ³GE Global Research, Niskayuna, NY, United States, ⁴University of California San Francisco, San Francisco, CA, United States*
- We describe a novel PET/MR attenuation correction (AC) method based on zero TE MR imaging that is fast, robust and accounts for bone. The method, termed ZT-AC, was tested for N=10 PET/MR patients in the head and compared relative to gold-standard CT-AC and atlas-based AC methods.
-
- 3560
Computer #37 Evaluation of ZTE localization accuracy for PET/MR hardware attenuation correction
Gaspar Delso¹, Mohammad Mehdi Khalighi², Sabrina Epp³, Felipe de Galiza Barbosa³, Tetsuro Sekine³, Edwin ter Voert³, and Patrick Veit-Haibach³
- ¹GE Healthcare, Zurich, Switzerland, ²GE Healthcare, Stanford, CA, United States, ³University Hospital, Zurich, Switzerland*
- One challenge of PET/MR imaging is the correction of photon attenuation caused by hardware in the field-of-view. For the particular case of MR local coil attenuation, a solution based on stored templates is provided by commercially available clinical PET/MR systems. This solution, however, is limited to rigid coils docked in a pre-defined position. A more general method encompassing other coil types would be desirable to improve the accuracy of PET images. The goal of the present study is to investigate the accuracy of fast ZTE acquisitions for the correction of local coil attenuation.
-
- 3561
Computer #38 Implementation of an 84 Channel Actively Shielded Matrix Gradient Coil
Sebastian Littin¹, Feng Jia¹, Kelvin J. Layton¹, Huijun Yu¹, Stefan Kroboth¹, and Maxim Zaitsev¹
- ¹Radiology, Medical Physics, University Medical Center Freiburg, Freiburg, Germany*
- In this abstract, we present an 84 channel actively shielded matrix gradient coil. This coil was built and integrated into our 3T MRI scanner. Functionality and characterization measurements such as high voltage tests, eddy current and field map measurements were successfully performed. This system allows for generating spatial encoding fields in a highly flexible fashion, which enables the development of novel imaging techniques.
-
- 3562
Computer #39 Evaluation of Multileaf Collimator performance in high magnetic fringe fields for MRI-Linac development
Bin Dong^{1,2}, Gary P. Liney^{1,2,3,4}, Kevin K. Zhang^{1,4}, Lois Holloway^{1,2,3,4,5}, Peter E. Metcalfe^{1,2}, and Paul J. Keall^{1,5}
- ¹Ingham Institute for Applied Medical Research, Liverpool, Australia, ²Centre for Medical Radiation Physics (CMRP), University of Wollongong, Wollongong, Australia, ³Department of Medical Physics, Cancer Therapy Centre, Liverpool Hospital, Liverpool, Australia, ⁴South Western Sydney Clinical School, University of New South Wales, Liverpool, Australia, ⁵Radiation Physics Laboratory, Sydney Medical School, The University of Sydney, Camperdown, Australia*
- Hybrid systems combining an MRI with a linear accelerator for image guided radiation treatment are being implemented world-wide. As part of our own development we investigated the effect of increasing magnetic field on the performance of a multi-leaf collimator (MLC) motor and encoder from the treatment head of a linear accelerator. Measurements were made at various locations in the fringe field of a 3T scanner with the MLC positioned to replicate both in-line and perpendicular treatment beam to B₀ directions. Results show a static field threshold and speed reduction which is position dependent which can be improved significantly with shielding.
-
- 3563
Computer #40 Adaptive Integrated Parallel Reception, Excitation, and Shimming (iPRES) with Bipolar Junction Transistors.
Dean Darnell¹, Trong-Kha Truong¹, and Allen Song¹
- ¹Brain Imaging and Analysis Center, Duke University, Durham, NC, United States*
- An integrated parallel reception, excitation, and shimming coil array with N DC shim loops within each RF coil, termed iPRES(N), improves the shimming of local B₀ inhomogeneities relative to the original iPRES design with one loop per coil, but requires N times more power supplies which adds complexity and cost. A new adaptive iPRES design is proposed that uses bipolar junction transistors to generate different DC current paths, and hence different B₀ fields for local shimming, within each coil using one power supply per coil, thus maintaining the shimming flexibility of iPRES(N) while reducing the number of power supplies.
-
- 3564
Computer #41 WITHDRAWN
Dean Darnell¹, Trong-Kha Truong¹, and Allen Song¹
- ¹Brain Imaging and Analysis Center, Duke University, Durham, NC, United States*
-

- 3565
Computer #42 Lenz lenses: RF field amplification and increased sensitivity using passive inductive elements
Peter T. While^{1,2}, Nils Spengler^{3,4}, and Jan G. Korvink³
- ¹Department of Radiology and Nuclear Medicine, St. Olav's University Hospital, Trondheim, Norway, ²IMTEK - Laboratory for Simulation, University of Freiburg, Freiburg, Germany, ³Institute of Microstructure Technology, Karlsruhe Institute of Technology, Karlsruhe, Germany, ⁴IMTEK - Laboratory for Microactuators, University of Freiburg, Freiburg, Germany*
- Lenz lenses are discrete elements that focus magnetic flux by virtue of their configuration. By the principle of reciprocity, Lenz lenses may be used to increase both B_1 -field strength and receiver sensitivity in an NMR experiment. We present the theory that describes Lenz lenses and their geometrical optimization, plus some preliminary experimental results that demonstrate a three-fold increase in local SNR.
-
- 3566
Computer #43 A prototype low field dental MRI system
Martyn Paley¹, Andreas Hopfgartner², and Steven Reynolds¹
- ¹Immunity, Infection and Cardiovascular Disease, University of Sheffield, Sheffield, United Kingdom, ²University of Wurzburg, Wurzburg, Germany*
- A prototype dental MRI magnet system has been designed, developed and tested. Initial results show the magnet design agrees well with the predicted field using electromagnetic modelling.
-
- 3567
Computer #44 Comparison of preemphasis based on a broadband filter vs. a standard exponential model for higher-order dynamic shimming
Signe Johanna Vannesjo¹, Yuhang Shi¹, Klaas P Pruessmann², Andrew Dewdney³, Karla L Miller¹, and Stuart Clare¹
- ¹FMRIB centre, NDCN, University of Oxford, Oxford, United Kingdom, ²Institute for Biomedical Engineering, University of Zurich and ETH Zurich, Zurich, Switzerland, ³Magnetic Resonance, Siemens Healthcare GmbH, Erlangen, Germany*
- Traditionally, shim preemphasis filters to compensate for eddy current fields have consisted of a sum of exponentially decaying terms. It has recently been proposed to instead implement a non-parametric preemphasis filter based on the shim impulse response function. This can address features that are not captured with the exponential model, such as oscillatory responses. We here compared the two preemphasis approaches for higher-order dynamic shim updating. The non-parametric filter yielded an improved frequency response of the system and about 10 ms faster shim settling, as well as suppression of field oscillations after a shim step.
-
- 3568
Computer #45 COSI Magnet: Halbach Magnet and Halbach Gradient Designs for Open Source Low Cost MRI
Lukas Winter¹, Antonia Barghoorn¹, Peter Blümler², and Thoralf Niendorf^{1,3,4}
- ¹Berlin Ultrahigh Field Facility (B.U.F.F.), Max Delbrück Center for Molecular Medicine, Berlin, Germany, ²Institute of Physics, University of Mainz, Mainz, Germany, ³Experimental and Clinical Research Center (ECRC), a joint cooperation between the Charité Medical Faculty and the Max Delbrück Center for Molecular Medicine, Berlin, Germany, ⁴MRI.TOOLS GmbH, Berlin, Germany*
- Cost effective open source imaging (COSI) is a collaborative initiative currently building an affordable low field open source MR scanner with the technical documentation available at www.opensourceimaging.org. As part of this initiative uniform Halbach magnets have been evaluated in absolute B_0 , field homogeneity, magnet mass and costs. Halbach quadrupoles are introduced, that produce an adjustable constant gradient field for spatial encoding removing the need for high power gradient amplifiers. Combining these efforts an imaging magnet ($B_0=0.3T$, $d=180mm$) design is presented that can incorporate a Halbach gradient of 157mT/m. The results are encouraging for low cost low field MR applications.
-
- 3569
Computer #46 Crosstalk between gradient coils
Fangfang Tang¹, Fabio Freschi^{1,2}, Maurizio Repetto^{1,2}, Feng Liu¹, and Stuart Crozier¹
- ¹School of Information Technology and Electrical Engineering, The University of Queensland, Brisbane, Australia, ²Department of Energy, Politecnico di Torino, Torino, Italy*
- In MRI, gradient coil switching generates eddy currents in surrounding conductors including intra-coil eddy currents in the surrounding gradient coils (crosstalk). In order to investigate the intra-coil eddy currents, a set of gradient coils with differing track widths has been designed for use in a cylindrical MRI system. It was found that the surrounding coils with wide tracks produced significantly larger eddy currents than the cold shield. It is therefore necessary to take into account the crosstalk between coils when evaluating coil performance. We found that the optimal track width to use in gradient coil design is around 14 mm.
-
- 3570
Computer #47 Theoretical investigation of gradient pulse alterations for acoustic noise reduction in an MRI-LINAC system
Yaohui Wang¹, Fangfang Tang¹, Yu Li¹, Feng Liu¹, and Stuart Crozier¹
- ¹The University of Queensland, Brisbane, Australia*
- A theoretical acoustic noise control method was proposed through gradient pulse alterations. This method can remove the resonant-frequency components of the gradient pulse and keep the pulse form. This method is easily implemented without reassembling the MRI system elements. Simulation shows that the noise reduction effect using this method is significant. Imaging quality will be evaluated on

future experimental measurements.

3571

Computer #48

The forgotten planar gradient coil
Hector Sanchez Lopez¹

¹*Department of Electrical Engineering, Universitas Dian Nuswantoro, Semarang, Indonesia*

This work present two methods for designing simple and compact planar coils. The length of a constant wire width is minimized using Euclidian and Manhattan distance. Euclidian coils exhibit smooth patterns of slightly lower resistance than that of square-shape coils obtained using Manhattan distance. Manhattan coils show straight conductors which minimizes the force and facilitate the coil manufacturing. The coil sensitivity increases up to 1.8 times when placed in the iron poles but in detriment of the coil slew rate. Compact transverse coils architected using both distance minimization induces a residual eddy current smaller than 0.05% within the DSV.

Electronic Poster

Interventional 1

Exhibition Hall

Tuesday, May 10, 2016: 17:00 - 18:00

3572

Computer #1

In-Bore MRI-Guided Transperineal Prostate Biopsy using 4-DOF Needle-Guide Manipulator

Junichi Tokuda¹, Kemal Tuncali¹, Gang Li², Nirav Patel², Tamas Heffter³, Gregory S Fischer², Iulian I Iordachita⁴, Everette Clif Burdette³, Nobuhiko Hata¹, and Clare M Tempamy¹

¹*Department of Radiology, Brigham and Women's Hospital, Boston, MA, United States*, ²*Department of Mechanical Engineering, Worcester Polytechnic Institute, Worcester, MA, United States*, ³*Acoustic MedSystems Inc., Savoy, IL, United States*, ⁴*Department Of Mechanical Engineering, Johns Hopkins University, Baltimore, MD, United States*

We present the clinical feasibility of our MRI-compatible 4-DOF needle-guide manipulator for in-bore MRI-guided transperineal prostate biopsy. Total 11 men were biopsied in a 3T MRI scanner using this manipulator. All 11 procedures were successfully performed in 102.6±24.5 minutes with targeting errors of 4.9±2.9 mm. The targeting errors were consistent with other clinical studies. Pathology results confirmed prostate cancer with Gleason score ≥ 6 in 5/6 men with previous negative TRUS biopsies, and upgraded 2/5 men on active surveillance to clinically significant cancer with Gleason score 7. In conclusion, In-bore MRI-guided prostate biopsy using the manipulator was feasible.

3573

Computer #2

Motion compensated high resolution MR Imaging of Vagus and Recurrent Laryngeal Nerves with Novel Phase-based Navigation Sequences

Ravi Teja Seethamraju¹, Jayender Jagadeesan², Vera Kimbrell², Aida Faria², Thomas C Lee², and Daniel T Ruan³

¹*MR R&D, Siemens Healthcare, Boston, MA, United States*, ²*Radiology, Brigham and Women's Hospital, Boston, MA, United States*, ³*Endocrine Surgery, Brigham and Women's Hospital, Boston, MA, United States*

Diagnostic imaging of the recurrent laryngeal (RLN) and vagus nerves (VN) could help in surgical planning and in minimizing the risk of damage to the nerves. However, imaging these nerves is technically challenging due to their size, location, and physiological motions such as breathing and swallowing. The RLN and VN can be visualized on the CISS and T2 TSE, however with a novel phase navigator, the nerves are better delineated on the motion-compensated T2 TSE compared to the CISS which is un-navigated.

3574

Computer #3

Geometry of Basal Ganglia nuclei in QSM and Histology in Parkinson's disease brains

Carsten Stueber^{1,2}, Alexey Dimov¹, Kofi Deh¹, David Pitt², and Yi Wang¹

¹*Weill Cornell Medical College, New York, NY, United States*, ²*Yale School of Medicine, Yale University, New Haven, CT, United States*

Quantitative susceptibility mapping (QSM) provides a quantitative MRI contrast, which reflects the local iron concentration. Thus, QSM allows to determine the geometries of iron-rich deep grey matter nuclei including substantia nigra (SN) and subthalamic nucleus (STN). These basal nuclei are of particular interest in Parkinson's disease. However, the measured dimensions need to be validated in histology using post-mortem human brain tissue. In this work, we show the concordance of the geometries measured in QSM and histology using Perl's iron stain, which opens the door to use QSM as a pre-surgical mapping for deep brain stimulation targeting the STN.

3575

Computer #4

Multi-parametric MRI Characterization of a Polymer Gel Dosimetry Phantom for Non-Invasive 3D Visualization of Radiation Deposition in Gamma Knife Therapy

Ivan E Dimitrov^{1,2} and Strahinja Stojadinovic³

¹*Philips Medical Systems, Dallas, TX, United States*, ²*Advanced Imaging Research Center, UT Southwestern Medical Center, Dallas, TX, United States*, ³*Radiation Oncology, UT Southwestern Medical Center, Dallas, TX, United States*

Radiation therapy aims to maximize dose delivery to tumor areas while minimizing the exposure to healthy tissue. Quality control is required to ensure that the delivered dose closely matches the calculated dose. We performed a patient-specific quality assurance for

cranial radiotherapy using MRI to visualize delivered radiation dose. We utilized an anthropomorphic 3D printed head phantom filled with polymer gel that was scanned before and after exposure to Gamma Knife irradiation. Irradiation changed the polymerization state of the gel and multi-parametric (T1, T2, MR Spectroscopy, CEST) quantitative dose-imaging maps were generated that may lead to optimized patient-specific dose delivery planning.

-
- 3576
Computer #5
TOLD MRI Validation of Reversal of Tumor Hypoxia in Glioblastoma with a Novel Oxygen Therapeutic
Heling Zhou¹, David Wilson², Jason Lickliter³, Jeremy Ruben⁴, Natarajan Raghunand⁵, Michael Sellenger⁶, Ralph P Mason⁷, and Evan Unger^{2,8}
- ¹UT Southwestern Medical Center, Dallas, TX, United States, ²NuvOx Pharma, Tucson, AZ, United States, ³Nucleus Networks, Melbourne, Australia, ⁴William Buckland Radiotherapy Centre, Melbourne, Australia, ⁵Moffitt Cancer Center, Tampa, FL, United States, ⁶Alfred Hospital, Prahran, Australia, ⁷Radiology, UT Southwestern Medical Center, Dallas, TX, United States, ⁸Medical Imaging, The University of Arizona, Tucson, AZ, United States*
- Glioblastoma multiforme (GBM) is known to be a hypoxic tumor and hypoxia adversely affects response to radiation therapy. Dodecafluoropentane emulsion (DDFPe) can improve oxygenation. Tissue oxygen level dependent (TOLD) MRI is an oxygen sensitive imaging technique which is used in this study to assess the improvement of oxygenation after administration of DDFPe. Two different doses were tested and each showed decreased T₁ indicating improved oxygenation.
-
- 3577
Computer #6
Towards DWI Guidance of Percutaneous Biopsies using Dual Echo Steady State Sequence: Qualitative Assessment in Liver
Elena A Kaye¹, Kristin L Granlund², Stephen B Solomon², and Majid Maybody²
- ¹Medical Physics, Memorial Sloan Kettering Cancer Center, New York, NY, United States, ²Radiology, Memorial Sloan Kettering Cancer Center, New York, NY, United States*
- Acquisition of a viable tissue sample is critical to success of a biopsy. DWI could help differentiate between viable and necrotic tissue during the procedure, however, EPI-DWI is not suitable in a percutaneous-biopsy setting due to geometric distortions. DW Dual Echo Steady State (DESS) sequence allows acquisition of 3D undistorted DWI images. This study evaluated the application of DW-DESS during an MR-guided liver biopsy in two patients. Using single breath-hold acquisition, DW-DESS image depicted a liver lesion sharper and less distorted than EPI-DWI. DW-DESS also allowed DWI in the presence of a biopsy needle without distortions of EPI.
-
- 3578
Computer #7
Scannerless real-time MRI
Frank Preiswerk¹, Cheng-Chieh Cheng¹, Sanjay S. Yengul^{1,2}, Lawrence P. Panych¹, and Bruno Madore¹
- ¹Radiology, Brigham and Women's Hospital, Harvard Medical School, Boston, MA, United States, ²Mechanical Engineering, Boston University, Boston, MA, United States*
- MRI can provide favorable image quality for image-guided interventions, but both magnetic field of the scanner and limited patient access inside the bore impose many limitations on image-guidance endeavors. The aim of this work was to estimate MRI of respiratory organ motion outside the scanner, which allows for a wider range of interventional applications. A single-element ultrasound transducer was used as a surrogate for the MR scanner outside the bore, after the correlation between both signals had been learned in a preceding training phase. Validation of estimated MR images outside the bore was performed using tracked 2D ultrasound.
-
- 3579
Computer #8
Real-Time Golden Angle Radial iSSFP for Interventional MRI
Samantha Mikael^{1,2}, Thomas Boyd Martin^{1,2}, Kyung Sung^{1,2}, and Holden H Wu^{1,2}
- ¹Radiological Sciences, University of California, Los Angeles, Los Angeles, CA, United States, ²Biomedical Physics, University of California, Los Angeles, Los Angeles, CA, United States*
- Real-time visualization is crucial to the success of MRI-guided minimally invasive cancer interventions. In this work we combine iSSFP with a golden-angle(GA) ordered radial trajectory and non-Cartesian parallel imaging to create a new real-time MRI sequence with good tissue contrast while suppressing bSSFP banding artifacts. Phantom and volunteer data were acquired and reconstructed using a combined sliding-window SPIRiT algorithm, at different frame rates, showing the capability of the sequence to achieve real-time imaging. These advantages of GA Radial iSSFP show its potential for improving real-time MRI-guided interventions.
-
- 3580
Computer #9
The Development of Tissue Mimicking Gels
Peter Andrew Hardy¹, Christopher J Norsigian², Walter Witschey³, and Luke H Bradley²
- ¹Radiology, University of Kentucky, Lexington, KY, United States, ²Anatomy & Neurobiology, University of Kentucky, Lexington, KY, United States, ³Smilow Center for Translational Research, University of Pennsylvania, Philadelphia, PA, United States*
- Developing tissue mimicking materials can be helpful in reducing the cost and duration of experiments which otherwise require animals. We tested a variety of agarose gels of different gel strength as suitable tissue mimicking material for convection enhanced delivery. The results demonstrate a significant difference in infusion volume and we relate that, through MR measurements, to the mechanical stiffness of the gels.
-
- 3581
A four-layer boundary element model for MRI-guided transcranial magnetic stimulation

Computer #10 Aapo Nummenmaa¹ and Matti Stenroos²

¹Athinoula A. Martinos Center for Biomedical Imaging, Department of Radiology, Massachusetts General Hospital, Charlestown, MA, United States, ²Department of Neuroscience and Biomedical Engineering, Aalto University, Espoo, Finland

MRI-guided targeting and dosing has the potential increase the consistency and efficacy of transcranial magnetic stimulation (TMS). We propose a boundary element method (BEM) approach for estimating the TMS-induced cortical electric fields (E-fields). The method can be applied based on standard T1/T2-weighted MRI data and can incorporate the cerebrospinal fluid (CSF) as a separate conductivity compartment. Our results show that the CSF layer may increase the estimated E-field amplitudes up to 25%. The effect of the CSF depends on the location and orientation of the TMS coil/target in a rather intricate manner, highlighting the importance of individualized, realistically shaped models.

3582 Computer #11 Measurement and Simulation of Susceptibility Artifacts in Variable-TE Radial MRI: Application in an MR-safe Guidewire
Katharina E. Schleicher¹, Stefan Kroboth¹, Klaus Düring², Michael Bock¹, and Axel Joachim Krafft^{1,3,4}

¹Dept. of Radiology - Medical Physics, University Medical Center Freiburg, Freiburg, Germany, ²MaRVIS Medical GmbH, Hannover, Germany, ³German Cancer Consortium (DKTK), Heidelberg, Germany, ⁴German Cancer Research Center (DKFZ), Heidelberg, Germany

A simulation framework is presented to optimize radial acquisition schemes with variable echo times which are designed to minimize the directional anisotropy of the artifact of an MR-safe guidewire. The simulation results are compared to measurements. We could theoretically and experimentally verify that the homogeneity of the artifact can be improved via the variable-TE method.

3583 Computer #12 First steps towards concurrent, high rate imaging and MR tracking using an inertial measurement unit (IMU)
Robert Darrow¹, Mauricio Castillo-Effen¹, Eric Fiveland¹, Elizabeth Morris², and Ileana Hancu¹

¹GE Global Research Center, Niskayuna, NY, United States, ²Memorial Sloan Kettering Cancer Center, New York City, NY, United States

Tissue motion during MR guided interventional procedures leads to the desire to perform simultaneous high speed tracking of the surgical instrument and imaging. In this work, a novel approach for concurrent tracking and imaging, based on an inertial measurement unit (IMU) and technology from plane/missile tracking, is presented. While using infrequent position updates for the IMU (that could be provided by MR tracking), we have showed fast tracking (166Hz) of the IMU sensor with ~2mm rms error.

3584 Computer #13 Interventional device visualisation using the coupling mode of a PTx transmit array
Francesco Padormo¹, Arian Beqiri¹, Joseph V Hajnal¹, and Shaihan Malik¹

¹Division of Imaging Sciences and Biomedical Engineering, King's College London, London, United Kingdom

We propose a novel method to visualise guidewires in interventional MRI procedures using the coupling mode of a PTx array.

3585 Computer #14 Automatic high temporal and spatial resolution position verification of an HDR brachytherapy source using subpixel localization and SENSE
Ellis Beld¹, Marinus A. Moerland¹, Frank Zijlstra², Jan J.W. Lagendijk¹, Max A. Viergever², and Peter R. Seevinck²

¹Department of Radiotherapy, UMC Utrecht, Utrecht, Netherlands, ²Image Sciences Institute, UMC Utrecht, Utrecht, Netherlands

In order to verify the positions of a high-dose-rate (HDR) brachytherapy source during treatment, fast imaging and post-processing are needed. To get high temporal resolutions, the use of lower spatial resolutions in combination with subpixel source localization and the use of parallel imaging were introduced. MR artifacts were simulated and correlated to the experimentally obtained artifacts (by phase-only cross correlation) to determine the position of the HDR source. It was shown that the described method was fast enough for localization of an HDR brachytherapy source in real-time and high accuracy and precision (submillimeter scale) were achieved.

3586 Computer #15 Hindered diffusion of Gadolinium-based Contrast Agents in rat brain extracellular micro-environment after ultrasound-induced delivery
Allegra Conti^{1,2}, Rémi Magnin^{1,3}, Matthieu Gerstenmayer¹, François Lux⁴, Olivier Tillement⁴, Sébastien Mériaux¹, Stefania Della Penna², Gian Luca Romani², Erik Dumont³, Denis Le Bihan¹, and Benoît Larrat¹

¹CEA/DSV/I2BM/NeuroSpin, Gif Sur Yvette, France, ²Department of Neuroscience, Imaging and Clinical Sciences, G. D'Annunzio, University of Chieti and Pescara, Chieti, Italy, ³Image Guided Therapy, Pessac, France, ⁴Université Lyon 1, Lyon, France

We present here a new method to study the diffusion process of Gadolinium-based Contrast Agents within the brain extracellular space after the artificial Blood-Brain Barrier opening induced by ultrasound. Four compounds were tested (MultiHance, Gadovist, Dotarem and AGuIX). By estimating the Free Diffusion Coefficients from *in vitro* studies, and the Apparent Diffusion Coefficients from *in vivo* experiments, an evaluation of the tortuosity (λ) in the right striatum of 11 Sprague-Dawley rats has been performed. The values of λ are in agreement with literature and demonstrate that the chosen permeabilization protocol maintains the integrity of brain tissue.

3587 Computer #16 3D Histogram Analysis of Apparent Diffusion Coefficient Maps Predicts Relief of Fibroid Symptoms after MR Imaging-guided High-Intensity Focused Ultrasound Ablation
HAO FU^{1,2}, Chenxia Li¹, Rong Wang¹, Jianxin Guo¹, Bilgin Keserci³, and Jian Yang¹

¹Department of Radiology, the First Affiliated Hospital of Xi'an Jiaotong University, xi'an, China, People's Republic of, ²MR Marketing, Philips Healthcare, xi'an, China, People's Republic of, ³MR Therapy Clinical Science, Philips Healthcare, Seoul, Korea, Republic of

The aim of the study was to investigate the variation among screening fibroids through analysis of ADC histogram, in order to predict fibroids residual NPV proportion (residual NPV%=NPV at 6 months follow up/ NPV immediately after treatment) and patients Symptom Severity Score (SSS). Thirty five patients who accepted MRgHIFU ablation were divided into group 1 (residual NPV%≥20%) of 19 patients and group 2 (residual NPV%<20%) of 16 patients, respectively. The SSS of patients were obtained at two time-point, screening and 6 months follow up. ADCmean, ADCq, kurtosis and skewness are derived from ADC histogram. The results showed that values of ADCmean, ADCq and kurtosis were significant difference between two groups. The average SSS reduction of group 1 between pre and post treatment was more obvious than that of group 2. Therefore, histogram analysis of ADC maps can provide the quantitative information to predict fibroids ablation outcome and patients symptom relief, which may be indicated as a useful screening tool to guide patients selection for MRgHIFU ablation.

3588 Computer #17 Real-time MRI-guided interventions using rolling-diaphragm hydrostatic actuators
Samantha Mikael^{1,2}, James Simonelli³, David Lu¹, Kyung Sung^{1,2}, Tsu-Chin Tsao³, and Holden H Wu^{1,2}

¹Radiological Sciences, University of California, Los Angeles, Los Angeles, CA, United States, ²Biomedical Physics, University of California, Los Angeles, Los Angeles, CA, United States, ³Mechanical and Aerospace Engineering, University of California, Los Angeles, Los Angeles, CA, United States

In this work we investigate a new rolling-diaphragm-based hydrostatic actuator design to achieve smooth remote manipulation without fluid leakage for MR-compatible robotic systems. We show that the actuators exhibit negligible impact on MR image fidelity and SNR, the actuator provides a linear displacement response over the fluid lines, and we were able to use the master/slave actuator pair to insert and retract the needle in a phantom with no leakage and no noticeable friction issues. Our new rolling-diaphragm hydrostatic actuators can potentially enable physicians to remotely perform real-time MRI-guided interventions.

3589 Computer #18 A Simple Scanner Control Technique for Device Localization during MRI-Guided Percutaneous Procedures
Matthew Alexander MacDonald^{1,2}, Adam C. Waspe^{3,4}, Joao Amaral^{3,4}, and Samuel Pichardo^{1,2}

¹Electrical Engineering, Lakehead University, Thunder Bay, ON, Canada, ²Thunder Bay Regional Research Institute, Thunder Bay, ON, Canada, ³Medical Imaging, University of Toronto, Toronto, ON, Canada, ⁴Hospital for Sick Children, Toronto, ON, Canada

An experiment demonstrates a simple technique for a clinician operator to interactively align scan planes to an interventional device within the scan room during an MRI guided procedure. Input is collected using foot pedal switches to select axial/device intersection points to specify a virtual line of best fit about which auxiliary views are aligned automatically. Volunteer operators position a biopsy needle within an ex vivo porcine specimen while interactively tracking the needle position and measurements are taken to assess the technique's efficiency.

3590 Computer #19 Experimental study of MR Compatible RF Hyperthermia System
Han-Joong Kim¹, Jong-Min Kim¹, Young-Seung Jo^{1,2}, Suchit Kumar¹, Seong-Dae Hong¹, Chulhyun Lee², and Chang-Hyun Lee¹

¹Electronics and Information Engineering, Korea University, Seoul, Korea, Republic of, ²The MRI Team, Korea Basic Science Institute, Cheongju, Korea, Republic of

Many reports suggest that hyperthermia is very effective treatment for tumor therapy. In this work, MR compatible RF hyperthermia system is presented for a 3.0 T MRI. Phantom and animal experiments have been conducted and the results compared with the simulations results for tumor and tissue model. They are in very good coincidence with each other, which confirms the utility and feasibility of the MR compatible RF hyperthermia system with capacitive driving.

3591 Computer #20 Tracking of a Robotic Device by Controlling the Visibility of Markers from the Robot Control
Junmo An¹, Eftychios G. Christoforou², Karen Chin³, Jeremy Hinojosa³, Dipan J. Shah³, Andrew G. Webb⁴, and Nikolaos V. Tsekos¹

¹University of Houston, Houston, TX, United States, ²University of Cyprus, Nicosia, Cyprus, ³Houston Methodist, Houston, TX, United States, ⁴Leiden University Medical Center, Leiden, Netherlands

Integrated control system of the manipulator and marker control is important for localization and tracking of multiple optically detunable MR markers on MR-compatible manipulators. Selecting which markers are visible on MR images by the motion of the maneuvering portion of the MR-compatible manipulators allows unambiguous identification of a combination of markers and simplifies both the data acquisition and the post processing. This proposed technique can be employed to track multiple marker positions on interventional devices such as the steerable catheters and the end-effectors of the MR-compatible manipulator.

3592 Computer #21 Visualization of interventional devices by transient, local magnetic field alterations using bSSFP sequences
Frank C Eibofner¹, Hansjörg Graf¹, and Petros Martirosian¹

¹University Hospital Tübingen, Tübingen, Germany

A technique for the visualization of interventional devices by use of transient, local magnetic field alterations and bSSFP sequences is

presented. It allows the generation of distinct artifacts with controllable dimension. The instrument is visualized in the phase image obtained in the same scan as the undisturbed anatomical image. Localization is done by subsequent superposition.

3593
Computer #22 On Demand Reprogramming of MR Sequence Parameters Using MatMRI
Samuel Pichardo^{1,2}, Charles Mougnot³, Steven Engler^{1,4}, Adam C. Waspe^{5,6}, and James Drake^{5,6}

¹Thunder Bay Regional Research Institute, Thunder Bay, ON, Canada, ²Electrical Engineering, Lakehead University, Thunder Bay, ON, Canada, ³Philips Healthcare, Toronto, ON, Canada, ⁴Computer Science, Lakehead University, Thunder Bay, ON, Canada, ⁵University of Toronto, Toronto, ON, Canada, ⁶The Hospital For Sick Children, Toronto, ON, Canada

For dynamic studies, it is often desirable to adjust parameters in “real time” depending on decisions made by user-defined algorithms. We performed a modification to the software tool MatMRI to develop a method that allows changing on demand multiple MR sequence parameters. We present results of this new method when applied to the modification of sequence parameters for MR-Acoustic Radiation Force Imaging. Our results demonstrate that it is feasible to reprogram MR sequence parameters dynamically using existing technology for the control of scanners.

3594
Computer #23 Efficient respiratory navigator-based 4D MRI
Sascha Krueger¹ and Tim Nielsen¹

¹Philips GmbH, Innovative Technologies, Research Laboratories, Hamburg, Germany

4D image data are used in radiation therapy planning to estimate motion of the tumor or regions at risk. Today 4D CT is commonly used for this purpose. Due to better soft tissue contrast and quantitative and functional imaging, a clinical demand for MRI in therapy planning exists. Consequently, there is also a growing interest in 4D MRI techniques. A scan-time-efficient 4D MRI method utilizing the MRI Navigator as motion sensor with high geometric fidelity is proposed.

3595
Computer #24 MR imaging patterns of Cholangiocarcinoma and post-intervention features: A case-based approach
Juan C Camacho¹, Courtney Moreno¹, Peter Harri¹, and Pardeep Mittal¹

¹Department of Radiology and Imaging Sciences, Emory University School of Medicine, Atlanta, GA, United States

Cholangiocarcinoma may demonstrate typical imaging manifestations and common patterns of organ involvement, guiding diagnosis, and facilitating imaging follow up after therapy. Adequate knowledge of tumoral biology in cholangiocarcinoma and current image-guided therapeutic approaches, along with imaging appearance of cholangiocarcinoma before and after image-guided interventions is crucial for adequate diagnosis and surveillance. MR imaging plays a key role for patient management, assessing therapy response and patient surveillance.

Electronic Poster

Interventional 2

Exhibition Hall

Tuesday, May 10, 2016: 17:00 - 18:00

3596
Computer #25 Real-Time Monitoring of Focused Ultrasound Induced Inertial Cavitation on Microbubbles by Using Gradient Echo MRI: in Vitro and in Vivo Experiments
Chen-Hua Wu¹, Shih-Tsung Kang¹, Chih-Kuang Yeh¹, Wen-Shiang Chen², and Hsu-Hsia Peng¹

¹Biomedical Engineering and Environmental Sciences, National Tsing Hua University, Hsinchu City, Taiwan, ²Physical Medicine and Rehabilitation, National Taiwan University Hospital, Taipei, Taiwan

This study aims to real-time monitor inertial cavitation on microbubbles (MBs) while transmitting focused ultrasound (FUS) with various duty cycle and pulse repetitive frequency (PRF) by gradient echo MRI. For in vitro experiments, with increasing duty cycle, more significant signal intensity (SI) changes or prolonged SI drop duration were shown. For in vivo experiment, two SI drop peaks were observed, reflecting the two IC events. In conclusion, FLASH has been proved to be a useful technique for real-time monitoring of IC when transmitting FUS pulses to MBs for in vitro and in vivo experiments.

3597
Computer #26 Multi-Contrast Late Enhancement Out-Performs Conventional Late Gadolinium Enhancement for Myocardial RFA Lesion Characterization
Philippa Krahn^{1,2}, Haydar Celik³, Venkat Ramanan², Jennifer Barry², and Graham A Wright^{1,2}

¹Medical Biophysics, University of Toronto, Toronto, ON, Canada, ²Physical Sciences, Sunnybrook Research Institute, Toronto, ON, Canada, ³Sheikh Zayed Institute for Pediatric Surgical Innovation, Washington, DC, United States

In this work we evaluated the quality and accuracy of myocardial RFA lesion visualization using the MCLE sequence. To compare MCLE to the standard LGE, we imaged 29 acute lesions in 11 pigs. Lesion sizes measured from each set of images were highly correlated, yet MCLE consistently achieved higher CNR than LGE. Our relaxometry maps from MCLE suggested a dramatic variation in T₁ after contrast injection, which will alter the optimal TI for LGE. Therefore, we demonstrated that MCLE, with the varied TIs in each acquisition, is a more

robust sequence for visualizing even the most subtle lesions.

-
- 3598
Computer #27 Improved Thermometry Based on a Fast Spin Echo Sequence
Yuval Zur¹
- ¹GE Healthcare, Haifa, Israel
- A time shifted Fast Spin Echo (FSE) thermometry sequence which is insensitive to B0 inhomogeneity is used in conjunction with restricted FOV module and parallel imaging to reduce scan time and increase the number of slices. Up to 5 slices are acquired in 3 sec. This sequence works well on a clinical Focused Ultrasound brain system. The temperature signal to noise ratio (TSNR) of this FSE sequence is approximately 2 times higher than the conventional Gradient Echo (GRE) sequence used today. 3 to 5 slices are acquired in 3 sec, rather than 1 slice with GRE.
-
- 3599
Computer #28 Prostate Focal Prostate Laser Ablation under MRI Guidance
Alexander Squires¹, Sheng Xu², Reza Seifabadi², Yue Chen¹, Harsh Agarwal³, Marcelino Bernardo², Ayele Negussie², Peter Pinto², Peter Chokye², Bradford Wood², and Zion Tsz Ho Tse¹
- ¹College of Engineering, University of Georgia, Athens, GA, United States, ²National Institutes of Health, Bethesda, MD, United States, ³Philips Research North America, Briarcliff Manor, NY, United States
- MRI-guided focal laser ablation (FLA) shows promise as an effective treatment for prostate cancer, but presents challenges related to accurate catheter positioning and ablation monitoring. A catheter positioning robot was designed to overcome these problems by positioning the catheter optimally for ablation and monitoring the ablation via MRI thermometry. A remote insertion guide allows the surgeon to perform the procedure without removing the patient from the MRI bore, saving time and increasing accuracy. Treatment planning software iteratively plans optimal catheter positioning. Preliminary tests show the robot can greatly improve efficiency and accuracy without sacrificing image quality.
-
- 3600
Computer #29 PRF Thermometry for Monitoring Small Temperature Changes during Very Long Thermal Therapies: Field Drift Compensation Using FID Navigators
Tetiana Dadakova¹, Axel Joachim Krafft^{1,2,3}, Jan Gerrit Korvink⁴, Stephan Meckel⁵, and Michael Bock¹
- ¹Dept. of Radiology - Medical Physics, University Medical Center Freiburg, Freiburg, Germany, ²German Cancer Consortium (DKTK), Heidelberg, Germany, ³German Cancer Research Center (DKFZ), Heidelberg, Germany, ⁴Institute of Microstructure Technology, Karlsruhe Institute of Technology, Karlsruhe, Germany, ⁵Department of Neuroradiology, Neurocenter, University Medical Center Freiburg, Freiburg, Germany
- Proton resonance frequency shift thermometry uses phase MR images to calculate temperature change in tissue during thermal therapies. Temporal and spatial changes of local magnetic field influence the phase images and can mimic temperature change. In order to correct for temperature errors due to magnetic field drift with time the FID navigators were used before and after imaging readout. Field-drift related phase slope during each repetition was calculated and used to correct the imaging data. This correction method is especially useful for the long thermometry procedures during which the temperature change is small and high temperature precision is needed.
-
- 3601
Computer #30 MR-guided focal laser ablation as primary treatment for prostate cancer: Preliminary results
Joyce GR Bomers¹, Christiaan G Overduin¹, Sjoerd FM Jenniskens¹, Michiel Sedelaar², and Jurgen J Futterer¹
- ¹Radiology, Radboud University Medical Center, Nijmegen, Netherlands, ²Urology, Radboud University Medical Center, Nijmegen, Netherlands
- Focal therapy offers great hopes in terms of cancer control and decreased morbidity (i.e. impotence and incontinence) for patients with localized low- and intermediate grade prostate cancer (PCa). Transrectal MR-guided focal laser ablation of newly diagnosed PCa was successfully performed in 5 patients. It was technically feasible and safe. PSA level decreased in all patients and follow-up MRI showed no residual or recurrent cancer; indicating local cancer control, without compromising with increased morbidity or a decrease in quality of life. Initial results are promising and more patients have to be included with longer follow-up.
-
- 3602
Computer #31 MR Thermometry-guided Prostate Hyperthermia with Real-time Ultrasound Beamforming and Power Control
Eugene Ozhinsky¹, Vasant A. Salgaonkar², Chris J. Diederich², and Viola Rieke¹
- ¹Radiology and Biomedical Imaging, University of California San Francisco, San Francisco, CA, United States, ²Radiation Oncology, University of California San Francisco, San Francisco, CA, United States
- We have developed and evaluated a real-time MR thermometry-guided system for acoustic power output and beam pattern control for prostate hyperthermia therapy. It was designed to be integrated with a commercial focused ultrasound ablation system and supports real-time ultrasound phase pattern switching and MR thermometry for monitoring and automated power adjustment.
-
- 3603
Computer #32 Zero TE based MR thermometry
Silke Lechner-Greite¹, Matthew Tarasek², Desmond Teck Beng Yeo², and Florian Wiesinger¹
- ¹GE Global Research, Munich, Germany, ²GE Global Research, Albany, NY, United States

Monitoring temperature changes in the human skull is important in clinical transcranial MR-guided focused ultrasound, as it can absorb a large amount of energy during sonication and thereby produce heat. We propose to extract relative temperature information from proton density weighted zero TE imaging and additionally calibrate the T₁ signal contamination effect.

3604
Computer #33 Evaluation of common proton resonance frequency shift based MR Thermometry methods in the pancreas
Cyril J Ferrer¹, Clemens Bos¹, Marijn van Stralen¹, Baudoin Denis de Senneville², Chrit T.W Moonen¹, and Lambertus W Bartels¹

¹University Medical Center Utrecht, Utrecht, Netherlands, ²Mathematical Institute of Bordeaux, Talence, France

MR-guided High Intensity Focused Ultrasound has recently been suggested to provide non-invasive alternative treatment options for pancreatic cancer patients. To successfully apply PRFS MR Thermometry in the pancreas motion correction techniques have to be applied. For other moving organs, several solutions have already been proposed to this end: gating, multibaseline and referenceless. However, due to specific properties of the pancreas, there was still a need to evaluate the performance of these methods in this organ. Our results show that all the evaluated techniques improved thermometry in the pancreas to a level that is sufficient to monitor thermal ablation.

3605
Computer #34 MR Guided Microwave Thermal Ablation: Guidance and Monitoring for Extending the Physics of Thermal Therapy
Michael Simonson¹, Peng Wang², Christopher Brace^{1,2,3}, and Walter Block^{1,2,3}

¹Biomedical Engineering, UW - Madison, Madison, WI, United States, ²Radiology, UW - Madison, Madison, WI, United States, ³Medical Physics, UW - Madison, Madison, WI, United States

Monitoring microwave ablation with thermometry could extend the application of this clinical procedure into territories where greater control is necessary to protect healthy tissue, such as the spine. MRI thermometry could also provide useful insights to generate and validate new thermal models based on the fundamentally different mode of dielectric heating utilized by microwave ablation. We present here a platform consisting of 1) a high power MR compatible microwave ablation system based on a FDA-approved design, 2) real-time applicator guidance during applicator insertion and 3) high frame rate MR thermometry and tissue monitoring.

3606
Computer #35 T2-based Temperature Monitoring in Bone Marrow for MR-guided Focused Ultrasound
Eugene Ozhinsky¹, Matthew D. Bucknor¹, and Viola Rieke¹

¹Radiology and Biomedical Imaging, University of California San Francisco, San Francisco, CA, United States

Current clinical protocols for bone treatments rely on measurement of the temperature change of adjacent muscle to estimate the temperature of the bone. In this study we have demonstrated for the first time that T2-based thermometry can be used in vivo to measure the heating in the marrow during bone ablation. The ability to monitor the temperature within the bone marrow allowed visualization of the heat penetration into the bone, which is important for local lesion control and treatment of osteoid osteomas.

3607
Computer #36 Monitoring of Stable Cavitation of Microbubbles by Using MRI
Cheng-Tao Ho¹, Chen-Hua Wu¹, Shih-Tsung Kang¹, Chih-Kuang Yeh¹, Wen-Shiang Chen², Hau-Li Liu³, and Hsu-Hsia Peng¹

¹Biomedical Engineering and Environmental Science, National Tsing Hua University, Hsinchu, Taiwan, ²Physical Medicine and Rehabilitation, National Taiwan University Hospital, Taipei, Taiwan, ³Electrical Engineering, Chang-Gung University, Taoyuan, Taiwan

Gas-filled microbubbles (MBs) can be locally cavitated by spatially focused ultrasound (FUS) to trigger stable cavitation (SC) and inertial cavitation (IC) to induce blood-brain barrier (BBB) opening; therefore, magnetic resonance imaging (MRI) may provide useful imaging information to real-time monitor the process of FUS cavitation on MBs. In this study, a HASTE (Half Fourier Acquisition Single Shot Turbo Spin Echo) sequence was used to observe the signal changes during SC for in vitro experiments. Experiments with different acoustic pressure, pulse repetitive frequency, and duty cycle were performed to clarify the SC effect on MR images.

3608
Computer #37 The effect of sonication duration on ablation depth during MR-guided focused ultrasound of bone: acute findings with MR in a swine model
Matthew Bucknor¹, Rutwik Shah¹, Eugene Ozhinsky¹, and Viola Rieke¹

¹Radiology and Biomedical Imaging, University of California, San Francisco, San Francisco, CA, United States

One challenge in magnetic resonance guided focused ultrasound ablation of bone lesions is extending the ablation zone deep to the cortical surface in order to cover the full intramedullary extent of the lesion. Extension of the ablation zone is important for complete treatment of for example, osteoid osteomas, and improved local control of metastatic bone disease. This study used a swine model to compare differences in the depth of the ablation zone between two protocols using short versus longer sonications, respectively, while maintaining the same overall sonication energy (by adjusting acoustic power).

3609
Computer #38 Assessments of Flow Velocity Changes by Phase-Contrast MRI Near Acoustic Radiation Force Aggregated Bubbles
Zhe-Wei Wu¹, Wu Chen-Hua², Hsu Po-Hong³, Hao-Li Liu³, Yeh Chic-Kuang², and Peng Hsu-Hsia²

¹Biomedical Engineering and Environmental Sciences, Nation Tsing Hua University, Hsinchu, Taiwan, ²Biomedical Engineering and

The aim of this study was to real-time assess flow velocity changes in the neighboring pixels of acoustic radiation force (ARF) aggregated bubbles by using phase-contrast MRI (PC-MRI). The flow velocity increased with the increase of microbubbles (MBs) concentrations, which might be attributed to the increase of aggregated bubbles size, narrowing the chamber diameter and thus presenting higher flow velocity. In conclusion, we verified the feasibility of using PC-MRI to assess flow velocity changes on pixels near ARF aggregated bubbles. In the future, a systematic investigation shall be conducted to comprehend the association between bubble size and the flow velocity.

3610 Computer #39 Prior Image based Temporally Constrained Reconstruction for Magnetic Resonance guided HIFU
Jaya Prakash¹, Nick Todd², and Phaneendra K Yalavarthy³

¹Institute for Biological and Medical Imaging, Helmholtz Zentrum Munich, Munich, Germany, ²Wellcome Trust Centre for Neuroimaging, UCL Institute of Neurology, University College London, London, United Kingdom, ³Supercomputer Education and Research Centre, Indian Institute of Science, Bangalore, India

Prior image based temporally constrained reconstruction (PITCR) algorithm was found to obtain accurate temperature maps with better volume coverage, and spatial, and temporal resolution than other algorithms using highly undersampled data in magnetic resonance (MR) thermometry. PITCR method is compared with the standard temporally constrained reconstruction (TCR) algorithm using ex-vivo pork muscle sample. It was seen that the PITCR method showed superior performance compared to the TCR approach with highly undersampled datasets.

3611 Computer #40 Phase artifact correction for improved ARFI displacement mapping using a short FID navigator
Tetiana Dadakova¹, Ali Caglar Özen¹, Axel Joachim Krafft^{1,2,3}, Jan Gerrit Korvink⁴, and Michael Bock¹

¹Dept. of Radiology - Medical Physics, University Medical Center Freiburg, Freiburg, Germany, ²German Cancer Consortium (DKTK), Heidelberg, Germany, ³German Cancer Research Center (DKFZ), Heidelberg, Germany, ⁴Institute of Microstructure Technology, Karlsruhe Institute of Technology, Karlsruhe, Germany

MR-guided acoustic radiation force imaging (ARFI) is used for the focal spot localization during high intensity focused ultrasound (HIFU) therapies. The acoustic radiation force related tissue displacement is measured with help of motion encoding gradients (MEG). While MEGs are sensitive enough to detect micrometer-scale displacement, the images acquired using MR-ARFI pulse sequences are often corrupted with artifacts. The method described uses very short FID navigator readout for correction of ARFI images without any manual interaction. ARFI displacement maps corrected by FID navigator have substantially less artifacts, 2.5 times higher SNR, and clearly visible HIFU focal spot.

3612 Computer #41 TREATMENT OF SMALL VASCULAR MALFORMATIONS USING MR GUIDED HIGH INTENSITY FOCUSED ULTRASOUND: PRELIMINARY RESULTS AFTER FOUR PATIENTS
Pejman Ghanouni¹, Sirish Kishore¹, Matthew Lungren¹, David Mohler², Raffi Avedian², and David Hovsepian¹

¹Radiology, Stanford University, Stanford, CA, United States, ²Orthopaedic Surgery, Stanford University, Stanford, CA, United States

Low flow vascular malformations are typically treated with ultrasound-guided percutaneous sclerotherapy, but not all of these lesions are visible sonographically. MR guided focused ultrasound (MRgFUS) combines the ability of MRI to delineate these tumors with the use of FUS to ablate the tumor non-invasively. We report our technical and clinical results after using MRgFUS to treat four patients with small intramuscular low flow vascular malformations in the lower extremities.

3613 Computer #42 First clinical evaluation of real-time cardiac MR thermometry
Valéry Ozenne¹, Solenn Toupin^{1,2}, Pierre Bour¹, Baudouin Denis de Senneville³, Alexis Vaussy², Matthieu Matthieu Lepetit-Coiffé², Pierre Jais^{1,4}, Hubert Cochet^{1,4}, and Bruno Quesson¹

¹Institut Hospitalier Universitaire : LIRYC Institut de Rythmologie et Modélisation Cardiaque, Bordeaux, France, ²Siemens France, Saint Denis, France, ³Mathematical Institute of Bordeaux, Bordeaux, France, ⁴Centre Hospitalier Universitaire de Bordeaux, Bordeaux, France

Catheter ablation using radiofrequency is commonly used to treat cardiac arrhythmia. However, direct assessment of lesion formation with MRI thermometry during RF delivery may improve safety and efficiency of the therapeutic procedure. Despite recent studies demonstrating the feasibility on volunteers or animal models, there are no reports regarding the possibility of doing cardiac thermometry on patient in the context of arrhythmias. The purpose of the present study was to evaluate the uncertainty of temperature estimate on patients depicting potential arrhythmic episodes, which may alter the precision of the method relying on an ECG-triggered acquisition.

3614 Computer #43 Using simultaneous multi-slice imaging for PRFS thermometry
Pim Borman¹, Clemens Bos², Sjoerd Crijns¹, Bas Raaymakers¹, and Chrit Moonen²

¹Radiotherapy, UMC Utrecht, Utrecht, Netherlands, ²Imaging Division, UMC Utrecht, Utrecht, Netherlands

PRFS thermometry is important for guidance of thermal therapies. Here we show that the thermometry sequence can be accelerated by the novel parallel imaging technique SMS-CAIPIRINHA and we compare it to an unaccelerated sequence and a SENSE accelerated sequence. Heating was applied by means of HIFU and LITT. A good agreement was seen between temperature curves from SMS-

CAIPIRINHA and those from the unaccelerated sequence. Furthermore, the noise level was significantly lower compared to temperature curves from the SENSE accelerated sequence.

3615
Computer #44 Fully automatic in-vivo localization of LDR brachytherapy seeds for post-implant dosimetry using MR simulations and template matching
Frank Zijlstra¹, Job G Bouwman¹, Marinus A Moerland², and Peter R Seevinck¹

¹Image Sciences Institute, UMC Utrecht, Utrecht, Netherlands, ²Department of Radiotherapy, UMC Utrecht, Utrecht, Netherlands

We present a method which can accurately localize brachytherapy seeds in MRI using fast MR simulations and template matching. In 5 patients we correctly detected and localized 298 out of 307 seeds. Using this method an MRI-only approach to post-implant dosimetry will be possible, which should increase accuracy by not requiring CT to MRI image registration.

3616
Computer #45 Towards Real-Time In Vivo Volumetric MR Thermometry
Samuel Fielden¹, Matthew Geeslin², Xue Feng¹, Wilson Miller², Kim Butts Pauly³, and Craig Meyer^{1,2}

¹Biomedical Engineering, University of Virginia, Charlottesville, VA, United States, ²Radiology & Medical Imaging, University of Virginia, Charlottesville, VA, United States, ³Radiology, Stanford University, Palo Alto, CA, United States

A rapid volumetric MR thermometry sequence, using a stack-of-spirals acquisition, was implemented on a real-time platform in order to support animal model experiments. The performance of the sequence, as measured by the maximum and mean recorded temperature as well as the sequence accuracy, was assessed against a clinically used 2DFT sequence in vivo. The use of efficient spiral trajectories supports rapid generation of volumetric thermometry maps and allows the visualization of the entire insonication as well as correlation with post-ablation imaging of lesion size and location.

3617
Computer #46 Accuracy of PRFS Temperature Mapping using Fast Interleaved Sequences for MR-HIFU Thermal Therapies
Steffen Weiss¹, Jochen Keupp¹, and Edwin Heijman²

¹Tomographic Imaging, Philips Research, Hamburg, Germany, ²Oncology Solutions, Philips Research, Eindhoven, Netherlands

MR-HIFU therapies require stable PRFS-based temperature monitoring over the treatment duration (>30min). Drift effects may be corrected using independent temperature information e.g. based on T2 or T1 maps and simultaneously obtained using fast interleaved sequences. As interleaves may impact PRFS-accuracy, a dynamic on-off-interleaved sequence pattern is introduced to selectively measure their influence on the PRFS phase. The mechanism of the phase variations is explored using multiple variants of the interleaved sequence. It is shown that eddy currents induced during the interleaved sequences represent the main cause of the phase variation. The spatio-temporal characteristics of the effect are explored as a first step towards compensation.

3618
Computer #47 Automatic temperature control during MR guided catheter based radiofrequency ablation of the heart
Valery Ozene¹, Thibaud Troadec¹, Pierre Bour¹, Solenn Toupin^{1,2}, Erik Dumont³, and Bruno Quesson¹

¹Institut Hospitalier Universitaire : LIRYC Institut de Rythmologie et Modélisation Cardiaque, Bordeaux, France, ²Siemens France, Saint Denis, France, ³Image Guided Therapy, Bordeaux, France

Although catheter-based radiofrequency (RF) ablation is increasingly used to treat cardiac arrhythmia, insufficient temperature increase may lead to incomplete treatment whereas excessive local energy deposition may result in severe adverse effects (e.g. esophageal fistulas or tamponade due to steam pop). Since MR thermometry can monitor in real-time the temperature distribution in the cardiac muscle, automatic regulation of RF energy deposition from temperature images, using well established proportional, integral controller algorithms, may improve safety and efficiency of the therapeutic procedure.

3619
Computer #48 TREATMENT OF OSTEIOD OSTEOMA USING MR GUIDED HIGH INTENSITY FOCUSED ULTRASOUND: PRELIMINARY RESULTS AFTER FOUR PATIENTS
Pejman Ghanouni¹, Sirish Kishore¹, David Mohler², Matthew Lungren¹, Raffi Avedian², and Nishita Kothary¹

¹Radiology, Stanford University, Stanford, CA, United States, ²Orthopaedic Surgery, Stanford University, Stanford, CA, United States

Osteoid osteoma is currently most frequently treated with CT guided radiofrequency ablation (CTgRFA), which is effective, but invasive and exposes the typical young patient population with osteoid osteomas to radiation. Our preliminary results are presented describing MR guided focused ultrasound (MRgFUS) for the treatment of patients with osteoid osteomas. As also reported in two European studies, in our experience, MRgFUS is effective at eliminating pain in these patients. These data form the basis for a proposed clinical trial directly comparing the safety and efficacy of MRgFUS and CTgRFA for treatment of osteoid osteoma.

Electronic Poster

MR Engineering Beyond RF Coils

Exhibition Hall

Tuesday, May 10, 2016: 17:00 - 18:00

- 3620 Computer #49 55Mn Fiducial Markers for Automated Coil Localization and Sensitivity Determination for Use With Hyperpolarized ¹³C MRI
Michael Ohliger¹, Cornelius von Morze¹, Lucas Carvajal¹, Irene Marco-Rius¹, Jao Ou¹, and Daniel Vigneron¹
¹Radiology and Biomedical Imaging, University of California San Francisco, San Francisco, CA, United States
- RF coil arrays are critically important for hyperpolarized C-13 imaging because of increased sensitivity, coverage, and speed. A major limitation preventing widespread use of coil arrays is the difficulty measuring coil sensitivity profiles due to low C-13 natural abundance. We propose to solve this problem by using fiducial markers filled with 55Mn to determine coil location and then calculate coil sensitivities. We show proof-of-principle using a single RF coil and ethylene glycol phantom. Coil sensitivities derived from fiducial markers and quasistatic calculations closely match those acquired through experiment.
-
- 3621 Computer #50 "Domino" Feed Board for Receive Coils
Victor Taracila¹, Miguel Navarro¹, and Fraser Robb¹
¹GE Healthcare, Aurora, OH, United States
- The physical size of the on-coil electronics could be one of the major obstacles in building high density RF coils. First, there is a clear mechanical desire to reduce its size in order to make the coils lighter and thinner; second, bulky electronics placed on small loops can disturb the sensitivity profile; third, for MR-PET applications the RF coils, in addition to the requirements mentioned above, have to be transparent to PET radiation. In order to achieve these critical to quality objectives we propose completely embedding all of the lumped components into a common printed circuit board (PCB).
-
- 3622 Computer #51 Modified Class E Amplifiers Used For Two Channel Digital RF Transmit Array System With Integrated Coil
Redi Poni^{1,2}, Berk Silemek², Umut Gündoğdu², Taner Demir², Niyazi Koray Ertan^{1,2}, and Ergin Atalar^{1,2}
¹Electrical and Electronics Engineering, Bilkent University, Ankara, Turkey, ²National Magnetic Resonance Research Center UMRAM, Bilkent University, Ankara, Turkey
- In this work we show a two-channel digitally controlled on coil high efficiency modified Class E amplifier for RF excitation easily tunable for 1.5 and 3 T. The amplifiers coupling in dual channel outside the scanner was investigated to show how the operation integrity of nearby amplifiers is affected. MR experiment in a 3 T scanner was conducted in order to test the two-channel system and showed the feasibility of the system for larger number of channels.
-
- 3623 Computer #52 Gradient Amplifier Design with Advanced Power Semiconductor Devices and Simple Topology
Ruxi Wang¹, Juan Sabate¹, Eladio Delgado¹, Xiaohu Liu¹, and Fengfeng Tao¹
¹GE global research center, Niskayuna, NY, United States
- Gradient Amplifier is one of the key components in a MRI system to supply the gradient coil with large current (>1000A) and high voltage (>2000V) to achieve strong gradient field and fast slew rate. In this paper, a high efficiency two H-bridge in cascaded gradient driver design with 1700V SiC MOSFET is designed and fabricated. The power module switching frequency is 31.25 kHz and amplifier total output ripple frequency is 125 kHz. The amplifier loss and efficiency (around 99.5%) is verified in experimental results.
-
- 3624 Computer #53 A High Power RF Gated Wireless Power Transfer System
Kelly Byron¹, Pascal Stang², Shreyas Vasanawala³, John Pauly¹, and Greig Scott¹
¹Electrical Engineering, Stanford University, Stanford, CA, United States, ²Procyon Engineering, San Jose, CA, United States, ³Radiology, Stanford University, Stanford, CA, United States
- If wireless patient coils could be realized, they would reduce setup time and reduce worry about the liability of the connectors on coils. Battery powering these coils would limit scan time, so it is desirable to use wireless power transfer (WPT), which uses inductively coupled resonant coils to transmit and receive power at a particular frequency. With RF gating, imaging while receiving up to 11W is demonstrated and shown to have minimal impact on image quality.
-
- 3625 Computer #54 gr-MRI: GNU Radio extensions for MRI using software-defined radios
Christopher J Hasselwander^{1,2} and William A Grissom^{1,2}
¹Biomedical Engineering, Vanderbilt University, Nashville, TN, United States, ²Vanderbilt University Institute of Imaging Science, Nashville, TN, United States
- Software defined radios have been shown to be a highly configurable, low cost alternative to traditional MRI spectrometers. They are well supported by the open-source GNU Radio software, however there are currently no GNURadio extensions to enable their use for MRI. In this work we describe a library of GNU Radio extensions for MRI, which implements all of the basic capabilities of an MR spectrometer in an SDR. The software will enable users to develop custom, low-cost MR spectrometer systems without requiring custom hardware design. We demonstrate its use via its built-in spin echo, gradient echo, and inversion recovery sequences.
-
- 3626 Magnetic field stability and homogeneity of high-temperature superconducting magnet with REBCO tapes measured using dedicated

Computer #55 field camera system
Shin-ichi Urayama¹, Taizo Tosaka², Hiroshi Miyazaki², Yasumi Ootani², So Noguchi³, Hiroshi Ueda⁴, Atsushi Ishiyama⁵, Shunji Nomura², Tsutomu Kurusu², and Hidenao Fukuyama¹

¹Kyoto University, Kyoto, Japan, ²Toshiba corporation, Tokyo, Japan, ³Hokkaido University, Sapporo, Japan, ⁴Osaka University, Osaka, Japan, ⁵Waseda University, Tokyo, Japan

Because of the rapid rise of helium price in recent years, we started a project targeting to produce high-temperature superconducting ultra-high-field MRI systems with REBCO (Rare-earth - Barium - Copper Oxide) tapes and as the first step, we developed a middle-size 1T-REBCO magnet and evaluated its magnetic field stability and homogeneity with dedicated field camera system with 16ch NMR probes. Inhomogeneity was up to 800 ppm and stability with linear trend correction was ± 1 ppm, and the causes were investigated.

3627 Computer #56 The Study of Quench Propagation for a MgB₂ 1.5 T MRI Magnet Design at Different Operating Temperatures
Charles R. Poole¹, Tanvir Baig¹, Robert J. Deissler¹, David Doll², Michael Tomsic², and Michael A. Martens¹

¹Department of Physics, Case Western Reserve University, Cleveland, OH, United States, ²Hyper Tech Research Inc., Columbus, OH, United States

To reduce the usage of liquid helium, conduction cooled MRI magnets using high temperature magnesium diboride (MgB₂) have been considered. Because the thermal normal zone propagation velocity (NZPV) of MgB₂ is much slower compared to NbTi wire, active quench protection is needed. The temperature rise in the magnet design was modeled using Douglas-Gunn method to solve the governing heat equation for operating temperatures ranging from 10 to 18 K. It was shown that the temperature rise is slower for higher operating temperatures, and thus better for quench protection.

3628 Computer #57 Very-high order shimming in the human spinal cord using a dedicated 24-channel array coil
Ryan Topfer¹, Grégoire Germain¹, Jason P. Stockmann², Karl Metzemaekers³, Hoby Hetherington⁴, Raphaël Paquin⁵, Piotr Starewicz³, Nikola Stikov^{1,6}, and Julien Cohen-Adad^{1,7}

¹NeuroPoly Lab, Institute of Biomedical Engineering, École Polytechnique de Montréal, Montreal, QC, Canada, ²Athinoula A. Martinos Center for Biomedical Imaging, Department of Radiology, Massachusetts General Hospital, Charlestown, MA, United States, ³Resonance Research Inc., Billerica, MA, United States, ⁴Department of Radiology, University of Pittsburgh, Pittsburgh, PA, United States, ⁵Siemens Healthcare Ltd., Montreal, QC, Canada, ⁶Montreal Heart Institute, Université de Montréal, Montreal, QC, Canada, ⁷Functional Neuroimaging Unit, CRIUGM, Université de Montréal, Montreal, QC, Canada

Pathologies of the spinal cord are a primary cause of functional disability and chronic pain. Although MRI already plays a role in the evaluation of these pathologies, it continues to be hampered by artifacts due to magnetic field inhomogeneity. This study reports the first results applying a specially designed 24-channel shim array to correct magnetic field inhomogeneity in the human spinal cord. Shimming using the custom array improved field homogeneity in the thoracic spinal cord of the two initial subjects by 53.6 % and 31.4 % respectively.

3629 Computer #58 Dedicated High-Performance, Lightweight, Low-Cryogen Compact 3.0T MRI System for Advanced Brain Imaging
Thomas Foo¹, Mark Vermilyea¹, Minfeng Xu¹, Paul Thompson¹, Ye Bai¹, Gene Conte¹, Christopher Van Epps¹, James Rochford¹, Christopher Immer¹, Seung-Kyun Lee¹, Ek Tsoon Tan¹, Dominic Graziani¹, Christopher Hardy¹, John Schenck¹, Eric Fiveland¹, Yunhong Shu², John Huston III², Matt Bernstein², Wolfgang Stautner¹, Justin Ricci¹, and Evangelos Laskaris¹

¹GE Global Research, Niskayuna, NY, NY, United States, ²Mayo Clinic, Rochester, MN, United States

A high-performance, lightweight, low-cryogen compact 3.0T MRI system for imaging the brain has been developed. This system has a gradient performance of 80 mT/m and 700 T/m/s, and has a magnet weight of less than 2,000 kg and has a 5 Gauss fringe field area of 24 m². This novel system has produced images that are equivalent if not better than that encountered in whole-body 3.0T scanners. This was demonstrated in imaging tests in healthy volunteers. Clinical evaluation is scheduled for a patient population.

3630 Computer #59 A design of a mobile, homogeneous and efficient electromagnet with a large field-of-view for neonatal low field MRI
Steffen Lothar¹, Steven Schiff², Thomas Neuberger³, Peter M. Jakob^{1,4}, and Florian Fidler¹

¹Research Center Magnetic-Resonance-Bavaria (MRB), Wuerzburg, Germany, ²Center of Neural Engineering, Departments of Engineering Science and Mechanics, Neurosurgery, and Physics, Penn State University, University Park, PA, United States, ³High Field MRI Facility, Huck Institutes of the Life Sciences, Penn State University, University Park, PA, United States, ⁴Department for Experimental Physics 5 (Biophysics), University of Wuerzburg, Wuerzburg, Germany

A mobile and effective electromagnet prototype with a large field-of-view for neonatal magnetic resonance imaging at 23 mT is presented. The efficient implementation succeeded by exploiting the use of steel plates as a housing system. This results in a design that ensures an optimum between large sample volumes, high homogeneity, high B₀ field, low power consumption, light weight, without the necessity of a dedicated water cooling system. Simulations and measurements are shown, which illustrate the functionality and quality of this imaging system. There are multiple paths to clinical and medical applications for such low cost devices.

3631 RF coil configurations for a RF-penetrable PET insert for simultaneous PET/MR

Computer #60 Brian J Lee^{1,2}, Ronald D Watkins², Alexander M Grant^{2,3}, Chen-Ming Chang^{2,4}, and Craig S Levin^{2,3,5,6}

¹Mechanical Engineering, Stanford University, Stanford, CA, United States, ²Radiology, Stanford University, Stanford, CA, United States, ³Bioengineering, Stanford University, Stanford, CA, United States, ⁴Applied Physics, Stanford University, Stanford, CA, United States, ⁵Physics, Stanford University, Stanford, CA, United States, ⁶Electrical Engineering, Stanford University, Stanford, CA, United States

Simultaneous acquisition of MRI and PET shows great promise for disease characterization as it enables concurrent collection of complementary molecular and anatomical information. To overcome the limited dissemination of integrated PET/MRI systems due to the high cost, we have developed an RF-penetrable PET insert integrated with custom RF coils that can be inserted into any existing MRI system for simultaneous PET/MRI acquisition. The RF-penetrable PET/RF-receiver insert enables the use of the built-in body coil for more uniform transmit RF field, fast acquisition using parallel imaging, and high SNR MR and PET images.

3632

Computer #61 A low cost home-built gradient amplifier for matrix gradient coils
Huijun Yu¹, Frank Huehe², Sebastian Littin¹, Kelvin J. Layton¹, Feng Jia¹, Stefan Kroboth¹, and Maxim Zaitsev¹

¹Dept. of Radiology, Medical Physics, University Medical Center Freiburg, Freiburg, Germany, ²Dept. of Clinical Neurology and Neurophysiology, University of Freiburg, Freiburg, Germany

To address the increased cost of high numbers of amplifiers for matrix gradient coils, a low cost home-built 100A/100V gradient amplifier is proposed. The water cooling amplifier consists of several parts: a controller that interfaces to a waveform generator and provides the current control signal; an H-bridge circuit that generates constant current to the load; and a ripple cancellation filter that reduces the inevitable ripple current. The switching frequency and peak ripple current of amplifier is 100 kHz and 300 mA, respectively. The amplifier can be operated with maximum continuous current (100A) for at least 1 min.

3633

Computer #62 Low-Field Permanent Magnet MR Systems in the Developing World: A Review of Clinical and Research Applications
Christina Louise Sammet^{1,2}, Godwin Ogbole³, and Steffen Sammet⁴

¹Radiology, Northwestern University, Chicago, IL, United States, ²Medical Imaging, Ann & Robert H. Lurie Children's Hospital of Chicago, Chicago, IL, United States, ³Department of Radiology, University of Ibadan, Ibadan, Nigeria, ⁴Department of Radiology, University of Chicago, Chicago, IL, United States

Low-field permanent magnet MR systems will be increasingly utilized in resource-limited settings due to their independence from helium and power supply infrastructure. Optimization of available systems for clinical imaging will greatly improve diagnostics and lead to unique opportunities to study health concerns in developing countries. This exhibit summarizes the state-of-the art in permanent magnet MRI to encourage interest in the improvement of existing systems and their utilization for collaborative imaging research in the developing world.

3634

Computer #63 A simple digital MRI system using a digital oscilloscope
Makoto Tsuda¹ and Katsumi Kose¹

¹University of Tsukuba, Tsukuba, Japan

A digital MRI system was developed using a digital oscilloscope that had a waveform generator function. An RF pulse with 43.85 MHz Larmor frequency was successfully output using this oscilloscope and the NMR signal was captured using the undersampling technique (144 ns dwell time, 6.94 MHz sampling frequency). The acquired a set of 3D MR image using a 1.0 T permanent magnet MRI system demonstrated the validity of our approach.

3635

Computer #64 An Active Quench Protection System for a 1.5 T MgB₂ Conduction-Cooled Magnet
Robert J. Deissler¹, Tanvir Baig¹, Charles R. Poole¹, David Doll², Michael Tomsic², and Michael A. Martens¹

¹Department of Physics, Case Western Reserve University, Cleveland, OH, United States, ²Hyper Tech Research Inc., Columbus, OH, United States

A numerical simulation of the heat equation was performed for a 10 coil persistent mode 1.5 T MgB₂ conduction-cooled magnet. A hot spot was initialized by allowing a section of wire to become resistive on one coil. An active protection system consisting of surface heaters on all the coils was initiated at 100 mV. Using a standard wire, the temperature was found to reach nearly 300 K, which may damage the coil. By increasing the amount of copper, using Glidcop instead of Monel, or increasing the thermal conductivity of the insulation, the temperature is kept within safe limits.

3636

Computer #65 DETECTION OF MR SIGNAL DURING RF EXCITATION USING FULL DUPLEX RADIO SYSTEM
Maryam Salim^{1,2}, Ali Caglar Ozen³, Michael Bock³, and Ergin Atalar^{1,2}

¹Electrical and Electronics Engineering Department, Bilkent University, Ankara, Turkey, ²National Magnetic Resonance Research Center (UMRAM), Bilkent University, Ankara, Turkey, ³Department of Radiology - Medical Physics, University Medical Center Freiburg, Freiburg, Germany

In this work, we demonstrated feasibility of MRI with concurrent excitation and acquisition (CEA) using our decoupling method which is potentially useful for MRI of tissues with ultra-short T2*. We have used the concepts used in the full-duplex radio system to suppress the Tx signal coupled on the Rx coil. We could achieve up to 100 dB decoupling between Tx and Rx coils using the cancellation circuit. 3D pulse radial scan was conducted using CEA. Deconvolved MR signal response from a rubber phantom and image of it in coronal slice

orientation is demonstrated as the feasibility of the proposed method.

-
- 3637
Computer #66 Evaluation and Integration of a Dual-Tuned $^{13}\text{C}/^1\text{H}$ Headcoil into PET/MR Hybrid Imaging
Mark Oehmigen¹, Maik E. Lindemann¹, Michael Sauer², Titus Lanz², and Harald H. Quick^{1,3}
- ¹High Field and Hybrid MR Imaging, University Hospital Essen, Essen, Germany, ²Rapid Biomedical GmbH, Rimpf, Germany, ³Erwin L. Hahn Institute for MR Imaging, University Duisburg-Essen, Essen, Germany*
- A dual tuned $^{13}\text{C}/^1\text{H}$ radiofrequency head coil was evaluated towards its potential use in integrated PET/MR hybrid imaging. The amount of PET-signal attenuation due to the head coil was quantified in phantom experiments. A CT-based 3D template μ -map of the hardware components was generated and evaluated for attenuation correction (AC). The head coil homogeneously attenuates the PET signal by 10%. Attenuation correction homogeneously reduced this attenuation bias to below 1%. These results were confirmed in PET/MR measurements of six patients. The RF head coil was successfully integrated into PET/MR hybrid imaging and can now be used for multinucleus hybrid imaging.
-
- 3638
Computer #67 Open Source Imaging Initiative
Lukas Winter¹, Haopeng Han¹, Antonia Barghoorn², Werner Hoffmann³, Stefan Hetzer⁴, Simone Winkler⁵, Larry Wald⁶, Andrew Webb⁷, Peter Blümler⁸, and Thoralf Niendorf^{1,9,10}
- ¹Berlin Ultrahigh Field Facility (B.U.F.F.), Max Delbrück Center for Molecular Medicine, Berlin, Germany, ²Department of Physics, Technische Universität Berlin, Berlin, Germany, ³Physikalisch Technische Bundesanstalt (PTB), Berlin, Germany, ⁴Berlin Center for Advanced Neuroimaging, Charité - Universitätsmedizin, Berlin, Germany, ⁵Department of Radiology, Stanford University, Stanford, CA, United States, ⁶Athinoula A. Martinos Center for Biomedical Imaging, Harvard Medical School, Massachusetts General Hospital, Charlestown, MA, United States, ⁷Gorter Center for High Field MRI, Leiden University Medical Center, Leiden, Netherlands, ⁸Institute of Physics, University of Mainz, Mainz, Germany, ⁹Experimental and Clinical Research Center (ECRC), a joint cooperation between the Charité Medical Faculty and the Max Delbrück Center for Molecular Medicine, Berlin, Germany, ¹⁰MRI.TOOLS GmbH, Berlin, Germany*
- Regardless public or private healthcare system, MR costs determine healthcare outcomes. There is a high demand for affordable MR technology around the world to improve patient diagnosis and treatment. The aim of the open source imaging initiative (www.opensourcimg.org) is to collaboratively build an affordable MR scanner and make its technical documentation available according to the standards of open source hardware. Combining innovation and open source allows major reduction of investment and operational costs with the ideal: From the community to the community.
-
- 3639
Computer #68 Decoupling Scheme for a Cryogenic Rx-Only RF Coil for ^{13}C Imaging at 3T
Juan D. Sánchez-Heredia¹, Esben Søvsø Szocska Hansen^{2,3}, Christoffer Laustsen², Vitaliy Zhurbenko¹, and Jan H. Ardenkjær-Larsen¹
- ¹Department of Electrical Engineering, Technical University of Denmark, Kgs Lyngby, Denmark, ²MR Research Centre, Department of Clinical Medicine, Aarhus University, Aarhus, Denmark, ³Danish Diabetes Academy, Odense, Denmark*
- In this study we evaluate the different active decoupling schemes that can be used to drive an Rx-only coil, in order to determine the optimal design for ^{13}C MRI at 3T. Three different circuit schemes are studied: two known ones (with regular series and parallel tuning respectively), and a novel one which we found to be optimal for this case. The circuits have been cooled to 77K to reduce coil noise. Preliminary tests with the preamplifier cooled to 77K for reduction of noise figure, are also reported.
-
- 3640
Computer #69 Development of Rotary Magnet MRI for Free Radical Imaging
Ryoma Kobayashi¹, Hideo Utsumi¹, Atsushi Iikura², Eiji Sugiyama³, Yuji Ohkubo⁴, Kazuhiro Ichikawa¹, Tatsuya Naganuma⁵, and Hidenori Kajiwara²
- ¹Innovation Center for Medical Redox Navigation, Kyushu university, Fukuoka, Japan, ²FUJI ELECTRIC CO., LTD., Tokyo, Japan, ³NOEMAX ENGINEERING Co., LTD, Gunma, Japan, ⁴MEIKO Co., LTD., Yamanashi, Japan, ⁵Japan Redox Limited, Fukuoka, Japan*
- poster file
-
- 3641
Computer #70 A hybrid RF shielding for PET inserts using carbon fiber and slotted copper layers
Antonio Javier Gonzalez¹, Luis Fernando San Sebastian¹, Sebastian Stanculovic², Reineiry Emilio Garcia³, Ralph Wissmann², Sven Junge², and Jose Maria Benlloch¹
- ¹Institute for Instrumentation in Molecular Imaging, i3M, Valencia, Spain, ²Preclinical Imaging, Bruker BioSpin, Ettlingen, Germany, ³Institute of Design and Manufacture, Valencia, Spain*
- A novel approach for radio-frequency shielding using hybrid carbon fiber materials and slotted copper layers. A proof of concept has been built and tested in high frequency MR scanners. The purpose is to use it to shield the MR RF field on PET electronics, allowing simultaneous PET-MR acquisitions.
-
- 3642
Computer #71 Optimization of DWI sequences using a dynamic consumption energy simulation model for large bore Actively Shielded Gradient Coil
Sho Kawajiri¹, Naoyuki Furudate¹, Yutaka Machii¹, Motohiro Miura¹, and Masashi Hori¹

¹MRI development department, Toshiba Medical Systems corp., Otawara, Tochigi, Japan

Estimating the accurate consumption energy of gradient power supply and gradient coil leads to advantage on an optimized power supply for environment and to achieve an economical system. In addition, providing sufficient power supply permits a flexibility in pulse sequences. The gradient power energy consumption depends on the gradient waveform. Because the gradient coil resistance is affected by frequency of gradient waveform, a simulation model is proposed to estimate the dynamic consumption energy with equivalent circuit for the gradient coil and evaluated actual and simulated consumption energy of DWI imaging with various conditions to ensure accuracy of the model.

3643 Computer #72 Accuracy and long-term stability measurements of a motion estimation sequence for hybrid PET-MR systems
Gaspar Delso¹, Mehdi Khalighi², Dan Rettmann³, Michel Tohme⁴, and David Goldhaber⁴

¹GE Healthcare, Zurich, Switzerland, ²GE Healthcare, Stanford, CA, United States, ³GE Healthcare, Rochester, MN, United States, ⁴GE Healthcare, Waukesha, WI, United States

One of the known potential benefits of integrated positron emission and magnetic resonance (PET/MR) scanners is the possibility of using MR data to monitor patient motion.

The present work evaluates the performance of a new pulse sequence designed exclusively for PET/MR head tracking. By assuming that all the required imaging data is provided by the PET subsystem, the MR sequence can be optimized exclusively for the task of providing accurate motion estimates over long periods of time (e.g. 30-60min). Data management, SAR and noise concerns are therefore minimized.

Electronic Poster

MR Safety

Exhibition Hall

Tuesday, May 10, 2016: 17:00 - 18:00

3644 Computer #73 DEVELOPMENT OF A SET OF GENERIC NUMERICAL BIRDCAGES FOR COMPREHENSIVE EVALUATIONS OF INDUCED RF FIELDS FOR IMPLANT SAFETY
Eugenia Cabot¹, Earl Zastrow^{1,2}, and Niels Kuster^{1,2}

¹IT'IS Foundation, Zurich, Switzerland, ²ETHZ, Zurich, Switzerland

A study of *in vivo* radiofrequency exposure of a group of human models to a reduced set of birdcages that cover clinical scanner variability was performed at 64 MHz, with a view to the assessment of implant safety during magnetic resonance imaging. Finite-difference time-domain simulations were run for combinations of human model/landmark/birdcage for quadrature fed coils representing closed-bore systems with respect to RF exposure. The evaluation of the E-fields for the Tier 3 of TS10974¹ shows large variations in the tangential E-field values obtained with the different coils.

3645 Computer #74 Uncertainty of RF Induced Heating Tests of a Generic Orthopedic Implant in Different Phantoms
Mahdi Abbasi^{1,2}, Yacine Noureddine¹, Gregor Schaefer^{1,3}, and Daniel Erni²

¹MR:comp GmbH, Gelsenkirchen, Germany, ²Faculty of Engineering/ATE, Duisburg-Essen University, Duisburg, Germany, ³MRI-STaR GmbH, Gelsenkirchen, Germany

comparison study has been implemented for a generic orthopedic implant (GOI) in ASTM and Elliptical phantom as well as in homogeneous and heterogeneous Duke model in terms of RF induced heating to evaluate the uncertainty of RF induced heating tests in phantoms. The parameters to be evaluated to track the hotspots at the surrounding tissue of the GOI were assessed.

3646 Computer #75 Decoupling a prosthetic hip implant from a parallel transmit array using different numbers of transmit channels
Arian Beqiri¹, Joseph V Hajnal^{1,2}, and Shaihan J Malik¹

¹Imaging Sciences and Biomedical Engineering, King's College London, London, United Kingdom, ²Centre for the Developing Brain, King's College London, London, United Kingdom

Ensuring safe imaging around metallic implants is paramount to safety in MRI. Parallel transmission offers the possibility of electromagnetically decoupling metallic implants from an RF coil. Here the impact of the number of transmit channels used is assessed in terms of reduction of SAR around the implant and improvement in the homogeneity of the B₁⁺ imaging field.

3647 Computer #76 The Effect of Field Strength on Wire-tip Heating: Simulation and Direct Measurements at 1.5T and 3T
Volkan Acikel¹ and Daniel B Ennis^{1,2}

¹Department of Radiological Sciences, University of California Los Angeles, Los Angeles, CA, United States, ²Department of Bioengineering, University of California Los Angeles, Los Angeles, CA, United States

MRI presents several potential risks for patients with implanted devices and one of the main concerns is RF induced heating of devices and nearby tissues. The aim of this study was to compare the RF induced heating characteristic of wires at 1.5T and 3T using simulations and direct measurements. Greater heating (SAR amplification) can be observed at lower field strengths for longer wires.

-
- 3648
Computer #77 Genetic damage investigations after repeated exposures to 7 T Magnetic Resonance Imaging
Mahsa Fatahi¹, Annika Reddig², Vijayalaxmi Vijayalaxmi³, Bjoern Friebe⁴, Dirk Roggenbuck^{5,6}, Dirk Reinhold², and Oliver Speck^{1,7,8,9}
- ¹Biomedical Magnetic Resonance, Otto-von-Guericke-University Magdeburg, Magdeburg, Germany, ²Institute of Molecular and Clinical Immunology, Otto-von-Guericke-University Magdeburg, Magdeburg, Germany, ³Department of Radiology, University of Texas Health Science Center, San Antonio, TX, United States, ⁴Department of Radiology and Nuclear Medicine, Otto-von-Guericke-University Magdeburg, Magdeburg, Germany, ⁵Faculty of Natural Sciences, Brandenburg University of Technology Cottbus-Senftenberg, Senftenberg, Germany, ⁶Medipan GmbH, Dahlewitz/Berlin, Berlin, Germany, ⁷Leibniz Institute for Neurobiology, Magdeburg, Germany, ⁸Center for Behavioral Brain Sciences, Magdeburg, Germany, ⁹German Center for Neurodegenerative Disease, Magdeburg, Germany
- Synopsis.** Ultra-high field magnetic resonance imaging (UHF MRI) is a technological development which is now only used for research purpose. Healthy individuals working with UHF MRI scanners as well as those participating in research investigations are repeatedly exposed to high field strengths, which can be >2-fold greater than those regularly used in clinics. In this study, we have examined the extent of genetic damage in peripheral blood mononuclear cells (PBMC) obtained from such individuals exposed to 7T MRI.
-
- 3649
Computer #78 Large volume distributed temperature measurements using MRI-compatible Raman spectroscopy
Paul de Bruin¹, Wouter Teeuwisse¹, Andrew Webb¹, and Rolf Hut²
- ¹Leiden University Medical Centre, Leiden, Netherlands, ²Technical University Delft, Delft, Netherlands
- A new method of monitoring temperature non-invasively within an MRI scanner is introduced. This method is based on Raman backscattering, with the sensor consisting of a long length of thin optical fibre which can be arranged in any desired geometry. The major advantage over existing techniques is that a wide area of surface temperatures can be monitored simultaneously. Preliminary feasibility of the approach is shown here for localized and global temperature measurements.
-
- 3650
Computer #79 Accurate and precise dynamic contrast enhanced (DCE) measurements with reduced gadolinium toxicity by lengthening pre-injection baseline
Samuel Barnes¹, Thomas Ng², and Russell Jacobs³
- ¹Radiology, Loma Linda University Medical Center, Loma Linda, CA, United States, ²Radiology, Brigham and Women's Hospital, Boston, MA, United States, ³Caltech, Pasadena, CA, United States
- For increased patient safety it is desirable to acquire dynamic contrast enhanced (DCE) MRI data with the lowest passable Gd contrast agent (CA) dose. However, a lower CA dose generally leads to smaller signal changes and lower quality studies. Through simulations we show that lower CA doses (up to 1/2 dose) can be compensated for by extending the pre-injection baseline acquisition time to maintain similar accuracy and precision of the fitted K_{trans} values.
-
- 3651
Computer #80 Effect of Renal Function on T1 signal changes in deep brain nuclei
Yan Cao¹, Yang Zhang^{1,2}, George Shih¹, Yan Zhang¹, and Martin R Prince^{1,3}
- ¹Radiology, Weill Cornell Medical Center, New York, NY, United States, ²Radiology, Qilu Hospital, Shandong University, Jinan, China, People's Republic of, ³Radiology, Columbia University, New York, NY, United States
- Dialysis patients had 3 times the signal increase on unenhanced T1-weighted images compared to a control population with near normal renal function undergoing the identical number of GBCA administrations. Although any clinical consequence to GBCA administration would be expected to be magnified in dialysis patients, no clinical effect of receiving GBCA could be identified in the nephrologist/nursing notes recorded 3 times a week in the 30 days following GBCA administration.
-
- 3652
Computer #81 Safety and diagnostic efficacy of Dotarem® (gadoteric acid) for MR mammography: Diagnosis vs. cytological findings
Matthias Hackenbroch¹, De Hua Chang¹, and David Maintz¹
- ¹Radiology, University Clinic of Cologne, Cologne, Germany
- A non-interventional post-marketing surveillance study carried out between January 2012 and October 2013 on 1,537 patients in 15 centres showed that Dotarem® (Guerbet, Roissy, France) is an effective contrast agent for the identification of invasive ductal carcinomas. An MR mammography with the diagnosis of invasive ductal carcinoma was confirmed in 93.5% of all cases by means of a subsequent cytological examination. Overall, a diagnosis was able to be made in 99.2% of the cases. Adverse reactions occurred in 5 patients (0.3%). In 4 out of 5 of the patients the adverse events were not serious and in one patient the adverse events were serious.
-
- 3653
Computer #82 Influences of 3.0 Tesla MRI noise on neonates and young adults: a longitudinal study
Huan Li¹, Chao Jin¹, Jianxin Guo¹, Miaomiao Wang¹, and Jian Yang¹

The temporary or permanent effects of strong noise from MRI devices on hearing functions, especially for different age populations (e.g. neonate and adult) remain unclear. Here we conduct a longitudinal study targeting 3T MRI to disclose such effects on hearing functions of young adults and neonates. Results indicate that due to immaturity of hearing nerve system, neonates show weaker sensitivity to acoustic noise than adults. The 3T MRI noise resulted in transient decrease of young adults' hearing function (i.e. temporary threshold shift), whereas showed rarely effects on neonates.

3654 Computer #83 Robust Simulation of MRI Gradient Field-Induced Vibration of an Implantable Medical Device
Ihsan Zainul¹, Mahdi Abbasi^{1,2}, and Gregor Schaefer^{1,3}

¹MR:comp GmbH, Gelsenkirchen, Germany, ²Faculty of Engineering/ATE, Duisburg-Essen University, Duisburg, Germany, ³MRI-STaR GmbH, Gelsenkirchen, Germany

The interaction between the gradient induced eddy current and the static magnetic field in the MRI system generates force and torque to a conductive implant if the eddy current magnetic moment and static magnetic field are misaligned. A frequency-domain solver (F-solver) of full-wave simulator CST studio suite 2015 was employed as an initial step to calculate the surface current induced due to the gradient field-induced switching.

3655 Computer #84 Measuring Gradient-Induced Vibration of a Conductive Device using Laser Doppler Vibrometry at 3T
Daniel J Martire¹, Krzysztof Wawrzyn¹, William Bradfield Handler¹, and Blaine A Chronik¹

¹Physics and Astronomy, Western University, London, ON, Canada

In this project, a method to quantify the gradient-induced vibration of a medical device in an MR system using a laser Doppler vibrometer is presented. A copper annulus was suspended in a 3T scanner, at a position chosen to maximize the x-component of the x-gradient. The displacement of the device was measured at different gradient field strengths. Typical observations were understood, which should lead towards helping establish a test standard for gradient induced vibrations of implanted medical devices.

3656 Computer #85 Effects of breast tissue density, size, and positioning on SAR at 7T
Joseph Vincent Rispoli¹

¹Weldon School of Biomedical Engineering, Purdue University, West Lafayette, IN, United States

It is common practice to perform full-wave electromagnetic modeling to characterize RF transmit coils and establish safety parameters limiting power and SAR to comply with guidelines for pre-clinical use with human volunteers. Currently-available female voxel models are unsuitable for simulating the filling factor of breast coils designed for women in the prone position. Accurate breast modeling is further confounded by variability of lipid and fibroglandular tissues, with modeling implications owing to disparate conductivity and permittivity values. This work presents simulations at 7T using high-resolution, anatomically-correct breast phantoms exhibiting varying proportions of fatty and fibroglandular tissues, as well as breast tissue girth, length, and positioning within the RF coil, demonstrating the effects of these variables in projected SAR for breast imaging.

3657 Computer #86 Potential Effects of MR-induced Temperature Increase on PET Signal during MR/PET: Simulations of a Worst-Case Scenario
Giuseppe Carluccio^{1,2}, Yu-Shin Ding^{1,2}, Jean Logan^{1,2}, and Christopher Michael Collins^{1,2}

¹Radiology, Center for Advanced Imaging Innovation and Research (CAI2R), New York, NY, United States, ²Radiology, Bernard and Irene Schwartz Center for Biomedical Imaging, New York, NY, United States

We explore the possibility that SAR-related temperature increase could affect metabolic rates enough to alter FDG signal in MR/PET. Using numerical simulations, we calculate the distributions of SAR, temperature, metabolic rates, FDG concentration ([FDG]), and PET signal throughout the human body. Calculation of [FDG] utilizes a two-compartment model considering metabolic rate through time. Results are calculated for injection time one hour before the onset of imaging and for injection time simultaneous with the onset of imaging. Even for worst-case scenario (max allowable whole-body SAR for the duration of the scan), there is little observable effect on PET signal.

3658 Computer #87 Local Q-matrix computation for parallel transmit MRI using optimal channel combinations
Arian Beqiri¹, Jeffrey W Hand¹, Joseph V Hajnal^{1,2}, and Shaihan J Malik¹

¹Imaging Sciences and Biomedical Engineering, King's College London, London, United Kingdom, ²Centre for the Developing Brain, King's College London, London, United Kingdom

Computing 10g averaged local SAR Q-matrices for parallel transmission MRI using self-implemented code is complex and computationally expensive. Here we present a simple method for computing Q-matrices using channel combinations of 10g SAR calculated with electromagnetic field simulation software and then simply constructed into Q-matrices from these combinations.

3659 Computer #88 Heating Reduction in Unilateral And Bilateral Implanted Leads At 3T Using Parallel Radiofrequency Transmission in a Heterogeneous Head Model

Clare McElcheran¹, Laleh Golenstani-Rad², and Simon Graham³

¹University of Toronto, Toronto, ON, Canada, ²Massachusetts General Hospital, Charlestown, MA, United States, ³Sunnybrook Health Sciences Centre, Toronto, ON, Canada

Long implanted wires, such as deep brain stimulation (DBS) implants, are subject to radiofrequency (RF) heating during MRI. In previous work, RF shimming was used to tailor the electric and magnetic fields creating optimal excitation and minimal heating in a uniform cylindrical medium with a single, straight, implanted copper wire at 3T. This work extends the methodology to a complex, heterogeneous head model with one or two implanted, curved copper wire(s). A substantial improvement in both B_1^+ -field homogeneity and E-field reduction is achieved when compared with a transmit/receive birdcage coil in both the single wire and bilateral wire case.

3660

Computer #89

Database Construction for Local SAR Prediction: Preliminary Assessment of the Intra and Inter Subject SAR Variability in Pelvic Region
Ettore Flavio Meliadori¹, Alexander J.E Raaijmakers¹, Matthew C. Restivo¹, Matteo Maspero¹, Peter R. Luijten¹, and Cornelis A.T. van den Berg¹

¹Center for Image Sciences, University Medical Center Utrecht, Utrecht, Netherlands

A reliable technique to assess the 10g averaged Specific Absorption Rate is necessary for parallel transmit ultra-high field body MRI. We believe that the best solution is to build a database with many different models. We have created nine dedicated body models and performed FDTD simulations on them to evaluate the inter-subject variability for prostate imaging at 7T using fractionated dipole antennas. Maximum SAR_{10g} ranges from 1.64 to 2.48W/kg with 8x1W input power. No relationship was found between BMI and maximum SAR_{10g}. Intra-subject variability (caused by slight antenna positioning variability, +/-2cm) was also investigated showing up to 67.8% SAR variability.

3661

Computer #90

Synthesis and SAR Assessment of Multi-slice PINS SLR RF Pulses for Wideband MRI: A Simulation Study
Fu-Hsing Wu¹, Edzer L. Wu¹, and Jyh-Horng Chen¹

¹Interdisciplinary MRI/MRS Lab, Department of Electrical Engineering, National Taiwan University, Taipei, Taiwan

The multislice RF pulse excitation is required in some simultaneous multi-slice (SMS) methods. The aim of this study was to investigate the synthesis method and SAR (Specific Absorption Rate) of multislice PINS (Power Independent of Number of Slices) SLR RF pulses for Wideband MRI and other SMS methods.

The relative values of SAR of the standard SLR and PINS SLR RF pulses with different number of slices W are presented. It can be found that the values of SAR of PINS SLR pulses were greatly reduced compared to that of the standard SLR pulses. For example, The SAR of PINS SLR with $W = 5$ is only 38% of that of standard SLR with $W = 5$. And The SAR of PINS SLR with $W = 5$ is only 1.9 times of that of standard SLR with $W = 1$.

3662

Computer #91

A Multi-Channel Real-Time Power Monitoring System for SAR Estimation Using FPGA in High Field MRI
Xinqiang Yan^{1,2}, Lei Shi³, Baotong Feng², Zhe Wang¹, Shujun Wei², Chuangxi Ma², Long Wei², and Rong Xue¹

¹State Key Laboratory of Brain and Cognitive Science, Beijing MRI Center for Brain Research, Institute of Biophysics, Chinese Academy of Sciences, Beijing, China, People's Republic of, ²Key Laboratory of Nuclear Radiation and Nuclear Energy Technology, Institute of High Energy Physics, Chinese Academy of Sciences, Beijing, China, People's Republic of, ³State Key Laboratory of Magnetic Resonance and Atomic and Molecular Physics, Wuhan Institute of Physics and Mathematics, Chinese Academy of Sciences, Wuhan, China, People's Republic of

Specific absorption rate (SAR) is a limiting factor for high field MRI due to excess RF power deposition in human subjects. In this study, we developed a multi-channel real-time RF power monitoring system for global and local SAR estimation using FPGA to ensure patient safety. The major components of the monitoring system include multiple dual directional couplers, demodulating logarithmic power sensors, analog to digital converters and a FPGA fast signal processing unit, etc. The deviation of the power measurement was less than 0.5dB after calibration for system errors over a dynamic RF signal range of 100dB.

3663

Computer #92

Local SAR increase in the human head induced by high-permittivity pads at the sodium (²³Na) resonance frequency at 7 Tesla
Thomas M. Fiedler¹, Mark E. Ladd^{1,2}, and Andreas K. Bitz¹

¹Medical Physics in Radiology, German Cancer Research Center (DKFZ), Heidelberg, Germany, ²Erwin L. Hahn Institute for Magnetic Resonance Imaging, University Duisburg-Essen, Essen, Germany

It has been shown that specific configurations of high-permittivity pads can lead to an increase of local SAR. So far, the effects of high-permittivity pads on RF fields have been investigated only for ¹H imaging at 7 Tesla. For X-nuclei imaging typically dual-tuned coils are applied. In this work, we investigate the effect of high-permittivity pads, typically utilized to optimize RF fields for ¹H imaging, for ²³Na imaging at 7T. RF simulations were performed for two body models to determine under which conditions SAR elevations are likely to occur or can be avoided.

3664

Computer #93

RF Heating Studies on Anesthetized Pigs by Using Fractionated Dipole Antennas at 7T

Yigitcan Eryaman¹, Patrick Zhang¹, Lynn Utecht¹, Russell L Lagore¹, Arcan Erturk¹, Angel Torrado-Carvajal^{2,3}, Esra Abaci Turk^{3,4}, Lance Delabarre¹, Gregory J. Metzger¹, and J. Thomas Vaughan¹

¹CMRR, Radiology, University of Minnesota, Minneapolis, MN, United States, ²Medical Image Analysis and Biometry Laboratory, Universidad Rey Juan Carlos, Mostoles, Madrid, Spain, ³Madrid-MIT M+Vision Consortium in RLE, Massachusetts Institute of Technology, Boston, MA, United States, ⁴Boston Children's Hospital, Harvard Medical School, Boston, MA, United States

We present our results regarding electromagnetic & thermal simulations as well as temperature measurement studies in anesthetized pigs. Pig models were generated by segmenting tissues from CT images. Fractionated dipole antennas were used to deliver RF energy in the pigs body. Power levels used for RF excitation were monitored. Temperature measurements were made using 4 fiber optic probes at locations which are visible in the digital pig model. Simulation and Experiment results were compared.

3665 Computer #94 E-field Comparison of 1.5T Transmit Head and Extremity Coils to 1.5T Body Coils – Implications for Implantable Cardiac Pacemaker and Defibrillator RF Heating and Unintended Stimulation
Shiloh Sison¹, Xin Huang², Shi Feng³, Ji Chen², Richard Williamson³, and Gabriel Mouchawar³

¹St. Jude Medical, Sunnyvale, CA, United States, ²University of Houston, Houston, TX, United States, ³St. Jude Medical, Sylmar, CA, United States

E-fields tangential to implantable cardiac pacemakers and defibrillators were analyzed at Normal and First Level Controlled Operating Modes as well as 30uT peak B1+. 1.5T body transmit and head and extremity transmit RF coils were simulated. A comparison of the Etans generated by the body transmit coils is made to those generated by head and extremity transmit coils. If RF heating and voltage can be shown to be safe with unrestricted body coils then no additional analysis is necessary for head and extremity coils since there is a 9x margin in RF heating and 3x margin in voltage.

3666 Computer #95 RF safety assessment of a 7 Tesla breast coil: SAR versus tissue temperature limits
Thomas M. Fiedler¹, Mark E. Ladd^{1,2}, and Andreas K. Bitz¹

¹Medical Physics in Radiology, German Cancer Research Center (DKFZ), Heidelberg, Germany, ²Erwin L. Hahn Institute for Magnetic Resonance Imaging, University Duisburg-Essen, Essen, Germany

RF safety of Tx coils can be assessed based on SAR or temperature limits; however, temperature is directly correlated to tissue damage and enables a more precise RF exposure assessment. Both safety assessments were compared for a 7T breast coil. Temperature depends on the individual thermoregulation system and was taken into account using three different temperature-dependent blood perfusions. Results for a subject with impaired thermoregulation showed that temperature limits are exceeded by up to 6.17 °C even when SAR limits are complied with. For a healthy subject, up to 40% higher input power is allowed if temperature limits are applied instead of SAR.

3667 Computer #96 Globally Applicable MR Safety Course for Medical Students
Steffen Sammet¹ and Christina Louise Sammet^{2,3}

¹Department of Radiology, University of Chicago Medical Center, Chicago, IL, United States, ²Department of Radiology, Northwestern University, Chicago, IL, United States, ³Department of Medical Imaging, Ann & Robert H. Lurie Children's Hospital of Chicago, Chicago, IL, United States

We propose an educational magnetic resonance (MR) safety course for instructing medical students world-wide about basic MR and patient-related safety. The MR safety course material can be implemented as a traditional didactic or interactive lecture in combination with hands-on safety demonstrations and will prepare medical students for patient screening and safety consultations when ordering MR studies. This course can be implemented globally by various medical school programs to ensure consistent quality of teaching materials and MR safety standards.

Electronic Poster

Hyperpolarized MR (non-gaseous)

Exhibition Hall

Wednesday, May 11, 2016: 10:00 - 11:00

3668 Computer #1 Measuring Perfusion with a Hyperpolarised Ultra-Long T1 15N Glutamine Compound
Rolf F Schulte¹, Enrico Chiavazza^{2,3}, Axel Haase², Silvio Aime³, Marion I Menzel¹, Markus Schwaiger², and Markus Durst^{1,2}

¹GE Global Research, Munich, Germany, ²Technische Universität München, Munich, Germany, ³Università di Torino, Turin, Italy

An experimental setup for 15N was established on a clinical 3T whole-body scanner, in order to measure perfusion with an ultra-long T1 15N compound. The substance α -trideuteromethyl[15N]glutamine was synthesised, polarised and injected into healthy rats to study the perfusion of the kidneys. With a T1 time in vivo of 146s, it was possible to acquire perfusion images for over 5 minutes.

3669 Computer #2 In vivo 3D mapping of intracellular pH using hyperpolarized [1-13C]pyruvate in the rodent heart
Angus Zoen Lau^{1,2}, Jack Miller^{2,3}, and Damian J Tyler^{1,2}

¹Cardiovascular Medicine, University of Oxford, Oxford, United Kingdom, ²Department of Physiology, Anatomy, and Genetics, University of Oxford, Oxford, United Kingdom, ³Department of Physics, Clarendon Laboratory, Oxford, United Kingdom

Intracellular pH can be measured *in vivo* by taking the ratio between hyperpolarized HCO_3^- and CO_2 produced from $[1-^{13}\text{C}]$ pyruvate, but to date, low CO_2 signal has limited this method to whole-heart assessment. We propose a 3D imaging approach using spectrally-selective excitation which exploits the rapid exchange between HCO_3^- and CO_2 to produce *in vivo* myocardial pH_i maps. The intracellular pH_i is found to be 7.15 ± 0.04 in the healthy rodent heart. Increased cardiac workload via continuous dobutamine infusion resulted in a decreased intracellular pH of 6.90 ± 0.06 .

-
- 3670
Computer #3
Branched-chain α -keto acid decarboxylation and transamination assessment in mouse liver and kidney using hyperpolarized α -keto $[1-^{13}\text{C}]$ isocaproate MRS
Celine A.J. Baligand¹, Irene Marco-Rius¹, Zhen Jane Wang¹, Daniel B. Vigneron¹, John Kurhanewicz¹, and Michael Ohliger¹
¹Radiology and Biomedical Imaging, UCSF, San Francisco, CA, United States
- The branched-chain α -keto acid dehydrogenase (BCKDH) is an important regulator of branched chain amino acid (BCAA) catabolism. In several diseases including liver cirrhosis, decreased BCKDH activation results in increased BCAA breakdown through the branched-chain amino transferase (BCAT) and subsequent protein and energy deficiency. We show that both hyperpolarized Leucine and HCO_3^- signals can be detected in liver *in vivo* at 14.1 T as byproducts of $[1-^{13}\text{C}]$ KIC metabolism. This provided information on BCAT/BCKDH activities in mouse liver and kidney, consistent with literature values. Assessing the effect of BCAA supplementation on liver cirrhosis has the potential to impact patient monitoring and treatment.
-
- 3671
Computer #4
Hyperpolarized Carbon-13 Ketoisocaproate Reveals Dysfunction in Branched-Chain Amino Acid Metabolism in Liver Cancer
Philip Lee¹, Xing Qi Teo¹, and Way Cherng Chen¹
¹FUNCTIONAL METABOLISM GROUP, SINGAPORE BIOIMAGING CONSORTIUM, Singapore, Singapore
- Complex reprogramming of cellular metabolism to support tumorigenesis & survival is a hallmark of cancer. Recently Ericksen et al observed that the suppression of branched-chain amino acids (BCAA) catabolic enzymes is a unique signature in human hepatocellular carcinomas (HCC), and the degree of downregulation correlates strongly with tumor grades and survival outcomes¹. Specifically the metabolic activity of the branched-chain keto-acid dehydrogenase (BCKDH) complex was significantly reduced. We hypothesize that this modulation can be measured *in vivo* by tracking the metabolism of hyperpolarized carbon-13 ketoisocaproate.
-
- 3672
Computer #5
Noninvasive *in vivo* assessment of cytosolic redox-state in rat liver using hyperpolarized $[1-^{13}\text{C}]$ alanine
Jae Mo Park¹, Ralph E Hurd², Shie-Chau Liu¹, and Daniel M Spielman¹
¹Radiology, Stanford University, Stanford, CA, United States, ²Applied Sciences Laboratory, GE Healthcare, Menlo Park, CA, United States
- Intracellular [lactate]:[pyruvate] is an important biomarker of cytosolic redox-state, directly reflecting free cytosolic [NADH]:[NAD⁺]. Hyperpolarized $[1-^{13}\text{C}]$ alanine, which can be also transported across the plasma membrane, is useful to measure relative concentrations of intracellular pyruvate and lactate. In this work, we propose a simple method to assess *in vivo* cytosolic redox-state using hyperpolarized $[1-^{13}\text{C}]$ alanine, and demonstrate the ethanol-induced redox change in rat liver.
-
- 3673
Computer #6
In-vivo Assessment of Lung Injury Using Hyperpolarized Carbon-13 MRI in a Two-hit Model of Acid Aspiration and VILI
Mehrdad Pourfathi^{1,2}, Yi Xin¹, Stephen J Kadlecek¹, Maurizio Cereda³, Harrilla Profka¹, Sarmad M Siddiqui^{1,4}, Hooman Hamedani^{1,4}, and Rahim R Rizzi¹
¹Radiology, University of Pennsylvania, Philadelphia, PA, United States, ²Electrical and Systems Engineering, University of Pennsylvania, Philadelphia, PA, United States, ³Anesthesiology and Critical Care, University of Pennsylvania, Perlmans School of Medicine, Philadelphia, PA, United States, ⁴Bioengineering, University of Pennsylvania, Philadelphia, PA, United States
- Ventilator induced lung injury (VILI) results from mechanical trauma and secondary inflammatory responses. Previous imaging studies focused on the effects of ventilator settings on structural or functional changes; however, no MRI studies have been conducted to elucidate the metabolic changes during VILI. In this study, the potential of HP $[1-^{13}\text{C}]$ -pyruvate and its conversion to $[1-^{13}\text{C}]$ -lactate as a marker for the lung inflammation was investigated in a two-hit model of acid aspiration and VILI.
-
- 3674
Computer #7
Zymonic acid - a novel ^{13}C enriched biosensor for *in vivo* pH-imaging
Christian Hundshammer^{1,2}, Stephan Düwel¹, Malte Gersch³, Benedikt Feurecker¹, Axel Haase⁴, Markus Schwaiger¹, Steffen J. Glaser³, and Franz Schilling¹
¹Department of Nuclear Medicine, Klinikum rechts der Isar, München, Germany, ²Department of Chemistry, Technische Universität München, München, Germany, ³Department of Chemistry, Technische Universität München, Garching, Germany, ⁴Department of Medical Engineering, Technische Universität München, Garching, Germany
- $[1,5-^{13}\text{C}_2]$ Zymonic acid is derived from carbon 13 labelled pyruvic acid and can be easily deuterium enriched for spin lattice relaxation time prolongation. The molecule exhibits pH dependent NMR shifts and can be used for pH *in vivo* mapping. Phantom measurements on human blood on a 7T preclinical MRI system indicate that $[1,5-^{13}\text{C}_2]$ ZA is a suitable pH sensor for pre-clinical and potentially also for clinical applications.
-

- 3675
Computer #8 pH Dependent Kinetics of the Decarboxylation of Pyruvate for pH Mapping Experiments
Nicholas Drachman¹, Stephen J. Kadlec¹, Yi Xin¹, and Rahim R. Rizi¹
¹Radiology, University of Pennsylvania, Philadelphia, PA, United States
- We have shown that the kinetic rate of the production of bicarbonate from pyruvate is heavily pH dependent. An increase in the rate by a factor of ~10 can be achieved by maintaining the pH of the reaction always above 10.3, the pKa of bicarbonate. This discovery will allow researchers to quickly produce hyperpolarized bicarbonate to be used for in vivo pH mapping experiments.
-
- 3676
Computer #9 *In Vivo* Hyperpolarized ¹³C Diffusion Weighted MRI Measures Lactate Efflux and Changes in MCT4 Expression in Prostate Cancer
Jeremy W Gordon¹, Hecong Qin¹, Renuka Sriram¹, Robert Bok¹, Peder EZ Larson¹, Daniel B Vigneron¹, and John Kurhanewicz¹
¹Radiology & Biomedical Imaging, University of California - San Francisco, San Francisco, CA, United States
- Dissolution DNP provides a 10,000-fold signal enhancement to carbon-13 nuclei and enables real-time metabolic imaging. In addition to the Warburg Effect, many malignant cancers overexpress MCT4, the monocarboxylate transporter responsible for lactate efflux and extracellular acidification. Because of microenvironmental differences, diffusion weighted imaging (DWI) with hyperpolarized substrates may provide unique information on lactate efflux and MCT4 expression. Here we show that DWI with hyperpolarized substrates is sensitive to changes in MCT4 expression, as lactate ADC is increased by >40% in late-stage TRAMP tumors. This technique may potentially provide a novel way to assess metabolite compartmentalization and transporter expression in malignant disease.
-
- 3677
Computer #10 Early diabetic kidney maintains the cortico-medullary urea and sodium gradient
Haiyun Qi¹, Thomas Stokholm Nørting¹, Per Mose Nielsen¹, Lotte Bonde Bertelsen¹, Yafang Xu¹, Fredrik Palm², Hans Stødkilde-Jørgensen¹, and Christoffer Laustsen¹
¹MR Research Centre, Aarhus University, Aarhus N, Denmark, ²Department of Medical Cell Biology, Uppsala University, Uppsala, Sweden
- To investigate the essential intrarenal electrolyte gradients in early diabetic kidneys, hyperpolarized ¹³C urea was applied to measure urea and sodium gradients. No differences in either intrarenal urea or sodium gradients were observed in early diabetes compared to healthy controls. These results indicate that the early metabolic and hypertrophic changes occurring in the diabetic kidney prelude the later functional alterations in diabetic kidney function, thus driving the increased metabolic demand commonly occurring in the diabetic kidney.
-
- 3678
Computer #11 Accelerating hyperpolarized metabolic imaging of the rat heart using k-t PCA and k-t SPARSE
Patrick Wespi¹, Jonas Steinhauser¹, Grzegorz Kwiatkowski¹, and Sebastian Kozerke¹
¹Institute for Biomedical Engineering, University and ETH Zurich, Zurich, Switzerland
- Hyperpolarized metabolic imaging of the heart suffers from limited spatial specificity in current protocols. In this work two algorithms, k-t PCA and k-t SPARSE, that allow accelerated metabolic imaging are compared in simulations and used to acquire in-vivo metabolic maps in rats at one millimeter in-plane resolution.
-
- 3679
Computer #12 Sampling Hyperpolarized Substrates using a 1 Tesla Permanent Magnet.
Sui-Seng Tee¹, Valentina Digialleonardo¹, Hannah Nikki Aldeborgh¹, Julio Alvarez¹, Alex Poot¹, and Kayvan Rahimi Keshari¹
¹Radiology, MSKCC, New York, NY, United States
- Hyperpolarized MRI quantifies metabolic fluxes non-invasively. One limitation is the rapid loss of polarized signal, decaying according to its longitudinal relaxation (T₁) time. We propose the use of a permanent, 1 Tesla spectrometer to lengthen T₁s. We show longer T₁ values across different functional groups. Scalar couplings were also visible and these advantages were translatable to biologically-relevant settings using perfused bioreactors. As more clinical trials are performed, it is essential to understand the behavior of HP molecules at field strengths similar to hospital magnets. Sampling HP substrates using permanent magnets is simple and cost-effective and will directly benefit clinical imaging.
-
- 3680
Computer #13 Hyperpolarized ¹³C-labeled 5,5-dimethyl-1-pyrroline-N-oxide for in vivo detection of reactive oxygen species
Keita Saito¹, Shingo Matsumoto², Deepak Sail³, Shun Kishimoto¹, Hellmut Merkle⁴, Marcelino Bernardo⁵, Rolf Swenson³, James B. Mitchell¹, and Murali C. Krishna¹
¹Radiation Biology Branch, National Cancer Institute, Bethesda, MD, United States, ²Graduate School of Information Science and Technology, Hokkaido University, Sapporo, Japan, ³Imaging Probe Development Center, National Heart, Lung, and Blood Institute, Rockville, MD, United States, ⁴National Institute of Neurological Disorder and Stroke, Bethesda, MD, United States, ⁵Molecular Imaging Program, National Cancer Institute, Bethesda, MD, United States
- 5,5-Dimethyl-1-pyrroline-N-oxide (DMPO) is a spin trap agent used to detect reactive oxygen species (ROS). We synthesized ¹³C-labeled DMPO, and investigated feasibility of hyperpolarized ¹³C-DMPO to detect ROS generated in living animals. Hyperpolarized ¹³C-DMPO gave us a single peak at 76 ppm on the ¹³C-spectrum, and ¹³C-DMPO was distributed through the mouse body immediately after intravenous injection. The results indicate hyperpolarized ¹³C-DMPO provided sufficient magnitude of the ¹³C signal to be detected in the mouse body, and can be applied to some disease models to evaluate the capability for detection of ROS in vivo.

-
- 3681
Computer #14 Time-course metabolic changes in high-fat diet-induced obesity in rats: hyperpolarized 13C MRS
Gwang-Woo Jeong^{1,2}, Chang-Hyun Oh³, Gwang-Won Kim², Chung-Man Moon², Xiao-Li Song¹, Yun-Hyeon Kim¹, Kyu-Youn Ahn⁴, and Heoung-Keun Kang¹
- ¹Department of Radiology, Chonnam National University Medical School, Gwang-ju, Korea, Republic of, ²Research Institute of Medical Imaging, Chonnam National University Medical School, Gwang-ju, Korea, Republic of, ³Department of Electronics and Information Engineering, Korea University, Gwang-ju, Korea, Republic of, ⁴Department of Anatomy, Chonnam National University Medical School, Gwang-ju, Korea, Republic of
- Non-alcoholic fatty liver is an increasing common liver disease in world population. Recent hyperpolarized 13C magnetic resonance spectroscopy (HP 13C MRS) studies revealed the cellular metabolite changes associated with the various liver diseases in animals. However, a study for high-fat diet(HFD)-induced obesity using HP 13C MRS in animal model has not yet been performed until now. The purpose of this study was to investigate the time-course metabolic changes based on HP 13C MRS in HFD-induced obesity in rats and their correlations with serum enzyme levels.
-
- 3682
Computer #15 Noninvasive biomarkers for the diagnosis of hepatic ischemia reperfusion injury: A real-time in vivo hyperpolarized 13C MRS and IVIM-DWI
Chung-Man Moon¹, Gwang-Won Kim¹, Heoung-Keun Kang², Yun-Hyeon Kim², Kyu-Youn Ahn³, and Gwang-Woo Jeong^{1,2}
- ¹Research Institute for Medical Imaging, Chonnam National University Hospital, Gwangju, Korea, Republic of, ²Radiology, Chonnam National University Medical School, Gwangju, Korea, Republic of, ³Anatomy, Chonnam National University Medical School, Gwangju, Korea, Republic of
- Hepatic ischemia reperfusion injury (IRI) induces cellular damage and causes cell death. It can lead to acute liver failure accompanied with biochemical changes, microcirculatory disturbances and/or histopathologic changes. Early detection of impaired liver function is vital for effective therapeutic interventions and thus prevents its progression to liver failure. However, an *in vivo* study of hepatic IRI model in combination with hyperpolarized ¹³C magnetic resonance spectroscopy (¹³C MRS) and diffusion-weighted imaging (DWI) has not yet been attempted until now. The purpose of this study was to investigate the cellular metabolite change, diffusion of water molecules and microcirculation of blood in rat model with hepatic IRI and their correlations with enzyme levels.
-
- 3683
Computer #16 Multi-modal and multi-scale measurement of metabolism in breast cancer cells both in vitro and in vivo
Benjamin L Cox^{1,2,3}, Joseph M Szulczewski⁴, Kai D Ludwig¹, Erin B Adamson¹, David R Inman⁴, Stephen A Graves¹, Justin J Jeffery⁵, Jason D McNulty⁶, Patricia J Keely⁴, Kevin W Eliceiri^{2,3,7}, and Sean B Fain^{1,7,8}
- ¹Medical Physics, University of Wisconsin at Madison, Madison, WI, United States, ²Morgridge Institute for Research, Madison, WI, United States, ³Laboratory for Optical and Computational Instrumentation, University of Wisconsin at Madison, Madison, WI, United States, ⁴Cell and Regenerative Biology, University of Wisconsin at Madison, Madison, WI, United States, ⁵UW Carbone Cancer Center, Madison, WI, United States, ⁶Mechanical Engineering, University of Wisconsin at Madison, Madison, WI, United States, ⁷Biomedical Engineering, University of Wisconsin at Madison, Madison, WI, United States, ⁸Radiology, University of Wisconsin at Madison, Madison, WI, United States
- A system and workflow for spatially registered *in vivo* optical microscopy, MRI, and PET of breast tumor metabolism is described. The system is coupled with a bioreactor designed to compare cellular metabolism *in vitro* using both optical microscopy and MR spectroscopy with the behavior of tumor cells in the *in vivo* tumor microenvironment. Results from enzyme reactions are shown, demonstrating the temperature control capabilities of the bioreactor. A proof of concept *in vivo* experiment is also described, with optical microscopy data of a mammary tumor acquired in conjunction with MRI and PET data, on the same animal.
-
- 3684
Computer #17 LED induced 19F-MR-signal enhancement at 7T
Markus Plaumann¹, Thomas Trantschel¹, Joachim Bargon², Ute Bommerich¹, and Johannes Bernarding¹
- ¹Department for Biometrics and Medical Informatics, Otto-von-Guericke University Magdeburg, Magdeburg, Germany, ²Institute for Physical and Theoretical Chemistry, University of Bonn, Bonn, Germany
- ¹⁹F containing substrates serve as attractive reporter molecules for NMR and MRI studies. Applications for in vivo studies are limited by low spin densities due to restricted concentrations. Using hyperpolarization techniques, such as Chemically Induced Dynamic Nuclear Polarization (CIDNP), this constrained can be overcome. So far, ¹⁹F hyperpolarization generated in D₂O, which is a prerequisite for an in vivo application, could only be documented using laser photo-CIDNP. In this study the successful hyperpolarization of a ¹⁹F nucleus in 3-fluoro-DL-tyrosine in its free and a complexed form using D₂O as a solvent is presented using a simple LED photo-CIDNP device.
-
- 3685
Computer #18 A Method to Identify and Correct for Blurring Artifacts in Hyperpolarized Metabolic Imaging
Stephen J. Kadlecek¹, Mehrdad Pourfathi^{1,2}, Harrilla Profka¹, and Rahim R. Rizi¹
- ¹Radiology, University of Pennsylvania, Philadelphia, PA, United States, ²Electrical and Systems Engineering, University of Pennsylvania, Philadelphia, PA, United States
- Hyperpolarized imaging sequences are subject to potential bias and spread of apparent signal to neighboring voxels due to the time-dependence of magnetization as RF pulses are applied and as polarization is lost through spin-lattice relaxation. In this abstract, we discuss a method to detect and correct for artifacts and demonstrate it using chemical shift imaging. The method utilizes periodic resampling of nonselective spectra to correct for signal dynamics. We show that this technique results in a higher fidelity, "de-blurred"

image.

-
- 3686
Computer #19
Hyperpolarized 1-13C Pyruvate Imaging of Porcine Cardiac Metabolism shift by GIK Intervention
Esben Søvsø Szocska Hansen^{1,2}, Rasmus Stilling Tougaard^{1,3}, Emmeli Mikkelsen¹, Thomas Stokholm Nørtinger¹, Lotte Bonde Bertelsen¹, Steffen Ringgaard¹, Hans Stødkilde-Jørgensen¹, and Christoffer Laustsen¹
- ¹MR Research Centre, Aarhus University, Aarhus N, Denmark, ²Danish Diabetes Academy, Odense, Denmark, ³Cardiology, Aarhus University Hospital, Aarhus N, Denmark*
- Cardiac metabolism has gained considerable attention worldwide lately, both as a diagnostic and prognostication tool, as well as a novel target for treatment. As human trials involving hyperpolarized MR in the heart are imminent, we employed a clinically relevant, large animal model, and sought to evaluate the general feasibility to detect an imposed shift in metabolic substrate utilization during metabolic modulation with glucose, insulin and potassium (GIK) infusion. This study demonstrates that hyperpolarized ¹³C-pyruvate, in a large animal, is a feasible method for cardiac studies, and, in combination with GIK intervention; that it is able to detect imposed metabolic shifts.
-
- 3687
Computer #20
Para-Hydrogen Induced Polarization: Advances in Amino Acid Polarization and Hyperpolarization in Heterogeneous Phase
Stefan Glögler¹, Alex Grunfeld², Jeff McCormick², Yavuz Ertas², Phillipp Schleker³, Shawn Wagner⁴, and Louis-Serge Bouchard²
- ¹University of Southampton, Southampton, United Kingdom, ²University of California Los Angeles, Los Angeles, CA, United States, ³RWTH Aachen University, Aachen, Germany, ⁴Cedars Sinai Medical Center, Los Angeles, CA, United States*
- We present new amino acid derivatives that can be hyperpolarized with the Para-Hydrogen Induced Polarization method (PHIP). Furthermore, we report on the highest achieved polarization of amino acid derivatives in biocompatible medium (water) to date with relevance for in vivo applications. Moreover, the first heterogeneous catalyst for PHIP in water will be presented that leads to significant levels of polarization. This poses the possibility of a quick filtration step to yield clean PHIP-polarized contrast agents for future in vivo studies.
-
- 3688
Computer #21
First hyperpolarization of quaternary pyridinium salts using PHIP
Frederike Euchner¹, Rainer Ringleb¹, Joachim Bargon², Ute Bommerich¹, Johannes Bernarding¹, and Markus Plaumann¹
- ¹Department for Biometrics and Medical Informatics, Otto-von-Guericke University Magdeburg, Magdeburg, Germany, ²Institute for Physical and Theoretical Chemistry, University of Bonn, Bonn, Germany*
- Quaternary ammonium substrates are of huge interest in the pharmaceutical field. Here, the hyperpolarization of new fluorinated pyridinium ions was examined. The effect of the positive charged nitrogen relating to the polarization transfer inside the molecule was proven and compared with the ¹H, ¹³C and ¹⁹F hyperpolarization examinations of 2-(3-fluoro-phenyl)-3-buten-2-ol. The observed effect can be used for localization of polarization and for the synthesis of extended MR signal enhancements.
-
- 3689
Computer #22
Hyperpolarized [1-13C]pyruvate and [1-13C]lactate observed using a single shot 3D pulse sequence in vivo
Jiazheng Wang¹, Alan Wright¹, De-en Hu¹, Richard Hesketh¹, and Kevin M. Brindle^{1,2}
- ¹Cancer Research UK Cambridge Institute, University of Cambridge, Cambridge, United Kingdom, ²Department of Biochemistry, University of Cambridge, Cambridge, United Kingdom*
- We have developed a single-shot 3D sequence for hyperpolarized ¹³C MRI, with a spatial-spectral (SpSp) pulse for excitation and a stack-of-spirals acquired in interleaved fashion during two spin echoes. The sequence achieved a resolution of 1.25x1.25x2.5 mm³ in vivo on a 7T animal system, where hyperpolarized [1-¹³C]pyruvate and [1-¹³C]lactate were imaged alternately at a frame rate of 2 s per metabolite. Variations are allowed in the design of the acquisition train to balance the in-plane and through-plane resolutions. This sequence allows higher temporal resolution and less RF depletion of the polarization than pulse sequences described previously.
-
- 3690
Computer #23
First-in-woman study of in vivo breast cancer metabolism using hyperpolarized [1-13C] pyruvate
Kristin L Granlund^{1,2}, Elizabeth A Morris³, Hebert A Vargas³, Serge K Lyashchenko⁴, Phillip J DeNoble⁴, Virgilio A Sacchini⁵, Ramon A Sosa³, Matthew A Kennedy³, Duane Nicholson³, YanWei W Guo³, Albert P Chen⁶, James Tropp⁷, Hedvig Hricak^{2,3}, and Kayvan A Keshari^{2,3}
- ¹Radiology, Memorial Sloan Kettering, New York, NY, United States, ²Molecular Pharmacology, Memorial Sloan Kettering Cancer Center, New York, NY, United States, ³Radiology, Memorial Sloan Kettering Cancer Center, New York, NY, United States, ⁴Radiochemistry & Imaging Probes (RMIP) Core, Memorial Sloan Kettering Cancer Center, New York, NY, United States, ⁵Surgery, Memorial Sloan Kettering Cancer Center, New York, NY, United States, ⁶GE Healthcare, Toronto, ON, Canada, ⁷GE Healthcare, Fremont, CA, United States*
- This is a first-in-woman study of hyperpolarized (HP) pyruvate to study in vivo cancer metabolism. A patient with biopsy-proven breast cancer has been scanned with a 2D dynamic hyperpolarized pyruvate protocol. This study aims to evaluate the feasibility and repeatability of HP breast cancer imaging. HP pyruvate imaging may be useful for evaluating treatment response before and after targeted as well as chemo-therapy or radiation treatment.
-
- 3691
1H-13C Independently Tuned RF Surface Coil Applied for In vivo Hyperpolarized MRI

¹Department of Radiology, University of California at San Francisco, San Francisco, CA, United States

This study aimed to develop a lump-element double-tuned common-mode-differential-mode (CMDM) radiofrequency (RF) surface coil with independent frequency tuning capacity for MRS and MRI applications. This CMDM coil maintained intrinsically decoupled magnetic fields, which provided sufficient isolation between the two resonators. The results from in vivo experiments demonstrated high sensitivity of both the ¹H and ¹³C resonators.

Electronic Poster

Molecular Imaging & Contrast Agents

Exhibition Hall

Wednesday, May 11, 2016: 10:00 - 11:00

3692
Computer #25 Imaging in vitro and in vivo pH with ioversol by CEST MRI
Miaomiao Chen¹, Xiaolei Zhang¹, Yanzi Chen¹, Zhiwei Shen¹, Wei Hu¹, Xilun Ma¹, and Renhua Wu¹

¹Radiology Department, Second Affiliated Hospital, Shantou University Medical College, Shantou, China, People's Republic of

We have developed a CEST MRI method that can measure pH using ioversol, a contrast agent that is clinically approved for X-ray imaging and has been repurposed for CEST MRI studies. Using ioversol as a CEST agent, we have measured pH over a range of 6.0 - 7.8 pH units by a novel ratiometric pH MRI method, in a concentration-independent manner. We also have used this agent and CEST MRI method to measure the extracellular pH (pHe) within the liver of healthy SD rats.

3693
Computer #26 ¹⁵N Heteronuclear Chemical Exchange Saturation Transfer MRI Imaging
Haifeng Zeng^{1,2}, Jiadi Xu^{1,2}, Nirbhay N Yadav^{1,2}, Michael T McMahon^{1,2}, Bradley Harden³, Dominique Frueh³, and Peter C.M van Zijl^{1,2}

¹Russell H. Morgan Department of Radiology and Radiological Science, Johns Hopkins University School of Medicine, Baltimore, MD, United States, ²F.M. Kirby Research Center for Functional Brain Imaging, Kennedy Krieger Research Institute, Baltimore, MD, United States, ³Department of Biophysics and Biophysical Chemistry, Johns Hopkins University School of Medicine, Baltimore, MD, United States

A two-step heteronuclear enhancement approach to magnify ¹⁵N MRI signal through indirect detection of water is described. Chemical Exchange Saturation Transfer (CEST) works by continuously perturbation of the spin magnetization of the exchangeable spins, and then through chemical exchange to accumulate this perturbation on water proton for signal magnification. This perturbation is mainly limited to saturation or excitation pulse on the exchangeable protons. In this work, the signal of ¹⁵N is detected indirectly through the water signal by first inverting selectively protons scalar-coupled to ¹⁵N in the urea molecule, followed by chemical exchange of the amide proton to bulk water.

3694
Computer #27 Quantification of macrophage recruitment in double and single hit head and neck cancer using fluorine-19 MRI
Aman Khurana¹, Fanny Chapelin¹, Hongyan Xu¹, Partick McConville², Quyen Nguyen³, and Eric Ahrens¹

¹Radiology, University of California, San Diego, San Diego, CA, United States, ²Molecular Imaging Inc. La Jolla, San Diego, CA, United States, ³Head & Neck Surgery, University of California, San Diego, San Diego, CA, United States

Head and neck carcinoma is a source of significant mortality worldwide, two prevalent subtypes include double and single hit tumors. We aimed to evaluate the role of infiltrating immune cells in worse clinical outcomes with double-hit tumor patients. A novel 19-Fluorine containing perfluorocarbon (PFC) emulsion was used to tag macrophages with high specificity and sensitivity and no background. The average number of 19F spins within the double hit tumors were approximately double compared to the single hit group. This quantifies the tumor associated macrophage burden of head and neck cancer using a PFC emulsion and proton/19F MRI.

3695
Computer #28 Simultaneously Trace Blood Perfusion and Glymphatic Passage by Analyzing Deuterium Oxide Perfusion Imaging with a Two-Compartment Parallel Model
Cheng-He Li¹, Zi-Min Lei¹, Sheng-Min Huang¹, Chin-Tien Lu¹, Kung-Chu Ho², and Fu-Nien Wang¹

¹Biomedical Engineering and Environmental Sciences, National Tsing Hua University, Hsinchu, Taiwan, ²Nuclear Medicine, Chang Gung Memorial Hospital, Linkou, Taoyuan, Taiwan

This study tried to simultaneously trace blood perfusion and glymphatic passage by applying two-compartment parallel model (2CPM) on D₂O perfusion using the new imaging strategy. Six rats were injected with D₂O, and both F₁ and F₂ were quantified from 2CPM. The results show that F₁ is highly coordinated with cerebral blood flow, while F₂ is much irrelevant. Only regions near several arteries show significant F₂ values, which is speculated as the paravascular pathway of CSF regulated by glymphatic system. Therefore, using 2CPM for tracing D₂O might noninvasively reveal the information of both blood and CSF dynamics.

3696
Computer #29 Cellulose-triacetate Nanoparticles as Smart Contrast Agents for Single Cell Detection.
Laura Szkolar-Sienkiewicz¹, Christiane Mallett², and Erik M Shapiro¹

It was demonstrated that enzymatically degradable cellulose triacetate particles offer a novel approach to contrast modulation. The use of such materials as smart contrast agents has been discussed and evidence of cellular uptake and relaxivity modification shown.

-
- 3697
Computer #30
Development of intravascular SPION with tunable pharmacokinetics and relaxivity for preclinical fMRI and micro-MRA
Manasmita Das^{1,2}, Esteban Oyarzabal¹, Heather Decot¹, Xiopeng Zong¹, Neal Shah¹, Sung Ho Lee¹, Jonathan Edward Frank¹, Nazar A Filnov³, and Yen-Yu Ian Shih^{1,2}
- ¹Biomedical Research Imaging Center, UNC Chapel Hill, Chapel Hill, NC, United States, ²Department of Neurology, University of North Carolina Chapel Hill, Chapel Hill, NC, United States, ³SOP-CNDD, UNC Chapel Hill, Chapel Hill, NC, United States
- We have developed a simple, inexpensive method to synthesize high-performance intravascular SPION in house. We were able to tune the relaxivity and PK profile of our home-made SPION via careful surface functionalization control and came up with an optimal formulation that offered very robust and stable contrast for high resolution cerebromicroangiography and steady state CBV functional imaging. Our future studies will focus on developing novel MR-detectable inflammation markers using our home-made iron oxide as the platform material.
-
- 3698
Computer #31
Assessment of brain development in children with developmental delay using amide proton transfer weighted (APT_w) MRI
Xiaolu Tang¹, Hong Zhang¹, Xuna Zhao^{2,3}, Jinyuan Zhou², and Yun Peng¹
- ¹Imaging Center, Beijing Children's Hospital, Capital Medical University, Beijing, China, People's Republic of, ²Neurosection, Division of MR Research, Department of Radiology, Johns Hopkins University, Baltimore, MD, United States, ³Philips Healthcare, Beijing, China, People's Republic of
- Amide proton transfer weighted (APT_w) imaging is a novel molecular MRI technique that can noninvasively detect cytosolic endogenous mobile proteins and peptides in myelination process. However it is not well known to brain developments in children with developmental delay using APT_w MRI. The aim of our work is to explore the brain development in children with developmental delay (DD) using APT_w MRI. The final conclusion shows that APT_w MRI is a promising technique to assess children with DD at a molecular level.
-
- 3699
Computer #32
Magnetic/Upconversion Fluorescent Nanoparticle-Based Dual-Modal Molecular Probes for Imaging of Lymph Node Metastasis From Pancreatic Cancer in vivo
Kai Cao¹, Ruirui Qiao², and Huimin Wei³
- ¹Radiology, Changhai Hospital, Shanghai, China, People's Republic of, ²Chemistry, Chinese Academy of Sciences, Beijing, China, People's Republic of, ³Clinic and Translational Medicine Center, Changhai Hospital, Shanghai, China, People's Republic of
- Construction of the specific pancreatic cancer probe based on upconversion nanoparticles. The probes taking biocompatibility upconversion nanoparticles with unique magnetic properties as a carrier, conjugated with ATF peptide specifically targeting the uPAR. Then, its effect of detection of tumor and lymph node metastasis would be further validated in an orthotopic human pancreatic cancer xenograft model by pathology and dual-modal imaging.
-
- 3700
Computer #33
Dynamic PET and cortical thickness comparison between healthy controls and epilepsy patients using simultaneous PET/MR
Yu-Shin Ding^{1,2}, Shaunak Ohri¹, Jean Logan¹, Thomas Koesters¹, James Babb¹, and Orrin Devinsky³
- ¹Radiology, NYU School of Medicine, New York, NY, United States, ²Psychiatry, NYU School of Medicine, New York, NY, United States, ³Neurology, NYU School of Medicine, New York, NY, United States
- Our results suggest that 1) simultaneous PET/MR imaging provides a useful imaging tool to identify regional abnormalities; 2) more information can be rendered from dynamic PET data; 3) SUV_{mean_late} and cortical thickness are independent biomarkers for epilepsy. In general, Freesurfer and SPM are more robust in orientation and segmentation than FSL.
-
- 3701
Computer #34
MRI-Guided Thermosensitive Liposomal Drug Delivery for Cancer Therapy
Po-Wah So¹, Maral Amrahli², Michael Wright², Miguel Centelles², Wladyslaw Gedroyc³, Andrew Miller², and Maya Thanou²
- ¹Neuroimaging, King's College London, London, United Kingdom, ²Institute of Pharmaceutical Sciences, King's College London, London, United Kingdom, ³Experimental Medicine, Imperial College London, London, United Kingdom
- We have designed and synthesised a novel liposome formulation, capable of releasing encapsulated drug on targeting/heating by focussed ultrasound (FUS) for cancer therapy and being visualised by MRI due to the incorporation of gadolinium chelates. We show the novel liposomes are targeted to tumours by FUS and MRI-visible *in vivo* and thus, suitable for theranostic applications in cancer.
-
- 3702
Computer #35
Towards Early Detection of Pancreatic Cancers by Active Feedback MR Molecular Imaging
Chaohsiung Hsu¹, Zhao Li¹, Ryan Quiroz¹, Raymond Ngo¹, and Yung-Ya Lin¹

¹Department of Chemistry and Biochemistry, UCLA, Los Angeles, CA, United States

Early detection of pancreatic cancers using enhanced MRI techniques increases not only the treatment options available, but also the patients' survival rate. This can be achieved with antibody-conjugated superparamagnetic iron oxide (SPIO) nanoparticles capable of binding to early stage pancreatic cancer cells to improve imaging specificity and innovation methods that can sensitively detect SPIO to improve imaging sensitivity. The enhanced contrast from SPIO can then be used to visually assess the distribution and magnitude of SPIO-targeted tumor cells. In vivo subcutaneous and orthotopic xenografts mouse models validated the superior contrast/sensitivity and robustness of this approach towards early pancreatic cancers detection.

3703
Computer #36 Real Time Detection of Pancreatic Cancer-induced Cachexia using a Fluorescent Myoblast Reporter and ¹H MRS Metabolic Analysis
Paul Thomas Winnard Jr¹, Santosh Bharti¹, Marie-France Penet¹, Radharani Marik¹, Yelena Mironchik¹, Flonne Wildes¹, Anirban Maitra², and Zaver M Bhujwala¹

¹Russell H. Morgan Department of Radiology and Radiological Science, Johns Hopkins University School of Medicine, Baltimore, MD, United States, ²MD Anderson Cancer Center, Houston, TX, United States

Therapeutic options for cancer-induced cachexia are limited and therefore, efforts to identify signs of precachexia in cancer patients are necessary for early intervention. Here, we generated a myoblast cell line expressing a dual dTomato:GFP construct that was grafted onto the muscle of mice bearing human pancreatic cancer xenografts to provide noninvasive live imaging of events associated with cancer-induced cachexia (i.e., weight loss). ¹H MRS revealed that weight loss in cachectic animals was associated with a depletion of plasma lipid, cholesterol, and valine, and decreased skeletal muscle alanine levels, which may provide informative biomarkers of cachexia.

3704
Computer #37 The effect of SNR optimization on cell quantification accuracy for fluorine-19 MRI sequences: bSSFP, FSE, and FLASH
Kai D. Ludwig¹, Erin B. Adamson¹, Christian M. Capitini^{2,3}, and Sean B. Fain^{1,4,5}

¹Medical Physics, University of Wisconsin-Madison, Madison, WI, United States, ²Pediatrics, University of Wisconsin-Madison, Madison, WI, United States, ³Carbone Cancer Center, University of Wisconsin-Madison, Madison, WI, United States, ⁴Radiology, University of Wisconsin-Madison, Madison, WI, United States, ⁵Biomedical Engineering, University of Wisconsin-Madison, Madison, WI, United States

Several MRI data acquisition methods have been used for fluorine-19 (¹⁹F) MRI cell tracking and optimizing the image SNR helps mitigate low sensitivity. An optimization workflow is presented for three ¹⁹F pulse sequences based upon relaxation parameters measured in a ¹⁹F reference phantom. Bloch simulations reveal signal differences between the reference phantom and pure ¹⁹F cellular label for SNR-optimized bSSFP, FSE, and FLASH. The simulated relative errors in ¹⁹F signal suggest SNR optimization can compromise signal quantification and thus in vivo cell quantification but could provide insight for improved methods to balance the degree of spin-density weighting and SNR.

3705
Computer #38 Effect of exposure in hypoxia environment caused by high altitude on magnetic susceptibility in human brain assessed by quantitative susceptibility mapping
Dandan Zheng¹, Wenjia Liu², Bing Wu¹, and Lin Ma²

¹MR Research China, GE Healthcare, Beijing, China, People's Republic of, ²Radiology Department, Beijing Military General Hospital, Beijing, China, People's Republic of

Cerebrospinal fluid fraction, CBF and T2 decay have been reported to be related with hypoxia caused by high altitude in previous studies. All these biomarkers maybe associate with tissue homogeneous magnetism changes, which may result in the magnetic susceptibility changes. Quantitative susceptibility mapping (QSM) is a novel technique that allows mapping of tissue magnetic susceptibility. It has the potential to be more sensitive with respect to magnetic tissue properties than conventional magnitude-based techniques such as transverse relaxation rates. This study was designed to reveal the effect of exposure in hypoxia environment on magnetic susceptibility in human brain assessed by QSM.

3706
Computer #39 Iron accumulation in rat brain with frequent USPIO administration
Kofi Deh¹, Andrew Gorman², Caspar Schwiedrzik³, Pascal Spincemaille¹, Martin Prince¹, and Yi Wang¹

¹Weill Cornell Medical College, New York, NY, United States, ²Tri-Institutional Training Program in Laboratory Animal Medicine and Science, New York, NY, United States, ³The Rockefeller University, New York, NY, United States

An observation of signal loss on functional MRI images of primates following repeated administration of ultra-small super-paramagnetic iron oxide (USPIO) particles, led us to test a hypothesis of iron accumulation in the brain by performing weekly quantitative susceptibility mapping (QSM) of rats receiving daily USPIO injections for 9 weeks. We observed rapid increase in the susceptibility values in brain ventricles and choroid plexus confirmed by serum iron measurements and histology. In light of a similar report in the literature, we recommend monitoring patients receiving iron therapy with a susceptibility imaging technique such as QSM.

3707
Computer #40 Comparison Study between T2*, Quantitative Susceptibility Mapping (QSM), and Histology for Postmortem Human Substantia Nigra
Jae-Hyeok Lee¹, Sun-Yong Baek², YoungKyu Song³, Sujeong Lim³, Hansol Lee³, Minh Phuong Nguyen⁴, Eun-Joo Kim⁵, Gi Yeong Huh⁶, Se Young Chun⁴, and Hyungjoon Cho³

¹Department of Neurology, Research Institute for Convergence of Biomedical Science and Technology, Pusan National University Yangsan

Hospital, Yangsan, Korea, Republic of, ²Department of Anatomy, Pusan National University School of Medicine, Yangsan, Korea, Republic of, ³Department of Biomedical Engineering, Ulsan National Institute of Science and Technology, Ulsan, Korea, Republic of, ⁴Department of Electrical and Computer Engineering, Ulsan National Institute of Science and Technology, Ulsan, Korea, Republic of, ⁵Department of Neurology, Pusan National University Hospital, Busan, Korea, Republic of, ⁶Department of Forensic Medicine, Pusan National University School of Medicine, Yangsan, Korea, Republic of

Selective iron deposition in the substantia nigra (SN) along with the gradual loss of neuromelanin cell (NMC) is known to be associated with neurodegenerative diseases, such as Parkinson's disease. Postmortem 40-year-old male and 70-year-old female SN tissues were scanned at various spatial resolutions with 7T MRI. The association of $T2^*$ and QSM-derived susceptibility values with quantitative NMC and iron from Perl's Prussian blue staining were investigated with precise co-registration of MRI and histology. We identified that $T2^*$ and susceptibility values for NMC and iron regions, which were segmented from histology were significantly different from corresponding values of background tissue area.

3708

Computer #41

Arterial spin labeling can detect discreet changes of renal perfusion after oral application of the pain medication diclofenac in healthy subjects

Susanne Tewes¹, Marcel Gutberlet¹, Van Dai Vo Chieu¹, Dagmar Hartung¹, Sebastian Rauhut², Matti Peperhove¹, Frank Wacker¹, Faikah Gueler², and Katja Hueper¹

¹Institute for Diagnostic and Interventional Radiology, Hannover Medical School, Hannover, Germany, ²Clinic for Nephrology, Hannover Medical School, Hannover, Germany

Diclofenac is a nonsteroidal anti-inflammatory drug that is frequently prescribed to reduce inflammation and pain. It reduces the prostaglandin-synthesis and may consequently have an effect on renal perfusion. We investigated whether arterial spin labeling can detect reduction of renal perfusion after oral and topical application of diclofenac compared to baseline measurements. Ten healthy subjects underwent functional MRI of the kidney. After oral application of diclofenac renal perfusion was reduced compared to baseline measurements (321 ± 13 vs. 345 ± 16 ml/(min*100g), $p < 0.01$). No significant changes were found after topical application. In conclusion, ASL can detect discreet changes of renal perfusion that occur after application of diclofenac.

3709

Computer #42

Drug Distribution Kinetics in the Eye assessed by 1H-MRI and 19F-MRS

Christina R Haeuser¹, Alfred Ross¹, Markus von Kienlin¹, and Basil Künnecke¹

¹Roche Pharma Research and Early Development, F. Hoffmann-La Roche Ltd, Basel, Switzerland

Drug treatment of vision impairing diseases often involves intraocular drug injection into the vitreous humour, a highly viscous gel-like matter. Drug transport within the vitreous humour has remained rather elusive although transport processes are acknowledged to play a pivotal role for treatment efficacy and adverse effects in the target tissue. Here, we devised a potentially translational approach based on contrast-enhanced 1H-MRI and 19F-MRS to quantitatively ascertain intravitreal drug distribution kinetics at the macro-scale. We provided proof-of-concept for the small drug-like molecule trifluoroethanol in isolated porcine eyes.

3710

Computer #43

Ultra-high field MRI enables the in vivo quantification of the efficacy of candidate promyelinating molecules in the cuprizone mouse model

Isaac Mawusi Adanyeguh¹, Emilie Poirion¹, Daniel García-Lorenzo², Marie-Stephane Aigrot¹, Brahim Nait-Oumesmar¹, Boris Zalc¹, Alexandra Petiet^{1,2}, and Bruno Stankoff^{1,3}

¹Inserm U 1127, CNRS UMR 7225, Sorbonne Universités, UPMC Univ Paris 06 UMR S 1127, Brain and Spine Institute, ICM, F-75013, Paris, France, Paris, France, ²Center for Neuroimaging Research (CENIR), Brain and Spine Institute, 75013 Paris, France, Paris, France, ³AP-HP, Saint Antoine Hospital, Department of Neurology, 184 bd Faubourg Saint Antoine, 75012 Paris, Paris, France

Endogenous remyelination can potentially restore rapid axonal-conduction and confer neuroprotection in chronic demyelinating diseases such as multiple sclerosis. We used T_2 mapping to evaluate the ability of two candidate pharmacological agents to promote remyelination in cuprizone-demyelinated mice. Demyelination was associated with increase in signal intensity and T_2 values in the corpus callosum and external capsules. T_2 values showed spontaneous recovery after discontinuation of cuprizone treatment, an effect accelerated following administration of the two compounds tested. This study confirms that *in vivo* MRI can be used to select pharmacological agents for their therapeutic potential on remyelination.

3711

Computer #44

MRI Assessment of Acute Pathologic Process after Myocardial Infarction: Role of Magnetic Nanoparticle-based MRI

Cheongsoo Park^{1,2}, Eun-Hye Park³, Jongeun Kang^{1,4}, Kiyuk Chang³, and Kwan Soo Hong^{1,4,5}

¹Korea Basic Science Institute, Cheongju, Korea, Republic of, ²The Catholic University of Korea, Seoul, Korea, Republic of, ³Seoul St. Mary's Hospital and College of Medicine, Seoul, Korea, Republic of, ⁴Chungnam National University, Daejeon, Korea, Republic of, ⁵University of Science and Technology, Daejeon, Korea, Republic of

Myocardial infarction (MI) is the major cause of sudden death in most industrialized society. Imaging of early disease progression and investigation of relationship between myocardial necrosis and successive inflammatory response are needed for optimal treatment of MI. We conducted cardiac MR imaging of disease progression in acute MI by using three different MRI methods of Gd (LGE), Mn (ME), and iron oxide nanoparticles (MNP)-based MRI for estimation of infarcted and inflammatory regions.

3712	Computer #45	<p>APT MRI of Intracranial Mass Lesions at 3T and Comparison with DCE Perfusion Parameters Ayan Debnath¹, Prativa Sahoo², Pradeep Gupta³, Rakesh Gupta³, and Anup Singh¹</p> <p><i>¹Centre for Bio-Medical Engineering, Indian Institute of Technology Delhi, Delhi, India, ²Philips India Limited, New Delhi, India, ³Radiology, Fortis Memorial Research Institute, New Delhi, India</i></p> <p>In the current study, Amide Proton Transfer (APT) and T1-weighted DCE perfusion MRI was performed on patients with intra-cranial mass lesions (low and high grade tumors, CNS tuberculoma, CNS lymphoma) at 3T MRI. APT maps provided a significant difference between lesion and its contra-lateral side. From the preliminary study it was observed that APT contrast was low in infection lesion followed by tumor and lymphoma. APT values showed a significant ($P < 0.01$) difference between low and high grade tumors. A weak Inter-class correlation was observed between APT and perfusion parameters (like cbf, cbv, K_{tr}, K_{ep}, v_e). Therefore, APT mapping might improve diagnostic value either alone or in combination with other MRI parameters.</p>
3713	Computer #46	<p>Nuclear Overhauser Enhancement (NOE) mediated Chemical Exchange Saturation Transfer (CEST) imaging in glioma with different progression at 7T Tang Xiangyong¹, Dai Zhuozhi¹, Shen Yuanyu¹, Hu Wei¹, Zhang Zhiyan¹, and Wu Renhua¹</p> <p><i>¹2nd Affiliated Hospital, Shantou University Medical College, Shantou, China, People's Republic of</i></p> <p>Nuclear Overhauser Enhancement (NOE) mediated Chemical Exchange Saturation Transfer (CEST) imaging in glioma with different progression at 7T</p>
3714	Computer #47	<p>A Comparison between the UTE and PETRA Pulse Sequences for Fluorine-19 MRI at 3 Tesla Roberto Colotti¹, Jean Delacoste¹, Giulia Ginami¹, Maxime Pellegrin², Tobias Kober^{1,3,4}, Yutaka Natsuaki⁵, David Grodzki⁶, Ulrich Flögel⁷, Matthias Stuber^{1,8}, and Ruud B. van Heeswijk¹</p> <p><i>¹Department of Radiology, University Hospital (CHUV) and University of Lausanne (UNIL), Lausanne, Switzerland, ²Division of Angiology, University Hospital of Lausanne (CHUV), Lausanne, Switzerland, ³Advanced Clinical Imaging Technology, Siemens Healthcare IM BM PI, Lausanne, Switzerland, ⁴LTSS, École Polytechnique Fédérale de Lausanne, Lausanne, Switzerland, ⁵Siemens Medical Solutions, NAM USA DI MR COLLAB WE, Los Angeles, CA, United States, ⁶Siemens Healthcare GmbH, HC DI MR R&D PLH, Erlangen, Germany, ⁷Department of Cardiovascular Physiology, Heinrich Heine University, Düsseldorf, Germany, ⁸Center for Biomedical Imaging (CIBM), Lausanne, Switzerland</i></p> <p>Fluorine-19 (¹⁹F) MRI of perfluorocarbon emulsions (PFCs) with multiresonant spectra is challenging due to destructive phase interference that leads to short T₂ relaxation times (<10 ms). Pulse sequences with very short echo times (≤ 100 μs) can be used to overcome this challenge. In this study, in vitro and in vivo ¹⁹F MRI obtained with both UTE and PETRA were acquired and quantitatively compared.</p>
3715	Computer #48	<p>On the Feasibility of Quantitative Dynamic Whole Body PET/MR Imaging Hyungseok Jang^{1,2}, Hyung-Jun Im¹, Arman Rahmim³, Steve Y Cho¹, and Alan B McMillan¹</p> <p><i>¹Department of Radiology, University of Wisconsin, Madison, WI, United States, ²Department of Electrical and Computer Engineering, University of Wisconsin, Madison, WI, United States, ³Department of Radiology, Johns Hopkins University, Baltimore, MD, United States</i></p> <p>In this study we investigate the feasibility of FDG PET/MR as a platform for whole body dynamic quantitative PET imaging. The ability of PET/MR systems to provide truly simultaneous imaging is advantageous compared to PET/CT for serial whole body PET acquisitions in that simultaneously acquired MR images can provide additional information to PET data, such as the application of motion parameters estimated from MR images to PET images to correct for misregistration which is not possible with PET/CT. Further improvements in workflow can allow integration of multiple MR contrasts, making dynamic whole body PET/MR a highly feasible and compelling methodology.</p>
Electronic Poster		
<h2>fMRI: Acquisition</h2> <p>Exhibition Hall Wednesday, May 11, 2016: 10:00 - 11:00</p>		
3716	Computer #49	<p>Combined T2*-Weighted Measurements of the Human Brain and Cervical Spinal Cord with Partial Multi-Band Acceleration Jürgen Finsterbusch¹</p> <p><i>¹Systems Neuroscience, University Medical Center Hamburg-Eppendorf, Hamburg, Germany</i></p> <p>Recently, an echo-planar imaging approach has been presented that covers the human brain and cervical spinal cord in the same acquisition in order to investigate the functional connectivity of the two regions. However, the repetition time of this approach (TR) usually exceeds 3 s which is not optimal for a connectivity analysis. Multi-band acceleration is a promising technique to speed up acquisitions, but most neck coil geometries limit its applicability for the cervical spinal cord. In this study, multi-band acceleration is applied to the brain slices only yielding a significantly reduced TR while retaining a good image quality in the cervical spinal cord.</p>

- 3717
Computer #50 Comparison of Physiological Noise in Multiband-EPI and Regular EPI fMRI
Zahra Faraji-Dana^{1,2}, Ali Golestani³, Yasha Khatamian³, Simon Graham^{1,2}, and J. Jean Chen^{1,3}
¹Department of Medical Biophysics, University of Toronto, Toronto, ON, Canada, ²Sunnybrook Research Institute, Sunnybrook Health Science Centre, Toronto, ON, Canada, ³Rotman Research Institute, Baycrest Health Science Centre, Toronto, ON, Canada
- Simultaneous multi-slice echo-planer imaging (EPI) or otherwise known as multiband (MB) EPI provides high temporal and/or spatial resolution in resting-state fMRI (rs-fMRI) studies by modulating and simultaneously imaging multiple slices. However, the effect of slice acceleration on "physiological noise" induced by respiration, cardiac pulsation, variations in respiratory-volume (RVT) and cardiac-rate (CRV) is still unknown. Similar to conventional parallel imaging techniques, residual aliasing occur in MB slice acceleration that could introduce spurious signals into fMRI data. We hypothesize that since a given group of simultaneously acquired slices samples the physiological noise at the same time, the effect of physiological noise may be amplified in MB-EPI. In this study we experimentally verify this hypothesis, and identify the physiological-correction strategy that best corrects this effect.
-
- 3718
Computer #51 Feasibility of line scanning BOLD fMRI on human subjects
Daniel Spitzer¹, Jochen Bauer¹, and Cornelius Faber¹
¹Department of Clinical Radiology, Muenster, Germany
- Line scanning fMRI is a novel technique to probe the BOLD signal with high temporal resolution, which has been previously demonstrated in small animals. Here, we implement line scanning fMRI on a clinical 3 T scanner and probe the BOLD response in human brain with 100 ms temporal resolution. From our data the hemodynamic response can be derived, perfectly matching the response function as observed with conventional fMRI detection methods.
-
- 3719
Computer #52 High resolution gradient-echo EPI using a shim insert coil at 7T: Implication for BOLD fMRI.
Tae Kim¹, Yoojin Lee¹, Tiejun Zhao², Hoby Hetherington¹, and Jullie Pan¹
¹University of Pittsburgh, Pittsburgh, PA, United States, ²Siemens Medical Solution USA, INC, Pittsburgh, PA, United States
- High degree/order shimming was applied to improve field homogeneity thereby reducing susceptibility-induced distortion in high resolution gradient-echo EPI using a shim insert coil at 7T. Use of the shim insert improved the overall homogeneity across the entire brain by 30% in comparison to conventional 1st&2nd degree/order shimming. The susceptibility-induced displacement improved by more than 2cm and the number of activated pixels increased by 150% with higher degree shimming in regions such as the anterior temporal and frontal lobes. Our study demonstrates that the use of higher order/degree shims improves GE-EPI BOLD signal at high field.
-
- 3720
Computer #53 DANTE-EPI for CSF Suppression in Cervical Spinal Cord BOLD fMRI at 7T
Alan Charles Seifert^{1,2}, Hadrien Dyvorne^{1,2}, Joo-won Kim^{1,2}, Bei Zhang³, and Junqian Xu^{1,2,4}
¹Translational and Molecular Imaging Institute, Icahn School of Medicine at Mount Sinai, New York, NY, United States, ²Department of Radiology, Icahn School of Medicine at Mount Sinai, New York, NY, United States, ³Department of Radiology, NYU Langone Medical Center, New York, NY, United States, ⁴Department of Neuroscience, Icahn School of Medicine at Mount Sinai, New York, NY, United States
- A major challenge in spinal cord fMRI is physiological noise due to pulsating CSF, which confounds detection of BOLD signal. In this work, we adapt DANTE to reduce CSF signal contamination in spinal cord BOLD fMRI at 7T. Absolute signal intensity, temporal SNR, and temporal cross-correlation between left and right spinal cord gray matter were measured in DANTE-EPI images at multiple pulse-train lengths and flip angles. Aggressive DANTE preparation suppresses CSF signal, but also significantly reduces spinal cord signal. More conservative DANTE preparation yields an optimal tradeoff between adequate CSF attenuation and preservation of spinal cord signal.
-
- 3721
Computer #54 Optimization of EPI protocols for maximum BOLD sensitivity through numerical simulations
Steffen Volz¹, Martina F. Callaghan¹, Oliver Josephs¹, and Nikolaus Weiskopf^{1,2}
¹Wellcome Trust Centre for Neuroimaging, UCL Institute of Neurology, UCL, London, United Kingdom, ²Department of Neurophysics, Max Planck Institute for Human Cognitive and Brain Sciences, Leipzig, Germany
- fMRI studies can suffer substantially from BOLD sensitivity loss due to susceptibility-related magnetic field inhomogeneities. We developed an automated algorithm for optimising arbitrary EPI protocols with respect to BOLD sensitivity based on numerical simulations and a multi-subject field map database, saving time and expensive measurements. In contrast to previous experimental optimization approaches that were limited e.g. to z-shim, gradient polarity and slice tilt for a specific EPI protocol, this algorithm optimizes on a larger parameter space including resolution, echo time and slice orientation. Results were compared to earlier experimental approaches and verified by BOLD sensitivity measurements in healthy volunteers.
-
- 3722
Computer #55 Improved detection of fMRI activity in ventromedial prefrontal cortex using multi-echo EPI
Brice Fernandez¹, Laura Leuchs², Phillip G. Sämann², Michael Czisch², and Victor I. Spoormaker²
¹Applications and Workflow, GE Healthcare, Munich, Germany, ²Neuroimaging Unit, Max Planck Institute of Psychiatry, Munich, Germany
- Standard fMRI suffers from signal loss in the ventromedial and orbital prefrontal cortex, a region of special interest in affective

neuroimaging. Multi-echo EPI (MEPI) is known to have several advantages over EPI. In this work, we test if MEPI is able to reach better performance in detecting task-induced activation in the ventromedial prefrontal cortex (vmPFC) during fear conditioning, known for eliciting activity in this area. We demonstrate that MEPI (by means of the weighted sum combination approach) outperforms standard EPI in vmPFC, which is highly relevant for affective neuroscience and psychiatry given its critical role in emotion regulation.

3723
Computer #56 Submillimeter spatial and 1 second temporal resolution in fMRI using 3D-EPI-CAIPI with cylindrical excitation
Wietske van der Zwaag^{1,2}, Mayur Narsude³, Olivier Reynaud², Dan Gallichan², and José P. Marques⁴

¹Spinoza Centre for Neuroimaging, Amsterdam, Netherlands, ²EPFL, Lausanne, Switzerland, ³Lausanne, Switzerland, ⁴Donders Institute for Brain, Cognition and Behaviour, Nijmegen, Netherlands

3D-EPI-CAIPI was combined with a cylindrical excitation profile to reduce the brain area from which signal is generated, and hence, the parallel imaging undersampling artefacts and signal loss. This 3D-EPI-CAIPI with cylindrical excitation can be used to acquire fMRI data with submillimetre spatial resolution, 1-second temporal resolution and very high BOLD sensitivity.

3724
Computer #57 Single vs Multi Echo EPI: a Head-to-Head, Within-Session Cross-Over Comparison for Task Evoked and Seed Based Connectivity Analysis
Jed Wingrove¹, Stephen J Wastling¹, Prantik Kundu², Gareth Barker¹, Donal Hill¹, Owen O'Daly¹, and Fernando Zelaya¹

¹Department of Neuroimaging, King's College London, London, United Kingdom, ²Brain Imaging Center, Mount Sinai Hospital, New York, NY, United States

Resting state fMRI data is highly susceptible to low frequency noise fluctuations from motion and pulsatile physiological movement leading to inaccuracies in observed connectivity. In this study we directly compare conventional single echo EPI against a multi echo EPI (ME-EPI) acquisition and analysis method which denoises and cleans acquired fMRI time series. Task evoked and rs-fMRI data was acquired in 8 volunteers and showed improved spatial localisation and discrete clustering in ME-EPI analysis in comparison to single echo data. Furthermore, this work demonstrates the benefits of using ME-EPI for both functional activation and resting state connectivity investigations.

3725
Computer #58 Echo-Time Optimization in Spin Echo EPI using Hypercapnic Manipulation at 3T
Don Marcial Ragot^{1,2} and Jean Chen^{1,2}

¹Medical Biophysics, University of Toronto, Toronto, ON, Canada, ²Roman Research Institute, Toronto, ON, Canada

The optimal echo time (TE) for spin-echo EPI (SE-EPI) BOLD is assumed to be near the tissue T₂ (65–100ms at 3 T), but this was never experimentally tested. In this study, we use a hypercapnia paradigm with SE-EPI at different TEs to identify the TE that maximizes BOLD detection at 3 T. Based on the normalized percent change in BOLD signal ($\Delta\text{BOLD\%/mmHg}$), BOLD contrast-to-noise ratio (CNR/mmHg) and temporal signal-to-noise ratio (tSNR), we concluded that the optimal SE-EPI TE may be much shorter than the tissue T₂, and the optimal TE at 3 T is near 50ms.

3726
Computer #59 A comparison of time-series SNR and Nyquist ghosting with different parallel imaging autocalibration acquisition schemes in 7 T fMRI with a chin task
Pedro Lima Cardoso¹, Jonathan R. Polimeni², Benedikt Poser³, Markus Barth⁴, Siegfried Trattnig¹, and Simon Daniel Robinson¹

¹High Field MR Center, Department of Biomedical Imaging and Image-guided Therapy, Medical University of Vienna, Vienna, Austria, ²Athinoula A. Martinos Center for Biomedical Imaging, Department of Radiology, Harvard Medical School, Massachusetts General Hospital, Charlestown, MA, United States, ³Maastricht Brain Imaging Center, Maastricht University, Maastricht, Netherlands, ⁴Center for Advanced Imaging, University of Queensland, Brisbane, Australia

The present study assesses time-series SNR and residual aliasing (ghosting) levels in accelerated EPI acquisitions at 7 T using single-shot (SS), multi-shot (MS), FLASH and FLEET autocalibration signal acquisition schemes for GRAPPA reconstruction in resting-state and in a chin task (commonly used in fMRI for presurgical planning), which elicits head motion and, consequently, changes in ΔB_0 . FLASH and FLEET acquisitions yielded significantly higher average tSNR values compared to SS and MS in the chin task and no significant residual aliasing enhancement in both resting-state and chin tasks.

3727
Computer #60 The dependence of the BOLD response transients on stimulus type and echo time
Martin Havlicek¹, Dimo Ivanov¹, Benedikt A Poser¹, and Kamil Uludag¹

¹Cognitive Neuroscience, Maastricht University, Maastricht, Netherlands

Adaptation and post-stimulus undershoot observed in the BOLD signal can originate from both active neuronal and passive vascular mechanisms. Using a multi-echo GE-EPI functional MRI sequence with two distinct visual stimuli, we are able to show that not only the BOLD response magnitude but also its shape is affected by the echo-time (TE). As pure oxygenation changes predict approximately a linear scaling of the BOLD signal with TE, this finding indicates that the composition of the underlying physiological mechanisms contributing to the fMRI signal (i.e. CBF, CBV, and CMRO₂) varies over time.

3728
Computer #61 Multiband integrated-SSFP for functional imaging at 7T with reduced susceptibility artifacts
Kaibao Sun^{1,2}, Zhentao Zuo¹, Hanyu Shao¹, Zhongwei Chen^{1,2}, Bo Wang¹, Thomas Martin³, Yi Wang³, Peng Zhang¹, Rong Xue¹, and

Danny JJ Wang³

¹State Key Laboratory of Brain and Cognitive Science, Beijing MRI Center for Brain Research, Institute of Biophysics, Chinese Academy of Sciences, Beijing, China, People's Republic of, ²Graduate School, University of Chinese Academy of Sciences, Beijing, China, People's Republic of, ³Laboratory of fMRI Technology (LOFT), Department of Neurology, UCLA, Los Angeles, CA, United States

BOLD fMRI based on echo-planar imaging (EPI) suffers from susceptibility artifacts that impair imaging in specific brain regions, especially severe at ultrahigh fields. Integrated-SSFP (iSSFP), which is modified from balanced SSFP (bSSFP), shows constant magnitude regardless of frequency shift and is proposed to overcome the obstacle. In our 1st experiment, iSSFP achieved better image quality without banding artifacts and more stable signal changes in visual cortex than bSSFP. In our 2nd experiment, using semantic processing task, more tissue signal and greater activations in the inferior portion of the anterior temporal lobe were detected by multiband iSSFP compared to EPI fMRI.

3729

Computer #62

Calibrated BOLD fMRI with an Optimized ASL-BOLD Dual-Acquisition Sequence

Maria A. Fernandez-Seara¹, Zachary B. Rodgers², Erin K. Englund², Hee-Kwon Song², John A. Detre³, Michael C. Langham², and Felix W. Wehrli²

¹Radiology, University of Navarra, Pamplona, Spain, ²Radiology, University of Pennsylvania, Philadelphia, PA, United States, ³Neurology, University of Pennsylvania, Philadelphia, PA, United States

Calibrated fMRI techniques estimate task-induced changes in the cerebral metabolic rate of oxygen (CMRO₂) based on simultaneous measurements of cerebral blood flow (CBF) and blood-oxygen-level-dependent (BOLD) signal changes evoked by stimulation. To determine the calibration factor M (corresponding to the maximum possible BOLD signal increase), BOLD signal and CBF are measured in response to a gas breathing challenge (CO₂, O₂). Here we describe an ASL dual-acquisition sequence that combines a background-suppressed 3D readout with 2D multi-slice EPI. In five subjects we found an average gray matter M-value of 8.71±1.03 and fractional changes of CMRO₂ of 12.5±5% in response to a bilateral motor task.

3730

Computer #63

Comparison of IVIM and pCASL in the brain

Hannah Hare¹ and Daniel Bulte^{1,2}

¹FMRI, NDCN, University of Oxford, Oxford, United Kingdom, ²Department of Oncology, University of Oxford, Oxford, United Kingdom

IVIM has been proposed as a method of imaging blood volume fraction and perfusion in the brain. In this study we directly compared both the images and the values measured with IVIM to a multi post label delay pCASL sequence in the same imaging session. Although the units are not directly comparable, the images can be visually compared, and it was hypothesised that inter-subject variability in resting CBF in grey matter across subjects would result in a positive correlation between measures from the 2 modalities. Although visually similar, no correlation was observed in the quantitative data.

3731

Computer #64

The effect of diffusion on quantitative BOLD parameter estimates acquired with the Asymmetric Spin Echo technique

Nicholas P Blockley¹, Naomi C Holland¹, and Alan J Stone¹

¹FMRI Centre, Nuffield Department of Clinical Neurosciences, University of Oxford, Oxford, United Kingdom

The results of a recently described streamlined quantitative BOLD (qBOLD) technique suggest that this method may overestimate the deoxygenated blood volume (DBV), leading to an underestimate of the oxygen extraction fraction (OEF). We hypothesise that this is due to the effect of diffusion, which is assumed to be zero in the analytical qBOLD model. In this study we performed Monte Carlo simulations to investigate this hypothesis and found that DBV and OEF measurements were vessel size dependent. However, the R₂' measurements which underlie qBOLD were found to be a reliable measure of deoxyhaemoglobin content above a vessel radius of 10µm.

3732

Computer #65

Submillimeter resolution fMRI in the midbrain: measuring T2* changes to a stop-task

Gilles de Hollander¹, Robert Trampel², Birte Forstmann¹, and Wietske van der Zwaag³

¹Universiteit van Amsterdam, Amsterdam, Netherlands, ²Max Planck Institute for Human Cognitive and Brain sciences, Leipzig, Germany, ³Spinoza Centre for Neuroimaging, Amsterdam, Netherlands

Multi-echo GRE was used to visualise BOLD signal changes in the midbrain, specifically targetting the subthalamic nucleus and substantia nigra, with submillimeter resolution. Midbrain clusters were very small and often only bordered the STN or SN, rather than falling robustly inside it, emphasizing the need for high spatial resolution.

3733

Computer #66

Characterization of ultra-high resolution Gradient Echo and Spin Echo BOLD fMRI in the human visual cortex at 7 Tesla

Catarina Rua^{1,2}, Mauro Costagli^{2,3}, Mark R Symms⁴, Laura Biagi³, Mirco Cosottini^{2,5}, Alberto Del Guerra¹, and Michela Tosetti^{2,3}

¹Department of Physics, University of Pisa, Pisa, Italy, ²Imago7 Research Center, Pisa, Italy, ³IRCCS Stella Maris, Pisa, Italy, ⁴GE Healthcare, Pisa, Italy, ⁵Department of Translational Research and New Technologies in Medicine and Surgery, University of Pisa, Pisa, Italy

This study compared GRE-EPI and SE-EPI sequences with different spatial resolutions at 7T for fMRI in the visual cortex. It is demonstrated that SE-EPI yields higher specificity than GRE-EPI. However, the decreasing temporal signal-to-noise at submillimeter

acquisitions affected significantly the extension of the activated volume in a SE acquisition. At this level, GRE-based functional maps showed significant increased specificity compared to standard resolutions, and a preserved cluster volume. The reduction of partial volume effects allowed the selection of an activation sub-cluster excluding the highest z-scores, which co-localized preferably in non-gray matter, potentially increasing the performance of UHF high-resolution fMRI.

-
- 3734
Computer #67
Whole brain measurements of the hemodynamic response function variability during a finger tapping task at 7T show regional differences in hrf profiles.
Yohan Boilat¹, Rolf Gruetter^{1,2,3}, and Wietske van der Zwaag^{1,4}
¹Ecole Polytechnique Fédérale de Lausanne, Lausanne, Switzerland, ²Universite de Lausanne, Lausanne, Switzerland, ³Universite de Geneve, Geneva, Switzerland, ⁴Spinoza Centre for Neuroimaging, Amsterdam, Switzerland
- The temporal properties of the BOLD response, including inter-trial variability, were studied using a 3D-EPI-CAIPI acquisition at 7T with TR=400ms. The HRFs of six different brain regions in the motor network were characterized, showing a reduced post-stimulus undershoot in the cerebellar regions of interest, as well as differences in peak height, with higher response amplitude in M1 than any other region and onset time, with the cerebellar lobule VIII response starting later than the other ROIs. Trial-to-trial variability was highest in CVIII and lowest in SI.
-
- 3735
Computer #68
The impact of through-slice acceleration on the optimum TE in BOLD-based fMRI: a simulation study
Wietske van der Zwaag¹, David G. Norris², and José P. Marques²
¹Spinoza Centre for Neuroimaging, Amsterdam, Netherlands, ²Donders Institute for Brain, Cognition and Behaviour, Nijmegen, Netherlands
- In this simulation study we evaluate the TE that offers the optimum BOLD contrast per unit time for a given field strength (taking into account the field-specific T_1 , T_2^* and ΔT_2^* values) as a function of the number of slice excitations to acquire the volume (minimum TR achievable), using the Ernst angle for excitation. Generally, optimum BOLD sensitivity is found at TEs closer to T_2^* when shorter TRs (higher multiband acceleration factors) are employed. At longer TRs efficiency constraints tend to make the optimum TE shorter with this effect being more pronounced at lower static fields.
-
- 3736
Computer #69
Evaluation of PCASL Imaging and T2* Mapping for the Assessment of Cerebrovascular Reactivity in the Hippocampus
Xiefeng Li¹, Nicholas Evanoff², Lynn E. Eberly³, Anne M. Murray⁴, Gregory J. Metzger¹, and Donald R. Dengel²
¹Center for Magnetic Resonance Research, School of Medicine, University of Minnesota, Minneapolis, MN, United States, ²Laboratory of Integrative Human Physiology, School of Kinesiology, University of Minnesota, Minneapolis, MN, United States, ³Division of Biostatistics, School of Public Health, University of Minnesota, Minneapolis, MN, United States, ⁴Berman Center for Clinical Research, Hennepin County Medical Center, Minneapolis, MN, United States
- The hippocampus is significantly affected in cognitive impairment, including Alzheimer's disease. Cerebrovascular endothelial dysfunction (CeV-ED) plays an essential role in the initiation and progression of cerebrovascular disease (CeV-D) and cognitive decline. CeV-ED can be assessed with the evaluation of cerebrovascular reactivity (CeV-R) by performing MRI studies with a respiratory challenge, such as the manipulation of end-tidal partial pressure of CO₂ (PetCO₂) and O₂ (PetO₂). In the presented studies, ASL imaging and T₂* mapping were evaluated for the assessment of the CeV-R in the hippocampus to determine the benefits and disadvantages of each imaging method and to facilitate the imaging method selection for future application studies.
-
- 3737
Computer #70
Functional Resolution of Gradient Echo, Asymmetric Spin Echo, and Spin Echo in Functional MRI
Eun Soo Choi¹ and Gary Glover²
¹Electrical Engineering, Stanford University, Stanford, CA, United States, ²Radiology, Stanford University, Stanford, CA, United States
- In BOLD fMRI, gradient-echo and spin-echo pulse sequences have been widely used due to their higher functional sensitivity and spatial specificity, however, fair comparison between SE and GRE methods has often not been made properly. In this study, we defined "functional resolution" as a quantitative metric to evaluate spatial specificity of BOLD contrast fMRI and measured it in SE, asymmetric spin-echo, and GRE. Then we conducted spatial smoothing to equalize their functional resolution and compare their functional sensitivity under the equivalent conditions.
-
- 3738
Computer #71
High resolution IVIM in brain using readout-segmented EPI
Hannah Hare¹, Robert Frost¹, and Daniel Bulte^{1,2}
¹FMRIB, NDCN, University of Oxford, Oxford, United Kingdom, ²Department of Oncology, University of Oxford, Oxford, United Kingdom
- 1mm isotropic diffusion-weighted images were acquired with readout-segmented EPI at 3T to investigate the effects of partial voluming on the IVIM-derived measures of perfusion and blood volume. The maps produced showed no contrast between white and grey matter, and very high signal from CSF. Both the grey and white matter curves were adequately fitted using a monoexponential model, and only the CSF required a biexponential to fit the data. This suggests that the biexponential signal behaviour typically observed at lower resolutions may arise primarily from the CSF rather than the blood compartment.
-
- 3739
Reduction of run-to-run variability of temporal SNR in accelerated EPI time-series data through FLEET-based robust autocalibration

¹Athinoula A. Martinos Center for Biomedical Imaging, Department of Radiology, Harvard Medical School, Massachusetts General Hospital, Charlestown, MA, United States, ²Siemens Medical Solutions USA Inc., Charlestown, MA, United States, ³Harvard-MIT Division of Health Sciences and Technology, Massachusetts Institute of Technology, Cambridge, MA, United States

Temporal signal-to-noise ratio (tSNR) provides a crucial metric determining sensitivity of the acquisition to BOLD fMRI measurements. It has been shown that tSNR may vary dramatically between multiple runs of accelerated single-shot EPI acquisitions using single- or multi-shot EPI to acquire autocalibration or ACS data. We applied noise-to-noise ratio (NNR) measure to map run-to-run variability of acquisitions using conventional multi-shot EPI ACS data as well as recently proposed Fastlow-angle excitation echo-planar technique (FLEET) ACS. tSNR variability between multiple runs improved in acquisitions using FLEET-ACS, providing the potential to increase sensitivity of BOLD fMRI experiments.

Electronic Poster

Brain Connectivity with fMRI

Exhibition Hall

Wednesday, May 11, 2016: 10:00 - 11:00

3740



Computer #73 Identifying Foci of Brain Disorders from Effective Connectivity Networks
D Rangaprakash¹, Gopikrishna Deshpande^{1,2,3}, Archana Venkataraman⁴, Jeffrey S Katz^{1,2,3}, Thomas S Denney^{1,2,3}, and Michael N Dretsch^{5,6}

¹AU MRI Research Center, Department of Electrical and Computer Engineering, Auburn University, Auburn, AL, United States, ²Department of Psychology, Auburn University, Auburn, AL, United States, ³Alabama Advanced Imaging Consortium, Auburn University and University of Alabama Birmingham, Birmingham, AL, United States, ⁴Department of Diagnostic Radiology, Yale University, New Haven, CT, United States, ⁵U.S. Army Aeromedical Research Laboratory, Fort Rucker, AL, United States, ⁶Human Dimension Division, HQ TRADOC, Fort Eustis, VA, United States

Brain connectivity studies report statistical differences in pairwise connection strengths. While informative, such results are difficult to interpret, since our understanding of the brain relies on region information, rather than connections. Given that large effects in natural systems are likely caused by few pivotal sources, we employed a novel framework to identify sources of disruption from directional connectivity. Using resting-state fMRI, we employed static and time-varying effective connectivities in a probabilistic framework to identify affected foci and associated affected connections. We illustrate its utility in identifying disrupted foci in Soldiers with post-traumatic stress disorder and mild traumatic brain injury.

3741

Computer #74 Brain Connectivity Network Dynamics Are Correlated with Cognitive Performance in Multiple Sclerosis
Sue-Jin Lin^{1,2}, Aiping Liu³, Alex MacKay^{4,5}, Brenda Kosaka⁶, Samantha Beveridge⁷, Irene Vavasour⁵, Anthony Traboulsee⁸, and Martin J McKeown^{1,2,8}

¹Graduate Program in Neuroscience, University of British Columbia, Vancouver, BC, Canada, ²Pacific Parkinson's Research Centre, University of British Columbia Hospital, Vancouver, BC, Canada, ³Department of Electrical and Computer Engineering Program, University of British Columbia, Vancouver, BC, Canada, ⁴Department of Physics and Astronomy, University of British Columbia, Vancouver, BC, Canada, ⁵Department of Radiology, University of British Columbia Hospital, Vancouver, BC, Canada, ⁶Department of Psychiatry, University of British Columbia Hospital, Vancouver, BC, Canada, ⁷Graduate Program in Counselling Psychology, University of British Columbia, Vancouver, BC, Canada, ⁸Neurology, Faculty of Medicine, University of British Columbia, Vancouver, BC, Canada

Brain connectivity networks are usually estimated with the assumption that neural networks do not change over time. However, functional connectivity is inherently non-stationary, changing across time from seconds to minutes. In healthy subjects, dynamic reconfiguration of functional connectivity assessed by fMRI has been estimated and has been linked to cognitive tests, indicating that flexibility of connectivity normally contributes to cognitive performance. In this study, we applied a novel time-varying analysis to study network dynamics in healthy controls and subjects with Multiple Sclerosis (MS).

3742

Computer #75 Parcellation-based connectome assessment by using structural and functional connectivity
Ying-Chia Lin¹, Tommaso Gili^{2,3}, Sotirios A. Tsaftaris^{1,4}, Andrea Gabrielli⁵, Mariangela Iorio³, Gianfranco Spalletta³, and Guido Caldarelli¹

¹IMT Institute for Advanced Studies Lucca, Lucca, Italy, ²Enrico Fermi Centre, Rome, Italy, ³IRCCS Fondazione Santa Lucia, Rome, Italy, ⁴Institute of Digital Communications, School of Engineering, The University of Edinburgh, Edinburgh, United Kingdom, ⁵ISC-CNR, UOS Sapienza, Dipartimento di Fisica, Universita Sapienza, Rome, Italy

Connectome analysis of the human brain structural and functional architecture provides a unique opportunity to understand the organization of brain networks. In this work, we investigate a novel large scale parcellation-based connectome, merging together information coming from resting state fMRI (rs-fMRI) data and diffusion tensor imaging (DTI) measurements.

3743

Computer #76 Group NMF Analysis for Resting State fMRI
Bhushan Patil¹, Mahesh Panicker¹, Radhika Madhavan¹, and Suresh Joel¹

¹Global Research, General Electric Global Research, Bangalore, India

Clustering of resting state fMRI signals for extraction of functional brain networks has been showed to provide value in recent times. Independent component analysis (ICA) is the most commonly used technique to extract functional brain networks. More recently non-negative matrix factorization (NMF) has been successfully utilized for identification of brain functional networks in single-subject resting state fMRI data. NMF may provide complementary information for analyzing resting state fMRI data. However, the technique has not been extended to provide group inferences. This is non-trivial, since the components obtained from single subject NMF is not ordered. Using temporal concatenation, similar to group ICA, we introduce a new framework for back reconstruction of individual subject from group analysis using NMF. This framework will make comparisons between groups possible for NMF.

-
- 3744
Computer #77
Mixed ICA and Clustering Method Introduced to Study the Life Span Changes in the Within-Network Functional Connectivity of the Default Mode Network
Isa Costantini¹, Ottavia Dipasquale^{1,2}, Laura Pelizzari^{1,2}, Maria Marcella Laganà², Francesca Baglio², and Giuseppe Baselli¹
¹Department of Electronics, Information and Bioengineering, Politecnico di Milano, Milan, Italy, ²IRCCS, Don Gnocchi Foundation, Milan, Italy
- This study combines the independent component analysis and a local clustering method in order to study the within-network functional connectivity of the default mode network (DMN). Our results strongly support the hypothesis that the long-range FC between anterior and posterior DMN increases from the childhood to the young adulthood and slowly decreases with aging. This joint approach allowed us to obtain more detailed information about within-network FC changes among the DMN sub-regions.
-
- 3745
Computer #78
A novel sparse partial correlation method for simultaneous estimation of functional networks in group comparisons
Xiaoyun Liang¹, David Vaughan^{2,3}, Alan Connelly^{1,4}, and Fernando Calamante^{1,4}
¹Imaging Division, Florey Institute of Neuroscience and Mental Health, Melbourne, Australia, ²Epilepsy Division, Florey Institute of Neuroscience and Mental Health, Melbourne, Australia, ³Department of Neurology, Austin Health, Melbourne, Australia, ⁴Department of Medicine, University of Melbourne, Melbourne, Australia
- We propose a novel approach, Graphical-Lasso with Stability-Selection (GM-GLASS), by employing sparse group penalties for simultaneously estimating networks from healthy control and patient groups. Simulations demonstrate that both GM-GLASS and JGMSS outperform Fisher Z-transform. Our in vivo results further show that GM-GLASS yields highest contrast of network metrics between groups, demonstrating the superiority of GM-GLASS in detecting significance group differences over JGMSS and Fisher Z-transform. Overall, by controlling confounding variations between subjects, and therefore enhancing the statistical power, our simulated and in vivo results demonstrate that GM-GLASS provides a robust approach for conducting group comparison studies.
-
- 3746
Computer #79
Characterizing cross session coherence in the resting-state human brain
Shuqin Zhou¹, Xiaopeng Song¹, Yue Cai¹, Xuemei Fu¹, and Jiahong Gao²
¹Department of Biomedical Engineering, Peking University, Beijing, China, People's Republic of, ²Center for MRI Research and Beijing City Key Lab for Medical Physics and Engineering, Peking University, Beijing, China, People's Republic of
- Previous studies suggested that the BOLD signal might be a mixture of different frequency components, but the neurophysiological basis of these components is still unclear. In this study, we attempted to quantify the similarity of the frequency profiles of the resting-state BOLD signals in different sessions by computing the cross session coherence (CSC) of these components. Our results suggested that different frequency components of BOLD signal in the brain might be associated with distinct intrinsic neuronal oscillations rather than random noise.
-
- 3747
Computer #80
Dynamic Reconfiguration of Intrinsic Functional Connectivity: A Probabilistic Framework
Dazhi Yin¹, Kristina Zeljic¹, Zhiwei Wang¹, Qian Lv¹, and Zheng Wang¹
¹Institute of Neuroscience, Chinese Academy of Sciences, Shanghai, China, People's Republic of
- Neural basis enabling flexible behavior remains largely unknown. Based on the spatiotemporal dynamics of intrinsic functional connectivity, we proposed a probabilistic modeling framework to quantify the functional flexibility and integration of different brain regions. We then applied this framework to investigate the functional representation of hand preference. Our findings revealed higher functional flexibility and integration for the preferred hand that controls cognitive-motor requirements for skilled movements.
-
- 3748
Computer #81
The long-term reproducibility of stimulation and resting state fMRI in the mouse
Yi-Ching Lynn Ho^{1,2}, Fiftarina Puspitasari¹, and Kai-Hsiang Chuang¹
*¹Singapore Bioimaging Consortium, Agency for Science, Technology & Research (A*STAR), Singapore, Singapore, ²Interdisciplinary Institute of Neuroscience & Technology (ZIINT), Zhejiang University, Hangzhou, China, People's Republic of*
- There is a need to evaluate the long-term reproducibility of stimulation and resting state fMRI in the mouse, given the technical challenges of mouse fMRI. We compared 2 sessions of scans done between 3-9 weeks apart on 7 C57BL/6 mice. The intraclass correlation (ICC) indicated significant absolute agreement for forepaw stimulation fMRI results. Interhemispheric functional connectivity scores for a large subcortical area like the CPU were also found to be reproducible, but in a small cortical area like the S1FL, reproducibility did not reach significance. Possible reasons include data coregistration mismatches due to distortion and susceptibility artifacts.

-
- 3749
Computer #82 Effects of Anesthesia on Functional Connectivity in Primary Somatosensory Cortex in Monkeys
Tung-Lin Wu^{1,2}, Arbinda Mishra¹, Feng Wang^{1,3}, Li Min Chen^{1,3}, and John C. Gore^{1,2,3}
- ¹Vanderbilt University Institute of Imaging Science, Nashville, TN, United States, ²Biomedical Engineering, Vanderbilt University, Nashville, TN, United States, ³Radiology and Radiological Sciences, Vanderbilt University, Nashville, TN, United States*
- Low-frequency fluctuation of resting state functional MRI (rsfMRI) signals have been linked to changes in the spontaneous neuronal activity, but their relationships have not been established. Anesthesia is known to suppress neuronal activity. Thus, by examining the effects of different levels of anesthesia on changes in inter-regional functional connectivity and the power spectra, we will be able to assess the neuronal origins of the rsfMRI signals. We carried out live anesthetized squirrel monkey experiments that measure how low frequency fluctuations and inter-regional functional connectivity within a small local network (primary somatosensory cortex) vary as isoflurane levels are altered in a small range.
-
- 3750
Computer #82 Chronic RF-coil and electrode implantation approach for long-term EEG-fMRI studies in rodents
Tiina Pirttimäki¹, Artem Shatillo¹, Mikko Kettunen¹, Jaakko Paasonen¹, Raimo Salo¹, Alejandra Sierra Lopez¹, Kimmo Jokivarsi¹, Ville Leinonen², Simon Quittek³, Asla Pitkänen¹, and Olli Gröhn¹
- ¹Neurobiology, A.I.Virtanen Institute for Molecular Medicine, University of Eastern Finland, Kuopio, Finland, ²Institute of Clinical Medicine - Neurosurgery, University of Eastern Finland and Neurosurgery of NeuroCenter, Kuopio University Hospital, Kuopio, Finland, ³RAPID Biomedical GmbH Technologiepark Wuerzburg-Rimpar, Rimpar, Germany*
- Simultaneous EEG-fMRI is routinely used in clinical settings as it provides better temporal and spatial information for example when locating seizure onset zones. In pre-clinical research with small rodents, obtaining simultaneous EEG-fMRI in longitudinal studies has been challenged by a number of problems including issues related to magnetic susceptibility artifacts. Here, we demonstrate a modified method for permanent MRI coil and EEG electrode implantation that is suitable for long-term chronic follow-up studies on epileptogenesis with improved data consistency across imaging and video-EEG monitoring sessions.
-
- 3751
Computer #84 Longitudinal resting-state fMRI and 1H-MRS characterization in the mouse brain during development of a chronic pain state
David Bühlmann^{1,2}, Joanes Grandjean¹, Giovanna Diletta Ielacqua¹, Jael Xandry³, and Markus Rudin^{1,3}
- ¹Institute for Biomedical Engineering, ETH and University of Zurich, Zurich, Switzerland, ²Neuroscience Center Zurich, Zurich, Switzerland, ³Institute of Pharmacology & Toxicology, University of Zurich, Zurich, Switzerland*
- We performed longitudinal resting-state fMRI and single voxel ¹H-MRS in a mouse model of chronic pain derived from bone cancer. Linear mixed model analysis of independent components revealed significant functional changes mostly in limbic but also cortical networks. These findings were reproducible across strains and mirror findings from clinical studies on chronic back pain patients. ¹H-MRS in the affected ventral hippocampus yielded significant decreases in glutamate, myo-inositol and glycerylphosphorylcholine concentrations in tumor-animals as well as increased glutamine levels. Given the translatability, these readouts could potentially be used to evaluate novel treatments specifically for chronic pain.
-
- 3752
Computer #85 Monitoring longitudinal functional reorganization of a capsular infarct rat model using resting-state fMRI
Chun-Qiang Lu¹ and Shenghong Ju^{1,2}
- ¹Southeast University, Nanjing, China, People's Republic of, ²ZhongDa Hospital, Nanjing, China, People's Republic of*
- Many resting-state fMRI studies in stroke patients claim that rs-fMRI measurements is behaviorally relevant. However, most of these studies enroll stroke patients with high heterogeneity. In this study, twenty-three rats underwent photothrombotic stroke lesioning in the PLIC with minimal affect to the nearby area. We monitor longitudinal resting-state brain activity and behavior change in this highly homogeneous white matter infarct rat model by using fcMRI and rat behavior test and try to find out the most behaviorally relevant fcMRI measurements. This project is still going on.
-
- 3753
Computer #86 Metabolic and functional connectivity of the rat brain during resting state assessed by simultaneous [18F]FDG-PET/MR
Andre Thielcke¹, Mario Amend¹, Suril Gohel², Bharat Biswal², Bernd J. Pichler¹, and Hans F. Wehr¹
- ¹Department of Preclinical Imaging and Radiopharmacy, Werner Siemens Imaging Center, Eberhard Karls University of Tuebingen, Tuebingen, Germany, ²Department of Biomedical Engineering, New Jersey Institute of Technology, Newark, NJ, United States*
- Recent advancement in hardware and software has enabled researchers to study systems level neuroscience using simultaneous PET/MRI. In this study, simultaneous PET/MR was used to investigate resting state networks (RSN) in rats, comparing [18F]FDG PET vs. BOLD-fMRI. RSNs such as default mode network (DMN) have been shown to be disrupted in clinical populations. ICA and ROI-analysis was used to elucidate the complementary nature between PET/MR and visualize brain connectivity. ICA PET and MR data showed prominent RSNs. However, ROI-analysis illustrated different connectivity between network-involved areas. This work suggests the complementary nature of metabolic connectivity mapping (Cometomics).
-
- 3754
Computer #87 Decoupling flow effects on functional connectivity using R2* resting-state fMRI
Venkata Veerendranadh Chebrolu¹, Brice Fernandez², Suresh E Joel¹, Bharath Sundar¹, Luca Marinelli³, Rakesh Mullick¹, Victor I

Spoormaker⁴, Michael Czisch⁴, and Thomas K Foo³

¹GE Global Research, Bangalore, India, ²GE Healthcare, Munich, Germany, ³GE Global Research, Niskayuna, NY, United States, ⁴Max Planck Institute of Psychiatry, Munich, Germany

In this work we compare whole brain functional connectivity (FC) estimates from R2* resting-state fMRI (rs-fMRI) with BOLD rs-fMRI. Thirty-two healthy subjects were imaged using three-echo multi-echo echo-planar-imaging (MEPI) under institutional guidelines. FC matrices based on structural and functional brain parcellation schemes were computed for individual BOLD echoes, R2* and M (initial magnetization approximated by BOLD signal at TE=0). Results tend to show that M might be helpful to decouple flow effects. Positive between network connectivity was observed in BOLD, M and R2* derived matrices. Anti-correlations observed between networks in BOLD and M were significantly lesser in R2* derived matrices.

3755

Computer #88

Evaluation of Resting State Network by Pupil Diameter Monitoring during fMRI Measurements – The Relationship between the Stability of the Pupil Diameter and the Activation in the Posterior Cingulate

Toshiharu Nakai¹, Keiji Matsuda², Sachiko Kiyama¹, and Ichiro Takashima²

¹NeuroImaging & Informatics, NCGG, Ohbu, Japan, ²Human Informatics Research Institute, AIST, Tsukuba, Japan

The status of the resting state performance was evaluated by using pupil diameter monitoring during fMRI sessions. The activation in the posterior cingulate was higher in the subjects who kept constant pupil diameters than those with time decay, suggesting that attempts to keep eyes open and fix them to the cross mark target may demand higher consciousness level. In other resting state networks (RSNs), no significant effect was confirmed suggesting that the RSNs are robust and not strongly affected by the tension or eye closing for a short time.

3756

Computer #89

Resting-state fMRI fails to detect disease progression in a multicenter randomized clinical trial of Alzheimer's disease

Coimbra Alexandre¹, Farshid Faraji¹, Alexander de Crespigny¹, Lee Honigberg¹, Robert Paul¹, and David Clayton¹

¹Research and Early Development, Genentech, South San Francisco, CA, United States

RS-fMRI was implemented in two multicenter clinical trials of a novel therapeutic for AD. Although data of good quality were acquired, none of three functional connectivity metrics (FCMs) showed significant progression associated with disease in placebo-treated patients: changes in connectivity in this mild-to-moderate AD population were less than the measurement precision. Significant cognitive decline and brain atrophy were observed. Test-retest precision was similar to other single-center studies. Operational and acquisition improvements could increase data quality (though difficult in multicenter trials), but more sensitive analysis will be needed for RS-fMRI to be a useful tool for the development of AD therapeutics.

3757

Computer #90

Increased functional connectivity associates with the improved emotion regulation after 8-week mindfulness-based stress reduction (MBSR) training using resting-state fMRI analysis

Yao-Chia Shih^{1,2}, Chang-Le Chen^{2,3}, Shih-Chin Fang⁴, Tzung-Kuen Wen⁵, Da-Lun Tang⁶, Si-Chen Lee⁷, and Wen-Yih Issac Tseng^{2,3,8}

¹Institute of Biomedical Engineering, National Taiwan University, Taipei, Taiwan, ²Institute of Medical Device and Imaging, National Taiwan University College of Medicine, Taipei, Taiwan, ³Graduate Institute of Brain and Mind Sciences, College of Medicine, National Taiwan University, Taipei, Taiwan, ⁴Department of Neurology, Cardinal Tien Hospital Yonghe Branch, New Taipei City, Taiwan, ⁵Department of Buddhist Studies, Dharma Drum Institute of Liberal Arts, New Taipei City, Taiwan, ⁶Department of Mass Communication, Tamkang University, Taipei, Taiwan, ⁷Department of Electrical Engineering, National Taiwan University, Taipei, Taiwan, ⁸Molecular Imaging Center, National Taiwan University, Taipei, Taiwan

Mindfulness-based stress reduction (MBSR) is modified from Buddhist traditions and aims to improve self-regulation. In this study, we employed the resting-state functional MRI to investigate changes of functional connectivity (FC) before and after MBSR practice, and before and after 8-week MBSR training. We hypothesized that changes in FC may reflect improvements of self-regulation after MBSR training. We found MBSR strengthened FC couplings of right subgenual anterior cingulate cortex and lateral middle orbitofrontal cortex with posterior cingulate cortex in the beginners after 8-week MBSR training. Our findings reveal an underlying neural mechanism of positive effects of MBSR practice on emotional regulation.

3758

Computer #91

Pattern classification reveals functional connectivity differences in expert and novice meditators

Roberto Guidotti^{1,2}, Mauro Gianni Perrucci^{1,2}, Cosimo Del Gratta^{1,2}, Antonino Raffone³, and Gian Luca Romani^{1,2}

¹Neuroscience, Imaging, and Clinical Sciences, Gabriele D'Annunzio University Chieti-Pescara, Chieti, Italy, ²Institute for Advanced Biomedical Technologies, Gabriele D'Annunzio University Chieti-Pescara, Chieti, Italy, ³Psychology, La Sapienza University Rome, Rome, Italy

In this work we explored how experience modulates ROI-based fMRI functional connectivity patterns in two different meditators groups: experts and novices. We recorded fMRI data during two styles of meditation (focused attention (Samatha), and open monitoring (Vipassana)), in two groups of subjects (Buddhist Theravada Monks, and novices), and we calculated the connectivity pattern between ROIs from the AAL90 atlas. We then used a pattern classification approach to discriminate these groups and find which connections and nodes are important to classify subject experience. Regions having a role in decoding were those implicated in self-awareness and attention control.

3759

Computer #92

Long-term and acute cannabis effects on brain networks

Isabelle Berger^{1,2,3}, Philippe Maeder¹, Jean-Marie Annoni⁴, Haithem Chtioui⁵, Christian Giroud⁶, Bernard Favrat⁷, Kim Dao⁵, Marie Fabritius⁶, Jean-Frédéric Mall⁸, Giovanni Battistella^{1,9}, Reto Meuli¹, and Eleonora Fornari^{1,2}

¹Department of Radiology, Centre Hospitalier Universitaire Vaudois (CHUV), and University of Lausanne, Lausanne, Switzerland, ²CIBM (Centre d'Imagerie Biomédicale), Centre Hospitalier Universitaire Vaudois (CHUV) unit, Lausanne, Switzerland, ³Department of Neurology, Besançon University Hospital, Besançon, France, ⁴Neurology Units, Department of Medicine, University of Fribourg, Fribourg, Switzerland, ⁵Department of Clinical Pharmacology and Toxicology, Centre Hospitalier Universitaire Vaudois CHUV, Lausanne, Switzerland, ⁶CURML (University Center of Legal Medicine), UTFC (Forensic Toxicology and Chemistry Unit), Lausanne, Switzerland, ⁷CURML (University Center of Legal Medicine), UMPT (Unit of Psychology and Traffic Medicine), Lausanne, Switzerland, ⁸Department of Psychiatry, SUPAA (Service Universitaire de Psychiatrie de l'Age Avancé), CHUV, Lausanne, Switzerland, ⁹Department of Neurology, Icahn School of Medicine at Mount Sinai, New York, NY, United States

The purpose of our study was to reveal the changes in functional networks due to chronic and acute cannabis use, and to highlight the anterior insula specific involvement. We explored changes in functional connectivity by means of ICA and seed-based methods. Long-term cannabis use leads to an attenuation of the engagement of the Salience Network regions. The further decrease of activity after acute consumption can reflect the decrease of subject awareness in their performances, or a modulation of networks interplay. Modifications revealed by seed-based connectivity analysis support and clarify the insular role in cannabis addiction.

3760

Computer #93

Wavelet variance analysis of brain resting state temporal dynamics reveals role of precuneus to reach and sustain abnormal default-mode network activity in major depressive disorder

Masaya Misaki¹, Hideo Suzuki¹, Jonathan Savitz^{1,2}, Brett McKinney³, and Jerzy Bodurka^{1,4}

¹Laureate Institute for Brain Research, Tulsa, OK, United States, ²Dept. of Medicine, Tulsa School of Community Medicine, University of Tulsa, Tulsa, OK, United States, ³Tandy School of Computer Science, Dept. of Mathematics, University of Tulsa, Tulsa, OK, United States, ⁴College of Engineering, University of Oklahoma, Tulsa, OK, United States

We investigated temporal dynamics of resting-state brain activation in BOLD resting-state networks (RSNs) in patients with major depressive disorder (MDD) and healthy controls (HC). The wavelet variance analysis was applied to the RSNs time courses to assess frequency specific temporal fluctuations. Comparing to HC, MDD subjects had significantly lower fluctuation in the default-mode network (DMN) and the high-visual network in 0.031-0.125Hz and higher fluctuation in the language/auditory and the cerebellum networks in 0.125-0.25Hz and 0.0156-0.031Hz. The low DMN fluctuation in MDD was associated with high precuneus activity that triggered increase of DMN activity.

3761

Computer #94

Staging Alzheimer's Disease Risk by Sequencing Brain Function and Structure, Cerebrospinal Fluid, and Cognition Biomarkers

Guangyu Chen¹, Hao Shu¹, Gang Chen¹, Barney Douglas Ward¹, Piero G Antuono², and Shi-Jiang Li¹

¹biophysics, medical college of wisconsin, milwaukee, WI, United States, ²Neurology, medical college of wisconsin, milwaukee, WI, United States

A robust temporal ordering sequence of biomarkers for staging the Alzheimer's disease (AD) progression risk is revealed by integrating brain function and structure, cerebrospinal fluid (CSF), and cognition biomarkers into an event-based model. In this study, we found that functional abnormality in the hippocampus and posterior cingulate cortex networks is the earliest event in the preclinical phase of AD, even antedating the detectable CSF A β and p-tau abnormalities; this sheds light on the link between preclinical AD status and its symptomatic onset for accurately identifying progressive AD trajectories along the disease course, given the condition that disease onset is insidious.

3762

Computer #95

The effect of preterm birth on the thalamocortical development during the neonatal stage: A resting-state fMRI study

Yue Cai¹, Xiushuang Wu², Yuan Shi³, Lizhi Xie⁴, and Jiahong Gao⁵

¹Biomedical Engineering, Peking University, Beijing, China, People's Republic of, ²Department of Pediatrics, Daping Hospital, Third Military Medical University, Chong Qing, China, People's Republic of, ³Department of Pediatrics, Daping Hospital, Third Military Medical University, Chongqing, China, Chong Qing, China, People's Republic of, ⁴GE Healthcare, MR Research China, Beijing, Beijing, China, People's Republic of, ⁵Center for MRI Research and Beijing City Key Lab for Medical Physics and Engineering, Peking University, Beijing, China, People's Republic of

Preterm birth is a leading cause of cognitive impairment in childhood and is associated with cerebral gray and white matter abnormalities. Using the resting-state fMRI imaging analysis, we tested the hypothesis that preterm birth might to some extent affect the thalamo-cortical connections particularly in the thalamo-SM and thalamo-SA projections. Reduced thalamo-SM and increased thalamo-SA connectivity were found in the preterm newborns, and preterm with punctate white matter lesions (PWMLs) exhibited a more sever trend in the thalamo-SA projection.

3763

Computer #96

Aberrant functional connectivity of resting state networks in subclinical hypothyroidism

Mukesh Kumar¹, Ritu Tyagi¹, Prabhjot Kaur¹, Subash Khushu¹, Maria M D'souza¹, Tarun Sekhri², Ratnesh Kanwar², and Poonam Rana¹

¹NMR Research Center, Institute of Nuclear Medicine and Allied Science, Delhi, India, ²Thyroid research centre, Institute of Nuclear Medicine and Allied Science, Delhi, India

Cognitive deficit in Subclinical hypothyroidism (SCH) patient is still a topic to research work upon. The present study was conducted to examine resting state networks (RSNs) in SCH using rsfMRI. SCH patients showed significantly decreased functional connectivity in right fronto-parietal network and anterior default mode network (DMN) as compared with control subjects. Our finding suggests cognitive impairment in resting state networks related to attention and emotional processing in SCH patients

fMRI Multimodal

Exhibition Hall

Wednesday, May 11, 2016: 11:00 - 12:00

-
- 3764 **Computer #1** Altered gray matter volume, cerebral blood flow and functional connectivity in chronic stroke patients: a multi-modal MRI study
Peifang Miao¹, Caihong Wang¹, Peng Li¹, Jingliang Cheng¹, Dandan Zheng², and Zhenyu Zhou²
- ¹MRI, The First Affiliated Hospital of Zhengzhou University, Zhengzhou, China, People's Republic of, ²GE Healthcare MR Research, Beijing, China, People's Republic of
- In order to investigate the cerebral plasticity in chronic stroke patients well-recovered in global motor function, 29 patients and 30 healthy subjects were recruited to undergo multi-modal MRI techniques. Group comparisons in gray matter volume(GMV), cerebral blood flow(CBF) and resting-state functional connectivity(rsFC) were assessed. Compared with healthy controls, patients exhibited increased GMV in contralesional supplementary motor area, increased CBFs in contralesional superior frontal gyrus and supramarginal gyrus, and increased rsFC in contralesional middle temporal gyrus. The results suggested cerebral structure plasticity, perfusion aberrant and functional reorganization coexist in well-recovered subcortical stroke patients, which may underlie functional recovery of stroke patients.
-
- 3765 **Computer #2** Machine learning approach to classify Alzheimer disease and Vascular Dementia using MRI quantitative metrics
Elia Tagliani¹, Gloria Castellazzi^{1,2}, Andrea De Rinaldis^{1,2}, Fulvia Palesi^{2,3}, Letizia Casiraghi^{2,4}, Elena Sinforiani⁵, Paolo Vitali⁶, Nicoletta Anzalone⁷, Giovanni Magenes¹, Claudia AM Gandini Wheeler-Kingshott^{2,8}, Giuseppe Miceli⁹, and Egidio D'Angelo^{2,4}
- ¹Department of Electrical, Computer and Biomedical Engineering, University of Pavia, Pavia, Italy, ²Brain Connectivity Center, C. Mondino National Neurological Institute, Pavia, Italy, ³Department of Physics, University of Pavia, Pavia, Italy, ⁴Department of Brain and Behavioral Sciences, University of Pavia, Pavia, Italy, ⁵Neurology Unit, C. Mondino National Neurological Institute, Pavia, Italy, ⁶Brain MRI 3T research center, C. Mondino National Neurological Institute, Pavia, Italy, ⁷Scientific Institute H. S. Raffaele, Milan, Italy, ⁸NMR Research Unit, Queen Square MS Centre Department of Neuroinflammation, UCL Institute of Neurology, London, United Kingdom, ⁹Department of Emergency Neurology, C. Mondino National Neurological Institute, Pavia, Italy
- Despite the large number of studies on dementia, efforts to define a clear profile of cognitive impairment for Vascular Dementia (VaD), as well as its differentiation from Alzheimer Disease (AD), are still poor. In this study we tested the power of imaging metrics and adopted a data mining approach, based on Diffusion Tensor Imaging and resting state fMRI, to assess the reliability of machine learning approaches for the automated diagnosis of AD and VaD. Our results show that machine learning algorithms are able to discriminate VaD from AD, representing a suitable approach to build an automated diagnostic system for dementia-like diseases.
-
- 3766 **Computer #3** A Preliminary Study of Major Depressive Disorder Using Simultaneous PET/fMRI with Two MID Tasks in a Single Scan
Fuyixue Wang¹, Paul Hamilton², Brian Knutson², Ian Gotlib², Matthew Sacchet², Hershel Mehta², Christina Schreiner², Dawn Holley³, Fred Chin³, Bin Shen³, Greg Zaharchuk³, Mehdi Khalighi⁴, and Gary Glover³
- ¹Department of Biomedical Engineering, Tsinghua University, Beijing, China, People's Republic of, ²Department of Psychology, Stanford University, Stanford, CA, United States, ³Department of Radiology, Stanford University, Stanford, CA, United States, ⁴Applied Science Lab, GE Healthcare, Menlo Park, CA, United States
- The release of dopamine during reward tasks is modulated by major depressive disorder (MDD). In this study of MDD, we used simultaneous PET/fMRI to detect the neurochemical changes of dopamine and neurovascular activity through BOLD contrast during two sequential monetary incentive delay tasks in a single scan. Several modeling methods were proposed and evaluated for dynamic PET data. Six participants with MDD were studied. The results of the group analysis of PET and fMRI show significant effects of dopamine release in ventral striatum bilaterally, close to the nucleus accumbens, and significant BOLD signals in putamen bilaterally during reward tasks.
-
- 3767 **Computer #4** EEG-fMRI at 7T using simultaneous multislice 2D-EPI: safety and functional sensitivity at the single-subject level
João Jorge^{1,2}, Frédéric Grouiller³, Patricia Cotič⁴, Wietske van der Zwaag⁵, Patrícia Figueiredo², and Rolf Gruetter^{1,6,7}
- ¹École Polytechnique Fédérale de Lausanne, Lausanne, Switzerland, ²ISR-Lisboa/LARSyS/Department of Bioengineering, Instituto Superior Técnico, Lisbon, Portugal, ³Biomedical Imaging Research Center, University of Geneva, Geneva, Switzerland, ⁴Institute of Mathematics, Physics and Mechanics, Ljubljana, Slovenia, ⁵Spinoza Centre for Neuroimaging, Amsterdam, Netherlands, ⁶Department of Radiology, University of Lausanne, Lausanne, Switzerland, ⁷Department of Radiology, University of Geneva, Geneva, Switzerland
- The enhanced BOLD sensitivity available at 7T can bring significant advantages for EEG-fMRI studies, and the use of accelerated fMRI sequences such as SMS-EPI could further boost sensitivity. This work investigated whether SMS-EPI can be safely acquired with EEG at 7T, and whether the resulting sensitivity is favorable for combined EEG-fMRI approaches. The adopted SMS-EPI sequence (1.8mm isotropic resolution, whole-brain, TR_{vol}=1.57s) produced no temperature increases when combined with EEG. In a human, eyes-open/closed and resting-state activity patterns could be robustly detected in both modalities, and EEG-derived timecourses produced consistent BOLD predictions, even at a single-subject level with minimal spatial smoothing.

-
- 3768
Computer #5
- A simultaneous fMRI-EEG acquisition to minimize the MR gradient artifact on human auditory system
Kevin Wen-Kai Tsai^{1,2}, Hsin-Ju Lee², Ching-Po Lin², Li-Wei Ko³, Wen-Jui Kuo², Toni Auranen⁴, Simo Särkkä⁵, and Fa-Hsuan Lin⁶
- ¹Aim for the Top University Project, National Taiwan Normal University, Taipei, Taiwan, ²Institute of Neuroscience, National Yang-Ming University, Taipei, Taiwan, ³Institute of Bioinformatics and Systems Biology, National Chiao Tung University, Hsinchu, Taiwan, ⁴Advanced Magnetic Imaging Centre, Low Temperature Laboratory, Aalto University, Espoo, Finland, ⁵Department of Electrical Engineering and Automation, Aalto University, Espoo, Finland, ⁶Institute of Biomedical Engineering, National Taiwan University, Taipei, Taiwan
- Simultaneous fMRI-EEG acquisition provides a good spatial and temporal resolution from MRI and EEG respective to study the human brain function. However, the EEG signal is impaired due to the strong magnetic gradient switching of concurrent MR imaging. A simultaneous interleaved MR InI-EEG recording strategy is proposed to minimize the distortion of the EEG. Our results suggest that the proposed acquisition strategy can reveal similar BOLD contract activation but preserve better auditory evoked potentials than conventional EPI-EEG acquisition.
-
- 3769
Computer #6
- Multimodal elucidation of rat brain function using BOLD-fMRI and CMRO₂ [15O]O₂-PET
Hans F Wehr^{1,2}, Jun-ichiro Enmi¹, Mario Amend², Kazuhiro Koshino¹, Masako Kunimi¹, Takashi Temma¹, and Hidehiro Iida¹
- ¹Department of Investigative Radiology, National Cerebral and Cardiovascular Center Research Institute, Suita City, Osaka, Japan, ²Department of Preclinical Imaging and Radiopharmacy, Werner Siemens Imaging Center, Eberhard Karls University of Tuebingen, Tuebingen, Germany
- The complex interplay of CMRO₂, CBF and CMRO₂ changes that constitute the BOLD effect are not fully understood. Here we study rat brain activation using combined BOLD-fMRI and CMRO₂ proportional [¹⁵O]O₂-PET during the same anesthesia session. To our knowledge, such combined measurements have not been obtained before in small animals. We observed a spatial mismatch between the main activation centers as well as additional activated regions in the CMRO₂-PET, not present in BOLD-fMRI. However, statistical significances of activation sites were higher in BOLD-fMRI compared to [¹⁵O]O₂-PET. This work points towards a complementary nature of both methods in certain brain areas.
-
- 3770
Computer #7
- A novel, single scanning session approach to image rat brain activity applying simultaneous [¹⁸F]FDG-PET and BOLD-fMRI
Mario Amend¹, Tadashi Watabe², André Thielcke¹, Bernd J Pichler¹, and Hans F Wehr¹
- ¹Department of Preclinical Imaging and Radiopharmacy, Werner Siemens Imaging Center, Eberhard Karls University, Tuebingen, Germany, ²Department of Nuclear Medicine and Tracer Kinetics, Osaka University Graduate School of Medicine, Osaka, Japan
- Functional and metabolic processes during brain activity are still not fully understood. We established a novel protocol to image rat brain activation in a single scanning session, enabling optimal comparison of PET/fMRI data. Performing activation and baseline scans in one single scanning session is challenging due to the half-life (here [¹⁸F]FDG: 109.8 min) and decay time of PET-tracers. Applying [¹⁸F]FDG-PET and BOLD-fMRI, spatial and quantitative correlations but also mismatches between the glucose proportional PET and the fMRI activation data were found. Our results provide the basis for further studies of brain function and point towards the complementary nature of PET/MR.
-
- 3771
Computer #8
- Simultaneous, trimodal MR-PET-EEG at 3T in humans: Glutamate drives energy consumption in the default mode network
Irene Neuner^{1,2,3}, Jörg Mauler¹, Ravichandran Rajkumar^{1,2,3}, Ezequiel Farrher¹, Elena Rota Kops¹, Lutz Tellmann¹, Jürgen Scheins¹, Frank Boers¹, Karl Josef Langen^{1,3,4}, Hans Herzog^{1,2,3}, and N. Jon Shah^{1,3,5}
- ¹Institute of Neuroscience and Medicine 4 (INM 4), Forschungszentrum Juelich GmbH, Juelich, Germany, ²Department of Psychiatry, Psychotherapy and Psychosomatics, RWTH Aachen University, Aachen, Germany, ³JARA-BRAIN, Translational Medicine, Aachen, Germany, ⁴Department of Nuclear Medicine, RWTH Aachen University, Aachen, Germany, ⁵Department of Neurology, RWTH Aachen University, Aachen, Germany
- Within the scope of this explorative pilot trial we focus on the role of GABA and glutamate within the default mode network with regard to energy consumption. In one simultaneous session MR, FDG-PET and EEG data were recorded at a 3T hybrid MR-BrainPET scanner (Siemens, Germany) equipped with a 32 channel MR-compatible EEG system (Brain Products, Germany) in 11 healthy volunteers. The Pearson correlation showed a statistically significant positive correlation between glutamate ratio and mean CMRglu in the DMN ($r = 0.678$, $n = 11$, $p = 0.022$) but none to GABA.
-
- 3772
Computer #9
- Pharmacological Modulation of Static and Dynamic Functional Connectivity: a Simultaneous PET/MRI Study
Hsiao-Ying Wey¹, R Matthew Hutchison², Bruce R Rosen¹, and Joseph B Mandeville¹
- ¹A. A. Martinos Center, Department of Radiology, Massachusetts General Hospital, Harvard Medical School, Charlestown, MA, United States, ²Center for Brain Science, Harvard University, Cambridge, MA, United States
- In this study, we present simultaneous PET/MRI study with pharmacological challenges targeting the μ -opioid receptor system in nonhuman primates to determine the effects of opioid drug on static and dynamic functional connectivity. μ -opioid receptor occupancy (quantified with PET) and CBV-fMRI signals show dose-dependent reductions to opioid antagonist (naloxone) challenges. Using brain regions showing PET signal changes as seeds, static FC analysis shows an increase in local (within the seed region) and distal (motor cortex) connectivity with putamen after naloxone. Dynamic FC patterns were also modulated with naloxone as indicated by weaker pairwise correlations and larger number of dynamic state transitions.

-
- 3773
Computer #10 Real-time ICA-based artifact correction of EEG data recorded during functional MRI
Ahmad Mayeli^{1,2}, Vadim Zotev¹, Hazem Refai², and Jerzy Bodurka^{1,3}
- ¹Laureate Institute for Brain Research, Tulsa, OK, United States, ²Electrical and Computer Engineering, University of Oklahoma, Tulsa, OK, United States, ³College of Engineering, University of Oklahoma, Tulsa, OK, United States
- Recording EEG signals during fMRI acquisition result EEG signals contamination from imaging and BCG artifacts in addition to other types of artifacts. In this abstract we introduced a novel method for detecting and reducing artifacts using second order blind separation in real time. The algorithm was tested on EEG signals from 12 subjects and it has proven successful for reducing various types of artifacts. The proposed algorithm can be applied in real time after the average artifact subtraction of imaging and BCG artifacts for various applications that require a real-time EEG & fMRI system.
-
- 3774
Computer #11 Automatic EEG-assisted retrospective fMRI head motions correction improves rs-fMRI connectivity analysis
Chung-Ki Wong¹, Vadim Zotev¹, Masaya Misaki¹, Raquel Phillips¹, Qingfei Luo¹, and Jerzy Bodurka^{1,2,3}
- ¹Laureate Institute for Brain Research, Tulsa, OK, United States, ²College of Engineering, University of Oklahoma, Norman, OK, United States, ³Center for Biomedical Engineering, University of Oklahoma, Norman, OK, United States
- We utilized an automatic EEG-assisted retrospective motion correction (aE-REMCOR) to improve rs-fMRI connectivity analysis. The aE-REMCOR utilizes EEG data to automatically correct for head movements in fMRI on a slice-by-slice basis. We compared the results of seed-based (posterior cingulate cortex) default-mode network (DMN) connectivity analysis performed with and without aE-REMCOR. The aE-REMCOR reduced the motion-induced position-dependent error in the DMN connectivity analysis. The results show the importance of slice-by-slice fMRI motion corrections to improve rs-fMRI connectivity accuracy especially when the entire group of subjects exhibits rapid head motions, and also provide incentive for conducting simultaneous EEG&fMRI.
-
- 3775
Computer #12 Detecting visual evoked responses in simultaneous EEG-fMRI using Reference Layer Artefact Subtraction (RLAS)
Glyn S. Spencer¹, Muhammad E. H. Chowdhury^{1,2}, Karen J. Mullinger^{1,3}, and Richard Bowtell¹
- ¹Sir Peter Mansfield Imaging Centre, School of Physics and Astronomy, University of Nottingham, Nottingham, United Kingdom, ²Electrical Engineering, Qatar University, Doha, Qatar, ³Birmingham University Imaging Centre, School of Psychology, University of Birmingham, Birmingham, United Kingdom
- Simultaneous EEG-fMRI is limited by large artefacts in EEG recordings resulting from time-varying field gradients, cardiac-related motion and head movement within the magnetic field. Reference layer artefact subtraction (RLAS) reduces artefacts at source by subtraction of artefact voltages recorded from a reference layer on which the EEG leads and electrodes are replicated. Since RLAS does not require prior knowledge of the timing of artefact occurrences, it is an ideal method for correcting pulse and movement artefacts. Here, we apply RLAS in EEG-fMRI experiments for the first time, particularly focusing upon recovery of single-trial, low-frequency, visual-evoked responses from artefact-corrupted data.
-
- 3776
Computer #13 Assessing the stability of neurovascular coupling: A combined fMRI/MEG approach
Marek Allen¹, Valentina Tomassini², Kevin Murphy¹, Suresh Muthukumaraswamy³, Krish D. Singh¹, and Richard G. Wise¹
- ¹Cardiff University Brain Research Imaging Centre, Cardiff University, Cardiff, United Kingdom, ²Institute of Psychological Medicine and Clinical Neurosciences, Cardiff University, Cardiff, United Kingdom, ³Faculty of Medical and Health Sciences, University of Auckland, Auckland, New Zealand
- Neurovascular coupling (NVC) is crucial to maintaining the structural and functional integrity of the brain. Using a graded contrast visual stimulus applied in magnetoencephalography (MEG) and functional MRI (fMRI), we assessed the stability of visual evoked fields (VEFs), gamma power and MRI blood flow responses. A power law was used to relate responses to stimulus contrast and describe the relationship between neuronal responses and blood flow. VEF amplitude was temporally unstable across time points. Gamma power and blood flow (ASL) responses remained stable, making gamma power-based NVC and ASL MRI measures a promising method for testing and exploring NVC in disease states.
-
- 3777
Computer #14 EEG-fMRI derived DMN-microstate quantifies meditation induced altered consciousness
Rose Dawn Bharath¹ and Rajanikant Panda¹
- ¹Neuroimaging and Interventional Radiology, National Institute of Mental Health and Neurosciences, Bangalore, India
- Fluctuations in the ICA derived resting state networks can be visualized using simultaneous EEG fMRI. This method can thus be used to understand human consciousness which is the result of synchronous oscillation between multiple networks. EEG fMRI derived "DMN microstate" is seen to accurately assess meditation induced altered consciousness in the current study.
-
- 3778
Computer #15 New perspectives in simultaneous EEG-fMRI using multiband and quiet pulse sequences
Beatriz Dionisio Parra^{1,2}, Nicolas Hehn¹, Xin Liu^{1,2}, Matthew Middione³, Anne Menini¹, Darius Burschka², Florian Wiesinger¹, and Ana Beatriz Solana¹
- ¹GE Global Research, Munich, Germany, ²TUM (Technical University Munich), Munich, Germany, ³GE Healthcare, California, CA, United States

Three novel fMRI pulse sequences are evaluated together with simultaneous EEG acquisition, with the aim to reduce the induced EEG Gradient Artifacts (GA), increase the spatio-temporal resolution of fMRI and reduce the acoustic noise during scanning: sinusoidal GE-EPI, multiband blipped-CAPI and single shot T₂-prep RUFIS.

Remarkable results were found for the T₂-prep RUFIS sequence, with a significantly reduced gradient artifact amplitude, high temporal resolution and low acoustic noise level, providing eminent advantages to this multimodal technique.

3779

Computer #16 Mapping dynamics of epileptic seizures in GAERS using simultaneous BOLD fMRI and optical Ca²⁺ recordings
Lydia Wachsmuth¹, Florian Schmid¹, Franziska Albers¹, Annika Lüttjohann², Thomas Budde², and Cornelius Faber¹

¹Department of Clinical Radiology, University of Münster, Münster, Germany, ²Institute of Physiology I, University of Münster, Münster, Germany

Simultaneous BOLD fMRI and optical Ca²⁺ recordings using the genetically encoded calcium indicator GCaMP were performed in a rat model of absence epilepsy (GAERS) for seizure mapping. Spike-and-wave discharge onset times and durations were derived from Ca²⁺ recordings and used for an event-related analysis with different hemodynamic response functions. BOLD maps showed large scale activations in cortical and subcortical areas, with delayed responses in subcortical areas. In contrast to electrophysiological recordings, Ca²⁺ recordings are not disturbed by MRI. They allow for cell-specific correlation with the hemodynamic response and provide a tool to obtain epileptic seizure maps with higher specificity.

3780



Computer #17 A novel test bed for non-BOLD functional MRI
Ruiliang Bai^{1,2}, Tim Bellay³, Andreas Klaus³, Craig Stewart³, Sinisa Pajevic⁴, Uri Nevo⁵, Hellmut Merkle⁶, Dietmar Plenz³, and Peter J Basser¹

¹Section on Quantitative Imaging and Tissue Science, DIBGI, NICHD, National Institutes of Health, Bethesda, MD, United States, ²Biophysics Program, Institute for Physical Science and Technology, University of Maryland, College Park, MD, United States, ³Section on Critical Brain Dynamics, LSJ, NIMH, National Institutes of Health, Bethesda, MD, United States, ⁴Mathematical and Statistical Computing Laboratory, Division of Computational Bioscience, Center for Information Technology, National Institutes of Health, Bethesda, MD, United States, ⁵Department of Biomedical Engineering, Tel-Aviv University, Tel-Aviv, Israel, ⁶Laboratory for Functional and Molecular Imaging, NINDS, National Institutes of Health, Bethesda, MD, United States

Several fMRI contrast mechanisms have been proposed to measure neuronal activity more directly and accurately than BOLD fMRI. Conclusive findings supporting these non-BOLD fMRI methods have been difficult to obtain, mainly because of the dearth of a reliable and robust test system to vet and validate them. Here we describe the development and testing of a test bed for non-BOLD fMRI, in which calcium fluorescence imaging and MR acquisition can be performed simultaneously on the same organotypic cortical cultures. This experimental design makes it possible to directly correlate any candidate fMRI signal to a robust optical indicator of neuronal activity.

3781



Computer #18 Anesthesia increases water diffusion in wakefulness/sleep brain regions in the rat brain
Yoshifumi Abe¹, Tomokazu Tsurugizawa¹, and Denis Le Bihan¹

¹NeuroSpin, Commissariat à l'Energie Atomique-Saclay Center, Gif-sur-Yvette, France

Diffusion fMRI (DfMRI) has been shown to reflect neuronal activation more directly than BOLD fMRI, showing neuronal responses even when neurovascular coupling is abolished. We compared resting state ADC and BOLD fMRI time courses under different anesthesia conditions. While BOLD fMRI showed a widespread signal increase with isoflurane and a decrease with medetomidine, the ADC increased significantly with both agents in specific regions, notably in the wakefulness/sleep network. The amount of ADC increase was correlated with the dose of anesthetic agent, suggesting the suitability of DfMRI to investigate brain resting state or pharmacological challenges quantitatively and without vascular confounding effects.

3782

Computer #19 Recruitment of Distinct Cortical and Subcortical Activations by Layer and Frequency Specific Optogenetic Stimulation in Primary Visual Cortex
Russell W Chan^{1,2}, Alex TL Leong^{1,2}, Patrick P Gao^{1,2}, Leon C Ho^{1,2}, Kevin K Tsia², and Ed X Wu^{1,2}

¹Laboratory of Biomedical Imaging and Signal Processing, The University of Hong Kong, Hong Kong, China, People's Republic of, ²Electrical and Electronic Engineering, The University of Hong Kong, Hong Kong, China, People's Republic of

Different layers in mammalian cortex have specific projections and circuit dynamics. However, how optogenetic stimulation frequencies at different infragranular layers contribute to widespread and large-scale cortical and subcortical activities remains largely unexplored. In this study, optogenetic fMRI is used to investigate layer and frequency dependent activities by stimulating excitatory neurons in different infragranular layers of visual cortex. Our results showed that layer and frequency specific optogenetic stimulation recruits distinct widespread and large-scale cortical and subcortical activations. Spatiotemporally varying optogenetic stimulation in combination with fMRI presents unique opportunities in studying the underlying mechanisms of long-range neural circuits and brain functional networks.

3783

Computer #20 Light-induced activation of the visual network by optogenetic fMRI (ofMRI)
Florian Schmid¹, Lydia Wachsmuth¹, Franziska Albers¹, Nathalie Just¹, Miriam Schwalm², Albrecht Strohm², and Cornelius Faber¹

¹Department of Clinical Radiology, University of Münster, Münster, Germany, ²Research Group Molecular Imaging and Optogenetics, Johannes Gutenberg-University Mainz, Mainz, Germany

Optogenetic fMRI is a novel tool in neurophysiology and neuroimaging. However, ofMRI is prone to light-induced artifacts. Here, the unspecific activation of the visual pathways in ofMRI in rats was investigated. It was caused by the stimulation light and was also detected in naïve rats without the presence of opsins. Visual stimulation of the eyes resulted in similar activation. Visual pathway activation by intrabrain illumination could be suppressed by additional low-level constant light applied to the eyes. We provide evidence that the activation of the visual pathways is at least partly caused by light scattered diffusely inside the brain.

3784

Computer #21

Development of Carbon Nanotube Optrodes to Acquire LFP and BOLD Concurrently with Optogenetic Stimulation
Corey Cruttenden¹, Jennifer M. Taylor², Xiao-Hong Zhu², Yi Zhang², Hannes M. Wiesner², Anders Asp³, Erin Larson³, Wilson Yu³, Rajesh Rajamani¹, Mark Thomas³, Esther Krook-Magnuson³, and Wei Chen²

¹Mechanical Engineering, University of Minnesota, Minneapolis, MN, United States, ²Center for Magnetic Resonance Research (CMRR), University of Minnesota, Minneapolis, MN, United States, ³Neuroscience, University of Minnesota, Minneapolis, MN, United States

Carbon nanotube optrodes are under development for simultaneous optogenetics, neural recording, and fMRI BOLD signal acquisition. First-generation devices demonstrate capability in combining optogenetic stimulation and neural recording *in vivo*, but *in vitro* MR-images reveal severe susceptibility artifacts generated by terminal silver leads. New devices utilize carbon fiber wires in place of silver. Initial *in vitro* images of the second-generation device show a dramatic reduction of image artifacts, indicating that BOLD signal should be obtainable around the optrodes. The new devices will enable the combination of the aforementioned techniques, providing a platform for novel brain investigations.

3785

Computer #22

Concurrent 32-channel electrophysiological recording and fMRI in bilateral rat striatum
Saul Jaime^{1,2}, Hanbing Lu¹, Jose Cavazos^{2,3}, and Yihong Yang¹

¹Neuroimaging Research Branch, National Institute on Drug Abuse, NIH, Baltimore, MD, United States, ²Physiology, Uni. Texas Health Science Center-San Antonio, San Antonio, TX, United States, ³Neurology, Uni. Texas Health Science Center-San Antonio, San Antonio, TX, United States

Despite the high clinical and pre-clinical value of fMRI, its success depends on the identification of the underlying neurophysiological basis of the fMRI BOLD signal. In previously reported simultaneous electrophysiology and fMRI studies, experiments were limited by the poor spatial resolution or poor source localization of intra-cranial or surface EEG techniques employed to record neural activity. In order to overcome these limitations, we have developed a method that allows concurrent whole brain fMRI acquisition and 32-channel intracerebral electrophysiological recording in the rat brain.

3786

Computer #23

MRI-compatible wireless multi-purpose game controller for social neuroscience fMRI experiments
Ying-Hua Chu¹, Yi-Cheng Hsu¹, Pu-Yeh Wu¹, Kevin W.-K. Tsai², Wen-Jui Kuo², and Fa-Hsuan Lin¹

¹Institute of Biomedical Engineering, National Taiwan University, Taipei, Taiwan, ²Institute of Neuroscience, National Yang Ming University, Taipei, Taiwan

We developed a MRI-compatible wireless multi-purpose game controller. With the presence of the game controller, EPI shows minimal distortion and time-domain SNR degradation. Subjects' responses were successfully recorded from a two-person hyper-scanning experiment.

3787

Computer #24

A new way of looking at brain connectivity. pH fMRI: myth or reality?
Vitaliy Khlebnikov¹, Jeroen CW Siero¹, Alex Bhogal¹, Peter R Luijten¹, Dennis WJ Klomp¹, and Hans Hoogduin¹

¹Radiology, University Medical Center Utrecht, Utrecht, Netherlands

A new way of looking at brain connectivity. pH fMRI: myth or reality?

Electronic Poster

fMRI: Application

Exhibition Hall

Wednesday, May 11, 2016: 11:00 - 12:00

3788

Computer #25

Loss of functional specificity in basal ganglia in Parkinson's disease: a rs-fMRI study
Anne-Charlotte PHILIPPE¹, Pierre BERROIR¹, Marie VIDAILHET², and Stéphane LEHERICY¹

¹Brain and Spine Institute, CENIR, INSERM U1127/CNRS UMR7225, Sorbonne Universités, UPMC, CHU Pitié-Salpêtrière, Paris, France, ²Brain and Spine Institute, INSERM U1127/CNRS UMR7225, Sorbonne Universités, UPMC, CHU Pitié-Salpêtrière, Paris, France

Loss of neuronal specificity in the basal ganglia (BG) has been reported in Parkinson's disease (PD)[1]. However, loss of specificity has not been characterized using non-invasive methods in PD. We proposed an innovative method to characterize the functional specificity of BG. We tested the hypothesis that loss of specificity may result in larger spatial extent of overlap between anatomo-functional

territories in the BG. We performed population statistics to compare the extent of overlap between PD subjects and controls. As expected, the motor territories had larger extent of overlap in PD subject than in controls revealing a loss of specificity of the BG in PD.

-
- 3789
Computer #26
Increased activation of precuneus and posterior cingulate cortex in resting state fMRI in patients with functional movement disorders after undergoing a motor retraining program
Kwan-Jin Jung¹, Sarah Mufti², and Kathrin LaFaver²
¹Radiology, University of Louisville, Louisville, KY, United States, ²Neurology, University of Louisville, Louisville, KY, United States
- Functional movement disorders (FMD) can be significantly reduced with a one-week motor retraining program. Our study compared resting state fMRI before and after treatment of 6 FMD patients. We found increased activity in the posterior default mode network, specifically the precuneus and posterior cingulate cortex, in 4 out of 6 patients after treatment, which correlated with clinical improvement of motor symptoms. Our findings suggest that restoration of normal movements in FMD patients are accompanied by increased default mode network activation.
-
- 3790
Computer #27
Demonstration of brain tumor-related NVU in both task-based fMRI and resting state fMRI
Shruti Agarwal¹, Noushin Yahyavi-Firouz-Abadi¹, Haris I. Sair¹, Raag Airan¹, and Jay J. Pillai¹
¹Division of Neuroradiology, Russell H. Morgan Department of Radiology and Radiological Science, Johns Hopkins University School of Medicine, Baltimore, MD, United States
- The phenomenon of neurovascular uncoupling (NVU) is a limitation of clinical fMRI, particularly in presurgical mapping. A previous study using task-based motor activation (tbfMRI) and breath hold cerebrovascular reactivity (BH CVR) mapping demonstrated that BH CVR was capable of detecting NVU in low-grade peritumoral tumors. In this study we demonstrated the effect of NVU on resting state fMRI (rsfMRI) data within the sensorimotor network through comparison to both BH CVR and task-based fMRI data.
-
- 3791
Computer #28
Why a clinical sign does not always correlate with lesion location?
Rajanikant Panda¹, Rose Dawn Bharath¹, Shriram Varadharajan^{1,2}, Sankalp Tikoo¹, Sarbesh Tiwari³, Surabhi ramawat¹, Shiva Karthik¹, Indira Devi Bhagavatula⁴, and Arun Gupta¹
¹Department of Neuroimaging & Interventional Radiology, National Institute of Mental Health and Neurosciences (NIMHANS), Bangalore, India, ²Bangalore, India, ³Department of Neuroimaging & Interventional Radiology, National Institute of Mental Health and Neurosciences (NIMHANS), Bangalore, India, ⁴Department of Neurosurgery, National Institute of Mental Health and Neurosciences (NIMHANS), Bangalore, India
- Understanding the degree of functional reserve in patient with brain tumor, when lesion is located in the eloquent cortex is important in presurgical evaluation to predict the surgical outcome as well reducing postoperative neurological deficits. For achieving this, a detailed knowledge of the functional topography and connectivity in whole brain level is crucial. In this study, our aim to understand the brain hyper and hypo connectivity in patients with high grade tumor who have deficits and who do not have deficits.
-
- 3792
Computer #29
Functional brain changes in breachers following a blast-overpressure: an acute longitudinal assessment with MRI
Fatima Nasrallah^{1,2}, Trina Kok¹, Mary Stephenson¹, Jiesen Wang³, Alexandre Schaefer³, You Jin¹, Benjamin Thomas¹, Pamela Pun Boon Li⁴, Melissa Teo Ai Ling⁴, Julie Yeo Su Li⁴, Jia Lu⁴, John Tottman¹, and David Townsend⁵
*¹Clinical Imaging Research Centre, NUS/A*STAR, Singapore, Singapore, ²Queensland Brain Institute, Queensland, Australia, ³Clinical Imaging Research Centre, NUS, Singapore, Singapore, ⁴Defense Singapore Organisation, DSO, Singapore, Singapore, ⁵Clinical Imaging Research Centre, NUS/A*STAR, Singapore, Singapore*
- Blast injury is one of the most common types of mild traumatic brain injury. In this work we have investigated the longitudinal changes induced by a blast-overpressure injury in breacher trainers using resting state functional connectivity MRI. We show that reductions in connectivity in the Thalamic and Cerebellar regions at Day 1 following a blast are regained and increased 1 month post blast.
-
- 3793
Computer #30
Parkinson's disease laterality impact onto the default mode network deactivation by the audio-motor transformation
Oleksii Omelchenko¹, Zinayida Rozhkova², and Iryna Karaban³
¹Human and Animal Physiology, Taras Shevchenko National University of Kyiv, Kyiv, Ukraine, ²Radiology, Medical Clinic BORIS, Kyiv, Ukraine, ³Department of extrapyramidal disorders, D. F. Chebotarev Institute of Herontology, Kyiv, Ukraine
- Asymmetry of motor symptoms is considered a crucial criterion for PD and influence hemisphere-associated cognitive functions. DMN was shown to loose its functional connectivity in PD. We hypothesized that AMT play important role in switching DMN to task-related deactivation state. AMT exploration for PD laterality specific DMN connectivity analysis during movements was done. AMT and movement execution in PD evokes activation auditory cortex, SMN and pC. In PD patients DMN deactivates exceptionally at the period of motor activity. pC participates as a DMN 'hub' and DMN deactivation 'switching' trigger during AMT. PD symptoms lateralization play important role in DMN functioning.
-
- 3794
Computer #31
Evaluation in brain function and the correlation with depression and anxiety of obese patients using resting-state fMRI
Cheng-Jui Li^{1,2}, Vincent Chin-Hung Chen³, Hse-Huang Chao⁴, Ming-Chou Ho⁵, and Jun-Cheng Weng^{1,2,6}

¹Department of Medical Imaging and Radiological Sciences, Chung Shan Medical University, Taichung, Taiwan, ²Department of Biomedical Sciences, Chung Shan Medical University, Taichung, Taiwan, ³Department of Psychiatry, Chang Gung Memorial Hospital, Chiayi, Taiwan, ⁴Tiawan Center for Metabolic and Bariatric Surgery, Jen-Ai Hospital, Taichung, Taiwan, ⁵Department of Psychology, Chung Shan Medical University, Taichung, Taiwan, ⁶Department of Medical Imaging, Chung Shan Medical University Hospital, Taichung, Taiwan

Obesity has reached epidemic proportions globally to become a major public health problem. Obesity-related health problems are numerous including strokes, cardiovascular disease, diabetes mellitus, and increased risk for developing cancer. Reward mechanism of obese patients regarding functional connectivity has been declared by several studies, but few studies mentioned about the correlation between functional images and clinical indices. Thus, our study aimed to find out abnormal functional connectivity over obese patients based on amplitude low frequency fluctuation (ALFF) and regional homogeneity (ReHo) using voxel-based analysis, and the correlation between functional images and clinical indices, including body mass index (BMI) and hospital anxiety and depression scale (HADS). We found the brain functional abnormality in the obese patients compared to healthy controls, and the correlation with depression and anxiety. The potential functional imaging markers may provide guidance for managing obesity and disordered eating behaviors.

3795
Computer #32 Local and Distant Functional Connectivity Density Alteration in Primary Open-angle Glaucoma: A Resting-state functional MRI Study
Zhenyu Liu¹ and Ting Li²

¹Key Laboratory of Molecular Imaging, Institute of Automation, Beijing, China, People's Republic of, ²Beijing Tongren Hospital, Beijing, China, People's Republic of

To measure functional connectivity density maps were applied with resting-state functional MRI. Twenty-one patients and twenty-two age- and gender-matched healthy controls were evaluated by 3T MRI using resting-state blood oxygenation level dependent imaging. POAG patients showed decreased FCD values in visual cortices and increased FCD values of DMN components. This study demonstrates POAG can induce reorganization of brain function in multiple brain regions, including visual cortices and DMN.

3796
Computer #33 Altered Amplitude of Low-Frequency Fluctuation and functional connectivity in High Myopia: A Resting-State fMRI Study
Xue-wei Zhang^{1,2}, Wei-hong Zhang², and Qin Long³

¹Department of Interventional Radiology, China Meitan General Hospital, Beijing, China, People's Republic of, ²Department of Radiology, Peking Union Medical College Hospital, Beijing, China, People's Republic of, ³Department of Ophthalmology, Peking Union Medical College Hospital, Beijing, China, People's Republic of

High myopia (HM) can result in serious vision problems. To date, the pathophysiologic mechanism remains unknown. The authors tried to explore the potential locations which involved in the brain abnormalities of HM patients, through observing altered ALFF of different bands and functional connectivity of the brain by rs-fMRI. The results showed that, not only visual cortex but also multiple brain regions were noted to have abnormal changes in the brain of HM patients. In conclusion, the findings indicated that high myopia affects many functional networks, and different bands of ALFF may provide a new way to explore the underlying mechanism.

3797
Computer #34 Accuracy of Functional Localization in Pre-surgical Function MRI
Mu-Lan Jen¹, Islam S. Hassan², Ping Hou¹, Guang Li¹, Ashok J. Kumar², Colen R. Rivka², and Ho-Ling Liu¹

¹Department of Imaging Physics, The University of Texas M. D. Anderson Cancer Center, Houston, TX, United States, ²Department of Diagnostic Radiology, The University of Texas M. D. Anderson Cancer Center, Houston, TX, United States

This study evaluates the errors associated with the spatial transformation process by using algorithms commonly applied for clinical pre-surgical fMRI. The images from nine right-handed patients with brain tumors were retrospectively analyzed. Significant differences ($P < 0.05$) were found when comparing results from automated registration (AR) vs. coordinate matching (CM) and AR vs. AR with manual adjustment (AR, adjusted). No statistical significance was found between CM and AR, adjusted. This study established a platform for evaluating the functional localization accuracy in pre-surgical fMRI, and highlighted the necessity of quality control for the AR processing as a clinical routine.

3798
Computer #35 Action observation network in children with unilateral cerebral palsy: an fMRI study.
Laura Biagi¹, Giuseppina Sgandurra¹, Leonardo Fogassi², Andrea Guzzetta^{1,3}, Giovanni Cioni^{1,3}, and Michela Tosetti¹

¹IRCCS Stella Maris, PISA, Italy, ²Department of Neuroscience, University of Parma, Parma, Italy, ³Department of Clinical and Experimental Medicine, University of Pisa, PISA, Italy

Mirror Neuron System (MNS) activation constitutes a powerful mechanism for recovery of motor deficits after stroke. We studied with fMRI the MNS (re)-organization in children with congenital unilateral cerebral palsy (UCP), using a goal-directed hand action stimulus. With respect to age-matched controls, UCP children present differences, appearing more lateralized to the dominant hemisphere as adults. The subject-specific pattern of lateralization seems related to the type and extension of the lesion and correlates negatively with the severity of the hand impairment. This paradigm might be useful to explore MNS in UCP and to monitor possible motor improvements in response to therapy.

3799
Computer #36 Resting-State Functional Connectivity in Patients with Treatment-Resistant Depression
Jia Liu¹, Mingrui Xia², Qiyong Gong¹, and Yong He²

¹Huaxi MR Research Center (HMRRRC), Department of Radiology, West China Hospital of Sichuan University, Chengdu, China, People's Republic of,

We used a data-driven graph theoretical approach—whole-brain functional connectivity strength (FCS) mapping to investigate functional connectivity patterns in 24 patients with RDD, 40 patients with NDD, and 48 healthy comparison subjects. Our study indicated that when compared with HC, the alteration of FCS in NDD group was mainly located in the medial frontal gyrus while the alterations of RDD group were located in the non-medial frontal areas and NDD demonstrated lower FCS in the limbic regions which was not obvious in the RDD group. Meanwhile, lower FCS in the default mode network and visual recognition network was observed in the group with NDD when compared with the group with RDD.

3800 Computer #37 When mint smells blue and diagonal: an fMRI study on olfactory synesthesias
Helena Melero¹, Susana Borrromeo¹, Alexandra Cristobal-Huerta¹, Eva Manzanedo¹, and Juan Antonio Hernandez-Tamames¹

¹Universidad Rey Juan Carlos, Madrid, Spain

Neuroimaging experiments on grapheme-color synesthesia have provided evidence of structural and functional peculiarities in the synesthetic brain and several explanatory models have been proposed. Nevertheless, data from other modalities are needed in order to test their predictions. For the first time, we investigated brain activity in response to olfactory stimuli in multiple synesthetes. Results showed differential activity in areas that participate in high level visual processing, memory, language, lexical meaning and emotion. These findings suggest that the Conceptual Mediation Model and the Emotional Binding Theory may be complementary and reinforce the idea that meaning and emotion are intrinsically related processes.

3801 Computer #38 Data-driven model for evaluation of cerebrovascular-reserve measurement with hypercapnia BOLD
Lenka Vondráčková^{1,2}, Pawel Krukowski³, Johannes Gerber³, Jennifer Linn³, Jan Kybic², and Jan Petr¹

¹Institute of Radiopharmaceutical Cancer Research, Helmholtz-Zentrum Dresden-Rossendorf, Dresden, Germany, ²Center for Machine Perception, Faculty of Electrical Engineering, Czech Technical University in Prague, Prague, Czech Republic, ³Department, University Hospital Carl Gustav Carus, Dresden, Germany

Hypercapnia BOLD with the breath-holding task is a technically easier and more clinically available alternative to cerebrovascular reserve (CVR) mapping than administration of CO₂ enriched air using an air-tight mask. The disadvantage is complicated data evaluation in case the subject does not adhere to the breathing protocol completely. Here, a data-driven approach for evaluation is presented that is more robust to protocol deviations and produces a reasonable CVR map in most cases where the standard model-driven approach fails. This is demonstrated on randomized evaluation of CVR maps of a group of 86 subjects with stenosis or vessel occlusion.

3802 Computer #39 Multi Voxel Pattern Analysis (MVPA) classification reveals distributed neural presentations of specific finger movement sequences in the human striatum: a task-based functional MRI study.
Kasper Winther Andersen¹, Kristoffer H Madsen¹, Tim B Dyrby¹, and Hartwig R Siebner^{1,2}

¹Danish Research Centre for Magnetic Resonance, Centre for Functional and Diagnostic Imaging and Research, Copenhagen University Hospital Hvidovre, Denmark, Copenhagen, Denmark, ²Department of Neurology, Copenhagen University Hospital Bispebjerg, Copenhagen, Denmark

The basal ganglia is a group of subcortical nuclei, which receives connections from almost the entire cerebral cortex. Here, we investigated the involvement of the striatum, which is the input structure of the basal ganglia, in a sequential finger movement task using fMRI. Sixteen healthy controls performed finger sequences with different complexities. Multi Voxel Pattern Analysis was used to discriminate the distributed signal in striatum and cortex. We found that the distributed signals in contra-lateral striatum are discriminative of the finger sequence performed, which points to a significant role of the basal ganglia in the control of finger sequences.

3803 Computer #40 Heterogeneity of hemodynamic response dynamics across the subcortical-cortical visual pathway
Laura Lewis^{1,2}, Kavin Setsompop^{2,3}, Bruce R Rosen^{2,3}, and Jonathan R Polimeni^{2,3}

¹Society of Fellows, Harvard University, Cambridge, MA, United States, ²Athinoula A. Martinos Center for Biomedical Imaging, Massachusetts General Hospital, Boston, MA, United States, ³Department of Radiology, Harvard Medical School, Boston, MA, United States

The hemodynamic response is nonlinear in response to short duration stimuli, and this nonlinearity varies across cortex. To study the nonlinearities in subcortical vs. cortical structures, we performed high-resolution fMRI at 7 Tesla to characterize responses to short visual stimuli in superior colliculus (SC), lateral geniculate nucleus (LGN) and primary visual cortex (V1). Response nonlinearity was increased in SC, and response timecourses were consistently narrower in LGN than in V1. We conclude that analysis of subcortical activations using fMRI will require flexible models of the hemodynamic response, and suggest future studies to identify the neural and vascular factors contributing to these nonlinearities.

3804 Computer #41 Morphological component analysis of functional MRI data based on sparse representations and dictionary learning
Hien M. Nguyen¹, Jingyuan Chen², and Gary H. Glover³

¹Department of Electrical Engineering & Information Technology, Vietnamese - German University, Binh Duong New City, Vietnam, ²Department of Electrical Engineering, Stanford University, Stanford, CA, United States, ³Department of Radiology, Stanford University, Stanford, CA, United States

A data-driven method for identifying functional connectivity networks utilizing sparse representations is presented. Specifically, fMRI signals are decomposed into morphological components which have sparse spatial overlap. Allowing sparse spatial overlap between components is more physically plausible than the statistical independence assumption of the Independent Component Analysis (ICA) method. The proposed formulation is related to the Morphological Component Analysis (MCA) and uses a K-Singular Value Decomposition (SVD) algorithm for dictionary learning. Experimental results prove that the MCA-KSVD method can identify functional networks in task and resting-state fMRI and thus can be used as an alternative method for investigating brain functional connectivity.

3805
Computer #42 fMRI activation patterns during Successful Face-Name Recognition
Yunqing Li¹, Prasanna Karunanayaka¹, and Qing X Yang^{1,2}

¹Radiology, Penn State College of Medicine, Hershey, PA, United States, ²Neurosurgery, Penn State College of Medicine, Hershey, PA, United States

The contributions of distinct anatomical brain regions within the medial temporal lobe (MTL) during successful learning and recognition is poorly understood. In this research, we attempt to unravel how the MTL brain structures interact and integrate information during successful memory recall under different conditions during the performance of a face-name fMRI task.

3806
Computer #43 Long-term intensive training induced cortical thickness alterations in world class gymnasts
Meng Li¹, Min Lu², Shumei Li¹, Junjing Wang³, Bin Wang³, Guihua Jiang¹, Ruibin Zhang³, Xue Wen³, Jun Wang⁴, and Ruiwang Huang³

¹Department of Medical Imaging, Guangdong No. 2 Provincial People's Hospital, Guangzhou, China, People's Republic of, ²Key Laboratory of Mental Health, Institute of Psychology, Chinese Academy of Sciences, Beijing, China, People's Republic of, ³Center for the Study of Applied Psychology, Key Laboratory of Mental Health and Cognitive Science of Guangdong Province, South China Normal University, Guangzhou, China, People's Republic of, ⁴State Key Laboratory of Cognitive Neuroscience and Learning, Beijing Normal University, Beijing, China, People's Republic of

World class gymnasts are typical elite athletes whose motor skills and experience are much more than non-athletes. Therefore, changes in brain structure may be expected to occur after long-term intensive training. Thus, we utilized the vertex-wise and ROI-wise methods to investigate the alterations in the cortical thickness of gymnasts. We found the increased thickness in some regions of parietal, occipital, and frontal cortex in the gymnasts, and the significant correlation between thickness with years of training in right superior frontal cortex. Our study indicates that in response to long-term training, neuroanatomical adaptations and plastic changes occur in gymnasts' cortical thickness.

3807
Computer #44 Effects of Hyperglycemia and Hyperinsulinemia on Amplitude of Low Frequency Fluctuations in Medial Frontal and Posterior Cingulate Cortices in Healthy Non-Diabetic Subjects
Nicolas R. Bolo^{1,2}, Alan M. Jacobson³, Brandon Hager¹, Gail Musen^{2,4}, Matcheri Keshavan^{1,2}, and Donald C. Simonson^{5,6}

¹Psychiatry, Beth Israel Deaconess Medical Center, Boston, MA, United States, ²Psychiatry, Harvard Medical School, Boston, MA, United States, ³Research Institute, Winthrop University Hospital, Mineola, NY, United States, ⁴Research Division, Joslin Diabetes Center, Boston, MA, United States, ⁵Division of Endocrinology, Brigham and Women's Hospital, Boston, MA, United States, ⁶Harvard Medical School, Boston, MA, United States

Our goal is to elucidate the independent effects of hyperglycemia and hyperinsulinemia on brain function. We measured whole-brain amplitude of low frequency fluctuations (ALFF) in slow-band 5 (SB5: 0.01-0.027Hz) and slow-band 4 (SB4: 0.027-0.073Hz) in 10 healthy non-diabetic subjects using resting state fMRI during fasting baseline euglycemia (EU), hyperglycemia (HG) and euglycemic hyperinsulinemia (EU-HI). SB5 fractional ALFF was decreased in the left medial frontal gyrus and right posterior cingulate/cuneus/precuneus cortices during HG, but not during EU-HI, relative to EU. Our findings may help understand brain functional adaptations to chronic hyperglycemia in diabetes, and their implications for comorbid neuropsychiatric complications.

3808
Computer #45 ECG-derived respiratory signal for physiological noise correction in simultaneous EEG-fMRI for enhanced mapping of epileptic activity
Rodolfo Abreu¹, Sandro Nunes¹, Alberto Leal², and Patrícia Figueiredo¹

¹ISR-Lisboa/LARSyS and Department of Bioengineering, Instituto Superior Técnico, Universidade de Lisboa, Lisboa, Portugal, ²Department of Neurophysiology, Centro Hospitalar Psiquiátrico de Lisboa, Lisboa, Portugal

We propose a physiological noise model where respiratory-induced BOLD signal fluctuations were extracted from a surrogate of the respiratory signal estimated by Empirical Mode Decomposition. We optimized this model on a subject-specific basis, and evaluate its impact EEG-correlated fMRI mapping of epileptic networks, by comparing the epileptic maps obtained with and without physiological noise correction. This assessment was performed in terms of specificity and sensitivity, having been obtained not only substantial improvements for both measures, but also plausible and patients' semiology concordant epileptic networks.

3809
Computer #46 Pelvic floor muscles contraction assessed by fMRI
Joel Daouk¹, Ludovic Viart², Fabien Saint², and Olivier Baledent^{1,3}

¹Bioflow Image, University of Picardie Jules Verne, Amiens, France, ²Urology, CHU Amiens, Amiens, France, ³Medical image processing, CHU Amiens, Amiens, France

In this work, we compared two fMRI paradigms to assess the volunteer pelvic floor muscles contraction.

Paradigms suited the block-design method and the action phases consisted in contraction of the pelvic floor muscles (continuously in "Continuous" paradigm and repeated in "pulsed" paradigm) and rest phases were complete relaxation.

Results showed that there was no significant difference in cluster size between "continuous" and "pulsed" paradigms. However, Z-max was significantly higher in the "pulsed" paradigm than in the "continuous" one ($p < 0.001$). fMRI, with a pulsed paradigm, is a suitable technique to assess volunteer pelvic floor muscles contraction.

3810

Computer #47

A Brain Resting State network specific T_2^* Study in neonatal infants

Maryam Abaei¹, Tomoki Arichi^{1,2}, Anthony Price¹, Eugene P Duff³, Emer Hughes¹, Giulio Ferrazzi¹, Jacques-Donald Tournier¹, Jonathan O'Muircheartaigh^{1,4}, Serena Counsell¹, A David Edwards^{1,5}, Steve M Smith³, Daniel Rueckert⁶, and Joseph V Hajnal^{1,5}

¹Centre for the Developing Brain, King's College London, London, United Kingdom, ²Department of Bioengineering, Imperial College, London, United Kingdom, ³Department of Clinical Neurosciences, Oxford University, Oxford, United Kingdom, ⁴Institute of Psychiatry, Kings College London, London, United Kingdom, ⁵Division of Imaging Sciences and Biomedical, King's College London, London, United Kingdom, ⁶Biomedical Image Analysis Group, Department of Computing, Imperial College, London, United Kingdom

Previous studies reported that, although the majority of RSNs are present at the time of normal birth, but they appear to mature at different rates with the "higher-order" networks developing later than primary sensory. T_2^* in neonates are up to 2 times longer than those typically seen in the mature adult brain and decrease with increasing gestational age at scan. In this study we assessed T_2^* for different RSNs and hypothesized that those which mature earlier on structural MRI would have shorter T_2^* than networks in cortical regions that develop later in gestation.

3811

Computer #48

How feedback, verbal instruction and reward influence learning brain self-regulation? A real-time fMRI study.

Pradyumna Sepulveda^{1,2}, Ranganatha Sitaram^{3,4,5,6}, Mohit Rana³, Cristián Montalba¹, Cristián Tejos^{1,2}, and Sergio Ruiz^{3,5}

¹Biomedical Imaging Center, Pontificia Universidad Católica de Chile, Santiago, Chile, ²Department of Electrical Engineering, Pontificia Universidad Católica de Chile, Santiago, Chile, ³Institute of Medical Psychology and Behavioral Neurobiology, University of Tübingen, Tübingen, Germany, ⁴Sree Chitra Tirunal Institute of Medical Sciences and Technology, Trivandrum, India, ⁵Department of Psychiatry, Faculty of Medicine, Interdisciplinary Center for Neuroscience, Pontificia Universidad Católica de Chile, Santiago, Chile, ⁶Institute for Biological and Medical Engineering, Pontificia Universidad Católica de Chile, Santiago, Chile

Explicitly instructing subjects to use mental imagery and giving monetary reward are two strategies used to complement contingent neurofeedback (NF) in the process of learning to self-regulate BOLD signal with real-time fMRI NF. However, it is yet to be defined which is the optimal protocol design in rtfMRI-NF studies, critical step for potential clinical applications. The present study compares the influence of these two strategies in NF learning. Results showed a positive effect of monetary reward in BOLD signal change. Mental imagery had no significant impact in rtfMRI learning. Despite variation of strategies, brain patterns during NF training were similar.

Electronic Poster

fMRI: Analysis & Models

Exhibition Hall

Wednesday, May 11, 2016: 11:00 - 12:00

3812

Computer #49

Improved Characterization of Low-Frequency Fluctuations in Resting-State fMRI using GLM Correction of Baseline and Physiological Noise

Olivia Viessmann¹, Peter Jezzard¹, and Harald Moeller²

¹Nuffield Department of Clinical Neuroscience, University of Oxford, FMRIB Centre, Oxford, United Kingdom, ²Max-Planck Institut fuer Kognitions-und Neurowissenschaften, Leipzig, Germany

We present a method to correct multiband rs-fMRI frequency spectra for baseline and physiological noise components using a GLM in the frequency domain. We acquired short-TR (32ms) rs-fMRI whole-brain data in a group of younger and older subjects to compare the fractional amplitude of low frequency fluctuations (fALFF) between 0.01 and 0.1 Hz that is thought to decline with age. We tested the ability of the GLM approach to minimise baseline and physiological noise contributions to the fALFF. GLM post-processing increased the statistical significance of the group fALFF difference.

3813

Computer #50

Nonlinear kernel canonical correlation analysis (kCCA) in fMRI

Zhengshi Yang¹, Xiaowei Zhuang¹, Tim Curran², and Dietmar Cordes^{1,3}

¹Cleveland Clinic Lou Ruvo Center for Brain Health, Las Vegas, NV, United States, ²Department of Psychology and Neuroscience, University of Colorado Boulder, Boulder, CO, United States, ³Department of Radiology, University of Colorado-Denver, Denver, CO, United States

Kernel representation is an efficient method to extract nonlinear features without significantly increased computational complexity. Linear kernel CCA has been applied to fMRI data but the performance of nonlinear kernel CCA is still not clear. Here we investigate the accuracy of five types of kernel on simulated fMRI data and then apply Gaussian kernel CCA on real fMRI data. It provides a more sensitive and specific way to detect activation pattern.

- 3814
Computer #51 Addressing multi-centre image registration of 3T arterial spin labeling images from the GENetic Frontotemporal dementia Initiative (GENFI)
Henk Mutsaerts¹, David Thomas², Jan Petr³, Enrico de Vita², David Cash², Matthias Van Osch⁴, Paul Groot⁵, John Van Swieten⁶, Robert Laforce Jr⁷, Fabrizio Tagliavini⁸, Barbara Borroni⁹, Daniela Galimberti⁸, James Rowe¹⁰, Caroline Graff¹¹, Giovanni Frisoni⁹, Elizabeth Finger¹², Sandro Sorbi¹³, Alexandre Mendonça¹⁴, Martin Rossor², Jonathan Rohrer², Mario Masellis¹, and Bradley MacIntosh¹
- ¹Sunnybrook Research Institute, Toronto, ON, Canada, ²London, United Kingdom, ³Dresden, Germany, ⁴Leiden, Netherlands, ⁵Amsterdam, Netherlands, ⁶Rotterdam, Netherlands, ⁷Quebec City, QC, Canada, ⁸Milan, Italy, ⁹Brescia, Italy, ¹⁰Cambridge, United Kingdom, ¹¹Stockholm, Sweden, ¹²London, ON, Canada, ¹³Florence, Italy, ¹⁴Lisbon, Portugal
- One obstacle in multi-centre arterial spin labeling (ASL) studies is the variability attributed to differences between vendor- or site-specific ASL implementations. This multi-centre study compares spatial registration methods from ASL to 3D-T1, to reduce the between-subject variability of cerebral blood flow (CBF) maps. Our results demonstrate that choices of image registration have profound effects on ASL data collected using different pulse sequences and/or sites. A rigid-body registration of CBF images to segmented gray matter images produced the most robust similarity outcome as a standard approach across the different ASL implementations.
-
- 3815
Computer #52 The Novel Anisotropic Filtering Method for Noise Reduction in fMRI Utilizing Phase Information
Vahid Malekian^{1,2,3}, Danny JJ Wang⁴, Gholam-Ali Hossein-Zadeh^{2,5}, and Abbas Nasiraei Moghaddam^{1,2}
- ¹Biomedical Engineering, Amirkabir University of Technology (Tehran Polytechnic), Tehran, Iran, ²School of Cognitive Sciences, Institute for Research in Fundamental Sciences (IPM), Tehran, Iran, ³Donders Institute for Brain, Cognition and Behaviour, Radboud University, Nijmegen, Netherlands, ⁴Neurology, UCLA, Los Angeles, CA, United States, ⁵School of Electrical and Computer Engineering, University of Tehran, Tehran, Iran
- To minimize noise and artifacts in fMRI studies, authors have mostly focused on magnitude-based filtering methods and have neglected phase data due to its noisy nature. However, fMRI is a complex-valued data with also valuable phase information. Here, we propose a novel spatial weighted averaging method which uses the phase information along with magnitude to create a reference signal and utilize it iteratively to update weights. We evaluate the method on experimental A-BOSS fMRI dataset and compared with conventional smoothing methods. The results indicate that the approach can suppress noise effectively and preserve the boundaries of active regions.
-
- 3816
Computer #53 Regional optimization of physiological noise models improves functional connectivity measurements in resting-state fMRI at 7T
Sandro Nunes¹, Marta Bianciardi², Afonso Dias¹, Luís M. Silveira³, Lawrence L. Wald², and Patrícia Figueiredo¹
- ¹ISR-Lisboa/LARSyS and Department of Bioengineering, Instituto Superior Técnico – Universidade de Lisboa, Lisbon, Portugal, ²Department of Radiology, A.A. Martinos Center for Biomedical Imaging, MGH and Harvard Medical School, Boston, MA, United States, ³INESC-ID, Instituto Superior Técnico – Universidade de Lisboa, Lisbon, Portugal
- We develop physiological noise models based on cardiac/respiratory recordings, with lag optimization at various levels of specificity (group, dataset, regional and voxel), where regional optimization was achieved by clustering the lagged BOLD responses across the brain. We compare these models, both in terms of the spurious variance explained in the data and the specificity and reproducibility of functional connectivity measurements from three well-known resting-state networks in rs-fMRI at 7T. Voxelwise models explain the most variance in the data; however, connectivity strength specificity and test-retest reproducibility indicate that optimization at the regional/cluster level produces the most accurate networks.
-
- 3817
Computer #54 CSF Signal as a Complex-Valued RETROICOR Regressor Removes Unwanted Physiological Signal and Increases the Accuracy of Spatial Correlation in Complex-Valued fMRI
Mary Kociuba¹ and Daniel Rowe^{1,2}
- ¹Mathematics, Statistics, and Computer Science, Marquette University, Milwaukee, WI, United States, ²Biophysics, Medical College of Wisconsin, Milwaukee, WI, United States
- Discarding the phase component of the time-series removes relevant biological information from a complex-valued signal. Although, commonly implemented retrospective image correction techniques fail to account for physiological artifacts in both the magnitude and phase components of the time-series. Using the CSF signal, observed during the data acquisition, as a complex-valued regressor increases the statistical power of fMRI analysis, through reducing unwanted physiological variability in the complex-valued signal of interest. The improved performance of implementing the complex-valued image correction methods is demonstrated with a comparison of magnitude-only and complex-valued spatial correlations.
-
- 3818
Computer #55 An overcomplete and efficient ICA for BOLD-fMRI.
Michael Hütel^{1,2}, Andrew Melbourne¹, Jonathan Rohrer², and Sebastien Ourselin^{1,2}
- ¹Translational Imaging Group, University College London, London, United Kingdom, ²Dementia Research Centre, University College London, London, United Kingdom
- Independent Component Analysis (ICA) has been proven to produce compact representations of recurrent patterns in BOLD-fMRI imaging data. Most ICA implementations used in BOLD-fMRI, however, optimize for spatial sparse decompositions rather than independent decompositions. We describe a neural-network ICA framework that optimizes directly for sparsity and also allows for

-
- 3819
Computer #56
- Sample entropy (SampEn) differentiate patients with Major Depressive Disorder (MDD) from healthy controls and explores mechanism of MDD
Kai Wang¹, Yunwen Shao¹, Tongxin Chen¹, Chuangjian Cai¹, Yan Zhu², and Kui Ying^{3,4}
- ¹Department of Biomedical Engineering, Tsinghua University, Beijing, China, People's Republic of, ²Psychiatry Department, Yu Quan Hospital, Tsinghua University, Beijing, China, People's Republic of, ³Department of Engineering Physics, Tsinghua University, Beijing, China, People's Republic of, ⁴Key Laboratory of Particle and Radiation Imaging, Ministry of Education, Beijing, China, People's Republic of*
- Entropy indicates system irregularity. Sample Entropy (SampEn), an estimation of entropy in a relatively robust way, was used to differentiate patients with Major Depressive Disorder (MDD) from healthy controls and to explore the mechanism of MDD. In this work, we found five clusters with significantly different SampEn in MDD group from that of control group, located in left frontal lobe, left parietal lobe, left temporal lobe, cerebellum and occipital lobe respectively, and the overall accuracy obtained with linear support vector machine formed by SampEn of those regions was 86.7%(p=0.000).
-
- 3820
Computer #57
- Useful Metrics to Facilitate Clinical Application of Resting-state fMRI
Tie-Qiang Li¹, Guochun Fu², and Peter Aspelin³
- ¹Department of Medical Physics, Karolinska University Hospital, Stockholm, Sweden, ²Department of CLINTEC, Karolinska Institute, Stockholm, Sweden, ³Department of Radiology, Karolinska University Hospital, Stockholm, Sweden*
- Resting-state fMRI is useful for studying functional networks in the human brain and the abnormalities associated with various neuropsychiatric disorders. However, a lack of quantitative metrics closely associated with underlying neurophysiological characteristics has made its translation to clinical settings difficult. In this study, we propose two voxel-based metrics, namely the functional connection counter index (CCI) and connection strength index (CSI). These metrics depicts high contrast between different brain tissues and can be used for quantitative data-driven analysis to detect changes in functional connectivity related to neuropathology.
-
- 3821
Computer #58
- A Novel Model-based Segmentation Approach for Improved Activation Detection in fMRI studies
Wei-Chen Chen¹ and Ranjan Maitra²
- ¹pbdr Core Team, Silver Spring, MD, United States, ²Statistics, Iowa State University, Ames, IA, United States*
- Functional Magnetic Resonance Imaging (fMRI) provides a popular approach to imaging cerebral activation in response to stimuli. Reliably detecting activation is, however, not an easy proposition because only a very small proportions of voxels show true activation. These truly activated voxels are known to be spatially localized, yet incorporating this information is challenging to implement practically. We provide a model-based approach that incorporates spatial context in a practical and methodologically sound manner while postulating our a priori expectation that a certain proportion of voxels is truly active. Results on simulation experiments for different noise levels are uniformly encouraging. The methodology is also illustrated on a sports imagination experiment and shows its potential in making possible the adoption of fMRI as a clinical tool to detect awareness and improve treatment in individual patients in persistent vegetative state, such as traumatic brain injury survivors.
-
- 3822
Computer #59
- Estimating directed functional connectivity through autoregressive models and orthogonal Laguerre basis functions
Andrea Duggento¹, Gaetano Valenza^{2,3}, Luca Passamonti^{4,5}, Maria Guerrisi¹, Riccardo Barbieri^{3,6}, and Nicola Toschi^{1,7}
- ¹Department of biomedicine and prevention, University of Rome "Tor Vergata", Rome, Italy, ²Department of Information Engineering, and Research Centre "E. Piaggio", University of Pisa, Pisa, Italy, ³Massachusetts General Hospital and Harvard Medical School, Boston, MA, United States, ⁴Institute of Bioimaging and Molecular Physiology, National Research Council, Catanzaro, Italy, ⁵Department of Clinical Neurosciences, University of Cambridge, Cambridge, United Kingdom, ⁶Department of Electronics, Informatics and Bioengineering, Politecnico di Milano, Milano, Italy, ⁷Department of Radiology, Martinos Center for Biomedical Imaging and Harvard Medical School, Boston, MA, United States*
- Classical multivariate Granger causality-based approaches to estimating effective functional connectivity are almost exclusively based on linear autoregressive models. In order to better represent the nonlinear, multiple-time scales interactions which concur to the formation of the BOLD signals, we present a novel approach to Granger causality based on a Volterra-Wiener decomposition with use of the discrete-time, orthogonal Laguerre basis. After validation in synthetic noisy oscillator networks, we analyze timeseries data from the "HCP-500-Subjects PTN Release", revealing a clear-cut, directed interactions between components which highlights strong driving roles of the posterior occipital-inferior parietal networks, superior parietal as well as of the novel "cognitive" cerebellar regions.
-
- 3823
Computer #60
- A Software as a Service Cloud-based Platform for integrated analysis of T1-based segmentation and structure-based resting-state fMRI Processing
Yue Li¹, Hangyi Jiang^{1,2}, Can Ceritoglu³, James Pekar^{2,4}, Michael I Miller^{1,3}, Susumu Mori^{1,2}, and Andreia Vasconcellos Faria²
- ¹AnatomyWorks, LLC, Baltimore, MD, United States, ²Department of Radiology and Radiological Science, Johns Hopkins University, Baltimore, MD, United States, ³Center for Imaging Science, Johns Hopkins University, Baltimore, MD, United States, ⁴F. M. Kirby Research Center for Functional Brain Imaging, Kennedy Krieger Institute, Baltimore, MD, United States*
- Brain resting state fMRI (rs-fmri) is a useful tool for research, although its clinical impact is still limited, mainly because data from single subjects is low in power. We have shown that this limitation can be addressed by "borrowing strength" from the population, specifically

by eschewing voxel-based analyses in favor of assessing connectivity between atlas parcels [1]. We now present user-friendly software for signal processing, integrated with structural analysis, under a web-based platform "BrainGPS" (<https://braingps.mricloud.org>). Users can submit data and download results (co-registered structural and functional images, rs-fMRI time-courses, and parcel-based correlation matrices) in a few minutes.

3824
Computer #61 Sparse Estimation of Quasi-periodic Spatiotemporal Components in Resting-State fMRI
Alican Nalci^{1,2}, Bhaskar D. Rao², and Thomas T. Liu¹

¹Center for Functional MRI, University of California, San Diego, La Jolla, CA, United States, ²Electrical and Computer Engineering, University of California, San Diego, La Jolla, CA, United States

Recent studies suggest the presence of complex recurrent spatiotemporal patterns in resting-state fMRI. These patterns may affect the performance of existing preprocessing and analysis approaches, such as global signal regression and ICA. In this work we present an approach for the sparse estimation of quasi-periodic spatiotemporal components in resting state fMRI. Our algorithm successfully estimates spatiotemporal components in a sample resting-state fMRI dataset and our results suggest that the removal of these components may represent an alternative to global signal regression.

3825
Computer #62 Alzheimer's Disease is Associated with Hypo-Brain Entropy
Zhengjun Li¹ and Ze Wang^{1,2}

¹Psychiatry, University of Pennsylvania, Philadelphia, PA, United States, ²Center for Cognition and Brain Disorders, Hangzhou Normal University, Hangzhou, China, People's Republic of

Brain entropy (BEN) mapping provides a way to characterize temporal brain dynamics, and thus the health of regional brain functionality. In this study, we aimed to examine its sensitivity for differentiating Alzheimer's disease (AD) from healthy controls, as well as its relationship to AD severity. We found reduced BEN in the limbic and prefrontal area in AD compared to controls, and a negative correlation between BEN and AD severity in a widespread area of neural cortex. These results suggest BEN as a potential biomarker for AD.

3826
Computer #63 Task-Driven Functional Connectivity of White Matter in Projection Pathways of the Human Brain
Xi Wu¹, Wuzhong Bi¹, Stephen K Bailey², Laurie E Cutting^{3,4}, Jiliu Zhou¹, Adam W Anderson^{4,5,6}, John C Gore^{4,5,6}, and Zhaohua Ding^{5,6,7}

¹Department of Computer Science, Chengu University of Information Technology, Chengdu, China, People's Republic of, ²Brain Institute, Vanderbilt University, Nashville, TN, United States, ³Kennedy Center, Chengu University of Information Technology, Nashville, TN, United States, ⁴Department of Radiology and Radiological Sciences, Vanderbilt University, Nashville, TN, United States, ⁵Institute of Imaging Science, Vanderbilt University, Nashville, TN, United States, ⁶Department of Biomedical Engineering, Vanderbilt University, Nashville, TN, United States, ⁷Department of Electrical Engineering and Computer Science, Vanderbilt University, Nashville, TN, United States

Functional MRI has proven to be most effective in detecting neural activity in brain cortices on the basis of hemodynamic responses, but meanwhile has poor sensitivity in detecting neural activity in white matter. In this study, we demonstrate that MRI signals in the projection pathways have significant correlations to the primary motor cortex in finger tapping conditions, and distributions of the correlations bear clear relations with the sidedness of the task. This indicates that MRI signals in white matter may also encode neural activity, which may be detectable with sensitive methods.

3827
Computer #64 Differences in slow drift among echoes in multiband multiecho EPI data compromise TE-dependent analysis
Kun Lu¹, Javier Gonzalez-Castillo², Matthew Middleton³, Brice Fernandez⁴, Valur Olafsson⁵, Prantik Kundu⁶, Ajit Shankaranarayanan⁷, and Thomas Liu¹

¹Center for Functional Magnetic Resonance Imaging, University of California, San Diego, La Jolla, CA, United States, ²Laboratory of Brain and Cognition, Section on Functional Imaging Methods, National Institutes of Health, Bethesda, MD, United States, ³Applied Sciences Laboratory West, GE Healthcare, Menlo Park, CA, United States, ⁴Applications and Workflow, GE Healthcare, Munich, Germany, ⁵Neuroscience Imaging Center, University of Pittsburgh, Pittsburgh, PA, United States, ⁶Brain Imaging Center, Icahn Institute of Medicine at Mt. Sinai, New York, NY, United States, ⁷Applications and Workflow, GE Healthcare, Menlo Park, CA, United States

We recently observed differences in slow signal drift between multiple echoes in multiband multiecho EPI data. Such differences in drift compromise the TE dependence model and could impact the TE dependence analysis (e.g. Multiecho Independent Component Analysis ME-ICA). We first designed a metric MEQA to quantitatively measure the observed drift differences, then investigated the effects of the drift differences on ME-ICA analysis.

3828
Computer #65 Reproducibility of low frequency components in scan-rescan resting state fMRI data
Katherine A Koenig¹, Wanyong Shin¹, Sehong Oh¹, and Mark J Lowe¹

¹Imaging Sciences, The Cleveland Clinic, Cleveland, OH, United States

This work investigates the reproducibility of low frequency fluctuations by assessing the relationship of scan-rescan timeseries data taken during a resting state fMRI. We look at the relationship between various cortical regions and white matter and CSF.

3829
Computer #66 High Resolution fMRI with Constrained Evolution Reconstruction
Xuesong Li¹, Lyu Li¹, Xiaodong Ma¹, Xue Zhang¹, Zhe Zhang¹, Bida Zhang², Sen Song³, and Hua Guo¹

¹Center for Biomedical Imaging Research, Department of Biomedical Engineering, School of Medicine, Tsinghua University, Beijing, China, People's Republic of, ²Healthcare Department, Philips Research China, Shanghai, China, People's Republic of, ³Department of Biomedical Engineering, School of Medicine, Tsinghua University, Beijing, China, People's Republic of

fMRI with high temporal and/or spatial resolution is beneficial for psychology and neuroscience studies, but is limited by various factors. Compressed Sensing (CS) based methods for accelerating fMRI data acquisition are promising, however, it may be problematic because the over-smoothing effects may contaminate the hemodynamic oscillation of fMRI data. This study aimed to develop a new method, Dual Extended TRACER (DUET), based on Temporal Resolution Acceleration with Constrained Evolution Reconstruction (TRACER), for accelerating fMRI acquisitions using golden angle variable density spiral. Results show DUET can recover fMRI hemodynamic signals in even 14 fold under-sampling. Compared with other methods, DUET provides better signal recovery, higher fMRI signal sensitivity and more reliable activity maps.

3830
Computer #67 Complex-Valued Correlation Increases Sensitivity and Specificity in the Analysis of Low Contrast-to-Noise fMRI Time-Series
Mary Kociuba¹ and Daniel Rowe^{1,2}

¹Mathematics, Statistics, and Computer Science, Marquette University, Milwaukee, WI, United States, ²Biophysics, Medical College of Wisconsin, Milwaukee, WI, United States

The standard in fMRI is a magnitude-only statistical analysis of the data, despite evidence of task related change in the phase time-series. This study demonstrates the increased sensitivity and specificity of implementing complex-valued correlation models for low magnitude and phase contrast-to-noise ratio (CNR) values in fMRI data sets.

3831
Computer #68 Modeling Resting Cerebral Perfusion from BOLD Signal Dynamics During Hyperoxia
M. Ethan MacDonald¹, Avery J.L. Berman^{1,2}, Erin L. Mazerolle¹, Rebecca J. Williams¹, and G. Bruce Pike¹

¹Departments of Radiology & Clinical Neurosciences, University of Calgary, Hotchkiss Brain Institute, Seaman Family MR Research Centre, Foothills Medical Centre, Calgary, AB, Canada, ²Montreal Neurological Institute, Montreal, QC, Canada

In this work we demonstrate the use of BOLD-fMRI during hyperoxia to obtain perfusion parameters, including CBF, CBV, and MTT. During BOLD imaging, subjects breathing from a respiratory circuit inhaled air whose oxygen content was increased from 21% to 70%. The exhaled oxygen concentration was processed to obtain an arterial input function, and the concentration of bound oxygen in the venous blood was determined by modeling the BOLD time series. Through deconvolution modeling we were able to obtain measurements of CBF, venous CBV, and MTT within expected ranges.

3832
Computer #69 Mean-Shift Clustering Technique For fMRI Activation Detection
Leo Ai¹ and Jinhu Xiong²

¹University of Minnesota, Minneapolis, MN, United States, ²University of Iowa, Iowa City, IA, United States

It has been shown the application of Mean-Shift Clustering (MSC) to fMRI analysis can increase detection sensitivity in low contrast to noise situations. In this study, MSC was utilized with a feature space containing both temporal and spatial features to further increase its detection power. If successful, the proposed technique can improve detection in techniques that inherently have low CNR, such as non-proton fMRI or non-BOLD fMRI.

3833
Computer #70 Deterministic Estimation of Spatiotemporal Motifs in Resting-State fMRI
Alican Nalci^{1,2} and Thomas Liu²

¹Electrical and Computer Engineering, University of California San Diego, La Jolla, CA, United States, ²Center for Functional MRI, University of California San Diego, La Jolla, CA, United States

In resting-state fMRI data, dynamic quasi-periodic spatio-temporal patterns have previously been identified in both animal and humans with potential links to infra slow electrical activity. These prior studies used an iterative pattern-finding algorithm that employed heuristic learning rules for the dynamic adjustment of correlation thresholds. Here we present a novel deterministic non-iterative approach for estimating spatiotemporal motifs in resting-state fMRI data without the need for heuristic learning rules.

3834
Computer #71 A Systematic Investigation on the BOLD Contrast in S1- and S2-SSFP fMRI
Mahdi Khajehim¹ and Abbas Nasiraei Moghaddam^{1,2}

¹Biomedical Engineering, Amirkabir University of Technology, Tehran, Iran, ²School of Cognitive Sciences, Institute for Research in Fundamental Sciences (IPM), Tehran, Iran

Non-balanced SSFP can provide banding artifact free images, with reduced sensitivity to B1 inhomogeneity and SAR level. Recently, non-balanced SSFP which is known by the S1 and S2 signals, has been utilized for fMRI. In this study to model the BOLD contrast in S1- and S2-SSFP fMRI a Monte Carlo simulation has been performed. It will enable us to accurately investigate the dependence of the BOLD contrast on vessel size and acquisition parameters. Results are in accordance with the reported experimental values and show the

increased sensitivity to capillary-sized vessels for only S2 signal.

3835

Computer #72 Monte Carlo Simulation for A-BOSS fMRI
Mahdi Khajehim¹ and Abbas Nasiraei Moghaddam^{1,2}

¹Biomedical Engineering, Amirkabir University of Technology, Tehran, Iran, ²School of Cognitive Sciences, Institute for Research in Fundamental Sciences (IPM), Tehran, Iran

Averaged-BOSS fMRI has been proposed as an alternative to BOSS fMRI to eliminate its spatial coverage problem. The feasibility of A-BOSS has been previously investigated. Due to the complexity presented in A-BOSS fMRI, in this work a Monte Carlo simulation has been performed for a comprehensive investigation on its achievable functional contrast and to compare the results with S1 and S2 SSFP fMRI. The obtained results show the superior absolute signal change for A-BOSS and demonstrate the desirable acquisition parameters.

Electronic Poster

Hepatobiliary 1: Quantitative

Exhibition Hall

Wednesday, May 11, 2016: 13:30 - 14:30

3836

Computer #1 Motion insensitive quantification of liver proton density fat-fraction using a single-shot 2D technique
Jeannine A. Ruby¹, Diego Hernando¹, Camilo A. Campo¹, Ann Shimakawa², Karl K. Vigen¹, James H. Holmes³, Kang Wang³, and Scott B. Reeder^{1,4,5,6,7}

¹Radiology, University of Wisconsin-Madison, Madison, WI, United States, ²Global MR Applications and Workflow, GE Healthcare, Menlo Park, CA, United States, ³Global MR Applications and Workflow, GE Healthcare, Madison, WI, United States, ⁴Medicine, University of Wisconsin-Madison, Madison, WI, United States, ⁵Medical Physics, University of Wisconsin-Madison, Madison, WI, United States, ⁶Biomedical Engineering, University of Wisconsin-Madison, Madison, WI, United States, ⁷Emergency Medicine, University of Wisconsin-Madison, Madison, WI, United States

In this study, we developed and validated a "single-shot" sequential 2D-chemical shift-encoded MRI (CSE-MRI) technique for motion-insensitive quantification of liver proton density fat fraction (PDFF). A phantom of 11 vials with varying PDFF demonstrated equivalent PDFF between 2D- and 3D-CSE-MRI. Fifteen subjects underwent five different CSE-MRI acquisitions: 3D-single-breathhold (BH), slice-interleaved 2D-single-BH and free-breathing (FB), and sequential 2D-single-BH and FB. PDFF was measured and averaged across all nine Couinaud liver segments. Good agreement was observed in PDFF between all 2D-CSE-MRI acquisitions and 3D-CSE-MRI. Qualitative motion artifact evaluation demonstrated significantly superior scores for free-breathing "single-shot" sequential 2D-CSE-MRI compared to free-breathing slice-interleaved 2D-CSE-MRI.

3837



Computer #2 Free-Breathing Liver Fat Quantification Using an Undersampled Multi-Echo 3D Stack-of-Radial Technique
Tess Armstrong^{1,2}, Isabel Dregely^{1,3}, Alto Stemmer⁴, Yutaka Natsuaki⁵, and Holden Wu^{1,2}

¹Radiological Sciences, University of California, Los Angeles, Los Angeles, CA, United States, ²Physics and Biology in Medicine, University of California, Los Angeles, Los Angeles, CA, United States, ³Biomedical Engineering, King's College London, London, United Kingdom, ⁴Siemens Healthcare, Erlangen, Germany, ⁵Siemens Healthcare, Los Angeles, CA, United States

Non-alcoholic fatty liver disease is the leading cause of chronic liver disease. Multi-echo Cartesian MRI methods can non-invasively quantify liver fat, but are susceptible to motion artifacts and limited by breath hold (BH) imaging. We have developed a new free-breathing (FB) liver fat quantification method using non-Cartesian 3D stack-of-radial imaging. To reduce scan time, we undersampled data up to a factor of R=3. In healthy subjects, mean fat quantification was statistically equivalent among different R. Initial comparisons with spectroscopy show good agreement. Our new technique can potentially achieve accurate whole-liver fat quantification within a fast 1-minute FB scan.

3838



Computer #3 Detection of Reduction in Liver Stiffness as a Result of Weight Loss Surgery using MR Elastography
Curtis N. Wiens¹, Alan B. McMillan¹, Nathan S. Artz^{1,2}, Rashmi Agni³, Michael Peterson⁴, Nikolaus Szeverenyi⁵, William Haufe⁵, Catherine Hooker⁵, Luke Funk⁶, Jacob Greenberg⁶, Guilherme M. Campos⁷, Santiago Horgan⁸, Garth Jacobsen⁸, Tanya Wolfson⁹, Claude Sirlin⁵, and Scott B. Reeder^{1,10,11,12,13}

¹Radiology, University of Wisconsin, Madison, WI, United States, ²Diagnostic Imaging, St. Jude Children's Research Hospital, Memphis, TN, United States, ³Pathology, University of Wisconsin, Madison, WI, United States, ⁴Tacoma General Pathology, Tacoma, WA, United States, ⁵Radiology, University of California, San Diego, CA, United States, ⁶Surgery, University of Wisconsin, Madison, WI, United States, ⁷Virginia Commonwealth University, Surgery, VA, United States, ⁸Surgery, University of California, San Diego, CA, United States, ⁹Computational and Applied Statistics Laboratory, University of California, San Diego, CA, United States, ¹⁰Medical Physics, University of Wisconsin, Madison, WI, United States, ¹¹Biomedical Engineering, University of Wisconsin, Madison, WI, United States, ¹²Medicine, University of Wisconsin, Madison, WI, United States, ¹³Emergency Medicine, University of Wisconsin, Madison, WI, United States

This study tracked changes in liver stiffness in morbidly obese patients undergoing bariatric surgery. 22 patients undergoing bariatric surgery were recruited for MRI studies including MR elastography (MRE) at 2 time points: 1-2 days prior to and 6 months after bariatric surgery. Changes in liver stiffness as measured by MRE were compared to intraoperative biopsies which were performed to assess relevant histological features (steatosis, inflammation and fibrosis) and their relation to liver stiffness. Follow-up measurement of liver stiffness 6 months after bariatric surgery showed statistically significant reductions in liver stiffness. Patients with biopsy confirmed liver

fibrosis, inflammation and features of NASH exhibited the largest reductions in liver stiffness.

-
- 3839
Computer #4
- Is fat a confounding factor for MOLLI T1 measurements in the liver at 3 Tesla?
Ferenc E Mozes¹, Elizabeth M Tunnicliffe¹, Michael Pavlides^{1,2}, and Matthew D Robson¹
- ¹RDM Cardiovascular Medicine, University of Oxford, Oxford, United Kingdom, ²Translational Gastroenterology Unit, University of Oxford, Oxford, United Kingdom
- The balanced steady-state free precession (bSSFP) sequence at 3T causes water and fat signals to be out of phase when TR=2.3 ms. Since the modified Look-Locker inversion recovery (MOLLI) mapping uses bSSFP readouts, the T1 of voxels that contain both fat and water is influenced by the choice of this TR. Simulations, phantom experiments and measurements collected from patients undergoing bariatric surgery were used to assess the impact of hepatic lipid content on liver MOLLI T1 values.
-
- 3840
Computer #5
- Feasibility of utilizing heterogeneity of hepatic stiffness in 3D MR elastography to improve detection of liver fibrosis in pediatric patients with nonalcoholic fatty liver disease
Kang Wang¹, Paul Manning¹, Tanya Wolfson², Michael S. Middleton¹, Jeffrey Schwimmer³, Kimberley Newton³, Cynthia Behling³, Janis Durelle³, Melissa Paiz³, Jorge Angeles³, Meng Yin⁴, Kevin Glaser⁴, Richard Ehman⁴, and Claude Sirlin¹
- ¹Liver Imaging Group, Department of Radiology, University of California, San Diego, School of Medicine, San Diego, CA, United States, ²Computational and Applied Statistics Laboratory, University of California, San Diego, San Diego, CA, United States, ³Department of Pediatric, University of California, San Diego, San Diego, CA, United States, ⁴Departments of Radiology, Mayo Clinic, Rochester, MN, United States
- We evaluated the feasibility of utilizing heterogeneity of hepatic stiffness in 3D MR elastography to improve detection of liver fibrosis in a cohort of 70 children with NAFLD. Children were dichotomized into two classes of fibrosis. We characterized the heterogeneity of hepatic stiffness by fitting a bi-Gaussian model to the histogram of hepatic stiffness. Features from the bi-Gaussian model and the known class labels were used to develop a support vector machine (SVM) classification model to predict fibrosis. We demonstrated that the SVM model has better overall classification performance than the calculated mean hepatic stiffness as measured by AUROC.
-
- 3841
Computer #6
- Proton-density fat-fraction quantification of the liver in the presence of ferumoxytol at 1.5T and 3T
Camilo A Campo¹, Diego Hernando¹, Tilman B Schubert¹, Utaroh Motosugi^{1,2}, Samir D Sharma¹, Shane A Wells¹, and Scott B Reeder^{1,3,4,5,6}
- ¹Radiology, University of Wisconsin-Madison, Madison, WI, United States, ²Radiology, University of Yamanashi, Yamanashi, Japan, ³Medical Physics, University of Wisconsin-Madison, Madison, WI, United States, ⁴Biomedical Engineering, University of Wisconsin-Madison, Madison, WI, United States, ⁵Medicine, University of Wisconsin-Madison, Madison, WI, United States, ⁶Emergency Medicine, University of Wisconsin-Madison, Madison, WI, United States
- This study evaluated the accuracy of liver proton-density fat-fraction (PDFF) quantification in the presence of ferumoxytol. Seven healthy subjects underwent MRI scans immediately before injection of ferumoxytol and one day after injection. Our results indicate that confounder-corrected chemical shift-encoded MRI PDFF estimates exhibit a small but significant bias in the presence of ferumoxytol. This bias could be due to differential shortening in the T2* of water and fat signals. Therefore, investigators attempting to create human models of iron and fat within the liver by administering ferumoxytol to patients with fatty liver should be aware of this potential source of bias.
-
- 3842
Computer #7
- Impaired hepatic arterial buffer response in a rodent model of chronic liver disease: assessment using caval subtraction phase-contrast MRI at 9.4T
Manil Chouhan¹, Alan Bainbridge², Nathan Davies³, Simon Walker-Samuel⁴, Shonit Punwani¹, Mark Lythgoe⁴, Rajeshwar Mookerjee³, and Stuart Taylor¹
- ¹UCL Centre for Medical Imaging, University College London, London, United Kingdom, ²Department of Medical Physics, University College London Hospitals NHS Trust, London, United Kingdom, ³UCL Institute for Liver and Digestive Health, University College London, London, United Kingdom, ⁴UCL Centre for Advanced Biomedical Imaging, University College London, London, United Kingdom
- Total liver blood flow (TLBF) is closely regulated in health so that reductions in portal venous (PV) flow are buffered by compensatory rises in hepatic arterial (HA) flow. In this study we use caval subtraction phase-contrast MRI to estimate TLBF and HA flow in cirrhotic rats and demonstrate an impaired HA buffer response after administering terlipressin, a vasopressin analogue used clinically used to reduce PV flow in portal hypertension.
-
- 3843
Computer #8
- Effect of choosing an in-phase vs. a default echo time in 2D MR elastography to estimate hepatic stiffness
Kang Wang¹, William Haufe¹, Nikolaus Szeverenyi¹, Alexandra Schlein¹, Tanya Wolfson², Michael S. Middleton¹, Jeffrey Schwimmer³, Kimberley Newton³, Cynthia Behling³, Janis Durelle³, Melissa Paiz³, Jorge Angeles³, Len Lazar⁴, Diana De La Pena⁴, Carolyn Hernandez⁴, Rohit Loomba⁴, Meng Yin⁵, Kevin Glaser⁵, Richard Ehman⁵, and Claude Sirlin¹
- ¹Liver Imaging Group, Department of Radiology, University of California, San Diego, School of Medicine, San Diego, CA, United States, ²Computational and Applied Statistics Laboratory, University of California, San Diego, San Diego, CA, United States, ³Department of Pediatric, University of California, San Diego, San Diego, CA, United States, ⁴NAFLD Translational Research Unit, Division of Gastroenterology, University of California, San Diego, San Diego, CA, United States, ⁵Departments of Radiology, Mayo Clinic, Rochester, MN, United States

To investigate the effect of different echo times (TE) in 2D MR elastography (2D MRE) to estimate hepatic stiffness, two 2D MRE scans were acquired in 50 patients using a 3T GE scanner, one with a default TE value of 20.1 ms (default-TE), and with a nearest in-phase TE value of 20.6 ms (IP-TE). Wave-image quality of each scan was measured quantitatively by ROI size. We demonstrated that 2D MRE with an in-phase TE provides slightly higher wave-image quality in patients with high PDFF, and potentially may be advantageous for fibrosis assessment in NAFLD.

-
- 3844
Computer #9
Deferiprone has a dose-dependent effect on liver iron concentration assessed by MRI
Antonella Meloni¹, Vincenzo Positano¹, Gianluca Valeri², Gennaro Restaino³, Chiara Tudisca⁴, Paolo Preziosi⁵, Elisabetta Chiodi⁶, Maria Giovanna Neri¹, Stefano Pulini⁷, Basilia Piraino⁸, Petra Keilberg¹, and Alessia Pepe¹
- ¹Fondazione G. Monasterio CNR-Regione Toscana, Pisa, Italy, ²Azienda Ospedaliero-Universitaria Ospedali Riuniti "Umberto I-Lancisi-Salesi", Ancona, Italy, ³Fondazione di Ricerca e Cura "Giovanni Paolo II", Campobasso, Italy, ⁴Policlinico "Paolo Giaccone", Palermo, Italy, ⁵Policlinico "Casilino", Roma, Italy, ⁶Arcispedale "S. Anna", Ferrara, Italy, ⁷Ospedale Civile "Spirito Santo", Pescara, Italy, ⁸Policlinico "G. Martino", Messina, Italy*
- The aim of this multi-centre study was to retrospectively assess in thalassemia major (TM) if deferiprone (DFP) had a dose-dependent effect on liver iron concentration (LIC) assessed by quantitative magnetic resonance imaging (MRI). We found out that the percentage of patients that worsened their status was significantly higher in patients with ≤ 75 mg/kg/d than in patients with > 75 mg/kg/d (26.6% vs 7.7%; $P=0.016$). So, the worsening in MRI LIC can be prevented by increasing the dose of deferiprone above the widely used regimen of 75 mg/kg body weight.
-
- 3845
Computer #10
Standardized approach for region-of-interest-based measurements of proton-density fat-fraction and R2* in the liver
Camilo A Campo¹, Diego Hernando¹, Candice Bookwalter^{1,2}, Tilman B Schubert¹, and Scott B Reeder^{1,3,4,5,6}
- ¹Radiology, University of Wisconsin-Madison, Madison, WI, United States, ²Radiology, Mayo Clinic, Rochester, MN, United States, ³Medical Physics, University of Wisconsin-Madison, Madison, WI, United States, ⁴Biomedical Engineering, University of Wisconsin-Madison, Madison, WI, United States, ⁵Medicine, University of Wisconsin-Madison, Madison, WI, United States, ⁶Emergency Medicine, University of Wisconsin-Madison, Madison, WI, United States*
- This study evaluated the reproducibility of different region-of-interest (ROI) sampling methods for MRI-based proton-density fat-fraction (PDFF) and R2* (1/T2*) measurements in the liver. 53 patient liver MRI datasets were retrospectively analyzed using ROI sampling methods that have been previously reported. Patients were not suspected of having hepatic steatosis or liver iron overload. Our results demonstrate improved measurement repeatability when the sampling area of the liver is increased by using multiple, large ROIs. Therefore, ROI-based measurements of liver PDFF and R2* should strive to sample the largest possible area of liver by using ROIs that are large in size and number.
-
- 3846
Computer #11
R2* of liver fat and water compared to proton density fat fraction estimated by 1H MRS
Gavin Hamilton¹, Alexandra N Schlein¹, Adrija Mamidipalli¹, Michael S Middleton¹, Rohit Loomba², and Claude B Sirlin¹
- ¹Department of Radiology, University of California, San Diego, San Diego, CA, United States, ²Department of Medicine, University of California, San Diego, San Diego, CA, United States*
- MRI based methods of estimating hepatic proton density fat fraction (PDFF) measure only one R2* value, as the R2* of fat and water are assumed to be identical. MRS can estimate the R2* of both fat and water. Liver MRS spectra were fitted with constraints derived from those used in MRI, and water R2* and fat R2*^{eff} (the effective fat R2* that would be measured by MRI) were compared to PDFF. We found that water R2* was independent of PDFF, while fat R2*^{eff} was weakly and inversely correlated with PDFF.
-
- 3847
Computer #12
The Feasibility Study of Liver Cirrhosis Stage Using Quantitative 3D Whole-Liver T1p Mapping at 3.0T
Xin Chen¹, Weibo Chen^{2,3}, Guangbin Wang⁴, Shanshan Wang⁴, Tao Gong¹, and Sai Shao¹
- ¹Shandong University, Jinan, China, People's Republic of, ²Shanghai Key Laboratory of Magnetic Resonance and Department of Physics, East China Normal University, China, People's Republic of, ³Shangdong Medical Imaging Research Institute, Jinan, China, People's Republic of*
- Liver cirrhosis is an abnormal liver condition that the liver would repair it through the deposition of collagen, proteoglycans, and other macromolecules. Invasive method that can objectively and simply assessment and grade the liver fibrosis is clinically required. T1p relaxation time has been proven to be an invasive biomarker to investigate liver fibrosis. The first whole-liver study was carried out on 1.5T MR Scanner [3]. The purpose of our study was to implement the method to initially apply the method to evaluate severity of whole-liver cirrhosis non-invasively at 3.0T.
-
- 3848
Computer #13
Liver parenchymal T1: repeatability and studies in a rodent model of chronic liver disease at 9.4T
Manil Chouhan¹, Rajiv Ramasawmy², Adrienne Campbell-Washburn², Alan Bainbridge³, Nathan Davies⁴, Shonit Punwani¹, Rajeshwar Mookerjee⁴, Simon Walker-Samuel², Mark Lythgoe², and Stuart Taylor¹
- ¹UCL Centre for Medical Imaging, University College London, London, United Kingdom, ²UCL Centre for Advanced Biomedical Imaging, University College London, London, United Kingdom, ³Department of Medical Physics, University College London Hospitals NHS Trust, London, United Kingdom, ⁴UCL Institute for Liver and Digestive Health, University College London, London, United Kingdom*
- There is a growing interest in the use of hepatic parenchymal T1 for the assessment of hepatic fibrosis. Using Look-Locker T1 measurements at 9.4T in a rat model of cirrhosis, we demonstrate that these measurements are repeatable and significantly different in

animals with and without chronic liver disease.

-
- 3849
Computer #14 Feasibility of Breath-hold Quantitative Susceptibility Mapping on Hepatic Iron quantification
Huimin Lin¹, Hongjiang Wei², Chunlei Liu², Xu Yan³, Caixia Fu⁴, and Fuhua Yan¹
- ¹Radiology, Ruijin Hospital, Shanghai Jiao Tong University School of Medicine, Shanghai, China, People's Republic of, ²Brain Imaging and Analysis Center, Duke University, Durham, NC, United States, ³MR Collaboration NE Asia, Siemens Healthcare, Shanghai, China, People's Republic of, ⁴Siemens Shenzhen Magnetic Resonance Ltd, Shenzhen, China, People's Republic of
- The purpose of this study was to estimate the Quantitative susceptibility mapping (QSM) in hepatic iron evaluation, compared with R2 based Liver concentration estimation (Ferriscan LIC). 7 Patients were scanned on a 1.5 T MR System using a GRE sequence and a SE sequence, for QSM and Ferriscan analysis respectively. QSM algorithm provided susceptibility values estimate. Approximate slices were selected according to the corresponding cross-section on the Ferriscan LIC report. Then ROIs were drawn on QSM images according to LIC maps. Significant positive correlation was observed between QSM and Ferriscan LIC ($R^2 = 0.8$).
-
- 3850
Computer #15 THE EVALUATION OF PORTAL HYPERTENSION USING QUANTITATIVE MAGNETIC RESONANCE IMAGING (MRI)
Eleanor F Cox¹, Naaventhana Palaniyappan², Andrew Austin³, Richard O'Neill⁴, Greg Ramjas⁴, Simon Travis⁴, Hilary White⁴, Rajeev Singh³, Peter Thurley³, Indra Neil Guha², Guruprasad Padur Aithal², and Susan T Francis¹
- ¹SPMIC, School of Physics & Astronomy, University of Nottingham, Nottingham, United Kingdom, ²NIHR Nottingham Digestive Diseases Biomedical Research Unit, Nottingham University Hospitals NHS Trust and University of Nottingham, Nottingham, United Kingdom, ³Royal Derby Hospital, Derby, United Kingdom, ⁴Department of Radiology, Nottingham University Hospitals NHS Trust, Nottingham, United Kingdom
- The hepatic venous pressure gradient (HVPG) is the only validated measure to assess portal pressure but this is invasive and not widely available. Here, we use non-invasive MR parameters as a surrogate for portal pressure. Longitudinal relaxation time (T1) measures of the liver and spleen, phase contrast measures of splanchnic and collateral flow, and ASL measures of perfusion are correlated against HVPG measures in 30 patients. Liver tissue T1 is shown to be positively correlated with HVPG ($p < 0.001$). Combining T1 measures with splenic artery velocity using a simple linear model, it is shown that HVPG can be non-invasively assessed.
-
- 3851
Computer #16 MRI Evaluation of Acetaminophen Induced Liver Failure in Mice using T1 Mapping and Stable Gadodetate Disodium Administration
Christiane Mallett¹, Matthew Latourette¹, Anna Kopec², James Luyendyk², and Erik Shapiro¹
- ¹Radiology, Michigan State University, East Lansing, MI, United States, ²Pathobiology & Diagnostic Investigation, Michigan State University, East Lansing, MI, United States
- We are developing an MRI method to measure acetaminophen toxicity in the liver. We obtained T1 maps using the clinically approved contrast agent gadodetate disodium (Eovist). The contrast agent was administered by infusion to maintain a steady liver concentration throughout the T1 mapping. Mice with acetaminophen toxicity had higher T1 and heterogeneous gadodetate disodium uptake compared to healthy controls. This is a promising method for quantifying drug induced liver damage in vivo.
-
- 3852
Computer #17 Comparison of R2* of liver water and fat using 1H MRS
Gavin Hamilton¹, Alexandra N Schlein¹, Adrija Mamidipalli¹, Michael S Middleton¹, Rohit Loomba², and Claude B Sirlin¹
- ¹Department of Radiology, University of California, San Diego, San Diego, CA, United States, ²Department of Medicine, University of California, San Diego, San Diego, CA, United States
- To estimate hepatic proton density fat fraction (PDFF), MRI techniques acquire multi-echo, gradient-echo images, assuming the R2* of fat and water to be identical. Liver MRS spectra were fitted with constraints derived from those used in MRI to examine this assumption. We compared fat R2*^{eff} (the effective fat R2* that would be measured by MRI) with water R2* and found that water R2* and fat R2*^{eff} were correlated. There was no significant difference between water R2* and fat R2*^{eff}, supporting the assumption that when measuring PDFF using MRI, fat and water R2* can be treated as identical.
-
- 3853
Computer #18 Iron measurements by quantitative MRI-R2* at 3.0 and 1.5 T
Jin Yamamura¹, Sarah Keller¹, Regine Grosse², Bjoern Schoennagel¹, Peter Nielsen³, Zhiyue Jerry Wang⁴, Joachim Graessner⁵, Hendrick Kooijman⁶, Gerhard Adam¹, and Roland Fischer^{3,7}
- ¹Diagnostic and Interventional Radiology, University Medical Center Hamburg-Eppendorf, Hamburg, Germany, ²Hematology and Oncology, University Medical Center Hamburg-Eppendorf, Hamburg, Germany, ³Biochemistry, University Medical Center Hamburg-Eppendorf, Hamburg, Germany, ⁴Radiology, University of Texas Southwestern Medical Center, Dallas, TX, United States, ⁵Siemens Healthcare AG, Hamburg, Germany, ⁶Philips Medical Care, Hamburg, Germany, ⁷Radiology, Children's Hospital & Research Center Oakland, Oakland, CA, United States
- We are investigating the suitability of a 3.0 T imager for iron measurements over the whole range of possible iron concentrations in the liver and spleen iron. For liver iron measurements in severely overloaded patients with LIC > 2400 µg/g liver or > 15 mg/g dry weight, 1.5 Tesla imagers are better suited than 3.0 Tesla systems.
-
- 3854
A prospective study comparing R2* derived Liver iron concentration(LIC) with noise-corrected post processing of data against FerriScan

Computer #19 reported LIC in patients with liver iron overload.
Kartik Jhaveri¹, Stephan Kannengiesser², Nima Sadougi³, Marshall Sussman¹, Hooman Hosseini-Nik³, Leila Zahedi³, and Richard Ward¹

¹UHN, University of Toronto, Toronto, ON, Canada, ²Siemens Germany, Erlangen, Germany, ³UHN, Toronto, ON, Canada

MRI is currently utilised as a non-invasive method for liver iron concentration (LIC) estimation and has essentially replaced liver biopsy. FerriScan derived LIC is considered the “gold standard” but has associated increased costs and delay results from required external data transmittal. There is no universal agreement or standardization of R2* derived LIC methods. We describe an optimized R2* method with noise corrected post processing of data for LIC estimation with simultaneous comparison to FerriScan derived LIC. Our results show very good correlation between R2* LIC and FerriScan LIC with potential for substitution of the latter with our R2* technique.

3855
Computer #20 Agreement between MRE-estimated liver stiffness using 2D GRE and 2D SE-EPI pulse sequences at 3T
Adrija Mamidipalli¹, Jonathan Hooker¹, Nikolaus Szevenyi¹, Alexandra Schlein¹, William Hauffe¹, Tanya Wolfson², Gavin Hamilton¹, Michael Middleton¹, and Claude Sirlin¹
¹Liver Imaging Group, UCSD, San Diego, CA, United States, ²Computational and Applied Statistics Laboratory, San Diego Supercomputer, UCSD, San Diego, CA, United States

In this study, agreement between MRE-estimated liver stiffness using 2D GRE and SE-EPI pulse sequences at 3T was examined in 30 adults with histology-confirmed nonalcoholic fatty liver disease (NAFLD) enrolled in a research registry. Results show that liver stiffness values obtained from both the sequences agree closely across a range of liver stiffness values for adults with NAFLD, although agreement tends to diverge at higher stiffness values. Differences at higher liver stiffness values were not explained by differences in image wave quality.

3856
Computer #21 Assessment of liver fibrosis by MRI tagging of cardiac-induced motion: preliminary results
Leonie Petitclerc^{1,2}, Guillaume Gilbert^{2,3,4}, Claire Wartelle-Bladou⁵, Giada Sebastiani⁶, Bich Nguyen^{7,8}, and An Tang^{1,2,4}
¹Centre de recherche du Centre hospitalier de l'Université de Montreal, Montreal, QC, Canada, ²Department of Radiology, Radio-Oncology and Nuclear Medicine, Université de Montreal, Montreal, QC, Canada, ³Philips Healthcare Canada, Montreal, QC, Canada, ⁴Centre hospitalier de l'Université de Montreal, Montreal, QC, Canada, ⁵Department of Gastroenterology and Hepatology, Université de Montreal, Montreal, QC, Canada, ⁶Department of Medicine, Division of Gastroenterology, McGill University Health Centre, Montreal, QC, Canada, ⁷Department of Pathology, Centre hospitalier de l'Université de Montreal, Montreal, QC, Canada, ⁸Department of Pathology and Cellular Biology, Université de Montreal, Montreal, QC, Canada

Elastography for the staging of liver fibrosis is optimized for the right liver and requires additional hardware. Using MRI tagging, the displacement and strain of liver tissue induced by cardiac motion was quantified with the Harmonic Phase (HARP) method. Of the four schemes tested for the extraction of a single measure of strain, one was especially promising, as it showed high correlation with fibrosis stages (Spearman's $\rho=0.913$), as well as a significant p -value for dichotomized diagnosis of $\geq F3$ fibrosis ($p=0.03$). These preliminary results suggest that strain measurements could be used as a diagnostic tool for the staging of liver fibrosis.

3857
Computer #22 Assessment of fibrotic liver using T1rho mapping: a rat model study
Qihua Yang¹, Taihui Yu¹, Hui Zhang², Hua Guo², Yingjie Mei³, Ziliang Cheng¹, Jingwen Huang¹, and Biling Liang¹
¹Radiology Dept, Sun Yat-sen Memorial Hospital, Guangzhou, China, People's Republic of, ²Center for Biomedical Imaging Research, Department of Biomedical Engineering, School of Medicine, Tsinghua University, Beijing, China, People's Republic of, ³Philips Healthcare, Guangzhou, China, People's Republic of

To find out the relationship among T1rho, liver fibrosis stages and liver function, MRI including T1rho sequence was performed in 32 CCl4 induced liver fibrosis SD rat models and 12 SD rats of control group. Laboratory test related to liver function were done before execution and liver was taken out for pathology evaluation. Liver fibrosis was staged according to staging systems for rodents. Results showed that T1rho could be used to diagnose early liver fibrosis ($>F2$) and correlation was significant between T1rho values and both liver fibrosis stage and blood serum parameters.

3858
Computer #23 The effect of long diffusion time on the diffusion measurements of fibrotic human liver
Hui Zhang¹, Pairash Saiviroonporn², Ed X Wu^{3,4}, and Hua Guo¹
¹Center for Biomedical Imaging Research, Department of Biomedical Engineering, School of Medicine, Tsinghua University, Beijing, China, People's Republic of, ²Department of Radiology, Faculty of Medicine Siriraj Hospital, Mahidol University, Bangkok, Thailand, ³Laboratory of Biomedical Imaging and Signal Processing, The University of Hong Kong, Hong Kong SAR, China, People's Republic of, ⁴Department of Electrical and Electronic Engineering, The University of Hong Kong, Hong Kong SAR, China, People's Republic of

To examine whether different diffusion times would yield different sensitivities in detecting the pathological alterations in tissue microstructure during liver fibrogenesis in human livers at 3 T. MRI including single-shot SE and simulated echo acquisition mode (STEAM) DWI EPI sequences were performed on 10 healthy volunteers and 19 liver fibrotic patients. One-way ANOVA with Turkey's multiple comparison tests were employed to compare quantitative measurements between the volunteers and patients with different diffusion times. Results showed that diffusion measurements with higher diffusion times will be more sensitive as a biomarker to detect the pathological alterations in tissue microstructure in fibrotic patients.

¹Biomedical Engineering, University of Southern California, Sierra Madre, CA, United States, ²Cardiology, Boston Children's Hospital, Boston, MA, United States, ³Pediatrics, Harvard School of Medicine, Boston, MA, United States, ⁴Cardiology, Children's Hospital of Los Angeles, Los Angeles, CA, United States, ⁵Biomedical Engineering, University of Southern California, Los Angeles, CA, United States

CPMG-based R2 (1/T2) estimates are traditionally insensitive to tissue iron load. We show that the application of a T1-corrected, skeletal muscle-based proton density constraint increases the sensitivity of R2 for iron quantitation in phantoms and human subjects. This method leads to a fundamentally different R2-LIC (liver iron concentration) calibration curve than has previously been applied to CPMG fit data.

Whole Body & Male Pelvis

- 3860
Computer #25 Accelerated Segmented Diffusion-Weighted Prostate Imaging for Higher Resolution, Better Geometric Fidelity, and Multi-b Perfusion Quantification
Pelin Aksit Ciris¹, Jr-yuan George Chiou², Andriy Fedorov², Hualei Shelley Zhang², Clare Mary Tempany-Afdhal², Bruno Madore², and Stephan Ernst Maier^{2,3}

¹Department of Biomedical Engineering, Akdeniz University, Antalya, Turkey, ²Department of Radiology, Brigham and Women's Hospital, Harvard Medical School, Boston, MA, United States, ³Department of Radiology, University of Gothenburg, Gothenburg, Sweden

An accelerated multi-shot diffusion imaging sequence and reconstruction scheme was developed for prostate imaging, allowing improvements in spatial resolution, geometric-fidelity and b -factor coverage to be achieved within a short scan time. Two-fold improvement in spatial resolution and three-fold improvement in geometric fidelity were obtained as compared to single-shot EPI, in twelve prostate cancer patients. In contrast to the standard protocol, which involves separate scans with high ($b=1400$ and 0 s/mm²) and intermediate ($b=500$ and 0 s/mm²) diffusion weighting, the proposed accelerated protocol yielded an additional 8 b -factors in half the scan time (5 min 43 s vs. 11 min 48 s).

- 3861
Computer #26 Bone Metastasis of Prostate Cancer: Comparing Readout-Segmented EPI (RESOLVE) Whole-Body DWI with ECT
Qingsong Yang¹, Zhen Wang¹, Luguang Chen¹, Yukun Chen¹, Chao Ma¹, Caixia fu², Xu Yan³, Hui Liu³, and Jianping Lu¹

¹Radiology Department, Changhai Hospital, Shanghai, China, People's Republic of, ²Application Department, Siemens Shenzhen Magnetic Resonance Ltd., Shenzhen, China, People's Republic of, ³MR Collaboration NE Asia, Siemens Healthcare, Shanghai, China, People's Republic of

Bone metastasis is a leading cause of morbidity and mortality for patients with metastatic prostate cancer. Early detection of bone metastasis plays a key role in the assessment of treatment methods and prognosis. This study aims to evaluate the diagnostic efficiency of readout-segmented whole body diffusion weighted imaging in the detection of bone metastases for patients with newly diagnosed high-risk or biochemical recurrent prostate cancer. The result shows that RESOLVE whole-body DWI has higher sensitivity, specificity and accuracy in bone metastasis detection than bone scintigraphy using ^{99m}Tc-MDP (BS).

- 3862
Computer #27 Restriction spectrum imaging improves MRI-based prostate cancer detection
Kevin Charles McCammack¹, Natalie M Schenker-Ahmed¹, Nathan S White¹, Shaun R Best², Robert M Marks³, Jared Heimbigner³, Christopher J Kane⁴, J Kellogg Parsons⁴, Joshua M Kuperman¹, Hauke Bartsch¹, Rahul S Desikan¹, Rebecca A Rakow-Penner¹, Michael A Liss⁵, Daniel JA Margolis⁶, Steven S Raman⁶, Ahmed Shabaik⁷, Anders M Dale¹, and David S Karow¹

¹Radiology, UCSD, San Diego, CA, United States, ²Kansas City, KS, United States, ³Radiology, Naval Medical Center San Diego, San Diego, CA, United States, ⁴Urology, UCSD, San Diego, CA, United States, ⁵Urology, UT San Antonio, San Antonio, TX, United States, ⁶Radiology, UCLA, Los Angeles, CA, United States, ⁷Pathology, UCSD, San Diego, CA, United States

Restriction Spectrum Imaging is an advanced, multiple b -value, diffusion technique which allows improved reader performance in the identification of prostate cancer when combined with current standard of care imaging, or performs comparably to current imaging practice when used alone.

- 3863
Computer #28 Inter-scanner reproducibility of parameters from advanced models of DW-MRI in a multi-centre study
Jessica M Winfield^{1,2}, David J Collins^{1,2}, Matthew R Orton², Jennifer C Wakefield^{1,2}, Andrew N Priest³, Rebecca A Quest⁴, Susan Freeman³, Andrea G Rockall⁴, and Nandita M deSouza^{1,2}

¹MRI, Royal Marsden Hospital, Sutton, United Kingdom, ²Division of Radiotherapy and Imaging, Cancer Research UK Cancer Imaging Centre, Institute of Cancer Research, London, United Kingdom, ³Department of Radiology, Addenbrooke's Hospital, Cambridge University Hospitals NHS Foundation Trust, Cambridge, United Kingdom, ⁴Imaging Department, Imperial College Healthcare NHS Trust, London, United Kingdom

The repeatability and inter-scanner reproducibility of fitted parameters from mono-exponential and non-mono-exponential (stretched exponential, kurtosis and bi-exponential) models of diffusion-weighted MRI signal attenuation were assessed in healthy volunteers and patients with advanced ovarian cancer imaged using MRI scanners from three manufacturers.

Repeatability of ADC estimates, evaluated in abdominal organs in healthy volunteers, was good on all three scanners. Estimates of DDC and α from the stretched exponential model, D_k from the kurtosis model and D from the bi-exponential model showed comparable repeatability to ADC on all three scanners; the standard deviation of differences in k was comparable across three scanners. Repeatability of f , D^* and fD^* was poor on all three scanners.

ADC estimates showed no significant differences between the three scanners in data from patients or healthy volunteers. Significant differences were observed between scanners in α , k , D and f in data from healthy volunteers. In lesions, there was a significant difference in k between scanners. Differences between parameters estimated from different scanners should be considered in multi-centre studies.

-
- 3864
Computer #29 In vivo prostate cancer detection and grading using Restriction Spectrum Imaging
Kevin Charles McCammack¹, Chris J Kane², J Kellogg Parsons², Nathan S White¹, Natalie M Schenker-Ahmed¹, Kuperman M Joshua¹, Hauke Bartsch¹, Rahul S Desikan¹, Rebecca A Rakow-Penner¹, Dennis Adams³, Michael A Lliss⁴, Robert F Mattrey¹, William G Bradley¹, DJA Margolis⁵, Steven Raman⁵, Ahmed Shabaik³, Anders M Dale¹, and David S Karow¹
- ¹Radiology, UCSD, San Diego, CA, United States, ²Urology, UCSD, San Diego, CA, United States, ³Pathology, UCSD, San Diego, CA, United States, ⁴Urology, UT San Antonio, San Antonio, TX, United States, ⁵Radiology, UCLA, Los Angeles, CA, United States
- Restriction Spectrum Imaging, an advanced multiple b-value diffusion technique, demonstrates greater sensitivity and specificity for discriminating between tumor and normal prostate than conventional ADC or Ktrans.
-
- 3865
Computer #30 MR Apparent Diffusion Coefficient (ADC) Quantification is an Imaging Biomarker Predicting Gleason Score grade in Patients with Prostate Cancer undergoing MRI-guided prostate biopsy
Juan C. Camacho^{1,2}, Nima Kokabi¹, Peter A. Harri¹, Tracy E. Powell², and Sherif G. Nour^{1,2}
- ¹Radiology and Imaging Sciences, Emory University School of Medicine, Atlanta, GA, United States, ²Interventional MRI Program, Emory University Hospital, Atlanta, GA, United States
- The study objective is to investigate magnetic resonance Apparent Diffusion Coefficient Quantification (ADC) in prostate lesions and to correlate the values with the results of MRI-guided prostate targeted sampling. A prospective cohort of patients presenting with persistently elevated or rising serum prostate specific antigen (PSA) and at least one lesion suspicious for prostate cancer that underwent MRI guided targeted biopsy was evaluated. Thirty-five consecutive patients were recruited presenting with 179 suspicious lesions. ROC curve analysis demonstrates that ADC predicts the presence of malignancy and allows grade stratification and therefore, behaves as a non-invasive imaging biomarker.
-
- 3866
Computer #31 Differences in perfusion fraction in different grade of prostate cancer assessed by DWI
Rossella Canese¹, Davide Fierro², Francesca Romana Giura², Gianmauro Palombelli¹, Elena Lucia Indino², Vincenzo Salvo², Carlo Catalano², and Valeria Panebianco²
- ¹Cell Biology and Neurosciences, Istituto Superiore di Sanita', Rome, Italy, ²Radiological Sciences, Oncology and Pathology, Sapienza University of Rome, Rome, Italy
- To date, most clinical DW-MRI studies have employed a monoexponential model for data analysis, which produces the ADC parameter for assessing diffusion characteristics whose value correlate with Gleason scores in prostate cancer. The intravoxel incoherent motion (IVIM) model introduce a fast diffusing component in the signal due to perfusion effects, but the application of this method is not yet widespread included in clinical practice. This study was aimed at measuring the water diffusion in tissue separating and estimating the perfusion component by adopting a simple protocol easy to be implemented in clinical practice and evaluating its diagnostic performance
-
- 3867
Computer #32 Prostate Cancer Detection and Gleason Upgrading on 3T In-Bore MRI-guided Prostate Biopsy Compared to TRUS Prostate Biopsy in Men with Elevated PSA
Nelly Tan¹, Wei-Chen Lin¹, and Steven S Raman¹
- ¹UCLA, Los Angeles, CA, United States
- MR guided Prostate Biopsy (MRgBx) yielded a Gleason upgrading in 37.5% of the patients with prior GS6 biopsy tumors. Overall diagnostic yield of MRI guided prostate biopsy was 58.3%. Men with positive MRgBx had tumors which were larger in size, lower ADC value, and higher T2, DWI and overall score compared to men with negative MRgBx. PIRADS reporting is an accurate measure to predict positive MR guided biopsy targets.
-
- 3868
Computer #33 Fast T2 mapping for the diagnosis of prostate cancer by using 3.0T MRI
Danyan Li¹, Qinglei Zhang¹, Harsh K Agarwal², Weibo Chen², and Bin Zhu¹
- ¹Radiology, The Affiliated Drum Tower Hospital of Nanjing University Medical School, Nanjing, China, People's Republic of, ²Phillips Research NA,

Quantitative T2 values has the potential to reliably and reproducibly differentiate prostate abnormalities, such as prostate cancer (PCa), benign prostate hyperplasia (BPH) and normal prostate tissue (NPT). We used k-t-T2 technique to obtain the T2 maps and tested the diagnostic performance of T2 mapping in differentiating PCa from NPT and BPH in the peripheral zone. We found the T2 values is quite useful for cancer discrimination with, for example, a threshold T2 of 68.3 ms yielded a sensitivity of 94% and a specificity of 98% for PCa discrimination.

-
- 3869 Computer #34 Objective response following interventional oncology treatments: A practical approach to apply response criteria through MR imaging
Juan C Camacho¹, Courtney Moreno¹, Peter Harri¹, and Pardeep Mittal¹

¹Radiology and Imaging Sciences, Emory University School of Medicine, Atlanta, GA, United States

MR plays a key role in patients with abdominal visceral malignancies, regarding management, assessing therapy response and surveillance. Standardized follow-up criteria and imaging techniques should be applied to patients with abdominal malignancies, taking into account the primary neoplasm and current therapeutic strategies. Adequate knowledge of response evaluation criteria for malignancies including WHO, EASL, RECIST and mRECIST criteria is crucial for adequate patient surveillance.

-
- 3870 Computer #35 Clinical Utility of mDIXON TSE and mDIXON FFE in Pediatric and Fetal, Neuro, Body, and Musculoskeletal MRI
Dianna M. E. Bardo¹, Patricia Cornejo¹, Jeffrey Miller¹, Amber Porkorney¹, Mittun Patel¹, Craig Barnes¹, Johnathan M Chia², and Houchun Harry Hu¹

¹Radiology, Phoenix Children's Hospital, Phoenix, AZ, United States, ²MRI, Philips Healthcare, Highland Heights, OH, United States

mDixon sequences allow for improved MR imaging in Pediatric MR.

-
- 3871 Computer #36 Feasibility of an automated tissue segmentation technique in a longitudinal weight loss study
William M Haufe¹, Jonathan Charles Hooker¹, Alexandra N Schlein¹, Nikolaus Szeverenyi¹, Magnus Borga², Olof Dahlqvist Leinhard², Thobias Romu², Patrik Tunon², Santiago Horgan³, Garth Jacobsen³, Jeffrey B Schwimmer⁴, Scott B Reeder⁵, and Claude B Sirlin¹

¹Radiology, UCSD, San Diego, CA, United States, ²AMRA, Linköping, Sweden, ³Surgery, UCSD, San Diego, CA, United States, ⁴UCSD, San Diego, CA, United States, ⁵University of Wisconsin, Madison, Madison, WI, United States

To address the problems inherent in manual methods, a novel, semi-automated tissue segmentation image analysis technique has been developed. The purpose of this study was to demonstrate the feasibility and describe preliminary observations of applying this technique to quantify and monitor longitudinal changes in abdominal adipose tissue and thigh muscle volume in obese adults during weight loss. Abdominal adipose tissue and thigh muscle volume decreased during weight loss. As a proportion of body weight, adipose tissue volumes decreased during weight loss. By comparison, as a proportion of body weight, thigh muscle volume increased.

-
- 3872 Computer #37 Body Composition Analysis In Large Scale Population Studies using Dixon Water-Fat Separated Imaging
Janne West^{1,2}, Olof Dahlqvist Leinhard^{1,2}, Thobias Romu^{2,3}, E. Louise Thomas⁴, Magnus Borga^{2,3}, and Jimmy D. Bell⁴

¹Department of Medical and Health Sciences (IMH), Linköping University, Linköping, Sweden, ²Center for Medical Image Science and Visualization (CMIV), Linköping, Sweden, ³Department of Biomedical Engineering, Linköping University, Linköping, Sweden, ⁴Department of Life Sciences Faculty of Science and Technology, University of Westminster, London, United Kingdom

Water-fat separated MRI, based on Dixon imaging techniques enables high soft-tissue contrast and the separation of fat and muscle compartments. This study investigate the feasibility and success-rate of one recently described method for MR data-acquisition and body composition analysis, in a large-scale population study. The first 1,000 subjects in the UK Biobank imaging cohort were scanned, quality assured and included for body composition analysis. Volumes of visceral adipose tissue, abdominal subcutaneous tissue, and thigh muscles were calculated. This study showed that the rapid MR-examination was sufficiently robust to achieve very high success-rate for body composition analysis.

-
- 3873 Computer #38 Automated MR Scanner Workflow of combined Chest, Abdomen and Pelvis Exams: First Clinical Experience
Caecilia S Reiner^{1,2}, Bernd Kuehn³, Daniel Nanz², Berthold Kiefer³, and Gustav Andreisek^{1,2}

¹Institute of Diagnostic and Interventional Radiology, University Hospital Zurich, Zurich, Switzerland, ²University of Zurich, Zurich, Switzerland, ³Oncology Application Predevelopment, Siemens Healthcare, Erlangen, Germany

An increasing demand for time-efficient and standardized MRI drives the development of automated MRI-workflows. The purpose of this study was to evaluate the feasibility of such a novel automated scanner-workflow for multi-station MRI. The scanner automatically detects the body regions selected and sequences are automatically adjusted to patient's size and breath-holding capacity to generate optimal image quality. In 20 patients scanned with a multi-station protocol (chest, abdomen, and/or pelvis), image quality was good to excellent and complete body region coverage was achieved in 95% of patients. This nearly "single-button" automated multi-station MRI could open new possibilities in the diagnostic process.

- 3874
Computer #39 MR based body composition analysis correlates ayurvedic phenotyping
Rama Jayasundar¹, Somenath Ghatak¹, Ariachery Ammini², Ashok Mukhopadhyaya³, and Arundhati Sharma⁴
¹NMR, All India Institute of Medical Sciences, New Delhi, India, ²Endocrinology, All India Institute of Medical Sciences, New Delhi, India, ³Laboratory Medicine, All India Institute of Medical Sciences, New Delhi, India, ⁴Anatomy, All India Institute of Medical Sciences, New Delhi, India
- The world is entering an era of personalised medicine and phenotyping individuals is gaining much attention. In this context, genetic basis of the comprehensive phenotyping in ayurveda, the indigenous medicine of Indian subcontinent has drawn much scientific interest. This study reports an innovative application of MR in providing the much needed objective parameters for some of the phenotyping indices. Interestingly, the results show that the phenotypes mentioned in ayurveda as being predisposed to diabetes are found to not only have increased localised fat deposition (abdomen and thigh) (measured by MRI) and triglyceride levels but also lower insulin sensitivity.
-
- 3875
Computer #40 High resolution imaging of pelvic lymph nodes at 7 Tesla
Bart W.J. Philips¹, Stephan Orzada², Ansje Fortuin¹, Marnix C. Maas¹, and Tom W.J. Scheenen^{1,2}
¹Radiology and Nuclear Medicine, Radboud University Medical Centre, Nijmegen, Netherlands, ²Erwin L. Hahn Institute for Magnetic Resonance Imaging, Essen, Germany
- MRI of the pelvis at a high spatial resolution has potential to assess lymph node status in oncological diseases. We propose to use spectrally selective 3D gradient echo imaging in combination with TIAMO at 7 Tesla to improve upon spatial resolution using the SNR increase that ultra high field MRI provides. The method is shown to robustly obtain homogeneous, large FOV body imaging of the pelvic lymph nodes with a spatial resolution of 0.66x0.66x0.66 mm³, both for T2* weighted as well as lipid selective imaging.
-
- 3876
Computer #41 Development of Relaxometry Methods and Hardware for Routine Determination of Volume Status: Dialysis Pilot Study
Lina Avancini Colucci¹, Matthew Li¹, Kristin Corapi², Andrew Allegretti², Raynuma Ahmed², Herbert Y. Lin², and Michael J. Cima³
¹Health Sciences and Technology (HST), MIT, Cambridge, MA, United States, ²Division of Nephrology, Massachusetts General Hospital, Boston, MA, United States, ³Materials Science and Engineering, MIT, Cambridge, MA, United States
- Incorrect assessment of clinical volume status leads to increased mortality and healthcare costs yet there are no accurate, non-invasive, and quantitative methods to assess this health metric. We evaluated the ability of a portable NMR sensor and relaxometry techniques to detect fluid changes in hemodialysis (HD) patients during the course of HD treatment. There was a significant difference between relaxation values of HD patients compared to healthy subjects.
-
- 3877
Computer #42 ¹⁹F ZTE MR Imaging of ¹⁹F labeled calcium phosphate cement at 11.7T
Weiqiang Dou¹, Simone Mastrogiacomo², Olga Koshkina³, Andor Veltien¹, Mangala Srinivas³, X. Frank Walboomers², and Arend Heerschap¹
¹Radiology, Radboud University Medical Centre, Nijmegen, Netherlands, ²Biomaterials, Radboud University Medical Centre, Nijmegen, Netherlands, ³Tumor Immunology, Radboud University Medical Centre, Nijmegen, Netherlands
- To enhance the MR image contrast of calcium phosphate cement (CPC) to bone, it was tagged with a ¹⁹F loaded nanoparticle as a contrast agent. ¹⁹F zero echo time (ZTE) MRI was applied for the first time for ¹⁹F imaging of this CPC in bone at 11.7T. The T₁ and T₂^{*} relaxation times of the ¹⁹F nanoparticles were measured for optimal settings of ¹⁹F ZTE MRI. We demonstrate overlaid ¹H+¹⁹F ZTE images of in vitro and ex vivo CPC/bone samples with hyperintense ¹⁹F signals allowing a qualitative and quantitative evaluation of these samples.
-
- 3878
Computer #43 Reproducibility of whole body ADC in a non-optimized multi-centre trial: Effectiveness of normalisation method
Jagadish Kalasthry¹, Stuart Taylor¹, David Atkinson², Alan Bainbridge³, Shonit Punwani¹, Anna Barnes⁴, and On behalf of STREAMLINE investigators⁵
¹Imaging, University College Hospital, London, United Kingdom, ²Centre for Medical Imaging, University College London, London, United Kingdom, ³Medical Physics and Biomedical Engineering, University College Hospital, London, United Kingdom, ⁴Clinical Physics, Institute of Nuclear Medicine, University College Hospital, London, United Kingdom, ⁵NIHR, National Institute for Health Research, London, United Kingdom
- Diffusion-Weighted (DW) MRI can be used as a quantitative tool but there is limited data documenting accuracy and reproducibility on different MRI scanners with non-identical protocols. We investigated the variation in ADC measurements in normal tissue in datasets acquired as part of a pragmatic multicentre study of whole body MRI cancer and tested the impact of normalisation methods. We found large variations in ADC within both the same platform, and between different MRI platforms. Normalisation had limited benefit and only for one platform. Fat suppression seemed to be the predominant driver of variation particular in tissues outside the brain.
-
- 3879
Computer #44 Abdominal FASE-DWI
Takeshi Yoshikawa¹, Katsusuke Kyotani², Yoshiharu Ohno¹, Yoshimori Kassai³, Hisanobu Koyama⁴, Kouya Nishiyama², Shinichiro Seki⁴, and Kazuro Sugimura⁴
¹Advanced Biomedical Imaging Research Center, Kobe University Graduate School of Medicine, Kobe, Japan, ²Radiology, Kobe University Hospital, Kobe, Japan, ³Toshiba Medical Systems Co., Otawara, Japan, ⁴Radiology, Kobe University Graduate School of Medicine, Kobe, Japan

To reduce distortion on abdominal EPI-DWI, we developed Fast Advanced Spin Echo (FASE)-DWI for abdominal 3T imaging. We found FASE-DWI can provide additional diagnostic information in evaluation of various abdominal diseases and be used as an alternative to EPI-DWI.

3880
Computer #45 Deep Learning of MR Imaging Patterns in Prostate Cancer
Nelly Tan¹, Noah Stier¹, Steven Raman¹, and Fabien Scalzo¹

¹*UCLA, Los Angeles, CA, United States*

This demonstrates the feasibility of using Deep Learning to characterize prostate cancer lesions in an automatic fashion. The translation and development of this method into a decision support tool may provide more objective criteria for clinicians during diagnosis.

3881
Computer #46 Can Lack of Marked Restricted Diffusion Downgrade the PI-RADS Score?
Amany Aziz¹, Khalid Alsabban¹, Steven M Shea¹, Ari Goldberg¹, Gopal Gupta¹, and Joseph H Yacoub¹

¹*Radiology, Loyola University Medical Center, Maywood, IL, United States*

~
Retrospective evaluation of the impact of DWI on PI-RADS scoring of TZ lesions. A blinded radiologist evaluates lesions based on only the DWI sequence and again only on the T2 TSE sequence, in separate occurrences, in patients who underwent targeted biopsy. New PI-RADS scores are given for each of the lesions. The given scores are then correlated with their corresponding Gleason scores. Of the 55 lesions studied, the DWI score downgraded four lesions from a higher T2 score. DWI could play a role in evaluation of TZ lesions, however our data lacked statistical significance.

3882
Computer #47 Effect of Prostate Deformity Due to Endorectal coil on Targeting Outcomes
Khalid Alsabban¹, Steven M Shea¹, Amany Aziz¹, Bryan Bisnaz², Everardo Arias², Ari Goldberg¹, Gopal Gupta³, and Joseph H Yacoub¹

¹*Radiology, Loyola University Medical Center, Maywood, IL, United States*, ²*Stitch School of Medicine, Maywood, IL, United States*, ³*Urology, Loyola University Medical Center, Maywood, IL, United States*

The method of using an endorectal coil in a Prostate Magnetic Resonance Imaging has been an area of debate between radiologists for some time now, with a majority of research projects done to compare this method with the use of phased array coils. In this retrospective project our main objective is to identify if the temporary deforming effects caused by the use of the endorectal coil in a Prostate Magnetic Resonance Imaging (MRI) procedure may affect biopsy targeting. We will collect the dimensions measured by the MRI and compare it to the dimensions measured using the Transrectal Ultrasound procedure (TRUS).

3883
Computer #48 Synthesized versus acquired high b-value (1200 s/mm²) diffusion-weighted magnetic resonance imaging for detection of peripheral zone lesions in the prostate using PI-RADS version 2
Stephanie T. Chang¹, Andreas M. Loening¹, and Shreyas S. Vasanawala¹

¹*Radiology, Stanford University, Palo Alto, CA, United States*

Greater diffusion weighting is generally thought to increase performance of MRI for prostate cancer detection. We compared acquired high b-value (1200 s/mm²) diffusion-weighted MRI against b-1200 images synthesized from b ≤ 800 acquisitions for detection of peripheral zone lesions in the prostate for 50 consecutive patients undergoing prostate MRI and biopsy using two blinded independent readers. Although subjective image quality was rated slightly but significantly worse for synthesized DWI compared to acquired DWI images, no significant difference in detection of peripheral zone lesions, PI-RADS version 2 lesion categorization, or confidence scores of interpretation were observed.

Electronic Poster

Renal/Female Pelvis/Fetal

Exhibition Hall

Wednesday, May 11, 2016: 13:30 - 14:30

3884
Computer #49 Clinical application of susceptibility-weighted MR sequences in the female pelvis
Mayumi Takeuchi¹, Kenji Matsuzaki^{1,2}, and Masafumi Harada¹

¹*Department of Radiology, University of Tokushima, Tokushima, Japan*, ²*Department of Radiological Technology, Tokushima Bunri University, Sanuki, Japan*

Susceptibility-weighted (SW) magnetic resonance (MR) sequences have exquisite sensitivity to the blood products within various gynecologic pathologies, and may provide helpful information for the differential diagnosis. In this exhibit we demonstrate the role of SW sequences in diagnosing various pathologies in the female pelvis such as hemorrhagic cysts (endometrioma vs non-endometriotic

cyst), extra-ovarian endometriosis and adenomyosis, gestation-associated lesions (ectopic pregnancy and retained products of conception), red degeneration of uterine leiomyoma, high-grade malignancy such as uterine sarcomas with hemorrhagic necrosis, and ovarian torsion.

- 3885
Computer #50 Assessment of metabolism in the placenta by hyperpolarized MRI
Emmeli F. R. Mikkelsen¹, Per Mose Nielsen², Haiyun Qi¹, Thomas S. Nørlinger¹, Hans Stødkilde-Jørgensen¹, Niels Uldbjerg³, Michael Pedersen¹, Puk Sandager³, and Christoffer Laustsen¹
- ¹MRI Research Centre, Aarhus University Hospital, Aarhus N, Denmark, ²Department of Clinical Medicine, Aarhus University Hospital, Aarhus N, Denmark, ³Department of Obstetrics and Gynaecology, Aarhus University Hospital, Aarhus N, Denmark
- Glucose is the main energy source for the placenta and the fetus and is essential for normal growth and development of the fetus. It has previously been shown that the placenta itself consumes about half of the glucose supplied, metabolizing a great amount to lactate. Hyperpolarized Magnetic Resonance Imaging (MRI) is a novel non-harmful method for monitoring metabolic processes in tissues in real time. We evaluate the metabolism of [1-¹³C]-pyruvate in the placenta and fetus in a novel pregnancy rodent model by the use of hyperpolarized MRI.
-
- 3886
Computer #51 Evaluation of retained products of conception by arterial spin labeling-MRI: Clinical feasibility and initial results
Nobuyuki Kosaka¹, Yasuhiro Fujiwara², Masayuki Kanamoto³, Tsuyoshi Matsuda⁴, Tatsuya Yamamoto¹, Kazuhiro Shimizu¹, Kanako Ota⁵, Yoshio Yoshida⁵, Tetsuji Kurokawa⁵, and Hirohiko Kimura¹
- ¹Department of Radiology, University of Fukui, Eiheiji, Japan, ²Department of Medical Imaging, Kumamoto University, Kumamoto, Japan, ³Radiological Center, University of Fukui Hospital, Eiheiji, Japan, ⁴Global MR Applications and Workflow, GE Healthcare Japan Corporation, Hino, Japan, ⁵Department of Obstetrics and Gynecology, University of Fukui, Eiheiji, Japan
- In this study, arterial spin-labeling (ASL)-MRI was used to evaluate the vascularity of retained products of conception (RPOCs). In 5 of 7 cases, high signals on ASL-MRI were observed, and therapeutic response could be evaluated by ASL-MRI. However, these findings of ASL-MRI were not completely identical to those of other conventional imaging modalities, such as dynamic contrast-enhanced MRI and Doppler-US. ASL-MRI is clinically feasible and can be used to assess therapeutic response. Although its clinical advantages over conventional imaging need to be evaluated, ASL-MRI has clinical potential for non-invasive assessment of RPOCs.
-
- 3887
Computer #52 Diffusion tensor imaging and fiber tractography in evaluation of the levator ani muscle change in pelvic organ prolapse patients
yu jiao zhao¹, can cui², yu zhang³, and wen shen⁴
- ¹Department of Radiology, Tianjin First Center Clinical College, Tianjin Medical University, Tianjin, Tianjin, China, People's Republic of, ²Department of Radiology, Tianjin First Center Clinical College, Tianjin Medical University, Tianjin, Tianjin, China, People's Republic of, ³Philips Healthcare, Beijing, China, Beijing, China, People's Republic of, ⁴Department of Radiology, Tianjin First Center Hospital, Tianjin, China, Tianjin, China, People's Republic of
- Levator ani muscle(LAM) dysfunction may cause pelvic organ prolapse(POP). DTI and fiber tracking was used to display the general morphology and microstructure changes of LAM in POP patients. We compared the FA, ADC values of pelvic floor muscles and fiber bundles shape between normal and prolapse group in this study. The results showed that the FA values of LAM muscle in prolapse group were lower than that of control and ADC values were opposite. DTI can realize the assessment of the status of LAM in patients with POP and guide the choice of operation methods.
-
- 3888
Computer #53 A reasoned approach to explore single shot FSE acquisition for fetal MRI
Maelene Lohezic^{1,2}, Joshua van Amerom^{1,2}, Kelly Pegoretti², Laura McCabe², Christina Malamateniou², Olivia Carney², Matthew Fox², Joanna Allsop², Mary Rutherford², and Joseph Hajnal^{1,2}
- ¹Department of Biomedical Engineering, King's College London, London, United Kingdom, ²Centre for the Developing Brain, King's College London, London, United Kingdom
- Fetal MRI is a growing field but it is still far from being a standard examination and setting up a protocol demands careful optimization. Here we explore some factors to consider when choosing an appropriate slice acquisition order pattern to mitigate the effect of crosstalk between temporally consecutive slices and the partial saturation from the excitation of the adjacent slice, while taking moderate range of fetal motion into account.
-
- 3889
Computer #54 The feasibility of red bone marrow segmentation based on MR Dixon only.
Anna Andreychenko¹, Petra S. Kroon¹, Matteo Maspero¹, Ina Jürgenliemk-Schulz¹, Astrid de Leeuw¹, Marnix Lam¹, Jan J.W. Legendijk¹, and Cornelis A.T. van den Berg¹
- ¹UMC Utrecht, Utrecht, Netherlands
- In this study a (semi-)automatic tool for red bone marrow segmentation in the pelvis was developed. The tool is solely based on MR Dixon imaging. It is intended for the dose planning for radiotherapy with the hematologic active bone marrow sparing. The optimization and validation of the tool was performed by means of FDG-PET scans of nine cervical cancer patients.
-

- 3890
Computer #55 HOW TO MAP PELVIC AUTONOMIC NERVES: VALUE OF A 3D HIGH-RESOLUTION MR NEUROGRAPHY SEQUENCE
Céline Giraudeau¹, Arthur R Wijsmuller^{1,2}, Carter C Lebares^{1,2}, Jacques Marescaux^{1,2}, and Didier Mutter^{1,2}
¹IHU Strasbourg, Institute of image-guided surgery, Strasbourg, France, ²IRCAD, Research Institute Against Digestive Cancer, Strasbourg, France
- The goal of this study was to investigate the value of a 3D high-resolution sequence with a particular contrast to visualize and delineate pelvic autonomic nerves in a healthy volunteer. Through segmented images and the corresponding 3D reconstruction, we show that our method offers interesting results for the delineation of the hypogastric plexus and the pudendal nerves that are frequently impacted by pelvic surgery. These results are promising for individualized preoperative mapping of autonomic innervation and could provide a valuable support to guide surgeons during interventions when combined with augmented reality.
-
- 3891
Computer #56 Feasibility of Fetal Fat Volume Assessment using 3D Water-Fat MRI
Stephanie Giza¹, Craig Olmstead², Kevin Sinclair¹, Charles A McKenzie^{1,3}, and Barbra de Vrijer^{3,4}
¹Medical Biophysics, Western University, London, ON, Canada, ²Schulich School of Medicine and Dentistry, Western University, London, ON, Canada, ³Division of Maternal, Fetal and Newborn Health, Children's Health Research Institute, London, ON, Canada, ⁴Obstetrics and Gynecology, Western University, London, ON, Canada
- Conventional ultrasound techniques perform adequately in assessment of fetal size in obese mothers but fail to identify the fetus that is chronically stressed inside the womb. A reliable MRI measurement of fetal fat volume and distribution would therefore be a powerful tool in the assessment of fetal condition. Using a 3D LAVA-Flex sequence during maternal breath hold, fat signal fraction images were generated to measure the fat volume of the fetus, while correcting for partial volume effects. 3D water-fat MRI was found to provide a reliable measurement of fetal fat volumes that could be used to assess size and growth.
-
- 3892
Computer #57 A pre-processing pipeline for bias field correction and rigid and elastic motion compensation in Placental-Fetal BOLD MRI
Esra Abaci Turk^{1,2}, Jie Luo^{1,2}, Borjan Gagoski¹, Carolina Bibbo³, Julian N. Robinson³, P. Ellen Grant¹, Elfar Adalsteinsson^{2,4,5}, Polina Golland^{4,6}, and Norberto Malpica^{2,7}
¹Fetal-Neonatal Neuroimaging and Developmental Science Center, Boston Children's Hospital, Harvard Medical School, Boston, MA, United States, ²Madrid-MIT M+Vision Consortium in RLE, Massachusetts Institute of Technology, Cambridge, MA, United States, ³Maternal and Fetal Medicine, Brigham and Women's Hospital, Harvard Medical School, Boston, MA, United States, ⁴Department of Electrical Engineering and Computer Science, Massachusetts Institute of Technology, Cambridge, MA, United States, ⁵Harvard-MIT Health Sciences and Technology, Massachusetts Institute of Technology, Cambridge, MA, United States, ⁶Computer Science and Artificial Intelligence Laboratory (CSAIL), Massachusetts Institute of Technology, Cambridge, MA, United States, ⁷Medical Image Analysis and Biometry Laboratory, Universidad Rey Juan Carlos, Madrid, Spain
- Abnormal oxygen transport through the placenta is thought to be a major etiologic factor in intrauterine growth restriction (IUGR). Blood-oxygen-level-dependent (BOLD) magnetic resonance imaging (MRI) with oxygen exposure is a non-invasive technique that can estimate oxygenation changes in specific organs. However, applying this technique to placentae and fetal organs can be challenging due to non-uniform signal and unpredictable fetal and maternal motion. This study presents a preprocessing pipeline to mitigate signal non-uniformities and motion, to enable automated regional analysis of placenta and fetal body for BOLD MRI studies.
-
- 3893
Computer #58 In Vitro and in Vivo MR measurement of fetal blood oxygen saturation
Fabian Kording¹, Hendrik Kooijman², Jin Yamamura¹, Manuela Tavares³, Mathias Kladeck¹, Kurt Hecher³, Gerhard Adam¹, and Bjoern Schoennagel¹
¹Department of Diagnostic and Interventional Radiology, University Medical Center Hamburg-Eppendorf, Hamburg, Germany, ²Philips Medical Systems, Hamburg, Germany, ³Department of Obstetrics and Fetal Medicine, University Medical Center Hamburg-Eppendorf, Hamburg, Germany
- Intrauterine growth restriction is associated with a decreased oxygen availability. In clinical practice, indicators such as Doppler changes of the ductus venosus and umbilical artery are measured and a direct measurement using MR oximetry would be desirable. The relationship between T2 relaxation time and oxygen saturation (sO₂) is determined in in-vitro fetal blood samples and the feasibility of a noninvasively determination of fetal sO₂ is evaluated. The calculated fetal sO₂ highly correlated with measured sO₂ values and determined parameters were successfully evaluated in-vivo in the left fetal ventricle.
-
- 3894
Computer #59 Real-time Chest MRI within the Neonatal Intensive Care Unit
Yu Y. Li¹, Wolfgang Loew¹, Ronald Pratt¹, Randy Giaquinto¹, Stephanie Merhar¹, Jean Tkach¹, and Charles Dumoulin¹
¹Radiology, Cincinnati Children's Hospital Medical Center, Cincinnati, OH, United States
- The presented work investigates a real-time imaging approach to chest MRI on a 21.8cm bore scanner dedicated for neonatal examination within the neonatal intensive care unit (NICU). This approach is based on the development of a 10-channel small coil array, a fast imaging pulse sequence, and an iterative image reconstruction algorithm. It is experimentally demonstrated that real-time imaging can provide high-quality cardiac and pulmonary images for improved clinical diagnosis in premature babies within the NICU.
-
- 3895
Computer #60 Shortened Fatty Acid Chains in Cervical Cancer using 1H MRSI at 7T
Catalina S. Arteaga de Castro¹, Jacob P. Hoogendam², Alexander Raaijmakers¹, Irene M.L. van Kalleveen¹, Wouter B. Veldhuis³, Ronald P. Zweemer², Peter R. Luijten¹, and Dennis W.J. Klomp¹

¹Imaging Division, University Medical Center Utrecht, Utrecht, Netherlands, ²Gynaecological oncology, University Medical Center Utrecht, Utrecht, Netherlands, ³Radiology, University Medical Center Utrecht, Utrecht, Netherlands

The feasibility of MRSI at 7T to image fatty acid composition in cervical cancer patients was investigated. A relatively high 2.1 ppm fatty acid signal was only observed in tumor tissue. Tumor free cervix showed predominantly the 1.3 ppm lipids signal. Metabolic maps of the 2.1 ppm fatty acid showed heterogeneity within the tumor, which coincided with a hyper-intense area within the T2-weighted image, that may indicate local necrosis.

-
- 3896
Computer #61 First Trimester Alcohol Exposure Alters Placental Perfusion and Fetal Oxygen Transport in a Pregnant Non-Human Primate Model
Jamie O. Lo¹, Matthias C. Schabel¹, Victoria H.J. Roberts², Xiaojie Wang², Kathleen A. Grant², Antonio E. Frias^{1,2}, and Christopher D. Kroenke^{1,2}
- ¹Oregon Health & Science University, Portland, OR, United States, ²Oregon National Primate Research Center, Beaverton, OR, United States
- Alcohol consumption in pregnancy adversely affects fetal growth and development, likely secondary to altered placental perfusion resulting in decreased fetal oxygen availability. We developed a novel MRI technique that allows *in-vivo* assessment and correlation of placental perfusion and oxygenation. Our study demonstrated reduced placental perfusion and oxygenation with first trimester ethanol exposure in a pregnant nonhuman primate model using a novel MRI method and Doppler ultrasound. Impaired fetal growth was also observed. These findings suggest that discontinuation of alcohol consumption after the first trimester is associated with decreased placental perfusion and oxygenation subsequently affecting fetal growth and development.
-
- 3897
Computer #62 Quantitative evaluations of placental function using Half-Fourier acquisition single-shot turbo spin-echo comparing with T2-relaxation time.
Kyoko Kameyama¹, Aki Kido¹, Yuki Himoto¹, Ko Suginami², Sachiko Minamiguchi³, Ikuo Konishi², and Kaori Togashi¹
- ¹Diagnostic Imaging and Nuclear Medicine, Graduate School of Medicine, Kyoto University, Kyoto, Japan, ²Gynecology and Obstetrics, Graduate School of Medicine, Kyoto University, Kyoto, Japan, ³Diagnostic Pathology, Graduate School of Medicine, Kyoto University, Kyoto, Japan
- Half-Fourier acquisition single-shot turbo spin-echo (HASTE) imaging is now widely used for placental and fetal imaging due to its rapidity and its low sensitivity to fetal movement. We aimed to investigate the index of placental dysfunction using HASTE imaging by comparing T2-relaxation time, which is known to be one of the noninvasive biomarkers for IUGR. The placental SIR to the maternal psoas muscle (SIR_{pl/psoas muscle}) showed significant correlation with placental T2 relaxation time. There was possibility that SIR_{pl/psoas muscle} may have relation with fetal well-beings.
-
- 3898
Computer #63 MRI Features of Placenta Percreta: Evaluation of the Features for 46 Patients Using Surgical and Histopathological Correlations
Xin Chen¹, Guangbin Wang², Shanshan Wang², Tao Gong¹, Sai Shao², and Tianyi Qian³
- ¹Shandong University, Jinan, China, People's Republic of, ²Shandong Medical Imaging Research Institute, Jinan, China, People's Republic of, ³MR Collaborations
- The objective of the study was to identify valuable features to distinguish placenta percreta from placenta accreta and increta by retrospectively review state precession sequence were included in the MR exam protocol. Two experienced radiologists evaluated seven MRI features using surgical and histo
-
- 3899
Computer #64 Diffusional Kurtosis Imaging of Kidneys in Children with Chronic Kidney Disease: Initial Experience
Yang Wen¹, Yun Peng¹, Dan Dan Zheng², Zhi Chen³, Guang Heng Yin¹, Yan Qiu Lv¹, Chen Xu¹, and Yang Fan²
- ¹Department of Radiology, Beijing Children's Hospital Affiliated to Capital Medical University, Beijing, China, People's Republic of, ²GE Healthcare, MR Research China, Beijing, China, People's Republic of, ³Department of Nephrology, Beijing Children's Hospital Affiliated to Capital Medical University, Beijing, China, People's Republic of
- To evaluate the feasibility of DKI in assessment of renal functions in children with chronic kidney disease (CKD). Materials and Methods: This study was IRB approved and informed consent was obtained. Fifteen pediatric patients with CKD and nine children without renal diseases underwent DKI of kidneys. Maps of fractional anisotropy (FA), mean diffusivity (MD), mean kurtosis (MK), radial kurtosis (K_r) and axial kurtosis (K_a) were produced. Results: There is a significant difference of kurtosis metrics and FA of renal medulla compared to those of renal cortex in both the control group and CKD group. FA, MD, K_r and MK values of both the cortex and medulla of kidney have significant differences between patients with CKD and control group. Conclusion: DKI could be a useful tool in the evaluation of renal function in children with CKD.
-
- 3900
Computer #65 Estimation of Oxygen Saturation in Renal Blood Using Intravoxel Incoherent Motion (IVIM) Imaging by FLAIR DWI
Tatsuo Nagasaka¹, Hideki Ota², and Hajime Tamura³
- ¹Radiology, Tohoku University Hospital, Sendai, Japan, ²Diagnostic Radiology, Tohoku University Graduate School of Medicine, Sendai, Japan, ³Graduate School of Medicine, Tohoku University, Sendai, Japan
- We aimed to apply IVIM imaging to estimate blood oxygen saturation in kidneys with extraction of glomerular filtrate fraction by using fluid-attenuated inversion recovery diffusion-weighted imaging (FLAIR DWI). A 3-compartment model (renal tissue, blood and water) was considered for the estimation. Combination of DWI and FLAIR DWI provided renal tissue T1. Images were acquired with two TEs to provide blood T2 which allows for estimation of blood oxygen saturation. Our model generated estimation of glomerular filtrate

fraction, blood R2 and blood oxygen saturation. FLAIR DWI has a potential to estimate blood oxygen saturation with extracting glomerular filtrates fractions in kidneys.

3901



Computer #66 Renal ischemia and reperfusion assessment with 3D hyperpolarized ¹³C urea
Per Mose Nielsen¹, Esben Søvsø Szocska Hansen², Thomas Nørting³, Rikke Nørregaard³, Lotte Bonde Bertelsen⁴, Hans Stødkilde Jørgensen⁵, and Christoffer Laustsen³

¹Clinical medicine, Aarhus university, Aarhus C, Denmark, ²MR Research Centre, institute of clinical medicine, Aarhus C, Denmark, ³Institute of clinical medicine, Aarhus C, Denmark, ⁴institute of clinical medicine, Aarhus C, Denmark, ⁵MR Research Centre, Institute of clinical medicine, Aarhus C, Denmark

Renal homeostasis is determined by the active transport of water and waste products, and the key to this is the active intra-renal transport of ions, creating the needed osmotic gradient. The maintenance of this cortico-medullary ion gradient is believed to be a measurement of kidney function. We investigated 3D hyperpolarized ¹³C, ¹⁵N-urea for mapping of this intra-renal gradient in a unilateral ischemic reperfusion renal rat model. A 3D balanced steady state sequence with an isotropic 1.25 mm resolution was used to image renal ischemic reperfusion injury. We revealed a significant reduction in the intra-renal ion gradient in the ischemic kidney.

3902

Computer #67 Lactate dehydrogenase activity, a novel renal cortical imaging bio-marker of tubular injury.
Per Mose Nielsen¹, Christoffer Laustsen¹, Haiyun Qi¹, Thomas Nørting¹, Emmeli Mikkelsen¹, Rikke Nørregaard¹, and Hans Stødkilde Jørgensen¹

¹institute of clinical medicine, Aarhus C, Denmark

Renal I/R-I is a leading cause of AKI in several disease states; there is a current lack of precise methods to directly assess cortical tubular injury. In the present study, we investigated the in situ alterations of metabolic conversion of pyruvate to lactate in a unilateral I/R-I rat model using [1-¹³C]pyruvate magnetic resonance. A significantly reduced lactate-to-pyruvate ratio of 25% as compared to control was found in the I/R-I kidney, concomitant with a reduced LDH activity, which was specific for the I/R-I kidney. The lowered lactate-to-pyruvate ratio and LDH activity strongly correlated with general tissue damage.

3903

Computer #68 Antioxidant treatment attenuates renal lactate production in diabetic nephropathy
Christoffer Laustsen¹, Thomas Stockholm Nørting¹, Haiyun Qi¹, Per Mose Nielsen¹, Jakob Appel Østergaard^{2,3}, Allan Flyvbjerg², Jan Henrik Ardenkjaer-Larsen⁴, Fredrik Palm⁵, and Hans Stødkilde Jørgensen¹

¹Department of Clinical Medicine, MR-Research Centre, Aarhus University, Aarhus, Denmark, ²Department of Endocrinology and Internal Medicine and Department of Clinical Medicine, Aarhus University, Aarhus, Denmark, ³The Danish Diabetes Academy, Odense, Denmark, ⁴Department of Electrical Engineering, Technical University of Denmark, Kgs Lyngby, Denmark, ⁵Department of Medical Cell Biology, Uppsala University, Uppsala, Sweden

Early diabetic nephropathy (DN) disease progression is notoriously difficult to detect and quantify before substantial histological damage has occurred. Recently, hyperpolarized [1-¹³C]pyruvate has demonstrated increased lactate production, implying increased lactate dehydrogenase activity, in the kidney early after the onset of diabetes as a consequence of increased nicotinamide adenine dinucleotide (NADH) substrate availability due to elevated flux through the polyol pathway. Here we investigated whether this deranged metabolic profile can be reversed by antioxidant treatment targeting the pseudohypoxic condition.

3904

Computer #69 Quantitative Estimation of Renal Blood PO₂ using BOLD MRI in Rat Kidneys.
Jon Thacker¹, Jeff Zhang², Tammy Franklin³, and Pottumarthi Prasad³

¹Northwestern University, Evanston, IL, United States, ²University of Utah, Salt Lake City, UT, United States, ³NorthShore University HealthSystem, Evanston, IL, United States

Blood oxygen level dependent (BOLD) MRI measurements generally use the transverse relaxation rate, R₂^{*}, as an indirect measure of oxygenation. While it has been shown to be related to tissue PO₂, and sensitive to changes in oxygenation induced by pharmaceutical maneuvers, R₂^{*} is sensitive to other physiological parameters (e.g. hydration, hematocrit, blood perfusion) and hence not a great measure of the physiologically parameters of interest. In this study, we apply a quantitative model to BOLD MRI measurements in rodent kidneys and derive regional values for hemoglobin saturation and blood PO₂. The MRI derived blood PO₂ measurements are in agreement with literature.

3905

Computer #70 Renal Ischemia/Reperfusion necrosis monitoring with hyperpolarized fumarate
Per Mose Nielsen¹, Abubakr Eldirdiri², Lotte Bonde Bertelsen¹, Haiyun Qi¹, Hans Stødkilde Jørgensen¹, Jan Henrik Ardenkjaer-larsen², and Christoffer Laustsen¹

¹institute of clinical medicine, Aarhus C, Denmark, ²Lyngby, Denmark

Renal I/R-I is a leading cause of AKI in several disease states; there is a current lack of precise methods to directly assess cortical tubular injury. In the present study, we investigated the in situ conversion of fumarate to malate in a unilateral Ischemia/reperfusion model, which is correlated with renal tubular necrosis. We saw a strong binary [1,4-¹³C₂]malate signal in the I/R-I kidney and a strong binary [1,4-¹³C₂]fumarate signal in the healthy CL kidney. This was correlated with histological examinations indication renal tubular necrosis. As well as compartmentalized fumarase activity specific for I/R-I.

-
- 3906
Computer #71 Renal [1-13C]-acetate turnover mapping with hyperpolarized MRI
Emmeli F. R. Mikkelsen¹, Thomas S. Nørlinger¹, Haiyun Qi¹, Ulrich Koellisch², Rolf F. Schulte³, Michael Pedersen¹, Hans Stødkilde-Jørgensen¹, and Christoffer Laustsen¹
- ¹MRI Research Centre, Aarhus University Hospital, Aarhus N, Denmark, ²Institute of Medical Engineering, Technische Universität München, Munich, Germany, ³GE Global Research, Munich, Germany
- Positron Emission Tomography (PET) using carbon-11 acetate has previously been used to reveal the oxidative metabolism in the kidneys. It has been found that renal carbon-11 acetate turnover measured by PET was significantly correlated with renal oxygen consumption and tubular sodium reabsorption measured by an invasive approach. Hyperpolarized MRI is an alternative method to obtain similar intracellular measures of acetate, and the aim of this study was therefore to evaluate the rate constants of hyperpolarized [1-¹³C]-acetate in rat kidneys. The intrarenal oxygen level was altered by diuretics, and measures of acetate rate constants were calculated before and after injection of furosemide.
-

- 3907
Computer #72 Exploring Intratumoral Heterogeneity of Lipid Metabolism in Clear Cell Renal Cell Carcinoma with Dixon-based MRI
Yue Zhang¹, Payal Kapur^{2,3,4}, Jin Ye⁵, Qing Yuan¹, Ananth Madhuranthakam^{1,6}, Ivan Dimitrov⁷, Yin Xi¹, Takeshi Yokoo^{1,6}, Jeffrey Cadeddu^{1,3}, Vitaly Margulis³, Andrea Pavia-Jiménez^{4,8}, James Brugarolas^{4,8,9}, Robert E. Lenkinski^{1,6}, and Ivan Pedrosa^{1,4,6}
- ¹Radiology, UT Southwestern Medical Center, Dallas, TX, United States, ²Pathology, UT Southwestern Medical Center, Dallas, TX, United States, ³Urology, UT Southwestern Medical Center, Dallas, TX, United States, ⁴Kidney Cancer Program, Simmons Comprehensive Cancer Center, UT Southwestern Medical Center, Dallas, TX, United States, ⁵Molecular Genetics, UT Southwestern Medical Center, Dallas, TX, United States, ⁶Advanced Imaging Research Center, UT Southwestern Medical Center, Dallas, TX, United States, ⁷Philips Medical Systems, Cleveland, OH, United States, ⁸Internal Medicine, UT Southwestern Medical Center, Dallas, TX, United States, ⁹Developmental Biology, UT Southwestern Medical Center, Dallas, TX, United States
- We investigated the correlation between *in vivo* fat fraction (FF) measurements by Dixon-based MRI in clear cell renal cell carcinoma (ccRCC) and both intracellular fat accumulation at histopathology and lipidomic profile in the same tumor by mass spectrometry. Quantitative targeted fat fraction measures were obtained from representative areas within each tumor and correlated with the percentage of cells containing fat in fresh tissue samples from the same location of the tumor. Lipidomic analysis of additional tissue samples was performed. Quantitative FF measures correlated with lipid accumulation in ccRCC and provide a tool for assessing heterogeneous metabolic pathways in these tumors.
-

Electronic Poster

Metabolism

Exhibition Hall

Wednesday, May 11, 2016: 13:30 - 14:30

-
- 3908
Computer #73 Effect of a two week hyper energetic matched high carbohydrate vs high fat diet on hepatic fat stores and metabolic blood markers: A ¹H MRS Study
Stephen Bawden^{1,2}, Carolyn Chee³, Peter Mansell³, Francis Stephens³, Sally Cordon³, Mehri Kaviani², Caroline Hoad², Luca Marciani¹, Penny Gowland², Guruprasad Aithal¹, and Ian Macdonald³
- ¹NIHR Nottingham Digestive Diseases Research Unit, University of Nottingham, Nottingham, United Kingdom, ²Sir Peter Mansfield Imaging Centre, University of Nottingham, Nottingham, United Kingdom, ³School of Life Sciences, University of Nottingham, Nottingham, United Kingdom
- This study used ¹H MRS to investigate the effects of a two week hyper-energetic 25% excess overfeeding diet of either high carbohydrate or high fat content on liver fat in 20 healthy overweight volunteers. Significant increases were found in whole group and in the high carbohydrate group, with smaller non-significant increases observed in the high fat group. Other blood measures and body fat were investigated also.
-
- 3909
Computer #74 Effects of lifestyle intervention on liver volume, intrahepatic fat and body weight: What are the metabolic benefits?
Malte Niklas Bongers¹, Norbert Stefan², Andreas Fritsche², Claus Claussen¹, Hans-Ulrich Häring², Konstantin Nikolaou¹, Fritz Schick³, and Jürgen Machann^{3,4,5}
- ¹Department of Diagnostic and Interventional Radiology, University Hospital of Tübingen, Tübingen, Germany, ²Department of Endocrinology, Metabolism, Clinical Chemistry, Nephrology and Angiology, University Hospital of Tübingen, Tübingen, Germany, ³Department of Diagnostic and Interventional Radiology, Section on Experimental Radiology, University Hospital of Tübingen, Tübingen, Germany, ⁴Institute for Diabetes Research and Metabolic Diseases (IDM) of the Helmholtz Center Munich at the University of Tübingen (Paul Langerhans Institute Tübingen), Tübingen, Germany, ⁵German Center for Diabetes Research (DZD), Tübingen, Germany
- Using MRI, the quantification of liver volume and identification of several compartments of adipose tissue with varying impact on metabolism is reliably possible. ¹H-MRS is established as non-invasive 'gold standard' to quantify the amount of ectopic lipids in the liver. Lifestyle interventions show differing effects on the compartments of physiological and ectopic lipids. Caloric restriction during lifestyle interventions leads to reduced liver volume, caused by a decrease of intrahepatic lipids (IHL). The decrease of IHL shows gender specific effects on liver enzymes, primarily resulting in lowered gamma-glutamyl transferase in females and lowered alanine transaminase in males. Only in females, the decrease of IHL seems to influence the systemic low-grade inflammation positively.

- 3910
Computer #75 Racial Differences in Visceral Fat and Hepatic Fat Fraction in Men with HIV, Hepatitis C, or HIV/Hepatitis C Co-infection
Natalie Korn¹, Susan Noworolski¹, Linda Nix², Kyle Tillinghast¹, and Phyllis Tien^{3,4}
- ¹Radiology and Biomedical Imaging, University of California, San Francisco, San Francisco, CA, United States, ²Northern California Institute for Research and Education, San Francisco, CA, United States, ³University of California, San Francisco, San Francisco, CA, United States, ⁴Department of VA Medical Center, San Francisco, CA, United States
- The purpose of this work is to compare differences in visceral fat volume (by IDEAL imaging) and hepatic fat fraction (FF) (by single-voxel MRS) between African American (AA) and Caucasian (CA) men with HIV, HCV, or co-infection (HIV/HCV) against an age-matched control population. We observe AA men to have a trend towards less MR-measured visceral fat and hepatic FF than CA men in a control population. This difference was enhanced and was significant in the HIV population, while there was no observable difference in the HCV or HIV/HCV populations, indicating a need to consider both race and disease status prior to interpretation of visceral or hepatic FF findings.
-
- 3911
Computer #76 Portosystemic shunts in C57BL/6J mice are associated with high levels of hepatic lipids and glucose intolerance
Ana Francisca Soares¹, Hongxia Lei^{2,3}, and Rolf Gruetter^{1,2,3,4}
- ¹Laboratory of Functional and Metabolic Imaging (LIFMET), Swiss Federal Institute of Technology Lausanne (EPFL), Lausanne, Switzerland, ²Center for Biomedical Imaging (CIBM), Lausanne, Switzerland, ³Department of Radiology, University of Geneva (UNIGE), Geneva, Switzerland, ⁴Department of Radiology, University of Lausanne (Unil), Lausanne, Switzerland
- C57BL/6J mice widely used in preclinical research exhibit sporadic congenital portosystemic shunts that prevent normal delivery of nutrients and hormones to the liver. We used MRI to diagnose portosystemic shunts in mice, and furthermore showed that their hepatic lipid content, as determined by ¹H-MRS *in vivo* is abnormally high. Also, compared with healthy cage mates, mice with portosystemic shunts displayed lower fasting glucose and insulin levels, with a less efficient glucose clearance after a glucose gavage. Hence, hepatic metabolism is significantly altered in mice with portosystemic shunts with consequences to whole-body glucose homeostasis.
-
- 3912
Computer #77 Quantification of liver metabolites in a rat model of high-fat-diet-induced nonalcoholic fatty liver disease with 1H MRS using internal standard method
Kyu-Ho Song¹, Chi-Hyeon Yoo¹, Song-I Lim¹, and Bo-Young Choe¹
- ¹Department of Biomedical Engineering, and Research Institute of Biomedical Engineering, The Catholic University of Korea College of Medicine, Seoul, Seoul, Korea, Republic of
- Our results of noninvasive *in vivo* proton magnetic resonance spectroscopy are based on accurate monitoring of the changes in lipid content, which were verified using the data on saturated fatty acids and unsaturated fatty acids.
-
- 3913
Computer #78 Subcutaneous fat unsaturation is negatively associated with liver fat fraction
Christian Cordes¹, Thomas Baum¹, Julia Clavel², Stefan Ruschke¹, Michael Dieckmeyer¹, Daniela Franz¹, Hendrik Kooijman³, Ernst J. Rummeny¹, Hans Hauner², and Dimitrios Karampinos¹
- ¹Department of Diagnostic and Interventional Radiology, Technische Universitaet Muenchen, Munich, Germany, ²Else Kroener Fresenius Center for Nutritional Medicine, Technische Universitaet Muenchen, Munich, Germany, ³Philips Healthcare, Hamburg, Germany
- Obesity, metabolic syndrome and diabetes are public health problems leading to increased morbidity and mortality. The present study performed fatty acid profiling of the abdominal adipose tissue by using MRS and found inverse correlations between SAT and liver fat fraction and regional distribution of adipose tissue (i.e. SAT and VAT volumes) assessed by chemical shift encoding-based water-fat MRI. This study allowed interesting insights into the obese phenotype and the reported findings may play an important role to identify different obese phenotypes, e.g. metabolically benign and insulin-resistant obese, which has clinical implications on patient treatment.
-
- 3914
Computer #79 Manganese-Enhanced Magnetic Resonance Imaging of Pancreatic Function in Mice
Smaragada Lamprianou¹, Jennifer Jung^{2,3}, Laurent Vinet¹, Rolf Gruetter^{4,5,6}, Paolo Meda¹, and Hongxia Lei^{3,6}
- ¹Dept of Cell Physiology and metabolism, University of Geneva, Geneva, Switzerland, ²Dept of Biomedical Engineering, Imperial College, London, United Kingdom, ³Animal Imaging and Technology CIBM-AIT, Ecole Polytechnique Fédérale de Lausanne, Lausanne, Switzerland, ⁴Laboratory of functional and metabolic imaging LIFMET, Ecole Polytechnique Fédérale de Lausanne, Lausanne, Switzerland, ⁵Radiology, University of Lausanne, Lausanne, Switzerland, ⁶Radiology, University of Geneva, Geneva, Switzerland
- Magnetic Resonance Imaging (MRI) at high magnetic field, with the help of manganese, a calcium analogue and a T₁ shortening contrast agent in MRI, could be beneficial for imaging murine pancreatic function.
-
- 3915
Computer #80 Automated Multi-Atlas Segmentation of Suspected Brown Adipose Tissue from Water-Fat MRI: Initial Evaluation
Elin Lundström¹, Robin Strand^{1,2}, Anders Forslund^{3,4}, Peter Bergsten⁵, Daniel Weghuber^{6,7}, Matthias Meissnitzer⁸, Håkan Ahlström¹, and Joel Kullberg¹
- ¹Department of Radiology, Uppsala University, Uppsala, Sweden, ²Department of Information Technology, Uppsala University, Uppsala, Sweden, ³Department of Women's and Children's Health, Uppsala University, Uppsala, Sweden, ⁴Children Obesity Clinic, Uppsala University Hospital,

Segmentation of brown adipose tissue (BAT) from water-fat MR images generally requires time-consuming manual delineation. In this work a fully automated method, based on multi-atlas registration, for segmentation of human cervical-supraclavicular adipose tissue (suspected BAT) was evaluated using a semi-automated reference method, based on manual delineation. The presented method shows promising results for automated segmentation that allows time-efficient and objective measurements of BAT in large cohort research studies.

-
- 3916
Computer #81
Longitudinal Evaluation of Brown Adipose Tissues in Rats By Multi-Modal Imaging
Sanjay Kumar Verma¹, Bhanu Prakash KN¹, Jadedgoud Yaligar¹, Julian Goggi¹, Venkatesh Gopalan¹, Swee Shean Lee¹, Tian Xianfeng¹, Shigeki Sugii², Melvin Khee Shing Leow^{3,4}, Kishore Bhakoo¹, and S. Sendhil Velan¹
- ¹Laboratory of Molecular Imaging, Singapore Bioimaging Consortium, Singapore, ²Laboratory of Metabolic Medicine, Singapore Bioimaging Consortium, Singapore, ³Singapore Institute for Clinical Sciences, Singapore, ⁴Department of Endocrinology, Tan Tock Seng Hospital, Singapore
- There are two types of fat tissues, white adipose tissue (WAT) and brown adipose tissue (BAT), which essentially perform opposite functions in whole body energy metabolism. Cold exposure activates adrenergic receptor in the brown adipose tissues, and improve the separation of WAT and BAT. In this study we have evaluated the longitudinal changes of fat fraction (FF), and relaxation times (T₂ and T₂*) of interscapular brown adipose tissue (BAT) of rats under thermoneutral and short term cold exposure, and validated with histology and UCP1. PET-CT was performed to visualize the activated BAT.
-
- 3917
Computer #82
Repeatability and accuracy of a novel, MRI-based, semi-automated analysis method for quantifying abdominal adipose tissue and thigh muscle volumes
Michael Simca Middleton¹, William Haufe¹, Jonathan Hooker¹, Magnus Borga^{2,3,4}, Olaf Dahlqvist Leinhard^{2,3,5}, Thobias Romu^{2,3,4}, Patrik Tunon², Nickolas Szeverenyi⁶, Gavin Hamilton⁶, Tanya Wolfson^{6,7}, Anthony Gamst^{6,7}, Rohit Loomba⁸, and Claude B. Sirlin¹
- ¹Department of Radiology, UCSD, San Diego, CA, United States, ²Advanced MR Analytics AB (AMRA), Linköping, Sweden, ³Center for Medical Image Science and Visualization, Linköping University, Linköping, Sweden, ⁴Department of Biomedical Engineering, Linköping University, Linköping, Sweden, ⁵Department of Medicine and Health, Linköping University, Linköping, Sweden, ⁶Radiology, UCSD, San Diego, CA, United States, ⁷Computational and Applied Statistics Laboratory (CASL), UCSD, San Diego, CA, United States, ⁸Department of Medicine, UCSD, San Diego, United Kingdom
- Current MRI methods to estimate body tissue compartment volumes rely on manual segmentation, which is laborious, expensive, not widely available outside specialized centers, and not standardized. To address these concerns, a novel, semi-automated image analysis method has been developed. Image acquisition takes about six minutes, and uses widely available MRI pulse sequences. We found that this method permits comprehensive body compartment analysis and provides high repeatability and accuracy. Current and future clinical and drug development studies may benefit from this methodology, as may clinical settings where monitoring change in these measures is desired.
-
- 3918
Computer #83
A Preliminary Study on Brown Adipose Tissue Detection Using PET/MR
Andrew Meeker McCallister^{1,2}, Le Zhang^{1,3}, Alex Burant^{1,2}, Abbie Smith-Ryan⁴, Laurence Katz⁵, and Rosa Tamara Branca^{1,3}
- ¹Physics, UNC Chapel Hill, Chapel Hill, NC, United States, ²Biomedical Research Imaging Center, UNC Chapel Hill, Chapel Hill, NC, United States, ³Biomedical Research Imaging Center, Chapel Hill, NC, United States, ⁴Department of Exercise and Sports Science, UNC Chapel Hill, Chapel Hill, NC, United States, ⁵Department of Emergency Medicine, UNC Chapel Hill, Chapel Hill, NC, United States
- A hybrid PET-MR scanner was used to compare proposed MR techniques to the FDG PET gold standard for brown adipose tissue detection. The subjects were cooled inside of the magnet while PET and MR fat fraction and BOLD techniques were obtained. It was found that MR techniques alone are not sufficient to accurately predict BAT volume but can be used to increase along side PET to increase BAT specificity.
-
- 3919
Computer #84
The effect of flip-angle on body composition using calibrated water-fat MRI.
Thobias Romu^{1,2}, Janne West^{2,3}, Anna-Clara Spetz Holm⁴, Hanna Lindblom³, Lotta Lindh-Åstrand⁴, Mats Hammar⁴, Magnus Borga^{1,2}, and Olof Dahlqvist Leinhard^{2,3}
- ¹Department of Biomedical Engineering, Linköping University, Linköping, Sweden, ²Center for Medical Image Science and Visualization (CMIV), Linköping University, Linköping, Sweden, ³Department of Medical and Health Sciences (IMH), Linköping University, Linköping, Sweden, ⁴Department of Clinical and Experimental Medicine, Linköping University, Linköping, Sweden
- This study tested how the flip angle affects body composition analysis by MRI, if adipose tissue is used as an internal intensity reference. Whole-body water-fat images with flip angle 5° and 10° were collected from 29 women in an ongoing study. The images were calibrated based on the adipose tissue signal and whole-body total adipose, lean and soft tissue volumes were measured. A mean difference of 0.29 L, or 0.90 % of the average volume, and a coefficient of variation of 0.40 % was observed for adipose tissue.
-
- 3920
Computer #85
Infant size-for-gestational age, obesity and ethnicity are associated with intramyocellular lipid content in Asian preschoolers
Navin Michael¹, Suresh Anand Sadananthan¹, Mya Thway Tint², Kuan Jin Lee³, Jay Jay Thuang Zaw², Khin Thu Zar Hlaing², Pang Wei Wei²,

Lynette Pei-Chi Shek⁴, Yap Kok Peng Fabian^{5,6}, Peter D. Gluckman^{1,7}, Keith M. Godfrey⁸, Yap Seng Chong^{1,2}, Melvin Khee-Shing Leow^{9,10}, Yung Seng Lee^{1,4}, Christiani Jeyakumar Henry⁹, Marielle Valerie Fortier¹¹, and S. Sendhil Velan^{1,3}

¹Singapore Institute for Clinical Sciences, A*STAR, Singapore, ²Department of Obstetrics & Gynaecology, Yong Loo Lin School of Medicine, National University of Singapore, Singapore, ³Singapore Biomed Imaging Consortium, A*STAR, Singapore, ⁴Department of Paediatrics, Yong Loo Lin School of Medicine, National University of Singapore, Singapore, ⁵Department of Paediatric Endocrinology, KK Women's and Children's Hospital, Singapore, ⁶Lee Kong Chian School of Medicine, Nanyang Technological University, Singapore, ⁷Liggins Institute, University of Auckland, Auckland, New Zealand, ⁸MRC Lifecourse Epidemiology Unit & NIHR Southampton Biomedical Research Centre, University of Southampton & University Hospital Southampton NHS Foundation Trust, Southampton, United Kingdom, ⁹Clinical Nutrition Research Centre, Singapore Institute for Clinical Sciences, A*STAR, Singapore, ¹⁰Department of Endocrinology, Tan Tock Seng Hospital, Singapore, ¹¹Department of Diagnostic and Interventional Imaging, KK Women's and Children's Hospital, Singapore

The goal of this study was to understand the contribution of ethnicity, obesity and early developmental factors on IMCL determined in Asian preschoolers. Prior works on IMCL in children have found IMCL to be positively associated with childhood obesity and maternal hyperglycemia. We show that, while children with higher BMI-for-age have higher IMCL, children born SGA also have higher IMCL at 4.5 years, despite being less obese, and despite having lower maternal BMI and maternal fasting glucose than children born AGA. We also found higher IMCL in 4.5 year-old Indian children than in Chinese and Malay children.

3921

Computer #86

Comparison of abdominal fat volume and fat cell hypertrophy in ex-SGA and AGA Asian preschoolers

Suresh Anand Sadananthan¹, Navin Michael¹, Mya Thway Tint², Kuan Jin Lee³, Jay Jay Thauang Zaw², Khin Thu Zar Hlaing², Pang Wei Wei², Lynette Pei-Chi Shek⁴, Yap Kok Peng Fabian^{5,6}, Peter D. Gluckman^{1,7}, Keith M. Godfrey⁸, Yap Seng Chong^{1,2}, Melvin Khee-Shing Leow^{9,10}, Yung Seng Lee^{1,4}, Christiani Jeyakumar Henry⁹, Marielle Valerie Fortier¹¹, and S. Sendhil Velan^{1,3}

¹Singapore Institute for Clinical Sciences, A*STAR, Singapore, ²Department of Obstetrics & Gynaecology, Yong Loo Lin School of Medicine, National University of Singapore, Singapore, ³Singapore Biomed Imaging Consortium, A*STAR, Singapore, ⁴Department of Paediatrics, Yong Loo Lin School of Medicine, National University of Singapore, Singapore, ⁵Department of Paediatric Endocrinology, KK Women's and Children's Hospital, Singapore, ⁶Lee Kong Chian School of Medicine, Nanyang Technological University, Singapore, ⁷Liggins Institute, University of Auckland, Auckland, New Zealand, ⁸MRC Lifecourse Epidemiology Unit & NIHR Southampton Biomedical Research Centre, University of Southampton & University Hospital Southampton NHS Foundation Trust, Southampton, United Kingdom, ⁹Clinical Nutrition Research Centre, Singapore Institute for Clinical Sciences, A*STAR, Singapore, ¹⁰Department of Endocrinology, Tan Tock Seng Hospital, Singapore, ¹¹Department of Diagnostic and Interventional Imaging, KK Women's and Children's Hospital, Singapore

Children born small-for-gestational age (SGA) are at an increased risk of developing diabetes and obesity. In vitro studies have shown higher lipid content in adipocytes differentiated from mesenchymal stem cells obtained from the umbilical cord of SGA neonates compared to appropriate-for-gestational age (AGA) infants. However, validating this in children is difficult as assessment of adipocyte hypertrophy has traditionally necessitated adipose tissue biopsies. In earlier studies, we have shown that hydrolipidic ratio (HLR) determined using MRS is negatively associated with adipocyte hypertrophy. In this work, we examined the size-for-gestational age specific differences in abdominal subcutaneous fat and HLR in Asian preschoolers.

3922

Computer #87

Dietary Fat Content Modulates the Effect of Long-term Exercise on Intramyocellular and Intrahepatic Lipids but not on Weight or Insulin Sensitivity

Venkatesh Gopalan¹, Jadegoud Yaligar¹, Navin Michael², Lee Swee Shean¹, Suresh Anand Sadananthan², Anna Ulyanova¹, Bhanu Prakash KN¹, and S Sendhil Velan¹

¹Laboratory of Molecular Imaging, Singapore Bio-Imaging Consortium, BioMedical Sciences, Singapore, Singapore, ²Singapore Institute for Clinical Sciences, Singapore, Singapore

The goal of this study was to investigate how dietary fat intake modulates the effect of long term exercise training on body weight, intrahepatic and intramyocellular lipids (IHL & IMCL), and effect on insulin sensitivity in an animal model of long-term exercise. Long term exercise was found to result in significant elevations in IMCL and IHL under low fat background diet, and significant reductions in IMCL and IHL under a high fat background diet, compared to sedentary diet-matched controls. Dietary fat content did not modulate the effect of exercise on insulin sensitivity.

3923

Computer #88

Longitudinal and Cross-Sectional Assessment of Proton Density Fat Fraction and Metabolic Syndrome in Obese Patients undergoing Weight Loss Surgery

Curtis N. Wiens¹, Alan B. McMillan¹, Nathan S. Artz^{1,2}, William Haufe³, Camilo A. Campo¹, Alexandria Schlein³, Luke Funk⁴, Jacob Greenberg⁴, Guilherme M. Campos⁵, Claude Sirlin³, and Scott B. Reeder^{1,6,7,8,9}

¹Radiology, University of Wisconsin, Madison, WI, United States, ²Diagnostic Imaging, St. Jude Children's Research Hospital, Memphis, TN, United States, ³Radiology, University of California, San Diego, CA, United States, ⁴Surgery, University of Wisconsin, Madison, WI, United States, ⁵Surgery, Virginia Commonwealth University, Richmond, VA, United States, ⁶Medical Physics, University of Wisconsin, Madison, WI, United States, ⁷Biomedical Engineering, University of Wisconsin, Madison, WI, United States, ⁸Medicine, University of Wisconsin, Madison, WI, United States, ⁹Emergency Medicine, University of Wisconsin, Madison, WI, United States

The purpose of this work was to determine the relationship between proton density fat fraction (PDFF) and metabolic syndrome (MetS) in obese patients. Patients were recruited for an MRI study 1-2 days prior to weight loss surgery (WLS). A subset of these patients with biopsy confirmed hepatic steatosis were recruited for a second MRI 6 months post WLS. A cut-off PDFF of 7.5% had a sensitivity of 77% and specificity of 80% for predicting MetS prior to undergoing WLS. At 6 months follow-up, patients with confirmed hepatic steatosis had significantly decreased prevalence of MetS (91% to 52%). Additionally, other metabolic, biometric, and imaging (PDFF) markers related to MetS were significantly reduced.

-
- 3924
Computer #89 Assessment of Fat Accumulation and Mobilization during obesity and weight-loss Interventions in Rodents
Bhanu Prakash KN¹, Venkatesh Gopalan¹, Swee Shean Lee¹, and Sendhil Velan S^{1,2}
- ¹Laboratory of Metabolic Imaging, Singapore Bioimaging Consortium, Singapore, Singapore, ²Singapore Institute for Clinical Sciences, Singapore, Singapore*
- Quantification of adipose tissue distribution within the abdomen is fundamental for investigations in obesity and diabetes. Distribution of fat within the body, and its accumulation in the abdominal cavity, exert different physiologic effects based on their anatomical location. Calorie-restriction and exercise interventions improve obesity risk factors. Fat accumulation and mobilization can vary depending on the type and quality of fat in different locations. We have investigated the quantitative changes in fat volumes at different positions in the abdomen in diet induced obese rats.
-
- 3925
Computer #90 Longitudinal imaging of interscapular brown adipose tissues in high fat diet induced obese rats
Jadegoud Yaligar¹, Sanjay Kumar Verma¹, Bhanu Prakash KN¹, Tian Xianfeng¹, Venkatesh Gopalan¹, Swee Shean Lee¹, Suresh Anand Sadananthan², Navin Michael², Ong Wee Kiat³, Shigeki Sugii³, and S Sendhil Velan¹
- ¹Laboratory of Metabolic Imaging, Singapore Bioimaging Consortium, A*STAR, Singapore, ²Singapore Institute for Clinical Sciences, A*STAR, Singapore, ³Fat Metabolism and Stem Cell Group, Singapore Bioimaging Consortium, A*STAR, Singapore*
- Obesity and diabetes are major metabolic disorders associated with dietary intake. Brown adipose tissue (BAT) is major site for adaptive thermogenesis involving uncoupling protein-1. We performed longitudinal imaging of fat fraction (FF) of interscapular BAT in control and high fat diet fed rats under thermoneutral and cold exposure conditions on Wistar rats of 7, 11 and 15 weeks. High fat diet results in increased fat fraction in iBAT. Histology shows increased size of brown adipocytes which may alter BAT function and influence thermogenic potential. UCP1 was upregulated in HFD groups. With cold exposure FF reduced significantly in control and HFD groups.
-
- 3926
Computer #91 Quantitative Magnetic Resonance Imaging of Renal Steatosis in Obesity and Type II Diabetes Mellitus
Haley R Clark¹, Ivan Pedrosa^{1,2}, Ildiko Lingvay^{3,4}, Muhammad Beg³, Ion A Bobulescu³, and Takeshi Yokoo^{1,2}
- ¹Radiology, University of Texas Southwestern Medical Center, Dallas, TX, United States, ²Advanced Imaging Research Center, University of Texas Southwestern Medical Center, Dallas, TX, United States, ³Internal Medicine, University of Texas Southwestern Medical Center, Dallas, TX, United States, ⁴Clinical Science, University of Texas Southwestern Medical Center, Dallas, TX, United States*
- In this retrospective pilot study, proton-density fat fraction (PDFF) of kidneys was compared in 40 and 29 adult subjects without and with type 2 diabetes mellitus (DM2), respectively. Median PDFF was significantly higher in DM2 (2.18%) than non-DM2 subjects (0.78%), with p=0.0008. Statistically significant correlation was found between renal PDFF and body-mass-index (BMI; r=0.2661, p=0.027). After correcting for age, sex, and BMI, PDFF difference due to DM2 remained statistically significant with p=0.0045.
-
- 3927
Computer #92 Multimodal MRI protocol for characterization of fat quantity and composition as well as cardiac parameters in patients with long-chain fatty acid oxidation defects (LCFAOD)
Martin Buechert¹, Frederike Wilbert², Thomas Lange³, Sara Tucci², and Ute Spiekerkoetter²
- ¹Magnetic Resonance Development and Application Center (MRDAC), University Medical Centre, Freiburg, Germany, ²Department of Pediatrics, Adolescent Medicine and Neonatology, University Medical Center, Freiburg, Germany, ³Medical Physics, Department of Radiology, University Medical Center, Freiburg, Germany*
- Deficiency of very-long-chain acyl-CoA dehydrogenase is the most common inherited disorder of mitochondrial β -oxidation of LCFAs with an incidence of about 1:50,000 to 1:100,000 newborns. The clinical phenotype is very heterogeneous, involving organs and tissues that mostly rely on fatty acid β -oxidation for energy production. In order to develop new monitoring and treatment strategies various approaches to characterize such patients are tested. Here a multimodal MR-approach already applied in a pre-clinical setting is transferred to humans within a pilot study. Cardiac MRI is combined with Dixon-fat/water MRI and liver MR-spectroscopy.
-
- 3928
Computer #93 ORBITAL FAT VOLUMETRY AND FAT FRACTION MEASUREMENT USING ITERATIVE DECOMPOSITION OF WATER AND FAT WITH ECHO ASYMMETRY AND LEAST-SQUARES ESTIMATION-FAST SPIN ECHO (IDEAL -FSE)
Keizo Tanitame¹, Yuji Takahashi², Yoko Kaichi³, Akira Naito¹, and Kazuo Awai³
- ¹Radiology, Chugoku Rosai Hospital, Kure, Japan, ²Clinical radiology, Hiroshima University Hospital, Hiroshima, Japan, ³Diagnostic Radiology, Hiroshima University Hospital, Hiroshima, Japan*
- We believe that the quantitative evaluation of orbital fat proliferation and edema is useful for diagnosing and monitoring Graves' ophthalmopathy. We demonstrate the feasibility of orbital fat volumetry and fat fraction measurement using iterative decomposition of water and fat with echo asymmetry and least-squares estimation-fast spin echo (IDEAL-FSE) and analyze preliminary data from healthy adults.
-
- 3929
Computer #94 T2* and T1 assessment of abdominal tissue response to graded hypoxia and hypercapnia using a controlled gas mixing circuit for small animals



Tameshwar Ganesh^{1,2}, Marvin Estrada³, James Duffin⁴, and Hai-Ling Margaret Cheng^{1,2,5,6}

¹Leslie Dan Faculty of Pharmacy, University of Toronto, Toronto, ON, Canada, ²Physiology & Experimental Medicine, Hospital for Sick Children Research Institute, Toronto, ON, Canada, ³Lab Animal Services, Hospital for Sick Children, Toronto, ON, Canada, ⁴Anesthesia, University of Toronto, Toronto, ON, Canada, ⁵Institute of Biomaterials & Biomedical Engineering, University of Toronto, Toronto, ON, Canada, ⁶The Edward S. Rogers Sr. Department of Electrical & Computer Engineering, University of Toronto, Toronto, ON, Canada

Inspiring gases with altered O₂ and CO₂ levels is an approach to assess the health of the cerebral vasculature. However, application of this technique in the body is new and less well understood compared to its application in the brain. In this study, we adopt a comprehensive approach to investigate the MR signatures of abdominal tissue response to a wide spectrum of gas challenges. Results in the liver, kidney, and muscle of healthy rats confirmed T₂* as a robust marker of blood oxygen saturation but suggested that T₁, other than its conventional association to tissue oxygenation, may a marker of blood volume changes.

3930 Computer #95 Water-Fat MRI Detects Increased Brown Adipose Tissue Volume In Anticipation of Hibernation in Ground Squirrels
Amanda D MacCannell¹, Kevin J Sinclair², Lanette J Friesen-Waldner², Charles A McKenzie², and James F Staples¹

¹Biology, Western University, London, ON, Canada, ²Medical Biophysics, Western University, London, ON, Canada

During winter, brown adipose tissue (BAT) is the primary source of heat production in hibernating animals. White adipose tissue volumes increase and BAT-specific genes are upregulated in autumn even when temperatures are warm, but the rhythm of changes in BAT volume is unknown. Water-fat MRI was used to measure total BAT volume in hibernating squirrels two months after arousing from hibernation in spring and again at 18 days following the first MRI scan. BAT volumes increased significantly in this 20 day time period.

3931 Computer #96 Imaging of Dermal White Adipose Tissue in Mice
Diego Hernando¹, Ildiko Kasza², Scott B Reeder^{1,3,4,5,6}, and Caroline M Alexander²

¹Radiology, University of Wisconsin-Madison, Madison, WI, United States, ²McArdle Laboratory for Cancer Research, University of Wisconsin-Madison, Madison, WI, United States, ³Medical Physics, University of Wisconsin-Madison, Madison, WI, United States, ⁴Biomedical Engineering, University of Wisconsin-Madison, Madison, WI, United States, ⁵Medicine, University of Wisconsin-Madison, Madison, WI, United States, ⁶Emergency Medicine, University of Wisconsin-Madison, Madison, WI, United States

Dermal white adipose tissue (DWAT) has only recently been recognized as a distinct adipocyte depot, with the potential to influence metabolism and physiology. In this study, we introduce a fat-water MRI approach for noninvasive quantification of the DWAT layer in mice on a clinical 3T scanner, and validate this approach using histology. As shown by MRI and histology, DWAT is thinner in Sdc1^{-/-} mice compared to wild type. Interestingly, DWAT was dramatically thicker in an obese mouse model.

Electronic Poster

MRSI & Non-Proton Imaging

Exhibition Hall

Wednesday, May 11, 2016: 14:30 - 15:30

3932 Computer #1 Simultaneous Determination of Metabolite Concentrations, Longitudinal and Transverse Relaxation Times
Li An¹, Shizhe Li¹, and Jun Shen¹

¹National Institute of Mental Health, National Institutes of Health, Bethesda, MD, United States

A data acquisition and quantification approach is proposed for simultaneous measurement of concentration, T₁, and T₂ of metabolites. The concentration, T₁, and T₂ of NAA, creatine, choline, glutamate and myo-inositol were determined reliably in less than 9 min using single voxel MRS at 7 Tesla.

3933 Computer #2 MR spectroscopy in the differentiation of benign, borderline and malignant cystic epithelial ovarian tumors
Feng-Hua Ma¹, Guo-Fu Zhang¹, Jin-Wei Qiang², Ya-Min Rao³, Song-Qi Cai⁴, and Hai-Min Li⁴

¹Department of Radiology, Obstetrics & Gynecology Hospital, Shanghai Medical College, Fudan University, Shanghai, China, People's Republic of, ²Department of Radiology, Jinshan Hospital, Shanghai Medical College, Fudan University, Shanghai, China, People's Republic of, ³Department of Radiology, Obstetrics & Gynecology Hospital, Shanghai Medical College, Fudan University, Shanghai, China, People's Republic of, ⁴Department of Radiology, Jinshan Hospital, Shanghai Medical College, Fudan University, Shanghai, China, People's Republic of

Because of the overlap in the imaging appearances of the benign, borderline, and malignant tumors, a considerable portion of cystic epithelial ovarian tumors (EOT) cannot be correctly diagnosed on conventional MR imaging. Recently, the rapid development of software and hardware has enabled the increasing application of proton magnetic resonance spectroscopy (¹H-MRS) in ovarian tumors. However, ¹H-MRS studies are still preliminary. To our knowledge, in vivo ¹H-MRS differentiation of a single type of histopathological and morphological tumors has not yet been studied. We prospectively performed in vivo ¹H-MRS of 86 patients with cystic EOT to understand the spectroscopic characteristics of different types of tumors and to investigate the ability of ¹H-MRS in the differentiation of benign, borderline and malignant EOT. The results shows that ¹H-MRS patterns of benign, borderline and malignant cystic EOT are different. The Cho/Cr ratio increases with the higher malignancy and a high Cho peak indicates a malignant tumor. A significantly elevated NAA peak indicates a borderline tumor.

-
- 3934
Computer #3
Prostate MRSI with reduced acquisition time and improved multichannel spectral processing
Jong Bum Son¹, Sooyoung Shin¹, Ralph Noeske², Ersin Bayram³, Jingfei Ma¹, and Haesun Choi¹

¹The University of Texas MD Anderson Cancer Center, Houston, TX, United States, ²GE Healthcare Technologies, Potsdam, Germany, ³GE Healthcare Technologies, Waukesha, WI, United States
- Prostate MR spectroscopic imaging (MRSI) is limited with long acquisition time and need for an endorectal coil. Using an acquisition-weighted spectroscopic imaging sequence with an odd symmetric sampling scheme and a sorted singular value decomposition method for spectral processing of data from a multiple receive channels, we demonstrated that *in vivo* prostate MRSI can be performed at 3T in a substantially reduced scan time and without using an endorectal coil. Our proposed technique has the potential to help substantially expand the clinical use of prostate MRSI.
-
- 3935
Computer #4
Accelerated Magnetic Resonance Spectroscopic Imaging (MRSI) using Magnetic Resonance Fingerprinting (MRF)
Rashmi Reddy¹, Imam Shaik¹, Arush Honnedeavasthana¹, Pavan Poojar¹, and Sairam Geethanath¹

¹Dayananda Sagar Institutions, Bangalore, India
- Magnetic Resonance Spectroscopic Imaging (MRSI) is used as a tool to quantify metabolites in human brain and other organs. It is extensively used in clinical imaging and clinical research applications¹. However, the major drawback of this technology is its long acquisition time which is the primary reason for not being used in the clinics. A novel approach of accelerating MRSI using Magnetic Resonance Fingerprinting (MRF) has been proposed in the current work.
-
- 3936
Computer #5
31P MRSI of Human Calf muscles Using Flyback Echo Planar Spectroscopic Imaging (EPSI) Readout Gradients
Alejandro Santos Diaz¹, Alireza Akbari¹, and Michael Noseworthy^{1,2,3}

¹School of Biomedical Engineering, McMaster University, Hamilton, ON, Canada, ²Imaging Research Centre, St Joseph's Healthcare, Hamilton, ON, Canada, ³Electrical and Computer Engineering, McMaster University, Hamilton, ON, Canada
- Long acquisition time due to the low sensitivity is one of the main constrains for using 31P MRSI on a regular basis. Different methods have been proposed to accelerate the acquisition showing advantages and limitations. In this work we present for the first time an *in vivo* experiment using flyback-Echo Planar Spectroscopic Imaging readout and compare it with the traditional fidCSI sequence. Results suggest that the technique might be suitable for clinical applications.
-
- 3937
Computer #6
Improved Stability of the Inverse Laplace Transform with Non-negativity Constraints through Extension into a Second Dimension, with Applications to Magnetic Resonance Relaxometry of Tissue
Ariel Hafftko^{1,2}, Hasan Celik¹, Wojciech Czaja², and Richard G. Spencer¹

¹Laboratory of Clinical Investigation, National Institute on Aging, National Institutes of Health, Baltimore, MD, United States, ²Department of Mathematics, University of Maryland, College Park, MD, United States
- Magnetic resonance (MR) relaxometry and related experiments provide useful information about tissues. These experiments reveal the distribution of a parameter, such as T2-relaxation, in a sample. The process required to recover the distribution from the observed data, an inverse Laplace transform (ILT), is highly ill-conditioned, meaning that small amounts of noise can create huge changes in the solution. Recent work has shown using simulations that 2D MR experiments result in a problem substantially more stable than in 1D. We present a theorem quantifying stability of the ILT and use it to explain the improved performance in 2D.
-
- 3938
Computer #7
31P MR Imaging with Radial bSSFP Data Acquisition and 1H Constraint Iterative Reconstruction
Kristian Rink¹, Moritz C. Berger¹, Nadia Benkhedah¹, Christine Gnahn¹, Peter Bachert¹, and Armin M. Nagel^{1,2}

¹German Cancer Research Center (DKFZ), Heidelberg, Germany, ²University Medical Center Ulm, Ulm, Germany
- Phosphorus (³¹P)-containing biomolecules play a crucial role in the energy metabolism of all cells. Since the *in vivo* MR signal of ³¹P is four orders of magnitude smaller compared to hydrogen, strategies to improve the signal-to-noise (SNR) are required. Therefore, this study focuses on the development of a signal-effective ³¹P acquisition in combination with a constraint iterative reconstruction applying prior knowledge from recorded hydrogen (¹H) data.
-
- 3939
Computer #8
A Comparison of Rapid Acquisition Sodium T1 Mapping Techniques at 3T
James Grist¹, Martin J Graves¹, Josh Kaggie¹, Mary Mclean², Frank Riemer¹, and Ferdia A Gallagher¹

¹Radiology, University of Cambridge, Cambridge, United Kingdom, ²Cancer Research UK Cambridge Institute, University of Cambridge, Cambridge, United Kingdom
- Sodium T₁ maps from three different Variable Flip Angle (VFA) methods were assessed against Inversion Recovery (IR) data, showing that the estimated method of slopes (eMOS) is superior to both linear and non-linear fitting methods in the healthy brain. eMOS requires two flip angle data sets to produce volumetric T₁ maps of the brain, in comparison to other techniques which require 4 or more data sets to produce maps, and therefore allows for shortening of the overall time spent scanning. Furthermore, T₁ maps may also give

further insight in to the underlying tissue structure surrounding sodium nuclei.

-
- 3940
Computer #9
Assessment of benefit to use a non-Cartesian trajectory and nonlinear reconstruction method compared to a Cartesian strategy for Fast 31P MRI
Arthur Coste¹, Nicolas Chauffert^{1,2}, Alexandre Vignaud¹, Philippe Ciuciu^{1,2}, Fawzi Boumezeur¹, Pierre Weiss³, Sandro Romanzetti⁴, Denis Le Bihan¹, and Cécile Lerman¹

¹MR Imaging and Spectroscopy Unit, NeuroSpin, Gif sur Yvette, France, ²Parietal, INRIA Saclay, Saclay, France, ³Institut des Technologies Avancées du Vivant, Toulouse, France, ⁴University Clinic RWTH Aachen, Aachen, Germany
- This work illustrates the application of a wavelet based least square regularized image reconstruction for non-Cartesian MR sampling trajectories in the framework of low concentration Phosphorus Imaging. We compared performances between 3D Cartesian Fast Imaging with Steady-state free Precession (FISP) and the TPI (FISP) sequence and show that in equivalent acquisition durations we are able to produce better images with the TPI sequence. Prospective sub-sampling was also performed and results open exciting possibilities to reduce acquisition time without impacting image quality for non-proton MRI.
-
- 3941
Computer #10
Fast PCr Imaging of Rat Calf Muscles Using Spiral-In/Out bSSFP
Yuchi Liu¹, Yun Jiang¹, Charlie Yi Wang¹, Mark Alan Griswold^{1,2}, and Xin Yu^{1,2,3,4}

¹Biomedical Engineering, Case Western Reserve University, Cleveland, OH, United States, ²Radiology, Case Western Reserve University, Cleveland, OH, United States, ³Physiology and Biophysics, Case Western Reserve University, Cleveland, OH, United States, ⁴Case Center for Imaging Research, Case Western Reserve University, Cleveland, OH, United States
- In this study, a fast phosphocreatine (PCr) imaging method was developed by combining spectrally selective bSSFP with single-shot spiral-in/out encoding for measuring PCr distribution in vivo. 2 min acquisition yielded an SNR of ~9 in rat calf muscles with high spatial resolution (1.25 mm×1.25 mm×5 mm) at 9.4T. The SNR was increased to 25.5 with 30 min acquisition. This method also has the potential for imaging other metabolites such as ATP with a different carrier frequency, dynamic PCr imaging in exercise-recovery or ischemia-reperfusion studies, and quantification of the absolute metabolite concentration with appropriate T₁, T₂, and flip angle calibration/correction.
-
- 3942
Computer #11
Sensitivity Comparison of Ultrahigh-field Oxygen-17 MRS Imaging between 7T and 10.5T using a Human Head Size Phantom and Quadrature Surface Coil
Hannes Michel Wiesner¹, Xiao-Hong Zhu¹, Kamil Ugurbil¹, and Wei Chen¹

¹CMRR, Radiology, University of Minnesota Medical School, Minneapolis, MN, United States
- In vivo ¹⁷O MRS imaging provides a valuable tool for quantitatively imaging the cerebral rate of oxygen metabolism, cerebral blood flow and oxygen extraction fraction from a brief inhalation of ¹⁷O-isotope labeled oxygen gas. In this study, we conducted a pilot test to examine the ¹⁷O sensitivity using the human head size water phantom in the world's first 10.5T whole-body human scanner at the CMRR, then compared it with that at 7T. We found approximately doubled ¹⁷O sensitivity at 10.5T after careful consideration signal and noise contributions at both fields.
-
- 3943
Computer #12
A Beating Heart Simulation for Sequence Optimization of Sodium MRI
Simon Konstandin¹ and Matthias Günther^{1,2}

¹MR-Imaging and Spectroscopy, University of Bremen, Bremen, Germany, ²Fraunhofer MEVIS, Bremen, Germany
- Sodium MRI can act as a biomarker for heart tissue viability. However, several aspects (blurring behavior of non-Cartesian ultra-short echo time sequences, blurring because of heart motion, small myocardial infarction (MI) regions) complicate MI detection due to resolution reasons. Optimal sequence parameters are difficult to find since many subject parameters (e.g., relaxation times, heart motion) must be considered. The presented simulation model of a beating heart can be used to optimize sequence parameters, among other things, for better visualization of MI and can be adapted to any kind of motion and to different subject/physiological parameters.
-
- 3944
Computer #13
31P MR Imaging and Concentration Measurements
Arthur Coste¹, Alexandre Vignaud¹, Philippe Ciuciu^{1,2}, Fawzi Boumezeur¹, Franck Mauconduit³, Alexis Amadon¹, Sandro Romanzetti⁴, Denis Le Bihan¹, and Cécile Lerman¹

¹MR Imaging and Spectroscopy Unit, NeuroSpin, Gif sur Yvette, France, ²Parietal, INRIA Saclay, Saclay, France, ³Siemens Healthcare, Saint Denis, France, ⁴University Clinic RWTH Aachen, Aachen, Germany
- This work describes a novel method accounting for MR acquisition properties (B₀, B₁⁺, B₁⁻, T₁, T₂^{*}) to perform concentration measurements in the framework of *in vitro* Phosphorus MRI. Our pipeline uses a non-Cartesian 3D sequence for efficient signal sampling and a wavelet regularized least square method for reconstruction. We demonstrated within an acceptable time for human experiment, for 5mm isotropic resolution, that we are able to calibrate and measure absolute ³¹P concentrations.
-
- 3945
Computer #14
Mapping of sodium and water content ratio in vivo in the human calf
Anja M. Marschar¹, Moritz C. Berger¹, Mark E. Ladd¹, Peter Bachert¹, and Armin M. Nagel^{1,2}

¹Medical Physics in Radiology, German Cancer Research Center (DKFZ), Heidelberg, Germany, ²Diagnostic and Interventional Radiology, University Medical Center Ulm, Ulm, Germany

Both lower legs of three male healthy volunteers were examined at 3 T and 7 T by means of ¹H and ²³Na MRI to obtain quantitative maps of the sodium and water content in muscle tissue. Corrections for T₂^{*} and T₁ relaxation and RF profiles (B₁⁺, B₁⁻) were performed. The resulting water content value in calf muscle tissue was in the range of 75–85 mol/l, the level of sodium was 15–21 mmol/l (sodium-to-water content ratio: 0.20–0.27 %).

3946 Computer #15 Phase Modulated Array Coil Image Reconstruction: A means to correct B₁[±] signal modulations for sodium Tx/Rx Array Coil at 3T
Yongxian Qian¹, Tiejun Zhao², Steven Baete¹, Karthik Lakshmanan¹, Graham Wiggins¹, and Fernando E Boada¹

¹Radiology, New York University, New York, NY, United States, ²Siemens Medical Solutions USA, New York, NY, United States

A transmit/receive (Tx/Rx) array coil has high efficiency in transmission and thus reduces specific absorption rate (SAR), which is highly desired in clinical applications for sodium (²³Na) MR imaging. However, a Tx/Rx array coil at 3T usually produces a spatially-varying excitation (B₁⁺) field and does not provide a uniform sum-of-squares of coil sensitivities (B₁⁻ fields) for quantitative sodium MRI. Here we present a solution to this problem and demonstrate its effectiveness with studies on phantoms and subjects with neurological disorders such as multiple sclerosis (MS), epilepsy, and mild traumatic brain injury (mTBI).

3947 Computer #16 Spectral Quantification of MRSI Data Using Spatiospectral Constraints
Qiang Ning^{1,2}, Chao Ma², Fan Lam², Bryan Clifford^{1,2}, and Zhi-Pei Liang^{1,2}

¹Electrical and Computer Engineering, University of Illinois, Urbana-Champaign, Urbana, IL, United States, ²Beckman Institute for Advanced Science and Technology, University of Illinois, Urbana-Champaign, Urbana, IL, United States

A new method is proposed for spectral quantitation of MRSI data. The method has two main features: 1) incorporation of prior spectral knowledge in the form of basis functions obtained by quantum simulation, and 2) incorporation of prior spatial knowledge by penalizing smoothness within each type of tissue. An efficient algorithm is also proposed to solve the underlying optimization problem, and its effectiveness for extracting quantitative spectral information from noisy MRSI data is demonstrated by comparing it with one of the state-of-the-art methods.

3948 Computer #17 Flexible flyback EPSI Waveform Generation under the Constraint of Peripheral Nerve Stimulation
Ralph Noeske¹ and Rolf F Schulte²

¹GE Healthcare, Potsdam, Germany, ²GE Global Research, Munich, Germany

Echo-Planar Spectroscopic Imaging (EPSI) reduces the long acquisition time of Chemical Shift Imaging. “Flyback” trajectories sampling the lobe only along one direction are commonly used for robustness and artifact reasons. Main challenge in the design is that there is no analytic solution for an SNR optimized readout/flyback trapezoid pair. The goal of this work was to implement a fast SNR optimized algorithm that takes Peripheral Nerve Stimulation into account to calculate waveforms on the fly for any given spectral and spatial resolution and therefore doesn’t require pre-calculated waveforms.

3949 Computer #18 A pilot validation of compressed sensing four dimensional multi-echo based echo-planar J-resolved spectroscopic imaging in human brain
Manoj Kumar Sarma¹, Zohaib Iqbal¹, Rajakumar Nagarajan¹, and M. Albert Thomas¹

¹Radiological Sciences, UCLA School of Medicine, Los angeles, Los Angeles, CA, United States

Phase encoded MR spectroscopic imaging (MRSI) is a time-consuming protocol because there is a large number of phase encodings to be collected. Non-uniform undersampling (NUS) and Compressed Sensing (CS), which has been widely used in MRI/MRS can be used to speed up the acquisition further. In this study, we have implemented a novel CS based multi-echo echo planar J-Resolved spectroscopic imaging (ME-EP-JRESI) acquisition and CS reconstruction in in human brain at 3T. We were able to detect and quantify several metabolites using a modified ProFit algorithm. The CS reconstructed spectra were of high quality, with metabolite ratios matching the fully encoded data closely.

3950 Computer #19 Accelerated Five-Dimensional Echo Planer J-resolved spectroscopic imaging: Pilot findings in untreated and CPAP treated Obstructive Sleep Apnea
Manoj Kumar Sarma¹, Paul Michael Macey², Zohaib Iqbal¹, Rajakumar Nagarajan¹, Ravi Aysola³, and M. Albert Thomas¹

¹Radiological Sciences, UCLA School of Medicine, Los angeles, Los Angeles, CA, United States, ²School of Nursing, UCLA School of Medicine, Los angeles, Los Angeles, CA, United States, ³Division of Pulmonary and Critical Care Medicine, UCLA School of Medicine, Los angeles, Los Angeles, CA, United States

With the rise of people with obesity and older age, obstructive sleep apnea (OSA) has become a potentially disabling health problem. Continuous positive airway pressure (CPAP) is the most common treatment method for OSA patients. Here we examined neurochemical changes of untreated and CPAP treated OSA patients versus healthy controls in several brain region including parietal gray/white,

insular cortex and frontal gray/white regions to demonstrate the nature of tissue changes using an accelerated five-dimensional (5D) echo-planar J-resolved spectroscopic imaging (EP-JRESI) sequence. We observed statistically significant differences between OSA patients and healthy control subjects in the occipital gray NAA/Cr, frontal gray Ch/Cr and ml/Cr, and occipital white Ch/Cr regions. Most of the differences were seen to be reversed in the OSA patients' with CPAP cohort except that the differences in occipital gray NAA/Ch and frontal gray ml/Cr remained significance. To validate our findings, further longitudinal studies using a large cohort of OSA subjects before and after CPAP are required. These pilot findings demonstrate that the 5D EP-JRESI sequence can be easily combined with any MRI protocol.

3951
Computer #20 2D MR Spectroscopic Imaging of the Pediatric Brain using Compressed Sensing
Rohini Vidya Shankar¹, Houchun Harry Hu², John C Chang³, and Vikram D Kodibagkar¹

¹Biomedical Engineering, Arizona State University, Tempe, AZ, United States, ²Radiology, Phoenix Children's Hospital, Phoenix, AZ, United States, ³Banner MD Anderson Cancer Center, Gilbert, AZ, United States

The spatial variations in brain metabolite concentrations can be mapped using magnetic resonance spectroscopic imaging (MRSI). The long scan times in MRSI do not permit its inclusion in pediatric imaging protocols. MRSI accelerated by compressed sensing was used to image the pediatric brain for various acceleration factors 2X-5X. The retrospectively undersampled reconstructions showed high data fidelity for up to 80% undersampling when compared with the fully sampled reference dataset. Studies are underway to prospectively acquire and validate CS accelerated MRSI data in pediatric patients.

3952
Computer #21 WITHDRAWN
Maryam Vareth^{1,2}, Yan Li², and Sarah Nelson^{1,2}

¹UCBerkeley/UCSF Joint Graduate Group in Bioengineering, University of California Berkeley, Berkeley, CA, United States, ²Department of Radiology and Biomedical Imaging, Surbeck Laboratory of Advanced Imaging, San Francisco, CA, United States

This work investigates the feasibility of using GRAPPA-EPSI based reconstruction of the short-echo 3D MRSI to shorten the acquisition time and to increase the spatial resolution for future routine clinical purposes. Fully sampled data were retrospectively under-sampled to achieve effective acceleration rate of 2, 3 and 4 using variety of sampling patterns. GRAPPA algorithm was modified to take advantage of the FID time points and handle the arbitrary sampling patterns. Additional technique was also developed to prospectively under-sample in-vivo data with various patterns for future studies.

3953
Computer #22 Enhanced T2 Spectroscopic Imaging Using Backprojections (SI-WEB): A Simulation Study
Zohaib Iqbal¹ and M. Albert Thomas¹

¹Radiological Sciences, University of California - Los Angeles, Los Angeles, CA, United States

Measuring the transverse relaxation times (T_2 s) of metabolites from different regions of the brain provides important insight into different pathologies, but requires long acquisition. A novel k-space acquisition using a hybrid technique involving both echo planar spectroscopic imaging (EPSI) and concentric circular echo planar trajectories (SI-CONCEPT) was applied to simulated brain tumor spectroscopic imaging data. In addition, an algorithm incorporating the backprojection information from the EPSI scan was developed to enhance the spectroscopic images. This novel acquisition and reconstruction technique, called SI-WEB, decreases the total duration of the scan while producing similar results when compared to the true T_2 spectroscopic images.

3954
Computer #23 Compressed Sensing 3D Echo Planar Spectroscopic Imaging of HIV Adults
Rajakumar Nagarajan¹, Zohaib Iqbal¹, Manoj K Sarma¹, Mario Guerrero², Vanessa Correa², Eric S Daar², and M. Albert Thomas¹

¹Radiological Sciences, University of California Los Angeles, Los Angeles, CA, United States, ²Department of Medicine, Harbor-UCLA Medical Center, Torrance, CA, United States

HIV affects more than 1 million individuals in the US and over 40 million people worldwide. CNS is commonly involved in the early stage HIV infection. Conventional 3D MRSI is time-consuming because it involves a large number of phase encodings. EPSI approaches have been used to reduce the long acquisition time required for multiple spatial encoding steps. In our study, non-uniformly undersampled (NUS) semi LASER based 3D EPSI was used to quantify changes in brain metabolites, NAA, Cr, Cho and myo-inositol in a group of HIV adults in comparison to age matched control sample using compressed sensing reconstruction by minimizing total variation.

3955
Computer #24 Denoising of MR Spectroscopic Imaging Data Using Statistical Selection of Principal Components (SSPC)
Abas Abdoli¹, Radka Stoyanova², and Andrew A. Maudsley¹

¹Radiology, University of Miami, Miami, FL, United States, ²Radiation Oncology, University of Miami, Miami, FL, United States

In this study we evaluate a new principal components analysis (PCA) based denoising method for volumetric MRSI data that employs a statistical test for the selection of the significant noise-free principle components (PCs).

Heteronuclear MRS

Exhibition Hall

Wednesday, May 11, 2016: 14:30 - 15:30

-
- 3956
Computer #25
- A Subspace-Based Approach to High-Resolution 31P-MRSI
Chao Ma¹, Fan Lam¹, Qiang Ning^{1,2}, Bryan A. Clifford^{1,2}, Ryan Larsen¹, and Zhi-Pei Liang^{1,2}
- ¹Beckman Institute, University of Illinois Urbana-Champaign, Urbana, IL, United States, ²Electrical and Computer Engineering, University of Illinois Urbana-Champaign, Urbana, IL, United States
- Conventional Fourier based phosphorus (31P)-MRSI methods have been limited by spatial resolution due to the low concentrations of phosphate-contained chemical compounds in the human body and the relatively low sensitivity of 31P NMR. This work presents a subspace-based data acquisition and reconstruction method to achieve accelerated, high-resolution 31P-MRSI. The feasibility of the proposed method is demonstrated using both phantom and in vivo experimental studies on a 3T scanner, which have yielded very promising results. The proposed method can be used in a range of 31P-MRSI applications.
-
- 3957
Computer #26
- 31P Magnetic Resonance Fingerprinting Method for Efficient Measurement of Creatine Kinase Mediated High Energy Phosphate Metabolism
Charlie Yi Wang¹, Yuchi Liu¹, Shuying Huang¹, Mark Alan Griswold^{1,2}, and Xin Yu^{1,2}
- ¹Biomedical Engineering, Case Western Reserve University, Cleveland, OH, United States, ²Radiology, Case Western Reserve University, Cleveland, OH, United States
- We propose a novel ³¹P Creatine Kinase encoding Magnetic Resonance Fingerprinting method (CK-MRF) to efficiently measure high energy phosphate metabolism through creatine kinase (CK). Measurement reproducibility of CK rate constant ($k_{f,CK}$) using CK-MRF was compared with both conventional ³¹P saturation transfer method, and Four Angle Saturation Transfer method in rat hind limb. CK-MRF measurement showed comparable or superior reproducibility using 20 s experiment time compared to 160 s experiment time of either comparison method. Changes in $k_{f,CK}$ following Ischemia/Reperfusion (IR) were also measured.
-
- 3958
Computer #27
- Citrate production in prostate cancer metastasis cell lines LNCaP and VCaP
Frits H.A. van Heijster¹, Vincent Breukels¹, Kees (C.) J. Jansen², Jack A. Schalken², and Arend Heerschap¹
- ¹Radiology and Nuclear Medicine, Radboud University Medical Center, Nijmegen, Netherlands, ²Urology, Radboud University Medical Center, Nijmegen, Netherlands
- Citrate production by prostate cancer cell lines LNCaP and VCaP were studied with ¹³C-NMR spectroscopy. Glucose acts as carbon source for citrate production in LNCaP and VCaP cell lines, but not aspartate, in contrast to expectation. Also pyruvate and glutamine can act as carbon sources for citrate production in LNCaP. Anaplerosis via pyruvate carboxylase is found to be low in these cells. Glutamine label only ends up in citrate via isocitrate instead of downstream in the Krebs cycle. These typical features of citrate metabolism might serve as valuable biomarkers for transition from healthy prostate cells to malignant cells.
-
- 3959
Computer #28
- Myocardial energetics in patients with degenerative mitral regurgitation studied by 31P MRS
Limiao Jiang¹, Mary C Stephenson¹, John J Totman¹, Stephanie Marchesseau¹, Arthur Mark Richards², and Lieng H. Ling²
- ¹Clinical Imaging Research Center, A*STAR & National University of Singapore, Singapore, Singapore, ²Department of Medicine, Yong Loo Lin School of Medicine and Cardiovascular Research Institute, National University Health System, Singapore, Singapore
- 31P MRS can noninvasively reflect the *in vivo* energy metabolism without using ionizing radiation. It has been widely applied in the clinical studies of cardiac energetics under different pathophysiological conditions. The aim of the present study was to evaluate the myocardial energetics in 30 patients with moderate or severe degenerative mitral regurgitation (DMR) using 31P MRS.
-
- 3960
Computer #29
- Measurement of ATP Synthesis in Human Brain by 31P Localized Band Inversion Transfer at 7T
Jimin Ren¹, A. Dean Sherry¹, and Craig R. Malloy¹
- ¹Advanced Imaging Research Center, University of Texas Southwestern Medical Center, Dallas, TX, United States
- Despite recent advances in measuring ATP energy metabolism using 31P magnetization transfer, there is still a lack of localized techniques capable of assessing the regional ATP synthesis. The importance of measuring regional ATP rates and fluxes in the human brain is highlighted by the heterogeneity in normal brain functions and also in many cerebral metabolic abnormalities. In this study, we demonstrate that, by combining wide-band inversion transfer with image selected in vivo spectroscopy (ISIS), quantitative information regarding ATP synthesis reaction $P_i \Rightarrow \gamma\text{-ATP}$ can be obtained from the localized regions in the human brain.
-
- 3961
Computer #30
- 7T allows correct measurement of PDE in the human liver without decoupling
Lucian A. B. Purvis¹, William T. Clarke¹, Michael Pavlides¹, Matthew D. Robson¹, and Christopher T. Rodgers¹
- ¹OCMR, Department of Cardiovascular Medicine, University of Oxford, Oxford, United Kingdom
- Phosphomonoesters (PME) and phosphodiesteres (PDE) are emerging biomarkers in cirrhosis and fatty liver disease. In this study,

phosphorus (^{31}P) liver metabolite concentrations were quantified at 7T for 10 healthy volunteers using a 28 minute, 3D UTE-CSI sequence and an endogenous 2.5mM ATP reference. The inorganic phosphate concentration was $1.95 \pm 0.18\text{mM}$ (1.25-2.43mM in the literature). Summing individual ester peaks, the total PME and PDE concentrations were $1.90 \pm 0.29\text{mM}$ (cf. 1.98-3.89mM) and $4.31 \pm 0.80\text{mM}$ (cf. 8.01-11.40mM). We attribute this apparent reduction in PDE to a broadening of the underlying phospholipid bilayer resonance and the increased spectral resolution at 7T.

-
- 3962
Computer #31 Simultaneous Assessment of Abnormal Glycolysis and Oxidative Metabolisms in Brain Tumor using In Vivo Deuterium MRS Imaging
Ming Lu¹, Xiao-Hong Zhu¹, Yi Zhang¹, Walter Low², and Wei Chen¹
- ¹Center for Magnetic Resonance Research, University of Minnesota, Minneapolis, MN, United States, ²Neurosurgery, University of Minnesota, Minneapolis, MN, United States
- Recently, we developed a novel 3D-Deuterium MR (DMR) approach able to simultaneously image glucose consumption rate and TCA cycle flux in rat brain at ultrahigh field. To evaluate its sensitivity in detecting altered metabolism, in this study, we acquired localized DMR spectra in rat brains with gliosarcoma following a brief infusion of deuterated glucose at 16.4 T. We observed accelerated glucose consumption and lactate accumulation accompany with decreased glutamate/glutamine turnover in brain regions with tumor. This pilot study demonstrates the feasibility of the *in vivo* DMR imaging approach for investigating abnormal glucose metabolism in brain tumor at ultrahigh field.
-
- 3963
Computer #32 In Vitro Oxygen-17 NMR Spectroscopy of Cellular Metabolism at Ultra High Field
Ruomin Hu¹, Andreas Neubauer¹, Jorge Chacón-Caldera¹, Javier Uranga Solchaga¹, Christian Schuch², Tilo Gläser², Cordula Nies³, Eric Gottwald³, Stefan Giselsbrecht⁴, and Lothar R. Schad¹
- ¹Computer Assisted Clinical Medicine, Medical Faculty Mannheim, Heidelberg University, Mannheim, Germany, ²NUKEM Isotopes Imaging GmbH, Alzenau, Germany, ³Institute for Biological Interfaces 5, Karlsruhe Institute of Technology, Eggenstein-Leopoldshafen, Germany, ⁴Department of Complex Tissue Regeneration, MERLIN Institute for Technology-Inspired Regenerative Medicine, Maastricht University, Maastricht, Netherlands
- In this work we present a novel *in vitro* oxygen-17 NMR method using ^{17}O -labeled glucose to investigate the metabolic process of cells cultivated in a MR-compatible microreactor. The metabolization of ^{17}O -labeled glucose was demonstrated to produce MR-detectable H_2^{17}O on the one hand and to not intervene with the inherent cellular physiology on the other hand, thus proving the method to serve as a neutral observation platform. The presented method has the potential to aid the modeling of fundamental physiological processes and to become a key element in cellular vitality assessment applications.
-
- 3964
Computer #33 Initial investigation of glucose metabolism in mouse brain using enriched ^{17}O -glucose and dynamic ^{17}O -MRS
Robert Borowiak^{1,2}, Wilfried Reichardt^{1,2}, Dmitry Kurzhunov¹, Christian Schuch³, Jochen Leupold¹, Thomas Lange¹, Marco Reiser¹, Axel Krafft^{1,2}, Elmar Fischer¹, and Michael Bock¹
- ¹University Medical Center Freiburg, Dept. of Radiology - Medical Physics, Freiburg, Germany, ²German Cancer Consortium (DKTK), German Cancer Research Center (DKFZ), Heidelberg, Germany, ³NUKEM Isotopes Imaging GmbH, Alzenau, Germany
- In this work, we demonstrate the feasibility of monitoring glucose uptake in mouse brain using direct ^{17}O -MRS at 9.4 Tesla for the first time. Time-resolved ^{17}O -MRS spectra (temporal resolution: 42 s) are acquired *in vivo* after injection of D-glucose with ^{17}O -labeled hydroxyl groups. The cerebral rate of glucose metabolism CMR_{Glc} is estimated using a pharmacokinetic model in an anesthetized (1.25% isoflurane) mouse to $0.43 \pm 0.21 \mu\text{mol/g/min}$, which is of the same order of magnitude as reported by ^{18}F -FDG PET.
-
- 3965
Computer #34 Evaluation of High Temporal and Spatial Resolution ^{17}O -MRI
Sebastian C. Niesporek¹, Reiner Umathum¹, Thomas M. Fiedler¹, and Armin M. Nagel^{1,2}
- ¹Medical Physics in Radiology, German Cancer Research Center (DKFZ), Heidelberg, Germany, ²Diagnostic and Interventional Radiology, University Medical Center Ulm, Ulm, Germany
- Functional information of cell and tissue viability can be obtained via dynamic ^{17}O -MRI. The quantification of H_2^{17}O -concentration as a turnover product of oxidative phosphorylation in combination with $^{17}\text{O}_2$ -inhalation enables mapping of the cerebral metabolic rate of oxygen consumption (CMRO_2). Due to low MR-sensitivity of the ^{17}O -nucleus, spatial as well as temporal resolution is limited. Induced partial volume effects hinder accurate and stable signal quantification which is essential for dynamic studies. High resolution ^{17}O -data with $(4.5\text{mm})^3$ was acquired with a Golden Angle acquisition scheme which allowed reconstruction of arbitrary time-frames. A partial volume correction algorithm was applied to test correction capability of data of different temporal resolution.
-
- 3966
Computer #35 Iterative Approach for Partial Volume Corrected T_2^* Determination in ^{17}O -MRI
Sebastian C. Niesporek¹, Reiner Umathum¹, Thomas M. Fiedler¹, and Armin M. Nagel^{1,2}
- ¹Medical Physics in Radiology, German Cancer Research Center (DKFZ), Heidelberg, Germany, ²Diagnostic and Interventional Radiology, University Medical Center Ulm, Ulm, Germany
- The energy balance of a cell is closely connected to in-vivo H_2^{17}O -concentration which also is the turnover product of oxidative phosphorylation. ^{17}O -MRI during inhalation of $^{17}\text{O}_2$ enables localized mapping of cerebral metabolic rate of oxygen consumption (CMRO_2). Larger voxel sizes due to a low MR-sensitivity and short relaxation times induce partial volume effects which reduce quantification accuracy. For accurate signal correction exact T_2^* -values are essential. A partial volume correction algorithm for improved

T_2^* -determination where T_2^* -values are adapted iteratively is presented. Consistent results to simulations were obtained for phantom and in-vivo data. The iteratively corrected in-vivo T_2^* -values were used for improved ^{17}O -MRI-signal quantification.

3967
Computer #36 Random under-sampling and spectra reconstruction for in vivo ^{13}C magnetic resonance spectroscopy
Ningzhi Li¹, Shizhe Steve Li¹, and Jun Shen¹

¹National Institute of Mental Health, Bethesda, MD, United States

The present study proposes and evaluates a novel under-sampled decoupling strategy in which no decoupling was applied during randomly selected segments of data acquisition. By taking advantage of the sparse spectral pattern of carboxylic/amide region of *in vivo* ^{13}C spectra of brain, an iterative algorithm was developed to reconstruct spectra from under-sampled data. Simulations and *in vivo* experiments show that this novel decoupling and data processing strategy can effectively reduce decoupling power deposition by >30%.

3968
Computer #37 Energy metabolism in the rat cortex under thiopental anaesthesia measured in vivo by ^{13}C MRS at 14.1T
Sarah Sonnay¹, Nathalie Just², Rolf Gruetter³, and João M.N. Duarte⁴

¹Laboratory of Functional and Metabolic Imaging (LIFMET), Ecole Polytechnique Fédérale de Lausanne (EPFL), Lausanne, Switzerland, ²Universitätsklinikum Münster, Münster, Germany, ³Center for Biomedical Imaging (CIBM) and Laboratory of Functional and Metabolic Imaging (LIFMET), Ecole Polytechnique Fédérale de Lausanne (EPFL), Lausanne, Switzerland, ⁴Laboratory of Functional and Metabolic Imaging (LIFMET), Ecole Polytechnique Fédérale de Lausanne (EPFL), Lausanne, Switzerland

Cerebral function relies on cooperative interaction between neuronal and glial cells. Anaesthetics modulate basal neuronal activity, and therefore the so-called neurometabolic coupling, by targeting different receptors, such as γ -aminobutyric acid type A (GABA_A) receptors, in the case of thiopental or α -chloralose anaesthesia. We investigated cortical metabolism *in vivo* using ^{13}C magnetic resonance spectroscopy (MRS) during infusion of [1,6- ^{13}C]glucose under thiopental anaesthesia. Data indicate glycolysis inhibition, decreased mitochondrial oxidative metabolism and possible oxidation of three-carbon molecules, namely lactate, which plasma concentration increased two-fold (compared to α -chloralose anaesthesia).

3969
Computer #38 In vivo measurement of metabolic fluxes in mouse dorsal hippocampus using ^1H -[^{13}C] NMR spectroscopy at 14.1 Tesla
Antoine Cherix¹, Blanca Lizarbe¹, Hongxia Lei^{2,3}, and Rolf Gruetter^{1,2,4}

¹Laboratory for Functional and Metabolic Imaging (LIFMET), Ecole Polytechnique Fédérale de Lausanne, Lausanne, Switzerland, ²Department of Radiology, University of Geneva, Geneva, Switzerland, ³Animal Imaging and Technology Core (AIT), Center for Biomedical Imaging (CIBM), Ecole Polytechnique Fédérale de Lausanne, Lausanne, Switzerland, ⁴Department of Radiology, University of Lausanne, Lausanne, Switzerland

^1H -[^{13}C] MRS was applied in a mouse dorsal hippocampus to investigate brain metabolism *in vivo*. The measured fractional enrichments allowed to measure metabolic fluxes using a one compartment model of glucose metabolism. Results were similar to previous study using a 3 times bigger voxel. This study shows that metabolism of the mouse dorsal hippocampus, which is one of the most studied structures of the brain, can be assessed *in vivo*.

3970
Computer #39 Measuring Glycolysis versus Oxidative Phosphorylation in Human Sperm by ^{13}C MR Spectroscopy
Steven Reynolds¹, Sarah Calvert², Jack Pearson², Allan Pacey², and Martyn Paley¹

¹Academic unit of radiology, University of Sheffield, Sheffield, United Kingdom, ²Academic Unit of Reproductive and Developmental Medicine, University of Sheffield, Sheffield, United Kingdom

Two main metabolic pathways provide energy for sperm swimming: glycolysis and oxidative phosphorylation, producing different biomarkers, including lactate (glycolysis) and bicarbonate/ CO_2 (Oxphos) that can be detected by MR spectroscopy. By incubating ^{13}C labeled exogenous metabolites with human spermatozoa we identify metabolic pathways and quantify rates of metabolism in spermatozoa. The rate constants for glucose and pyruvate conversion to lactate were estimated as $1.1 \pm 0.5 \times 10^{-6} \text{s}^{-1}$ and $2.4 \pm 1.1 \times 10^{-6} \text{s}^{-1}$ per million sperm respectively (mean \pm SD, n=4). Metabolic pathways used by live sperm were assessed and work is being done to estimate the relative importance of different metabolic activity in sperm of normozoospermic and asthenozoospermic patients.

3971
Computer #40 Towards direct detection of natural abundance glycogen C2-C6 resonances by localized ^{13}C MRS at 7T.
Eulalia Serés Roig^{1,2}, Lijing Xin³, and Rolf Gruetter^{4,5}

¹Laboratory of Functional and Metabolic Imaging (LIFMET), Ecole Polytechnique Fédérale de Lausanne (EPFL), Lausanne, Switzerland, ²Image Guided Interventions Laboratory, Radiology Department, University of Geneva (UNIGE), Geneva, Switzerland, ³Centre d'Imagerie Biomédicale - Animal and Imaging Technology (CIBM-AIT), Lausanne, Switzerland, ⁴Department of Radiology, University of Lausanne (UNIL), Lausanne, Switzerland, ⁵Department of Radiology, University of Geneva (UNIGE), Geneva, Switzerland

Glycogen is the main energy store in the human body, while its concentration is particularly abundant in muscle tissue. *In vivo* ^{13}C MRS is unique for investigating glycogen metabolism, as it allows the non-invasive measurement of natural abundance glycogen C₁ resonance in the human muscle. However, spatial localization is desirable to detect glycogen C₂-C₆ resonances due to their overlap with the glycerol C₂ and C₁, C₃ resonances. In this study, we designed a pulse-acquire sequence for localized ^{13}C MRS using ISIS-1D and OVS schemes. The localization performance of the sequence was validated *in vitro* and *in vivo* in human muscle at 7T.

3972

Computer #41

Comparison of in vivo potassium, chloride and sodium TQ effects at 21.1 T
Victor Schepkin¹, Andreas Neubauer², Armin Nagel³, and Thomas Budinger⁴

¹NHMF/FSU, Tallahassee, FL, United States, ²University of Heidelberg, Mannheim, Germany, ³German Cancer Research Center (DKFZ), Heidelberg, Germany, ⁴Lawrence Berkeley National Laboratory/UCB, Berkeley, CA, United States

A comparison of the TQ MR signals without filtration from three in vivo ions was performed in a rat head at 21.1 T using a time proportional phase increment. A strong and competitive binding of potassium relative to sodium was demonstrated and confirmed using agarose samples. The TQ signal from in vivo chloride was the lowest. Our results support a model that normal cells have similar ion binding in intracellular and extracellular spaces. Visualization of TQ magnetization was demonstrated using matching angular dependence of spherical harmonics and corresponding irreducible tensors.

3973

Computer #42

Does Tempol enter the brain with an unpaired electron?
Miho C Emoto¹, Hideo Sato-Akaba², and Hirotsada G Fujii¹

¹Center for Medical Education, Sapporo Medical University, Sapporo, Japan, ²Osaka University, Osaka, Japan

Nitroxides have unique biochemical properties, and thus they have been used for many biomedical applications. However, although piperidine nitroxide (4-hydroxy-2,2,6,6-tetramethylpiperidin-1-oxyl: Tempol) has been presently tested in clinical trials, details concerning the distribution and kinetics of Tempol in vivo have not been thoroughly studied. In particular, it is not clear whether Tempol enters the brain as paramagnetic materials with an unpaired electron. To examine this matter, electron paramagnetic resonance (EPR) imaging study of mouse brains was conducted using a modified EPR imager. The obtained EPR images clearly showed that Tempol could enter the brain with an unpaired electron.

3974



Computer #43

Comparison of a 30-channel head array with a birdcage for ²³Na MRI at 7 Tesla

Jonathan M. Lommen¹, Frank Resmer², Nicolas G.R. Behl¹, Michael Sauer², Nadia Benkhedah¹, Andreas K. Bitz¹, Reiner Umathum¹, Mark E. Ladd¹, Titus Lanz², and Armin M. Nagel^{1,3}

¹Medical Physics in Radiology, German Cancer Research Center (DKFZ), Heidelberg, Germany, ²Rapid Biomed, Rimplar, Germany, ³Diagnostic and Interventional Radiology, University Medical Center Ulm, Ulm, Germany

A 30 channel Rx array for ²³Na MRI at 7 Tesla is compared with a reference Tx/Rx birdcage. Strong SNR improvement by the array technology is acknowledged and good B₁ homogeneity could be found. Images were reconstructed using der adaptive combine algorithm which provides a near perfect channel combination.

3975

Computer #44

Reconstruction of asymmetrically undersampled high-resolution ²³Na-MRI data after homodyne processing
Nicolas G.R. Behl¹, Peter Bachert¹, Mark E. Ladd¹, and Armin M. Nagel^{1,2}

¹Medical Physics in Radiology, German Cancer Research Center (DKFZ), Heidelberg, Germany, ²Diagnostic and Interventional Radiology, University Medical Center Ulm, Ulm, Germany

Due to the low concentration of ²³Na in the human body, ²³Na-MRI suffers from long acquisition times T_{acq}, especially for high nominal spatial resolutions. In this work we investigated the performance of homodyne data processing prior to the iterative 3D-Dictionary-Learning Compressed Sensing reconstruction (3D-DLCS) for the reconstruction of asymmetrically undersampled radial ²³Na-data, in order to take advantage of the point-symmetry in k-space.

3976

Computer #45

The venous contribution to sodium (²³Na) MRI signals in human brain
Ian D Driver¹, Robert W Stobbe², Richard G Wise¹, and Christian Beaulieu²

¹CUBRIC, School of Psychology, Cardiff University, Cardiff, United Kingdom, ²Department of Biomedical Engineering, University of Alberta, Edmonton, AB, Canada

We show for the first time that venous sodium MRI signals in the human brain are elevated with respect to grey and white matter in vivo. These results have implications for studies using sodium MRI signals to investigate pathologies such as stroke and cancer, with abnormal cerebrovasculature. Observed signal changes in these groups may be partially due to changes in vascular structure, rather than metabolic dysfunction or disruption of cell integrity. Also, potential studies aiming to use sodium MRI for direct detection of neuronal activity will need to account for functional hyperaemia changing the venous sodium signal.

3977

Computer #46

Development and Application of a ²³Na Elliptical Body Coil for 7 Tesla
Tanja Platt¹, Thomas M Fiedler¹, Armin M Nagel^{1,2}, Andreas K Bitz¹, Peter Bachert¹, Mark E Ladd^{1,3}, and Reiner Umathum¹

¹Medical Physics in Radiology, German Cancer Research Center (DKFZ), Heidelberg, Germany, ²Diagnostic and Interventional Radiology, University Medical Center Ulm, Ulm, Germany, ³Erwin L. Hahn Institute for Magnetic Resonance Imaging, University Duisburg-Essen, Essen, Germany

Up to now only a few ²³Na abdominal MRI studies have been performed at 7T. In this work, a versatile ²³Na transceive elliptical-shaped body coil for 7T with a large FOV and a high transmit/receive efficiency was designed, simulated, and implemented on a 7T scanner. The

setup was applied for in-vivo imaging of the human torso. The obtained 3D ^{23}Na image data set contains ^{23}Na signals from heart to pelvis. High regional ^{23}Na signals are especially present in the areas of kidney, liver, cartilage, vessels, vertebral disks, spinal canal, and heart.

- 3978
Computer #47
Standardisation and quantification of ^{23}Na -MRI: repeatability and reproducibility of sodium imaging across two independent sites
Damien J. McHugh^{1,2}, Frank Riemer^{2,3}, Hamied A. Haroon¹, Geoff J.M. Parker^{1,2,4}, and Ferdia A. Gallagher^{2,3}
- ¹Centre for Imaging Sciences, The University of Manchester, Manchester, United Kingdom, ²CRUK & EPSRC Cancer Imaging Centre in Cambridge & Manchester, United Kingdom, ³Department of Radiology, University of Cambridge, Cambridge, United Kingdom, ⁴Bioxydyn Ltd., Manchester, United Kingdom*
- This work investigates the repeatability and reproducibility of total sodium concentration (TSC) estimates in the human brain. Healthy volunteers were scanned twice at two different sites using comparable 3D Cones acquisitions, and region of interest TSC values were compared. Consistent TSC estimates were observed across repeated scans at different sites, and, for robust multi-site comparisons, a need was identified for standardisation of non-Cartesian data reconstruction. These preliminary results provide an initial step in the technical validation of sodium MRI-derived cancer biomarkers.

- 3979
Computer #48
Development of translational simple multinuclear MRI system for ultra high-field
Chang-Hoon Choi¹, YongHyun Ha¹, Pandichelvam Veeraiah¹, Jörg Felder¹, Klaus Möllenhoff¹, and N. Jon Shah^{1,2}
- ¹Institute of Neuroscience and Medicine-4, Research Centre Juelich, Juelich, Germany, ²Faculty of Medicine, Department of Neurology, JARA, RWTH Aachen University, Aachen, Germany*
- Non-proton MRI has recently been of great interest with the increased availability of ultra high-field MRI system. A translational multinuclear MRI system for ^1H , ^{13}C , ^{17}O , ^{19}F , ^{23}Na and ^{31}P was developed using six optimised single-tuned RF resonator sets and implemented at the home-assembled 9.4T small animal MRI scanner. This system demonstrated its capability of identifying the concentration difference and sensitivity of these X-nuclei without signal-to-noise-ratio loss for any nuclei, subject interruption and degrading in the static shim condition.

Electronic Poster

MRS Methods & Applications

Exhibition Hall

Wednesday, May 11, 2016: 14:30 - 15:30

- 3980
Computer #1
Whole body broadband and uniform ^{31}P MRSI with sub-second power calibration at 7T.
Dennis WJ Klomp¹, Joost Löring¹, Joep WM van Oorschot¹, Peter R Luijten¹, and Wybe JM van der Kemp¹
- ¹Radiology, UMC Utrecht, Utrecht, Netherlands*
- We have integrated a body RF coil tuned at the ^{31}P frequency in a 7T MR system that includes pick-up probes for fast and reliable power calibration. With this setup, full body and broadband ^{31}P MRSI can be obtained in single breath-holds. When averaged over less than 5 minutes, excellent ^{31}P spectra can be shown from liver and heart as demonstrated in healthy volunteers.
- 3981
Computer #2
31P MRS Signal-to-Noise Ratio in Human Brain at 3, 7, and 9.4 Tesla Using Dual Tuned Head RF Coils
Marek Chmelik^{1,2}, Diana Bencikova³, Christian Mirkes⁴, Christopher T. Rodgers⁵, Gunamony Shajan⁴, Klaus Scheffler^{4,6}, Siegfried Trattnig^{1,2}, and Wolfgang Bogner¹
- ¹High Field MR Centre, Department of Biomedical Imaging and Image-guided Therapy, Medical University of Vienna, Vienna, Austria, ²Christian Doppler Laboratory for Clinical Molecular MR Imaging, Vienna, Austria, ³Department of Nuclear Physics and Biophysics, Faculty of Mathematics, Physics and Informatics, Comenius University, Bratislava, Slovakia, ⁴High-Field MR Center, Max Planck Institute for Biological Cybernetics, Tuebingen, Germany, ⁵OCMR, RDM Cardiovascular Medicine, University of Oxford, Oxford, United Kingdom, ⁶Department for Biomedical Magnetic Resonance, University of Tuebingen, Tuebingen, Germany*
- The purpose of this study was to quantitatively compare the SNR of brain ^{31}P -MRS coils capable of covering the whole brain at various B_0 field strengths. SNR was compared using phantoms and in vivo in clinically acceptable measurement times at 3T (birdcage), 7T (23ch-array) and 9.4T (27ch-array). Data showed approximately 3-fold higher SNR at 7T than at 3T. 9.4T provided an additional -more than linear- increase. WSVD coil combination outperformed Brown's coil combination. Especially with the 7T coil the necessity of advanced coil combination algorithms is apparent.
- 3982
Computer #3
In vivo comparison of quadrupole splitting of potassium resonance with dipole-dipole splitting of total creatine resonance in proton MR spectroscopy of human calf muscle
Manuela Barbara Rösler^{1,2}, Nicolas G.R. Behl¹, Nadia Benkhedah¹, Armin Michael Nagel^{1,3}, and Reiner Umathum¹
- ¹Medical Physics in Radiology, German Cancer Research Center, Heidelberg, Germany, ²Institute for Biomedical Engineering, University and ETH Zurich, Zurich, Switzerland, ³Diagnostic and Interventional Radiology, University Medical Center Ulm, Ulm, Germany*

Theory predicts that the residual quadrupole interaction of spin-3/2 nuclei with electrical field gradients and the dipole-dipole interaction of coupled spin-1/2 nuclei depend similarly on the angle between the privileged direction and the static magnetic field. In this work, we compare the splitting of the ^{39}K resonance with the splitting of the total creatine resonance in ^1H MR spectroscopy in vivo at human calf muscle. We find similar behavior under variation of the angle between B_0 and tibia. Therefore we conclude that the potassium ions and creatine are located in an equivalent electromagnetic environment.

-
- 3983
Computer #4
Model-based fitting of *in vivo* ^{129}Xe spectra in mice reveals five robust dissolved-phase peaks
Rohan S. Virgincar¹, Scott H. Robertson², Simone Degan³, Geoffrey Schrank⁴, Mu He⁵, John Nouls⁴, and Bastiaan Driehuys⁴
- ¹Biomedical Engineering, Duke University, Durham, NC, United States, ²Medical Physics Graduate Program, Duke University, Durham, NC, United States, ³Center for Molecular and Biomolecular Imaging, Duke University, Durham, NC, United States, ⁴Radiology, Duke University, Durham, NC, United States, ⁵Electrical and Computer Engineering, Duke University, Durham, NC, United States
- Inhaled ^{129}Xe exhibits chemical shifts which carry useful information about the underlying physiology. However, their resonant frequencies have been reported with a variability of 2-3 ppm likely attributable to using simplistic peak finding methods and inconsistent reference frequencies. In this work, we use robust non-linear curve fitting of the complex dissolved-phase spectrum in mice to identify resonances, and report shifts relative to an accurate reference frequency. At short ^{129}Xe replenishment times curve fitting identified two peaks at 197.4 ± 0.9 and 193.0 ± 0.7 ppm, but as replenishment time was increased, five distinct peaks became apparent at 198.4 ± 0.4 , 195.5 ± 0.4 , 193.9 ± 0.2 , 191.3 ± 0.2 , and 190.7 ± 0.3 ppm.
-
- 3984
Computer #5
Dynamic ^1H MRS study of water T_2^* and water concentration contributions to water signal intensity changes in premotor cortex of the norm and in early stage schizophrenia during hemodynamic response to a single stimulus.
Svetlana Sergeevna Batova¹, Andrei Valerievich Manzhurtsev², Maxim Vadimovich Ublinskii^{2,3}, Irina Sergeevna Lebedeva⁴, Tolibjon Abdullaevich Akhadov³, Petr Evgenievich Menshchikov⁵, and Natalia Alexandrovna Semenova^{2,3,5}
- ¹Lomonosov Moscow State University, Moscow, Russian Federation, ²Emanuel Institute of Biochemical Physics of Russian Academy of Sciences, Moscow, Russian Federation, ³Radiology, Scientific Research Institute of Children's Emergent Surgery and Trauma, Moscow, Russian Federation, ⁴Scientific Centre of Mental Health, Moscow, Russian Federation, ⁵Semenov Institute of Chemical Physics of Russian Academy of Sciences, Moscow, Russian Federation
- Using dynamic ^1H MRS we have separated T_2^* and water concentration contributions to changes of MRS detectable water signal in motor cortex after activation by a single short stimulus. We revealed effects of schizophrenia on both parameters in the period of hemodynamic response to stimulation. Decreased changes of T_2^* and water concentration in schizophrenia might reflect a lower vasodilation caused by a single short stimulus.
-
- 3985
Computer #6
Assessment of the glutamatergic activity changes induced by Schizophrenia on rat model: An In Vivo Proton Magnetic Resonance Spectroscopy (^1H MRS) Study at 9.4 T
Chi-Hyeon Yoo^{1,2}, Do-Wan Lee¹, Kyu-Ho Song¹, Song-I Lim^{1,2}, Dong-Cheol Woo², and Bo-Young Choe¹
- ¹Department of Biomedical Engineering, and Research Institute of Biomedical Engineering, The Catholic University of Korea College of Medicine, Seoul, Korea, Republic of, ²Asan Institute for Life Science, Asan Medical Center, Seoul, Korea, Republic of
- To investigate schizophrenia (SZ)-induced effects in the glutamatergic activity on prefrontal cortex of rat, we used proton magnetic resonance spectroscopy (^1H MRS) to estimate the concentration of glutamate (Glu) and glutamine (Gln). With a short echo time (TE) and 9.4 T of our study, Glu, Gln and glutamate-complex (Glx) were reliably quantified with a low Cramer-Raw low bound (CRLB) value, and Glu, Glx showed significant increase. As our results the SZ-induced change in the glutamatergic activity can be reliably detected by ^1H MRS.
-
- 3986
Computer #7
Chronic pain related alterations of regional and interregional glutamate and GABA associations in the human brain
Alexander Gussew¹, Lisa Janetzki², Marianne Cleve¹, Constanze Borys³, and Jürgen Reichenbach¹
- ¹Medical Physics Group, Institute of Diagnostic and Interventional Radiology, Jena University Hospital - Friedrich Schiller University Jena, Jena, Germany, ²Institute of Psychosocial Medicine and Psychotherapy, Jena University Hospital - Friedrich Schiller University Jena, Jena, Germany, ³Department of Psychiatry and Psychotherapy, Jena University Hospital - Friedrich Schiller University Jena, Jena, Germany
- ^1H -PRESS and MEGA-PRESS spectroscopy was performed in anterior cingulate cortex (aCC), insula (Ins) and posterior cortex (PC) of 13 matched pairs of chronic low back pain patients and healthy volunteers to quantify regional and interregional Glx and GABA associations in the resting state. Volunteers had negative correlations between GABA in aCC and Glx in Ins and PC ($\rho < -0.55$) as well as positive correlations between Glx in aCC, Ins and PC ($\rho > 0.65$). In contrast, patients had no any comparable metabolic associations, which may be ascribed to disordered functional pathways between brain regions due to the disease.
-
- 3987
Computer #8
The Influence of Varenicline on Repeated Nicotine-Induced Rats: In Vivo Proton Magnetic Resonance Spectroscopy at 9.4T
Song-I Lim^{1,2}, Kyu-Ho Song¹, Chi-Hyeon Yoo^{1,2}, Dong-Cheol Woo², and Bo-Young Choe¹
- ¹Department of Biomedical Engineering, and Research Institute of Biomedical Engineering, The Catholic University of Korea College of Medicine, Seoul, Korea, Republic of, ²Asan Institute for Life Sciences, Asan Medical Center, Seoul, Korea, Republic of
- Nicotine effects the activation of nicotinic acetylcholine receptors (nAChRs) in multiple areas of the brain. Varenicline is a partial agonist

acting at the $\alpha 4\beta 2$ nAChRs. The purpose of the study is to compare the *in vivo* effects of nicotine and varenicline that contribute to the reward system. The results show the tendency of increased Glu level in nicotine group. Moreover, GSH and NAA levels tended to decrease in the nicotine group. It satisfies that high resolution and short TE component adequately split the overlapped metabolite spectra and quantify the cerebral neurochemicals. We found that varenicline effectively inhibits the reward cycle.

3988
Computer #9 Choline metabolism is reprogrammed differently in mutant IDH1 cells
Pavithra Viswanath¹, Jose Izquierdo-Garcia¹, Larry Cai¹, Joanna Phillips², Russell Pieper², and Sabrina M Ronen¹

¹Radiology, University of California San Francisco, San Francisco, CA, United States, ²Neurological Surgery, University of California San Francisco, San Francisco, CA, United States

Abnormal choline metabolism with increased levels of phosphocholine (PC) driven by overexpression of choline kinase α is considered a hallmark of cancer. For the first time, we show that glioma cells with the IDH1 mutation reprogram choline metabolism differently. Using ¹³C-MRS to quantify [1,2-¹³C]-choline flux to PC in IDH1 mutant cells from two genetically engineered glioma models, we show that reduced PC synthesis is characteristic of mutant IDH1 cells. Furthermore, reduced PC synthesis is driven by down-regulated choline kinase α expression. Our study points to unusual reprogramming of choline metabolism in IDH1 mutant glioma cells, pointing to novel therapeutic opportunities.

3989
Computer #10 Reciprocity based metabolite quantification at 3T
Niklaus Zoelch¹, Andreas Hock^{1,2}, and Anke Henning^{1,3}

¹Institute for Biomedical Engineering, UZH and ETH Zurich, Zurich, Switzerland, ²Department of Psychiatry, Psychotherapy and Psychosomatics, University of Zurich, Zurich, Switzerland, ³Max Planck Institute for Biological Cybernetics, Tuebingen, Germany

At 1.5 T reciprocity principle based quantification strategies have been successfully used to quantify brain metabolites. But these methods all rely on the assumption that the magnitude of the RF transmission field B_1^+ and the reception field B_1^- are equal at all points in the subject. This is not true at higher field strengths and for example differences in the concentrations measured in the left and right hemisphere are observed when these methods are directly applied at higher fields. Here a further development is presented, proposing a correction for deviations of B_1^+ from B_1^- to allow concentration measurements at 3T and even higher field strength without the need of assumptions about concentrations of an internal reference. The obtained metabolite concentrations *in vivo* in 31 healthy volunteers highly agree with values estimated with internal water referencing, demonstrating the capabilities of this new method, which might make concentration measurements in diseased tissue more reliable.

3990
Computer #11 In vivo metabolite quantification using ERETIC with corrections for changes in the RF transmission and reception field
Niklaus Zoelch¹, Andreas Hock^{1,2}, and Anke Henning^{1,3}

¹Institute for Biomedical Engineering, UZH and ETH Zurich, Zurich, Switzerland, ²Department of Psychiatry, Psychotherapy and Psychosomatics, University of Zurich, Zurich, Switzerland, ³Max Planck Institute for Biological Cybernetics, Tuebingen, Germany

With ERETIC (Electric Reference To access In vivo Concentrations) metabolite signals measured *in vivo* are referenced to a signal measured in a phantom while directly correcting for differences in the coil loading conditions between the *in vivo* and *in vitro* measurement. This is beneficial compared to using an internal reference because no assumption about the concentration or the relaxation rate of the internal reference is needed. However in contrast to the signal of an internal reference the ERETIC signal contains no information about B_1 during transmission or reception and changes in B_1 between the *in vivo* and *in vitro* measurement or at different positions are misinterpreted as metabolite concentration changes. The aim of this work was to tackle this problem by incorporating reception sensitivity corrections into the ERETIC method and by using a volume based power optimization to avoid differences during transmission. As a result, the obtained metabolite concentrations agree well with the values obtained with internal water referencing in healthy volunteers.

3991
Computer #12 Using partially suppressed water signal to improve J-edited proton MRS
Zhengchao Dong^{1,2}, Joshua Kantrowitz^{1,2}, and Hong Wang^{1,3}

¹Columbia University, New York, NY, United States, ²New York State Psychiatric Institute, New York, NY, United States, ³Tianjin University, Tianjin, China, People's Republic of

Magnetic field drift and subject motion during J-editing proton MRS scan will not only cause frequency and phase drifts in the spectrum but also alter the linewidth and lineshape. When the linewidths/shapes of edit-on and edit-off spectra do not match, the J-difference spectrum will have residue of Cr peaks; even when edit-on/off spectra match each other, the linebroadening and distortion will deteriorate the quality of the difference spectrum. In this study, we used the partially suppressed water signals to match and to transform the edit-on and edit-off spectra so as to improve the quality of the J-edited spectrum.

3992
Computer #13 Echo-time optimization for J-difference editing of glutathione at 3T
Kimberly L Chan^{1,2,3}, Nicolaas AJ Puts^{2,3}, Karim Snoussi^{2,3}, Ashley D Harris^{2,3,4,5,6}, Peter B Barker^{2,3}, and Richard AE Edden^{2,3}

¹Biomedical Engineering, Johns Hopkins School of Medicine, Baltimore, MD, United States, ²Radiology and Radiological Science, Johns Hopkins School of Medicine, Baltimore, MD, United States, ³F.M. Kirby Center for Functional Brain Imaging, Kennedy Krieger Institute, Baltimore, MD, United States, ⁴Radiology, University of Calgary, Calgary, AB, Canada, ⁵Hotchkiss Brain Institute and Alberta Children's Hospital Research Institute, University of Calgary, Calgary, AB, Canada, ⁶CAIR Program, Alberta Children's Hospital Research Institute, University of Calgary, Calgary,

AB, Canada

Glutathione is involved in maintaining redox balance, and can be detected in vivo in brain tissue using MEGA-PRESS editing. In literature to-date, echo times from 68 to 131 ms have been stated as optimal; in this abstract, the TE-dependence of MEGA-edited GSH signals is investigated using simulations, and phantom and in vivo experiments. It is shown that, in vivo, there is a moderate (15%) benefit of detecting GSH at TE 120 ms over 68 ms. We also demonstrate that the longer echo time allows the use of higher-bandwidth, more rectangular slice-selective refocusing pulses, giving a further 57% gain in signal.

3993

Computer #14 Post acquisition frequency correction in GABA editing
Jan Willem van der Veen¹, Stefano Marengo², Karen Berman², and Jun Shen¹

¹Magnetic Resonance Spectroscopy Core, NIH, NIMH, Bethesda, MD, United States, ²NIH, NIMH, CTNB, Bethesda, MD, United States

Patient motion and magnetic field drift may shift the frequency of the GABA editing pulse relative to that of metabolites. Using the frequency location of the residual water we corrected for changes caused by frequency variations by using averaged reference signals simulated at specific editing frequency offsets. Our analysis also showed that GABA editing with a top-hat editing pulse is highly robust in the presence of frequency variations.

3994

Computer #15 Macromolecule Suppressed GABA Editing using MEGA-SPECIAL Sequence with Spectral-spatial RF Pulse
Meng Gu¹, Adam Kerr², Ralph Hurd³, and Daniel Spielman¹

¹Radiology, Stanford University, Stanford, CA, United States, ²Electrical Engineering, Stanford University, Stanford, CA, United States, ³GE Healthcare, Menlo Park, CA, United States

MEGA PRESS has been used to edit the GABA resonance at 3ppm. Due to the wide transition bandwidth of the editing pulse, macromolecule resonances are coedited. To suppress macromolecule signals, a symmetric suppression method has been proposed resulting in reduced GABA signal. We present a new editing method by incorporating spatial and spectral selectivity into the SPECIAL refocusing RF pulses to achieve both GABA editing and macromolecule suppression. Phantom studies showed higher edited GABA signal compared with MEGA PRESS and 90% macromolecule suppression. In-vivo studies demonstrated significantly higher edited GABA signal compared with MEGA PRESS.

3995

Computer #16 Dual J-difference editing of glutathione and lactate at 3T
Kimberly L Chan^{1,2,3}, Karim Snoussi^{2,3}, Richard AE Edden^{2,3}, and Peter B Barker^{2,3}

¹Biomedical Engineering, Johns Hopkins School of Medicine, Baltimore, MD, United States, ²Radiology and Radiological Science, Johns Hopkins School of Medicine, Baltimore, MD, United States, ³F.M. Kirby Center for Functional Brain Imaging, Kennedy Krieger Institute, Baltimore, MD, United States

Glutathione (GSH), a redox metabolite, and lactate, a product of anaerobic energy metabolism, can both be detected in the human brain using J-difference editing. Editing each will usually co-edit the other to some degree, as the GSH editing target spin is at 4.56 ppm and the lactate spin is at 4.1 ppm. In this abstract, we investigate optimal simultaneous detection of both metabolites, using a combination of simulations, and phantom and in vivo experiments. We demonstrate a new acquisition protocol applying 10 ms editing pulses at 4.35 ppm, which successfully edits both GSH and lactate signals with near maximal efficiency.

3996

Computer #17 J-Difference Editing of 2-Hydroxyglutarate
Kimberly L Chan^{1,2,3}, Richard AE Edden^{2,3}, and Peter B Barker^{2,3}

¹Biomedical Engineering, Johns Hopkins School of Medicine, Baltimore, MD, United States, ²Radiology and Radiological Science, Johns Hopkins School of Medicine, Baltimore, MD, United States, ³F.M. Kirby Center for Functional Brain Imaging, Kennedy Krieger Institute, Baltimore, MD, United States

2-hydroxyglutarate (2HG) is formed in some brain tumors due to a mutation of isocitrate dehydrogenase (IDH), and is becoming an important biomarker for tumor classification. Various approaches have been proposed for the in vivo measurement of 2HG using MR spectroscopy, including spectral-editing using the MEGA-PRESS technique. This abstract investigates 2HG editing at 3T using density-matrix simulations and phantom experiments. It is demonstrated that MEGA-PRESS detection of 2HG is best performed at an echo time of 100 ms, applying editing pulses to the 1.9 ppm spins and detecting the 4.0 ppm signal, and employing high-bandwidth refocusing pulses.

3997

Computer #18 Volumetric Navigated MEGA-SPECIAL for real-time zero- and first-order shim and motion corrected GABA MRS
Muhammad Gulamabbas Saleh¹, Jamie Near², A Alhamud¹, Lindie du Plessis¹, André J.W. van der Kouwe³, and Ernesta M Meintjes¹

¹Human Biology, MRC/UCT Medical Imaging Research Unit, University of Cape Town, Cape Town, South Africa, ²Douglas Mental Health University Institute and Department of Psychiatry, McGill University, Montreal, QC, Canada, ³Athinoula A. Martinos Center for Biomedical Imaging, Massachusetts General Hospital, Charlestown, MA, United States

During macromolecule (MM) suppressed GABA MRS acquisition, subject motion may cause the spectra to be acquired at an incorrect region of interest and with suboptimal shim. Furthermore, effective MM-suppression requires the editing pulses to be applied consistently at 1.7 ppm, necessitating real-time frequency updates, which can be exacerbated in the presence of motion. We

demonstrate that a pair of 3D EPI volumetric navigators acquired once per TR is able to perform accurate motion and magnetic field inhomogeneity correction in real time during MM-suppressed MEGA-SPECIAL GABA MRS.

3998
Computer #19 Simultaneous MEGA-PRESS editing of valine and lactate
Thomas Lange¹, Cheng-Wen Ko², Shang-Yueh Tsai³, Martin Buechert⁴, and Ping-Hong Lai⁵

¹Medical Physics, Department of Radiology, University Medical Center Freiburg, Freiburg, Germany, ²Dept. of Computer Science and Engineering, National Sun Yat-sen University, Kaohsiung, Taiwan, ³Graduate Institute of Applied Physics, National Chengchi University, Taipei, Taiwan, ⁴Magnetic Resonance Development and Application Center, University Medical Center Freiburg, Freiburg, Germany, ⁵Dept. of Radiology, Veterans General Hospital Kaohsiung, Kaohsiung, Taiwan

The MEGA-PRESS sequence allows difference editing of J-coupled metabolites on the basis of their specific coupling behavior. In this work, we demonstrate MEGA-PRESS editing of valine and lactate from a large background of lipid signal. Exploiting the very similar J-coupling constants of valine and lactate, it is demonstrated that both metabolites can be edited simultaneously with an echo time of 142 ms, allowing an editing efficiency of 100% with negligible lipid co-editing. Simultaneous valine/lactate editing is validated in vitro and successfully demonstrated in one brain abscess patient. The method may prove clinically useful for distinguishing brain abscesses from brain tumors.

3999
Computer #20 Optimized B1-robust Outer Volume Suppression for MR Spectroscopy
Martin A Janich¹, Ralph Noeske², Timo Schirmer¹, and Rolf F Schulte¹

¹GE Global Research, Munich, Germany, ²GE Healthcare, Potsdam, Germany

Outer Volume Suppression (OVS) applied to MR spectroscopy improves voxel localization and suppresses undesired signals. Goal of this work was the numerical optimization of a train of broadband SLR pulses for B₁-robustness and T₁ effects and its application to PRESS in the human brain at 3T. The technique improved localization and better suppressed subcutaneous fat at around 1.5ppm in MRS voxels close to the scalp.

4000
Computer #21 Quantitative Imaging of ATP Production Rates and their Functional Changes in Healthy Human Brain
Xiao-Hong Zhu¹, Byeong-Yeul Lee¹, and Wei Chen¹

¹CMRR, Radiology Department, University of Minnesota, Minneapolis, MN, United States

We established a practical protocol for quantitatively imaging the cerebral metabolic rates of ATP production via ATPase and creatine kinase (CK) reactions in human brain at 7T using three dimensional (3D) chemical shift imaging (CSI) and *in vivo* ³¹P MR spectroscopy (MRS) in combine with magnetization transfer (MT) approach. Subsequently, we applied this 3D ³¹P-MT imaging protocol to quantify the regional phosphorous metabolites concentrations, ATPase and CK reaction rate constants and fluxes and the intracellular pH in human brain at rest and during visual stimulation. The results of this study provide the values of key parameters relevant to ATP metabolism in absolute scale, which allow quantitative evaluation of regional cerebral energetics in resting human brain and its functional changes.

4001
Computer #22 CSF fraction calculation for single voxel spectroscopy: comparison of water signal T2 biexponential fitting and image segmentation in a pediatric population
Frances C Robertson¹, Martha J Holmes¹, Francesca Little², Mark F Cotton³, Els Dobbels³, Andre JW van der Kouwe^{4,5}, Barbara Laughton³, and Ernesta M Meintjes¹

¹Department of Human Biology, University of Cape Town, Cape Town, South Africa, ²Department of Statistical Sciences, University of Cape Town, Cape Town, South Africa, ³Department of Paediatrics & Child Health, Stellenbosch University, Stellenbosch, South Africa, ⁴A.A. Martinos Centre for Biomedical Imaging, Massachusetts General Hospital, Charlestown, MA, United States, ⁵Department of Radiology, Harvard Medical School, Boston, MA, United States

For partial volume correction in ¹H-MRS the voxel fraction of brain matter (BM) and cerebral spinal fluid (CSF) can be calculated via biexponential fitting of T2 relaxation of the unsuppressed water signal or via segmentation of a high-resolution structural image. We compared voxel CSF percentages obtained using these two methods and investigated whether discrepancies could be explained by head movement between voxel positioning and MRS acquisition. Subjects with large differences in CSF% between methods tended to show greater displacement than those with no difference between methods. Inconsistencies may be due to segmentation inaccuracy in particular regions or subject motion.

4002
Computer #23 Rotation optimization for semi-LASER implementation under the constraint of maximum gradient strength
Ralph Noeske¹

¹GE Healthcare, Potsdam, Germany

The semi-LASER sequence is less prone to chemical shift displacement errors and shows higher B₁-robustness compared to PRESS. To achieve short echo times high amplitude crusher gradients are used to suppress unwanted coherence signals. Goal of this work was to implement an algorithm that prevents violation of gradient strength constraints due to unrestricted rotation of the voxel while optimizing for shortest possible echo time.

4003
Computer #24 Hepatic lipid metabolite changes in high-fat diet induced liver steatosis model by in vivo 1H-MRS at 9.4T
Joo-Yeon Kim¹, Yeong-Jae Jeon^{1,2}, Sang-Woo Kim^{1,2}, and Hyeon-Man Baek^{1,2}

¹Bioimaging Reseach Team, Korea Basic Science Institute, Ochang, Korea, Republic of, ²Bio-Analytical Science, University of Science and Technology, Ochang, Korea, Republic of

The aim of this study was to characterize hepatic lipid metabolites changes in high-fat diet induced liver steatosis model using in vivo 1H-MRS. MR imaging an single-voxel 1H-MRS was performed using a PRESS sequence at 9.4T. Significant increase in lipid signals at 0.9, 1.3, 2.1, 2.3, 2.8, 4.1, 4.3, and 5.3 ppm was found in mice with high-fat diet ($p < 0.001$). TL, TUB, UI, and Cho were increased with high-fat diet. Therefore, 1H-MRS is useful in detecting and characterizing various hepatic lipid alterations at early phase in mouse liver steatosis prior to development of fibrosis.

Electronic Poster

MRS Applications

Exhibition Hall

Wednesday, May 11, 2016: 14:30 - 15:30

4004
Computer #73 On the composition of Glx in MEGA-PRESS measurements at 3T, is it glutamate?
Tamar M van Veenendaal^{1,2}, Walter H Backes^{1,2}, Richard AE Edden^{3,4}, Nicholaas AJ Puts^{3,4}, Dominique M Ijff^{2,5}, Albert P Aldenkamp^{2,5}, and Jacobus FA Jansen^{1,2}

¹Radiology and Nuclear Medicine, Maastricht University Medical Center, Maastricht, Netherlands, ²School for Mental Health and Neuroscience, Maastricht University, Maastricht, Netherlands, ³Russel H. Morgan Department of Radiology and Radiological Science, Johns Hopkins University, Baltimore, MD, United States, ⁴F.M. Kirby Center for Functional Brain Imaging, Kennedy Krieger Institute, Baltimore, MD, United States, ⁵Epilepsy Center Kempenhaeghe, Heeze, Netherlands

Some authors claim that the 3.7 ppm Glx peak, measured with MEGA-PRESS, constitutes predominantly glutamate. This claim was tested measuring nine phantoms with different glutamate, glutamine, and GABA concentrations using a MEGA-PRESS sequence on a 3T MR scanner. The spectra were analyzed with Gannet (to measure the Glx peak) and LCModel (as an alternative approach). The results show that both glutamate and glutamine attribute to the Glx peak, but that an exclusive estimation of glutamate and glutamine is possible by using LCModel for analysis.

4005
Computer #74 The anterior cingulate cortex GABA levels with varied tissue composition measured by in vivo single voxel MRS
Meining Chen¹, Gaiying Li¹, Zhuwei Zhang¹, Luguang Chen¹, Mengchao Pei¹, Xu Yan², and Jianqi Li¹
¹Shanghai Key Laboratory of Magnetic Resonance and Department of Physics, East China Normal University, Shanghai, China, People's Republic of, ²MR Collaboration NE Asia, Siemens Healthcare, Shanghai, China, People's Republic of

Owing to relatively low concentration of GABA in the brain, a large voxel size is normally applied in MRS to achieve a high signal-to-noise ratio, but with combined signal from white matter, gray matter and cerebrospinal fluid. The tissue contribution in GABA measurement remains to be resolved. GABA levels from three closely adjacent voxels with varied tissue composition in the anterior cingulate cortex were acquired by using MEGA-PRESS. GABA level was found to be significantly higher in gray matter than in white matter.

4006
Computer #75 Quadrature ³¹P and single ¹H dual-tune coil for cardiac ³¹P-MRS at 7T
Benoit Schaller¹, Watcharaphol Paritmongkol¹, Arthur W Magill², Matthew D Robson¹, and Christopher T Rodgers¹
¹RDM Cardiovascular Medicine, University of Oxford, OXFORD, United Kingdom, ²Institute of Neuroscience and Medicine - 4, Forschungszentrum Juelich GmbH, Juelich, Germany

Phosphorus spectroscopy is a powerful tool for cardiac metabolism studies. Working at 7T gives a significant (2.8x) gain in SNR compared to 3T. However, with existing RF coils, it is hard to excite the heart uniformly and with sufficient peak B₁₊. In this work we simulated 8 candidate coil designs and identified the best one for cardiac ³¹P-MRS. We built this quadrature pair of 15cm loops for ³¹P and a single 10cm loop for ¹H, decoupled with LCC traps, performed safety tests, validated its B₁₊ in phantoms and recorded spectra in vivo in the human leg, liver and heart.

4007
Computer #76 Metabolite diffusion up to very high b in the mouse brain in vivo: revisiting the correlation between relaxation and diffusion properties
Clemence Ligneul^{1,2}, Marco Palombo^{1,2}, and Julien Valette^{1,2}

¹CEA/DSV/I2BM/MIRcen, Fontenay aux Roses, France, ²CNRS Université Paris-Saclay UMR 9199, Fontenay aux Roses, France

Diffusion-weighted magnetic resonance spectroscopy is performed in a large voxel in the mouse brain at two diffusion times, up to very high b-values. We combine different echo times and mixing times to investigate the potential interplay between relaxation properties and diffusion attenuation. Under current experimental conditions, we don't observe any significant dependence of metabolite diffusion properties on TE/TM, except for water (and possibly NAA at very high b-values), which supports the interpretation and modeling of metabolite diffusion based primarily on geometry, irrespective of relaxation properties.

- 4008
Computer #77 MEGA-PRESS Single-voxel Spectroscopy for GABA J-editing with Real-time Frequency Adjustment
Sinyeob Ahn¹, Tongbai Meng², Dieter J Meyerhoff^{3,4}, and Gerhard Laub¹
- ¹Siemens Healthcare, San Francisco, CA, United States, ²Siemens Healthcare, Baltimore, MD, United States, ³Radiology and Biomedical Imaging, UCSF, San Francisco, CA, United States, ⁴CIND, Veterans Affairs Medical Center, San Francisco, CA, United States
- Spectroscopy scan is highly sensitive to frequency drift during the acquisition. Although most spectroscopy sequences do not create large frequency drift themselves, it is problematic when they are run immediately after sequences with high gradient duty-cycle, as the frequency still drifts due to gradient cooling. In this paper, realtime frequency adjustment was implemented for MEGA-PRESS sequence for GABA J-editing. FID signal was read during water suppression and used to calculate and update the system frequency every TR cycle. It was tested on a phantom and in vivo and showed effectiveness by providing insensitivity to the frequency drifts during the acquisition.
-
- 4009
Computer #78 Toolbox for automatic localization of volume of interest in MRS (ALLVOI)
Po-Yu Peng¹, Shang-Yueh Tsai^{2,3}, and Yi-Ru Lin¹
- ¹Electronic and Computer Engineering, National Taiwan University of Science and Technology, Taipei, Taiwan, ²Graduate Institute of Applied Physics, National Chengchi University, Taipei, Taiwan, ³Research Center for Mind, Brain and Learning, National Chengchi University, Taipei, Taiwan
- Magnetic Resonance Spectroscopy (MRS) data were usually acquired with single voxel spectroscopy techniques (SVS), which is used to access metabolites concentrations from a predefined volume of interest (VOI). Currently, MRS has been linked to fMRI studies to access metabolic information. Therefore, it's important to define the VOI on standard space (template) and transform the predefined VOI from standard space to subject space for each MRS scan. In this study, we developed a tool to guide the definition of VOI on template before MRS scan then automatically calculate VOI in subject space.
-
- 4010
Computer #79 Downfield spectra of human brain obtained with and without water suppression at 9.4T
Nicole D Fichtner^{1,2}, Ioannis Giapitzakis³, Nikolai Avdievich³, Anke Henning^{2,3}, and Roland Kreis¹
- ¹Depts. Radiology and Clinical Research, University of Bern, Bern, Switzerland, ²Institute for Biomedical Engineering, UZH and ETH Zurich, Zurich, Switzerland, ³Max Planck Institute for Biological Cybernetics, Tuebingen, Germany
- Ultra high field strengths offer the benefit of higher signal to noise ratio as well as improved separation of metabolites in spectroscopy, which is beneficial for evaluating downfield peaks. In the current work, the metabolite cycling technique is implemented at 9.4T in order to evaluate the downfield part of the human brain spectrum. The 9.4T spectra confirm the 3T findings on exchanging peaks, and indicate that the higher field strength improves metabolite separation, allowing for better quantification of exchanging peaks, which is also of great interest for chemical exchange dependent saturation transfer experiments.
-
- 4011
Computer #80 1H MRS of gray and white matter in the human brain using B0 Adjusted Sensitivity Encoded Spectral Localization by Imaging (BASE-SLIM)
Peter Adany¹, Phil Lee^{1,2}, and In-Young Choi^{1,2,3}
- ¹Hoglund Brain Imaging Center, University of Kansas Medical Center, Kansas City, KS, United States, ²Department of Molecular & Integrative Physiology, University of Kansas Medical Center, Kansas City, KS, United States, ³Department of Neurology, University of Kansas Medical Center, Kansas City, KS, United States
- Reliable localization of ¹H MRS in gray and white matter of the human brain was achieved using the BASE-SLIM technique. Distinctive spectral patterns of gray and white matter were measured from all subjects using BASE-SLIM, which were consistent with those measured in both tissue types using single-voxel ¹H MRS. BASE-SLIM spectroscopy promises 1) accurate and robust acquisition of MR spectra from gray and white matter with minimum cross contamination from other compartments, 2) shorter scan time and 3) flexibility in compartmental shapes that match anatomical structures.
-
- 4012
Computer #81 Parameter optimization for reproducible cardiac 1H-MR Spectroscopy at 3 T
Paul de Heer¹, Maurice B Bizino², Hildo J Lamb², and Andrew G Webb¹
- ¹CJ Gorter Center, Radiology, Leiden University Medical Center, Leiden, Netherlands, ²Radiology, Leiden University Medical Center, Leiden, Netherlands
- Cardiac proton MR spectroscopy is a challenging technique to perform in a reliable manner. In this study data acquisition parameters are optimized in terms of signal-to-noise and reproducibility. The optimal protocol was determined to be a PRESS localized scan, local power optimization, pencil beam B0 shimming, a cardiac trigger delay of 200 ms, MOIST water suppression and pencil beam navigator-based respiratory compensation. With these parameters high intra- ($r=1.000$, $p<0.0001$) and inter- ($r=1.000$, $p=0.0004$) session reproducibilities were achieved. Bland-Altman analysis showed limits of agreement from -0.11 to 0.04 (intra) and -0.15 to 0.9.
-
- 4013
Computer #82 Potential of NMR metabonomics of Small Intestinal Mucosa in assessing Marsh Grade in patients with Celiac Disease
Deepti Upadhyay¹, Uma Sharma¹, Govind Makharia², Prasenjit Das³, Siddharth Datta Gupta³, and Naranamangalam R Jagannathan¹
- ¹Department of NMR & MRI Facility, All India Institute of Medical Sciences, New Delhi, India, ²Department of Gastroenterology and human Nutrition, All India Institute of Medical Sciences, New Delhi, India, ³Department of Pathology, All India Institute of Medical Sciences, New Delhi, India

This study illustrates the potential of proton NMR based metabonomics in determining biomarkers for assessing severity of villous abnormality in patients with celiac disease (CeD). CeD patients with Grade 3c showed significantly higher concentration of pyruvate, alanine and succinate compared to Grade 3b patients, suggesting more impaired oxidative phosphorylation in Grade 3c compared to Grade 3b patients. Increased acetoacetate in Grade 3c compared to Grade 3b patients indicated utilization of ketone bodies by intestinal mucosa for energy generation. Higher level of creatine seen in Grade 3c patients may probably be related to increased intestinal dysbiosis compared to Grade 3b patients.

-
- 4014
Computer #83 ¹H-MRS ultra-long echo time PRESS detects omega-3 fatty acids *in vivo* at 7T
Martin Gajdošík^{1,2}, Lukas Hingerl¹, Petr Šedivý³, Miloslav Drobný³, Monika Dezortová³, Michael Krebs⁴, Siegfried Trattnig^{1,2}, Wolfgang Bogner¹, and Martin Kržšák^{1,2,4}
- ¹High-field MR Centre, Department of Biomedical Imaging and Image-guided Therapy, Medical University of Vienna, Vienna, Austria, ²Christian Doppler Laboratory for Clinical Molecular MR Imaging, Vienna, Austria, ³MR Unit, Institute for Clinical and Experimental Medicine, Prague, Czech Republic, ⁴Division of Endocrinology and Metabolism, Department of Internal Medicine III, Medical University of Vienna, Vienna, Austria*
- Omega-3 (n-3) fatty acids are essential to human health. However, the knowledge about their tissue concentrations is not well established. The spectral dispersion at 7T yields a sufficient spectral separation of n-3 (n-3 CH₃) and non n-3 methyl (CH₃) groups. Large differences in the T₂ relaxation and J-modulation of outer triplet lines allowed for excellent separation of the n-3 CH₃ signal and for estimation of its relative concentration in adipose tissue for the detection by ¹H MR PRESS with TE of 1000ms.
-
- 4015
Computer #84 Broadband NOE for 7T 31-Phosphorous MRS of Human Brain
Shizhe Steve Li¹, Li An¹, Maria Ferraris Araneta¹, Christopher Johnson¹, and Jun Shen¹
- ¹National Institute of Mental Health, National Institutes of Health, Bethesda, MD, United States*
- To further increase SNR of 7T Phosphorus (³¹P) MRS in human brain, Nuclear Overhauser Effect (NOE) has been utilized where WALTZ waveform was often applied during relaxation time with low RF peak power and long pulse width with inherent narrow bandwidth. At higher field with larger chemical shift dispersion of the protons, broadband saturation of protons is desirable. This study demonstrated the feasibility of broadband NOE at 7 Tesla for ³¹P MRS of human brain.
-
- 4016
Computer #85 Using Proton MR Spectroscopy and Quantitative Susceptibility Mapping (QSM) at 7 Tesla to Decipher Mitochondrial Membrane Protein-Associated Neurodegeneration (MPAN)
Ralf Mekte¹, Florian Schubert¹, Thoralf Niendorf², Till Huelnhagen², Antje Else², Simon Daniel Robinson³, Bernd Ittermann¹, Vince Madai⁴, Marta Skowronska⁵, Petr Dusek^{6,7}, Jens Wuerfel⁸, and Susanne A. Schneider⁹
- ¹Physikalisch-Technische Bundesanstalt (PTB), Braunschweig and Berlin, Germany, ²Berlin Ultrahigh Field Facility (B.U.F.F.), Max Delbrück Center for Molecular Medicine in the Helmholtz Association, Berlin, Germany, ³High Field MR Centre, Department of Biomedical Imaging and Image-guided Therapy, Medical University of Vienna, Vienna, Austria, ⁴Department of Neurology and Center for Stroke Research Berlin, Charité Universitaetsmedizin, Berlin, Germany, ⁵2nd Department of Neurology, Institute of Psychiatry and Neurology, Warsaw, Poland, ⁶Department of Neurology and Centre of Clinical Neuroscience, First Faculty of Medicine and General University Hospital in Prague, Charles University in Prague, Prague, Czech Republic, ⁷Institute of Neuroradiology, University Medicine Goettingen, Goettingen, Germany, ⁸Medical Image Analysis Center, Basel, Switzerland, ⁹Neurology Department, University of Kiel, Kiel, Germany*
- ¹H MR spectroscopy (MRS) in the white matter (WM) of the precentral region and quantitative susceptibility mapping (QSM) of basal ganglia acquired at 7 Tesla in patients (homozygotes), non-manifesting heterozygotes, and control subjects were used to investigate mitochondrial membrane protein-associated neurodegeneration (MPAN). MPAN is a rare, but severe disorder from the neurodegeneration with brain iron accumulation (NBIA) group. Comparison of results for the different subject groups showed no abnormalities in heterozygotes. In contrast, metabolic changes in patients detected by MRS, in particular an increase in glutamate, suggests an underlying mechanism for MPAN related to neurotransmission in corticospinal pathway.
-
- 4017
Computer #86 Investigating the effects of decoupling on *in vivo* 13C MRS to optimize acquisition in glycogen studies
Stephen Bawden^{1,2}, Paul Glover¹, Peter Morris¹, Guruprasad Aithal², and Penny Gowland¹
- ¹Sir Peter Mansfield Imaging Centre, University of Nottingham, Nottingham, United Kingdom, ²NIHR Nottingham Digestive Diseases Research Unit, University of Nottingham, Nottingham, United Kingdom*
- In this study the decoupling efficiency of *in vivo* 13C MRS measurements of glycogen levels was assessed. Due to SAR restrictions and surface coil decoupling field inhomogeneity, this study showed that short TR coupled spectroscopy provides improved SNR and better defined spectral parameters for fitting, whereas decoupled spectra reduces the number of averages in the same timeframe and runs the risk of varying residual coupling constants across a large field of view with inhomogeneous B₂
-
- 4018
Computer #87 Longitudinal relaxation time editing for acetylcarnitine detection with 1H-MRS
Lucas Lindeboom^{1,2}, Yvonne M.H. Bruls^{1,2}, Petronella A. van Ewijk¹, Matthijs K.C. Hesselink², Joachim E. Wildberger¹, Patrick Schrauwen², and Vera B. Schrauwen-Hinderling^{1,2}
- ¹Radiology, Maastricht University Medical Center, Maastricht, Netherlands, ²Human Biology and Human Movement Sciences, Maastricht*

The use of a long TE enables detection of acetylcarnitine with ^1H -MRS. However, in (very) obese subjects, suppression of overlapping lipid resonances becomes problematic, even with long TE. We here show short T_1 metabolites, such as lipids, can additionally be suppressed with a new T_1 editing approach.

-
- 4019
Computer #88
- Kinetic modelling of hyperpolarized ^{13}C -pyruvate metabolism in Canines using a model-based input function
Nikolaos Dikaaios¹, Shonit Punwani¹, Henrik Gutte², Majbrit ME Larsen³, Annemarie T Kristensen³, Andreas Kjær², David Atkinson⁴, and Adam E Hansen²
- ¹Centre of Medical Imaging, UCL, London, United Kingdom, ²Nuclear Medicine & PET and Cluster for Molecular Imaging, Rigshospitalet, University of Copenhagen, Copenhagen, Denmark, ³Department of Veterinary Clinical and Animal Sciences, Faculty of Health and Medical Sciences, University of Copenhagen, Copenhagen, Denmark, ⁴Centre for Medical Imaging, UCL, London, United Kingdom*
- Mathematical models based on kinetic parameters allow us to investigate ^{13}C -pyruvate metabolism. Metabolic exchanges between pyruvate and its metabolites can differentiate benign from malignant tissue but their quantification is limited by the estimation of the arterial input function (AIF). This work suggests to model the AIF using a Gaussian pdf to account for the time pyruvate needs to travel and dispersion effects. The proposed AIF fits the measured data better than the commonly used box-car AIF, and is in agreement with the model-free formalism which approximates the kinetics using the ratios of AUC of the injected and product metabolites.
-
- 4020
Computer #89
- Visualizing lactate in the ischemic hindleg of mice using localized proton 2D correlation spectroscopy (UHF-P-COSY) at ultrahigh field.
Devashish Das¹, Andor Veltien¹, and Arend Heerschap¹
- ¹Radiology, Radboud University Nijmegen, Nijmegen, Netherlands*
- Lactate is associated with mitochondrial and neuromuscular diseases. Therefore, its methylene (CH₂) and methyl (CH₃) proton assignment is necessary in the skeletal muscle. In particular for understanding mechanisms associated with the skeletal muscle ischemia in rodents. Unambiguous detection of lactate resonances in the ischemic and/or hypoxic rodent muscle remains challenging, however, necessary for the assessment of treatment in the dysfunctional muscle of transgenic animals. *In vivo* lactate resonances remain hidden under lipid pool. However, by tuning spinecho delays in the localized 2D proton correlation sequence we are able to separate lactate CH₂ and CH₃ protons from the lipid resonances in the F1 dimension of the 2D-spectrum.
-
- 4021
Computer #90
- Study of MS Tissue Injury and Repair with In Vivo MR Spectroscopy of Lipids and Proteins - First Results
Christoph Juchem¹, Hetty Prinsen¹, Kevin L Behar¹, Robert K Fulbright¹, and Douglas L Rothman¹
- ¹Yale University, New Haven, CT, United States*
- Altered lipid and protein contents have been detected with MR spectroscopy in acute multiple sclerosis lesions and speculated to reflect de- and remyelination processes. To date, however, neither the metabolites involved nor their pathological relevance have been satisfactorily described. Hofmann et al. introduced an elegant concept for the separation of biochemicals of varying metabolic weight based on differences in T₁ relaxation behavior (MRM 46, 2001). Here, we describe T₁-encoded MR spectroscopy at 7 Tesla, the extraction of individual, spectroscopically overlapping lipid/protein signals by two-dimensional processing and initial applications to the study of the pathological processes associated to multiple sclerosis tissue injury and repair.
-
- 4022
Computer #91
- Metabolic profiling of normal hepatocyte and hepatocarcinoma cell lines related to metastasis potentials by ^1H NMR spectroscopy and chemometrics
Yang Chen¹, Jianghua Feng¹, Naishun Liao², Ying Su³, Changyan Zou³, and Zhong Chen¹
- ¹Department of Electronic Science, Xiamen University, Xiamen, China, People's Republic of, ²The United Innovation of Mengchao Hepatobiliary Technology Key Laboratory of Fujian Province, MengChao Hepatobiliary Hospital of Fujian Medical University, Fuzhou, China, People's Republic of, ³Laboratory of Radiobiology, Fujian Provincial Tumor Hospital, Fuzhou, China, People's Republic of*
- To explore metabolic characteristics of hepatocarcinoma cell lines associated with different metastasis potentials, ^1H NMR-based metabolomics conjugated with multivariate statistical analysis were performed to determine the molecular mechanisms of metastasis. Characteristic metabolites from both cell extracts and cultured medium were identified. Our results provide evidences that cells with different metastasis potentials exhibit different levels of glucose consumption, as well as the products of some intermediates of glycolysis.
-
- 4023
Computer #92
- Simultaneous absolute quantitation of glutamate and GABA on highly resolved 2D constant time PRESS spectra using 2D FT with shared time domain data
Hidehiro Watanabe¹ and Nobuhiro Takaya¹
- ¹Center for Environmental Measurement and Analysis, National Institute for Environmental Studies, Ibaraki, Japan*
- Absolute quantitation framework on highly resolved 2D CT-PRESS spectra with ^1H decoupling was proposed for measurement of concentration of glutamate and GABA. Although peaks of these metabolites are clearly resolved on the spectra, long constant time delay (T_{cd}) requires T_2 correction. To overcome this, we proposed a fast T_2 correction method using 2D FT with shared time domain data. After curve fitting of series of spectra with varied T_{cd} 's, we obtained series of peak volumes that can be expressed as an exponential decay of

T₂. In phantom experiments, we could measure the concentrations of glutamate and GABA by our method.

-
- 4024
Computer #93
- Localized in-phase one-dimensional proton MRS
Liangjie Lin¹, Yanqin Lin¹, Zhiliang Wei¹, and Zhong Chen¹
- ¹*Electronic science, Xiamen University, Xiamen, China, People's Republic of*
- Magnetic resonance spectroscopy (MRS) is a powerful noninvasive tool in diagnoses, progressive monitoring, and studies of disease states of humans and animals. In this study, we present a MRS pulse sequence for localized one-dimensional in-phase proton MRS. The proposed pulse sequence can be utilized to reduce undesired broad resonances with short T₂s and increasing signal intensity of *J* coupling metabolites. Moreover, it provides an approach of direct measurement of non-overlapping *J* coupling peaks at achievable arbitrary TEs and of their transverse relaxation times (T₂).
-
- 4025
Computer #94
- Grey and white matter signal separation in the single voxel NMR spectroscopy at 7T
Donghyun Hong¹, Jack JA van Asten², Seyedmorteza Rohani Rankouhi¹, Jan-Willem Thielen¹, and David G. Norris^{1,3}
- ¹*Erwin L. Hahn Institute for Magnetic Resonance Imaging, University of Duisburg-Essen, Essen, Germany*, ²*Department of Radiology and Nuclear Medicine, Radboud University Medical Center, Nijmegen, Netherlands*, ³*Donders Institute for Brain, Cognition and Behavior, Radboud University, Nijmegen, Netherlands*
- GABA spectroscopy has two potential confounds widely ignored by the spectroscopic community: 1) a potential 5-10Hz frequency shift between grey and white matter shown in imaging experiment and 2) the fact that the GABA is circa 9 times more concentrated in grey matter. To investigate whether these confounds could affect GABA spectroscopy at 7T, we compute grey and white matter lineshapes by frequency mapping. We found a slight frequency shift and lineshape which can be ignored. Hence, we conclude that we can probably safely use a single lineshape for fitting using LCModel.
-
- 4026
Computer #95
- Potential of 3T fMRS to detect dynamic changes of glutamate related to activation in visual cortex
Miguel Martínez-Maestro¹, Christian Labadie², Karsten Mueller¹, and Harald E. Möller¹
- ¹*NMR Group, Max Planck Institute for Human Cognitive and Brain Sciences, Leipzig, Germany*, ²*Charité - Berlin Center for Advanced Neuroimaging (BCAN), Berlin, Germany*
- Dynamic changes of metabolite concentrations in the human brain have been successfully detected in response to stimulus at 7T. The present study focus on characterize the detection limits at 3T. 20min fMRS paradigm alternated 5min intervals with stimulus OFF/ON/OFF/ON. A significant intra-individual increase in glutamate+glutamine (Glx) was found in the group analysis (1.83%, p = 0.017). The cross-subjects averaged time course also indicated 1.98% concentration increase during the ON periods. A direct correlation between subtle changes of Glx concentrations and the application of a visual stimulus could be shown consistent with reports from ultra-high field studies.
-
- 4027
Computer #96
- GABA+ levels in postmenopausal women with mild-to-moderate depression: A Preliminary Study
Zhensong Wang^{1,2}, Aiying Zhang³, Jie Gan², Guangbin Wang¹, Bin Zhao¹, Huifang Qu⁴, Weibo Chen⁵, Bo Liu⁶, Fei Gao¹, Tao Gong⁷, and Richard A.E. Edden^{8,9}
- ¹*Shandong Medical Imaging Research Institute, Jinan, China, People's Republic of*, ²*Second Affiliated Hospital of Shandong University of Traditional Chinese Medicine, Jinan, China, People's Republic of*, ³*Affiliated Eye Hospital of Shandong University of Traditional Chinese Medicine, Jinan, China, People's Republic of*, ⁴*Shandong Chest Hospital, Jinan, China, People's Republic of*, ⁵*Philips Healthcare, Shanghai, China, People's Republic of*, ⁶*Qilu Hospital of Shandong University, Jina, China, People's Republic of*, ⁷*Shandong Medical Imaging Research Institute, Shandong University, Jinan, China, People's Republic of*, ⁸*Russell H. Morgan Department of Radiology and Radiological Science, The Johns Hopkins University School of Medicine, Baltimore, MD, USA, Baltimore, MD, United States*, ⁹*FM Kirby Center for Functional Brain Imaging, Kennedy Krieger Institute, Baltimore, MD, USA, Baltimore, MD, United States*
- The present study hypothesized that the GABA levels would be lower in postmenopausal women with mild-to-moderate depression. We investigate the cerebral GABA levels in postmenopausal women using the edited MRS technique MEGA-PRESS. 18 postmenopausal women with mild-to-moderate depression and 11 healthy controls with the age- and body index-, educationally matched were enrolled. GABA+ levels were quantified in the anterior cingulate cortex/medial prefrontal cortex (ACC/mPFC) and the posterior cingulate cortex (PCC). Water-scaled GABA+ levels were significantly lower in the ACC/mPFC regions of patients group than in healthy controls, which suggesting that dysfunctional GABAergic system may be involved in depression in postmenopausal women.
-

Electronic Poster

Alzheimer's Dementia

Exhibition Hall

Wednesday, May 11, 2016: 16:00 - 17:00

-
- 4028
Computer #1
- Simultaneous assessment of cerebral iron load, as estimated by Quantitative Susceptibility Mapping, and Amyloid- β plaque density, as measured by 18F-Flutemetamol, in Super-agers
Jiri M.G. van Bergen¹, Xu Li², Frances C. Quevenco¹, Anton F. Gietl¹, Valerie Treyer^{1,3}, Rafael Meyer¹, Sandra E. Leh¹, Alfred Buck³, Roger

Nitsch¹, Peter C.M. van Zijl², Christoph Hock¹, and Paul G. Unschuld¹

¹Psychiatry Research and Psychogeriatric Medicine, University of Zurich, Zurich, Switzerland, ²F.M. Kirby center for Functional Brain Imaging, Kennedy Krieger Institute and Johns Hopkins School of Medicine, Baltimore, MD, United States, ³Division of Nuclear Medicine, University of Zurich, Zurich, Switzerland

We investigated “super-agers” (a minority of elderly subjects that display significantly higher cognitive performance levels) for the interaction of A β -plaque burden and iron load, using Quantitative Susceptibility Mapping and simultaneous 18F-Flutemetamol measures in the PET-MR. We found significant increased iron load in the putamen and caudate nucleus of subjects with a high A β -plaque burden, but no regional correlations between the two markers in gray matter. This suggests that while super-agers are affected by common age-related brain pathologies, such as cortical A β -plaque burden and increased striatal iron load, these might exert less neurotoxic damage.

4029 Computer #2 The glutamine and glutamate complex measured by functional MRS alters during a face-name association task in patients with MCI and AD

Geon-Ho Jahng¹, Janghoon Oh¹, Hyug-Gi Kim¹, Do-Wan Lee², Chanhee Lee¹, Hak Young Rhee³, Chang-Woo Ryu¹, Wonchul Shin³, Jong-Woo Paik⁴, Kyung Mi Lee⁵, Soonchan Park¹, Bo-Young Choe², and Dal-Mo Yang¹

¹Department of Radiology, Kyung Hee University Hospital at Gangdong, Kyung Hee University, Seoul, Korea, Republic of, ²Department of Biomedical Engineering, The Catholic University of Korea, Seoul, Korea, Republic of, ³Department of Neurology, Kyung Hee University Hospital at Gangdong, Kyung Hee University, Seoul, Korea, Republic of, ⁴Department of Mental Health, Kyung Hee University Hospital, Kyung Hee University, Seoul, Korea, Republic of, ⁵Department of Radiology, Kyung Hee University Hospital, Kyung Hee University, Seoul, Korea, Republic of

To investigate the metabolite changes in subjects with AD, MCI, and cognitively normal (CN) elderly during a memory task using dynamic MRS at a 3T MRI system, we included 95 subjects who included: 23 young normal control (YC), 24 cognitively normal (CN) elderly, 24 aMCI, and 24 mild and probable AD. The functional MRS data were measured during the face-name association task with the stimulation paradigm of fixation, novel, and repeat conditions. The fMRS data were analyzed using the LCModel software. Glx was altered during the stimulation conditions, which can be used in neuronal dysfunction for a patient with dementia.

4030 Computer #3 Abnormal Grey Matter Arteriolar Cerebral Blood Volume and its Association with the Presence of E4 Allele of the Apolipoprotein E (APOE) Gene in Elderly Subjects at Risk for Alzheimer's Disease (AD)

Jun Hua^{1,2}, SeungWook Lee³, Nicholas I.S. Blair³, Michael Wyss⁴, Simon J Schreiner⁵, Stefanie C Steininger⁵, Sandra Leh⁵, Roger Nitsch⁵, Klaas P Pruessmann⁴, Peter C.M. van Zijl^{1,2}, Marilyn Albert⁶, Christoph Hock⁵, and Paul G Unschuld⁵

¹F.M. Kirby Research Center for Functional Brain Imaging, Kennedy Krieger Institute, Baltimore, MD, United States, ²Neurosection, Div. of MRI Research, Dept. of Radiology, Johns Hopkins University School of Medicine, Baltimore, MD, United States, ³Department of Biomedical Engineering, Johns Hopkins University, Baltimore, MD, United States, ⁴Institute for Biomedical Engineering, University of Zürich and ETH Zürich, Zürich, Switzerland, ⁵Division of Psychiatry Research and Psychogeriatric Medicine, University of Zürich and ETH Zürich, Zürich, Switzerland, ⁶Department of Neurology, Johns Hopkins University School of Medicine, Baltimore, MD, United States

Cerebrovascular dysfunction has been associated with mild-cognitive-impairment (MCI) and Alzheimer's Disease (AD). Recent animal studies in aging show that abnormalities in pial arteries and arterioles start before other blood vessels and blood flow are affected. We show that cerebral-blood-volume of pial arteries and arterioles (CBVa), measured with the inflow-based vascular-space-occupancy (iVASO) MRI, is significantly altered in various brain regions in MCI patients compared to healthy elderly controls. CBVa in the orbitofrontal cortex significantly correlated with APOE-e4 carrier-status, the major genetic risk factor for sporadic AD. Our results suggest CBVa as a potential biomarker at an early stage of the disease.

4031 Computer #4 Sildenafil improves vascular and metabolic function in patients with Alzheimer's Disease

Hanzhang Lu¹, Min Sheng², Peiyong Liu¹, Harshan Ravi¹, Shin-Lei Peng¹, Ramon Diaz-Arrastia³, Michael D. Devous Sr.⁴, and Kyle B. Womack⁵

¹Department of Radiology, Johns Hopkins University School of Medicine, Baltimore, MD, United States, ²Advanced Imaging Research Center, University of Texas Southwestern Medical Center, Dallas, TX, United States, ³Center for Neuroscience and Regenerative Medicine, Uniformed Services University of the Health Sciences, Bethesda, MD, United States, ⁴Avid Radiopharmaceuticals, Inc., Philadelphia, PA, United States, ⁵Department of Neurology, University of Texas Southwestern Medical Center, Dallas, TX, United States

Alzheimer's disease (AD) is the leading cause of degenerative dementia in the aging population. Patients with AD have alterations in cerebral hemodynamic function. Therefore, improved cerebrovascular function may be an attractive goal for pharmaceutical intervention in AD. Our study applied several novel non-invasive MRI techniques to investigate the alterations of CBF, cerebral metabolic rate of oxygen (CMRO2) and cerebrovascular reactivity (CVR) after a single dose of sildenafil administration in order to assess its physiological effects in AD patients. Our data suggest that a single dose of sildenafil improves cerebral hemodynamic function and increases cerebral oxygen metabolism in patients with AD.

4032 Computer #5 Multi-Parametric Imaging Assessment of Alzheimer's Disease Pathology

Eva-Maria Ratai^{1,2}, Kimberly A. Stephens^{1,2}, Alison E. Goldblatt^{1,2}, Jean-Philippe Coutu^{1,2}, Ciprian Catana^{1,2}, Diana Rosas^{2,3}, and David Salat^{1,2}

¹Radiology, Massachusetts General Hospital, Boston, MA, United States, ²A. A. Martinos Center for Biomedical Imaging, Charlestown, MA, United States, ³Neurology, Massachusetts General Hospital, Boston, MA, United States

The purpose of this study was to find associations between metabolites measures by MRS and glucose metabolism using FDG PET and cerebral blood flow (CBF) measured by ASL MRI in the assessment of Alzheimer's Disease. Our study shows an association between increased myo-inositol, a marker of glial inflammation, and hypo-metabolism measured by FDG as well hypo-perfusion measured by ASL. Linear regression analysis revealed that creatine, a marker of altered energy metabolism positively correlated with increased glucose uptake by FDG PET. Increased levels of glutamate+glutamine (contributing to excitotoxicity) were related to decreased metabolic activity by PET and decreased CBF.

-
- 4033 Computer #6 Functional connectome architecture of Alzheimer's disease, mild cognitive impairment and behavioral variant of frontotemporal dementia: a graph analysis study.
Elisa Canu¹, Federica Agosta¹, Silvia Basaia¹, Alessandro Meani¹, Sebastiano Galantucci¹, Francesca Caso¹, Giuseppe Magnani², Roberto Santangelo², Monica Falautano², Giancarlo Comi², Andrea Falini³, and Massimo Filippi^{1,2}
- ¹Neuroimaging Research Unit, San Raffaele Scientific Institute, Vita-Salute San Raffaele University, Milan, Italy, ²Department of Neurology, San Raffaele Scientific Institute, Vita-Salute San Raffaele University, Milan, Italy, ³Department of Neuroradiology, San Raffaele Scientific Institute, Vita-Salute San Raffaele University, Milan, Italy*
- This is a graph analysis study applying a new parcellation approach, which combines the need for equal sized nodes with respecting brain anatomy, on resting state fMRI data from a population of 247 patients with neurodegenerative cognitive impairment (early [EO] and late onset [LO] Alzheimer's disease (AD), behavioural frontotemporal dementia [bvFTD], mild cognitive impairment [MCI]) and 86 controls. Compared to other groups, AD patients showed disrupted global network connectivity, while MCI had specific regional changes, suggesting that graph-analysis is promising to detect early features of neurodegeneration. Global and regional graph network properties were able to distinguish EOAD and bvFTD.
-
- 4034 Computer #7 Investigating the correspondence of clinical diagnostic grouping with underlying neurobiological and phenotypic clusters using unsupervised learning: An application to the Alzheimer's spectrum
Xinyu Zhao¹, D Rangaprakash¹, D Narayana Dutt², and Gopikrishna Deshpande^{1,3,4}
- ¹Electrical and Computer Engineering, AU MRI Research Center, Auburn, AL, United States, ²Medical Electronics, Dayananda Sagar College of Engineering, Bangalore, India, ³Psychology, Auburn University, Auburn, AL, United States, ⁴Alabama Advanced Imaging Consortium, Auburn University and University of Alabama Birmingham, Auburn, AL, United States*
- Many brain-based disorders are traditionally diagnosed based on clinical interviews and behavioral assessments. Using Alzheimer's spectrum (i.e. mild cognitive impairment [MCI] and Alzheimer's disease [AD]) as a test case, we investigated whether clinical diagnostic grouping is grounded in underlying neurobiological and phenotypic clusters. In order to do so, three unsupervised learning methods were applied on resting-state fMRI connectivity measures obtained from subjects with MCI and AD. High similarity was achieved between connectivity and phenotypic clusters while similarity was low with clinical diagnosis. It shows that neurobiological and phenotypic markers could be used to improve the precision of clinical diagnosis.
-
- 4035 Computer #8 Imaging vascular alterations in a mouse model of Down's syndrome using magnetic resonance angiography with tensor-based morphometry
Holly E Holmes¹, Nick Powell², James M O'Callaghan¹, Jack A Wells¹, Ian F Harrison¹, Da Ma², Ozama Ismail¹, Victor LJ Tybulewicz³, Frances Wiseman⁴, Sebastian Ourselin², Elizabeth M Fisher⁴, and Mark F Lythgoe¹
- ¹Centre for Advanced Biomedical Imaging, University College London, London, United Kingdom, ²Centre for Medical Image Computing, University College London, London, United Kingdom, ³National Institute for Medical Research, London, United Kingdom, ⁴Institute of Neurology, University College London, London, United Kingdom*
- Magnetic resonance angiography (MRA) is an established MRI technique for visualising the cerebral vasculature. Interpretation of MR angiograms is often reliant on visual inspection of the data;¹ however, it is possible to misinterpret flow artefacts (e.g. signal voids) as vascular alterations.² In this work, we have used a novel combination of MRA and advanced registration as well as statistical algorithms to explore vascular alterations in the Tc1 mouse model of Down's syndrome. We identified operator-independent local disturbances in the vascular architecture, which supports previous work in this mouse model as well as observations in the wider DS population.
-
- 4036 Computer #9 Probing white matter abnormalities in preclinical and early Alzheimer's disease
Qing Wang^{1,2}, Yong Wang^{1,3,4}, Joshua S Shimony¹, Anne M Fagan^{2,5}, John C Morris^{5,6}, and Tammie L.S. Benzinger^{1,6,7}
- ¹Mallinckrodt Institute of Radiology, Washington University in St. Louis, St. Louis, MO, United States, ²Knight Alzheimer's Disease Research Center, St. Louis, MO, United States, ³Obstetrics and Gynecology, Washington University in St. Louis, St. Louis, MO, United States, ⁴Biomedical Engineering, Washington University in St. Louis, St. Louis, MO, United States, ⁵Neurology, Washington University in St. Louis, St. Louis, MO, United States, ⁶Knight Alzheimer's Disease Research Center, St. Louis, MO, United States, ⁷Neurosurgery, Washington University in St. Louis, St. Louis, MO, United States*
- Robust neuroimaging biomarker sensitive to the early white matter abnormalities could provide novel insights into the pathogenesis of Alzheimer's disease (AD), and serve as surrogate measures for disease progression. We demonstrated that novel DBSI white matter abnormality biomarkers strongly correlate with invasive CSF measures of neuronal injuries, and provide specific preclinical measures of WM abnormalities for early diagnostics and accurate assessment of disease-modifying therapies targeting neuro-protection in AD.
-

- 4037
Computer #10 White matter lesion volume does not affect the relationship between CSF A β 42 and cerebral amyloid deposition assessed with PET
Danielle van Westen¹, Sebastian Palmqvist², Henrik Zetterberg³, Niklas Mattsson², Lennart Minthon², Katarina N agg a², Erik Stomrud²,
The Swedish BioFINDER study², Kaj Blennow³, and Oskar Hansson²
- ¹Diagnostic Radiology, Lund University, Lund, Sweden, ²Memory Clinic, Lund University, Lund, Sweden, ³The Sahlgrenska Academy at University
of Gothenburg, Clinical Neurochemistry Laboratory, Institute of Neuroscience and Physiology, Gothenburg, Sweden
- White matter lesions (WML) are abundant in the elderly and even more so in Alzheimer's disease (AD). Previous studies indicate that
WML affect the level of cerebrospinal fluid (CSF) A β 42 and this in turn might affect the validity of CSF A β 42 as biomarker of the
pathological hallmark of AD, namely cerebral amyloid deposition. Therefore, we studied the influence of WML on the association
between CSF A β 42 and amyloid deposition measured with [18F]-flutemetamol positron emission tomography (PET).
-
- 4038
Computer #11 Voxel-Based Analysis of Cerebral Perfusion in Subcortical Ischemic Vascular Dementia and Alzheimer's Disease Dementia: a Multi-
Parametric Multi-TI Arterial-Spin-Labeling Study
Shuang Yang¹, Tianyi Qian², Yao Meng³, Fei Gao¹, Josef Pfeuffer⁴, Guangbin Wang¹, and Bin Zhao¹
- ¹Shandong Medical Imaging Research Institute, Shandong University, Jinan, China, People's Republic of, ²Siemens Healthcare, MR Collaborations
NE Asia, Beijing, China, People's Republic of, ³Shandong provincial Hospital, Shandong University, Jinan, China, People's Republic of, ⁴Siemens
Healthcare, Application Development, Erlangen, Germany
- This study aims to present the feasibility of multi-TI (mTI)-ASL in distinguishing between AD and SIVD patients in cerebral perfusion.
Nineteen SIVD subjects, twelve AD subjects, and ten controls were included in the study. There was no significant difference in CBF
between SIVD and HCs, and between SIVD and AD patients. However, significant differences of BAT were detected among all three
groups. The mTI-ASL could evaluate the cerebral perfusion of AD and SIVD patients. Compared with CBF, the BAT could better detect
perfusion differences and demonstrated better efficiency.
-
- 4039
Computer #12 Dynamic Dysfunction of DMN in AD and MCI: a Time Point-Based Network Analysis
Tianyi Qian¹, Peipeng Liang², and Kuncheng Li²
- ¹MR Collaborations NE Asia, Siemens Healthcare, Beijing, China, People's Republic of, ²Radiology, Xuanwu Hospital, Capital Medical University,
Beijing, China, People's Republic of
- In recent years, the study of dynamic changes within brain functional networks has become a trend topic in the fields of neuroscience
and neuroradiology. In this study, we proposed a time-point based analysis method to search for dynamic pattern changes in normal
controls, AD and two MCI stages. We aim to investigate whether the DMN deficit we observed in previous studies is related to changes of
activity frequency of micro-state network condition. The results show that the dynamic patterns obtained by the time point-based
analysis could detect several DMN micro-states and the frequency of the appearance of these micro-states changes during the progress
of cognitive impairment.
-
- 4040
Computer #13 Temperature effects in post mortem structural MRI of human brain in situ
Gunther Helms^{1,2}, Arne Wrede³, Peter Dechent², and Walter Schulz-Schaeffer³
- ¹Medical Radiation Physics, Lund University, Lund, Sweden, ²Cognitive Neurology, G ttingen University Medical Center, G ttingen, Germany,
³Neuropathology, G ttingen University Medical Center, G ttingen, Germany
- Structural 3D MRI and FLASH-based mapping of T_1 and magnetization transfer (MT) at 3T was performed in situ on 11 subjects with
probable Creutzfeldt-Jacob disease prior to autopsy. The mean diffusivity in ventricles yielded temperatures between 6°C and 29°C. T_1
contrast in the deep brain decreased with temperature and vanished under refrigerated conditions. T_1 of gray matter lowered towards
the normal white matter's T_1 which did not change. The MT saturation was generally independent of temperature, except in normal WM
below 13°C. Above 13°C, MT maps yield a high contrast and can be used for quantitative assessment of structural changes.
-
- 4041
Computer #14 Histological correlates of MRI contrast in patients with Alzheimer's Disease
Marjolein Bulk¹, Walid M. Abdelmoula¹, Linda M. van der Graaf¹, Mark A. van Buchem¹, Pieter Voorn², Jouke Dijkstra¹, and Louise van
der Weerd^{1,3}
- ¹Radiology, Leiden University Medical Center, Leiden, Netherlands, ²Department of Anatomy and Neurosciences, VU University Medical Center,
Amsterdam, Netherlands, ³Human Genetics, Leiden University Medical Center, Leiden, Netherlands
- Investigating the histological correlates of MRI contrasts in patients with Alzheimer's disease (AD) will give more insight into the
pathological correlates of T2* and SWI. Using 7T MRI and histology of post-mortem brain tissue we showed that the frontal cortex of AD
patients has a different imaging phenotype compared to non-demented controls, which spatially correlates to changes in iron
deposition and grey matter myelin organization. Most importantly, within the AD group the early-onset AD patients are distinguishable
on MRI from the late-onset AD patients, and these differences are mirrored in the underlying pathology of these AD subtypes.
-
- 4042
Computer #15 Probing the effects of elevated glucose level on the integrity of white matter in Alzheimer's disease using diffusion kurtosis imaging
Weiwei Wang¹, Jing Jing¹, Bing Wu², Ailian Liu¹, Qingwei Song¹, and Yanwei Miao¹
- ¹Radiology Department, the First Affiliated Hospital of Dalian Medical University, Dalian, China, People's Republic of, ²GE Healthcare MR

AD concomitant with hyperglycemia is commonly observed during clinical work, and it was known that AD and disorder of glucose metabolism are related. However, the factor of glucose level in AD patients have not yet been taken into consideration in the past studies, which might be of clinical significance in learning the AD progression. In this work, DKI is used to probe the likely effects of elevated glucose level in the white matter microstructure of AD patients.

-
- 4043
Computer #16 The effect of physical exercise on cerebral blood flow in Alzheimer's disease
Lisa A. van der Kleij¹, Esben T. Petersen², Hartwig R. Siebner², Jeroen Hendrikse¹, Kristian S. Frederiksen³, Nanna A. Sobol⁴, Steen G. Hasselbalch³, and Ellen Garde²
- ¹Department of Radiology, UMC Utrecht, Utrecht, Netherlands, ²Danish Research Centre for Magnetic Resonance, Centre for Functional and Diagnostic Imaging and Research, Copenhagen University Hospital Hvidovre, Hvidovre, Denmark, ³Danish Dementia Research Centre, Department of Neurology, Rigshospitalet, Copenhagen University Hospital, Copenhagen, Denmark, ⁴Musculoskeletal Rehabilitation Research Unit and Institute of Sports Medicine, Bispebjerg Hospital, University of Copenhagen, Copenhagen, Denmark*
- The purpose of this study was to determine the effect of moderate-to-high-intensity aerobic exercise on cerebral blood flow in patients with Alzheimer's disease (AD). In the ADEX trial, patients with mild to moderate AD participated in aerobic exercise for 16 weeks. Pulsed Arterial Spin Labeling was performed at baseline and at 16 weeks. CBF in the anterior cingulate cortex was significantly lower at 16 weeks in the control group, but it remained unchanged in the intervention group. Our results suggest that even brains affected by mild to moderate Alzheimer's disease may still benefit from regular exercise.
-
- 4044
Computer #17 TDP43 correlates of amygdala volume in aging with ex-vivo MRI
Junxiao Yu¹, Aikaterini Kotrotsou¹, Arnold M. Evia¹, Julie A. Schneider², Sue E. Leurgans², David A. Bennett², and Konstantinos Arfanakis¹
- ¹Department of Biomedical Engineering, Illinois Institute of Technology, Chicago, IL, United States, ²Rush Alzheimer's Disease Center, Rush University Medical Center, Chicago, IL, United States*
- Transactive response DNA-binding protein 43 (TDP43) pathology was the primary protein abnormality in amyotrophic lateral sclerosis (ALS) and frontotemporal lobar degeneration (FTLD). Recent findings showed that TDP43 pathology is common in old age and strongly associated with cognition, cognitive decline and increased risk of dementia beyond the contributions of other age-related neuropathologies. TDP43 pathology in aging is mainly found in the medial temporal lobes with the being one of the first regions to be affected. The purpose of this project was to study associations of TDP43 in aging with amygdalar volume for the first time in a large community cohort.
-
- 4045
Computer #18 Gender Based Analyses of Cortical Thickness and Structural Networks Connectivity in Parkinson's Disease
Santosh Kumar Yadav¹, Georgia Vasileiou², Anup Singh³, Elias R Melhem⁴, Ena Wang¹, Francesco M Marincola¹, Arijitt Borthakur⁵, and Mohammad Haris¹
- ¹Division of Translational Medicine, Sidra Medical and Research Center, Doha, Qatar, ²Department of Medical physics, University college of London, London, United Kingdom, ³Center for Biomedical Engineering, Indian institute of Technology, Delhi, India, ⁴Department of diagnostic Radiology and Nuclear Medicine, University of Maryland, Baltimore, MD, United States, ⁵Center for Magnetic Resonance and Optical Imaging, Department of Radiology, University of Pennsylvania, Philadelphia, PA, United States*
- We evaluated the gender based differences in cortical thickness and structural brain network connectivity in PD patients. Significantly reduced cortical thicknesses and disrupted structural networks connectivity appeared in PD males compared to PD females suggestive of more brain tissue changes in PD males than PD females. These male-specific cortical thickness changes and disrupted structural networks connectivity may contribute to or derive from physiological and genetically differences between males and females and may have significant implications in diagnosing and treating PD among the gender.
-
- 4046
Computer #19 Investigating pathology-related functional connectivity in cognitively normal super-agers
Frances-Catherine Quevenco¹, Jiri van Bergen¹, Xu Li², Anton F. Gietl¹, Valerie Treyer^{1,3}, Rafael Meyer¹, Sandra E. Leh¹, Alfred Buck³, Roger Nitsch¹, Peter C. M. van Zijl², Christoph Hock¹, and Paul G. Unschuld¹
- ¹Psychiatric Research, University of Zurich, Zurich, Switzerland, ²F.M. Kirby center for Functional Brain Imaging, Kennedy Krieger Institute and Johns Hopkins School of Medicine, Baltimore, MD, United States, ³Division of Nuclear Medicine, University of Zurich, Zurich, Switzerland*
- To investigate early stages of preclinical Alzheimer's, this study investigates the functional connectivity of 25 cognitively healthy elderly participants ("super agers") in relation to cortical iron (using QSM) and cortical amyloid-beta load (18F-Flutemetamol PET). Functional connectivity analysis with the posterior cingulate cortex (PCC) as a seed found significant regional and temporal overlaps in primary DMN regions for groups with high iron and high amyloid. Despite the network synchronicities, a contrast between high iron and high amyloid networks found significant FC differences between the PCC, precuneus, hippocampus and parahippocampus which are DMN connections known to be affected by A β -burden.
-
- 4047
Computer #20 Deformation Based Classification of Alzheimer's Disease
Thomas Bonde Larsen¹, Akshay Pai¹, and Sune Darkner¹
- ¹Computer Science, University of Copenhagen, Copenhagen, Denmark*

Effective and accurate diagnosis of Alzheimer's disease (AD) purely based on structural magnetic resonance imaging (MRI) is a very pertinent clinical problem. We present a simple but highly accurate registration-based method to discriminate between the three classes of healthy controls (HC), mild cognitively impaired (MCI) and AD. The method uses the norm of the tangent space of the deformation in a K-nearest neighbor KNN classifier. The result show that for 60 subjects, 20 in each class using n-fold cross-validation an overall accuracy of 81.6% with 75% for HC, 85% MCI and 85% for AD.

4048 Computer #21 A follow-up study of hippocampal subfield atrophy in mild cognitive impairment with automatic segment method
XIANGZHU ZENG¹, HUI SHU YUAN¹, YING LIU¹, and ZHENG WANG¹

¹RADIOLOGY, PEKING UNIVERSITY THIRD HOSPITAL, BEIJING, China, People's Republic of

Mild cognitive impairment (MCI) is often considered as an intermediate stage between normal aging and dementia, as reflected by a higher rate of conversion to clinical Alzheimer's disease (AD) than in the normal elderly population. The hippocampal formation is a complex brain region with a primary role in memory function and vulnerable to neurodegenerative diseases. The aim of this research is to investigate the atrophy feature of hippocampal subfield and follow up the changes of hippocampal subfield in about two years by using automatic segmentation tool in patients with MCI. Our results suggest that compared to ICV, hippocampal subfield could be a more sensitive to detect cerebral changes of MCI. CA1, CA3 and left entorhinal cortex may be main subfields involved during MCI stage. Volumes of hippocampal subfield decreased in MCI patients and were positive correlation with clinical scores. There were also decreases in volumes of hippocampal subfield in MCI patients with the progress of the disease.

4049 Computer #22 4D Flow MRI for assessing cerebral venous flow, a potential surrogate marker for capillary pulsatility in Alzheimer's disease
Leonardo A Rivera-Rivera¹, Tilman Schubert², Kevin M Johnson¹, Sterling C Johnson³, Patrick Turski², and Oliver Wieben^{1,2}

¹Medical Physics, University of Wisconsin Madison, Madison, WI, United States, ²Radiology, University of Wisconsin Madison, Madison, WI, United States, ³Medicine, University of Wisconsin Madison, Madison, WI, United States

Cerebral arteries are often morphologically altered and dysfunctional in Alzheimer's disease. In this study, 4D flow MRI was used to assess cerebral venous flow, particularly mean blood flow and pulsatility index in patients with AD, and in healthy age matched controls. We found a statistically significant increase in pulsatility index and decrease in mean flow for the AD in most venous segments. With the large volume coverage and high temporal and spatial resolution, 4D flow MRI can provide additional biomarkers of vascular health that can contribute to the identifying patients who could benefit from interventions to improve circulatory system functions.

4050 Computer #23 Evaluation of blood brain barrier permeability in Alzheimer's disease with DCE-MRI
Rexford Newbould¹, Brandon Whitcher², Christopher Long³, Shaila Shabbir⁴, Paul Matthews⁵, Andrew Lockhart⁴, Craig Ritchie⁵, and Eugeniu Ilan Rabiner¹

¹Imanova, London, United Kingdom, ²Klarismo, London, United Kingdom, ³MIT Sloan School of Management, Cambridge, MA, United States, ⁴GSK, Brentford, United Kingdom, ⁵Imperial College London, London, United Kingdom

DCE 3T MRI data acquired from 6 subjects with previous diagnoses of AD, 2 subjects with vascular dementia, and 7 healthy controls group-matched for age and gender. Radiofrequency transmit (B1) field corrected Gd concentration values were calculated via dual-temporal resolution dynamic T1 mapping during and over 45 minutes post rapid Gd infusion. The extended Tofts model was used to determine the volume and rate transfer constants of BBB permeability in 11 regions of interest. No differences were detected between groups, implying BBB leakage in AD is slower than detectable in this experiment, or that BBB permeability in AD is moderated by an active transport mechanism.

4051 Computer #24 Quantitative Susceptibility Mapping in Alzheimer's Disease using Joint background-field removal and segmentation-Enhanced Dipole Inversion
Jakob Meineke¹, Fabian Wenzel¹, Iain D. Wilkinson², and Ulrich Katscher¹

¹Philips Research Europe, Hamburg, Germany, ²University of Sheffield, Sheffield, United Kingdom

Quantitative Susceptibility Mapping (QSM) is used to study the deep gray-matter nuclei of patients with Alzheimer's Disease (AD) and healthy control subjects. QSM is performed using "Joint background-field removal and segmentation-Enhanced Dipole Inversion" (JEDI), which leverages the information from automated model-based segmentation and allows the compact single-step formulation of the ill-posed inversion problem of QSM. The tissue magnetic susceptibility shows a trend for increase in the amygdala and the putamen of AD patients as compared to healthy control subjects, in agreement with previous studies.

Electronic Poster

Multiple Sclerosis: General

Exhibition Hall

Wednesday, May 11, 2016: 16:00 - 17:00

4052 Computer #25 Effect of patient motion on the visibility of small veins in T2*w imaging: A simulation experiment with implications for the study of the central-vein-sign (CVS) theory in MS

¹Buffalo Neuroimaging Analysis Center, Department of Neurology, Jacobs School of Medicine and Biomedical Sciences, The State University of New York at Buffalo, Buffalo, NY, United States, ²High Field Magnetic Resonance Centre, Department of Biomedical Imaging and Image-guided Therapy, Medical University of Vienna, Vienna, Austria, ³MRI Molecular and Translational Research Center, Jacobs School of Medicine and Biomedical Sciences, The State University of New York at Buffalo, Buffalo, NY, United States

FLAIR* is a fusion of T2-FLAIR and 3D-T2*w images and it is used to assess the central-vein-sign, a recent promising research direction in MRI-based study of Multiple Sclerosis. However in this experiment we show that researchers should be aware that slight patient movement during acquisition can produce blurring effect in 3D-T2*w images. This subtle artifact can mask small vessels even in case which the overall quality of the image is not substantially degraded.

4053
Computer #26 Combined Anatomic and Functional Connectivity Metric for Tracking Disease Progression in MS
Mark J Lowe¹, Katherine Koenig¹, Erik Beall¹, Jian Lin¹, Ken Sakaie¹, Lael Stone², and Micheal D. Phillips¹

¹Imaging Institute, Cleveland Clinic, Cleveland, OH, United States, ²Neurologic Institute, Cleveland Clinic, Cleveland, OH, United States

Based on the observation that anatomic and functional connectivity measures in multiple sclerosis (MS) are correlated, but not highly correlated, we propose to combine these metrics into an imaging based measure of disease progression. We show that this metric is sensitive to disease progression in a cohort of MS patients over a time period of one year.

4054
Computer #27 Assessment of ferritin in the multiple sclerosis brain using temperature induced R2* changes
Christoph Birkel¹, Daniele Carassiti², Christian Langkammer¹, Christian Enzinger¹, Franz Fazekas¹, Klaus Schmierer^{2,3}, and Stefan Ropele¹

¹Department of Neurology, Medical University of Graz, Graz, Austria, ²Blizard Institute (Neuroscience), Queen Mary University of London, London, United Kingdom, ³Barts Health NHS Trust, Emergency Care and Acute Medicine Clinical Academic Group (Neuroscience), London, United Kingdom

Evidence for a possible role of iron in the pathogenesis and progression of multiple sclerosis (MS) has raised interest in iron mapping techniques. However, current approaches are not reliable in white matter because of the diamagnetic properties of myelin. We recently proposed a new method for iron mapping which is based on the temperature dependency of the paramagnetic susceptibility. Here, the temperature coefficient of R2* (TcR2*) as a measure of iron content was assessed in three post-mortem MS brain samples. Validation of TcR2* mapping was done with immunohistochemistry using cell counting on ferritin light-chain stains.

4055
Computer #28 Longitudinal mcDESPOT Shows Contrasting Patterns of Change in Multiple Sclerosis and Neuromyelitis Optica Cervical Cord
Anna Combes¹, Lucy Matthews², Gareth J Barker¹, Steven CR Williams¹, Katrina McMullen³, Janet Lam⁴, Anthony Traboulsee³, David KB Li^{3,4}, Jacqueline Palace², and Shannon Kolind³

¹Neuroimaging, King's College London, London, United Kingdom, ²Nuffield Department of Clinical Neurosciences, University of Oxford, Oxford, United Kingdom, ³Medicine, University of British Columbia, Vancouver, BC, Canada, ⁴Radiology/UBC MS/MRI Research Group, University of British Columbia, Vancouver, BC, Canada

Neuromyelitis optica (NMO) severely affects the optic nerves and spinal cord and shares features with multiple sclerosis (MS). Ongoing diffuse neurodegeneration, however, is thought to be absent in NMO between relapses. We collected cervical cord mcDESPOT at baseline and one-year follow-up in patients and matched controls. While there were no significant changes in controls and MS patients, the NMO group showed a loss of cord volume, decrease in T₁ and increase in myelin water fraction. We hypothesize that continuing atrophy in lesioned areas reduces the amount of damaged tissue relative to healthy tissue, and is responsible for the observed changes.

4056
Computer #29 White Matter Water Content in Multiple Sclerosis and Neuromyelitis Optica
Irene Vavasour¹, Sandra Meyers², Praveena Manogaran³, Shuhan Xiao³, Anika Wurl³, Katrina McMullen³, David Li¹, Anthony Traboulsee³, and Shannon Kolind³

¹Radiology, University of British Columbia, Vancouver, BC, Canada, ²Physics and Astronomy, University of British Columbia, Vancouver, BC, Canada, ³Medicine, University of British Columbia, Vancouver, BC, Canada

Multiple sclerosis (MS) and neuromyelitis optica (NMO) are both autoimmune diseases of the central nervous system. Normal appearing white matter is known to be affected by diffuse tissue damage in MS whereas damage in NMO is thought to be restricted to acute lesions. Surprisingly, in this study, water content within whole white matter and white matter tracts of subjects with neuromyelitis optica (NMO) was found to be higher than in healthy matched controls and similar to MS. Both NMO and MS lesions had a higher water content compared to normal appearing white matter.

4057
Computer #30 A randomized controlled trial on the efficacy of cognitive training in MS reveals functional connectivity changes
Ottavia Dipasquale^{1,2}, Jamie Campbell³, Camila Callegari Piccinin⁴, Dawn Langdon⁵, Waqar Rashid⁶, and Mara Cercignani³

¹IRCCS, Don Gnocchi Foundation, Milan, Italy, ²Department of Electronics, Information and Bioengineering, Politecnico di Milano, Milan, Italy, ³Clinical Imaging Sciences Centre, Brighton and Sussex Medical School, Brighton, United Kingdom, ⁴Neuroimaging Laboratory, University of Campinas, Cidade Universitária, Campinas, Brazil, ⁵Psychology Department, Royal Holloway, University of London, Egham, United Kingdom, ⁶Department of Neurology, Brighton and Sussex University Hospitals NHS Trust, Brighton, United Kingdom

We investigated the resting-state functional connectivity (FC) changes induced after 6 weeks of computerised, home-based cognitive rehabilitation in patients with multiple sclerosis (MS) in a randomized controlled trial. The intervention and control groups were evaluated at baseline (T1), after a 6-week intervention period (T2) and a 12-week follow-up period (T3). Out of the 94 regions investigated, many memory-, attention- and motor-related areas strengthened their FC at T2 and T3 in the intervention group. This study supports the hypothesis that this cognitive rehabilitation is a feasible and effective approach in patients with MS and confirms that fMRI is a useful tool for mapping plastic changes.

-
- 4058
Computer #31
Quantitative T2 mapping detects pathology in normal-appearing brain regions of relapsing-remitting MS patients
Timothy Shepherd^{1,2}, Ivan Kirov^{1,2}, James S Babb^{1,2}, Mary T Bruno², Robert E Charlson³, Jacqueline Smith², Kai Tobias Block^{1,2}, Daniel K Sodickson^{1,2}, and Noam Ben-Eliezer^{1,2}
- ¹Center for Advanced Imaging Innovation and Research (CAI2R), New York University School of Medicine, New York, NY, United States, ²The Bernard and Irene Schwartz Center for Biomedical Imaging, Department of Radiology, New York University School of Medicine, New York, NY, United States, ³Department of Radiology, New York University School of Medicine, New York, NY, United States*
- Accurate quantification of T₂ values in vivo is a long-standing challenge hampered by the inherent inaccuracy associated with rapid multi-SE sequences. This inaccuracy is, moreover, not constant and depends on both the pulse sequence scheme and parameter-set employed, resulting in different vendors or scanners yielding different results! We used a recently developed novel T₂ mapping technique, the **EMC** algorithm, to quantify T₂ changes in different brain regions of MS patients. Our results demonstrate that the robustness of the EMC approach allows the detection of subtle, but statistically significant T₂ differences in normal appearing brain regions for MS patients.
-
- 4059
Computer #32
Ultra-high Resolution MRSI of Multiple Sclerosis at 7T
Bernhard Strasser¹, Gilbert Hangel¹, Michal Považan¹, Stephan Gruber¹, Marek Chmelik¹, Assunta Dal-Bianco², Fritz Leutmezer², Siegfried Trattnig^{1,3}, and Wolfgang Bogner¹
- ¹MRCE, Department of Biomedical Imaging and Image-guided Therapy, Medical University of Vienna, Vienna, Austria, ²Department of Neurology, Medical University of Vienna, Vienna, Austria, ³Christian Doppler Laboratory for Clinical Molecular MR Imaging, Vienna, Austria*
- In this study fourteen MS patients were measured with an FID-based MRSI sequence at 7T with resolutions of 64x64 and 100x100. Metabolic maps of total NAA, total Choline, total Creatine, and myo-Inositol were compared to FLAIR images. All patients had lesions with decreased tNAA, and eight had increased myo-Inositol levels. However, not all lesions showed decreased tNAA values. Two patients showed decreased tNAA levels with no visible lesion on the FLAIR image. In average, a decrease of 26% in tNAA and an increase of 42% in myo-Inositol were observed in comparison to normal appearing white matter.
-
- 4060
Computer #33
BA 4p BOLD response profile distinguishes low and high MS morbidity
Adnan A.S. Alahmadi^{1,2}, Matteo Pardini^{1,3}, Rebecca S. Samson¹, Egidio D'Angelo^{4,5}, Karl J. Friston⁶, Ahmed T. Toosy^{1,7}, and Claudia Angela Michela Gandini Wheeler-Kingshott^{1,5}
- ¹NMR Research Unit, Queen Square MS Centre, Department of Neuroinflammation, UCL Institute of Neurology, London, United Kingdom, ²Department of Diagnostic Radiology, Faculty of Applied Medical Science, KAU, Jeddah, Saudi Arabia, ³Department of Neurosciences, Ophthalmology and Genetics, University of Genoa, Genoa, Italy, ⁴Department of Brain and Behavioral Sciences, University of Pavia, Pavia, Italy, ⁵Brain Connectivity Center, C.Mondino National Neurological Institute, Pavia, Italy, Pavia, Italy, ⁶Wellcome Centre for Imaging Neuroscience, UCL, Institute of Neurology, London, United Kingdom, ⁷NMR Research Unit, Department of Brain Repair and Rehabilitation, Queen Square MS Centre, UCL Institute of Neurology, London, United Kingdom*
- This study investigates how multiple sclerosis (MS) selectively affects regional BOLD response to variable grip forces (GF). It is known that the anterior and posterior BA4 areas are anatomically and functionally distinguishable – and that in healthy subjects there are linear and non-linear BOLD response components. After modelling BOLD responses with a polynomial expansion of the applied GF during task, we showed that in BA4a MS subjects respond like healthy subjects. BOLD response in BA4p, instead, was altered in MS, with those with greatest disability showing the greatest deviations from the non-linear profile of the healthy response.
-
- 4061
Computer #34
Functional cognitive control load in multiple sclerosis
Paola Valsasina¹, Maria Assunta Rocca¹, Laura Vacchi¹, Alessandro Meani¹, Mariaemma Rodegher², Vittorio Martinelli², Giancarlo Comi², Andrea Falini³, and Massimo Filippi¹
- ¹Neuroimaging Research Unit, San Raffaele Scientific Institute, Vita-Salute San Raffaele University, Milan, Italy, ²Department of Neurology, San Raffaele Scientific Institute, Vita-Salute San Raffaele University, Milan, Italy, ³Department of Neuroradiology, San Raffaele Scientific Institute, Vita-Salute San Raffaele University, Milan, Italy*
- In this study, we investigated behavioral and functional MRI (fMRI) correlates of a N-back task in 72 patients with multiple sclerosis (MS). We found a load-dependent alteration of executive network recruitment, varying according to the disease phenotype. Increased recruitment of frontal regions was associated to the early phase of MS. Conversely, the modulation of regions belonging to the default mode network was more evident in patients with long-lasting disease and was related to the global cognitive profile, suggesting an increased need of cognitive resources to cope with task-demand.
-
- 4062
Formation of transient and persistent multiple sclerosis lesions: serial follow-up with quantitative MR imaging and spectroscopy

Computer #35 Ivan Kirov^{1,2}, Shu Liu^{1,2}, Assaf Tal³, William E. Wu^{1,2}, Matthew S. Davitz^{1,2}, James S. Babb^{1,2}, Henry Rusinek^{1,2}, Joseph Herbert⁴, and Oded Gonen^{1,2}

¹Center for Advanced Imaging Innovation and Research (CAI2R), New York University School of Medicine, New York, NY, United States, ²Bernard and Irene Schwartz Center for Biomedical Imaging, New York University School of Medicine, New York, NY, United States, ³Chemical Physics, Weizmann Institute of Science, Rehovot, Israel, ⁴Neurology, New York University Langone Medical Center, New York, NY, United States

Using MR imaging and proton spectroscopy, we follow the evolution of transient and persistent multiple sclerosis lesions from pre-lesional state to long-term (over 2 years post-formation) status. The main finding was that the sharp drop in *N*-acetyl-aspartate associated with the formation of an acute lesion was reversible in resolving, but not in persisting black holes, substantiating the idea that transient new lesions revert to pre-lesional axonal state. The additional findings were a decrease in creatine after the appearance of a persisting lesion and the lack of metabolic differences between pre-lesional tissue giving rise to resolving versus persisting lesions.

4063
Computer #36 Assessment of grey matter cortical lesions in Multiple Sclerosis using high resolution ASL at 7T
Richard J Dury¹, Molly G Bright¹, Yasser Falah², Penny A Gowland¹, Nikos Evangelou², and Susan T Francis¹

¹Sir Peter Mansfield Imaging Centre, University of Nottingham, Nottingham, United Kingdom, ²Nottingham University Hospital, University of Nottingham, Nottingham, United Kingdom

Grey matter cortical lesions have been associated with physical disability, cognitive impairment and fatigue in Multiple Sclerosis. Only one previous study has assessed cerebral blood flow (CBF) and cerebral blood volume (CBV) within cortical lesions. Here we use high spatial resolution 7T FAIR TrueFISP ASL to assess the perfusion in grey matter cortical lesions and compare this to surrounding normal appearing grey matter. Cortical lesions showed a significant 32% reduction in perfusion signal compared to normal appearing grey matter. This ASL method can be used to evaluate longitudinal perfusion changes in new and chronic cortical lesions.

4064
Computer #37 Energy dysregulation and neuro-axonal dysfunction in multiple sclerosis measured in-vivo with diffusion-weighted spectroscopy
Benedetta Bodini¹, Francesca Branzoli^{1,2}, Emilie Poirion¹, Daniel Garcia-Lorenzo^{1,2}, Elisabeth Maillart¹, Julie Socha¹, Geraldine Bera¹, Itamar Ronen³, Stephane Lehericy^{1,2}, and Bruno Stankoff¹

¹Brain and Spine Institute, INSERM U1127, Sorbonne Universités, UPMC, CHU Pitié-Salpêtrière, Paris, France, ²Brain and Spine Institute, Center for Neuroimaging Research (CENIR), CHU Pitié-Salpêtrière, Paris, France, ³C.J. Gorter Center for High Field MRI, Radiology, Leiden University Medical Center, Leiden, Netherlands

Diffusion-weighted spectroscopy (DWS), allowing to measure in-vivo the diffusion properties of endogenous intracellular metabolites such as total *N*-acetyl-aspartate (tNAA) and total creatine (tCr), offers the opportunity to explore the early phase of neuronal structural damage and energetic mismatch in multiple sclerosis (MS). We compared the apparent diffusion coefficient (ADC) of tNAA and tCr in 25 patients with MS and 20 healthy volunteers, and found a reduced diffusivity of both metabolites in patients, both in the corona radiata and in the thalami. These results may reflect an ongoing neuro-axonal damage and a simultaneous energy dysregulation affecting neurons and/or glial cells in MS.

4065
Computer #38 *N*-acetyl aspartate predicts disease severity in an animal model of multiple sclerosis (MS)
Amber Michelle Hill¹, Mohamed Tachrount², David L Thomas³, Kenneth J Smith⁴, Xavier Golay⁵, and Olga Ciccarelli¹

¹NMR Research Unit, Queen Square MS Centre, Department of Neuroinflammation, UCL Institute of Neurology, University College London, London, United Kingdom, ²Department of Brain Repair and Rehabilitation, UCL Institute of Neurology, University College London, London, United Kingdom, ³Leonard Wolfson Experimental Neurology Centre, UCL Institute of Neurology, University College London, London, United Kingdom, ⁴Department of Neuroinflammation, Queen Square MS Centre, UCL Institute of Neurology, University College London, London, United Kingdom, ⁵Department of Brain Repair and Rehabilitation, Queen Square MS Centre, UCL Institute of Neurology, University College London, London, United Kingdom

EAE, an animal model of MS, can be investigated with MR to address the clinical need to understand mechanisms of the MS disease course. Longitudinal MR studies with EAE are currently under-explored. This study investigated longitudinal changes in metabolite concentrations and lesion development, in relation to neurological deficits in EAE, using 9.4T MRI and ¹H-MRS. Five time-points of EAE disease progression were assessed. The results suggest that before visible signs of neurological deficits, higher [NAA] predicts the severity of late-stage neurological deficits in EAE. Considering NAA is predominantly associated with neuronal mitochondria, this may reflect relevant pathological processes in MS.

4066
Computer #39 Longitudinal follow-up of chronic multiple sclerosis lesions with quantitative MR imaging and partial volume-corrected proton MR spectroscopy
Ivan Kirov^{1,2}, Shu Liu^{1,2}, Assaf Tal³, William E. Wu^{1,2}, Matthew S. Davitz^{1,2}, James S. Babb^{1,2}, Henry Rusinek^{1,2}, Joseph Herbert⁴, and Oded Gonen^{1,2}

¹Center for Advanced Imaging Innovation and Research (CAI2R), New York University School of Medicine, New York, NY, United States, ²Bernard and Irene Schwartz Center for Biomedical Imaging, New York University School of Medicine, New York, NY, United States, ³Chemical Physics, Weizmann Institute of Science, Rehovot, Israel, ⁴Neurology, New York University Langone Medical Center, New York, NY, United States

We describe the evolution of chronic multiple sclerosis lesions from a quantitative MR imaging and spectroscopy perspective. Metabolite concentrations were obtained along with measures of lesion T1-hypointensity and size. Moderately hypointense lesions were more metabolically active than severely hypointense lesions, driving an increase in the glial marker myo-inositol. Correlational analyses

revealed that lesion size is a better predictor of axonal health than T1-hypointensity, with lesions larger than 1.5 cm³ exhibiting terminal axonal injury. A positive correlation between changes in choline and in lesion size in moderately hypointense lesions implied that changes in lesion size are mediated by chronic inflammation.

-
- 4067
Computer #40 2D Localised Correlated Spectroscopy (L-COSY): A potential tool for identifying biochemical changes in Multiple Sclerosis
Jameen ARM¹, Scott Quadrelli², Karen Ribbons³, Jeanette Lechner-Scott³, and Saadallah Ramadan⁴
- ¹Imaging, HMRI, Newcastle, Australia, ²Imaging, TRI Brisbane, Brisbane, Australia, ³Neurology, John Hunter Hospital, Newcastle, Australia, ⁴Faculty of Health and Medicine, University of Newcastle, Newcastle, Australia*
- ¹H Magnetic Resonance Spectroscopic techniques (1H-MRS) have been utilised to assess inflammatory nature of both acute and chronic lesions as well as normal appearing brain tissue to understand the neuro degenerative irreversible component of multiple sclerosis (MS) from early stages¹⁻³. However, due to high spectral overlap in one-dimensional (1D) ¹H-MRS, it has been challenging to establish a standard specific spectral pattern in plaques or normal appearing brain tissues. L-COSY might provide the needed spectral dispersion
-
- 4068
Computer #41 Multiple Sclerosis: Assessment of normal-appearing white matter hypoperfusion with DCE MRI
Michael Ingrischi¹, Steven Sourbron², Moritz Schneider¹, Sina Herberich³, Tania Kumpfel⁴, Reinhard Hohlfeld⁴, Maximilian Reiser³, and Birgit Ertl-Wagner³
- ¹Josef-Lissner-Laboratory for Biomedical Imaging, Institute for Clinical Radiology, Ludwig-Maximilians-University Munich, Munich, Germany, ²Leeds Institute of Cardiovascular and Metabolic Medicine, University of Leeds, Leeds, United Kingdom, ³Institute for Clinical Radiology, Ludwig-Maximilians-University Munich, Munich, Germany, ⁴Institute for Clinical Neuroimmunology, Ludwig-Maximilians-University Munich, Munich, Germany*
- Several studies have reported diffuse hypoperfusion in normal-appearing white matter (NAWM) in patients with relapsing-remitting multiple sclerosis (RR-MS). Here, we investigate this issue using dynamic contrast-enhanced (DCE) MRI. The statistical power of a DCE-MRI acquisition to reveal hypoperfusion was estimated for n=16 patients at 96% using a Monte-Carlo simulation. 24 patients with RR-MS and 16 healthy controls underwent a DCE-MRI examination and cerebral blood flow (CBF), cerebral blood volume (CBV) and permeability-surface area product (PS) were quantified in NAWM, revealing no significant differences between groups. This indicates that, in our patient cohort, NAWM hypoperfusion is much less pronounced than in previous DSC studies.
-
- 4069
Computer #42 Structural connectivity in multiple sclerosis and simulation of disconnection
Elisabetta Pagani¹, Maria Assunta Rocca^{1,2}, Ermelinda De Meo¹, Bruno Colombo², Mariaemma Rodegher², Giancarlo Comi², Andrea Falini³, and Massimo Filippi^{1,2}
- ¹Neuroimaging Research Unit, San Raffaele Scientific Institute, Vita-Salute San Raffaele University, Milan, Italy, ²Department of Neurology, San Raffaele Scientific Institute, Vita-Salute San Raffaele University, Milan, Italy, ³Department of Neuroradiology, San Raffaele Scientific Institute, Vita-Salute San Raffaele University, Milan, Italy*
- Aim of the study was to quantify structural connectivity integrity in multiple sclerosis (MS) patients with different clinical phenotypes, to simulate a disconnection due to T2 visible lesions and to test its effect on network based measures. Diffusion tensor MRI was obtained from 239 MS patients and 131 healthy controls; connectivity matrices were produced and then artificially disconnected based on T2 visible lesion distribution. Global and nodal network metrics were calculated for both cases. Crucial nodes of the network were found to be different in strength between MS phenotypes. Disconnection simulation highlighted the role of T2 lesions in determining structural connectivity abnormalities.
-
- 4070
Computer #43 Preliminary Experience Using Magnetic Resonance Fingerprinting in Multiple Sclerosis
Anagha Deshmane¹, Kunio Nakamura², Deepti K Guruprakash², Yun Jiang¹, Dan Ma³, Jar-Chi Lee⁴, Elizabeth Fisher⁵, Richard A. Rudick⁵, Jeffrey A. Cohen⁶, Mark J. Lowe⁶, Daniel Ontaneda⁶, Mark A. Griswold^{1,3}, and Vikas Gulani^{1,7}
- ¹Biomedical Engineering, Case Western Reserve University, Cleveland, OH, United States, ²Biomedical Engineering, Cleveland Clinic, Cleveland, OH, United States, ³Radiology, Case Western Reserve University, Cleveland, OH, United States, ⁴Quantitative Health Sciences, Cleveland Clinic, Cleveland, OH, United States, ⁵Biogen, Boston, MA, United States, ⁶Mellen Center for Multiple Sclerosis Research and Treatment, Cleveland Clinic, Cleveland, OH, United States, ⁷Radiology, University Hospitals, Cleveland, OH, United States*
- Magnetic Resonance Fingerprinting (MRF) is used to simultaneously map T₁, T₂, and spin density in the normal appearing white matter and normal appearing grey matter of multiple sclerosis patients and healthy controls. Relaxation parameters measured by MRF are found to be significantly different between MS subjects and healthy controls, to distinguish between relapsing remitting MS and secondary progressive MS in certain brain structures, and to correlate with clinical measures of function and disability.
-
- 4071
Computer #44 QSM is sensitive to myelin changes just beyond the boundaries of conventional T2 lesion detection
Sneha Pandya¹, Yan Zhang¹, Thanh Nguyen¹, Yi Wang¹, Susan A Gauthier², and Sneha Pandya¹
- ¹Department of Radiology, Weill Cornell Medicine, New York, NY, United States, ²Department of Neurology, Weill Cornell Medicine, New York, NY, United States*
- MRI-derived measures of lesion accrual and tissue loss have acquired a central role in the understanding of MS disease evolution, pathogenesis of symptoms, and prediction of clinical outcome. Conventional MRI imaging is highly sensitive for detection of MS lesions,

which are characteristically hyperintense on a T2 weighted images, however this technique lacks pathological specificity. QSM can help identify myelin and iron content changes during an MS lesion's lifetime.

-
- 4072
Computer #45 Influence of cognitive impairment and depression on cortical thinning in patients with multiple sclerosis
Paola Valsasina¹, Maria Assunta Rocca¹, Emanuele Pravata^{1,2}, Gianna Riccitelli¹, Giancarlo Comi³, Andrea Falini⁴, and Massimo Filippi¹
- ¹Neuroimaging Research Unit, San Raffaele Scientific Institute, Vita-Salute San Raffaele University, Milan, Italy, ²Department of Neuroradiology, Neurocenter of Southern Switzerland, Lugano, Switzerland, ³Department of Neurology, San Raffaele Scientific Institute, Vita-Salute San Raffaele University, Milan, Italy, ⁴Department of Neuroradiology, San Raffaele Scientific Institute, Vita-Salute San Raffaele University, Milan, Italy
- In this study, we investigated cortical thickness abnormalities associated with cognitive impairment and depression in 126 patients with multiple sclerosis (MS). Compared with controls, MS patients exhibited a widespread bilateral cortical thinning involving all brain lobes. While cognitive impairment was associated with atrophy of regions located in the fronto-parietal lobes (including the middle and superior frontal gyrus, the inferior parietal lobule and the precuneus), depression was linked to atrophy of the orbitofrontal cortex. This study shows that cortical thickness analysis was able to detect specific effects of clinical symptoms on cortical atrophy in MS.
-
- 4073
Computer #46 CE-MRV with concordant 4D flow MRI and ultrasound reveals no internal jugular venous outflow obstruction in multiple sclerosis
Eric Schrauben¹, Sarah Kohn², Samuel Frost², Oliver Wieben^{2,3}, and Aaron Field²
- ¹Centre for Advanced MRI, University of Auckland, Auckland, New Zealand, ²Radiology, University of Wisconsin - Madison, Madison, WI, United States, ³Medical Physics, University of Wisconsin - Madison, Madison, WI, United States
- Contrast-enhanced MR venography scoring in internal jugular veins is performed and compared with 4D flow MRI and ultrasound assessment in patients with multiple sclerosis, patients with other neurological disorders and healthy controls. Narrowing assessment is shown to be more variable in flow MRI and ultrasound.
-
- 4074
Computer #47 Multimodal Characterization of Grey Matter Alterations in Neuromyelitis Optica
Yaou Liu¹, Yunyun Duan², Huiqing Dong², Tianyi Qian², Frederik Barkhof³, Jinhui Wang⁴, and Kuncheng Li²
- ¹Xuanwu Hospital, Capital Medical University, Beijing, China, People's Republic of, ²Beijing, China, People's Republic of, ³Amsterdam, Netherlands, ⁴Hanzhou, China, People's Republic of
- Combining double-inversion-recovery (DIR), high-resolution structural MRI, diffusion tensor imaging (DTI) and resting-state functional MRI (rs-fMRI), this study systematically investigated structural and functional alterations in grey-matter (GM) structures in thirty-five neuromyelitis optica (NMO) patients compared with healthy controls. We demonstrated that NMO exhibits both structural and functional alterations of GM in the cerebrum and cerebellum. Multimodal MRI techniques complementary worked to capture NMO-related GM abnormalities. GM alterations, especially diffusion abnormalities, correlated with cognitive impairment in NMO. These findings have important implications for understanding the roles of GM damage and also for highlighting multimodal MRI techniques as objective biomarkers in NMO.
-
- 4075
Computer #48 A longitudinal assessment of brain iron using quantitative susceptibility mapping (QSM) in multiple sclerosis (MS) over 2 years
Ferdinand Schweser^{1,2}, Nicola Bertolino¹, Michael G Dwyer¹, Jesper Hagemeier¹, Paul Polak¹, Niels P Bergsland^{1,3}, Andreas Deistung⁴, Bianca Weinstock-Guttman⁵, Jürgen R Reichenbach^{4,6}, and Robert Zivadinov^{1,2}
- ¹Buffalo Neuroimaging Analysis Center, Department of Neurology, Jacobs School of Medicine and Biomedical Sciences, The State University of New York at Buffalo, Buffalo, NY, United States, ²MRI Molecular and Translational Research Center, Jacobs School of Medicine and Biomedical Sciences, The State University of New York at Buffalo, Buffalo, NY, United States, ³MR Research Laboratory, IRCCS Don Gnocchi Foundation ONLUS, Milan, Italy, ⁴Medical Physics Group, Department of Diagnostic and Interventional Radiology, Jena University Hospital - Friedrich Schiller University Jena, Jena, Germany, ⁵Department of Neurology, Jacobs School of Medicine and Biomedical Sciences, The State University of New York at Buffalo, Buffalo, NY, United States, ⁶Michael Stifel Center for Data-driven and Simulation Science Jena, Friedrich Schiller University Jena, Jena, Germany
- Quantitative susceptibility mapping (QSM) is the most sensitive technique currently available to study brain iron *in vivo*. The technique opens the door to a longitudinal assessment of brain iron, bearing the potential to understand and disentangle factors resulting in the large scatter of reported iron concentrations in later decades of life.
- In the present work, we investigated longitudinal changes of brain magnetic susceptibility in a cohort of 40 healthy controls (HCs) and 160 multiple sclerosis (MS) patients over a period of 2 years.
-

Electronic Poster

Neuroimaging: Novel Techniques

Exhibition Hall

Wednesday, May 11, 2016: 16:00 - 17:00

-
- 4076
Computer #49 LONG TERM EFFECTS OF SINGLE VS. REPEATED LOW INTENSITY PULSED FOCUSED ULTRASOUND TREATMENT WITH MICROBUBBLES
Zsofia I. Kovacs¹, Tsang-Wei Tu¹, Georgios Z. Papadakis^{1,2}, William C. Reid², Dima A. Hammoud², and Joseph A. Frank^{1,3}

¹Frank Laboratory, Radiology and Imaging Sciences, National Institutes of Health, Bethesda, MD, United States, ²Center for Infectious Disease Imaging (CID), Radiology and Imaging Sciences, National Institutes of Health, Bethesda, MD, United States, ³National Institute of Biomedical Imaging and Bioengineering, National Institutes of Health, Bethesda, MD, United States

One potential issue for using MR-guided pulsed Focused Ultrasound (pFUS) to open the blood brain barrier (BBB) is the lack of data on the long term effects. Safety determination in the brain have been limited to the MR characterization after repeated BBB opening that can be achieved without hemorrhage, edema and behavioral changes in non-human primates (Arvanitis, et al. 2015; Downs, et al. 2015). We use multimodal imaging technics to characterize long term effects of pFUS + MB in the rat brain.

4077

Computer #50

MRI of Peripheral Nerve: MT of Short T2 Components, Susceptibility and Diffusion Weighting of Collagen Components
Sameer Shah¹, Qun He¹, Micheal Carl², Justin Brown¹, Mark Mahan³, Graeme M. Bydder¹, and Nikolaus M. Szevenenyi¹

¹University of California, San Diego, San Diego, CA, United States, ²Global MR Applications & Workflow, General Electric, San Diego, CA, United States, ³Clinical Neurosciences Center, University of Utah, Salt Lake City, UT, United States

The objective of this paper is to describe the use of several new approaches for magnetic resonance (MR) imaging of peripheral nerves. MR examinations were performed on fresh human median, tibial and sciatic nerve samples, as well as cadaveric forearms at 3T and/or 11.7T as well as one fresh human median nerve sample. Application of MR techniques used elsewhere in the body, and the use of MR microscopy show a variety of new imaging findings in peripheral nerve. This approach is likely to improve understanding of the MR appearances of peripheral nerve and lead to improved experimental and clinical studies.

4078



Computer #51

Convex Optimized Diffusion Encoding (CODE) for Improved SNR in Diffusion-Weighted Neuro MRI
Eric Aliotta^{1,2}, Holden H Wu^{1,2}, and Daniel B Ennis^{1,2}

¹Radiological Sciences, UCLA, Los Angeles, CA, United States, ²Biomedical Physics IDP, UCLA, Los Angeles, CA, United States

Spin Echo EPI Diffusion Weighted MRI (SE-EPI DWI) is widely used for neuro applications because of its speed. Conventional SE-EPI DWI approaches, however, often require long echo times (TE) which degrade SNR. Because SNR is inherently limited in high b-value DWI, TE must be kept as short as possible to ensure high-quality DWI. A Convex Optimized Diffusion Encoding (CODE) framework was developed to design waveforms which eliminate sequence dead times and minimize TE. CODE gradients were designed and implemented on a 3.0T scanner and demonstrated improved SNR in neuro DWI for healthy volunteers.

4079

Computer #52

Role of MR cerebrospinal fluid flow study in assessment of Ventriculomegaly in the Elderly
Mona ElSheikh¹, AbdelAziz ElNekiedy¹, Ihab Samy Reda¹, and Tarek Rashad Saleh¹

¹Radiology, Alexandria University Hospitals, Alexandria, Egypt

Elderly patients often present with ventriculomegaly, not only with normal aging, but also due to a multitude of neurological disorders. The aim of this work was to study the role of MR CSF flow studies in assessment of elderly patients with ventriculomegaly. We identified variable underlying causes of ventriculomegaly in 20 elderly subjects including communicating hydrocephalus, obstructive hydrocephalus, and age-related cerebral atrophy.

4080

Computer #53

Morphometric analysis of cerebrospinal fluid alterations by MRI for spontaneous intracranial hypotension patients before and after treatments

Hui-Feng Ho^{1,2}, Hung-Chieh Chen², Hsin Tung³, Yi-Hsin Tsai⁴, Yi-Ying Wu², Jyh-Wen Chai^{2,4}, Clayton Chi-Chang Chen², Shin-Lei Peng¹, Wu-Chung Shen¹, and Tzu-Ching Shih¹

¹Biomedical Imaging and Radiological Science, China Medical University, Taichung, Taiwan, ²Radiology, Taichung Veterans General Hospital, Taichung, Taiwan, ³Neurological Institute, Taichung Veterans General Hospital, Taichung, Taiwan, ⁴College of Medicine, China Medical University, Taichung, Taiwan

Cerebrospinal fluid (CSF) is the fluid circulating through the subarachnoid space and providing a neuroprotective function as a hydraulic cushion for the brain and the spinal cord. CSF not only plays a vital role for normal brain function, but also serves numerous important functions in the central nervous system. However, CSF leaks are a key cause of new-onset headaches. Despite numerous reports characterizing CSF and its circulation in subarachnoid space, our understanding of CSF leakage remains limited. In this study, we calculate the CSF volumes in the brain and the spine of SIH patients using T2-weighted MRI images.

4081

Computer #54

Magnetic resonance spectroscopy reveals oral lactobacillus promotion of increases in brain GABA, N-acetyl aspartate and glutamate
Rafal Janik¹, Lysie A.M. Thomason², and Greg J. Stanisz^{1,2,3}

¹Medical Biophysics, University of Toronto, Toronto, ON, Canada, ²Physical Sciences, Sunnybrook Research Institute, Toronto, ON, Canada, ³Department of Neurosurgery and Pediatric Neurosurgery, Medical University of Lublin, Lublin, Poland

We previously have demonstrated that administration of Lactobacillus rhamnosus (JB-1) to healthy male BALB/c mice, promotes consistent changes in GABA-A and -B receptor subtypes in specific brain regions, accompanied by reductions in anxiety and depression-related behaviours. In the present study, using magnetic resonance spectroscopy (MRS), we quantitatively assessed two clinically

validated biomarkers of brain activity and function, glutamate + glutamine (Glx) and total N-acetyl aspartate + N-acetylaspartylglutamic acid (tNAA), as well as GABA, the chief brain inhibitory neurotransmitter.

-
- 4082
Computer #55
Analysis of brain volume in a 19 year-old extremely-preterm born cohort
Andrew Melbourne¹, Eliza Orasanu¹, Zach Eaton-Rosen¹, Manuel J Cardoso¹, Joanne Beckmann², Lorna Smith³, David Atkinson³, Neil Marlow², and Sebastien Ourselin¹
- ¹Medical Physics and Biomedical Engineering, University College London, London, United Kingdom, ²Institute for Women's Health, University College London, London, United Kingdom, ³University College Hospital, London, United Kingdom*
- This abstract presents an analysis of brain tissue volume in a cohort of 69 extremely preterm born young adults and 50 term-born controls at 19 years of age.
-
- 4083
Computer #56
MEMRI Detection of Neuronal Activity Following Acute and Chronic Nicotine Exposure in Rats
Aditya N Bade¹, Jingdong Dong², Howard E Gendelman¹, Michael D Boska^{1,3}, and Yutong Liu^{1,3}
- ¹Department of Pharmacology and Experimental Neuroscience, University of Nebraska Medical Center, Omaha, Omaha, NE, United States, ²Second Affiliated Hospital, Dalian Medical University, Dalian, China, People's Republic of, ³Department of Radiology, University of Nebraska Medical Center, Omaha, Omaha, NE, United States*
- Rats with acute and chronic nicotine exposure were studied using manganese-enhanced MRI (MEMRI). Neuronal activity was found on nucleus accumbens and hippocampus in rats with acute nicotine exposure, and on nucleus accumbens and hippocampus, prefrontal and insular cortex. The neuronal activity was confirmed by immunohistology. The above-mentioned brain regions are believed to play roles in drug addiction. We demonstrate that MEMRI can be used to assess neuroadaptations from nicotine addiction.
-
- 4084
Computer #57
Mapping of Time and Space Spatial Preferences in the Hippocampus
Shir Hofstetter¹ and Yaniv Assaf²
- ¹sagol school of neuroscience, tel aviv university, tel aviv, Israel, ²tel aviv university, tel aviv, Israel*
- The hippocampus plays an important role in spatial and non-spatial episodic memory. Using DTI, a micro-structural probe sensitive to rapid neuroplasticity, and the Morris water maze, we investigated spatial preference for place and time in the hippocampus as revealed by changes in diffusion indices induced by learning of a specific location in the maze and the overall training experience. We were able to find a system-level mapping of space and time in the rat hippocampus.
-
- 4085
Computer #58
Cortical folding patterns in extremely preterm born young adults
Eliza Orasanu¹, Andrew Melbourne¹, Zach Eaton-Rosen¹, David Atkinson², Alexandra Saborowska³, Joanne Beckmann⁴, Neil Marlow⁴, and Sebastien Ourselin¹
- ¹Translational Imaging Group, Centre for Medical Image Computing, University College London, London, United Kingdom, ²University College London, London, United Kingdom, ³University College Hospital, London, United Kingdom, ⁴Institute for Women's Health, University College London, London, United Kingdom*
- Preterm born individuals may be subject to abnormal gyrification, associated with behavioural-cognitive deficit. In this work we perform a cortical folding analysis of the white-grey matter boundary in extremely preterm born young adults when compared to their term born peers, through a groupwise analysis using joint spectral matching. The results show that there are significant differences in folding in the temporal lobe, results which could be connected with poor executive function and language deficits in the extremely preterm cohort.
-
- 4086
Computer #59
Evaluation of Whole-Body Iron Loading in Transfusion-Dependent Patients with Quantitative Susceptibility Imaging
Zhang Xiaoqi¹, Ni Hongyan¹, and Qian Tianyi²
- ¹Tianjin First Central Hospital, Tianjin, China, People's Republic of, ²MR Collaboration NE Asia, Siemens Healthcare, Beijing, China, People's Republic of*
- To quantify the iron loading in the whole body among transfusion-dependent patients, 32 transfusion-dependent patients and 32 healthy volunteers were recruited to participate in this study. The quantitative susceptibility mapping was processed to get the susceptibility of the ROIs in the brain, and T2* values of their livers, pancreas and myocardium. Significantly higher iron levels in the putamen were found in transfusion-dependent patients (right/left=0.147±0.066/0.149±0.811 ppm) compared with healthy controls(right/left=0.064±0.037/0.060±0.326ppm) ($P=0.021/0.011$). A ROC curve was performed, and the results suggested that liver T2* and pancreas T2* values can be great predictors to diagnose the iron overload in the brain (AUC=0.877, 0.974, $P<0.01$).
-
- 4087
Computer #60
Reproducibility of Cerebral Blood Flow Measurements Across MR Systems: A Matter of Magnet Geometry
Bogdan G Mitrea¹, Ralf B Loeffler¹, Ruitian Song¹, and Claudia M Hillenbrand¹
- ¹Diagnostic Imaging, St Jude Children's Research Hospital, Memphis, TN, United States*

For longitudinal investigations reproducibility and accuracy of ASL measurements are of essence. The purpose of this study is to investigate how magnet design and labeling position within the magnet impact CBF quantification. Our results indicate that CBF values are not always reproducible in our ultra-short wide bore scanner. Great variability may be introduced by the actual position of the labeling slice with respect to the magnet isocenter. The exact cause of this difference requires further investigation. However, positioning the labeling slice in isocenter provided a simple solution to overcome this issue and to measure reproducible CBF values.

4088
Computer #61 Quantitative pH using chemical exchange saturation transfer and phosphorous spectroscopy
Zhuozhi Dai^{1,2}, Phillip Zhe Sun³, Gang Xiao⁴, Gen Yan², Yanlong Jia², Zhiwei Shen⁵, Alan H. Wilman¹, and Renhua Wu^{2,5}

¹Biomedical engineering, University of Alberta, Edmonton, AB, Canada, ²Medical Imaging, 2nd Affiliated Hospital of Shantou University Medical College, Shantou, China, People's Republic of, ³Athinoula A. Martinos Center for Biomedical Imaging, Department of Radiology, MGH and Harvard Medical School, Charlestown, MA, United States, ⁴Math and Information Technology, Hanshan Normal University, Chaozhou, China, People's Republic of, ⁵Provincial key laboratory of medical molecular imaging, Shantou, China, People's Republic of

pH is a very important biochemical property that changes in many pathological states. Monitoring pH is of significance in early diagnosis and treatment therapy. However, there is lack of non-invasive methods to image pH in vivo effectively. Our study quantified the pH value using a chemical exchange saturation transfer (CEST) method in rat brain and established a strong correlation of pH between CEST and 31P-MRS in vivo, Pearson correlation factor is 0.819, $P < 0.01$. Because CEST imaging has superior spatial resolution to 31P-MRS, CEST may provide an alternative, straightforward, and effective way to obtain quantitative pH images in vivo.

4089
Computer #62 Double-tuned (¹H/²³Na) vs. clinically used ¹H coil – Intraindividual comparison of image quality
Melissa M Ong¹, Alexander Schmidt¹, Daniel Hausmann¹, Stefan O Schoenberg¹, and Stefan Haneder¹

¹Institute of Clinical Radiology and Nuclear Medicine, University Medical Center Mannheim, Mannheim, Germany

Although ²³Na-MRI can offer additional information regarding tissue function and viability compared to ¹H-MRI several obstacles have impeded its clinical implementation, including hardware costs and technical challenges. One step towards a more widespread clinical use of ²³Na-MRI would be the use of double-tuned (¹H/²³Na) coils. This would require morphologic and functional images with diagnostic image quality. The purpose of this study was therefore to prospectively compare image quality of a double-tuned (¹H/²³Na) vs. a clinically used ¹H head coil in healthy subjects. Image data of both coils showed excellent image quality with no significant differences in SNR.

4090
Computer #63 Diffusion-weighted MR Imaging and Spectroscopy reveal brain tissue alterations induced by ionizing radiation in the mouse brain
Elodie A. Pérès^{1,2}, Fawzi Boumezbeur¹, Olivier Etienne², Antoine Grigis¹, François D. Boussin², and Denis Le Bihan¹

¹UNIRS, NeuroSpin, I2BM, Life Sciences Division, Commissariat à l'Energie Atomique, Gif-sur-Yvette, France, ²Laboratoire de Radiopathologie, SCSR, iRCM, UMR 967, Life Sciences Division, Commissariat à l'Energie Atomique, Fontenay-aux-Roses, France

Patients frequently suffer from cognitive impairments following brain radiotherapy. Ionizing radiations are known to induce various brain alterations and impair neurogenesis. Following whole cerebral irradiation (3X5 Gy), we found significant changes in non-Gaussian water diffusion parameters (ADC₀ and kurtosis) and related S-index, a new diffusion biomarker sensitive to changes in tissue microstructure, in the subventricular zone, a site of adult neurogenesis and in the olfactory bulbs. MRS exhibited a longitudinal decrease in taurine specifically in the olfactory bulbs. These results suggest that diffusion MRI and MRS could be used to monitor changes induced by radiation injury.

4091
Computer #64 Magnetic Resonance Imaging de-noising using the squared eigenfunctions of the Schrödinger operator: Application to brain MRI data.
Jiayu Zhang¹, Taous Meriem Laleg¹, Stephanie Bogaert², Rik Achten^{2,3}, and Hacene Serrai^{2,3}

¹Computer, Electrical and Mathematical Sciences and Engineering, King Abdullah University of Science and Technology (KAUST), Thuwal, Saudi Arabia, ²Department of Radiology, University Hospital of Gent, gent, Belgium, ³University of Gent, Gent, Belgium

A magnetic resonance imaging denoising method based upon the spectral analysis of the shrodinger operator is proposed. The method called semi-classical signal analysis SCSA, employs an adaptive filter to represent the MRI image as a set of useful vectors and others representing noise. The separation between signal and noise vectors is achieved using a soft and efficient threshold. Method validation is achieved on anatomical brain images acquired with low signal to noise ratio. The obtained results demonstrate that the SCSA is efficient in reducing noise while preserving image details necessary for accurate image diagnosis.

4092
Computer #65 Susceptibility Weighted Imaging in the Early Stages of Hypoxia
Sarah C Wayne¹, Victoria Sherwood¹, Ravjit Sagoo¹, Eddie Ng'andwe¹, Charles E Hutchinson^{1,2}, and Christopher HE Imray^{1,2}

¹University Hospitals Coventry and Warwickshire, Coventry, United Kingdom, ²Warwick Medical School, Warwick University, Coventry, United Kingdom

The apparent changes in venous calibre on susceptibility weighted imaging (SWI) of six normal volunteers pre-hypoxia, during the first 12 minutes of hypoxia, and at 30 and 60 minutes were investigated. For all subjects there was a step increase in apparent venous calibre on SWI which occurred within the first few minutes of hypoxia, and this was maintained up to 60 minutes. The apparent increase in

venous calibre occurred too rapidly after hypoxia induction to be entirely due to an increase in vessel volume. The vessels appear dilated because of the greater magnetic susceptibility of deoxyhaemoglobin than oxyhaemoglobin.

4093
Computer #66 Imaging of Nicotinamide adenine dinucleotide (NAD⁺) in vitro using CEST
Puneet Bagga¹, Kevin D'Aquila¹, Mohammad Haris², Hari Hariharan¹, and Ravinder Reddy¹

¹Department of Radiology, University of Pennsylvania, Philadelphia, PA, United States, ²Research Branch, Sidra Medical and Research Center, Doha, Qatar

Nicotinamide adenine dinucleotide (NAD⁺) is a ubiquitous molecule present in all cells and tissues of the body with an important role in the redox reactions and metabolism. Small changes in NAD levels may lead to oxidative stress and may be a cause for various disorders. Currently, NAD can be detected *in vivo* only by ³¹P NMR spectroscopy. Chemical Exchange Saturation Transfer (CEST) MRI is an imaging technique which exploits the properties of exchangeable protons on the molecule for imaging. In the present study, we have shown the *in vitro* CEST effect of solution containing NAD⁺.

4094
Computer #67 Frontal-parieto-temporal white matter integrity in chronic HIV infection reflects a complex combination of education level, immune recovery, antiretroviral brain penetration and current neurocognitive functioning
Lucette A Cysique¹, James R Soares², John Geng³, Maia Scarpetta^{3,4}, Bruce J Brew^{2,5}, Roland Henry⁶, and Caroline D Rae⁷

¹UNSW Australia, NeuRA, Sydney, Australia, ²UNSW Australia, Sydney, Australia, ³NeuRA, Sydney, Australia, ⁴Reed College, Portland, WA, United States, ⁵St. Vincent's Hospital, Sydney, Australia, ⁶UCSF, San Francisco, CA, United States, ⁷The University of New South Wales, Randwick, Australia

DTI was performed in 40 HIV- men and 82 HIV+ men with comparable demographics and life styles. The study was designed to recruit chronic HIV+ participants with successful viral control. DTI was 32 directions; FA values were quantified in each participant in 12 skeleton regions of interest, which have been associated with HIV-related brain injury. The study present first evidence for complex brain repair processes in treated and chronic HIV infection arguing for careful multilevel characterization of HIV+ samples in neuroHIV DTI studies. The association of neurocognitive function with FA suggests ongoing vulnerability despite successful treatment.

4095
Computer #68 Evaluation of Cerebral Venous Oxygen Saturation in Patients with Long-Term Haemodialysis using Susceptibility Mapping
Chao Chai¹, Linlin Fan², Chao Zuo³, Mengjie Zhang³, Lei Liu³, Zhiqiang Chu⁴, Tianyi Qian⁵, E Mark Haacke⁶, Shuang Xia³, and Wen Shen³

¹Department of Radiology, Tianjin First Central Hospital, Tianjin Medical University First Central Clinical college, Tianjin, China, People's Republic of, ²Department of Prophylactic Inoculation, Tianjin First Central Hospital, Tianjin Medical University First Central Clinical College, Tianjin, China, People's Republic of, ³Department of Radiology, Tianjin First Central Hospital, Tianjin Medical University First Central Clinical College, Tianjin, China, People's Republic of, ⁴Department of Haemodialysis, Tianjin First Central Hospital, Tianjin Medical University First Central Clinical college, Tianjin, China, People's Republic of, ⁵MR Collaboration NE Asia, Siemens Healthcare, Beijing, China, People's Republic of, ⁶Department of Radiology, Wayne State University, Detroit, MI, United States

The aim of this study was to explore cerebral venous oxygen saturation changes in long-term hemodialysis (HD) patients using susceptibility mapping (SWIM). SWIM was reconstructed from phase data of SWI and used to measure the susceptibility of cerebral veins in HD patients and healthy controls respectively. The results suggested that SWIM was a feasible and reliable method to measure the venous oxygen saturation. It can show the decrease of CMRO₂ in HD patients and the susceptibility value of the left cerebral cortical vein is positively correlated with MMSE scores.

4096
Computer #69 Reduced Creatine Concentrations in Severe Short-sleep Insomnia Disorder
Christopher B Miller¹, Caroline D Rae², Michael Green², Brendon Yee^{1,3}, Christopher J Gordon^{1,4}, Nathaniel S Marshall¹, Simon D Kyle⁵, Colin A Espie⁵, Ronald R Grunstein¹, and Delwyn J Bartlett¹

¹NeuroSleep and Woolcock Institute of Medical Research, The University of Sydney, Sydney, Australia, ²The University of New South Wales, Randwick, Australia, ³Department of Respiratory and Sleep Medicine, RPAH, Sydney, Australia, ⁴Sydney Nursing School, Sydney, Australia, ⁵Nuffield Department of Clinical Neurosciences and Sleep & Circadian Neuroscience Institute, The University of Oxford, Oxford, United Kingdom

We investigated 31 subjects with Insomnia Disorder grouped by hierarchical cluster analysis into long (N = 19) or short (N = 12) sleep duration insomnia and 16 healthy, good sleeping controls using an asymmetric PRESS MRS sequence at 3T in the left occipital cortex. A super metabolite variable constructed from creatine, Asp, Glu and Gln separated short sleeping insomnia from long sleeping and controls, positively correlated with total sleep duration and negatively with wake-time after sleep onset. Short sleep is associated with reduced creatine concentration.

4097
Computer #70 Decreased Cortical GABA in Youth with Tourette's Disorder
Rachel D. Freed¹, Barbara J. Coffey¹, Xiangling Mao², Guoxin Kang², Nora Weiduschat², Dikoma C. Shungu², and Vilma Gabbay¹

¹Psychiatry, Icahn School of Medicine at Mount Sinai, New York, NY, United States, ²Weill Medical College of Cornell University, New York, NY, United States

γ-aminobutyric acid (GABA), the major inhibitory neurotransmitter in the central nervous system, may play a role in the pathophysiology of Tourette's disorder (TD). We used ¹H MRS to measure GABA in the anterior cingulate cortex (ACC) and striatum of adolescents with TD and healthy controls (HC). Adolescents with TD had lower GABA spectra in the ACC than HC, suggesting a role for dysregulated ACC

neurotransmitter function. Within the TD group, ACC GABA was positively associated with tic severity, potentially related to attempts at regulating or suppressing tics. Findings provide evidence for dysfunction of the central GABAergic system in TD.


- 4098
Computer #71 Neurotoxic side effects of immunosuppressive in patients after liver transplantation: Preliminary results of a brain 31P-MRS study
Birte Schmitz¹, Anita B. Tryc², Karin Weißenborn², Henning Pflugrad², Heinrich Lanfermann¹, and Xiao-Qi Ding¹
- ¹Institute for Neuroradiology, Hannover Medical School, Hannover, Germany, ²Institute for Neurology, Hannover Medical School, Hannover, Germany
- Patients treated with immunosuppressive calcineurin inhibitors (CNI) for at least 3 years after liver transplantation were studied by using non-localized whole brain 31P-MRS at 3T to evaluate possible chronic neurotoxic side effects of the CNI. Global concentrations of brain high-energy metabolites Adenosine-5'-triphosphate (ATP) and phosphocreatine (PCr) were estimated. The values of the patient with different doses of CNI were compared with those of age-matched healthy volunteers. In our preliminary results significant lower concentrations of ATP and PCr were found in patients treated both with standard and low doses of CNI, indicating possible neurotoxic side effects.
-
- 4099
Computer #72 Quantitative Susceptibility Mapping – Comparison of Silent and Conventional Acquisitions
Pauline W Worters¹, Dirk Beque², Robert D Peters³, Dominic Graziani⁴, Michael Carl⁵, Graeme C McKinnon³, and Christopher J Hardy⁴
- ¹GE Healthcare, Menlo Park, CA, United States, ²GE Global Research, Munich, Germany, ³GE Healthcare, Waukesha, WI, United States, ⁴GE Global Research, Niskayuna, NY, United States, ⁵GE Healthcare, San Diego, CA, United States
- A silent 3D multi-echo gradient-echo pulse sequence is developed for quantitative susceptibility mapping (QSM). The new, silent sequence is compared to the standard acquisition and gives comparable susceptibility values. The silent acquisition gives the benefit of patient comfort and workflow ease at some cost to SNR and acquisition time.

Electronic Poster

Neuroimaging: Novel Findings

Exhibition Hall

Wednesday, May 11, 2016: 16:00 - 17:00

- 4100
Computer #73 Mapping of ex-vivo human cervical spinal cord using magnetic resonance micro-imaging
Abdullah Asiri^{1,2}, Charles Watson³, Shalini Nair⁴, Gary Cowin¹, Marc Ruitenber⁵, and Nyoman Kurniawan¹
- 
- ¹Centre for Advanced Imaging, University of Queensland, Brisbane, Australia, ²Najran University, Najran, Saudi Arabia, ³Faculty of Health Sciences, Curtin University of Technology, Perth, Australia, ⁴National University Hospital Systems, Kent Ridge, Singapore, ⁵School of Biomedical sciences, The University of Queensland, Brisbane, Australia
- Imaging the spinal cord is normally performed at lower magnetic field with limited resolution. In this study, 13 *ex-vivo* cervical spinal cords have been scanned at 9.4T to provide high-resolution images. A variation of the position of the rostral brachial motoneurons among the cords was used to classify the samples into normal and pre-fixed types. For each segment, the length and GM/WM total areas were measured. A high resolution MRI template of the normal type samples was created to assist registration and delineation of spinal cord structures and improve the accuracy of diagnostic radiology.
-
- 4101
Computer #74 Increased Apparent Diffusion Coefficient And Thickness In The Optic Nerve Is Associated With Visual Acuity Loss In Optic Pathway Glioma
Patrick W. Hales¹, Kshitij Mankad², Patricia O'Hare², Victoria Smith², Darren Hargrave², and Christopher Clark¹
- ¹Developmental Imaging & Biophysics Section, University College London Institute of Child Health, London, United Kingdom, ²Great Ormond Street Children's Hospital, London, United Kingdom
- Conventional MRI sequences have so far failed to provide imaging biomarkers that reliably differentiate asymptomatic optic pathway glioma (OPG) tumours from those which cause visual impairment. ADC maps are now acquired as standard in most institutions, and despite their typically limited resolution, may provide quantitative assessment of tumour invasion of the optic nerve. We measured ADC and optic nerve thickness using standard clinical imaging sequences in OPG patients, in conjunction with visual assessment. We found that the product of ADC and nerve thickness showed a significant correlation with visual acuity, and was significantly increased in patients who had gone blind.
-
- 4102
Computer #75 Interleaved acquisition of high resolution 3D susceptibility-weighted and FLAIR MRI
Refaat E Gabr¹, Amol S Pednekar², and Ponnada A Narayana¹
- ¹Department of Diagnostic and Interventional Imaging, The University of Texas Health Science Center at Houston (UTHealth), Houston, TX, United States, ²Philips Healthcare, Cleveland, OH, United States
- Combining the contrast of susceptibility weighted imaging (SWI) and fluid-attenuated inversion recovery (FLAIR) allows simultaneous visualization of multiple sclerosis lesions and the penetrating veins and iron deposition. However, the need for image registration, to

account for patient motion between the scans, adds to the complexity of the post-processing pipeline, and introduces undesirable blurring of the image. We have developed an interleaved sequence for simultaneous acquisition of 3D FLAIR and SWI data, which produces self-registered images in a clinically feasible time, greatly simplifying the post-processing steps and eliminating interpolation effects. The interleaved time delays in between the FLAIR and SWI modules provide a degree of freedom for further optimization of the image contrast. Experiments in MS patients show the utility of the proposed sequence.

-
- 4103
Computer #76 Improved reproducibility in subcortical gray matter atrophy measurement using FIRST and FreeSurfer
Houshang Amiri¹, Antoine Meijerman¹, Martijn D. Steenwijk^{1,2}, Ronald A. van Schijndel³, Frederik Barkhof^{2,3}, Keith S. Cover¹, and Hugo Vrenken^{1,2}
- ¹Department of Physics and Medical Technology, VU University Medical Center, Amsterdam, Netherlands, ²Department of Radiology and Nuclear Medicine, VU University Medical Center, Amsterdam, Netherlands, ³Image Analysis Center, VU University Medical Center, Amsterdam, Netherlands*
- Interest in measuring brain atrophy in neurodegenerative diseases such as Multiple Sclerosis (MS) and Alzheimer's disease (AD) is growing. To this end, FreeSurfer and FSL-FIRST are widely used as fully automated algorithms for quantification of the brain volume and volume change in both cross-sectional and longitudinal MRI studies. We have tested reproducibility of these methods in measuring deep gray matter atrophy rates in a group of subjects consisting of healthy aging, mild cognitive impairment and AD. We showed that using longitudinal mode for FreeSurfer and highest number of modes for FIRST provides the best reproducibility that is similar for FreeSurfer and FIRST.
-
- 4104
Computer #77 A SEMI-AUTOMATIC METHOD TO SEGMENT MULTIPLE SCLEROSIS LESIONS ON DUAL-ECHO MAGNETIC RESONANCE IMAGES
Loredana Storelli¹, Elisabetta Pagani¹, Maria Assunta Rocca^{1,2}, Paolo Preziosa^{1,2}, Antonio Gallo^{3,4}, Gioacchino Tedeschi^{3,4}, Maria Laura Stromillo⁵, Nicola De Stefano⁵, Hugo Vrenken⁶, David Thomas⁷, Laura Mancini⁷, Christian Enzinger⁸, Franz Fazekas⁸, and Massimo Filippi^{1,2}
- ¹Neuroimaging Research Unit, San Raffaele Scientific Institute, Vita-Salute San Raffaele University, Milan, Italy, ²Department of Neurology, San Raffaele Scientific Institute, Vita-Salute San Raffaele University, Milan, Italy, ³MRI Center "SUN-FISM", Second University of Naples and Institute of Diagnosis and Care "Hermitage-Capodimonte, Naples, Italy, ⁴Division of Neurology, Department of Medical, Surgical, Neurological, Metabolic and Aging Sciences, Second University of Naples, Naples, Italy, ⁵Department of Neurological and Behavioral Sciences, University of Siena, Siena, Italy, ⁶Department of Radiology and Nuclear Medicine, MS Centre Amsterdam, VU University Medical Centre, Amsterdam, Netherlands, ⁷NMR Research Unit, Queen Square MS Centre, UCL Institute of Neurology, London, United Kingdom, ⁸Department of Neurology, Medical University of Graz, Graz, Austria*
- Aim of the study was to develop a semi-automatic method for the segmentation of hyperintense multiple sclerosis (MS) lesions on dual-echo (DE) PD/T2-weighted scans. DE MRI scans were obtained from 6 different European centers from 52 MS patients with a mean lesion load of 10.3 (\pm 11.9) ml. The method was based on a region growing approach initialized by manual identification of lesions and a priori information. The segmentation results with the new method showed high accordance with the ground truth and a low misclassification of lesion voxels. Furthermore, operator time required for lesion segmentation was drastically reduced.
-
- 4105
Computer #78 Subcortical brainstem changes in the motor system in patients with chronic spinal cord injury revealed by quantitative MRI protocols
Patrick Grabher¹, Claudia Blaiotta², Armin Curt¹, John Ashburner², and Patrick Freund^{1,2,3,4}
- ¹Spinal Cord Injury Center Balgrist, University of Zurich, Zurich, Switzerland, ²Wellcome Trust Centre for Neuroimaging, UCL Institute of Neurology, London, United Kingdom, ³Department of Brain Repair and Rehabilitation, UCL Institute of Neurology, London, United Kingdom, ⁴Department of Neurophysics, Max Planck Institute for Human Cognitive and Brain Sciences, Leipzig, Germany*
- Neurodegeneration and neuroplasticity within the brainstem is poorly understood in patients suffering from spinal cord injury (SCI). We acquired quantitative MRI data of the brainstem using a multi-parameter mapping protocol to assess trauma-induced volumetric and microstructural changes after SCI. We show focal atrophic changes within different subregions of the brainstem in chronic SCI patients and their correlation with clinical outcomes. Neuroimaging biomarkers using quantitative MRI at the brainstem level could be applied to complement clinical assessments during rehabilitation and interventional studies.
-
- 4106
Computer #79 Comparison of CEST and [18F]-FDG Imaging in Patients with Brain Tumor: A hybrid PET/MR Study
Xuna zhao^{1,2}, Hongzan Sun³, Jun Xin³, Shanshan Jiang¹, Yansong Zhao⁴, Yi Zhang¹, Dong-Hoon Lee¹, Hye-Young Heo¹, and Jinyuan Zhou¹
- ¹Department of Radiology, Johns Hopkins University, Baltimore, MD, United States, ²Philips Healthcare, Beijing, China, People's Republic of, ³Department of Radiology, Shengjing Hospital, Shenyang, China, People's Republic of, ⁴Philips Healthcare, Cleveland, OH, United States*
- Hybrid PET/MR provides a high resolution anatomical and metabolic imaging approach to evaluate human brain tumors. As a novel molecular MRI technique, CEST MRI has been successfully employed in clinical practice. The combination of [18F]-FDG and CEST images will provide further supplementary information on the study of clinic and molecular mechanism for human brain tumors.
-
- 4107
Computer #80 Fast and full coverage dual-venic 4D flow MRI: can time-averaged acquisition be useful?
Maria Aristova¹, Michael Markl², John C Carr², Sameer A Ansari², Can Wu³, and Susanne Schnell²
- ¹Biomedical Engineering, Northwestern University, Chicago, IL, United States, ²Radiology, Northwestern University Feinberg School of Medicine, Chicago, IL, United States, ³Biomedical Engineering, Northwestern University Feinberg School of Medicine, Chicago, IL, United States*

This work compares the utility of time-averaged vs. time-resolved dual-venic 4D flow MRI to look at intracranial blood flow distribution for applications such as evaluation of cerebral arteriovenous malformation (AVM). Time-averaged scans provide larger FOV, no additional time for image reconstruction after the scan and net flow distributions that correlate well with time-resolved scans.

-
- 4108
Computer #81
Intraoperative MRI Guided Resection for Glioblastoma Results in Increased Short-term Survival Compared to Conventional Surgery
Mark Oswood^{1,2}, Bridget Ho³, Aditi Gupta⁴, Todd DeFor⁵, and Nilanjana Banerji⁴
- ¹Radiology, HCMC, Minneapolis, MN, United States, ²Radiology, University of Minnesota, Minneapolis, MN, United States, ³John Nasseff Neuroscience Institute, Allina Health, St. Paul, MN, United States, ⁴John Nasseff Neuroscience Institute, Allina Health, Minneapolis, MN, United States, ⁵MCC Biostatistics Core, University of Minnesota, Minneapolis, MN, United States
- A retrospective analysis of survival after resection of glioblastoma was performed comparing use of intraoperative MRI with conventional surgery. There was a significant difference in extent of resection, with more gross total resections achieved with iMRI. There was a significant improvement in overall survival at 6 months with iMRI. The groups had equivalent survival from 12-36 months. Younger age was correlated with longer overall survival.
-
- 4109
Computer #82
Metabolic and morphological characterization of the triple transgene mouse model of Alzheimer disease: effects of palmitoylethanolamide on the onset and progression of the AD-pathology
Rossella Canese¹, Giulia Carpinelli¹, Gianmauro Palombelli¹, Caterina Scuderi², Luca Steardo², and Tommaso Cassano³
- ¹Cell Biology and Neurosciences, Istituto Superiore di Sanita', Roma, Italy, ²Department of Physiology and Pharmacology "Vittorio Erspamer", University of Rome SAPIENZA, Rome, Italy, ³Dipartimento di Medicina Clinica e Sperimentale, Università degli Studi di Foggia, Foggia, Italy
- Alzheimer disease (AD) is characterized clinically by progressive cognitive decline, and pathologically by the presence in the brain of senile plaques composed primarily of amyloid-beta peptide and neurofibrillary tangles containing hyperphosphorylated tau protein. Here we investigated the effects of a naturally occurring amide of ethanolamine and palmitic acid (PEA), abundant in the CNS to contrast the AD phenotype in triple transgene (PS1, APP and Tau) mice model, by in vivo 1H MRI and MRS and histology. Our data indicate that PEA treatment affects brain metabolism as a function of age and that PEA rescues altered molecular pathways that can mimic some traits of AD
-
- 4110
Computer #83
Network-wide longitudinal atrophic covariance after ischaemic stroke
Michele Veldsman¹, Amy Brodtmann¹, Graeme Jackson², and Evan Curwood²
- ¹Stroke Division, The Florey Institute of Neuroscience and Mental Health, Heidelberg, Australia, ²Epilepsy Division, The Florey Institute of Neuroscience and Mental Health, Heidelberg, Australia
- Brain atrophy is common after stroke. The extent and pattern of atrophy has not been well investigated and has been limited to localised atrophy and cross-sectional studies, despite network-wide effects of stroke on brain structure and function. We examined correlations in the rate of longitudinal cortical thickness change in stroke patients, compared to healthy age-matched controls. We aimed to investigate whether patterns of neurodegeneration occur in healthy networks as in aging and dementia. We provide evidence of correlations in the rate of cortical atrophy within the DMN suggesting a process of network-based degeneration one year after stroke.
-
- 4111
Computer #84
Experimentally Optimizing Labeling Position in Pseudo-continuous ASL in the Presence of Carotid Artery Stenting
Chien-Yuan Eddy Lin^{1,2}, Ai-Chi Chen³, David Yen-Ting Chen³, Ying-Chi Tseng³, and Chi-Jen Chen³
- ¹GE Healthcare, Taipei, Taiwan, ²GE Healthcare MR Research China, Beijing, China, People's Republic of, ³Department of Radiology, Taipei Medical University - Shuang Ho Hospital, New Taipei City, Taiwan
- Pseudo-continuous arterial spin labeling (pCASL) has been recently used for investigating cerebral hemodynamic change on the patient receiving carotid artery stenting (CAS) because it permits repeated measurement of absolute cerebral blood flow in a short interval without MR contrast agent or radioactive material. However, labeling efficiency of pCASL has been proved to be dependent on B₀ inhomogeneity. Labeling position may need to be carefully applied after CAS. The aim of this study was to experimentally determine the optimal labeling position for pCASL with minimal frequency shift caused by stent in exploring cerebral perfusion in the patient with CAS treatment.
-
- 4112
Computer #85
Assessment of Moyamoya Disease by Using Vessel Wall Imaging with MSDE Technique: Feasibility and Implication
Akira Kunitatsu¹, Yasushi Watanabe², Mitsuharu Miyoshi³, Yuichi Suzuki², Kouhei Kamiya¹, Hiroyuki Kabasawa³, Harushi Mori¹, and Kuni Ohtomo¹
- ¹Department of Radiology, The University of Tokyo, Tokyo, Japan, ²Department of Radiology, The University of Tokyo Hospital, Tokyo, Japan, ³Global MR Applications and Workflow, GE Healthcare, Tokyo, Japan
- We assessed diagnostic feasibility of vessel wall imaging with MSDE-prepared, 3D T1-weighted variable refocusing flip angle fast spin echo MR imaging (CUBE T1) in differentiation between moyamoya disease (MMD) and intracranial atherosclerotic disease (ICAD), both of which can cause stenosis of the intracranial arteries. MSDE-prepared CUBE T1 enabled correct differentiation in our cohorts and may be helpful to differentiate MMD from ICAD when luminal narrowing is found on conventional brain MRA.

- 4113
Computer #86 The integrity and atherosclerosis of Circle of Willis detected by bright-blood and black-blood MRI are associated with severity of stroke
Le He¹, Rui Li¹, Xihai Zhao¹, Shuo Chen¹, and Huijun Chen¹
¹Center for BioMedical Imaging Research, Tsinghua University, Beijing, China, People's Republic of
- Circle of Willis (CoW) is an important source of collateral blood flow, which may influence the severity of ischemia stroke. However, traditional methods only evaluate the luminal conditions of CoW. This study evaluate the luminal and vessel wall conditions of CoW using bright- and black-blood MRI. We found that most stroke patients have incomplete CoW, and patients with atherosclerotic CoW tends to have larger ischemic infraction. More importantly, the infarction size in stroke patients was significantly associated with integrity&atherosclerosis of CoW, suggesting that the integrity and atherosclerosis of CoW may be a risk factor for stroke severity.
-
- 4114
Computer #87 Characterization of Asymptomatic Intracranial Atherosclerosis using 3D High Resolution Contrast-enhanced MRI
Huan Yang^{1,2}, Xuefeng Zhang^{1,3}, Li Liu¹, Qing Hao⁴, Victor Urrutia⁴, Qin Qin^{1,5}, Bruce A. Wasserman¹, and Ye Qiao¹
¹The Russell H. Morgan Department of Radiology and Radiological Sciences, The Johns Hopkins Hospital, Baltimore, MD, United States, ²Shandong Medical Imaging Research Institute, Shandong University, Jinan, China, People's Republic of, ³Inner Mongolia Autonomous Region People's Hospital, Inner Mongolia, China, People's Republic of, ⁴Department of Neurology, The Johns Hopkins Hospital, Baltimore, MD, United States, ⁵F.M. Kirby Research Center for Functional Brain Imaging, Kennedy Krieger Institute, Baltimore, MD, United States
- Although most of strokes occur in asymptomatic patients, most studies have been conducted in symptomatic cohort. Here we aimed to characterize ICAD in stroke-free participants and compare with stroke patients using 3D high-resolution contrast-enhanced BBMRI. Nineteen asymptomatic and 15 stroke patients were included and underwent a standardized protocol which contains 3D TOF MRA and pre- and post-contrast 3D BBMRI imaging. Plaque enhancement was categorized, and morphology and signal-based measurements were compared. The results showed that asymptomatic plaques demonstrated lower contrast-enhancement compared with symptomatic plaques. Contrast-enhancement of ICAD may serve as a marker for plaque stability, providing insight into stroke risk.
-
- 4115
Computer #88 Contralateral Cerebro-Cerebellar White Matter Pathways for Verbal Working Memory: A Combined Diffusion Spectrum Imaging and fMRI Study
Monika Sobczak-Edmans¹, Yu-Chun Lo², Yung-Chin Hsu², Yu-Jen Chen², Fu Yu Kwok¹, Kai-Hsiang Chuang^{3,4}, Wen-Yih Isaac Tseng^{2,5,6,7}, and SH Annabel Chen^{1,8}
¹Psychology, Nanyang Technological University, Singapore, Singapore, ²Institute of Medical Device and Imaging, National Taiwan University College of Medicine, Taipei, Taiwan, ³The Queensland Brain Institute, The University of Queensland, Brisbane, Australia, ⁴The Centre for Advanced Imaging, The University of Queensland, Brisbane, Australia, ⁵Institute of Brain and Mind Sciences, National Taiwan University College of Medicine, Taipei, Taiwan, ⁶Department of Radiology, National Taiwan University College of Medicine, Taipei, Taiwan, ⁷Molecular Imaging Center, National Taiwan University, Taipei, Taiwan, ⁸Centre for Research And Development in Learning, Nanyang Technological University, Singapore, Singapore
- Diffusion spectrum imaging was employed to establish structural connectivity between cerebro-cerebellar regions co-activated during verbal working memory. IFG, IPL, pons, thalamus, superior cerebellum and inferior cerebellum were used as seed points to reconstruct the white matter cerebro-cerebellar circuitry. The reconstructed pathways were examined further to establish the relationship between structural and effective connectivity as well as the relationship between structural connectivity and verbal working memory performance. It was found that structural connectivity is indirectly related to effective connectivity but does not predict it. Additionally, it was demonstrated that the integrity of the ponto-cerebellar tract is an important factor in explaining individual differences in verbal working memory. The findings of the study furthered our understanding of the relationship between structural and functional connectivity and provided insight to the variability in verbal working memory performance.
-
- 4116
Computer #89 Interpreting patterns of BOLD responses to carbon dioxide through flow resistance
James Duffin^{1,2}, Olivia Sobczyk³, Adrian P Crawley⁴, Julien Poublanc⁴, Paul Dufort³, Lashmi Venkatraghavan⁵, David J Mikulis^{3,4}, and Joseph A Fisher^{1,2,3}
¹Department of Physiology, University of Toronto, Toronto, ON, Canada, ²Departments of Anaesthesia, University Health Network, Toronto, ON, Canada, ³Institute of Medical Sciences, University of Toronto, Toronto, ON, Canada, ⁴Joint Department of Medical Imaging and the Functional Neuroimaging Laboratory, University Health Network, Toronto, ON, Canada, ⁵Department of Anaesthesia, University Health Network, Toronto, ON, Canada
- The patterns of BOLD changes in response to a ramp CO₂ stimulus ranging from hypocapnia to hypercapnia can be classified into four types, based on the two linear slopes fitted to each range. We describe the physiology underlying the different response patterns using a simple model of two vascular beds competing for the same limited blood supply; deriving the sigmoidal resistance changes in each branch of the model from measured BOLD responses. We illustrate the use of the model to analyse the BOLD responses in an example patient.
-
- 4117
Computer #90 Relationship between the position of the plaque signal intensity identified by 3D-FSE T1W MR plaque imaging and development of microembolic signals on transcranial Doppler during exposure procedure of carotid arteries in endarterectomy
Yasushi Ogasawara¹, Kuniaki Ogasawara¹, Yuiko Sato¹, Shinsuke Narumi², Makoto Sasaki³, Masakazu Kobayashi¹, Shunrou Fujiwara¹, Kenji Yoshida¹, Yasuo Terayama², and Akira Ogawa¹
¹Department of Neurosurgery, Iwate Medical University, Morioka, Japan, ²Department of Neurology and Gerontology, Iwate Medical University,

Preoperative 2D MR carotid plaque imaging can assess plaque vulnerability. It may allow improved risk stratification for patients considered for CEA and may be associated with development of MES during CEA. On the other hand, it is unclear what position of high signal intensity in the plaque, especially at the position showing maximum stenosis or maximum signal intensity, is deeply associated with MES, and it is difficult to validate it by the 2D plaque imaging. The aim of the present study was to determine where in the plaque is deeply associated with development of MES on TCD during CEA in carotid artery stenosis, using 3D-FSE T1W plaque imaging.

4118 Computer #91 A semi-automatic workflow of constructing printable 3D models for cerebrovascular surgical planning based on MR angiography and CT data

Huaiqiang Sun¹, Haoyang Xing¹, Jiayu Sun¹, Lu Ma², Ji Bao³, Youjin Zhao¹, and Qiyong Gong¹

¹Huaxi MR Research Center, Department of Radiology, West China Hospital, Chengdu, China, People's Republic of, ²Department of Neurosurgery, West China Hospital, Chengdu, China, People's Republic of, ³Laboratory of Pathology, West China Hospital, Chengdu, China, People's Republic of

A semi-automatic workflow, which can be done within one hour and need minimal manual intervention, was proposed for constructing printable 3D models for cerebrovascular surgical planning based on MR angiography and CT data. The constructed models were consistent with the findings of MR angiography and have the potential to help surgeons to rehearse the operation beforehand and reduce operative risk.

4119 Computer #92 Z-shim with Parallel-Transmit Methods (pTX) in MR Neuro Applications
Lukas Mario Gottwald¹, Rainer Schneider¹, and Josef Pfeuffer¹

¹MR Application Development, Siemens Healthcare, Erlangen, Germany

In clinical 3T imaging, gradient-echo-based sequences often suffer from signal loss induced by patient-specific susceptibility artifacts. To tackle this problem, a proposed local signal recovery z-shim method using parallel transmission was implemented for a clinical setup. The approach was further extended by an automated slice-specific delay-time calculation to ensure user-friendly operation as well as maximal signal gain in artifact regions. Studies in humans were carried out using commonly used GRE and EPI sequences. Signals could be nearly fully recovered in artifact regions; tSNR gain maps for EPI time series showed an increase up to 148%.

4120 Computer #93 Noninvasive imaging of oxygen extraction fraction in adults with sickle cell anemia
Lori Jordan¹, Melissa Gindville¹, Allison Scott¹, Meher Juttukonda¹, Megan Strother¹, Adetola Kassim¹, Sheau-Chiann Chen¹, Hanzhang Lu², Sumit Pruthi¹, Yu Shyr¹, and Manus J. Donahue¹

¹Vanderbilt University Medical Center, Nashville, TN, United States, ²Johns Hopkins University, Baltimore, MD, United States

The goal of this work is to apply hemo-metabolic MRI to evaluate relationships between oxygen extraction fraction (OEF), cerebral blood flow (CBF), and clinical impairment in adults with sickle cell anemia (SCA). Healthy (n=11) and sickle cell anemia (n=34) participants received neurological evaluation, head/neck-angiography, structural-MRI, CBF-weighted-MRI, and T2-relaxation-under-spin-tagging (TRUST)-MRI. CBF and OEF were elevated (P<0.05) in SCA relative to control participants; OEF (P<0.0001) but not CBF was increased in SCA participants with higher clinical impairment. Data provide support for TRUST-MRI being able to quickly and noninvasively detect elevated OEF in SCA participants with high levels of clinical impairment.

4121 Computer #94 Clinical Evaluation of TOF-MRA with Sparse Undersampling and Iterative Reconstruction (Sparse TOF) for Cerebral Aneurysms.
Yasutaka Fushimi¹, Tomohisa Okada^{1,2}, Akira Yamamoto¹, Takayuki Yamamoto¹, Aurelien Stalder³, Michaela Schmidt³, Yutaka Natsuaki³, and Kaori Togashi¹

¹Kyoto University Graduate School of Medicine, Kyoto, Japan, ²Human Brain Research Center, Kyoto University Graduate School of Medicine, Kyoto, Japan, ³Siemens, Erlangen, Germany

Sparse TOF has demonstrated the potential to accelerate TOF MRA. We conducted comparison study targeting patients with cerebral aneurysms to check the clinical relevance of evaluation of aneurysms on Sparse TOF 3X, 5X and TOF with parallel imaging (PI TOF). MIP images of patients with cerebral aneurysms were blindly evaluated by one neuroradiologist, and the sum of grades were compared among Sparse TOF 3X, 5X and PI-TOF 3X. Sparse TOF 3X and 5X were reconstructed with clinically acceptable time, and cerebral aneurysms were visible in both Sparse TOF 3X and 5X with equivalent quality as PI TOF.

4122 Computer #95 A probabilistic atlas based on 168 subjects for labeling of brain arteries
Tora Dunås¹, Anders Wåhlin^{1,2}, Khalid Ambarki^{1,3}, Laleh Zarrinkoob⁴, Jan Malm⁴, and Anders Eklund^{1,2,3}

¹Department of Radiation Sciences, Umeå University, Umeå, Sweden, ²Umeå Center for Functional Brain Imaging, Umeå University, Umeå, Sweden, ³Centre for Biomedical Engineering and Physics, Umeå University, Umeå, Sweden, ⁴Department of Clinical Neuroscience, Umeå University, Umeå, Sweden

The cerebral arterial system is complex with large inter-individual spatial variations, which are potentially challenging for automatic methods. The objective of this work was to construct an artery specific probabilistic atlas of 16 large cerebral arteries, based on 168 subjects, and to investigate if the regional specificity of vascular branches was sufficient to permit atlas based arterial labeling. Voxels of

the arterial centerlines was labeled according to the highest probability at the corresponding location in the atlas. The rate of correctly labeled voxels was over 80% for all arteries, which should be sufficient to permit atlas based arterial labeling.

- 4123
Computer #96 Magnetic Resonance imaging features of normal and abnormal fetal Ganglionic Eminence. A pictorial essay.
Giorgio Conte^{1,2}, Claudia Cesaretti¹, Giana Izzo¹, Cecilia Parazzini¹, and Andrea Righini¹

¹Radiology and Neuroradiology, Children's Hospital V. Buzzi, Milan, Italy, ²Radiology Institute, University of Milan, Milan, Italy

Ganglionic eminence (GE) is the main proliferative structure of the ventral telencephalon and contributes to GABA-ergic cortical interneuron population; GE imaging characterization in normal and abnormal conditions is poor. After searching a 3500 cases fetal MR database, we illustrate normal GE features, its abnormalities and its possible associations. GE malformations are divided: 1) bilateral symmetric cavitations as inverted C shape separating GE from parenchyma; 2) GE volume increase associated or not with the above mentioned cavitation. About half of cases are associated with micro-lissencephaly, the others with minor-moderate anomalies. As group apart are presented clastic GE lesions, featuring haemorrhagic changes.

Electronic Poster

Psychiatric Disorders: Psychosis

Exhibition Hall

Wednesday, May 11, 2016: 17:00 - 18:00

- 4124
Computer #1 Magnetic Resonance Imaging of hippocampal subfield in a large sample of posttraumatic stress disorder
Lianqing Zhang¹, Xingyu Hu¹, Shiguang Li², Lei Li¹, Lizhou Chen¹, Qi Liu¹, Lu Lu¹, Qiyong Gong¹, and Xiaoqi Huang¹

¹Huaxi MR Research Center (HMRRCC), radiology department, West China Hospital of Sichuan University, Chengdu, China, People's Republic of, ²radiology department

We analysis hippocampal subfields volume changes in a relatively large sample of adult patients with post-traumatic stress disorder and same stressor e the responsive change of hippocampus after stress which cause cellular edema or at a early stage of the disorder. The second find is the difference betw

- 4125
Computer #2 Redox Dysregulations in Schizophrenia Revealed by in vivo NAD⁺/NADH Measurement
Sang-Young Kim^{1,2}, Bruce Cohen³, Scott Lukas⁴, Cagri Yuksel², Dost Ongur², and Fei Du^{1,2}

¹McLean Imaging Center, McLean Hospital, Harvard Medical School, Belmont, MA, United States, ²Psychotic Disorders Division, McLean Hospital, Harvard Medical School, Belmont, MA, United States, ³Program for Neuropsychiatric Research, McLean Hospital, Harvard Medical School, Belmont, MA, United States, ⁴Behavioral Psychopharmacology Research Laboratory, McLean Hospital, Harvard Medical School, Belmont, MA, United States

In this work, we demonstrated the feasibility of 31P MRS-based in vivo intracellular redox state quantification at 4 T. We applied this novel method to investigate oxidative stress in the frontal lobe of chronic and first-episode SZ as well as first-episode BD patients. We found evidence for striking Rx reductions in SZ, with every chronic SZ patient showing an Rx of at least one standard deviation below the control mean. Rx reduction was of even greater magnitude among first-episode SZ patients. This study illustrates the power of examining in vivo brain redox dysregulation (measured as Rx) in psychiatric disorders.

- 4126
Computer #3 Functional Disconnectivity in Schizophrenia Patients with Auditory Hallucinations: a Dynamic Resting-State Functional MRI Study with a Multiband EPI Sequence
Wenjing Zhang¹, Wei Deng², Siyi Li¹, John Sweeney³, Qiyong Gong¹, and Su Lui¹

¹Huaxi MR Research Center (HMRRCC), Department of Radiology, West China Hospital of Sichuan University, Chengdu, China, People's Republic of, ²Department of Psychiatry, West China Hospital of Sichuan University, Chengdu, China, People's Republic of, ³Department of Psychiatry, UT Southwestern Medical Center, Dallas, TX, United States

A simultaneous multi-slice multiband EPI sequence, which could significantly increase temporal resolution for the fMRI scanning, was adopted to investigate the dynamic functional connectivity in the schizophrenia patients with auditory hallucinations. We found that, relative to traditional static functional connectivity calculation, dynamic analysis evaluated with multiband EPI provides much more information, including more widespread aberrant functional connectivity maps across different states and their temporal variability over time. The expanded information may help to give better insight into the pathological processes and subsequently reveal the spontaneous model of affected networks in schizophrenia.

- 4127
Computer #4 Glutamatergic metabolism and disease severity in Schizophrenia: a 7T MRS study
Subechhya Pradhan¹, Laura M. Rowland², S. Andrea Wijtenburg², Stephanie Korenic², Sarah Nosinger², L. Elliot Hong², and Peter B. Barker^{1,3}

¹The Russell H. Morgan Department of Radiology and Radiological Science, Johns Hopkins University School of Medicine, Baltimore, MD, United States, ²Department of Psychiatry, University of Maryland School of Medicine, Baltimore, MD, United States, ³Radiology, Kennedy Krieger Institute, Baltimore, MD, United States

Imbalance in the glutamatergic system is implicated in the pathophysiology of schizophrenia. Various previous MRS studies have

reported altered levels of glutamate and/or glutamine in schizophrenia, however most of these studies have been performed at 3T or lower where separation from Glu from Gln is challenging, and few have looked at correlations with disease severity or cognitive impairment. The purpose of this study was to investigate neurochemical differences in participants with and without schizophrenia using high-resolution 7T MRS in multiple brain regions, and to exam correlations with measures of cognitive impairment, function and symptom severity.

4128 Computer #5 Microstructural alterations detected by dMRI in KO mouse model showing schizophrenic like phenotype
Nicolas Kunz¹, Alexandre Bacq², Jocelin Grosse², Rolf Gruetter^{1,3}, and Carmen Sandi²

¹CIBM-AIT, École Polytechnique Fédérale de Lausanne, EPFL, Lausanne, Switzerland, ²Laboratory of Behavioral Genetics, École Polytechnique Fédérale de Lausanne, EPFL, Lausanne, Switzerland, ³Department of Radiology, University of Geneva and Lausanne, Geneva, Lausanne, Switzerland

Schizophrenia is a severe mental disorder that afflicts 1% of the world's population. However, the cause of this disorder remains unknown. Increasing evidence points toward a neurodevelopmental mechanism, which implicates genes involved in neuronal proliferation, migration, or synapse formation. We investigate microstructural changes by ex-vivo diffusion MRI in PSA-KO mice brain. Trends of microstructural alterations were visible in a few fiber tracts such as ST, ST-post, AC and FX. These preliminary results suggest that altered plasticity during development of the PSA-KO mice, presenting schizophrenic like phenotype and altered sociability, creates long term effects and structural alterations depicted by dMRI.

4129 Computer #6 Prediction of treatment response with multi-modality MRI in first-episode antipsychotic-naive schizophrenia
Lu Liu¹, Yuan Xiao¹, Wenjing Zhang¹, and Su Lui²

¹Huaxi MR Research Center (HMRRRC), Department of Radiology, West China Hospital of Sichuan University, Chengdu, China, People's Republic of, ²Huaxi MR Research Center (HMRRRC), Department of Radiology, West China Hospital of Sichuan university, Chengdu, China, People's Republic of

Using SVM to characterize structural and functional pattern implicated in antipsychotic-naive schizophrenia to predict the response of anti-psychotic treatment and also to examine the structural neuroanatomy and functional activity. And revealed that anatomical and functional changes revealed by Multi-modality MRI in first-episode schizophrenia patients before treatment showed the potential in predicting the one year treatment response, which could help psychiatrists to make treatment strategy for individual patient in future.

4130 Computer #7 ³¹P MRS study of schizophrenia induced changes of energy metabolism in activated cerebral cortex.
Andrei Valerievich Manzhurtsev¹, Maxim Vadimovich Ublinskii^{1,2}, Irina Sergeevna Lebedeva³, Tolibjon Abdullaevich Akhadov², Petr Evgenievich Menshchikov⁴, and Natalia Alexandrovna Semenova^{1,2,4}

¹Emanuel Institute of Biochemical Physics of Russian Academy of Sciences, Moscow, Russian Federation, ²Radiology, Scientific Research Institute of Children's Emergent Surgery and Trauma, Moscow, Russian Federation, ³Scientific Centre of Mental Health, Moscow, Russian Federation, ⁴Semenov Institute of Chemical Physics of Russian Academy of Sciences, Moscow, Russian Federation

³¹P MRS in the period of neuroactivation allows direct analysis of metabolic response on energy consuming processes. In this study we revealed decreased creatine kinase system response in visual cortex of early stage schizophrenia patients in the period of videostimulation: while PCr in normal activated cortex is reduced for ATP regeneration during activation, no PCr decrease was observed in patients. The data obtained allowed to offer a new neuronal metabolism scheme in response to stimulation at early stage of schizophrenia.

4131 Computer #8 A novel framework for global comparison of tract-topology between subjects reveals callosum shape variations in first episode psychosis
Greg D Parker¹, George J.A. Evans², and Derek K Jones^{1,3}

¹CUBRIC, School of Psychology, Cardiff University, Cardiff, United Kingdom, ²School of Medicine, Newcastle University, Newcastle, United Kingdom, ³Neuroscience and Mental Health Research Institute (NMHRI), School of Medicine, Cardiff University, Cardiff, United Kingdom

Changes in the size and shape of white matter tracts are known to be associated with the onset or progress of various brain disorders. Common techniques for characterising tract shape include measuring cross sectional area or thickness¹⁻³, Fourier descriptors⁴ and measures of streamline dispersion⁵. Here we present a novel principal component analysis (PCA)-based method and demonstrate two ways in which those representations may be used to examine inter-group differences in tract shape. As an example, we compare 30 first-episode psychosis patients with age/sex matched controls and find significant shape differences in the genu of the callosum.

4132 Computer #9 Common Pattern of Gray Matter Changes in First Episode Schizophrenia Patients with and without Antipsychotics: VBM Meta-analyses Using Signed Differential Mapping
Chandan Shah¹, Wenjing Zhang¹, Yuan Xiao², Li Yao², Xin Gao², Lu Liu², Jieke Liu², Siyi Li², Qiyong Gong², and Su Lui²

¹Radiology, Sichuan University, Chengdu, China, People's Republic of, ²Chengdu, China, People's Republic of

Current study provides an insight about the brain morphological changes of first episode schizophrenia patients at drug-naive state and after antipsychotic treatment. Our study reveals that GM changes in frontal, temporal and insular regions are the fundamental regions of pathologic GM changes in first-episode schizophrenia irrespective of antipsychotic medication. This common pattern of GM changes in first episode schizophrenia patients with and without antipsychotics suggest the anatomical deficits involved in the fronto-temporal

and limbic regions are likely to be the trait- instead of state-related changes at the early course of illness in schizophrenia. Until now only assumptions have been made about the potential effects of antipsychotics rather than making a strong statement due to lack of proper investigation methods and also due to difficulty in gaining access to a satisfactory number of drug naïve and medicated patients group of the same age. We therefore hope this study would be helpful in providing important information about the pathology of the schizophrenic brain after the early course of treatment with antipsychotics.

-
- 4133
Computer #10
Reduced gamma-amino butyric acid and elevated Glu/Gln complex in the anterior cingulate cortex of medicated schizophrenic patients
Pui Wai Chiu¹, Queenie Chan², Sai-yu Lui³, Karen Shee Yueng Hung³, Raja Rizal Azman Raja Aman⁴, Raymond Chor Kiu Chan⁵, Pak Chung Sham⁶, Eric Fuk Chi Cheung³, Richard A Edden⁷, and Henry Ka Fung Mak¹

¹Diagnostic Radiology, The University of Hong Kong, Hong Kong, Hong Kong, ²Philips Healthcare, Hong Kong, Hong Kong, Hong Kong, ³Institute of Mental Health, Castle Peak Hospital, Hong Kong, Hong Kong, ⁴Biomedical Imaging, University of Malaya, Kuala Lumpur, Malaysia, ⁵Neuropsychology and Applied Cognitive Neuroscience Laboratory, Chinese Academy of Sciences, Beijing, China, People's Republic of, ⁶Psychiatry, The University of Hong Kong, Hong Kong, Hong Kong, ⁷Radiology and Radiological Sciences, Johns Hopkins University, Baltimore, MD, United States

Gamma-amino butyric acid (GABA) is thought to play an important role in the pathophysiology of schizophrenia. The anterior cingulate cortex (ACC) has been reported to exhibit functional and morphological abnormalities in schizophrenic patients compared to healthy controls(HC). In this pilot study, absolute concentrations of GABA([GABA]_{abs}) and Glx([Glx]_{abs}) were measured in the ACC of 9 schizophrenic patients and 14 HC at 3.0T. Significant lower [GABA]_{abs} level in ACC of schizophrenic patients might provide evidence of abnormalities in GABAergic neurotransmission in schizophrenia. Significant positive correlation between [Glx]_{abs} and positive symptoms subscale might indicate Glx level is specific for positive symptoms in ACC.

-
- 4134
Computer #11
A 7T MRS Study of First Episode Psychosis: glutamatergic abnormalities and correlations with symptom severity
Subechhya Pradhan¹, Anouk Marsman¹, Rebecca Ward², Candice Ford², Ashley Lloyd², David Schretlen^{1,2}, Akira Sawa², and Peter B. Barker^{1,3}

¹The Russell H. Morgan Department of Radiology and Radiological Science, Johns Hopkins University School of Medicine, Baltimore, MD, United States, ²Department of Psychiatry and Behavioral Sciences, Johns Hopkins University School of Medicine, Baltimore, MD, United States, ³Radiology, Kennedy Krieger Institute, Baltimore, MD, United States

Imbalance in glutamatergic systems is implicated in the pathophysiology of psychosis. The purpose of this study was to assess differences in metabolite levels between subjects with a first episode of psychosis (FEP) and healthy controls, and to study correlations between metabolites and measures of disease severity, including neuropsychological scales, positive and negative symptoms.

-
- 4135
Computer #12
Glutamatergic metabolite concentrations in the superior temporal gyrus in schizophrenia are increased and glutamate predicts neuroticism
Florian Schubert¹, Ralf Mекle¹, Johanna Balz², Julian Keil², Yadira Roa Romero², Bernd Ittermann¹, Jürgen Gallinat³, and Daniel Senkowski²

¹Physikalisch-Technische Bundesanstalt (PTB), Braunschweig and Berlin, Germany, ²Charité Universitätsmedizin Berlin, Berlin, Germany, ³Universitätsklinikum Hamburg-Eppendorf, Hamburg, Germany

Findings of deviant glutamate (Glu) and glutamine (Gln) levels in brain of patients support the glutamate hypothesis of schizophrenia. Thickness and volume of the left superior temporal gyrus (STG) are established endophenotypes of schizophrenia. We quantified glutamatergic metabolites using proton MRS with SPECIAL in the left STG of schizophrenic patients and controls, and investigated the relationships between Glu and personality traits. Glu was significantly higher in patients than in controls, Gln likewise but with a weak trend only. Glu predicted neuroticism in patients. Our results suggest dysfunctional glutamatergic neurotransmission in STG and confirm widespread Glu increases in cortical regions in schizophrenia.

-
- 4136
Computer #13
Cortical GluCEST in Schizophrenia and Youth at Clinical High Risk for Psychosis
Ravi Prakash Reddy Nanga¹, David R. Roalf², Petra Rupert², Megan Quarmley², Hari Hariharan¹, Mark Elliott¹, Raquel E. Gur², Paul J. Moberg², Ravinder Reddy¹, and Bruce I. Turetsky²

¹Radiology, University of Pennsylvania, Philadelphia, PA, United States, ²Psychiatry, University of Pennsylvania, Philadelphia, PA, United States

In this glutamate Chemical Exchange Saturation Transfer (GluCEST) study, typically developing individuals and youth at clinical high risk for psychosis exhibit subtle, but significant, abnormalities in brain glutamate, similar to patients with schizophrenia in the entire cortical area. GluCEST technique holds distinct promise for understanding neurodevelopmental contributions to schizophrenia pathophysiology.

-
- 4137
Computer #14
Hippocampal metabolic abnormalities in Schizophrenia: a 3D multi-voxel MR spectroscopic imaging study
Ivan I. Kirov^{1,2}, Emma J. Meyer^{1,2}, Assaf Tal³, Matthew S. Davitz^{1,2}, Dolores Malaspina^{4,5}, and Oded Gonen^{1,2}

¹Center for Advanced Imaging Innovation and Research (CAI2R), New York University School of Medicine, New York, NY, United States, ²Bernard and Irene Schwartz Center for Biomedical Imaging, New York University School of Medicine, New York, NY, United States, ³Chemical Physics, Weizmann Institute of Science, Rehovot, Israel, ⁴Psychiatry, New York University School of Medicine, New York, NY, United States, ⁵Institute for Social and Psychiatric Initiatives (InSPIRES), New York University Langone Medical Center, New York, NY, United States

The objective of this study was to test the hypothesis that schizophrenia patients' hippocampi are metabolically different from healthy controls'. Twenty-four patients and seven controls were studied with proton MR spectroscopic imaging at 3 T. Hippocampal volumes were also obtained. The findings were increased choline concentration in patients' hippocampi compared with controls, but no statistically significant changes in n-acetyl-aspartate or total creatine. While contrary to previous (mostly single-voxel) proton MR spectroscopy studies, these findings are nevertheless consistent with neuropathology reports of neither gliosis nor net neuronal loss. Bilateral hippocampal volume was 10% lower in the patients, consistent with previous reports.

4138
Computer #15 Altered cortical thickness related to the SNPs on the major histocompatibility complex in never-medicated schizophrenia
Bo Tao¹, Yuan Xiao¹, Lu Liu¹, Li Yao¹, Wenjing Zhang¹, and Su Lui¹

¹Radiology, West China Hospital of Sichuan University, Chengdu, China, People's Republic of

In summary, the present study provided evidence that single nucleotide polymorphisms (SNPs) on the major histocompatibility (MHC) relate with cortical thickness deficits in several regions, which support the critical role of immune system in the pathology of schizophrenia via modulation the development of the cerebral cortical structure.

4139
Computer #16 Reduced clustering co-efficient in structural connectivity of schizophrenia patients analyzed using diffusion tensor imaging
Merry Mani¹, Nancy Andreasen¹, and Vincent Magnotta¹

¹University of Iowa, Iowa City, IA, United States

Schizophrenia is a psychiatric illness characterized by failure of functional integration. To shed light on the underlying pathophysiology, the complex networks of the brain have to be studied comprehensively. This study used network analysis tools to study the topological features of the brain in schizophrenia. Using diffusion tensor imaging, we generated the graph network of schizophrenia patients and controls. We defined 68 cortical regions as nodes and used streamlines derived from deterministic fiber tracking to define the edges of the graph. A permutation testing was used to test differences between topological measures derived from the graphs of schizophrenia patients and controls.

4140
Computer #17 Reduced amygdala and hippocampal fractional anisotropy in methamphetamine use with psychosis
yadi li¹, Haibo Dong¹, Feng Li¹, Gaoyan Wang¹, Wenwen Shen², Wenhua Zhou², Jianbing Zhang², Longhui Li², and Chaogan Yan³

¹The Affiliated Ningbo Medical Treatment Center Lihuili Hospital of Ningbo University, Ningbo, China, People's Republic of, ²Ningbo Addiction Research and Treatment Center, Ningbo, China, People's Republic of, ³Institute of psychology, Chinese academy of sciences, Beijing, China, People's Republic of

This study detected microstructural changes of amygdala and hippocampus in methamphetamine(METH) users with psychosis by analyzing FA index on diffusion weighted imaging, while these users presented no evident volume reduction in these 2 structures. These 2 structures play a vital part in METH psychosis

4141
Computer #18 Age-related abnormalities of the corpus callosum in autism spectrum disorder: A diffusion spectrum imaging study using template-based tract-specific analysis
Chien-Hung Lu¹, Yu-Jen Chen², Yu-Chun Lo², Yu-Chun Hsu², Susan Shur-Fen Gau^{3,4}, and Wen-Yih Isaac Tseng^{2,4}

¹School of Medicine, National Taiwan University, Taipei, Taiwan, ²Institute of Medical Device and Imaging, National Taiwan University, Taipei, Taiwan, ³Department of Psychiatry, National Taiwan University College of Medicine, Taipei, Taiwan, ⁴Molecular Imaging Center, National Taiwan University, Taipei, Taiwan

The corpus callosum (CC) has been the most investigated white matter tract in autism spectrum disorder (ASD). However, whether the development of the CC is altered in ASD is not clearly identified. In this study, we performed diffusion spectrum imaging using tract specific analysis to measure the generalized fractional anisotropy of 16 segments of the CC. A GFA-age hyperbolic model was applied to test the age effect. The CC connecting bilateral temporal lobes was significantly different between ASD and TD. Our results identify the unique time trajectory of the CC in ASD.

4142
Computer #19 Application of the Mahalanobis Distance for Depicting the Neuroanatomical Variability within Autism Spectrum Disorders
Douglas C Dean III¹, Nicholas Lange², Brittany Travers¹, Nagesh Adluru¹, Do Tromp¹, Daniel Destiche¹, Abigail Freeman¹, Danica Samsin¹, Brandon Zielinski³, Molly Prigge³, P.T. Fletcher³, Jeffery Anderson³, Erin Bigler⁴, Janet Lainhart¹, and Andrew Alexander¹

¹Waisman Center, University of Wisconsin-Madison, Madison, WI, United States, ²McLean Hospital, Boston, MA, United States, ³University of Utah, Salt Lake City, UT, United States, ⁴Brigham Young University, Provo, UT, United States

To date, the heterogeneity of neuroimaging findings has made it challenging to identify specific brain-related phenotypes within autism spectrum disorder (ASD). In particular, a quantitative index of individual deviation across a set of brain measurements may be informative for constructing distributions of brain variation and identifying individuals who may or may not have abnormal brain structure. To this end, we investigated the use of the Mahalanobis distance to characterize multidimensional brain measures in individuals with and without ASD and to demonstrate that patterns of brain features distinguishing individuals with ASD are multidimensional and likely encompass differing cortical and sub-cortical characteristics.

-
- 4143
Computer #20
- One-Class Classifiers detect a specific endophenotype in young children with Autism Spectrum Disorders
Alessandra Retico¹, Ilaria Gori^{1,2}, Alessia Giuliano^{1,3}, Piernicola Oliva^{1,2}, Michela Tosetti⁴, Filippo Muratori^{3,4}, and Sara Calderoni⁴
- ¹National Institute of Nuclear Physics, Pisa, Italy, ²University of Sassari, Sassari, Italy, ³University of Pisa, Pisa, Italy, ⁴IRCCS Stella Maris Foundation, Pisa, Italy*
- Binary classifiers are widely used to analyze brain MRI features and to identify useful biomarkers of pathology. Strong challenges arise when dealing with extremely heterogeneous conditions such as Autism Spectrum Disorders (ASD). We propose the use of the One-Class Classifier (OCC) method that, in contrast to two-class classification, is based on the description of the positive class only. A test of similarity of new cases to the positive examples is then performed, and they are eventually considered as outliers. The application of OCC to Freesurfer-based brain MRI features identified a specific endophenotype in young children with ASD.
-
- 4144
Computer #21
- Identification of Novel Gene-Specific Bioimaging Markers in Autism Spectrum Disorder
Judith A. Gadge¹ and John-Paul J. Yu^{1,2}
- ¹Department of Radiology, University of Wisconsin School of Medicine and Public Health, Madison, WI, United States, ²Department of Biomedical Engineering, University of Wisconsin School of Medicine and Public Health, Madison, WI, United States*
- Autism spectrum disorder (ASD) is a complex genetic neurodevelopmental disorder. Differential expression patterns, splice-variants, and mutations in Neurexin1 (Nrxn1) have been implicated in the neurodevelopment of ASD. New targeted genome editing technologies have yielded the first cogent genetic animal models of ASD with animals harboring biallelic deletions of Nrxn1, allowing for the assessment of gene-specific perturbations in white matter composition and organization. Interrogating changes in brain structure attributable to a specific genetic allele is the first step towards the development and validation of an objective imaging biomarker, which can contribute to the diagnosis of ASD.
-
- 4145
Computer #22
- Abnormal brain structure is associated with depression and anxiety in obese patients using DTI
Yi-Chun Liu¹, Vincent Chin-Hung Chen², Hse-Huang Chao³, Ming-Chou Ho⁴, and Jun-Cheng Weng^{1,5}
- ¹Department of Medical Imaging and Radiological Sciences, Chung Shan Medical University, Taichung, Taiwan, ²Department of Psychiatry, Chang Gung Memorial Hospital, Chiayi, Taiwan, ³Taiwan Center for Metabolic and Bariatric Surgery, Jen-Ai Hospital, Taichung, Taiwan, ⁴Department of Psychology, Chung Shan Medical University, Taichung, Taiwan, ⁵Department of Medical Imaging, Chung Shan Medical University Hospital, Taichung, Taiwan*
- Since there is more and more delicious food in our daily life, people cannot resist the attraction to food. Therefore, obesity has become an important issue in modern society. Previous studies used food pictures to stimulate obese patients and used functional MRI to find the brain regions with increased activity. However, few studies mentioned about particular brain structure changes in obese patient. Noninvasive diffusion tensor imaging (DTI) are able to observe the water diffusion in the brain on the microscopic level for the early detection of white matter structural changes. Therefore, we used DTI to find the differences of brain structures between obese patients and healthy controls. The correlation between clinical and the DTI indices were also calculated and discussed. The clinical indices included body mass index (BMI), and measures of anxiety and depression.
-
- 4146
Computer #23
- Mapping Cerebral Oxidative Metabolism of Oxygen in Patients with Post-Stroke Apathy
Xiang He¹, Kenneth Wengler^{1,2}, Ananth Narayanan³, Chuan Huang¹, Christine DeLorenzo³, Ramin Parsey³, Mark Schweitzer¹, and Andrew Goldfine³
- ¹Radiology, Stony Brook University School of Medicine, Stony Brook, NY, United States, ²Biomedical Engineering, Stony Brook University, Stony Brook, NY, United States, ³Psychiatry, Stony Brook University School of Medicine, Stony Brook, NY, United States*
- Five post-stroke apathy patients underwent simultaneous ¹⁸F-FDG-PET/MRI to determine brain metabolic rates. PET data was used to determine whole brain metabolic rate of glucose (MR_{Glu}). Quantitative BOLD and arterial spin labeling MRI was used to determine cerebral metabolic rate of oxygen (CMRO₂). Metabolic rates were compared for the two modalities to determine useful information associated with post-stroke apathy. The prefrontal cortex showed decreased metabolic rates for both CMRO₂ and MR_{Glu} potentially indicating apathy. MR qBOLD-derived CMRO₂ measurements demonstrated good correlation with PET ¹⁸F-FDG metabolism, providing strong support for its adoption as a non-invasive mapping of brain metabolism in patients with post-stroke apathy.
-
- 4147
Computer #24
- Cerebellar microstructural abnormalities in bipolar depression and unipolar depression: a diffusion kurtosis and perfusion imaging study
Lianping Zhao¹, Ying Wang¹, Yanbin Jia¹, Shuming Zhong¹, Yao Sun¹, Zhifeng Zhou¹, and Li Huang^{1,2}
- ¹Jinan university, Guangzhou, China, People's Republic of, ²Guangzhou, China, People's Republic of*
- Depression in the context of bipolar disorder (BD) is often misdiagnosed as unipolar depression (UD), leading to mistreatment and poor clinical outcomes. However, little is known about the similarities and differences in cerebellum between BD and UD. Patients with BD (n = 35) and UD (n = 30) during a depressive episode as well as 40 healthy controls underwent diffusional kurtosis imaging (DKI) and three dimensional arterial spin labeling (3D ASL). The DKI parameters including mean kurtosis (MK), axial kurtosis(Ka), radial kurtosis (Kr),fractional anisotropy (FA), mean diffusivity (MD), axial diffusivity (Da) and radial diffusivity (Dr) and 3D ASL parameters (i.e. cerebral blood flow) was measured by using regions-of-interest (ROIs) analysis in the superior cerebellar peduncles(SCP), middle cerebellar

peduncles (MCP) and dentate nuclei (DN) of cerebellum. Patients with UD exhibited significant differences from controls for DKI measures in bilateral SCP and MCP and cerebral blood flow (CBF) in bilateral SCP and left DN. Patients with BD exhibited significant differences from controls for DKI measures in the right MCP and left DN and CBF in the left DN. Patients with UD showed significantly lower MD values compared with patients with BD in the right SCP. Correlation analysis showed there were negative correlations between illness duration and MD and Dr values in the right SCP in UD, and negative correlations between illness duration and CBF in bilateral SCP in BD. Our findings provide new evidence of microstructural changes in cerebellum in BD and UD. The two disorders may have overlaps in microstructural abnormality in MCP and DN during the depressive period. Microstructural abnormality in SCP may be a key neurobiological feature of UD.

Electronic Poster

Psychiatric Disorders: General

Exhibition Hall

Wednesday, May 11, 2016: 17:00 - 18:00

-
- 4148
Computer #25
- Abnormal brain volume and shape are associated with aspects of inhibitory control and implicit attitude toward betel nut in chewers
Deborah Xiu-Ning Lin¹, Shu-Wei Chu¹, Ming-Chou Ho², and Jun-Cheng Weng^{1,3}
- ¹Department of Medical Imaging and Radiological Sciences, Chung Shan Medical University, Taichung, Taiwan, ²Department of Psychology, Chung Shan Medical University, Taichung, Taiwan, ³Department of Medical Imaging, Chung Shan Medical University Hospital, Taichung, Taiwan
- Betel nut is the seed of the betel palm, which grows in the tropical or subtropical regions, especially in Taiwan, India, China and parts of east Africa. It has been confirmed that chewing betel nuts can be addictive to it and is also carcinogenic to humans. Chewing betel nuts lead to a greatly increased risk of developing a range of serious diseases, including oral and esophagus cancers. In Taiwan, 88% of people who were diagnosed to oral cancer have the habit of chewing betel nuts, but very few researches studied on how chewing betel nuts effects brain structure. Therefore, in this study we tried to find out the structural volume and shape changes in the brain between betel nut chewers and healthy controls with voxel-based morphometry (VBM) and vertex-wise shape analyses. In addition, the relationship between brain structural volume size and implicit attitude or inhibitory control were also discussed.
-
- 4149
Computer #26
- Glutamate level change in anterior cingulate elicited by alcohol cues in alcohol use disorder
Hu Cheng¹, Derek Kellar¹, Ulrike Dydak^{2,3}, Peter Finn¹, Allison Lake¹, Shalmali Dharmadhikari^{2,3}, George Rebec¹, and Sharlene Newman¹
- ¹Psychological and Brain Sciences, Indiana University, Bloomington, IN, United States, ²School of Health Sciences, Purdue University, West Lafayette, IN, United States, ³Department of Radiology and Imaging Sciences, Indiana University School of Medicine, Indianapolis, IN, United States
- Evidence indicates that glutamate neurotransmission plays a critical role in alcohol and other substance addiction. This study investigated the dynamic change of glutamate level elicited by alcohol cues in individuals with alcohol use disorder (AUD). Both the absolute value of glutamate concentration and its ratio to total creatine measured decreased significantly for AUD subjects after they viewed the pictures of alcoholic beverages. A high correlation ($r = -0.90$) between baseline glutamate level and alcohol problem counts was observed for AUD subjects. This cue induced decrease of glutamate is not a direct translation from animal studies.
-
- 4150
Computer #27
- Disadvantage of social sensitivity: Interaction of oxytocin receptor genotype (OXTR rs53576) and childhood maltreatment on limbic gray matter
Harald Kugel¹, Udo Dannlowski^{2,3}, Dominik Grotegerd², Ronny Redlich², Nils Opel², Katharina Dohm², Dario Zaremba², Anne Groegler², Juliane Schwieren², Thomas Suslow⁴, Patricia Ohrmann², Jochen Bauer^{1,2}, Axel Krug³, Tilo Kircher³, Christa Hohoff², Katharina Domschke⁵, Andreas Jansen³, Pienie Zwitserlood⁶, Markus Heinrichs^{7,8}, Volker Arolt², Walter Heindel¹, and Bernhard T. Baune⁹
- ¹Department of Clinical Radiology, University of Muenster, Muenster, Germany, ²Department of Psychiatry, University of Muenster, Muenster, Germany, ³Department of Psychiatry, University of Marburg, Marburg, Germany, ⁴Department of Psychosomatics and Psychotherapy, University of Leipzig, Leipzig, Germany, ⁵Department of Psychiatry, University of Wuerzburg, Wuerzburg, Germany, ⁶Department of Psychology, University of Muenster, Muenster, Germany, ⁷Department of Psychology, University of Freiburg, Freiburg, Germany, ⁸Freiburg Brain Imaging Center, University of Freiburg, Freiburg, Germany, ⁹School of Medicine, Discipline of Psychiatry, University of Adelaide, Adelaide, Australia
- Oxytocin is a pro-social and anxiolytic neuropeptide, especially if the G-allele of a common polymorphism (rs53576) in the oxytocin receptor gene is present. Recent studies suggest, however, a detrimental role of this allele in the context of childhood maltreatment. Structural MRI data show reduced gray matter volumes of the ventral striatum, fMRI shows increased amygdala responsiveness associated with increased CTQ (maltreatment) score. Thus for individuals with adverse childhood experiences the G-allele may be a vulnerability factor.
-
- 4151
Computer #28
- Differences in the structural brain network analysis between internet addicted adolescents and healthy adolescents
Min-Hee Lee¹, Yoon Ho Hwang¹, Aream Min¹, Dong Youn Kim¹, Bong Soo Han², and Hyung Suk Seo³
- ¹Department of Biomedical Engineering, Yonsei University, Wonju, Korea, Republic of, ²Department of Radiological Science, Yonsei University, Wonju, Korea, Republic of, ³Department of Radiology, Korea University Ansan Hospital, Ansan, Korea, Republic of
- Although Internet addiction (IA) has been increasingly considered as a serious public health issue for adolescents, its neurobiological

mechanisms remain poorly understood. Therefore, new biomarkers are needed to understanding IA. Using diffusion tensor images for IA and healthy adolescents, we analyzed brain network to reveal structural alterations in brain of IA adolescents. IA adolescents showed increase of regional efficiency in bilateral superior orbitofrontal cortex, right rectus and parahippocampal gyrus. Severity of IA is correlated with regional efficiency of brain regions which showed differences between groups. The brain network analysis can be used to disclose potential functional deficits in IA.

-
- 4152
Computer #29
Alteration of white matter microstructure within the reward circuit revealed by neurite orientation dispersion and density imaging (NODDI)
Kouhei Kamiya¹, Naohiro Okada², Yuichi Suzuki³, Ryusuke Irie¹, Takatoshi Kubo¹, Yudai Nakai⁴, Yasumasa Nippashi¹, Daisuke Koshiyama², Kentaro Morita², Kingo Sawada², Yoshihiro Satomura², Shinsuke Koike^{2,5}, Harushi Mori¹, Akira Kunimatsu¹, Kiyoto Kasai², and Kuni Ohtomo¹
- ¹The Department of Radiology, The University of Tokyo, Tokyo, Japan, ²The Department of Neuropsychiatry, The University of Tokyo, Tokyo, Japan, ³The Department of Radiological Technology, The University of Tokyo Hospital, Tokyo, Japan, ⁴The Department of Radiology, Teikyo University School of Medicine, Tokyo, Japan, ⁵Office for Mental Health Support, Division for Counseling and Support, The University of Tokyo, Tokyo, Japan
- This study aimed to investigate the brain microstructural alteration in patients with major depressive disorder (MDD) using neurite orientation dispersion and density imaging (NODDI). Nineteen MDD patients and 13 controls were involved. The TBSS analyses revealed significant increase in orientation dispersion index (ODI) in patients with MDD, distributed in bilateral frontal lobes and right occipital lobe, right internal capsule, bilateral thalamus and hypothalamus, right nucleus accumbens, and midbrain tegmentum, suggesting involvement of the reward circuit. The neurite density was not significantly altered, arousing interest on further study focusing on treatment response, whether the ODI increase is reversible or not.
-
- 4153
Computer #30
Alterations of neural correlates in drug-naïve first episode pediatric patients with posttraumatic stress disorder: An optimized voxel-based morphometry study
Lei Li¹, Xinyu Hu¹, Du Lei¹, Xiaoqi Huang¹, and Qiyong Gong¹
- ¹Huaxi MR Research Center (HMRR), Department of Radiology, West China Hospital of Sichuan University, Chengdu, China, People's Republic of
- The current study used voxel-based morphometry (VBM)-diffeomorphic anatomical registration through exponentiated lie algebra (DARTEL) algorithm to investigate the gray matter abnormalities in drug-naïve first-episode pediatric patients with posttraumatic stress disorder (PTSD) using high resolution structural MRI. Meanwhile, we investigated the association between altered neural correlates and symptom severity as measured by clinician-administered PTSD scale (CAPS) and PTSD checklist (PCL) scores with the age as a covariate. The current study provided the preliminary evidence that the intrinsic abnormalities of neural correlates in pediatric PTSD patients were mainly in fear circuit and default mode network.
-
- 4154
Computer #31
Altered whole brain functional connectivity in drug-naïve patients with obsessive-compulsive disorder: A resting-state functional magnetic resonance imaging study
Xinyu Hu¹, Xi Yang², Yanchun Yang², Qiyong Gong¹, and Xiaoqi Huang¹
- ¹Huaxi MR Research Center (HMRR), Department of Radiology, West China Hospital of Sichuan University, Chengdu, China, People's Republic of, ²Department of Psychiatry, West China Hospital of Sichuan University, Chengdu, China, People's Republic of
- We analysis whole brain connectivity in a relatively large sample of drug-naïve patients with obsessive-compulsive disorder (OCD) using a novel graph-theory approach known as functional connectivity strength (FCS) to identify brain regions displaying high-degree centrality of connectivity. Based on the new approach of FCS, our findings demonstrated obvious significant hyperactivity of default mode network (DMN) in OCD patients at resting state. Furthermore, our results provided evidence that besides the prevailing model of cortical-striatal-thalamic-cortical circuits in OCD, the disequilibrium between the DMN and the salience network (SN) might be associated with the pathophysiology of OCD.
-
- 4155
Computer #32
Altered Intrinsic Brain Functional Connectivity in Suicidal Patients with Major Depressive Disorder
Ziqi Chen¹, Mingrui Xia², Jia Liu¹, Zhiyun Jia^{1,3}, Xin Xu^{1,4}, Weihong Kuang⁴, Yong He², and Qiyong Gong^{1,5}
- ¹Huaxi MR Research Center (HMRR), Department of Radiology, West China Hospital of Sichuan University, Chengdu, China, People's Republic of, ²State Key Laboratory of Cognitive Neuroscience and Learning, Beijing Normal University, Beijing, China, People's Republic of, ³Department of Nuclear Medicine, West China Hospital of Sichuan University, Chengdu, China, People's Republic of, ⁴Department of Psychiatry, West China Hospital of Sichuan University, Chengdu, China, People's Republic of, ⁵Department of Psychology, School of Public Administration, Sichuan University, Chengdu, China, People's Republic of
- The underlying neural correlates of suicide attempts in major depressive disorder (MDD) at the connectivity or circuit level remains incompletely understood. Therefore, we utilized a graph-theory approach—functional connectivity strength (FCS) to identify resting-state functional connectivity alterations of whole-brain networks in MDD patients with a history of suicide attempts. Relative to healthy controls, two MDD patient groups (attempters and non-attempters) showed overlapping reduced FCS in the middle and inferior occipital gyrus (IOG), insula, superior temporal gyrus, thalamus and limbic regions, while attempters showed more decreased FCS in right insula and left IOG. The depression severity was positively correlated with FCS in right thalamus in suicide attempters. Disconnection of the insula and IOG could be biological correlates of impaired decision making and emotional information processing in MDD patients with a history of suicide attempt.

- 4156
Computer #33 Functional connectivity and neuroanatomical differences in a stress susceptible and resilient mouse model
Victoria X Wang¹, Caroline Menard², Cheuk Ying Tang³, Frances Marks¹, Johnny C Ng¹, Lazar Fleysher¹, Zahi A Fayad¹, and Scott Russo²
¹Radiology, Translational and Molecular Imaging Institute at Mount Sinai, New York, NY, United States, ²Neuroscience, Icahn School of Medicine at Mount Sinai, New York, NY, United States, ³Radiology & Psychiatry, Translational and Molecular Imaging Institute at Mount Sinai, New York, NY, United States
- We studied functional and structural connectivity in a stress susceptible and resilient mouse model using rsfMRI and DTI. We also investigated the integrity of the Blood Brain Barrier using Gd-DTPA. We found hyperactivity in the susceptible mice which had also several regions in the brain with compromised BBB. We also detected increased structural connectivity in the resilient mice.
-
- 4157
Computer #34 Altered Dynamic Functional Connectivity of Amygdala in Major Depressive Disorder
Lihua Qiu^{1,2}, Mingrui Xia³, Yong He³, and Qiyong Gong²
¹Radiology, The Second People's Hospital of Yibin, Yibin, China, People's Republic of, ²West China Hospital of Sichuan University, Chengdu, China, People's Republic of, ³Beijing Normal University, Beijing, China, People's Republic of
- Neuroimaging studies have shown that MDD is accompanied by functional abnormalities in amygdala and related connections; yet, little is known about amygdala subregion dynamic functional connectivity alterations of the whole-brain networks in MDD patients. In this work, general linear model analysis were used to assess the between-group differences of amygdalar subregion dynamic functional connectivity alterations in MDD patients. We found the altered amygdaloid projection were mainly in brainstem, cerebellum, thalamus, temporal and orbital cortical areas. These areas belong to limbic-thalamo-cortical circuitry which play important role in MDD and may associated with the impaired emotional modulation ability in MDD.
-
- 4158
Computer #35 Increased pregenual anterior cingulate glucose and lactate concentrations in major depressive disorder
Andreas Hock^{1,2}, Jutta Ernst², Anke Henning^{1,3}, Erich Seifritz², Heinz Boeker², and Simone Grimm^{2,4}
¹Institute for Biomedical Engineering, University and ETH Zurich, Zurich, Switzerland, ²Department of Psychiatry, Psychotherapy and Psychosomatics, Hospital of Psychiatry, University of Zurich, Zurich, Switzerland, ³Max Planck Institute for Biological Cybernetics, Tuebingen, Germany, ⁴Department of Psychiatry, Charité, Berlin, Germany
- Proton magnetic resonance spectroscopy (¹H-MRS) was used to test whether patients with major depressive disorder have increased glucose and lactate levels in the pregenual anterior cingulate cortex (PACC) compared to healthy controls. Therefore, forty healthy and depressed participants spectra were acquired from the PACC using a maximum echo JPRESS protocol. Results show significant increases of glucose and lactate in patients, which are also associated with depression severity. These findings indicate impaired brain energy metabolism in MDD with increased fraction of energy utilization via glycolysis and reduced mitochondrial oxidative clearance of lactate.
-
- 4159
Computer #36 Increase of grey matter following bifrontal rTMS in drug resistant major depressive disorder patients: A VBM study
Elisa Kallioniemi^{1,2}, Mervi Könönen^{1,3}, Juhana Hakumäki³, Esa Mervaala¹, Heimo Viinamäki⁴, Ritva Vanninen³, and Minna Valkonen-Korhonen⁴
¹Department of Clinical Neurophysiology, Kuopio University Hospital, Kuopio, Finland, ²Department of Applied Physics, University of Eastern Finland, Kuopio, Finland, ³Department of Clinical Radiology, Kuopio University Hospital, Kuopio, Finland, ⁴Department of Psychiatry, Kuopio University Hospital, Kuopio, Finland
- Repetitive transcranial magnetic stimulation (rTMS) is able to induce long-term excitatory and inhibitory effects on cortical functions if applied repeatedly over several days. Thus, rTMS possesses a great potential in therapeutic applications and several promising therapies have already been developed. Whether rTMS causes structural neuroplasticity, however, remains mainly unknown. In this study, we found that bifrontal rTMS applied to dorsolateral prefrontal cortex (DLPFC) elicited structural changes in major depressive disorder patients. The increase in grey matter was found in the right post- and precentral gyri, which are both functionally connected to DLPFC.
-
- 4160
Computer #37 Neurochemical alterations detected in Irritable Bowel Syndrome using 2D L-COSY
Scott Quadrelli^{1,2}, Gerald Holtmann³, Nicholas Talley², Saadallah Ramadan², and Carolyn Mountford⁴
¹Queensland University of Technology, Brisbane, Australia, ²The University of Newcastle, Newcastle, Australia, ³The University of Queensland, Brisbane, Australia, ⁴Translational Research Institute, Brisbane, Australia
- IBS is a characterised intermittent chronic abdominal pain and altered bowel habit in the absence of an organic cause. Neurochemical changes may play a role in the pathophysiology of IBS.
- Our pilot studies indicate that in vivo neuro 2D L-COSY monitors alterations to neurochemical pathways associated with IBS.
-
- 4161
Computer #38 Amygdala down-regulation with fMRI neurofeedback in healthy subjects and BPD patients
Christian Paret¹, Matthias Ruf¹, Traute demirakca¹, Christian Schmahl², and Gabriele Ende¹
¹Neuroimaging, Central Institute of Mental Health, Mannheim, Germany, ²Department of Psychosomatic Medicine and Psychotherapy, Central

fMRI neurofeedback on emotion-related brain activation via a brain-computer interface can improve brain self-regulation. We could show that neurofeedback is associated with amygdala down-regulation and alterations in frontolimbic functional connectivity in healthy female participants and female patients with borderline personality disorder. Real-time fMRI neurofeedback may in future help patients with severe emotion dysregulation to improve control over emotion-related brain networks.

-
- 4162
Computer #39 White matter microstructure is associated with auditory and tactile processing in children with and without sensory processing disorder
Yi-Shin Chang¹, Mathilde Gratiot¹, Julia Owen¹, Anne Brandes-Aitken¹, Shivani Desai¹, Susanna Hill¹, Anne Arnett¹, Julia Harris¹, Elysa Marco¹, and Pratik Mukherjee¹

¹University of California in San Francisco, San Francisco, CA, United States

Sensory processing disorders (SPD) affect 5-16% of school-aged children, and can cause downstream deficits of intellectual and social development. In this study, we use diffusion tensor imaging to study a cohort of 41 children with SPD and 41 typically developing children ages 8-12. We confirm and generalize results from our prior pilot study indicating disrupted posterior white matter in SPD, and further demonstrate a relationship between direct measurements of tactile and non-linguistic auditory function and white matter microstructure -- not just in SPD, but also in typically developing children.

-
- 4163
Computer #40 Intra-hippocampal Diffusion Tensor Imaging Identifies Dendritic Abnormalities After Early-life Stress
Jenny Molet¹, Pamela M Maras¹, Eli Kinney-Lang^{1,2}, Fasial Rashid², Neil Harris³, Autumn Ivy¹, Ana Solodkin^{1,4}, Tallie Z Baram^{1,5}, and Andre Obenaus^{2,5}

¹Anatomy/Neurobiology, University of California, Irvine, Irvine, CA, United States, ²Pediatrics, Loma Linda University, Loma Linda, CA, United States, ³Neurosurgery, University of California, Los Angeles, Los Angeles, CA, United States, ⁴Neurology, University of California, Irvine, Irvine, CA, United States, ⁵Pediatrics, University of California, Irvine, Irvine, CA, United States

The effects of early-life adversity observed in the brain anatomy of rodents might be instructive about the human condition. Chronic early life stress in a rodent model results in dendritic pruning in the dorsal hippocampus. High resolution volumetric MRI found hippocampal volume loss and DTI measures of microstructure found increased fractional anisotropy. Structural MRI measures can be used to find microstructural abnormalities related to dendritic morphological abnormalities. Thus, MRI metrics could be subsequently tested clinically to monitor adolescents at risk for neuropsychiatric illness.

-
- 4164
Computer #41 Sensitivity of MT and T1 VBM to subcortical morphometric alterations in adult ADHD
Arjun Sethi¹, Hugo Critchley¹, Neil A Harrison¹, and Mara Cercignani¹

¹Brighton & Sussex Medical School, Brighton, United Kingdom

Attention Deficit Hyperactivity Disorder (ADHD) is robustly associated with striatal abnormalities in childhood, though results in adults have been less definitive. Whilst this may reflect maturational normalisation, studies in adults have also typically been smaller. To enhance sensitivity to such changes we employ VBM analysis to MT saturation maps in adult ADHD, which have been shown to enhance localisation and segmentation of subcortical structures. In comparing these results to VBM analysis performed with T1 images in the same subjects, we show that MT-VBM is sensitive to striatal morphometric alterations that are not detected using T1-VBM.

-
- 4165
Computer #42 Assessment of chemotherapy-induced brain volume and shape changes in breast cancer patients using voxel-based morphometry and vertex-wise shape analysis
Ren-Horng Wang¹, Vincent Chin-Hung Chen², Dah-Cherng Yeh³, and Jun-Cheng Weng^{1,4}

¹Department of Medical Imaging and Radiological Sciences, Chung Shan Medical University, Taichung, Taiwan, ²Department of Psychiatry, Chang Gung Memorial Hospital, Chiayi, Taiwan, ³Department of Breast Surgery, Taichung Veterans General Hospital, Taichung, Taiwan, ⁴Department of Medical Imaging, Chung Shan Medical University Hospital, Taichung, Taiwan

Recent advances in breast cancer treatment have improved the long-term survival rate in cancer patients. The success in primary breast cancer treatment marks the importance of the post-treatment care. Cancer-related trauma after chemotherapy have been widely reported by breast cancer survivors. Previous study showed the decreased gray matter volume one month after chemotherapy completion, especially in frontal regions which is known for cognitive function. Another study indicated that there is reduction in cerebellar regions and right thalamus after the chemotherapy. However, several studies focused on the change of brain volume, but did not mention about the change of brain shape. Thus, in the study we aim to find out the differences of both brain volume and shape between chemotherapy-treated breast cancer patients and healthy subjects based on voxel-based morphometry (VBM) and vertex-wise shape analysis, respectively. In our results, reduced gray matter volume of right thalamus and white matter volume of cerebellum, and altered shape of left amygdala, bilateral thalamus, and bilateral hippocampus was found in the chemotherapy-treated breast cancer patients compared to normal controls.

-
- 4166
Computer #43 Neurobiological Quantification of Stress-Induced Sleep-Perturbation in Rats using In Vivo Proton MR Spectroscopy and In Vitro Liquid Chromatography-Tandem Mass Spectrometry (LC-MS/MS)
Do-Wan Lee^{1,2}, Seockhoon Chung³, Hyun Ju Yoo⁴, Su Jung Kim⁴, Chul-Woong Woo², Sang-Tae Kim², Kyungwon Kim⁵, Jeong-Kon Kim⁵, Jin Seong Lee⁵, Choong Gon Choi⁵, Woo Hyun Shim⁵, Dong-Hoon Lee¹, Yoonseok Choi², and Dong-Cheol Woo²

¹Department of Radiology, Johns Hopkins University School of Medicine, Baltimore, MD, United States, ²MR Core Laboratory, Asan Institute for Life Sciences, Asan Medical Center, Seoul, Korea, Republic of, ³Department of Psychiatry, Asan Medical Center, University of Ulsan College of Medicine, Seoul, Korea, Republic of, ⁴Biomedical Research Center, Asan Institute for Life Sciences, Asan Medical Center University of Ulsan College of Medicine, Seoul, Korea, Republic of, ⁵Department of Radiology, Asan Medical Center, University of Ulsan College of Medicine, Seoul, Korea, Republic of

The aim of this study was to quantitatively assess the differences on the cerebral metabolites and to identify factors determining the alterations of endogenous biomolecules on stress-induced sleep disturbance in rats using in vivo 1H-MRS and in vitro LC-MS/MS. The GABA, Gln concentrations, Gln/Glu, Gln/tCr, and GABA/Glu ratios were significantly higher in SSP rats than in CNTLs. The serotonin concentrations were significantly lower in SSP rats than in CNTLs. Our in vivo 1H MRS and in vitro LC-MS/MS results suggest that the various metabolites and endogenous biomolecule signals in hippocampal region are particularly sensitive and vulnerable to stress-induced sleep perturbation.

4167

Computer #44

Quantitative prediction of symptom progression in drug-naïve individuals with obsessive-compulsive disorder using resting-state functional magnetic resonance imaging

Xinyu Hu¹, William Pettersson-Yeo², Lizhou Chen¹, Xi Yang³, Yanchun Yang³, Qiyong Gong¹, and Xiaoqi Huang¹

¹Huaxi MR Research Center (HMRR), Department of Radiology, West China Hospital of Sichuan University, Chengdu, China, People's Republic of,

²Department of Psychosis Studies, Institute of Psychiatry, King's College London, London, United Kingdom, ³Department of Psychiatry, West China Hospital of Sichuan University, Chengdu, China, People's Republic of

Neuroimaging techniques hold the promise that they may one day aid the clinical assessment of individual psychiatric patients. However, the vast majority of studies published so far have been based on average differences between groups. The current study aimed to apply a novel multivariate pattern analysis technique known as relevance vector regression to evaluating the potential of resting-state functional magnetic resonance imaging for making accurate predictions about symptom progression in a relatively large sample of drug-naïve patients with obsessive-compulsive disorder.

4168

Computer #45

Parcellation of nigrostriatal and mesolimbic midbrain components in adults ADHD: Relationship to waiting impulsivity and motivation

Arjun Sethi¹, Valerie Voon², Hugo Critchley¹, Neil A Harrison¹, and Mara Cercignani¹

¹Brighton & Sussex Medical School, Brighton, United Kingdom, ²Department of Psychiatry, University of Cambridge, Cambridge, United Kingdom

The substantia nigra/ventral tegmental area (SN/VTA) is central to the modulation of dopaminergic networks implicated in Attention Deficit Hyperactivity Disorder (ADHD). However, little is known of its specific contribution to the disorder. Whilst motivational abnormalities and impulsivity are known to be related to the structure, it is not clear whether SN/VTA subcomponents differentially contribute to these deficits. Using diffusion MRI tractography parcellation of the SN/VTA, we show that increased waiting impulsivity in ADHD is related to the microstructure of the mesolimbic SN/VTA, whilst trait motivation is related to the nigrostriatal component. Unlike previous reports in unmedicated ADHD, we detect no motivational abnormalities in this medicated cohort. However, we report that patients who have been medicated longer show alterations in microstructure consonant with increased motivation.

4169

Computer #46

Longitudinal VBM of downregulation in mice with striatum-specific D2R overexpression

Claudia Falfan-Melgoza¹, Anne Stephanie Mallien², Lei Zheng^{1,3}, Alexander Sartorius^{1,2}, Christoph Kellendonk⁴, Peter Gass², and Wolfgang Weber-Fahr¹

¹RG Translational Imaging, Central Institute of Mental Health, Medical Faculty Mannheim, University of Heidelberg, Mannheim, Germany,

²Department of Psychiatry, Central Institute of Mental Health, Medical Faculty Mannheim, University of Heidelberg, Mannheim, Germany,

³Department of Radiation Oncology, Medical Faculty Mannheim, University of Heidelberg, Mannheim, Germany, ⁴Department of Pharmacology, Columbia University, New York, NY, United States

Striatal D2R overexpression has been linked to the pathophysiology of schizophrenia. We used longitudinal voxel based morphometry on a transgenic mouse model before and after switching off the striatal D2R overexpression using doxycycline. Longitudinal registration showed a significant volume gain after the treatment in large areas covering frontal, prefrontal, striatal and temporal regions in the animals with D2R overexpression. The areas with volume increase over time show a remarkable plasticity as a result of the D2R downregulation within three weeks and correspond largely to regions with decreased gray matter volume commonly found in VBM studies on schizophrenia patients.

4170

Computer #47

Brain cortical thickness abnormalities in untreated, first-episode adult patients with major depressive disorder

Youjin Zhao¹, Huaiqiang Sun¹, Su Lui¹, and Qiyong Gong¹

¹Huaxi MR Research Center (HMRR), Department of Radiology, West China Hospital of Sichuan University, Chengdu, China, People's Republic of

The present study aimed to use surface-based morphometric analysis to characterize the alteration of cortical thickness in first-episode never-medicated adult MDD patients. 37 MDD patients and 41 healthy controls were enrolled. Results showed increased cortical thickness ($p < 0.05$, False Discovery Rate) in left anterior and posterior cingulate cortex extending to medial superior frontal cortex, bilateral precentral cortex, left paracentral cortex, bilateral superior parietal cortex, left temporal poles, and right lateral occipital cortex in MDD patients than HC group. The data provide evidence that even early in the course of depression brain regions involved in mood regulation show cortical thickness abnormalities.

4171

Computer #48

Whole-brain volume alteration and its correlation with anxiety severity in patients with obsessive compulsive disorder and generalized anxiety disorder
Gwang-Won Kim¹, Chung-Man Moon¹, Tae-Hoon Kim¹, and Gwang-Woo Jeong^{1,2}

¹Research Institute of Medical Imaging, Chonnam National University Medical School, Gwang-ju, Korea, Republic of, ²Department of Radiology, Chonnam National University Medical School, Gwang-ju, Korea, Republic of

Obsessive compulsive disorder (OCD) and generalized anxiety disorder (GAD) are associated with abnormalities in the processing and regulation of anxiety. The purpose of this study was to evaluate gray matter (GM) and white matter (WM) volume alterations over whole-brain structures in healthy controls vs. patients with OCD vs. GAD using voxel-based morphometry (VBM), and further to assess the correlations of the GM and WM volume variations with the scores for anxiety severity in OCD and GAD.

Electronic Poster

Human Brain Tumours 1: Diagnosis & Response to Therapy

Exhibition Hall

Wednesday, May 11, 2016: 17:00 - 18:00

4172

Computer #49

Multiparametric MR imaging of oxygen metabolism and angiogenesis for detection of recurrence or grade increase in glioma patients
Andreas Stadlbauer¹, Max Zimmermann¹, Karl Rössler¹, Stefan Oberndorfer², Michael Buchfelder¹, and Gertraud Heinz³

¹Department of Neurosurgery, University of Erlangen, Erlangen, Germany, ²Department of Neurology, University Clinic of St. Pölten, St. Pölten, Austria, ³Department of Radiology, University Clinic of St. Pölten, St. Pölten, Austria

Early detection of recurrence is crucial in patient care, but differentiation of treatment related necrosis from recurrent neoplasm is often difficult with conventional MRI (cMRI). We evaluated the usefulness for glioma recurrence grade increase detection of a multiparametric MRI for combined examination of oxygen metabolism and microvessel architecture. Forty-one patients with suspected recurrent glioma and one patient under antiangiogenic therapy were examined using vascular architecture mapping (VAM) and multiparametric quantitative BOLD (mp-qBOLD). 57% of LGG-patients, 22% of glioma WHO^oIII, and 32% of glioblastoma patients which were diagnosed as unsuspecting showed changes in oxygen metabolism and microvasculature indicative for recurrence.

4173

Computer #50

MCT down-regulation contributes to reduced conversion of hyperpolarized [1-13C]-pyruvate to [1-13C]-lactate in IDH1 mutant glioma cells
Pavithra Viswanath¹, Jose Izquierdo-Garcia¹, Chloe Najac¹, Larry Cai¹, Russell Pieper², and Sabrina M Ronen¹

¹Radiology, University of California San Francisco, San Francisco, CA, United States, ²Neurological Surgery, University of California San Francisco, San Francisco, CA, United States

In this study we used hyperpolarized ¹³C-MRS to investigate pyruvate to lactate flux in IDH1 mutant cells. We found reduced hyperpolarized [1-¹³C]-lactate production from hyperpolarized [1-¹³C]-pyruvate in IDH1 mutant cells compared to wild-type. While there was no difference in lactate dehydrogenase A activity or NAD⁺/NADH, IDH1 mutant cells and patient samples showed reduced expression of monocarboxylate transporters MCT1 and MCT4. Comparison of hyperpolarized [1-¹³C]-lactate production between IDH1 wild-type and mutant lysates confirmed that reduced MCT expression was responsible for reduced hyperpolarized [1-¹³C]-lactate production. Thus, our study indicates that reduced MCT expression is a metabolic feature of the IDH1 mutation.

4174

Computer #51

Assessment of changes in structural connectivity of the central executive network during cranial radiotherapy in children treated for medulloblastoma
Wilburn E Reddick¹, John O Glass¹, Elizabeth C Duncan¹, Jung Won Hyun², Qing Ji¹, Yimei Li², and Amar Gajjar³

¹Diagnostic Imaging, St. Jude Children's Research Hospital, Memphis, TN, United States, ²Biostatistics, St. Jude Children's Research Hospital, Memphis, TN, United States, ³Oncology, St. Jude Children's Research Hospital, Memphis, TN, United States

Diffusion tensor imaging from 30 childhood medulloblastoma patients were analyzed to assess changes in structural connectivity of the central executive network (CEN) in response to cranial irradiation. Significant drops in fractional anisotropy and axial diffusivity (AX) were demonstrated in most of the CEN subnetworks after irradiation. Furthermore, patients receiving the highest CRT dose had significantly decreased AX in all subnetworks of the CEN. These findings suggest significant reduction in the microstructural integrity within the CEN immediately after CRT in this population and support the use of the CEN model for evaluating changes in cerebral white matter early in therapy.

4175

Computer #52

Slip interface imaging: a novel MR-elastography based imaging method for assessing the surgical plane of cleavage in meningiomas
Ziyang Yin¹, Kevin J. Glaser¹, Armando Manduca², Jamie J. Van Gompel³, Arvin Arani¹, Joshua D. Hughes³, Anthony Romano⁴, Richard L. Ehman¹, and John Huston III¹

¹Radiology, Mayo Clinic, Rochester, MN, United States, ²Physiology and Biomedical Engineering, Mayo Clinic, Rochester, MN, United States, ³Neurosurgery, Mayo Clinic, Rochester, MN, United States, ⁴Naval Research Laboratory, Washington, WA, United States

The preoperative assessment of the surgical cleavage plane at the tumor-brain interface in meningiomas is important for surgical planning. A recently developed slip interface imaging (SII) technique is uniquely capable of directly assessing the degree of tumor



adherence at the tumor-brain interface. In this study, SII was applied to assess the surgical cleavage plane between the tumor and the underlying brain in meningiomas. The correlation between the SII results and the surgical plane of cleavage was statistically significant ($p=0.0014$). The presence of a complete slip interface suggests the tumor can be removed using a dissection plane outside the pia mater.

-
- 4176
Computer #53 High grade intracranial gliomas exhibit widespread impaired cerebrovascular reactivity
Christiaan Hendrik Bas van Niftrik¹, Marco Piccirelli², Jan-Karl Burkhardt¹, Athina Pangalu², Antonio Valavanis², Michael Weller³, Oliver Bozinov¹, Luca Regli¹, and Jorn Fierstra¹
- ¹Department of Neurosurgery, University Hospital Zurich, Zurich, Switzerland, ²Department of Neuroradiology, University Hospital Zurich, Zurich, Switzerland, ³Department of Neurology, University Hospital Zurich, Zurich, Switzerland
- Neurovascular uncoupling (false negative BOLD activation) can be found in patients with high grade gliomas. An underlying mechanism could be impaired cerebrovascular reactivity. We determined overall cerebrovascular reactivity (CVR) as well as the perifocal CVR and used a healthy control group. We applied an automated tumor masking with determination of CVR in 7 consecutive rings of 3 mm. We found an overall impaired CVR as well as significantly impaired intratumoral CVR and perifocal up to 12 mm. No such trend was found on the contralateral hemisphere, after flipping of the tumor mask.
-
- 4177
Computer #54 Fractional Motion Diffusion Model for Differentiation of Low- and High-Grade Pediatric Brain Tumors
Muge Karaman¹, Ying Xiong^{1,2}, He Wang³, Frederick C Damen^{1,4}, Yuhua Li⁵, and X. Joe Zhou^{1,6}
- ¹Center for MR Research, University of Illinois at Chicago, Chicago, IL, United States, ²Department of Radiology, Tongji Hospital, Tongji Medical College, Huazhong University of Science and Technology, Wuhan, China, People's Republic of, ³Philips Research China, Shanghai, China, People's Republic of, ⁴Department of Radiology, University of Illinois at Chicago, Chicago, IL, United States, ⁵Department of Radiology, Xinhua Hospital, Shanghai, China, People's Republic of, ⁶Departments of Radiology, Neurosurgery, and Bioengineering, University of Illinois at Chicago, Chicago, IL, United States
- It has been well-recognized that the complexity of biological tissues, particularly the brain tumors with high degree of structural heterogeneity, requires more sophisticated diffusion models than a simple mono-exponential model due to the non-Gaussian behavior. Among these, a newly introduced model to MRI, the fractional motion (FM) model has been the focus of many biophysical studies at the *molecular* level. While the FM model has been demonstrated at the voxel-level, it has not been utilized to address a clinical question. In this study, we investigate the utility of FM model for differentiating low-grade and high-grade pediatric brain tumors.
-
- 4178
Computer #55 Association of Apparent Diffusion Coefficient with PFS for recurrent Astrocytoma and Generation of Maps to aid in Defining Tumor Pathology
Evan Neill¹, Manisha Dayal¹, Joanna Phillips², Llewellyn Jalbert¹, Soonme Cha¹, Annette Molinaro², Susan Chang², and Sarah Nelson¹
- ¹Radiology and Biomedical Imaging, University of California, San Francisco, San Francisco, CA, United States, ²Neurological Surgery, University of California, San Francisco, San Francisco, CA, United States
- Patients with recurrent low-grade Astrocytomas may experience a large variety of clinical disease courses and outcomes. Diffusion MR imaging and its associations with patient and tumor level characteristics provide an opportunity to use images as maps of tumor aggression and therefore prognosis. This study examines the relationships between the Apparent Diffusion Coefficient (ADC), histology and progress free survival in order to develop a colormap that highlights regions of the tumor with more aggressive characteristics. The colormaps provide an easier way for neuro-oncologists and neurosurgeons to interpret ADC images that can aid them in making decisions about how to manage their patients.
-
- 4179
Computer #56 Whole-brain echo planar spectroscopic imaging distinguishes recurrent tumor versus pseudoprogression in glioblastoma patients
Gaurav Verma¹, Suyash Mohan¹, Sanjeev Chawla¹, Sumei Wang¹, Andrew Maudsley², Ronald Wolf¹, Steven Brem³, Robert Lustig⁴, Arati Desai⁵, and Harish Poptani⁶
- ¹Department of Neuroradiology, University of Pennsylvania, Philadelphia, PA, United States, ²Department of Radiology, University of Miami, Miami, FL, United States, ³Department of Neurosurgery, University of Pennsylvania, Philadelphia, PA, United States, ⁴Department of Radiation Oncology, University of Pennsylvania, Philadelphia, PA, United States, ⁵Department of Hematology/Oncology, University of Pennsylvania, Philadelphia, PA, United States, ⁶Department of Cellular and Molecular Physiology, University of Liverpool, Liverpool, United Kingdom
- Differentiating brain tumor recurrence (True Progression, TP) from treatment effect (pseudoprogression, PsP) among enhancing neoplasms following radiation therapy by non-invasive imaging may directly inform treatment strategies, yet similar imaging patterns makes this difficult leading to invasive biopsy or repeat surgery. Three-dimensional echo-planar spectroscopic imaging (EPSI) facilitates region-of-interest analysis with high-resolution metabolic data. In this study, we compared seven patients with PsP and seven with recurrent tumor using EPSI. Higher choline was detected from the contrast-enhancing, peritumoral and distal peritumoral regions in TP patients compared to PsP.
-
- 4180
Computer #57 ASL, DCE, DSC and IVIM: A 4-way comparison of perfusion imaging in brain tumours
Lawrence Kenning¹, Martin D Pickles², Martin Lowry³, Chris Roland Hill⁴, Shailendra Achawal⁴, and Chittoor Rajaraman⁴
- ¹Centre for MR Investigations, Hull York Medical School, Hull, United Kingdom, ²Centre for MR Investigations, Hull York Medical School at University of Hull, Hull, United Kingdom, ³Hull York Medical School at University of Hull, Hull, United Kingdom, ⁴Hull and East Yorkshire Hospitals

This study aimed to compare Intravoxel Incoherent Motion (IVIM) to more established measures of perfusion; Arterial Spin Labelling (ASL), Dynamic Contrast Enhanced (DCE) and Dynamic Contrast Susceptibility (DSC) imaging, both in tumours and white matter. Mean and 95th percentile values for f , D^* , fD^* , CBF, K^{trans} , v_e , v_b , rCBV and K_2 were calculated. Multiple correlations were observed. Significant correlations of note include CBF vs. fD^* , v_b vs. rCBV and K^{trans} vs. K_2 . Spatial registration of the 4 different methods yielded acceptable agreement given technical differences.

4181

Computer #58

Myoinositol as a predictive baseline biomarker for overall survival of patients with recurrent glioblastoma treated with Bevacizumab: A 1H-magnetic resonance spectroscopy study.

Eike Steidl^{1,2,3}, Oliver Baehr^{2,3}, Joachim P. Steinbach^{2,3}, Michael W. Ronellenfitsch^{2,3}, Friedhelm Zanella¹, Elke Hattingen¹, and Ulrich Pilatus¹

¹Institute of Neuroradiology, Frankfurt am Main, Germany, ²Dr. Senckenberg Institute of Neurooncology, Frankfurt am Main, Germany, ³German Cancer Consortium (DKTK) and German Cancer Research Center (DKFZ), Heidelberg, Germany

Myoinositol is an organic osmolyte, with intracellular concentration changes depending on the extracellular osmolality. Since Bevacizumab reduces tumor edema, we asked whether the Myoinositol concentration changes during therapy.

We used ¹H-MRS to measure the Myoinositol concentrations in the tumor and contralateral control of patients with recurrent glioblastomas treated with Bevacizumab (n=30) and CCNU/VM26 (n=9).

Pre-therapeutic Myoinositol concentrations in the contralateral control were predictive of overall survival in patients treated with Bevacizumab. Furthermore our data confirm that recurrent glioblastoma show a strong metabolic reaction to Bevacizumab and support the hypothesis that Myoinositol might be a marker for early tumor cell invasion.

4182

Computer #59

Comparison of tumor microstructure derived NODDI and DTI metrics to histopathology in different grades of brain tumor

Prasanna Parvathaneni¹, Qiuting Wen², Joanna J Phillips^{3,4}, Soonmee Cha^{1,4}, Susan M Chang⁴, Sarah J Nelson^{1,5}, and Janine M Lupo¹

¹Department of Radiology and Biomedical Imaging, University of California San Francisco (UCSF), San Francisco, CA, United States, ²Indiana University, Indianapolis, IN, United States, ³Department of Pathology, University of California San Francisco (UCSF), San Francisco, CA, United States, ⁴Department of Neurological Surgery, University of California San Francisco (UCSF), San Francisco, CA, United States, ⁵Department of Bioengineering and Therapeutic Sciences, University of California San Francisco (UCSF), San Francisco, CA, United States

New non-Gaussian measurement techniques like neurite orientation dispersion and density imaging (NODDI) that allow quantification of specific tissue microstructure features can provide meaningful biophysical indices to overcome the low specificity of DTI. In this study we applied three compartment model based NODDI and DTI to histopathology and explored the correlation with tumor cellularity between non-enhancing and contrast enhancing lesions. Unlike in normal brain where V_{in} represents the neurite density, it was positively correlated with tumor grade and tumor score in tissue samples from the tumor region, indicating the association of V_{in} with tumor cellularity. Although NODDI is not directly built on tumor, it brings parameters that were sensitive to tumor cellularity, which may complement the conventional DTI model and adds specificity. Thus NODDI, when combined with DTI, could add value in understanding the heterogeneity of tissue microstructure in brain tumors.

4183

Computer #60

Axial diffusivity is more sensitive in detecting white matter injury in adult survivors of childhood brain tumors: a DTI study using tract-based spatial statistics

Silun Wang¹, Jianming Ni², Liya Wang¹, Tricia King³, and Hui Mao¹

¹Department of Radiology and Imaging Sciences, EMORY UNIVERSITY, ATLANTA, GA, United States, ²Medical Imaging Center, The Second Hospital of Wuxi, Wuxi, China, People's Republic of, ³Department of Psychology & Neuroscience Institute, Georgia State University, Atlanta, GA, United States

White matter injury is considered as a major contributory factor of treatment-induced neurotoxicity prevalent among childhood cancer survivors. DTI study with TBSS analysis shows significantly lower FA, $\lambda_{//}$ and higher λ_{\perp} in survivors compared to controls. DTI indices show unmatched white matter regions with significant difference. In comparison of FA, $\lambda_{//}$ may be more sensitive to detect white matter injury. Combining analysis of DTI indices provide additional information to explore white matter injury induced by radiotherapy or chemotherapy.

4184

Computer #61

Diagnostic value of 2-hydroxyglutarate detection by 1H MR spectroscopy in patients with glioma

Francesca Branzoli^{1,2}, Anna Luisa Di Stefano^{2,3,4}, Malgorzata Marjanska⁵, Romain Valabregue^{1,2}, Stephane Lehericy^{1,2}, and Marc Sanson^{2,3}

¹Brain and Spine Institute (ICM), Center for Neuroimaging Research (CENIR), F-75013, Paris, France, ²INSERM U1127/CNRS UMR7225, Sorbonne Universités, UPMC Univ Paris 06, ICM, F-75013, Paris, France, ³AP-HP, GH Pitié-Salpêtrière, Service de Neurologie 2, F-75013, Paris, France, ⁴Division of Neurology, Foch Hospital, Paris, France, ⁵Center for Magnetic Resonance Research and Department of Radiology, University of Minnesota, Minneapolis, MN, United States

Reliable quantification by magnetic resonance spectroscopy of the oncometabolite 2-hydroxyglutarate (2HG) has important implications in diagnosis of IDH mutation, prognosis, as well as assessment of the efficacy of anti-IDH targeted therapies. In this study, we employed two approaches for 2HG detection previously described, e.g., difference spectroscopy and optimized for 2HG detection conventional

spectroscopy, in order to assess for the first time the specificity and sensitivity of the two methods, and to relate these results to the natural history and the neuroradiological status of patients with glioma.

-
- 4185
Computer #62 Correlated MR imaging and ultramicroscopy (MR-UM) is a tool kit to assess the dynamics of glioma angiogenesis
Michael Breckwoldt¹, Julia Bode², Felix Kurz¹, Angelika Hoffmann¹, Martin Ott², Katrin Deumelandt², Gergely Solecki², Sara Chiblak², Amir Abdollahi², Frank Winkler², Michael Platten², Sabine Heiland¹, Martin Bendszus¹, and Björn Tews²
- ¹Neuroradiology, University of Heidelberg, Heidelberg, Germany, ²German Cancer Research Center, Heidelberg, Germany*
- Gliomas are malignant brain tumors that depend on neoangiogenesis. Novel imaging methods are required to assess vascularization status, treatment effects and disease progression. We developed a combined MR and optical vascularization “tool kit” to study neoangiogenesis in mouse glioma models. We use T2* post contrast imaging (iron oxide nanoparticle or Gd-based) of vascular susceptibility signals and innovative ultramicroscopy (UM) of cleared brains. T2* imaging identifies single arterioles and venules in glioma development. Correlated UM of fluorescently labeled microvessels shows typical features of pathological vessels (increased caliber, density and tortuousness). Thus, MR-UM facilitates the preclinical search for more effective antiangiogenic agents.
-
- 4186
Computer #63 Automatic acquisition of dynamic susceptibility contrast and dynamic contrast enhanced images using a single contrast dose
Yufen Chen¹ and Todd B Parrish¹
- ¹Radiology, Northwestern University, Chicago, IL, United States*
- In clinical settings, dynamic susceptibility contrast (DSC) and dynamic contrast enhanced (DCE) data are rarely acquired together as both require a full single dose for optimal contrast-to-noise-ratio (CNR). However, both techniques offer complementary information that aid in the assessment of tumors. Current double acquisition methods acquire the DCE scan first with a half dose to minimize leakage effects in the subsequent DSC scan, compromising both scans. Here, we demonstrate the feasibility of an automatically switching DSC-DCE scan sequence by monitoring the signal intensity of the DSC scan, allowing acquisition of both datasets with a single contrast dose.
-
- 4187
Computer #64 Characterization of Pediatric Brain Tumors and Treatment Effect using Magnetic Resonance Fingerprinting: Initial Experience
Peter de Blank^{1,2}, Dan Ma², Chaitra Badve², Shivani Pahwa², Sara Dastmalchian³, Duncan Stearns^{1,2}, Deborah Rukin Gold^{2,4}, Krystal Tomei^{2,5}, Jill S Barnholtz-Sloan², Andrew Sloan^{2,5}, Vikas Gulani^{2,6}, and Mark Griswold²
- ¹Pediatrics, University Hospitals, Cleveland, OH, United States, ²Case Western Reserve University, Cleveland, OH, United States, ³University Hospitals, Cleveland, OH, United States, ⁴Neurology, University Hospitals, Cleveland, OH, United States, ⁵Surgery, University Hospitals, Cleveland, OH, United States, ⁶Radiology, University Hospitals, Cleveland, OH, United States*
- This study uses magnetic resonance fingerprinting to investigate relaxometry values in pediatric and young adult primary brain tumors. Six children with primary brain tumors were scanned: 3 with low-grade tumors and 3 with high-grade tumors. T1 and T2 values of tumor were significantly different from contralateral white matter. T1, T2 quantification of tumor were also significantly different between high- and low-grade tumors. Three subjects underwent serial observations: 2 received therapy and 1 did not. Subjects that underwent surgical decompression and chemotherapy appeared to have larger changes in T1 values than those that were only observed.
-
- 4188
Computer #65 Assessment of Global and Regional Cerebral White Matter Changes Induced by Cranial Radiotherapy in Childhood Brain Tumor Patients Using a Structural Connectivity Network Approach
Qing Ji¹, John O. Glass¹, Elizabeth C. Duncan¹, Amar Gajjar², and Willburn E. Reddick¹
- ¹Diagnostic Imaging, St.Jude Children's Research Hospital, Memphis, TN, United States, ²Oncology, St.Jude Children's Research Hospital, Memphis, TN, United States*
- Global and regional cerebral white matter changes induced by cranial radiotherapy (CRT) were analyzed by comparing Pre-CRT and Post-CRT diffusion tensor imaging (DTI) from 30 childhood medulloblastoma patients using a structural connectivity network model and graph theory approaches. At the global level, global network efficiency and character path were significantly changed for the whole network. At the regional level, 17 of 82 network nodes had significantly decreased local efficiencies, and 14 of those nodes also had significantly decreased clustering coefficients. These findings suggest significant reduction in the microstructural integrity immediately after CRT in this population.
-
- 4189
Computer #66 Characteristics of apparent relative oxygen extraction fraction (rOEF) in human high grade glioma
Christine Preibisch^{1,2}, Mathias Lukas³, Anne Kathrin Kluge¹, Claus Zimmer¹, Stefan Förster^{3,4}, and Thomas Pyka³
- ¹Dept. of Neuroradiology, Technische Universität München, Munich, Germany, ²Clinic for Neurology, Technische Universität München, Munich, Germany, ³Clinic for Nuclear Medicine, Technische Universität München, Munich, Germany, ⁴Clinic for Nuclear Medicine, Klinikum Bayreuth, Bayreuth, Germany*
- Hypoxia plays an important role in prognosis and therapy response of cancer. This study explores the characteristics of multi-parametric measurements of relative oxygen extraction fraction (rOEF) in a sample of 36 mostly high grade glioma patients. This study confirms previous results in human glioma where rOEF values were found to increase with tumor grade but does not find a similar

increase of a supposedly hypoxic tumor area with tumor grade. According to present results, high rOEF values, supposedly corresponding to a high oxygen extraction, prevail in edematous tissue with low rCBV. Whether this translates into tissue hypoxia, needs further investigation.

-
- 4190
Computer #67
Altered Frontal Functional Networks in Adult Survivors of Pediatric Brain Tumors
Liya Wang^{1,2}, Hongbo Chen^{1,3}, Tricia Z King⁴, and Hui Mao¹
- ¹Radiology and Imaging Sciences, Emory University School of Medicine, Atlanta, GA, United States, ²Radiology, Cancer Hospital Chinese Academy of Medical Sciences at Shenzhen, Shenzhen, China, People's Republic of, ³School of Life and Environmental Sciences, Guilin University of Electronic Technology, Guilin, China, People's Republic of, ⁴Psychology and Neuroscience Institute, Georgia State University, Atlanta, GA, United States*
- Pediatric brain tumors and associated treatment affect brain development and functional network. We investigated the functional connectivity (FC) of adult survivors of pediatric brain tumors using resting-state functional MRI and independent component analysis to better understand the neural mechanisms underlying long term cognitive outcomes of the survivors. It was found that survivors exhibited differences in the FC in executive control network, default mode network and salience network compared to demographically-matched controls with increased number of effective functional connectivities and increased FC strength in survivors compared the controls.
-
- 4191
Computer #68
Differentiation of Central Nervous System Lymphoma and Gliomas using Dynamic Susceptibility Contrast and Dynamic Contrast-Enhanced MRI
Kazuhiro Murayama¹, Takahiro Ueda¹, Takashi Fukuba², Shigeharu Ohyu³, Ayako Ninomiya³, Masato Ikedo³, Kazuhiro Katada⁴, and Hiroshi Toyama¹
- ¹Radiology, Fujita Health University, Toyoake, Japan, ²Radiology, Fujita Health University Hospital, Toyoake, Japan, ³Toshiba Medical Systems, Otawara, Japan, ⁴Joint Research Laboratory of Advanced Medical Imaging, Fujita Health University, Toyoake, Japan*
- A combination of Ktrans, Ve, and rCBV would be useful in differentiating between central nervous system lymphoma and gliomas. Dynamic contrast-enhanced MRI parameters have been successfully applied to obtain quantitative estimates of the permeability of brain tumors for characterization of the vascular microenvironment.
-
- 4192
Computer #69
Diffusion kurtosis imaging can efficiently assess the glioma grade, cellular proliferation and survival
Rifeng Jiang¹, Jingjing Jiang¹, Jingjing Shi¹, Yihao Yao¹, Nanxi Shen¹, Changliang Su¹, Ju Zhang¹, and Wenzhen Zhu¹
- ¹Radiology, Tongji Hospital, Wuhan, China, People's Republic of*
- Compared with conventional diffusion metrics, the kurtosis metrics derived from DKI in the solid region of the tumors were better diagnostic factors in distinguishing HGGs from LGGs and identifying grade II, III and IV gliomas. The kurtosis metrics offered great potential to noninvasively predict the cellular proliferation of gliomas. DKI was also useful to evaluate the survival of glioma patients, and MK was a significant death risk in glioma patients.
-
- 4193
Computer #70
Comparison of ferumoxytol and gadolinium enhancement changes in response to Avastin in high grade glioma patients
Andrea Horváth^{1,2,3}, Csanád Várallyay¹, Daniel Schwartz¹, Prakash Ambady¹, Péter Bogner⁴, and Edward Neuwelt¹
- ¹Department of Neurology, Oregon Health and Science University, Portland, OR, United States, ²Department of Neurosurgery, University of Pécs, Pécs, Hungary, ³Diagnsotic Center of Pécs, Pécs, Hungary, ⁴Department of Radiology, University of Pécs, Pécs, Hungary*
- Ferumoxytol is an alternative, investigational, iron-based MRI contrast agent, which might be beneficial in the accurate diagnosis of treated glioma patients. In this study we investigated how gadolinium and 24 hour ferumoxytol enhancement change as a result of Avastin treatment. The enhancement volumes and normalized signal intensities before and after Avastin treatment were calculated with histogram analysis and were compared between contrast agents. Changes in enhancement volumes and in signal intensities in response to Avastin were not different between contrast agents. Ferumoxytol shows good potential in brain tumor imaging.
-
- 4194
Computer #71
Application of diffusion kurtosis imaging for a structural differentiation of the brain metastasis and primary glioblastomas
Aram Tonoyan¹, Ezequiel Farrher², Ivan Maximov³, Farida Grinberg^{4,5}, Elena Lyubimova⁶, Ludmila Fadeeva¹, Eduard Pogosbekyan¹, Nadim Joni Shah^{2,5}, and Igor Pronin¹
- ¹Neuroimaging, Burdenko Neurosurgery Institute, Moscow, Russian Federation, ²Institute of Neuroscience and Medicine – 4, Medical Imaging Physics, Forschungszentrum Juelich GmbH, Juelich, Germany, ³Experimental physics III, TU Dortmund University, Dortmund, Germany, ⁴Institute of Neuroscience and Medicine – 4, Medical Imaging Physics, Forschungszentrum Juelich GmbH, Juelich, Germany, ⁵Faculty of Medicine, Department of Neurology, RWTH Aachen University, JARA, Aachen, Germany, ⁶Radiology, Krasnodar Regional Hospital, Krasnodar, Russian Federation*
- MRI allows one to detect and visualize the primary and metastatic tumours in the brain. However, conventional methods suffer from a poor contrast. In turn, it leads to a problem in proper diagnostics of the tumour origins. In the present work we demonstrated the potential of kurtosis imaging technique in the tumour differentiation of primary tumour and metastasis cancers.

4195
Computer #72 How much microvascular anatomy is in T1-DCE MRI? – A computerized analysis of meningioma microvasculature correlated to kinetic parameters applying the extended Tofts model
Vera Catharina Keil¹, Kanishka Hiththetiya², Gerrit H. Gielen³, Matthias Simon⁴, Bogdan Pintea⁴, Anna Vogelgesang¹, Juergen Gieseke^{1,5}, Burkhard Maedler⁵, Hans Heinz Schild¹, and Dariusch Reza Hadizadeh¹

¹Department of Radiology, Universitätsklinikum Bonn, Bonn, Germany, ²Center for Pathology, Universitätsklinikum Bonn, Bonn, Germany, ³Department of Neuropathology, Universitätsklinikum Bonn, Bonn, Germany, ⁴Clinic for Neurosurgery and Stereotaxy, Universitätsklinikum Bonn, Bonn, Germany, ⁵Philips Healthcare, Best, Netherlands

Tissue perfusion is co-defined by anatomical factors of the microvasculature. If and how kinetic parameters of T1w dynamic-contrast enhanced (T1-DCE) MRI fit into this anatomical perfusion model, is a topic of on-going discussion. Based on the extended Tofts model (ETK) we therefore performed a focal analysis of kinetic parameters in meningioma and surgically retrieved precisely corresponding tissue specimens. Their microvasculature underwent multimodal computerized analysis. Kinetic parameters were found to correlate poorly and inconsistently with the microvascular anatomy on both an inter- and intra-individual level.

Electronic Poster

Sparse & Low-Rank MRI: Theory & Applications

Exhibition Hall

Thursday, May 12, 2016: 10:30 - 11:30

4196
Computer #1 Rapid high-resolution T1 mapping using highly accelerated radial steady-state free-precession acquisition
Zhitao Li¹, Benjamin Paul Berman², Jean-Philippe Galons³, Ali Bilgin^{4,5}, Maria I. Altbach³, and Diego R. Martin³

¹Electrical and Computer Engineering, The University of Arizona, Tucson, AZ, United States, ²Program in Applied Mathematics, the University of Arizona, Tucson, AZ, United States, ³Department of Medical Imaging, the University of Arizona, Tucson, AZ, United States, ⁴Electrical and Computer Engineering, the University of Arizona, Tucson, AZ, United States, ⁵Biomedical Engineering, the University of Arizona, Tucson, AZ, United States

A golden angle radial steady-state free-precession technique and a principle component based iterative algorithm are developed for the reconstruction of high resolution T1 maps from highly undersampled data. The total acquisition time is < 3 seconds per slice.

4197
Computer #2 Concentration time-course Model-based Angiogram SEparation (MASE) for dynamic contrast-enhanced magnetic resonance angiography
Eun Ji Lim^{1,2} and Jaeseok Park²

¹Center for Neuroscience Imaging Research, Institute for Basic Science (IBS), Suwon, Korea, Republic of, ²Department of Biomedical Engineering, Sungkyunkwan University, Suwon, Korea, Republic of

Dynamic contrast-enhanced (DCE) 3D MRA has been widely used for diagnostic assessment of vascular morphology and hemodynamics in a clinical routine. It acquires a series of time-resolved images, revealing details on contrast dynamics. To extract angiograms while eliminating unwanted background tissues, subtraction between the reference (pre-contrast) and DCE images in each time frame is typically employed. However, in the presence of non-stationary background signal transition such as subject motion and time-varying magnetic field, subtraction results in incomplete background suppression and noise amplification. Due to the inherent, subtraction sparsity in either between the reference and each dynamic image or between neighboring time frames, compressed sensing (CS) is well suited to DCE MRA to enhance spatial and temporal resolution. Nevertheless, these approaches remain suboptimal due to the inherent limitation of subtraction. In this work, we propose a new, DCE MRA method called "concentration time-course Model-based Angiogram SEparation (MASE)", in which DCE signals in the temporal direction are directly modeled and reconstructed with sparsity priors while background signals are attenuated.

4198
Computer #3 Entangled Compressed Sensing for Highly Accelerated 4D Flow MRI
Adrian Emmanuel Georg Huber¹, Christian Binter¹, Claudio Santelli¹, and Sebastian Kozerke¹

¹Institute for Biomedical Engineering, University and ETH Zurich, Zurich, Switzerland

Entangled denoising (eSPARSE) was developed for highly undersampled 4D Flow MRI, combining both k-t SPARSE-SENSE and 3D-L1-Wavelets. Undersampling factors of 8 and 10 were studied in healthy volunteers. The proposed algorithm improves the reconstruction of fluid vector fields in the aorta compared to k-t SPARSE-SENSE. The relative RMSE velocity is reduced by up to 16% for an undersampling rate of R = 8 and by up to 19% for R = 10. Entangled denoising (eSPARSE) is a promising approach to accelerate 4D Flow MRI while preserving key features of the flow field.

4199
Computer #4 High resolution CBV assessment with PEAK-EPI and PS-SPIRiT-EPI
Rebecca Ramb¹, Anthony G. Christodoulou^{2,3}, Irina Mader⁴, Maxim Zaitsev¹, Zhi-Pei Liang², and Jürgen Hennig¹

¹University Medical Center Freiburg, Dept. of Radiology - Medical Physics, Freiburg, Germany, ²Beckman Institute, Dept. of Electrical and Computer Engineering, University of Illinois at Urbana-Champaign, Urbana, IL, United States, ³Heart Institute and Biomedical Imaging Research Institute, Cedars-Sinai Medical Center, Los Angeles, CA, United States, ⁴University Medical Center Freiburg, Dept. of Neuroradiology - Freiburg

This work is to provide perfusion parameters such as cerebral blood volume at high spatial resolution, for detailed delineation of tumor borders and to guide stereotactic surgery biopsies in locating the most aggressive tumorous tissue. This is achieved with an k-t-undersampled EPI acquisition and PEAK-GRAPPA reconstruction. Additionally, an advanced iterative reconstruction method is developed incorporating partial separability constraint into parallel imaging with SPIRiT kernels (PS-SPIRiT). Two half-dose first-pass perfusion acquisitions in tumor patients allow direct comparison of the standard clinical protocol with the proposed acquisition and reconstruction schemes.

4200 Computer #5 Sliding-window Reconstruction Strategy for Accelerating the Acquisition of MR Fingerprinting
Xiaozhi Cao¹, Congyu Liao¹, Zhixing Wang¹, Huihui Ye¹, Ying Chen¹, Hongjian He¹, Song Chen¹, Hui Liu², and Jianhui Zhong¹

¹Center for Brain Imaging Science and Technology, Department of Biomedical Engineering, Zhejiang University, Hangzhou, Zhejiang, China, People's Republic of, ²MR Collaboration NE Asia, Siemens Healthcare, Shanghai, China, People's Republic of

The original MRF method uses one spiral interleaf acquired within each time point to reconstruct one image, leading to dramatic fluctuation in the signal evolution caused by undersampling error. In this work, a sliding window is utilized to select multiple interleaves to generate one full-sampled image for each step so that the fluctuation in signal evolution could be significantly alleviated. Therefore our proposed method can reach an expected result with reduced time points. The results demonstrate that the proposed method can reduce the acquisition time from about 11s to 5.6s or even less.

4201 Computer #6 Improving temporal resolution in fMRI using 3D spiral acquisition and low-rank plus sparse image reconstruction
Andrii Y Petrov¹, Michael Herbst^{1,2}, and V Andrew Stenger¹

¹Department of Medicine, University of Hawaii, Honolulu, HI, United States, ²Department of Radiology and Medical Physics, University Medical Center Freiburg, Freiburg, Germany

Recent advances in dynamic MRI propose low-rank plus sparse (L+S) matrix decomposition for image reconstruction from reduced data acquisition. The L+S method has been successfully applied to multiple applications including cardiac MRI, perfusion, angiography and recently to denoise resting-state fMRI data, suggesting that it might be promising for improving temporal resolution in task-based fMRI. We propose to use 3D spiral acquisition, undersampled in k_z -t domain, and L+S method for image reconstruction. Our results indicate that proposed approach allows 4x acceleration for the data acquisition and improved statistical significance of activation maps in the S component from an increased temporal resolution and eliminating physiological noise in the L component.

4202 Computer #7 Accelerated 3D Coronary Vessel Wall MR Imaging Based on Compressed Sensing with A Novel Block-Weighted Total Variation Regularization
Chen Zhongzhou¹, Zhang Xiaoyong¹, Zheng Hairong¹, Liu Xin¹, Fan Zhaoyang², and Xie Guoxi¹

¹Lauterbur Research Center for Biomedical Imaging, Shenzhen Institutes of Advanced Technology, CAS, Shenzhen, China, People's Republic of, ²Biomedical Imaging Research Institute, Cedars-Sinai Medical Center, Los Angeles, CA, United States

Coronary vessel wall MR imaging has great potential to detect coronary plaques which can be important for heart disease diagnosis. However, the imaging is always time-consuming because it needs a large amount of data for clear vessel wall depiction. In this work, a novel method based on compressed sensing (CS) with block-weighted total variation (BWTV) was proposed to accelerate coronary vessel wall imaging. Simulation and in vivo experiment results demonstrated that the proposed method can significantly decrease the amount of data for image reconstruction without compromising the depiction of the tiny coronary vessel wall.

4203 Computer #8 Non-rigid Motion Correction using Localized PROPELLER and Low-Rank Minimization
Joseph Y. Cheng¹, Mariya Doneva², Tao Zhang¹, John M. Pauly³, Shreyas S. Vasanawala¹, and Michael Lustig²

¹Radiology, Stanford University, Stanford, CA, United States, ²Electrical Engineering & Computer Sciences, University of California, Berkeley, CA, United States, ³Electrical Engineering, Stanford University, Stanford, CA, United States

A major obstacle in MRI is artifacts from patient motion. This is especially challenging for pediatric imaging where anesthesia is often required to obtain diagnostic image quality from uncooperative patients. Thus, we developed a PROPELLER-based method to correct for non-rigid motion. Simple localized motion is estimated for each spatial region by first applying a spatial window to the image data. Low-rank minimization is used to iteratively estimate the motion without the need of determining a reference motion state and to potentially enable higher-resolution navigation. The final image is constructed via autofocusing. This approach is demonstrated in free-breathing abdominal scans of healthy and patient volunteers.

4204 Computer #9 MRI acceleration using correlation imaging with tissue boundary sparsity
Yu Y. Li¹

¹Radiology, Cincinnati Children's Hospital Medical Center, Cincinnati, OH, United States

In MRI data acquisition, gradient encoding introduces a non-uniform distribution of tissue contrast and boundary information in k-space. As a result, data correlation increases with tissue boundary sparsity from the center to the outer k-space. The presented work investigates a new approach to accelerating MRI by taking advantage of non-uniform k-space data correlation. In this approach, k-space

data are collected and reconstructed in a region-by-region fashion using a previously developed high-speed imaging framework, "correlation imaging"^{1,2}. It is demonstrated that region-by-region correlation imaging can introduce a gain over parallel imaging in imaging acceleration by utilizing more information.

4205
Computer #10 Projected Fast Iterative Soft-thresholding Algorithm for Tight Frames in Compressed Sensing Magnetic Resonance Imaging
Xiaobo Qu¹, Yunsong Liu¹, Zhifan Zhan¹, Jian-Feng Cai², Di Guo³, and Zhong Chen¹

¹Department of Electronic Science, Xiamen University, Xiamen, China, People's Republic of, ²Department of Mathematics, Hong Kong University of Science and Technology, Hong Kong SAR, Hong Kong, ³School of Computer and Information Engineering, Xiamen University of Technology, Xiamen, China, People's Republic of

Redundant sparse representations can significantly improve the MRI image reconstruction with sparsity constraint. An appropriate sparse model is very important to improve image quality even with the same sparsifying transforms and undersampled data. We propose a new fast, stable, compatible and simple iterative thresholding algorithm to solve the analysis sparse models that can obviously improve the image reconstruction for tight-frame-based sparsifying transform in compressed sensing MRI. We theoretically prove the convergence of the proposed projected fast iterative soft-thresholding algorithm (pFISTA). Numerical results show that pFISTA achieves better reconstruction than state-of-art FISTA for synthesis sparse model and more stable and compatible than the state-of-art SFISTA.

4206
Computer #11 On-scanner sparse sampling for high resolution structural imaging of the human brain at 7T
Matthan W.A. Caan^{1,2}, Abdallah G. Motaal¹, Bram F. Coolen¹, Wouter V. Potters¹, Kerry Zhang¹, Pieter Buur², and Aart J. Nederveen¹

¹Radiology, Academic Medical Center, Amsterdam, Netherlands, ²Spinoza Centre for Neuroimaging, Amsterdam, Netherlands

We aimed to increase spatial resolution while maintaining scanning time for 3D-T1 weighted imaging by on-scanner undersampling at 7T. A 3DT1-weighted structural scan with a resolution of 0.5 mm³ was acquired with 4 times variable poisson disc compressed sensing (CS) undersampling. For comparison, scans with resolutions of 0.5 and 0.7 mm³ were acquired, with SENSE undersampling adapted to match scanning time. The CS-reconstructed scan showed no streaking artifacts, was less hampered by noise in deep brain regions, had better contrast between gray matter and CSF and less partial voluming effects.

4207
Computer #12 Promoting incoherence of radial x-f point spread functions using randomly perturbed golden angles
Mark Chiew¹, Nadine N Graedel¹, and Karla L Miller¹

¹FMRIB Centre, University of Oxford, Oxford, United Kingdom

In this work we propose a simple method for increasing the spatio-temporal incoherence of a golden angle radial time-series acquisition by mildly perturbing the golden angles with a random variable. Despite its quasi-random distribution of golden angle samples, x-f point spread function analysis reveals strong coherence along the frequency domain. When the golden angles are slightly jittered using a normal random variable with small variance, the x-f point spread functions take on a more diffuse, noise-like appearance, making the acquisition scheme more appropriate for k-t reconstruction methods relying on incoherence, while maintaining its favourable spatial properties.

4208
Computer #13 Accelerated Dynamic MRI Reconstruction with Sequential Low Rank Matrix Completion and Parallel Imaging
Eric G Stinson¹, Stephen J. Riederer¹, and Joshua D. Trzasko¹

¹Radiology, Mayo Clinic, Rochester, MN, United States

Multi-level (uniform + non-uniform) sampling for accelerated dynamic MRI either solves a computationally expensive full regression problem, or breaks the problem into two separate steps for each sampling operator. Here, the latter approach is taken, with low-rank matrix completion used as a pre-processing step to complete the non-uniform sampling operator before SENSE reconstruction unfolds the effects of the uniform sampling operator. It is shown that both spatial and temporal resolution are retained with LRMC + SENSE in comparison with more traditional pre-processing steps.

4209
Computer #14 Optimized image reconstruction for high resolution cerebral blood volume mapping with Ferumoxytol
R. Marc Lebel^{1,2,3}, Csanad G Varallyay⁴, and Edward A Neuwelt⁴

¹GE Healthcare, Calgary, AB, Canada, ²Radiology, University of Calgary, Calgary, AB, Canada, ³Biomedical Engineering, University of Calgary, Calgary, AB, Canada, ⁴Neurology, Oregon Health and Science University, Portland, OR, United States

Quantitative or semi-quantitative mapping of cerebral blood volume typically involves complex modeling of a dynamic gadolinium-enhanced acquisition. Off-label use of ferumoxytol is being explored as a mechanism for high-resolution quantification of cerebral blood volume. Acquisition involves high-resolution pre- and post-contrast T₂*-weighted scans; quantification is straightforward and does not require fitting. We present a multi-echo acquisition and optimal quantification algorithm for improved detection of ferumoxytol-based blood volume measurements. Our approach provides high dynamic range and minimal noise amplification.

4210 Improved Temporal Resolution TWIST Reconstruction using Annihilating Filter-based Low-rank Hankel Matrix

Computer #15 Eun Ju Cha¹, Kyong Hwan Jin¹, Dong-Wook Lee¹, Eung Yeop Kim², Seung-Hong Choi³, and Jong Chul Ye¹

¹KAIST, Daejeon, Korea, Republic of, ²Gacheon University Gil Medical Center, Incheon, Korea, Republic of, ³Seoul National University Hospital, Seoul, Korea, Republic of

In dynamic contrast enhanced (DCE) MRI, temporal and spatial resolution can be improved by time-resolved angiography with interleaved stochastic trajectories (TWIST). However, due to view sharing, the temporal resolution of TWIST is not a true one. To overcome this limitation, we employ recently proposed annihilating filter-based low rank Hankel matrix approach (ALOHA) that interpolates the missing k-space data by performing low-rank matrix completion of weighted Hankel matrix. In vivo results showed considerably better temporal resolution than standard TWIST reconstruction.

4211

Computer #16 Accelerated Dynamic MRI Using Tensor Dictionaries Learning
Jinhong Huang^{1,2}, Biaoshui Liu¹, Gaohang Yu^{1,2}, Yanqiu Feng¹, and Wufan Chen¹

¹School of Biomedical Engineering and Guangdong Provincial Key Laboratory of Medical Image Processing, South Medical University, Guangzhou, China, People's Republic of, ²School of Mathematics and Computer Science, Gannan Normal University, Ganzhou, China, People's Republic of

Conventional CS methods treat a 2D/3D image to be reconstructed as a vector. However, many data types do not lend themselves to vector data representation, and this vectorization based model may lose the inherent spatial structure property of original data and suffer from curse of dimensionality that occurs when working with high-dimensional data. In this work, we introduce a novel tensor dictionary learning method for dynamic MRI reconstruction. Numerical experiments on synthetic data and in vivo data show approximately 2 dB improvement in PSNR presented by the proposed scheme over existing method with overcomplete dictionary learning.

4212

Computer #17 A combined Compressed Sensing Super-Resolution Diffusion and gSlider-SMS acquisition/reconstruction for rapid sub-millimeter whole-brain diffusion imaging
Lipeng Ning^{1,2}, Kawin Setsompop^{2,3}, and Yogesh Rathi^{1,2}

¹Brigham and Women's Hospital, Boston, MA, United States, ²Harvard Medical School, Boston, MA, United States, ³Massachusetts General Hospital, Boston, MA, United States

We introduce a new method for rapid acquisition of sub-millimeter whole-brain diffusion imaging. Our method combines the gSlider-SMS acquisition method and the compressed-sensing super-resolution reconstruction algorithm. We demonstrate that this proposed approach is able to increase the resolution to 860 μ m iso in an effective acquisition time of 12 min.

4213

Computer #18 Accelerating MR measurement of liver steatosis using combined compressed sensing and parallel imaging: quantitative evaluation for clinical trials
Louis W Mann¹, David M Higgins², Carl N Peters¹, Sophie Cassidy¹, Ken K Hodson¹, Anna Coombs¹, Roy Taylor¹, and Kieren Grant Hollingsworth¹

¹Institute of Cellular Medicine, Newcastle University, Newcastle upon Tyne, United Kingdom, ²Philips Healthcare, Guildford, United Kingdom

We compared hepatic fat fractions quantified with accelerated magnetic resonance (MR) imaging reconstructed with combined compressed sensing and parallel imaging (CS-PI) with conventional acquisitions. Undersampled data at ratios of 2.6 \times , 2.9 \times , 3.8 \times , and 4.8 \times were prospectively acquired from eleven subjects with type 2 diabetes and a healthy control. Fat fraction maps were calculated using CS-PI and Bland-Altman analysis. Inter- and intrarater analysis was performed. The fat fractions from the accelerated acquisitions had tight 95% limits of with no bias. The fat fractions were acceptable up to a factor of 3.8 \times , shortening the breath-hold from 17.7s to 4.7s.

4214

Computer #19 Under-sampled multi-shot diffusion data recovery using total variation regularized structured low-rank matrix completion
Merry Mani¹, Mathews Jacob², Douglas Kelley³, and Vincent Magnotta⁴

¹Dept. of Psychiatry, University of Iowa, Iowa City, IA, United States, ²Dept. of Electrical and Computer Engineering, University of Iowa, Iowa City, IA, United States, ³General Electric Healthcare Technologies, San Francisco, CA, United States, ⁴Dept. of Radiology, University of Iowa, Iowa City, IA, United States

Multi-shot diffusion imaging holds great potential for enabling high spatial resolution diffusion imaging as well as short echo time imaging to enhance studies at higher field strengths. However, the imaging throughput of multi-shot diffusion scheme is low. To increase the efficiency, under-sampled multi-shot acquisitions can be employed. However the conventional multi-shot diffusion-weighted imaging reconstructions that rely on motion-induced phase estimates are not appropriate for such acquisitions since the phase estimates will be highly corrupted due to the under-sampling. Here we propose a new total-variation regularized reconstruction for under-sampled multi-shot diffusion data using an annihilating filter bank formulation in a weighted k-space domain.

4215

Computer #20 Reconstruction Using Compressed Sensing with Edge Preservation for High Resolution MR Characterization of Myocardial Infarction: In-Vivo Preclinical Validation
Li Zhang^{1,2}, Jennifer Barry², Mihaela Pop^{1,2}, and Graham A Wright^{1,2}

Multi-contrast late enhancement (MCLE)¹ images offer better visualization of myocardial infarction (MI) than conventional IR-FGRE. However, current MR images either with IR-FGRE or MCLE provide an inferior spatial resolution of 1.6-2.0mm in-plane with a slice thickness of 5-8mm in the clinical setting. Characterization of infarct heterogeneity requires high spatial resolution. We propose a novel method to reconstruct MCLE images at a high spatial resolution from a highly accelerated dataset acquired prospectively with three-dimensional (3D) MCLE. The method was validated in a preclinical model, producing an isotropic resolution of 1.5mm within a single breath-hold.

4216 Computer #21 Accelerated MP2RAGE Imaging Using Sparse Iterative Reconstruction
Emilie Mussard^{1,2,3}, Tom Hilbert^{1,2,3}, Reto Meuli², Jean-Philippe Thiran^{2,3}, and Tobias Kober^{1,2,3}

¹Advanced Clinical Imaging Technology (HC CMEA SUI DI BM PI), Siemens Healthcare AG, Lausanne, Switzerland, ²Department of Radiology, University Hospital (CHUV), Lausanne, Switzerland, ³LTSS, École Polytechnique Fédérale de Lausanne, Lausanne, Switzerland

MP2RAGE is a T1 imaging method providing greatly reduced B1 bias as well as less T2* and PD-contributions. It requires, however, long acquisition time (standard protocol with GRAPPAx3: ~8min) which hampers its clinical application. This work proposes to use sparse iterative reconstruction techniques to shorten MP2RAGE acquisition times. Resulting images are benchmarked using contrast assessment, changes in obtained T1 values as well as evaluating the effect of undersampling on an automated brain morphometry algorithm. Acceptable penalty in image quality and morphometric outcome was achieved with up to 5-fold acceleration, yielding a measurement time of 3.8min compared to fully sampled 20min.

4217 Computer #22 Estimation and Correction of Systematic Bias Inherent in Sparsely Undersampled Sodium Imaging of the Human Brain at High-Field
Yasmin Blunck¹, Sonal Josan², Brad A. Moffat³, Shawna Farquharson⁴, Roger J. Ordidge³, and Leigh A. Johnston¹

¹Electrical & Electronic Engineering, University of Melbourne, Melbourne, Australia, ²Siemens Healthcare, Melbourne, Australia, ³Anatomy & Neuroscience, University of Melbourne, Melbourne, Australia, ⁴Florey Institute of Neuroscience and Mental Health, Melbourne, Australia

Sodium plays a vital role in various physiological processes and functions due to the delicate balance between intra- and extracellular sodium concentration. Disturbance to this electrochemical gradient is considered to be a sensitive, early indicator of cell breakdown and provide an insight into cellular integrity. Iterative reconstruction of sparsely undersampled data has been shown to cause inaccuracies in the estimation of tissue sodium content. This work investigates the bias in sodium concentration estimates and presents a method for correction that recovers the quantitative property of sodium imaging for high undersampling factors.

4218 Computer #23 Highly accelerated fat-fraction measurements for clinical trials in muscular dystrophy
Thomas Loughran¹, David M Higgins², Anna Coombs¹, Michelle McCallum³, Volker Straub³, and Kieren Grant Hollingsworth¹

¹Institute of Cellular Medicine, Newcastle University, Newcastle upon Tyne, United Kingdom, ²Philips Healthcare, Guildford, United Kingdom, ³Institute of Genetic Medicine, Newcastle University, Newcastle upon Tyne, United Kingdom

Fat frac[on measurement in muscular dystrophy is important for therapy trials. Accelerated acquisi[on reconstructed by combined compressed sensing and parallel imaging (CS-PI) can improve pa[ent compliance. Eight pa[ents with Becker muscular dystrophy were recruited and prospec[vely undersampled data at ra[os of 3.65x, 4.94x, and 6.42x were acquired in addi[on to fully sampled data. The CS-PI reconstruc[ons were of sufficient quality at 3.65x and 4.94x accelera[on. Compared to fully sampled data, non-significant bias and 95% limits of agreement of 1.65%, 1.95% and 2.22% were found for the three CS-PI reconstruc[ons, significantly outperforming conven[onal parallel imaging alone.

4219 Computer #24 Evaluation of highly undersampled contrast-enhanced MR angiography (SPARSE CE-MRA) in intracranial applications
Marcel Gratz^{1,2}, Marc Schlamann^{3,4}, Sophia Göricke⁴, Stefan Maderwald², and Harald H. Quick^{1,2}

¹High Field and Hybrid MR Imaging, University Hospital Essen, Essen, Germany, ²Erwin L. Hahn Institute for Magnetic Resonance Imaging, University Duisburg-Essen, Essen, Germany, ³Neuroradiology, University Hospital Giessen and Marburg GmbH, Giessen, Germany, ⁴Department of Diagnostic and Interventional Radiology and Neuroradiology, University Hospital Essen, Essen, Germany

Highly undersampled contrast-enhanced intracranial MR angiography (SPARSE CE-MRA) was evaluated regarding the vascular visibility and image quality in a clinical setting on a 3T MRI system for 23 patients with various pathologies. The overall performance is comparable to TOF MR angiography, yet with much shorter acquisition times and a high-resolution whole-head coverage in both arterial and venous phase. However, a strong dependence of the obtained MRA quality on the bolus timing of the contrast agent was found and needs to be properly addressed by the operators to minimize the arterio-venous overlap in the imagery for best diagnostic quality.

Computer #25 Yawen Huang¹, Leandro Beltrachini¹, Ling Shao², and Alejandro Frangi¹

¹Department of Electronic and Electrical Engineering, The University of Sheffield, Sheffield, United Kingdom, ²Department of Computer Science and Digital Technologies, Northumbria University, Newcastle, United Kingdom

Multi-modality MRI protocols are becoming standard in the everyday clinical practise. The advantages of such acquisitions were shown to be fundamental in a wide range of applications, such as medical diagnosis and image segmentation. However, the implementation of these protocols tends to be time-consuming, consisting in one key limitation. In this paper we address this problem by presenting a novel method for synthesising any MRI modality from a single acquired image. This is done using machine learning techniques for dictionary learning. Results show that our approach can lead to significant performance over the state-of-the-art methods.

4221 Computer #26 Fast Dynamic MRI from Undersampled Acquisitions Using Weighted, Adaptive Model Consistency Reconstruction (WI-MOCCO) Julia Velikina¹ and Alexey Samsonov²

¹Medical Physics, University of Wisconsin, Madison, WI, United States, ²Radiology, University of Wisconsin, Madison, WI, United States

We describe next generation of Model Consistency COndition (MOCCO) reconstruction which makes use of new Weighted low-rank models and attains high image quality through Iterative model adaptation to complexity of the local temporal dynamics (WI-MOCCO).

4222 Computer #27 Accelerating Intravoxel Incoherent Motion Imaging of the Brain using k-b PCA Georg Spinner¹, Johannes Frieder Matthias Schmidt¹, and Sebastian Kozerke¹

¹Institute for Biomedical Engineering, ETH Zurich, Zurich, Switzerland

In vivo Intravoxel Incoherent Motion (IVIM) parameter mapping in the brain is particularly challenging because of inherent noise amplification of parallel imaging. To address this limitation, correlations in space and in the b-value dimension may be jointly exploited. To this end, an iterative approach of k-t PCA was adapted to allow image reconstruction from undersampled IVIM data. Reconstruction and parameter estimation errors of the proposed k-b PCA approach relative to parallel imaging were assessed. Mean absolute parameter errors of k-b PCA were lower compared to CG-SENSE (R=4): $1.3 \pm 1.9 \cdot 10^{-4} / 1.8 \pm 2.0 \cdot 10^{-4}$ mm²/s (D) $0.068 \pm 0.083 / 0.085 \pm 0.101$ (f) and $6.4 \pm 16.9 \cdot 10^{-2} / 7.6 \pm 18.3 \cdot 10^{-2}$ mm²/s (D*). It is concluded that k-b PCA is a promising alternative to parallel imaging to reduce scan times while maintaining the quality of diffusion and perfusion parameter maps in brain exams.

4223 Computer #28 An Improved Tissue-Fraction MRF (TF-MRF) with Additional Fraction Regularization Xiaozhi Cao¹, Congyu Liao¹, Zhixing Wang¹, Huihui Ye¹, Ying Chen¹, Hongjian He¹, Song Chen¹, Hui Liu², and Jianhui Zhong¹

¹Center for Brain Imaging Science and Technology, Department of Biomedical Engineering, Zhejiang University, Hangzhou, Zhejiang, China, People's Republic of, ²MR Collaboration NE Asia, Siemens Healthcare, Shanghai, China, People's Republic of

MR fingerprinting has been used for estimating the intra-voxel tissue component fractions by resolving the equation $\mathbf{S}_{\text{voxel}} = \mathbf{D}\mathbf{w}$. In this study, potential fractions of interested components are used for building dictionary instead of T1 and T2, changing the solution of $\mathbf{S}_{\text{voxel}} = \mathbf{D}\mathbf{w}$ into an optimization problem with regularization terms. The results demonstrate that the proposed method could provide more robust quantification of tissue composition and estimation of partial volume effects.

4224 Computer #29 Effect of a Low-Rank Denoising Algorithm on Quantitative MRI-Based Measures of Liver Fat and Iron Brian C Allen¹, Felix Lugauer², Dominik Nickel², Lubna Bhatti¹, Randa A Daffalla¹, Brian M Dale³, Tracy A Jaffe¹, and Mustafa R Bashir^{1,4}

¹Radiology, Duke University Medical Center, Durham, NC, United States, ²MR Application Predevelopment, Siemens Healthcare GmbH, Erlangen, Germany, ³MR R&D Collaborations, Siemens Healthcare, Cary, NC, United States, ⁴Center for Advanced Magnetic Resonance Development, Duke University Medical Center, Durham, NC, United States

Applying the described low-rank denoising algorithm to a liver fat/iron quantification technique reduces image noise in PDFF and R2* maps without adversely affecting mean values of the quantitative measures or reader assessment of edge sharpness.

4225 Computer #30 Steady-State Magnetic Resonance Fingerprinting Thomas Amthor¹, Peter Koken¹, Karsten Sommer¹, Mariya Doneva¹, and Peter Börner¹

¹Philips Research Europe, Hamburg, Germany

We propose an acceleration technique for MR Fingerprinting measurements based on Cartesian or otherwise segmented sampling. We show that quick repetition of MR Fingerprinting sequences leads to stationary signal responses. Instead of waiting for the spin system to relax completely before the start of the next fingerprint sequence, we take the evolution of the spin system into account and calculate a dictionary of steady-state fingerprints. We present a Cartesian fingerprint measurement with a SENSE factor of four. Using our method, additional acceleration by more than a factor of two could be achieved, without reducing the match accuracy.

4226 Computer #31 Reconstructing all physical quantities from time-domain data of a very short sequence Alessandro Sbrizzi¹, Annette van der Toorn¹, Hans Hoogduin¹, Peter R Luijten¹, and Cornelis AT van den Berg¹

Magnetic Resonance Spin Tomography in Time-domain (MR-STAT) aims at reconstructing all physical quantities (T1, T2, PD, etc) directly from the data in the time-domain. By solving a large scale nonlinear inversion problem, the parameters can be inferred. The spatial encoding is entangled implicitly in the time response of the system. A very quick acquisition can be performed and processed to derive all system parameters, including electromagnetic field maps like B0 and B1. We illustrate MR-STAT at high resolution for a realistic numerical phantom and we show high precision reconstructions of quantitative maps.

4227
Computer #32 Acceleration of MR Fingerprinting with Low Rank and Sparsity Constraint
Congyu Liao¹, Xiaozhi Cao¹, Huihui Ye¹, Ying Chen¹, Hongjian He¹, Song Chen¹, Qiuping Ding¹, Hui Liu², and Jianhui Zhong¹

¹Center for Brain Imaging Science and Technology, Zhejiang University, Hangzhou, China, People's Republic of, ²MR Collaboration NE Asia, Siemens Healthcare, Shanghai, China, People's Republic of

In this study, a low rank and sparsity based MRF reconstruction scheme (L&S MRF) is proposed for reducing the artifacts of each time point with a fraction of acquisition times.

4228
Computer #33 Highly Accelerated Chemical Exchange Saturation Transfer (CEST) MRI Using Combination of Compressed Sensing and Sensitivity Encoding
Hye-Young Heo^{1,2}, Yi Zhang¹, Dong-Hoon Lee¹, Shanshan Jiang¹, Xuna Zhao¹, and Jinyuan Zhou^{1,2}

¹The Russell H. Morgan Department of Radiology and Radiological Science, Johns Hopkins University School of Medicine, Baltimore, MD, United States, ²F.M. Kirby Research Center for Functional Brain Imaging, Kennedy Krieger Institute, Baltimore, MD, United States

Chemical exchange saturation transfer (CEST) imaging is a unique contrast enhancement technique that enables the indirect measurement of endogenous metabolites with water-exchangeable protons. The measurement of a complete Z-spectrum using standard imaging acquisition scheme is time consuming because a large number of the RF saturation frequency offset followed by MR signal readout is inevitable to obtain the full Z-spectrum. In this study, the feasibility of accelerated CEST imaging using combined CS and SENSE technique (CS-SENSE) was demonstrated in healthy volunteers and glioma patients at 3 T.

4229
Computer #34 Multi-shot sensitivity encoded diffusion data recovery using structured low-rank matrix completion (MUSSELS)
Merry Mani¹, Mathews Jacob², Douglas Kelley³, and Vincent Magnotta⁴

¹Dept. of Psychiatry, University of Iowa, Iowa City, IA, United States, ²Dept. of Electrical and Computer Engineering, University of Iowa, Iowa City, IA, United States, ³General Electric Healthcare Technologies, San Francisco, CA, United States, ⁴Dept of Radiology, University of Iowa, Iowa City, IA, United States

Multi-shot diffusion imaging holds great potential for enabling high spatial resolution diffusion imaging as well as short echo time imaging to enhance studies at higher field strengths. Conventional reconstructions rely on motion-induced phase estimates to recover the diffusion-weighted images from multi-shot acquisitions. Since a good estimate of phase cannot be obtained in many situations either due to noisy data or high under-sampling, these methods are unreliable in such situations. Here we propose a new reconstruction for multi-shot diffusion imaging that recovers the missing k-space data of the multiple shots by formulating the recovery as a structured low-rank matrix completion problem.

4230
Computer #35 Two-step adaptive reconstruction of multichannel phase images
Peng Wu¹ and Hua Guo¹

¹Center for Biomedical Imaging Research, Department of Biomedical Engineering, School of Medicine, Tsinghua University, Beijing, China, People's Republic of

Adaptive reconstruction (AR) can be used to combine multichannel images without acquiring coil sensitivity information. It can improve the SNRs of combined magnitude and phase images. But the reconstructed phase images may suffer from open-ended fringe artifacts when coil-sensitivity maps vary a lot. We propose a two-step adaptive reconstruction method to combine multichannel images. This method is shown to be more robust than the traditional AR method and can still maintain the high SNR.

4231
Computer #36 Improved Time Fidelity in Sparse ADMM Reconstruction via Tempered Data Weighting
Eric A. Borisch¹, Joshua D. Trzasko¹, and Stephen J. Riederer¹

¹Mayo Clinic, Rochester, MN, United States

By adding an age-of-sample dependent weighting to the data fidelity penalty of an Alternating Direction Method of Multipliers sparse reconstruction of a view-shared accelerated acquisition, improved temporal fidelity is observed in a time-resolved motion-controlled phantom study.

4232
Computer #37 Reference-guided CS-MRI with Gradient Orientation Priors
Xi Peng¹, Shanshan Wang¹, Qingyong Zhu¹, and Dong Liang¹

In various MR applications, a pre-scan is usually practicable that extra morphology information can be extracted from the reference image. However, with a reference image obtained from a different contrast mechanism, the signal variation in the reference may differ from that in the target image. In this work, we propose to exploit gradient orientation information, which is closely related to the anatomical structures but less dependent on the image contrast, to enable superior CS-based reconstruction. The proposed method was validated using multi-scan experiment data and is shown to provide high speed and high quality imaging.

4233 Computer #38 Temporal point spread function interpretation of low rank, dictionary learning models in dynamic MRI
Sajan Goud Lingala¹, Sampada Bhawe², Yinghua Zhu¹, Krishna Nayak¹, and Mathews Jacob²

¹Electrical Engineering, University of Southern California, Los Angeles, CA, United States, ²Electrical and Computer Engineering, University of Iowa, Iowa city, IA, United States

A number of dynamic MRI applications have seen the adaptation of data-driven models for efficient de-noising and reconstruction from under-sampled data. In this work, we develop a novel temporal point spread function interpretation of two data-driven models: low rank, and dictionary-learning. Through this interpretation, we show (a) the low rank model to perform spatially invariant non-local view-sharing, and (b) the dictionary-learning model to perform spatially varying non-local view-sharing. Both the models can be viewed as efficient data-driven retrospective binning techniques. We provide demonstrations using the application of de-noising real-time MRI speech data.

4234 Computer #39 Kernelized Low-Rank: Improve Low-Rank with Adaptive Nonlinear Kernel for Dynamic MRI
Enhao Gong¹, Tao Zhang¹, Joseph Cheng¹, Shreyas Vasanaawala², and John Pauly¹

¹Electrical Engineering, Stanford University, Stanford, CA, United States, ²Radiology, Stanford University, Stanford, CA, United States

Low-Rank methods are widely applied to improve reconstruction for Dynamic Contrast Enhanced (DCE) MRI by imposing linear spatial-temporal correlation in global, local or multiple scales. This assumption does not fully capture the highly nonlinear spatial-temporal dynamics of DCE signals. We proposed a generalized Kernelized-Low-Rank model, assumed Low-Rank property after nonlinear transform and solved it by Regularizing singular-values with Adaptive Nonlinear Kernels. The proposed method captures the spatial-temporal dynamics as a sparser representation and achieves more accurate reconstruction results. Kernelized-Low-Rank model can be easily integrated to provide significant improvements to Global Low-Rank, Locally Low-Rank, LR+S and Multi-scale LR models.

4235 Computer #40 Efficient algorithm for maximum likelihood estimate and confidence intervals of T_1 from multi-flip, multi-echo FLASH
M. Dylan Tisdall^{1,2} and André J. W. van der Kouwe^{1,2}

¹Athinoula A. Martinos Center for Biomedical Imaging, Massachusetts General Hospital, Charlestown, MA, United States, ²Radiology, Harvard Medical School, Boston, MA, United States

Multi-flip, multi-echo 3D FLASH is routinely used to estimate T1. We present a novel, efficient algorithm for finding both the ML estimate and a confidence interval for T1, given full, multi-channel data from such an experiment. Finding the ML estimate is based on minimizing a cost function. The ends of the CI are a threshold value for the same cost function, where the threshold is determined via Monte Carlo experiment based on the protocol and desired confidence level. Results from a phantom study are shown, demonstrating the value of CIs in interpreting the validity of the ML estimates.

4236 Computer #41 Advances in Model-Based Reconstruction of High Resolution T1 maps
Volkert Roeloffs¹, Xiaoqing Wang¹, and Jens Frahm¹

¹Biomedizinische NMR Forschungs GmbH, Max Planck Institute for Biophysical Chemistry, Goettingen, Germany

Fast and accurate determination of T1 values can be accomplished by Look-Locker type MRI sequences. Here, we formulate T1 mapping as a nonlinear optimization problem which we subsequently solve by the iteratively regularized Gauss Newton (IRGN) method. Our choice of the model parameterization allows to exploit smoothness of the spatial flip angle distribution as additional prior knowledge. This model-based reconstruction allows accurate and precise reconstruction of high resolution T1 maps from radial, highly undersampled data as validated in phantom studies and demonstrated in the human brain.

4237 Computer #42 Whole-Brain Gray Matter Imaging Exploiting Single-Slab 3D Dual-Echo TSE With Relaxation Modulation: Comparison With Double Inversion Recovery Gray Matter Imaging
Hyunyeol Lee¹ and Jaeseok Park²

¹Center for Neuroscience Imaging Research, Institute for Basic Science, Suwon, Korea, Republic of, ²Department of Biomedical Engineering, Sungkyunkwan University, Suwon, Korea, Republic of

In this work we propose a novel, GM-selective single-slab 3D dual echo TSE with relaxation modulation (no long IR), in which white matter signals remain nulled before signal encoding while CSF signals are modulated to be cancelled during residual reconstruction between echoes with sparsity prior. We demonstrate the effectiveness of the proposed method over conventional DIR in that the former can achieve 1mm-isotropic whole-brain GM acquisition in 5-6 min. without apparent artifacts.

4238 Computer #43 Dynamic Tagged Liver MRI Exploiting Tag-Constrained Sampling and Separation: Assessment of Liver Stiffness
Hyunkyung Maeng^{1,2} and Jaeseok Park²

¹Center for Neuroscience Imaging Research, Institute for Basic Science (IBS), Suwon, Korea, Republic of, ²Department of Biomedical Engineering, Sungkyunkwan University, Suwon, Korea, Republic of

It is important to assess liver stiffness and monitor the progression of fibrosis in patients with liver diseases using non-invasive imaging. Exploiting the fact that the motion of the heart during cardiac cycle is an intrinsic driving source to deform the liver, dynamic tagged MRI can be employed to measure the cardiac motion induced displacements using harmonic phase images and thereby evaluate the corresponding strain maps in the liver. In this work, we propose a novel framework of compressed sensing (CS) for dynamic tagged liver MRI, in which: 1) data is acquired using tag-constrained, incoherent undersampling in k-t space, 2) a time series of morphologies is decomposed into transient tag-only images and stationary tag-free liver images, 3) both morphological components are then reconstructed directly from the tag-constrained, undersampled k-t space, and 4) the transient tag-only images are employed to estimate time-varying displacements and the corresponding strain maps while the stationary tag-free liver images are used as a structural roadmap.

4239 Computer #44 Dynamic Contrast-Enhanced MRA with Robust Background Suppression Exploiting Motion Subspace Learning and Sparsity Priors
Suhung Park¹ and Jaeseok Park²

¹Center for Neuroscience Imaging Research, Institute for Basic Science (IBS), Suwon, Korea, Republic of, ²Department of Biomedical Engineering, Sungkyunkwan University, Suwon, Korea, Republic of

Dynamic contrast-enhanced magnetic resonance angiography(DCE-MRA) has been widely used for diagnostic assessment in clinical practices. To enhance the conspicuity of arteries relative to unwanted background tissues, subtraction between the pre-contrast and the post-contrast images was typically performed displaying maximum intensity projection images(MIP). Nevertheless, if there exists non-stationary signal transition due to time-drifting field inhomogeneity, and subject motion etc, the subtraction leads to incomplete background suppression, impairing the detectability of arteries as well as small vessel particularly at high reduction factors. In this work, we propose a novel DCE-MRA method exploiting motion subspace learning and sparsity priors for robust angiogram separation, in which the motion subspace is learned using partial Casorati matrix without any motion information while image reconstruction with sparsity priors is performed to jointly estimate motion-induced artifacts and DCE angiograms of interest under the framework of the decomposition. Simulation and experimental studies show that the proposed method is highly competitive with the competing methods including subtraction and fast reconstruction techniques.

4240 Computer #45 High Spatiotemporal Resolution 3D Dynamic MRI using Spiral Acquisition and Compressed Sensing with L0 Homotopic Minimization
Lyu Li¹, Sheng Fang², Pascal Spincemaille³, Bida Zhang⁴, Yi Wang^{3,5}, and Hua Guo¹

¹Center for Biomedical Imaging Research, Department of Biomedical Engineering, School of Medicine, Tsinghua University, Beijing, China, People's Republic of, ²Institute of nuclear and new energy technology, Tsinghua University, Beijing, China, People's Republic of, ³Radiology, Weill Cornell Medical College, New York, NY, United States, ⁴Healthcare Department, Philips Research China, Shanghai, China, People's Republic of, ⁵Biomedical Engineering, Cornell University, New York, NY, United States

High spatiotemporal resolution 3D imaging is a desired technique for detecting dynamic information of detailed anatomy and getting accurate modeling parameters. In this abstract, we developed a method using golden angle spiral and compressed sensing with L0 homotopic minimization for high resolution 3D imaging. In this method, a high undersampling rate and high motion insensitivity can be achieved. In clinical applications such as dynamic contrast enhanced MRI, this new method is very promising to achieve high spatiotemporal resolution without breath-hold.

4241 Computer #46 Improved Field-Map Estimation and Deblurring for MAVRIC-SL
Brady Quist^{1,2}, Xinwei Shi^{1,2}, Hans Weber¹, and Brian A Hargreaves^{1,2}

¹Department of Radiology, Stanford University School of Medicine, Stanford, CA, United States, ²Department of Electrical Engineering, Stanford University, Stanford, CA, United States

In order to image in the large B₀ field inhomogeneity near metallic implants, multi-spectral imaging sequences, such as MAVRIC-SL, acquire images at multiple spectral bins to reduce distortion while imaging the entire anatomy. However, blurring is introduced when these overlapping bins are combined. While a deblurring method, which uses a field-map estimated from the bin images, does exist, the resulting images are subject to increased noise and distortion. Here we propose both a better field-map estimation method along with an improved deblurring algorithm, both of which are less sensitive to noise and help provide excellent deblurring without distortion.

4242 Computer #47 Free-breathing 3D Cine Whole-heart Magnetic Resonance Imaging using Compressed Sensing Parallel Image Reconstruction
Mehdi Hedjazi Moghari^{1,2}, Jonathan I Tamir³, John Axerio-Cilies³, Tal Geva^{1,4}, and Andrew J Powell^{1,4}

¹Pediatrics, Harvard Medical School, Boston, MA, United States, ²Cardiology, Boston Children's Hospital, Boston, MA, United States, ³Arterys, San Francisco, CA, United States, ⁴Cardiology, Boston Children's Hospital, Boston, MA, United States

We developed and evaluated a variable density Poisson disc undersampling technique and compressed sensing image reconstruction algorithm for free-breathing 3D cine steady-state free precession whole-heart imaging. In 10 patients, we found good agreement between 3D cine and conventional breath-hold 2D cine imaging measurements of ventricular volumes.

4241



4243
Computer #48 Accelerated 3D coronary MRA using non-rigid motion corrected regularized reconstruction
T. Correia¹, G. Cruz¹, R. M. Botnar¹, and C. Prieto¹

¹Division of Imaging Sciences and Biomedical Engineering, King's College London, London, United Kingdom

Accelerated 100% scan efficiency whole-heart 3D coronary MR angiography (CMRA) is achieved by combining undersampling and non-rigid motion correction in a unified regularized reconstruction. 3D undersampled CMRA is performed using a golden-step spiral-like Cartesian trajectory. Motion correction is achieved in two steps: beat-to-beat 2D translational correction with motion estimated from interleaved image navigators, and bin-to-bin 3D non-rigid correction with motion estimated from the data itself. A generalized matrix formalism with total variation regularization is used to perform the non-rigid correction directly in the reconstruction. This approach produces good quality images, comparable to those of a navigator-gated approach, but in a ~5x shorter scan time.

Electronic Poster

Motion Correction

Exhibition Hall

Thursday, May 12, 2016: 10:30 - 11:30

4244
Computer #49 Impact of non-rigid registration and retrospective image correction (RETROICOR) on detecting BOLD fMRI vasomotor response in the breast
Tess E. Wallace¹, Andrew J. Patterson², Roie Manavaki¹, Martin J. Graves¹, and Fiona J. Gilbert¹

¹Department of Radiology, University of Cambridge, Cambridge, United Kingdom, ²Cambridge University Hospitals NHS Foundation Trust, Cambridge, United Kingdom

Physiological fluctuations and motion artifacts are expected to be dominant sources of noise in BOLD fMRI experiments to assess tumor oxygenation and angiogenesis. This work assesses the impact of a non-rigid registration algorithm and retrospective image correction (RETROICOR) on the detection of activation signals in the breast, both at resting state and in response to a modulated respiratory stimulus paradigm. Our results suggest that correction for motion artifacts is associated with a reduction in false-positive activation effects, which can be further improved by the addition of RETROICOR, confirming the importance of these physiological corrections in functional parameter estimation.

4245
Computer #50 Prospective Motion Correction in Brain Imaging Using a Passive Magnetic Sensor
Mahamadou Diakite¹, Steve Roys², Taehoon Shin², Jiachen Zhuo², Jaydev P. Desai³, and Rao P. Gullapalli²

¹Radiology, Center for Metabolic Imaging and Therapeutics, University of Maryland, School of Medicine, Parkville, MD, United States, ²Radiology, Center for Metabolic Imaging and Therapeutics, University of Maryland, School of Medicine, Baltimore, MD, United States, ³Department of Mechanical Engineering, University of Maryland, College Park, Maryland, United States, Baltimore, MD, United States

We present a prospective motion correction (PMC) technique using a miniature passive magnetic sensor. The motion sensor can virtually work with any imaging technique that is sensitive to motion. Especially techniques such as fMRI, DTI and spectroscopy sequences are likely to benefit greatly when dealing with non-cooperative subjects.

In this study, the GRE sequence was initially modified by adding three bipolar gradients along the read, phase, and slice-selection directions respectively. The bipolar gradients were used to trigger the position and orientation tracking sensor. A dynamic feedback loop mechanism was implemented into the sequence to receive the sensor position and orientation for real-time update of the imaging slice using an in-house developed application.

We demonstrate that our PMC method in brain imaging using a passive magnetic sensor is capable of tracking the patient head motion with high accuracy.

4246
Computer #51 Synchronization of longitudinal multi time-point breast DCE data using a group-wise registration approach
Chandan Aladahalli¹, KS Shriram¹, Dattesh Shanbhag¹, Rakesh Mullick¹, Reem Bedair², Fiona Gilbert², Andrew Patterson², and Martin Graves²

¹GE Global Research, Bengaluru, India, ²University of Cambridge, Cambridge, United Kingdom

Multi-parametric longitudinal imaging is an important tool to monitor therapy response at tumor locations. The key challenge in longitudinal data is the synchronization of volumes across time points, as large variations are seen due to therapy response, weight loss/gain, patient positioning, and surgery. We employ a group-wise registration approach to synchronize the longitudinal volumes and compare/contrast it with a more typical pair-wise registration approach. Group-wise approach results in consistent registration across time-points as it does not require a reference image. The group-wise non-rigid registration approach is demonstrated on longitudinal MRI data used for assessing breast tumor therapy response.

4247
Computer #52 Outer volume suppression improves motion tracking and image quality in self-navigated whole heart cardiac MRI: results from a moving phantom and healthy volunteers
Andrew J Coristine¹, Jerome Chaptin¹, Giulia Ginami¹, Gabriele Bonanno¹, Simone Coppo¹, Ruud B van Heeswijk¹, Davide Piccini^{1,2}, and

Matthias Stuber^{1,3}

¹Department of Radiology, University Hospital (CHUV) / University of Lausanne (UNIL), Lausanne, Switzerland, ²Advanced Clinical Imaging Technology, Siemens Healthcare, Lausanne, Switzerland, ³CardioVascular Magnetic Resonance (CVMR) research centre, Centre for Biomedical Imaging (CIBM), Lausanne, Switzerland

In respiratory self-navigation (SN), static structures, such as the arms or chest wall, may complicate motion detection due to the superposition of signal originating from different tissues. Even if motion detection is successful, the subsequent motion correction may introduce streaking artefacts when applied to static structures. Suppressing signal from those tissues may therefore improve image quality. In this study, we address the hypothesis that SN coronary MRA will benefit from the introduction of an outer volume suppressing "2D-T-Prep", and present results from a moving cardiac phantom and 10 healthy volunteers.

4248 Computer #53 Reconstruction of under-sampled Propeller gradient-echo image using projection onto convex sets based multiplexed sensitivity-encoding (POCSMUSE)
Hing-Chiu Chang^{1,2}, Mei-Lan Chu², and Nan-Kuei Chen²

¹Department of Diagnostic Radiology, The University of Hong Kong, Hong Kong, Hong Kong, ²Brain Imaging and Analysis Center, Duke University Medical Center, Durham, NC, United States

The Propeller technique is a useful acquisition scheme and reconstruction method to reduce motion artifact. However, the higher specific absorption rate (SAR) of RF pulse at high-field magnetic strength can limit the number of multiple slices for a given TR, which in turn reduces the efficiency of acquisition, especially for Propeller-FSE sequence. A possible solution is to reduce the echo-train-length with under-sampling of data of each blade. In this study, we propose to apply POCSMUSE instead of SENSE reconstruction and Propeller reconstruction, to reconstruct the image from all under-sampled blade data with reduced noise amplification. The data acquired from brain and liver using Propeller-GRE will be used to test purposed POCSMUSE algorithm.

4249 Computer #54 Respiratory Motion Compensation for Simultaneous PET/MR Using Strongly Undersampled MR Data
Christopher M Rank¹, Thorsten Heußer¹, Andreas Wetscherek¹, Martin T Freitag², Heinz-Peter Schlemmer², and Marc Kachelrieß¹

¹Medical Physics in Radiology, German Cancer Research Center (DKFZ), Heidelberg, Germany, ²Radiology, German Cancer Research Center (DKFZ), Heidelberg, Germany

To allow for MR acquisition times as short as 1 minute per bed, we propose a new method for PET/MR respiratory motion compensation (MoCo), which is based on strongly undersampled radial MR data. We acquired simultaneous PET/MR data of the thorax of three patients. Motion vector fields were estimated with a newly-developed algorithm, which alternates between MR image reconstruction and motion estimation. Subsequent 4D MoCo PET reconstructions employing the motion vector field derived from strongly undersampled MR data yielded a considerable visual and quantitative improvement compared to standard 3D PET and 4D gated PET reconstructions.

4250 Computer #55 Motion Correcting Complete MR-PET Exams Via Plot Tone Navigators
Thomas Koesters¹, Ryan Brown¹, Tiejun Zhao², Mattias Fenchel³, Peter Speier³, Li Feng¹, Yongxian Qian¹, and Fernando Emilio Boada¹

¹Radiology, New York University, New York, NY, United States, ²Siemens Medical Systems, Malvern, PA, United States, ³Siemens Medical Systems, Erlangen, Germany

We demonstrate the use of an external RF signal as a mean to provide motion tracking information for motion-state sorting of k-space line during dynamic MRI scans.

4251 Computer #56 High temporal resolution retrospective motion and B_0 correction using FIDNavs and segmented FatNavs at 7T.
Frédéric Gretschi¹, Tobias Kober^{2,3,4}, Maryna Waszak^{2,3,4}, José P. Marques⁵, and Daniel Gallichan¹

¹CIBM, EPFL, Lausanne, Switzerland, ²Advanced Clinical Imaging Technology (HC CMEA SUI DI BM PI), Siemens Healthcare AG, Lausanne, Switzerland, ³Department of Radiology, University Hospital (CHUV), Lausanne, Switzerland, ⁴LTSS, EPFL, Lausanne, Switzerland, ⁵Donders Centre for Cognitive Neuroimaging, Radboud University, Netherlands

FID navigators (FIDNavs) and a few lines of highly accelerated double-echo 3D fat navigators (FatNavs) were measured each TR of a high-resolution 3D-GRE acquisition. High temporal resolution B_0 variations and motion parameters could be estimated by the FIDNavs using the lower temporal resolution FatNavs to derive calibration data. The cardiac cycle pattern emerged clearly in these estimates and retrospectively corrected images were of clearly improved quality, thereby demonstrating the potential for this hybrid approach.

4252 Computer #57 Self-navigated real-time motion tracking of the abdomen in free-breathing single-shot EPI data using the Extended Kalman Filter.
Nathan White¹, Josh Kuperman¹, Neal Corson¹, Kazim Narisinh¹, Hauke Bartsch¹, David Karow¹, Ajit Shankaranarayanan², and Anders Dale^{1,3}

¹Department of Radiology, University of California, San Diego, San Diego, CA, United States, ²Global Applied Sciences Lab, GE Healthcare, Menlo Park, CA, United States, ³Department of Neuroscience, University of California, San Diego, San Diego, CA, United States

Free-breathing single-shot EPI data in the abdomen is confounded by respiratory motion artifact. Previous work has demonstrated the utility of using the Extended Kalman Filter (EKF) for real-time image-based tracking of spiral-navigated scans in brain. This study we demonstrate the feasibility of using the EKF framework for real-time self-navigated motion tracking in the abdomen.

4253
Computer #58 Motion-resolved 3D dynamic contrast enhanced liver MRI
Dominik Nickel¹, Xiao Chen², Boris Mailhe², Qiu Wang², Yohan Son³, Jeong Min Lee⁴, and Berthold Kiefer¹

¹Siemens Healthcare GmbH, Erlangen, Germany, ²Medical Imaging Technologies, Siemens Healthcare, Princeton, NJ, United States, ³Siemens Healthcare Ltd., Seoul, Korea, Republic of, ⁴Department of Radiology, Seoul National University Hospital, Seoul, Korea, Republic of

Free-breathing dynamic contrast-enhanced liver MRI is explored using a Cartesian spoiled Volume-Interpolated Breath-hold Examination (VIBE) GRE sequence that also acquires a navigation signal. Images are iteratively reconstructed using a hard-gating approach as well as resolving the motion-states using an additional dimension. With both approaches yielding promising results, the latter appears to be more motion robust at the cost of computational effort.

4254
Computer #59 Prospective motion correction for MRI using EEG-equipment
Mads Andersen^{1,2}, Kristoffer H. Madsen¹, and Lars G. Hanson^{1,2}

¹Danish Research Center for Magnetic Resonance, Copenhagen University Hospital Hvidovre, Hvidovre, Denmark, ²DTU Elektro, Technical University of Denmark, Lyngby, Denmark

A new prospective motion correction technique is presented that is based on signals from gradient switching, in an EEG-cap with interconnected electrodes the subject wears during scanning. The method has no line-of-sight limitations as optical methods, requires no interleaved navigator modules or additional hardware for sites already doing EEG-fMRI. Instead a training scan is performed where signals recorded with the EEG-system are correlated with motion parameters estimated by image realignment. Initial results from application of the method in a phantom are promising.

4255
Computer #60 Motion Correction Using Orthogonal Images
Niranchana Manivannan¹, Bradley D. Clymer¹, Anna Bratasz^{2,3}, and Kimerly A. Powell^{2,4}

¹Department of Electrical and Computer Engineering, The Ohio State University, Columbus, OH, United States, ²Small Animal Imaging Shared Resources, The Ohio State University, Columbus, OH, United States, ³Davis Heart & Lung Research Institute, The Ohio State University, Columbus, OH, United States, ⁴Department of Biomedical Informatics, The Ohio State University, Columbus, OH, United States

In most small animal imaging studies both long axis (coronal or sagittal) and short axis (axial) images of the region of interest are obtained. The goal of this study is to explore whether combining two orthogonal views obtained with different slice-select directions could reduce the motion artifacts and improve image quality. The advantages of this method are that no a priori knowledge or external hardware is needed and it doesn't increase the acquisition time. The results show that it is advantageous to use the available orthogonal image(s) to improve the image quality by reducing ghosting artifacts caused by motion.

4256
Computer #61 Image Registration and Robust Fitting for Motion Insensitive Magnetic Resonance Fingerprinting (MRF)
Bhairav Bipin Mehta¹, Dan Ma¹, and Mark Alan Griswold¹

¹Radiology, Case Western Reserve University, Cleveland, OH, United States

Motion is one of the biggest challenges in clinical MRI. The recently introduced Magnetic Resonance Fingerprinting (MRF) has been shown to be less sensitive to motion. However, it is still susceptible to patient motion primarily occurring in the early stages of the acquisition. In this study, we propose a novel reconstruction algorithm for MRF, which uses robust fitting and image registration algorithms to decrease the motion sensitivity of MRF. The evaluation was performed in numerical phantoms with simulated rigid motion.

4257
Computer #62 Dynamic, T2-Weighted, Single-Shot Fast Spin Echo with Variable Refocusing Flip Angle and Cylindrical Navigator for Retrospective Respiratory Compensation
Daniel V Litwiller¹, Erik Tryggstad², Kiaran McGee³, Yuji Iwadata⁴, Lloyd Estkowski⁵, and Ersin Bayram⁶

¹Global MR Applications & Workflow, GE Healthcare, New York, NY, United States, ²Department of Radiation Oncology, Mayo Clinic, Rochester, MN, United States, ³Department of Radiology, Mayo Clinic, Rochester, MN, United States, ⁴Global MR Applications & Workflow, GE Healthcare, Hino, Tokyo, Japan, ⁵Global MR Applications & Workflow, GE Healthcare, Menlo Park, CA, United States, ⁶Global MR Applications & Workflow, GE Healthcare, Houston, TX, United States

Here we present a multi-slice, multi-phase, single-shot fast spin echo sequence with variable refocusing flip angle and interleaved cylindrical reference navigator for retrospective respiratory-guided image sorting for the purpose of managing motion in the context of MR-guided radiation therapy treatment planning.

- 4258
Computer #63 Beyond high resolution MPRAGE: In vivo T1-weighted imaging at 7T with 250 μm isotropic resolution using prospective motion correction
Falk Lüsebrink¹, Alessandro Sciarra¹, Hendrik Mattern¹, Renat Yakupov¹, and Oliver Speck^{1,2,3,4}
- ¹Biomedical Magnetic Resonance, Otto-von-Guericke University, Magdeburg, Germany, ²Leibniz Institute for Neurobiology, Magdeburg, Germany, ³Center for Behavioral Brain Sciences, Magdeburg, Germany, ⁴German Center for Neurodegenerative Disease, Magdeburg, Germany*
- Increasing the spatial resolution is of major importance to structural imaging as this may build bridges to optical microscopy and may lead to superior diagnostics and segmentations. Increasing the spatial resolution with sufficient SNR usually prolongs time of acquisition. This inevitably introduces more motion artifacts even with experienced subjects. However, this can be compensated by prospective motion correction. Increasing the resolution to a few hundred micrometers inherently reduces SNR such that reconstruction by sum of squares is not adequate anymore. Here we demonstrate our work on the acquisition and reconstruction of the currently highest resolution in vivo MPRAGE at 7T.
-
- 4259
Computer #64 Low rank and sparsity on MR-based PET motion correction using simultaneous PET/MRI: a patient study
Yixin Ma¹, Yoann Petibon², Joyita Dutta², Xucheng Zhu³, Rong Guo¹, Georges El Fakhri², Kui Ying¹, and Jinsong Ouyang²
- ¹Key laboratory of Particle and Radiation Imaging, Ministry of Education, Tsinghua University, Beijing, China, People's Republic of, ²Center for Advanced Medical Imaging Sciences, Division of Nuclear Medicine and Molecular Imaging, Department of Imaging, Massachusetts General Hospital, Boston, MA, United States, ³UCSF/UC Berkeley Bioengineering Graduate Group, University of California Berkeley, Berkeley, CA, United States*
- In this work, we exploited the low-rank and sparse properties of dynamic MRI data to accelerate the MR acquisition and assessed its impact on MR-based PET respiratory motion using a PET/MR oncologic patient study. PET/MR motion correction workflow was accomplished, and good performance of partially sampled MR based motion correction attests the possibility of faster PET/MR data acquisition and better lesion estimation.
-
- 4260
Computer #65 High Efficiency Coronary MRA: Beyond the Quiescent Period
Jianing Pang¹, Yuhua Chen^{1,2}, and Debiao Li^{1,3}
- ¹Biomedical Imaging Research Institute, Cedars-Sinai Medical Center, Los Angeles, CA, United States, ²Department of Computer and Information Science, University of Pennsylvania, Philadelphia, PA, United States, ³Bioengineering, University of California, Los Angeles, CA, United States*
- Current motion compensation strategies for whole-heart coronary MRA only accept data acquired during specific motion phases, thus significantly reduce the imaging efficiency. In this work, we developed a reconstruction framework based on 4D coronary MRA that allowed one to increase the cardiac gating efficiency by accepting cardiac phases beyond the quiescent period, while minimizing the associated cardiac motion artifacts through non-rigid motion correction. Preliminary results from healthy subjects showed that the proposed method significantly improved the imaging efficiency, aSNR, and coronary sharpness compared with images reconstructed from the quiescent period.
-
- 4261
Computer #66 Motion Tracking using Nonlinear Gradient Fields: Experimental Verification and Oblique Slices
Emre Kopanoglu¹, Haifeng Wang¹, Gigi Galiana¹, and Robert Todd Constable^{1,2}
- ¹Diagnostic Radiology and Biomedical Imaging, Yale University, New Haven, CT, United States, ²Neurosurgery, Yale University, New Haven, CT, United States*
- Motion navigation using nonlinear gradient fields is demonstrated experimentally. The method makes use of the simultaneous multi-dimensional encoding capabilities of nonlinear gradient fields. A two-dimensional navigator image is obtained from a single-echo encoded using a nonlinear gradient field and multiple receiver coils. Without exceeding the maximum field generated by the linear gradient fields of a 3T scanner inside a 20cm isotropic field-of-view, the navigator can be acquired in under one millisecond, including its rewind. The method can track both translational and rotational in-plane rigid body motion, as demonstrated in phantom experiments. Simulations show the method is applicable in oblique angles.
-
- 4262
Computer #67 3D Stack-of-Stars Dixon Fat-Only Signal for Respiratory Motion Detection
Thomas Martin^{1,2}, Andres Saucedo¹, Tess Armstrong¹, Holden Wu², Danny Wang³, and Kyunghyun Sung²
- ¹Biomedical Physics, UCLA, Los Angeles, CA, United States, ²Radiological Sciences, UCLA, Los Angeles, CA, United States, ³Neurology, UCLA, Los Angeles, CA, United States*
- Respiratory motion is one of the biggest confounders of liver DCE-MRI. There are methods that use a 3D radial self-gated signal (SGS) to compensate for respiratory motion. However, SGS includes both respiratory motion and contrast uptake in DCE-MRI, and it is not trivial to perfectly separate the two from SGS, leading to inaccuracies of respiratory motion. In this work, we propose a method to extract the respiratory motion only from SGS using golden angle radial acquisition with two-point Dixon separation. The proposed method utilizes the fact the fat-only SGS does not include contrast uptake while including the same respiratory motion.
-
- 4263
Computer #68 Navigator-Free Motion Correction for Cartesian FSE
Yilong Liu^{1,2}, Mengye Lyu^{1,2}, Yanqiu Feng^{1,2}, Victor B. Xie^{1,2}, and Ed X. Wu^{1,2}

¹Laboratory of Biomedical Imaging and Signal Processing, The University of Hong Kong, Hong Kong, China, People's Republic of, ²Department of Electrical and Electronic Engineering, The University of Hong Kong, Hong Kong, China, People's Republic of

A navigator-free motion correction method for Cartesian FSE is proposed for intermittent motion compensation. It first divides all shots into several motion-free groups, then estimates and corrects inter-group motion. In vivo imaging results show that this approach has decent performance in dealing with intermittent motion problems. Though only demonstrated with Cartesian acquisition, it is also applicable for non-Cartesian acquisitions, such as spiral and radial acquisitions.

4264 Computer #69 Phantom pose detection with spherical navigator echoes for calibration of optical tracking systems in MRI
Denis Kokorin¹, Cris Lovell-Smith¹, Benjamin Knowles¹, Michael Herbst¹, Jürgen Hennig¹, and Maxim Zaitsev¹

¹Medical Physics, University Medical Center Freiburg, Freiburg, Germany

In this work, we present a new k-space based approach for position and rotation detection to improve calibration of optical tracking systems used for prospective motion correction in MRI. 3D radial acquisition was employed to detect motion of a custom built phantom. The integrated method was tested for different motion types and showed a high precision along with a good robustness for rotation detection.

4265 Computer #70 Respiratory Motion Corrected 3D Patch based Reconstruction of Under-sampled Data for Liver 4D DCE-MRI
Dongxiao Li^{1,2}, Juerong Wu¹, Kofi M. Deh², Thanh D. Nguyen², Martin R. Prince², Yi Wang^{2,3}, and Pascal Spincemaille²

¹College of Information Science and Electronic Engineering, Zhejiang University, Hangzhou, China, People's Republic of, ²Department of Radiology, Weill Cornell Medical College, New York, NY, United States, ³Department of Biomedical Engineering, Cornell University, Ithaca, NY, United States

Liver dynamic contrast enhanced MRI (DCE-MRI) requires high spatial and temporal resolution such that all relevant enhancement phases are clearly visualized. Image quality is compromised when breathing occurs during the acquisition. This abstract presents a novel 4D respiratory Motion corrected Patch based Reconstruction of Under-sampled Data (M-PROUD) which uses 3D patch based local dictionaries for sparse coding and simultaneously estimates 3D nonrigid motion. Results on in vivo data demonstrated that the proposed method can significantly reduce motion blurring artifacts and preserve more details at a sub-second temporal frame rate in free breathing liver 4D DCE-MRI.

4266 Computer #71 Motion-Robust Abdominal DCE-MRI Using Respiratory-Gated Golden-Angle Radial Sparse Parallel MRI
Robert Grimm¹, Dominik Nickel¹, Qiu Wang², Boris Mailhe², Berthold Kiefer¹, Kai Tobias Block³, and Tobias Heye⁴

¹Siemens Healthcare GmbH, Erlangen, Germany, ²Medical Imaging Technologies, Siemens Healthcare, Princeton, NJ, United States, ³Radiology, New York University School of Medicine, New York City, NY, United States, ⁴Klinik für Radiologie und Nuklearmedizin, Universitätsspital Basel, Basel, Switzerland

Although the radial sampling scheme of GRASP DCE-MRI leads to inherent motion robustness, strong respiration can still impair the image quality of free-breathing abdominal examinations. We propose to combine GRASP with respiratory gating to minimize motion artifacts within and between temporal frames, without prolonging the reconstruction time and maintaining a high spatio-temporal resolution. A validation in 10 clinical patients confirmed the improved sharpness of the gated reconstruction.

4267 Computer #72 Investigating the temporal stability of phase offsets at 7T for field mapping and multi-channel phase combination.
Barbara Dymerska¹, Siegfried Trattig¹, and Simon Daniel Robinson¹

¹High Field MR Centre, Department of Biomedical Imaging and Image-guided Therapy, Medical University of Vienna, Vienna, Austria

A common assumption for phase combination and dynamic distortion correction is that phase offsets (\$\$\$\Phi_0\$\$\$), i.e. the phase of coil sensitivities, are temporally stable. We investigate the validity of this assumption at 7T for long measurements (40min) and large head rotations (up to 12°) made with multi-channel coils. We show that changes in separate-channel \$\$\$\Phi_{0,ch}\$\$\$ have little effect on the combined phase images (unwarping errors of 0.2 voxel, reduction in phase matching quality by 2%). We thus conclude that the assumption of \$\$\$\Phi_0\$\$\$ temporal stability holds and methods based on this assumption should work at 7T with substantial motion.

Electronic Poster

Mapping & Manipulating Fields

Exhibition Hall

Thursday, May 12, 2016: 11:30 - 12:30

4268 Computer #1 Off-Resonance Map Extrapolation Using Image Inpainting
Ashley G Anderson III¹ and James G Pipe¹

¹Imaging Research, Barrow Neurological Institute, Phoenix, AZ, United States

An inpainting technique using the fast marching method was used to implement a fast, robust algorithm for extrapolating \$\$\$\Delta

-
- 4269
Computer #2
Measuring Magnetic Field Inhomogeneity From Spatial Distortion of Echo Planar Images
Peter Andrew Hardy¹ and Erfan Akbari²
¹Radiology, University of Kentucky, Lexington, KY, United States, ²Radiation Medicine, University of Kentucky, Lexington, KY, United States
- We developed an imaging and analysis method to use the spatial distortion in echo planar images to estimate the magnetic field inhomogeneity. The method requires the acquisition of two images from an unmodified echo planar sequence with the direction of the phase encode reversed between the two. After combining the images appropriately an undistorted and a displacement image are produced. The displacement image is a map of the local magnetic field inhomogeneity.
-
- 4270
Computer #3
Real time shimming over multiple regions across the DTI volume with motion correction using a multislab navigated DTI sequence
A Alhamud¹, Ernesta M. Meintjes¹, and André J.W. van der Kouwe²
¹Human Biology, MRC/UCT Medical Imaging Research Unit, University of Cape Town, Cape Town, South Africa, ²Massachusetts General Hospital, Charlestown, MA, United States
- Most DTI acquisitions are based on 2D multislice EPI sequences. The spatial distribution of the field inhomogeneity may differ from region to region within the DTI volume. While the scanner and traditional prospective shimming methods shim over the whole volume, this may not be optimal for DTI. Further, changes in the shim in different regions across DTI volume in the presence of subject motion are yet to be explored. In this work, we introduce a technique to measure and correct the changes in the static field from region to region and for different sized regions across the DTI volume
-
- 4271
Computer #4
Multiband DREAM: Multi-Slice B₁⁺ Mapping in a Single Shot
Kay Nehrke¹, Arthur Felipe Nisti Grigoletto Borgonovi², and Peter Börnert^{1,3}
¹Philips Research, Hamburg, Germany, ²Philips Healthcare, Best, Netherlands, ³Radiology, LUMC, Leiden, Netherlands
- Simultaneous multi-slice imaging has been employed for the DREAM B₁⁺ mapping approach, allowing a multi-slice B₁⁺ map to be acquired in a fraction of a second. Basic feasibility has been shown in experiments on phantoms and in vivo using a clinical 3T MRI system. The presented approach potentially allows free-breathing multi-slice B₁⁺ mapping, freezing respiratory motion in a short single shot acquisition window.
-
- 4272
Computer #5
Signal-domain optimization metrics for MPRAGE RF pulse design in parallel transmission at 7 Tesla
Vincent Gras¹, Alexandre Vignaud¹, Franck Mauconduit², Michel Luong³, Alexis Amadon¹, Denis Le Bihan¹, and Nicolas Boulant¹
¹Neurospin, CEA/DSV/I2BM, Gif-sur-Yvette, France, ²Siemens Healthcare, Saint-Denis, France, ³IRFU, CEA/DSM, Gif-sur-Yvette, France
- The standard approach to design radiofrequency pulses in MRI is to minimize the deviation of the flip angle from a target value. An alternative approach is proposed here for the MPRAGE sequence which uses the signal as a surrogate of the flip angle in the optimization of the excitation and inversion pulses. The results obtained in simulation and in the brain in vivo on a parallel transmission enabled 7T scanner show two possible applications of the method: an improvement in image quality or a significant reduction of the SAR at equivalent image quality.
-
- 4273
Computer #6
Spiral trajectories for 2D parallel excitation of limited slice profiles
Denis Kokorin¹, Jürgen Hennig¹, and Maxim Zaitsev¹
¹Medical Physics, University Medical Center Freiburg, Freiburg, Germany
- In this study, the feasibility of 2D spiral-encoded parallel excitation of limited slice profiles was investigated. The imaging experiments were performed in phantoms on a 3T MRI system with 8 RF channels for transmission and compared to 2D parallel excitation using EPI encoding. The resulting profiles revealed that 2D spiral-encoded parallel excitation is more robust against B₁ deviations compared to EPI.
-
- 4274
Computer #7
Transmit SENSE on a whole-body 10.5 Tesla system using 16 RF channels: initial results
Xiaoping Wu¹, Gregor Adriany¹, Eddie J. Auerbach¹, Sebastian Schmitter¹, Kamil Ugurbil¹, and Pierre-Francois Van de Moortele¹
¹CMRR, Radiology, University of Minnesota, Minneapolis, MN, United States
- Increased signal to noise ratio and tissue contrast are strong incentive for pushing toward higher magnetic fields. However, as the magnetic field increases, transmit B₁ fields become more and more non-uniform, leading to spatially varying contrast and local signal dropouts. This problem can be addressed with parallel RF transmission (pTx). We have recently made operational the first 10.5 Tesla whole body MRI scanner which holds promise for a wide range of biomedical applications. In this study, we assessed the performance of the installed 16-channel pTx system by designing 2D Transmit SENSE pulses. Our results suggest that high fidelity excitation patterns can be attained after correction of system imperfections.

-
- 4275
Computer #8 Optimization of the k_T-points placement under explicit SAR and power constraints in the large flip angle regime
Vincent Gras¹, Michel Luong², Alexis Amadon¹, and Nicolas Boulant¹
- ¹Neurospin, CEA/DSV/I2BM, Gif-sur-Yvette, France, ²IRFU, CEA/DSM, Gif-sur-Yvette, France*
- The k_T-points parametrization is a powerful technique to mitigate the RF inhomogeneity at ultra-high field which can also be used to achieve homogeneous non-selective inversion profiles with less SAR than adiabatic RF pulses. The large flip angle regime thus is an interesting domain of application of the k_T-points technique. However, to fully exploit it, it is necessary to optimize the placement of the k_T-points in k-space. In this work, the simultaneous optimization of the RF and k-space trajectory coefficients is proposed and validated, whereby SAR and power constraints are handled explicitly.
-
- 4276
Computer #9 Frequency shimming with local excitation coils improves fat suppression in breast MRI at 7 T
Tijl van der Velden¹, Peter R Luijten¹, and Dennis W.J. Klomp¹
- ¹Radiology, UMC Utrecht, Utrecht, Netherlands*
- Using multiple local excitation coils for different parts of the body, such as bilateral breast coils, opens up the possibility to perform frequency shimming: using multiple carrier frequencies to excite the different body parts without gradient based localization. In this work we demonstrate frequency shimming to improve fat suppressed breast MRI at 7 T.
-
- 4277
Computer #10 A parallel transmit VERSE RF pulse design method using dynamic field monitoring
Mustafa Cavusoglu¹, Klaas Paul Pruessmann¹, and Shaihan Malik²
- ¹Institute of Biomedical Engineering, ETH Zurich, Zurich, Switzerland, ²Kings College London, London, United Kingdom*
- Variable-rate selective excitation (VERSE) is a powerful method to control RF power and SAR that bounds to a key condition as retaining the RF-to-gradient amplitude ratio at each sample that preserves the rotational behavior of on-resonance spins (1). The maintenance of VERSE condition strictly depends on the fidelity of the local gradient fields implying that any deviation from the nominal VERSE'd gradients will modulate the spin rotations similar to off-resonances ultimately resulting excitation errors and the RF pulse to converge to a significantly different peak RF power.
-
- 4278
Computer #11 3D volumetric parallel excitation at 9.4T using the trajectory container concept
Tingting Shao¹, Nikolai I. Avdievich¹, and Anke Henning^{1,2}
- ¹Max Planck Institute for Biological Cybernetics, Tübingen, Germany, ²Institute of Biomedical Engineering, University and ETH, Zürich, Switzerland*
- This work presents experimental results of 3D volumetric parallel excitation at a 9.4T human whole-body MRI scanner. The approach and concept of a "trajectory container" is adopted to match practical considerations. The "trajectory container" is used to shape the k space trajectory and restrict it to a limited traversing area in the k space and therefore to constrain the pulse duration. A simplified and direct way of the definition of the "trajectory container" is proposed and verified with promising experimental results.
-
- 4279
Computer #12 Distortions during excitation and acquisition in zoomed DWI combined with parallel transmission
Denis Kokorin¹, Jürgen Hennig¹, and Maxim Zaitsev¹
- ¹Medical Physics, University Medical Center Freiburg, Freiburg, Germany*
- In this work, we discuss off-resonance effects observed in zoomed DWI combined with 2D pulses based on EPI trajectories. Our main focus is placed on the use of parallel excitation (PEX) for shortening 2D pulses and further minimizing the distortion. Experimental data were obtained using a 3T MRI system with an 8-channel TxArray extension and analyzed in detail. We conclude that the use of PEX improves the matching between excitation and acquisition in zoomed EPI applications.
-
- 4280
Computer #13 Optimisation of Post-processing Correction of Transmit Field Inhomogeneity in R₁ Maps by Relaxometry Modelling
Martina F Callaghan¹, Frederic Dick², Patrick Grabher³, Tim Keller⁴, Patrick Freund^{1,3,5}, and Nikolaus Weiskopf^{1,5}
- ¹Wellcome Trust Centre for Neuroimaging, UCL Institute of Neurology, London, United Kingdom, ²Birkbeck/UCL Centre for Neuroimaging, London, United Kingdom, ³Spinal Cord Injury Center Balgrist, University Hospital Zurich, Zurich, Switzerland, ⁴Department of Psychology, Carnegie Mellon University, Pittsburgh, PA, United States, ⁵Department of Neurophysics, Max Planck Institute for Human Cognitive and Brain Sciences, Leipzig, Germany*
- Unified segmentation based correction of R₁ brain maps for RF transmit field inhomogeneities (UNICORT) has previously been shown to reduce bias in R₁ maps caused by inhomogeneity in the RF transmit field (B₁⁺). This approach simultaneously estimates the B₁⁺ inhomogeneities and R₁ values from the uncorrected R₁ maps without the need for additional B₁⁺ calibration data. It employs a probabilistic framework that incorporates a physically informed generative model of smooth transmit field inhomogeneities and their multiplicative effect on R₁ estimates. However, different systems may require different priors, depending on the particular transmit coil

used. Here we show that these parameters can be estimated using a linear relaxometry model framework, without the need to acquire B_1^+ mapping data.

- 4281
Computer #14 Single point based techniques for rapid and robust gradient measurement
Hyungseok Jang^{1,2} and Alan B McMillan¹
- ¹Department of Radiology, University of Wisconsin, Madison, WI, United States, ²Department of Electrical and Computer Engineering, University of Wisconsin, Madison, WI, United States
- Accurate knowledge of the k-space trajectory is critical for artifact-free MR imaging, particularly in non-Cartesian imaging. In this study we propose a new gradient measurement technique based on single point imaging (SPI), which allows simple, rapid, and robust measurement of k-space trajectory. In the proposed technique, the zoom-in/out effect of SPI is used for k-space trajectory measurement. First, 1D SPI data are acquired from a targeted gradient in each axis, and then relative FOV scaling factors between encoding times are found, which represents relative k-space position. Improvements in image quality are demonstrated for UTE, spiral, and ramp-sampled IDEAL imaging.
-
- 4282
Computer #15 Multi-slice spiral imaging trajectory mapping using high density 25-channel field probe array
Ying-Hua Chu¹, Yi-Cheng Hsu¹, and Fa-Hsuan Lin¹
- ¹Institute of Biomedical Engineering, National Taiwan University, Taipei, Taiwan
- We use a dense 2D field probe array with 24 probes moving over a 3D volume to estimate magnetic field distribution dynamically and demonstrate that trajectory calibration is slice-dependent. The image reconstructed using measured dynamic magnetic field information 7 cm away shows similar l_2 norm error as the image reconstructed without any dynamic magnetic field information.
-
- 4283
Computer #16 Linear Gradient Characterization Using A Rapid Thin-slice Measurement
Ryan K Robison¹ and James G Pipe¹
- ¹Imaging Research, Barrow Neurological Institute, Phoenix, AZ, United States
- Gradient impulse response functions can predict gradient behavior in the presence of eddy currents and other sources of error. This work presents a rapid method for generating the 0th and 1st order gradient impulse response functions using existing software measurement techniques. The proposed method is applied to spiral imaging but could be similarly applied to EPI, projection reconstruction, or any other imaging sequence.
-
- 4284
Computer #17 Chemical Shift based Fat-Water Separation using a Variational Approach for B_0 -field Correction
Andreas Lesch¹, Kristian Bredies², Clemens Diwoky³, and Rudolf Stollberger^{1,4}
- ¹Institute of Medical Engineering, Graz University of Technology, Graz, Austria, ²Institute of Mathematics and Scientific Computing, University of Graz, Graz, Austria, ³Institute of Molecular Biosciences, University of Graz, Graz, Austria, ⁴BioTechMed Graz, Graz, Austria
- In this work we present an approach for chemical shift based fat/water-separation using variational methods for the estimation of the underlying B_0 -field inhomogeneity. We show that the fat/water-problem can be solved by the application of total-generalized-variation (TGV) regularization on the underlying B_0 -field to enforce piecewise smoothness. With this approach we are able to model huge B_0 -deviations as well as discontinuities in the B_0 -field at tissue boundaries with different susceptibility parallel to the main-field. This is shown on different datasets, including two of the ISMRM fat/water-challenge of 2012.
-
- 4285
Computer #18 Reduction of Ghosting Due to Respiration Induced B_0 Variation in Double Echo Steady State (DESS) Imaging in the Breast with a DC Navigator and Image Entropy Metric
Catherine J Moran¹, Bragi Sveinsson^{1,2}, Brady Quist², Marcus T Alley¹, Bruce Daniel¹, and Brian A Hargreaves¹
- ¹Radiology, Stanford University, Stanford, CA, United States, ²Electrical Engineering, Stanford University, Stanford, CA, United States
- The double echo steady state (DESS) acquisition has the potential to provide high-resolution and distortion-free T2 and diffusion-weighted images in the breast. Initial investigations of DESS in the breast have been limited by the presence of ghosting artifacts. Respiratory-induced B_0 variation is one source of these artifacts. A method utilizing an in-vivo time-varying off-resonance estimate along with an image entropy metric to assess the level of artifact is described and investigated for correction of ghosting due to respiration-induced B_0 variation in DESS in the breast.
-
- 4286
Computer #19 Gradient Pre-Emphasis Correction for First-order Concomitant Field on Head-only Asymmetric Gradient MRI System
Shengzhen Tao¹, Paul T Weavers¹, Joshua D Trzasko¹, Yunhong Shu¹, Seung-Kyun Lee², Lou Frigo³, Scott Hinks³, and Matt A Bernstein¹
- ¹Radiology, Mayo Clinic, Rochester, MN, United States, ²GE Global Research, Niskayuna, NY, United States, ³GE Healthcare, Milwaukee, WI, United States
- Based on Maxwell's equation, the spatial encoding gradient fields must be accompanied by spatially-varying higher-order concomitant

fields. Different from conventional gradient systems whose concomitant fields contain second-order and higher spatial dependence, some MRI platforms employ asymmetric gradient systems, and their concomitant fields also include zero- and first-order terms. The first-order terms cause artifacts including image blurring and ghosting in spiral acquisition and echo shifting in EPI. Here, an efficient gradient pre-emphasis scheme suitable for real-time implementation is demonstrated to simultaneously correct all the first-order concomitant fields with a real-time implementation on gradient firmware typically used for eddy current compensation.

4287

Computer #20 Gradient Unwarping: Reverse Engineering the Warpfield with Spherical Harmonics
Paul Polak^{1,2}, David Lindner¹, Jannis Hanspach¹, Michael Dwyer¹, Niels Bergsland¹, Nicola Bertolino^{1,2}, Robert Zivadinov^{1,2}, and Ferdinand Schweser^{1,2}

¹Neurology, Buffalo Neuroimaging Analysis Center, State University of New York at Buffalo, Buffalo, NY, United States, ²Molecular and Translational Imaging, Clinical Translational Research Center, Buffalo, NY, United States

Gradient “unwarping” is the removal of image distortions caused by non-linearity of the imaging gradient fields. Exasperated by increasing distance from isocenter, the unwarping process is applied to every image by the manufacturer and generally is a “black-box” process occurring near the end of the image processing pipeline. This is problematic for researchers who source their data from a more primitive step, e.g. from raw k-space, since this data is generally “warped”. Presented here is a method to reverse engineer the spherical harmonic coefficients that describe the warp field and are used by the vendor’s black-box process, allowing the researcher to perform the gradient unwarping off-line as a post-processing step.

4288

Computer #21 Rapid whole body B₁ mapping using continuously moving table imaging at 3 Tesla
Saikat Sengupta¹, David S Smith¹, and Edward Brian Welch¹

¹Department of Radiology, Vanderbilt University, Nashville, TN, United States

In this abstract, we present an approach for rapid mapping of the whole body B₁ field at 3 Tesla. We use a combination of dual interleaved TR B₁ mapping with continuously moving table imaging to measure the B₁ field in the whole body in 90 seconds. Considerable variation is observed in the B₁ distribution in different sections of the body. This measurement will serve as the basis for dynamic B₁ field shimming with the moving table for whole body imaging in future work.

4289

Computer #22 Automatic Gradient Predistortion Applied to Clinical 2D-UTE
Kevin D Harkins¹, Mary Katherine Manhard^{1,2,3}, William A Grissom^{1,2,3}, and Mark D Does^{1,2,3,4}

¹Institute of Image Science, Vanderbilt University, Nashville, TN, United States, ²Biomedical Engineering, Vanderbilt University, Nashville, TN, United States, ³Electrical Engineering, Vanderbilt University, Nashville, TN, United States, ⁴Radiology and Radiological Sciences, Vanderbilt University, Nashville, TN, United States

Transient gradient waveform errors can degrade MRI quality. This work presents an automatic implementation of gradient waveform predistortion, which has been applied to half-pulse excited 2D-ultrashort echo time imaging. The predistortion method reliably improves image quality and quantification of ultrashort T₂ species by reducing out-of-slice signal that contaminates half-pulse excited images.

4290

Computer #23 Assessment of geometric distortion in six clinical scanners using a 3D-Printed Grid Phantom
Maysam M Jafar¹, Christopher E Dean¹, Malcolm J Birch¹, and Marc E Miquel¹

¹Clinical Physics, Barts Health NHS Trust, City of London, United Kingdom

Major hardware-related geometric distortions in MRI arise from gradient field non-linearity and static field inhomogeneity. For an accurate mapping of geometrical distortion in 3D, the number of control points must be sufficiently large to provide a comprehensive mapping of the spatial variation of distortion and the positional accuracy of these control points must be ensured. In this study, the spatial accuracy of coordinates in 3D space is assessed across six clinical MRI scanners at both 1.5T and 3T field strengths using a previously reported 3D-printed grid phantom. This is a cost-effective approach to determine the spatial accuracy of control points.

4291

Computer #24 Characterising and Modelling Susceptibility Artifacts in the Mouse Brain at 9.4 T
Rosie Goodburn¹, Nicholas Powell^{2,3}, James O’Callaghan², Simon Walker-Samuel², and Karin Shmueli¹

¹Department of Medical Physics and Biomedical Engineering, University College London, London, United Kingdom, ²UCL Centre for Advanced Biomedical Imaging, Division of Medicine, London, United Kingdom, ³UCL Centre for Medical Imaging Computing, London, United Kingdom

Susceptibility artifacts hamper gradient-echo MRI of the mouse brain at 9.4 Tesla. Here, we characterised and modelled magnetic field maps aiming to improve preclinical mouse MRI. To characterise field perturbations, we measured and coregistered field maps in 7 mice to create a group-average field map. Next, a Fourier forward model was used to simulate a field map based on a susceptibility distribution constructed from the group-average magnitude image. The measured and modelled field maps showed similar qualitative field patterns, especially around the aural air cavities, but had quantitative differences. Work is ongoing to improve the accuracy of the model.

Contrast Mechanisms & Artefacts: System Imperfections & Implants

Exhibition Hall

Thursday, May 12, 2016: 11:30 - 12:30

- 4292
Computer #25 Zero Echo Time imaging of ocular tumours at 7T
Jan-Willem Beenakker¹, Joep Wezel¹, Gregorius Luyten¹, Andrew Webb¹, and Peter Boerner^{1,2}
- ¹Leiden University Medical Centre, Leiden, Netherlands, ²Philips Research Laboratories, Hamburg, Germany*

MRI is becoming an increasingly valuable non-invasive tool in ocular tumour assessment and treatment planning. ophthalmology. High resolution images acquired at high field provide multi-dimensional information on tumour size. However, image quality is often compromised by eye motion which is often triggered by gradient noise In the present work the use of magnetization prepared 3D Zero Echo Time imaging (ZTE) is proposed, enabling for almost silent volumetric scanning at isotropic resolution. An initial validation showing the potential of the ZTE approach at 7T for is shown in volunteers and tumour patients.

- 4293
Computer #26 In-vivo detection of oscillatory magnetic field with an oscillatory-selective detection (OSD)
Yuhui Chai¹, Jingwei Sheng¹, Bing Wu², Yang Fan², and Jia-Hong Gao¹
- ¹Center for MRI Research, Peking University, Beijing, China, People's Republic of, ²GE Healthcare, MR Research China, Beijing, China, People's Republic of*

In-vivo detection of oscillatory magnetic field may lead to fundamental development of functional MR imaging. The recently developed spin-lock oscillatory excitation (SLOE) method exhibited sub-nanotesla level of sensitivity. However its application in vivo is troubled by main field inhomogeneity. In this work, an oscillatory-selective detection (OSD) is proposed to overcome this limitation and hence to improve sensitivity of in-vivo detection of oscillatory magnetic field. OSD has also been verified as a viable tool in mapping transcranial alternating current.

- 4294
Computer #27 Simultaneous Spin Echo and Gradient Echo Imaging with Controlled Aliasing and Parallel Imaging Reconstruction
Mengye Lyu^{1,2}, Victor B. Xie^{1,2}, Patrick G. Peng^{1,2}, Edward Hui³, and Ed X. Wu¹
- ¹Laboratory of Biomedical Imaging and Signal Processing, The University of Hong Kong, Hong Kong SAR, China, People's Republic of, ²Department of Electrical and Electronic Engineering, The University of Hong Kong, Hong Kong SAR, China, People's Republic of, ³Department of Diagnostic Radiology, The University of Hong Kong, Hong Kong SAR, China, People's Republic of*

We propose a method to simultaneously acquire spin echo and gradient echo and form two images with distinct contrasts. The spin echo and gradient echo are created by phase-cycled RF pulses, so that they are shifted from each other in image space. In reconstruction, coil sensitivity information can be used to separate them. This study demonstrates the feasibility of extracting multiple echo components using controlled aliasing and parallel imaging reconstruction.

- 4295
Computer #28 Single-shot T2 mapping through overlapping-echo detachment planar imaging (OLED) sequence
Congbo Cai¹, Yuchuan Zhuang², Shuhui Cai³, Jianhui Zhong², and Zhong Chen³
- ¹Department of Communication Engineering, Xiamen University, Xiamen, China, People's Republic of, ²Department of Imaging Sciences, University of Rochester, ROCHESTER, NY, United States, ³Department of Electronics Science, Xiamen University, Xiamen, China, People's Republic of*

Magnetic Resonance parameters mapping can provide useful quantitative information for characterization of tissue properties. However, the long acquisition time usually hinder the real-time MR parameter mapping. In this abstract, a novel single-shot T2 mapping method was proposed based on spin-echo EPI method. Two overlapping echo signals with the different T2 weighting were obtained simultaneously. A detachment algorithm based on joint sparsity constraint was proposed to separate the two echo signals. The robustness and efficiency of the sequence were demonstrated through phantom experiments. The reliable T2 mapping can be obtained in the order of milliseconds.

- 4296
Computer #29 Simultaneous Quantification of T1, T2 and Diffusion with Diffusion-weighted drive-equilibrium prepared Magnetic Resonance Fingerprinting
Yun Jiang¹, Jesse I. Hamilton¹, Katherine L. Wright², Dan Ma², Nicole Seiberlich¹, Vikas Gulani^{1,2}, and Mark A. Griswold^{1,2}
- ¹Department of Biomedical Engineering, Case Western Reserve University, Cleveand, OH, United States, ²Department of Radiology, Case Western Reserve University, Cleveand, OH, United States*

The purpose of this study is to develop a method for simultaneous quantification of T₁, T₂, and diffusion within the MR Fingerprinting (MRF) framework. Multiple diffusion-weighted driven-equilibrium modules are inserted into the MRF-FISP acquisition in this study. The results from the prostate show the promising ability of this combination of MRF-FISP and diffusion preparation modules to quantify relaxation parameters along with diffusion in one scan.

- 4297
Computer #30 Multi-shot Magnetic Resonance Fingerprinting using Saturation Recovery Preparation Pulse
Xiao Chen¹, Christopher C. Cline^{1,2}, Boris Mailhe¹, Qiu Wang¹, and Mariappan S. Nadar¹
- ¹Medical Imaging Technologies, Siemens Healthcare, Princeton, NJ, United States, ²Biomedical Engineering, University of Minnesota, Minneapolis, MN, United States
- In MRF, a single image is reconstructed from data collected from each short TR due to the non-repeatable magnetization history. The highly-undersampled single-shot imaging leads to high levels of noise and artifacts. In this study, an SR preparation module was introduced to MRF, enabling multi-shot MRF without a waiting time for magnetization recovery. The SR prepared multi-shot MRF can achieve similar or even better accuracy than the original single-shot IR prepared MRF with the same amount of data collected.
-
- 4298
Computer #31 Optimizing MRI contrast with optimal control theory
Eric Van Reeth¹, H el ene Ratiney¹, Michael Tesch², Steffen Glaser², and Dominique Sugny³
- ¹CREATIS, Universit e de Lyon ; CNRS UMR5220 ; Inserm U1044 ; INSA-Lyon ; Universit e Claude Bernard Lyon 1, Lyon, France, ²Department of Chemistry, Technische Universit at M unchen, Munich, Germany, ³Laboratoire Interdisciplinaire Carnot de Bourgogne (ICB), UMR 5209 CNRS-Universit e de Bourgogne, Dijon, France
- Magnetic Resonance Imaging (MRI) uses the difference in tissue relaxation times to create contrast. Various image weightings can be obtained by tuning acquisition parameters which are usually empirically defined. In this article, optimal control theory is used to design excitation pulses that produce the optimal contrast between given tissues. The designed pulses are tested on numerical phantoms with and without magnetic field inhomogeneities and for the first time in vitro on a small-animal MRI. The reasonable match between simulation and real experiments is promising for the development of such pulses in further in vivo applications.
-
- 4299
Computer #32 Correction of Phase Offset Induced From Eddy Current in MR Phase Contrast Cine Flow Measurement of Cerebrospinal Fluid in the Cervical Spine
Kwan-Jin Jung¹, Andrea Willhite², and Susan Harkema²
- ¹Radiology, University of Louisville, Louisville, KY, United States, ²Neurosurgery, University of Louisville, Louisville, KY, United States
- The phase offset in the phase contrast MR flow imaging was corrected using an image-based method in order to account for the spatially inhomogeneous and subject-dependent phase offset. The phase shift on the flow region was estimated iteratively from the phase shift of the stationary tissue using the low spatial distribution of the phase offset. This phase offset correction method with an automated segmentation and iterative estimation of the phase offset allowed us to study the cerebrospinal fluid flow in the spinal subarachnoid space of ten healthy and ten spinal cord injury participants reliably without elaborate manual effort.
-
- 4300
Computer #33 MR artifacts removal using sparse + low rank decomposition of annihilating filter based Hankel matrix
Kyong Hwan Jin¹, Dongwook Lee¹, Paul Kyu Han¹, Juyoung Lee¹, Sung-Hong Park¹, and Jong Chul Ye¹
- ¹Dept. of Bio and Brain Engineering, KAIST, Daejeon, Korea, Republic of
- In this paper, we propose a sparse and low-rank decomposition of annihilating filter-based Hankel matrix for removing MR artifacts such as motion, RF noises, or herringbone artifacts. Based on the observation that some MR artifacts are originated from k-space outliers, we employ a recently proposed image modeling method using annihilating filter-based low-rank Hankel matrix approach (ALPHA) to decompose the sparse outliers from the low-rank component. The proposed approach can be applied even for static images, because the k-space low rank component comes from the intrinsic image properties. We demonstrate that the proposed algorithm clearly removes several types of artifacts such as impulse noises, motion artifacts, and herringbone artifacts.
-
- 4301
Computer #34 Gradient Nonlinearity and B0-induced Distortion Corrections of Prospective Motion Correction Data at 7T MRI
Uten Yarach¹, Daniel Stucht¹, Hendrik Mattern¹, Frank Godenschweger¹, and Oliver Speck¹
- ¹Department of Biomedical Magnetic Resonance, Otto-von-Guericke University Magdeburg, Magdeburg, Germany
- Patient motion during an MRI of the brain can result in non-diagnostic image quality. Even with perfect prospective motion (PMC) tracking and correction, the varying coil sensitivity, gradient non-linearity, and B0 field shift can cause significant artifacts that cannot be corrected prospectively. Recently, a model-based MR image reconstruction via iterative solver was employed to minimize the sensitivity misalignment due to physiological movement. In this study, we extended the mentioned model by gradient-warped and B0-induced distortion corrections to reconstruct the PMC MR data. The result shows the improvement that is remarkably reduced artifacts after a few iterations of the proposed technique.
-
- 4302
Computer #35 Referenceless high order EPI calibration based on multiplexed SENSE
Jiazheng Wang¹, Bing Wu², and Yongchuan Lai³
- ¹Radiology Department, University of Cambridge, Cambridge, United Kingdom, ²GE healthcare MR Research China, Beijing, China, People's Republic of, ³GE healthcare China, Beijing, China, People's Republic of
- Usually aper-volume or even per-slice basis reference scan is usually needed for correcting the phase inconsistency between odd and even shots attributed to eddy current in EPI. The phase correction is usually first order. In this work, the concept of multiplexed SENSE

(MUSE) is extended for EPI N/2 ghost calibration.

- 4303
Computer #36
Improving functional imaging of the fetal brain using constrained image-based shimming to suppress maternal fat
Andreia S Gaspar^{1,2}, Giulio Ferrazzi¹, Rita G Nunes^{1,2}, Emer J Hughes^{3,4}, Shaihan J Malik¹, Laura McCabe^{3,4}, Kelly Pegoretti^{3,4}, Mary A Rutherford^{3,4}, Joseph V Hajnal^{1,4}, and Anthony N Price^{1,4}
- ¹Biomedical Engineering, King's College London, London, United Kingdom, ²Instituto de Biofísica e Engenharia Biomédica, Faculdade de Ciências, Universidade de Lisboa, Lisbon, Portugal, ³Perinatal Imaging and Health, King's College London, London, United Kingdom, ⁴Centre for the Developing Brain, King's College London, London, United Kingdom*
- Effective suppression of maternal fat is critical for functional imaging of the fetal brain with echo planar imaging (EPI). Localized image-based shimming (IBS) for the fetal brain is required but can provoke high field variation in maternal adipose regions causing fat suppression to fail. We have addressed this issue by using IBS of the fetal brain with linear constraints across maternal fat regions and optimization of saturation pulse frequency offset. The results showed that is possible to obtain more complete fat suppression when combining an optimized pulse offset with a constrained shimming approach without compromising fetal brain shim.
-
- 4304
Computer #37
Sparse Parameter Global Signal Correction for Resting State fMRI Analysis
Xueqing Liu¹, Zhihao Li², Shiyang Chen², and Xiaoping Hu²
- ¹Department of Biomedical Engineering, Columbia University, New York, NY, United States, ²Coulter Department of Biomedical Engineering, Georgia Tech and Emory University, Atlanta, Georgia*
- We describe a novel global signal removal method, sparse parameter global signal regression (SP-GSR), for fMRI data preprocessing. We assume the global signal to be low-rank and the remaining signal can be decomposed into orthogonal regressors with spatially sparse parameters. We demonstrated by simulation that SP-GSR can remove global signal and recovery true correlations without introducing anti-correlations. Application of this method to experimental data led to a more prominent and focused default mode network with isolated negative correlations.
-
- 4305
Computer #38
Data Acquisition Strategies for Reducing Eddy-Current and Transient Oscillation Artifacts in Balanced Steady-State Free Precession
Hyun-Soo Lee¹, Seung Hong Choi², and Sung-Hong Park¹
- ¹Department of Bio and Brain Engineering, Korea Advanced Institute of Science and Technology, Daejeon, Korea, Republic of, ²Department of Radiology, Seoul National University College of Medicine, Seoul, Korea, Republic of*
- The quality of balanced steady-state free precession is vulnerable to eddy-currents and transient oscillations. However, the conventional centric phase-encoding (PE) scheme makes these artifacts severe, thus needs additional compensation strategies. In this study, we propose an improved PE scheme where k-space is encoded from center to periphery in a group-wise manner (PE-grouping). This reduces related artifacts by preventing big jumps in k-space along PE direction. Also proposed were various averaging strategies that could further eliminate the residual artifacts by averaging two full images acquired not only with the PE-grouping, but also with the conventional centric and pairing schemes.
-
- 4306
Computer #39
An effective way of overcoming TE variation in single-refocusing spatiotemporal-encoding imaging.
JaeKyun Ryu^{1,2}, Joonsung Lee^{1,2}, Seong-gi Kim^{1,2}, and Jang-Yeon Park^{1,2}
- ¹Center for Neuroscience Imaging Research, Institute for Basic Science, Suwon, Korea, Republic of, ²Department of Biomedical Engineering, Sungkyunkwan University, Suwon, Korea, Republic of*
- RASER(Rapid Acquisition by Sequential Excitation and Refocusing) sequence acquires all the echoes with same TE by using two refocusing pulses [1], whereas other spatiotemporal-encoding(SPEN) techniques using a single-refocusing pulse offers a shorter effective TE than RASER but with varying TE, thereby causing signal variation in the SPEN dimension [2]. Here, we propose an effective way of overcoming this problem of TE variation in single-refocusing SPEN imaging.
-
- 4307
Computer #40
Improved gradient warping correction for large field-of-view imaging and application to radiation therapy planning
Paul T. Weavers¹, Shengzhen Tao¹, Kieran McGee¹, Joshua Trzasko¹, Yunhong Shu¹, Erik Tryggstad², Ken-Pin Hwang³, Seung-Kyun Lee⁴, Thomas KF Foo⁴, and Matt Bernstein¹
- ¹Mayo Clinic, Rochester, MN, United States, ²Radiation Oncology, Mayo Clinic, Rochester, MN, United States, ³MD Anderson, Houston, TX, United States, ⁴GE Global Research, Niskayuna, NY, United States*
- Radiation therapy, especially proton beam therapy requires exacting spatial accuracy to deliver a sterilizing dose of ionizing radiation to the target volume with confidence. The superior soft tissue contrast afforded by MRI vs. CT has increased interest in using MRI for treatment planning. However, gradient non-linearities reduce the spatial accuracy of MRI. We have developed a fiducial phantom based calibration procedure to map these gradient nonlinearities on a system-specific basis and generate up to 9th order spherical harmonic coefficients for correction. These coefficients show improved spatial accuracy vs. standard 5th order, especially at distances >400mm from magnet and gradient isocenter.
-
- 4308
Calibration-free EPI trajectory error correction by k-space data consistency

Computer #41 Julianna D. Ianni^{1,2} and William A. Grissom^{1,2,3,4}

¹Department of Biomedical Engineering, Vanderbilt University, Nashville, TN, United States, ²Vanderbilt University Institute of Imaging Science, Vanderbilt University, Nashville, TN, United States, ³Department of Radiology and Radiological Sciences, Vanderbilt University, Nashville, TN, United States, ⁴Department of Electrical Engineering, Vanderbilt University, Nashville, TN, United States

A method for automatic correction of EPI trajectory errors is presented. The method is an iterative parallel imaging reconstruction which uses k-space data consistency to correct image artifacts. An advantage of the method is that it requires no calibration data and allows correction of non-static errors such as those due to gradient coil heating.

4309
Computer #42 Measurement of magnetic susceptibility of commonly implanted metals from commercial prostheses
Matthew Robert Smith¹, Jin Jung Kweon², Eun Sang Choi², Curtis Wiens¹, Nathan Artz³, and Scott B Reeder^{1,4}

¹Radiology, University of Wisconsin, Madison, WI, United States, ²Florida State University, Tallahassee, FL, United States, ³St. Jude's Children's Hospital, Memphis, TN, United States, ⁴Medical Physics, University of Wisconsin, Madison, WI, United States

Despite important recent development, further progress of MR imaging around metallic prostheses is dependent on the ability to model the field perturbations surrounding the prostheses. These calculations require knowledge of the magnetic susceptibility of the metal which is not reported by the manufacturers. The purpose of this work was to estimate the magnetic susceptibility of commonly implanted metal alloys by measuring the magnetic moment across a range of clinical field strengths (0-5 Tesla) using a SQUID (Superconducting QUantum Interference Device) magnetometer. Linearity of the susceptibility across field strengths was also assessed.

4310
Computer #43 Phase drift effect correction for MR Thermometry using magnetic field monitoring
Daniel Daniel Hernandez¹, Eric Michel¹, Ki Soo Kim¹, and Soo Yeol Lee¹

¹Bio-medical engineering, Kyung Hee University, Yogin, Korea, Republic of

We propose a method to correct phase drift artifact from MR thermometry measurements with the use of Magnetic field monitoring (MFM). Field variations are measured with an array of MFM probes and correction maps are computed from the frequency shifts of FID signals. This method allows to have better resolution and can be used with any MR thermometry pulse sequence.

4311
Computer #44 Reference-free Nyquist ghost removal in single-shot SPEN MRI using phase-corrected partial Fourier reconstruction
Ying Chen¹, Song Chen¹, Hui Liu², Zhong Chen³, and Jianhui Zhong^{1,4}

¹Center for Brain Imaging Science and Technology, Zhejiang University, Hangzhou, China, People's Republic of, ²MR Collaboration Northeast Asia, Siemens Healthcare, Shanghai, China, People's Republic of, ³Department of Electronic Science, Xiamen University, Xiamen, China, People's Republic of, ⁴Collaborative Innovation Center for Diagnosis and Treatment of Infectious Diseases, Zhejiang University, Hangzhou, China, People's Republic of

Single-shot SPEN MRI is a technique capable of retaining the time efficiency of single-shot EPI but with significantly reduced geometric distortions. Akin to EPI, the phase inconsistency between even and odd echoes also result in Nyquist ghosts in SPEN images. This work is to present a scheme with more reliable performance than the previously reported Nyquist ghost correction method. Experimental results of human brains and in vivo rats show that the proposed method can remove ghosts without introducing blurring, and unwarping procedures can be conducted on the ghost-corrected data for further distortion correction.

4312
Computer #45 Comparison of methods for choosing radial spoke directions in 3D UTE
Mark BYDDER¹, Wafaa Zaaraoui¹, and Jean-Philippe Ranjeva¹

¹Aix Marseille Université, MARSEILLE, France

Several algorithms for choosing the radial spoke directions were evaluated for use in 3D UTE imaging. It was observed that methods that produce a highly regular set of directions result in higher aliasing than those that are more irregular.

4313
Computer #46 Flow-induced artifacts in two-point Dixon MRI: Incidence, severity and potential diagnostic pitfalls.
Tilman Schubert¹, Peter Bannas², Samir Sharma³, Sonja Kinner¹, Mahdi Rahimi³, Frank Korosec³, and Scott Reeder¹

¹Radiology, University of Wisconsin Madison, Madison, WI, United States, ²Radiology, University Medical Center Hamburg-Eppendorf, Hamburg, Germany, ³Medical Physics, University of Wisconsin Madison, Madison, WI, United States

Chemical shift based two-point "Dixon" MRI with bipolar readout gradients may produce flow induced fat-water misallocation artifacts. These artifacts have the potential to mimic intravascular thrombus. We reviewed 100 cases of two-point body MRI exams to characterize the incidence, location and severity of these artifacts. Artifacts appeared in 46% of the cases, with severe artifacts in 20% and mild artifacts in 26% of the patients. Given this high number of potentially thrombus-mimicking, flow-induced artifacts, radiologists should be aware of this potential pitfall when using two-point fat-water separation methods.

4314
Computer #47 Two-Step Generic Referenceless Phase Combination (GRPC) for accurate phase image reconstruction from multiple receiver coils
Francesco Santini^{1,2}, Mathieu D Santin³, Paulo Loureiro de Sousa⁴, and Oliver Bieri^{1,2}

¹Radiological Physics, University of Basel Hospital, Basel, Switzerland, ²Department of Biomedical Engineering, University of Basel, Basel, Switzerland, ³Institut du Cerveau et de la Moelle épinière, Hôpital Pitié-Salpêtrière, Paris, France, ⁴CNRS, ICube Laboratory, FMTS, Université de Strasbourg, Strasbourg, France

This work presents a method to combine the signal from multiple coils in order to obtain a coherent phase image. The methods is agnostic to the acquisition protocol and the coil geometry, and does not require operator interaction.

4315
Computer #48 Image-based phase correction for dual-band EPI with slice-GRAPPA using point-by-point procedures in k-space
Hiroshi Toyoda¹, Sosuke Yoshinaga², Naoya Yuzuriha², and Hiroaki Terasawa²

¹CiNet, NICT, Suita, Japan, ²Department of Structural Bioluminescence Imaging, Kumamoto University, Kumamoto, Japan

We proposed an Image-based phase correction for dual-band EPI with slice-GRAPPA using point-by-point procedures in k-space. The results showed the usefulness and robustness of the proposed method compared with the conventional approach.

Electronic Poster

Image Processing & Analysis

Exhibition Hall

Thursday, May 12, 2016: 11:30 - 12:30

4316
Computer #49 A combinatorial model approach for feature selection from multimodal MRI data
Xiaowei Zhuang¹, Virendra Mishra¹, Karthik Sreenivasan¹, Charles Bernick¹, Sarah Banks¹, and Dietmar Cordes^{1,2}

¹Cleveland Clinic Lou Ruvo Center for Brain Health, Las Vegas, NV, United States, ²Department of Psychology and Neuroscience, University of Colorado Boulder, Boulder, CO, United States

Clinical applications of brain abnormality detection with supervised machine learning techniques are limited due to less and unbalanced sample sizes as compared to rich feature sets in patient population. We proposed a new combinatorial model approach, fs-RBFN, involving sampling from multivariate joint distribution, LASSO feature selection, RBFN cross validation, and inverse probability weighting to solve this problem. The proposed approach was validated against a ground truth phantom and further tested on a multimodal MRI dataset for cognitively impaired and non-impaired professional fighters. Our results suggest superior performance of this technique over several other out-of-the-bag feature selection algorithms.

4317
Computer #50 Three-dimensional lung tumour motion tracking using an advanced template matching technique: Texture Reformatted Angle Correlation (TRAC)
Kevin K. Zhang^{1,2}, Shivani Kumar^{2,3}, Robba Rai³, Armia George³, Bin Dong^{1,4}, and Gary P. Liney^{1,2,3,4}

¹Ingham Institute for Applied Medical Research, Sydney, Australia, ²South Western Sydney Clinical School, University of New South Wales, Sydney, Australia, ³Department of Medical Physics, Cancer Therapy Centre, Liverpool Hospital, Sydney, Australia, ⁴Centre for Medical Radiation Physics (CMRP), University of Wollongong, Sydney, Australia

Real-time lung tumour tracking and motion analysis is important in MRI-based radiotherapy planning to inform treatment margins and to permit accurate delivery for developing MR-Linac technology. This work describes a template matching approach to provide 3D motion assessment of lung tumours from real-time 2D images. Compared to previous work the TRAC technique utilises a multi-angled correlation analysis of the target region to correctly identify the tumour position. Results in both a moving phantom and in lung cancer patients show that the technique is feasible, accurate and can be easily adopted in widely used single plane cine imaging.

4318
Computer #51 Renal segmentation from non-contrast T1-weighted MR images
Nicole Wake¹, Jeremy C Lim², Artem Mikheev¹, Jas-mine Seah³, Elissa Botterill², Shawna Farquharson⁴, Henry Rusinek¹, and Ruth P Lim^{2,5}

¹Bernard and Irene Schwartz Center for Biomedical Imaging, Center for Advanced Imaging Innovation and Research, Department of Radiology, New York University School of Medicine, New York, NY, United States, ²Department of Radiology, Austin Health, Melbourne, Australia, ³Department of Endocrinology, Austin Health, Melbourne, Australia, ⁴Florey Neuroscience Institute, Melbourne, Australia, ⁵The University of Melbourne, Melbourne, Australia

A semi-automatic renal segmentation technique for non-contrast T1-weighted MR images was developed. Renal segmentation and volumetric analysis was tested in ten healthy volunteers and ten Type I diabetic patients. We found that this segmentation tool is fast, reliable, and requires minimal user interaction. Upon further validation, this method has clinical potential for monitoring renal status in appropriate patient populations.

4319
Computer #52 Exploring abnormal arch shape patterns using CMR-based hierarchical 3D shape clustering: Application to a generic imaging population of repaired coarctation of the aorta
Jan L Bruse¹, Abbas Khushnood¹, Tain-Yen Hsia¹, Andrew M Taylor¹, Vivek Muthurangu¹, and Silvia Schievano¹

¹Centre for Cardiovascular Imaging, UCL Institute of Cardiovascular Science & Great Ormond Street Hospital for Children, London, United Kingdom

Kingdom

We present a novel method for hierarchical 3D shape clustering of aortic arch shape models segmented and reconstructed from CMR imaging data. We apply the method to a cohort of 45 patients post aortic coarctation repair in order to explore previously unknown arch shape patterns that may relate to clinical outcome. Exploring a pathologic shape population using data mining and statistical shape modeling techniques can provide novel insight for improved diagnosis and treatment strategies and can thereby assist in clinical decision making when analysing complex cases.

4320
Computer #53 Direct CT conversion from a single ultra-short echo sequence
Soumya Ghose¹, Jason Dowling¹, Robba Rai², Benjamin Schmitt³, and Gary Liney^{2,4,5,6}

¹eHealth, CSIRO, Brisbane, Australia, ²Liverpool Cancer Therapy Centre, Liverpool, Australia, ³Siemens Healthcare Pty Ltd, Macquarie Park, Australia, ⁴Medical Physics, Ingham Institute, Liverpool, Australia, ⁵UNSW Australia, Liverpool, Australia, ⁶University of Wollongong, Wollongong, Australia

Accurate conversion of MRI into attenuation correction maps is of current interest in PET-MR and MR-only radiotherapy planning in particular, where electron density calculation is particularly demanding and usually derived from CT. MRI methods to date have usually involved building a patient atlas and/or use of multiple imaging sequences and are time intensive. We propose a new single sequence approach based on ultra-short echo time to identify tissue classes of air, bone and soft-tissue in combination with a dynamic clustering regression based model that provides a direct CT conversion which is both efficient and accurate.

4321
Computer #54 Non-invasive estimation of arterial input function for imaging of cerebral blood flow on a PET/MR scanner
Mohammad Mehdi Khalighi¹, Audrey Peiwen Fan², Gaspar Delso³, Praveen K. Gulaka², Bin Shen⁴, Aileen Hoehne⁴, Prachi Singh², Jun-Hyung Park⁴, Dawn Holley², Frederick T. Chin^{2,4}, and Greg Zaharchuk^{2,4}

¹Applied Science Lab, GE Healthcare, Menlo Park, CA, United States, ²Radiology Department, Stanford University, Stanford, CA, United States, ³Applied Science Lab, GE Healthcare, Zurich, Switzerland, ⁴Molecular Imaging Program, Stanford University, Stanford, CA, United States

Accurate measurement of Arterial Input Function (AIF) is essential in quantitative analysis of cerebral blood flow (CBF) using ¹⁵O-H₂O PET imaging. The time-of-flight enabled Signa PET/MR scanner (GE Healthcare, Waukesha, WI, USA) provides quality PET images during the arrival of ¹⁵O-H₂O tracer to the brain arteries, which can be used for carotid artery segmentation. The optimal time frame to segment these brain arteries for image-based AIF, is found by binning the PET list file every second and plotting the total number of true and scatter coincident events over time.

4322
Computer #55 Partial volume correction of quantitative susceptibility maps for oxygen extraction fraction measurements.
Phillip G. D. Ward^{1,2}, Audrey P. Fan³, Parnesh Raniga¹, David G. Barnes^{2,4}, David L. Dowe², and Gary F. Egan^{1,5}

¹Monash Biomedical Imaging, Monash University, Clayton, Australia, ²Faculty of Information Technology, Monash University, Clayton, Australia, ³Lucas Center for Imaging, Department of Radiology, Stanford University, Stanford, CA, United States, ⁴Monash eResearch Centre, Monash University, Clayton, Australia, ⁵ARC Centre of Excellence for Integrative Brain Function, Melbourne, Australia

Partial volume effects impede the use of quantitative susceptibility maps for assessing small veins. Oxygen extraction fraction measures are particularly sensitive to these effects. We propose a geometric technique for calculating partial volume from binary venograms. The technique is able to calculate accurate partial volume maps, and vessel geometry, on simulated veins of sub-voxel radius. These partial volume maps are used to adjust for partial volume effects in estimating venous magnetic susceptibility.

4323
Computer #56 Improving Tissue Segmentation of Brain MRI through Sparsity-guided Super-resolution Imaging
Jean-Christophe Brisset¹, Louise E Pape¹, Ricardo Otazo¹, and Yulin Ge¹

¹Radiology, New York University School of Medicine, New York, NY, United States

Since human gray matter cortex is a relatively thin structure and has a complex folding pattern blended with white matter and cerebrospinal fluid (CSF), partial volume effect is always considered a challenging issue for precise tissue segmentation. Super-resolution (SR) is a common method that is often used in the picture world to recover a high-resolution image from low-resolution images. This study was performed to test whether a newly developed sparsity-guided SR algorithm can be adapted on standard clinical MRI images to improve brain tissue segmentation by decreasing partial volume effect.

4324
Computer #57 Data and cluster-extent based thresholding to analyze statistical parametric maps in the study of knee articular cartilage biochemical composition.
Allison B Randolph V¹, Valentina Pedita¹, Lorenzo Nardo¹, and Sharmila Majumdar¹

¹Radiology & Biomedical Imaging, UCSF, San Francisco, CA, United States

Voxel-based relaxometry (VBR) allows for MR relaxation time analysis without the sometimes deleterious assumptions of traditional ROIs. However, VBR introduces potentially new analysis issues, such as noise and map heterogeneity. In this study we propose to use VBR significance thresholding in conjunction with cluster-extent based thresholding to define data-driven regions of interest (ROIs) that include the most critical information in Statistical Parametric Maps (SPM), controlling the aforesaid issues. The results suggests that the data driven voxel cluster ROIs and predefined traditional ROIs have unique, separate anatomical locations, and that the data-driven

clusters perform better when correlated to osteoarthritis (OA) disease markers.

-
- 4325
Computer #58
Automatic organ-specific localization and quantification of fat in abdominal chemical shift encoding-based water-fat MRI: application to weight-loss in obesity
Jun Shen¹, Thomas Baum², Christian Cordes², Beate Ott³, Claudia Eichhorn³, Thomas Skurk^{3,4}, Hendrik Kooijman⁵, Ernst J Rummeny², Hans Hauner^{3,4}, Bjoern H Menze¹, and Dimitrios C Karampinos²
- ¹Department of Computer Science, TU Munich, Munich, Germany, ²Department of Radiology, TU Munich, Munich, Germany, ³Else Kröner Fresenius Center for Nutritional Medicine, TU Munich, Munich, Germany, ⁴ZIEL Research Center for Nutrition and Food Sciences, TU Munich, Munich, Germany, ⁵Philips Healthcare, Hamburg, Germany*
- The accumulation and regional distribution of abdominal adipose tissue and organ fat plays an important role in several diseases including obesity, metabolic syndrome and diabetes. The present work proposes a fully automatic method for abdominal organ segmentation and adipose tissue classification and measurement based on chemical shift encoding-based water-fat MR images. The results from the automatic method showed very good agreement with the manually created references. The developed automatic algorithm allowed the detection of regional differences in changes of adipose tissue depots in a study of 20 obese women undergoing a calorie restriction intervention.
-
- 4326
Computer #59
Semi-Automatic Comparison of Myocardial Tissue Injury using a Non-Rigid Registration Method in patients with non-ischemic disease
Leili Riazzy¹, Simone Fritzsche^{2,3}, Arthur Stötzner^{2,3}, Fabian Mühlberg^{2,3}, Luisa Schmach^{2,3}, Matthias Dieringer^{1,2,4}, Florian von Knobelsdorff-Brenkenhoff^{2,3}, Thoralf Niendorf^{1,2}, and Jeanette Schulz-Menger^{2,3}
- ¹Berlin Ultrahigh Field Facility (B.U.F.F.), Max-Delbrueck Center for Molecular Medicine, Berlin, Germany, ²Working Group on Cardiovascular Magnetic Resonance, Experimental and Clinical Research Center (ECRC), Berlin, Germany, ³Department of Cardiology and Nephrology, HELIOS Klinikum Berlin Buch, Berlin, Germany, ⁴Siemens Healthcare GmbH, Erlangen, Germany*
- Late Gadolinium Enhancement (LGE) is the noninvasive gold standard for focal fibrosis, parametric mapping with and without contrast-media enable detection of diffuse fibrosis. We developed a non-rigid registration method to superimpose LGE images and T1-Maps allowing for pixel-wise comparison of LGE extent and abnormal T1 times. We observed significantly larger regions of ECV, T1 native and post-contrast abnormalities than LGE positive areas. However, LGE was not always completely covered by abnormalities of any of the mentioned parameters.
-
- 4327
Computer #60
MRI-guided PET image denoising using a non-local means filter
Marie Anne Richard¹, Réjean Lebel¹, Jérémie P. Fouquet¹, and Martin Lepage¹
- ¹Centre d'imagerie moléculaire de Sherbrooke, Université de Sherbrooke, Sherbrooke, QC, Canada*
- Positron emission tomography (PET) images suffer from statistical noise, especially in short time frames. For applications requiring high temporal resolution, such as dynamic studies, efficient edge-preserving denoising algorithms such as the non-local means filter (NLMF) are needed. Because this filter relies on structural data, coregistered MR images were used to guide the NLMF. This novel method was compared to conventional PET-guided NLMF and proved superior in terms of increased contrast-to-background ratio and signal-to-noise ratio in a phantom model. It also increased small structure resolution in a rat model.
-
- 4328
Computer #61
THOMAS: Thalamus Optimized Multi-Atlas Segmentation at 3T
Jason Su¹, Thomas Tourdias², Manojkumar Saranathan³, Pejman Ghanouni⁴, and Brian Rutt⁴
- ¹Electrical Engineering, Stanford University, Stanford, CA, United States, ²Neuroradiology, Bordeaux University Hospital, Bordeaux, France, ³Radiology, University of Arizona, Tucson, AZ, United States, ⁴Radiology, Stanford University, Stanford, CA, United States*
- The efficacy of the Thalamus Optimized Multi-Atlas Segmentation (THOMAS) algorithm for segmentation of thalamic nuclei with white-matter-nulled MP-RAGE images is studied in 3T and 7T variants of the image contrast. 5 subjects are evaluated at both field strengths and ground truth manual delineations of nuclei are performed on the 7T images. We demonstrate that the algorithm performs as well on 3T images as on 7T within a dice coefficient of ± 0.1 as evaluated against the ground truth. This indicates that THOMAS can now reach a much wider audience of interested groups.
-
- 4329
Computer #62
Evaluation of feature-driven clustering of dynamic contrast enhanced and oxygen enhanced MRI data to assess tumour microenvironment heterogeneity
Adam K Featherstone^{1,2}, James P B O'Connor^{2,3}, Ross A Little¹, Yvonne Watson¹, Sue Cheung¹, Kaye J Williams^{2,4}, Julian C Matthews^{1,2}, and Geoff J M Parker^{1,2,5}
- ¹Centre for Imaging Sciences, The University of Manchester, Manchester, United Kingdom, ²CRUK & EPSRC Cancer Imaging Centre in Cambridge and Manchester, Cambridge and Manchester, United Kingdom, ³Institute of Cancer Sciences, The University of Manchester, Manchester, United Kingdom, ⁴School of Pharmacy, The University of Manchester, Manchester, United Kingdom, ⁵Bioxydyn Ltd., Manchester, United Kingdom*
- DCE-MRI and OE-MRI scans were performed on 8 preclinical U87 tumour xenografts. Heuristic features (area-under-curve and rate-of-enhancement) were calculated from tumour voxel enhancement curves for each imaging modality. Clustering algorithms (k-means clustering and Gaussian mixture modelling) were applied to these features and native tissue T₁ to investigate their utility in

characterising physiological heterogeneity in tumours. Efficacy in identifying large regions where there is agreement between features is shown. Further optimisation is needed to optimise the approach to characterise smaller, and potentially important, regions where there is a lack of concordance between features.

-
- 4330
Computer #63 Automatic sodium maps reconstruction using PatchMatch algorithm for phantom detection
Ferran Prados^{1,2}, Bhavana S Solanky², Patricia Alves Da Mota², Manuel Jorge Cardoso¹, Wallace J Brownlee², Niamh Cawley², David H Miller², Xavier Golay³, Sebastien Ourselin¹, and Claudia Angela Michela Gandini Wheeler-Kingshott^{2,4}
- ¹Translational Imaging Group, Medical Physics and Biomedical Engineering, University College London, London, United Kingdom, ²NMR Research Unit, Queen Square MS Centre, Department of Neuroinflammation, UCL Institute of Neurology, University College London, London, United Kingdom, ³Brain Repair & Rehabilitation, UCL Institute of Neurology, University College London, London, United Kingdom, ⁴Brain Connectivity Center, C. Mondino National Neurological Institute, Pavia, Italy*
- Quantitative sodium magnetic resonance imaging (²³Na-MRI) enables the non-invasive measurement of in vivo total ²³Na concentration (TSC) in the human brain. This involves a complex process of reconstructing datasets acquired to calculate a TSC map. Quantitative TSC map calibration relies on external reference phantoms with known concentration for linear calibration. This commonly involves manually segmenting the phantoms by trained raters, hindering automatic image analysis, and presenting a bottleneck in the TSC computation. We propose to substitute the manual segmentation by OPAL, a novel, fast, robust and reliable technique for segmenting sodium phantoms that allows fully-automatic reconstruction of TSC maps.
-
- 4331
Computer #64 Dynamic Whole-Brain Connectivity underlying Abnormal Brain States in Late-onset Depression
Mingze Xu^{1,2}, Shiyang Chen², Bing Ji^{2,3}, Jiuquan Zhang⁴, Huaiqiu Zhu¹, Yi Zhang⁵, Yonggui Yuan⁶, Jiahong Gao¹, Yijun Liu¹, and Xiaoping Hu²
- ¹Biomedical Engineering, Peking University, Beijing, China, People's Republic of, ²Biomedical Engineering, Emory University & Georgia Institute of Technology, Atlanta, GA, United States, ³University of Shanghai for Science & Technology, Shanghai, China, People's Republic of, ⁴Department of Radiology, Southwest Hospital, Third Military Medical University, Chongqing, China, People's Republic of, ⁵School of Life Science and Technology, Xidian University, Shaanxi, China, People's Republic of, ⁶Department of Psychosomatics and Psychiatry, ZhongDa Hospital, School of Medicine, Southeast University, Nanjing, China, People's Republic of*
- We conducted dynamic whole-brain connectivity analysis in Late-onset depression (LOD) to investigate alterations in brain networks. All subjects' ROI-to-ROI dynamic FC were explored using a data-driven method to obtain the most explanatory states. Each state indicate a particular ROI-to-ROI FC pattern. The property of each state were determined based on its scores across time. Besides decreased FC in normal state, we found LOD patients switch between brain states more frequently and tend to enter LOD-risk states, due to and its high states variance and dominating increased FC in LOD-risk states. These results suggest neural mechanisms of disorder from dynamic perspective.
-
- 4332
Computer #65 Application of Partial Least Squares regression for Fast and Robust Dictionary Matching for Magnetic Resonance Fingerprinting
Shivaprasad Ashok Chikop¹, Vimal Chandran², Imam Shaik¹, Rashmi Rao¹, Mauricio Antonio Reyes Aguirre², and Sairam Geethanath¹
- ¹Medical Imaging Research Center, Dayananda Sagar Institutions, Bangalore, India, ²Institute of Surgical Technology and Biomechanics, University of Bern, Bern, Switzerland*
- The step size of the parameters used for simulation of dictionary determines the parameters being determined. Partial Least squares (PLS) can be used as a general frame work for fast and robust dictionary matching. Regression co-efficient matrix obtained from PLS can be used for localizing the different brain tissue types thus avoiding iterative searching. The increase in contrast between the grey matter and white matter can be attributed to the intermediate values generated by PLS based matching. PLS matches comparatively better at low SNR images compared to the straight forward dot product method.
-
- 4333
Computer #66 Cluster Analysis of Dynamic Contrast-Enhanced MRI Pharmacokinetic Parameters for Prostate Cancer Risk Stratification: a Step towards Practical Translation
Saba N Elias¹, Guang Jia², Firas G Petros³, Huyen Nguyen¹, Debra L Zynger⁴, Zarine K Shah⁵, Ronney Abaza⁶, and Michael V Knopp¹
- ¹Radiology/Wright Center of Innovation, The Ohio State University, Columbus, OH, United States, ²Department of Physics & Astronomy, Louisiana State University, Baton Rouge, LA, United States, ³Urology, The Ohio State University, Columbus, OH, United States, ⁴Pathology, The Ohio State University, Columbus, OH, United States, ⁵Radiology, The Ohio State University, Columbus, OH, United States, ⁶Robotic Urologic Surgery, OhioHealth Dublin Methodist Hospital, Dublin, OH, United States*
- Feasibility of classifying PCa into clusters based on microcirculatory features has the potential to predict outcome and assist in therapeutic treatment of PCa.
-
- 4334
Computer #67 Pulmonary Imaging Biomarkers of COPD for Personalized Treatment and Better Outcomes
Dante PI Capaldi¹, Anthony Lausch², Khadija Sheikh¹, Fumin Guo¹, David G McCormack³, and Grace Parraga¹
- ¹Robarts Research Institute, The University of Western Ontario, London, ON, Canada, ²Credit Valley Hospital, Mississauga, ON, Canada,*

In this proof-of-concept demonstration, we developed and generated multimodal-parametric-response-mapping (mPRM) from CT and MRI pulmonary measurements to phenotype chronic obstructive pulmonary disease (COPD). We performed principal component analysis of the voxel distribution generated from co-registered inspiration or expiratory CT with ³He MRI SV cluster maps and ³He MRI ADC maps for ex-smokers with and without COPD. Further work is necessary to determine the appropriate combination of imaging biomarkers generated from MRI and CT to provide useful information in deeply phenotyping COPD.

4335
Computer #68 Brain Connectivity Analysis of Parkinson's Disease and "Scans Without Evidence for Dopaminergic Deficit" Patients
Tiago Constantino^{1,2,3}, André Santos Ribeiro⁴, Ricardo Maximiano³, John Mcgonigle⁴, David Nutt⁴, and Hugo Alexandre Ferreira³

¹Lisbon School of Health Technology-ESTeSL, Lisbon, Portugal, ²Spitalzentrum Biel, Biel, Switzerland, ³Institute of Biophysics and Biomedical Engineering, Faculty of Sciences of the University of Lisbon, Lisbon, Portugal, ⁴Centre for Neuropsychopharmacology, Imperial College London, London, United Kingdom

In this work we propose a comparison study between "Scans Without Evidence for Dopaminergic Deficit" (SWEDD) and Parkinson's Disease (PD) patients against healthy subjects using the MIBCA toolbox. Here, we studied the difference in imaging and connectivity metrics obtained from anatomical (T1-weighted) and structural (Diffusion Tensor Imaging) data between the three groups. Results showed increased mean diffusivity in the frontal pole, rostral middle frontal gyrus and superior frontal gyrus between SWEDD and PD patients, which can be related with the dopaminergic mesocortical pathway degeneration in PD. These preliminary results help clarify the differences between SWEDD and PD patients.

4336
Computer #69 Resolving ambiguity in T1 mapping using complex MRI data
Kees M. van Hesp¹, Dirk H.J. Poot^{1,2}, Harm A. Nieuwstadt¹, and Stefan Klein¹

¹Departments of Medical Informatics and Radiology, Erasmus MC, Rotterdam, Netherlands, ²Imaging Science and Technology, Delft University of Technology, Delft, Netherlands

We have recently developed an optimized T₁ mapping protocol for carotid atherosclerotic plaque imaging, using a combination of inversion and recovery prepared acquisitions. This protocol requires less images to be taken (and thus shorter acquisition time) for precise T₁ estimation than conventional inversion-prepared or saturation-prepared acquisition schemes. However, estimating T₁ from magnitude data, acquired with the optimized settings, causes bimodality of T₁ estimates, due to the ambiguity in sign of the inversion prepared magnitude images. Simulations and experiments on a hardware phantom and a volunteer show that the ambiguity resolves when we fit a complex-valued model to the complex data.

4337
Computer #70 Comparing MRI texture heterogeneity with MTR and myelin water fraction as measures of myelin integrity
Tim Luo¹, Shrushrita Sharma², Mark Polivchuk³, Peng Zhai⁴, and Yunyan Zhang⁴

¹Bachelor of Health Sciences, University of Calgary, Calgary, AB, Canada, ²Biomedical Engineering Program, University of Calgary, Calgary, AB, Canada, ³Computer Science, University of Calgary, Calgary, AB, Canada, ⁴Radiology and Clinical Neurosciences, University of Calgary, Calgary, AB, Canada

Changes in myelin integrity are associated with many neurological diseases. We acquired 9.4T MRI from healthy mouse brain to evaluate the utility of texture heterogeneity in T2-weighted MRI for assessing myelin integrity, in comparing with proposed measures including magnetic transfer ratio and myelin water fraction. Measurements were focused on the corpus callosum, with both anatomical (genu, body, splenium) and hemispheric (left, center, right) locations evaluated. All 3 methods showed the uniformity of myelin in corpus callosum between hemispheres, and no significant differences between anatomical locations were detected. Texture heterogeneity showed the best consistency between animals and deserves further verification.

4338
Computer #71 Color mapping in medical imaging - you're (probably) doing it wrong
Jan-Gerd Tenberge¹

¹University of Münster, Münster, Germany

Some imaging software packages do not accurately display datasets due to difficulties in color mapping. We show some of the shortcomings an three of the most widely used tools (FSL, SPM, FreeSurfer) and provide an easy fix that can be applied to correct the images output by these tools.

4339
Computer #72 T1 Mapping through Bayesian Analysis with Spatial Information Collaboration (BASIC) using Steady-State-Based Imaging Data
Mustapha Bouhrara¹ and Richard G. Spencer¹


¹NIA, NIH, Baltimore, MD, United States

We introduce two Bayesian-based analyses that use spatial information as a prior to improve the quality of voxel-by-voxel T₁-mapping from spoiled gradient recalled echo (SPGR) imaging data. These approaches, called BASIC, combine voxel-by-voxel fitting with region-of-interest (ROI) parameter estimation. ROI parameters act as a constraint, while voxel fitting mitigates blurring and detail loss. The results were compared with those derived using a conventional nonlinear least-squares-based algorithm. Estimation of T₁ from SPGR imaging data was markedly improved through use of the BASIC methods.

Human Brain Tumours 2: Response to Treatment

Exhibition Hall

Thursday, May 12, 2016: 13:30 - 14:30

-
- 4340
Computer #1
- Investigation of Varied Readout Sequences Impact on the Amide Proton Transfer Contrast
Chien-Yuan Eddy Lin^{1,2}, Bing Wu², Rui Li³, and Ma Lin³
- ¹GE Healthcare, Taipei, Taiwan, ²GE Healthcare MR Research China, Beijing, China, People's Republic of, ³PLA general hospital, Beijing, China, People's Republic of
- The aim of this study was to understand whether amide proton transfer (APT) contrast on brain tumor patient will be impacted by applying three different imaging sequences, spin-echo EPI, single-shot FSE, and a recent developed 3D FSE spiral. Although our finding on APT contrast appears to be similar among various sequences, careful consideration may be required when choosing the appropriate CEST readout sequences for your own applications.
-
- 4341
Computer #2
- 
- 2HG Optimized PRESS MRS for Metabolic Profiling of IDH-mutant Gliomas in Patient-Derived Orthotropic Mouse Model of Human Brain Tumor
Vivek Tiwari¹, Tomoyuki Mashimo², Sandeep Kumar Ganji¹, Zhongxu An¹, Keith Hulse³, Vamsidhara Vemireddy², Shanrong Zhang¹, Elizabeth Maher², Robert Bachoo², and Changho Choi¹
- ¹Advanced Imaging Research Center, UT Southwestern Medical Center, Dallas, TX, United States, ²Department of Internal Medicine, UT Southwestern Medical Center, Dallas, TX, United States, ³Department of Radiology, UT Southwestern Medical Center, Dallas, TX, United States
- 2-Hydroxyglutarate (2HG) is elevated in gliomas harboring IDH1 or IDH2 mutations, and can be a biomarker for the diagnosis of IDH-mutant gliomas. The present study was undertaken to develop PRESS MRS Methodology for 2HG-detection with enhanced precision, and studying 2HG kinetics together with metabolic profiling in Patient-Derived Xenograft Orthotropic Mouse model. *In-vivo* PRESS MRS was performed at an optimized long-TE of 96ms. A large inverted-signal of 2HG at 2.25-ppm was obtained from IDH-mutant gliomas, well separated from neighboring signals of positive-polarity, with minimal interference from macromolecules. The method was successfully employed to detect 2HG and brain metabolism with tumor progression.
-
- 4342
Computer #3
- Cerebral blood volume MRI elucidates the impact of ERK1 on high grade glioma growth and invasion
Min-Chi Ku¹, Andreas Pohlmann¹, Sonia Waiczies¹, Joao dos Santos Periquito¹, Till Huelnhagen¹, and Thoralf Niendorf¹
- ¹Berlin Ultrahigh Field Facility, Max Delbrück Center for Molecular Medicine in the Helmholtz Association, Berlin, Germany
- Glioma progression involves complex interactions of tumor vasculature and infiltrating anti-tumor immune cells. As we previously found that mouse lacking ERK1 formed significantly smaller tumors, it was still not clear whether ERK1 deletion in the tumor vascular architecture might influence the outcome of glioma growth. To further study this, we examined the relative cerebral blood volume (rCBV) in the glioma tumor. R_2^* changes induced by a blood-pool contrast agent, ferumoxytol, were quantified. Here, we established a model system to noninvasively monitor brain tumor angiogenesis, and found evidence supporting the role of ERK1 in regulating glioma growth via angiogenesis.
-
- 4343
Computer #4
- Dynamic Contrast Enhanced perfusion MRI in pediatric brain tumors
Rupsa Bhattacharjee¹, Prativa Sahoo², Pradeep Kumar Gupta³, and Rakesh Kumar Gupta³
- ¹Healthcare, Philips India Ltd, Gurgaon, India, ²Healthcare, Philips India Ltd, Bangalore, India, ³Radiology and Imaging, Fortis Memorial Research Institute, Gurgaon, India
- Perfusion Studies in Pediatric Brain Tumors is a less explored area due to technical challenges of performing contrast enhanced perfusion in infant and children. This study is the first preliminary study reported in Dynamic Contrast Enhanced MRI perfusion involving both high grade and low grade brain tumors. Purpose of this study is to quantify the range of various perfusion metrics in high and low grade tumor as well as normal gray and white matter regions of brain. This ongoing study shows significant statistical difference in cerebral blood volume and fractional plasma volume in high grade and low grade tumor population.
-
- 4344
Computer #5
- Adiabatic T₂-Prepared 3D Fast Gradient Echo Imaging for Brain Tumor Studies at 7T
Peng Cao¹, Angela Jakary¹, Yan Li¹, Sarah J. Nelson¹, Doug Kelley², and Peder E. Z. Larson¹
- ¹Department of Radiology, University of California at San Francisco, San Francisco, CA, United States, ²GE Healthcare, Waukesha, WI, United States
- Mechanisms to create a homogenous T₂ contrast at 7T should be robust to both B₀ and B₁ inhomogeneities. This issue was addressed by applying a zero-degree BIR-4 adiabatic pulse for T₂ preparation. Simulation and in vivo experiments in mouse brain verified the robustness and contrast of the preparation scheme at 7T. Application of this method was further demonstrated in a study of a patient with a brain tumor. The adiabatic T₂ weighting showed high intensity in the region of the tumor, suggesting that the proposed method is

likely to be useful in screening and characterizing tumors.

-
- 4345
Computer #6
Comparing the CEST imaging of Cerebral Glioma using APT and LOVARS
Taiyuan Liu¹, Yan Bai², Xiaolei Song³, Jinyuan Zhou³, Panli Zuo⁴, Benjamin Schmitt⁵, and Meiyun Wang²
¹Henan Provincial People's Hospital, Zhengzhou, China, People's Republic of, ²Zhengzhou, China, People's Republic of, ³Baltimore, MD, United States, ⁴Beijing, China, People's Republic of, ⁵Macquarie Park, Australia
- To evaluate the value of length and offset varied saturation (LOVARS) in the diagnosis of gliomas, and compared with amide proton transfer (APT), We performed the study using LOVARS and APT imaging technique .And we found that APT images is useful in distinguishing low-grade and high-grade glioma, while LOVARS phase images shows better contrast between glioma and peripheral tissue, and the internal heterogeneous components of the glioma.
-
- 4346
Computer #7
Chemotherapy increases anti-correlation between default mode and attention networks
Suresh Emmanuel Joel¹, Roberto Garcia Alvarez², Juan Bachiller Egea³, Lucia Gonzalez Cortijo⁴, Vincente Martinez de Vega³, Rakesh Mullick¹, and Mar Jimenez de la Pena³
¹General Electric Global Research, Bangalore, India, ²General Electric Healthcare, Madrid, Spain, ³Departamento Diagnostico por la imagen, Hospital Universitario Quiron, Madrid, Spain, ⁴Departamento de Oncología Médica, Hospital Universitario Quiron, Madrid, Spain
- More than three-fourth of chemotherapy treated cancer survivors have cognitive impairment, including memory loss, inability to think, lasting several years after completion of therapy, sometimes labelled as 'chemobrain'. Previously, the default mode network (DMN) has been shown to be specifically vulnerable to chemotherapy. In this study we study changes in DMN connectivity after chemotherapy within the same patients. In healthy adults, the DMN is anti-correlated to task positive networks. We observe an increase in this anti-correlation between DMN regions and task positive network regions post-chemotherapy.
-
- 4347
Computer #8
Predicting overall survival in glioblastoma patients from DTI, DCE and DSC MRI data acquired prior to surgery and post-chemoradiotherapy
Lawrence Kenning¹, Martin Lowry², Martin D Pickles¹, Chris Roland Hill³, Shailendra Achawal³, and Chittoor Rajaraman³
¹Centre for MR Investigations, Hull York Medical School at University of Hull, Hull, United Kingdom, ²Hull York Medical School at University of Hull, Hull, United Kingdom, ³Hull and East Yorkshire Hospitals NHS Trust, Hull, United Kingdom
- DTI, DCE and DSC MRI parameters obtained pre-surgery and post-chemoradiotherapy were used to predict overall survival in a cohort of patients with glioblastoma multiforme. Results suggest that preoperative diffusivity measurements contain prognostic information about survival. Following chemoradiotherapy, K^{trans} , v_e , rCBV and tumour volumes were found to have significant prognostic value with higher values associated with shorter overall survival. Cox regression analysis identified 2 volumes and 2 MR parameters, confirming the Kaplan-Meier findings that preoperative DTI and post-chemoradiotherapy DCE parameters have added prognostic value to more traditional prognostic features such as tumour volume.
-
- 4348
Computer #9
Optimizing Magnetization Prepared Rapid Gradient Echo (MPRAGE) for Brain Tumor Detection
Jinghua Wang¹, Mark Smith², and Lili He³
¹The Ohio State University, Columbus, OH, United States, ²Radiology, Nationwide Children's Hospital, Columbus, OH, United States, ³Center for Perinatal Research, Nationwide Children's Hospital, Columbus, OH, United States
- Gadolinium based contrast agents decrease T_1 times in pathologic regions of the brain and improve image contrast and lesion visualization with increased sensitivity and specificity. Magnetization Prepared Rapid Gradient Echo (MPRAGE) sequence offer thinner slices, near seamless reformatting options, and lower specific absorption rates than 2D spin-echo based technique. In this study, we optimize MPRAGE sequence using computer simulation to improve brain tumor enhancement and detection. Compared with a Siemens default MPRAGE sequence, our optimized protocol greatly shortened scan time by around 60% without sacrificing tumor detection sensitivity.
-
- 4349
Computer #10
Diffusional kurtosis imaging for differentiating between high-grade glioma and primary central nervous system lymphoma
Haopeng Pang¹, Yan Ren¹, Zhenwei Yao¹, Jingsong Wu¹, Chengjun Yao¹, Xuefei Dang², Yong Zhang³, and Xiaoyuan Feng¹
¹Affiliated Huashan Hospital of Fudan University, Shanghai, China, People's Republic of, ²The 307th Hospital of Chinese People's liberation Army, Beijing, China, People's Republic of, ³MR Research China, GE Healthcare, Beijing, China, People's Republic of
- This study provided a new non-invasive method to better discriminate between high-grade gliomas and primary nervous system lymphomas. We found the kurtosis parameters (MK and $K_{//}$) showed more obvious differences that can be used for differentiating between these two types of tumors than diffusion parameters (FA, MD, $\lambda_{//}$ and λ_{\perp}). The ROC curve analysis showed MK and $K_{//}$ had the largest area under curve, which further confirmed that the kurtosis parameters MK and $K_{//}$ could better separate these tumors than traditional diffusion parameters.
-
- 4350
Computer #11
Automated extraction of glioblastoma tumor sub-components using multi-modal MRI
Sushmita Datta¹, Jay-jiguang Zhu², Roy F Riascos-Castaneda¹, and Ponnada A Narayana¹

¹Diagnostic and Interventional Imaging, The University of Texas Health Science Center at Houston, Houston, TX, United States, ²Neurosurgery, The University of Texas Health Science Center at Houston, Houston, TX, United States

Automated quantification of tumors and its components are important in monitoring disease status in glioblastoma patients. We have proposed an automatic segmentation procedure based on morphological grayscale reconstruction techniques to classify and identify tumor sub-regions using multi-modal MRI.

4351
Computer #12 Characterizing metabolic profiles in non-enhancing gliomas using 3D MRSI
Yan Li¹, Tracy L Luks¹, Jason C Crane¹, Sarah J Nelson¹, and Tracy R McKnight²

¹Department of Radiology and Biomedical Imaging, University of California, San Francisco, CA, United States, ²Tobacco-Related Disease Research Program, University of California, Oakland, CA, United States

This study evaluated the metabolite profiles that were acquired using short and long echo time (TE) magnetic resonance spectroscopic imaging (MRSI) for forty patients with non-enhancing gliomas, including 25 grade 2 and 15 grade 3 gliomas. Metabolite differences were detected between the lesions and white matter, as well as between grades. There were also differences in the T2 values between metabolites within the lesions that could influence the Cho/NAA ratios between short and long TE MRSI.

4352
Computer #13 Enhanced brain labeling by atlas registration in Neuro-oncology using virtual tumor shrinking
Hariharan Ravishankar¹, Igor Barani², Sheshadri Thiruvankadam¹, Marc Mabray², KS Shriram¹, SoonMee Cha², Rakesh Mullick³, and Suresh Emmanuel Joel³

¹General Electric Global Research, Bangalore, India, ²University of California at San Francisco, San Francisco, CA, United States, ³Diagnostic Imaging and Biomedical Technologies, General Electric Global Research, Bangalore, India

In this work, we address the problem of registration of brain images to atlases in presence of large, space-occupying tumor pathologies. We provide an integrated registration framework to address two types of tumors - a) infiltrating tumors - which penetrate the surrounding tissues b) extrinsic tumors - which grow and compress the surrounding tissues. We propose a mathematical model to shrink extrinsic tumors before registration, thereby reversing the compression effects.

4353
Computer #14 Improved Modeling of Glioblastoma Proliferation and Necrosis using Growth Parameters Derived from MRI
Vishal Patel¹ and Leith Hathout²

¹University of California, Los Angeles, Los Angeles, CA, United States, ²Harvard University, Boston, MA, United States

We outline a new model for the proliferation and necrosis of glioblastoma multiforme. Our approach uniquely accounts both for the anisotropic migration of tumor cells through brain parenchyma and for central tumor necrosis. Model parameters relating to cell division, cell migration, and tumor necrosis are estimated directly from serial MR imaging to generate a customized growth profile for each tumor. The proposed model is shown to replicate observed tumor growth more closely than existing techniques. We anticipate that improved modeling of tumor growth profiles will enable more effective tailoring of treatment regimens.

4354
Computer #15 Quantitative DCE-MRI for differentiating high grade glioma recurrence from treatment-related changes: Effect of T1 mapping method
Greg O. Cron^{1,2,3}, Beckie Manouchehri⁴, Andrew Boivin³, Nader Zakhari^{1,3}, Brandon Zanette^{5,6}, Gerard H. Jansen^{1,2,3}, John Woulfe^{1,2,3}, Rebecca E. Thornhill^{1,2,3}, Andreas Greiser⁷, Ian G. Cameron^{1,2,3,4}, and Thanh B. Nguyen^{1,2,3}

¹The Ottawa Hospital, Ottawa, ON, Canada, ²Ottawa Hospital Research Institute, Ottawa, ON, Canada, ³University of Ottawa, Ottawa, ON, Canada, ⁴Carleton University, Ottawa, ON, Canada, ⁵University of Toronto, Toronto, ON, Canada, ⁶Peter Gilgan Centre for Research and Learning, The Hospital for Sick Children, Toronto, ON, Canada, ⁷Siemens Healthcare GmbH, Erlangen, Germany

After a patient has received treatment for a high grade glioma, a new enhancing lesion presents a common diagnostic dilemma: Malignant tumor recurrence and benign treatment-related changes (TRC) appear similar on conventional MRI. MRI tracer kinetic studies may help distinguish recurrence from TRC. We investigated whether Ktrans measurements using quantitative DCE-MRI can accurately diagnose recurrence. We also studied the effect of the DCE T1 mapping method (VFA versus LL). Ktrans values in recurrent tumor were higher than in TRC, providing sensitivity of 69-77%, specificity of 100%. The choice of T1 mapping had little effect on diagnostic accuracy.

4355
Computer #16 Differentiation of Glioblastoma from Brain Metastasis: Qualitative and Quantitative Analysis using Pseudo-continuous Arterial Spin Labeling MR Imaging
Leonard Sunwoo^{1,2}, Tae Jin Yun^{2,3}, Roh-Eul Yoo^{2,3}, Soo Chin Kim^{2,4}, and Hye Young Sun^{2,4}

¹Radiology, Seoul National University Bundang Hospital, Seongnam, Korea, Republic of, ²Seoul National University College of Medicine, Seoul, Korea, Republic of, ³Radiology, Seoul National University Hospital, Seoul, Korea, Republic of, ⁴Radiology, Seoul National University Healthcare System Gangnam Center, Seoul, Korea, Republic of

Arterial spin labeling (ASL) magnetic resonance (MR) imaging could be used to assess the tumor blood flow (TBF). To distinguish glioblastoma (GBM) from brain metastasis, we compared TBF between the two groups by using visual grading and quantitative analyses. Both intratumoral and peritumoral blood flow were significantly higher in GBM than in brain metastasis. We propose that ASL-TBF can

-
- 4356
Computer #17
- Changes in DTI and DSC Parameters as Markers for Assessing Treatment Response in Glioblastomas
Sumei Wang¹, Sanjeev Chawla¹, Maria Martinez-Lage², Tianyu Yin¹, Gaurav Verma¹, Robert A Lustig³, Steven Brem⁴, Suyash Mohan¹, Ronald L Wolf¹, Arati Desai⁵, and Harish Poptani⁶
- ¹Radiology, University of Pennsylvania, Philadelphia, PA, United States, ²Pathology and Laboratory Medicine, University of Pennsylvania, Philadelphia, PA, United States, ³Radiation Oncology, University of Pennsylvania, Philadelphia, PA, United States, ⁴Neurosurgery, University of Pennsylvania, Philadelphia, PA, United States, ⁵Hematology-Oncology, University of Pennsylvania, Philadelphia, PA, United States, ⁶Cellular and Molecular Physiology, University of Liverpool, Liverpool, United Kingdom
- The study was performed to determine whether changes in DTI and DSC parameters can aid in differentiating glioblastomas with pseudo-progression (PsP) from true-progression (TP) and partial response. MRI data from thirty patients with these diagnoses (based on pathological evaluation and clinical follow-up) were included. All patients underwent two MR scans before pathological confirmation. A significant increase in median rCBV and rCBV_{max} value was noted in TP compared with PsP, while none of the DTI parameters showed significant differences between groups. Our preliminary results indicate that changes in rCBV may be helpful in identifying PsP from TP.
-
- 4357
Computer #18
- Which is the best predictor for histological grade of glioma: DWI, MRS, 11C-methionine -, and 18F-fluorodeoxyglucose -PET
Keiichi Kikuchi¹, Yoshiyasu Hiratsuka¹, Shiro Ohue², Shohei Kohno², and Teruhito Mochizuki¹
- ¹Radiology, Ehime University School of Medicine, Ehime, Japan, ²Neurosurgery, Ehime University School of Medicine, Ehime, Japan
- Various imaging modalities are commonly used for preoperative examinations of brain tumors. Here we evaluated the specificity of ADC, MRS, and PET-CT to predict the WHO glioma grade and identified potential correlations with the Ki-67 index as a marker of tumor cell proliferation. In this limited patients series, minimum ADC was the best predictor of the histological glioma grade and it was also significantly negatively correlated with the Ki-67 index indicating its potential as a reliable marker of cellular proliferation.
-
- 4358
Computer #19
- Histogram analytics and data mining of multiparametric FMRI (perfusion, diffusion) in preoperative histologic prediction of posterior fossa tumors.
Shanker Raja¹, Ali Daghriri², Sadeq Wasil Al Dandan³, Tariq Ahmad Wani⁴, Muhammad Usman Manzoor⁵, Abdullah Ali Alrashed², Sarah Farooq⁶, William Plishker⁷, and Sharad George⁸
- ¹Radiology, Baylor College of Medicine, Bellaire, TX, United States, ²Medical Imaging, King Fahad Medical City, Riyadh, Saudi Arabia, ³Pathology and Laboratory Medicine, King Fahad Medical City, Riyadh, Saudi Arabia, ⁴KFMC-Riyadh, Riyadh, Saudi Arabia, ⁵Radiology, King Fahad Medical City, Riyadh, Saudi Arabia, ⁶King Fahad Medical City, Riyadh, Saudi Arabia, ⁷IGI Technologies, College Park, MD, United States, ⁸Johns Hopkins Aramco Healthcare, Dhahran, Saudi Arabia
- Histogram metrics derived from a combination preoperative MRI: AFDC and perfusion maps, appear to be promising in differentiation of posterior tumors
-
- 4359
Computer #20
- Perfusion MRI as the predictive/prognostic and Pharmacodynamic Biomarkers in Recurrent Malignant Glioma Treated with Bevacizumab: A Systematic Review and a time-to-event meta-analysis
Kyung Won Kim¹, Sang Hyun Choi¹, Seung Chai Jung¹, Ja Youn Lee², Ho Sung Kim¹, and Seong Ho Park¹
- ¹Radiology, Asan Medical Center, University of Ulsan College of Medicine, Seoul, Korea, Republic of, ²National Evidence-based Healthcare Collaborating Agency, Seoul, Korea, Republic of
- The current evidence in the literature shows that the rCBV of DSC-MRI is the most widely used perfusion MRI parameter. The rCBV can be used to predict disease progression and overall survival in patients with recurrent malignant glioma treated with BVZ. Various perfusion MRI parameters from DSC-MRI and DCE-MRI could play a role as pharmacodynamic biomarkers to evaluate the drug's anti-angiogenic effect on tumor.
-
- 4360
Computer #21
- Is there an optimal acquisition delay for postcontrast quantitative MRI of brain metastasis?
Koung Mi Kang¹, Seung Hong Choi¹, Moonjung Hwang², Soo Chin Kim³, Ji-Hoon Kim⁴, Tae Jin Yun⁴, and Chul-Ho Sohn⁴
- ¹Seoul National University Hospital, Seoul, Korea, Republic of, ²MR Applications and Workflow, GE Healthcare, Seoul, R.Korea, Seoul, Korea, Republic of, ³SNUH healthcare system gangnam center, Seoul, Korea, Republic of, ⁴Department of Radiology, Seoul National University Hospital, Seoul, Korea, Republic of
- In the brain metastasis, T1 shortening after the administration of gadolinium contrast agent may vary with the timing of contrast administration. Synthetic MRI enables quantitative measurements with relatively short times. Our study aimed to determine the optimal acquisition delay for quantitative imaging of brain metastases with contrast-enhanced synthetic MRI. This study revealed that there was no significant difference and relationship in the histogram parameters between three different delay time points of immediately, 8 minutes and 20 minutes after the contrast injection. Therefore, postcontrast quantitative MRI might be acquired regardless of time within 20 minutes.
-

- 4361
Computer #22
Differentiating radiation-induced brain necrosis from glioma recurrence: using 3-Dimensional arterial spin labeling and dynamic susceptibility contrast perfusion MR imaging
YULIN WANG¹ and LIN MA¹

¹Radiology, PLA General Hospital, Beijing, China, People's Republic of
- Perfusion made it possible to obtain measurements of vascularity within brain lesions. The vascularity of malignant tumor differs dramatically from that of radiation necrosis. Thus, tumor recurrence within irradiated lesions may be differentiated from regions of radiation necrosis with perfusion. 64 patients were prospectively entered into the study on the basis of the following criteria: previous treatment with radiation therapy after surgical resection for intraaxial tumors; new development of enhancing lesions within the radiation field. To compare 3D-ASL with DSC and to see whether 3D ASL-derived CBF values can be used as an alternative to DSC for their differentiation.

- 4362
Computer #23
Can cerebral lymphomas and glioblastomas be differentiated based on histogram parameters on contrast-enhanced T1-weighted images?
Tatsuya Yamamoto¹, Yuriko Ohtani², and Hirohiko Kimura¹

¹Department of Radiology, University of Fukui, Fukui, Japan, ²Division of Radiology, University of Fukui Hospital, Fukui, Japan
- Cerebral lymphomas are sometimes difficult to distinguish from glioblastomas based on routine magnetic resonance (MR) examination. Therefore, this study assessed the utility of a histogram analysis of the intratumoral enhanced region, using contrast-enhanced T1WI (CET1WI) with a 3D-spoiled gradient recalled acquisition in the steady state (SPGR) sequence, for cerebral lymphomas and glioblastomas, to determine whether the histogram parameters differed between the two tumors. There was significant difference ($p < 0.01$) in skewness between lymphomas and glioblastomas. This suggests the possibility of differential diagnosis of cerebral lymphomas and glioblastomas by histogram analysis of CET1WI.

- 4363
Computer #24
Multiparametric quantitative MRI of meningiomas (H2O, T1, T2*, kurtosis) for microscopic tissue characterization
A.M. Oros-Peusquens^{1,2}, M. Zimmermann³, E. Iordanishvili¹, O. Nikoubashman⁴, F. Jablawi⁴, B. Ulus⁴, G. Neuloh⁴, H. Cluesmann⁵, M. Wiesmann⁴, and N.J. Shah¹

¹Institute of Medicine and Neuroscience (INM-4), Research Centre Juelich, Juelich, Germany, ²Institute of Neuroscience and Medicine 4 (INM-4), Research centre Juelich, Juelich, Germany, ³Institute of Medicine and Neuroscience (INM-4), Research Centre Juelich, Juelich, Georgia, ⁴University Hospital Aachen, Aachen, Germany, ⁵University Hospital Aachen, Aachen, Germany
- Differentiation between meningioma types has implications in preoperative planning but is seldom achieved by conventional MRI. We investigate a multiparameter quantitative characterization of meningioma in clinically acceptable measurement times characterizing each tumour by its "qMRI fingerprint". The parameters included are water content, T1, T2* and diffusion maps (MD, FA, MK, axonal water fraction, tortuosity) derived from a diffusion kurtosis acquisition. The "qMRI fingerprints" are distinct for each tumour.

Electronic Poster

Neuromuscular Disease & Stroke

Exhibition Hall

Thursday, May 12, 2016: 13:30 - 14:30

- 4364
Computer #25
Cell treatment improves recovery after stroke in type two diabetic rats measured by MRI
Guangliang Ding¹, Jieli Chen¹, Michael Chopp^{1,2}, Lian Li¹, Tao Yan^{1,3}, Esmaeil Davoodi-Bojd¹, Qingjiang Li¹, Chengcheng Cui¹, Siamak P.N. Davarani¹, and Quan Jiang¹

¹Neurology, Henry Ford Health System, Detroit, MI, United States, ²Physics, Oakland University, Rochester, MI, United States, ³Tianjin Geriatrics Institute, Tianjin Medical University General Hospital, Tianjin, China, People's Republic of
- With a suture 2-hour occlusion and reperfusion stroke model and a low dose Streptozotocin injection combined with a high fat food diet diabetic model of young adult Wistar rats, longitudinal measurements of MRI demonstrated that bone marrow stromal cell treatment of stroke in type 2 diabetes mellitus rats, compared with the saline treated control rats, not only significantly reduced blood-brain barrier leakage and hemorrhagic spots starting from 1 week and 3 weeks after stroke ($p < 0.05$) measured by contrast enhanced T1WI with Gd-DTPA and identified by SWI, respectively; but also significantly improves white matter remodeling after stroke measured by DSI.

- 4365
Computer #26
The MIPP study: Monitoring Intracranial atherosclerotic Plaque Progression using high resolution MRI - initial results
Chengcheng Zhu¹, Xuefeng Zhang², Andrew J Degnan³, Qi Liu², Luguang Chen², Zhongzhao Teng⁴, David Saloner¹, and Jianping Lu²

¹Radiology, University of California, San Francisco, San Francisco, CA, United States, ²Radiology, Changhai Hospital, Shanghai, China, People's Republic of, ³Radiology, University of Pittsburgh, Pittsburgh, PA, United States, ⁴Radiology, University of Cambridge, Cambridge, United Kingdom

Intracranial large artery atheroma is a major cause of stroke, however its natural history is still poorly understood. In this study we followed 63 symptomatic patients who had intracranial atherosclerotic plaque for up to 3 years. Multi-contrast black blood vessel wall MRI and clinical brain imaging were performed. Initial results included 22 patients who were followed for 6 months showed an overall plaque volume progression rate of 0.8%, however with a large standard deviation (20.1%) and range (-45.9% to 40.1%). Patients with



hypertension or low HDL tended to progress faster. The feasibility of MRI for monitoring intracranial plaque pathological changes was demonstrated.

- 4366
Computer #27 Simultaneous Time-Encoding for Bi-Polar (STEP) MRA combining Arterial Spin Labeling (ASL) and Phase-Sensitive Inversion Recovery Black-Blood (PSIR-BB)
Tokunori Kimura¹, Naotakata Sakashita¹, and Mitsue Miyazaki²

¹Toshiba Medical Systems, Otawara, Japan, ²Toshiba Medical Research Institute, Vernon Hills, IL, United States

We proposed and assessed a simultaneous time-encoding for bipolar MRA technique (STEP-MRA), combining both the 4DASL-MRA of nulling background signals and PSIR BB-MRA with preserving Mz polarities and background stationary signals, which allows simultaneously providing using the same acquired data as the standard 4DASL-MRA. In addition, vessel visualization and SNR were improved by synthesizing multiple T1 data. Although further parameter optimization and clinical evaluation are required, our proposed method has a potential to provide various information with limited acquisition data.

- 4367
Computer #28 High-resolution intracranial vessel wall magnetic resonance imaging in an elderly asymptomatic population: comparison of 3.0T and 7.0T
Anita A. Hartevelde¹, Anja G. van der Kolk¹, H. Bart van der Worp², Nikki Dieleman¹, Jeroen C.W. Siero¹, Hugo J. Kuijff³, Catharina J.M. Frijns², Peter R. Luijten¹, Jaco J.M. Zwanenburg^{1,3}, and Jeroen Hendrikse¹



¹Radiology, University Medical Center Utrecht, Utrecht, Netherlands, ²Neurology, University Medical Center Utrecht, Utrecht, Netherlands, ³Image Sciences Institute, University Medical Center Utrecht, Utrecht, Netherlands

In recent years, multiple intracranial vessel wall MRI sequences have been developed for direct evaluation of the intracranial vessel wall and its pathology in vivo. These studies have mainly been performed on 3T and 7T field strengths. In the current study, we compared 3T and 7T MRI for visualizing both healthy intracranial arterial vessel wall as well as possible vessel wall lesions. Vessel wall visibility was significantly better at 7T even though there were more artefacts hampering assessment. Overall, more lesions were scored on 7T images; however – surprisingly – only half of all 3T lesions were seen at 7T.

- 4368
Computer #29 High Resolution Whole Brain Intracranial Vessel Wall Imaging at 3T and 7T
Chengcheng Zhu¹, Henrik Haraldsson¹, Karl Meisel², Nerissa Ko², Michael Lawton³, John Grinstead⁴, Sinyeob Ahn⁴, Gerhard Laub⁴, Christopher Hess¹, and David Saloner¹



¹Radiology, University of California, San Francisco, San Francisco, CA, United States, ²Neurology, University of California, San Francisco, San Francisco, CA, United States, ³Neurological Surgery, University of California, San Francisco, San Francisco, CA, United States, ⁴Siemens Healthcare, San Francisco, CA, United States

High resolution MRI of the intracranial vessel wall provides important capabilities for the assessment of intracranial vascular disease including atherosclerotic plaques and aneurysms. This study developed and optimized 3D high resolution (0.5mm isotropic) techniques for intracranial vessel wall imaging at 3T and 7T. The abilities of 3T clinical scanners and 7T research scanners were systematically compared through theoretical simulations and in vivo patient studies. We found 3D T1-weighted SPACE sequence could be used for whole brain intracranial vessel wall evaluation at both 3T and 7T. 7T provides significantly better image quality and improves the confidence of diagnosis.

- 4369
Computer #30 Altered Temporal Dynamics in BOLD Measurements of Vascular Reserve in Children with Sickle Cell Disease
Jackie Leung¹, James Duffin², and Andrea Kassner^{1,3}

¹Physiology and Experimental Medicine, The Hospital for Sick Children, Toronto, ON, Canada, ²Physiology, University of Toronto, Toronto, ON, Canada, ³Medical Imaging, University of Toronto, Toronto, ON, Canada

Cerebrovascular reactivity (CVR) measured with BOLD MRI can be robustly acquired by altering blood flow with a square-wave CO₂ stimulus. However, the BOLD response to a step change is confounded by a temporal lag and transient period of signal change. Differences in temporal response between different tissues can lead to CVR underestimation. Transfer function analysis (TFA) provides a frequency domain analysis of CVR that is less sensitive to temporal variations. This study compares the results of TFA to conventional CVR analysis in children with and without sickle cell disease.

- 4370
Computer #31 Diffusion Corrected Aneurysm Wall Permeability as a Measure of Rupture Risk
Charles G Cantrell¹, Parmede Vakili^{1,2}, Sameer A Ansari³, and Timothy J Carroll^{1,3}

¹Biomedical Engineering, Northwestern, Chicago, IL, United States, ²College of Medicine, University of Illinois, Chicago, IL, United States, ³Radiology, Northwestern, Chicago, IL, United States

We report the first evidence of diffusion corrected DCE-MRI modeled contrast permeability in intracranial aneurysms and show the diffusion model more accurately represents physiology than previous methods. Permeability metrics, as measured in 23 patients, demonstrate a statistically significant trend with rupture risk as defined by anatomic imaging and clinical risk factors.

- 4371 Estimation of the Evolution of Cerebral Ischemia by MRI with T1 Relaxation Time in Rotating Frame and Apparent Diffusion Coefficient

Computer #32 Yuefa Tan¹, Ruiying Chen¹, Bin Chen¹, Juan Xu¹, Daokun Ren¹, Yingjie Mei², Queenie Chan³, Yuankui Wu¹, and Yikai Xu¹

¹Department of Medical Imaging Center, Nanfang Hospital, Southern Medical University, Guangzhou, China, People's Republic of, ²Philips Healthcare, Guangzhou, China, People's Republic of, ³Philips Healthcare, HongKong, China, People's Republic of

This study was to evaluate the abilities of T1p and ADC to estimate the duration of ischemia in human, and focus on clinical application. We take a cross-sectional study to collect patients with brain ischemia in period of time(March 2014 to February 2015), and exploit the characteristics of ADC and T1p in brain ischemia in various stages of ischemia and uncover their relationships with ischemia stages. Our results indicate that T1p parametric results were elevated in the ischemic lesion, and increased over time of ischemia in a linear fashion.

4372

Computer #33 Assessment of cortical cerebrovascular permeability using 3-dimension pseudo-continuous arterial spin labeling and T1 dynamic contrast enhancement magnetic resonance imaging in moyamoya disease
Yan Ren¹, Qian Zhou¹, Haopeng Pang¹, Yong Zhang², Zihua Su³, and Zhenwei Yao¹

¹Huashan Hospital, Fudan University, Shanghai, China, People's Republic of, ²MR Research, GE Healthcare, Shanghai, China, People's Republic of, ³Advanced application, GE Healthcare, Beijing, China, People's Republic of

In moyamoya disease (MMD), the compensatory collateralization from external cerebral artery or bypass artery is essential to evaluate the severity of disease and perfusion efficacy of surgical revascularization. And the leptomeningeal anastomoses were regarded as significant contributors to the collateral blood supply. However, the characteristic of the compensatory collateralization has not been clarified up to now, such as the permeability of vessels, which could be the reason of rehemorrhage and other complications after the surgical revascularization for MMD. We hypothesize the high permeability of collateralization leads to rehemorrhage in MMD. In this work, quantitative assessment of 3D-pCASL and DCE-MRI suggests no significant increased permeability in the cortical areas with collateral neovascularization in MMD.

4373

Computer #34 T1 weighted, black blood variable flip angle spin echo imaging utilizing variable density, distributed spirals and a low rank reconstruction
Kevin M Johnson¹, Leonardo Rivera-Rivera¹, and Patrick A Turski²

¹Medical Physics, University of Wisconsin - Madison, Madison, WI, United States, ²Radiology, University of Wisconsin - Madison, Madison, WI, United States

Summary

4374



Computer #35 Intracranial vessel wall and cerebrovascular reactivity imaging provides evidence for mechanistic differences in atherosclerotic and non-atherosclerotic stenotic disease
Petrice M Cogswell¹, L Taylor Davis¹, Megan K Strother², Carlos C Faraco¹, Lori C Jordan³, Blaise deB Frederick⁴, Jeroen Hendrikse⁵, and Manus J Donahue¹

¹Radiology, Vanderbilt University, Nashville, TN, United States, ²DXP Imaging, Louisville, KY, United States, ³Neurology, Vanderbilt University, Nashville, TN, United States, ⁴McLean Hospital, Boston, MA, United States, ⁵University Medical Center Utrecht, Utrecht, Netherlands

No study to date has assessed the relationship between intracranial vessel plaque and wall thickening and its impact on tissue-level function. A novel intracranial vessel wall imaging protocol and BOLD imaging were applied in patients with intracranial stenosis secondary to atherosclerosis and moyamoya disease (non-atherosclerotic stenosis). The time of maximum correlation of BOLD data with the applied stimulus, the CVR time, calculated using a novel time regression technique, is prolonged in vascular territories with a proximal vessel wall lesion for both atherosclerosis and moyamoya patients. The maximum z-statistic, a qualitative metric of CVR, is decreased in vascular territories with a proximal vessel wall lesion in moyamoya patients only.

4375

Computer #36 Neurovascular Reactivity in Smokers and Nonsmokers Measured by High-Speed MR Flow Mapping During Volitional Apnea
Felix W Wehrli¹, Yongxia Zhou¹, Zachary B Rodgers¹, and Michael C Langham¹

¹Department of Radiology, University of Pennsylvania, Philadelphia, PA, United States

Smoking is well known to cause vasoconstriction as a result of the formation of reactive oxygen species, which reduce nitric oxide availability. Vasomotor reactivity can be measured in terms of the change in cerebral blood flow in response to a hypercapnic challenge. Here we measured the change in superior sagittal sinus flow at 2-second temporal resolution during breath-hold (a predominantly hypercapnic stimulus) and computed a breath-hold index (BHI) as the slope of the flow velocity-time curve in 20 nonsmokers and 13 chronic smokers. The data suggest reduced BHI in the smoking group (0.252±0.097 vs. 0.306±0.098 cm/s², p<0.07) indicative of dysregulation of vascular reactivity.

4376

Computer #37 Non-contrast enhanced 4D intracranial MR angiography based on pseudo-continuous arterial spin labelling (PCASL) with the keyhole technique
Makoto Obara¹, Osamu Togao², Tomoyuki Okuaki³, Shuhei Shibukawa⁴, Masami Yoneyama¹, and Marc Van Cauteren³

¹Healthcare, Philips Electronics Japan Ltd., Tokyo, Japan, ²Department of Clinical Radiology, Graduate School of Medical Science, Kyushu University, Fukuoka, Japan, ³Philips Healthcare, Tokyo, Japan, ⁴Department of Radiology, Tokai University Hospital, Kanagawa, Japan

A non-contrast enhanced intracranial three-dimensional dynamic magnetic resonance angiography (4D-MRA) based on pseudo-continuous arterial spin labelling with the keyhole technique (4D-PACK) was implemented. Images acquired from three volunteers were compared with the data acquired without the keyhole technique. We show that the 4D-PACK can accelerate acquisition speed, while keeping flow dynamics information.

4377



Computer #38 Feasibility of Combining Perforating Artery Imaging and Whole Brain Vessel Wall Imaging at 7T
Zihao Zhang^{1,2}, Qi Yang^{3,4}, Zhaoyang Fan³, Xianchang Zhang^{1,2}, Yujiao Yang⁴, Jing An⁵, Zhentao Zuo¹, and Rong Xue^{1,6}

¹State Key Laboratory of Brain and Cognitive Science, Beijing MR Center for Brain Research, Institute of Biophysics, Chinese Academy of Sciences, Beijing, China, People's Republic of, ²Graduate School, University of Chinese Academy of Sciences, Beijing, China, People's Republic of, ³Biomedical Imaging Research Institute, Cedars-Sinai Medical Center, Los Angeles, CA, United States, ⁴Xuanwu Hospital, Beijing, China, People's Republic of, ⁵Siemens Shenzhen Magnetic Resonance Ltd., Shenzhen, China, People's Republic of, ⁶Beijing Institute for Brain Disorders, Beijing, China, People's Republic of

In this study, we improved TOF-MRA and T1w-SPACE to a higher resolution for imaging perforating arteries and intracranial vessel walls at 7T. With the combination of the two techniques, we are for the first time able to depict the position of perforators and the vessel wall lesion in patients with ICAD. Small changes within the vessel wall may be revealed, and the certainty of the diagnosis may become better established, enabling better therapeutic management.

4378

Computer #39 High-resolution whole-brain intracranial vessel wall MRI at 3T: Technical considerations toward a clinically practical imaging approach to stroke etiology assessment
Zhaoyang Fan¹, Qi Yang^{1,2}, Zixin Deng^{1,3}, Shlee Song⁴, Xiuhai Guo⁵, Wouter Schievink⁶, Xiaoming Bi⁷, Gerhard Laub⁷, Patrick Lyden⁴, and Debiao Li^{1,3}

¹Biomedical Imaging Research Institute, Cedars-Sinai Medical Center, Los Angeles, CA, United States, ²Radiology, Xuanwu Hospital, Beijing, China, People's Republic of, ³Bioengineering, University of California, Los Angeles, CA, United States, ⁴Neurology, Cedars-Sinai Medical Center, Beijing, CA, United States, ⁵Neurology, Xuanwu Hospital, Beijing, China, People's Republic of, ⁶Neurosurgery, Cedars-Sinai Medical Center, Los Angeles, CA, United States, ⁷MR R&D, Siemens Healthcare, Los Angeles, CA, United States

High-resolution MR using variable-flip-angle 3D fast spin-echo (FSE) has emerged as a promising intracranial vessel wall imaging technique. However, its typical implementations on clinically available MR systems have several limitations. This work aimed to develop a 3D FSE-based method that allows for CSF-attenuated T1-weighted whole-brain vessel wall imaging within 8 min. Volunteer studies were performed during technical optimization. Preliminary clinical validation was conducted in patients with various vessel wall pathologies. The technique demonstrated excellent vessel wall delineation quality, diagnostic accuracy, and patient tolerance. It may potentially become a clinically practical imaging approach to stroke etiology assessment.

4379



Computer #40 Iterative algorithm for the temporal decomposition of the cerebrovascular reactivity dynamic response in neurovascular patients.
Marco Piccirelli¹, Christiaan Hendrik Bas van Niftrik², Oliver Bozinov², Athina Pangalu¹, Antonio Valavanis¹, Luca Regli², and Jorn Fierstra²

¹Department of Neuroradiology, University Hospital Zurich, Zurich, Switzerland, ²Department of Neurosurgery, University Hospital Zurich, Zurich, Switzerland

Our iterative algorithm evaluates transient phases of BOLD fMRI signal dynamics during a CO₂ pseudo-square wave challenge and optimizes CO₂ arrival time determination to increase sensitivity and reliability of cerebrovascular reactivity analysis. On 25 healthy controls and unilateral internal carotid occlusion patients, all BOLD-derived parameters maps are normalized in MNI space and combined for reference atlases and assess alterations within single patient. The transient phase durations, temporal delay maps and dynamic and static CVR maps were calculated. We determined the optimal CO₂ arrival time and found that excluding the transient phases resulted in the best fit to the physiological data.

4380

Computer #41 Patterns of bold signal responses to progressive hypercapnia enhance the interpretation of underlying cerebrovascular pathologies
Joseph A Fisher^{1,2,3}, Olivia Sobczyk¹, Adrian P Crawley⁴, Julien Poubanc⁴, Paul Dufort¹, Lashmi Venkatraghavan⁵, David J Mikulis^{1,4}, and James Duffin^{2,3}

¹Institute of Medical Sciences, University of Toronto, Toronto, ON, Canada, ²Department of Physiology, University of Toronto, Toronto, ON, Canada, ³Departments of Anaesthesia, University Health Network, Toronto, ON, Canada, ⁴Joint Department of Medical Imaging and the Functional Neuroimaging Laboratory, University Health Network, Toronto, ON, Canada, ⁵Department of Anaesthesia, University Health Network, Toronto, ON, Canada

We surveyed the varied patterns of BOLD changes in response to a ramp CO₂ stimulus ranging from hypocapnia to hypercapnia in 10 healthy individuals and 10 patients with steno-occlusive disease. The patterns of response fell into 4 types, based on the two linear slopes fitted to each range. Maps of these types on a voxel by voxel basis were compared to cerebrovascular reactivity (CVR) calculated as the linear slope over the whole ramp. We suggest that for assessing cerebrovascular reactivity, CVR and type scoring enhance the interpretation of each other, and that modeling the possible underlying patho/physiologies to explain the type patterns is the portal to further work.

4381

Evaluation of the cross flow for anterior communicating artery aneurysms using 4D-Flow MRI

Computer #42 Yoshiyuki Watanabe¹, Hiroto Takahashi¹, Hisashi Tanaka¹, Atsuko Arisawa¹, Chisato Matsuo¹, Eri Yoshioka¹, Hajime Nakamura², and Noriyuki Tomiyama¹

¹Radiology, Osaka University, Suita, Japan, ²Neurosurgery, Osaka University, Suita, Japan

The purpose of this study was to elucidate in vivo analysis of the flow dynamics of ACOM aneurysms from both A1 arteries using 4D-Flow and digital subtraction angiography (DSA). 2 out of 8 ACOM aneurysms showed intra-aneurysm flow from both A1 arteries and 6 other patients showed the unilateral A1 inflow. Inflow findings of all patients are consistent with 4D-Flow and DSA. 4D-FLOW MRI is able to visualize cross flow in ACOM aneurysms.

4382 Computer #43 Functional Reorganization of the Brain in Ischemic Stroke Patients after the Repetitive Transcranial Magnetic Stimulation: a fMRI Study
Jing Li¹, Xuewei Zhang², Jie Lu¹, Zhentao Zuo³, Rong Xue³, Yong Fan⁴, Yuzhou Guan⁵, and Weihong Zhang¹

¹Department of Radiology, Peking Union Medical College Hospital, Peking Union Medical College, Beijing, China, People's Republic of, ²Department of Interventional Radiology, China Meitan General Hospital, Beijing, China, People's Republic of, ³State Key Laboratory of Brain and Cognitive Science, Beijing MR Center for Brain Research, Institute of Biophysics, Chinese Academy of Sciences, Beijing, China, People's Republic of, ⁴Department of Radiology, School of Medicine, University of Pennsylvania, Philadelphia, PA, United States, ⁵Department of Neurology, Peking Union Medical College Hospital, Peking Union Medical College, Beijing, China, People's Republic of

It is a resting-state fMRI(rs-fMRI) study of patients with motor disturbance after acute ischemic stroke. We assessed the functional connectivity (FC) changes of the ipsilesional primary motor cortex (M1) within the brain before and after the repetitive transcranial magnetic stimulation (rTMS) by rs-fMRI. The research not only gave theoretical support of the rTMS treatment in stroke patients but also investigated the cerebral functional changes in motor recovery.

4383 Computer #44 Evaluation of perfusion and hypoxia parameters in healthy subjects and patients with high-grade carotid artery stenosis
Stephan Kaczmarz¹, Jens Göttler¹, Anne Kluge¹, Dimitrios C. Karampinos², Claus Zimmer¹, and Christine Preibisch^{1,3}

¹Department of Neuroradiology, Technische Universität München, Munich, Germany, ²Department of Radiology, Technische Universität München, Munich, Germany, ³Clinic for Neurology, Technische Universität München, Munich, Germany

Severe intracranial arterial stenosis (SIAS) is a major health issue as it often accounts for strokes. Here, we present preliminary data from a clinical study in patients with SIAS compared to healthy controls. The major aim was to evaluate the reliability of perfusion and oxygenation related measures by analyzing their hemispheric symmetry to assess their potential diagnostic capabilities. Preliminary results imply symmetry of all measures between hemispheres of healthy controls. Regarding patients, only pCASL-based CBF implies a reduced perfusion on the side of carotid artery stenosis which is in accordance to recent literature and is currently under further investigation.

4384 Computer #45 Arterial Spin Labeling MRI Evaluation of Cerebrovascular Reserve with Acetazolamide in Patients with Sickle Cell Disease
Lena Václavů¹, Henk Mutsaerts², Pim van Ooij¹, Bart J Biemond³, John C Wood⁴, Charles BLM Majoie¹, Ed van Bavel⁵, and Aart J Nederveen¹

¹Radiology, Academic Medical Center, Amsterdam, Netherlands, ²Sunnybrook Research Institute, Toronto, ON, Canada, ³Internal Medicine, Academic Medical Center, Amsterdam, Netherlands, ⁴Cardiology, Children's Hospital Los Angeles, Los Angeles, CA, United States, ⁵Biomedical Engineering and Physics, Academic Medical Center, Amsterdam, Netherlands

Arterial spin labelling perfusion MRI was employed with an acetazolamide challenge to probe the cerebrovascular physiology in patients with sickle cell disease and matched controls. Cerebral blood flow was estimated at baseline and cerebrovascular reserve(CVR) was calculated after vasodilation with acetazolamide. We found that patients had limited CVR compared to controls, and that the patients with the highest CBF at baseline also had the smallest response to acetazolamide. ASL-based CBF measurements with ACZ showed robust CVR results indicating the cerebral hemodynamics of some patients may be impaired.

4385 Computer #46 Amide Proton Transfer-Weighted MR Imaging Signal as Predictor of Non Thrombolysis Treatment Efficiency for Stroke
Chunmei Li¹, Guodong Song¹, Yuhui Chen¹, Xuna Zhao², Jinyuan Zhou², and Min Chen¹

¹Beijing Hospital, Beijing, China, People's Republic of, ²Johns Hopkins University, Baltimore, MD, United States

This study is to evaluate the longitudinal Amide Proton Transfer-weighted (APT_w) signal changes in patients with stroke after treatment. APT weighted images of stroke patients was acquired, including non-treatment and post treatment. 91.7% patients (22/24) showed gradual increased APT values with the extension of time, accompanied with the clinical symptoms improvement. The other 2 patients (8.3%) showed further decreased APT values in the second scan (the first scan after treatment), accompanied with the clinical symptoms aggravation. The increase of APT weighted signal may indicate the improvement of clinical symptoms while the decrease may indicate the aggravating of clinical symptoms.

4386 Computer #47 Diffusion kurtosis imaging for preliminary analysis of micro-structural changes of brain tissue affected by acute ischemic stroke
LiuHong Zhu¹, Zhongping Zhang², Qihua Cheng¹, Phillip Zhe Sun³, and Gang Guo¹

¹Radiology, Xiamen Second Hospital, Xiamen, China, People's Republic of, ²MR Research China, GE Healthcare, Beijing, China, People's Republic of, ³Athinoula A. Martinos Center for Biomedical Imaging, Department of Radiology, Massachusetts General Hospital and Harvard Medical

School, Charlestown, MA, United States

One hundred and thirteen patients with acute ischemic stroke underwent DKI sequence scanning. 131 lesions were outlined and divided into six groups. The changed percentages of DKI indices (FA%, MD%, Da%, Dr%, MK%, Ka%, Kr%) relative to normal contra-lateral ROI were computed. The statistical analysis results illustrated that there was a trend that when the acute ischemic stroke affected tissue mostly contained white matter, the complexity of micro-structure changes of the tissue was much higher than other affected locations. Also, the kurtosis-derived parameters presented to have greater potential in distinguishing each group.

4387
Computer #48 Evaluation of Retrograde Embolization in Cryptogenic Stroke by Aortic 4D flow MRI and 3D TOF MRA
Michael Markl¹, Edouard Semaan¹, LeRoy Stromberg¹, James Carr¹, Shyam Prabhakaran¹, and Jeremy Collins¹

¹Northwestern University, Chicago, IL, United States

The purpose of this study was to employ aortic 4D flow MRI and brain TOF MRA for the evaluation of retrograde diastolic flow from the descending aorta into the supra-aortic vessels as a mechanism for embolic stroke. In 35 cryptogenic stroke patients, 4D flow MRI demonstrated close to 50% concordance with stroke location on imaging with retrograde diastolic flow into the feeding vessels of the affected cerebral area, identifying a potential etiology for cryptogenic stroke. Our findings further document the importance of taking into account variants in cerebrovascular anatomy which identified retrograde embolization risk in an additional 14% of subjects.

Electronic Poster

Spine Imaging

Exhibition Hall

Thursday, May 12, 2016: 13:30 - 14:30

4388
Computer #49 Characterization of Regional and Longitudinal Changes in Z-spectra of Spinal Cord Injury
Feng Wang^{1,2}, Zhongliang Zu^{1,2}, Tung-Lin Wu^{2,3}, John C. Gore^{1,2,3}, and Li Min Chen^{1,2}

¹Radiology and Radiological Sciences, Vanderbilt University, Nashville, TN, United States, ²Institute of Imaging Science, Vanderbilt University, Nashville, TN, United States, ³Biomedical Engineering, Vanderbilt University, Nashville, TN, United States

Non-human primates provide a valuable pre-clinical model for studying spinal cord injuries. Here we examine the fingerprints in the Z-spectra of abnormal tissues and cysts surrounding the lesion site after spinal cord injury, regionally and longitudinally. Characteristic chemical exchange saturation transfer (CEST) and nuclear Overhauser enhancement (NOE) effects extracted from Z-spectra may enable the non-invasive assessment of spontaneous recovery from traumatic injury.

4389
Computer #50 In Vivo Proton Magnetic Resonance Spectroscopy Reveals Metabolite Changes in a Rat Model of Kainic Acid Induced Spinal Cord Injury
Mingming Zhu¹, Alice H Shum-Siu², Emily Martin³, David S Magnuson², and Chin K Ng¹

¹Department of Diagnostic Radiology, University of Louisville School of Medicine, Louisville, KY, United States, ²Departments of Neurological Surgery, Anatomical Sciences & Neurobiology, and Bioengineering, University of Louisville School of Medicine, Louisville, KY, United States, ³Department of Bioengineering, University of Louisville School of Medicine, Louisville, KY, United States

Current study was to focus on the proton MRS detection of metabolite profile of spinal cord gray matter just caudal to a kainic acid injury in rats 14 days after administration of the excitotoxic agent, and further to correlate the MRS findings to the histopathology of the animal model. Quantitative evaluations of different metabolites were also performed to identify potential MR based biomarkers of neurotoxicity.

4390
Computer #51 In vivo T1 mapping of the spinal cord using a reduced Field-of-View Inversion Recovery sequence (IR-ZOOM-EPI)
Marco Battiston¹, Torben Schneider², Claudia Angela Michela Gandini Wheeler-Kingshott^{1,3}, and Rebecca S Samson¹

¹NMR Research Unit, Queen Square MS Centre, Department of Neuroinflammation, UCL Institute of Neurology, University College London, London, United Kingdom, ²Philips Healthcare, Guildford, United Kingdom, ³Brain Connectivity Center, C. Mondino National Neurological Institute, Pavia, Italy

The T₁ relaxation time is a fundamental quantitative Magnetic Resonance parameter widely used to characterize healthy and pathological tissue. However, investigation of quantitative T₁ in the human spinal cord has been limited to date. In this work, we propose a scan time efficient protocol in the spinal cord for Inversion Recovery T₁ mapping, which is considered the "gold-standard" method. The mean (± standard deviation) T₁ for white matter and grey matter in the cervical spinal cord were found to be respectively 1096 (±26) ms and 1153 (±24) ms.

4391
Computer #52 Demyelination and remyelination: frequency shift assessment in lysolecithin rat model
Evan I Wen Chen¹, Andrew Yung², Barry Bohnet¹, Alexander Rauscher^{1,3}, and Piotr Kozlowski^{1,3}

¹MRI Research Center, University of British Columbia, Vancouver, BC, Canada, ²Research Scientist, University of British Columbia, Vancouver, BC, Canada, ³Radiology, University of British Columbia, Vancouver, BC, Canada

GRE images provide strong gray/white matter contrast that is determined by the local MR resonance frequency, which has been shown to be strongly influenced by the local tissue microstructure. While studies have looked at well-defined architectures in rat spinal cord to study this biophysical mechanism, the specific effects of axon/myelin microstructure on frequency shifts is difficult to evaluate independently. Using lyssolecithin to induce chemical demyelination while preserving axonal integrity, we assess predominantly myelin-related effects on frequency shifts in rat dorsal column as it demyelinates/remyelinates, providing insight important to applications of frequency shift mapping to demyelinating diseases such as multiple sclerosis.

-
- 4392
Computer #53 A comprehensive assessment of cervical cord lesions in patients with multiple sclerosis on T1-MPRAGE at 3T: relationship with cord atrophy and disability
Paola Valsasina¹, Maria Assunta Rocca¹, Paolo Preziosa¹, Mohammad Ahmad Abdullah Ali Aboulwafa^{1,2}, Mark Andrew Horsfield³, Giancarlo Comi⁴, Andrea Falini⁵, and Massimo Filippi¹
- ¹Neuroimaging Research Unit, San Raffaele Scientific Institute, Vita-Salute San Raffaele University, Milan, Italy, ²Clinical Neurology Department, Faculty of Medicine, Al-Azhar University, Cairo, Egypt, ³Xinapse System Ltd, West Bergholt, Essex, United Kingdom, ⁴Department of Neurology, San Raffaele Scientific Institute, Vita-Salute San Raffaele University, Milan, Italy, ⁵Department of Neuroradiology, San Raffaele Scientific Institute, Vita-Salute San Raffaele University, Milan, Italy
- In this study, we performed a comprehensive assessment of cervical cord lesions in 133 patients with multiple sclerosis (MS) on 3D T1-weighted scans at 3.0 T. Lesion occurrence, regional distribution, influence on cord atrophy and disability were evaluated. T1 lesions were detected in a large proportion (85%) of MS patients, with a higher frequency of cord lesions in the progressive than in the relapsing forms of the disease. There was only a modest correlation between cord T1 lesions and atrophy. Both cord T1 lesions and atrophy were significant and independent contributors to patient disability.
-
- 4393
Computer #54 Single acquisition multiple contrast spine MRI using accelerated quantitative mapping
Suchandrima Banerjee¹, Ken-Pin Hwang^{2,3}, Peng Lai¹, Marcel Warntjes⁴, and Ajit Shankaranarayanan¹
- ¹Global MR Applications & Workflow, GE Healthcare, Menlo Park, CA, United States, ²Global MR Applications & Workflow, GE Healthcare, Houston, TX, United States, ³Department of Imaging Physics, University of Texas M.D. Anderson Cancer Center, Houston, TX, United States, ⁴Synthetic MR Technologies AB, Stockholm, Sweden
- Recently, several techniques for rapid simultaneous mapping of proton density and T1, T2 relaxation parameters from a single acquisition and generation of synthetic images of any desired image contrast have been demonstrated, mostly in the brain. Such an approach could potentially shorten a spine MRI exam which typically consists of multiple 2D acquisitions with different contrast weightings. But even routine spine MRI is fraught with technical challenges such as motion and inhomogeneity. So in this work we explore the feasibility of obtaining synthetic MRI images of usable image quality in the spine using a 2D quantitative mapping technique.
-
- 4394
Computer #55 Detection of Stellate Ganglion and Thoracic Sympathetic Chain Ganglia on Non-contrast CISS MRI
Ammar Chaudhry¹, Arash Kamali², Daniel Herzka³, Kenneth C Wang⁴, John carrino⁵, and Ari Blitz²
- ¹Diagnostic Radiology, Johns Hopkins Medical Institute, Elkridge, MD, United States, ²Neuroradiology, Johns Hopkins Medical Institute, Baltimore, MD, United States, ³Radiology, Johns Hopkins Medical Institute, Baltimore, MD, United States, ⁴Radiology, Johns Hopkins, Baltimore, MD, United States, ⁵Radiology, Hospital of Special Surgery, New York, NY, United States
- Thoracic sympathetic chain ganglia can be readily seen and well characterized on pre-contrast 3D-CISS MRI. This technique can aid in initial evaluation of potential stellate and/or SCG pathology as well allow for post-treatment follow-up.
-
- 4395
Computer #56 Magnetisation Transfer Ratio (MTR) Measurements in the Lumbar cord: A Pilot Study using ZOOM-EPI at 3T
Rebecca Sara Samson¹, Marco Battiston¹, Claudia Angela Michela Gandini Wheeler-Kingshott^{1,2}, and Marios C Yiannakas¹
- ¹NMR Research Unit, Queen Square MS Centre, Department of Neuroinflammation, UCL Institute of Neurology, University College London, London, United Kingdom, ²Brain Connectivity Center, C. Mondino National Neurological Institute, Pavia, Italy
- The Magnetisation Transfer Ratio (MTR), and quantitative Magnetisation Transfer (MT) parameters have proven to be sensitive to the diseased spinal cord (SC), however in vivo quantitative imaging of the cord is challenging. Rapid acquisition sequences such as Echo Planar Imaging (EPI) are desirable but may suffer from artefacts and image distortions. Here we present results from the use of single-shot ZOOM-EPI to reduce acquisition time and distortions in SC MTR mapping. The mean SC MTR value for 9 subjects was 38.8 (±4.05). The mean scan-rescan coefficient of variation for measuring SC MTR (from 5 subjects) was 4.39%.
-
- 4396
Computer #57 Functional connectivity in spinal cord for clinical translation
Robert L Barry^{1,2}, Benjamin N Conrad¹, Seth A Smith^{1,2}, and John C Gore^{1,2}
- ¹Vanderbilt University Institute of Imaging Science, Nashville, TN, United States, ²Department of Radiology and Radiological Sciences, Vanderbilt University Medical Center, Nashville, TN, United States
- Spinal cord functional magnetic resonance imaging studies have previously used task-based paradigms, but we recently showed the existence of resting state networks within the cord at 7 Tesla. More recently we have successfully translated the acquisition, preprocessing, and analysis methods developed at 7 Tesla to more clinically relevant 3T scanners. Our results suggest that a run of approximately 6 mins is sufficient at 3T if resting state signals undergo bandpass filtering with frequencies up to 0.17 Hz. Thus,

functional connectivity measures in the cervical cord are practical for widespread clinical applications for studying diseases of the central nervous system.

- 4397
Computer #58 MRI of the thoracic spinal cord in multiple sclerosis at 7T
Jennifer Lefeuve^{1,2}, Qi Duan¹, Jacco A de Zwart¹, Peter van Gelderen¹, Stéphane Lehericy², Steven Jacobson¹, Daniel S Reich¹, and Govind Nair¹

¹NINDS, NIH, Bethesda, MD, United States, ²INSERM U1127/CNRS UMR7225, CENIR, Brain and Spine Institute, Paris, France

MRI of the thoracic spinal cord (t-spine) is challenging especially due to motion, flow, and susceptibility artifacts. Improving the image quality and resolution in t-spine has the potential to improve visualization of anatomy, as well as lesions in neurodegenerative diseases such as multiple sclerosis (MS). Towards this end, we have developed high-resolution t-spine imaging techniques at 7T with a custom built RF transmit-receive coil and navigator based frequency correction.

- 4398
Computer #59 Spinal Perimedullary Vein Enlargement Sign: An Added Value for the Differentiation between Intradural-Extramedullary and Intramedullary Tumors on MR Imaging
Tao Gong¹, Guangbin Wang¹, and Weibo Chen²

¹Shandong University, Jinan, China, People's Republic of, ²Shanghai, China, People's Republic of

Magnetic resonance imaging (MRI) is widely used to narrow the differential diagnosis in the preoperative study of spinal cord tumors. The use of a medium in MRI is preferred to improve visualization of tumor's intrinsic characteristics and boundaries, and to identify reactive changes (such as cysts and dilated veins) in adjacent tissues. Most times, it is easy to determine whether a lesion arises from the spinal cord itself or from the IDEM space according to common MRI findings, however, at other times, this might be difficult. There have been reported cases of schwannoma located at IDEM space misdiagnosed with IMT. Thus, radiologists must discern the characteristic imaging features of IDEMs to distinguish them from IMTs. The presence of vein enlargement is often a sign in some cases of intradural spinal tumors, most of which are extramedullary. A perimedullary vein enlargement sign around an intradural spinal tumor (without dilated veins in the tumor) has not been reported, which might be an imaging mark to differentiate IDEMTs from IMTs. The purpose of this study was to determine the added value of the perimedullary spinal vein enlargement sign on MRI in helping to distinguish IDEMTs from IMTs.

- 4399
Computer #60 Comparison of 3D FSE Cube and 3D Fiesta-c sequences for image contrasts of the tissues on T2-weighted images in cervical spine MRI
Yumi Koizumi¹, Masaru Sonoda¹, Tsutomu Inaoka², Hideki Nagatomo¹, and Hitoshi Terada²

¹Division of Radiology, Seirei Sakura Citizen Hospital, Sakura, Japan, ²Department of Radiology, Toho University Sakura Medical Center, Sakura, Japan

Currently, various 3D MR sequences such as 3D FSE, GRE, and steady-state sequences have been developed and used to obtain MR images of submillimeter thicknesses in the spine. However, the question, "which 3D sequence has a better image contrast of the tissues in spinal MRI?", has come up. Therefore, we examined optimal imaging parameters of variable refocus flip angle 3D FSE (Cube) and 3D Fiesta-c sequences for T2-weighted images in cervical spine MRI and compared the two different 3D sequences for better image contrasts of the tissues on T2-weighted images in cervical spine MRI. In conclusion, 3D FSE Cube T2-weighted images has excellent image contrasts between the spinal cord versus other tissues except cerebrospinal fluid, vertebral body, and subcutaneous fat in the cervical spine compared to 3D Fiesta-c T2-weighted images. Therefore, 3D FSE Cube sequence is believed to be more appropriate for T2-weighted images in cervical spine MRI compared to 3D Fiesta-c sequence.

- 4400
Computer #61 fMRI of lumbar spinal cord during electrical stimulation in diabetic patients
Zhiwei Shen¹, Yanlong Jia¹, Tingting Nie¹, Tao Zhang¹, Gen Yan¹, and Renhua Wu¹

¹The 2nd Affiliated Hospital of Shantou University Medical College, Shantou, China, People's Republic of

Diabetic peripheral neuropathy (DPN) is one of the main complications of long-term diabetes and the incidence is 60% to 90%. However, there is no objective noninvasive method to detect the degree of damage of DPN and its pathogenesis remains unknown. Functional magnetic resonance imaging (fMRI) has the advantages of high spatial and temporal resolution, which had been used to detect neuron activity. In this study, the activation in the lumbar spinal cord of by electric stimulation were detected. Elevated activation percentage changes of DPN were found and the activation changes have the correlated relationship with blood biochemical indexes such as glucose, the total cholesterol and haemoglobin A1c.

- 4401
Computer #62 The feasibility study of imaging lumbosacral spinal nerve roots by IDEAL sequence at 3.0T MR
Lihua Sun¹, Yunlong Song², Huisheng Zheng¹, and Lizhi Xie³

¹Radiology Department, The Second Affiliated Hospital of Anhui Medical University, HeFei, China, People's Republic of, ²Department of CT & MRI, Air Force General Hospital, Beijing, China, People's Republic of, ³GE Healthcare, MR Research China, Beijing, Beijing, China, People's Republic of

The IDEAL acquisition can generate a water, fat, in-phase and out-phase data sets for clear tissue differentiation in a single sequence. It offers a great opportunity for imaging the nerve root compression. In this work, we demonstrated the feasibility of IDEAL sequence to image the anatomic structure and the whole contour of the lumbosacral nerve roots as well as the microstructural of lumbosacral nerve

on the canals of lumbar spinal nerves is possible. IDEAL imaging on lumbosacral nerve roots can be valuable for clinical diagnosis to estimate the nerve compression, and provide detailed information for the right treatment at early-stage.

-
- 4402
Computer #63
Reduced Field-of-View Diffusion-Weighted Imaging of the Lumbosacral Enlargement: A Pilot In Vivo study of the healthy spinal cord using a clinical 3T MR system
Marios C Yiannakas¹, Polymnia Louka¹, Francesco Grussu¹, Ferran Prados^{1,2}, Rebecca S Samson¹, Marco Battiston¹, Sebastien Ourselin², David H Miller^{1,3}, and Claudia Angela Michela Gandini Wheeler-Kingshott^{1,4}
- ¹NMR Research Unit, Queen Square MS Centre, Department of Neuroinflammation, UCL Institute of Neurology, University College London, London, United Kingdom, ²Translational Imaging Group, Medical Physics and Biomedical Engineering, University College London, London, United Kingdom, ³NIHR Biomedical Research Centre, UCL-UCLH, London, United Kingdom, ⁴Brain Connectivity Center, C. Mondino National Neurological Institute, Pavia, Italy
- The use of imaging methods to study the lower spinal cord has been hindered by a number of technical challenges; hence the relative contribution of pathology affecting the lower spinal cord to the observed clinical symptoms remains largely unexplored. In this pilot study, we investigate the feasibility of obtaining tissue-specific (grey matter and white matter) diffusion tensor imaging metrics within the lumbosacral enlargement in vivo in healthy volunteers using reduced field-of-view echo planar imaging on a clinical 3T MRI system. Preliminary results show that such measures may be obtained reliably and within clinically acceptable scan times.
-
- 4403
Computer #64
Right-handedness is associated with myelination asymmetry of the motor tracts in the human spinal cord
Manuel Taso^{1,2,3,4}, Oliver M. Girard^{1,3}, Guillaume Duhamel^{1,3}, Maxime Guye^{1,3}, Jean-Philippe Ranjeva^{1,3,4}, and Virginie Callot^{1,3,4}
- ¹CRMBM UMR 7339, Aix-Marseille Université, CNRS, Marseille, France, ²LBA UMR T 24, Aix-Marseille Université, IFSTTAR, Marseille, France, ³CEMEREM, AP-HM, Pôle d'imagerie médicale, Marseille, France, ⁴Lab-Spine international associate laboratory, Marseille/Montréal, France
- Handedness is known to influence brain structure. However, no evidences of such influence in the spinal cord (SC) exist. Hence, we propose to use multi-parametric MRI (DTI and inhomogeneous MT, both sensible to microstructural properties), combined with atlas-based analysis in specific fascicles, to assess the influence of handedness on the SC structure. Results demonstrated that right-handers presented higher ihMTR/MTR values in the right motor tracts, suggesting an asymmetric myelination while left-handers did not present differences between left and right regions. This is consistent with brain findings suggesting that right-handedness is associated with higher structural asymmetry in the central nervous system.
-
- 4404
Computer #65
Ultra-high-resolution postmortem imaging of marmoset EAE spinal cords
Jennifer Lefeuve^{1,2}, Joseph R Guy¹, Nick Luciano¹, Emily Leibovitch¹, Mathieu D Santin², Afonso C Silva¹, Steve Jacobson¹, Stéphane Lehericy², Daniel S Reich¹, and Pascal Sati¹
- ¹NINDS, NIH, Bethesda, MD, United States, ²INSERM U1127/CNRS UMR7225, CENIR, Brain and Spine Institute, Paris, France
- Multiple sclerosis (MS) is a demyelinating disease that affects the entire central nervous system, with more than 90% of patients showing focal or diffuse abnormalities in the spinal cord (SC). Experimental autoimmune encephalomyelitis (EAE) in marmosets is an attractive animal model of MS due to its radiological presentation with brain lesions that mimic MS¹. However, spinal cord lesions in marmoset EAE have not yet been well characterized. The proposed methodology allows high-quality, high-resolution imaging of SC lesions in autopsied marmosets with EAE. The artifact-free images allowed accurate detection of focal and confluent rim lesions along the edges of the SC.
-
- 4405
Computer #66
Multiband Excitation Enables Diffusion Tensor Imaging of Brain Stem and Cervical Spinal Cord in Clinically Feasible Scan Times at 3T
Samantha By^{1,2}, Ed Mojahed^{2,3,4}, Robert L. Barry^{2,4}, and Seth A. Smith^{2,4}
- ¹Biomedical Engineering, Vanderbilt University, Nashville, TN, United States, ²Vanderbilt University Institute of Imaging Science, Vanderbilt University, Nashville, TN, United States, ³Phillips Healthcare, Cleveland, OH, United States, ⁴Radiology and Radiological Sciences, Vanderbilt University, Nashville, TN, United States
- Multiband excitation with diffusion tensor imaging (DTI) was implemented at 3T to enable characterization of the cervical spinal cord and brainstem in a clinically feasible scan time. The efficiency of the multiband acquisition (9 minutes) was compared to a standard acquisition (18 minutes), which included all of the same parameters except no multiband was applied. Results with multiband generated high-resolution images with similar SNR to the standard (whole cord: multiband – 6.60, no multiband – 6.14). Additionally, DTI measurements from the multiband acquisition were in good agreement to the standard, yielding a percent difference of less than 3% for the cervical spine.
-
- 4406
Computer #67
Diffusion basis spectrum imaging (DBSI) reveals axon loss on spinal cord in RRMS and NMO
Peng Sun¹, Kim J. Griffin¹, Robert T. Naismith², Anne H. Cross², and Sheng-Kwei Song¹
- ¹Radiology, Washington University in St. Louis, St. Louis, MO, United States, ²Neurology, Washington University in St. Louis, St. Louis, MO, United States
- DTI failed to detect the extent of axonal loss which plays a significant role in irreversible neurological impairments in MS and NMO patients. Our results suggest diffusion basis spectrum imaging (DBSI) may serve as a useful method to quantify the extent of axonal loss and confounding pathologies in RRMS and NMO.

-
- 4407
Computer #68 Correlation of DTI Metrics to Spinal Cord Cross Sectional Area in Pediatric Subjects with Spinal Cord Injury
Devon M Middleton¹, Shiva Shahrapour¹, Scott H Faro¹, Sona Saksena², Mahdi Alizadeh¹, Chris J Conklin², Winston Liu³, Govind Nair⁴, Laura Krisa², MJ Mulcahey², and Feroze B Mohamed²
- ¹Temple University, Philadelphia, PA, United States, ²Thomas Jefferson University, Philadelphia, PA, United States, ³University of Maryland, College Park, MD, United States, ⁴National Institutes of Health, Bethesda, MD, United States*
- As more advanced imaging techniques are used for the spinal cord (such as DTI) it is important to examine potential relationships to other injury biomarkers. This study was to examine correlations between DTI metrics and spinal cord cross sectional area in pediatric subjects with spinal cord injury. Cord cross section data was acquired using a recently developed technique for semi-automated spinal cord segmentation and measurement of spinal cord cross sectional area. Fractional anisotropy was found to be strongly significantly correlated with spinal cord cross sectional area in the injured subjects.
-
- 4408
Computer #69 A Simple and Fast Approach for Spinal Cord Imaging at 3T with High In-Plane Resolution and Good Contrast
Matthias Weigel¹ and Oliver Bieri¹
- ¹Dept. of Radiology, Radiological Physics, University of Basel Hospital, Basel, Switzerland*
- For fast spinal cord images of high in-plane resolution and estimable contrast, an image combination of different inversion recovery (IR) prepared balanced steady state free precession (bSSFP) images acquired by a Modified Look Locker IR (MOLLI) sequence with fixed RR-intervals is suggested. The strength of the approach lies in its simplicity and that for short acquisition times of currently about 2mins per slice already a good contrast can be achieved at the high in-plane resolution of 0.4mm.
-
- 4409
Computer #70 Multisite feasibility study of spinal cord gray matter and total cord areas measurements on 2D Phase Sensitive Inversion Recovery images
Nico Papinutto¹, Esha Datta¹, Alyssa H Zhu¹, Julio Carballido-Gamio², Regina Schlaeger^{1,3}, Sinyeob Ahn⁴, Kevin Johnson⁴, Lara Stables⁵, William A Stern¹, Gerhard Laub⁴, and Roland G Henry¹
- ¹Neurology, University of California San Francisco, San Francisco, CA, United States, ²Radiology and Biomedical Imaging, University of California San Francisco, San Francisco, CA, United States, ³Neurology, University Hospital Basel, University of Basel, Basel, Switzerland, ⁴Siemens Healthcare USA, San Francisco, CA, United States, ⁵Neuroscience Imaging Center, University of California San Francisco, San Francisco, CA, United States*
- The goal of the present work was to test the reliability of the C2-C3 spinal cord gray matter and total cord areas measurements performed using a 2D-PSIR sequence. Nine healthy subjects were scanned twice with repositioning in between the scans (test/retest) on three different 3T scanners with different hardware. On the phase sensitive-reconstructed images, total cord area was measured in a semi-automated way and gray matter area was estimated by using an automatic segmentation method. Evaluations of contrast to noise ratio, intra-scanner and inter-scanner reliability suggest that multicenter studies using a 2D-PSIR sequence are feasible.
-
- 4410
Computer #71 Automatic Gray Matter Segmentation of the Spinal Cord in 2D Phase-Sensitive Inversion Recovery Images
Esha Datta¹, Nico Papinutto¹, Regina Schlaeger¹, Julio Carballido-Gamio¹, Alyssa Zhu¹, and Roland G Henry¹
- ¹UCSF, San Francisco, CA, United States*
- This study demonstrates the accuracy and reliability of a new method for automatic segmentation of spinal cord gray matter in 2D PSIR images at 3T of the C2-C3 spinal cord level in healthy controls. This method deforms an initial contour, based on registration from a template, using an active contours algorithm to ultimately obtain the final gray matter segmentation. When comparing the automatic segmentations with manual segmentations in 12 subjects, the Dice coefficients ranged from .82 to .93, with an average of .88. In 8 additional subjects that were scanned twice, the percent changes ranged from 1% to 6%.
-
- 4411
Computer #72 Towards Tissue Characterization of the Spinal Cord: High-Resolution T1 Relaxometry with Precise B1+-Mapping of the Spinal Cord at 3T
Matthias Weigel¹, Orso Pusterla¹, Monika Gloor¹, and Oliver Bieri¹
- ¹Dept. of Radiology, Radiological Physics, University of Basel Hospital, Basel, Switzerland*
- A high-resolution T1 mapping protocol for the spinal cord (SC) based on ultra-fast RF spoiled gradient echo sequences with initial precise B1-Tx mapping was developed. The measured T1 values for white matter (WM-SC) of 976ms and for gray matter (GM-SC) of 1154ms deviate notably from the corresponding T1 values found for the human cerebellum at 3T. This finding may partially explain the relatively low contrast between GM-SC and WM-SC frequently observed in SC imaging. Furthermore, the knowledge of these precise T1 values will allow to set up dedicated SC imaging protocols with an optimized GM-SC/WM-SC contrast in the future.
-

-
- 4412
Computer #73
- Improving the Quality of Neonatal Brain Structural MRI with Shorter Acquisition Train Length
Lili He¹, Jinghua Wang², Mark Smith³, Zhong-Lin Lu², and Nehal A Parikh^{1,4}
- ¹Center for Perinatal Research, Nationwide Children's Hospital, Columbus, OH, United States, ²The Ohio State University, Columbus, OH, United States, ³Radiology, Nationwide Children's Hospital, Columbus, OH, United States, ⁴Department of Pediatrics, The Ohio State University College of Medicine, Columbus, OH, United States*
- Three-dimensional (3D) T₁-weighted sequences such as MP-RAGE are invaluable for evaluation of neonatal and infant brain injury/development. Sequence optimization for neonates has been historically challenging because neonatal brains exhibit reversed white matter–gray matter (WM-GM) contrast on T₁-weighted scans, and the contrast is much lower than that of adult brains. In this study, we show in preterm neonates that shortening the acquisition train length of the MP-RAGE sequence significantly improved SNR and CNR efficiencies. The proposed optimization methodology can be easily extended to other populations (e.g. term infants, adults and elders), and different organs, field strengths and MR sequences.
-
- 4413
Computer #74
- HASTE imaging with EPI volumetric navigators for real-time fetal head motion detection
Borjan Gagoski^{1,2}, Patrick McDaniel³, André J. W. van der Kouwe^{2,4}, Himanshu Bhat⁵, Lawrence L. Wald^{2,4,6}, Elfar Adalsteinsson^{3,6}, P. Ellen Grant^{1,2}, and M. Dylan Tisdall^{2,4}
- ¹Fetal Neonatal Neuroimaging and Developmental Science Center, Boston Children's Hospital, Boston, MA, United States, ²Radiology, Harvard Medical School, Boston, MA, United States, ³Electrical Engineering and Computer Science, Massachusetts Institute of Technology, Cambridge, MA, United States, ⁴Athinoula A. Martinos Center for Biomedical Imaging, Massachusetts General Hospital, Charlestown, MA, United States, ⁵Siemens Medical Solutions USA Inc, Charlestown, MA, United States, ⁶Harvard-MIT Health Sciences and Technology, Institute of Medical Engineering and Science, Massachusetts Institute of Technology, Cambridge, MA, United States*
- Although heavily used in clinical fetal imaging due to its encoding efficiency, the image quality of T₂-weighted single-shot fast-spin-echo (ss-FSE, or HASTE) acquisitions is often compromised by fetal head motion. We have implemented and tested an enhanced version of the HASTE acquisition scheme that includes EPI-based volumetric navigators (EPI-vNavs) played each TR, enabling detection and estimation of fetal head motion along six degrees of freedom in real time, while maintaining equivalent T₂ contrast in the fetal head compared to the original HASTE acquisition.
-
- 4414
Computer #75
- Free-breathing T1-weighted gradient-echo imaging for fetus brain
bin zhang¹
- ¹Department of Radiology, Xijing Hospital, xi'an, China, People's Republic of*
- Magnetic resonance (MR) imaging appears to be increasing used for the diagnosis of abnormalities in fetuses because of the absence of ionizing radiation and superior contrast of soft tissues. However, the T₁-weighted 3D MR imaging for fetus remains very challenging due to the respiratory motion of the mother and the movement of the fetus. In this study, we evaluated the feasibility of a free-breathing 3D T₁-weighted gradient-echo imaging with radial data sampling for fetus imaging, and compared with a standard breath-hold imaging with Cartesian k-space acquisition
-
- 4415
Computer #76
- HARDI Acquisition in Neonates and Children using Modular Multiband Multi-shell Sequence
Vincent Kyu Lee¹, Meredith Monsour², Sudhir Pathak², Vincent Schmithorst³, Catherine Fissell², Ashok Panigrahy^{1,3}, and Walt Schneider²
- ¹Radiology, University of Pittsburgh, Pittsburgh, PA, United States, ²University of Pittsburgh, Pittsburgh, PA, United States, ³Children's Hospital of Pittsburgh, Pittsburgh, PA, United States*
- High angular-resolution diffusion imaging (HARDI) is the best imaging technique to distinguish crossing fibers and high turning angle neuronal tracts, which is critical for identifying and characterizing the microstructural changes in neuro pathology and traumatic brain injury. Its main disadvantage has been the lengthy scan time needed to acquire analyzable images – a challenge especially in children and neonates who do not tolerate long scanning sessions. This study presents the preliminary fiber tractography of healthy neonatal and pediatric subjects acquired using multiband multi-shell HARDI sequence within a practicable scan time without sacrificing image quality.
-
- 4416
Computer #77
- Gender-specific attention system subnetwork vulnerability in prematurely born children
Elda Fischi-Gomez^{1,2}, Lana Vasung¹, Sebastien Urben^{3,4}, Cristina Borradori-Tolsa¹, François Lazeyras⁵, Jean-Philippe Thiran^{2,6}, and Petra Susan Hüppi¹
- ¹Division of Development and Growth, Department of Pediatrics, University Hospital of Geneva, Geneva, Switzerland, ²Signal Processing Laboratory 5, École Polytechnique Fédérale de Lausanne (EPFL), Lausanne, Switzerland, ³Child Clinical Neuropsychology Unit, Department of Psychology, University of Geneva, Geneva, Switzerland, ⁴Research Unit, University Service of Child and Adolescent Psychiatry, Department of Psychiatry, University Hospital of Lausanne (CHUV), Lausanne, Switzerland, ⁵Department of Radiology and Medical Informatics, Faculty of Medicine, University of Geneva, Geneva, Switzerland, ⁶Department of Radiology, University Hospital Center (CHUV) and University of Lausanne (UNIL), Lausanne, Switzerland*
- Within preterm-born children, being born male and at a lower gestational age have both been associated with a heightened risk for developmental difficulties. However, in this population little is known about the combined effect and the influence of these risk factors

on the structural networks subserving attention and executive. Using a diffusion-based brain connectome approach, in this work we analyze the effect of these two factors in the brain networks of school-age preterm born children and provide evidence of a gender-specific vulnerability in the executive attentional subnetwork.

-
- 4417
Computer #78 White Matter Structural Alterations in Children with HIV Infection and Exposure
Marcin Jankiewicz¹, Paul A. Taylor^{1,2,3}, Martha Holmes¹, Mark F. Cotton⁴, Barbara Laughton⁴, Andre J.W. van der Kouwe⁵, and Ernesta M. Meintjes¹
- ¹MRC/UCT Medical Imaging Research Unit, Department of Human Biology, University of Cape Town, Cape Town, South Africa, ²Scientific and Statistical Computing Core, National Institutes of Health, Bethesda, MD, United States, ³African Institute for Mathematical Sciences, Muizenberg, South Africa, ⁴Children's Infectious Diseases Clinical Research Unit, Department of Pediatrics and Child Health, Stellenbosch University, Cape Town, South Africa, ⁵Athinoula A. Martinos Center for Biomedical Imaging, Massachusetts General Hospital, Charlestown, MA, United States
- In this work we examine WM alterations in HIV infected children at age 7 years and compare those who initiated ART before and after 12 weeks of age.
-
- 4418
Computer #79 Drum Training induces MR visible changes in the Cerebellum and Cortex
Muriel M.K. Bruchhage¹, Ali Amad¹, Stephen B. Draper², Jade Seidman¹, Flavio Dell'Acqua³, Luis Lacerda³, Pedro Luque Laguna³, Ruth G. Lowry⁴, Andrew Robertson⁵, Marcus S. Smith⁴, and Steven C.R. Williams¹
- ¹Department of Neuroimaging, King's College London, The Institute of Psychiatry, Psychology and Neuroscience, London, United Kingdom, ²School of Sport and Exercise, University of Gloucestershire, Chichester, United Kingdom, ³NatBrainLab, Department of Neuroimaging, King's College London, The Institute of Psychiatry, Psychology and Neuroscience, London, United Kingdom, ⁴Department of Sport and Exercise, University of Chichester, Chichester, United Kingdom, ⁵Centre for Digital Music, School of Electronic Engineering and Computer Science, Queen Mary University, London, United Kingdom
- Cerebellar networks show long-term plasticity and motor training has been shown to change cerebellar microstructure and cortical thickness. We used a combination of neuroimaging measures to visualise plastic changes in drumming - a demanding multilimb training method: cerebellar lobular volume and shape analysis, cortical thickness and diffusion tensor imaging. Drum training reorganises and reshapes the posterior cerebellum, expanding to connected parietal and prefrontal cortical structures through the inferior cerebellar white matter pathway. Thus, it may offer a novel method for cerebellar and cortical plasticity, relevant as an intervention method for psychiatric disorders connected to cerebellar dysfunction, including autism spectrum disorder.
-
- 4419
Computer #80 Absolute metabolite concentration of Creatine in the deep gray matter measured using short echo 1H-MRS predict long-term prognosis of neonatal hypoxic-ischemic encephalopathy as excellent as NAA concentration
Noriko Aida^{1,2}, Jun Shibasaki³, Moyoko Tomiyasu^{1,2}, Yuri Nishi^{1,4}, Naho Morisaki⁴, Takeo Fujiwara⁴, Katsuaki Toyoshima³, and Takayuki Obata²
- ¹Radiology, Kanagawa Children's Medical Center, Yokohama, Japan, ²Research Center for Charged Particle Therapy, National Institute of Radiological Sciences, Chiba, Japan, ³Neonatology, Kanagawa Children's Medical Center, Yokohama, Japan, ⁴Social Medicine, National Research Institute for Child Health and Development, Tokyo, Japan
- Absolute metabolite concentrations of N-acetylaspartate (NAA), Choline(Cho) and Creatine(Cr) in the deep gray matter of 44 near term neonates with hypoxic-ischemic encephalopathy (HIE), measured using PRESS method short echo 1H-MRS within 2 weeks after birth, showed excellent prognostic values (AUC; NAA: 0.98, Cho: 0.96, Cr: 0.99) with the adverse outcomes having significantly lower measurements compared to those with favorable outcomes, while Lactate was less efficient (AUC 0.74). Moreover NAA and Cr concentrations measured at 24-96 hours revealed perfect prognostic values (AUC 1.00). Early measurement of absolute Cr and NAA concentrations can be excellent biomarkers of infants suffered with neonatal HIE.
-
- 4420
Computer #81 Iron deposition in the globus pallidus of healthy youth
Karthik Prabhakaran¹, David Roalf¹, Mark Elliott¹, Simon Vandekar¹, Kosha Ruparel¹, Ryan Hopson¹, Efstathios D Gennatas¹, Jeffrey Valdez¹, Chad Jackson¹, Theodore Satterthwaite¹, Raquel Gur¹, and Ruben Gur¹
- ¹University of Pennsylvania, Philadelphia, PA, United States
- R2*, the transverse relaxation rate was used to measure iron deposition in the globus pallidus of 815 youth and young adults between the ages of 8 and 22. Significant iron deposition occurs in the globus pallidus between the ages of 8 and 22 in accordance with previously described models of iron deposition in the brain throughout the lifespan. Among adolescents (age 12-16) females had lower iron deposition in the globus pallidus (p < 0.001) as compared to males, this may be related to adolescent females being especially susceptible to dietary iron deficiency because of poor dietary intake in conjunction with high iron requirements related to rapid growth and menstrual blood loss.
-
- 4421
Computer #82 Parcellation of neonatal brain MRI into 107 regions using atlas propagation through intermediate time points in childhood.
Manuel Blesa¹, Ahmed Serag¹, Alaistir G Wilkinson², Devasuda Anblagan^{1,3}, Emma J Telford¹, Rozalia Patak¹, Sarah A Sparrow¹, Gillian Macnaught⁴, Scott I Semple⁴, Mark E Bastin³, and James P Boardman^{1,3}
- ¹MRC Centre for Reproductive Health, University of Edinburgh, Edinburgh, United Kingdom, ²Department of Radiology, Royal Hospital for Sick Children, Edinburgh, United Kingdom, ³Centre for Clinical Brain Sciences, University of Edinburgh, Edinburgh, United Kingdom, ⁴Clinical Research

We created a neonatal brain atlas of healthy subjects that can be applied to multi-modal MRI data. Structural and diffusion 3T MRI scans were acquired after birth from 25 neonates born at term. The SRI24/TZO atlas was propagated to the neonatal data using temporal registration via childhood templates (NIHPD), with the final atlas (the Edinburgh Neonatal Atlas, ENA25) constructed using iterative averaging of T1-weighted volumes. The computed transformations were applied to T2-weighted data, diffusion maps and tissue probability maps to provide a multi-modal atlas with 107 anatomical regions; and we have generated a symmetric version to facilitate studies of laterality.

4422 Computer #83 Assessing the effects of pediatric subject motion on T2 relaxation under spin tagging (TRUST) cerebral oxygenation measurements using volume navigators (vNavs)

Jeffrey N Stout¹, M. Dylan Tisdall², Patrick McDaniel³, Borjan Gagoski⁴, Divya S Bolar^{2,5}, Patricia Ellen Grant⁴, and Elfar Adalsteinsson^{1,3,6}

¹Harvard-MIT Health Sciences and Technology, Massachusetts Institute of Technology, Cambridge, MA, United States, ²Martinos Center for Biomedical Imaging, MGH/Harvard Medical School, Boston, MA, United States, ³Department of Electrical Engineering and Computer Science, Massachusetts Institute of Technology, Cambridge, MA, United States, ⁴Fetal-Neonatal Neuroimaging and Developmental Science Center, Boston Children's Hospital, Boston, MA, United States, ⁵Department of Radiology, Massachusetts General Hospital, Boston, MA, United States, ⁶Institute for Medical Engineering and Science, Cambridge, MA, United States

When using the T₂-relaxation under spin tagging (TRUST) technique on non-compliant subjects, motion has an unknown effect on estimations of cerebral oxygenation that are derived from an empirical mapping between T₂ and blood oxygen saturation. Incorporating low resolution 3D-EPI volume navigators into the TRUST pulse sequence permits independent measurements of motion during scanning. We show that for static scans vNav modules have only small effects on resulting venous blood T₂ estimates, that poor exponential goodness of fit is not a sufficient indicator of motion, and that T₂ is biased upwards with increasing motion.

4423 Computer #84 Congenital sensorineural hearing loss affects the development of corpus callosum
Weiwei Men¹, Tianbing Song², Shuang Xia³, Yaoyu Zhang¹, Jing Che⁴, and Jia-Hong Gao¹

¹Center for MRI Research, Academy for Advanced Interdisciplinary Studies, Peking University, Beijing, China, People's Republic of, ²Beijing cancer hospital, Beijing, China, People's Republic of, ³Tianjing First Central Hospital, Tianjing, China, People's Republic of, ⁴Aerospace Central Hospital, Beijing, China, People's Republic of

Congenital sensorineural hearing loss (CSHL) is a common disease in newborns, which can affect the development of corpus callosum (CC). In this study, a novel method of CC thickness analysis was employed to compare the CC difference between deaf and control groups. The results indicate that after 24 months deaf group has thinner CC thickness in the anterior splenium of CC compared to control group, which means the development of deaf anterior splenium is slowed down. Our study suggests that 12-24 month old is the best time period for CSHL treatment and intervention.

4424 Computer #85 Age-specific gray and white matter DTI atlas for human brain at 33 and 36 postmenstrual weeks
Lei Feng^{1,2}, Hang Li^{1,3}, Kenichi Oishi⁴, Virendra Mishra⁵, Minhui Ouyang¹, Tina Jeon¹, Yun Peng³, Shuwei Liu², and Hao Huang^{1,6}

¹Department of Radiology, Children's Hospital of Philadelphia, Philadelphia, PA, United States, ²Research Center for Sectional and Imaging Anatomy, Shandong University School of Medicine, Jinan, China, People's Republic of, ³Department of Radiology, Beijing Children's Hospital Affiliated to Capital Medical University, Beijing, China, People's Republic of, ⁴Department of Radiology and Radiological Science, Johns Hopkins University, Baltimore, MD, United States, ⁵Advanced Imaging Research Center, University of Texas Southwestern Medical Center, Dallas, TX, United States, ⁶Department of Radiology, Perelman School of Medicine, University of Pennsylvania, Philadelphia, PA, United States

The large brain morphological differences of the preterm brain at 33 or 36 postmenstrual week (PMW) to that at 40 PMW makes it necessary to establish age-specific atlases for preterm brains. In this study, with diffusion MRI (dMRI) data acquisition of 82 preterm and term normal neonates, we aimed to establish a comprehensive digital atlas including labeling of gray and white matter for preterm brains at 33 and 36 PMW. We demonstrated these atlases and showed the differences of the major neural structures including ganglionic eminence and uncinate fasciculus by comparison to JHU-neonate-SS atlas for brains at around 40PMW.

4425 Computer #86 Variable Refocusing Flip Angle Single Shot Imaging For Anesthesia-Free Brain MRI
Kristen W. Yeom¹, Valentina Taviani¹, Andreas M. Loening¹, Michael Iv¹, and Shreyas S. Vasanawala¹

¹Stanford University, Stanford, CA, United States

Conventional single shot fast spin echo (SSFSE) and variable refocusing flip angle SSFSE (vrfSSFSE) were compared for fast sedation-free pediatric brain MRI (N=33). Two neuroradiologists independently and blindly evaluated SSFSE and vrfSSFSE images for motion, perceived resolution (sharpness), contrast and lesion conspicuity on a five-point scale. vrfSSFSE gave less motion and misregistration artefacts than conventional SSFSE, due to the shorter scan duration. As for the other image quality metrics, vrfSSFSE was found to be either comparable or superior to conventional SSFSE.

4426 Computer #87 Distortion correction of fetal EPI using registration of orthogonal stacks with Laplacian constraint
Maria Kuklisova Murgasova¹, Georgia Lockwood Estrin¹, Rita G. Nunes^{1,2}, Mary Rutherford¹, and Jo Hajnal¹

¹King's College London, London, United Kingdom, ²Instituto de Biofisica e Engenharia Biomedica, Faculdade de Ciencias, Universidade de Lisboa,

We present a novel method for correction of geometric distortions induced by static B0 field in fetal EPI. The method estimates distortion by including a distortion-correction step in the slice to volume reconstruction of orthogonal EPI stacks with orthogonal phase encoding directions, in the form of non-rigid registration with a Laplacian constraint. We show that the proposed method achieves better consistency with reconstructed ssFSE volumes than EPI volumes constructed from data corrected by B0 field map. The registration-based distortion correction is thus a viable alternative to acquisition of B0 field map.

-
- 4427
Computer #88 Age-related white matter changes on phase difference enhanced imaging in children
Tetsu Niwa¹, Tetsuya Yoneda², Shuhei Shibukawa¹, Toshiki Kazama¹, Taro Takahara³, and Yutaka Imai¹

¹Radiology, Tokai University School of Medicine, Isehara, Japan, ²Medical Physics in Advanced Biomedical Sciences, Kumamoto University, Kumamoto, Japan, ³Biomedical Engineering, Tokai University School of Engineering, Isehara, Japan

Recent reports suggest that phase shift in the white matter may be related to myelin content. We assessed the age-related phase changes of the white matter in small children (age range, 0–6 years) on phase difference enhanced imaging (PADRE). PADRE showed progression of the phase changes in the white matter along with age, particularly in the pyramidal tract and subcortical region in Rolandic area. Whereas, less phase changes were noted in the subcortical white matter in the temporal lobe. PADRE showed age-related white matter phase shift, suggesting progression of myelination and myelin content.

-
- 4428
Computer #89 A simple method for myelin mapping using T1-weighted, T2-weighted and PD-weighted images
J-Donald Tournier^{1,2}, Rui Pedro A. G. Teixeira^{1,2}, Maria Murgasova^{1,2}, A. David Edwards^{2,3}, Joseph V. Hajnal^{1,2}, and Serena J. Counsell^{2,3}

¹Biomedical Engineering, King's College London, London, United Kingdom, ²Centre for the Developing Brain, King's College London, London, United Kingdom, ³Perinatal Imaging and Health, King's College London, London, United Kingdom

Myelin mapping is of great interest, particularly to study brain development. However, existing methods are time consuming and/or noisy. We propose a simple method to obtain semi-quantitative maps of myelin from routinely acquired T1-, T2- and proton density weighted images, by modelling the signal as a linear combination of non-exchanging tissue types: lipid, tissue water and free water. The method is calibrated empirically from the signal intensities in the data themselves. We show promising results in neonatal scans, showing the expected pattern of myelination in infants at term-equivalent age.

-
- 4429
Computer #90 Reduced GABA levels and altered sensory function in children with Autism Spectrum Disorder
Nicolaas AJ Puts^{1,2}, Ericka L Wodka^{3,4}, Ashley D Harris^{1,2,5,6}, Deana Crocetti⁷, Mark Tommerdahl⁸, Richard AE Edden^{1,2}, and Stewart H Mostofsky^{3,7,9}

¹Radiology and Radiological Science, Johns Hopkins University, Baltimore, MD, United States, ²F.M. Kirby Center for Functional Brain Imaging, Kennedy Krieger Institute, Baltimore, MD, United States, ³Center for Autism and Related Disorders, Kennedy Krieger Institute, Baltimore, MD, United States, ⁴Psychiatry and behavioral sciences, Johns Hopkins University, Baltimore, MD, United States, ⁵Alberta Children's Hospital Research Institute, University of Calgary, Calgary, AB, Canada, ⁶Radiology, University of Calgary, Calgary, AB, Canada, ⁷Laboratory for Neurocognitive and Imaging Research, Kennedy Krieger Institute, Baltimore, MD, United States, ⁸Biomedical Engineering, University of North Carolina at Chapel Hill, Chapel Hill, NC, United States, ⁹Neurology, Johns Hopkins University, Baltimore, MD, United States

Children with Autism often show difficulties processing sensory stimuli, but the underpinnings are poorly understood. Multiple lines of evidence suggest that GABA, the main inhibitory neurotransmitter in the brain, plays a role in the pathophysiology of ASD. Here we show reduced GABA levels in children with ASD, which is associated with abnormal performance on vibrotactile tasks related to inhibition. We show that alterations in GABA can contribute to alterations in sensory processing in ASD.

-
- 4430
Computer #91 Microstructural organization of the language connectome in typically developing left-handed children: a DTI tractography study
Marjolein Verly¹, Robin Gerrits¹, Lieven Lagae², Inge Zink¹, Stefan Sunaert³, and Nathalie Rommel¹

¹Dept. Neurosciences, KU Leuven, Leuven, Belgium, ²Dept. Pediatrics, UZ Leuven, Leuven, Belgium, ³Dept. Translational MRI, KU Leuven, Leuven, Belgium

The main objective of this study was to investigate the relationship between the microstructural properties of language-related white matter (WM) tracts and hand preference in typically developing school-aged children. Our DTI tractography results provide evidence for a different structural connectivity pattern of the language connectome in left-handed children. Whereas right-handed children show a clear left-lateralized structural language network, our group of left-handed children seems to have a more bilateral organized language system. Those observed differences in WM microstructure and lateralization might reflect an interaction between handedness and the neural processing of language in children.

-
- 4431
Computer #92 Optimal Slice Planning of the Fetal Brain Using Interactive Real-Time MRI
Lau Brix^{1,2}, Steffen Ringgaard¹, Puk Sandager³, Olav Bjørn Petersen³, Thomas Sangild Sørensen^{4,5}, Erik Lundorf¹, and Brian Stausbøl-Grøn¹

¹MR Research Centre, Aarhus University Hospital, Skejby, Aarhus N, Denmark, ²Department of Procurement & Clinical Engineering, Region Midt, Aarhus N, Denmark, ³Department of Obstetrics and Gynecology, Aarhus University Hospital, Skejby, Aarhus N, Denmark, ⁴Department of Clinical Medicine, Aarhus University, Aarhus N, Denmark, ⁵Department of Computer Science, Aarhus University, Aarhus N, Denmark

Diagnostic image quality of MRI can be hampered by fetal movements during data acquisition which may limit its diagnostic use (1;2). We propose an interactive real-time MRI technique which may serve as an alternative to traditional fetal MRI for anthropometrics or as a supplement for representation of fetal brain structures in cases in which fetal motion causes challenges in relation to obtaining optimal slice planes using conventional MRI techniques.

4432 Computer #93 A hybrid premature neonatal segmentation pipeline for clinical brain imaging acquired without dedicated neonatal coils.
Zachary Hill¹, Mengyuan Liu¹, Sandra Juul², and Colin Studholme³

¹Bioengineering, University of Washington, Seattle, WA, United States, ²Pediatrics, University of Washington, Seattle, WA, United States, ³Pediatrics, Bioengineering, Radiology, University of Washington, Seattle, WA, United States

Due to the difference in individual cases, larger multi-site studies of brain injury after premature birth may be needed, but dedicated neonatal imaging technology isn't always available. The use of older scanners with coils not specifically aimed at imaging neonatal brains introduces a severe intensity variation across the field of view, which can cause conventional image analysis pipelines to fail. A robust hybrid tissue segmentation pipeline was developed and shown to improve tissue segmentations of four test subjects with manual segmentations for reference. This enables automated and consistent analysis to better quantitatively study early human brain development.

4433 Computer #94 Utilization of Simultaneous Multi-slice Accelerated Turbo Spin Echo in Pediatric Epilepsy
Michael Kean^{1,2}, Lee Coleman^{2,3}, Simone Mandelstam³, Sonal Josan⁴, Benjamin Schmitt⁴, and Dingxin Wang^{5,6}

¹Children MRI Centre, Royal Childrens Hospital, Parkville, Australia, ²Murdoch Childrens Research Institute, Parkville, Australia, ³Royal Childrens Hospital, Parkville, Australia, ⁴Siemens Healthcare, Bayswater, Australia, ⁵Centre for Magnetic Resonance Research, University of Minnesota, Minneapolis, MN, United States, ⁶Siemens Medical Solutions, Malvern, PA, United States

The objective of our prospective study was to examine the clinical utility of Simultaneous Multi-Slice(SMS) Accelerated TSE at 3T imaging paediatric patients who present with seizures. A randomly selected cohort of patients were enrolled in the protocol covering a broad spectrum of clinical entities.

A direct comparison was undertaken with anatomically matched conventional TSE and SMS TSE acquisitions with matched in-plane and through plane resolution, echo train lengths and echo spacing.

Analysis of the data confirmed that although there were minimal variations in the quantitative measures recorded both sequences provided images of consistent image quality and diagnostic confidence with a significant scan time reduction attributed to the SMS TSE acquisition.

4434 Computer #95 Amide proton transfer imaging of neonatal brain development and brain injury: a preliminary study
Yang Zheng¹, Xiaoming WANG¹, Xuna Zhao², and Jinyuan Zhou³

¹Department of Radiology, Shengjing Hospital of China Medical University, Shenyang, China, People's Republic of, ²Philips Healthcare, Beijing, China, Beijing, China, People's Republic of, ³Division of MR Research, Department of Radiology, Johns Hopkins University, Maryland, USA, Baltimore, MD, United States

Yang Zheng M.D. Department of Radiology, Shengjing Hospital of China Medical University, No. 36, Sanhao Street, Heping District, Shenyang 110004, PR China E-mail address: jingshenbing0702@gmail.com Tel.: +86 13889830846

4435 Computer #96 Effects of pediatric HIV/antiretroviral therapy on basal ganglia metabolite-volume relationships
Frances C Robertson¹, Martha J Holmes¹, Emmanuel C Nwosu¹, Francesca Little², Mark F Cotton³, Els Dobbels³, Andre JW van der Kouwe^{4,5}, Barbara Laughton³, and Ernesta M Meintjes¹

¹Department of Human Biology, University of Cape Town, Cape Town, South Africa, ²Department of Statistical Sciences, University of Cape Town, Cape Town, South Africa, ³Department of Paediatrics & Child Health, Stellenbosch University, Stellenbosch, South Africa, ⁴A.A. Martinos Centre for Biomedical Imaging, Massachusetts General Hospital, Charlestown, MA, United States, ⁵Department of Radiology, Harvard Medical School, Boston, MA, United States

HIV is associated with structural deficits in the basal ganglia (BG). Volumes from structural MRI may relate to metabolic changes measurable with magnetic resonance spectroscopy. We investigated the relationship between BG NAA and Glutamate/Glutamine and caudate, putamen, nucleus accumbens and subcortical gray matter (GM) volumes in 7-year old HIV-infected children on antiretroviral therapy and uninfected controls. Higher NAA was associated with smaller accumbens and left putamen in all children. Higher Glutamate/Glutamine was associated with greater subcortical GM in controls, but not HIV-infected children. Relationships between brain metabolites and volumes add to the description of effects of HIV/ART on the BG.

4436



Computer #49

Mapping Glutamate Changes in the Brain: GluCEST as a Biomarker to Study Localized Glial Function Derangements
Puneet Bagga¹, Rachele Crescenzi¹, Guruprasad Krishnamoorthy¹, Ravi Prakash Reddy Nanga¹, Damodara Reddy¹, Sidarth Garimall¹, Kevin D'Aquilla¹, Joel Greenberg², John A Detre², Hari Hariharan¹, and Ravinder Reddy¹

¹Department of Radiology, University of Pennsylvania, Philadelphia, PA, United States, ²Department of Neurology, University of Pennsylvania, Philadelphia, PA, United States

MPTP (1-methyl-4-phenyl-1,2,3,6-tetrahydropyridine) causes selective dopaminergic death in the substantia nigra and striatum leading to dopamine loss in the basal ganglia. Here, we apply glutamate chemical exchange saturation transfer (GluCEST), a novel non-invasive MRI technique, to investigate glutamate changes in MPTP mouse model. The data suggests elevation in GluCEST contrast in striatum and motor cortex of MPTP treated mice. Immunostaining experiments showed elevation of glial markers in the striatum, which correlates with the GluCEST contrast. Also, motor function was found to be negatively correlated with GluCEST.

4437



Computer #50

Acute pressure changes in the brain are measurable with MR Elastography: Initial feasibility in an in vivo porcine model
Arvin Arani¹, Paul Min¹, Nikoo Fattahi¹, Nicholas M Wetjen¹, Clifford Jack¹, Kendall H Lee¹, Richard L Ehman¹, and John Huston III¹

¹Mayo Clinic, Rochester, MN, United States

Hydrocephalus is a common medical condition that results from obstruction to the flow of cerebral spinal fluid (CSF) or resorption of CSF. No non-invasive method offers direct measurement of intracranial pressure (ICP). Magnetic resonance elastography (MRE) is capable of non-invasively measuring brain tissue stiffness in-vivo, and may act as a surrogate to ICP. The objective of this study was to investigate the impact of ICP on brain stiffness using MRE in a porcine model. This study shows that MRE brain stiffness changes directly correspond to changes in ICP, motivating future investigation into shunt-therapy monitoring in a patient population.

4438



Computer #51

Long term high fat diet modifications of the neurochemical profile of the mouse hypothalamus
Blanca Lizarbe¹, Joao M. N. Duarte¹, Ana Francisca Soares¹, and Rolf Gruetter^{1,2,3}

¹Laboratory for Functional and Metabolic Imaging (LIFMET), Ecole Polytechnique Fédérale de Lausanne, Lausanne, Switzerland, ²Department of Radiology, University of Lausanne, Lausanne, Switzerland, ³Department of Radiology, University of Geneva, Geneva, Switzerland

Obesity is a complex disorder that leads to reduced life expectancy, with increased risk of heart disease, type-2 diabetes, high blood pressure and some type of cancers. To understand the mechanisms of obesity development, several animal models, such as high fat diet administered rodents, are being studied. We designed a longitudinal study to investigate the short and long term effects of high caloric diet intake in two populations of mice -high fat or regular fed- during 6 months, evaluating *in vivo* the changes in the neurochemical profile of the hypothalamus by ¹H MRS.

4439

Computer #52

A 3D HIGH RESOLUTION MRI ATLAS OF THE SHEEP BRAIN
Arsene Longin Ella¹, José Delgadoillo¹, Philippe Chemineau¹, and Matthieu Keller¹

¹Laboratory of Reproductive Physiology and Behavior, INRA - Centre Val de Loire, Nouzilly, France

The sheep model was first used in the field of reproductive physiology in agronomy to improve milk and meat production, and then was brought into fundamental and preclinical neurosciences. Since a decade, MR studies performed on this model are increasingly reported. To play an important role in MR translational neuroscientific research, a brain template and an atlas are therefore necessary. Simultaneously, two MR templates were proposed in 2015. To complete the set of MR tools, we computed a high resolution 3D in-vivo sheep brain atlas including: i) gyri and sulci ii) inner structures iii) main external structures.

4440

Computer #53

TBM and DTI reveal structural changes by memantine treatment in YAC128 mouse model of Huntington disease
Xin Hong¹, Marta Garcia-Miralles², Ling Yun Yeow¹, Xuan Vinh To¹, Benjamin Chaik Meng Yeo¹, Fiftarina Puspitasari¹, Katrianne Bethia Koh², Liang Juin Tan², Mahmoud Abdul Pouladi^{2,3}, and Kai-Hsiang Chuang¹

¹Singapore Bioimaging Consortium, Agency for Science, Technology and Research, Singapore, Singapore, ²Translational Laboratory in Genetic Medicine, Agency for Science, Technology and Research, Singapore, Singapore, ³Department of Medicine, National University of Singapore, Singapore, Singapore

T2 weighted structural and diffusion MRI together with behavioral tests were conducted to evaluate the effects of memantine treatment in YAC128 mouse model of Huntington disease. In low-dose (2 mg/kg)-treated YAC128 mice, cognitive functions improved, and increased fractional anisotropy was found in major fiber tracts including the corpus callosum, anterior commissure, and internal capsule. No significant gray matter volume change was detected in treatment groups, though the relative caudate putamen volume showed increasing trend with dose. Our results suggest that low dose memantine treatment had protective effects on white matter in YAC128 mice.

4441

Computer #54

A step towards developing MR elastography and diffusion tensor imaging as complementary MR tools to improve the management of hydrocephalus.
Lauriane Jugé^{1,2}, Alice C. Pong¹, Andre Bongers³, Ralph Sinkus⁴, Lynne E. Bilston^{1,5}, and Shaokoon Cheng⁶

¹Neuroscience Research Australia, Randwick, NSW, Australia, ²School of Medical Sciences, University of New South Wales, Kensington, NSW, Australia, ³Biological Resources Imaging Laboratory, University of New South Wales, Kensington, NSW, Australia, ⁴BHF Centre of Excellence, Division of Imaging Sciences and Biomedical Engineering, King's College London, London, United Kingdom, ⁵Prince of Wales Clinical School, University of New South Wales, Kensington, NSW, Australia, ⁶Department of Engineering, Faculty of Science, Macquarie University, North Ryde, NSW, Australia

Hydrocephalus is characterised by enlarged ventricles resulting in compression of surrounding tissues. Conventional imaging techniques depict ventricle size accurately. However, they are limited to detect changes in brain microstructure. The aim of this work was to quantify changes in brain mechanical and diffusion properties during the development of hydrocephalus in rats, using MR Elastography and Diffusion Tensor Imaging. Results showed that both techniques have the potential to be complementary imaging tools for tracking the effects of hydrocephalus on the tissue microstructure and provided new insights on how the brain changes during the course of the disease.

4442

Computer #55

Glymphatic clearance impaired in a mouse model of tauopathy: captured using contrast-enhanced MRI

Ian F Harrison¹, Asif Machhada¹, Niall Colgan¹, Ozama Ismail¹, James M O'Callaghan¹, Holly E Holmes¹, Jack A Wells¹, Alexander V Gourine², Tracey K Murray³, Zeshan Ahmed³, Ross A Johnson⁴, Emily C Collins⁴, Michael J O'Neill³, and Mark F Lythgoe¹

¹Centre for Advanced Biomedical Imaging, University College London, London, United Kingdom, ²Department of Neuroscience, Physiology & Pharmacology, University College London, London, United Kingdom, ³Eli Lilly and Company, Windlesham, United Kingdom, ⁴Eli Lilly and Company, Indianapolis, IN, United States

The 'glymphatic' clearance system is a brain-wide pathway for removal of waste solutes from the brain. It has recently been implicated in Alzheimer's disease (AD), due to discovery that both amyloid and tau, accumulations of which lead to AD development, can be cleared from the brain via this pathway. We therefore hypothesise that an impairment of 'glymphatic' clearance occurs in the initial stages of disease development, leading to accumulation of amyloid and tau in the brain. Here, we determine whether this is the case, by using dynamic contrast-enhanced MRI to quantify glymphatic clearance in the brain of a mouse model of AD.

4443

Computer #56

High Field MR Demonstrates Effect of Glucocorticoids in a Novel Murine Model of VEGF-Induced Vasogenic Brain Edema

Roger Muray¹, Martin Piazza¹, Jeeva Munasinghe¹, Nancy Edwards¹, Stuart Walbridge¹, Marsha Merrill¹, and Prashant Chittiboina¹

¹Surgical Neurology Branch/NINDS, National Institutes of Health, Bethesda, MD, United States

The molecular mechanisms mediating the formation of peritumoral vasogenic brain edema (VBE) and its abrogation from glucocorticoid treatment is poorly understood. In order to study the molecular underpinnings and temporal evolution of these processes we successfully developed a murine model of VBE confirmed by high field MRI and histopathologic studies. Furthermore, we demonstrate a differential effect of systemic glucocorticoids on blood-brain-barrier breakdown and edema formation. This in-vivo model will allow for further investigation into the molecular mechanisms of VBE formation and potentially provide additional targets for its treatment.

4444

Computer #57

Gray Matter Atrophy in A Rat Model of Chronic Hypoperfusion and The Effects of Environmental Enrichment: A Voxel-based Morphometry Study

Xuxia Wang¹, Ronghui Li¹, and Hao Lei¹

¹National Center of Magnetic Resonance in Wuhan, State Key Laboratory of Magnetic Resonance and Atomic and Molecular Physics, Wuhan Institute of Physics and Mathematics, Chinese Academy of Sciences, Wuhan, China, People's Republic of

Permanent bilateral common carotid arteries occlusion (2VO) rat model can induce pathological changes in brain, do these changes induce MRI visible structural changes? The enriched environment, an useful paradigm of increasing brain structural plasticity, may have a structural effect on 2VO rat brain. In this study the structural changes of 2VO rat brain with and without enriched environment (EE) were studied by in vivo MRI. Our results showed that sensorimotor cortex, dorsolateral striatum, cingulate cortex and dentate gyrus represented significant atrophy after 2VO and EE effectively protected against the gray matter atrophy.

4445

Computer #58

Neuroprotective Effects of Acetyl-L-Carnitine on Neonatal Hypoxia-Ischemia Induced Brain Injury in Rats

Shiyu Tang^{1,2}, Jaylyn Waddell³, Mary C. Mckenna³, Su Xu^{1,2}, Prashant Raghavan¹, and Gullapalli P. Rao^{1,2}

¹Diagnostic Radiology & Nuclear Medicine, University of Maryland School of Medicine, Baltimore, MD, United States, ²Core for Translational Research in Imaging, University of Maryland School of Medicine, Baltimore, MD, United States, ³Department of Pediatrics, University of Maryland School of Medicine, Baltimore, MD, United States

Cerebral hypoxia ischemia (HI) is a primary cause of perinatal brain injury. Infants surviving HI face risk of abnormal neurodevelopment, motor and intellectual disability. Acetyl-L-carnitine (ALCAR) is neuroprotective while its efficacy in perinatal HI treatment has yet to be shown. To test the neuroprotective efficacy of ALCAR and potential sex differences, we performed *in vivo* MRI and behavioral tests in a rat model of neonatal HI. Results revealed that ALCAR is neuroprotective in both morphological and behavioral outcomes. Males exhibit more consistent HI-induced functional impairments. ALCAR was effective in ameliorating functional impairments in both males and females.

4446

Computer #59

Sensitivity and specificity of susceptibility weighted imaging to cerebral microbleeds: A radiologic-neuropathologic correlation study

Karthikeyan Subramanian¹, David Utriainen¹, Ewart Mark Kaacke¹, Charbel Habib¹, John Beaver², and Rajasimhan Rajagovindan²

This study uses cynomolgus macaques, a non-human primate, as an animal model for cerebral microbleeds (CMBs). The intent is to leverage histological slices stained for iron detection against an MRI protocol with susceptibility weighted imaging (SWI) systematically collected over the course of several weeks. The radiologic-neuropathologic assessment of the CMBs was done separately on SWI, T2WI, T2*, SWI phase, and susceptibility weighted imaging and mapping (SWIM). SWIM was also used to quantify the iron content in the basal ganglia structures, such as the caudate nucleus. A quantified increase in CMBs and iron content was observed.

4447

Computer #60

Acute high altitude exposure induces ADC change in rat brain
Sunil Koundal^{1,2}, Sonia Gandhi¹, Tanzeer Kaur², and Subash Khushu¹

¹NMR Research Centre, Institute of Nuclear Medicine and Allied Sciences (INMAS), Delhi, India, ²Department of Biophysics, Panjab University, Chandigarh, India

High altitude hypoxia poses a serious threat to human health. In the present study, rats were exposed to acute simulated high altitude exposure which resulted in apparent diffusion coefficient changes in brain regions including corpus callosum and hippocampus. The study suggested the occurrence of vasogenic edema in corpus callosum and delayed cytotoxic edema in hippocampus region of brain due to acute high altitude exposure. This study has potential in setting new insights to address high altitude related health problems effectively.

4448

Computer #61

Identification of the nigrostriatal and pallidothalamic fiber tracts by high-resolution probabilistic diffusion tractography in Squirrel monkey
Mathieu David Santin^{1,2}, Thomas Samoyeau², Romain Valabrègue^{1,2}, Elodie Laffrat², Chantal François², and Stéphane Hunot²

¹Centre de NeuroImagerie de Recherche - CENIR, Paris, France, ²Inserm U 1127, CNRS UMR 7225, Sorbonne Universités, UPMC Univ Paris 06 UMR S 1127, Institut du Cerveau et de la Moelle épinière, ICM, Paris, France

This work presents tractography of an *ex vivo* brain of a primate model. Parkinson's disease related tracts were clearly identified and can serve as biomarkers in our primate model.

4449

Computer #62

MR GluCEST Study of Neuroinflammation
Chen Yanzi¹, Dai Zhuozhi¹, Shen Zhiwei¹, Chen Miaomiao¹, Ma Xilun¹, and Wu Renhua¹

¹2nd Affiliated Hospital, Shantou University Medical College, Shantou, China, People's Republic of

Glutamate (Glu) plays a crucial role in the early stage of neuroinflammation, which requires early diagnosis and treatment. This study aimed to explore Glu concentration changes in rats brain abscess model and patients with neuroinflammation using chemical exchange saturation transfer (CEST) MRI.

4450

Computer #63

MR spectroscopy predicts injury in a variable rat model of epilepsy
Yijun Wu¹, Patrice S Pearce², Amedeo Rapuano³, Kevin Kelly², Nihal de Lanerolle³, and Jullie W Pan⁴

¹Developmental Biology, University of Pittsburgh, Pittsburgh, PA, United States, ²Pittsburgh, PA, United States, ³New Haven, CT, United States, ⁴University of Pittsburgh, Pittsburgh, PA, United States

MR spectroscopy in a variable rat status epilepticus (kainate induced) model of epilepsy is shown to segregate between mildly and severely injured animals. As measured 3 days after status epilepticus, animals with NAA/tCr values of less than 1.0 (kainate more injured, KMI) segregated with greater increases in Inositol/tCr, Glutamine/tCr and Lac/tCr, with these changes predicting the metabolic measured 3 weeks after status. Although Inositol/tCr was elevated in the kainate less injured KLI group, the KLI group showed milder changes at 3 days and at 3 weeks. This metabolic classification was also sustained into histologic studies.

4451

Computer #64

Assessment of intrauterine growth restriction on pup rat brain by DTI and NODDI at 9.4T
Yohan van de Looij^{1,2}, Aline Rideau Batista Novais³, Olivier Baud³, Petra S Hüppi¹, and Stéphane V Sizonenko¹

¹Division of Child Growth & Development, Department of Pediatrics, University of Geneva, Geneva, Switzerland, ²Laboratory for Functional and Metabolic Imaging, Ecole Polytechnique Fédérale de Lausanne, Lausanne, Switzerland, ³Inserm U1141 - DHU PROTECT, Robert Debré Hospital, Paris, France

Experimental studies of intrauterine growth restriction (IUGR) in the rat, induced by protein or caloric restriction, have shown to have extensive effects on brain development including white and grey matter structural changes [1]. The aim of this work was to establish offspring cerebral structural changes following low protein diet in rats during gestation by using DTI and NODDI. LPD microstructural consequences on pup rats at P10/P21 were characterized. At P10, structural changes were mainly found in the white matter whereas at P21 cortical structure was abnormally developed. DTI and NODDI give accurate probing of the cerebral impairment following IUGR.

4452

Probiotics as possible treatment in Chronic Liver Disease-induced Hepatic Encephalopathy, an in vivo longitudinal ¹H MRS study in a rat

Computer #65 model
Veronika Rackayova¹, Olivier Braissant², Corina Berset³, Jocelyn Grosse⁴, Daniela Capobianco⁵, Paola Mastromarino⁵, Valérie A. McLin⁶, and Cristina Cudalbu³

¹Laboratory of Functional and Metabolic Imaging, Center for Biomedical Imaging, Ecole Polytechnique Fédérale de Lausanne (EPFL), Lausanne, Vaud, Switzerland, Lausanne, Switzerland, ²Service of Biomedicine, University Hospital of Lausanne, Lausanne, Vaud, Switzerland, Lausanne, Switzerland, ³Center for Biomedical Imaging, Ecole Polytechnique Fédérale de Lausanne (EPFL), Lausanne, Vaud, Switzerland, Lausanne, Switzerland, ⁴Laboratory of behavioral genetics, Ecole Polytechnique Fédérale de Lausanne (EPFL), Lausanne, Vaud, Switzerland, Lausanne, Switzerland, ⁵Sapienza University of Rome, Department of Public Health and Infectious diseases, Section of Microbiology, Rome, Italy, Rome, Italy, ⁶Swiss Center for Liver Disease in Children, Department of Pediatrics, University Hospitals Geneva, Geneva, Switzerland, Geneva, Switzerland

We investigated potential therapeutic effect of probiotic treatment with anti-inflammatory properties (VSL#3) in a rat model of Chronic Liver Disease induced Hepatic Encephalopathy (HE). ¹H MRS at 9.4T revealed significantly lower increase of glutamine (typical sign of HE) and better osmoregulation in the hippocampus together with overall better performance in behavioural tests in treated animals. These results are very promising.

4453
Computer #66 Monitoring Treatment Response to Gene Therapy in a Feline Model of Alpha-mannosidosis using 1H MRS
Sanjeev Chawla¹, Manoj Kumar^{1,2}, Sea-Young Yoon³, Harish Poptani⁴, and John H Wolfe³

¹Radiology, Perelman School of Medicine at the University of Pennsylvania, Philadelphia, PA, United States, ²Center for Perinatal Research, The Research Institute, and Nationwide Children's Hospital, Columbus, OH, United States, ³Abramson Research Center, Children's Hospital of Philadelphia, Philadelphia, PA, United States, ⁴Department of Cellular and Molecular Physiology, University of Liverpool, Liverpool, United Kingdom

To evaluate the potential of *in vivo* proton MR spectroscopy (¹H MRS) in monitoring treatment response to adeno-associated viral (AAV) gene therapy to the cisterna-magna in a cat model of alpha-mannosidosis. Normal (n=3), untreated (n=3) and AAV-treated (n=3) cats underwent multivoxel ¹H MRS. Significant elevations in resonances due to mannose-rich oligosaccharides (OG) and N-acetylated sugars (Glc-NAC) were observed in brain of untreated cats compared to normal controls. AAV treated cats demonstrated a decrease (normalization) in the OG and Glc-NAC resonances, which were not significantly different from untreated cats indicating some degree of positive response to this therapy.

4454
Computer #67 Prenatal exposure to common insecticide Malathion selectively alters micro-structural architecture in male guinea pigs
Su Xu^{1,2}, Shiyu Tang^{1,2}, Roger J Mullins^{1,2}, Edna FR Pereira³, Edson X Albuquerque³, and Rao P Gullapalli^{1,2}

¹Radiology, University of Maryland School of Medicine, Baltimore, MD, United States, ²Core for Translational Research in Imaging @ Maryland, Baltimore, MD, United States, ³Department of Epidemiology & Public Health, University of Maryland School of Medicine, Baltimore, MD, United States

To test the hypothesis that prenatal exposure of guinea pigs to malathion, one of the few organophosphate insecticides that is still in residential use in the USA, disrupts axonal integrity. After the sub-acute maternal exposure to malathion, male offspring of exposed mothers had significantly decreased diffusion metrics and anisotropy in the corpus callosum. The findings reveal the lasting effect of prenatal exposure to malathion and the danger of mother to child transmission of malathion in the environment.

4455
Computer #68 Radiation induced sub-acute, early delayed and late delayed changes in hippocampus: A successive MRS, DTI and behavioral evaluation after whole body radiation
Poonam Rana¹, Mamta Arya Gupta¹, Seenu Haridas², Kailash Manda², B S Hemanth Kumar¹, and Subash Khushu¹

¹NMR Research Centre, INMAS, Delhi, India, ²Division of Radiation Biosciences, INMAS, Delhi, India

Nuclear accidents or terrorist activities may lead to moderate dose whole body radiation exposure to a mass population. Whole body radiation exposure may influence brain function but it has not been extensively studied. Present study was conducted on mice to look for whole body radiation induced delayed behavioural, metabolic and microstructural changes. The results illustrated changes in recognition memory, MRS and MD values till 8 months post-irradiation. At later time points (10 and 12 months post-irradiation), no profound effect of radiation exposure was observed which indicates that 5Gy whole body radiation dose exposure does not have late delayed radiation injury.

4456
Computer #69 R1 Relaxation Mapping of Manganese Uptake and Wash-out in a Non-Human Primate Model of Chronic Mn Exposure
Chien-Lin Yeh^{1,2}, Jennifer McGlothlan Dziedzic³, Tomas R. Guilarte³, and Ulrike Dydak^{2,4}

¹School of Health Sciences, Purdue University, West Lafayette, IN, United States, ²Radiology and Imaging Sciences, Indiana University School of Medicine, Indianapolis, IN, United States, ³Department of Environmental Health Sciences, Columbia University Mailman School of Public Health, New York, NY, United States, ⁴School of Health Sciences, Purdue University, West Lafayette, IN, United States

High exposure to manganese (Mn) causes motor impairments resembling Parkinson's disease. Using R1 mapping we investigated the dynamics of brain Mn accumulation during and after chronic manganese exposure in nonhuman primates. The R1 in whole brain displayed a significant increase after 27-41 wks of exposure. The visual cortex was found to have continuous Mn accumulation over exposure duration, while R1 of substantia nigra was decrease at 66-81 wks. Some select brain areas still show hyperintensities ten months after cessation of exposure. Understanding the regional uptake and retention may help elucidating the relation of Mn exposure

4456



- 4457
Computer #70 Follow-up analyses on the effects of long-term use of high fat diet on hippocampal volumes and hippocampal metabolite concentrations in Wistar rats: a voxel based morphology and 1H MRS approach
Piotr Majka¹, Bartosz Kossowski², Jarosław Orzeł², Piotr Bogorodzki², Zuzanna Setkiewicz³, and Stefan P. Gazdzinski⁴

¹Nencki Institute for Experimental Biology, Warsaw, Poland, ²Warsaw University of Technology, Warsaw, Poland, ³Neuroanatomy, Jagiellonian University, Krakow, Poland, ⁴CNS Lab, Military Institute for Aviation Medicine, Warsaw, Poland

Our study of long-term use of high fat diet inducing mild ketonemia in Wistar rats showed improvements in learning and memory, as well as larger hippocampi and higher concentrations of tNAA (marker of neuronal viability), tCho (involved in metabolite turnover), and tCr (involved in cell energetics). Here, we applied voxel based morphometry (VBM) for structural images and used TARQUIN for ¹H MRS data obtained at 7T. Results of VBM and TARQUIN provided results consistent with previous analyses. However, the use of a literature-based template lead to tissue contractions not detectable with study specific template.

- 4458
Computer #71 Feasibility of 50µm in vivo MR microscopy (µMRI) of mouse brain at 9.4 Tesla
Ferdinand Schweser^{1,2}, Claire M Modica^{1,3}, Nicola Bertolino¹, Paul Polak¹, Marilena Preda^{1,2}, and Robert Zivadinov^{1,2}

¹Buffalo Neuroimaging Analysis Center, Department of Neurology, Jacobs School of Medicine and Biomedical Sciences, The State University of New York at Buffalo, Buffalo, NY, United States, ²MRI Molecular and Translational Research Center, Jacobs School of Medicine and Biomedical Sciences, The State University of New York at Buffalo, Buffalo, NY, United States, ³Neuroscience Program, Jacobs School of Medicine and Biomedical Sciences, The State University of New York at Buffalo, Buffalo, NY, United States

The technique of MR microscopy (µMRI) has evolved into an important tool for morphologic phenotyping and computational neuroanatomy research. However, due to the inherent challenges of mouse imaging, µMRI of mouse brain has so far mostly been limited to *post mortem* tissue, often relying on perfusion with a mixture of saline and a T1-shortening constant agent, which increases the MRI sampling efficiency.

In this work, we demonstrate the feasibility of *in vivo* µMRI of mouse brain at 9.4 Tesla with a resolution of 50µm using a cryogenic brain coil and an optimized imaging sequence.

- 4459
Computer #72 Effect of dystrophin levels on brain volumes in Duchenne muscular dystrophy mouse models
Bauke Kogelman¹, Artem Khmelinskii^{2,3}, Maaïke van Putten⁴, and Louise van der Weerd^{1,4}

¹Department of Radiology, Leiden University Medical Center, Leiden, Netherlands, ²Division of Image Processing, Dept. of Radiology, Leiden University Medical Center, Leiden, Netherlands, ³Percurus B.V., Enschede, Netherlands, ⁴Department of Human Genetics, Leiden University Medical Center, Leiden, Netherlands

Besides muscle, Duchenne muscular dystrophy also affects the brain, resulting in memory and behavior problems. The consequences of dystrophinopathy on gross macroscopic alterations in the mouse brain are unclear. We used a number of mouse models that express either 0% (*mdx*), 100% (B10-WT) or a low amount of dystrophin (*mdx-XistΔhs*). We showed that while whole brain volume does not significantly differ between *mdx* and B10-WT mice, there are differences in volumes of individual brain substructures. These results are in line with human data, where brain volume was found to be reduced only in patients lacking both full-length dystrophin and the shorter isoform Dp140.

Electronic Poster

Bone & Soft Tissue

Exhibition Hall

Thursday, May 12, 2016: 14:30 - 15:30

- 4460
Computer #25 Image Fusion of Ultrasound and Magnetic Resonance Imaging for Regional Anesthesia of the Hip: The Influence of MRI Scanning Position for Fusion Accuracy and Post Anesthesia Visualization of Anatomical Distribution of Local Anesthetics
Jennie Maria Christin Strid¹, Erik Morre Pedersen², Olga Vendelbo², Niels Dalsgaard¹, Yousef Nejatbakhsh³, Jens Randel Nyengaard⁴, Kjeld Søballe⁵, and Thomas Fichtner Bendtsen¹

¹Department of Anesthesiology, Aarhus University Hospital, Aarhus C, Denmark, ²Department of Radiology, Aarhus University Hospital, Aarhus C, Denmark, ³Hospital Pharmacy, Aarhus University Hospital, Aarhus C, Denmark, ⁴Electron Microscopy Lab and Stereology, Institute of Clinical Medicine, Aarhus University, Aarhus C, Denmark, ⁵Department of Orthopedic Surgery, Aarhus University Hospital, Aarhus C, Denmark

Ultrasound guided lumbar plexus blocks holds the potential for reducing anesthesia related complications in hip surgery in the elderly punctum. The ultrasound guidance is, however, imprecise and associated with epidural spread of local anesthetic due to limited visualization. It is the overall aim of this study to improve the quality of lumbar plexus blocks using Fusion imaging between MRI and ultrasound. Here we report preliminary results of the impact of different MR scanning positions for the accuracy of fusion imaging and report on the feasibility of using gadolinium doped anesthetics for studying the distribution of local anesthetic fluid using MRI.

- 4461
Computer #26 PET/MRI molecular imaging in sports medicine: Assessment of ACL graft viability with combined 18F-FDG and 3T MR imaging
Katherine Binzel¹, Robert Magnussen², Christopher Kaeding², David C Flanigan², Wenbo Wei¹, Melanie U Knopp³, and Michael V Knopp¹
- ¹Radiology, The Ohio State University, Columbus, OH, United States, ²Sports Medicine, The Ohio State University, Columbus, OH, United States, ³Sports Medicine, Pepperdine University, Malibu, CA, United States
- Evaluation of ACL graft healing by combined PET/MR imaging is readily feasible but has limited quantitative accuracy with use of conventional PET systems. The application of next generation digital photon counting in PET improves the quantitative accuracy and precision of assessment of graft metabolic activity. This advanced imaging modality also holds potential for ultra-low dose PET imaging, enhancing the clinical utility of such a combined imaging approach for detailed assessment of ACL graft viability after reconstructive surgery.
-
- 4462
Computer #27 Diffusion Tensor Imaging of the brachial plexus as an aid to the diagnosis of inflammatory neuropathies: preliminary results.
Jos Oudeman¹, Filip Eftimov², Gustav J Strijkers³, Martijn Froeling⁴, Matthan W. A. Caan¹, Ivo N. van Schaik², Mario Maas¹, Aart J Nederveen¹, Marianne de Visser², and Camiel Verhamme²
- ¹Radiology, Academic Medical Center, Amsterdam, Netherlands, ²Neurology, Academic Medical Center, Amsterdam, Netherlands, ³Biomedical Engineering and Physics, Academic Medical Center, Amsterdam, Netherlands, ⁴Radiology, University Medical Center, Utrecht, Utrecht, Netherlands
- Diagnosing -treatable- inflammatory neuropathies such as chronic inflammatory demyelinating polyradiculoneuropathy (CIDP) and multifocal motor neuropathy (MMN) can be challenging, especially differentiating MMN from -untreatable- focal spinal muscular atrophy (fSMA). One of the reasons is that conduction studies cannot evaluate reliably the proximal part of the brachial plexus. Therefore we investigated DTI of the brachial plexus in patients with CIDP, MMN, fSMA and healthy controls and found significant differences, indicating DTI might be a valuable diagnostic tool in the clinic.
-
- 4463
Computer #28 Comparison of vertebral bone marrow water ADC between young and old subjects: DW-MRS versus DWI
Michael Dieckmeyer¹, Stefan Ruschke¹, Hendrik Kooijman², Ernst J. Rummeny¹, Jan S. Kirschke³, Thomas Baum¹, and Dimitrios C. Karampinos¹
- ¹Diagnostic and Interventional Radiology, Technische Universität München, Munich, Germany, ²Philips Research Laboratory, Hamburg, Germany, ³Neuroradiology, Technische Universität München, Munich, Germany
- The apparent diffusion coefficient (ADC) of vertebral bone marrow has been proposed as a useful biomarker for differentiating between benign and malignant vertebral compression fractures and could potentially be beneficial for the understanding of physiological as well as pathological bone marrow changes. In this work we exploit the spectral resolution of diffusion weighted magnetic resonance spectroscopy (DW-MRS) to exclusively quantify the ADC of the bone marrow water component and compare it to DWI based measurements. The results of two age groups are compared.
-
- 4464
Computer #29 Using hyperpolarised 13C-MRS to explore murine skeletal muscle metabolism during exercise
M. Kate Curtis¹, Brianna J Stubbs¹, Vicky Ball¹, Lowry E Cochlin², Mark A Cole³, Jack J Miller^{1,4}, David P O'Neill¹, Kieran Clarke¹, Peter A Robbins¹, and Damian J Tyler^{1,5}
- ¹Physiology, Anatomy and Genetics, University of Oxford, Oxford, United Kingdom, ²PulseTeq Ltd, Surrey, United Kingdom, ³Queen's Medical Centre, University of Nottingham Medical School, Nottingham, United Kingdom, ⁴Physics, University of Oxford, Oxford, United Kingdom, ⁵Radcliffe Department of Medicine, University of Oxford, Oxford, United Kingdom
- Previous techniques used to determine the hierarchy of skeletal muscle metabolic fuel selection have been unable to directly describe the changes in cellular metabolic flux during exercise. The aim of this project was to develop a technique that allows the simultaneous assessment of metabolism and function in exercising skeletal muscle in real-time, in an intact mouse, using hyperpolarized [1-¹³C] pyruvate MRS. Our results demonstrate that the technique is sensitive enough to distinguish differences in metabolic flux between the resting and exercising states shown by a significant increase in ¹³C label incorporation into bicarbonate during exercise.
-
- 4465
Computer #30 Radiation-induced Early Temporal Changes of IVIM-based Diffusion and Perfusion Patterns of Bone Marrow Predict the Likelihood of Hematological Toxicity
Elaine Yuen Phin Lee¹, Jian He², Jose Angelo Udal Perucho¹, and Queenie Chan³
- ¹The Department of Diagnostic Radiology, Li Ka Shing Faculty of Medicine, The University of Hong Kong, Hong Kong, Hong Kong, ²Department of Radiology, Nanjing Drum Tower Hospital, The Affiliated Hospital of Nanjing University Medical School, Nanjing, China, People's Republic of, ³Philips Healthcare, Hong Kong, Hong Kong
- Intravoxel incoherent motion (IVIM) diffusion-weighted MRI offers the unique opportunity to simultaneously study the diffusion and perfusion changes in the bone marrow following whole-pelvis radiotherapy. We prospectively studied twenty-eight patients with cervical cancer who had paired IVIM MRI examinations before and at week-4 of treatment. We observed a distinctive positive trend of D (true diffusion coefficient) in patients who suffered hematological toxicity (HT), whilst D remained relatively stable in patients who did not suffer HT. In addition, *f* (perfusion fraction) increased following treatment, but this pattern was not unique to patients who suffered HT.

- 4466
Computer #31 The value of BOLD-MRI in early diagnosis of osteonecrosis of the femoral Head in patients with steroid treatment
Jing Li¹, Zhuoli Zhang², Yu Zhang³, Quan Zhang¹, and Fei Yuan⁴
¹Pingjin Hospital, Tianjin, China, People's Republic of, ²Northwestern Univeristy, Chicago, IL, United States, ³Philips Healthcare, Beijing, China, People's Republic of, ⁴MRI, Pingjin Hospital, Tianjin, China, People's Republic of
- This study attempted to compare BOLD with conventional MRI sequences for determining the onset of osteonecrosis of the femoral head following steroid-related osteonecrosis. 112 patients who had received steroid treatment were scanned using conventional MRI and BOLD. The manifestation in BOLD-MRI is in accordance with the pathology of ONFH, which would allow early treatment of ONFH.
-
- 4467
Computer #32 Associations between quantitative MRI biomarkers in the lumbar spine and pain in chronic low back pain patients with disc degeneration
Volkan Emre Arpinar¹ and L Tugan Muftuler^{1,2}
¹Neurosurgery, Medical College of Wisconsin, Milwaukee, WI, United States, ²Center for Imaging Research, Medical College of Wisconsin, Milwaukee, WI, United States
- Associations between quantitative MRI biomarkers in the lumbar spine and pain in chronic low back pain patients (CLBP) were studied. These biomarkers are currently being explored as quantitative metrics of disc degeneration. Since most CLBP cases are associated with pathologic disc degeneration processes, these biomarkers might provide clues about the actual source of pain. For analysis, the discs from each subject were pooled from the least to the most degenerated one using a semi-quantitative metric. Results showed that these biomarkers might aid in identifying the source of pain in CLBP patients.
-
- 4468
Computer #33 Quantitative assessment of lumbar disc degeneration by non-Gaussian diffusion-weighted imaging
Masaki Katsura^{1,2}, Yuichi Suzuki², Akihiro Kasahara², Harushi Mori¹, Akira Kunimatsu¹, Yoshitaka Masutani³, Masaaki Hori⁴, Shigeki Aoki⁴, and Kuni Ohtomo¹
¹Radiology, Graduate School of Medicine, The University of Tokyo, Tokyo, Japan, ²Radiology, The University of Tokyo Hospital, Tokyo, Japan, ³Intelligent Systems, Graduate School of Information Sciences, Hiroshima City University, Hiroshima, Japan, ⁴Radiology, School of Medicine, Juntendo University, Tokyo, Japan
- We performed q-space imaging(QSI) analyses for lumbar intervertebral discs(IVDs) in patients suffering from lower back pain with different stages of degeneration. We evaluated the correlation between the quantitative QSI measurements and the qualitative grading(Pfirrmann's scale) of disc degeneration. Our results suggest that the degenerative process of IVDs involves narrowing of the space for free water movement and a generally higher degree of microstructural complexity, in which we are unable to assess with conventional quantitative MR measurements. QSI may provide sensitive biomarkers for IVD degenerative microstructural changes and can potentially become a tool to allow characterization of various IVD pathologies.
-
- 4469
Computer #34 B1-insensitive high-resolution isotropic T2 mapping of the lumbar plexus with a T2-prepared 3D TSE
Dominik Weidlich¹, Barbara Cervantes¹, Nico Sollmann², Hendrik Kooijman³, Jan S. Kirschke⁴, Ernst J. Rummeny¹, Axel Haase⁵, and Dimitrios C. Karampinos¹
¹Department of Diagnostic and Interventional Radiology, Technische Universität München, Munich, Germany, ²Department of Neurosurgery, Technische Universität München, Munich, Germany, ³Philips Healthcare, Hamburg, Germany, ⁴Section of Neuroradiology, Technische Universität München, Munich, Germany, ⁵Zentralinstitut für Medizintechnik, Technische Universität München, Garching, Germany
- T2 mapping is a great candidate for quantitatively assessing inflammatory changes in peripheral nerves. However, measuring T2 of the lumbar nerve roots is challenging because of the need for high isotropic resolution and the sensitivity of the region to transmit B1 inhomogeneities. The present work proposes a T2 preparation, based on a modified BIR-4 pulse, and combined with 3D TSE imaging for B1-insensitive high-resolution isotropic T2 mapping of the lumbar plexus. The feasibility of the method is shown in five healthy volunteers and a variation of T2 along the nerve root course is observed.
-
- 4470
Computer #35 Feasibility of brachial plexus assessment using 3D fat suppression T2-weighted Cube combined with double inversion recovery at 3T
Shuji Nagata¹, Hiroshi Nishimura², Kimberly K Amrami³, Kazutaka Nashiki¹, Tatsuyuki Tonan¹, Uchiyama Yusuke¹, Kiminori Fujimoto¹, and Toshi Abe¹
¹Kurume University Hospital, Kurume, Japan, ²Saiseikai Futsukaichi Hospital, Chikushino, Japan, ³Mayo Clinic, Rochester, MN, United States
- A high-resolution MR neurography using 3D fat suppression T2-weighted Cube combined with double inversion recovery (3D FS DIR Cube) was evaluated the feasibility of brachial plexus assessment. 15 normal volunteers were scanned 3D FS DIR Cube, 3D FS T2-weighted Cube (3D FS T2 Cube), and 2D IDEAL water on a 3T MRI scanner using a GEM NV coil. The 3D FS DIR Cube can provide excellent contrast between brachial plexus branch and surrounding tissues and increase the conspicuity of the nerves delineation with uniformed fat suppression and vessels signal suppression compared with 3D FS T2 Cube and 2D IDEAL water.
-
- 4471
Computer #36 Quantitative MR Imaging of Vertebral Disc and Bone Marrow in Chronic Kidney Disease: A Rat Model Study
Chao-Ying Wang¹, Yu-Juei Hsu², Yi-Jen Peng³, Yi-Chih Hsu⁴, Shih-Wei Chiang^{4,5}, Ming-Huang Lin⁶, Hsiao-Wen Chung⁵, and Guo-Shu

Huang^{4,7}

¹Department and Institute of Biology and Anatomy, National Defense Medical Center, Taipei, Taiwan, ²Division of Nephrology, Department of Internal Medicine, Tri-Service General Hospital, National Defense Medical Center, Taipei, Taiwan, ³Department of Pathology, Tri-Service General Hospital, National Defense Medical Center, Taipei, Taiwan, ⁴Department of Radiology, Tri-Service General Hospital, National Defense Medical Center, Taipei, Taiwan, ⁵Graduate Institute of Biomedical Electronics and Bioinformatics, National Taiwan University, Taipei, Taiwan, ⁶Institute of Biomedical Sciences, Academic Sinica, Taipei, Taiwan, ⁷Department of Medical Research, Tri-Service General Hospital, National Defense Medical Center, Taipei, Taiwan

An animal study to investigate bone marrow changes in the lumbar spine by quantitative Magnetic Resonance Imaging

-
- 4472
Computer #37
Differentiation of spinal lesions using monoexponential, biexponential, and gamma distribution diffusion-weighted MR Imaging: Initial clinical results
Miyuki Takasu¹, Yuji Akiyama¹, Chihiro Tani¹, Yoko Kaichi¹, Takayuki Tamura¹, Koichi Oshio², and Kazuo Awai¹

¹Diagnostic Radiology, Hiroshima University Hospital, Hiroshima-shi, Japan, ²Department of Diagnostic Radiology, Keio University School of Medicine, Tokyo, Japan
- The purpose of this study was to quantitatively compare various diffusion parameters obtained from monoexponential, biexponential, and gamma distribution models in differentiating vertebral lesions in human subjects. All MR parameters, except for ADC_{fast} and $\frac{f}{3}$, were significantly different between normal bone marrow and lesions. Water molecular diffusion parameters may provide additional information and improve the differentiation of spinal lesions compared with conventional diffusion parameters. This also refers to differentiation of malignant lesions from acute spinal fracture, in which both PG (D) calculated from gamma distribution model and perfusion fraction f of the biexponential model proved to be useful.
-
- 4473
Computer #38
Predictive patient assessment via T2 Mapping of the Lumbar Intervertebral Disc at 3T: Correlation of T2 values with clinical reports, morphological grading, RMDQ, and VAS at a 5-year follow-up in patients with low back pain
Marcus Raudner¹, David Stelzener², Claudia Kronnerwetter¹, Vladimir Juras¹, Karin Pieber³, Reinhard Windhager², and Siegfried Trattnig¹

¹High Field MR Centre, Department of Biomedical Imaging and Image-guided Therapy, Medical University of Vienna, Vienna, Austria, ²Department of Orthopaedics, Medical University of Vienna, Vienna, Austria, ³Department of Physical Medicine and Rehabilitation, Medical University of Vienna, Vienna, Austria
- Anatomical determination of cause for low back pain often remains impossible in the majority of patients. This study examined the diagnostic and predictive capabilities of T2 values of the lumbar intervertebral discs (IVDs). Twenty-five symptomatic patients were examined via magnetic resonance imaging (MRI) at 3T at baseline and 5-year follow-up (FU). Combining radiological reports, morphological grading, region-of-interest (ROI) analysis and patient assessment (VAS and Roland-Morris-Disability-Questionnaire), significant predictive capabilities were identified.
-
- 4474
Computer #39
High-Resolution DWI of the Lumbar Plexus using B1-insensitive Velocity-Compensated Diffusion-Prepared 3D TSE
Barbara Cervantes¹, Dominik Weidlich¹, Hendrik Kooijman², Ernst Rummeny¹, Axel Haase³, Jan S Kirschke⁴, and Dimitrios C Karampinos¹

¹Diagnostic and Interventional Radiology, Technische Universität München, Munich, Germany, ²Philips Healthcare, Hamburg, Germany, ³Zentralinstitut für Medizintechnik, Garching, Germany, ⁴Neuroradiology, Technische Universität München, Munich, Germany
- Diffusion weighted imaging (DWI) can describe the microstructure of nerve fibers and is therefore a powerful tool in the study of neuropathic changes. Diffusion imaging in the body faces challenges with motion and B0 and B1 field effects. Particularly, imaging of nerves has resolution requirements that can limit the performance of the acquisition method. The lumbar plexus is a particularly difficult region to image due to the complexity of the nerve geometry there and its susceptibility to motion and field inhomogeneity. Therefore, careful considerations need to be taken in the design of a diffusion-prepared sequence for imaging the lumbar plexus. The present work proposes an adiabatic diffusion preparation module in combination with a 3D TSE readout to achieve high-resolution DWI of the lumbar plexus.
-
- 4475
Computer #40
Is intravoxel incoherent motion (IVIM) more helpful for differentiating benign from malignant vertebral bone marrow lesions comparing with the conventional DWI?
Xiaodong Zhang¹, Yingjie Mei², Jiewen Yan¹, Yanjun Chen¹, Yinxia Zhao¹, and Shaolin Li¹

¹Department of medical radiology, The Third Affiliated Hospital of Southern Medical University, Guangzhou, China, People's Republic of, ²Philips Healthcare, Guangzhou, China, People's Republic of
- The aim of this study is to evaluate the value of intravoxel incoherent motion (IVIM) for the differentiation between benign and malignant vertebral bone marrow lesions. The results of our study show that IVIM is potentially a promising and valuable non-invasive method in differentiating the spinal benign and malignant diseases.
-
- 4476
Computer #41
Postoperative Spinal Imaging Metal Artefact Reduction Using Ultrashort Echo Time MRI: A Feasibility Study
Amy Ming-Chun Tsai Sevaio¹, Alistair Young¹, Benjamin Schmitt², Hament Pandya³, Karen Billington³, Anthony Doyle³, David Grodzki⁴, and Brett Cowan⁵

Post-operative spine imaging with metal implants in situ are problematic because of the significant metal artefacts, in both CT due to beam hardening, and MRI from signal loss. Ultrashort Echo Time (UTE) MRI has potential to significantly reduce metal artefacts because of its method of acquisition. Significant differences in metal artefacts between conventional MR and UTE are found in our study, imaging sheep spine with spinal fusion hardware in situ, with important clinical implications.

4477

Computer #42

Rapid and Distortion-Free Diffusion Tensor Imaging for Evaluation of Lumbar Nerve Roots Using Direct Coronal Single-Shot Turbo Spin-Echo Diffusion Sequence

Takayuki Sakai¹, Atsuya Watanabe^{2,3}, Kiichi Nose¹, Daichi Murayama¹, Shigehiro Ochi¹, Masami Yoneyama⁴, and Noriyuki Yanagawa¹

¹Eastern Chiba Medical Center, Chiba, Japan, ²Chiba university graduate school of medicine, Chiba, Japan, ³Orthopaedic surgery, Eastern Chiba Medical Center, Chiba, Japan, ⁴Philips Electronics Japan, Tokyo, Japan

The purpose of this study was to visualize the lumbar nerve roots and to measure their FA values in healthy volunteers and in patients with neurological symptom of leg by using TSE-DTI. Tractography of the patients with symptomatic side of lumbar nerve roots indicated abnormalities such as narrowing, deformation, and disruption. The FA values of the symptomatic side of lumbar nerve roots were significantly lower than those of the asymptomatic side. TSE-DTI might more accurately evaluate compressed lumbar nerve roots compared to conventional EPI-DTI. Additionally, tractography of TSE-DTI enables visualization of abnormal nerve tracts and has a lower geometric distortion for diagnosing lumbar nerve compression than EPI-DTI.

4478

Computer #43

Quantification of vertebral bone marrow fat fraction using time-interleaved multi-echo gradient-echo water-fat MRI: preliminary experience in children

Stefan Ruschke¹, Amber Pokorney², Holger Eggers³, Jan S. Kirschke⁴, Thomas Baum⁵, Dimitrios C. Karampinos¹, and Houchun Harry Hu²

¹Diagnostic and Interventional Radiology, Technische Universität München, Munich, Germany, ²Radiology, Phoenix Children's Hospital, Phoenix, AZ, United States, ³Philips Research, Hamburg, Germany, ⁴Section of Diagnostic and Interventional Neuroradiology, Technische Universität München, Munich, Germany, ⁵Department of Diagnostic and Interventional Radiology, Technische Universität München, Munich, Germany

In this work, we describe our preliminary clinical experience using a previously reported time-interleaved six-echo gradient-echo (TIMGRE) acquisition for water-fat chemical-shift encoded MRI. The acquisition scheme involved two interleaves that acquired three echoes each with fly-back gradients. The pulse sequence was used to quantify vertebral bone marrow fat fraction in a pilot cohort of 12 pediatric patients (age range: 1-13 years) at 3T with 1.2-1.6 mm in-plane resolution and 1.2-3 mm slices. The knowledge on bone marrow fat fraction may provide insight into adverse effects on bone health later in life, given that there is clinical relevance of vertebral osteoporotic fractures in adults.

4479

Computer #44

UTE-T2* detects matrix changes in Achilles tendon after tendon allograft reconstruction for old Achilles tendon rupture and the correlation with clinical score: a preliminary study

Hongyue Tao¹, Yong Zhang², Yang Qiao¹, Ziyang Wu³, Kui Ma³, Yinghui Hua³, and Shuang Chen¹

¹Radiology, Huashan Hospital, Fudan University, Shanghai, China, People's Republic of, ²GE Healthcare, MR Research China, Shanghai, China, People's Republic of, ³Sports Medicine, Huashan Hospital, Fudan University, Shanghai, China, People's Republic of

This preliminary study used UTE-T2*, a novel quantitative technique with potential short-T2* relaxations that are not well captured by standard T2 mapping, to investigate T2* value in Achilles tendon (AT) after tendon allograft reconstruction (AT-R) and analyze the correlation between T2* value and AOFAS score. Six patients with AT-R and 6 sex, age, and BMI matched healthy controls were recruited for comparison. The results showed T2* values of middle (MID) and muscle-tendon junction (MTJ) regions in AT-R patients were statistically lower compared with the matched regions of controls and T2* value of MID region was negatively correlated with AOFAS score, which suggest T2* may be a promising marker for the detection of matrix changes in AT after AT-R.

4480

Computer #45

MR properties of cadaveric Achilles tendon enthesis with ultrashort echo time (UTE) sequences and correlate with biomechanics

Bimin Chen^{1,2}, Erik Dorthe³, Michael Carl⁴, Hongda Shao¹, Yajun Ma¹, Darryl D'Dlima³, Graeme M Bydder¹, and Jiang Du¹

¹Radiology Department, UCSD, San Diego, CA, United States, ²Radiology Department, The first affiliated hospital of Jinan University, Guangzhou, China, People's Republic of

Entheses are sites where tendons, ligaments, and joint capsules attach to bone. They may be fibrous or fibrocartilaginous. Entheses are adapted at both

4481

Computer #46

Accuracy evaluation of pulse sequences using inversion recovery pulse for T1 measurement.

Noriyuki Tawara^{1,2}, Kanokvalee Ponkanist², Shuichi Shiratori², Anchali Krisanachinda², and Toru Yamamoto¹

¹Faculty of Health Sciences, Hokkaido University, Sapporo, Japan, ²Faculty of Medicine, Chulalongkorn University, Bangkok, Thailand

It has been reported that T₁ in skeletal muscles is proportional to the percentage of type I fibers which would be a determinant for athletic performance. However, the precision of the measured T₁ values is unclear due to various pulse sequences used for the measurement. In this study, we evaluated the reliability of T₁ measured by pulse sequences with inversion recovery technique that is

believed to be most accurate in T₁ measurement. A value of goodness of fitting was employed for the quantitative evaluation of the obtained data. The influence of SNR on the T₁ measurement was also examined.

- 4482
Computer #47
Depiction of deep fascia, epimysium and periosteum in 3 dimensional Ultrashort Echo Time MR Imaging (3D UTE) with histologic correlation in porcine model
Ah Rhm Woo¹, Yeo Ju Kim¹, Mi Young Kim¹, Jang Gyu Cha², Michael Carl³, Sangwoo Lee⁴, Moonjung Hwang⁴, and Dong Eun Kim⁴
- ¹Department of radiology, Inha University Hospital, Incheon, Korea, Republic of, ²Department of radiology, Soonchunhyang University Hospital, Bucheon, Korea, Republic of, ³GE Healthcare, San Diego, CA, United States, ⁴GE Healthcare, Seoul, Korea, Republic of*
- We evaluated the ability of depiction of deep fascia, epimysium and periosteum in 3 dimensional Ultrashort Echo Time MR Imaging (3D UTE) with histologic correlation in porcine model. In our study, the 3D UTE might depict deep fascia and periosteum as high signal intensities whereas the ability of visualization of epimysium was uncertain and high signal intensity of artifact remains in naked cortex without periosteum.

- 4483
Computer #48
The Advantages of Spectrally Calibrated 3D-MSI in Assessments of Symptomatic Spinal Fusion
S Sivaram Kaushik¹, Abhishiek Sharma², Rajeev Mannem¹, Cathy Marszalkowski¹, Scott Rand¹, Dennis Maiman², and Kevin M Koch¹
- ¹Radiology, Medical College of Wisconsin, Milwaukee, WI, United States, ²Neurosurgery, Medical College of Wisconsin, Milwaukee, WI, United States*
- Failed back surgery syndrome (FBSS) is a commonly encountered clinical condition for which the root cause often remains elusive after lengthy clinical assessment. While MRI provides great potential utility for uncovering the causes of failed back surgery syndrome, it also is confounded by metal-induced artifacts. This study explores the benefits of a prospectively calibrated 3D-MSI metal artifact reduction technique in assessing instrumented FBSS. Residual artifacts and clinical diagnostic impact were assessed on a cohort of symptomatic FBSS subjects. The results of the study indicate diagnostic advantages using calibrated 3D-MSI, even in the presence of lower-susceptibility titanium spinal hardware.

Electronic Poster

Cartilage & Joints

Exhibition Hall

Thursday, May 12, 2016: 14:30 - 15:30

- 4484
Computer #49
Multiparametric quantitative MRI of cartilage composition and bone blood perfusion applied in a case-control study of patellofemoral pain.
Rianne A van der Heijden^{1,2}, Dirk HJ Poot^{1,3,4}, Melek Ekinci², Esther E Bron^{1,4}, Jasper van Tiel^{1,5}, Stefan Klein^{1,4}, Peter LJ van Veldhoven⁶, Gabriel P Krestin¹, Jan AN Verhaar⁵, Sita MA Bierma-Zeinstra^{2,5}, Marienke van Middelkoop², and Edwin HG Oei¹
- ¹Radiology, Erasmus University Medical Center, Rotterdam, Netherlands, ²General Practice, Erasmus University Medical Center, Rotterdam, Netherlands, ³Imaging Science and Technology, Delft University of Technology, Delft, Netherlands, ⁴Medical informatics, Erasmus University Medical Center, Rotterdam, Netherlands, ⁵Orthopedics, Erasmus University Medical Center, Rotterdam, Netherlands, ⁶Sports medicine, MC Haaglanden, Leidschendam, Netherlands*
- Diminished patellofemoral cartilage composition and vascular problems are potential pathogenic mechanisms in patellofemoral pain (PFP). These mechanisms can be studied in depth using advanced MRI techniques. We are the first to successfully apply a wide range of quantitative MRI techniques for cartilage composition and bone blood perfusion in a case-control study on PFP. The results show no significant differences in patellofemoral cartilage composition and patellar bone blood perfusion between PFP patients and healthy controls.

- 4485
Computer #50
MR texture analysis of subchondral bone in osteoarthritis
James MacKay¹, Samantha Low¹, Philip Murray¹, Bahman Kasmai¹, Glyn Johnson², Simon Donell^{2,3}, and Andoni Toms^{1,2}
- ¹Radiology, Norfolk & Norwich University Hospital, Norwich, United Kingdom, ²Norwich Medical School, University of East Anglia, Norwich, United Kingdom, ³Trauma & Orthopaedics, Norfolk & Norwich University Hospital, Norwich, United Kingdom*
- Subchondral bone (SB) plays an important role in osteoarthritis (OA). Texture analysis (TA) is a method of quantifying changes in SB and may be a useful OA biomarker. The optimum MR method to allow TA of SB is unclear. We compared TA using two sequences which demonstrated promise in depicting SB structure in three groups of participants: normal controls (n=10), individuals with early OA (n=10) and individuals with advanced OA (n=10). TA using a 2D T1-weighted spin echo sequence demonstrated more significant differences in texture features between groups and improved classification accuracy compared to a 3D gradient echo sequence.

- 4486
Computer #51
T1 bi-component analysis across whole articular cartilage depth - from calcified cartilage to superficial cartilage
Hongda Shao¹, Soorena Azam ZAnganeh¹, Eric Chang¹, Graeme Bydder¹, and Jiang Du¹
- ¹Radiology, University of California, San Diego, San Diego, CA, United States*

Articular cartilage is a highly ordered tissue with an organized layered structure that can be functionally and structurally divided into the superficial, transitional, radial and the calcified cartilage. By exploiting intrinsic magnetic resonance (MR) properties of cartilage, current techniques allow for the non-invasive assessment of many of the structural components. More recently, ultrashort echo time (UTE) imaging sequences have been used to investigate the T2* relaxation times of bound and free water components in different layers of articular cartilage. However, the depth dependence of longitudinal relaxation times, or T1s are still unknown. In this study we aim to study the T1s of bound and free water in different layers of patella cartilage using UTE imaging sequences on a clinical 3T scanner.

4487
Computer #52 T1p imaging in hip cartilage: A comparative study in hips with and without cam type deformity
Gerd Melkus^{1,2}, Helen Anwander³, Kawan S Rakhra^{1,2}, and Paul E Beaulé^{3,4}

¹Medical Imaging, The Ottawa Hospital, Ottawa, ON, Canada, ²Radiology, University of Ottawa, Ottawa, ON, Canada, ³Orthopaedic Surgery, The Ottawa Hospital, Ottawa, ON, Canada, ⁴Faculty of Medicine, University of Ottawa, Ottawa, ON, Canada

In this study we systematically investigated the analysis of hip cartilage T1p images in healthy as well as asymptomatic and symptomatic subjects with cam deformities. Hips with cam-type deformity showed a significant T1p prolongation compared to the healthy subjects indicating loss of proteoglycan in the lateral third of the anterosuperior quadrant. A significant correlation between entire hip cartilage T1p values and WOMAC subscore pain was found. The study shows that in the presence of a cam deformity, T1p has the ability to detect proteoglycan depletion, the earliest stage of cartilage degeneration, even before to symptoms occur.

4488
Computer #53 Buy One, Get Two for Free: Simultaneous Knee T2 Mapping and Morphological Analysis On Synthetic Images Using GRAPPATINI
Patrick Omoumi¹, Tom Hilbert^{1,2,3}, Marion Roux¹, Jean-Baptiste Ledoux¹, Ruud B Van Heeswijk¹, Reto Meuli¹, and Tobias Kober^{1,2,3}

¹Radiology, Lausanne University Hospital, Lausanne, Switzerland, ²Advanced Clinical Imaging Technology (HC CMEA SUI DI BM PI), Siemens Healthcare AG, Lausanne, Switzerland, ³LTSS, Ecole Polytechnique Fédérale de Lausanne, Lausanne, Switzerland

A fast quantitative T2 mapping technique that additionally provides synthetic images for morphological assessment was validated by two experienced radiologists regarding (1) the T2 values through a phantom experiment and (2) the image quality through a quantitative and qualitative assessment for the knee joint in five healthy volunteers.

4489
Computer #54 Isotropic Three-Dimensional T₂ Mapping of Knee Cartilage with T₂-Prepared Segmented Gradient Echo at 3T
Roberto Colotti¹, Patrick Omoumi¹, and Ruud B. van Heeswijk¹

¹Department of Radiology, University Hospital (CHUV) and University of Lausanne (UNIL), Lausanne, Switzerland

An isotropic three-dimensional T₂ mapping technique with adiabatic T₂ magnetization preparation for T₂ relaxation time quantification was implemented and validated at 3T in phantoms and 6 healthy volunteers.

4490
Computer #55 Repeatability and reproducibility of in vivo magnetic resonance T1rho relaxation time measurements of hip cartilage at 3T
Angéline Nemeth¹, Lucy Di Marco², Denis Grenier¹, Michaël Sdika¹, Olivier Beuf¹, and Jean-Baptiste Pialat³

¹CREATIS, Université de Lyon ; CNRS UMR5220 ; Inserm U1044 ; INSA-Lyon ; Université Claude Bernard Lyon 1, Lyon, France, ²Radiologie et Imagerie médicale diagnostique et thérapeutique, Hôpital François Mitterrand, Dijon, France, ³Radiologie Pavillon B, Hôpital Edouard Herriot, Hospices Civils de Lyon, INSERM U1033 and Université Lyon 1, Lyon, France

To detect early changes in cartilage, quantification methods were developed with Magnetic Resonance Imaging. T1rho sequence is a valuable tool to quantitatively access the proteoglycans content, complementary to T2 mapping technique that is correlated with the collagen content. The thin cartilage thickness and deep location of the hip joint require a strong compromise between SNR, pixel size and acquisition time. The aim of this study is to test the repeatability and reproducibility of in vivo (magnetic resonance) T1rho and T2 relaxation times measures in the hip joint cartilage of thirty healthy asymptomatic volunteers.

4491
Computer #56 Osteochondral lesion depth on MRI can help predict the need for a sandwich procedure
Razmara Nizak¹, Joris Bekkers¹, Pim de Jong², and Daniel Saris¹

¹Orthopedics, UMC Utrecht, Utrecht, Netherlands, ²Radiology, UMC Utrecht, Utrecht, Netherlands

Autologous subchondral bone grafting combined with ACI (sandwich procedure) is a well-accepted procedure for the treatment of osteochondral lesions of the knee. This requires a different surgical technique and preoperative planning. Also pain from bone marrow donor site location is expected and should be part of patient consent and expectations. This study evaluates whether MRI is able to predict the need for a sandwich procedure to help in optimizing the preoperative planning and consent.

4492
Computer #57 7 Tesla quantitative hip MRI: A comparison between TESS and CPMG for T2 mapping
Oliver Kraff¹, Andrea Lazik-Palm^{1,2}, Rahel Heule^{3,4}, Oliver Bieri^{3,4}, and Harald H Quick^{1,5}

¹Erwin L. Hahn Institute for MRI, University Duisburg-Essen, Essen, Germany, ²Department of Diagnostic and Interventional Radiology and Neuroradiology, University Duisburg-Essen, University Hospital, Essen, Germany, ³Division of Radiological Physics, Department of Radiology, University of Basel Hospital, Basel, Switzerland, ⁴Department of Biomedical Engineering, University of Basel, Basel, Switzerland, ⁵High Field and Hybrid MR Imaging, University Duisburg-Essen, University Hospital, Essen, Germany

Purpose was the assessment of TESS T2 relaxometry in comparison to standard CPMG as a potential candidate to improve workflow in quantitative hip MRI protocols at 7T. A total of 8 healthy volunteers were included. T2 relaxation times were measured by manually drawing regions of interest in both acetabular and femoral cartilage in multiple regions of the hip joint. Compared to CPMG, TESS provides systematically reduced T2 values in both hip cartilage layers, in line with previously reported values. Nevertheless, with a 5-fold increase in spatial coverage TESS seems to be a good candidate to improve hip protocols at 7T.

4493
Computer #58 Repeatability of R1 ρ , R2, and R2* in Knee Cartilage
Joshua Kaggie¹, Scott Reid², Gavin Houston², Kevin F King³, Ferdia Gallagher¹, and Martin Graves¹

¹Radiology, University of Cambridge, Cambridge, United Kingdom, ²GE Healthcare, Amersham, United Kingdom, ³GE Healthcare, Milwaukee, WI, United States

R1 ρ , R2, and R2* imaging have been considered as biomarkers of degenerative cartilage diseases. In order to ensure the reliability of these measurements, we acquired data in eight subjects twice and compared measurements of variability. R1 ρ -measurements had lower variability (CVRMS=21%) and a higher correlation to age (r2-value=0.566) when compared to R2 (r2-value=0.183; CVRMS=25%) and R2* (r2-value=0.092; CVRMS=38%). These measurements suggest that R1 ρ is a more sensitive biomarker than R2 or R2*.

4494
Computer #59 Diffusion Weighted MRI of the Fibrous Structure of the Meniscus of the Knee: In Vitro Studies at 11.7T
Qun He^{1,2}, Jihye Baek¹, Daryl D'Lima¹, Jiang Du¹, Nikolaus M. Szevenenyi¹, and Graeme Bydder¹

¹University of California, San Diego, San Diego, CA, United States, ²Ningbo Jansen NMR Technology Co., Ltd., Cixi, Zhejiang, China, People's Republic of

In vitro high resolution diffusion weighted imaging of the meniscus of the knee at 11.7T shows detailed structure of fiber groups that has not previously be seen with MRI. There were clearly differentiated from cartilaginous areas of the meniscus. The diffusion contrast adds to that which results from the magic angle effect. This acts as a T₂ filter. The diffusion contrast has more flexibility than magic angle contrast since it is not dependent on B₀ and in principle any diffusion direction can be used. The results may be translatable to high field clinical systems.

4495
Computer #60 Spotlight on gagCEST imaging in human menisci with MR-microimaging on ultra-high field 7T - a pilot study
Benedikt Hager^{1,2,3}, Sonja Walzer³, Matthew DiFranco⁴, Vladimir Juras^{1,5}, Vladimir Mlynarik^{1,2}, Markus Schreiner³, Martin Zalaudek¹, Stefan Domayer³, Esau Poblador Rodriguez¹, Andreas Berg⁴, Reinhard Windhager³, and Siegfried Trattnig^{1,2}

¹High Field MR Centre, Department of Biomedical Imaging and Image-guided Therapy, Medical University of Vienna, Vienna, Austria, ²Christian Doppler Laboratory for Clinical Molecular MR Imaging, Vienna, Austria, ³Department of Orthopaedic Surgery, Medical University of Vienna, Vienna, Austria, ⁴Center for Medical Physics and Biomedical Engineering, Medical University of Vienna, Vienna, Austria, ⁵Department of Imaging Methods, Institute of Measurement Science, Slovak Academy of Sciences, Bratislava, Slovakia

The purpose of this study was to examine whether gagCEST imaging reflects the histopathological changes concerning glycosaminoglycan in human meniscus in vitro. All MRI acquisitions were performed on 7T MRI with a microimaging system. Histological staining using safranin-O was performed for correlation to imaging findings. Qualitatively, the gagCEST map and the corresponding safranin-O image show the same relative regional intensity of glycosaminoglycans. In sum, gagCEST imaging in a 7T microimaging system allows a very detailed look into the glycosaminoglycan distribution in the human meniscus.

4496
Computer #61 Diffusion Weighted 3D UTE in the Posterior Cruciate Ligament
Michael Carl¹, Yajun Ma², Graeme M Bydder², and Jiang Du²

¹Global MR Applications & Workflow, General Electric, San Diego, CA, United States, ²University of California San Diego, San Diego, CA, United States

In this work, we used a stimulated echo prepared diffusion 3DUTE sequence to image the posterior cruciate ligament. Volunteer scans in the knee were performed. We found that stimulated echo based diffusion weighted 3DUTE MR imaging can be used effectively to achieve useful b-values in short T2 MSK tissues. This initial proof-of-principle study shows good quantitative agreement with clinical EPI diffusion sequences.

4497
Computer #62 Open MRI of FAI: Reader agreement of a new method for quantifying femoroacetabular clearance for hips in an impingement posture
Lawrence L Buchan^{1,2}, Honglin Zhang^{1,2}, Mark Harmon³, Elaine Ni Mhurchu³, Morgan Barber⁴, Shannon Jennifer Patterson⁵, Jacek Kopec⁴, Hubert Wong⁶, John Esdaile⁴, Jolanda Cibere⁴, Charles R Ratzlaff⁴, Bruce B Forster³, and David R Wilson¹

¹Orthopaedics, University of British Columbia, Vancouver, BC, Canada, ²Centre for Hip Health and Mobility, Vancouver, BC, Canada, ³Radiology, University of British Columbia, Vancouver, BC, Canada, ⁴Arthritis Research Canada, Richmond, BC, Canada, ⁵Vancouver Coastal Health, Vancouver, BC, Canada, ⁶University of British Columbia, Vancouver, BC, Canada

In this study, we describe a novel open MRI method for evaluating femoroacetabular impingement (FAI) in subjects with and without symptomatic FAI. First, we acquired images of subjects in postures suspected of inducing impingement using a T1-weighted gradient echo MR sequence. Second, readers measured β -angle to quantify clearance between the femur and acetabulum. Reader agreement for β -angle was equivalent or better to agreement when measuring α -angle, a similar structural measure. The open MRI method has the potential to assess functional relationships between the femur and acetabulum that otherwise cannot be assessed with closed-bore MRI scanners and conventional imaging protocols. This approach may be useful in addressing fundamental questions in FAI.

4498 Computer #63 Rapid T2 Relaxometry of the Meniscus, Tendons, and Ligaments with an Ultrashort Echo-Time Double-Echo Steady State Sequence
Akshay S Chaudhari^{1,2}, Bragi Sveinsson^{1,3}, Marcus T Alley¹, Emily J McWalter¹, Garry E Gold^{1,2}, and Brian A Hargreaves^{1,2,3}

¹Radiology, Stanford University, Stanford, CA, United States, ²Bioengineering, Stanford University, Stanford, CA, United States, ³Electrical Engineering, Stanford University, Stanford, CA, United States

Quantitative MR imaging has the potential to provide information regarding the biochemical state of tissues and to track biochemical changes before the onset of morphological changes. However, with current MRI techniques, it is challenging to obtain signal from tissues with short-T₂ relaxation times in the knee, let alone to perform quantitative imaging on them. Ultrashort echo-time double-echo in steady state (UTEDESS) is a pulse sequence that offers echo times of 50 μ s, and high resolution imaging with high SNR efficiencies. In this study, UTEDESS was also used to measure T₂ relaxation times of the menisci, tendons, and ligaments in human knees.

4499 Computer #64 μ MRI T₂* mapping of degenerated human meniscal specimens compared to histology
Benedikt Hager^{1,2,3}, Sonja Walzer², Vladimir Juras^{1,4}, Andreas Berg⁵, Matthew DiFranco⁵, Vladimir Mlynarik^{1,3}, Markus Schreiner², Martin Zalaudek¹, Stefan Domayer², Joachim Friske¹, Reinhard Windhager², and Siegfried Trattnig^{1,3}

¹High Field MR Centre, Department of Biomedical Imaging and Image-guided Therapy, Medical University of Vienna, Vienna, Austria, ²Department of Orthopaedic Surgery, Medical University of Vienna, Vienna, Austria, ³Christian Doppler Laboratory for Clinical Molecular MR Imaging, Vienna, Austria, ⁴Department of Imaging Methods, Institute of Measurement Science, Slovak Academy of Sciences, Vienna, Austria, ⁵Center for Medical Physics and Biomedical Engineering, Medical University of Vienna, Vienna, Austria

In this study, T₂* maps of degenerated meniscal specimens were obtained using MRI on an ultra-high field scanner in combination with an MR microscopy insert and these images were compared to histological findings. The results showed that all five investigated menisci specimens had very similar morphological appearance when comparing histological images, T₂* weighted images and T₂* maps.

4500 Computer #65 Measurement of Fast T2* of the ACL Using 3D UTE Imaging
Kenneth Wengler^{1,2}, Mingqian Huang², Elaine Gould², Mark Schweitzer², Seth Korbin³, James Paci³, and Xiang He²

¹Biomedical Engineering, Stony Brook University, Stony Brook, NY, United States, ²Radiology, Stony Brook University School of Medicine, Stony Brook, NY, United States, ³Orthopaedic Surgery, Stony Brook University School of Medicine, Stony Brook, NY, United States

3D-UTE imaging was utilized to estimate the fast T₂* component of ACL after graft repair surgery. The average fast T₂* component in the grafted ACL 3 months post-surgery for eight subjects is 1.66 +/- 0.4 ms. Two subjects currently have both 3 and 6 month post-surgery images. The ACL average fast T₂* component went from 2.55ms to 1.81ms at three and six months post-surgery respectively for the first subject, and 1.39ms to 1.24ms for the second subject. The results demonstrate promise for 3D-UTE T₂* mapping of bound water to evaluate ACL repair.

4501 Computer #66 Variable angle GLCM analysis for T2 maps of osteoarthritic knee cartilage with endpoint analysis: Oulu Knee Osteoarthritis study
Arttu Peuna^{1,2,3}, Joonas Hekkala^{1,3}, Marianne Haapea^{1,2}, Jana Podlipska^{1,3}, Simo Saarakkala^{1,2,3}, Miika T Nieminen^{1,2,3}, and Eveliina Lammentausta^{1,2}

¹Medical Research Center, University of Oulu and Oulu University Hospital, Oulu, Finland, ²Department of Diagnostic Radiology, Oulu University Hospital, Oulu, Finland, ³Research group of Medical Imaging, Physics and Technology, University of Oulu, Oulu, Finland

Texture analysis methods based on gray level co-occurrence matrices can be optimized to probe the spatial information from knee MR T2 maps and of the changes caused by osteoarthritis. Curvature of the cartilage surfaces and relatively low resolution in relation to cartilage thickness set special requirements for texture analysis tools. Here we report an optimized analysis tool with customized point-wise offset angle and endpoint extrapolation for cartilage texture analysis. Method provides excellent performance compared to traditional texture analysis implementation.

4502 Computer #67 Comparing The Performance Of 3D T1W-WATS Sequence With 2D T2* FFE Sequence In Cartilage Changes Of Pediatric Hemophilic Joints
Yanqiu Lv¹, Hua Cheng¹, Ningning Zhang¹, Kaining Shi², Guangheng Yin¹, Di Hu¹, Huiying Kang¹, Xiaojuan Tao¹, Feng Guan¹, Yang Wen¹, and Yun Peng¹

¹Beijing Children's Hospital Affiliated To Capital Medical University, Beijing, China, People's Republic of, ²Imaging systems Clinical Science, Philips Healthcare, Beijing, China, People's Republic of

Comparing the performance of 3D T1W-WATS sequence with 2D T2*W FFE sequence in the evaluation of cartilage damage in Pediatric hemophilia joints. 16 hemophilic joints including 8 knees and 8 ankles were scanned on a 3.0 T, signal to noise of Cartilage, relative contrast between cartilage and surrounding tissue and the impact of hemosiderin were employed to compare. Our result showed that 3D T1W-WATS sequence had better relative contrast between cartilage and surrounding tissues and the immunity to hemosiderin

compared with 2D T2*W sequence.3DT1W-WATS sequence can be performed in the evaluation of cartilage damage in hemophilia patients.

-
- 4503
Computer #68 Effects of the acquisition window length on articular cartilage sodium MR image quality
Alireza Akbari^{1,2} and Michael Noseworthy^{1,2,3}
- ¹School of Biomedical Engineering, McMaster University, Hamilton, ON, Canada, ²Imaging Research Centre, St Joseph's Healthcare, Hamilton, ON, Canada, ³Electrical and Computer Engineering, McMaster University, Hamilton, ON, Canada*
- We assessed articular cartilage sodium MR image SNR and blurring as a function of acquisition window length. Increasing the acquisition window dramatically improved the SNR with minimal reduction in image quality as shown by minimal blurring.
-
- 4504
Computer #69 Simultaneous Extraction of ADC and T2: Validation of Quantified DESS Sequence at 3T and 7T
Forrest Howell¹, Haonan Wang¹, Daniel Park², Meredith Taylor¹, Bragi Sveinsson³, and Neal Bangerter¹
- ¹Electrical Engineering, Brigham Young University, Provo, UT, United States, ²Biomedical Imaging, Electrical Engineering, University of Oxford, Oxford, United Kingdom, ³Radiology, Stanford University, Palo Alto, CA, United States*
- A modification of the dual-echo steady state (DESS) pulse sequence was recently proposed that allows the extraction of both T2 and apparent diffusion coefficient (ADC) maps from a pair of DESS acquisitions (termed quantitative DESS, or qDESS). A careful validation of the accuracy of the qDESS T2 and ADC estimates has not yet been performed. The qDESS sequence produces accurate, high-resolution ADC and T2 maps. This is especially notable at 7T, where transmit B1 inhomogeneity makes it very difficult to produce reasonable T2 maps using typical multi-echo spin echo techniques. The qDESS technique shows great promise in providing both high-resolution morphological data and maps of T2 and ADC at 3 and 7 Tesla.
-
- 4505
Computer #70 Diffusion MRI models for Cartilage: beyond the Diffusion Tensor
Uran Ferizi¹, Ignacio Rossi², Christian Glaser³, Jenny Bencardino¹, and Jose Raya¹
- ¹Department of Radiology, New York University School of Medicine, New York, NY, United States, ²Department of Orthopaedic Surgery, New York University School of Medicine, New York, NY, United States, ³Radiologisches Zentrum München-Pasing, Munich, Germany*
- The current DTI model has shown promise in capturing the early trends of change in cartilage. However, the model is very sensitive to the noise in the signal, hence blurring the contrast in the the anisotropy maps. Here we propose a simplification of the 6-parameter model to a 4-parameter one, called the "Zeppelin". The biophysical description that the Zeppelin makes remains the same and, additionally, provides fits that are more stable and provide better contrast. We also propose a new and simple 4-parameter multicompartment model (which is already known in neuroimaging). This provides an even more robust model fitting to the data, producing parameters that are analogous to those of Zeppelin, and promising more specificity to the early changes that occur in cartilage.
-
- 4506
Computer #71 Loading Significantly Influences the Zonal T1 of Medial Tibial Cartilage Topographically
Ji Hyun Lee^{1,2}, Farid Badar^{1,2}, John Matyas³, and Yang Xia^{1,2}
- ¹Physics, Oakland University, Rochester, MI, United States, ²Center for Biomedical Research, Oakland University, Rochester, MI, United States, ³Univeristy of Calgary, Calgary, AB, Canada*
- This study aims to quantify the loading-modified T1 in articular cartilage using a canine model of early osteoarthritis (OA) at different degradation stages, at a 17.6µm resolution and with the use of Gd contrast agent. Both lesion and mechanical compression were found to alter T1 in cartilage at each sub-tissue zone and topographically, which provide a better understanding of the MRI properties of cartilage during joint loading. This result could help to design effective protocols in clinical MRI to better detect and manage the osteoarthritic diseases.
-
- 4507
Computer #72 Chondral Injury from ACL Injury: Monitoring Disease Progression
Matthew F. Koff¹, Hollis G. Potter¹, Sonja Eagle¹, Scott Rodeo², Kimberly Amrami³, Aaron Krych³, Xiaojuan Li⁴, and Sharmilla Majumdar⁴
- ¹Department of Radiology and Imaging - MRI, Hospital for Special Surgery, New York, NY, United States, ²Sports Medicine and Shoulder Service, Hospital for Special Surgery, New York, NY, United States, ³Mayo Clinic, Rochester, MN, United States, ⁴University of California San Francisco, San Francisco, CA, United States*
- this is a synopsis
-

Electronic Poster

Muscle & Functional Imaging

Exhibition Hall

Thursday, May 12, 2016: 14:30 - 15:30

- 4508
Computer #73
Functional Changes in Medial Gastrocnemius from Unilateral Limb Suspension Induced Acute Atrophy: a 2D Strain Rate Study during Isometric Contraction
Vadim Malis¹, Usha Sinha², Robert Csapo³, and Shantanu Sinha³
- ¹Physics, University of California at San Diego, San Diego, CA, United States, ²Physics, San Diego State University, San Diego, CA, United States, ³Radiology, University of California at San Diego, San Diego, CA, United States
- Unilateral limb suspension is a controlled method to generate acute atrophy. The loss of muscle force with acute atrophy may be due to changes in contractile elements and extracellular matrix (ECM); a study of the strain rate (SR) patterns could provide information on these changes. Subjects were assessed at baseline (pre-ULLS) and post-ULLS using dynamic velocity encoded phase contrast MR imaging. The indices extracted from the SR tensor show at post-ULLS (i) a decrease in the asymmetry of deformation in the fiber cross-section and (ii) larger SR-muscle fiber angles. These findings may reflect a loss of integrity in the ECM.
-
- 4509
Computer #74
Physiological insights into medial gastrocnemius function during eccentric contraction in normal and in acute atrophy – Quantification of 2D strain rate indices from Velocity Encoded Phase Contrast MR Imaging.
Usha Sinha¹, Vadim Malis², Robert Csapo³, and Shantanu Sinha³
- ¹Physics, San Diego State University, San Diego, CA, United States, ²Physics, University of California at San Diego, San Diego, CA, United States, ³Radiology, University of California at San Diego, San Diego, CA, United States
- In-vivo studies of muscle function under different motion paradigms can elucidate the physiology of acute atrophy. This study maps the 2D strain rate tensor in subjects performing eccentric contractions before and after Unilateral Limb Suspension induced acute atrophy. As expected, strain rate values are smaller during eccentric compared to isometric contractions, since in the eccentric mode, muscle contraction occurs under lengthening conditions resulting in a net smaller local elongation. Changes of SR indices with atrophy are negligible possibly due to a balance of force loss from atrophy and greater force generation from a potentially stiffer matrix.
-
- 4510
Computer #75
Feasibility study of interleaved multi-nuclear acquisitions on a 3 T clinical NMR scanner without hardware modifications
Alfredo Liubomir Lopez Kolkovsky^{1,2}, Benjamin Marty^{1,2}, Eric Giacomini¹, and Pierre G Carlier^{1,2}
- ¹NMR Laboratory, Institut of Myology, Paris, France, ²NMR Laboratory, CEA/DSV/I2BM/MIRCen, Fontenay-aux-Roses, France
- NMR allows to investigate multiple aspects of physiological parameters like regional perfusion, blood and tissue oxygenation, intracellular pH or high-energy phosphate metabolism. In the past, interleaved multiparametric multinuclear dynamic NMR imaging and spectroscopy of skeletal muscle was developed on prototype scanners. Here we evaluated an interleaved pulse sequence combining the NMR acquisition of a ¹H image and ³¹P spectrum on a clinical system without any hardware modifications from the customer. Having the possibility to run interleaved multinuclear sequences on unmodified clinical systems will greatly facilitate simultaneous measurements of tissue perfusion, oxygen content and mitochondrial ATP production in clinical research studies.
-
- 4511
Computer #76
Comparison of T2-prepared 3D TSE with multi-echo spin-echo sequences for T2 mapping of thigh muscles in healthy volunteers
Elisabeth Klupp¹, Dominik Weidlich², Thomas Baum², Barbara Cervantes², Marcus Deschauer³, Hendrik Kooijman⁴, Ernst J. Rummeny², Claus Zimmer¹, Jan S. Kirschke¹, and Dimitrios C. Karampinos²
- ¹Neuroradiology, Technische Universität München, München, Germany, ²Radiology, Technische Universität München, München, Germany, ³Neurology, Technische Universität München, München, Germany, ⁴Philips Healthcare, Hamburg, Germany
- There is a growing interest for applying T2 mapping for non-invasively tracking inflammatory changes in patients with neuromuscular diseases. T2 has been traditionally quantified using multi-echo spin-echo (MESE) sequences with known problems related to the refocusing pulses in presence of B1-inhomogeneity and slice profiles effects. The present work proposes the combination of an adiabatic T2-preparation with 3D TSE for B1-insensitive T2 mapping. The proposed method is compared with 2D-MESE and 3D-MESE, in terms of reproducibility on T2 quantification and sensitivity to B1 effects, in the thigh musculature of ten healthy subjects.
-
- 4512
Computer #77
T2* Mapping of Lower Leg Muscles Following Single Brief Contractions at 3 T
Prodromos Parasoglou¹, Tiejun Zhao², Oleksandr Khagai¹, Xuejiao Che¹, and Jill M Slade³
- ¹Department of Radiology, New York University School of Medicine, New York, NY, United States, ²Siemens Medical Solutions USA, Siemens Healthcare, New York, NY, United States, ³Department of Radiology, Michigan State University, East Lansing, MI, United States
- Microvascular function in the skeletal muscle can be assessed through blood oxygenation level dependent (BOLD) MRI signal changes after performing a brief exercise or following a period of induced ischemia. Such BOLD related relaxation changes are mainly attributed to intravascular mechanisms, such as changes in the hemoglobin content and oxygen saturation levels. In this work, we developed and implemented a rapid echo-planar imaging (EPI) method to map T₂* changes, following a single maximum voluntary contraction on a 3 T whole body clinical scanner.
-
- 4513
Computer #78
Quantitative Assessment of Muscle Fat in Sarcopenia Using Magnetic Resonance Imaging (MRI) and Spectroscopy (MRS)
Alexandra Grimm^{1,2}, Heiko Meyer², Mathias Nittka², Esther Raithel², Andreas Friedberger¹, Marc Teschler¹, Michael Uder³, Wolfgang Kemmler¹, Klaus Engelke¹, and Harald H. Quick^{1,4}
- ¹Institute of Medical Physics, Erlangen, Germany, ²Product Definition & Innovation, Siemens Healthcare GmbH, Erlangen, Germany, ³Institute of

Sarcopenia describes muscle degeneration. In particular with increasing age, muscle tissue is replaced by fatty infiltrations. We developed an MRI sequence protocol (T₁w TSE, PDw SPACE, PDw TSE Dixon, q-Dixon, and HISTO) for quantifying this degradation and applied it twice to 54 patients suffering from sarcopenia. Between both measurements three months of whole body electromyostimulation (EMS) training were performed. Initial results show that image data can be used for muscle segmentation and determination of muscle volumes, fat fractions, and fat distribution within the muscles. Muscle fat fractions correlate with muscle strength. In spectroscopy accurate voxel repositioning is challenging.

4514

Computer #79 Foot Oximetry Angiosomes with MRI
Jie Zheng¹, David Muccigrosso¹, Xiaodong Zhang², Hongyu An¹, Andrew R Coggan¹, Charles F Hildebolt¹, Chandu Vemuri³, Patrick Geraghty³, Mary K Hastings⁴, and Michael J Mueller⁴

¹Radiology, Washington University in St. Louis, St. Louis, MO, United States, ²Radiology, Peking University First Hospital, Beijing, China, People's Republic of, ³Surgery, Washington University in St. Louis, St. Louis, MO, United States, ⁴The Program in Physical Therapy, Washington University in St. Louis, St. Louis, MO, United States

The objective of this study was to develop a non-contrast MRI based oximetry approach to assess the skeletal muscle microcirculation in diabetic and healthy feet. In both healthy and subjects with diabetes, the feasibility of the foot oximetry was examined when the subjects were at rest and during a toe-flexion isometric exercise. The percent difference in the areas of the oxygen extraction fraction within the 0.7 - 1.0 range between rest and exercise was significantly different between healthy subjects and subjects with diabetes. This is the first MRI foot oximetry developed for assessing regional skeletal muscle oxygenation.

4515

Computer #80 Correlation between sodium and T1ρ dispersion in human calf muscle
Ping Wang^{1,2}, Henry Zhu^{1,2}, Hakmook Kang³, and John C. Gore^{1,2}

¹Institute of Imaging Science, Vanderbilt University Medical Center, Nashville, TN, United States, ²Department of Radiology and Radiological Sciences, Vanderbilt University Medical Center, Nashville, TN, United States, ³Department of Biostatistics, Vanderbilt University Medical Center, Nashville, TN, United States

Simultaneous acquisitions of sodium concentrations and T_{1ρ} in muscles from different aged individuals show that sodium values increase with age and are accompanied by increases in the dispersion of spin-lock relaxation rates (i.e. the difference in R_{1ρ} = 1/T_{1ρ} at low and high locking frequencies). A previous study has suggested that such differences in R_{1ρ} at different fields reflects the contribution of chemical exchange to relaxation, which is known to dominate transverse relaxation at high fields, and potentially reflects GAG concentration in cartilage. In this study, we found ΔR_{1ρ} in muscle was smaller than in cartilage at 3T but was measurable and showed a strong correlation with sodium content in muscle. The increase in sodium with age possibly corresponds to the loss of muscle mass and increase in extracellular volume within a voxel, but this appears to be accompanied by an increase in exchangeable protons as well.

4516

Computer #81 Automatic segmentation for volume quantification of quadriceps muscle head in athletes during an extreme mountain ultra-marathon
Benjamin Gilles¹, Charles de Bourguignon², Pierre Croisille³, Grégoire Millet⁴, Magalie Viallon³, and Olivier Beuf⁵

¹LIRMM; CNRS (UMR 5506) Université de Montpellier, Montpellier, France, ²Radiology Dept, CHU de Saint Etienne, Saint Etienne, France, ³CREATIS, Université de Lyon ; CNRS UMR5220 ; Inserm U1044 ; INSA-Lyon ; Université Claude Bernard Lyon 1, Saint Etienne, France, ⁴Institute of Sport Sciences, University of Lausanne, Lausanne, Switzerland, ⁵CREATIS, Université de Lyon ; CNRS UMR5220 ; Inserm U1044 ; INSA-Lyon ; Université Claude Bernard Lyon 1, Villeurbanne, France

Acute loss of skeletal muscle mass is a common feature of several pathologies such as stroke, cancer, chronic obstructive pulmonary disease. Having a non-invasive method to accurately quantify muscle mass is of crucial interest to follow procedure that could prevent muscle wasting and restore physical capacity, mobility and optimize motor recovery. The aim of the current study is to propose an automatic segmentation technique to quantify muscle mass. The automatic segmentation of 3D quadriceps volumes was performed using a deformable registration technique applied to 3D isotropic in-phase (IN), out-phase (OUT), and calculated fat (F) and water (W) images obtained using a double-echo gradient echo Dixon coronal acquisition in order to test the best contrast channel for segmentation. The method was tested in a longitudinal study in athletes enrolled for the most extreme mountain ultra-marathon (The Tor des Géants, Courmayeur, Italy: +24000 positive elevation, 330km). 51 athletes were scanned at departure, 27 finishers at the arrival and 2 days after recovery, leading to 105 datasets that were segmented in total. The best automatic segmentation accuracy was obtained when using the calculated Water image (DSC=0,946).

4517

Computer #82 Simultaneous quantitative susceptibility, PDFF and transversal relaxation time mapping in dystrophic skeletal muscle
Benjamin Leporq^{1,2}, Arnaud Le Troter³, Yann Le Fur³, Emmanuelle Salort-Campana⁴, Maxime Guye³, Olivier Beuf², and David Bendahan^{3,5}

¹Center of Research on inflammation; Inserm U1149, Université Paris Diderot, Paris, France, ²CREATIS CNRS UMR 5220; Inserm U1044, Université de Lyon, Villeurbanne, France, ³CRMBM; CNRS UMR 7339, Aix-Marseille University, Marseille, France, ⁴Genétique Médicale et Génomique Fonctionnelle; Inserm UMR S_910, Aix Marseille University, Marseille, France, ⁵CEMEREM, Hôpital de la Timone, Pôle d'imagerie médicale, AP-HM, Marseille, France

We have developed a dedicated algorithm allowing to quantify, from a single MR acquisition fat and muscle fractions together with magnetic susceptibility and transverse relaxation time (T₂*). This approach was linked to a dedicated segmentation algorithm allowing to quantify specific indices which could be of interest for the assessment of disease severity and progression. Our results showed the

feasibility of quantitative susceptibility mapping (QSM) in thigh muscles and demonstrated that its implementation into the fat-water separation reconstruction pipeline is possible. For dystrophies assessment, magnetic susceptibility-related information might provide a useful supplementary materials in comparison to relaxometry and fat fraction measurements.

4518

Computer #83 Evaluation of Cuff-Induced Skeletal Muscle Microvascular Perfusion of Lower Extremity by ASL and IVIM MRI techniques
Qing Lu¹, Shiteng Suo¹, Hui Tang¹, Jianxun Qu², Yong Zhang², and Jianrong Xu¹

¹Department of Radiology, Ren Ji Hospital, School of Medicine, Shanghai Jiao Tong University, Shanghai, China, People's Republic of, ²GE Healthcare China, Shanghai, China, People's Republic of

Arterial spin labeling (ASL) and intravoxel incoherent motion (IVIM) are both noninvasive MRI techniques that offer quantitative perfusion measurements. The current study showed that the ASL perfusion decreased while the IVIM vascular volume fraction increased compared to baseline under cuff compression paradigm in the lower extremity muscle, indicating that the two MRI techniques based on two completely distinct mechanisms provide complementary tissue perfusion characteristics.

4519

Computer #84 Quantitative MR evaluation of fatty infiltration and edema-like processes in skeletal muscles of Myotonic Dystrophy type 1
Linda Heskamp¹, Marlies van Nimwegen², Barbara Janssen¹, Baziel van Engelen², and Arend Heerschap¹

¹Department of Radiology and Nuclear Medicine, Radboud university medical center, Nijmegen, Netherlands, ²Department of Neurology, Radboud university medical center, Nijmegen, Netherlands

We used quantitative MR to evaluate the extent of fatty infiltration and edema-like processes in muscles of patients with Myotonic Dystrophy type 1 (DM1). Fat fractions were obtained using a DIXON method and the T2 of muscle water (T2_{water}) was calculated using a bi-component extended phase graph model. The results show that fatty infiltration in DM1 is a slow gradual process whereby the distal part of the muscle is more heavily fat infiltrated than the proximal part. In addition, muscles that are in an active process of fatty infiltration have an elevated T2_{water}, possibly from reactive edema.

4520

Computer #85 Rapid High Resolution 3D Musculoskeletal Imaging at 7T: Contrast Optimization and Comparison of DESS, Phase-Cycled bSSFP, and 3D SPACE
Meredith Taylor¹, Haonan Wang¹, Antony JR Palmer², Andrew J Carr², Sion Glyn-Jones², Daniel Park², and Neal K Bangerter¹

¹Electrical Engineering, Brigham Young University, Provo, UT, United States, ²Nuffield Department of Orthopaedics, Rheumatology, and Musculoskeletal Sciences, University of Oxford, Oxford, United Kingdom

In this study, we (1) implemented a two-acquisition 3D phase-cycled bSSFP protocol at 7 Tesla that achieves 0.31mm isotropic resolution in under 9 minutes of scan time, (2) implemented a 3D DESS protocol at 7 Tesla that achieves 0.36mm isotropic resolution in just under 7 minutes, (3) performed a contrast optimization to identify flip angles that maximize both cartilage/muscle and cartilage/synovial fluid contrast, and (3) compared to a 3D SPACE acquisition at 7T that achieves 0.55mm isotropic resolution in a scan time of 11:37.

4521

Computer #86 ¹H MRS can detect and quantify acetylcarnitine in different human skeletal muscles at rest at 7T.
Radka Tušková^{1,2,3}, Ladislav Valkovič^{1,3,4,5}, Martin Gajdošík^{1,3}, Thomas Heckmann⁶, Norbert Bachl⁶, Harald Tschan⁶, Siegfried Trattnig^{1,3}, and Martin Krššák^{1,3,7}

¹High-Field MR Center, Department of Biomedical Imaging and Image-Guided Therapy, Medical University of Vienna, Vienna, Austria, ²Faculty of Chemical and Food Technology, Department of NMR Spectroscopy and Mass Spectrometry, Slovak University of Technology in Bratislava, Bratislava, Slovakia, ³Christian Doppler Laboratory for Clinical Molecular MR Imaging, Vienna, Austria, ⁴John Radcliffe Hospital, University of Oxford Centre for Clinical Magnetic Resonance Research, University of Oxford, Oxford, United Kingdom, ⁵Department of Imaging Methods, Institute of Measurements Science, Slovak Academy of Sciences, Bratislava, Slovakia, ⁶Center of Sport Science and University Sport, University of Vienna, Vienna, Austria, ⁷Division of Endocrinology and Metabolism, Department of Internal Medicine III, Medical University of Vienna, Vienna, Austria

Carnitine plays an important role in fat metabolism. A long-echo time (TE of 350ms) proton magnetic resonance spectroscopy protocol was implemented for detection of skeletal muscle acetylcarnitine at rest on a clinical 7T scanner in the calf (soleus) and thigh (vastus lateralis) muscle. T2 relaxation times of the 2.13 ppm signal of acetylcarnitine at 7T were assessed as 137.8±47.7ms. Concentrations of acetylcarnitine in vastus lateralis muscle in four healthy volunteers were found to be 1.69±0.21mmol/kg wet weight, whereas lower concentrations (i.e., 0.54±0.19mmol/kg) were found in soleus muscle.

4522

Computer #87 A Low-Cost MR Compatible Ergometer For Assessing Lower Leg Muscle Metabolism
Xuejiao Che¹, Ryan Brown^{1,2}, Leeor Alon^{1,2}, Ravinder R Regatte¹, and Prodomos Parasoglou¹

¹Department of Radiology, New York University School of Medicine, New York, NY, United States, ²NYU WIRELESS, Polytechnic Institute of New York University, Brooklyn, NY, United States

In this work, we designed and constructed an inexpensive MR compatible ergometer that can be used for studying lower leg muscle metabolism. This ergometer allows subjects to perform a plantar flexion exercise protocol while ³¹P-MR data are acquired. The device is easy to use, and it can be positioned inside the bore of the magnet in less than 10 min. The mechanical power exerted by the subject can be estimated from force and angle displacement signals that are continuously monitored, while the exercise intensity can be varied by changing the number and/or the material of the resistive elastic cords.

-
- 4523
Computer #88
What is the Relationship between Vascular Disease Distribution in PAD and Exercise-Induced Hyperemia Pattern in Calf Muscle?
Christopher J Hanrahan¹, Jeff L Zhang¹, Gwenael Layec², Corey Hart², Michelle Mueller³, Daniel Kim¹, Kristi Carlston¹, Russell S Richardson², and Vivian S Lee¹
- ¹Radiology, Utah Center for Advanced Imaging Research (UCAIR), University of Utah School of Medicine, Salt Lake City, UT, United States, ²Internal Medicine, Division of Geriatrics, Utah Vascular Research Lab (UVRL), University of Utah School of Medicine, Salt Lake City, UT, United States, ³Surgery, University of Utah School of Medicine, Salt Lake City, UT, United States
- Calf muscle perfusion by first-pass gadolinium MRI provides objective measures to help understand the relationship between vascular pathology and muscle dysfunction in peripheral arterial disease (PAD) patients. We compared perfusion in healthy and PAD subjects in exercise-recovery and, in the same PAD patients, related muscle perfusion pattern to hemodynamically significant vessel pathology found at MR arteriography. We found no relation between specific stenosis/occlusion and the expected muscle perfusion downstream, but calf vascular pathology significantly decreased perfusion in the superficial posterior compartment muscles compared to abdominopelvic/thigh vessel abnormality. Assessing muscle perfusion shows promise in assessing PAD disease severity and guiding treatment.
-
- 4524
Computer #89
Magnetic resonance imaging estimates of muscle volume and inter-muscular fat in the thigh in sarcopenia population: correlation with physical performances
Yu Xin Yang¹, Mei Sian Chong¹, Laura Tay¹, Suzanne Yew¹, Audrey Yeo¹, and Cher Heng Tan²
- ¹Institute of Geriatrics and Active Ageing, Tan Tock Seng Hospital, Singapore, Singapore, ²Department of Diagnostic Radiology, Tan Tock Seng Hospital, Singapore, Singapore
- This study presented using MRI to quantify muscle and fat volumes in thigh for sarcopenic and sarcopenic obese (SO) populations. The correlation between different thigh components and patients' physical performances was also assessed. Results show that MRI is a promising tool for early detection of sarcopenia and SO. This may translate to use in clinical trials and in clinical practice. MRI measurement of inter-muscular fat volume is a valuable component in thigh to monitor patients' physical performances.
-
- 4525
Computer #90
Comparison of relative RF power deposition for shoulder MRI at 3.0T and 7.0T using 3D dual echo steady state imaging
Marko Hoehne¹, Andreas Graessl², Antje Els², Thomas Herold³, and Thoralf Niendorf⁴
- ¹HELIOS Klinikum Berlin Buch, Radiology, Max Delbrück Center for Molecular Medicine (MDC) Berlin, Ultrahigh Field Facility (B.U.F.F.), Berlin, Germany, ²Max Delbrück Center for Molecular Medicine (MDC), Ultrahigh Field Facility (B.U.F.F.), Berlin, Germany, ³HELIOS Klinikum Berlin Buch, Radiology, Berlin, Germany, ⁴Max Delbrück Center for Molecular Medicine (MDC), Experimental and Clinical Research Center (ECRC), Charite Campus Berlin Buch, Humboldt University Berlin, Ultrahigh Field Facility (B.U.F.F.), Berlin, Germany
- Technology advances in ultra-high field systems improve significantly diagnose of different musculoskeletal structures. A challenge of this work examines relative RF power deposition for shoulder MRI with dual echo steady state imaging at 3.0T and 7.0T. Volunteers (n=10, mean age 36.5 ± 8.51 years) were investigated at 3.0 T and 7.0 T. The flip angle was varied for each field strength. A comparison of flip angle between 3.0T and 7.0T showed a SAR gain of approximately 2.6 for the local RF coil setup used at 7.0 T versus the body coil configuration employed at 3.0 T. It is important to considering a right choice of sequences and these parameters.
-
- 4526
Computer #91
Fat infiltration is non-uniform along the proximodistal muscle axis in Duchenne Muscular Dystrophy
Melissa Hooijmans¹, Nathalie Doorenweerd¹, Jedrek Burakiewicz¹, Jan Verschuuren², Constantin Anastasopoulos¹, Andrew Webb¹, Erik Niks², and Hermien Kan¹
- ¹Radiology, Leiden University Medical Center, Leiden, Netherlands, ²Neurology, Leiden University Medical Center, Leiden, Netherlands
- Progressive replacement of muscle tissue by fat is one of the main characteristics of DMD. This muscle degeneration process has been extensively studied in terms of differences between individual muscles, but not as a function of physical location within each individual muscle. This work showed non-uniform fat infiltration along the proximodistal muscle axis within individual muscles using the Dixon water/fat technique. These observations provide new insight into disease progression in DMD.
-
- 4527
Computer #92
Towards Fast and Robust Bilateral Brachial Plexus Imaging
Kang Wang¹, Ken-Pin Hwang^{2,3}, Zac Slavens⁴, Adriana Kanwischer⁵, Kevin King⁵, Suchandrima Banerjee⁶, Pauline Worters⁶, and Ersin Bayram²
- ¹Global MR Applications & Workflow, GE Healthcare, Madison, WI, United States, ²Global MR Applications & Workflow, GE Healthcare, Houston, TX, United States, ³Department of Imaging Physics, University of Texas M.D. Anderson Cancer Center, Houston, TX, United States, ⁴MR Engineering, GE Healthcare, Waukesha, WI, United States, ⁵Global MR Applications & Workflow, GE Healthcare, Waukesha, WI, United States, ⁶Global MR Applications & Workflow, GE Healthcare, Menlo Park, CA, United States
- MR imaging of bilateral brachial plexus has been challenging due to various reasons, such as fat suppression failures caused by B₀ inhomogeneity, arms wrapping in arms-down imaging for patient comfort, and long scan time, etc. In this work, these aforementioned challenges were addressed by combining and utilizing novel MR imaging techniques, and a fast and robust protocol for bilateral brachial plexus MR imaging is proposed.

- 4528
Computer #93 Fasciculation MR Imaging (faMRI) of the Lower Leg
Nikolaus M. Szevenyi¹ and Graeme M. Bydder¹
¹Radiology, University of California, San Diego, San Diego, CA, United States
- Fasciculations are brief spontaneous contractions affecting a small number of muscle fibers. We investigated how diffusion sensitized MR images were able to detect these contractions in the lower leg of healthy volunteers. Large intensity decreases were observed (at random times) in random areas of muscle on images, acquired repeatedly using single shot (diffusion sensitized) EPI acquisitions over the course of several minutes. Signal intensity reductions were attributed to intra-voxel incoherent-like motion due to displacement of tissue. Quantification compared activated areas to total muscle area and frequency of activation on a per pixel basis. Results were expressed as a fasciculation index parameter and in fasciculation frequency maps.
-
- 4529
Computer #94 Towards high temporal resolution Creatine Chemical Exchange Saturation Transfer (Cr-CEST) during plantar flexion exercise: Preliminary results at 7T
Esaú Poblador Rodriguez¹, Marek Chmélík^{1,2}, Vladimír Mlynárik^{1,2}, Siegfried Trattng^{1,2}, and Wolfgang Bogner¹
¹High Field MR Centre, Department of Biomedical Imaging and Image-guided Therapy, Medical University of Vienna, Vienna, Austria, ²Christian Doppler Laboratory for Clinical Molecular MR Imaging, Vienna, Austria
- Once the technical limitations are cleared, Cr-CEST could replace ³¹P-MRS, becoming a powerful tool for assessment of treatment outcomes and diagnosis of muscular disorders, due to its superior spatial resolution and sensitivity. Phantom measurements show how Cr concentration and pH are linearly correlated with CEST contrast maps. The preliminary *in-vivo* measurements, with a time resolution of 13.1s per repetition, produce an enhancement of gastrocnemius muscle of 12% during plantar flexion exercise. However, a further increased time resolution is anticipated for dynamic studies, close to those routinely used in dynamic ³¹P-MRS.
-
- 4530
Computer #95 High-Resolution DTI of Distal Peripheral Nerves Using Flow-Compensated Diffusion-Prepared 3D TSE
Barbara Cervantes¹, Qinwei Zhang², Kim van de Ven³, Hendrik Kooijman⁴, Ernst Rummeny¹, Axel Haase⁵, Gustav J Strijkers², Jan S Kirschke⁶, Aart J Nederveen², and Dimitrios C Karampinos¹
¹Diagnostic and Interventional Radiology, Technische Universität München, Munich, Germany, ²Radiology, Academic Medical Center, Amsterdam, Netherlands, ³Philips Healthcare, Best, Netherlands, ⁴Philips Healthcare, Hamburg, Germany, ⁵Zentralinstitut für Medizintechnik, Garching, Germany, ⁶Neuroradiology, Technische Universität München, Munich, Germany
- Quantitative MRI is becoming a promising tool in the assessment of peripheral nerve pathologies and anomalies. Peripheral neuropathy is frequently accompanied by neuropathic changes, which can be quantified with diffusion tensor imaging (DTI). Given the small sizes and oblique geometries of many peripheral nerves, peripheral-nerve DTI requires an acquisition method that can provide high-resolution, distortion-free images in acceptable clinical scanning times. The present work demonstrates isotropic- and sub-millimeter-resolution, artifact-free DTI of the nerves in the lower extremity using flow-compensated diffusion-prepared 3D turbo spin echo (TSE).
-
- 4531
Computer #96 Volumetric Brachial Plexus Imaging at 3T with Dual-echo Dixon TSE: comparison against 3D STIR and 3D SPAIR
Xinzeng Wang¹, Crystal E. Harrison¹, Yogesh K. Mariappan², Karthik Gopalakrishnan², Avneesh Chhabra^{1,3}, Robert E. Lenkinski^{1,3}, and Ananth J. Madhuranthakam^{1,3}
¹Radiology, UT Southwestern Medical Center, Dallas, TX, United States, ²Philips Innovation Campus, Philips Healthcare, Bangalore, India, ³Advanced Imaging Research Center, UT Southwestern Medical Center, Dallas, TX, United States
- Volumetric Brachial Plexus imaging at 3T often suffers from incomplete fat suppression and reduced SNR with standard STIR and SPAIR due to increased B1 and B0 inhomogeneities. Dual-echo Dixon TSE has been shown to achieve uniform fat suppression without increasing total scan time or SNR penalty by acquiring two echoes in the same repetition. In this work, we compared 3D dual-echo Dixon TSE against current standard of care 3D STIR and 3D SPAIR for brachial plexus imaging with respect to fat suppression, blood suppression, nerve visualization and SNR at 3T. Overall, the 3D dual-echo Dixon TSE showed significantly improved performance.
-
-